



42ND ANNUAL *MidWinter Meeting*

February 9 – 13, 2019



Baltimore Marriott Waterfront

Baltimore, Maryland, USA

ARO OFFICERS FOR 2018-2019

PRESIDENT:	Karen P. Steel, PhD (18-19) Kings College London Wolfson Centre for Age Related Diseases London, United Kingdom SE1 1UL
PRESIDENT ELECT:	Keiko Hirose, MD (18-19) Department of Otolaryngology Washington University School of Medicine 660 S Euclid Ave. St. Louis, MO 63110
PAST PRESIDENT:	John P. Carey, MD (18-19) Johns Hopkins School of Medicine Department of Otolaryngology-HNS 601 North Caroline Street, Room 6161A Baltimore, MD 21287-0910 USA
SECRETARY/ TREASURER:	Gabriel Corfas, PhD (17-20) The University of Michigan, Kresge Hearing Research Institute 1150 West Medical Center. Drive Medical Sciences 1 Bldg; RM 5424A Ann Arbor, MI 48109
COMMUNICATIONS OFFICER:	Donna M. Fekete, PhD (18-21) Purdue University 829 Lagrange Street West Lafayette, IN 47906
HISTORIAN:	Open
COUNCIL MEMBERS AT LARGE:	Gwenaelle S. Geleoc, PhD (17-20) Boston Children's Hospital 3 Balckfan Circle Boston, MA 02115 Shi Nae Park, MD, PhD (16-19) Professor, Dept of Otolaryngology – HNS Seoul St. Mary's Hospital The Catholic University of Korea College of Medicine 505 Banpo-dong, Seocho-su Seoul, Korea 137-040 Mark Warchol, PhD (18-21) Washington University of School of Medicine Department of Otolaryngology, Box 8115 660 South Euclid Ave St. Louis, MO 63110
ARO Executive Director:	Haley J. Brust Talley Management Group 19 Mantua Road Mt. Royal, NJ 08061 USA Ph: 1 (856) 423-7222 Ext. 103 Fax 1 (856) 423-0041 Email: hbrust@talley.com headquarters@aro.org



Conference Program of the 42nd Annual MidWinter Meeting

Welcome to Baltimore! Our Association continues to grow and thrive, and this year we have a record number of 1354 presentations. Ruth Litovsky and her team on the Program Committee have worked hard to organise these into a great program. This year, I encourage you to wander into sessions that are not your usual scene, as there is so much to learn from listening to alternative approaches.

We start on Saturday morning with the President's Symposium. This year I have chosen the topic Age-Related Hearing Loss; What we know and what we need to know to develop treatments. There are many challenges to getting to the point where someone with the first signs of hearing difficulties can go to a doctor, get a diagnosis of the primary problem, and come out with a medical treatment to stop further deterioration, but this will happen. The symposium includes a look at ageing processes in general, insights from human histopathology, steps towards diagnosis of the biology underlying hearing loss in individuals, approaches to delivering drugs and other agents to the inner ear, and finally two views from an industry perspective of developing therapeutics for deafness.

Young Investigators, don't miss the mentorship sessions arranged throughout the meeting, or the opportunity to participate in the many special spARO events during the meeting, for student and postdoc and other early-career ARO members.

Sadly we lost our Historian and Founder Member of the ARO, David Lim, last summer. On Monday we will hold a special symposium to reflect his scholarly contributions to middle and inner ear ultrastructural anatomy, otitis media, and inner/middle ear cell lines.

On Monday evening, Peter Narins will receive the Award of Merit, the premier award of our Association. We can look forward to an entertaining evening listening to his talk about how frogs and toads in rain forests and moles in deserts detect pertinent sounds and vibrations. We will also present the Geraldine Dietz Fox young investigator award to Srivatsun Sadagopan for his accomplishment and promise in research related to otolaryngology.

The External Affairs committee have been busy arranging events such as the Science Café on Friday evening, Sporting in Silence event featuring four-times Olympic Gold Medalist Tamika Catchings on Sunday evening, and an Elevator Pitch event in the poster hall throughout the meeting, where you can record a one-minute video about your science and why it matters to post on social media. This year we also plan to use Twitter for the first time to communicate the highlights of the meeting; look out for the details near the registration desk.

Over the past year, ARO Council have worked on a number of changes to the organisation, including renaming our Editor post as Communications Officer to reflect the current needs of our Association. This includes upgrading our website to make it more useful to members. Donna Fekete, our first Communications Officer, has worked closely with Haley Brust and Denise Smith at Talley Management to develop a new site which we will launch in the next few months.

At our business meeting on Sunday evening I will hand over to our new ARO President Keiko Hirose and thank retiring past-president John Carey, who has contributed much to our Association behind the scenes. Finally, I would like to thank all members who have contributed to ARO Council and committees over the past year and the new members who are starting their term for giving their time to making our Association such a key part of this research area and for making the annual meeting the place to be each year. See you next year in San Jose!

Karen P Steel
ARO President, 2018-19

MOBILE APP AND ONLINE WEBSITE

Be sure to download our mobile app to enhance your experience at the 2019 ARO MidWinter Meeting! You'll be able to plan your day by performing detailed abstract searches and can also view the schedule, browse exhibitors, sponsors, maps and general show info. *You must create an account in order to view abstracts/save talks to your itinerary.*

The app is compatible with iPhones, iPads, iPod Touches and Android devices. Search "ARO MWM" on the App Store/Google Play. You can also access the same information via our website version of the app through any browser on any device!

MOBILE DEVICES

As a courtesy to the speakers and your fellow attendees, please switch your mobile device(s) to silent while attending the sessions.

RECORDING POLICY

ARO does not permit audio or photographic recording of any research data presented at the meeting.

BREAKS

Complimentary coffee and tea will be available in the morning and at selected breaks.

ASSISTED LISTENING DEVICES

A limited amount of assisted listening devices are available at the ARO MidWinter Meeting Registration Desk, courtesy of Freeman.

A SPECIAL NOTE FOR THE DISABLED



ARO wishes to take steps that are required to ensure that no individual with a disability is excluded, denied services, segregated or otherwise treated differently than other individuals because of the absence of auxiliary aids and services. If you need any auxiliary aids or services identified in the Americans with Disabilities Act or any assistance please see the ARO staff at the Registration Desk.

ARO Committees

PROGRAM COMMITTEE

Chair:

Ruth Y. Litovsky, PhD (3/17-2/20)

Scientific Program Co-Chairs:

Carolina Abdala, PhD (3/17-2/20)

Christopher Shera, PhD (3/17 – 3/20)

Members:

Jose Antonio Lopez-Escamez, MD (3/17 – 2/20)

Martin Basch, PhD (3/18 – 2/21)

Maria Chait, PhD (3/17 – 2/20)

Monita Chatterjee, PhD (3/17 – 2/20)

Robert Froemke, PhD (3/18 – 2/21)

Gregory Frolenkov, PhD (3/18 – 2/21)

Nandini Iyer (3/17 – 2/20)

Ingrid Johnsrude, PhD (3/16-2/19)

Achim Klug, PhD (3/16-2/19)

Hubert Lim, PhD (3/16-2/19)

Rebecca Lim, PhD (3/17 – 2/20)

H. Heidi Nakajima, MD, PhD (3/16-2/19)

Kevin Ohlemiller, PhD (3/18 – 3/21)

Teresa Nicolson, PhD (3/18 – 2/21)

Konstantina Stankovic, MD, PhD (3/17 – 2/20)

Eric Thompson, PhD (3/17 – 2/20)

Mark Warchol, PhD (3/16-2/19)

Council Liaison: Ruth Y. Litovsky, PhD (3/17-2/20)

spARO Representative: Grace Kim

EX-OFFICIO COUNCIL MEMBER

International Committee Chair

Isabel Varela-Nieto, PhD (3/18 - 2/21)

Long Range Planning Committee Chair

Lisa Goodrich, PhD (3/17 – 2/20)

Mentoring – spARO Committee Chair

Catherine (Cat) Weisz, PhD (3/17 – 2/20)

Program Chair

Ruth Y. Litovsky, PhD Chair (3/17 - 2/20)

spARO Exiting Chair

Mishaela DiNino (3/18 – 2/19)

spARO Chair-Elect

Nicole Jiam (3/18 – 2/19)

BYLAW COMMITTEES

LONG RANGE PLANNING

Chair:

Lisa Goodrich, PhD (3/17 - 2/20)

Members:

Peter Barr-Gillespie, PhD (3/18 – 3/21)

R. Michael Burger, PhD (3/16 - 2/19)

Alan Cheng, MD (3/18 – 2/21)

Brandon Cox, PhD (3/8 – 2/21)

Judy Dubro (3/15 – 3/19)

Bernd Fritzsich, PhD (3/17 - 2/20)

Chris Plack, PhD (3/18 – 2/21)

Amy Poremba, PhD, NIDCD Rep.

Stephen Lomber, PhD (3/16 - 2/19)

Yilai Shu, MD, PhD (3/18 – 2/21)

Aleta Steevens, (3/18 – 2/21)

Catherine Weisz, PhD (3/18 – 2/21)

Past Chair: Steven Green, PhD (3/17 – 3/20)

Council Liaison: President-Elect: Keiko Hirose, MD, PhD (3/18-2/19)

Chair, International Committee: Isabel Varela-Nieto, PhD: Spain (3/18-2/21)

spARO Representative: Brandon Kamrava

NOMINATING

Chair:

John P. Carey, MD (3/18-2/19)

Members:

Andrew Griffith (3/18 – 2/19)

Christine Koepl (3/18 – 2/19)

Lisa Olson, PhD (3/18 – 2/19)

John Oghelai (3/18 – 2/19)

STANDING COMMITTEES

AWARDS COMMITTEE

Chair:

Ruth Anne Eatock, (3/17-2/20)

Members:

Kathleen Cullen, PhD (3/16-2/19)

Jutta Engel, PhD (3/18 – 2/21) j

Paul Fuchs, PhD (3/17 – 2/20)

Phil Joris (3/18 – 2/21)

Matt Kelley, PhD (3/18 – 2/21)

Anna Lysakowski, PhD (3/17 – 2/20)

Edwin Rubel, PhD (3/16-2/19)

Jenny Stone, PhD (3/18 – 2/21)

Deb Tucci, (3/18 – 2/21)

Sarah Wooley, (3/18 – 2/21)

Fan-Gang Zeng, PhD (3/16-2/19)

Council Liaison: Past-President John Carey, MD (3/18-2/19)

DIVERSITY & MINORITY AFFAIRS

Chair:

Ivan Lopez, PhD (3/18 – 2/21)

Members:

Kelsey Anbuhl (3/18 – 2/21)

Alain Dabdoub, PhD (3/18 – 2/21)

Amanda Lauer, PhD (3/16-2/19)

Ramnarayan Ramachandran (3/16-2/19)

Suhua Sha, MD (3/16-2/19)

Yi Zhou, PhD (3/18 – 2/21)

Council Liaison: Shi Nae Park, MD, PhD (3/17-2/19)

spARO Representative: Sara Talaei

ARO Committees

EXTERNAL RELATIONS

Chair:

Keith Duncan, PhD (3/18-2/21)

Allison Coffin, PhD (3/18-2/21)

Members:

Yuri Agrawal, MD (3/17 – 2/20) y

Dylan Chan, (3/18 – 2/21)

J. Chris Holt, PhD (3/16-2/19)

Stéphane Maison, PhD (3/16-2/19)

Michael Roberts, PhD (3-16 – 2/19)

Joel Snyder, PhD (3/16-2/19)

Council Liaison: Mark Worchol, PhD (3/18 – 2/21)

spARO Representative: Judith Kempfle

FINANCE AND INVESTMENT

Chair:

Erick Gallun, PhD (3/17-2/20)

Members:

Thomas Friedman, PhD (3/16-2/19)

Michael Anne Gratton, PhD (3/16-2/19)

Anna Lysakowski, PhD (3/18 – 2/21)

Lisa Olson, PhD (3/17 – 2/20)

Ex-officio: Secretary-Treasurer Gabriel Corfas, PhD
(3/17-2/20)

INTERNATIONAL

Chair:

Isabel Varela-Nieto, PhD (3/18 – 2/21)

Members:

Yun-Hoon Choung, MD, PhD: Korea (3/18 – 2/21)

W. Robert J. Funnell: Canada (3/16-2/19)

Jonathan Gale: UK (3/16-2/19)

Hannes Maier, PhD: Germany (3/16-2/19)

Takayuki Nakagawa, MD, PhD: Japan (3/18 – 2/21)

Ulla Pirvola, PhD: Finland (3/16-2/19)

Sonya Pyott, PhD: Netherlands (3/18 – 3/21)

Council Liaison: Gwen Geleoc, PhD (3/18 – 2/21)

spARO Representative: Patrick Atkinson, PhD

PUBLICATIONS

Chair:

Gregory I. Frolenkov, PhD (3/18-2/21)

Members:

Alan Cheng, MD (3/16-2/19)

Wade Chien, MD (3/16-2/19)

Ben Crane, MD, PhD (3/18 – 2/21)

Antje Ihlefeld, PhD (3/18 – 2/21)

Robert Froemke, PhD (3/18 – 2/21)

Hainan Lang, MD, PhD (3/16-2/19)

Saima Riazuddin, PhD (3/16-2/19)

Isabelle Roux, PhD (3/16-2/19)

JARO Editor: Paul B. Manis, PhD, ex officio

Springer Representative: Gregory Baer, ex officio

Secretary-Treasurer: Gabriel Corfas, PhD (3/17-2/20)

Council Liaison: Donna Fekete, PhD, PhD (3/18-2/21)

spARO Representative: Mary O'Sullivan

TRAVEL AWARDS

Chair:

Mike Bowl, PhD (3/17-2/20)

Members:

Samira Anderson (3/18 – 2/21)

Hela Azaiez, PhD (3/17 – 2/20)

Jonathan Bird, PhD (3/17 – 2/20)

JinWoong Bok, PhD (3/18 – 2/21)

Tom Coate, PhD (3/18 – 2/21)

Laura Corns, PhD (3/17 – 2/20)

Stephanie Eckrich (3/18 – 2/21)

Jeff Lichtenhan, PhD (3/17 – 2/20)

Manuel Malmierca, MD, PhD (3/18 – 2/21)

Jim Phillips, PhD (3/18 – 2/21)

Diana Peterson (3/18 – 2/21)

Maria Rubio, MD, PhD (3/18 – 2/21)

Regi Santos-Cortez, MD, PhD (3/16-2/19)

Martin Schwander (3/16-2/19)

Janet Cyr, PhD, NIDCD Dir ex officio

Council Liaison: Shi Nae Park, MD, PhD (3/17-2/21)

spARO Representative: Cathy Sung

JARO EDITORIAL BOARD

Paul B. Manis, PhD, Editor-in-Chief (2018 - 2019)

Associate Editors:

Julie Arenberg, PhD (2015 – 2019)

Alan M. Brichta, PhD (2015-2019)

Catherine E. Carr, PhD (2016-2019)

Paul Delano (2017 – 2021)

Mark A. Eckert, PhD (2013-2019)

Ana Belén Elgoyhen, PhD (2013-2019)

W. Robert J. Funnell, PhD (2013-2019)

Elisabeth Glowatzki, PhD (2015-2019)

Nace L. Golding, PhD (2016-2020)

Michael G. Heinz, PhD (2016-2020)

Ronna Hertzano, MD, PhD (2015-2019)

Richard F. Lewis, MD (2015-2019)

Ruth Y. Litovsky, PhD (2013-2019)

Christian Lorenzi, PhD (2016-2020)

Brigitte Malgrange, PhD (2015-2019)

Colette M. McKay, PhD (2016-2020)

John C. Middlebrooks, PhD (2015-2019)

Heidi Nakajima, MD, PhD (2017-2021)

Adrian Rees, PhD (2015-2019)

Suhua Sha, MD (2017-2021)

Xiaorui Shi, MD, PhD (2013-2019)

George A. Spirou, PhD (2014-2019)

Marcel van der Heijden, PhD (2014-2019)

Joseph P. Walton, PhD (2016-2020)

Robert H. Withnell, PhD (2015-2019)

ISSN-0742-3152

The Abstracts of the Association for Research in Otolaryngology is published annually and consists of abstracts presented at the Annual MidWinter Research Meeting. A limited number of copies of this book and previous books of abstracts (1978-2011) are available. Please address your order or inquiry to Association for Research in Otolaryngology Headquarters by calling (856) 423-0041 or emailing headquarters@aro.org.

This book was prepared from abstracts that were entered electronically by the authors. Authors submitted abstracts over the World Wide Web using Cadmium Abstract Management System. Any mistakes in spelling and grammar in the abstracts are the responsibility of the authors. The Program Committee performed the difficult task of reviewing and organizing the abstracts into sessions. The Program Committee; Program Committee Chair, Ruth Litovsky, PhD; and the President, Karen P. Steel constructed the final program. Cadmium and Marathon Printing electronically scheduled the abstracts and prepared Adobe Acrobat pdf files of the Program and Abstract Books. These abstracts and previous years' abstracts are available at www.aro.org.

Citation of these abstracts in publications should be as follows: **Authors, year, title, Assoc. Res. Otolaryngol. Abs.: page number.**

Table of Contents

	Abstract Number	Page No.
Presidential Symposium:		
Age-related Hearing Loss: What We Know and What We Need to Know to Develop Treatment.....	PRES SYMP 1-7	1-3
Poster Session 1:	PS 1-281	190-337
Auditory Brainstem I.....	PS 1-17	3-11
Auditory Cortex: Anatomy & Physiology I.....	PS 18-40	12-23
Auditory Nerve I.....	PS 41-58	24-33
Auditory Prostheses I: Novel Technologies & Applications.....	PS 59-69	34-40
Binaural Hearing in Non-Human Animals.....	PS 70-83	41-48
Central Vestibular Pathways.....	PS 84-94	48-55
Development I.....	PS 95-126	55-73
Human Auditory System: Electrophysiology.....	PS 127-148	74-85
Inner Ear: Membranes & Fluids.....	PS 149-163	86-94
Inner-Ear Mechanics I.....	PS 164-177	94-100
Noise Injury I.....	PS 178-192	101-108
Ototoxicity I.....	PS 193-205	109-116
Outer & Middle Ear: Biology.....	PS 206-220	117-125
Psychoacoustics: Some Current Trends.....	PS 221-234	125-132
Symptoms of Age-Related Hearing Loss in Humans.....	PS 234-253	132-143
Temporal Bone Pathology & Histology.....	PS 254-265	143-150
Tinnitus & Hearing Loss: Clinical Studies.....	PS 266-281	150-159
Symposium:		
Inner Ear Efferents: Form and Function.....	SYMP 1-7	160-162
Symposium:		
Mechanisms of Auditory Hypersensitivity in Fragile X Syndrome.....	SYMP 8-14	162-163
Podium:		
Auditory Cortex: From Sensation to Perception.....	PD 1-8	164-168
Symposium:		
Adaptive coding for efficient behavioral performance in the auditory system.....	SYMP 15-19	169-170
Podium:		
Development II.....	PD 9-16	170-174
Podium:		
Middle-Ear Mechanics.....	PD 17-24	175-178
Podium:		
Inner-Ear Therapeutics.....	PD 25-32	181-185
Podium:		
Tinnitus.....	PD 33-40	186-189
Poster Session 2	PS 282-548	190-337
Auditory Brainstem II.....	PS 282-302	192-200
Auditory Cortex: Anatomy & Physiology II.....	PS 303-320	201-209
Auditory Pathways: Midbrain.....	PS 321-341	210-221
Auditory Pathways: Midbrain, Thalamus & Cortex.....	PS 342-349	222-226
Auditory Prostheses II: Applications & Novel Technologies.....	PS 350-360	226-232
Auditory Prostheses III: Animal Models, Trauma & Survival.....	PS 361-377	233-242
Binaural Hearing: Real & Simulated Impairments.....	PS 378-386	242-247
Clinical Vestibular Applications.....	PS 387-404	247-247
Genetics of Hearing Loss.....	PS 405-432	258-274
Hair Cells: Mechanotransduction.....	PS 433-447	274-281
Hair Cells: Stereocilia.....	PS 448-454	282-284
Inner-Ear Therapeutics I.....	PS 455-469	285-294
Peripheral Vestibular System.....	PS 470-491	294-306
Psychophysical Characterization of Normal & Impaired Ears.....	PS 492-513	306-318
Speech Perception: Intelligibility.....	PS 514-532	319-328
Synaptopathy & Hidden Hearing Loss.....	PS 533-548	328-337

Table of Contents

	Abstract Number	Page No.
Symposium:		
Age-related hearing loss and cognitive decline	SYMP 26-30	338-340
Symposium:		
Beyond the Basilar Membrane: Measuring Cochlear Micromechanics	SYMP 31-36	340-341
Podium:		
Intracochlear Drug Delivery & Biomarkers	PD 41-48	341-345
Podium:		
Inferior Colliculus: Function, Connections & Plasticity	PD 49-56	346-348
Symposium:		
Benefits of Extended High Frequency Hearing	SYMP 37-43	350-353
Symposium:		
Kolliker's organ: BigGERer roles for an overlooked organ	SYMP 44-50	350-353
Symposium:		
Spontaneous Otoacoustic Emissions and Active Amplification	SYMP 51-57	353-355
Podium:		
Auditory Cortex: Human Studies	PD 57-64	355-359
Podium:		
Regeneration I	PD 65-72	359-363
Poster Session 3	PS 549-817	364-508
Auditory Cortex: Anatomy & Physiology III	PS 549-563	364-372
Auditory Nerve II	PS 564-582	373-382
Auditory Perception in Complex Environments	PS 583-600	383-391
Auditory Prostheses IV: Stimulus Coding & Nerve Survival	PS 601-614	392-399
Auditory Prostheses V: Music Perception & Binaural Hearing	PS 615-623	400-405
Binaural Hearing: Normal-Hearing Humans & Models	PS 624-643	406-417
Development III	PS 644-673	417-431
Genomics & Gene Regulation	PS 674-705	431-447
Inner Ear: Drug Delivery	PS 706-730	448-460
Noise Injury II	PS 731-743	461-467
Otoacoustic Emissions	PS 744-758	468-475
Outer & Middle Ear: Mechanics	PS 759-781	459-488
Speech Perception: Musicianship, Models & Mechanisms	PS 782-803	489-500
Tinnitus: Animal Models	PS 804-817	501-508
Symposium:		
Hearing in aging: Temporal Processing Deficits Throughout the Brain	SYMP 58-65	508-511
Symposium:		
Tribute to David Lim	SYMP 66-69	511-512
Podium:		
Inner-Ear Structure & Function	PD 73-80	513-516
Symposium:		
Beyond the Mouse: Comparative Approaches to Auditory Encoding	SYMP 70-74	517-518
Podium:		
Genetic Landscape of Hearing Loss	PD 81-88	518-522
Podium:		
Receptors, Afferents, Brains & Behaviors	PD 89-96	522-527
Symposium:		
Activity-Dependent Development of the Inner Ear	SYMP 75-80	527-528
Symposium:		
Benefits and Limitations of Perceptual Fusion Within and Across Modalities	SYMP 81-86	529-530
Podium:		
Hair Cells: Mechanotransduction & Synaptic Transmission	PD 97-104	530-534

Table of Contents

	Abstract Number	
Poster Session 4	PS 818-1092	535-687
Age-Related Hearing Loss in Animals	PS 818-841	535-548
Auditory Brainstem III	PS 842-862	549-561
Auditory Cortex: Plasticity	PS 863-882	561-571
Auditory Protheses VI: Audiovisual Integration & Speech Perception	PS 883-892	572-577
Auditory Protheses VII: Brainstem & Cortex	PS 893-908	578-586
Hair Cells: Anatomy & Function	PS 909-919	586-591
Hair Cells: Mechanics & Motility	PS 920-931	592-597
Hair Cells: Synapses	PS 932-945	598-605
Human Auditory System: Imaging & Behavior	PS 946-958	605-613
Human Development	PS 959-962	613-615
Inner Ear: Anatomy & Physiology	PS 963-981	616-626
Inner Ear: Innervation & Synaptic Transmission	PS 982-996	626-634
Inner-Ear Mechanics II	PS 997-1008	634-640
Inner-Ear Therapeutics II	PS 1009-1024	641-649
Ototoxicity II	PS 1025-1036	650-656
Prosthetic Devices	PS 1037-1043	656-660
Regeneration II	PS 1044-1070	661-674
Surgical Innovation	PS 1071-1080	675-680
Vestibular Testing	PS 1081-1092	680-687
Podium:		
Development IV	PD 105-111	687-690
Podium:		
Normal & Impaired Binaural Hearing	PD 112-119	691-695
Podium:		
Speech Perception	PD 120-127	695-699
Podium:		
Age-Related Changes in Humans & Mice	PD 128-135	699-703
Podium:		
Auditory Brainstem Jamboree	PD 136-143	705-708
Podium:		
Cochlear Mechanics: Facts & Fancies	PD 144-151	709-712
Podium:		
Auditory Cortical Plasticity	PD 152 - 160	712-717
Podium:		
Clinical Otolaryngology & Pathology	PD 161 - 168	717-721
Podium:		
Inner-Ear Genomics & Gene Regulation	PD 169 - 176	722-726

Presidential Symposium:

Age-Related Hearing Loss: What We Know and What We Need to Know to Develop Treatments

Chair: Karen Steel

PRES SYMP 1

Age-Related Hearing Loss: What We Know and What We Need to Know to Develop Treatments

Karen Steel

King's College London

Age-related hearing loss (ARHL) is one of the most common sensory deficits in the human population and has been associated with increased risk of social isolation, depression and dementia. There is no medical treatment currently available despite the need. Environmental factors such as noise or drug exposure undoubtedly have a role in causation but ARHL also has a strong genetic component. Genetics can give us useful clues to the underlying molecular mechanisms involved in progressive hearing loss. Modulating these key molecular pathways may be useful as treatments whatever the trigger for the hearing loss, genetic or environmental. In this symposium, we discuss what we know about ARHL and how we can move towards developing treatments to stop or slow down the progression.

PRES SYMP 2

Aging Interventions get Human-Preventing Age-related Changes

Brian Kennedy, *NUS Singapore and Buck Institute California*

PRES SYMP 3

Human Inner Ear Histopathology and Insights Into Mechanisms of Age-related Hearing Loss

M. Charles Liberman, *Mass. Eye and Ear Infirmary*

Correlating audiograms and histopathology in human temporal bones led Schuknecht and colleagues to posit four types of presbycusis: 1) "sensory", with precipitous high-tone audiometric loss and basal-turn hair cell loss, 2) "strial", with flat audiometric loss and degeneration of the stria vascularis, 3) "neural", with variable audiometric losses, poor speech discrimination and degeneration of the spiral ganglion without corresponding hair cell loss, and 4) "cochlear conductive", with sloping high-tone loss, no cochlear histopathology and a putative increase in cochlear mechanical stiffness.

Application of new techniques to human otopathology
ARO Abstracts

suggests this view of presbycusis needs revision. In classic otopathology, cochlear neural degeneration was assessed by counting spiral ganglion cells (SGCs), but animal work in noise-damaged and aging ears shows that many SGCs are disconnected from their hair cell targets. To look for this hidden hearing loss in humans, we counted hair cells, synapses and SGC peripheral axons in sections from archival cases in the Mass Eye and Ear collection, and microdissected wholmounts from new specimens. We found that primary neural degeneration is also a prominent feature of the normal-aging human: mean data from 21 cases shows < 10% loss of inner hair cells by age 60, yet > 50% loss of SGC peripheral axons. This neuropathy likely contributes to the decline in speech discrimination scores that is a hallmark of the aging ear. In classic otopathology, temporal bones are prepared as serial 20-micron sections, and cytochleograms are constructed by rating hair cells in each section as present or absent. This binary approach underestimates hair cell loss: for example, our immunostained wholmounts from humans > 65 yrs show mean fractional loss (~50%) of outer hair cells throughout the audiometric range. We are now re-deriving cytochleograms from the archival cases on which Schuknecht based his ideas about presbycusis, using high-N.A. objectives and DIC to optically section the material and compute fractional hair cell survival, rather than presence vs. absence. Our blinded analysis of "cochlear conductive" cases, i.e. no hair cell loss in the classic analysis, finds a clear apical-basal gradient of fractional hair cell loss that correlates well with the sloping audiometric pattern. We are currently examining cases of strial and neural presbycusis to determine if hair cell loss more generally explains the patterns of threshold shift in all four types of presbycusis.

Research supported by grants from the NIDCD (P50 DC015857 and R01 DC000188).

PRES SYMP 4

Developing Electrophysiologic Methods for Identifying Pathophysiology of Human Age-related Hearing Loss

Kelly C. Harris, *Medical University of South Carolina-Dept of Otolaryngology-Head & Neck Surgery*

Age-related hearing loss in humans is complex because many factors in addition to aging can produce hearing loss in older persons, such as the accumulated effects of a lifetime of exposure to noise, ototoxic drugs, or otologic disease. Thus, targeted treatments for age-related hearing loss must address the multiple sources of pathology and their complex impact on communication. Three primary sites of pathology, sensory cells and the stria vascularis in the cochlea, and the auditory nerve

(AN) underlie age-related changes in hearing thresholds and suprathreshold auditory function. However, current interventions, mainly amplification, treat only the symptom of hearing loss and disregard the underlying pathology. Diagnosis of the primary sites of pathology in an individual is crucial in testing the effectiveness of new treatments as they become available, and in determining the best course of intervention for an individual rather than a group. Attempts to classify the sites of pathology have been based largely on the configuration of the audiogram. These studies show classic patterns of hearing loss seen in animal models of sensory and strial deficits, and are consistent with demographic and noise history patterns. However, the audiogram represents only one aspect of functional abilities, ignores suprathreshold auditory processing, and is insensitive to neural loss. Thus, a multi-metric differential approach that incorporates multiple measures from each individual that may be validated in animal models may greatly improve sensitivity and specificity in identifying underlying pathologies. This electrophysiologic approach assumes that sensory cell and strial deficits differentially affect cochlear measures, including otoacoustic emissions and the cochlear microphonic. The effects of these cochlear deficits are predicted to propagate through the auditory system and result in unique patterns of AN dysfunction, as characterized by summing and compound action potentials (CAP). In contrast, neural deficits can be characterized by the CAP but will not affect cochlear measures. A strength of this electrophysiologic approach is the ability to compare results with animal models of known pathology, while reducing the impact of non-auditory factors, such as cognitive functioning. Establishing the appropriate set of measures for characterizing cochlear and AN dysfunction in older adults will help move beyond the audiogram to identify the underlying pathophysiology associated with age-related hearing loss. [Work supported by NIH/NIDCD].

PRES SYMP 5

Local Drug Therapy of the Inner Ear: Dependence on Molecular Properties

Alec Salt

Washington University Medical School

Treating the inner ear with locally-applied drugs is technically challenging to a degree that some therapies may be ineffective. A major factor controlling both the time course and spatial distribution of a drug in the ear is the rate of elimination (loss) from perilymph. Drugs that are rapidly eliminated do not distribute well to the apical regions of the ear. We have now accumulated pharmacokinetic data with enough molecules to

understand some of the general principles underlying drug distribution in the ear. For other biological barriers of the body, such as the gut or the blood-brain barrier, passage of molecules through the barrier is limited by their ability to pass through the lipid membranes of the cell layer. Both passage through membranes and aqueous solubility depend on the polar properties and lipid solubility of the specific molecule. Small, non-polar lipophilic molecules tend to have low aqueous solubility but readily pass through membranous barriers. In contrast, large, polar, hydrophilic molecules are more soluble but pass less easily through membranous barriers. Our studies show that similar considerations influence the passage of drugs from the middle ear to perilymph and from perilymph to the vasculature. When applied intratympanically, small lipophilic molecules, such as triamcinolone-acetonide and dexamethasone enter perilymph readily through the round window and stapes. However, they also pass through the blood-perilymph barrier and are rapidly lost from perilymph, limiting their apical distribution along the cochlear scalae. Larger, more-polar molecules such as gentamicin and dextran are retained better in perilymph, but also enter more slowly into perilymph when applied intratympanically. Unfortunately, dexamethasone-phosphate, the form of dexamethasone widely used for intratympanic therapy of humans, has an undesirable combination of pharmacokinetic properties. This polar form of the drug has higher aqueous solubility but its polar properties make it relatively impermeable through the boundaries from the middle ear so it enters perilymph relatively slowly. Within the ear it is then metabolized to the active, less-polar form, dexamethasone, which is more permeable though membranous boundaries and rapidly leaks from perilymph through the blood-labyrinth barrier. With these properties, dexamethasone-phosphate therapy is likely to provide only a brief exposure of vestibular and basal cochlear regions to the active drug. From the pharmacokinetic perspective, triamcinolone (distinct from the more common form triamcinolone-acetonide) is retained in perilymph better than dexamethasone and may therefore have more appropriate properties for steroid therapy of the inner ear.

Studies supported by NIH/NIDCD R01 DC001368

PRES SYMP 6

Refinement of ARHL Patient Populations and Targeted Treatments

Michael Su

Decibel Therapeutics

Presbycusis or age-related hearing loss (ARHL) is a societal condition that affects at least one third of

people over 70, making it the most prevalent sensory disorder in the elderly. The impact of ARHL on quality of life is profound and includes isolation, depression, and accelerated mental decline. The pathogenesis of ARHL is a complex mixture of genetic and environmental factors that can manifest in different ways, and methods for segmenting heterogeneous etiologies into distinct patient populations are still in their infancy.

Identification of therapeutics for ARHL requires improved understanding of genetics, risk factors, and pathophysiology in human patients, in addition to an end-to-end drug discovery platform built around relevant disease models and precise tools for testing target hypotheses and preclinical development. This talk will focus on how an integrated team of scientists at Decibel Therapeutics is paving a new path for solving these problems, highlighting multidisciplinary advances in translational research, human genetics, systems biology, pharmacology, and drug delivery.

To this end, Decibel has been evaluating the neurotrophins as a therapeutic target for diseases that affect the synapse between inner hair cells and Type I spiral ganglion neurons. A variety of studies have shown that afferent synapses are one of the most vulnerable elements of the cochlear circuit, irreversibly disconnecting after loud noise exposure and during natural aging. Furthermore, loss of synapses and neurons appears to accelerate ARHL by removing essential trophic signals for hair cells, leading to premature hair cell death. Neurotrophins regulate development and survival of spiral ganglion neurons and have been shown to have therapeutic potential for preventing or repairing noise-induced synaptic disconnection when delivered locally to the ear. Thorough evaluation of the clinical potential of this target has required a robust animal model, improved understanding of the disease biology, methods for consistent delivery and detection of a specific neurotrophin, confirmation of receptor engagement in target cells, clear histological and physiological readouts of efficacy, and establishment of disease relevance in humans. This work serves as an example of the scientifically rigorous approach Decibel is taking for discovering therapies for inner ear disorders, and it demonstrates how tackling ARHL will require more precise definitions of this heterogeneous, multifactorial disease.

PRES SYMP 7

Medicines Discovery for Age Related Hearing Loss: Right Drug, Right Dose, Right Time, Right Patient

Rick Cousins

UCL Ear Institute & Cinnabar Consulting Ltd

A review will be provided of the pharmaceutical industry perspective on medicine discovery and development and on the opportunities and challenges in developing therapies for age related hearing loss. The following aspects will be considered:

- How industry discovers and develops new medicines - key decision points and reality of probability of success.
- The historical learnings from drug discovery and development that drive better informed investment decisions, including the Three Pillars of Survival.
- What strategies to discover new drugs must consider - the end-to-end activities required to create and deliver a licensed medicine.
- How industry strategies are focused on predict first, to be able to deliver the right drug at the right dose at the right time to the right patient.
- The drug modalities that could be considered for age related hearing loss.
- The value of human genetic association for a potential biological target.
- The value of the risk-reward sharing alliances and collaboration to enable success in novel therapeutic areas.

Auditory Brainstem I

PS 01

Evidence for a neuronal network model of the cochlear nucleus and its implication for coding strategies in auditory prostheses

Andreas Bahmer

University Clinic Wuerzburg

A simulation study is presented that shows that the ability of humans to distinguish changes in pitch can be explained as a correlation analysis of temporal information in auditory signals. The correlation analysis is performed by a neuronal network in the auditory system located in the cochlear nucleus and the inferior colliculus. Parts of this network are chopper neurons in the brain stem. The connections between the chopper neurons construct neural oscillators that can discharge spikes at constant intervals, which are integer multiples of 0.4 ms, contributing to the temporal processing of auditory cochlear output. These constant intervals are found in measurements in different species and may be attributed to the smallest synaptic delay between interconnected chopper neurons. The neuronal network is triggered by the input of onset neurons. Broadband spectral input of onset neurons and of

narrowband spectral input of single auditory nerve fibers are integrated and utilized in the network. The topology of the network is the basis for new concepts of coding strategies in auditory prosthesis. The new concepts are patented and aim at various parameters for the electrical stimulation such as pulse shapes, pulse polarity, pulse amplitude sequences, and pulse train rates, e.g. the timing of pulses for apical electrodes to synchronize with periods of 0.4 ms.

PS 02

Selective Opsin-Mediated Excitation of T-Stellate Cells in the Ventral Cochlear Nucleus Using Serial AAV Infections

Gabriel E. Romero; Laurence O. Trussell
Oregon Health & Science University

T-stellate cells of the ventral cochlear nucleus (VCN) receive input from the auditory nerve, and are a major ascending pathway of the auditory system. In addition to local collaterals in the cochlear nucleus, T-stellate cells project widely to many brainstem and midbrain targets involved in hearing. However, there is currently no method that allows stimulation of only T-stellate cells while recording from neurons in distal nuclei, and thus many of the synaptic contacts between T-stellate cells and their targets have not been functionally characterized. Here we report a method to genetically manipulate T-stellate cells using an adeno-associated virus (AAV) with robust retrograde transgene delivery in order to perform virally driven tract tracing and functional optogenetic studies of auditory circuitry. Cre-recombinase expressing retrograde-AAV (rgAAV-pmSyn1-EBFP-Cre) was pressure injected into the inferior colliculus (IC) of P22 reporter mice expressing a Cre-dependent tdTomato (Ai9-tdTomato). Two weeks post injection, tdTomato expression was observed in VCN contralateral to the injection, and little tdTomato expression was observed in ipsilateral VCN. This is consistent with known T-stellate projections, as previous studies have shown that a large majority of T-stellate cells project to contralateral IC, whereas very few project to ipsilateral IC. Few positive fusiform neurons in the dorsal cochlear nucleus were observed, suggesting that this retrograde-AAV has selective tropism for particular neuronal subtypes. Whole-cell current clamp recordings of tdTomato positive neurons in VCN confirm that these retrograde-AAV infected neurons are T-stellate cells, as they exhibit sustained action-potentials in response to depolarizing current injections, and a hyperpolarization that sags toward rest in response to negative current injections, reflecting the activation of a hyperpolarization activated cation current. As a proof of concept, a second coincident AAV injection (AAV2-EF1a-DIO-hChR2-EYFP) was made in VCN contralateral to retrograde-

AAV IC injections. Ideally, this should unilaterally confine Cre-dependent channelrhodopsin(ChR2)-EYFP expression to T-stellate cells in VCN. Indeed, two weeks post-infection, expression of ChR2-EYFP was limited to T-stellate cells in VCN contralateral to retrograde-AAV IC injections, as EYFP positive neurons were also positive for tdTomato. In whole-cell voltage-clamp recordings of EYFP positive T-stellate neurons, ChR2-mediated currents were evoked in response to 2-ms flashes of blue light. In current-clamp mode, ChR2-mediated potentials were able to integrate and evoke action-potentials in response to bursts of light-stimulation. Optogenetic activation of T-stellate cells will enable experiments which will help define the functional significance of T-stellate projections.

PS 03

Two Distinct Inhibitory Circuits in the Dorsal Cochlear Nucleus

Tessa-Jonne Ropp¹; Michael Kasten²; Paul B. Manis³; ¹Dept of Otolaryngology, University of North Carolina-Chapel Hill; ²Department of Otolaryngology/Head and Neck Surgery, The University of North Carolina at Chapel Hill

With the rising incidence of environmental noise-induced hearing loss (NIHL), age-related hearing loss (ARHL) and tinnitus, understanding how the brain's circuits are affected is critical to developing treatments for auditory insults. The cochlear nucleus is the first locus of auditory processing in the brain. The ventral cochlear nucleus (VCN) is tightly coupled to the auditory nerve and is essential for rapid detection and translation of auditory input while the dorsal cochlear nucleus (DCN) receives weaker auditory nerve input and is implicated in spectral processing and early multisensory integration. NIHL and ARHL have been associated with altered DCN responses and tinnitus. DCN circuitry is complex, receiving excitatory input from auditory and other sensory modalities. Knowledge of the DCN principal neuron inputs and the complex inhibitory networks of the nucleus is limited. We hypothesize that each input modality utilizes a unique inhibitory network to regulate firing of principal neurons. We utilize optogenetics in the VGAT-ChR2 mouse line, together with laser scanning photostimulation and patch clamp recording to determine the responsiveness of, and the connectivity between, cells in the DCN. DCN principal neurons receive weak inhibition from deep-layer, auditory-based interneurons (tuberculoventral cells) but stronger inhibition from molecular-layer, multisensory-based interneurons (cartwheel cells). Both interneuron subtypes demonstrate strong recurrent activity, indicative of dis-inhibitory refinement of feedforward inhibition. Little crosstalk was seen between vertical and

cartwheel cells, demonstrating inhibition from separate modalities is independent. Multiple inhibitory networks exist in the DCN: auditory driven feed-forward inhibition from tuberculoventral cells, multimodal inhibition via cartwheel cells, and inhibition between cartwheel cells. Supported by NIH grant DC004551.

PS 04

Classification of Neurons in the Adult Mouse Cochlear Nucleus: Linear Discriminant Analysis of Intrinsic Excitability

Paul B. Manis¹; Michael Kasten²; Ruili Xie³

¹Department of Otolaryngology/Head and Neck Surgery, *The University of North Carolina at Chapel Hill*; ²Dept of Otolaryngology, *University of North Carolina-Chapel Hill*;

³Department of Otolaryngology, *Ohio State University*

The cochlear nucleus transforms the spikes trains of spiral ganglion cells into a new set of sensory representations that are essential for auditory discriminations and perception. These transformations require the coordinated activity of different classes of neurons that are embryologically derived from distinct sets of precursors. Decades of investigation have shown that the neurons of the CN are differentiated by their ion channel expression and intrinsic excitability. In the present study we have used linear discriminant analysis (LDA) to perform an unbiased analysis of measures of the responses of CN neurons to current injection to mathematically separate cells on the basis of both morphology and physiology. Recordings were made from cells in brain slices from CBA mice (28-69 days of age) and a transgenic mouse line based on the FVB strain (NF107, BAC transgenic), crossed against the Ai32 line, on an C56Bl/6J background (ages 31-166 days of age). For each cell, responses to current injections (100-500 msec duration, ranging from -1 to 1 or -0.5 to 0.5 nA) were analyzed for spike rate, spike shape (action potential height, afterhyperpolarization depth, first spike half-width), input resistance, resting membrane potential, membrane time constant and hyperpolarization sag and time constant. Cells were filled with dyes for morphological classification, and visually classified according to published accounts. The different morphological classes of cells were separated with the LDA. VCN bushy cells, T-stellate (planar multipolar) cells, and D-stellate (radiate multipolar) cells were in separate clusters, and were well separated from all of the neurons from the DCN. Within the DCN, the pyramidal and giant cells were overlapping, but largely separated from the distinct clusters of tuberculoventral cells and cartwheel cells. Cells for which morphological identification was either absent or ambiguous appeared as a cluster that partially overlapped with pyramidal and tuberculoventral cells. Other small populations (chestnut

cells, horizontal bipolar cells and type B cells of Lorente de No) were mixed within other DCN populations. Interestingly, the DCN cells largely fell along a plane in the first 3 principal axes, whereas the VCN cells were in 3 clouds well separated from this plane. VCN neurons from the two mouse strains were slightly separated, indicating either a strain dependence or the differences in slice preparation methods. We conclude that cochlear nucleus neurons can be objectively distinguished based on their intrinsic electrical properties. This work was supported by NIDCD grants R01 DC004551 to PBM and R03 DC013396 to RX.

PS 05

Auditory Brainstem Response Originating from Axonal Terminal Zones in the Auditory Brainstem of the Barn Owl

Paula T. Kuokkanen¹; Anna Kraemer²; Nadine Thiele³; Richard Kempter⁴; Christine Köppl⁵; Catherine Carr²

¹*Humboldt-Universität zu Berlin*; ²*University of Maryland College Park*; ³*Cluster of Excellence "Hearing4all"*; ⁴*Institute for Theoretical Biology, Humboldt-Universität zu Berlin*; ⁵*Department of Neuroscience, School of Medicine and Health Sciences, Carl von Ossietzky University Oldenburg*

The auditory brainstem response (ABR) is an extracranially recorded potential, which is used for diagnosis of hearing loss, especially among newborns. The ABR is generated in the auditory brainstem by local current sources, which also give rise to extracellular field potentials (EFPs). The origins of both the ABR and the EFP are not well understood. Traditionally synaptic dipoles have been attributed as the main sources for both. We have recently found that EFPs, especially their dipole behavior, may be dominated by the branching patterns and the activity of axonal terminal zones in the barn owl (McColgan et al., 2017). Furthermore, our model suggests that the dipoles from axonal terminal zones can be strong enough to contribute to extracranial potentials. To test the hypothesis that axonal arbors also shape the ABR, we used the well-described barn owl early auditory system. We recorded the ABR and a series of EFPs between the brain surface and nucleus laminaris (NL) in response to binaural clicks. We furthermore recorded extracellular single-cell responses in the nucleus magnocellularis (NM). The ABR and the EFP within and around NL are correlated, as are the NM spikes and ABR. Our model of the dipole sources in the auditory brainstem is in accordance with the data. Together, our data and model suggest that axonal dipoles within the barn owl nucleus laminaris contribute to the ABR wave III.

Acknowledgments: We acknowledge the help of G. Ashida and L. Kettler. Supported by NSF CRCNS IOS1516357, NIH DC00436, NIH P30 DC0466 to the UMD Center for the Evolut. Biol. of Hearing, the Bundesministerium fuer Bildung und Forschung (BMBF): as part of the NSF/NIH/ANR/BMBF/BSF CRCNS program, 01GQ1505A and 01GQ1505B
References: McColgan, T., Liu, J., Kuokkanen, P. T., Carr, C. E., Wagner, H., & Kempster, R. (2017). Dipolar extracellular potentials generated by axonal projections. *eLife*, 6. <http://dx.doi.org/10.7554/eLife.26106>

PS 06

Nitric Oxide-Mediated Plasticity in Inhibitory Neurons of the Ventral Cochlear Nucleus

Xiao-Jie Cao; Lin Lin; Donata Oertel

University of Wisconsin School of Medicine and Public Health

Inhibition by D stellate cells shapes responses to sound in T stellate cells that form an ascending pathway from the ventral cochlear nucleus (VCN) to the brainstem, midbrain and thalamus (Wenthold, 1987; Smith and Rhode, 1989; Oertel et al., 1990; Ferragamo et al., 1998). D stellate cells likely give T stellate cells inhibitory sidebands that enhance the encoding of spectral peaks and valleys (Blackburn and Sachs, 1990; May et al., 1998). T Stellate cells excite one another through interconnections whose strength is modulated by nitric oxide (NO) (Cao and Oertel, 2016, 2017, ARO Abstracts). Here we show that D stellate cells are also affected by NO signaling. D stellate cells are recognized by the shapes of action potentials evoked by depolarization and by the strong and rapid inward rectification evoked by hyperpolarization (Oertel et al., 1990; Ferragamo et al., 1998; Fujino and Oertel, 2001; Xie, 2017). When D stellate cells were held at -65 mV, only occasional mEPSCs (<100 pA) were observed. Surprisingly, after depolarizing pulses to +30 mV for ~1 min, bursts of EPSCs appeared that lasted roughly 30 sec and whose frequency decreased. The amplitude of those EPSCs was initially ~500 pA and then grew by about 40% before the burst stopped. Blockers of neuronal nitric oxide synthase (nNOS) and of NMDA receptors prevented the bursts of EPSCs. These results suggest that the entry of Ca²⁺ through NMDA receptors activated nNOS, resulted in release of NO, and activated signaling cascades pre- and possibly postsynaptically. nNOS acts presynaptically to initiate a burst of EPSCs. The growth of EPSCs could result postsynaptically from a recruitment of receptors or presynaptically from an increase in neurotransmitter release. What terminals are affected by nNOS? D stellate cells receive excitatory input from auditory nerve fibers as well as from other

sources (Cant, 1981; Xie, 2017); potentiation was not observed in bushy or octopus cell targets of auditory nerve fibers (Cao and Oertel, 2017, ARO Abstract). Our electrophysiological findings suggest that D stellate cells contain nNOS and that at least some of the surrounding terminals have receptors for NO. nNOS and NO-sensitive-guanylate cyclase has indeed been observed in the VCN where D stellate cells are found (Burette et al., 2001; Coomber et al., 2015). We find that nNOS α is strongly expressed in neurons whose distribution resembles that of D stellate cells. This work is supported by a grant from NIH 1R01DC016861.

PS 07

Cartwheel Cells in the Dorsal Cochlear Nucleus Process Multimodal Input by Adjusting their Inter-connectivity

Calvin Wu; Susan E. Shore

University of Michigan

The dorsal cochlear nucleus (DCN) receives multimodal input from somatosensory, vestibular, and pontine-reticular-motor systems. Multimodal input is relayed to DCN principal output neurons, fusiform cells (FC), and inhibitory interneuron, cartwheel cells (CWC), in a feed-forward and lateral inter-connected microcircuit (Roberts & Trussell, *J Neurophysiol* 2010). While the role of individual FCs in multimodal integration has been elucidated (Koehler & Shore, *J Neurosci* 2013), the role of the CWC network remains unknown. Here, we used multichannel in vivo CWC and FC recording during stimulation the pontine-cochlear nuclei pathways. Functional connectivity of multiple spike trains containing CWCs and FCs was computed using the Cox method of modulated renewal process (Masud & Borisyuk, *J Neurosci Methods* 2011), which provides a statistical estimation of interaction strength for all pairwise neurons. We found that CWCs exert a strong iso-frequency inhibitory influence on 4-7 FCs but <2 other CWCs at 0.5-1 octaves above best-frequency. Electrical stimulation of the pontine nuclei resulted in long-lasting adjustments of functional connectivity: CWC inhibition of FCs was weakened while inhibition amongst CWCs strengthened. Increased overall influence of CWCs after multimodal stimulation effectively regulates FC spontaneous firing rates. These findings suggest that CWCs play an important role in multimodal integration, and may significantly contribute to pathologies arising from FC spontaneous activity, such as tinnitus (Wu et al., *J Neurosci* 2016).

PS 08

Auditory Nerve Inputs Target Specific Cell Types in Dorsal Cochlear Nucleus

Michael Kasten¹; Tessa-Jonne Ropp¹; Paul B. Manis²
¹*Dept of Otolaryngology, University of North Carolina-Chapel Hill*; ²*Department of Otolaryngology/Head and Neck Surgery, The University of North Carolina at Chapel Hill*

Pyramidal and giant cells are the principal cells of the dorsal cochlear nucleus (DCN) and send extensive outputs to inferior colliculus, playing an important role in auditory processing. The circuitry regulating the firing of DCN principal cells remains unclear. While DCN principal cells respond to auditory nerve stimulation, responses are generally slower and weaker compared to bushy and stellate cells of the ventral cochlear nucleus (VCN). Smaller responses of DCN principal cells to auditory input could be due to dendritic filtering or weaker auditory nerve input. We utilized the NF107 (Colgalt2-cre) mouse line, in which the Cre driver is highly expressed in auditory nerve fibers but not in neurons of the cochlear nucleus, crossed to the Ai32-ChR2 mouse. Focal laser scanning photostimulation and in vitro patch-clamp recording was used to determine the properties of auditory nerve input to neurons of the cochlear nucleus. Recordings were obtained from neurons across a broad range of ages (p17-p177). All tested VCN bushy neurons demonstrated strong, fast, reliable responses to laser stimulation in NF107::Ai32 mice, showing that laser pulses successfully stimulated auditory nerve fibers. Surprisingly, DCN principal cells had weak or no response (~45% of cells) to laser photostimulation. As expected, cartwheel cells consistently lacked responses to laser photostimulation. The subset of tuberculoventral cells (~50%) that exhibited responses demonstrated stronger auditory nerve input than seen in pyramidal cells, and these inputs were sometimes sufficient to generate firing of these cells. These data suggest that within the DCN, the strength of auditory nerve input is segregated amongst different target cell types. This work was supported by NIDCD grant R01 DC004551 to PBM.

PS 09

The source of inhibition for spherical bushy cells - combining modeling and experiment

Christian Keine¹; Bernhard Englitz²
¹*Carver College of Medicine, Department of Anatomy and Cell Biology, University of Iowa*; ²*Computational Neuroscience Lab, Donders Institute for Brain, Cognition and Behavior, Radboud University*

Inhibition plays a crucial role in neural signal processing, shaping and limiting neuronal responses. In the auditory

system, inhibition already modulates second order neurons in the cochlear nucleus (CN), e.g. spherical bushy cells (SBCs). The cellular mechanisms underlying the inhibition have been described both in vitro and in vivo, including their functional consequences. However, the dense architecture of the cochlear nucleus has so far precluded to link physiological responses to the anatomical source of the inhibition. Given the spectral and temporal properties of inhibition and the predominantly glycinergic nature of inhibition onto SBCs, only a small number of cell types within the CN are reasonable candidates: the tuberculoventral and D-stellate cells.

To separate their influences on the activity of SBCs we combine our experimental recordings from SBCs under complex stimulus conditions with a recently published biophysical model of CN neurons (Manis & Campagnola 2018).. We constrain the model using recent findings from the literature to adapt it to the physiology of the gerbil auditory brainstem. In this configuration, the model creates realistic responses for the different cell types in the CN. We find that both tuberculoventral and D-stellate cells have a substantial influence on the SBC responses, which, however, differs in its spectral range, overall strength and their effective shape of inhibition, i.e. either subtractive or divisive.

PS 10

An Algorithm for Automatic Thresholding of Auditory Brainstem Responses (ABR) using Cross Covariance Analysis

Kirupa Suthakar¹; M. Charles Liberman²
¹*Eaton-Peabody Lab, Massachusetts Eye and Ear Infirmary, Harvard Medical School*; ²*Mass. Eye and Ear Infirmary*

The auditory brainstem response (ABR) is a sound-evoked neural response commonly used to assess auditory function in humans and laboratory animals. ABR thresholds are typically chosen by visual inspection, leaving ABRs susceptible to user bias. We sought to develop an algorithm to automate determination of ABR thresholds to eliminate such biases and standardize approaches across investigators and laboratories.

Two datasets of ABR waveforms versus level obtained from previously published studies of normal ears as well as ears with varying degrees of cochlear-based threshold elevations (Liberman et al 2014, J Neurosci 34:4599; Sergeyenko et al 2013, J Neurosci 33:13686) were reanalyzed using an algorithm based on cross-covariation analysis of adjacent level presentations. We used cross covariance rather than cross correlation as a convenient way to normalize mean waveform amplitude increases across successively higher-level

presentations, thereby optimizing the correlation-coefficient values obtained. The resultant correlation-coefficient vs. level function for each ABR level series was fit with either a sigmoidal or exponential function, from which threshold was interpolated at different criterion values of correlation coefficient ranging from 0 to 1. The criterion value of 0.35 was selected by comparing visual thresholds to computed thresholds across all frequencies tested. With such a criterion, the mean algorithm-computed thresholds did not differ significantly from the visual thresholds noted by two independent observers for each data set. The success of the algorithm was also qualitatively assessed by comparing averaged waveforms at the thresholds determined by the two methods, and quantitatively assessed by comparing peak 1 amplitude growth functions expressed as dB re each of the two threshold measures.

Here, we have shown that application of a cross-covariance analysis to ABR waveforms can emulate visual thresholding decisions made by highly trained observers. Unlike previous applications of similar methodologies using template matching, our algorithm performs only intrinsic comparisons within ABR sets, and therefore is more robust to equipment and investigator differences in waveforms, as evidenced by similar results across the two datasets.

Research supported by a grant from NIDCD (DC000188)

PS 11

A Simple Coincidence Detector Model to Simulate Temporal Coding of Bushy Cells in the Anteroventral Cochlear Nucleus

Go Ashida; Helen Heinermann; Jutta Kretzberg
University of Oldenburg

Bushy cells in the anteroventral cochlear nucleus transfer acoustic information from auditory nerves (ANs) to the superior olivary complex, where binaural neurons compute relevant cues for sound localization. Bushy cells are subdivided into two groups: globular bushy cells (GBCs) innervated by converging AN inputs (typically >10) and spherical bushy cells (SBCs) that receive a few large AN inputs via endbulb terminals. Reflecting this innervation pattern, spontaneous spike rates of SBCs are generally higher than those of GBCs. Both types of bushy cells show relatively irregular firing for high-frequency sounds, comparable to ANs. The peristimulus time histogram (PSTH) of a GBC

to repeated sound stimuli, however, shows a “primary-like-with-notch” pattern at high frequencies, while that of an SBC is “primary-like”. In response to low-frequency tones up to about 1 kHz, both cell types present an enhanced phase-locking and entrainment compared to their AN input. In the present study, we aim to simulate these physiological characteristics of bushy cells using a simple model of monaural coincidence detection. Sound-driven inputs from the ANs are computed by an auditory periphery model (Bruce et al. 2018, *Hear Res*), and are fed into a coincidence counting model (Ashida et al., 2016, *PLoS Comput Biol*) to generate an output spike sequence. After parameter fitting and a series of simulations, we find that the original version of the coincidence counting model cannot properly replicate the PSTH of a GBC, while other physiological responses (such as spontaneous rates, irregularity, enhancement of phase-locking and entrainment) are relatively well captured. This observation leads us to introducing an adaptive threshold to the model that suppresses the excessive excitability at the stimulus onset. This adaptive model enables us to simulate known physiological response patterns of GBCs, with much lower computational costs than conventional Hodgkin-Huxley-type models of bushy cells. These results suggest that our GBC model can be used as a simple alternative to complex models, especially when detailed intracellular dynamics need not to be explicitly considered. Prospective applications of this model include a large-scale simulation of the sound localization circuit, in which the activity of hundreds or thousands of neurons is computed. Fitting the model to SBCs will also be discussed in the presentation.

PS 12

Presynaptic GABAA Receptors Modulate Glutamatergic Transmission at the Endbulb of Held

Jana Nerlich; Stefan Hallermann; Ivan Milenkovic
Carl Ludwig Institute for Physiology, Faculty of Medicine, University of Leipzig

Background

Spherical bushy cells (SBCs) in the ventral cochlear nucleus integrate acoustically driven excitatory input from the auditory nerve with non-primary glycinergic and GABAergic inhibitory inputs to precisely encode the temporal structure of sounds. We have recently shown that some GABAergic terminals on SBCs apparently lack their postsynaptic counterparts expressing GABAAR (Nerlich et al., 2017). This suggests that the functional role of GABA may extend beyond the SBC inhibition. Indeed, GABABR at the endbulb can reduce synaptic strength of individual inputs and increase the requirement for their synchronicity (Chanda and Xu-

Friedman 2010). However, it remained elusive, whether the glutamate release at the endbulb terminal may be modulated by GABAA receptors.

Methods

Pre- and postsynaptic whole cell and gramicidin perforated recordings were performed in acute slices from P13-15 gerbils. Agonists (GABA, glycine) were pressure applied to the recorded presynaptic terminal. Action potentials were evoked by electrical stimulation of auditory nerve fibers. Postsynaptic EPSCs were recorded at the reversal potential for GABAAR (EGABA) to specifically investigate the effects of presynaptic GABAA receptors. All recordings were done with 3 μ M CGP55845 to block GABAB receptors.

Results

GABA evoked a prominent chloride conductance at the endbulb while glycine had no effect. Gramicidin perforated patch recordings revealed depolarizing chloride gradient within the terminal ($E_{Cl} = -28$ mV; estimated intraterminal $[Cl^-] = 40$ mM). The GABA-induced depolarization decreased the amplitude of APs evoked by electrical stimulation of auditory nerve fibers, in a concentration-dependent manner. The functional effect of presynaptic GABAAR onto glutamatergic transmission was assessed with postsynaptic EPSC recordings. To segregate the effects of pre- and postsynaptic GABAAR, each SBC was held at the experimentally-determined reversal potential for GABAAR ($V_{hold} = EGABA$), thus enabling to record isolated EPSC. Hence, GABA-puff elicited a membrane current only in the endbulb terminal. Brief application of GABA transiently reduced EPSC amplitudes. Such reduction of glutamate release also persists at P25 endbulbs, suggesting that the modulation is not constrained to immature synapses. The effect was blocked by the GABAAR antagonist SR95531. Puff application of glycine did not affect EPSCs, consistent with the lack of GlyR at the endbulb terminal.

Conclusion

The results suggest that GABAAR can modulate the strength of glutamatergic transmission at the endbulb of Held-SBC synapse. GlyR seem to be absent from the endbulb terminal.

References

Chanda, S., and Xu-Friedman, M.A. (2010). Neuromodulation by GABA converts a relay into a coincidence detector. *J Neurophysiol* 104, 2063–2074.
Nerlich, J., Rübtsamen, R., and Milenkovic, I. (2017). Developmental Shift of Inhibitory Transmitter Content at a Central Auditory Synapse. *Front Cell Neurosci* 11, 211.

PS 13

Bidirectional Long-Term Synaptic Zinc Plasticity at Glutamatergic Synapses in the Dorsal Cochlear Nucleus

Nathan W. Vogler; Thanos Tzounopoulos
Pittsburgh Hearing Research Center, Department of Otolaryngology, University of Pittsburgh

Synaptic zinc is coreleased with glutamate to modulate neurotransmission in many excitatory synapses. In the auditory cortex, synaptic zinc modulates sound processing by fine-tuning the neuronal response gain. In auditory, visual, and somatosensory circuits, sensory experience causes long-term changes in synaptic zinc levels and signaling. However, the mechanisms underlying long-term synaptic zinc plasticity and the effects of this plasticity on long-term glutamatergic plasticity remain unknown. To study these mechanisms, we used male and female mice and employed in vitro and in vivo models in zinc-rich, glutamatergic dorsal cochlear nucleus (DCN) synapses. High-frequency stimulation of DCN synapses, associated with long-term potentiation (LTP) of excitatory synaptic strength, induced long-term depression of synaptic zinc signaling (Z-LTD), as evidenced by reduced zinc inhibition of excitatory postsynaptic currents (EPSCs). Low-frequency stimulation, associated with LTD of synaptic strength, induced LTP of synaptic zinc signaling (Z-LTP), as evidenced by enhanced zinc inhibition of EPSCs. Thus, Z-LTD is a new mechanism of LTP and Z-LTP is a new mechanism of LTD. Pharmacological inhibition of Group 1 metabotropic glutamate receptors (G1 mGluRs) eliminated both Z-LTD and Z-LTP. Pharmacological activation of G1 mGluRs induced Z-LTD and Z-LTP, associated with bidirectional changes in presynaptic zinc levels. Furthermore, depletion of endoplasmic reticulum Ca^{2+} stores induced Z-LTD, suggesting a role of intracellular calcium signaling in zinc plasticity. Exposure of mice to loud sound caused G1 mGluR-dependent Z-LTD in DCN synapses, thus validating our in vitro results. Together, we show that G1 mGluR activation is necessary and sufficient for inducing bidirectional long-term synaptic zinc plasticity. Synaptic zinc plasticity is a previously unknown mechanism of LTP and LTD at zinc-containing glutamatergic synapses in the DCN. This work was supported by NIH grants F31-DC015924 (N.W.V.) and R01-DC007905 (T.T.).

Discovery of a Novel Inhibitory Cell Type in the Cochlear Nucleus

Tenzin Ngodup¹; Laurence O. Trussell²

¹OHSU; ²Oregon Health & Science University

In the ventral cochlear nucleus (VCN), inhibition is mediated by glycine. Feedforward inhibition provided by glycinergic cells is important for auditory processing by principal excitatory neurons in the VCN. However, only a single VCN glycinergic cell type has been described, the D-stellate or radiate cell. Previous studies have hinted at the existence of additional local glycinergic sources within the VCN but their identity has remained unknown. We used a well-characterized transgenic mouse line, GlyT2-EGFP, which labels all glycinergic neurons, to study the diversity of glycinergic cells in the VCN. With these transgenic mice, optical clearing (CUBIC MOUNT), whole-CN super resolution microscopy, and individual cell-fills, we discovered a surprisingly large population of inhibitory glycinergic GFP positive cells in the VCN that are distinctly different from the D-stellate cell class. Novel glycinergic cells are much smaller in soma size and dendritic area, but far larger in number, as compared with D-stellate cells. We also studied the cellular and synaptic properties of the novel inhibitory cell types using whole-cell patch-clamp recording in brain slices. The smaller inhibitory cell types showed some diversity in intrinsic properties, but generally could sustain action potentials at high rates. Interestingly, these cells show responses during long current injections that mimic in-vivo “chopper” responses to tones. To study responses to afferent auditory nerve (AN) fibers input, we electrically stimulated the AN root, and found that the novel cells received multiple AN fibers inputs. In addition to this primary input, these cells also received potent excitatory collaterals from local T-stellate cells. Previous studies have reported that D-stellate cells project to the contralateral CN. To test whether these cells are also commissural neurons, we injected retrobeads into the contralateral CN to label the commissural glycinergic cells. Large, presumptive D-stellate cells were labeled but no labeling was observed in smaller glycinergic cells, indicating that the latter are not commissural neurons. The small cells, but not D-stellate cells, were excited by carbachol, and bath application of carbachol triggered IPSCs in VCN principal cells, indicating that the small cells have local axonal projections. We term these novel inhibitory cells L-stellate cells as they project locally, and suggest that they could provide robust inhibition to principal cell types in the VCN.

Maturational Changes in Cholinergic Efferent Synapses in the ChAT-tauGFP Mouse Cochlea.

Anna Dondzillo; Samuel Gubbels

University of Colorado Anschutz Medical Campus

Presbycusis, or age-related hearing loss, affects one in four people of the US population aged 60-69 (2011-2012 survey¹). Age related changes occur in the entire auditory system at synaptic and cellular levels from sensory epithelium of the inner ear through the peripheral and central nervous systems. Hair cell death is well established as a causal factor of hearing loss with age. However, growing anatomical and physiological evidence suggests that the initial change seen in presbycusis might be caused by synaptic rearrangements at the hair cells.

The inner ear sends information to and receives feedback from the auditory brainstem. In the feedback system of the adult, the outer hair cells (OHCs) receive axosomatic input from contralateral Medial Olivocochlear (MOC) neurons. The inner hair cells (IHC) do not receive direct input, instead their afferents, which carry the signal out to the brain, receive inhibitory input from the ipsilateral Lateral Olivocochlear (LOC) neurons. In contrast, in young mammal's inner hair cells receive temporary, direct, inhibitory cholinergic input from the contralateral MOC neurons until around hearing onset in mice. In the last decade investigators using electron microscopy and whole cell electrophysiology have shown that those temporary cholinergic inhibitory synapses re-appear on IHCs in the aged cochlea (Lauer et al., 2012; Zachary and Fuchs, 2015). However, the number and synaptic ratio per hair cell, their brainstem area of origin, and finally their role in sound processing is not well understood.

In this study we identified and quantified synaptic connections between hair cells and efferent neurons at different ages in C57BL6/J and transgenic ChAT-tauGFP mice. We use presynaptic SV2 antibody, which has not been found in the chicken and mouse hair cell ribbon synapses, to identify efferent presynaptic terminals and anti-Myosin 7a antibody to identify hair cells. We also compare the usefulness of different tracers: Dextran Red MW 10 000, Lumafuor Nano beads, and Cholera toxin subunit B in retrograde labeling of the efferent somata in the auditory brainstem. Our preliminary data suggests, that at least in the C57BL6/J mice there is a reduction by one half of efferents per inner hair cell in one-year old mouse as compared with a postnatal day 14 mouse. Our tracer data suggests that the Cholera toxin subunit B labels the highest number of cells in the brainstem and is picked up by axo-somatic as well as axo-dendritic terminals.

Kainate Receptors Regulate the Excitability of Granule Cell Axons

Zheng-Quan Tang¹; Laurence O. Trussell²

¹Oregon Hearing Research Center at the Oregon Health and Science University; ²Oregon Health & Science University

Kainate receptors (KARs) modify excitability and synaptic efficacy in the CNS. Although widely expressed, the exact roles of KARs remain largely unknown. To address this, we examined KAR modulation in granule cells (GrCs) of the dorsal cochlear nucleus (DCN) and cerebellum in mice.

We performed whole-cell voltage-clamp recordings from DCN cartwheel cells in mouse brain slices (P16-42, 33°C) and recorded parallel fiber (i.e., GrC axon)-evoked EPSCs (Excitatory Postsynaptic Currents) in the presence of inhibitory receptor antagonists. Furthermore, taking advantage of the TCGO mouse line which expresses mCitrine in a subset of GrCs, we performed loose cell-attached voltage-clamp recordings from the soma of labeled GrCs in the DCN and cerebellum and recorded antidromic action currents (ACs) following electrical stimulation of labeled parallel fibers in the molecular layer, in the presence of selective GABAA, glycine, NMDA and AMPA receptors antagonists. Glutamate was locally puffed onto parallel fibers of GrCs.

We found that bath application of UBP-302, a GluK1-selective KAR antagonist, decreased the frequency of spontaneous EPSCs in cartwheel cells, but not the amplitude of EPSCs. By contrast, ATPA, a GluK1-selective KAR agonist, increased the frequency of spontaneous EPSCs. ATPA did not affect the frequency or amplitude of miniature EPSCs recorded in the presence of tetrodotoxin. Together, these data indicate that GluK1-KARs regulate the excitability of GrCs and/or their axons. Consistently, UBP-302 decreased the amplitude of EPSCs in cartwheel cells evoked by a train of stimulation of parallel fibers, without affecting their short-term plasticity. These data suggest that a tonic activation of GluK1-KARs on presynaptic granule cell axons maintains a positive tone of glutamate release onto cartwheel cell. We thus hypothesized that KARs regulate parallel fiber excitability and thereby facilitate transmission to target cells.

To address this hypothesis, we further examined whether activation of axonal KARs by local glutamate application affects the back propagation of antidromic ACs to the soma of GrCs. Puffing application of glutamate onto parallel fibers significantly increased the rate of antidromic ACs recorded at soma. Bath application of NBQX, an antagonist of kainate receptors, prevented the effects of glutamate on firing rate of antidromic ACs.

Our findings demonstrate that KARs can regulate

the axonal excitability of GrCs both in the DCN and cerebellum, and facilitate the propagation of ACs. By modulation the axonal excitability of GrCs, this mechanism may promote signaling during high-frequency sensory activity.

PS 17

The Human Cochlear Nucleus: Anatomical Characterization and Functional Considerations on 7 Tesla Diffusion Tensor Imaging

Lorenz Epprecht¹; Ahad A. Qureshi²; Elliott D. Kozin³; Alexander M. Huber⁴; Ron Kikinis⁵; Allan Johnson⁶; M. Christian Brown⁷; Katherine Reinshagen⁸; Daniel J. Lee⁹

¹Eaton Peabody Laboratories, Massachusetts Eye and Ear Infirmary, Department of Otolaryngology, Harvard Medical School; ²Eaton Peabody Laboratories, Massachusetts Eye and Ear Infirmary, Department of Otolaryngology, Harvard Medical School; ³Massachusetts Eye and Ear Infirmary; Department of Otolaryngology, Harvard Medical School; ⁴Department of Otorhinolaryngology and Head and Neck Surgery, University Hospital of Zurich; ⁵Surgical Planning Laboratory, Harvard Medical School; ⁶Duke Center for In Vivo Microscopy, Duke University School of Medicine; ⁷Eaton-Peabody Laboratories, Massachusetts Eye and Ear, Harvard Medical School, Harvard Program in Speech and Hearing Bioscience and Technology; ⁸Department of Radiology, Massachusetts Eye and Ear Infirmary and Harvard Medical School; ⁹Department of Otolaryngology, Harvard Medical School

Introduction: Patients with Neurofibromatosis type 2 (NF2) develop bilateral vestibular schwannomas that can influence cochlear nucleus (CN) structure and function via physical and chemical factors. Following tumor resection, these patients can be implanted with an auditory brainstem implant (ABI) that provides hearing sensations by stimulating the CN. During surgical planning, routine 3 Tesla (3T) structural and diffusion magnetic resonance imaging (MRI) do not resolve detailed anatomy of the CN. We hypothesize that diffusion tensor imaging (DTI) would enable structural and anatomical localization in vivo and allow quantitative analysis of the human CN.

Methods: We analyzed 7 Tesla (7T) DTI data from 100 young healthy normal hearing subjects (200 CN) who participated in the Human Connectome Project. Relevant anatomic structures were identified using an MRI brainstem atlas with submillimetric (50 µm) resolution. We analyzed diffusion scalar measures of fractional anisotropy (FA), mean diffusivity (MD) and

mode of anisotropy (Mode). Principal eigenvectors of the CN measured included the adjacent inferior cerebellar peduncle (ICP) inferiorly, medially and superiorly.

Results: On 7T DTI the human CN was a distinct structure lateral to the inferior cerebellar peduncle (ICP) with a microscopic lamellar structure and anterior-posterior fiber orientation. This fiber orientation was orthogonal to tracts of the adjacent ICP where fibers projected were oriented mainly inferior-superiorly. The CN had lower FA compared to the inferior, superior and medial aspect of the ICP (0.44 ± 0.09 vs. 0.64 ± 0.08 , $p < 0.001$).

Conclusions: 7T DTI enables distinction of the human CN and resolves its structural fidelity and spatial position from the adjacent ICP based on fiber orientation. This technique is possible with current state-of-the-art MRI scanners and would aid in the accurate placement of the ABI electrode array onto the CN.

Auditory Cortex: Anatomy & Physiology I

PS 18

Spatial Organization of Primary and Higher-Order Fields in the Mouse Auditory Cortex

Sandra Romero Pinto¹; Ariel E. Hight¹; Pooja Balaram²; Jennifer Resnick³; Kenneth E. Hancock³; Daniel B. Polley³

¹*Eaton-Peabody Laboratories, Massachusetts Eye and Ear; Program in SHBT, Division of Medical Sciences, Harvard Medical School;* ²*Allen Institute for Brain Science;* ³*Eaton-Peabody Laboratories, Massachusetts Eye and Ear; Dept. of Otolaryngology, Harvard Medical School*

Microelectrode mapping studies have identified two tonotopically organized fields in the mouse auditory cortex (ACTx), the primary ACTx (A1) and the anterior auditory field (AAF), surrounded by a secondary ACTx (A2), a dorsoposterior field (DP) and the insular auditory field (IAF). Interest in cortical organization at “mesoscale” resolution has been revived thanks to sensitive genetically encoded calcium indicators (GECIs) that offer a higher signal-to-noise ratio than intrinsic hemodynamic signals, flavoproteins or bulk-loaded calcium indicators. Widefield epifluorescence imaging of GECIs offers several advantages over traditional mapping approaches, including 1) performing measurements in awake animals, 2) deriving maps from all fields simultaneously, 3) repeatedly deriving maps from the same animal at multiple time points, 4) restricting GECI expression to particular cell types of interest. Here, we exploit all four of these advantages in a series of experiments that quantify the spatial

arrangement of cortical fields and their reliability over time. We characterized two commercially available transgenic mouse lines that express GCaMP6s in excitatory neurons but found that both have extreme, early-onset high-frequency hearing loss. We crossed one of these mouse lines (Thy1-GCaMP6s) to a strain with good hearing (CBA/CaJ) to establish a transgenic line with normal hearing and confirmed with immunohistochemistry that GCaMP6 expression was limited to CaMKII-expressing pyramidal neurons. We labeled points of interest with Di-I and identified several major discrepancies with ACTx boundaries published in widely used mouse brain atlases. We developed an objective, data-driven approach to parcel each field and observed a high-degree of precision and reliability of tonotopic mapping over a several weeks period, particularly in A1. In a subset of mice, we are performing 2-photon calcium imaging to determine whether local heterogeneity of preferred frequency tuning in individual layer 2/3 pyramidal neurons is found in regions with smoothly varying mesoscale tonotopic gradients. Finally, we presented more complex stimuli, including ripples, amplitude modulated noise and dynamic moving ripples to identify potential regions with preferential responses to more complex stimuli, and to determine whether there are more efficient stimuli for deriving tonotopic maps than pure tones. Collectively, these studies describe the functional organization of auditory fields in the mouse cortex at a variety of spatial scales, with a variety of stimulus types and relate this organization to neuroanatomical landmarks. We anticipate that these descriptive studies will facilitate future work in other labs studying mouse auditory cortex.

PS 19

Cell-Specific Intrinsic and Synaptic Plasticity of Auditory Cortical Neurons after Noise Exposure

Amanda Henton; Manoj Kumar; Thanos Tzounopoulos
Pittsburgh Hearing Research Center, Department of Otolaryngology, University of Pittsburgh

Exposure to loud sound induces death of cochlear hair cells and loss of synapses between hair cells and the auditory nerve, which contribute to loss of afferent input to the brain. While a reduction of input after noise exposure may be predicted to cause reduced responses to sound, it paradoxically increases excitatory responses in auditory cortex. This increased responsiveness to sound after noise exposure aids perception even with reduced input from the auditory periphery. This phenomenon has been termed auditory gain adaptation. A decrease in parvalbumin (PV) neuron-mediated inhibition to principal neurons has been suggested as a possible mechanism for gain adaptation after

noise exposure (Resnik & Polley, 2017). Additionally, 2-photon, in-vivo calcium imaging results from our lab show that PV interneurons increase their response gain after noise exposure, and that the PV neuron plasticity precedes the increase in principal neuron response gain. However, the intrinsic mechanisms of plasticity in auditory cortex after noise exposure are unknown. Here we describe the intrinsic plasticity of PV interneurons, and Corticocallosal neurons, which are a subclass of principal neurons that project axons via the corpus callosum to the contralateral auditory cortex to mediate intrahemispheric connectivity. Our results show that PV interneuron excitability is initially decreased one day after noise exposure, as evidenced by a reduced firing rate and a depolarized action potential threshold. However, seven days after noise exposure intrinsic excitability is increased, via a depolarization of the resting membrane potential. We did not observe any changes in the intrinsic excitability of Corticocallosal neurons. These results suggest that PV interneurons may serve as a crucial site of plasticity in auditory cortex after noise exposure. This work was supported by: F31-DC017635-01 (A.H), R01-DC007905 (T.T), and DOD W81XWH-14-1-0117 (T.T)

PS 20

A Versatile and Integrated LabVIEW Based System for High Throughput Auditory Behavior and Physiology

Wenhao Zhang; **Anton Banta**; Jack Shi; Matthew McGinley
Baylor College of Medicine

Recent advancements in electrophysiology, imaging, optogenetics, and computing power have led to a renaissance of in vivo ‘circuit busting’; in systems neuroscience, particularly using head-fixed approaches in mice. In order to tap into this convergence of advancements, an integrated software system for data-intensive, high-throughput experimentation is required. In addition, the auditory system presents unique challenges due to the high temporal and signal resolution needed for precise and accurate sound delivery.

To meet this need, we have developed a custom hardware and software system centered in LabVIEW. LabVIEW is customizable and easy to use, allowing for high throughput data acquisition and automated experimentation. We have constructed a general software architecture that can both interface with many hardware inputs and be adapted to fit the specific needs of different behavior paradigms. The software conducts real-time complex sound waveform construction and delivery with a 20 ms time buffer. This allows creation

of navigable auditory virtual reality, and closed loop manipulation of sound and brain stimulation driven by the animal's behavior. The software integrates sound delivery and behavior in tandem with two photon microscopy, vagus nerve stimulation, optogenetics, and/or high-channel count electrophysiology to combine behavioral and physiological approaches. All tasks are fully automated and require no user interaction once an experiment process is started.

The software design is primarily based on the Queued Message Handler (QMH) pattern. QMH is a flexible design pattern that can implement modular software process design and communicate between multiple processes. Multiple QMHs are used to execute and synchronize parallel processes that acquire or interact with different types of data, simultaneously. These include playing complex auditory stimuli (e.g. tone clouds with embedded, psychometrically manipulate temporal coherence), sensor data for detecting licking and administering rewards, rotary encoder data for tracking animal walking, and IR camera recording animal videography, such as for pupil measurement. A QMH is also used to manage and automatically stream experiment data to hard drives. All experiment setup parameters are logged for traceability purpose. Within LabVIEW, the priorities of different processes are configured to make full use of multicore CPUs and other computing resources. For example, we acquire high-definition high-speed video of the animal, with real-time compression using built-in codecs and chunked file saving. After experiments, videos are concatenated and further compressed using the robust multimedia framework, FFmpeg. Overall, our versatile and integrated LabVIEW-based system allows high-throughput behavior and physiology in diverse studies of the auditory system.



PS 21

Early Auditory Cortex Responds to Task-related Visual Events as early as Prefrontal Cortex

Ying Huang; Michael Brosch

Special Lab Primate Neurobiology, Leibniz Institute for Neurobiology

Many studies have shown that, during the performance of auditory tasks that consist of a sequence of events, neuronal activity in early auditory cortex can be related not only to sounds but also to task-relevant non-auditory events. However, the sources of such task-related non-auditory activity in auditory cortex have remained unclear. One possibility is that this activity in auditory cortex originates from some high-order brain areas, such as prefrontal cortex, which are known to represent multiple events of a sequential task and to play key roles in constructing temporal structures and mental programs for the task. If this is the case, we would expect to observe the first task-related neuronal activity later in auditory cortex than in high-order brain areas. To test this possibility, we conducted an electrophysiological study in two monkeys in which they performed two tasks. In both tasks, each trial started with a visual event which signaled the monkey that he could grasp a touch bar to trigger the presentation of auditory events and then make an appropriate action to obtain a small amount of water. Therefore, the first task-relevant event was the visual event. Spiking activity was recorded from the core fields of auditory cortex and also from the ventrolateral part of the prefrontal cortex while the monkeys performed the tasks. We observed the spiking activity that was related to the presentation of the visual event in both cortical areas, but in a task-specific way. We also found that such task-related spiking activity occurred in auditory cortex as early as in prefrontal cortex, about 90 ms after the event onset. Our results suggest that such task-related spiking activity in the core fields of auditory cortex unlikely originated from the ventrolateral part of the prefrontal cortex.

The work was supported by CBBS neuronetwork project, LIN special project, and DFG projects He1721/10-1 and 10-2.

PS 22

The Influence of Amygdalo-Auditory Cortex Direct Projections in Audition and Tinnitus: An Optogenetic Reversible Deactivation Study.

Diana C. Peterson

High Point University

The role of the amygdalar projection to auditory cortex (AM-AC) is currently unknown. It has been hypothesized

that AM-AC may help to manipulate descending control circuits for auditory attention. It could also serve a modulatory function in conjunction with the amygdalo-nucleus basalis-auditory cortex circuit to manipulate auditory conditioning and learning.

Methods (Experiment 1): To help elucidate the role of the direct amygdalo-auditory cortex pathway, optogenetic vectors (AAV-CaMKIIa-eNpHR3.0-EYFP) were placed into the amygdala of Long Evans rats to isolate and reversibly deactivate the pathway when a laser light was presented within auditory cortex. In the same animals, multichannel electrodes were implanted into auditory cortex. Auditory responses were then recorded from cortex in both normal and amygdalo-cortical light deactivation conditions.

In (Experiment 2), the role of the AM-AC in tinnitus perception was tested by inducing an acoustic tinnitus at the end of the surgery (see methods experiment 1 above). These animals were tested for their response to acoustic startle both with and without light deactivation of the circuit.

Results (Experiment 1): When the amygdalo-cortical circuit was deactivated with light, both single and multiunit activity was dramatically reduced for the duration of the light stimulation. However, the recording returned to normal levels immediately after the light was turned off. Experiment 2: Tinnitus behavior (a marked decrease in the startle versus gap acoustic reflex) was observed in the tinnitus induced animals. Light deactivation of the AM-AC caused the acoustic startle reflex to resemble the non-tinnitus behavior. The tinnitus behaviors immediately resumed when the light was turned off (i.e., AM-AC reactivation).

In both experiments, the location of the tracer was examined histologically after animals were euthanized. Results from these examinations revealed that the surgical locations for both recording and tracer injections were accurate. Examination of other brain regions revealed a few (very limited) neurons in the medial geniculate and nucleus basalis. Numerous labeled neurons were observed within the hippocampus.

Conclusions: The results from Experiment 1 indicate that the AM-AC has fairly profound but transient influences on cortical activity. This transient nature may indicate that it has a short-term modulatory influence on cortex to prime it for secondary circuits (e.g., amygdalo-nucleus basalis-auditory cortex).

While our results show that tinnitus was eliminated during deactivation of the pathway, the fact that deactivation had a profound influence on auditory activity during the

recording experiments may indicate that the animals'; overall perception was reduced during activation which influenced the results.

PS 23

Comparison of Auditory Responses in Old and Young Neurons in Ferret A1.

Jayalakshmi Viswanathan¹; Kai Lu²; Jonathan B. Fritz³; Shihab A. Shamma³

¹Neural systems lab, Institute for Systems Research, University of Maryland; ²Neural Systems Lab, Institute for Systems Research, University of Maryland; ³Neural Systems Laboratory, Institute for Systems Research, University of Maryland

Background: Age-related hearing loss (ARHL) is a highly prevalent social and health issue, with about 63% of adults over 70 years of age affected. ARHL is associated with impairment in several cognitive processes such as auditory perception, attention, spatial localization, temporal precision in encoding. These deficits in auditory skills often lead to difficulties in understanding speech and navigating in complex and noisy acoustic environments. Although ARHL is of great importance, especially in an aging population, the mechanisms of how these deficits emerge as a function of aging is poorly understood. Such understanding may lead approaches that can alleviate ARHL.

Methods: To elucidate age-related changes in response properties and characterize cortical plasticity in the aging brain, we have chosen to study the ferret, an animal model with a hearing range that is very similar to humans. We recorded neuronal responses from the primary auditory cortex (A1) in older ferrets and compared to responses in younger animals. We recorded single units (N>2000) from A1 of 24 female ferrets ranging from 1 year up to 8 years of age (comparable to 20-year-old up to 90-year-old humans). In these experiments, we recorded from A1 units in passively listening head-fixed ferrets as they were presented with a variety of acoustic stimuli, including speech in silent and noisy (white noise and reverberant) backgrounds. Single unit responses to speech in the different contexts were then used to reconstruct the stimuli. Stimuli reconstructed from young ferrets were compared with those reconstructed from the older ferrets.

Results: In characterizing the response properties of cortical neurons, we found that frequency selectivity deteriorates (bandwidth increases) with increasing age. Likely due to peripheral presbycusis, there was an overall shift in A1 responses to lower frequencies in older ferrets. A1 neurons from older animals also exhibited

sluggish phase-locked responses, also reflected by increased latency of responses. A likely contributing cause of these changes in response properties with aging may be a decrease in overall inhibition in older brains, that could also lead to difficulties in extracting speech in noise. We will also explore the possibility that there is less task-related plasticity in older brains resulting in sub-optimal sound processing. We discuss our results in the context of the computational challenge in extracting signal from noise with reduced inhibition and plasticity.

PS 24

Using Mesoscale Chronic Calcium Imaging to Track Cortical Map Reorganization Following Acoustic Trauma

Ariel E. Hight¹; Matthew McGill²; Daniel B. Polley³
¹Eaton-Peabody Laboratories, Massachusetts Eye and Ear Infirmary/ Program in Speech and Hearing Bioscience and Technology, Department of Medical Sciences, Harvard Medical School; ²Eaton-Peabody Laboratories, Massachusetts Eye and Ear Infirmary/ Program in Neuroscience, Department of Medical Sciences, Harvard Medical School; ³Eaton-Peabody Laboratories, Massachusetts Eye and Ear; Dept. of Otolaryngology, Harvard Medical School

Damage to restricted regions of the basilar membrane in adult ears has been linked to large-scale reorganization of cortical tonotopic maps. It has been nearly 30 years since Robertson and Irvine's seminal demonstration of large-scale map reorganization in the adult cortex, yet important questions remain unresolved due to inherent limitations of cortical mapping with microelectrode recordings. Here we monitor day-to-day changes in map reorganization over a two month period across three fields of the adult mouse auditory cortex and relate these changes to shifts in peripheral sensitivity and perception of tones assessed with an operant behavior. Chronic mapping of all fields within the mouse auditory cortex was accomplished with a widefield Ca²⁺ imaging system in awake-head fixed Thy1-GCaMP6s x CBA/CaJ transgenic mice, where the genetically encoded calcium indicator GCaMP6s is restricted to excitatory neurons in the auditory cortex. We recorded the day-to-day tone evoked fluorescence across the cortical surface in awake, head-fixed mice via a chronically implanted cranial window. We computed the preferred frequency for each pixel to reveal the boundaries and tonotopic organization of the primary auditory cortex (A1), anterior auditory field (AAF), and secondary auditory cortex (A2). Control animals showed stable tonotopy across days ($r > 0.7$, shuffled day-to-day correlations). We induced high-frequency cochlear trauma by exposing adult mice

to octave band noise (16-32 kHz, 103 dB SPL, 2-h). We quantified wave 1 of the ABR to confirm that noise exposure induced a permanent shift in high-frequency thresholds (>16 kHz, >20 dB SPL). In the ACtx we found fractional representation of high frequencies decreased across A1, AAF, and A2. We also found the number of non-responsive pixels increased hours after noise exposure but then decreased nearly to baseline levels within 5-days after exposure. We observed a commensurate increase in the fractional area and the growth function of spared 8 kHz regions following noise exposure. Using a Go-NoGo operant detection task in head-fixed mice, we found that pure tone detection thresholds were elevated on the day of noise exposure, but returned to baseline for 8 but not 32 kHz (~50 dB HL). Interestingly, the psychometric detection functions grew more steeply at 8 kHz after noise exposure, which could not be explained by ABR wave-1 growth functions. These experiments address the temporal dynamics of map reorganization in excitatory neurons at mesoscale resolution (~15 microns). We observe cortical map dynamics that more directly explain changes in sound perception after acoustic trauma than traditional measures of peripheral function.

PS 25

The Effects of Synaptic Zinc on Corticocollicular Neurons in the Auditory Cortex

Charles Anderson
WVU School of Medicine

Corticocollicular neurons in layer 5 of the auditory cortex send axons to subcortical areas of the ascending auditory pathway including the thalamus and inferior colliculus, as well as areas outside of the ascending auditory pathway including the striatum and amygdala. These corticofugal neurons show compensatory gain increases following hearing loss and are crucial for relearning auditory spatial location cues after monoaural ear plugging which suggests that they contribute to auditory system plasticity. Auditory cortex stimulation can alter the sound-encoding properties of neurons in the thalamus and inferior colliculus, suggesting that corticofugal inputs to these structures can shape receptive field properties. Although a good deal is known about the intrinsic properties of corticocollicular neurons and how they are integrated into local excitatory and inhibitory cortical microcircuits, it is less well understood how these factors contribute to the sound-encoding properties of these neurons. In particular, the effects of synaptic zinc – a powerful modulatory neurotransmitter system throughout the cortex – on corticocollicular neurons are unexplored. Synaptic zinc enhances the gain and sharpens the sound-frequency tuning of

principal neurons in layer 2/3, which in turn, provide a large amount of excitatory input to corticocollicular neurons in layer 5. Here, I am exploring the effects of synaptic zinc signaling on corticocollicular neurons in the auditory cortex using 2-photon calcium imaging in awake mice and electrophysiological recordings from identified neurons in acute brain slices.

PS 26

Cell-specific Modulation of Cortical Inhibition by Synaptic Zinc

Stylianos Kouvaros; Thanos Tzounopoulos
Pittsburgh Hearing Research Center, Department of Otolaryngology, University of Pittsburgh

Activation of inhibitory pathways in the cortex is essential for maintaining the balance between excitation and inhibition during normal cortical activity. Somatostatin-expressing-GABAergic neurons (SST), a major class of interneurons in the cortex provide strong cortical inhibition. Zinc is loaded into the synaptic vesicles and is a crucial element for synaptic function. The mRNA for ZnT3, the protein responsible for loading zinc into presynaptic vesicles, is highly and specifically expressed in SST neurons relative to other inhibitory neurons. In this study, we sought to study the effect of synaptically released zinc on inhibition mediated by SST interneurons onto pyramidal neurons (PNs) and parvalbumin (PV) interneurons in layers II/III of the mouse auditory cortex. By using in vitro optogenetics, we discovered that removal of synaptic zinc, by using a high-affinity extracellular zinc chelator, leads to a dramatic decrease of the SST-mediated inhibitory postsynaptic currents (IPSCs) onto PNs and PVs, in layers II/III. This effect was further confirmed by dual recordings between SSTs and PNs. Chelation of zinc also causes decrease of the amplitude of SST-mediated evoked desynchronized miniature IPSC when calcium is replaced with strontium. Interestingly, the PV-mediated IPSCs onto PNs did not alter after zinc²⁺ depletion indicating a cell-specific role of zinc. Furthermore, chelation of zinc does not alter either the pair-pulse ratio (PPR) or the quantal content (1/CV²) of the optogenetically evoked-IPSCs from SSTs to PNs. indicating a lack of contribution of presynaptic mechanisms in the zinc-mediated enhancement in IPSCs. These findings suggest that synaptic zinc is a key modulator of inhibitory cortical activity in the layers II/III of mouse auditory cortex.

Supported by NIDCD, R-01 DC007905 award to TT

PS 27

Neural Circuits Underlying Spectro-Temporal Integration of Sounds

Amber M. Kline; Destinee A. Aponte; Hiroyuki K. Kato
University of North Carolina at Chapel Hill, Department of Psychiatry and Neuroscience Center

The brain's capacity to integrate the features of sensory stimuli is essential to understand and respond to our environment. In the auditory system, even in the face of multiple sound sources, our brain binds acoustic components originating from the same source to reconstitute individual sound objects. In particular, integration of harmonic components is critical to accurately perceive physiologically relevant sounds such as language. In humans, one of the factors influencing the binding of harmonic components is timing of the spectral components'; onset within a 30-ms window. However, the neural circuits by which the auditory system integrates sounds in a timing-dependent manner remain unknown.

In this study, we investigated the temporal integration of harmonic sounds in mouse auditory cortex. Using macroscopic imaging of all auditory cortical areas, we determined that higher-order area, A2, preferentially responds to harmonic vocalizations over pure tones. Furthermore, using two-photon calcium imaging in awake mice, we found that A2 neurons display preferential response to non-shifted harmonics compared to harmonic tones whose onsets are shifted in time. This timing-dependence was not observed in primary area A1, suggesting that A2 plays a unique computational role in processing harmonics. Finally, we developed a Go/No-go task in which mice were trained to discriminate between non-shifted harmonics and time-shifted distractors. Interestingly, we found that mice have a similar 30-ms window for integrating harmonic components, suggesting conserved neural circuitry across species. In the future, we will manipulate A2 activity during this task to investigate its causal role in the perceptual integration of harmonics. Determining the mechanism by which the auditory cortex integrates harmonic sounds will contribute to our knowledge of how we process language, as well as inform us about how speech perception could be affected in neurodevelopmental disorders.

PS 28

Imbalanced Synaptic Charge Shapes Direction Selectivity in Primary Auditory Cortex

Destinee A. Aponte; Amber M. Kline; Hiroyuki K. Kato
University of North Carolina at Chapel Hill, Department of Psychiatry and Neuroscience Center

Frequency Modulation (FM) is a prevalent sound feature found in both human speech and animal vocalization. The brain's ability to detect the direction of frequency modulation is critical for vocal communication. Neurons in the primary auditory cortex (A1) have been reported to show selective firing to their preferred FM direction. However, it remains debated how direction selectivity maps spatially onto A1, and what circuit mechanisms underlie the selectivity.

Here, we determined the FM tuning properties of a large population of A1 neurons using in vivo two-photon Ca²⁺ imaging in awake mice. We found that more than 70% of A1 neurons show direction-selective firing, and that the selectivity was topographically ordered along the A1 tonotopic axis. Interestingly, neurons also showed robust direction selectivity to ethologically relevant slow-rate FM sweeps, which previous studies did not observe in anesthetized animals. To investigate the synaptic mechanism underlying the direction selectivity to slow FM sweeps, we measured synaptic currents using in vivo whole cell recordings. In contrast to previous models that explained direction selectivity based on different onset timings of EPSCs and IPSCs, we found that direction selectivity is rather driven by a difference in the total charge triggered by preferred and null directions. Null-direction FM sweeps evoked significantly attenuated EPSCs and IPSCs, which is explained by a suppression of recurrent circuits in the cortex - a phenomenon we recently reported as "network suppression". Taken together, our findings revealed a non-classical circuit mechanism that ensures direction selectivity of A1 neurons to slow FM sweeps which play important roles in our vocal communication.

PS 29

Immunocytochemistry for Glial and Neuronal Markers in the Rat Brain after Auditory Cortex Anodal Epidural Direct Current Stimulation

Ana Colmenarez¹; Ivan Diaz¹; Marianny Pernia¹; Ignacio Plaza¹; David Perez-Gonzalez²; Jose Maria Delgado-Garcia³; Miguel Merchan¹

¹*Instituto de Neurociencias de Castilla y Leon;*

²*University of Salamanca;* ³*Universidad Pablo de Olavide*

Electric neuromodulation of the brain was applied recently to neurological, psychiatric or otological disorders (tinnitus and auditory hallucinations).

The aims of this study were to analyze the effects of epidural electrical stimulation of the auditory cortex (AC) using immunocytochemistry of well characterized antibodies for glial cells (Iba-1 and GFAP) and neurons (c-Fos and GAD67). Also, corticofugal modulation of the olivocochlear reflex was explored by Auditory Brainstem Responses (ABRs), as a test to evaluate AC activation. Guided by stereotaxic coordinates a silver ball electrode of 1.3 mm was surgically inserted in contact with dura mater in the surface of the dura of primary AC. A protocol of continuous anodal, 100 μ Amp, 10 min direct current (DC) was applied 7 times in alternating days, starting 7 days after surgery (AS). ABRs were recorded before and 7 days AS and at the end (14 days AS) of the experiments. After the DC stimulation protocol an increase (up to 20 dB) in ABRs thresholds and a significant decrease about (~ 30%) waves amplitudes were shown.

Immunohistochemical analysis showed that astrocytes and microglial cells were locally activated following DC stimulation in an extension about 620 μ m², affecting mainly the superficial layers (I to V). No clear signs of lesional glial activation were observed in brain sections. c-Fos immunocytochemistry showed changes in distribution of positive neurons along cortical layers and along cortical subdivisions which suggest a global surface effect of electric currents on the brain. We conclude that multisession epidural 100 μ Amp stimulation allows to induce a global reorganization of the cortex without significant or extensive lesions. Also, our ABRs results pointed out that AC epidural stimulation could be applied as a tool for dynamic regulation of cochlear responses to sound.

PS 30

Role of synaptic zinc signaling in cell-specific plasticity of auditory cortical neurons after noise-induced hearing loss

Manoj Kumar; Thanos Tzounopoulos
Pittsburgh Hearing Research Center, Department of Otolaryngology, University of Pittsburgh

Noise-induced hearing loss (NIHL) is one of the most common types of sensorineural hearing loss, which reduces the auditory sensory inputs relayed from cochlea to auditory cortex (AC). To compensate for the loss of peripheral inputs, principal neurons in AC undergo homeostatic plasticity. Namely, principal neurons increase their response gain, the slope of

sound level against the neuronal response. Despite the established role of reduced GABAergic signaling in increased gain, the precise signaling mechanisms underlying the plasticity of distinct GABAergic neurons, including parvalbumin- (PV) and somatostatin-expressing (SOM) neurons, are unknown. My recent in-vivo studies in awake mice have shown that synaptic zinc (Syn-Zn²⁺), which is co-released with glutamate at many excitatory terminals and modulates NMDA and AMPA receptors in auditory circuits, fine-tunes the primary auditory cortex (A1) responsiveness to sound in a cell-specific manner. Namely, Syn-Zn²⁺ increases the gain of principal neurons but reduces the gain of PV and SOM neurons. Further, previous studies have shown that cortical Syn-Zn²⁺ levels increase after sensory deprivation and vice-versa. To identify the role and signaling mechanism of Syn-Zn²⁺ signaling in increased gain of A1 after NIHL, we have employed in-vivo wide-field Ca²⁺ imaging in awake mice to study the effect of pharmacological chelation of Syn-Zn²⁺ on principal, PV and, SOM neurons'; gain after 1, 3 and 10 days of NIHL. Our results are consistent with Syn-Zn²⁺ signaling contributing to the increased gain of A1 principal neurons after NIHL by enhancing the inhibition of PV neurons. Further, after 10 days of NIHL, Syn-Zn²⁺ signaling facilitates the reduction of increased gain of principal neurons by potentiating PV neurons'; gain via enhanced inhibition of SOM neurons. These findings may provide insights of AC plasticity occurring in hearing loss induced by ototoxic drugs, aging or ear diseases and in other pathologically increased central gain disorders, like tinnitus and hyperacusis.

Supported by NIDCD, R-01 DC007905 award to TT

PS 31

The role of interneurons in maintaining sensitivity to sensory cues in on-going sounds: the case of gap detection in the mouse primary auditory cortex

Bshara Awwad¹; Israel Nelken²

¹*The Edmond and Lily Safra Center for Brain Sciences and the Department Neurobiology, the Silberman Institute of Life Sciences, Hebrew University;*

²*Edmond and Lily Safra Center for Brain Sciences and Department of Neurobiology, Silberman Institute of Life Sciences, Hebrew University*

The mammalian auditory system is exquisitely sensitive to short silent gaps in broadband. We recently studied the cellular mechanism that underlies gap detection response in the rat auditory cortex. For gaps occurring shortly after the onset of the stimulus, the gap responses are almost exclusively onset responses to the noise burst following the gap. We demonstrated that gap responses

are potentiated through the recruitment of synaptic resources that are not activated at sound onset. For example, NMDA currents were more prominent during the onset response than during the gap response; the excitatory and the inhibitory inputs during the gap response were not as depressed as we expected from the known forward masking in auditory cortex; the excitatory-inhibitory balance varied between the onset and the gap response; and the gap response adapted differently than the onset response.

We suggest that the differential synaptic fingerprints of the onset and gap responses are due to the way PV+, SST+ and VIP+ inhibitory interneurons interact to provide inhibition and disinhibition in the cortical network. To check this hypothesis, we study gap responses in the mouse, enabling genetic access to the different subpopulations of inhibitory interneurons. We report here similar properties of the gap responses in mice and rats. By expressing the Arch-T opsin selectively in PV+ interneurons, we can suppress their activity only during sound presentations. We present preliminary results suggesting a role of PV+ interneurons in controlling the size of the gap responses

PS 32

Neuronal Network Structure in Primary Auditory Cortex Layer 2/3 During a Pure-tone Frequency Discrimination Task

Nikolas A. Francis¹; Alireza Sheikhattar²; Kevin Armengol³; Behtash Babadi⁴; Patrick O. Kanold¹
1Department of Biology, University of Maryland, College Park; 2Department of Electrical and Computer Engineering, University of Maryland, College Park; 3Neuroscience and Cognitive Science Program, University of Maryland, College Park; 4Institute for Systems Research, University of Maryland, College Park

Auditory communication critically depends on our ability to recognize behaviorally meaningful sounds. We have recently shown that pure-tone target detection involves small neuronal networks in primary auditory cortex (A1) layer 2/3 (L2/3) that are driven by the sum of sensory input, attentional gain, and behavioral choice (Francis et al. Neuron 2018). However, natural acoustic environments often require the listener to discriminate between target vs non-target sounds, and it remains unclear how the presence of non-targets affects the neural coding of task-related information in neuronal networks. Thus, we trained transgenic CBA x Thy1-GCaMP6s F1 mice to perform a go/no-go pure-tone frequency discrimination task, while we used in vivo 2-photon (2P) Ca²⁺ imaging during task performance to study how target and non-

target sounds are encoded in A1 L2/3. The mice learned to lick a waterspout if the pure-tone frequency was 7 or 9.9 Hz, and to withhold licking if the pure-tone frequency was 14 or 19.8 kHz. We performed 30 experiments in 6 mice, with a total population of >2000 neurons. For each experiment, we selected a different field of view (FOV) in A1, as determined from the rostro-caudal axis of tonotopy identified from individual wide-field imaging maps. During task performance, the mice successfully discriminated target vs. non-target tones (d' =1.6 on average across experiments). For each neuron, we separated responses during trials with behavioral hits (H), misses (M), false alarms (FA), and correct rejections (CR). Initial results indicate that neural response amplitudes depended on behavioral choice (i.e., H>FA>M>CR). This dependence emerged within the first few hundred milliseconds of the tone onset and occurred independently of reward outcome. Granger causality analysis indicates that within a 2P FOV, the effective connectivity between neurons was stronger for false alarm than for hit trials, while the size of neuronal subnetworks was smaller for false alarm than for hit trials. Together our results suggest that auditory targets and non-targets are differentially encoded within both the activity and functional connectivity of neuronal populations in A1 L2/3. Supported by NIH RO1DC9607 (POK) and NINDS U01NS090569 (POK).

PS 33

Effect of Developmental Hearing Loss on Behaviorally Gated Responses in Auditory Cortex

Justin Yao; Dan H. Sanes
New York University

Background

Developmental hearing loss (HL) is associated with perceptual deficits that may be due to both sensory and non-sensory factors. Therefore, one broad goal is to determine whether HL induces functional changes to the central nervous system that degrade sensory encoding or interfere with a cognitive mechanism, such as attention or working memory. Here, we consider two attributes of auditory cortex (ACx) processing. The first is the ACx representation of behaviorally relevant acoustic features. The second is the increased ACx sensitivity that is brought about by task engagement (e.g., Fritz et al., 2003).

Methods

We recorded telemetrically from ACx neurons in normal hearing gerbils (NH) gerbils, and those reared with conductive HL, both as they performed a Go-Nogo AM discrimination task, and while they were disengaged from the task, passively listening to the identical AM

stimuli. The Nogo stimulus consisted of AM broadband noise presented at 4 Hz, whereas Go stimuli consisted of AM broadband noise presented at rates from 4.5 to 12 Hz. ACx neural encoding of AM stimuli was assessed with changes in firing rate (FR), both during engaged and disengaged conditions. A neurometric FR d' was calculated at each Go value by normalizing the FR by the standard deviation (SD) pooled across all stimuli (z-score), and subtracting the Nogo FR from each Go stimulus evoked FR. In addition, we measured noise correlations between pairs of single units recorded during both engaged and disengaged sessions.

Results

Psychometric discrimination thresholds from animals reared with conductive HL were poorer than those obtained in NH animals. Approximately 30% of ACx units from each group displayed better neural sensitivity during task engagement. However, units from NH animals displayed greater improvement in firing rate-normalized response variability (CV) during task engagement, as compared to HL units. In addition, pairs of NH single-units with positively correlated tuning properties (r -tuning > 0) displayed reduced noise correlations during task engagement compared to corresponding disengaged sessions (r -noise engaged < r -noise disengaged). This was not observed for pairs of HL single-units.

Conclusion

These results demonstrate that developmental HL leads to non-sensory effects of task engagement that may contribute to diminished perceptual skills. We will further evaluate neural sensitivity across engaged versus disengaged conditions with population decoding techniques to assess how sensory and non-sensory inputs may lead to sensory encoding or downstream processing differences that can account for auditory perceptual performance.

PS 34

Examining the Accuracy of a Commonly-used Automated Cortical Parcellation/Labeling Process in Human Auditory Cortex

Barrett St George¹; Bryan Wong²; Frank Musiek²

¹The University of Arizona; ²University of Arizona Research Background

Evermore, researchers are using automated cortical parcellation/labeling techniques to study neuroanatomy and its associated functions. Automated techniques allow researchers to study large sample sizes without spending extra time and effort otherwise performing manual measurements, which requires extensive knowledge of inter- and intra-subject

neuromorphological variability exhibited in normal human brains. For these reasons, one can see the appeal of utilizing automated procedures, as they are efficient, accessible and unbiased.

It is unclear though, how automated parcellation/labeling procedures handle the complex macroanatomical variances of certain brain structures. Our previous work has shown that human auditory cortex exhibits pronounced structural variability. In this study we assess the accuracy of a widely-used automated cortical parcellation/labeling procedure compared to expert manual surface area measures for a principal component of auditory cortex - planum temporale (PT). We also examine how surrounding auditory cortex morphology affects the surface area of PT and more specifically, its structural hemispheric asymmetry in both measurement techniques.

Methods

High-resolution structural MRI brain scans of 50 healthy, right-handed young adults were sequentially drawn from the cross-sectional OASIS database. All MRIs were processed through an automated cortical reconstruction process, which includes skull-stripping, 3D cortical surface rendering and cortical parcellation.

Cortical surface area of PT, Heschl's gyrus (HG) and planum parietale (PP) were measured manually in all 50 brains (100 hemispheres): BrainVisa Anatomist neuroimaging software was used to define virtual clipping planes that exposed PT, HG and PP for subsequent surface area measurements. Automated surface area measures of PT were obtained from a widely-used cortical reconstruction process, using the Destrieux (2010) cortical parcellation atlas.

Results & Conclusion

A significant difference in cortical surface area and hemispheric asymmetry between manually- and automatically-defined labels of "PT" was found. Examples and discussion of four major issues in the automated process which leads to inaccurate anatomical localization of PT are provided.

These results demonstrate that researchers should exhibit caution when using automated cortical parcellation/labeling procedures to interpret human auditory cortex anatomy. It is clear that such automated methods, although time-efficient, are riddled with measurement error (in auditory cortex), especially at the single-subject level.

These results also confirm that the surface area of PT depends greatly on the morphology of neighboring perisylvian structures which principally explain its

structural asymmetry. This type of translational research affects how we draw structure-function correlations across brain image (i.e., subject) data, thusly influencing subsequent treatment protocols for individuals with neuroaudiological compromise.

PS 35

Parallel Systems for Sound Processing and Functional Connectivity among Layer 5 and 6 Auditory Corticothalamic Projection Neurons

Ross S. Williamson; Daniel B. Polley
Eaton-Peabody Laboratories, Massachusetts Eye and Ear; Dept. of Otolaryngology, Harvard Medical School

Corticofugal neurons in the deep layers of the auditory cortex (ACtx) innervate a wide range of targets both within and outside the central auditory pathway. Of the different corticofugal systems, the corticothalamic (CT) projection is the largest. Layer (L) 5 and L6 CT neurons exhibit markedly different morphological, intrinsic, and synaptic properties, suggesting that they comprise two parallel projection systems from the cortex to the thalamus. Until now, technical limitations have made it impossible to extend these observations to sensory processing in awake animals. Here, we leveraged recent advances in multi-channel electrophysiology and optogenetics to make targeted recordings from both layer 5 (L5 CT) and 6 (L6 CT) corticothalamic neurons in awake mice.

As a first step towards highlighting the differences in anatomical connectivity of L5 and L6 CT neurons, we used an intersectional viral strategy to label each cell type. While L6 CT neurons primarily targeted the ventral subdivision of the medial geniculate body (MGB), L5 CT neurons had more divergent connectivity, with collateral axons innervating the non-lemniscal regions of the MGB en route to the inferior colliculus. To characterize the sensory processing capabilities of these neurons, we developed an antidromic optogenetic “phototagging” approach to isolate individual L5 CT and L6 CT units on high-density multichannel probes in awake, head-fixed mice. L6 CT neurons exhibited shorter response latencies, narrower frequency tuning, and sparser stimulus selectivity than L5 CT neurons. Linear spectrotemporal receptive field (STRF) fits explained a higher percentage of response variance in L6 CT neurons, indicating a higher degree of linearity. The amount of additional variability that was explained when the nonlinear effects of acoustic context were modelled was larger in L5 CT neurons, suggesting a greater susceptibility to contextual nonlinearities. Analyses of functional connectivity revealed that L6 CT neurons powerfully regulate response gain across the deep layers of the ACtx via dense local connections with inhibitory subnetworks, while L5 CT neurons featured

far weaker feedforward excitation onto local columnar neurons.

Collectively, these findings suggest a dichotomy of sensory processing and functional connectivity in two corticothalamic cell-types. L6 CTs show sparse stimulus selectivity but can powerfully regulate the gain on local cortical processing, whereas L5 CTs integrate local circuit processing with dense, non-linear coding and “broadcast” signals out of the ACtx. Future work will entail recording from these projection neurons during task engagement to establish how these functional differences are adaptively used in service of goal-directed behavior.

PS 36

A Newly-Developed Timing Production Task For Guinea Pigs To Mimic Decodable Quick Actions of Human

Masataka Nishimura; Chi Wang; Yuta Shiromi; Wen-Jie Song
Kumamoto University

Background: Timing of quick actions can represent some meaning of action as we intentionally change timing of syllable in our speech or timing of note in music (Buhusi and Meck, 2005). For correct transmission of the meaning, the produced timing must be precise enough to decode the meaning by observers of action. To the best of our knowledge, no animal model mimicking such decodable quick actions of human has been established in conventional laboratory animals. Here we aimed to establish an animal model which allows decoding animal’s perception reliably from quick actions with guinea pigs.

Methods and Results: We developed an interactive training system of learning timing production for animals. The key feature of the training system is ‘adaptive reward-positive time window’;. In all tested animals, precision of timing production significantly varied in time. The adaptive window worked to encourage guinea pigs to make the timing more precisely and to prevent losing motivation to do the task by actively adjusting reward-positive time window based on the temporally local precision of timing. With the training system, we successfully trained three guinea pigs to produce 300 msec and 600 msec timings, depending on randomly presented cues, with several tens millisecond timing error. Observation rate of incorrect timing of action was < 5% when the data analysis focused on the better precision trials which were systematically identified with an algorithm established in this study ($p < 0.001$). Furthermore, a mathematical model of from-cue-to-

timing system demonstrated that observation probability of incorrect representation of cue and/or action timing at any stage of processing in the brain should be < 5% in the better precision trials.

Summary: In conclusion, we successfully established the animal model of decodable quick actions to study the brain mechanism of hundreds millisecond timing production with > 95% reliability of representation.

PS 37

Equivolumetric Normal Coordinate Systems for Structural Analysis of Feline Auditory Cortical Areas

Kwame Kutten¹; Peter Hubka²; Daniel Tward¹; Laurent Younes¹; Andrej Kral³; J. Tilak Ratnanather¹

¹*Johns Hopkins University*; ²*Institute of Audioneurotechnology & Department of Experimental Otolology, Hannover Medical School*; ³*Institute of AudioNeuroTechnology & Dept. of Experimental Otolology, ENT Clinics, Hannover Medical University*

Background

The congenitally deaf cat is a commonly used model for studying the effect of long-term hearing loss on the brain. Its primary and secondary auditory cortices have distinct functions and connectivity. It was shown that cortical activation pattern is compromised by the absence of auditory stimuli during development (Kral et al. 2002, Tillein et al. 2010) which also affected cortical layer thickness (Berger et al. 2017). Further it has been hypothesized that cortical layer thickness varies due to equivolumetric deformation (Bok 1929). Thus two pipelines for generating equivolumetric coordinate systems were developed to accurately represent the general pattern of auditory cortical lamination.

Methods

In the magnetic resonance imaging pipeline, image volumes were acquired for a deaf and a hearing cat. The right auditory cortical region was manually segmented in each cat. In the histological pipeline, brains of a different deaf cat and hearing cat were axially cut through the right auditory cortex at 1.0 mm intervals. After SMI-32 staining which visualize mainly pyramidal cells, six slices were imaged using light microscopy. These slices were reconstructed into a volume through rigid landmark alignment with a MRI atlas (Stolzberg et al. 2017). Manual segmentations of the right auditory cortex were then upsampled in the axial direction through diffeomorphic registration of adjacent slices (Beg et al. 2005). In both pipelines closed surfaces of the segmentation masks were created using restricted Delaunay triangulation. These surfaces were then cut

into inner and outer surfaces at the white and pial matter boundaries respectively. The inner surfaces were then diffeomorphically registered to their corresponding outer surfaces (Ratnanather et al. 2018). Intermediate surfaces generated were then reparametrized along the normal curves to create equivolumetric surfaces.

Results

By overlaying the surfaces on SMI-32 histology, equivolumetric surfaces closely followed the stained layers. This was also confirmed in depth verses intensity histograms where the darkly stained pyramidal layers created a distinct dip in intensity at a relative equivolumetric depth of 0.35. Layer IV, the site of major thalamocortical synapses, was found between these layers.

Conclusions

Equivolumetric normal coordinate systems can accurately describe the depths of cortical layers in auditory areas. Future work will involve quantitative comparison of equivolumetric surfaces with a focus on cortical laminar stratification and applications measuring cortical changes due to hearing loss.

Funding

This work was supported by National Institutes of Health (NIH) grant R01-DC016784 and Germany Federal Ministry of Education and Research (BMBF) grant 01GQ1703

PS 38

Multiscale Calcium Imaging of Auditory Cortex in Awake Marmoset Monkeys

Xindong Song; Yueqi Guo; Xiaoqin Wang
Johns Hopkins University

The common marmoset (*Callithrix jacchus*), a highly vocal New World monkey species, has emerged in recent years as a promising non-human primate model for neuroscience research. Because the marmoset brain is lissencephalic (smooth), nearly all cortical areas are accessible directly under the skull with optical imaging methods. Two-photon calcium imaging with genetically encoded calcium indicators (GECIs) has been previously implemented in marmoset somatosensory cortex. Two-photon imaging in the auditory cortex is technically challenging since a mechanically vibrating laser scanner can generate sounds that are audible to the animal and thus interferes with the experimental design. In the current study, we developed a flexible, agile, yet silent two-photon microscope based on an acousto-optical deflector (AOD) scanner. An optical window with a quarter-inch diameter was implanted over the auditory cortex of awake marmosets. A clear tonotopic structure

can be observed through intrinsic signal imaging at both green and blue wavelengths. Multiple virus injections carrying GCaMP were made through the silicone-based optical window. A dual-virus strategy was used to separate controls over expression specificity and expression level. A clear macroscopic wide-field fluorescence response was observed starting 10 days after virus injections, at sound levels as low as 10 dB lower than hearing thresholds. The tonal response recorded from wide-field fluorescence imaging was consistent with intrinsic signal imaging results and was also limited mainly within the primary auditory cortex. By using complex sound stimuli, such as music or marmoset vocalization recordings, strong and widespread cortical responses ($\Delta F/F > 10\%$) can be evoked in both primary and secondary cortical areas. The silicone-based window can be replaced by a glass coverslip-based window. And a customized silent two-photon microscope was used to measure responses of individual neurons at a microscopic scale. The general response patterns within each two-photon field-of-view were consistent with wide-field imaging results. However, individual neurons' responses can be heterogeneous even for close-by neurons. The multiscale calcium imaging approach reported here thus provides a new experimental paradigm for functional mapping of the marmoset auditory cortex in the awake condition in a high throughput way over conventionally electrophysiology methods.

PS 39

Responses to Cathodic-leading and Anodic-leading Biphasic Stimuli in Microstimulation of the Auditory Cortex

Mathias B. Voigt¹; Andrej Kral²

¹*Institute of AudioNeuroTechnology, Department of Experimental Otolaryngology, Hannover Medical School;*

²*Institute of AudioNeuroTechnology & Dept. of Experimental Otolaryngology, ENT Clinics, Hannover Medical University*

Electrical stimulation paradigms for neuroprosthetic applications frequently use symmetric biphasic current pulses. While the first phase of the stimulus elicits the desired neuronal activity, the second phase of opposite polarity is thought to remove the charge deposited during the stimulating phase so as to avoid tissue damage due to charge accumulation. According to simulations, monophasic cathodic stimuli preferentially activate fibrous cell compartments (axons, dendrites) while anodic stimuli preferentially activate cell somata in isolated neurons. Previously, we demonstrated the possibility to combine extracellular recordings and intracortical microstimulation (ICMS) to characterize the response of the auditory cortical network to different

types of acoustic and electric stimuli in vivo (Voigt et al., 2017, Brain Stim; Voigt et al., 2018, J Neurosci). Here we investigated the influence of the leading-phase polarity (cathodic- vs. anodic-leading) in single-pulse electrical microstimulation within a dense network of neurons in vivo - inside the auditory cortex.

Concurrent ICMS and extracellular recording was performed in vivo, in the auditory cortex of adult guinea pigs ($n = 15$) under ketamine/xylazine anesthesia. Recordings were performed using multi-electrode arrays inserted perpendicularly to the cortical surface in the primary auditory cortex (field A1), penetrating all cortical layers. We analyzed local field potentials, current source density (CSD) profiles and multi-unit activity in response to acoustic clicks (50 μ s condensation clicks, 15-95 dB) or single ICMS pulses (200 μ s/phase, biphasic, charge-balanced, 0.1-45.0 μ A) with either cathodic or anodic leading-phase.

Cathodic-leading ICMS resulted in significantly higher CSD sink amplitudes than anodic-leading ICMS (cathodic: 2.6 mV/mm², anodic: 1.3 mV/mm², $p = 0.002$). This was particularly pronounced in deep cortical layers, where anodic-leading stimulation, in contrast to cathodic-leading ICMS, failed to evoke local activity. In accordance with electrical stimulation in subcortical nuclei of the auditory pathway, the dynamic range of the cortical response was significantly reduced during ICMS compared to acoustic stimulation. Multi-unit activity provided evidence for a lower response latency in cathodic-leading stimulation, supporting simulations showing a preferential fiber activation with cathodic stimuli.

Together, the results demonstrate a robust difference in effectivity of cathodic and anodic-leading polarities with the conclusion that cathodic-leading biphasic stimuli are more effective in ICMS applications.

Supported by Deutsche Forschungsgemeinschaft (Exc 1077).

PS 40

Mapping Areal Organization of Mouse Auditory Cortex by Data-driven Decomposition of Responses to Naturalistic Sounds

Hiroki Terashima¹; Hiroaki Tsukano²; Shigeto Furukawa¹

¹*NTT Communication Science Laboratories;* ²*Niigata University*

Revealing the functional organization of the auditory cortex is one of the main goals in auditory neuroscience. Recent advances in imaging techniques have raised controversy about the areal organization of the mouse

auditory cortex. There is still no agreement about how many areas the auditory cortex has, which of them are tonotopic, and how tonotopy is organized in AAF and A1. The controversy mainly originated from two biases in previous hypothesis-driven studies: a bias in selecting limited types of synthetic stimuli and a bias in analysis methods. To address these issues, we drew a new map using naturalistic complex sounds and a data-driven method.

We recorded cortical responses to a set of naturalistic complex sounds. The Committee for Animal Care at Niigata University approved the experimental protocols used in this study. All data were recorded in male offspring obtained by crossing *Emx1-Cre* driver mice and *GCaMP8-flox* mice. Mice were anesthetized with urethane and the skull was exposed and kept transparent by paraffin. We recorded *GCaMP* signals in the right auditory cortex with a cooled CCD camera. We developed a set of naturalistic complex sounds for mice by pitch-shifting 165 natural sounds for humans (Norman-Haignere et al., 2015) by four octaves to fit to the hearing range of mice.

We decomposed the obtained responses using a data-driven method proposed in a human fMRI study (Norman-Haignere et al., 2015). Applying the matrix-decomposition technique, we extracted five major spatial components. We characterized the obtained components by comparing them with responses to pure tones and regression by acoustic features. We found areas that corresponded to low and high frequency regions of what were called AAF, A1, A2, and DM in previous studies. Non-tonotopic areas corresponded to what were called DA and DP. Moreover, we found an unidentified area on the rostradorsal side of the other areas.

To conclude, we drew a new areal map of the mouse auditory cortex using naturalistic sounds and a data-driven method. We reconfirmed some areas discussed in previous studies and found an unidentified area. The results indicate how effective the data-driven method is in depicting the organization of the auditory cortex and that the mouse auditory cortex has more complex organization than previously thought.

Auditory Nerve I

PS 41

Optimizing Auditory Brainstem Response Acquisition using Interleaved Frequencies

Brad N. Buran; Sean Elkins; J. Beth Kempton; Edward V. Porsov; John V. Brigande; Stephen V. David
Oregon Health & Science University

Auditory brainstem responses (ABRs) are an essential assay used to characterize a wide range of auditory

disorders. Hundreds of averages are required to obtain a measurable waveform and adaptation in the auditory nerve limits the rate at which responses to multiple frequencies and levels can be acquired. Previous studies developed a rapid acquisition paradigm in which a train of multiple frequencies and levels were interleaved¹. With careful ordering of the frequencies and levels in the stimulus train, adaptation in the auditory nerve can be minimized while increasing the rate at which tone bursts are presented. Widespread adoption of this paradigm has been hindered by the lack of available software. Here, we leverage an open-source data acquisition software framework, *psiexperiment*², to develop an ABR application that runs on the same National Instruments PXI Platform used with the Eaton-Peabody Laboratories Cochlear Function Test Suite software³. Consistent with prior studies, we demonstrate that careful design of a stimulus train reduces ABR acquisition time by more than half, with minimal effect on thresholds, wave amplitudes, and latencies in both the gerbil (1 to 8 kHz) and mouse (5.6 to 45.2 kHz).

In addition to optimizing the acquisition of ABRs, *psiexperiment* offers additional features including online filtering and artifact rejection and saving the full electroencephalogram signal to disk for offline analysis. Customization of the offline analysis is achieved by varying parameters of artifact rejection, band-pass filter settings, and segmentation of the trial epoch (e.g., from 1 msec before to 10 msec after tone burst onset). Critically, the modular design of *psiexperiment* allows its adaptation to other data acquisition systems (e.g., TDT's System 3).

1. Mitchell, Kempton, Creedon and Trune. Rapid acquisition of auditory brainstem responses with multiple frequency and intensity tone-bursts. *Hear Res* 99, 38-46 (1996).
2. Buran and David. ψ - *psiexperiment*. doi:10.5281/zenodo.1405144 (2018). <https://github.com/bburan/psiexperiment>.
3. Hancock, Stefanov-Wagner, Ravicz and Liberman. The Eaton-Peabody Laboratories Cochlear Function Test Suite. ARO Midwinter Meeting (2015).

PS 42

Phase Locking of Auditory-Nerve Fibers Reveals Stereotyped Distortions and a Dynamic Rather Than Static Peripheral Nonlinearity

Adam J. Peterson; Peter Heil
Leibniz Institute for Neurobiology

The phase locking of auditory-nerve-fiber (ANF) responses to the fine structure of acoustic stimuli is a hallmark of the auditory system's temporal precision and is important for many aspects of hearing. Period

histograms from phase-locked ANF responses to tones often exhibit spike-rate asymmetry in which increases above the spontaneous rate are greater than decreases below the spontaneous rate. They also often exhibit temporal asymmetry in which the leading edge of the peak is steeper than the trailing edge. Period histograms otherwise retain an approximately sinusoidal shape as stimulus level increases, even beyond the level at which the mean spike rate saturates. This is intriguing because apical cochlear mechanical vibrations show little compression and mechano-electrical transduction in the receptor cells is thought to obey a static sigmoidal nonlinearity, which should produce peak clipping at moderate and high stimulus levels. Here we analyze and model period histograms computed from the extracellularly recorded spike trains of 83 ANFs in five barbiturate-anesthetized adult cats in response to tones with frequencies below 5 kHz. We show that refractoriness has minimal effects on the shapes of period histograms. We demonstrate that the upper saturating portion of the sigmoidal nonlinearity is never reached and that the sigmoidal transfer function in the model can be replaced by an exponential transfer function, accounting for the spike-rate asymmetry of period histograms. We further demonstrate that stereotyped harmonic distortions underlie the temporal asymmetry of period histograms. Finally, we show that the lack of peak clipping is not due to spike-rate adaptation, but to the nonlinearity being dynamic, rather than static. This peripheral gain control saturates the mean spike rate while enabling the full range of instantaneous stimulus pressures to be coded by instantaneous spike rate.

Supported by grants of the Deutsche Forschungsgemeinschaft (Priority Program 1608 "Ultrafast and temporally precise information processing: Normal and dysfunctional hearing", He1721/11-1 and He1721/11-2 to PH).

PS 43

Photobiomodulation delays secondary degeneration of spiral ganglion neuron and demyelination after topical application of kanamycin

Jae-Hun Lee¹; Nathaniel Carpena²; So-Young Chang¹; Ji Eun Choi²; Min Young Lee²; Phil-Sang Chung²; Jae Yun Jung²

¹*Beckman Laser Institute Korea, College of Medicine, Dankook University;* ²*Department of Otorhinolaryngology-Head & Neck Surgery, College of Medicine, Dankook University*

Backgrounds and Objective:

Hair cells cannot be regenerated itself once damaged and causes an additional damage in auditory afferent

pathway which is called secondary degeneration. Cochlear implant has been used as the preferable way for the rehabilitation and the performance of cochlear implant highly relies on the survival of spiral ganglion neurons (SGN). Thus, maintaining the status of spiral ganglion neuron is important. Photobiomodulation (PBM) is a type of light therapy using broadband light, or LED. The neuroprotective and regenerative effect of PBM has been reported in various tissues and organs. These effects were also reported in spiral ganglion neurons and inner ear hair cells after various insults with ototoxic drug treatment or noise exposure. In the present study, we investigated the effect of PBM in the auditory nerves and SGN after hair cell loss induced by aminoglycoside.

Materials and Methods:

Twenty-eight Mongolian gerbils were divided into Sham PBM and PBM groups. Secondary degeneration was induced using kanamycin application at the RWM with gelfoam. For PBM, 808 nm wavelength diode laser was irradiated twice for five continuous days at two weeks after surgery. Hearing threshold and histological analysis were performed at two and three months after surgery.

Results:

Hearing threshold in both groups severely increased a week after drug administration. SGN in Sham PBM group showed damaged status whereas it was intact in PBM group. In the quantitative analysis, decrease of SGN number was significant in the basal and middle parts of the cochlea at two and three months after surgery. With PBM reduction of SGN was significantly less compared to sham PBM group. Immunostaining results showed a significant difference in myelination status of the auditory nerve and spiral ganglion neurons between these groups. Increased myelination of SGN was observed in PBM group compared to sham PBM group.

Conclusion:

These results indicate that PBM could maintain myelination and delay secondary degeneration of SGN after hair cell damage. This protective effect could improve the efficacy of cochlear implants.

Acknowledgements:

study was supported by the Ministry of Science, Information and Communications technology (ICT) and Future Planning grant funded by the Korean Government (NRF-2017R1D1A1B03033219), and supported by Leading Foreign Research Institute Recruitment Program through the National Research Foundation of Korea (NRF) funded by the Ministry of Science and ICT (MSIT) (NRF-2018K1A4A3A02060572).

PS 44

Differential Expression of Calcium-Buffering Protein Calretinin in Cochlear Afferent Fibers

Kushal Sharma¹; Young-Woo Seo²; Eunyong Yi¹

¹Mokpo National University; ²Korea Basic Science Institute Gwangju Center

The synaptic contacts of cochlear afferent fibers (CAFs) with inner hair cells (IHCs) are spatially segregated according to their firing properties. CAFs also exhibit spatially segregated vulnerabilities to noise. The CAFs contacting the modiolar side of IHCs tend to be more vulnerable. Noise vulnerability is thought to be due to the absence of neuroprotective mechanisms in the modiolar side contacting CAFs. In this study, we investigated whether the expression of neuroprotective Ca²⁺-buffering proteins is spatially segregated in CAFs. The expression patterns of calretinin, parvalbumin, and calbindin were examined in rat CAFs using immunolabeling. Calretinin-rich fibers, which made up ~50% of the neurofilament (NF)-positive fibers, took the pillar side course and contacted all IHC sides. NF-positive and calretinin-poor fibers took the modiolar side pathway and contacted the modiolar side of IHCs. Both fiber categories juxtaposed the C-terminal binding protein 2 (CtBP2) puncta and were contacted by synaptophysin puncta. These results indicated that the calretinin-poor fibers, like the calretinin-rich ones, were afferent fibers and probably formed functional efferent synapses. However, the other Ca²⁺-buffering proteins did not exhibit CAF subgroup specificity. Most CAFs near IHCs were parvalbumin-positive. Only the pillar-side half of parvalbumin-positive fibers coexpressed calretinin. Calbindin was not detected in any nerve fibers near IHCs. Taken together, of the Ca²⁺-buffering proteins examined, only calretinin exhibited spatial segregation at IHC-CAF synapses. The absence of calretinin in modiolar-side CAFs might be related to the noise vulnerability of the fibers.

PS 45

The Influence of the Spatial Summation on Cochleoneural Mass-potentials

Eric Verschooten; Philip X. Joris
University of Leuven

The compound action potential (CAP) and neurophonic (NP) recorded near the round window (RW) in human and macaque are smaller than in cat. The exact location and nature of the generators of these mass-potentials is still unclear. We examine the hypothesis that they are smaller in primates due to the longer length of the auditory nerve: generators are distributed along the nerve and their summation has a spatial filtering effect due to the relative short wavelength of the action potential. In this study we examine whether mass-potentials are affected

by spatial convolution.

RW-potentials and action potentials of single nerve fibers were recorded in cat and chinchilla. From these signals, RW-unit contributions were obtained by spike-triggered averaging (Kiang et al., 1976; Prijs, 1986). Additionally, CAPs to pip-tones at 6 kHz were obtained and compared with responses in human and macaque. A simple model was used to simulate the impact of spatial integration on the unit contribution and CAP. The model simulated the unit contribution of a traveling action potential by calculating the difference of the potentials summed across two adjoining stretches of the fiber, with increasing length of these stretches.

Comparison between the unit contribution and its action potential revealed that the former is strikingly similar in shape to the first derivative of the latter, but with a small (submillisecond) delay. This suggests that the unit contribution reflects a potential difference, rather than a spatial summation. The small size of the delay indicates that the origin of the unit contribution is close to the single-fiber recording site, likely near the internal meatus as proposed by Brown and Patuzzi (2010). This observation is supported by simultaneous recordings of the neurophonic at the RW and auditory nerve, showing a similar delay. Simulations with imposed spatial integration showed that, if present, it would affect the shape of the unit contribution and CAP for distances well within the anatomy of the cat. The lack of signs of spatial integration in cat and the similarity between CAP shapes of cat, monkey, and human indicates that the length of the AN has no influence on mass-potentials in human. We conclude that the unit contribution reflects a potential difference originating at a specific point near the internal meatus, rather than spatially distributed generators. Spatial integration is not a significant factor in cochlear mass potentials of cat and chinchilla and likely not in human and macaque either. Supported by FWO (G0B2917N), BOF (OT-14-118).

PS 46

The Effect of Masking Noise on the Envelope Following Responses (EFR)

Gerard Encina-Llamas¹; James M. Harte²; Bastian Epp¹

¹Hearing Systems, Technical University of Denmark;

²Interacoustics Research Unit

Background

Envelope following responses (EFR) have been proposed as a promising tool to investigate cochlear synaptopathy (i.e., the loss of auditory nerve (AN) fiber synapses without a permanent threshold elevation) both in mice and humans. In mice, it was shown that cochlear synaptopathy leads to a reduction of EFR magnitudes at supra-threshold stimulation levels. Corresponding

studies in human listeners are, however, inconclusive. In a previous study we used a computational model of the AN to investigate the effect of cochlear synaptopathy on EFRs. We concluded that the EFR evoked by a sinusoidally amplitude modulated (SAM) tone in quiet was dominated by off-frequency contributions (i.e., neuronal activity remote from the characteristic place of the stimulus carrier) and by high-spontaneous rate (SR) AN fibers. In this study, the effect of commonly used masking noises was systematically analyzed using the same computational model of the AN as in the previous study. The simulations were compared with EFR magnitude-level functions recorded in human listeners.

Methods

The humanized version of the AN model by Zilany et al. (2009, 2014) was used to simulate the AN activity for characteristic frequencies (CF) between 0.2 to 20 kHz. AN simulations were run for stimulation levels ranging from 5 to 100 dB SPL, for 5 modulation depths (100%, 85%, 50%, 25% and 12%), 5 SNR conditions (20, 10, 0, -10, -15 dB and in quiet), and for broadband and notched noise maskers. EFR magnitude-level functions were computed for each condition by summing the simulated AN activity across CFs.

Results

At positive SNRs, the presence of masking noise partially reduced the contribution of off-frequency AN fibers. At those SNRs and towards medium-to-high stimulus levels, the AN neurons contributing most to the total EFR were, however, still located off-frequency. At negative SNRs, the on-frequency AN neurons showed stronger encoding of the envelope than other CFs.

Conclusions

The simulations suggested that the use of masking noise to limit the dominance of off-frequency contribution onto the EFRs was effective at negative SNRs. At positive SNRs, the off-frequency contributions still dominated the response at medium-to-high stimulus levels but to a lesser extent than in quiet. Nevertheless, the use of such high masking noise levels might not be suitable for experiments.

Funding

This work was supported by the Oticon Centre of Excellence for Hearing and Speech Sciences (CHeSS) at the Technical University of Denmark.

PS 47

Estimating the Frequency Limit of Auditory Nerve Phase Locking from Round-Window Recordings in Birds

M. Queralt Caus-Capdevila¹; Lena Koepcke²; Rainer Beutelmann³; Nicolás Palanca-Castán⁴; Christine Köppl⁵
¹Cluster of Excellence "Hearing4all"; ²Department of Neuroscience; ³Cluster of Excellence "Hearing4all"; ⁴Centro Interdisciplinario de Neurociencia de Valparaíso (CINV); ⁵Department of Neuroscience, School of Medicine and Health Sciences, Carl von Ossietzky University Oldenburg

Background

Based on the observation that neural responses – compound action potential (CAP) and neurophonic (NP) – adapt when preceded by a masker, whereas hair-cell responses – cochlear microphonics (CM) – do not, Verschooten and Joris (2014, JARO 15:767-787) extracted neural phase-locking in mass potential recordings from the round window (RW). By presenting a stimulus of alternating phase and subtracting the responses from each other, the CAP is eliminated and the periodic CM and NP extracted. The NP is then singled out by subtracting the masked response from the probe-only response. The amplitude of the NP component is a correlate of mean single-unit vector strength in the cat (Verschooten et al., 2015, J Neurosci 35(5):2255-2268). The objective of this study was to determine if this method could be applied in birds. Our test cases were the barn owl, a known phase-locking specialist (Köppl, 1997, J Neurosci 17(9):3312-3321) and the chicken.

Methods

Preliminary experiments were conducted in four adult owls and five P21 chickens. Animals were anesthetized with ketamine/xylazine, and a silver-ball electrode was placed at the RW membrane. Pure tone probe stimuli at different frequencies (owl: 0.5 - 8 kHz; chicken: 0.5 - 4 kHz; 100 ms duration) with alternating phases were presented at levels between 0 and 40 dB above threshold. In masking trials, the probe was preceded by a 100 ms broadband noise with the level set between -10 and +20 dB relative to the probe. Data were analyzed with custom software following Verschooten and Joris (2014).

Results

In both chicken and owl, an NP component could be detected and its amplitude generally increased with probe level. The signal-to-noise ratio was considerably higher in the owl, such that an NP was detectable with fewer response averages. To sufficiently mask the NP, the masker level needed to be at least equal to the probe level. In chickens, an NP was observed at frequencies

up to 2 kHz. In owls, it persisted up to 8 kHz, with a consistent decrease in amplitude above 4 kHz.

Conclusions

Detection of a phase-locked neural (NP) component in RW recordings was possible in both owls and chickens. NP amplitude was considerably higher in the owl, consistent with its larger number of auditory-nerve fibers. Furthermore, consistent with the higher frequency limit of phase-locking of single auditory nerve fibers, the NP was observed at much higher frequencies in the owl than in the chicken.

Supported by the Deutsche Forschungsgemeinschaft (DFG), PP 1608

PS 48

Modeling the Concurrent Vowel Scores for a Shorter Duration

Harshavardhan Settibhaktini; Ananthakrishna Chintanpalli

Department of Electrical and Electronics Engineering, Birla Institute of Technology and Science

Background: A fundamental frequency (F0) difference is an important cue for normal-hearing listeners to segregate multiple speeches presented at the same time. Concurrent vowel identification is studied to understand the role of this F0 difference in identifying two simultaneously presented vowels. However, this ability could be reduced when stimuli, is presented for a shorter duration. It was found that normal-hearing listeners took advantage of F0 difference (quantified by F0 benefit) for identifying concurrent vowels that had 200-ms duration, when compared to 51.2-ms. For 200-ms, the identification score increased with increasing F0 difference and then asymptoted at higher F0 differences. In case of 51.2-ms, the scores were similar, indicating F0 benefit was near to zero. Thus, it is hypothesized that the absence of vowel segregation using F0 difference might contribute to zero-F0 benefit for shorter duration stimulus. The study here attempts to predict concurrent vowel scores across F0 difference for longer and shorter durations, using the population responses of auditory-nerve model and F0-segregation algorithm.

Methods: The vowel pairs were generated using five different vowels. Each vowel was presented at 65 dB SPL and either had 200 or 51.2-ms duration. The vowel pairs were created with six F0-difference conditions (0, 1.5, 3, 6, 12 and 26 Hz). To quantify the duration effects, a physiologically-based computational model was employed by cascading the auditory-nerve model with Meddis and Hewitt's F0-segregation algorithm. A

similar modeling-framework had been done primarily on vowel pairs that had longer durations, where the scores were qualitatively similar to normal-hearing listeners. The present work applies this model to study if it can predict concurrent vowel scores across F0 difference for shorter duration.

Results: Consistent with other studies, the computational model was able to predict the concurrent-vowel data as a function of F0 difference for 200-ms, qualitatively, using the parameters of F0-segregation algorithm. It predicted similar scores across F0 difference and negligible F0 benefit for 51.2-ms, by altering only one parameter, that contributed to absence of F0-based vowel segregation. For longer-duration, our preliminary model-predictions for listeners with sensorineural hearing loss suggested that the reduced concurrent vowel scores across F0 difference could be attributed to reduced functionalities of hair-cells and loss of number of high-spontaneous fibers from its population responses.

Conclusions: The computational modeling results suggest that absence of F0-based vowel segregation might have contributed to similar identification scores across F0 difference for shorter duration.

Work supported by OPERA and RI Grants.

PS 49

Nav1.9 Knockout Causes Auditory Neuropathy by Reduction of Auditory Signals Transduction in Primary Afferent Neurons

Mian Zu¹; Weiwei Guo²; Ning Yu³; Guowei Qi²; Shiming Yang²

¹Chinese PLA General Hospital; ²PLA General Hospital;

³General hospital of Chinese PLA

Background The exact molecular pathogenesis about auditory neuropathy (AN) is still unclear, owing to the lack of suitable animal model. The SCN11A gene encoded Nav1.9 resistant to TTX is well known by its highly expression in nociceptive neurons of dorsal root ganglia, which is a main effector of peripheral inflammation related pain. However, the expression pattern or function of Nav1.9 in peripheral auditory afferent neurons has never been determined. **Methods** In our present study, the expression of Nav1.9 in the murine cochlea was determined by qPCR and immunofluorescence staining. Furthermore, the morphological features of hair cells, ribbon synapse or spiral ganglion neurons (SGNs) of mice model with CRISPR-mediated knockout (KO) of Nav1.9 were observed by scanning electron microscope or laser scanning confocal microscope. Finally, auditory brainstem response (ABR) and the electrocochleograms

(ECochGs) of Nav1.9 KO mice were recorded, to explore the possible mechanism of action for Nav1.9 in auditory afferent neural circuit. **Results** Nav1.9 was found to be expressed in the primary afferent endings beneath IHCs and the SGNs body, as well as dorsal cochlear nucleus. The relative expression of Nav1.9 mRNA in modiolus remained unchanged from P0 to P60, except for the decline at P21. Compared with wildtype (WT) littermates, the number of Ctbp2 positive ribbon synapses in cochlea of Nav1.9 KO mice significantly decreased. Besides, the counting of SGNs in the basal turn of Nav1.9 KO mice was lower than that in WT, while no significant difference was found in the apical or middle turn. As for hair cells, the hair cell somas and stereociliary bundles were found to be intact. ABR threshold shifts at 12 and 16 kHz for tone bursts were found in Nav1.9 KO mice, versus heterozygote and WT. Furthermore, ABR threshold shifts at 16 kHz increased progressively ranging from P21 to P60, with decreased amplitudes for a series of vertex positive waves from Wave I to V. Nav1.9 KO induced a significant increase in CAP thresholds, a significant decrease in CAP N1 amplitudes, and no significant change in latencies. Last but not the least, the Nav1.9 KO mice and WT littermates shared similar recordings of microphonic potentials (CM). **Conclusions** In all, our study showed a novel murine model of AN caused by Nav1.9 KO with synaptic or post-synaptic dysfunction due to impairment of ribbon synapse or SGNs, resulting in failure transduction for the synchronous activation of the auditory nerve fibers.

PS 50

Ultrafast Optogenetic Stimulation of the Auditory Pathway by Targeting-optimized Chronos

Antoine Huet¹; **Daniel Keppeler**²; **David Lopez de la Morena**²; **Burak Bali**²; **Vladan Rankovic**³; **Tobias Moser**⁴
¹*Institute for Auditory Neuroscience and InnerEarLab;*
²*Institute for Auditory Neuroscience and InnerEarLab; Göttingen Graduate School for Neurosciences and Molecular Biosciences;*
³*Institute for Auditory Neuroscience and InnerEarLab; Collaborative Research Center 889 (DFG);*
⁴*Institute for Auditory Neuroscience, University Medical Center Göttingen; Synaptic Nanophysiology Group, Max Planck Institute for Biophysical Chemistry; Collaborative Research Center 889, University of Göttingen*

Optogenetic stimulation of spiral ganglion neurons (SGNs) in the ear provides a future alternative to electrical stimulation used in cochlear implants. As light can be conveniently confined in space, optical stimulation promises to increase the number of independent stimulation channels. However, most channelrhodopsins do not support the high temporal

fidelity pertinent to auditory coding because they require milliseconds to close after light-off. The opsin Chronos could overcome this main limitation by ultrafast closing kinetics (Klapoetke et al., 2014). Using a viral approach for in vivo transduction of SGNs, we successfully expressed Chronos in mice and gerbils. In order to enhance Chronos expression at the plasma membrane, we improved its trafficking to the plasma membrane (Chronos-ES/TS). Following efficient transduction of SGNs using early postnatal injection of the adeno-associated virus AAV-PHP.B into rodent cochlea, fiber-based optical stimulation elicited optical auditory brainstem responses (oABR) with minimal latencies of 1 ms, thresholds of 5 μ J and 100 μ s per pulse, and sizable amplitudes even at 1000 Hz of stimulation. Recordings from single SGNs demonstrated high temporal fidelity of light-evoked spiking. To conclude, efficient virus-mediated expression of targeting-optimized Chronos-ES/TS achieves ultrafast optogenetic control of neurons.

PS 51

Regulation of Quaking RNA Binding Proteins of Mouse Auditory Nerve Myelination and Hearing Onset

Clarisse H. Panganiban¹; **Carolyn M. McClaskey**¹; **Kelly C. Harris**²; **Hainan Lang**¹

¹*Medical University of South Carolina;* ²*Medical University of South Carolina-Dept of Otolaryngology-Head & Neck Surgery*

Myelination and nodes of Ranvier are necessary for rapid, saltatory conduction of electrical impulses along the auditory nerve (AN). Dysmyelination and improper nodal formation can lead to decreased conduction velocities and neural dyssynchrony. Work in our lab has identified the Quaking (QKI) gene as essential for maintenance of myelination of type I spiral ganglion neurons. We have shown that knockout of QKI isoforms, which encode the QKI RNA binding proteins (RBPs) QKI-5, -6, and -7, in young-adult mice result in severe dysmyelination and loss of hearing function. In developing mouse AN, peak activity of myelin formation occurs around postnatal day (P) 7, with complete myelination by P10-12, concurrent with hearing onset. Although the importance of QKI RBPs in myelin maintenance is unquestionable in young-adult AN, their role during AN postnatal development is less clear. This study aims to elucidate the effects of induced depletion of QKI isoforms around the critical period of myelination on formation of myelin, nodal assembly, and auditory functional development/maturation.

To analyze the effects of QKI depletion in auditory glial cells, QKIFL/FL;PLPCreERT (QKI-KO) pups were used with QKIFL/FL;- littermate controls. The

tamoxifen-induced depletion of QKI was generated via intraperitoneal injections for three consecutive days starting at P5 or P7. Physiological tests assessing AN and myelin function were conducted using a comprehensive multi-metric approach developed in our lab to characterize differences in conduction velocity and neural dyssynchrony. Cochleas were collected for quantitative immunohistochemical and ultrastructural analyses.

Depletion of QKI at P5 and P7 showed the complete disappearance of Pan-QKI protein reactivity in auditory glia at P14 in QKI-KO compared to controls. Depletion at P5 shows AN fiber abnormalities and improperly formed paranodes at P14 in QKI-KO. Surprisingly, for depletion beginning at P7, there was no significant dysmyelination seen around AN fibers of P14 in QKI-KO. Node of Ranvier formation, marked by nodal molecule NrCAM and paranodal Cntn1, were quite normal. Wave I thresholds at P14 were not significantly different between QKI-KO and controls after depletion at P7.

Our study shows that the effects of QKI depletion prior to peak myelination are greater than depletion at P7. QKI activity may be more important in the pre-myelination stages. These preliminary studies suggest a precise temporal regulation of QKI RBPs in AN myelination and nodal formation. Comprehensive analyses of wave I suprathreshold responses and AN firing synchrony are in progress.

PS 52

Auditory Nerve Responses to Electric Pulse Trains in Guinea Pigs and Humans

Dyan Ramekers; Ruben H.M. van Eijl; Henk A. Vink; Huib Versnel

University Medical Center Utrecht

The auditory nerve progressively degenerates following severe cochlear hair cell loss. Variability in auditory nerve degeneration is thought to be partly responsible for variability in speech perception among cochlear implant (CI) users (Kamakura and Nadol, 2016, *Hear Res* 339:132-141). An objective measure of auditory nerve degeneration could therefore give an indication of maximum achievable speech perception performance. In animal models advanced stimulation paradigms including pulse trains have yielded promising results in that derived eCAP measures correlate well with survival of the auditory nerve (Ramekers et al., 2015, *Hear Res* 321:12-24). In the current study we assess the potential clinical value of eCAPs in response to pulse trains by testing the same recording paradigms in human CI users and in deafened guinea pigs.

Twenty-three guinea pigs, either normal hearing or

deafened by systemic administration of kanamycin and furosemide, were implanted with a MED-EL PULSAR CI in the basal cochlear turn. A 100-ms pulse train with varying inter-pulse interval (IPI; 0.4 – 16 ms) was presented; eCAPs were recorded to each of the initial ten pulses and to each of the final ten pulses. The extent of auditory nerve degeneration was assessed by histological quantification of the spiral ganglion cells (SGCs). Using pulse trains with similar parameter settings as in the guinea pigs, we recorded eCAPs in 8 human subjects (14 – 45 years of deafness) with a MED-EL CI at both basal and apical electrodes, peroperatively and/or postoperatively. Speech perception was tested with consonant-vowel-consonant words in silence and noise and digit triplets in noise.

In guinea pigs the eCAP amplitudes modulated with successive pulses for IPIs between 0.5 and 1 ms, i.e., amplitudes were larger to odd than to even pulses. These modulations were negatively correlated to SGC survival. In human subjects we found similarly large eCAP amplitude modulations in the IPI range of 0.5-1 ms. However, some individuals did not tolerate pulse train stimulation at the current level required to evoke eCAPs, in particular for the final pulses of the 100-ms train.

In summary, useful information about the condition of the auditory nerve in CI users may be derived from eCAPs recorded to a pulse train with short IPIs. Recording the eCAPs to the first 10 pulses, as opposed to the last 10 pulses in a 100-ms pulse train, is more feasible in awake CI users.

PS 53

Effects of Prolonged Purinergic Receptor Activation in Cochlear Glial Cells

Silvia Prades; Katie E. Smith; Jonathan E Gale; Dan Jagger

UCL Ear Institute, University College London

The auditory nerve relays acoustic information to the auditory brain. The spiral ganglion neurons (SGNs) forming this primary afferent pathway are in close contact with different types of glial cells, but their functional interactions remain largely uncharacterized. Purinergic signaling is recognized as a regulator of auditory nerve physiology, following the detection of various P2Y and P2X receptors in SGNs (Housley et al., *Audiol Neurootol* 2002; Huang et al., *Purinergic Signal* 2010). In addition, we have demonstrated functional expression of P2X7 receptors (P2X7Rs) in cochlear glia (ARO MWM 2017). In the present study, we examine the downstream effects of prolonged P2YR and P2XR activation in cultured glia.

In agreement with previous work (Huang et al., Purinergic Signal 2010), immunofluorescence experiments using vibratome-sectioned cochlear tissue revealed expression of P2Y1Rs and P2Y4Rs in Schwann cells wrapping SGN peripheral neurites, and in satellite cells surrounding the SGN-soma. During ratiometric Fura-2 imaging, prolonged exposure to P2Y agonists (UTP, UDP and ADP) resulted in a significant increase in cytoplasmic calcium levels in cultured glia, with UTP being the most effective. These results are consistent with functional metabotropic purinergic signaling in cochlear glial cells.

We previously showed expression of P2X7Rs in Schwann cells and in satellite cells. Transient exposure to P2X7R agonists resulted in the activation of cationic currents. Prolonged exposure led to an increased permeability to fluorescent macromolecules, suggesting that P2X7Rs have the potential to mediate multiple cell-signaling pathways in cochlear glia. In other tissues P2X7Rs are recognized as activators of cell death pathways, and so P2X7R antagonists have been proposed as therapeutic targets in inflammatory conditions (Burnstock and Knight, Purinergic Signal 2017). In the present work we are investigating the consequences of prolonged P2X7R activation, and in particular their potential involvement in the control of cell death in the auditory nerve. Preliminary data will be presented on the extent of cell death caused by P2X7R activation in comparison to the effects of known pro-cell death agents (e.g. staurosporine).

The functional expression of P2YRs and P2XRs in glial cells within the peripheral portion of the auditory nerve raises the possibility that these receptors play specific roles in physiological and pathophysiological cochlear neuro-glial communication. In addition, the downstream effects of prolonged purinergic stimulation we describe suggest that P2YRs and P2XRs may both act as sensors of tissue stress during periods of damaging noise or ischemia.

This work was supported by an Action on Hearing Loss Studentship and a grant from the BBSRC.

PS 54

Enhanced Resolution Imaging of Excitable Microdomains in the Auditory Nerve during Development

Katie E. Smith; Dan Jagger
UCL Ear Institute, University College London

Type I spiral ganglion neurons (SGNs) in the auditory nerve transmit acoustic information from cochlear inner

hair cells (IHCs) to the brainstem in the form of action potentials. The ion channels responsible for action potential initiation and propagation are organized into discrete “microdomains” (Hossain et al., 2005; Smith et al., 2015; Kim and Rutherford, 2016), the assembly of which most likely depends on associated glial cells. These microdomains include the first heminode region located a short distance from the IHC synapse which is the spike generator of the auditory nerve, and nodes of Ranvier distributed along SGN neurites. The peripheral neurites of SGNs can degenerate substantially in severe cases of sensorineural hearing loss. Regenerative strategies aiming to regrow SGN neurites must recapitulate the complex organisation of the microdomains in order to fully restore function to the auditory nerve. Here we investigated the sequence of events leading to microdomain assembly and maturation during cochlear development.

Using enhanced resolution (Airyscan) confocal imaging, various nodal proteins including cell adhesion proteins and ion channels, were immunolocalized to developing microdomains in fixed cochlear vibratome sections from P4-P14 mice. The earliest detected proteins included the nodal proteins AnkyrinG and NF186 and the paranodal protein Caspr, which localized to immature clusters in the peripheral neurites of SGNs at ~P4. These proteins then formed heminodal arrangements by ~P6, with approaching heminodes observed along the same labelled neurite suggesting that nodal assembly most likely occurs by the fusion of two heminodes. Heminodal structures appeared later at the peri-somatic nodes of Ranvier within the spiral ganglion with fusion events in this area continuing to be observed at P12, after hearing onset. Refinement of the first heminodes which form the spike generator region also continued after hearing onset, as has been reported in the rat (Kim and Rutherford, 2016).

These results present a defined spatio-temporal pattern of microdomain formation during maturation of the auditory nerve and provide an insight into the mechanisms involved in microdomain assembly, a process that must be recapitulated in regenerative strategies targeting sensorineural hearing loss.

PS 55

Laminin Promotes Schwann Cell Migration and Neuronal Axon Growth In Vitro

Esperanza Bas; **Olena Bracho;** Paula Monje; Liliana Ein; Thomas R. Van De Water; Christine T. Dinh
University of Miami Miller School of Medicine

Background: Following nerve injury, myelinating

Schwann cells dedifferentiate and align in parallel tracks that provide physical scaffolds and trophic support for neurites to re-grow. Laminin is a component of the extracellular matrix that can promote migration and survival of Schwann cells. In this study, we investigate the effect of laminin on Schwann cell migration and neuronal axon growth and extension in vitro.

Methods: A migration assay was created by culturing adult rat Schwann cells and/or primary neurons against 0 or 1000 ug/ml of laminin in a two-well insert dish. Time-lapse light microscopy was performed daily to monitor Schwann cell migration and axonal extension toward the cell-free gap between cells and laminin conditions. At 96 hours, cells were fixed in 4% paraformaldehyde and immunofluorescence was performed using primary antibodies for tubulin β 3 (TUJ1, neuronal marker), S100 (Schwann cell marker) and DAPI (nuclei). Cell distribution and axonal length were analyzed with ImageJ software. One-way ANOVA with Bonferroni post-hoc testing was used for statistical analysis.

Results: Schwann cells migrated toward 1000 ug/ml laminin significantly more than control conditions without laminin ($p < 0.05$). In Schwann and neuronal cell co-cultures, there were significantly more Schwann cell migration events and axonal extension toward 1000 ug/ml of laminin compared to control conditions ($p < 0.05$). Laminin (1000 ug/ml) placement adjacent to co-cultures prevented cell clustering, spheroid formation, and detachment of cells from the plate.

Conclusions: Laminin is a trophic factor that can stimulate Schwann cell migration, promote axonal extension, and support health of Schwann and neuronal cells. These findings support further investigations into the mechanisms of how laminin can initiate Schwann-cell induced neuronal growth and has significant clinical implications such as in nerve injury and cochlear implantation.

PS 56

The Role of Mitochondrial Transport in Afferent Axon Structure and Function

Amrita Mandal¹; Katherine Pinter¹; Katie Kindt²; **Katie Drerup**¹

¹NICHHD; ²National Institute on Deafness and Other Communication Disorders

Afferent axons are the primary structure conveying information from hair cells to the cortex for perception of hearing and balance. These axons innervate the base of the hair cell and, to function correctly, must contain synaptic structures and organelles necessary

for neurotransmitter-mediated signal transduction. To properly place organelles and proteins through the axon, neurons utilize microtubule based motors. While a superfamily of Kinesin motors is responsible for plus end (axon terminal) directed axonal transport, the single molecular motor Cytoplasmic dynein accomplishes the bulk of retrograde (cell body directed) flow. One dynein cargo of particular importance is mitochondria. Clinical literature has suggested a strong correlation between abnormal mitochondrial localization and degenerative diseases of the nervous system; however, the impact of mitochondrial transport disruption on the structure and function of the afferent axons is unknown. First we determined the role of mitochondrial retrograde transport in the turnover of this organelle in axon terminals under normal conditions using zebrafish larvae. For this work, we utilized photoconversion of mitochondrially localized mEos in posterior lateral line afferent axon terminals and tracked the displacement of converted organelles over time. Our data illustrates a robust mitochondrial turnover in axon terminals, with complete turnover of this mitochondrial population within three hours. These organelles are not subject to immediate degradation but instead are repositioned within the axon, some being deposited at proximal axon terminals. In *actr10* mutants, which have defective retrograde transport, this turnover fails to occur. We next used live imaging of fluorescent reporters to determine if mitochondrial health or function are impacted by loss of retrograde mitochondrial transport in the *actr10* mutant line. Surprisingly, short-term trapping of mitochondria in the distal axon has little effect on either mitochondrial health or ATP production of axon terminal mitochondria. However, these neurons show a dramatic defect in cell body mitochondria: the overall mitochondrial load in the cell body is decreased with consequent loss of ATP production. Together, our data support a model in which mitochondrial retrograde transport is necessary to support a homeostatic balance of mitochondria in the neuron. Loss of normal retrograde movement leads to a decrease in neuronal cell body mitochondrial load and decreased energy production in this region. Future work will concentrate on the functional ramifications of disrupting homeostatic mitochondrial transport in afferent neurons with the long-term goal of linking this intracellular phenomena to neural circuit physiology in normal and disease states.

PS 57

Dual Action Potential Thresholds Characterize the Responses of SGNs to Dynamic Stimuli

Jeffrey Parra-Munevar¹; Charles E. Morse²; Mark R. Plummer²; Robin L. Davis¹

¹Rutgers University; ²Rutgers University

Spiral ganglion neurons (SGNs) display a remarkable level of heterogeneity, including the diversity of thresholds that correlate with spontaneous rate in vivo and APmax in vitro. When assessed with square-pulse depolarization current injections into (P1-14) neuronal somata in vitro, we found that slowly accommodating neurons were predominately low-threshold, whereas unitary or rapidly accommodating neurons were largely high-threshold (Crozier & Davis, 2014). This pattern of activity suggests that neurons within the ganglion fire in predictable ways depending upon their intrinsic depolarizing threshold level, yet we questioned whether this is a fixed property of the neurons or one that could be altered dynamically by changing the input stimulus.

To evaluate the possibility of intrinsic threshold modulation in SGNs, we assessed their action potential (AP) responses to the offset of 240ms hyperpolarizing square pulses. Not unexpectedly, the resultant rebound APs (APR) fired at thresholds that were significantly lower (51.0 ± 0.2 mV, $n=18$) than those evoked by depolarization (APD; -46.1 ± 0.3 mV, $n=18$; $p < 0.01$). The APD and APR thresholds were heterogeneous and positively correlated. The difference between APD and APR thresholds, however, was greater in high-threshold neurons as compared to the essentially overlapping values observed in low-threshold neurons.

The dynamic nature of SGN responsiveness was further evaluated with oscillatory stimuli ranging from 4.2 to 416.7 Hz in which the initial cycle was either depolarizing or hyperpolarizing. Input-output (I-O) functions resulting from this analysis showed unequivocally that neurons responded to the depolarizing phases of the stimulus at lower voltage levels when immediately preceded by a hyperpolarizing cycle. As predicted from our initial observations, this 'rebound excitation' behavior was more prominent in high-threshold neurons likely due to their divergent APD and APR thresholds. This dynamic sensitivity resulted in double, rather than single Boltzmann fits to the I-O relationships of many high-threshold neurons, as compared to their low-threshold counterparts.

Our analysis shows that SGNs are capable of firing APs to depolarizing and rebound stimuli, both at heterogeneous voltages. The dual nature of AP threshold levels in SGNs likely underlies the presence of rebound excitation observed in recordings from neurons injected with sinusoidal currents. Because the presence of rebound excitation can dynamically elevate the sensitivity of SGNs, we speculate that this type of behavior is likely an important substrate for integrating complex, time-dependent input to shape spiral ganglion output.

Funded by NIDCD RO1-DC01856 and Action on Hearing Loss, UK

PS 58

Endocytosis and Endocytotic Signaling in Spiral Ganglion Neurons

Shannon Doolittle¹; Eduardo Chavez²; Kwang Pak²; Arwa Kurabi¹; Allen F Ryan¹

¹UCSD Surgery/Otolaryngology; ²Department of Surgery / Otolaryngology, University of California, San Diego; San Diego VA Medical Center

Background: In transmembrane receptor signaling by tyrosine kinase receptors, ligand binding results in autophosphorylation and local signal transduction. Receptor/ligand internalization followed by degradation is the canonical model for limiting excessive receptor signaling. Alternatively, endosomes can function to recycle receptors back to the cell surface and maintain long-term signaling. However, current evidence indicates that receptor signaling may continue in endosomes. These "signaling endosomes" can traffic receptor signaling to distant cell sites. In neurons, neurite extension and direction can be controlled locally at the growth cone, where neurotrophin receptors are selectively expressed in the membrane. However, expression of genes important for neurite growth is controlled at the distant cell nucleus. Retrograde transport of signaling endosomes is a mechanism by which signals can reach the nucleus.

Methods: To explore how endosomes impact neurotrophin signaling in cochlear neurons, we first exposed explants of neonatal rat spiral ganglion to BDNF and NT-3. Neurite extension and neuritegenesis were then compared with and without exposure to Pitstop-2, a potent inhibitor of clathrin-mediated endocytosis; Dynasore, an inhibitor of clathrin-dependent and some clathrin-independent endocytosis; Wortmannin, an inhibitor of clathrin-independent endocytosis, and Mycolide B, an inhibitor of neuronal retrograde, but not anterograde transport.

Results: If endosomal degradation of neurotrophin receptors serves to limit signaling in cochlear neurons, inhibition would be expected to enhance the effects of neurotrophins, as has been shown in some circumstances for EGF. On the other hand, if receptor recycling by endosomes is important, as has been seen for insulin receptors, reduced neurite extension would be expected. If signaling endosomes are involved in transmitting signals to the cell nucleus, reduced neurite extension would be expected. The extension of neurites from SGNs was severely limited by clathrin-mediated endocytosis inhibition, in a dose-dependent manner. Clathrin-independent inhibition had no effect. Inhibition of retrograde transport completely blocked neurite extension.

Conclusions: The results indicate that endocytosis plays a critical role in enhancing the effects of neurotrophins on SGNs, most likely by increasing receptor recycling to the membrane. They also suggest that signaling endosomes mediate nuclear responses to neurotrophins.

Auditory Prostheses I: Novel Technologies & Applications

PS 59

Comparison of Inferior Colliculus Recordings Associated with Single Modality or Combined Electro-Optogenetic Stimulation of the Murine Cochlea

Fadhel El May¹; Xiankai Meng¹; Vivek V. Kanumuri¹; Florent-Valéry Coen²; Stephen McInturff³; Osama Tarabichi¹; Stéphanie P. Lacour²; Albert Edge⁴; M. Christian Brown⁵; Daniel J. Lee⁴
¹*Eaton-Peabody Laboratories, Massachusetts Eye and Ear, Harvard Medical School*; ²*École Polytechnique Fédérale de Lausanne*; ³*Eaton-Peabody Laboratories, Massachusetts Eye and Ear, Harvard Program in Speech and Hearing Bioscience and Technology*; ⁴*Department of Otolaryngology, Harvard Medical School*; ⁵*Eaton-Peabody Laboratories, Massachusetts Eye and Ear, Harvard Medical School, Harvard Program in Speech and Hearing Bioscience and Technology*

Introduction:

In developing a next-generation cochlear implant (CI), optical stimulation may address limitations of electrically-based devices, as light can be more spatially focused to create a greater number of independent channels. An optical CI uses light-driven stimulation of auditory neurons, which is now feasible using optogenetics. A first generation optical CI will likely be a hybrid device combining both electrical and optical modalities to increase spiral ganglion neurons (SGN) responses. Preliminary results from a mouse model of cochlear optogenetics showed co-stimulation (i.e. combined electrical and optical stimulation) resulted in larger auditory brainstem responses (eABRs) than those achieved by each of these modalities alone - with peak amplitudes that approximated the sum of those from each modality alone (El May et al, 2018 ARO abstr. # 924). Here, we further explored these interactions by recording the activity of the inferior colliculus (IC).

Methods:

Transgenic mice (n=8 mice) expressing channelrhodopsin 2 (ChR2) in SGNs driven by Cre-recombinase enzyme were used. Similar strain mice with no ChR2 expression were used as controls. Prior to surgery, we first assessed acoustically evoked ABRs. We then performed a cochleostomy distal to the round window niche using a

postauricular approach and inserted either: 1) a silver wire through the cochleostomy and a return silver wire through the round window, or 2) a conformable micro-electrode array (fabricated at École Polytechnique Fédérale de Lausanne) through the cochleostomy. To record IC activity, we performed a craniotomy and inserted a 16-electrode multichannel shank along the tonotopic axis of the contralateral IC. Stimulation was biphasic electrical pulses (with alternating polarity) and blue light (488nm) pulses. We examined the effect of different co-stimulation paradigms and combinations on IC activity, threshold and morphology.

Results / Conclusions:

Transgenic mice expressing ChR2 all showed evoked IC activity to either electrical or optical stimulation alone. Light addition to the electrical stimulation resulted in an increase in IC activity in the following pattern: sub-threshold levels of light did not result in a significant increase in IC activity, near and supra-threshold levels of light did result in a significant increase in IC activity until saturation of the neural response. Increases in response suggest that a hybrid electro-optical cochlear implant might be more effective than a device using just one modality.

PS 60

Establishment of In Vitro Model to Understand the Effect of Electrical Stimulation on Inner Ear

Zaid Al-Zaghal; Jeenu Mittal; Mario M. Perdomo; Elijah J. Horesh; Christopher O'toole; Jorge Bohorquez; Carolyn Garnham; Rahul Mittal; **Adrien A. Eshraghi**
University of Miami Miller School of Medicine

Introduction: While there is a trend to implant patients with residual hearing, cochlear implantation (CI) may cause some loss of this residual hearing. The direct effect of implantation of the electrode in affecting macroscopic structures of the inner ear is well described. Recently, a hybrid approach has been developed, where both residual hearing and electrical stimulation are used. However, the effect of the electrical field generated by the implant has not been investigated to date. There is a need to develop in vitro models of electrical stimulation of CI, which closely mimic human clinical conditions that will help in understanding the precise contribution of electrical stimulation in cochlear damage.

Materials and Methods: A custom stimulator circuit that allows to study several parameters, including stimulation amplitude, pulse width, and total stimulation duration was designed. The organ of Corti explant cultures from postnatal day three (P3) rats were used and placed in microchannel slide (Ibidi GmbH) in the incubator and

exposed to stimulation or left unstimulated. We also determined the efficacy of an otoprotective compound in providing protection against adverse effects of electrical stimulation. Parameters (amplitude, pulsewidth and duration) were changed one at a time. The organ of Corti explants were subjected to FITC phalloidin staining to visualize hair cells using confocal microscopy. The number of surviving hair cells were counted. The organ of Corti was also subjected to CellROX and cleaved caspase 3 staining to determine the levels of oxidative stress and apoptosis, respectively.

Result: In vitro testing suggests that the electrical stimulation may cause some damage to hair cells, mainly with higher stimulation levels and longer times of stimulation. The identified otoprotective compound provides significant protection against loss of hair cells in response to electrical stimulation. The molecule mechanisms behind otoprotection involves abrogation of activation of oxidative stress and apoptosis pathways. Conclusion: The stimulator circuit we designed and constructed very closely simulates the electrical field of a cochlear implant. It has enough task flexibility to be used as an in vitro model of electrical stimulation. The models developed in this study using electrical stimulation can be used to understand the effect of electrical field on inner ear sensory cells and to screen future otoprotective drugs for the preservation of residual hearing post CI using similar approach as used in this study.

Funding: MED-EL Corporation to Dr. AA Eshraghi

PS 61

Zwitterionic Coatings Reduce Bacterial Adhesion to Silastic Surfaces

Elise Cheng¹; Megan Foggia¹; Ryan Horne²; Na Shen¹; Braden Leigh³; Bradley Jones⁴; C. Allan Guymon³; Marlan R. Hansen¹

¹University of Iowa Department of Otolaryngology Head and Neck Surgery; ²University of Iowa Carver College of Medicine; ³University of Iowa Departments of Chemical and Biochemical Engineering; ⁴University of Iowa Department of Microbiology and Immunology

Introduction: Implantable medical devices, including cochlear implants (CI), must resist bacterial attachment and colonization on the device surface or risk device loss. Zwitterionic polymer systems have shown promise as anti-fouling materials, yet lack the mechanical properties to be used for medical devices. Here we explore the use of zwitterionic systems to provide a low-fouling surface coating of silastic materials that serve as housing/carrier for CI devices. The zwitterionic polymers, sulfobetaine methacrylate (SBMA) and carboxybetaine

methacrylate (CBMA), were UV-photografted to silastic to form an antibacterial hydrogel coating. Hydroxyethyl methacrylate (HEMA) was used as a low-fouling control. Zwitterionic coated and uncoated silastic samples were then exposed to two bacterial contaminants, *Staphylococcus aureus* (*S. aureus*) and *Staphylococcus epidermidis* (*S. epidermidis*), in vitro and in vivo to evaluate the antifouling properties of the coatings.

Methods: GFP-expressing *S. aureus* and *S. epidermidis* were cultured on silastic surfaces that were coated with CBMA or SBMA or remained uncoated. After 24 and 48 hours epifluorescent microscopy was used to count attached bacteria. The experiment was repeated under dry conditions by spraying bacterial suspension onto dry samples. To assess the effect of the coatings on bacterial adhesion in vivo, adult rats were divided into four groups: 1) uncoated silastic implanted subcutaneously, 2) uncoated silastic implanted transcutaneously, 3) CBMA coated-silastic implanted subcutaneously, and 4) CBMA coated-silastic implanted transcutaneously. GFP-expressing *S. aureus* was then injected around each polymer implant. Serial live, quantitative imaging of the GFP signal was obtained 0, 3, 7, 14 and 21 days following bacterial inoculation. At 21 days, the implants were removed and attached bacteria were scored with epifluorescent microscopy. Colony counts were also performed to verify the viability of attached bacteria.

Results: CBMA coatings significantly reduced bacterial adhesion to silastic in vitro under wet and dry conditions. SBMA coatings exhibited mixed results, with reduction of bacterial adhesion under some conditions, but not others. Uncoated silastic and HEMA developed large numbers of attached bacteria. Significantly fewer bacterial counts and colonies were found on CBMA-coated implants in vivo compared to uncoated implants. While biofilms developed on uncoated silastic after 3 weeks in vivo, they did not appear to form on CBMA-coated implants.

Conclusion: CBMA and SBMA applied as a UV photopolymerizable coating to silastic surfaces resist bacterial adhesion. CBMA is superior to SBMA. CBMA coatings on silastic could reduce the rate of bacterial infection, a difficult complication following cochlear implantation.

Validation of PTFE Artificial Cochlea Model for Insertion Force Measurements

Rolf Salcher¹; Martina Nullmeier²; Jakob Cramer²; Nick Pawsey²; Thomas Lenarz¹; Thomas S. Rau¹
¹Hannover Medical School; ²Cochlear Ltd.

One of the standard procedures in developing and characterizing cochlear implant electrodes is the measurement of insertion forces, as they are assumed to be correlated with trauma. To have a reproducible test setup, typically an artificial cochlea model (ACM) made of an easy to process and smooth material, like polytetrafluoroethylene (PTFE), in combination with various lubricants is used in these measurements. However it has not been demonstrated that such models accurately represent the conditions of the living cochlea. This study was conducted in order to validate the use of PTFE as a realistic cochlea model in respect to friction properties.

The friction conditions inside a cochlea are not easily measurable therefore we decided to compare insertion forces measured in fresh cochlea specimens with PTFE models of matching cochlear geometry. As a measurement in a human living patient is not possible the use of fresh never frozen temporal bones is the best available approach. The porcine cochlea is similarly proportioned to the human, provides straightforward surgical access and is readily available in contrast to human specimens.

We repeatedly measured insertion forces in porcine cochlea specimens and the corresponding ACMs with the same insertion speed. For these measurements a non-functional dummy electrode based on the Cochlear Slim Straight electrode was used and inserted up to a depth of 15 mm. A PTFE ACM was produced for each porcine cochlea, matching the size and shape based on CBCT data according to an in-house established method. We tested different lubricants in the PTFE model -saline solution, additional Healon, and soap solution- and compared the results to the measurements in the fresh cochleae. A good correlation between the insertion forces was found in a number of the specimens when saline solution was used as a lubricant in the PTFE model. However, there are also specimens with a poorer correlation match to forces in the corresponding PTFE model. Either the 2D shape of the PTFE model is an inappropriate oversimplification of the cochlear geometry or other factors impact insertion forces which are not identified at the moment.

A Method for Building Individualized Two-Dimensional Artificial Cochlea Models

Thomas S. Rau¹; Martina Nullmeier²; Jakob Cramer²; Silke Hüggl¹; Nick Pawsey²; Thomas Lenarz¹; Rolf Salcher¹
¹Hannover Medical School; ²Cochlear Ltd.

During the development process new electrode arrays for cochlear implant systems are frequently characterized by means of insertion force measurements. Although human cadaveric cochlea specimens are the most realistic models of the patient's cochlear geometry and friction conditions, also artificial cochlea models (ACM) are widely used due to their unlimited availability, low cost and, most important, reproducible conditions for repeated insertions. Typically, these ACMs are two-dimensional (2D) representations of an average human cochlea and may be milled out of polytetrafluoroethylene (PTFE). In order to justify the use of PTFE for ACMs we conducted a comparison study between cochlea specimens and geometrically corresponding ACMs. For this purpose we established a method to build a geometrically more realistic replica of the individual cochlea specimen.

In an initial study porcine cochlea specimens were used. Fresh, never frozen pig half heads were obtained from the slaughterhouse, cut into smaller pieces exclusively containing the cochlea and glued on a sample holder to ensure a well-controlled positioning. Cone-beam computed tomography (CBCT, Accuitomo, Morita, voxel size 0.08 mm) imaging was performed and the images processed in a custom-made DICOM viewer (COMET) featuring a rotating mid-modiolar slice plane. By rotating this plane in 22.5° steps around the central axis of the cochlea (modiolus) the shape of the inner and outer wall of scala tympani (ST) were segmented. Special focus was put on the basal part where segmentation was performed with tighter step wide. Afterwards, these contours were projected onto a plane perpendicular to the modiolar axis to derive the 2D equivalent of the original cochlear geometry. These contours were further processed using computer-aided design (CAD) software (Autodesk Inventor Professional 2015) and finally the geometry was milled out of a PTFE plate using a computer numerically controlled (CNC) milling machine. A thin PTFE sheet supported by an acrylic glass disk to cover the model was added to close the ST lumen and to enable visual documentation of the insertion process.

3D Printed Cochlea Model For Insertion Force Measurement Testbench

Guillaume Turrel¹; Caio Maciel J. Viera¹; Thomas Demarcy¹; Julie Foncy²; Laurent Malaquin²
¹Oticon Medical; ²LAAS-CNRS

Background

Lower the forces during the electrode's insertion in the cochlea is extremely important to avoid damaging the interior structures of the Scala tympani, as the basilar membrane, and, consequently, to avoid the loss of residual audition in patients [1] [2]. These force measurements can be performed in synthetic models or in cochleae of cadavers, for design verification purpose. The objective of this study was to develop a more realistic 3D printed cochlea model to integrate into our insertion force measurement tests, and then provide a tool for the evaluation of new electrode designs.

Methods

1- Parametric anatomical model of the cochlea [3]
 After analyzing 987 segmented tomography (CT) images, an analytical model was developed to generate different configurations of models of the cochlea (Fig. 1). This parametric model allowed the generation of cochlea's shapes in different sizes and anatomical conditions (Fig.2).

2- Workflow for preparation of the cochlea's model
 The proposed numerical treatment (Fig. 3) ensured an acceptable accuracy of the final 3D printed model (operation step / format file)

3- 3D printed cochlea model
 Cochlea models were 3D printed layer-by-layer using a 3D printer with a high-speed, high-precision stereolithography process (SLA) with a resolution down to 20 μ m (x,y,z). The systems uses a 405 nm laser controlled by galvanometers. All reported designs were fabricated using a commercial DS3000 photosensitive polymer (DWS) according to previously reported processes [4].

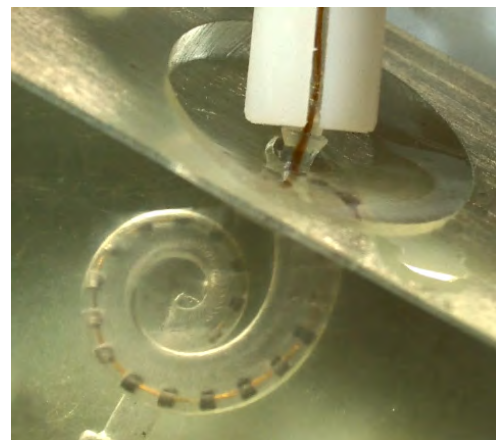
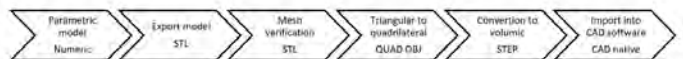
4- Test bench using the 3D cochlea model
 The 3D printed model is integrated onto an insertion force measurement test bench (Fig. 4). The following insertion parameters can be controlled: Speed, depth, angles, and lubricant.

Results

Electrode insertions (Fig. 5) have been performed according to several insertion conditions. The results showed that the insertion forces are consistent and enough accurate to comply with the expected use in development tool for electrode verification.

Conclusions

The 3D printed cochlea model brought a more realistic shape and behavior of the electrode insertion. Some limitations are induced by the design of the model with only scala tympani cavity engraved in the physical model. Some events occurring during the surgery, like tip foldover or bulking electrode, may not be revealed. For that reason, we expect to provide a 3D printed model comprising the ST, SV and BM.



PS 65

Insulin-like growth factor 1 attenuates hearing loss at low frequencies in animal models of cochlear implantation

Kohei Yamahara¹; Koji Nishimura²; Hideaki Ogita³; Juichi Ito³; Takayuki Nakagawa²; Ichiro Furuta²; Tomoko Kita²; Koichi Omori²; Norio Yamamoto²

¹*Dep. Otolaryngology, Head and Neck Surgery, Shizuoka City Shizuoka Hospital;* ²*Department of Otolaryngology-Head and Neck Surgery, Graduate School of Medicine, Kyoto University;* ³*Shiga Medical Center Research Institute*

(Background)

The electric-acoustic stimulation (EAS) or hybrid cochlear implant is applied to patients with a residual hearing at low frequencies. EAS covers high- and low- frequencies with electric and acoustic stimulation, respectively. The enhancement of the low-frequency hearing with acoustic stimulation contributes to the pitch perception or the detection of the intraural time difference by EAS. Thus, it is mandatory to preserve the low-frequency hearing during EAS cochlear implantation (CI). However, the cochlear implantation damages the cochlea partly due to the apoptosis of hair cells, resulting in the deterioration of residual-hearing and diminished the merit of the acoustic-hearing in many patients. To prevent hearing deterioration after CI, corticosteroids have been used clinically although their effects are limited. As a novel treatment of sensorineural hearing loss other than corticosteroids, we have reported that insulin-like growth factor 1 (IGF1) prevented the apoptosis of hair cells and was effective for hearing preservation in noise- or ischemia-induced hearing loss. In this study, the effects of IGF1 on hearing preservation after CI were examined on a normal-hearing guinea pig model.

(Methods)

The electrode was inserted in an atraumatic way through the round window membrane of guinea pigs with the application of a gelatin-sponge soaked with IGF1 or saline. The auditory brainstem response (ABR) was recorded preoperatively, immediately after CI, and 7, 14, 28, and 56 days after electrode insertion. After the final ABR measurement on day 56, all animals were euthanized and cochleae were dissected out for histological examination.

(Results)

The IGF1-treated group showed better hearing preservation than the saline-treated group at low

frequencies (2, 4 and 8 kHz), 7 days after surgery. The IGF1 application was effective at low frequencies (2 and 4 kHz) throughout the period of examination. Histological study revealed the less outer hair cell loss in the cochlear region responsible for low-frequency hearing and less fibrous tissue formation around the electrode in the IGF1-treated group. Both the outer hair cell numbers and the extent of fibrosis had a statistically significant correlation with the ABR threshold shifts at low frequencies.

(Conclusions)

These results indicate that IGF1 preserves low-frequency hearing after CI, suggesting its possible clinical use in CI surgeries requiring hearing preservation.

PS 66

Zwitterionic Coatings Mitigate the Foreign Body Response to Implanted Biomaterials

Elise Cheng¹; Megan Foggia¹; Ryan Horne²; Braden Leigh³; Marlan R. Hansen¹; C. Allan Guymon³

¹*University of Iowa Department of Otolaryngology Head and Neck Surgery;* ²*University of Iowa Carver College of Medicine;* ³*University of Iowa Departments of Chemical and Biochemical Engineering*

Introduction: Cochlear implant electrode arrays consist of platinum contacts and wires embedded in a poly(dimethyl siloxane) (PDMS) carrier. These materials generate a fibrotic/immune response when implanted, which can impair implant function and longevity. Zwitterionic polymers, including carboxybetaines (CBMA) and sulfobetaines (SBMA), show promise in reducing protein and biomolecule adsorption. We recently developed methods to durably coat PDMS surfaces with these zwitterionic polymers in an effort to blunt the foreign body response. We propose that these low-fouling coatings reduce early (protein adhesion), intermediate (macrophage recruitment), and late (fibroblast adhesion) events in the response to biomaterials.

Methods: PDMS was coated by photopolymerizing SBMA and CBMA monomers using various concentrations of benzophenone as a surface activator and various concentrations of cross-linking moieties. This resulted in zwitterionic hydrogels with a range of cross-link densities covalently photografted to PDMS surfaces. Protein adsorption and cell adhesion were assessed to evaluate the relationship between cross-link density and anti-fouling properties of zwitterionic coatings. SBMA and CBMA coated and uncoated PDMS substrates were exposed to human fibrinogen and protein adsorption was measured. Macrophages and fibroblasts

were cultured on coated and uncoated PDMS substrates to evaluate the ability of zwitterionic coatings to prevent cellular adhesion. To test in vivo durability of the anti-fouling properties, uncoated and coated PDMS substrates were implanted subcutaneously in rats for two weeks and then removed. Fibroblast adhesion was evaluated on the explanted materials. The ability of zwitterionic coatings to spatially control macrophage attachment to PDMS surfaces is currently being assessed.

Results: Shear adhesion experiments demonstrated that lower concentrations of benzophenone resulted in coating delamination from PDMS surfaces, while higher benzophenone concentrations resulted in covalent attachment and subsequent cohesive failure. Fibrinogen adsorption was significantly reduced for both pSBMA- and pCBMA-coated surfaces compared to uncoated PDMS. Patterning zwitterionic coatings using photomasks on glass and PDMS resulted in reduced fibroblast adhesion in unmasked (coated) regions. Further, the ability of CBMA thin films to reduce fibroblast adhesion after two weeks in vivo was comparable to the effects on unimplanted substrates, indicating that anti-fouling properties were retained. Results of macrophage adhesion to PDMS substrates are currently under review.

Conclusion: PDMS can be durably coated with SBMA and CBMA systems that dramatically reduce protein and cell adsorption. Ongoing work focuses on the effect of zwitterionic coatings on macrophage attachment to PDMS, an intermediate step in the foreign body response to CI materials.

PS 67

Laminin coated Cochlear Electrodes to promote Axonal Growth and Guidance

Esperanza Bas; Mir R Anwar; Stefania Goncalves; Christine T. Dinh; Olena R Bracho; Juan A Chiossone; **Thomas R. Van De Water**
University of Miami Miller School of Medicine

Background: The benefits of cochlear implant (CI) technology depend on the number of excitable neurons remaining and the distance between the electrodes and these sensory neurons. Among new designs, perimodiolar electrodes attempt to bring the electrodes closer to their neuronal targets allowing for decreased signal spread and power consumption. However, perimodiolar electrodes are not suitable for all patients because they may flex during insertion causing mechanical trauma. We have previously

demonstrated in a P-3 rat organ of Corti explant model that Schwann cells provide guidance of axonal growth towards laminin-coated surfaces. Here we explore the effectiveness of laminin-coated electrodes in promoting axonal outgrowth from auditory neurons towards matrix-coated electrode arrays and the reduction of electric ABR (eABR) thresholds.

Experimental procedure: 3 month-old Norway Brown rats were divided in 2 groups: uncoated cochlear implants (CI) and laminin-coated cochlear implants (CI-Laminin). CAPs, aABRs, eABRs and impedances were recorded on a weekly basis up to 4 weeks, then animals are euthanized and their cochleae processed for histology.

Results: Electrophysiology: Animals implanted with laminin-coated electrodes experienced significant decreases in eABR and aABR thresholds at selected frequencies, CAPs were not significantly affected. An increase in impedances was observed in laminin-coated electrode animals. Histology: In the early phase laminin-coated electrodes attracted Schwann cells and neuronal outgrowth towards the electrode analog (10 days). At 1 month we observe a greater number of neurons in the spiral ganglia of animals implanted with laminin-coated electrodes compared to the uncoated group and more axonal processes projecting into the scala tympani. Correlation analysis shows that a decrease in spiral ganglion neurons was correlated with an increase in eABR thresholds.

Discussion & Conclusions: These data suggest that Schwann cells are attracted to laminin coated electrodes and promote: 1) axonal outgrowth; 2) axonal guidance; and 3) post-insertion trauma survival of spiral ganglion neurons.

PS 68

Evaluation of Cochlear Duct Length Measurements From a 3D Analytical Cochlear Model Using Synchrotron Radiation Phase-Contrast Imaging

Luke W. Helpard¹; S. Alireza Rohani²; Hanif M. Ladak¹; Sumit K. Agrawal³

¹Western University; ²Department of Otolaryngology - Head and Neck Surgery, Western University; ³London Health Sciences Centre

Background: Accurate cochlear duct length (CDL) determination is required for cochlear implant electrode size selection and frequency map programming. Many CDL measurement techniques have been well established and validated in a research setting, however are time consuming and require resources that exceed

what is available in a standard clinical setting. The A value technique described in the literature is valuable in its ability to generate individual CDL estimates in a clinical setting, however does not capture apical variations in the cochlea and traditionally has not been used to model any geometric information aside from cochlear lengths. To overcome these problems, a 3D individualized cochlear model dependent on four basal turn distances was proposed in the literature. Initial validation of this model was done using corrosion casts of human cochlea. The objective of this work was to validate the 3D individualized cochlear model using synchrotron radiation phase-contrast imaging (SR-PCI) data. Compared to corrosion casts, SR-PCI provides higher discernment of both bone and soft tissue, and the ability to view cross sections of the cochlea during point placement.

Methods: SR-PCI data from 11 cadaveric human cochleae was obtained for validation purposes. From each SR-PCI sample, the reference CDL value, the reference number of cochlear turns, and the four model input distances were determined. The reference CDL values were compared with the CDL values generated by the 3D analytical model when the number of cochlear turns were automatically predicted based on the input distances, and when the number of cochlear turns were manually specified (based on SR-PCI reference values). Statistical and clinical metrics were used to determine the overall significance of the results.

Results: When the model automatically predicted the number of cochlear turns from the input distances, the mean absolute difference between reference and model CDL was 2.61 ± 1.56 mm, with three out of 11 samples having an error in the clinically acceptable range of ± 1.5 mm. When the number of cochlear turns were manually specified based on SR-PCI data, the mean absolute difference between reference and model CDL was 0.99 ± 0.64 mm, with eight out of 11 samples having a clinically acceptable error.

Conclusion: The 3D analytical model introduced in the literature is effective at modelling the 3D geometry of individual cochleae, however appears to require slight tuning in the cochlear turn estimation.

PS 69

Anatomical Correlates and Surgical Considerations for Localized Therapeutic Hypothermia Application in Cochlear Implantation Surgery

Enrique Perez¹; Andrea Viziano¹; Zaid Al-Zaghal²; Fred F. Telischi²; Rachele Sangaletti³; Weitao Jiang⁴; Curtis King⁵; Michael Hoffer⁶; Suhrud M. Rajguru⁷

¹University of Miami; ²University of Miami Miller School of Medicine; ³Department of Otolaryngology, University of Miami; ⁴Department of Biomedical Engineering, University of Miami; ⁵Lucent Technologies; ⁶Department of Otolaryngology and Neurological Surgery, University of Miami; ⁷Department of Biomedical Engineering and Otolaryngology, University of Miami

Background

Electrode insertion during cochlear implantation (CI) surgery can result in hair cell damage and may result in a loss of residual low-frequency hearing. Amongst hearing preservation strategies, local application of therapeutic hypothermia has shown promising results. Using a custom-designed probe and system, our group has demonstrated the feasibility of delivering controlled hypothermia to the inner ear without requiring modifications in the surgical approach. However, anatomical variations and suitability of different surgical approaches, including the standard facial recess (FR) approach versus a transtympanic approach need to be further investigated. The aim of the present study is to utilize anatomical and radiologic measurements and experimental outcomes from cadaveric human temporal bones to investigate the feasibility of delivering local hypothermia.

Methods

Ten human adult cadaveric temporal bones were scanned with micro-CT. By means of software analysis, distances between the chorda tympani and the facial nerve and FR height were measured and total FR area was derived. Further measurements predicting RW visibility were recorded. Each bone was drilled and a standard FR approach was developed. The St. Thomas classification (STC) was then used to record degree of RW visibility. This grading was repeated following further drilling for optimizing visualization of the RW or independent cochleostomy and placement of the cooling probe through the FR or myringotomy. Following previously published protocols, hypothermia was delivered through both approaches and temperatures recorded by thermistors placed inside the RW (Apex), at RW niche, over the lateral semicircular canal (LC) and the supero-lateral mastoid edge (M).

Results

The average FR area was 13.87 mm²(SD 5.52) ranging from 8.44 to 24.28 mm². Regarding STC grading, the introduction of the cooling probe through either approach did not impede full visualization of the RW or cochleostomy. The average maximum temperature decrease, using the FR approach, was 4.57 °C (SD \pm

1.68) for RW and 3.42 °C (SD ± 1.12) for Apex, while a transtympanic approach produced a mean decrease of 4.11 °C (SD ± 0,98) for RW and 3.22 °C (SD ± 0.95) for Apex. No significant differences were found between the two probe approaches.

Conclusion

Results show that local hypothermia delivery during CI surgery, using a customized probe, can be efficiently achieved both through a FR and transtympanic approach regardless of anatomical constraints and without limiting optimal surgical visualization.

Supported by Cochlear Grant to SMR

Binaural Hearing in Non-Human Animals

PS 70

Inhibitory Nuclei in the Auditory Pathway of the Barn Owl

Anna Kraemer; Catherine Carr
University of Maryland College Park

The barn owl is a good auditory model with relatively simpler auditory brainstem circuitry compared to mammals (review in Nothwang 2016). We have used this system to understand how inhibition regulates the excitatory brainstem nuclei. The superior olivary nucleus (SON) appears to play a large role (Burger et al., 2011; Tabor et al., 2012), and is the source of most inhibitory projections to excitatory brainstem nuclei (Carr et al., 1989; Burger et al., 2005). The ventral lateral lemniscal nuclei (LLV) may also provide inhibition. In zebra finches, LLV projects to the nucleus laminaris (NL) (Wild et al., 2010; Krutzfeld et al., 2010), although this projection has not been confirmed in barn owl (Takahashi & Konishi 1988). We therefore injected a retrograde fluorescent adeno-associated virus (Tervo et al., 2016) into NL and identified many retrogradely labeled neurons in SON and a few neurons in the LLV.

Although hypothesized to be important for regulating the sound localization circuit in chicks in vitro (Yang et al. 1999; Monsivais et al. 2000; Yang et al. 2012; review in Burger et al. 2011) and in vivo (Nishino et al. 2008), there has been little research on the barn owl SON (Moiseff and Konishi 1983). Moiseff & Konishi (1983) recorded SON single units in barn owl and suggested that their search criteria were biased to the ipsilateral ear, since the majority of their units were EO responsive, or only responded to ipsilateral stimuli (Moiseff and Konishi 1983). We therefore recorded single units in barn owl SON, with lesions to confirm the recording location. The majority of the units responded preferentially to binaural

noise and rarely responded to tones, showing broad frequency tuning with low spontaneous firing rates. Response types were heterogeneous, and included off-responses, on-off responses, sustained, suppressed, primary-like, and chopper units. Because the SON projects to the three brainstem excitatory nuclei and the inferior colliculus, and has separate projections to the contralateral SON, these heterogeneous response types may represent separate SON neuronal populations, projecting to different nuclei (Burger et al. 2005). Further experiments are needed to gain insight into the different roles that the SON plays in regulating the activity in the auditory brainstem of the barn owl.

Grant# NIDCD 000436

PS 71

The Barn Owl Minimum Audible Angle

Bianca Krumm¹; **Georg M. Klump**²; Christine Köppl³;
Ulrike Langemann¹

¹*Cluster of Excellence Hearing4all, Department of Neuroscience;* ²*Custer of Excellence Hearing4all, Department of Neuroscience, Carl von Ossietzky University;* ³*Department of Neuroscience, School of Medicine and Health Sciences, Carl von Ossietzky University*

Background

Sound localization is a crucial ability for the barn owl, a night hunting bird with an exceptional sense of hearing benefitting from accurate sound localization for successful hunting. Space-specific neurons in the ICx, form an auditory space map (Knudsen and Konishi 1978, *Science* 200: 795-797). The azimuthal spatial tuning of neurons in the barn owl IC is determined mainly by the interaural time difference (ITD) corresponding to the large variation of this acoustic cue with azimuth (Moiseff 1989, *J. Comp. Physiol. A.* 164: 629-636). In the barn owl, acoustic interaural level differences (ILD) vary only little with azimuth (Moiseff 1989, *J. Comp. Physiol. A.* 164: 629-636). The width of ITD tuning curves increases with increasing azimuth (Cazettes et al. 2016, *J. Neurosci.* 36: 2101-2110). Consistent with that, space specific neurons representing frontal space have more confined spatial receptive fields than peripheral neurons (Knudsen and Konishi 1978, *J. Neurophys.* 41: 870-884). Both observations predict better spatial acuity in perceiving frontal compared to lateral sounds. ITD tuning deteriorates with decreasing frequency (Cazettes et al. 2016) which predicts a reduced acuity at low frequencies.

Methods

Three barn owls were trained in a Go/NoGo paradigm, to report a perceived change in stimulus position in azimuth, i.e., we determined the minimum audible angle (MAA). Stimuli were narrowband noise signals with different center frequencies (0.5, 1, 2, 4, or 8 kHz, 40 Hz bandwidth) or a broadband noise (500 - 8000 Hz) to test the effect of frequency on the MAA. To compare frontal and lateral MAAs, reference stimuli were either presented from 0° or from +/- 45° in azimuth. The hit and false-alarm rate were measured to calculate the sensitivity d' ; and the discrimination threshold.

Results and conclusion

Behavioral sensitivity was related to signal frequency, angular separation between reference and test stimuli, and the position of the reference stimuli, with all effects being additive (no interactions). In general the owls' MAA linearly increased with decreasing frequency, from about 6° at 8000 Hz up to about 14° at 500 Hz. The comparison of frontal and lateral MAAs revealed smaller MAAs in the frontal sound field than at the side, irrespective of the signal frequency. These observations match the predictions based on the neuronal responses in the owl's auditory midbrain.

Funding

Funded by the DFG (TRR 31, EXC 1077).

PS 72

Enhancement of Spontaneous Excitatory Transmission by Group I mGluRs in Neurons of the Medial Nucleus of the Trapezoid Body

Kang Peng; Chun-Jen Hsiao; Yong Lu
Northeast Ohio Medical University

Background

Neuromodulation mediated by metabotropic glutamate receptors (mGluRs) regulates many brain functions, however, the modulatory roles of mGluRs in auditory processing are not well understood. The medial nucleus of the trapezoid body (MNTB) is a critical nucleus in the auditory brainstem circuits involved in sound localization. MNTB neurons are excited by glutamatergic inputs from bushy cells in the contralateral anteroventral cochlear nucleus (AVCN) via the giant calyx of Held synapse. MNTB neurons also receive inhibitory inputs mediated by GABA and glycine. The integration of these synaptic inputs determines the MNTB's output. Our recent study shows that group I mGluRs (mGluR I) exert neurotransmitter- and release-mode-specific modulation

on the inhibitory transmission in MNTB (Curry, Peng, and Lu, *The Journal of Neuroscience*, 2018). Here, we further investigated the modulatory effects of mGluR I on the excitatory transmission.

Methods

C57/B6 mice were purchased from the Jackson Laboratory and bred at NEOMED. Brainstem slices (250-300 μm) were prepared, and whole-cell voltage- and current-clamp recordings were performed at 35 °C. Calcium imaging was used to measure calcium signaling in response to mGluR I activation.

Results

In the presence of a GABAAR antagonist (gabazine, 10 μM) and a glycine receptor antagonist (strychnine, 1 μM), at the holding potential of -60 mV, activation of mGluR I by 3,5-DHPG (200 μM) produced an inward current, and increased glutamatergic sEPSC frequency and amplitude in MNTB neurons. The effect on sEPSCs was blocked by a voltage-gated sodium channel (Nav) antagonist (tetrodotoxin, 1 μM). Cadmium chloride (100 μM), a non-specific voltage-gated calcium channel (Cav) blocker, partially eliminated the modulatory effects. Accordingly, under current-clamp configuration, 3,5-DHPG depolarized MNTB neurons, increased sEPSP frequency and amplitude, and in some cells produced action potentials, which persisted after synaptic receptors were blocked. In AVCN bushy cells, after blocking the known synaptic receptors with a cocktail of blockers (APV, 50 μM ; DNQX, 50 μM ; gabazine, 10 μM ; strychnine, 1 μM), 3,5-DHPG (200 μM) depolarized the membrane without generating action potentials. 3,5-DHPG also increased intracellular free calcium concentration in AVCN neurons under this condition.

Conclusions

Presynaptic mGluR I enhance the spontaneous excitatory transmission in MNTB neurons, via a Nav- and Cav-dependent pathway. Postsynaptic mGluR I increase the excitability of MNTB neurons.

Supported by NIH/NIDCD R01DC016054.

PS 73

Soma-Axon Coupling Configurations that Enhance Neuronal Coincidence Detection

Joshua Goldwyn¹; Michiel Remme²; John Rinzel³
¹*Swarthmore College*; ²*Humboldt University Berlin*; ³*New York University*

Background

Coincidence detector neurons are cells that generate spikes preferentially to synaptic inputs that arrive (nearly) simultaneously. Principal cells of the medial superior olive (MSO) in the mammalian auditory brainstem are superb coincidence detectors. MSO neurons encode sound source location with high temporal precision by distinguishing submillisecond timing differences among inputs. Distinctive biophysical properties contribute to the remarkable temporal precision of MSO neurons.

Methods

We investigate structural specializations in coincidence detector neurons. Specifically, we develop a model of an MSO-like coincidence detector neuron that describes the connection between input regions (soma+dendrites) and output regions (axon) of a cell. With this model, we have parametric control of the coupling between these regions. Through systematic computer simulations and mathematical analysis of the model, we investigate the effects of soma-axon coupling on neural dynamics, spike generation, and coincidence detection sensitivity.

Results

We show that the electrical coupling between soma and axon, as well as the distribution of INa and IKLT in soma and axon regions of a model MSO neuron can be configured to enhance coincidence detection sensitivity. Specifically, we find that a two-compartment model with a “feedforward” configuration – one in which the input regions of a cell (soma and dendrites) strongly drive activity in the spike-generating output region (axon), but backpropagation from the axon into the soma is weak – is significantly advantageous for coincidence detection. In the feedforward configuration, spikes are generated with greater efficiency (fewer INa channels) than a one-compartment model. In addition, INa inactivates more than in models with weak feedforward coupling. The feedforward configuration can, therefore, more effectively enable INa inactivation to prevent spike-generation in response to non-coincident inputs. A dynamic IKLT current further enhances coincidence detection sensitivity in these models.

Conclusions

Our work provides a unifying view of structure, dynamics, and function in coincidence detector neurons. MSO neurons have been characterized as “feedforward neurons” – prior work has shown that the site of spike-generation is electrically isolated from the soma with weak backpropagation of action potentials (Scott et al 2007). Our findings elucidate the advantages of this structural specialization. Our modeling framework

could also provide useful insights for related systems. Coincidence detector neurons in the auditory brainstem of owls, for example, have also been modeled as two-compartment structures and display intriguing evidence of plasticity in the soma-axon connection.

PS 74

Linear and Nonlinear Components of the Interaction Between Ipsi- and Contralateral Inputs at the Medial Superior Olive

Yarmo Mackenbach¹; J. Gerard G. Borst²; Marcel van der Heijden¹

¹Erasmus MC; ²Erasmus Medical Center

To localize low-frequency sounds, a nucleus located in the brainstem called the Medial Superior Olive (MSO) compares the arrival times of excitatory signals from both cochlear nuclei. MSO principal neurons act as coincidence detectors, as they preferentially fire when inputs from both ears arrive simultaneously. This happens at the ‘best’; Interaural Time Difference (BITD), at which point a difference in arrival times compensates for the difference in internal travel time from either ear. MSO neurons receive not only excitatory inputs, which are segregated to different dendrites, but also inhibitory inputs, which target the soma; inputs from the ipsilateral ear arrive via the lateral nucleus of the trapezoid body, whereas inputs from the contralateral ear are contributed by the medial nucleus of the trapezoid body. Their function is still debated, and we tested here their possible involvement in coincidence detection at different sound intensities. We performed juxtacellular electrophysiological recordings on MSO cells using a ventral approach in anaesthetized gerbils, while presenting a new multi-tone ‘zwijs’ stimulus, in which the different sound frequencies are segregated to both ears. A comparison of the responses to monaural and binaural stimuli allowed us to estimate how the inputs from one ear affected those of the other. We observed that for low intensity wideband stimuli (30-40 dB SPL), there was little or no impact of the inputs from the other ear, whereas at high intensities (60-70 dB SPL), a sound frequency-dependent reduction in the size of the phase-locked response was typically observed, suggesting a sound level-dependent recruitment of synaptic inhibition. This inhibition could be asymmetrical with either of the ears dominant. In general, spike rates in response to binaural stimuli on average did not change between 40 and 60 dB SPL whereas spike rates in response to both ipsi- and contralateral stimulation did increase. Our data thus suggest a role for synaptic inhibition in keeping the MSO output within narrow boundaries for different sound intensities.

**Biosonar in Bats: Pulse-Echo Ambiguity
Suppression by a Novel Auditory Anticorrelation
SCAT Mechanism**

James Simmons¹; Stephanie Haro²; Chen Ming¹
¹Brown University; ²Harvard University

When bats fly in complex surroundings, each biosonar broadcast is followed by a series of echoes returned by objects comprising the scene, from the nearest potential targets or collision hazards to the farthest objects that return detectable echoes. Clutter interference caused by reception of multiple echoes for the same broadcast is a pervasive problem for sonar and radar systems operating in complex environments. Although echoes often arrive from the background of the scene after long delays, nearer objects may require rapid response-times, which implies the need to emit sounds as short intervals to guide flight, intercept targets, or keep track of potential collision hazards. A special case of clutter occurs when broadcasts are emitted at such short intervals that echoes from one transmitted sound are still arriving when a second sound is emitted and its echoes begin to arrive, too. Mixing of echo streams from successive broadcasts creates pulse-echo or range ambiguity about which echoes are related to which broadcasts. When echo streams overlap, long-delay echoes of the first broadcast can be misinterpreted as short-delay echoes of the second broadcast, giving rise to phantom objects at spurious close ranges. When interpulse intervals have to be very short to steer flight, one solution is to emit successive sounds at different frequencies so their respective echoes can be sorted and referred to the corresponding broadcasts. Big brown bats (*Eptesicus fuscus*) make small changes in the terminal, low-frequency end of their frequency-modulated (FM) broadcasts so that closely-spaced sounds alternate in their ending frequency. However, such changes amount to only a few kilohertz out of a transmitted bandwidth of 75-80 kHz, which is too small to segregate echoes for the corresponding broadcasts because the sounds are still highly correlated. Bats employ an additional, anticorrelation auditory mechanism that blanks out echoes of a sound with a high ending sweep frequency from being associated with a broadcast that contains a slightly lower ending frequency. A constellation of results obtained in psychophysical tests, flight tests of bats in dense clutter, and computational modeling of biosonar with the Spectrogram Correlation and Transformation (SCAT) model reveal how this process works and provide estimates of the degree of segregation of overlapping echo streams. (Work supported by ONR MURI)

**Interaural Time Difference Sensitivity For Pulsatile
Acoustic and Electric Stimuli in the Auditory
Midbrain of Unanesthetized Rabbits**

David R. Axe¹; Yoojin Chung²; Bertrand Delgutte²
¹Dept. of Otolaryngology, Mass. Eye and Ear Eaton-Peabody Lab; ²Dept. of Otolaryngology, Harvard Medical School; Eaton-Peabody Lab, Mass. Eye and Ear

BACKGROUND

Interaural time differences (ITDs) are an important cue for sound localization and speech reception in noisy environments. In patients with bilateral cochlear implants (CI), ITD sensitivity is poorer than normal, especially for the high pulse rates used as carriers in CI processing strategies. Neural ITD sensitivity in the auditory midbrain of animal models of bilateral CIs also declines rapidly for stimulation rates above 100-200 Hz. However, little is known about ITD sensitivity to trains of short broadband acoustic stimuli, similar to electrical pulses used in CIs, in the auditory system of normal hearing (NH) animals.

METHOD

We recorded from single units in the inferior colliculus (IC) of unanesthetized, NH rabbits in response to trains of short ($\leq 200 \mu\text{s}$) broadband noise pulses with varying repetition rates (20-640 Hz) and ITDs ($\pm 2000 \mu\text{s}$) presented at 45-65 dB SPL. Results were compared with those from the IC of rabbits that were bilaterally deafened and implanted as adults (Chung et al., *J Neurosci.* 36:5520). ITD sensitivity was quantified by the "signal-to-total variance ratio" (STVR), an analysis of variance metric representing the fraction of variance in neural firing rates due to variations in ITD.

RESULTS

In NH animals, the firing rate for the vast majority of neurons showed significant sensitivity to ITD to pulsatile stimuli for at least one repetition rate, regardless of their pure tone best frequency (0.3-12 kHz). The strength of ITD sensitivity varied with repetition rate. Half the neurons showed strongest sensitivity to repetition rates of 80-160 Hz, while about one quarter each were most sensitive to rates above and below this range, respectively. Strength of ITD sensitivity quantified by STVR, was significantly higher in NH rabbits than in deafened rabbits with bilateral CIs. Similarly, the fraction of units sensitive to ITD was significantly higher in NH rabbits than in implanted rabbits. This difference was particularly pronounced at higher repetition rates ($> 200 \text{ Hz}$) where ITD sensitivity for CI stimulation rolls off quickly.

CONCLUSION

IC neurons in NH rabbits do not show the steep decline in ITD sensitivity to pulsatile stimulation that occurs with bilateral CI stimulation for repetition rates above 200 Hz, consistent with previous studies demonstrating ITD sensitivity for pure tones up to ≥ 2000 Hz. Future work will test whether the steep decline with CI stimulation is due to the abnormal peripheral patterns of neural activity or to deafness-associated reorganization of the binaural circuits.

Supported by NIH Grant DC005775.

PS 77

Binaural Hearing in the Naked Mole-Rat

Elizabeth A. McCullagh¹; John Peacock²; Catherine Barone³; Thomas Park⁴; Achim Klug¹; Daniel J. Tollin⁵
¹University of Colorado Anschutz; ²University of Colorado School of Medicine, Department of Physiology and Biophysics; ³University of Illinois Chicago; ⁴Department of Biological Sciences, University of Illinois at Chicago; ⁵Department of Physiology & Biophysics, and Department of Otolaryngology, University of Colorado School of Medicine

The Naked mole-rat (*Heterocephalus glaber*) is increasingly being used as a laboratory mammal due to its resistance to aging and cancer, as well as other peculiar traits. The mole-rats live in eu-social, underground colonies of around 80 animals. The underground tunnels in which they live limit the range of acoustical information the animals are exposed to. Sounds attenuate rapidly through the burrow, and there are very limited sound localization cues. However the mole-rats do produce a wide range of vocalizations for communication, suggesting that sound, and thus hearing, play an important role in their lives.

Previous studies have suggested that the mole-rats have a degenerate hearing system. Published behavioral measurements show poor hearing thresholds, limited high frequency hearing, and poor sound localization abilities. And published anatomical measurements have shown intraspecific variations in middle and inner ear structures. Further studies have also shown that the mole-rats lack the HCN1 ion channel, which contributes to the integration of binaural inputs in the brainstem, thus potentially impeding their ability to effectively localize sounds.

In order to provide a more comprehensive understanding of hearing and sound localization ability in mole-

rats, we made various anatomical and physiological measurements. Specifically, we made measurements of the binaural interaction component (BIC) of the auditory brainstem response (ABR), which is a non-invasive electroencephalographic signature of neural processing of binaural sounds by brainstem neurons. We report that mole rats do have a measurable BIC of the ABR similar to other laboratory species commonly used for sound localization research. Additionally, we performed histological analysis to investigate the underlying neuroanatomy of the brainstem of these peculiar mammals. In conclusion, the naked mole rat may have a more refined auditory brainstem than previously shown, making them an interesting species for future sound localization research due to their unique ecology.

PS 78

The Effect of Anticipated Cue Reliability on Behavioral and Neural Adaptation in Barn Owls

Keanu Shadron; Roland Ferger; Jose L. Pena
Albert Einstein College of Medicine

The brain actively updates the representation of the environment through adaptation. An open question is whether this function is weighted by the predicted statistics of sensory information. Here we asked whether anticipated cue reliability affects the rate of adaptation in the auditory system of the barn owl.

The midbrain of the barn owl contains a map of auditory space, which uses the interaural phase difference to compute sound location in azimuth. Previous work showed that space-specific neurons in this map are tuned to the frequency range that is most reliable for its preferred location, an effect due to the acoustical properties of the head causing higher frequencies to convey interaural phase difference more reliably in frontal space and lower frequencies in the periphery.

We hypothesized that adaptation to sound location would differ between stimuli expected to be reliable or unreliable. We tested this hypothesis at the behavioral and neural-population levels. We measured the pupillary dilation response, an orienting response that readily adapts upon repetition of a stimulus. Tones were repeatedly presented through earphones to an awake barn owl, either from the front or periphery of the head to measure the habituation rate. To assess the strength of the novelty detection, a deviant in location was then presented to elicit a recovery of the PDR. Trials with higher cue reliability were compared to trials with low reliability to find trends in habituation. To assess this question at the neural-population level, we conducted recordings of multiple neurons in the space map using a

microelectrode array. Adapter and test stimuli were used to assess population activity and tuning of individual cells before and after adaptation. Frontal and peripheral neurons were compared to test the hypothesis that anticipated reliable and unreliable stimuli lead to different adaptation rates.

PS 79

Acoustic Cues to Sound Localization in the Common Ostrich (*Struthio camelus*)

Zoe Owruisky¹; John Peacock²; Nathaniel T. Greene³; Daniel J. Tollin⁴

¹University of Colorado Denver Anschutz Medical Campus; ²University of Colorado School of Medicine, Department of Physiology and Biophysics; ³University of Colorado School of Medicine, Department of Otolaryngology; ⁴Department of Physiology & Biophysics, and Department of Otolaryngology, University of Colorado School of Medicine

Background:

Terrestrial animals localize sound by having two ears on opposing sides of their head that receive sound with differential intensities, timing and spectral content. These differences depend on the size and shape of the head and external ear (pinna), as well as other anatomical features such as, for instance, a beak. The brain extracts these differences to determine the location of a sound; therefore, an animal's ability to localize sound depends in part on the available acoustic cues.

Sound localization ability varies considerably across species. Some differences can be understood in context of the range of acoustical information available to each species. Many studies have been conducted to measure the cues to sound localization available to various, mostly mammalian species.

Methods:

To extend these studies we made detailed measurements of the acoustic cues to sound localization in the common ostrich (*Struthio camelus*), a large flightless avian species in the ratite family. Measurements consisted of directional transfer functions (DTFs), the directional components of the head related transfer functions (HRTFs), in cadaveric ostrich heads. Probe-tube microphones were inserted (under the skin) into the ear canals near the tympanic membranes to measure sound pressure levels, simultaneously with tympanic membrane motion measured with laser Doppler vibrometers positioned bilaterally, when presented with sound from the full range of sound source locations, 775 locations in 7.5° steps in both azimuth and elevation. From the DTF

measurements, ITDs, ILDs, and spectral shape cues were computed.

Results:

Maximum ITDs calculated from low-pass filtered (below 2kHz) DTFs varied between +/-300 microseconds. ILDs likewise varied with source location and increased with frequency up to ~20 dB at 10kHz. As might be expected for an animal lacking pinnae, no distinct spectral notches were observed within the expected physiological range of hearing (< ~10 kHz). The spatial distribution of DTF amplitude gain spanned between 150-160° in elevation and 15-60° in azimuth, in line with the rearward-facing orientation and geometry of the ostrich ear canal.

Conclusions:

Overall, the acoustical information available to the ostrich is similar to predictions from a spherical head model. Based on the acoustical information alone, we might expect that it would be difficult for the ostrich to localize sound sources due to front-back confusions. However, like many non-mammals, the ostrich possesses other anatomical features such as interaural cavities that could enhance sound localization ability by allowing sound at one ear to alter responses at the other ear.

PS 80

Comparing Bat Biosonar with Generalized Soundfield Reconstruction and a Biosonar Model

Chen Ming¹; James Simmons¹; Michael Roan²

¹Brown University; ²Virginia Tech

While echolocating bats successfully carry out difficult tasks in complex surroundings, engineered sonars do not readily achieve such high performance, especially in cluttered conditions where clutter rejection is the primary problem for sonar or radar operation. Both bats and fast-moving autonomous vehicles that operate in airborne or underwater environments have to cope with clutter for reconstruction of sonar scenes and for guidance of locomotion to avoid collisions, find targets of interest, and register their positions in the overall scene. To acquire acoustic data for assessing the actual performance of bats in conjunction with a computational model of echolocation and also with generalized soundfield reconstruction methods, we devised a forward-looking sonar head with four ultrasonic microphones spaced in a square 23 mm on a side and surrounding the transmitting loudspeaker. For a robust design and easy swapping out of components, we chose a commercial high-frequency tweeter as the transmitter and commercial electret microphones preassembled with preamplification as

receivers. We broadcast simulated FM bat biosonar sounds and record both the broadcasts and all of the echoes that return from the surrounding scene. By performing crosscorrelation of signals pairwise from the four microphones with the broadcasts, both the direction and range of objects comprising the scene were determined and incorporated into images of the scene. The temporal evolution of the soundfield derived from generalized methods was used for reconstruction of the acoustic sonar scene and compared with the scene rendered by the sonar process. Besides registration of individual objects and the configuration of these objects in the scene, we introduce into the sonar processing stream a large-scale computer simulation model (Spectrogram Correlation and Transformation, or SCAT). The model is used to assess images obtained using algorithms derived from auditory research on bats compared to images obtained from conventional sonar processing, such as matched filtering. The SCAT model converts neurally-encoded pulse-echo stimuli into focused spatial images that depict the distance and direction of objects in the flight-path taken by the bat in flight tests. The model's capacity to "see" into a safe forward path through the scene is used to predict the bat's flight path. To bring the model into real condition, the complex acoustic backscatter from vegetation is measured to understand the bats'; perception of vegetation, and to simulate most foliage echoes by taking a few parameters that describe the vegetation.

PS 81

Near-field Sound Source Localization by the Plainfin Midshipman Fish

Nicholas Lozier¹; Jonathan Perelmuter²; Brooke Vetter³; Paul Forlano⁴; Joseph Sisneros³
¹UNIVERSITY OF WASHINGTON; ²CUNY Brooklyn College; ³University of Washington; ⁴Dept. of Biology, Brooklyn College, City University of New York; *Programs in Ecology, Evolution, and Behavior ; Neuroscience ; and Behavioral and Cognitive Neuroscience, The Graduate Center, City University of New York*

The plainfin midshipman fish (*Porichthys notatus*) has become a good model to explore how fishes localize underwater sounds because reproductive, gravid females exhibit innate, robust phonotactic responses to simulated male advertisement calls. Like most fishes, midshipman are thought to detect the particle motion component of sound using their inner ear otolithic end organs that essentially act as biological accelerometers. How and which end organs are used for sound source localization remains unclear. Here we present recent experiments that are part of a long term study

that examines the role of the inner ear auditory end organs (sacculle, lagena, and utricle) in sound source localization by the midshipman. Our recent experiments sought to test the hypothesis that binaural input from the sacculle and lagena is required for successful sound source localization. The otoliths from the sacculle and lagena (together) were either unilaterally or bilaterally removed in reproductive females that were then tested in a sound source localization assay. Sound source localization behavior was video recorded and later processed and analyzed in Image-J. Positive phonotactic responses were observed in the control (sham) group and observed in one case where both otoliths from the sacculle and lagena were unilaterally removed. None of the females with bilateral otolith removal of the sacculle and lagena (with bilateral utricle intact) were successful in the sound localization assay. Preliminary results suggest that binaural input of the sacculle and lagena may not be necessary for sound source localization in the midshipman. Alternative explanations for near-field sound source localization by the plainfin midshipman will be discussed.

PS 82

Neural Sensitivity to Dynamic Binaural Cues: Human EEG and Chinchilla Single-Unit Responses

Ravinderjit Singh¹; Hari Bharadwaj²; Mark Sayles¹
¹Purdue University; ²Speech, Language, & Hearing Sciences, and Weldon School of Biomedical Engineering, Purdue University

Animals typically encounter dynamic binaural timing information in broadband sounds such as speech and background noise. Dynamic binaural cues can result from: 1) moving sound sources, 2) self motion, or 3) reverberation. Most studies of inter-aural time delay (ITD) or inter-aural correlation (IAC) sensitivity have used static or sinusoidally varying inter-aural signals. However, neural sensitivity to change in ITD and IAC is rarely systematically addressed.

We used systems-identification techniques to characterize neural responses to the dynamics of changing ITDs and IACs in broadband sounds. We used a maximum length sequence (MLS) to modulate either the ITD, or the IAC of a broadband noise carrier. Neural responses were recorded from humans (electroencephalogram; EEG) and from single neurons in terminally anesthetized chinchillas (auditory nerve fibers; ANFs). IAC jumped between -1 and +1. ITD jumped between -0.5 and +0.5 ms for EEG, and between -0.5 cycles of CF and 0 ms for ANF experiments. Amplitude modulation (AM) was applied at the same rate as the resolution of the MLS so that phase discontinuities occurred at the troughs of the AM.

Single-unit ANF responses were obtained using standard in-vivo electrophysiological techniques. Spikes were recorded from ANFs in response to “ipsi” and “contra” channels, presented in an interleaved sequence. Sound level was varied over a 20-dB range from near threshold to near saturation. From these spike times, we performed across-ear coincidence analyses to predict responses of binaurally sensitive brainstem neurons (e.g., medial superior olive). From the predicted brainstem “coincidence” spikes we derived impulse responses describing the neuron’s response to changes in ITD and IAC using circular cross correlation techniques. EEG data was collected from humans using a 32-channel cap. Impulse responses were derived for each channel in the EEG using similar deconvolution methods applied in the single unit data.

ITD and IAC transfer functions estimated from ANF responses were low-pass, with corner frequencies in the range of several hundreds of Hz. EEG-based transfer functions, presumably reflecting cortical responses, were also low-pass, but with much lower corner frequencies in the region of tens of Hz.

In conclusion, broadband system-identification techniques are useful for characterizing neural sensitivity to dynamic binaural temporal cues. Future experiments will compare EEG- and single-unit derived cortical limits of dynamic tracking to human perceptual measures of detecting dynamic fluctuations in ITD and IAC and the ability to use these dynamics for unmasking.

Funding: NIH-T32DC016853, NIH-R01DC015989, Showalter Trust.

PS 83

Population Responses to Single and Competing Stimuli in the Barn Owl’s Auditory Space Map

Roland Ferger¹; Michael V. Beckert¹; Keanu Shadron¹; Brian J. Fischer²; Jose L. Pena¹

¹Albert Einstein College of Medicine; ²Seattle University

Since the discovery of a midbrain map of auditory space, the barn owl, a nocturnal hunter with outstanding sound localization abilities, has become a model organism to study neural circuits computing and representing binaural cues relevant for sound localization. Neurons in the owl’s midbrain respond maximally to acoustic stimuli with distinct combinations of interaural time and level differences (ITD, ILD). Together, these neurons form a topographic representation of auditory space which supports sound-orienting behavior. However, open questions regarding how the neural population

in the map is read out on a trial-by-trial basis remain unanswered. This work, using a microelectrode array to record multiple units across the map, reaches beyond responses of single neurons to investigate the relationship between the activity pattern across the neural population and behavior.

Recent work has shown that the read out of population activity by a population vector (PV) predicts orienting head saccades, and approximates Bayesian statistical inference by integrating the overrepresentation of frontal directions and the differential shape of spatial tuning curves across the map. We show that the trial-by-trial variability of neural activity matched predictions made under a Bayesian model, which matches a PV to the behavioral output. When a stimulus becomes less reliable (e.g. by decorrelation of the binaural signal) an animal’s performance becomes less accurate. The Bayesian model predicts that this should manifest in a broadening of the population response in the map. An alternative hypothesis that could explain this behavioral effect is that the reduced reliability induces shifts in the population response, which are indistinguishable from a response to a different ITD, termed differential correlations. We tested which model was better matched by the trial-by-trial population activity across a number of stimulus conditions. This analysis showed that the population activity and correlation structure matches predictions of the Bayesian/PV model.

Additionally, the PV model could break down when competing stimuli from different directions are presented at the same time. We explored whether the global inhibition network described in the owl’s optic tectum for selecting dominant stimuli, could restore population activity patterns consistent with a PV readout. We found that the population activity under two-sound stimulation remained consistent with predictions of a PV readout of the higher priority stimulus.

Central Vestibular Pathways

PS 84

MicroRNA expression in the vestibular nucleus after unilateral labyrinthectomy

Moo Kyun Park¹; Mun Young Chang²; Sohyeon Park³; Myung-Whan Suh¹; Jun Ho Lee¹; Seung Ha Oh⁴; Young-Kook Kim⁵; Young Ho Kim⁶

¹Seoul National University Hospital; ²Chung-Ang University College of Medicine; ³Seoul National University; ⁴Seoul National University College of Medicine; ⁵Chonnam National University Medical School; ⁶Seoul National University College of Medicine, Boramae Medical Center

Background: Vestibular compensation is a process of rebalancing of resting activities of bilateral vestibular nuclei neurons resulting in homeostasis of bilateral excitability. MiRNAs are abundant in the brain and play a crucial role in the development and function of the neuronal network including neurogenesis, synaptogenesis and regulation of morphogenesis. We investigate which miRNAs are involved in the vestibular compensation after UVD. This study could lay some foundation for future study of the functional mechanism of miRNA involved in vestibular compensation as well as neuronal plasticity.

Methods: This study consisted of seven steps: identification of the vestibular compensation course, microarray analysis, quantitative RT-PCR validation of miRNAs expression, validation study using oligomers of candidate miRNAs, target pathway analysis of candidate miRNAs, Luciferase assay of candidate miRNA, and Target RNA and Protein analysis. To make UVD, labyrinthectomy was performed at left side of SD rats. We measured the rotarod rod, spontaneous nystagmus, head roll tilt and postural asymmetry to identify the course of vestibular compensation. microarray was performed at two time points when vestibular compensation did not fully progress and reached the maximal level to select the candidate miRNAs. In microarray analysis, in addition to comparison between UL and SO groups, comparison between two time points in UL group was used as criteria for candidate selection. Then twelve miRNAs were selected as the candidate miRNAs and qRT-PCR was performed for validation. After that, miR-218a-5p, 219a-5p, 221-3p and 1298 were selected as the candidate miRNAs. To validate whether these four candidate miRNAs affected the vestibular compensation, we compared the results of rotarod test and immunohistochemistry for 5-bromo-2'-deoxyuridine (BrdU) after UVD between the control group and the groups that candidate miRNA oligomers were administered.

Result: The 218a-5p and 219a-5p groups showed both delayed recovery of rotarod scores and decreased neurogenesis in MVN. In the 221-3p group, recovery of rotarod scores were delayed though neurogenesis did not decrease. We performed the pathway analysis of miR-218a-5p, 219a-5p and 221-3p. Most miR-218a-5p pathways were related with signal transmission or neuronal system. Luciferase assay showed that miR-218a-5p controls the Robo1 gene expression. Expression of DRP-3 which is down streaming pathway of Robo1 was changed after labyrinthectomy.

Conclusions: Our findings indicate that miR-218a-5p, 219a-5p and 221-3p are important in regulating the vestibular compensation.

PS 85

Effects of hypergravity on changes in serotonin receptor expression of vestibular nuclei in rats

Kyu-Sung Kim¹; Hyun Ji Kim¹; Eun Hae Jeon²

¹Inha University Hospital; ²Inha University Hospital

Objectives: Motion sickness occurs as a result of a mismatch or conflict between the information arising from the vestibular system, the visual and proprioceptive inputs. Many different environments can cause motion sickness including travelling on land, sea or space. The activation or blockade of serotonin receptors is known to be closely related with migraine and motion sickness. In this study, we investigated the effects of hypergravity on vestibular function using VOR analysis and changes of gene expression of serotonin receptors in vestibular nuclei. **Methods:** Using an animal rotator, we assessed the vestibular function (recording the eye movement) after hypergravity loads(4G for 24hours, 4weeks) in rats(aged 7~8weeks, weighing 250-300gm). We estimated the VOR responses, gain, asymmetry and phase at 0.04, 0.08, 0.16, 0.32Hz on earth vertical axis rotation. And we also checked the recovery of the VOR response after stopping the hypergravity stimulation. We investigated the effects of the centrifugation-induced gravity changes on gene expression of serotonin receptors (5HT1B, 5HT2A,5HT1D, 5HT1F) in vestibular nuclei. **Results:** Under 4G for 24hrs stimulation for 4weeks, the gain at 0.04, 0.08, 0.16, 0.32 Hz were 0.463 ± 0.113 , 0.524 ± 0.455 , 0.494 ± 0.093 , 0.509 ± 0.198 respectively. They showed significant reduction of VOR gain compared to the control group. Decreased VOR gains were recovered to a normal range on 3~4days after stopping the hypergravity stimulation. 5-HTR expression was increased in the vestibular nuclei. Exposure to 4G for 4weeks showed differential modulation of gene expression of serotonin receptors in vestibular nuclei. **Conclusion:** By observing the data, hypergravity stimulation affects the vestibular function and modulation of gene expression in vestibular nuclei. We can induce the results that long-term hypergravity stimulation causes remarkable changes on VOR gain in rats. And this altered gravity also induced differential modulation of several target gene expression in vestibular nuclei in rats. (NRF-2018R1A6A1A03025523)

Wireless Inertial Measurement of Activity and Head Kinematics in a Rat Model of Acute Unilateral Vestibular Loss Reveal Persistent Dynamic Vestibular Deficit Symptoms

Viviana Delgado-Betancourt¹; Guillaume Dugué²; Pauline Liaudet¹; Vincent Descossy¹; Mathieu Petremann¹; **Jonas Dyhrfeld-Johnsen¹**

¹Sensorion; ²Institut de Biologie de l'École Normale Supérieure

Patients suffering acute unilateral vestibular loss employ different coping strategies to reduce vertigo and dizziness ranging from simple reduction of overall movement (immobility and bed rest) to more subtle and lasting postural, gait and in particular head kinematic modifications. As an example, recent follow-up of post-surgical vestibular schwannoma patients revealed persistent changes in head kinematics compared to healthy controls, including significant reduction in head turn velocity (Paul et al., 2018). Vertigo and non-evoked vestibular deficit evaluation in preclinical models has generally been restricted to evaluation of gross deficits compensated after the acute phase, using videonystagmography recordings, qualitative assessment of posturo-locomotor symptoms and static postural deviation as measures. We here report persistent changes in spontaneous activity level and head turns determined using a wireless inertial head-mounted sensor in a rat model of acute unilateral vestibular lesion.

A head-post was surgically implanted on 13 adult female Long-Evans rats (200-225 g) under tiletamine-zolazepam-xylozine anesthesia for mounting of the 9-axis digital inertial sensor with onboard battery and Bluetooth transmitter. Following a baseline recording (30 min) under open field conditions, an excitotoxic vestibular lesion was induced using transtympanic injection of 45 mM kainate under isoflurane anesthesia. Recordings were subsequently repeated 1 hour and 1/2/7/14/21/28 days after lesion induction.

The percentage of time spent immobile in the open field arena increased from 33% at baseline to 85% after vestibular lesion induction and remained significantly elevated (+11%) at D28 ($p=0.015$, 1-way repeated measures ANOVA). Similarly, the median spontaneous head turn velocity decreased from 39.5 deg/s at baseline to <1.5 deg/s at 1h after lesion and remained reduced at 23.5 deg/s at D28. The head turn velocity cumulative distribution functions remained significantly different at D28 ($p<0.001$, 1-way repeated measures ANOVA).

Contrary to other approaches quantitative posture-

locomotor evaluation such as video monitoring, the inertial sensor output is immediately quantitative, does not require large amounts of digital storage space and is easily treatable using mathematical transforms in broadly available software packages such as MatLab or R. The described persistent changes in spontaneous activity level and head kinematics demonstrate the ability of wireless inertial measurements in freely moving animal models to deliver translationally valid, clinically relevant outcome measures for evaluation of long-term effects of acute phase vertigo interventions as well as pharmaceutical strategies for enhancing central compensation.

PS 87

The expression of c-Fos in anxiety-related nuclei after intratympanic gentamicin administration

Feng Zhai¹; Jie Chen²

¹Shanghai Children's Medical Center; ²Department of Otolaryngology, Shanghai Children's Medical Center Affiliated with Shanghai Jiaotong University School of Medicine

Objectives: To research into the expression alterations of c-Fos in the anxiety-related nuclei (parabrachial nucleus (PBN), bed nucleus of stria terminalis (BNST) and dorsal raphe nucleus (DRN)) in the vestibular-impaired animal model through intratympanic gentamicin administration.

Materials and Methods: We injected gentamicin (30mg/ml) intratympanically into adult C57BL mice weighing from 22 to 25g and observed the expression alterations of c-Fos in PBN, BNST and DRN through immunohistochemical analysis 3 and 7 days after the injections. The data were analyzed through ANOVA and Bonferonni paired comparison method. Stata 12.0 software was used.

Results: Three days after gentamicin administration, the expression of c-Fos in BNST increased significantly and decreased to some extent 7 days after the injection, indicating elevated anxiety level; Three and 7 days after gentamicin administration, the expression of c-Fos in BNST increased significantly, indicating elevated arousal level; No significant differences in the expression of c-Fos in DRN were noted among the three different groups </p>

Conclusions: Peripheral vestibular impairment could activate the neurons in BNST and PBN, thereby increase the levels of anxiety and arousal. BNST and PBN might mediate the pathophysiological process of peripheral vertigo induced anxiety.

Key words: Peripheral vertigo; Anxiety; Parabrachial nucleus, Bed nucleus of stria terminalis; Dorsal raphe nucleus.

The Localization and Chemoanatomical Phenotype of Vestibular Nuclear Neurons with Direct Projections to Nucleus Tractus Solitarius (NTS).

Amelia H. Gagliuso¹; Emily K. Chapman¹; Giorgio P. Martinelli¹; Gay R. Holstein²

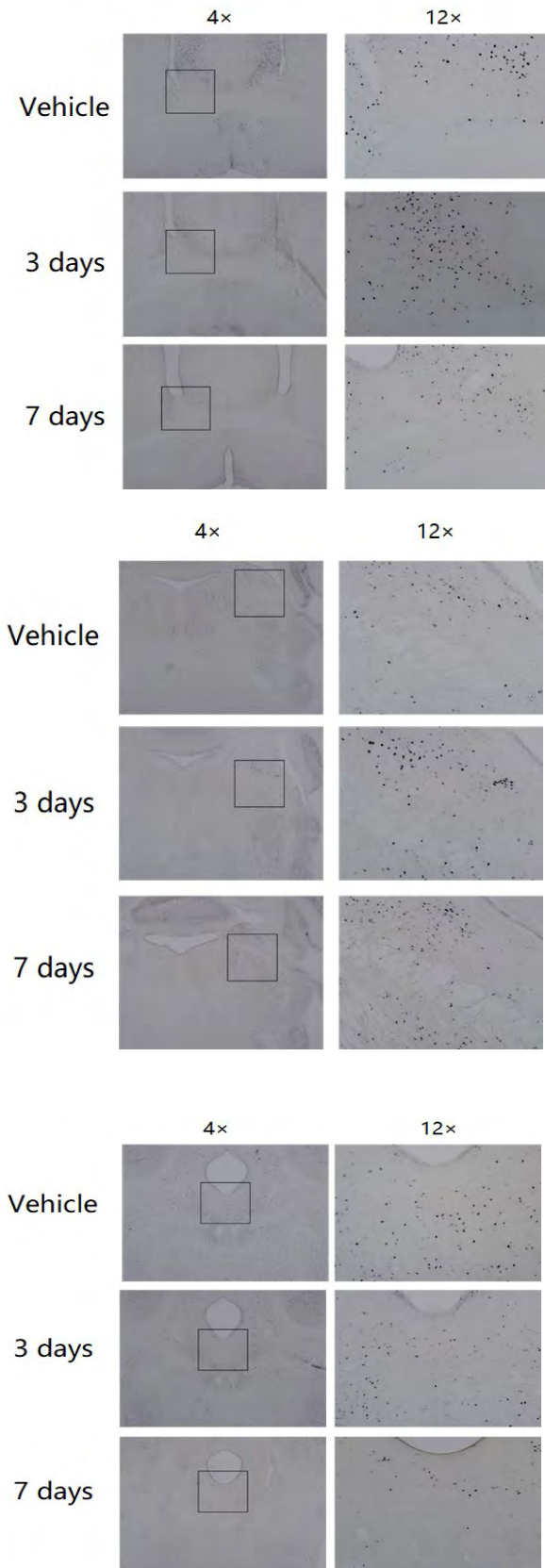
¹Icahn School of Medicine at Mount Sinai; ²Icahn School of Medicine Mount Sinai

Background: Consistent cerebral perfusion is necessary to provide the brain with a stable supply of oxygen and glucose. During a sudden change in posture or at the onset of movement, the vestibulo-sympathetic reflex (VSR) mediates a rapid change in blood pressure to compensate for the shift in body position. Over time, the baroreflex reasserts homeostatic control over cardiovascular function.

The VSR pathway initially conveys signals from vestibular end organs to areas of the vestibular nuclei (VN). In turn, neurons in these regions project to key pre-sympathetic sites for integration of cardiovascular signals such as the rostral and caudal ventrolateral medullary regions. The baroreflex pathway relays signals from arterial baroreceptors to NTS which, in turn, projects to the same pre-sympathetic sites as the VSR. The primary goal of the present study was to characterize the VN projection to NTS, which could provide an anatomical basis for direct vestibular control of the baroreflex.

Methods: Unilateral iontophoretic injections of the retrograde tracer FluoroGold (FG) were placed in the caudal NTS of 9 male Long-Evans rats. After 10 days, the animals were euthanized by mixed aldehyde perfusion and the brainstems were serially sectioned. Skip-serial section sets were used to map the tracer injection sites, characterize the FG-filled VN neurons, and visualize the principal amino acid neurotransmitter(s) of these VSR-related neurons.

Results: VN neurons with direct projections to NTS were located almost exclusively in the caudal portion of the medial vestibular nucleus (MVN). There were few FG-immunolabeled cells in the inferior vestibular nucleus, or in the more rostral VN cell groups. Most FG-labeled MVN neurons were located ipsilaterally. Immunofluorescence studies were conducted to localize glutamate, GABA and imidazoleacetic acid-ribotide (IAA-RP), a neuromodulator involved in blood pressure regulation, in FG-filled VN neurons. Most of the FG-labeled VN neurons co-localized glutamate-immunofluorescence, while only a small minority co-localized GABA. Many of the FG- and glutamate-immunofluorescent neurons also co-localized IAA-RP, and/or were surrounded by GABA-immunofluorescent puncta.



Conclusions: Direct VN projections to NTS exist and are derived primarily from neurons in the caudal region of the ipsilateral MVN. These neurons appear to utilize glutamate for neurotransmission, with IAA-RP present as a neuromodulator. Many of these neurons are under GABAergic inhibitory control. Overall, this study demonstrates an anatomical basis for direct vestibular control of the baroreflex.

Funding: Supported by NIH/NIDCD grant 1R01DC008846 (GRH).

PS 89

Comparison of Vestibular Nucleus Neurons Activated by Unilateral Electrical Stimulation of the Posterior Canal Nerve and by Pulsed Infrared Laser Stimulation (pIR) of the Posterior Canal

Emily K. Chapman¹; Amelia H. Gagliuso¹; Darrian L. Rice²; Suhrod M. Rajguru³; Giorgio P. Martinelli¹; Gay R. Holstein⁴

1Icahn School of Medicine at Mount Sinai; 2University of Miami; 3Department of Biomedical Engineering and Otolaryngology, University of Miami; 4Icahn School of Medicine Mount Sinai

Background: Rapid changes in head position are detected by the vestibular system and trigger modulations in blood pressure that serve to maintain consistent cerebral perfusion. These compensatory adjustments are mediated by the vestibulo-sympathetic reflex (VSR) pathway. This pathway can be activated experimentally by galvanic vestibular stimulation, tilt, and pIR. We have previously demonstrated that there are direct projections from the caudal vestibular nuclei (VNC) to several key pre-sympathetic sites in the ventrolateral medulla that mediate the VSR. Our current research seeks to determine the specific contributions of individual vestibular end organs to the VSR. Toward that end, the present study was conducted to identify the brainstem locations and cytology of VSR-related VNC neurons activated by stimuli specifically targeting the posterior canal (PC), and to compare the neuronal populations activated by unilateral pIR stimulation of the PC with those activated by unilateral electrical stimulation of the PC nerve.

Methods: pIR at 1863 nm, 250 pps baseline pulse frequency, and 200 μ s pulse duration was directed through the round window toward vestibular end organs in rats. Changes in blood pressure and heart rate were detected using a telemetric sensor implanted in the aorta and recorded using Ponemah software (DSI Inc.; MN). Evoked eye movements were recorded using video oculography. Cells that were activated by pIR

were identified by cFos/DAB immunohistochemistry. These cells were counted in skip-serial sections through the VNC, and the cell counts from each rat were mapped onto 16 representative rostro-caudal Bregma levels and normalized for comparison across subjects. In some animals, the retrograde tracer FluoroGold was placed in the pre-sympathetic medullary region two weeks prior to pIR stimulation. In three additional rats implanted with sensors, the PC nerve was activated by electrical stimulation (biphasic bipolar, 200Hz pulse rate, 0.05Hz modulation and responses were recorded as above.

Results: Following unilateral pIR activation of the PC, the highest density of cFos-positive cells was located in a narrow rostrocaudal belt between Bregma levels -11.40 and -11.88. These neurons were concentrated in the caudal medial vestibular nucleus contralateral to the stimulation site. A far more extensive pattern of activation was observed following PC electrical stimulation, including c-Fos-immunostained neurons in rostral regions of the vestibular nuclei.

Conclusions: The PC participates in the activation of the VSR through VNC neurons located in the contralateral MVN, and pIR provides significantly greater stimulus specificity than electrical stimulation.

Funding: NIH NIDCD 1R01DC008846 (GRH) and 1R01DC013798 (SMR).

PS 90

Vestibular Inputs are Processed Through Anatomically Distinct Mossy Fiber Pathways to Physiologically Distinct Subtypes of Unipolar Brush Cells in Cerebellum

Timothy S. Balmer¹; Laurence O. Trussell²
¹OHSU; ²Oregon Health & Science University

In the cerebellum, mossy fibers convey multimodal signals from diverse regions, converging in the granule cell layer. Unipolar brush cells (UBCs) are excitatory interneurons found within the granule cell layer of vestibular processing lobes and whose roles in cerebellar processing are not well understood. UBCs receive a single mossy fiber ending on their brush-like dendrite that slows the removal of glutamate from the synapse. Thus, this unique dendritic morphology causes prolonged glutamate exposure that dramatically transforms extrinsic mossy fiber activity before projecting to local granule cells and other UBCs through its own intrinsic mossy fiber axons. Recently, differences in UBC subtypes based on synaptic physiology separated UBCs into two categories- ON UBCs, whose glutamate responses are mainly AMPA receptor-mediated and

thus increase their firing in response to glutamate, and OFF UBCs that have large mGluR2-mediated inhibitory currents, which causes a decrease in firing. In order to understand the function of this transformation of extrinsic input, it is essential to know the sources of mossy fibers to each subtype of UBC. For example, if both subtypes receive common input, then the ON/OFF distinction in UBCs would allow mossy signals to diverge, setting up distinct processing pathways within the granule cell layer. On the other hand, if each subtype receives mossy fiber input that conveys a distinct vestibular modality, then ON and OFF UBCs would mediate modality-specific transformations of extrinsic inputs.

We investigated this question in the vestibular cerebellar nodulus (lobe X). Transgenic mouse lines and viruses were used to express channelrhodopsin specifically in primary or secondary vestibular mossy fiber sources. Retrograde AAVs were used to label axons in lobe X and were followed to their input hair cells in the vestibular end organs. This revealed that primary vestibular afferents to ON UBCs carry angular head acceleration signals from the semicircular canals. Postsynaptic recordings from UBCs in acute brain slices showed that ON UBCs receive direct primary afferent input from vestibular ganglion neurons and OFF UBCs do not. By contrast, secondary vestibular projections from the medial vestibular nucleus project to both UBC types. Striking differences were observed in the morphology of mossy fibers carrying primary vs secondary signals, as well as in the size of UBCs receiving these distinct inputs, regardless of their ON/OFF subtype. Thus, unlike the cerebellar granule cell that integrates multimodal signals, the different subtypes of UBC function to transform specific signals through distinct anatomical pathways.

PS 91

Vestibular Nucleus Activity is Correlated with Limb Movements of Rhesus Monkeys During Treadmill Walking

Erez Gugig; Kathleen E. Cullen
Johns Hopkins University

Locomotion is a natural behavior that is common across many species. To maintain balance during locomotion in everyday life, the sensorimotor system integrates inputs from multiple modalities, including the vestibular and proprioceptive systems, with motor-related information. In the vestibular system, the primary sensory afferents carry information from the vestibular sensors to neurons in the vestibular nuclei. In turn, the vestibular nuclei send direct and indirect projections via descending vestibulospinal pathways to the spinal cord. Previous experiments in alert cats have shown that vestibular nuclei

neurons are modulated during voluntary locomotion on a treadmill (Matsuyama and Drew 2000a,b). Typically, neurons discharge with a double peak pattern for each cycle of locomotion. However, a limitation of these prior studies was that head was not restrained. Consequently, it was not possible to dissociate whether the observed responses were activity correlated with limb motion or rather reflected responses to vestibular inputs. For example, during head unrestrained walking, vertical acceleration will likely be associated with the initiation of the stance phase of walking.

Accordingly, to understand the information encoded by the vestibular nuclei neurons during walking, we recorded from single neurons in monkeys while they walked on a treadmill with their heads held stationary relative to the world. Specifically, we determined whether and how neuronal activity is modulated during locomotion in the absence of accompanying vestibular stimulation. Limb movements were tracked via video and quantified with markerless tracking. We found that the average response of most neurons increased during treadmill walking compared to rest. Moreover, neuronal activity was modulated in phase with the locomotor rhythm. Notably, in contrast to prior reports in head-unrestrained cats, we found that vestibular nuclei cells respond with a single predominate peak per cycle during head-restrained treadmill walking (i.e. in the absence of vestibular stimulation). To address the possibility that the additional peak observed in cat might reflect vestibular rather than limb related responses, we recorded head motion during normal head unrestrained walking. We confirmed the presence of large vestibular inputs (i.e., vertical acceleration) at the initiation of the stance for each set of hind and forelimbs. Thus, in conclusion, our findings establish that the activity of vestibular nuclei neurons in rhesus monkeys is elevated relative to rest and correlated with limb movements during treadmill walking. We suggest this limb-related modulation of primate vestibulospinal pathways serves an important role in control and balance during locomotion.

PS 92

Encoding of Eye-related versus Vestibular Information by the Nucleus Prepositus of Mice during Voluntary Movements

Hui Ho Vanessa Chang¹; Shan Zhu²; Kathleen E. Cullen²
¹McGill University; ²Johns Hopkins University

The vestibular system plays a crucial role in our everyday life as it ensures gaze and postural stabilization and the sense of self-motion by detecting the head motion in space. To maintain a stable representation of spatial

orientation, visual and non-visual signals such as vestibular and proprioceptive signals are required. It has been proposed that the nucleus prepositus hypoglossi (NPH) and the supragenu nucleus (SGN) in brainstem relay vestibular information from the vestibular system to head direction (HD) network. Based on experiments in rodents, it has been suggested that this pathway produces an internal compass of the head's direction relative to space that is vital for spatial cognition. However, the NPH has also been long-known to comprise the oculomotor integrator which plays an essential role in eye movement control by holding the eye at eccentric position in the orbit after saccade. Further, a recent study in non-human primates (Dale & Cullen, 2013), established that neurons in the NPH predominantly encode eye-related rather than head-related movement signals during both passively-generated and voluntary head movements. To date, however, it remains unknown whether neurons in the NPH of rodents encode eye-related and/or head-related movement signals.

We hypothesized that NPH neurons in mouse, as in primate, preferentially encode eye-related rather than head-related signals during voluntary movement. To test this hypothesis, we developed a mouse model in which we could record eye movements both during head retrained behavioral protocols (Beraneck & Cullen, 2007) including: vestibular-ocular reflex (VOR), visuo-vestibular conflict (VORC), optokinetic reflex (OKR) and changes in static eye position (SEP), as well as during voluntary head movements. Notably, the mice were trained to make active head movements to the left and right in response to an auditory tone. Further, to measure mouse eye movement during active head movements, we used a MEMS based magnetic field sensor, which measured the location of a magnet implanted in the eye in the orbit. Our preliminary single unit recording experiments indicate that indeed consistent in non-human primate model, neuron in the NPH of mice output eye-related information during active head movement.

PS 93

Linear versus Nonlinear Vestibular Information Processing in Posterior Thalamocortical Vestibular Pathway; Implications for Self-motion Perception

Hamed Hooshangnejad¹; Jerome Carriot²; Maurice J. Chacron²; Kathleen E. Cullen¹

¹Johns Hopkins University; ²McGill University

In the vestibular system, head motion is first detected by the vestibular sensors in the inner ear and then transmitted to the vestibular nuclei by afferents. In turn, the vestibular nuclei send this information to cortical areas via two thalamocortical pathways, anterior and

posterior. Here we recorded the responses of single neurons in the ventral posterior lateral (VPL) thalamus of macaque monkeys to understand how the posterior thalamocortical vestibular pathway encodes vestibular information.

We first applied traditional linear analysis by testing neuronal responses to low amplitude (15 deg/s) sinusoidal yaw rotations and computing their response gains (0.5-17 Hz). The amplitude of the applied sinewaves was chosen to not induce obvious nonlinearities such as cut-off or saturation, while the frequency range was chosen to span that of natural movement (0-20 Hz). We found that VPL neuronal response gains ((sp/s)/(deg/sec)) typically reached values greater than in the earliest stages of vestibular processing (i.e., vestibular nuclei neurons and afferents that provide their peripheral input). Further, VPL neurons demonstrated "band pass" tuning (i.e., highest sensitivity for frequencies from 2 - 15 Hz), in contrast to vestibular nuclei neurons and afferents, which demonstrated "high pass" tuning over the same range. We then used two specific approaches to probe nonlinear coding in VPL neurons. We first again applied sinusoidal yaw rotations, but varied the amplitude for each frequency from 0 to 100 deg/s. Such stimuli elicited significant nonlinearities in these cells; neuronal response gains decrease markedly with increasing amplitude. We next tested whether the principle of superposition holds, by testing neuronal responses to stimulation using band-limited white noise whose frequency content was i) limited to a low frequency band (0-5 Hz), ii) limited to a high frequency band (15-20 Hz), and iii) comprised the low and high frequency band stimuli applied concurrently. Our results showed that neuronal responses were not linear, but rather neuronal sensitivities to low frequency stimulus were significantly attenuated (30%), when applied concurrently with high frequency stimulation.

Taken together, these findings emphasize that the thalamus is more than a simple relay station between early vestibular processing and cortex. We suggest that the increased sensitivity of VPL thalamic neurons in the posterior thalamocortical vestibular pathway to low amplitude movements facilitates self-motion perception by providing low detection threshold, while their tuning preferentially encodes information with frequency content associated with the self-motion experienced in everyday life.

PS 94

Spatio-temporal processing for motion perception by fully immersive visual scene according to scale of motion sickness

Sungkwang Hong; Jeong Hye Park; Euncheon Lim
Department of Otolaryngology, Hallym University
College of Medicine

Purpose of the study: Visual cues could lead to the illusory sensation of self-motion by relative motion difference between an observer and a scene. Our hypothesis is that different spatio-temporal processing may elicit for motion perception according to characteristics of the visual scene (constant vs. acceleration) and motion sickness scale. We attempted to explore the dynamics of spatio-temporal processing by motion sickness (MS) scale based on electrophysiological template obtained from healthy subjects.

Materials and methods: Twenty right-handed subjects without evidence of motion-sickness and 15 subjects with motion-sickness based on results of simulator sickness questionnaire (SSQ) and visual analog scale (VAS) were recruited. Head mount display integrated with infrared-based eye tracker display (SMI, Teltow, Germany USA) were used to embody an immersive virtual environment. During EEG acquisition (Brain product GmbH, Gilching, Germany), the participants performed the oddball tasks consisting of visual flow with acceleration and constant. MATLAB-based toolbox "eConnectome" were used for estimating over the directional interactions among functional areas of the brain.

Results: Theta oscillation was initiated from the right parieto-insular vestibular cortex (PIVC) at an earlier time, and PIVC consistently transmitted those signals into another brain area for acceleration condition while that transmission of theta oscillation from PIVC was only appeared at around 1s for constant stimulation. In addition, functional connectivity in subjects with high-MS scale revealed that PIVC may be a functional area. Interestingly, alpha oscillation from right PIVC was transmitted into another brain area regardless of speed gradient (acceleration vs. constant) or group difference.

Conclusion: we could conclude that PIVC work as modulation center for visually induced motion perception by selective inhibition and excitation of the neural signal from visual or motion-sensitive cortices.

Development I

PS 95

Generation of an Epitope-Tagged Human Embryonic Stem Cell Line for Modeling CHARGE Syndrome with Human Inner Ear Organoids

Jing Nie; Andro Botros; Eri Hashino
Indiana University School of Medicine

CHARGE syndrome is a congenital anomaly disorder that affects multiple organs. The most prevalent clinical feature is malformation of the inner ear structures, resulting in prelingual deafness and vestibular dysfunction. The main cause of CHARGE syndrome is dominant mutations in the CHD7 gene, which encodes an ATP-dependent chromatin remodeling protein that regulates the expression of a large number of genes through epigenetic modifications. We sought to investigate how mutations in CHD7 affect inner ear development using human embryonic stem (ES) cell-derived inner ear organoids as a model system. Elucidating the function of CHD7 protein requires a highly specific antibody. However, we found none of the widely used commercially available CHD7 antibodies were specific, as multiple cross-reacting bands were present on western blots, even with CHD7 null mutant ES cells. We therefore used CRISPR genome editing technology to knock in a 3xFlag tag to the C-terminus of the endogenous CHD7 allele. Human ES cells were transfected with a 3xFlag donor vector and a high fidelity Cas9 ribonucleoprotein complex specific to the CHD7 stop codon locus. The established CHD7-3xFlag ES cell lines were validated with PCR and Sanger sequencing for correct 3xFlag insertion, and were tested for pluripotency and off-target mutations. In both ES cells and ES cells-derived human inner ear organoids, anti-Flag antibody immunofluorescence signal overlapped with anti-CHD7 signal. Importantly, compared to the multiple non-specific anti-CHD7 bands, the anti-Flag antibody detected a single bright band at ~336 kDa on the western blot, demonstrating high specificity. The human 3xFlag-tagged CHD7 ES cells will serve as a valuable tool for studying the mechanisms underlying the pathophysiology of CHARGE syndrome in the inner ear and other organs.

In vivo simultaneous germline inactivation of multiple genes in mouse through CRISPR/Cas9-mediated base editing

He Zhang¹; Hong Pan¹; Changyang Zhou¹; Yu Wei¹; Wenqin Ying¹; Shuting Li¹; Guangqin Wang²; Chao Li²; Yifen Ren¹; Gen Li³; Xu Ding³; Yidi Sun⁴; Geng-Lin Li⁵; Lei Song³; Yixue Li⁴; Hui Yang⁶; **Zhiyong Liu**²

¹*Institute of Neuroscience, Chinese Academy of Sciences*; ²*Institute of Neuroscience, CAS Center for Excellence in Brain Science and Intelligence Technology, Shanghai Institutes for Biological Sciences, Chinese Academy of Sciences*; ³*Department of Otolaryngology-Head and Neck Surgery, Ninth People's Hospital, Shanghai Jiao Tong University School of Medicine*; ⁴*Key Lab of Computational Biology, CAS-MPG Partner Institute for Computational Biology, Chinese Academy of Sciences*; ⁵*University of Massachusetts, Amherst, MA, USA*; ⁶*Institute of Neuroscience, Chinese Academy of Sciences*

In vivo genetic mutations has become a powerful tool for dissecting gene function; however, multi-gene interaction and compensatory mechanisms involving can make findings from single mutations at best difficult to interpret, and at worst, misleading. Hence, it is necessary to establish an efficient way to disrupt multiple genes simultaneously. The CRISPR/Cas9-mediated base editing disrupts gene function by converting a protein coding sequence into a stop codon; this is referred to as CRISPR-stop. Its application in generating germline mutations in zygotes has not been well explored yet. Here, we firstly performed a proof-of-principle test by disrupting *Atoh1*, a gene critical for auditory hair cell generation. Next, we individually mutated *vGlut3*, *Otoferlin* and *Prestin*, three genes needed for normal hearing function. Finally, we successfully disrupted *vGlut3*, *Otoferlin* and *Prestin* simultaneously. Our results show that CRISPR-stop can efficiently generate single or triple homozygous F0 mice mutants, bypassing laborious mouse breeding. We believe that CRISPR-stop is a powerful method that will pave the way for high-throughput screening mouse developmental and functional genes, matching the efficiency of methods available for model organisms, such as *Drosophila*.

PS 97

Hair Cell Mechanotransduction Regulates Spontaneous Activity and Spiral Ganglion Subtype Specification in the Auditory System

Shuohao Sun¹; Travis A. Babola¹; Gabriela Pregernig²; Joseph C. Burns²; Ulrich Müller³

¹*Johns Hopkins University*; ²*Decibel Therapeutics*; ³*Johns Hopkins University School of Medicine*

Type I spiral ganglion neurons (SGNs) transmit sound information from cochlear hair cells to the CNS. Using transcriptome analysis of thousands of single neurons, we demonstrate that murine type I SGNs consist of subclasses that are defined by the expression of subsets of transcription factors, cell adhesion molecules, ion channels and neurotransmitter receptors. Subtype-specification is initiated prior to the onset of hearing during the time period when auditory circuits mature. Gene mutations linked to deafness that disrupt hair cell mechanotransduction or glutamatergic signaling perturb the firing behavior of SGNs prior to hearing onset and disrupt SGN subtype specification. We thus conclude that an intact hair cell mechanotransduction machinery is critical during the pre-hearing period to regulate the firing behavior of SGNs and their segregation into subtypes. Since deafness is frequently caused by defects in hair cells, our findings have significant ramifications for the etiology of hearing loss and its treatment.

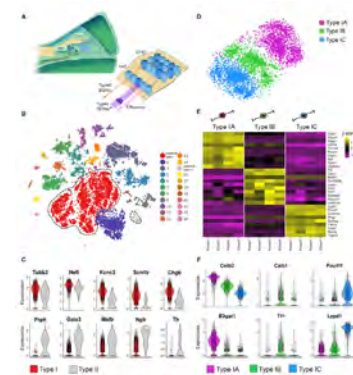
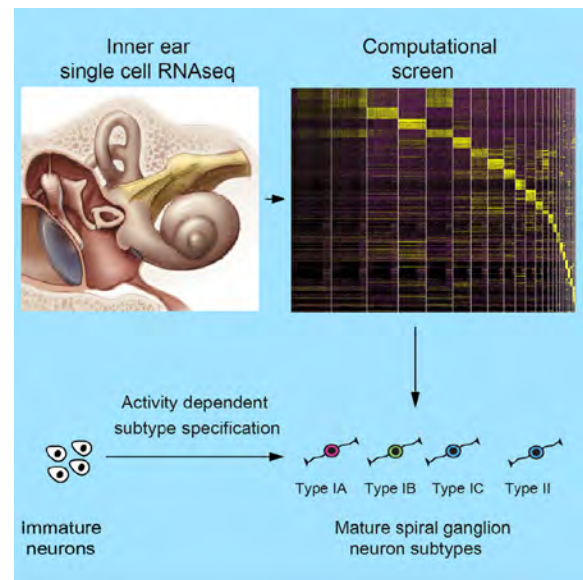
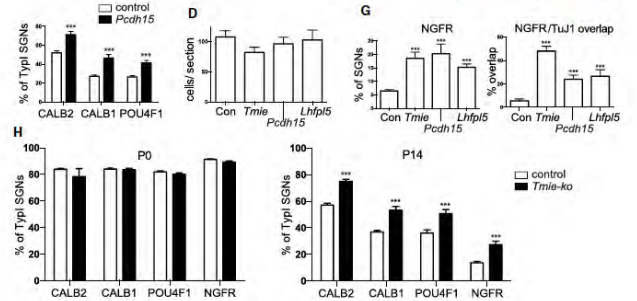
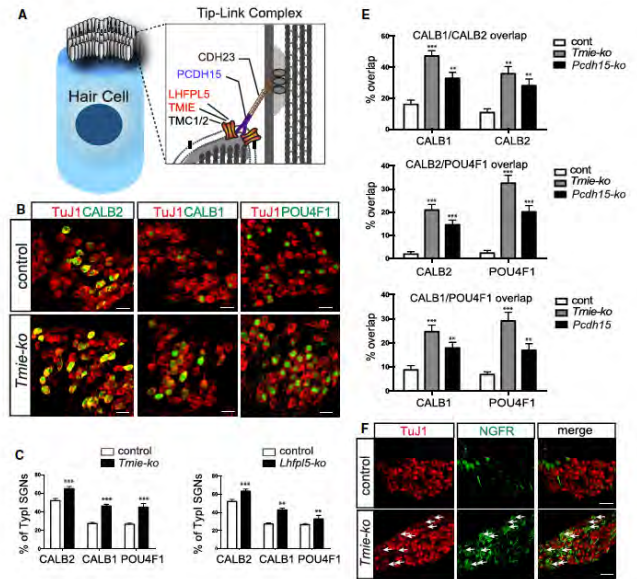
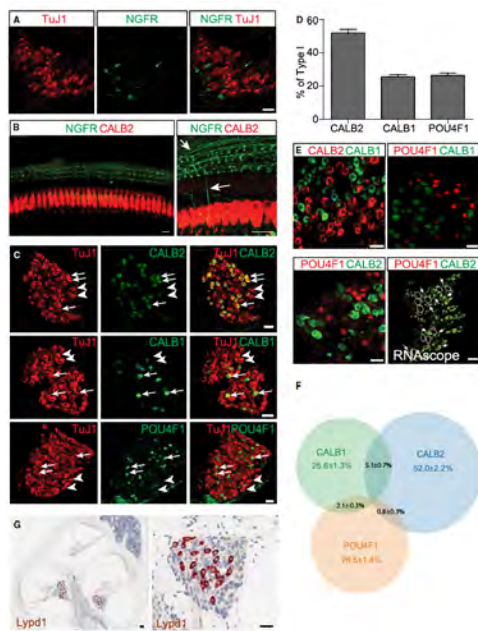
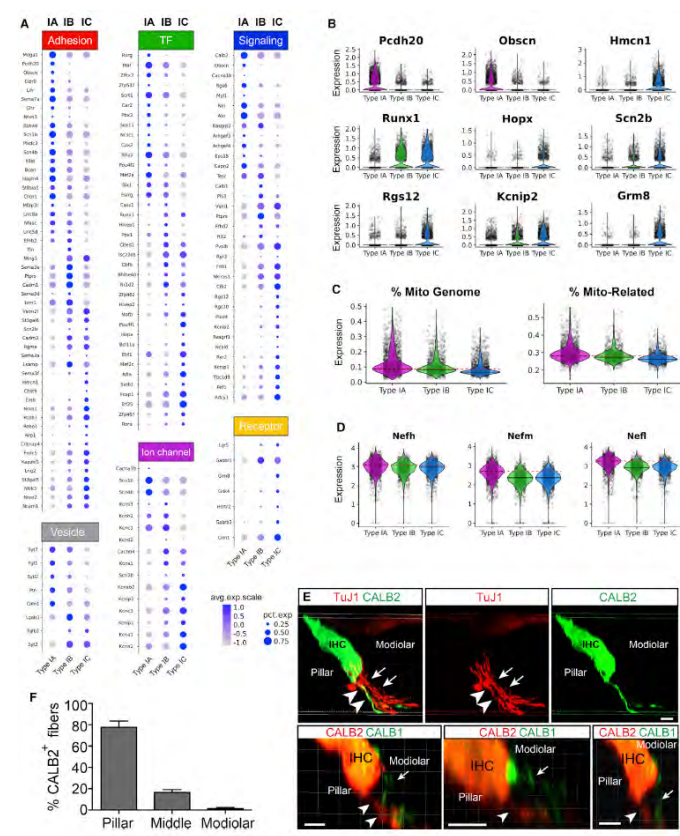


Figure 1. Identification of subtypes of type I SGNs. **A**, Schematic of the inner ear. **B**, t-SNE plot of single-cell RNA-seq data. **C**, Heatmap of gene expression across subtypes. **D**, Heatmap of gene expression across subtypes. **E**, Heatmap of gene expression across subtypes. **F**, Heatmap of gene expression across subtypes. **G**, Heatmap of gene expression across subtypes. **H**, Heatmap of gene expression across subtypes. **I**, Heatmap of gene expression across subtypes. **J**, Heatmap of gene expression across subtypes. **K**, Heatmap of gene expression across subtypes. **L**, Heatmap of gene expression across subtypes. **M**, Heatmap of gene expression across subtypes. **N**, Heatmap of gene expression across subtypes. **O**, Heatmap of gene expression across subtypes. **P**, Heatmap of gene expression across subtypes. **Q**, Heatmap of gene expression across subtypes. **R**, Heatmap of gene expression across subtypes. **S**, Heatmap of gene expression across subtypes. **T**, Heatmap of gene expression across subtypes. **U**, Heatmap of gene expression across subtypes. **V**, Heatmap of gene expression across subtypes. **W**, Heatmap of gene expression across subtypes. **X**, Heatmap of gene expression across subtypes. **Y**, Heatmap of gene expression across subtypes. **Z**, Heatmap of gene expression across subtypes.



PS 98
Characterization of Recently Identified Candidate Hearing Loss Genes
 Melissa McGovern¹; Basel Jazzar²; Andrew Groves³
¹Department of Neuroscience, Baylor College of Medicine; ²Baylor College of Medicine; ³Department of Neuroscience, Department of Molecular and Human Genetics, Baylor College of Medicine

Congenital hearing loss, which is prevalent throughout the world, results when the cochlea fails to develop and mature properly. Often, congenital hearing loss results from the inherited mutation of genes necessary for cell fate specification or mature cell function. Identification of genes related to hearing development and function have historically been identified when multiple patients with hearing loss present with a mutation of the same gene. As with many tissues, identification of novel genes that are integral to development of the hearing organ is important for the development of both prophylactic and therapeutic interventions. Recently, analysis of targeted genetic mutations developed by the International Mouse Phenotyping Consortium revealed 52 novel candidate hearing loss genes. When mutated, these genes caused ABR threshold shifts suggesting they play a role in



either the development, maturation, or normal function of the hearing system. To better understand the stage when each gene contributes to hearing, we performed in situ hybridization on frozen sections from wild type mouse cochleae at multiple time points during normal development and maturation of the hearing organ. At birth, most genes are expressed ubiquitously throughout the cochlea from the spiral ganglion throughout the sensory and non-sensory epithelium, and the lateral wall including the stria. One gene, DNase1 was specifically expressed within the stria while another gene, Basigin, had a higher level of expression in the stria compared to the rest of the cochlea. Adgrb1, Ube2b, and Med28 were specific to the spiral ganglion, while Odf3l2 and Baiap2l2 showed expression predominantly in the hair cells. Further investigation into two other time points is currently underway to understand how these genes change from development to maturation. Understanding the expression patterns of these novel hearing loss genes will enhance our understanding of how the cochlea develops, matures, and functions to be better prepared to develop strategies to combat hearing loss in the future.

PS 99

Investigation for roles of macrophages during embryonic development of the mouse cochlea

Ippei Kishimoto¹; Takayuki Okano²; Koichi Omori³
¹*Department of Otolaryngology-Head and neck surgery, Graduate School of Medicine, Kyoto University;* ²*Department of Otolaryngology-Head and Neck surgery, Graduate School of Medicine, Kyoto University;* ³*Department of Otolaryngology-Head and Neck Surgery, Graduate School of Medicine, Kyoto University*

Background

The role of cochlear resident macrophages are mostly unknown, but recent studies have reveal the functional aspects of cochlear macrophages such as cell clearance. We showed that the resident macrophages which might be originated from hematopoietic progenitors in the yolk sac appeared around the cochlea at embryonic day (E) 10.5 and appears to become matured during embryonic and early postnatal development with in situ proliferation potentials while changing their distribution in the cochlea (ARO 40th and 41st Annual MidWinter Meeting). Colony stimulating factor 1 (Csf1) is a growth factor that regulates the survival, proliferation and differentiation of the mononuclear phagocyte lineage. This time, we show results of the further study about macrophage in the cochlea investigating the roles of macrophage during embryonic development using Csf1 receptor (Csf1r) null mice.

Methods

The temporal bones of homozygous Csf1r-null and wild type mice at postnatal day (P) 0 were dissected out, and the specimens were perfused with 4% paraformaldehyde in phosphate buffer overnight and cryoprotected with 30% sucrose. Specimens were prepared for cryostat sections and the midmodiolar sections were provided for hematoxylin and eosin (H&E) staining and fluorescent immunohistochemistry (IHC). We used anti Iba-1 antibody as surface marker of macrophage. We performed comparison of morphologies of main structures in the cochlea between homozygous Csf1r null mice and wild type mice by IHC. That is, we assessed SG neurons with anti-neurofilament antibody, cochlear vascularity with anti-CD31 antibody, hair cells with anti-Myosin VIIA antibody. We also evaluated glial cells around SG neurons with anti-Sox10 antibody and performed quantitative comparison of Sox10-positive cell density in the SG.

Results

IHC using anti-Iba1 antibody showed that there were macrophages in the cochlea of wild type mice, while no macrophages in the cochlea of homozygous Csf1r null mice. Evaluation of cochlear morphology with H&E staining and IHC using anti-neurofilament, anti-CD31 and anti-MysinVIIA antibody showed no apparent difference among homozygous Csf1r-null and wild type mice. However, IHC using anti-Sox10 antibody showed a mild, but not significant, trend toward higher density of Sox10 positive cells in the cochlear SG of Csf1r null mice than that of wild types.

Conclusion

Resident cochlear macrophage doesn't seem to alter gross morphogenesis of the cochlea during embryonic development, however, it may contribute to auditory nerve refinement by regulating glial cell number in the SG.

PS 100

Exploring Tmprss3 Function in Stem-Cell Derived 3D Inner Ear Organoids

Pei-Ciao Tang¹; Karl Koehler¹; Jing Nie¹; Alpha Alex²; Jiyeon Lee¹; Eri Hashino¹; **Rick F. Nelson**¹
¹Indiana University School of Medicine; ²Indiana University

Mutations in the type II transmembrane serine protease 3 (Tmprss3) gene cause non-syndromic autosomal recessive deafness (DFNB8/10). Mouse harboring a truncation mutation in the C-terminal protease domain of Tmprss3 (Tmprss3Y260X) show normal inner ear hair

cell development followed by rapid hair cell degeneration between P12 and P14 (Fasquelle et al., 2011). Thus, *Tmprss3* is required for normal inner ear hair cell survival. To date, little is known about the physiologic function of *Tmprss3* in the inner ear.

Here we used three different approaches to examine the function of *TMPRSS3*: 1) embryonic stem cell (ESC) derived from *Tmprss3*^{Y260X} and control mice, 2) CRISPR/Cas9n engineered *Tmprss3* knockout-2A-nGFP knockin ESC line with isogenic controls, and 3) ESCs constitutively expressing 3XFLAG-tagged *TMPRSS3*.

ESC-derived inner ear organoids from *Tmprss3*-mutant mice and *Tmprss3*-knockout display normal hair cell development and uptake of FM-143. This is followed by progressive elevation in markers of apoptosis and rapid hair cell degeneration in *Tmprss3*-knockout organoids. Voltage gated potassium channel (BK channel) expression is reduced in *Tmprss3*-knockout hair cells. *Tmprss3* undergoes self-cleavage and localizes to the cytoplasm and cell membrane.

We conclude that functional *Tmprss3* is required for inner ear organoid hair cell survival in mouse ESC-derived inner ear organoids and genetically engineered inner ear organoids recapitulate in vivo pathophysiology.

PS 101

Sensorineural hearing loss in *Lrrtm3* mutant mice, a model for autism spectrum disorder

Han Seul Choi¹; Hyehyun Min¹; Ji Won Um²; Jinwoong Bok¹

¹Yonsei University College of Medicine; ²Daegu Gyeongbuk Institute of Science and Technology (DGIST)

Background

Autism spectrum disorder (ASD) is an early-onset neurodevelopmental disorder that is characterized by impaired social interaction and communication, repetitive behavior, and stereotyped patterns of interests. Some of the earliest signs of ASD involve atypical responses of auditory cortex to the sound, and recent studies reported increased hearing thresholds and decreased otoacoustic emissions in children with ASD in the mid-range frequencies. However, the etiology of hearing loss associated with ASD is unclear.

Methods

To understand the mechanism of hearing loss associated with ASD, we analyzed a knockout mouse model of *Lrrtm3* (leucine-rich repeat-containing transmembrane

protein 3), whose mutations have recently been associated with ASD in humans. *Lrrtm3* is a post-synaptic adhesion molecule, which is shown to interact with pre-synaptic proteins to form trans-synaptic complexes and contribute to the excitatory synapse development.

Results

When analyzed hearing function using auditory brainstem response (ABR) tests, the ABR thresholds were increased in *Lrrtm3* knockout mice as early as 3 weeks of age with incomplete penetrance. Thus, *Lrrtm3* knockout mice were divided into two groups based on hearing function; hearing loss (HL) and normal hearing (N). The hearing loss became progressively deteriorated with age in the HL group. Histological analyses revealed no obvious differences between HL and N groups in cochlear structures such as the organ of Corti and spiral ganglion neurons. The lack of structural defects led us to analyze the wave I amplitudes of ABR, which represent the signal intensities transmitted from the hair cells to spiral ganglion neurons. There was a significant reduction in the wave I amplitudes in the *Lrrtm3* knockout mice (HL) compared to wild type littermates. Immunofluorescent analysis using a presynaptic marker CtBP2 and a postsynaptic marker GluA2 showed that the synaptic morphology between hair cells and afferent fibers of spiral ganglion neuron was defective and the numbers of synapses were reduced. We also observed that stereocilia bundles of the inner and outer hair cells became progressively disorganized, which is followed by hair cell loss.

Conclusion

These results suggest that abnormal synapse formation and subsequent hair cell loss is the major causes of hearing loss in *Lrrtm3* deficient mice. We are currently investigating the mechanism of how *Lrrtm3* contributes to synapse formation and hair cell maintenance.

Supported by the Brain Korea 21 PLUS Project for Medical Science, Yonsei University

PS 102

Endodermal Signals Direct Neural Crest Cells to Form Specific Middle Ear Ossicles

Harinarayana Ankamreddy¹; Hyehyun Min¹; Jae Yoon Kim¹; Xiao Yang²; Eui-Sic Cho³; Un-Kyung Kim⁴; Jinwoong Bok¹

¹Yonsei University College of Medicine; ²Beijing Institute of Lifeomics; ³Chonbuk National University; ⁴Kyungpook National University

Background

The mammalian middle ear consists of a chain of ossicles: malleus, incus, and stapes. These ossicles transmit the sound waves from the outer ear to the inner ear in the form of mechanical vibrations. Defects in any of the ossicles can lead to conductive hearing loss. It is known that the middle ear ossicles are derived from neural crest cells (NCCs). NCCs from rhombomere (r) 1 and 2 migrate into pharyngeal arch (PA) 1 to form malleus and incus, while NCCs from r4 migrate into PA2 to form stapes. However, the molecular mechanism of how NCCs find their destinations and develop into specific ossicles is still unclear.

Methods

To investigate the roles of Sonic Hedgehog (SHH) or TGF- β signaling in NCC development into middle ear ossicles, a mediator of SHH (Smoothed; Wnt1-Cre; Smolox/lox) or a transcriptional mediator of TGF- β (Smad4; Wnt1-Cre; Smad4lox/lox) was specifically deleted in NCCs. To confirm the sources of the signaling molecules, Shh (Foxg1Cre; Shhlox/lox) or Bmp4 (Foxg1Cre; Bmp4lox/Tm1) was specifically deleted in the pharyngeal endoderm. Gene expression patterns, NCC lineage, cell proliferation, and cell death analyses were examined by in situ hybridization, R26R reporter, EdU analysis, and TUNEL analysis, respectively.

Results

Inactivation of responsiveness to SHH signaling in NCCs (Wnt1-Cre; Smolox/lox) or deletion of endodermal Shh expression (Foxg1Cre; Shhlox/lox) resulted in the loss of initial condensation of malleus-incus in PA1 but not of stapes in PA2 at embryonic day (E) 10.5, indicating that SHH signaling emanating from the endoderm of PA1 is specifically required for malleus-incus condensation. However, stapes condensation was lost in these mutants at E11.5 with increased cell death, suggesting that SHH signal was also required for further development of the ossicles by promoting cell survival. In contrast, inactivation of TGF- β /BMP signaling in NCCs by deleting Smad4 (Wnt1-Cre; Smad4lox/lox) or deletion of endodermal Bmp4 expression (Foxg1Cre; Bmp4lox/Tm1) resulted in the loss of initial condensation of stapes in PA2 but not of malleus-incus in PA1. NCC lineage cell were not observed in the prospective stapes region with no apparent cell death, suggesting that endodermal BMP4 signaling guides NCCs to migrate and differentiate into stapes in PA2.

Conclusion

Our results show that region-specific interactions between the migratory NCCs and the pharyngeal

endodermal play an important role in directing NCCs to differentiate into specific middle ear ossicle.

Supported by BK21 PLUS Project for Medical Science, Yonsei University College of Medicine

PS 103

In vivo Regulation of the Fragile X Mental Retardation Gene During Embryonic Development of the Auditory Brainstem

Diego AR Zorio¹, Xiaoyu Wang¹, Yuan Wang^{1, 2}

¹Florida State University, Department of Biomedical Sciences; ²Program in Neuroscience, Florida State University

Fragile X mental retardation protein (FMRP) is an mRNA-binding protein that regulates a multitude of synaptic proteins and signaling pathways involved in neurological diseases. Loss of FMRP leads to the fragile X syndrome (FXS), which is characterized with hyperactivity, intellectual disability, sensory dysfunction, and difficulties in social communication. However, how FMRP expression is regulated during normal brain development is not understood.

We have previously reported a highly dynamic expression of FMRP in the developing brainstems of mice and chickens. We discovered a stage-specific alternative splicing event that causes retention of intron 8 of Fmr1 RNA. Remarkably, this event is conserved with regard to its temporal association with developmental milestones of auditory circuits between mouse and chicken. Moreover, we demonstrated for the first time that FMRP is capable binding to the 3' region of its intron 8 in a very specific manner, leading to a hypothesis that FMRP protein inhibits its own expression by producing an mRNA with premature stop codons and this regulation is most distinct during certain developmental stages.

We continue our efforts to elucidate this mechanism at the cellular level by focusing on the chicken nucleus magnocellularis (NM), the avian analogue of the mammalian anteroventral cochlear nucleus (AVCN). We had three novel findings. First, recombinant chicken FMRP specifically binds its intron 8 in a way that competes with the binding of a splicing factor U2AF65 to the same site. Second, nuclear localization of FMRP in NM neurons is developmentally programmed in a way temporally overlapping with the intron retention event. Finally, exogenous Fmr1 transcripts do not increase FMRP levels in vivo when intron retention is intensively present, although they do at earlier or later ages, suggesting a strong posttranscriptional control. Taken together, we identified a novel FMRP auto-regulation mechanism in vivo that tightly regulates its own level during critical periods of circuit and synaptic development.

Transcriptional Profiling of Perinatal Spiral Ganglion Neurons Using Single Cell RNA-Seq

Tessa R. Sanders¹; Hanna E. Sherrill¹; Madison Mehlferber¹; Michael C. Kelly²; Matthew Kelley³

¹Laboratory of Cochlear Development, National Institute on Deafness and Other Communication Disorders, National Institutes of Health; ²Single Cell Analysis Facility, National Cancer Institute, National Institutes of Health; ³NIDCD

The afferent innervation to the cochlea is composed of the spiral ganglion neurons (SGNs), which transmit mechanosensory input from the hair cells centrally to the cochlear nucleus as an electrochemical signal. Despite its importance, relatively little is known about the degree of cellular diversity within the spiral ganglion (SG). Two populations of SGNs can be distinguished in the mammalian cochlea, based on their morphology: Type 1 SGNs which constitute 90-95% of the total population, and form contacts with inner hair cells (IHCs); and Type 2 SGNs which constitute the remaining 5-10% of the total population and form contacts with outer hair cells (OHCs). However, considering the complexity of auditory information that these neurons must encode, and in light of recent molecular studies of the entire adult SGN population, there appears to be more neuronal phenotypic diversity present in the SG than previously understood.

We undertook a FACS-based single cell RNA-Seq approach to profile the molecular diversity of the SGN population during the pre-hearing developmental period. A total of 121 and 187 single cells were sequenced at embryonic day 16 (E16) and postnatal day 1 (P1), respectively. At E16 the SGN population appears to be broadly heterogeneous, which is consistent with the developmental processes known to be occurring at this time point. At P1 unbiased clustering identified three transcriptionally distinct groups. However, these groups did not correspond to the three sub-groups of type 1 SGNs recently identified in the adult SG. Additionally, there was no evidence at this time point of transcriptionally distinct type 2 SGNs. Type 2 markers such as Tyrosine Hydroxylase were expressed more broadly across all three groups.

Overall this dataset indicates that at P1 SGNs have yet to mature into their distinct adult phenotypes. We are now determining the transcriptional trajectory of SGNs across the early postnatal period by utilizing single nucleus RNA-Seq which should reduce potential contamination from glia and mesenchymal cells. This approach will also enable us to sequence a much greater number of SGNs at each time point. Additionally,

it will provide us with transcriptional information of non-neuronal cells within the SG which should lead to better contextualization of the SGN across this developmental period.

PS 105

Differentiation of mouse embryonic stem cells into inner ear cell-like cells in co-culture with HEI-OC1 cells

Nathaniel Carpena¹; Jae-Hun Lee²; So-Young Chang²; Ji Eun Choi¹; Jae Yun Jung¹; Min Young Lee¹

¹Department of Otorhinolaryngology-Head & Neck Surgery, College of Medicine, Dankook University; ²Beckman Laser Institute Korea, College of Medicine, Dankook University

Background:

Recent attempts in generating inner ear hair cells from stem cells in vitro require several exogenous bioactive molecules, such as BMP4, TGF- β i, FGF2 and Wnt. The most straightforward and common ways to deliver these molecules to the culture system is via well timed and gradual addition of bulk molecules. Several studies also showed stem cells being able to differentiate when co-cultured with special cells or cultured in conditioned media. HEI-OC1 expresses specific markers of cochlear hair cells (HCs) and supporting cells which could represent a common progenitor for sensory and supporting cells of the organ of Corti. Several studies have provided evidence of damaging effects of archetypal ototoxic drugs to HEI-OC1 as well as the therapeutic effects of stem cells on them. However, it is unknown if HEI-OC1 cells can promote the differentiation of embryonic stem (ES) cells. The objective of this study is to determine whether the endogenous inductive factors from HEI-OC1 cells can induce the differentiation of ES cells into HC phenotype through co-culture.

Materials and Methods:

Embryonic bodies (EBs) were formed using ES cells via hanging drop technique. EBs and dissociated ES cells were co-cultured with a conditioned and inactivated layer of HEI-OC1 cells for 14 days. Differentiated cells were immune-stained for oct4, sox2 and myosin VIIa and quantified for gene expression using PCR and western blotting.

Results:

The dissociated ESCs coalesced into an EB like form yet smaller than the actual co-cultured EBs. Furthermore, both the co-cultured forms of ESCs expressed Myosin7a

and only in the periphery showed Sox2 expression. Co-cultured EBs developed organoid outgrowths with Myo7a and Sox2-positive cells after 14 days of contact co-culture with HEI-OC1 cells. Dissociated ESCs form dense EB-like aggregates and expressed Myo7a while Sox2-positive cells are only found around the periphery after 14 days of co-culture. ESCs and EBs were also cultured in conditioned medium (CM) from HEI-OC1 cells suspecting soluble factors alone could have a similar effect. However, the ESCs did not form into aggregates yet still showed to be Myo7a positive while the EBs degenerated.

Conclusions:

The present study suggests that cellular interaction between ES cells and HEI-OC1 cells may stimulate the differentiation of ES cells towards a HC-like cells. However, further work is needed to determine the viability of the differentiated cells to further develop in vivo.

Acknowledgements:

This study was supported by the Ministry of Science, Information and Communications technology (ICT) and Future Planning grant funded by the Korean Government (NRF-2016R1D1A1B0393624), and supported by Leading Foreign Research Institute Recruitment Program through the National Research Foundation of Korea (NRF) funded by the Ministry of Science and ICT (MSIT) (NRF-2018K1A4A3A02060572).

PS 106

Photobiomodulation enhanced stem cell differentiation to inner ear like organoid

So-Young Chang¹; Nathaniel Carpena²; Seyoung Mun³; Jae Yun Jung²; Hosup Shim³; Phil-Sang Chung²; Ji Eun Choi²; Min Young Lee²

¹Beckman Laser Institute Korea, College of Medicine, Dankook University; ²Department of Otorhinolaryngology-Head & Neck Surgery, College of Medicine, Dankook University; ³Department of Nanobiomedical Science & BK21 PLUS NBM Global Research Center for Regenerative Medicine, Dankook University

Background:

The study of cochlear hair cells regeneration which caused by irreversible hearing loss have been conducted around the world. Stem cell therapy is one of the potential therapeutic tools for inner ear diseases. However, differentiation process to generate cochlear hair cells from stem cells is relatively difficult and

complicated compare to other differentiation. Recent advances of adopting photobiomodulation (PBM) for the stem cell therapy showed that stem cells and progenitor cells have favorable responses to light. PBM has been shown to stimulate different types stem cells to migrate, proliferate and differentiate in vitro (Arany et al. 2014, Barboza et al. 2014, Kushibiki et al. 2015) and in vivo (Min et al. 2015, Soares et al. 2015). Meanwhile, very little is known about the effect of PBM on the differentiation of embryonic stem (ES) cells towards the otic lineage. In this study, we determined the optimal condition to differentiate the stem cell into the otic organoid. Different culture techniques and cell density has been tested and effect of photobiomodulation was analyzed.

Materials and Methods:

A mouse embryonic stem cell with GFP was used. Embryoid-body (EB) formation was obtained by two methods (monolayer culture and hanging drop technique). For the differentiation of inner ear like organoid, on the second day of differentiation, BMP4 and SB431542 were treated for Non-neural ectoderm induction and FGF2 and LDN193189 were treated for Pre-placodal ectoderm induction on the third day of differentiation to induce into ectoderm. They were cultured until differentiation Day 6 and were observed until day 18. LEDs (470 nm, 630 nm and 740 nm) were used in maturation phase (Day 6 to 8). The cells were directly irradiated at an intensity of 40 mW for 750 s per day. Epifluorescence (MyosinVIIa, ROS & intracellular calcium level), RT-qPCR and RNA-Seq were analyzed.

Results:

EB formed by hanging drop was much larger than monolayer culture. The diameter of EBs statistically increased with the increase of cellular density but the largest number of organoids was observed at the density of 4.0 x 10⁵. MyosinVIIa positive cells inside the organoid was observed and confirmed by RT-qPCR. Only 630 of LED irradiation increased the organoid formation rate. EBs with PBM (630 nm) showed higher expression of MyosinVIIa and lesser expression of Oct4 compared to differentiation without PBM. ROS was overexpressed as well. With the RNA seq analysis among the biological process, nervous system development-related processes are enriched with only down-regulated genes in PBM group. Among the down regulated genes Hes5 which inhibits the hair cell transdifferentiation process are negatively down-regulated in PBM group.

Conclusions:

EB formation was generated by hanging drop technique, and differentiation of EBs into inner ear hair cell-like cells were enhanced by PBM with

LED. Investigation on gene expression showed the factors that are responsible for the therapeutic effect of PBM in the formation of otic organoids.

Acknowledgements:

This study was supported by the Ministry of Science, Information and Communications technology (ICT) and Future Planning grant funded by the Korean Government (NRF-2016R1D1A1B0393624), and supported by Leading Foreign Research Institute Recruitment Program through the National Research Foundation of Korea (NRF) funded by the Ministry of Science and ICT (MSIT) (NRF-2018K1A4A3A02060572).

PS 107

Astrocyte Calcium Activity in the Developing Inferior Colliculus is mediated by mGluR5 Receptors

Vered Kellner; Travis A. Babola; Dwight Bergles
Johns Hopkins University

Patterned bursts of spontaneous neuronal activity occur in the auditory system of developing animals before the onset of hearing. This activity originates in the cochlea and propagates throughout the auditory system, including the inferior colliculus (IC). Neuronal activity in the developing IC occurs in discrete bands, corresponding to isofrequency zones apparent after hearing onset. Recent studies indicate that astrocytes in developing circuits mature in parallel with surrounding neurons to establish the tripartite relationship necessary to sustain synaptic activity. Moreover, astrocytes have the potential to affect synaptic development and maturation, through release of synaptogenic factors, such as hevin and thrombospondin. Astrocytes during this period of development express the metabotropic receptor mGluR5, which is well positioned to link neuronal activity to gene expression changes and secretion from astrocytes. Extrasynaptic receptors such as those on astrocyte membranes require bursts of presynaptic activity to raise the glutamate concentration high enough to enable activation. Thus, the patterns of spontaneous activity that occur in the developing auditory system are well suited to enable activation of astrocyte receptors.

To explore the role of astrocytes in the development of the auditory system, we imaged astrocyte calcium activity in the IC of awake mice using genetically encoded calcium indicators targeted specifically to astrocytes. We found that astrocyte calcium activity in the IC closely follows the spatial and temporal patterns of neuronal activity – these events were transient, bilateral and oriented along future isofrequency zones like those exhibited by neurons. However, the astrocyte calcium transients were less frequent and longer in duration than neuronal events, as expected due to the

higher threshold for activation of metabotropic receptors and the requirement for second messenger-dependent calcium release. Pharmacological inhibition of mGluR5 dramatically reduced spontaneous activity in astrocytes in the IC, but did not alter spontaneous activity of surrounding neurons, indicating that this metabotropic receptor is necessary for activation of astrocytes. Future studies using astrocyte-specific deletion of mGluR5 will help reveal the role of this receptor in generating astrocyte activity, and the involvement of this mode of neuron-astrocyte signaling in controlling the maturation of astrocytes and neuronal circuits.

PS 108

Proteolytic Targets of Caspase-3 in Auditory Brainstem Development

Forrest Weghorst¹; Yeva Mirzakhanyan¹; Kian Samimi¹; Mehron Dhillon¹; Paul D. Gershon¹; Karina S. Cramer²
¹*University of California, Irvine*; ²*University of California Irvine, Dept. of Neurobiology and Behavior*

Background: The computation of interaural time differences (ITDs) for azimuthal sound localization requires ultraprecise circuitry in the auditory brainstem. In the chick, this circuitry consists of the bifurcating axons of the cochlear nucleus, N. magnocellularis (NM), which project both ipsilaterally and contralaterally to the coincidence detector, N. laminaris (NL). We have previously shown that NM axons express the active form of an apoptotic protease, caspase-3, between embryonic days 7 and 13, a time that coincides with the formation of NM-NL synapses. We have also shown that pharmacological inhibition of caspase-3 activity in the brainstem causes both NM axonal mistargeting and NL morphological disruption prior to the period of developmental cell death in either nucleus. This suggested that caspase-3 acts in a non-apoptotic manner to ensure proper ITD circuit formation. However, little is known about the proteolytic targets of caspase-3 in developmental contexts. We thus sought to identify these targets using protein mass spectrometry of the ITD circuit during development.

Methods: A caspase-3 inhibitor or vehicle solution was injected into the IVth ventricle over the auditory brainstem on E9 and E10 in whole embryo cultures. Six hours after the final injection, brainstems were dissected, and the dorsorostral quadrant of the brainstem, which contains NM and NL, was isolated. Trypsinized samples were subjected to liquid chromatography tandem mass spectrometry (nanoLC-MS/MS), which yielded the peptide content of each sample. Peptides with non-tryptic termini were filtered for those with the D/E.X signature of caspase proteolysis (an aspartate

(D) or glutamate (E) residue immediately N-terminal to the cleavage site). Peptides observed exclusively in vehicle-treated brainstems were considered likely products of *in vivo* caspase cleavage in NM axons. We used functional annotation clustering of parent proteins to identify non-redundant enriched classes of proteins among the putative caspase targets. Results were validated by immunohistochemistry against representative proteins from enriched functional groups.

Results: We found a significant enrichment of proteins involved in translation, protein degradation and cell adhesion. Representative proteins from enriched classes colocalized with active caspase-3 in NM axons.

Conclusions: Our results suggest that caspase-3 influences ITD circuit development in part by cleaving the cellular machinery that regulates protein life cycle. This study also validated a novel approach to screen for targets of caspase proteolysis.

PS 109

Characterization of Cochlear Development using Single-Cell RNA-seq

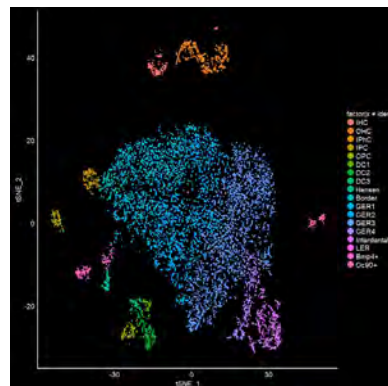
Likhitha Kolla¹; Michael C. Kelly²; Joseph Mays¹; Adam T. Palermo³; Kathy S. So³; Matthew Nguyen³; Joseph C. Burns³; Matthew Kelley⁴

¹NIDCD/NIH; ²NCI/NIH; ³Decibel Therapeutics; ⁴NIDCD

The sensory epithelium of the mature cochlea comprises an elaborate mosaic of sensory hair cells and non-sensory supporting cells which work together to mediate hearing. During cochlear development, individual otocyst-derived epithelial precursor cells must transition through multiple transcriptional states in order to acquire distinct cell-fates. To begin to identify the different cell states and the factors that mediate those transitions, we collected and sequenced in excess of 45,000 single cells from four embryonic and two postnatal time points using the 10X Chromium system and an Illumina NextSeq. Single-cell computational methods were used to map the heterogeneous landscape of the cochlear epithelium at each time point and to build unsupervised, diffusion-based developmental trajectories for specific cellular transitions. The analysis identified novel transcriptional markers for known cochlear cell-populations at each time point and provided insights regarding novel cellular subpopulations. In particular, at P1 the population of greater epithelial ridge cells (GER) is comprised of at least four transcriptionally distinct cell types. Whether these different GER cells are at different positions along a developmental continuum or functionally distinct cell types has not been determined. Ongoing analyses of cellular developmental trajectories will identify gene

modules that determine specific branchpoints leading to the specification of at least fifteen distinct cell-populations in the cochlear duct. Future studies will use a similar approach to examine cell type specific gene regulatory networks and transcriptional motifs that are disrupted following deletion of genes, such as *Atoh1*, that are known to regulate cochlear development.

This analysis will provide insights regarding the transcriptional decisions and molecular pathways that drive the development of specialized cell types with the cochlea and may identify novel targets for the development of regenerative gene therapies for the treatment of hearing loss disorders.



PS 110

Microglia Regulate Synaptic Pruning in the Mammalian Auditory Brainstem

Giedre Milinkeviciute¹; Caden M. Henningfield¹; Michael A. Muniak²; Kim N. Green¹; Karina S. Cramer³

¹University of California, Irvine; ²Garvan Institute of Medical Research, University of New South Wales;

³University of California Irvine, Dept. of Neurobiology and Behavior

Background

Sound localization relies heavily on the speed, precision and reliability of acoustic signal propagation in the auditory brainstem. These prerequisites are fulfilled by a chain of specialized synapses with unique morphological and electrophysiological characteristics. The assembly of these brainstem circuits and synapses requires precise developmental mechanisms. Glial cells have the potential to shape synaptic connections during development. They interact with neurons during the formation of neural circuits. In this project we investigated the role of microglia in auditory brainstem circuit assembly. We focused on synapse formation and pruning of calyces of Held in the medial nucleus of the trapezoid body (MNTB). Early in development multiple inputs are found to converge on a single MNTB neuron,

and synapses are systematically removed until exactly one input remains. We examined the development of this specialized synapse and innervation status of MNTB neurons in the absence of microglia.

Methods

Microglia were pharmacologically depleted early in development using an inhibitor of colony stimulating factor 1 receptor, which is essential for microglia survival. Brainstems of mice were examined prior to and after hearing onset, at postnatal days (P) 8 and P13, respectively. Brains were processed using standard histologic methods for visualization of an array of synaptic proteins and astrocytic markers using fluorescence microscopy. Axonal projections in MNTB were sparsely labeled using rhodamine dextran amine and analyzed using confocal microscopy and Imaris 7.5 software.

Results

The expression of excitatory and inhibitory synaptic proteins was not affected by the absence of microglia. However, we found an increase in the size of calyces of Held in experimental mice at P8 so that they resembled P13 calyces in size. Examination of the mono-innervation status revealed significantly more poly-innervated MNTB neurons at P13 than in controls, consistent with a defect in pruning. Interestingly, expression of glial fibrillary acidic protein (GFAP), a marker for astrocytes that populate the MNTB late in development, was significantly decreased in microglia depleted mice at P13, while other types of astrocytes were not affected.

Conclusions

Our results indicate that in the absence of microglia more MNTB neurons receive multiple inputs instead of a single calyx of Held. This effect could be a direct result of the absence of microglia, and may also reflect the delayed arrival of GFAP-positive astrocytes in MNTB. These findings highlight the role of glia in pruning during calyx of Held development.

PS 111

Identification of Candidate Genes Expressed in the Part of Sox2 Positive Region in the Developing Cochlea

Norio Yamamoto¹; Hiroe Ohnishi¹; Masahiro Fukui²; Ryosuke Yamamoto¹; Takayuki Nakagawa¹; Koichi Omori¹; Juichi Ito³

¹Department of Otolaryngology-Head and Neck Surgery, Graduate School of Medicine, Kyoto University; ²Institute for Virus Research, Kyoto University; ³Shiga Medical Center Research Institute

Background

Sox2 gene has important roles in the developing mammalian cochlear epithelia. Sox2 gene starts its expression from the otic placode stage of the inner ear and contributes to the establishment of progenitor cells in the sensory epithelia as well as neuronal formation in the cochlea. After that, its expression becomes limited to supporting cells and may have important roles to establish the cell fate within the cochlear epithelia. Considering that both hair and supporting cells are derived from the Sox2 positive region within the cochlear duct, this region should contain many different sub-populations. In this study, we performed comprehensive gene expression analysis from the single cochlear epithelial cells and tried to define the sub-population of the Sox2 positive region in the cochlea.

Methods

From the dissociated embryonic day 13 (E13) cochlear epithelia, we picked up a single cell using glass pipette. We extracted mRNA and performed linear cDNA amplification (Kurimoto et al. 2006). The expression of housekeeping genes was evaluated by RT-PCR to confirm the successful cDNA amplification. Sox2 expression was also checked.

Both Sox2 positive and negative samples (n = 47 and 34, respectively) were reacted onto microarray chips to gain the comprehensive gene expression data. We excluded the probes expressed in at least one of 34 Sox2 negative samples. After that, we picked up the probes that are expressed in more than 6 out of 47 Sox2 positive samples.

Results

Among 45000 probes on the microarray, we picked up 14424 probes that were never detected on all of 34 Sox2 negative samples. To detect the genes that are expressed in some Sox2 positive cells but not expressed in other Sox2 positive cells, we picked up the 28 probes that are expressed in more than 6 among 47 Sox2 positive samples.

Among the 28 genes of the selected probes, we picked up seven genes that are expressed differently in hair and supporting cells at later developmental stages or that are reported to have functions in the inner ear. We confirmed by RT-PCR that all seven genes were expressed in the developmental cochlea and by in situ hybridization that four genes were localized within the cochlea. One of the four genes was expressed in the part of the Sox2 positive region of E13.5 mouse cochlea.

Conclusion

We successfully identified a candidate gene that is expressed in the part of Sox2 positive cells within the E13.5 mouse cochlea.

PS 112

CRISPR gRNA Ablation of Candidate Genes in Chicken Basilar Papilla during Hair Cell Development

Weise Chang¹; Matthew Kelley²

¹Laboratory of Cochlear Development, National Institute on Deafness and Other Communication Disorders, National Institutes of Health; ²NIDCD

Modulation of gene expression represents a crucial approach for understanding normal hair cell development in the inner ear. Unfortunately, existing techniques for the deletion of specific genes are fairly laborious and, for the most part, are restricted to a limited number of vertebrate model systems (mice, zebrafish). Recently, CRISPR CAS9-gRNA gene editing approaches have been shown to act as an efficient method to delete specific genes through the generation of Indel mutations. The introduction of an expression construct expressing CAS9 and specific gRNAs can be used to rapidly generate mutated cells within explants or tissues

To examine the potential use of this technique as a method to screen for candidate genes that might be important for hair cell development, CAS9/gRNA constructs were electroporated into developing chick basilar papillae (BPs) using an in ovo approach. For proof-of-principle, we initially targeted ATOH1, which is required for hair cell formation, and two components of the notch pathway, RBPJ and NOTCH1, which act to inhibit hair cell formation. Following validation of specific deletion of target genes in HEK cells, constructs were electroporated along with a tdTomato reporter into developing chick basilar papillae at E5. Embryos were allowed to develop for 4 days and then harvested at E9. Initial results indicated that 28% of cells within the BP transfected with control tdTomato developed as hair cells. In contrast, only 1.5% of cells transfected with a CAS9-ATOH1 gRNA developed as hair cells. Loss of Atoh1 protein expression was confirmed by antibody labeling. We similarly tested CAS9-RBPj gRNA and CAS9-Notch1 gRNAs. Transfection of the CAS9-RBPj gRNA resulted in 89.04% of transfected cells developing as hair cells, while the CAS9-Notch1 gRNA induced an even higher 97.1% of cells to develop as hair cells. By comparison, only 33.20% of cells transfected with control tdTomato developed as hair cells. These results are consistent with the role of notch signaling in the mediation of lateral inhibition between developing hair cells and supporting

cells. Based on the results of previous RNA profiling studies, we also tested CAS9-gRNAs for transcriptions factors such as LHX3, GF11, and POU4f3 which have been proposed to act downstream of Atoh1. These results suggest that CAS9-gRNA gene editing can be used to efficiently screen candidate genes in Ovo in order to determine the effects of loss of gene function in the inner ear.

PS 113

Role of Neural Crest Cells in the Development of Inner Ear

Vibhuti Khan; William J. Davis; Martín L. Basch
Case Western Reserve University

The stria vascularis is a specialized epithelial structure of the mammalian cochlea that produces endolymph, the potassium-rich fluid responsible for the positive endocochlear potential. This positive extracellular potential is the major driving force for proper signal transduction by sensory cells in the ear, and thus normal hearing. Strial degeneration is estimated to cause more than 30% of the age-related hearing loss. The stria vascularis is composed of 4 types of cells, marginal cells, Intermediate cells, basal cells, and interspersed endothelial cells. Intermediate cells of the stria are originated from the migratory population of neural crest cells and are essential for normal hearing. Neural crest cells also give rise to the glial of the VIIIth ganglion and dark cells of the vestibular system. Intermediate cells of the stria vascularis and the dark cells of the vestibular system share about 95% of their transcriptome with melanocytes, which are a late-migrating subpopulation of neural crest cells. Skin melanocytes and glia originate from different subpopulations of neural crest cells. Mutations that affect neural crest cells migration often result in syndromes that include deafness. The present challenge is to understand how and when these neural crest cells migrate and integrate into the inner ear to form the glial cells of the VIIIth ganglion, intermediate cells of the stria vascularis and the dark cells of the vestibular system. In order to better understand the contribution of neural crest cells to the different cell types in the inner ear, we have used two transgenic mice lines: inducible Wnt1-CreER and Wnt1-Cre. We have set up a timed mating of these mice to the Ai3 reporter mice to label early and late-migrating subpopulations of neural crest cells and to map their contribution to the development of inner ear. Our preliminary data suggest that an early migrating population of neural crest cells gives rise to glial cells of the VIIIth ganglion and vestibular melanocytes, while intermediate cells of the stria vascularis originate from the late migratory population of neural crest cells.

PS 114

GRXCR2 Function in Hearing and Deafness

Chang Liu¹; Na Luo¹; Chun-Yu Tung²; Benjamin Perrin²; Bo Zhao¹

¹*Department of Otolaryngology-Head and Neck Surgery, Indiana University School of Medicine,*

²*Indiana University - Purdue University*

Mutations in human GRXCR2, which encodes a protein of undetermined function, cause hearing loss by unknown mechanisms. We found that mouse GRXCR2 localizes to the base of the stereocilia, which are actin-based mechanosensing organelles in cochlear hair cells that convert sound-induced vibrations into electrical signals. The stereocilia base also contains taperin, another protein of unknown function required for human hearing. We show that taperin and GRXCR2 form a complex and that taperin is diffused throughout the stereocilia length in *Grxcr2*-deficient hair cells. Stereocilia lacking GRXCR2 are longer than normal and disorganized due to the mislocalization of taperin, which could modulate the actin cytoskeleton in stereocilia. Thus, our findings suggest that GRXCR2 and taperin are in the same molecular pathway critical for the morphogenesis of stereocilia and auditory perception.

PS 115

Reconstructing the Transcriptional Network Downstream of GF11 in Hair Cell Development

Maggie Matern¹; Beatrice Milon¹; Yoko Ogawa¹; Andrew Tkaczuk¹; Mark McMurray¹; Yang Song¹; Ran Elkon²; Ronna Hertzano¹

¹*University of Maryland Baltimore-School of Medicine;*

²*Tel Aviv University, Sackler Faculty of Medicine*

Research into the control of inner ear development has indicated that early hair cell (HC) differentiation is dependent on the expression and normal function of the transcription factors ATOH1, POU4F3, and GF11. Additionally, the efficiency of producing HC-like cells from mouse embryonic stem cells in vitro is greatly increased by the combined expression of these transcription factors (Costa et al, 2015). However, while *Pou4f3* and *Gfi1* expression seems to be downstream of ATOH1, and the expression of *Gfi1* is known to be dependent on POU4F3, the signaling cascades downstream of the GF11 transcriptional repressor are completely unknown. To address this gap in knowledge, here we utilize the *Gfi1Cre/Cre* knock-in mouse inner ear to delineate the molecular consequences of loss of GF11 in neonatal cochlear and vestibular HCs.

We have previously shown that *Gfi1Cre/Cre* mice exhibit severe hearing and vestibular defects compared to

their heterozygous and wildtype littermates. Our further characterizations of this model show that, as with *Gfi1*^{-/-} mice, *Gfi1Cre/Cre* cochlear HCs degenerate in a basal to apical gradient after birth and express the neuronal marker TUBB3. Utilizing both the simultaneous ablation of *Gfi1* and HC-expressed Cre recombinase, we have performed an RNA-seq analysis of the cochlear and vestibular HCs of newborn *Gfi1Cre/Cre* mice and their heterozygous littermate controls using the RiboTag method. Through this analysis, we have identified 210 upregulated and 277 downregulated genes in *Gfi1Cre/Cre* cochlear HCs, and 223 upregulated and 76 downregulated genes in *Gfi1Cre/Cre* vestibular HCs compared to *Gfi1Cre/+* controls. Focusing on genes with upregulated expression in the mutant HCs in order to identify direct targets of GF11 mediated transcriptional repression, we observed a significant enrichment of genes involved in neuronal differentiation. Moreover, comparisons of our dataset to an RNA-seq dataset generated from E16 and P0 cochlear and utricular HCs (Scheffer et al., 2015) indicate that these upregulated neuronal genes are normally expressed in early HC development before being downregulated prior to birth. These data suggest that GF11 promotes proper HC development by repressing the expression of neuronal genes at its onset. Combining in silico regulatory motif prediction, viral gene delivery, as well as functional and histological analyses, we further reconstruct the downstream regulatory network of GF11 mediated transcriptional repression. Overall, this work identifies a novel transcriptional cascade downstream of GF11 in cochlear and vestibular HCs, and implicates the downregulation of several drivers of neuronal differentiation as a key step in embryonic HC development.

PS 116

Ear Transplants Can Identify Guidance Cues and their Persistence for Inner Ear Afferent Replacement Strategies

Karen Elliott Thompson¹; Jeremy Duncan²; Marlan R. Hansen³; Douglas Houston¹; Bernd Fritsch⁴

¹*University of Iowa;* ²*Western Michigan University;*

³*University of Iowa Department of Otolaryngology Head and Neck Surgery;* ⁴*University of Iowa Department of Biology*

Background: Inner ear afferents establish stereotyped connections between hair cells at the periphery and nuclei in the hindbrain. Loss of either hair cells and/or inner ear afferents results in hearing and balance defects. Current attempts at hearing restoration focus mostly on hair cells and their innervation, with less emphasis on how to reestablish correct central connections of

regenerated neurons. As a novel approach toward restoration of neuronal central connections, we focus on connecting inner ear afferents of transplanted otic vesicles with specific brainstem nuclei. Here we concentrate on inner ear afferent navigation to correct hindbrain nuclei following gene manipulation or from divergent entry points. From our previous studies, we hypothesize that Wnt/PCP signaling plays a role in inner ear afferent central pathfinding and that inner ear afferents can navigate using these signals to find the correct hindbrain nuclei when entering at novel entry points or at variable times.

Methods: To test the role of Wnt/PCP signaling, levels of the Wnt receptor, Fzd3, were manipulated in frogs and their inner ears were transplanted to replace the inner ear of wild type frogs. Dyes were used to reveal central neuronal projections. Phenotypes were confirmed by analyzing Fzd3 null mice. To test the ability of afferents to navigate from divergent entry points, ears were transplanted to other regions of similar Wnt expression (caudal), or to heterochronically replace ears from later stage tadpoles with developing otocysts. Behavior and central neuronal projections were assessed.

Results: Frog inner ear afferents show an increasing tendency to project more dorsally with increasing concentration of Fzd3 morpholino. Similarly, mice mutant for Fzd3 show aberrant central projections for auditory and vestibular afferents, indicating conservation of guidance cues across species. In addition, ears transplanted caudally toward the spinal cord, or heterochronically to replace an ear have neurons that are able to navigate to correct hindbrain nuclei, complete with forming functional connections.

Conclusions: These results implicate the Wnt pathway in dorsoventral targeting of inner ear afferents within the hindbrain and suggest that the Fzd3 receptor plays a role in directing inner ear afferents to the proper dorsoventral column. The ability of transplanted or replaced ears to have neurons that project to, and form functional connections with hindbrain nuclei suggests that neuronal and/or ear replacement strategies may function as novel therapies. Future work will determine the mechanism of guidance via Wnt/PCP signaling and extent that guidance molecules remain active in postnatal mice.

PS 117

Correlation of Emx2 Expression with Hair Bundle Orientation in Zebrafish Larvae with Disrupted Planar Cell Polarity, Notch or Wnt Signaling

Youngrae Ji; Doris Wu

National Institute on Deafness and other Communication Disorders

The neuromasts of the lateral line system allow aquatic animals to detect the direction of water flow for navigation. This function is mediated by hair bundles on the apical surface of sensory hair cells (HCs) within the neuromast. In each neuromast, hair bundles can be divided into two groups with opposite orientations. Previously, we have shown that this hair bundle pattern is established by the transcription factor Emx2, which is expressed in only half of the HCs within a neuromast and as a result, the hair bundle orientation in those HCs is reversed from the default position by approximately 180°. To investigate whether Emx2 expression is always robustly correlated with HCs of a specific orientation of hair cells, we investigated Emx2 expression in several type of zebrafish with disrupted HC number and/or bundle polarity pattern: *vangl2^{m209}* (a core planar cell polarity (cPCP) mutant) as well as larvae that were treated with a Notch inhibitor, DAPT, or a Wnt agonist, AZK. Our results showed that although the hair bundle orientation is random in *vangl2^{m209}* mutants, Emx2 expression is not altered, present in only half of the HCs within a neuromast, suggesting that the cPCP pathway and Emx2 regulate hair bundle polarity independently. It has been shown that blocking the Notch signaling pathway with DAPT resulted in an increased number of HCs in the neuromasts and the 1:1 ratio of the two opposite-direction HCs disrupted. Despite the disrupted ratio, our results showed that Emx2 expression remained correlated with HCs of a specific orientation as in wildtype. The increase in HC number in DAPT treatment could be due to an increase in Wnt signaling because Notch normally negatively regulates the proliferative effects of Wnts in regenerating neuromasts. We asked whether the reported increase in hair cell number with the Wnt agonist, AZK, affects hair bundle orientation and Emx2 expression differently. Our results showed that although the total number of HCs was increased in AZK-treated neuromasts, the ratio of hair bundle orientation and Emx2 expression remained similar to wildtype. Together, these results demonstrated that Emx2 expression is consistent with hair cell orientation despite disrupted hair bundle orientation pattern. Furthermore, our results suggest that Emx2 functions epistatic to the Notch signaling pathway.

Exploring Parallels in the Mechanisms of Hearing and Deafness Between the Fruit Fly, *Drosophila melanogaster*, and Humans

Daniel C. Sutton¹; Jonathan Andrews²; Shinya Yamamoto²; Andrew Groves³

¹Program in Molecular and Human Genetics, Department of Genetics, Baylor College of Medicine; ²Duncan Neurological Research Institute, Department of Molecular and Human Genetics; ³Department of Neuroscience, Department of Molecular and Human Genetics, Baylor College of Medicine

Background

There is remarkable evolutionary conservation of molecular and functional properties between *Drosophila* and vertebrates. Over 60% of all human disease genes have orthologs in the fruit fly and all major signaling pathways are conserved. The auditory system of the fly, Johnston's organ (JO), is located within the second segment of each antenna and is comprised of around 200 stretch receptor units called scolopidia. These scolopidia contain mechanosensitive neurons that respond to gravity and sound from vibrations of the outermost antennal segment. Although JO is morphologically different from the cochlea, the function of orthologs of some human deafness genes are known to be conserved. Orthologs of myosin VIIa and non-muscle myosin II (NMII) are both expressed within JO and are necessary for normal hearing. The ortholog of protocadherin-15 localizes to JO and genetically interacts with a hearing-impaired mutant of UBR3 in *Drosophila*. While many studies have drawn parallels between vertebrate and fly hearing mechanisms, no comprehensive study exploring orthologs of vertebrate deafness genes has been conducted in *Drosophila*.

Methods

Ortholog prediction software (DIOPT) was used to identify published human and mouse deafness genes with evolutionary conservation to *Drosophila*. Libraries of internally tagged *Drosophila* genes were used to determine expression and/or localization within JO. Fly lines internally tagged with a GAL4 transcription factor were crossed to UAS-GFP expressing lines to explore gene expression. Lines internally tagged with a fluorescent marker were used to explore protein localization. Confocal microscopy was performed to image JO 24 to 48 hours post-pupation.

Results

Data from the expression/localization screen

confirmed previous findings that myosin VIIa, NMII, and protocadherin-15 orthologs are expressed in JO. Orthologs of Usher syndrome proteins cadherin-23 and whirlin were also expressed in JO and partially colocalize with the myosin VIIa and protocadherin-15 orthologs. The ortholog of Usher syndrome genetic interactor ATP2B2 (PMCA2) is also expressed within JO. Orthologs of the LINC complex protein Nesprin-4 and the molecular motor Myosin-15 localize within JO.

Conclusions

The finding that other Usher syndrome proteins are expressed within JO suggests a molecular conservation between the Usher complex in humans and flies. The extent of these interactions and whether loss of function of these genes in *Drosophila* is sufficient to cause deafness has not yet been explored. The expression of other deafness gene orthologs within JO further indicates that the fly can be used as a model to quickly and efficiently study mechanisms of deafness.

PS 119

Identification of genes differentially-expressed between differentiating outer vs inner hair cells

Anne Duggan; Teerawat Wiwatpanit; John C. Clancy; **Jemma L. Webber**; Jaime Garcia-Anoveros
Northwestern University

Insm1 encodes a zinc-finger transcription factor transiently expressed in nascent OHCs (from E15.5 at the base of the cochlea to P2 at the apex) that is required to consolidate their fate (Lorenzen, et al., 2015, MOD; Wiwatpanit et al., 2018, Nature). We generated *Insm1*^{GFP.Cre/+}; *Atoh1*^{A1GFP/+}; *R26R*^{tdTomato/+} mice, in which all hair cells express GFP (from *Atoh1*^{A1GFP} and, in OHCs, from *Insm1*^{GFP.Cre}) but only OHCs express tdTomato following *Insm1*^{GFP.Cre} expression (throughout the cochlea by E18.5). We used these mice to collect by fluorescent activated cell sorting (FACS) separate pools of neonatal (P0) IHCs (green) and OHCs (green and red), and by RNAseq determined the transcriptomes of these differentiating cochlear hair cell types. We identified 922 IHC- and 676 OHC-enriched genes. Among these are the 12 genes previously shown (with immunohistochemistry, in situ hybridization or reporter alleles) to be expressed only or preferentially in IHCs or OHCs at embryonic to early postnatal stages. We also confirmed by TaqMan RT-qPCR differential expression of all 21 additional genes tested, further validating the reliability of our RNAseq-determined transcriptomes. A comparison among differentiating vs mature (previously identified by microarray technology; Liu et al., 2014, J Neurosci) IHC- or OHC-enriched genes

reveals very little overlap between the differentiating and mature stages (5.9% or 2% for IHC or OHC-enriched genes, respectively). These include some known genes characteristic of the mature stage (Vglut3 and Otof in IHCs and Prestin in OHCs) but whose expression is incipient at birth. However, the vast majority of the genes preferentially expressed in either cell type during differentiation are not expressed upon maturation, and vice versa. These results reveal that a complex transcriptome, involving hundreds of genes, is transiently active during OHC- and IHC-specific differentiation.

By RNAscope in situ hybridization we confirmed expression of many of these genes to IHCs or OHCs, and found that in general differentially expressed genes are not confined to the hair cells, but expressed in some supporting cells as well. By comparing with the neonatal transcriptomes of hair vs supporting cells (Cai et al., 2015, J Neurosci), we identified genes that were primarily expressed only in IHCs or OHCs. Among these, we found the transcription factors INSM2 (confirmed with an *Insm2*LacZ reporter mouse line), BCL11b (confirmed by immunohistochemistry) and NEUROD6, in addition to INSM1, to be specific to differentiating OHCs. We hypothesize that some of these factors participate with of INSM1 in specifying OHC fate and differentiation.

PS 120

INSM1 represses a core set of differentiating IHC-specific genes in embryonic OHCs

Chuan Zhi Foo; Sarah M. Lorenzen; Anne Duggan; John C. Clancy; Jemma L. Webber; Jaime Garcia-Anoveros
Northwestern University

INSM1, a zinc-finger transcription factor expressed transiently in nascent outer hair cells (OHCs), regulates OHC differentiation. In the absence of *INSM1*, embryonic OHCs switch fates and trans-differentiate into inner hair cells (IHCs). Only about half of the OHCs switch fate, and they do so in a graded fashion. OHCs of the neural rows are more likely to transform into IHCs than those at the abneural row. This suggests that a graded morphogen induces IHC-differentiation, and that normally *INSM1* prevents OHCs from responding to this gradient (Lorenzen et al., 2018, Nature). In order to elucidate how *INSM1* controls OHC vs IHC differentiation, we collected by FACS embryonic (E18.5) OHCs with (*Insm1*^{GFP.Cre/+}) and without (*Insm1*^{GFP.Cre/-}) *INSM1*, and then determined their transcriptomes by RNAseq. We tested ~300 candidate genes for differential expression by TaqMan RT-qPCR and some of them also by RNAscope in situ hybridization.

Among the genes confirmed to be regulated by *INSM1*

in embryonic OHCs were several encoding DNA-binding proteins like *Brip1* and *Tbx2*, others encoding proteins involved in signaling like *Fgf8* and *Smad3*, and some encoding uncharacterized proteins like *Lrrn1* and *Sez6l*. By comparing the genes potentially up or down-regulated by *INSM1* in differentiating OHCs with the genes differentially expressed between differentiating OHCs or IHCs, we found that *INSM1* represses in embryonic OHCs a small core set of early IHC-specific genes. Since embryonic OHCs expressing these few genes differentiate as IHCs, these genes are likely required for IHC differentiation. Hence, in addition to identifying *Insm1* as a critical gene for OHC differentiation, our results are also the first to identify candidate genes responsible for driving the specific differentiation of IHCs. Because all OHCs express *INSM1*, yet in its absence less than half trans-differentiate into IHCs, we expected two patterns of miss-expression by in situ hybridization. Some genes were upregulated in all OHCs lacking *INSM1*, as expected if repressed by *INSM1*. These (e.g., *Rprm*, *Id4*, *Lrrn1*, *Car13*, *Pink1* and *Brip1*) must include the genes whose disinhibition in the absence of *INSM1* renders embryonic OHCs susceptible to the gradient that induces IHC trans-differentiation. Other genes (e.g., *Fgf8* and *Tbx2*) were only upregulated in less than half of the OHCs lacking *INSM1*, presumably the OHCs trans-differentiating into IHCs. These genes are some of the earliest expressed in IHCs, and likely include regulators of IHC differentiation.

PS 121

Sound Experience during Development and The Maintenance of AIS structure in a Tonotopic Manner in the Auditory Brainstem

Eun Jung Kim; Jun Hee Kim
University of Texas Health Science Center

Continuous auditory input is necessary for proper development and maintenance in the auditory system. In particular, early auditory experiences within the critical period of auditory development, i.e. when the nervous system is especially sensitive to certain environmental sound stimuli, significantly influence structural plasticity and refinement of auditory neurons associated with central plasticity and auditory processing. A decline or complete loss of auditory inputs during the critical period could result in auditory processing disorders or reading/speaking disabilities. However, cellular mechanisms through which sound-evoked activity refines auditory brainstem circuits to maintain and fine-tune the temporal processing and developmental plasticity are not well understood. We investigate how sound input influences structural properties of axonal domains and physiological function of auditory neurons during development using

immunohistochemistry and electrophysiology. We found differential development of axon initial segment (AIS) structure and location along the tonotopic axis in the MNTB after exposure to different auditory environments, including sound stimulation and sound deprivation (deaf mice). Along the medial-lateral axis, AIS length is gradually increased from medial to lateral MNTB neurons. Medial MNTB neurons, which are high frequency-responding neurons, have shorter AIS that are distally located from the soma. Lateral neurons, responding to low frequency sound, have longer AIS that are proximally located from the soma. The tonotopy of AIS length and location appears distinctly around hearing onset and is progressively enhanced throughout adulthood. We examined the effect of sound-evoked activity on regulating AIS length and location in the MNTB in sound deprivation and enhancement mice. The length of the AIS in the MNTB was significantly decreased by ~20% in the sound stimulation group, whereas it was significantly increased by ~30% in deaf mice. In addition, AIS location in the sound stimulation group is proximal to the soma compared to control whereas it is distally located in sound deprivation model. Furthermore, we questioned whether altered AIS is associated with age-related hearing loss, a prominent phenotype of which is high-frequency hearing loss. In an age-related hearing loss model that displays a reduction of neuronal activity and an elevated threshold of auditory brainstem responses, AIS length was significantly lengthened compared to those in adult mouse. Taken together, these results demonstrate that structural plasticity of the AIS in auditory neurons is refined by sound-evoked neuronal activity, suggesting that auditory experience is essential to maintain topographical differences in AIS structure.

Funding: NIDCD R01 to J.H.K.

PS 122

Extracellular ATP Regulates Embryonic Spiral Ganglion Neuron Development via P2X3 Receptors

Zhirong Wang; Thomas M. Coate
Georgetown University

The mammalian cochlea undergoes a highly dynamic process of growth during development. This process includes the extension of the cochlear duct along with spiral ganglion neuron (SGN) migration, followed by their maturation and synaptic contact with hair cells (HCs). In mouse, this process commences around embryonic day 12 (E12) and continues through early postnatal stages. Upon hearing onset around postnatal day 10-12 (P10-P12), most of the connections between HCs and SGNs have been fine-tuned so that the cochlea can relay (to the brain) sound in a range of frequencies and intensities. Understanding the

molecular mechanisms of precise cochlear wiring will be critical for developing treatments for hearing loss because SGN/HC connections need to be reestablished. Extracellular ATP has been extensively investigated as a neurotransmitter and acts as a ligand for both ionotropic and metabotropic ATP receptors. However, little is known about their roles in development. By antibody staining, we have found that one of the ionotropic receptor family members, P2X3, is expressed at high levels in SGNs from E12.5 to P6 and in HCs from E15.5 until P4. Given that P2X3 as a dynamic membrane-bound ATP-gated ion channel, we hypothesize that P2X3 controls early SGN development and HC innervation via subsequent calcium signaling. We serendipitously found that Sox2-CreER; Rosa26-tdTomato alleles without tamoxifen treatment enables us to examine individual neuronal morphology. With this sparse labeling strategy, we found that loss-of-function of P2X3 in vivo results in more complex branching patterns along the axons near SGN cell bodies as well as at axonal terminals around P0. Additionally, our preliminary in vitro results showed that blocking P2X3 receptor leads to an increased terminal innervation pattern of SGNs. These data suggested that P2X3 normally mediates a pruning process to eliminate excessive branches during SGN development. Physiologically, using Fluo-4-AM dye, I documented calcium-based spontaneous neuronal activities ex vivo using E16.5 cochlear explants. Furthermore, P2X3 specific agonist, $\alpha, \beta, \text{me-ATP}$, potentiates such calcium events in a dose-dependent manner. This implied that embryonic calcium transients in SGNs are potentially mediated by P2X3 receptor-dependent ATP signaling. Previously, extracellular ATP and purinergic receptors have been implicated in spontaneous calcium action potentials to organize early developmental events of neural circuits prior to sensory input. Taken together, we concluded that SGN maturation requires P2X3 mediated extracellular ATP and intracellular calcium signaling.

PS 123

The evolutionary map of the cochlea revealed by single cell RNA seq

Na Xue¹; Lei Song²; Joseph Santos-Sacchi³; Hao Wu⁴; Dhasakumar Navaratnam⁵

¹*Department of Otolaryngology - Head & Neck Surgery, Shanghai Ninth People's Hospital, Shanghai JiaoTong University School of Medicine;* ²*Otolaryngology-Head and Neck Surgery, Shanghai ninth people's Hospital, Shanghai Jiao Tong University School of Medicine;* ³*Ear Institute, Shanghai JiaoTong University School of Medicine;* ⁴*Department of Surgery (Otolaryngology), Yale School Of Medicine;* ⁵*clinical auditory;* ⁵*Department of Neurology and Neuroscience, Yale University School of Medicine*

The postnatal cochlea changes significantly in morphology and physiology reaching maturity approximately at 20 days. To obtain a granular understanding of the molecular events underlying these changes, we undertook single cell RNA sequencing of the cochlea at different post natal time points (P0, P5, P10 and P20). Single cell RNA sequencing was done using the 10X genomics platform and subsequently analyzed post-hoc using a range of software suites including Seurat, Monocle, Magic and Phate.

In comparing different algorithms we determined that canonical correlation analysis (CCA) provided the most robust alignment of cell clusters from different time points (compared to principal component analysis). Among the cells types and the time points, there was considerable heterogeneity in gene expression. Surprisingly, we noted that expression of key genes that have been hitherto used to demarcate regions of the cochlea in embryonic development persisted into post-natal time points. These included Pax2, Lfng, Sox2, Fgf members, Bmp4, Otx1/2, and several other genes that also helped demarcate the anatomical location of these cell populations. Developmental changes pinpointed molecular changes of physiological importance in many cell types. For instance, in Schwann cells there were markers for myelination that were up regulated at P5 and P10, suggesting that myelination was most robust at these time points. In hair cells there were changes in the expression of proteins in different subcellular compartments that had developmental correlation (synaptic proteins, lateral wall proteins, and stereocilliary proteins). Since our datasets were large we were also able to make predictions of lineage and potential transcription factors and pathways that determine fates at branch points of lineage trajectories. Lastly, we explored algorithms of data imputation to overcome dropout of individual transcripts that further reinforced our findings.

Supported by NIH-NIDCD R01 DC007894, Shufro Foundation and National Natural Science Foundation of China 81770995

PS 124

The Role of LIN28B and Let-7 miRNAs in Cochlear Tonotopic Specialization

Meenakashi Prajapati-DiNubila¹; Angelika Doetzelhofer²

¹*The Solomon H. Snyder Department of Neuroscience and Center for Sensory Biology, Johns Hopkins University School of Medicine;* ²*Johns Hopkins Medical Institution*

The inner ear cochlea is the organ responsible for the detection of sound. Its spiral-shaped sensory epithelium contains mechano-sensory hair cells (HCs) that transduce sound waves into neuronal signals. This sensory epithelium is tonotopically organized such that it detects high frequency sounds at the base of the spiral and low frequency sounds at the apex. Features of this tonotopic specialization include graded differences in HC soma and stereocilia size as well as differences in HC-specific gene expression. Little is known of the mechanisms that produce tonotopic specialization in the mammalian cochlea. Here, we investigate the role of the RNA binding protein LIN28B and the let-7 family of miRNAs in cochlear tonotopic specialization. The mutual antagonistic LIN28B and let-7 miRNAs are post-transcriptional regulators that control the expression of large numbers of genes in a dose-dependent manner. In the developing cochlea opposing expression gradients of LIN28B and let-7s regulate the timing of cell cycle exit and HC differentiation (Golden et al., 2015). Interestingly, we found that these gradients persist during the maturation and tonotopic specialization of HCs, with let-7s being highest expressed in basal HCs, and LIN28B being highest expressed in apical HCs. To determine the role of LIN28B and let-7 miRNAs in the tonotopic specialization of HCs, we manipulated LIN28B/let-7 levels in maturing HCs using LIN28B or let-7g overexpressing transgenic mice. To determine if these manipulations disrupt frequency-specific HC function, we recorded Auditory Brainstem Responses (ABRs) from these mice. Our hypothesis predicts that LIN28B overexpression will result in a more 'apical' identity, which would disrupt the function of the basal (high frequency) region of the cochlea. Indeed, ABRs from these mice revealed a severe deficit specifically in high frequency hearing, compared to control littermates. Conversely, overexpressing let-7g during cochlear maturation show deficits specifically in low frequency hearing, compared to control littermates. Histological analyses confirmed that these deficits are not due to HC loss. Ongoing experiments are examining whether LIN28B and/or let-7 overexpression disrupted the graded differences in HC-specific gene expression and HC morphology along the tonotopic axis. In summary, our current results suggest that the LIN28B/let-7 pathway plays a critical role in tonotopic specialization, with LIN28B activity conferring a more 'apical' identity to HCs, while let-7 miRNAs impart a more 'basal' identity.

Funding: F31 DC016538 (MP) and David M. Rubenstein Fund for Hearing Research (AD)

Cytomegalovirus in newborn mice leads to delayed auditory development and early loss in spiral ganglion neurons

Cathy Yea Won Sung; William J. Britt
University of Alabama at Birmingham

Congenital HCMV infection can lead to moderate to severe sensorineural hearing loss (SNHL) in approximately 15% of infected newborns. However, the mechanism(s) of disease leading to SNHL in infants with congenital HCMV infection are not well understood. To study the pathogenesis of HCMV, we have developed a mouse model in which newborn mice (P0) are infected intraperitoneally (i.p.) with murine CMV (MCMV). In this model, we have previously shown that 50-60% of young mice (PNd32) infected as newborns exhibit elevated ABR, indicative of hearing loss. Histological analyses in mice with elevated thresholds revealed uniformly preserved hair cells and supporting cells. However, the number of spiral ganglion neurons (SGN) and synapses connecting cochlear hair cells and SGN nerve terminals were reduced and the stria vascularis exhibited altered morphology. These findings suggested that MCMV infection in newborn mice led to structural alterations in the cochlea that could contribute to impaired auditory function in the mature cochlea of PNd32 mice.

One mechanism that could account for these structural alterations in the cochlea of PNd32 MCMV-infected mice is the robust enhancement of proinflammatory cytokines and chemokines during early postnatal cochlear maturation, rather than direct virus cytopathology, as we have observed during cerebellar development. Coincidentally, virus-induced inflammatory response during postnatal development overlaps with the critical period of the auditory system development in mice (PNd5-14). During critical periods of postnatal development, neurons are susceptible to environmental growth cues that induce sequential events of cellular maturation and synaptogenesis that result in formation of functional pathways and hearing. Because insults during the critical period can impair the normal developmental processes leading to permanently altered cochlear structure and function, we sought to address whether virus infection and virus-induced inflammation in newborn mice impacted development of the auditory system during the critical period of auditory development in mice. Pre-synaptic ribbons from IHC, post-synaptic densities, as well as hair cells were visualized, respectively, with anti-CtBP2, anti-GluR2, and anti-myosin VIIa for quantification of synapses/IHC at PNd8 in the organ of Corti whole mounts. Additionally, PNd8 cochlear sections were immunostained for Tuj-1, labeling all SGNs in the Rosenthal's canal, and the

numbers of SGNs were quantified. Staining of the organ of Corti showed no morphological differences in the hair cells but exhibited excess synapses in the OHCs suggesting delayed synaptic pruning of OHCs. We have also observed reduced numbers of SGN soma as early as PNd8 in MCMV-infected mice. These data argue that MCMV infection during postnatal development alters normal development of auditory pathways early after infection and that morphological changes in cochlear structures in adult mice infected as newborns represent the sequelae of this infection.

PS 126

HDAC3 Is Required for Hair Cell Survival in the Developing Mouse Cochlea

Xiaoling Lu¹; Wen Li²; Yingzi He²; Huawei Li³
¹*Affiliated Eye and ENT hospital, Fudan University;*
²*Otorhinolaryngology Department of Affiliated Eye and ENT Hospital;* ³*ENT Institute and Otorhinolaryngology Department, Affiliated Eye and ENT Hospital, State Key Laboratory of Medical Neurobiology, Fudan University.*
2 NHC Key Laboratory of Hearing Medicine (Fudan University)

Histone deacetylases (HDACs) are involved in multiple developmental processes, but their roles in the development of mechanosensory organs are largely unknown. In this study, we reported the expression of histone deacetylase 3 (HDAC3) in mouse cochlea and investigated its role in hair cell survival and in neomycin-induced hearing loss in mice. HDAC3 mainly expressed in hair cells in mouse cochlea. Conditional knockout mice deficient for HDAC3 in cochlear HCs displayed severe hearing loss comparable to control mice and exhibited patched outer hair cell loss at postnatal day 30 under normal conditions. Furthermore, neomycin-induced hair cells death dramatically increased in HDAC3-cKO mice compared with those observed in wild-type control mice, indicating that HDAC3-cKO mice were more sensitive to neomycin-induced damage. Pharmacological inhibition of HDAC3 by RGFP966 caused caspase-dependent apoptosis as evidenced by the increased cleaved caspase-3 and TUNEL staining as well as expression of pro-apoptotic genes *in vitro*. Importantly, MitoSOX-red staining showed the levels of mitochondrial ROS markedly increased in hair cells of RGFP966-treated cochlear cultures, while the antioxidant N-acetylcysteine can rescue those hair cells from neomycin injury, suggesting that ROS accumulation was mainly responsible for the increased aminoglycosides sensitivity in HDAC3 inhibition hair cells. Our data demonstrate that HDAC3 plays an important role in hair cell survival in the cochlear sensory epithelium.

PS 127

Behavioral and Neural Measures of Auditory Selective Attention Suggest Diminished Top-Down Control in ADHD

Jasmine Kwasa¹; Laura Torres¹; Barbara Shinn-Cunningham²

¹Boston University; ²Carnegie Mellon University

Background: Selective attention is the ability to preferentially pay attention to a single stimulus within a complex sensory environment. This requires cognitive control, an ability that greatly varies between individuals. People with Attention Deficit Hyperactivity Disorder (ADHD or ADD) tend to have system-wide cognitive deficits that lead to distractibility and inefficiencies in organizing, vigilance, and inhibition. Therefore, we hypothesized that young adults with ADHD would exhibit deficits in auditory selective attention which would be evident in both behavioral and neural measures. Using 64-channel human electroencephalography (EEG), we compared subjects'; behavioral performance and their neural correlates on a set of psychoacoustics tasks.

Methods: Human participants listened to three time-staggered, spatially lateralized streams of speech consisting of permutations of the syllables bah, dah, and gah. Subjects were prompted to report the order of the syllables presented from the central "target" stream or the left "supertarget" stream and to always ignore the right "distractor" stream. The supertarget stream either did not appear at all (indicating that the subject should report the order of the central target stream instead) or it started at a delay. This paradigm produces two attentional states: focal attention, where only the central target stream was attended, and broad attention, where listeners had to monitor the target stream but prepare for a spatial attention switch to report the supertarget stream. A subset of ADHD participants performed this task twice: once while under the influence of their physician-prescribed stimulant medications and once while abstaining. No neurotypical participants took stimulant medications.

Results: There were no significant group differences in performance between ADHD and neurotypical participants for either attention condition. However, reaction times did negatively correlate to overall performance on the task, as expected, indicating individual differences in processing speed regardless of ADHD status. In contrast, reaction times did distinguish groups on average: ADHD participants had significantly longer reaction times than their neurotypical

counterparts, even when using stimulant medications. Additionally, there were group differences in the change in amplitude (modulation) of event-related potentials (ERPs) between the focused and broad conditions: N1 components evoked by the onsets of the supertargets modulate significantly less in ADHD participants than neurotypical controls, regardless of stimulant use. This consistent neural response to differing task demands along with longer reaction times points to a relative lack of top-down control of auditory attention in ADHD participants.

PS 128

Characterizing Deep Neural Networks Trained to Predict Neural Responses to Speech in Human Auditory Cortex

Menoua Keshishian¹; Hassan Akbari¹; Bahar Khalighinejad¹; Jose Herrero²; Ashesh Mehta³; Nima Mesgarani⁴

¹Columbia University; ²Feinstein Institute for Medical Research; ³The Feinstein Institute for Medical research; ⁴Zuckerman Institute for Brain Research, Columbia University, Program in Neurobiology and Behavior, Columbia University, Department of Electrical Engineering, Columbia University

There is a growing interest in characterizing the response properties of sensory neurons under natural stimulus conditions. The majority of previous studies have used linear models to relate the acoustic features of sound to neural responses. Linear models, however, cannot capture the inherent non-linearity of the processes in the brain. Recent advancements in machine learning and computational power have allowed us to utilize deep learning methods in a large variety of tasks. We investigate the utility of deep neural network models to predict neural responses to speech in human auditory cortex, with the goal of analyzing the learned networks to gain insight into the nonlinear mechanisms of the brain. The neural responses were recorded from the transverse and the superior temporal gyrus of five patients undergoing surgery for the treatment of epilepsy, as they listened to continuous speech. As deep neural networks (DNNs) have shown great promise in capturing non-linear relationships, we trained a DNN with a non-linearity in each layer using the time-frequency representation of the stimulus as the input and the envelope of the high-gamma activity of the neural responses as the output of the model. First, we started with a one-node one-layer fully connected network, which is equivalent to the commonly used spectrotemporal receptive field (STRF). We then proceeded by progressively adding nodes and layers, to study the effect of depth and complexity of the model, on prediction accuracy. To further study

the effect of artificial neural networks, we chose a convolutional neural network (CNN), a more state-of-the-art architecture, as our final model.

In comparison to the STRFs, the predicted responses from the neural networks had a higher correlation with the original responses. On average, using CNNs improved performance by 25%. To interpret the nonlinear function that the network applies to the stimulus, we analyze the linear equivalent of the function, at each time point. As a result, we observe three general classes of nonlinear behavior implemented by the network: gain change, feature memory, and shape diversity. The feature memory or “hold” can be interpreted as the network holding on to a response captured by the STRF. Finally, we quantify these three properties for all electrodes and try to explain the prediction improvement gained from using the CNN model, through these simple parameters. Furthermore, we studied the relation between these parameters and the electrodes’ anatomical locations along the auditory pathway.

PS 129

Effects of Spatial (In)congruence on Audio-Visual Integration as Revealed by the Pip and Pop Effect

Justin T. Fleming¹; Abigail L. Noyce²; Barbara Shinn-Cunningham³

¹Harvard University; ²Boston University; ³Carnegie Mellon University

In the pip and pop effect, visual search is improved by temporal synchrony between the visual target and a spatially uninformative auditory stimulus. For instance, in a visual search task where all the search items change color at random time intervals, search times are faster when target color changes are accompanied by a synchronous tone (Van der Berg et al., 2008). Previous research from our lab has demonstrated that the pip and pop effect is impervious to spatial incongruence between the visual target and the auditory stimulus. However, in the typical pip and pop paradigm, the auditory stimulus is related only to the visual target. It may be that spatial congruence plays a larger role in AV integration in more complex scenes, in which multiple auditory and visual targets compete for integration. To examine this possibility, we recorded 64-channel electroencephalography (EEG) while participants performed a version of the pip and pop paradigm in which there were two potential visual targets, one in the right hemifield and one in the left, embedded among several non-targets. One of the potential targets was the actual target and the other was a distractor; a pre-trial cue informed participants which hemifield contained the actual target. Target and distractor color changes were each accompanied by

synchronous auditory stimuli, presented via separate free-field loudspeakers. The target/distractor and their corresponding auditory stimuli were either Spatially Matched (target and synchronous tones in the same hemifield, same for distractor) or Spatially Mismatched (target and synchronous tones in opposite hemifields, same for distractor). Behaviorally, the addition of competing AV stimuli weakened but did not abolish the pip and pop effect. However, reaction time benefits of AV synchrony were only observed in the Spatially Matched condition. In the EEG data, event-related potential (ERP) results recapitulated the behavioral findings. In the Spatially Matched condition, the N100 component of ERPs evoked by tones synchronized to the target was larger than the N100 elicited by tones synchronized to the distractor. This was not the case in the Spatially Mismatched condition, suggesting that participants were less able to attend and integrate the synchronous AV stimuli when they were misaligned in space. While the pip and pop effect is driven by temporal coherence, these results suggest that other factors – particularly the effective deployment of spatial attention – are likely at play in real-world multisensory perception.

PS 130

Auditory Attention Decoding: What Anatomical Locations and Neural Frequency Bands Contribute?

James O’Sullivan¹; Jose Herrero²; Elliot Smith¹; Guy McKhann¹; Sameer Sheth³; Ashesh Mehta⁴; Nima Mesgarani⁵

¹Columbia University; ²Feinstein Institute for Medical Research; ³Baylor College of Medicine; ⁴The Feinstein Institute for Medical research; ⁵Zuckerman Institute for Brain Research, Columbia University, Program in Neurobiology and Behavior, Columbia University, Department of Electrical Engineering, Columbia University

Decoding an attended speaker from neural recordings (termed auditory attention decoding; AAD) has many applications. The most pertinent is probably the development of a cognitively controlled hearing aid that can automatically track and amplify an attended speaker. Such devices will likely be limited to either non-invasive or minimally invasive neural recordings. Non-invasive recordings such as electroencephalography (EEG) can typically only record from low frequency (LF; < 50Hz) neural data, and have relatively poor spatial resolution. However, multiple electrodes can be used to target cortical areas using source-localization signal processing strategies. Minimally invasive approaches can place a restricted number of electrodes over specific cortical areas, and can also record from higher neural frequencies (<200Hz). In both cases, knowledge of the

anatomical locations and neural frequency bands that contribute to AAD is crucial.

To investigate, we used an invasive recording methodology known as electrocorticography (ECoG) that can record from both low and high frequency (HF; < 200Hz) neural data, and can also localize neural activity to within ~3mm from both deep and surface brain regions, spanning the full extent of auditory cortex. We show that both LF and HF data, as well as deep and surface regions, can be used to decode attention. However, we found a dichotomy between the combinations of frequency band and anatomical location that could be used: when using HF data, the anatomical region that produced the most robust encoding of attended speech was superior temporal gyrus (STG; a surface brain region). Conversely, LF data was the best at decoding attention in Heschl's gyrus (HG; a deep brain region). Both of these combinations (LF data in HG, and HF data in STG) provided similar results in terms of decoding speed and accuracy. These results provide the first extensive exploration of the neural frequency bands and anatomical locations that contribute to AAD, and will inform future work on the development of cognitively controlled hearing aids.

PS 131

The Time Course and Acoustic Correlates of Early Neural Representations of Speakers and Vowels in MEG

Mattson Ogg; L. Robert Slevc
University of Maryland, College Park

Background:

Human speech carries a wealth of acoustic information related to both the linguistic content a speaker intends to convey as well as cues for identifying the individual who is speaking. How does the listener's auditory system manage this wealth of information as the perception of an utterance unfolds in time? Speaker normalization theories suggest that successfully perceiving linguistic content across speakers (phonemes, prosody, etc.) is achieved by accounting for speaker-specific qualities in the speech signal. If this is the case, then speaker specific aspects of an utterance should be represented early in cortical processing in support of later linguistic or perceptual functions. We tested this idea in MEG using pattern classifiers to decode different neural representations of labels (vowel, speaker, gender) associated with the same set of speech utterances over time.

Methods:

Listeners heard 100 repetitions of each of three vowels (/a/, /i/ and /u/) spoken by six different speakers (three males and three females) played back at a jittered rate of 1 per second while their neural responses were recorded in the MEG. Participants listened passively to the critical vowel sounds, however they had to respond whenever they heard an unrelated target sound (a cat vocalization which was not analyzed) to ensure they remained vigilant. Linear discriminant classifiers were trained and tested on how well they could associate neural responses with the different labels associated with each speech stimulus (speakers, vowels, or genders) in 5 millisecond steps. A representational similarity analysis was also conducted to determine what acoustic features were associated with these neural representations as they emerged over time.

Results:

Speaker decoding performance exceeded chance earliest, followed by gender and vowel decoding (all decoding $p < 0.05$ assessed via bootstrapped sign permutation testing and threshold-free cluster enhancement). Vowel decoding yielded the highest accuracy overall, but this peak accuracy occurred later than the peaks for speaker and gender decoding. The best decoding was obtained at frontotemporal sensor locations. Representational similarity analysis revealed that these results were correlated with how the stimuli differed in terms of their fundamental frequencies, different aspects of their formants and in their overall spectrotemporal variability.

Conclusion

These results suggest that speaker-related speech qualities are represented earliest in the neural response, likely supporting more robust representations of an utterance's linguistic content. Fundamental frequency and vocal tract cues appear to support these early representations along with auditory computations that are carried out in auditory cortex.

PS 132

Temporal Context Invariance Reveals Neural Processing Timescales in Human Auditory Cortex

Sam Norman-Haignere¹; Laura Long²; Orrin Devinsky³; Werner Doyle⁴; Adeen Flinker³; Nima Mesgarani⁵
¹*Zuckerman Institute for Brain Research, Columbia University, HHMI Postdoctoral Fellow of the Life Sciences Research Foundation*; ²*Zuckerman Institute for Brain Research, Columbia University, Program*

in Neurobiology and Behavior, Columbia University;
³*Department of Neurology, NYU Langone Medical Center, Comprehensive Epilepsy Center, NYU Langone Medical Center;*
⁴*Comprehensive Epilepsy Center, NYU Langone Medical Center, Department of Neurosurgery, NYU Langone Medical Center;*
⁵*Zuckerman Institute for Brain Research, Columbia University, Program in Neurobiology and Behavior, Columbia University, Department of Electrical Engineering, Columbia University*

Many basic questions about auditory cortical processing timescales remain debated: Do processing timescales increase along the cortical hierarchy as predicted by some computational models? Is there hemispheric specialization for processing information at different timescales? Are there distinct processing timescales for particular stimulus categories like speech or music? Answering these questions has been challenging because there is no general method for estimating the temporal integration period of a region: the time window within which stimulus features can alter the neural response. Spectrotemporal receptive fields can be used to estimate the integration period of the best-fitting linear model with respect to a spectrogram, but cortical responses are often highly nonlinear particularly in nonprimary regions. Temporal scrambling paradigms have revealed selectivity for intact temporal structure in nonprimary regions, but primary regions often show no difference between intact and scrambled stimuli, revealing a limitation of the method. Here, we introduce a simple experimental paradigm (the “temporal context invariance” or TCI paradigm) for inferring the integration period of any time-varying response. We present the same sound segment in two different contexts and we test how long the segment needs to be in order for the response to the segment to become invariant to the context. We tested the paradigm by collecting electrocorticography data from human epilepsy patients implanted with electrodes overlapping primary (near Heschl’s gyrus) and/or nonprimary auditory cortex (in superior temporal gyrus). We measured the high gamma response (70-140 Hz) to segments of natural sounds, ranging in duration from 30 milliseconds to 2 seconds. Each segment was presented in two different contexts and each context was repeated at least once to establish a noise ceiling. We then measured the segment duration at which each electrode’s response become invariant to the context. Preliminary results suggest that electrodes in primary auditory cortex exhibit integration periods between 50 and 200 ms, while electrodes in nonprimary regions show integration periods between 200 and 500 ms. With additional data, we expect to be able to test whether functionally specific regions, such as those selective for speech and music, exhibit distinctive timescales. Our empirical data will also be useful in

testing computational models, by making it possible to test whether the integration periods of the model match those measured experimentally.

PS 133

Specialized High-Level Processing of Speech and Music Revealed with EEG

Nathaniel J. Zuk¹; Emily S. Teoh²; Edmund C. Lalor¹
¹*University of Rochester;* ²*Trinity College Dublin*

Recent evidence with fMRI demonstrated specialized processing of speech and music in the auditory cortex of humans. This was revealed by using unsupervised methods to identify weightings across the cortex that best captured the variability in neural responses to a wide variety of sounds (Norman-Haignere et al, 2015, *Neuron*, 88:1281-1296). While there are clear spatial differences in neural activity for speech and music, the temporal responses are not well understood, and it is not clear if the temporal responses are unique for speech and music. We hypothesized that neural responses measured with electroencephalography (EEG) may capture unique and discriminable responses to speech and music stimuli resulting from high-level processing.

Subjects listened to 30 different two-second-long sounds, including speech, music, and other environmental sounds. EEG responses were recorded between 80 to 100 presentations of the sounds, randomly presented across trials. Using linear discriminant analysis to classify the two-second EEG responses to each sound, we found that the speech and music sounds, in addition to impact sounds, produced higher classification accuracies than all other environmental sounds. Separately, we repeated this experiment using scrambled versions of the speech, music, and impact sounds. The scrambled sounds were resynthesized using a model of low-level processing with identical spectrotemporal statistics to the originals (McDermott & Simoncelli, 2011, *Neuron*, 71:926-940). Scrambled impact sounds were classified identically to their original counterparts, showing that the EEG responses were dominated by the processing of low-level statistics. In contrast, scrambled music and speech sounds were classified worse than the originals. Additionally, the patterns of classification accuracy persisted when spatial information was removed by averaging the EEG data across channels.

Our study demonstrates that EEG captures temporally unique responses to speech and music more strongly than other environmental sounds. Furthermore, the unique responses are dominated by high-level processing in the brain. These results highlight the importance of using naturalistic sounds when using EEG

to study the neural processing of speech and music in humans.

PS 134

The Acoustic Change Complex in Cochlear Implant Users

Jan van Heteren¹; Bernard Vonck¹; Marc Lammers²; Huib Versnel¹

¹University Medical Center Utrecht; ²University of British Columbia

Cochlear implant (CI) users can reach impressive speech perception abilities, however, they show a large variability. The clinical audiometry measures to evaluate their hearing are subjective, age-dependent, and require linguistic skills. The acoustic change complex (ACC), which is a cortical auditory evoked potential to a sound change (Martin and Boothroyd, 2000, *J Acoust Soc Am* 107: 2155-2161), might be helpful to assess auditory performance and could even give an insight in cortical auditory processing capabilities. The aim of our study is to evaluate whether the ACC is predictive for hearing performance of CI users.

We recorded the ACC in 11 bilaterally and 5 unilaterally deaf adult CI users with more than one year of CI experience. The ACC was evoked by a pure tone stimulus directly presented in the center of the frequency band of the middle or apical CI electrode, with varying frequency increases corresponding to 1, 2 or 3 inter-electrode steps. Speech perception was tested with consonant-vowel-consonant words in silence and in noise, and digit triplets in noise. Frequency discrimination was assessed using a 3-interval, 2-alternative forced-choice, adaptive staircase procedure using the same reference frequency of the ACC stimuli.

In all subjects reliable ACCs could be evoked. Increasing frequency changes resulted in increasing N1-P2 amplitudes and decreasing N1 latencies. Speech perception in noise was positively correlated to the ACC amplitude for both the middle and apical electrode sites (Spearman's $r > 0.6$, $p < 0.05$). Only for the middle electrode, frequency discrimination was significantly correlated to the ACC amplitude ($r = 0.7$, $p < 0.05$).

In summary, the ACC is a potentially useful objective measure to contribute to better rehabilitation of CI users, as it is a non-attentive test, which correlates with postoperative hearing performance.

PS 135

Cortical Auditory Encoding of Reverberant Speech

Ramesh Kumar Muralimanohar¹; Marcin Wróblewski²; Jay Vachhani¹; Michelle R. Molis¹; Curtis J. Billings¹
¹VA RR&D NCRAR; ²Pacific University

Listeners, particularly those with hearing loss, face great difficulties communicating in daily situations involving reverberation and noise, even with hearing aids. Individuals with similar hearing thresholds also vary greatly in their ability to handle degraded speech. The underlying causes of variability and impaired performance in reverberation are poorly understood, preventing the development of effective rehabilitative strategies. Reverberation results in the temporal smearing, decreasing the contrasts required to successfully parse speech. Multiple N1-P2 responses can be evoked by acoustic changes like onsets that characterize continuous sounds/speech. The purpose of this study is to systematically analyze the effects of reverberation on the neural encoding of speech using cortical auditory evoked potentials (CAEP). We hypothesized that the temporal smearing due to increased reverberation would reduce amplitudes and increase latencies associated with the neural encoding of multiple acoustic changes within a stimulus.

A single 700-ms long /daba/ stimulus was used. It was created by concatenating /da/ and /ba/ syllables (both 350 ms in duration), with no gap between them. This stimulus was presented in both clean (anechoic) and reverberant contexts to passively elicit CAEPs in a group of young normally hearing adults. Reverberation time (T60) was varied to be between 400 and 1600 ms in 400 ms steps. The stimuli were presented monaurally at 80 dB SPL to the right ear through ER-3A insert earphones. Preliminary results indicate that reverberation changes the neural response to both the first and second syllables relative to the clean anechoic condition; however, the response to the second syllable was impacted more by the reverberation than the response to the first syllable. Also, increasing amounts of reverberation resulted in greater changes to the morphology of the response. Correlational analyses were completed to link response changes to the reverberation parameters that caused them. Speech identification scores in the same contexts will be obtained from these participants to link the patterns of neural encoding observed in this study to intelligibility scores. These data will help establish the baselines of changes in neural encoding due to reverberation and allow further study in populations with impairments.

[Work supported by R01 DC015240]

Resting State Connectivity Within and Beyond Auditory Cortex Across Awareness States: An Intracranial Electrophysiology Study

Matthew I. Banks¹; Kirill V. Nourski²; Hiroto Kawasaki³; Matthew Howard³

¹Department of Anesthesiology, University of Wisconsin School of Medicine and Public Health; ²The University of Iowa; ³Human Brain Research Laboratory, Department of Neurosurgery, The University of Iowa

Introduction: The sharing of information between nodes in the cortical network plays a central role in leading theories of consciousness. Disruption of connectivity across networks that subserve sensory processing has been proposed to occur upon loss of consciousness (LOC) during sleep and general anesthesia. However, whether LOC during these two conditions shares a common mechanism is unclear. To investigate this issue, functional connectivity between cortical regions of interest (ROIs) was compared across brain states during natural sleep and propofol anesthesia.

Methods: Subjects were neurosurgical patients implanted with intracranial electrodes placed to identify epileptic foci. A combination of multicontact subdural grid and depth electrodes provided dense coverage of temporal, parietal and frontal cortex, including core and non-core auditory cortex on the superior temporal plane (STP) and the superior temporal gyrus (STG), auditory-related cortex on the middle temporal (MTG), supramarginal, angular gyrus and insula, as well as prefrontal cortex (PFC), amygdala, hippocampus and parahippocampal gyrus (PHG). Resting state data were recorded in the same subjects during overnight natural sleep and during induction of general anesthesia with propofol. Six brain states were compared: wake (WS) and NREM stages 1 and 2 (N1, N2) during natural sleep, and pre-drug wake (WA), sedated/responsive (S) and unresponsive (U) during propofol anesthesia. Connectivity was computed as thresholded, weighted alpha (8-13 Hz) phase lag index. Assignment of recording sites to ROIs was made using MRI-based anatomical reconstructions of recording site locations. Connectivity values for recording sites within each ROI (n = 1 – 20) were averaged.

Results: In WS and WA conditions, connections within and between auditory core, non-core and auditory-related areas on STP, STG, MTG, angular gyrus and insula were dominant. This pattern was largely unchanged for the WS to N1 transition, but with increased connectivity between auditory areas and mesial temporal lobe (hippocampus and amygdala). A similar pattern was observed for transition from WA to

S, but with greater connectivity between auditory areas and PHG. In both sleep and anesthesia, transitions into unresponsive states (U, N2) were characterized by dramatic reduction in connectivity across auditory areas and greater connectivity with PFC.

Conclusions: Pronounced changes in network topology for the transitions S → U and N1 → N2 likely reflect changes in cortical connectivity mediating transition between conscious and unconscious states. The similarity in network topology between equivalent brain states during anesthesia and sleep suggests common mechanisms of LOC in these two conditions.

PS 137

Measuring Spread of Excitation Using the Masked Onset Response in Humans and Cats

Robert P. Carlyon¹; François Guérit²; Andrew Harland¹; John C. Middlebrooks³

¹MRC Cognition & Brain Sciences Unit; ²MRC Cognition and Brain Sciences Unit, University of Cambridge; ³University of California at Irvine

To understand the limitations on hearing, it is useful to compare psychophysical and physiological measurements to the same stimuli. Unfortunately, accurate physiological recordings are possible only in animals, and psychophysical measures are most reliable and easiest to obtain in humans. To bridge this gap we used scalp-based EEG recordings to measure spread of excitation from a noise masker in normal-hearing (NH) humans and cats. Because we ultimately wish to compare spread-of-excitation from CI electrodes, as a proof-of-principle we used two acoustic maskers that should produce narrow and broad spread-of-excitation, respectively. In humans these maskers were 1/8th and 1-octave bands of noise, geometrically centred on 4000 Hz, 13-seconds long, and combined with a low-pass pink noise designed to mask distortion products arising from the interaction between maskers and probes. Thirteen 70-dB-SPL 50-ms sinusoidal probes were presented every 1 sec starting at the onset of the masker. Responses to the last 12 of these probes were averaged within each masker, and averaged across 20 presentations of each masker. Five probe frequencies (Fp) were tested, corresponding to -0.5, -0.25, 0, 0.25, and 0.5 octaves re 4000 Hz. There was a 1-sec gap between each masker presentation. All stimuli were presented monaurally. The N1-P2 cortical evoked potential was expressed for each probe/masker combination as a percentage of the response to the unmasked probe and at noise levels of 48, 52, 56, and 60 dB SPL within the (human) 4-kHz auditory filter. EEG responses were recorded using an 8-channel BioSemi system and measured between

electrodes at Cz and at the mastoid contralateral to presentation. Subjects watched a silent TV programme during recordings. Average results from the first six subjects show the expected pattern with the two maskers producing equal N1-P2 at Fp=4000 Hz, which increased for the narrowband masker (only) at more distant probe frequencies. Data for cats were obtained under light ketamine anaesthesia using a subset of the stimulus conditions used for humans, shifted an octave higher in frequency. The cat and human EEG data will be compared to each other and to psychophysical spread-of-excitation curves obtained from humans using the same stimuli.

PS 138

Electrocorticographic Analysis of Human Superior Temporal Sulcus

Kirill V. Nourski¹; Mitchell Steinschneider²; Ariane Rhone¹; Hiroto Kawasaki³; Matthew Howard³

¹The University of Iowa; ²Albert Einstein College of Medicine; ³Human Brain Research Laboratory, Department of Neurosurgery, The University of Iowa

The superior temporal sulcus (STS) is a crucial hub in the cortical system subserving speech perception. To date, this area has been primarily examined with non-invasive functional neuroimaging (e.g. fMRI). In neurosurgical epilepsy patients, multicontact depth electrodes that target mesial temporal lobe structures such as the amygdala can traverse the upper or the lower bank of the STS. This offers a unique opportunity to study this region with high spatial and temporal resolution. The study sought to characterize fundamental electrophysiological properties of the STS using a variety of auditory stimuli presented under multiple task conditions in a large cohort of subjects (N = 25).

Subjects were patients undergoing chronic invasive monitoring for medically intractable epilepsy. Stimuli were non-speech (tones, click trains) and speech sounds, presented in passive-listening, target detection and dialog-based paradigms. ECoG data were simultaneously acquired from the STS as well as auditory cortex in Heschl's gyrus (HG), lateral superior and middle temporal gyri (STG, MTG). Event-related band power (ERBP) was examined between 4 and 150 Hz.

High (70-150 Hz) and low gamma (30-70 Hz) ERBP exhibited similar increases in response to the auditory stimuli. Increases in high frequency ERBP were paralleled by decreases in low frequency (4-14 Hz) ERBP. The STS was less responsive to non-speech sounds and degraded speech compared to clear speech. Responses in the STS had longer latencies than those

in the HG and on the STG, and shorter latencies than on the MTG. Responses were more robust and had shorter onset latencies in the upper bank of the STS compared to the lower bank. Comparable degrees of activity were elicited in the language-dominant and non-dominant hemispheres in a semantic classification task. High gamma responses were not consistently modulated by target condition (target and non-target words in the semantic task; non-target words in a control tone detection task). In contrast, results of a dialog-based paradigm demonstrated modulation of neural activity in both the upper and the lower banks of the STS by task-related features, including task direction, difficulty and affirmation of successful task completion. Sites in STS could preferentially respond to the subject's own speech over that of the interviewer's, reflecting their possible involvement in the audiomotor processing pathway.

We conclude that human STS can be effectively probed with ECoG, and that multiple experimental paradigms are necessary to adequately identify its response properties and the transformations that occur from earlier processing stages in auditory cortex.

PS 139

Neural Correlates of Enhanced Audiovisual Processing in the Bilingual Brain

Gavin Bidelman

University of Memphis

Bilingualism is associated with enhancements in perceptual and cognitive processing necessary for juggling multiple languages. Recent psychophysical studies demonstrate bilinguals also show enhanced multisensory processing and more restricted temporal binding windows for integrating audiovisual information. Here, we probed the neural mechanisms of bilinguals'; audiovisual benefits. We recorded neuroelectric responses in mono- and bi-lingual listeners to the double-flash paradigm in which auditory beeps concurrent with a single visual flash induces the perceptual illusion of multiple flashes. Relative to monolinguals, bilinguals showed less susceptibility to the illusion (fewer false perceptual reports) coupled with stronger and faster event-related potentials to audiovisual information. Source analyses of EEG data revealed monolinguals increased propensity for erroneously perceiving audiovisual stimuli was attributed to increased activity in primary visual (V1) and auditory cortex (PAC), increases in multisensory association areas (BA 37), but reduced frontal activity (BA 10). Regional activations were associated with an opposite pattern of behaviors: whereas stronger V1 and PAC activity predicted slower behavioral responses, stronger frontal BA10 responses

elicited faster judgments. Our results suggest bilinguals'; higher precision in audiovisual perception reflects more veridical sensory coding of physical cues coupled with superior top-down gating of sensory information to suppress the generation of false percepts. Findings underscore that the plasticity afforded by speaking multiple languages shapes extra-linguistic brain regions and can enhance audiovisual brain processing in a domain-general manner.

PS 140

Individual Differences in Listening Skills Modulate the Auditory Categorical Processing of Speech and Music

Kelsey Mankel; Jake Barber; Gavin Bidelman
University of Memphis

Successful perception of the world requires the human brain assemble diverse sensory information into common groupings, a process known as categorical perception (CP). Intense auditory experiences (e.g., musical training, language expertise) can shape categorical representations necessary for identifying speech and novel sound-to-meaning learning, but little is known concerning the role of innate hearing function in CP. Here, we asked whether listeners vary in their intrinsic abilities to categorize complex sounds (speech and music) with the goal of characterizing how individual differences in this core perceptual skill manifest in auditory brain mechanisms. To this end, we recorded neuroelectric brain activity in individuals without formal music training but who differed in their inherent auditory perceptual abilities (assessed via the Profile of Music Perception Skills [PROMS]) as they rapidly categorized sounds along speech and music continua. Behaviorally, listeners were more precise and faster at identifying (more familiar) speech than (less familiar) musical stimuli. Yet, individuals with naturally more adept listening skills ("musical sleepers") showed enhanced speech categorization in the form of faster identification. At the neural level, inverse modeling parsed EEG data into different sources to evaluate the contribution of region-specific activity (i.e., primary auditory cortex, PAC; inferior frontal gyrus, IFG) to categorical neural coding. We found limited differences in neural responses across speech tokens but stronger neural responses in the PAC for categorically ambiguous music stimuli compared to prototypical tokens. Music stimuli generated more robust neural activity than speech, particularly in the right PAC, suggesting listeners may have exerted greater listening effort for identification of the novel (but not overlearned speech) stimuli. Results suggest that listeners arrive at categorical sound labels using individual strategies, supported by a differential

engagement of the brain's auditory-linguistic network (PAC-IFG). More broadly, our data show that listeners with naturally more adept auditory skills can map sound to meaning more efficiently than their peers, which may aid novel sound learning related to language and music acquisition.

PS 141

Neural Speech Tracking in the Delta and Theta Frequency Bands Differentially Encodes Comprehension and Intelligibility of Speech in Noise

Octave Etard¹; Tobias Reichenbach²

¹*Department of Bioengineering, Imperial College London*; ²*Department of Bioengineering and Centre for Neurotechnology, Imperial College London*

Background: Humans excel at analysing complex acoustic scenes. Effective segregation of different competing speech signals is indeed often necessary for communication. Speech processing may be aided by cortical activity in the delta and theta frequency bands that has been found to track the speech envelope. Change of these neural responses with the intelligibility and comprehension of speech have previously been established. These studies employed speech that was acoustically degraded. It therefore remains unclear which aspects of neural speech tracking represent the processing of acoustic features, related to speech intelligibility, and which aspects reflect higher-level linguistic processing related to speech comprehension.

Methods: We employed electroencephalography (EEG) with 64 scalp electrodes to record neural responses of native English speakers listening to naturalistic continuous speech in varying conditions of noise (speech in quiet, competing speakers and different levels of speech-in-babble-noise). We obtained EEG recordings in response to English stimuli as well as in response to a foreign unknown language with similar acoustic properties (Dutch). When listening to English the subjects'; comprehension was systematically modulated by the noise level, but remained nil in the acoustically matched Dutch conditions. This allowed us to separate neural correlates of changes in the acoustic properties of the stimuli (intelligibility) and of speech comprehension. We used regularised linear spatio-temporal models in both a decoding and an encoding approach to relate intelligibility and comprehension to the neural responses.

Results: We were able to accurately reconstruct the stimulus envelopes, and to reliably predict speech comprehension and intelligibility in the different acoustic conditions. We investigated the relative importance of the delta, theta and alpha frequency

bands, and found that cortical tracking in the theta frequency band is mainly correlated to intelligibility, while the delta band contributed most to speech comprehension. Strikingly, we uncovered a neural component in the delta band that preceded the speech signal and that informed on comprehension, hinting at a predictive mechanism for language processing.

Conclusion: We have developed a procedure to infer speech-in-noise comprehension and intelligibility from neural responses to continuous speech in background noise. Our results disentangle the functional contributions of cortical speech tracking in the delta and theta bands to speech processing. The obtained results demonstrate that speech envelope, a low-level acoustic feature, can be used to recover comprehension, a high level cognitive construct. This approach may thus prove useful to investigate auditory processing disorders.

PS 142

On the Relationship between Cortical Oscillatory Activity and Inner Ear Amplification Gain

Heivet Hernandez Perez¹; Ronny Ibrahim¹; Catherine McMahon¹; Sriram Boothalingam²; Jessica J.M. Monaghan³

¹Macquarie University; ²University of Wisconsin-Madison; ³Macquarie University, Department of Linguistics

The role of the efferent system (descending projections from the auditory cortex to the lower auditory centres) in aiding speech processing and comprehension remains controversial in the auditory literature. In a previous approach (Hernandez-Perez et al., 2018), we addressed how the cochlear gain is differentially modulated by the efferent system depending on the auditory scene encountered (single vs multiple speech streams perception). To determine if this efferent control of the cochlear gain is related to word processing, we have explored in this study the relationship between oscillatory activity and amplification of the cochlear gain (measured using otoacoustic emissions: OAEs). In particular, we have focused our interest on the relationship between the cortical oscillatory activity in the theta band (4–8 Hz), that has been extensively linked to word processing (Ghitza, 2012; Ghitza, 2013), and amplification of the cochlear gain. Here concurrent EEG and OAE recording systems allowed us to monitor, at different stages of the auditory pathway, the effects of lexical decision-making as well as passive listening of words and non-words. In a series of three experiments, speech intelligibility was either manipulated by noise vocoding the speech signal or adding babble noise/

speech shaped noise to the clean speech. Our results show that theta band energy is stronger in the power spectrum when participants are performing the lexical decision compared to passive listening of speech. Changes in oscillatory activity could also be accompanied by suppression of Click-Evoked OAE magnitude depending on the type of stimuli being processed. This study contributes to our better understanding of the likely role that the auditory efferent system plays in speech processing and comprehension.

References

Ghitza, O. (2012). On the role of theta-driven syllabic parsing in decoding speech: intelligibility of speech with a manipulated modulation spectrum. *Frontiers in psychology*, 3, 238.

Ghitza, O. (2013). The theta-syllable: a unit of speech information defined by cortical function. *Frontiers in psychology*, 4, 138.

Hernandez-Perez H., McMahon C., Boothalingam S., Dhar. S., Poeppel D., Monaghan J. (2018). Does the way speech intelligibility is manipulated matter for the auditory efferent system? ARO 41st MidWinter Meeting, Podium presentation.

PS 143

Modulation Change Detection in Human Auditory Cortex: Evidence for Asymmetric, Nonlinear Edge Detection

Seung-Goo Kim¹; David Poeppel²; Tobias Overath¹
¹Duke University; ²New York University

Changes in modulation rate are important cues for parsing acoustic signals such as speech. We parametrically controlled modulation rate via the correlation coefficient (r) of amplitude variations across fixed frequency channels: modulation rate increases with decreasing r , and vice versa. Four levels of correlation coefficients roughly spaced by equal perceptual distances were used (i.e., $r = 0, 0.5, 0.8, 0.95$). By concatenating segments with different r , acoustic changes of various directions (e.g. changes to higher correlation coefficients, random-to-correlated, or vice versa) and sizes (e.g. low-to-high correlation, or vice versa) can be obtained (Figure 1). We recorded MEG data in 13 participants while they detected changes in correlation in 36-s sound blocks. Evoked responses (Figure 2) demonstrated 1) an asymmetric representation of change direction: random-to-correlated changes produced a prominent evoked field around 180 ms after change-onset, while correlated-to-random changes did not evoke any significant

responses; and 2) a highly non-linear representation of correlation structure, whereby even small changes involving segments with a high correlation coefficient (i.e., with slow modulation rates) are much more salient than relatively large changes that do not involve segments with high correlation coefficients. Specifically, the direction of changes significantly modulated the amplitude of peaks identified between 100–300 ms after onset (repeated-measures ANOVA with factors Change direction and Change size; $F[1,12] = 19.9$, $p = 0.0007$), confirming prominent responses by random-to-correlated changes. Moreover, the correlation coefficient of the target segment significantly affected the amplitude of the same peaks (repeated-measures ANOVA with nominal factors Previous correlation level and Current correlation level; $F[3,36] = 23.5$, $p < 10^{-9}$). This effect was not significant when modeled as a linear variable (a repeated-measures linear model with two continuous variables of Previous correlation level and Current correlation level, $F[1,12] = 0.7$, $p = 0.40$), reflecting the non-linear saliency of the slow modulation in detecting correlation structures. The results demonstrate a high sensitivity for low modulation rates in the human auditory cortex (Luo & Poeppel, 2007; Overath et al., 2008, 2012), both in terms of their representation and their segregation from other modulation rates (Cervantes Constantino et al., 2012).

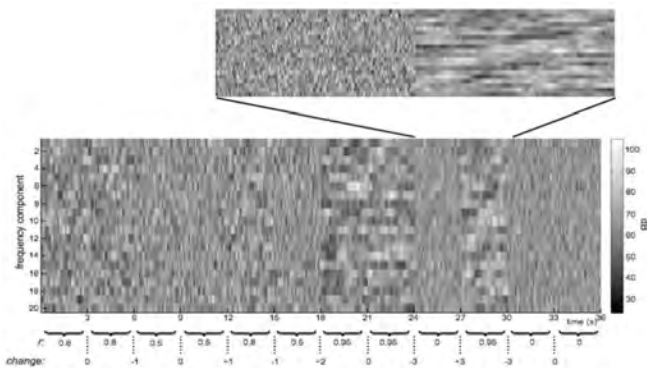


Figure 1: Example stimulus. The y-axis represents 20 (randomly selected) frequencies between 246–4435 Hz, gray-shading indicates their amplitude over time. Below the plot, r denotes the correlation coefficient governing each 3-s segment ($r = 0, 0.5, 0.8, 0.95$; total of four levels), while the corresponding change sizes between levels are noted at boundaries.

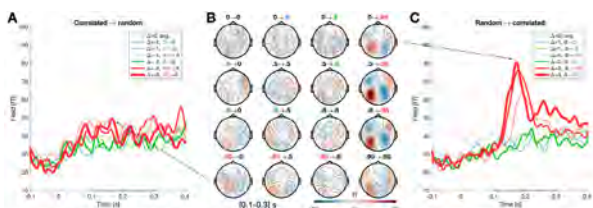


Figure 2: Grand-average evoked responses and topographies. A, C: Root-mean-squared (RMS) response of temporal channels (marked by black dots in the topographies in B) to changes from correlated to random (A) and random to correlated (C) temporal modulation. The thickness encodes absolute changes in correlation, the color encodes the maximal correlation involved. The latency range (0.1–0.3 s) to identify peaks is marked in a gray on the x-axis. B: Grand-average topographies constructed with the channels of interest within the latency range are given in a 4-by-4 grid of conditions (row = previous segment; column = current segment). Correlation coefficients of the previous and current segments are noted above each topography.

PS 144

Effects of vowel, emotion, and age in latency and amplitude of Cortical Auditory Evoked Potentials (CAEPs)

Kieun Lee; Hyunwook Song; Jiyeong Yun; Eunsung Lee; Jinsook Kim
Hallym University

Background: The cortical auditory evoked potentials (CAEPs) were categorized by either the exogenous or endogenous and were not investigated sufficiently. Among many variables affecting the results of CAEP, speech stimuli have been emerged to measure the degree of central nervous system maturity, the ability of central hearing processing and listening effort. Also, the emotional salience of the speech was found to be an element factor influencing the components of CAEP. Finally, CAEPs were known to reflect the cognitive changes of the geriatric population followed the deficiency of neurotransmission. The purpose of this study was to analyze the parameters that could affect the latencies and amplitudes of CAEPs and determine the characteristics more specifically with the composite responses of variables. The responses of younger and older adults according to the vowels, /u/, /a/, and /i/ representing low, middle, and high frequencies with emotional saliences, neutral(N), anger(A), happiness(H), and sadness(S) were observed.

Methods: 20 younger (mean: 22.1, range: 21–27) and 20 older (mean: 68.2, range 65–74) adults with normal hearing participated. To rule out any age-related cognitive impairment, the Korean version of Mini-Mental State Examination (MMSE) was conducted to the older group. The score 25 or above of MMSE was only accepted. Applying 4 emotions to 3 vowels, 12 stimuli were composed and utilized. To analyze CAEPs, the bipolar channel was used with channel A for measuring evoked responses and channel B for monitoring eye movement and blinking. The parameters were at a sweep at 200, a rate of 1.1, a sampling rate at 640Hz, a gain at 50K and 20K of channels A and B, a polarity at alternative, and a bandpass filter from 1 to 30 Hz. The intensity was 70 dB. **Results:** The main effects of age, vowel, and emotion showed significant differences. For A and H emotion, the shorter latencies for all the component the larger amplitudes for P1 and N2 were noted. Only N1 latency was significantly different depending on vowels. The shortest latency was noted in /a/ and /i/ and /u/ followed. The older adults showed longer P2 latency and reduced N2 amplitude as compared to younger adults. Additionally, the variables were influential to several interactions. **Conclusion:** The emotional valence of the stimuli has revealed the definite effect to all latencies and some amplitude of the components. Therefore, we could cautiously conclude that the endogenous factor is predominant to all the CAEP components except P1.

Lateralization of Parietal Alpha Power During Auditory Spatial Attention in Normal and Hearing Impaired Listeners

Lia Bonacci¹; Lengshi Dai¹; Barbara Shinn-Cunningham²
¹*Boston University*; ²*Carnegie Mellon University*

In noisy environments, spatial attention may be used to select target speech in one location while suppressing irrelevant sounds in another. However, if the spatial separation of sounds cannot be perceived, then spatial attention may not be used at all, making it difficult to communicate in complex auditory scenes. Electroencephalography (EEG) is often used to identify correlates of selective attention. In particular, lateralization of alpha (8-14 Hz oscillations) power over parietal sensors has been shown to reflect spatial focus of attention—greater alpha power ipsilateral to the attended location reflects suppression of stimuli in the ignored location. Hearing impaired (HI) listeners are less sensitive to spatial cues than normal hearing (NH) listeners. Therefore, the ability to use spatial attention may be degraded in HI listeners, which in turn may lead to degraded lateralization of EEG alpha. In this study, NH and HI listeners performed an auditory spatial attention task while we recorded 32-channel EEG. HI subjects had bilateral symmetrical sensorineural hearing loss with thresholds ≥ 25 dB hearing level (HL) at one or more frequencies from 250 Hz to 8,000 Hz; NH subjects had thresholds ≤ 20 dB HL across these frequencies. During the task, three melodies were presented simultaneously from left, right, and center using interaural time differences (ITDs). Left and right melodies were lateralized using symmetric ITD pairs that were either small (± 205 μ s) or large (± 799 μ s); the center melody had an ITD of 0 μ s. Notes in each melody changed pitch over time, with contours that were rising, falling, or zigzagging. Subjects were cued to attend either the left, right, or center melody and report its pitch contour. ITD thresholds were measured for each subject to quantify sensitivity to spatial cues. Overall, HI listeners had higher ITD thresholds than NH listeners, suggesting lower sensitivity to spatial cues. This is consistent with the fact that HI listeners performed worse on the spatial attention task than NH listeners. In NH listeners, alpha power was greater in parietal-occipital sensors ipsilateral to the attended location, and this lateralization was stronger in the large ITD condition. In HI listeners, we observed no lateralization of alpha power across these sensors in either small or large ITD condition. These results suggest that EEG correlates of spatial attention are degraded in hearing impaired listeners, likely reflecting a degraded ability to use spatial cues for suppressing irrelevant sounds in noisy settings.

Within-Subject Cortical Auditory Response Variability and Listening Performance

Anne Islam¹; Caren Armstrong¹; Mackenzie Cervenka¹; Sai Akanksha Punuganti²; Dana Boatman³

¹*Department of Neurology, Johns Hopkins School of Medicine*; ²*Department of Biomedical Engineering, Johns Hopkins School of Medicine*; ³*Departments of Neurology and Otolaryngology, Johns Hopkins School of Medicine*

Background

Increased within-subject variability is often considered a defining characteristic of individuals with listening impairment. However, prior cortical auditory electrophysiology studies based on scalp recordings have yielded equivocal findings. In this study, we used intracranial electrocorticographic (ECoG) recordings to measure within-subject variability in early cortical auditory evoked responses as a function of individual listening performance.

Methods

Test-retest ECoG recordings were acquired at 2-5 day intervals from 13 right-handed patients with focal epilepsy being evaluated for epilepsy surgery (mean age 34 yrs; 7 females) who had 8x8 electrode arrays implanted over the left hemisphere for seizure localization. All patients had electrode coverage of the posterior superior temporal gyrus (auditory) and confirmed normal hearing (≤ 25 dB, 0.5-4 kHz) and cognitive function (FSIQ > 80). Patients who scored ≥ 2 standard deviations below the mean on two or more behavioral speech-in-noise tests were classified as impaired listeners (N=7). ECoG recordings were acquired using a 300-trial passive listening paradigm with 200-ms duration pure tones (1000 Hz, N=246 trials; 1200 Hz, N=54 trials). Evoked responses were derived by trial-averaging in the time domain. Waveform measurements (latency, amplitude) focused on the evoked N1 response, occurring 75-120 ms post-stimulus, as was present consistently across all patients and sessions. For test-retest comparisons, peak waveform latencies and amplitudes were measured at electrode sites that showed the largest N1 responses to the 1000 Hz tone in both sessions.

Results

For normal listeners, mean N1 test-retest latencies (103 ms ± 10 and 105 ms ± 10 , respectively) and amplitudes (36 μ V and 34 μ V, respectively) were reproducible across sessions. Test-retest correlation coefficients for latency ($r=0.89$), and amplitude ($r=0.95$) indicated high reliability (p

Conclusions

These results indicate that early cortical auditory responses are highly reliable within subjects, despite individual differences in listening performance.

Funding

Supported by U.S. Army Research Laboratory Grant W911NF-10-2-0022 and the David M. Rubenstein Fund for Hearing Research.

PS 147

Lateralization of Parietal Alpha Power During Auditory Spatial Attention in the Presence of Strong Pitch Cues

Lia Bonacci¹; Barbara Shinn-Cunningham²
¹*Boston University*; ²*Carnegie Mellon University*

In order to communicate in noisy environments, an individual must select target stimuli while simultaneously suppressing distractors. If the location of the target is known, this can be performed using top-down spatial attention. Neural correlates of spatial attention have been found using electroencephalography (EEG), namely through measurement of event-related potentials (ERP) and alpha (8-14 Hz oscillations) power. Increased ERP amplitudes from auditory cortex reflect enhancement of stimuli in the attended location. Increased parietal alpha power ipsilateral to the attended location is associated with suppression of distractors in the ignored location. Alpha oscillations have been studied extensively in vision, but their role in auditory spatial attention is less clear. Furthermore, top-down spatial attention may not persist over the course of an auditory stream if pitch also differentiates target from distractors. We recorded EEG while subjects performed an auditory spatial attention task. Three melodies were presented simultaneously from left, right, and center using interaural time differences of -100 μ s, +100 μ s, and 0 μ s, respectively. Notes in each melody changed pitch over time, with contours that were rising, falling, or zigzagging. Subjects were cued to attend either the left or right melody and report its pitch contour. The center melody was always ignored. Experimental blocks alternated between two conditions that differed in the pitch separation of the competing melodies: one where the separation was large (~10 semitones) and one where it was small (~1 semitone). N1 amplitudes and alpha power were measured from the recorded EEG. In frontocentral sensors, N1s for a given note were larger when the note was attended than when it was ignored. Alpha power over parietal sensors varied with spatial attention focus such that it was larger ipsilateral to the attended melody. Importantly, while spatial attention focus changed alpha lateralization similarly in the two pitch conditions, this

modulation was stronger when pitch differences were small. We conducted an additional experiment with stimuli similar to those in the large pitch separation condition. The melody task was the same, but the spatial cue also contained information about the pitch of the target melody. Here, attentional modulation of the N1 occurred, but we observed no modulation of alpha power across parietal sensors. Our findings suggest that alpha modulation reflects suppression during auditory spatial selective attention. However, when pitch cues are strong, parietal alpha modulation is weak, likely reflecting the fact that pitch differences can be used to help focus attention.

PS 148

Active Tracking of Sound Textures: a Human Intracranial Study

Alexander J. Billig¹; Phillip E. Gander²; William Sedley³; Maria Chait¹; Hiroto Kawasaki⁴; Christopher K. Kovach⁴; Matthew Howard⁴; Timothy D. Griffiths⁵

¹*UCL Ear Institute, University College London*;

²*Department of Neurosurgery, Department of Otolaryngology, The University of Iowa*; ³*Institute of Neuroscience, Newcastle University*; ⁴*Human Brain Research Laboratory, Department of Neurosurgery, The University of Iowa*; ⁵*Wellcome Centre for Human Neuroimaging, University College London; Institute of Neuroscience, Newcastle University*

A network consisting of auditory cortex, hippocampus, and inferior frontal gyrus has been proposed to support auditory working memory (Kumar et al., *J Neurosci* 36:4492-4505, 2016). However, human intracranial recordings are yet to reveal hippocampal high gamma activity, a neural spiking correlate, during memory for tones. Recordings from the rat hippocampal complex indicate that cells that support navigation can also form discrete firing fields for particular sound frequencies (Aronov et al., *Nature* 543:719-722, 2017). Critically, this is the case only when the animal adjusts a sound to match the frequency of a remembered target, but not during passive listening. For humans performing such a task, recruitment of navigation circuits may stem from a cognitive association between height in pitch and in physical space (Rusconi et al., *Cognition* 99:113-129, 2006). Here, we study the neural underpinnings of memory for and tracking of sound textures that vary continuously in a single dimension but have no such spatial association. Subjects were patients implanted with electrodes to localize epileptic activity. Stimuli were concatenated chords, each containing between 4 and 100 simultaneous 200-ms tones randomly distributed in frequency over a 4-octave range. Fixing the number of simultaneous tones ("density") while varying their

frequencies from chord to chord gave rise to textures that were more “beep”-like at lower densities and more “noise”-like at higher densities (these terms were used to describe the sounds to subjects in language that avoided spatial metaphors). In each active trial, subjects listened to a 2-s sound of fixed target density, which they were to remember over a subsequent 2-s retention period. They then heard a 15-s texture, the density of which they adjusted using button presses to match the density of the target. Preliminary analyses of sound-induced neural activity revealed robust (high) gamma responses in Heschl’s gyrus and superior temporal gyrus, with concurrent low frequency (4-30 Hz) power decreases over a range of frontal, temporal, and parietal sites. (High) gamma responses were also observed in right hippocampus and right inferior frontal gyrus; these were greater during active adjustment than in a passive listening condition with similar auditory stimulation. Activity at one hippocampal site was also present during target presentation and the subsequent silent retention period. Ongoing work includes conducting motor/attention control experiments, and applying multivariate analyses to study the link between behaviour and the strength of target representations across the putative auditory working memory brain network.

Inner Ear: Membranes & Fluids

PS 149

Sound Stimulated Changes in Cochlear Blood Flow are Blocked by Ablation of the Superior Cervical Ganglion in Wild-type but not salsa Mice

Suzan Dziennis¹; George Burwood²; Teresa Wilson¹; Jianlong Yang¹; Gangjun Liu¹; Sarah Foster¹; Ruikang Wang³; Alfred Nuttall⁴

¹Oregon Health & Science University; ²Oregon Hearing Research Center; ³University of Washington, Seattle; ⁴OHSU

The cochlea is one of the most metabolically demanding organs in the body. In order to meet the high energy demand critical for hearing, cochlear microvasculature is tightly controlled to maintain optimal perfusion. However, when subjected to loud sound exposure (LSE), cochlear blood flow (CBF) becomes dysregulated and paradoxically decreases, leading to increased cell death and hearing loss. Whether this change in CBF is induced by local or systemic metabolic pathways, or direct mechanical insult to the lateral wall vessels is not known. The lateral wall of the cochlea is supplied by capillary networks and CBF is regulated by local metabolism though other evidence suggests that sympathetic innervation regulates blood flow in the main arterioles

and may potentiate hearing loss. We hypothesized that damage caused by sound stimulation would be attributed to the activation of mechanotransduction (MET) channels rather than physical forces applied to the organ of Corti leading to overactive and harmful metabolic pathways, ultimately leading to vasoconstriction. We have attempted to separate the metabolic and mechanical pathways to lateral wall flow regulation during loud sound exposure, by using Cadherin23-missense mutant mice (salsa) mice which lack Cadherin23 for tip links required for the activation of MET channels, but have intact outer hair cells (at p56). 8 week old male age-matched salsa and CBA/CaJ wild-type (WT) mice were exposed to 30 min of acute intense band limited noise followed by 30 min of recovery. Using optical coherence tomography angiography, CBF was measured, in both groups, from the lateral wall vessels directly through bone in the 16 kHz region of the cochlea during and after LSE. Furthermore, CBF was examined, with and without sympathetic cochlear innervation from the superior cervical ganglion (SCG) during and after LSE. LSE reduced CBF in WT and increased CBF in salsa mice. CBF in the contralateral cochlea was unaffected. SCG ablation partially ameliorated LSE-induced reduction in CBF in WTs and had no effect in salsa mice. Although compensatory mechanisms may occur, these results suggest that MET channel controlled hair cell stimulation is, in part, responsible for regulating cochlear blood flow. The SCG-mediated effect could mask flow changes from local metabolic feedback loops of unknown mechanism, as flow changes were not affected by SCG removal in the salsa mouse. Vascular treatment strategies aimed at stimulating local metabolism and preventing sympathetic-induced decreased CBF may improve hearing outcome after LSE, or as a prophylactic therapy. This work was supported by grants from the National Institute of Health NIDCD R01 DC000105.

PS 150

Glycerol Enhanced Drug Delivery to the Endolymphatic Sac: Preliminary Results

Daniel J. Brown

The University of Sydney

Background: Corticosteroids, such as Dexamethasone, can be delivered either intra-tympanically or systemically, to provide relief from the symptoms of Meniere’s disease. However, they are not effective in all sufferers, and the high-clearance rate of drugs from perilymph limits the extent to which they can treat deeper parts of the inner ear, such as the endolymphatic sac, thought to be inflamed in Meniere’s. Recently, clinical researchers have directly delivered dexamethasone to the endolymphatic sac in Meniere’s sufferers undergoing

sac-shunt surgery, demonstrating a greater relief from vertigo. A more effective treatment strategy could involve delivering steroids to the sac, without the need for surgery. Previous studies have demonstrated that inner ear fluid markers are transported into the sac, and this transport can be enhanced following the systemic delivery of osmotic diuretics such as glycerol. Our own research supports the increased fluid uptake into the sac following glycerol.

Objective: To visualize the diffusion of fluorescent markers delivered intratympanically or systemically, throughout the entire inner ear, with or without the adjunct use of glycerol.

Methods: Experiments were performed in anesthetised guinea pigs, without recovery. Round window compound action potential thresholds were continuously monitored during the experiment. Glycerol (50% saline, 2mls) was delivered intravenously. Two fluorescent fluid markers, either 4kDa FITC-dextran or FITC-Dexamethasone, were applied to either the round window, or intravenously, 20-30 minutes after intravenous glycerol (or saline as a control). An hour later, animals were euthanized via cardiac fixation, and temporal bones were harvested. Inner ears were chemically cleared and imaged in 3D using a light-sheet fluorescence microscope.

Results: Our preliminary results suggest that glycerol provides a modest enhancement to the diffusion of fluid markers into the sac, after they are either applied to the round window or systemically. Glycerol also induced a transient increase in compound action potential thresholds.

Conclusion: Whilst the present results are preliminary, and show only a minor enhancement of marker diffusion into the sac following adjunct glycerol therapy, this study suggests this approach may benefit inner ear drug delivery. Moreover, as both therapies are currently used in the treatment of Meniere's, their adjunct use is likely to be well tolerated.

PS 151

Chronic Endolymphatic Hydrops in a Guinea Pig after Antigen Injected into Scala Media.

Daniel J. Brown; Ljiliana Sokolic; Christopher Pastras
The University of Sydney

Background: It has been suggested that if antigen, or antigen presenting cells, persisted in the membranous labyrinth, chronic endolymphatic hydrops may develop, providing the basis of Meniere's disease. However, attempts to induce such effects in animals have failed,

with antigen injections typically inducing only temporary hydrops (2-3 weeks), along with significant cellular infiltration and fibrosis – thus providing a model of Labyrinthitis. Importantly, almost all previous studies have introduced antigen into the perilymphatic compartments (a few have placed antigen into the endolymphatic sac), but no previous studies have introduced antigen directly into scala media.

Objective: To inject Lipopolysaccharide (LPS) directly into scala media of guinea pigs, and monitor functional and morphological changes over 6 weeks. Our hypothesis is that antigen within scala media cannot be completely cleared effectively, and will result in chronic endolymphatic hydrops.

Methods: Various concentrations (0.1%, 0.05% & 0.01%) of LPS in 0.4ml of artificial endolymph were injected into scala media of anaesthetized guinea pigs via a glass micropipette, with subsequent recovery for 1 to 6 weeks. Artificial endolymph injections and contralateral ears served as controls. After the recovery period, cochlear and vestibular function was measured, and inner ears were imaged using light-sheet fluorescence microscopy. The relative volumes of scala media and the endolymphatic duct were quantified.

Results: Functional and morphological changes varied with LPS concentration, ranging from severe fibrosis and severe hearing loss (0.1% LPS), to no fibrosis with moderate to severe endolymphatic hydrops and mild hearing loss (0.01% LPS). Interestingly, fibrosis and hydrops in scala media coincided with an enlargement of the endolymphatic duct.

Conclusion Injections of 0.01% LPS produced hydrops lasting at least 6 weeks, without fibrosis or cellular infiltration, with morphological changes resembling those seen in Meniere's. However, hearing loss was still greater than 30dB, and there were no obvious signs of balance dysfunction, and thus this does not provide a sufficient animal model of Meniere's. That chronic hydrops can be induced with antigen placed in endolymph, without cellular infiltration, suggests the membranous labyrinth may be more immune-privileged than the perilymphatic space of the inner ear.

PS 152

Pharmacokinetics of Gentamicin in Perilymph of Guinea Pigs with Endolymphatic Hydrops

Xuanyi Li¹; Chunfu Dai²; Wei Li¹

¹*E&ENT hospital of Fudan university;* ²*Department of Otolaryngology, Eye Ear Nose & Throat Hospital*

Backgrounds:

The feature of pharmacokinetics of gentamicin in perilymph of guinea pigs has already been well researched. However, the pharmacokinetics of gentamicin in the presence of endolymphatic hydrops (EH) has not been reported.

Objective:

To study the feature of pharmacokinetics of gentamicin in perilymph in the presence of EH in guinea pigs with embolized endolymphatic sac.

Methods:

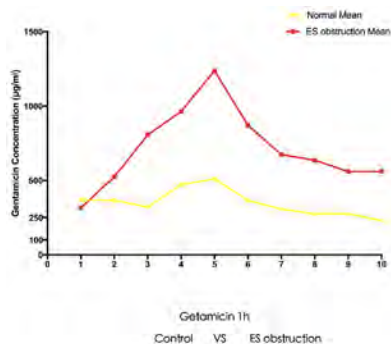
5 albino guinea pig accepted surgeries to embolize the right endolymphatic sac (ES). After 4 weeks, ten samples of 2 μ l perilymph were sequentially collected from each cochlear at the right lateral semicircular canal prominence 1 hour after 20 μ l gentamicin was locally applied to the right round window membrane. Those ten samples of 2 μ l perilymph which sequentially came from lateral semicircular canal (LSC), vestibule, scala vestibuli (SV), scala tympani (ST), and cerebrospinal fluid (CSF) were numerically infused into 150 μ l sterile saline. Concentration of gentamicin in each samples was detected by the Liquid chromatography–mass spectrometry and was compared to the control group of 5 guinea pigs which did not accept the surgery but were locally applied with 20 μ l gentamicin to the right round window membrane.

Results:

The feature of gentamicin distribution in perilymph was similar both in ES embolized group and control group. The concentration of gentamicin in vestibule and SV was much higher than that in LSC, ST and CSF. However, the concentration in perilymph of ES embolized group was much higher than that of control group ($p < 0.05$).

Conclusion:

After locally applied gentamicin, the presence of EH would not change the distribution feature that concentration of gentamicin was higher in vestibule and SV. However, as a result of EH and the decreased volume of perilymph, the concentration of gentamicin achieved a higher concentration gradient in perilymph.



PS 153

In-vitro Perforation of the Round Window Membrane via Direct 3-D Printed Microneedles

Aykut Aksit; Daniel N. Arteaga; Miguel Arriaga; Xun Wang; Hirobumi Watanabe; Karen E. Kasza; Anil K. Lalwani; Jeffrey W. Kysar
Columbia University

We report the use of Two-Photon-Polymerization (2PP) lithography to manufacture precision microneedles for the purpose of intracochlear drug delivery.

The cochlea, or inner ear, is a space fully enclosed within the temporal bone of the skull, except for two membrane-covered portals connecting it to the middle ear space. One of these portals is the round window, which is covered by the Round Window Membrane (RWM). A longstanding clinical goal is to deliver therapeutics into the cochlea to treat a plethora of auditory and vestibular disorders. Standard of care for several difficult to treat diseases calls for injection of a therapeutic substance through the tympanic membrane into the middle ear space, after which a portion of the substance diffuses across the RWM into the cochlea. The efficacy of this technique is limited by an inconsistent rate of molecular transport across the RWM.

A solution to this problem involves the introduction of one or more microscopic perforations through the RWM to enhance the rate and reliability of diffusive transport. Hence, ultra-sharp polymer microneedles specifically designed to perforate the RWM are made using direct 3D printing via 2PP lithography.

The needles are 3D printed, developed and mounted on sterile 23 Gauge blunt syringe tips for practical use. The needles are then used to perforate freshly excised guinea pig membranes. The perforation force is collected, and the resulting holes are analyzed via confocal microscopy, which has the benefit of visualizing the fibers that give the RWM its mechanical properties. The microneedle has tip radius of curvature of 500 nm and shank radius of 50 μ m. It perforates the RWM with a mean force of 1.19 mN. The resulting perforations performed in-vitro are lens-shaped with major axis equal to the microneedle shank diameter and minor axis about 25% of the major axis, with mean area 1670 μ m². The major axis is aligned with the direction of the connective fibers within the RWM. The fibers were separated along their axes without ripping or tearing of the RWM suggesting the main failure mechanism to be fiber-to-fiber decohesion.

The needles are imaged using a Scanning Electron Microscope (SEM) after use, and it is seen that the tips

of these microneedles are bent to some extent, limiting their reusability. Therefore, radii of curvature of the tips are systematically changed in order to find an optimal shape for the needles with the purpose of enhancing the mechanical strength and preventing blunting.

These results establish a foundation for the use of 2PP as a means to fabricate microneedles to perforate the RWM and other similar membranes requiring precision manufacturing of complex geometries. The small perforation area along with fiber-to-fiber decohesion are promising indicators that the perforations would heal readily following in-vivo experiments. An optimal needle geometry is currently being researched for the purpose of RWM perforation.

PS 154

LCCL peptide of cochlin in the inner ear has an immune-surveillance by conglomerating macrophages and neutrophils against Pseudomonas infection

Jinsei Jung; Jee Eun Yoo; Byung Wha No; Haiyue Lin; KyuMin Kim; Jae Young Choi
Yonsei University College of Medicine

Sensory organs such as the inner ear and the eye have an immune-privileged space filled with aqueous fluid. In the inner ear, endolymph surrounds the organ of Corti, which is important for hearing function. However, immune system in the endolymph of cochlea is still elusive. Here, we report that LCCL peptide of cochlin has a locally programmed surveillance immune response against bacterial infection in the cochlea. In vivo as well as ex vivo cochlea of Coch knock-out mice (Coch *-/-*) did not induce LCCL peptide cleavage of cochlin in response to *Pseudomonas* infection, which followed bacterial overgrowth and hearing deterioration. It revealed that LCCL peptide isolated and aggregated infected *Pseudomonas* in the perilymph of the cochlea to preserve hearing function in the organ of Corti. More importantly, increase of IL-1 β and IL-6 for the recruitment of macrophages and neutrophils into perilymph was strongly dependent on the cochlin secreted from resident dendritic cells in the cochlea. Taken together, LCCL peptide in the perilymph space has a role in immune surveillance to detect, segregate, and eliminate infected pathogens by recruiting innate immune cells.

PS 155

Pharmacokinetic Properties Compared for Native and Fluorescent Analogs of Dexamethasone and Gentamicin in the Inner Ear

Alec Salt¹; Jared J. Hartsock²; Ruth M. Gill²; Ting

Zhang³; Wei Li⁴; Chunfu Dai³; Fabrice Piu⁵; Jennifer Hou⁵; F. Bernhard Kraus⁶; Stefan Plontke⁷

¹*Washington University Medical School*; ²*Department of Otolaryngology, Washington University School of Medicine*; ³*Department of Otolaryngology, Eye Ear Nose & Throat Hospital*; ⁴*E&ENT hospital of Fudan university*; ⁵*Otonomy, Inc.*; ⁶*Zentrallabor, Department of Laboratory Medicine, University Hospital Halle*; ⁷*Department of Otorhinolaryngology, Head and Neck Surgery, Martin Luther University Halle-Wittenberg*

Fluorescent drug analogs have been widely used as a tool to monitor access and distribution of drugs in biological systems. In the current study, we have compared findings from quantitative pharmacokinetic studies of two drugs and their fluorescent analogs in the fluids of the inner ear of guinea pigs. The two drugs, dexamethasone and gentamicin, are both widely used in clinical otology. Both their native and fluorescent forms, fluorescein-labeled dexamethasone (FITC-Dex) and Texas red-labeled gentamicin (GTTR), have been extensively studied in the ear and are the subject of numerous reports in the literature. Entry into perilymph from the middle ear was assessed by applying the drugs to the RW niche of guinea pigs followed by perilymph sampling from the lateral semi-circular canal (SCC). Elimination of the drug from perilymph was assessed by loading perilymph by injection into the lateral SCC followed by perilymph sampling after varying delay times. In both types of experiment, perilymph was collected from the lateral SCC with a sequential-sampling technique in which 10 x 2 μ L samples representing perilymph from different regions of the ear were collected as quickly as possible. We found that for both drugs, the fluorescent analog exhibited entry and elimination kinetics completely different from the native drug. Entry from the middle ear into perilymph occurred 50x more slowly for GTTR than gentamicin and 360x more slowly for FITC-Dex than dexamethasone. For both fluorescent drugs, elimination measures showed characteristics of buffering or binding to inner ear tissues, which was not apparent for native forms. The perilymph measurements are in agreement with a considerable body of work showing the passage of drugs through membranous barriers depends on specific molecular properties, including the lipid solubility and polar surface area of the molecule. The fluorophore component increases the mass, the polar surface area and the lipophilicity of the molecule. Our findings demonstrate that these fluorescent drug analogs do not provide a meaningful indicator of pharmacokinetics in the inner ear for the native drug, although they may have value for other applications.

TRPV4 Receptors as Multimodal Sensors of Inner Ear Fluids

Gregory Heard¹; Dan Jagger²

¹*UCL Ear Institute*; ²*UCL Ear Institute, University College London*

The homeostasis of inner ear fluids is essential to normal hearing and balance. Endolymphatic hydrops and the symptoms of Ménière's disease might result from dysregulation of fluid homeostasis, which leads to severe vertigo, fluctuating hearing loss and discomfort. TRPV4 receptors are multimodal sensors of osmolarity, membrane stretch and temperature (White et al., *Physiol. Rev.* 2016). They have previously been localised to specific inner ear structures (Liedtke et al., *Cell* 2000; Karasawa et al., *J. Cell Sci.* 2008), and TRPV4 knockout results in delayed onset hearing loss and increased susceptibility to noise damage (Tabuchi et al., *Neurosci. Lett.* 2005). Therefore we are investigating TRPV4 receptors as potential sensors and regulators of inner ear fluid.

In cochlear sections from mice and rats, TRPV4 immunolabelling was detected in the lateral membranes of outer hair cells (OHCs) of the organ of Corti, basolateral membranes of stria vascularis marginal cells, the apical surface of Reissner's membrane epithelial cells (RMECs), and vestibular dark cells. Thus, the receptors seem well-placed to sense the ionic composition or osmotic pressure of the endolymphatic compartment. Using patch clamp electrophysiology, we identified candidate TRPV4-mediated currents in P8-P12 mouse organ of Corti explants. The TRPV4 agonist GSK1016790A elicited inward currents in OHCs, whose reversal potential was around 0mV, consistent with a non-selective cation current. These currents were inhibited by gadolinium, a broad-acting cation channel blocker. Some cells also featured a biphasic response consisting of a transient inward current followed by a sustained outward current.

In agreement with previous studies, we present preliminary evidence of functional TRPV4 receptors in cell types which face the endolymphatic compartment. Future experiments will determine which physiological stimuli activate TRPV4, and how downstream targets might influence fluid homeostasis.

This project is supported by grants from the Rosetrees Trust and the Ménière's Society.

Proteome of Normal Human Perilymph and Perilymph from People with Disabling Vertigo

Yin Ren¹; Hsiao-Chun Lin¹; Andrew Lysaght¹; Shyan-Yuan Kao¹; Konstantina M. Stankovic²

¹*Department of Otolaryngology, Harvard Medical School and Massachusetts Eye and Ear*; ²*Eaton-Peabody Laboratories, Massachusetts Eye and Ear & Department of Otolaryngology, Massachusetts Eye and Ear and Harvard Medical School & Speech and Hearing Bioscience and Technology Program*

The human perilymph, extracellular fluid that bathes most cell types in the inner ear, contains important proteins secreted by these cells that could serve as direct markers of inner ear pathologies that result in disorders of hearing and balance. Previous studies on the development of inner ear "liquid biopsies" have uncovered alterations in perilymph proteins that have been shown to be associated with unique etiologies of hearing loss. Nevertheless, existing efforts to quantitatively assess the human perilymph proteome have been constrained to specimens obtained from patients with various hearing pathologies, including patients with perilymphatic fistulas, those undergoing resection of vestibular schwannomas (VS), or patients undergoing cochlear implantation. While these studies have begun to elucidate the set of perilymph proteins unique to patients with profound hearing loss, we have not yet assembled the proteome of perilymph from patients with otherwise intact hearing. Furthermore, no complete characterization of perilymph from patients with vestibular dysfunction has been achieved. Here, using liquid-chromatography with tandem mass spectrometry (LC-MS/MS), we analyzed three samples of normal perilymph collected from patients without hearing loss. We identified 228 proteins with high confidence that were common across the samples, establishing a greatly expanded known proteome of normal human perilymph fluid. Further comparison to the perilymph obtained from patients with vestibular dysfunction showed 38 proteins with significantly differential abundance. The abundance of four protein candidates with previously unknown roles in inner ear biology was validated in murine cochleae: AACT, HGFAC, EFEMP1, and TGFBI. Together, these results motivate future work in characterizing the normal human perilymph and identifying potential biomarkers of inner ear disease.

Cochlear Pharmacokinetics - Transport Parameter Learning and Forward Model Estimations of Intracochlear Drug Concentrations for Cochleostomy Infusions

Sanketh S. Moudgalya¹; Kevin Wilson¹; Xiaoxia Zhu²; Mikalai M. Budzevich³; Gary V. Martinez³; Joseph P. Walton⁴; Nathan D. Cahill⁵; Robert D. Frisina²; David A. Borkholder¹

¹Rochester Institute of Technology; ²Medical Engineering Dept., Global Center for Hearing & Speech Research, University of South Florida; ³Moffitt Cancer Center; ⁴Communication Sciences & Disorders Dept., Medical Engineering Dept., Global Center for Hearing & Speech Research, University of South Florida; ⁵College of Science at Rochester Institute of Technology

Emerging methods in cochlear fluid pharmacokinetics simulate drug transport within cochlear regions and across compartments by first estimating the diffusion and transport coefficients from contrast agent concentrations within the cochlea. Local drug delivery will allow the utilization of many more drug options, as compounds that are efficacious often have systemic side effects. Our work focuses on learning the transfer coefficients within and across cochlear scalae including scala tympani (ST), scala vestibule (SV), scala media (SM), and clearance to blood by in vivo imaging the murine cochlea at multiple successive time instances during the delivery of a contrast agent (Isovue – Iopamidol). A previously established 3D image registration of the micro Computer Tomography (μ CT) to a high-resolution atlas enables transfer of the segmented regions in the atlas to the scan. The spatio-temporal concentration profile within each scalae is extracted along the medial axis for each scan, and subsequently used in a joint inverse-forward pharmacokinetics model to extract the transport coefficients. Our forward model simulates the concentrations in each scala using a random initialized value of transfer coefficients for the first iteration. Using optimizers (Stochastic Gradient Descent (SGD), Levenberg-Marquardt algorithm (LM)), the two models iteratively optimize the initial transfer coefficients by minimizing the error between extracted and simulated concentrations. To account for higher apical concentrations than predicted by pure diffusion, a concentration-dependent diffusion parameter is modeled as inversely proportional to the square of the concentration and is learned in the iterative inverse-forward model optimization. Time-dependent leakage at the cochleostomy site is also a learned parameter, and is essential to accurately model the time rate of change of peak concentration at the point of infusion. The forward model facilitates exploration of different delivery profiles through modeling of advective flow

from the cochleostomy site at the base of ST, to a sink at the cochlear aqueduct (CA). The resulting model with learned transport parameters has been used to optimize the delivery profile (flow rate and on/off times) for reduced concentration gradients within the cochlear scalae. Clinically this will enable control of a therapeutic concentration level while avoiding toxicity. While developed in the murine model, this approach can be extended to larger rodents and humans to advance inner ear drug delivery research and associated therapies, in conjunction with the development of new implantable micropumps for inner ear drug delivery.

Supported by NIH NIDCD award R01 DC014568.

PS 159

Cochlear Statistical Shape Modeling - Efficient Capture of Inter-Animal Scalae Variations

Sanketh S. Moudgalya¹; Kevin Wilson¹; Xiaoxia Zhu²; Mikalai M. Budzevich³; Gary V. Martinez³; Joseph P. Walton⁴; Nathan D. Cahill⁵; Robert D. Frisina²; David A. Borkholder¹

¹Rochester Institute of Technology; ²Medical Engineering Dept., Global Center for Hearing & Speech Research, University of South Florida; ³Moffitt Cancer Center; ⁴Communication Sciences & Disorders Dept., Medical Engineering Dept., Global Center for Hearing & Speech Research, University of South Florida; ⁵College of Science at Rochester Institute of Technology

Cochlear fluid pharmacokinetics make use of 1D and 3D diffusion models to simulate drug activity in the inner ear. Key regions of interest for these models include scala tympani (ST), scala vestibuli (SV), and scala media (SM). Both types of models are parameterized by transfer coefficients across the scalae and diffusion coefficients within the scalae, and 3D diffusion models additionally require accurately determining the scalae geometry. Micro computed tomography (μ CT) of the murine cochlea provides images that can aid in model development and validation: a baseline scan can be used to extract scalae geometry, and a sequence of scans collected during/after infusion of a contrast agent (Isovue) can be used to validate the models. Although geometry extraction could be performed manually by requiring an expert to identify pixel regions for each scalae in each slice of the 3D baseline scan, this would be extremely tedious. An easier, more automated approach would be to warp a manually constructed pre-defined template (cochlear atlas) onto the scans using deformable 3D registration. While this removes the need to manually identify scalae in every new baseline scan, the deformable registration step can be susceptible to inter-animal variations in the shape of the scalae. Our

work focuses on building a cochlear atlas that captures the anatomical variation between different animals by taking advantage of the statistical differences in the shape of the scalae. Statistical shape models of the cochlear atlas will simplify the subsequent deformable registrations step by only allowing deformations that follow the dominant directions of variability in scalae anatomy. Traditional approaches to creating statistical shape models would require performing principle component analysis (PCA) on scalae shapes extracted from a large number of baseline scans. Rather, we propose an incremental principal component analysis (IPCA) approach that initializes a shape model and then iteratively updates it using each new baseline scan, eliminating the need to have all scans in memory and improving computational efficiency. The resulting statistical shape models of scalae pave the way for improved concentration extractions within the cochlea from the μ CT scans, and for better spatially dependent transfer coefficients. The method is scalable and can be used to create statistical shape model to larger mammals in the future.

Supported by NIH NIDCD award R01 DC014568.

PS 160

In Vitro Pressure-Induced Deformation of the Guinea Pig Round Window Membrane

Wenbin Wang; Michelle Yu; Xun Wang; Miguel Arriaga; Harry Chiang; Daniel N. Arteaga; Karen Kasza; Anil K. Lalwani; Jeffrey W. Kysar
Columbia University

The round window membrane (RWM) is a thin layer of tissue dividing the inner and middle ear compartments. It provides a unique access point for treating diseases of the cochlea, an otherwise elusive structure almost entirely encased in bone. Recent studies, including several by these authors, have proposed novel surgical techniques for the treatment of inner ear diseases such as the application of Micro Perforations to the RWM to enhance drug delivery. As the RWM can deform significantly under pressure, understanding the mechanical properties of the round window membrane is critical for ensuring the safety of nearby structures and guiding surgical needle design. In this study, we introduce a new method for tracking the deformation of the RWM in vitro in response to pressure. Using a closed tubing system, we applied uniform pressure with phosphate-buffered saline to an isolated ex vivo guinea pig RWM. We then imaged fluorescent microbeads scattered onto the membrane with confocal microscopy and used digital volume correlation (DVC) to compute membrane deformation. To account for the effects of anatomical

asymmetry of the RWM, we applied both negative and positive pressures over a range of -2 kPa to 2 kPa in our experiments. Our experiments validate the use of fluorescent beads for tracking RWM deformation in vitro, and as expected, the responses of the RWM under positive and negative pressures are distinct. Moreover, we find regional behaviors in deformation of the RWM that coincide with variations in the orientation of elastic fibers within the RWM. As such, the orientation of fibers may play a key role in the mechanical properties of the guinea pig RWM.

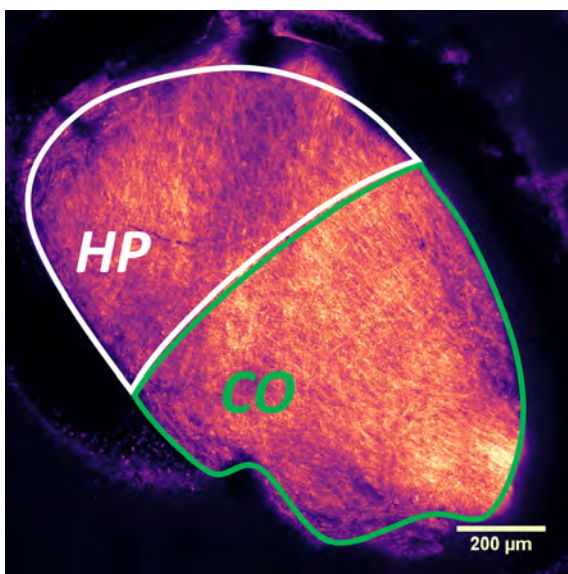
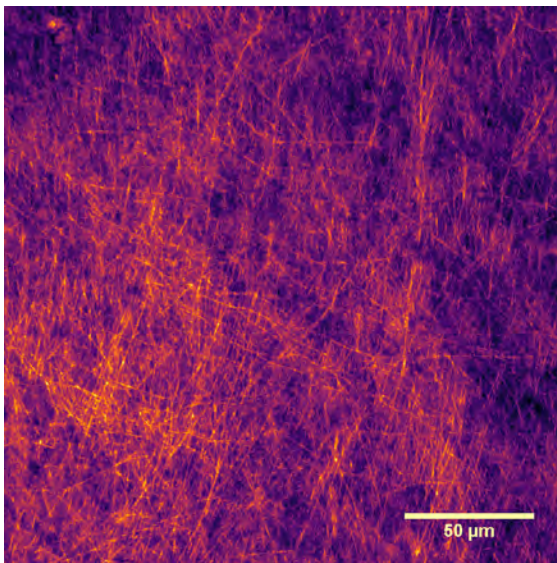
PS 161

Modelling the Round Window Membrane of the Guinea Pig: An Experimental Characterization of Fiber Distribution Based on Microscopic Imaging

Miguel Arriaga; **Dimitrios Fafalis**; Daniel N. Arteaga; Xun Wang; Wenbin Wang; Karen Kasza; Anil K. Lalwani; Jeffrey W. Kysar
Columbia University

The round window membrane (RWM) is a fibrous structure that separates the fluid-filled inner ear from the air-filled middle ear cavity, protecting the inner ear from middle ear pathology and modulating changes in perilymphatic pressure produced by the movement of the stapes. The RWM also represents a portal to the inner ear and is a promising candidate for delivery of therapy and collection of diagnostic samples with respect to the cochlea. Accessing the inner ear via the RWM, however, remains a significant challenge as the human RWM is small (diameter ~2mm), thin (thickness ~100 μ m), pre-stressed, and prone to tearing when manipulated using standard surgical tools. To aid in the development of new technologies for safe and reliable surgical handling of the RWM, it is essential to model the membrane's mechanical behavior, which is largely determined by a central layer of connective tissue. To this end, confocal microscopy was conducted on intact guinea pig RWMs in order to characterize for the first time the orientation and dispersion of the membrane's collagen and elastic fibers while preserving its underlying anatomic geometry. Images of the RWM were captured by confocal microscopy of the emitted signals due to second-harmonic-generation, auto-fluorescence and Rhodamine-B staining. An algorithm was developed and implemented in ImageJ to mathematically flatten the resulting images and to isolate the central fiber layer from the surrounding epithelial cells (Figure 1). A detailed description and quantitative analysis of fiber orientation and dispersion revealed that the orientation of fibers was variable across the membrane. Two principle regions were identified (Figure 2): [1] fibers

within the superficial RWM, which took the shape of a hyperbolic paraboloid (HP), and [2] fibers in the deep RWM, which took the shape of a cone (CO). Fibers in the superficial HP region, proximal to the surrounding bony niche, were highly dispersed and tended to follow the direction of zero curvature. Fibers in the deep CO region, extending into the cochlea, were highly aligned and tended to follow the generating line of the membrane's conical shape. In between, we observed a transition zone in which the alignment of fibers in the superficial HP region converged upon the alignment of fibers in the deep CO region. These efforts reveal how the fiber direction is informed by the membrane's unique geometry and represent a necessary step in providing the biomechanical parameters towards establishing a high-fidelity model of the RWM.



PS 162

Co-expression of Natriuretic Peptide Receptor A and Protein Kinase G2 (PRKG2) in Mouse Cochlea

Janet Fitzakerley¹; Patricia Kingsley²; Joel Madson²; George Trachte¹

¹University of Minnesota Medical School; ²University of Minnesota Duluth

Activation of the natriuretic peptide receptor A (NPR-A) by atrial natriuretic peptide (ANP) has both beneficial or harmful effects on hearing, but little is known about the downstream pathways that mediate these effects. NPR-A is a guanylyl cyclase, whose activation results in increased intracellular cyclic guanosine monophosphate (cGMP) concentrations. In other tissues, cGMP can activate several downstream effectors, including protein kinase G2 (PRKG2). Although microarray evidence indicates that it is present in the cochlea, little else is known regarding the role of PRKG2 in hearing. These experiments were designed to test the hypothesis that NPR-A and PRKG2 are co-localized in the cochlea.

The presence of PRKG2 in the cochlea and several control tissues was confirmed by multiplex qRT-PCR. Total RNA was isolated and amplified using standard primers for PRKG2 and the housekeeping gene RPLP0. In the immunohistochemistry experiments, CBA/J mice were perfused with a 4% paraformaldehyde/0.05% picric acid solution and cochlear sections were cut at a thickness of 10 microns on a cryostat. Commercially available antibodies against NPR-A and PRKG2 were used and visualized using confocal microscopy.

PRKG2 mRNA was present in the cochlea at levels similar to the heart, but less than the cerebellum and more than the kidney. PRKG2 was expressed in many regions of the cochlea including the organ of Corti, the modiolus and the potassium recycling systems. The highest level of expression was in the cells lining scala media. PRKG2 was found in the stria vascularis and in the interdental cells of the spiral limbus, as well as the type I, II and V fibrocytes of the lateral wall, but not in the fibrocytes of the limbus or in type III or IV fibrocytes. PRKG2 was found in both inner and outer hair cells, as well as supporting cells of the organ of Corti and cells lining the inner and outer sulci. PRKG2 was also found within the spiral ganglion. Many, but not all, of these cell types also expressed NPR-A. Within individual cells, the expression of these two proteins did not precisely overlap. For example, in Deiter's cells, NPR-A was found in the processes heading toward the reticular lamina, while PRKG2 expression was limited to the cell body. These results support the hypothesis that PRKG2 is a downstream effector of NPR-A in some, but not all, cells of the cochlea. Further physiological experiments are needed to determine the exact role of PRKG2 in hearing.

Inner Ear Aqueducts - anatomical study based on microCT

Kowther Hassan¹; S. Alireza Rohani²; Sumit K. Agrawal³; Nikolas Blevins⁴; **Yona Vaisbuch**⁴

¹*Department of Computer Science, University of Calgary;* ²*Department of otolaryngology - head and neck surgery, Western University;* ³*London Health Sciences Centre;* ⁴*Department of Otolaryngology-Head and Neck Surgery, Stanford University School of Medicine*

Background

The intricacies of the inner ear bony labyrinth anatomy has long been of interest due to the many hypotheses that link otological and vestibular conditions to abnormalities in the inner ear structure. Meniere's disease, a chronic condition characterized by hearing loss, vertigo, tinnitus, and other declines in auditory and vestibular functions, is postulated in some patients to be a consequence of anatomical deformities, including narrowing of the endolymphatic lumen and hypoplasia of the vestibular aqueduct. There is a lack of quantitative studies on the bony labyrinth.

Aim

To define the detailed anatomy, including size and relationship of the inner ear aqueducts

Methods

The data set consists of 54 cadaveric temporal bone specimens that were scanned using a micro-CT at 50-150 μm resolutions. Segmentations of the vestibular aqueduct and the cochlear aqueduct were made using ITK-SNAP, an open source semi-automatic segmentation software. It's active contour segmentation algorithm evolves user-positioned seed points that conform to the boundary of the anatomical structure of interest. The structure boundary is determined using thresholding. The segmentations were then manually edited to remove any imperfections generated from the algorithm. Volume and length of segmentations were calculated using open source imaging software 3DSlicer (BSD license). STATISMO open source software was used for statistical shape modeling to analyze the variations between the specimens.

Results

The volume of the vestibular aqueduct and cochlear aqueduct was found to be variable. The cochlear aqueduct had several anatomical variations in regards to shape and size. Different cross section areas were measured.

Discussion

Due to the complex and sub-millimeter nature of the

inner ear anatomy, which makes conventional imaging impractical in identifying some of the finer anatomical features. There have been some studies that employed histological sectioning to characterize the labyrinth. While histological slices give detailed anatomical images of the inner ear aqueducts, the sectioning by nature limits the ability to conduct spatial measurements. While in our study the data obtained pertains to the bony anatomy and not the membranous labyrinth anatomy, the results can be utilized in building an initial mathematical model, which would be valuable in understanding the mechano-physiology of the ear. High-resolution CT scans could become valuable diagnostic tool in different presentations of inner ear hydrops. Further studies that can volumetrically measure the membranous labyrinth are needed.

Inner-Ear Mechanics I

PS 164

Electromechanical Longitudinal Coupling and Nonreciprocity in the Cochlea

Amir Nankali¹; Aritra Sasmal²; Karl Grosh²

¹*University of Southern California;* ²*University of Michigan, Ann Arbor;*

Sound entering the mammalian cochlea generates a fluid-structure coupled wave that travels along the length of the cochlea and stimulates the microstructure of the organ of Corti (OoC). An active process based on outer hair cell somatic motility is hypothesized to amplify the response. Experimentally, in vivo electrical stimuli has been used to interrogate the contribution of the active process to cochlear transduction by providing a means of excitation different from acoustic stimulation. In this work, we use a 3D finite element model of the cochlea to interpret the experimental data [Grosh et al. (2004) J. Acoust. Soc. Am., He and Ren (2013) Sci. Rep.] and propose a mechanism that explains the difference between the forward and reverse traveling waves on the cochlear partition. We study the influence of longitudinal electrical coupling in the scalae during either acoustical or intracochlear electrical stimulation in order to test the hypothesis that the wave propagation in the cochlea is nonreciprocal with a preferred direction from base to apex. External acoustical stimulation gives rise to forward propagating waves on the partition, while intracochlear electrical excitation generates dispersive waves that are directionally biased due to the combination of the nearly instantaneous forcing introduced by the longitudinal electrical coupling and the electromechanical nonreciprocity of the mechano-electro-transducer channels. We discuss the implications of this nonreciprocity to the phase delay seen in otoacoustic emissions. This work was supported by NIH grants DC-004084 and T32DC-00011.

PS 165

Dual Velocity-Displacement Sensitive Behavior of Outer Hair Cells Determined by Tectorial Membrane Nanoscale Poroelasticity

Jonathan B. Sellon¹; Mojtaba Azadi²; Ramin Oftadeh³; Hadi T. Nia⁴; Roozbeh Ghaffari³; Alan J. Grodzinsky³; Dennis M. Freeman³

¹*Decibel Therapeutics*; ²*San Francisco State University*; ³*Massachusetts Institute of Technology*; ⁴*Massachusetts General Hospital, Harvard Medical School*

The inner ear separates sounds by their frequency content, and this separation underlies our remarkable ability to communicate and resolve speech in acoustically noisy environments. The mechanical interactions of outer hair cell (OHC) stereociliary bundles with the overlying tectorial membrane (TM) are thought to be essential to achieve this extraordinary sensitivity. OHC stereociliary bundles are embedded in the TM and are thus thought to act as displacement sensors that move in proportion to shearing motions between the TM and the reticular lamina. However, because the TM is 97% water by weight, interactions of interstitial fluid with the TM's elastic matrix may play a key role in hair cell stimulation. To better understand this nanoscale interaction, we apply nanoscale displacements to the TM at audio frequencies and measure the resulting forces on microscale probes. We observe that these probes are resisted by frequency dependent forces that are in phase with TM displacement at low and high frequencies, but are in phase with TM velocity at transition frequencies. The phase lead can be as much as a quarter of a cycle, thereby affecting the stability of micromechanical feedback paths and ultimately the sensitivity of hearing. Furthermore, this transitional phase lead in the force applied by the TM to a hair bundle occurs over a limited frequency range, suggesting the presence of an additional tuning mechanism whereby OHCs act as velocity sensors near their characteristic frequency rather than displacement sensors.

PS 166

Examining the link between the stability diagram and the fine structure of reflection otoacoustic emissions using a cochlear model

Haiqi Wen¹; Thomas Bowling¹; Julien Meaud²
¹*G.W.W. School of Mechanical Engineering, Georgia Institute of Technology*; ²*G.W.W. School of Mechanical Engineering and Petit Institute for Bioengineering and Bioscience, Georgia Institute of Technology*

Otoacoustic emissions (OAEs), have been extensively studied in scientific research and widely applied in

clinical practice due to their noninvasive characteristics. Depending on their generation mechanism, OAEs can be categorized as nonlinear distortion emissions and linear reflection emissions. In spite of different stimulus paradigm, Stimulus-frequency OAEs (SFOAEs), Spontaneous OAEs (SOAEs) and the reflection component of distortion product OAEs (DPOAEs) are believed to arise as reflections of the traveling wave due to impedance perturbations along the cochlea partition. Rapid amplitude variation separated by periodic frequency intervals that result in the peak and valley fluctuations across frequency, commonly referred to as "fine structure", has been observed in reflection emissions. Careful examination of the similarity and interrelationship between different the fine structure of different types of linear reflection emissions is expected to provide insights on the process of OAE generation. In this work, a state space-based time domain model of the gerbil cochlea is used to investigate the relationship between the fine structure of various reflection-type OAEs. Cochlear roughness is introduced by adding distributed inhomogeneities along the cochlea partition which causes the reflection of traveling waves due to impedance discontinuities. The state-space approach makes it possible to determine the linearly unstable modes and nearly unstable modes of the cochlea. SOAEs, SFOAEs and DPOAE generation are simulated in the time-domain. Analysis of model simulations demonstrate that SOAEs are linked to the presence of linearly unstable modes. Furthermore, both linearly unstable and nearly unstable modes appear as peaks in low level SFOAEs. Due to the saturation of the cochlear amplifier, these spectral peaks are not as prominent in higher level SFOAEs. In the case of the reflection component of DPOAEs, the peaks linked to unstable or nearly unstable modes tend to be attenuated due to two-tone suppression of the distortion product response by the primary tones. However, overall, the main aspects of the fine structure of these reflection-type OAEs are all similar and linked to the fundamental properties of the cochlea. Varying key model parameters that affect the reflection of forward propagating waves close to their peak, or the reflection of backward propagating waves at the stapes, affect the fine structure of reflection-type emissions in a similar manner.

PS 167

The Anatomy and Cochlear Partition Motion-Pattern of the Human is Different from those of Laboratory Animals: Optical Coherence Tomography (OCT) Measurements

Stefan Raufer¹; Nam-Hyun Cho²; John J. Guinan³; Sunil Puria⁴; Hideko H. Nakajima³

¹*Eaton-Peabody Laboratories, Massachusetts*

Eye and Ear; Graduate Program in Speech and Hearing and Bioscience and Technology, Harvard University; ²Harvard Medical School; ³Eaton-Peabody Laboratories, Massachusetts Eye and Ear; Graduate Program in Speech and Hearing and Bioscience and Technology, Harvard Medical School; ⁴Eaton-Peabody Laboratories

Background: The motion of the cochlear partition (CP) determines the mechanical input to the inner hair cells, which determine auditory nerve responses. In laboratory animals (typically rodents), the CP consists of the basilar membrane (BM) attached to the bony osseous spiral lamina (OSL), where the BM motion is similar to that of a simply-supported beam and is the primary contributor to the surface motion of the CP with the relative motion of the OSL being negligible. However, the anatomy of the larger human CP shows major differences from the anatomy of smaller laboratory animals: in the base, the OSL occupies the majority of the width of the CP. Furthermore, there exists a soft-tissue 'bridge'; between the OSL and the BM in the human, which has about the same width as the BM and which is absent in laboratory animals.

Methods: We measured the transverse motion of the CP in fresh human temporal bones at multiple radial locations, including along the OSL, the soft-tissue bridge, and the BM. Measurements were made through the intact round window membrane and after removing it. We used a ThorLabs Ganymede-III-905 nm center wavelength, spectral-domain OCT system combined with custom measurement system software VibOCT and SyncAv (Ravicz et al., 2018 AIP). Ear-canal sound-driven CP motion was measured along the CP with a spatial resolution of 10 μm and at each point from 0.1 to 10 kHz in 1/4th-octave steps below the best frequency of about 15 kHz.

Results: Our OCT measurements show that the dynamics of the human CP differ greatly from those of laboratory animals. In humans, the primary OSL vibrates considerably (consistent with a single-point measurement from Stenfelt et al. (2003)) and behaves like a stiff plate hinged near the modiolus. The maximum transverse CP motion is at the connection between the soft-tissue bridge and BM. All structures (OSL, bridge, BM) move in phase in the measured frequency range. These data are consistent with our recent measurements obtained with laser Doppler vibrometry and show that the classic view of simple-beam CP motion that is dominated by BM motion and applicable in laboratory animals, is not valid for the human CP. Because the CP motion greatly differs in humans, the mechanical process for sound transduction carried out by the organ of Corti sitting above the BM may also differ in humans.

[Supported by NIH/NIDC R01-DC013303, R01-DC007910, and American Otological Society]

PS 168

Optical Coherence Tomography and Spectral Domain Phase Microscopy Reveal Complex Differential Motion within the Cochlea.

C. Elliott Strimbu; Nathan C. Lin; Lisa Olson
Columbia University

Traditional cochlear vibrometry has been able to measure the motion of the basilar membrane (BM) or reticular lamina (RL) but not both simultaneously. Within the cochlea, however, mechano-electrical transduction relies on complex motion between different structures within the Organ of Corti (OoC). The ear relies on the nonlinear cochlear amplifier to boost its internal vibrations, sharpen the frequency response, and extend its dynamic range. Because the cochlear amplifier is generated by outer hair cell based forces, which are driven by mechano-electrical transduction, knowledge of the BM displacements alone is not sufficient to explain the input to the hair cells.

We use spectral domain phase microscopy (SDPM), a functional extension of optical coherence tomography (OCT), to measure vibrations at the base of the gerbil cochlea *in vivo*. SDPM allows us to simultaneously measure vibrations from multiple positions along the instrument's optical path yielding displacements from multiple axial locations within the hearing organ between the BM and OoC-complex. The ears are stimulated with either pure tones or multi-frequency "Zwuis" complexes which spanned the gerbil's audiometric range.

Similar to recent reports (He et al., *eLife* (2018) and Cooper et al., *Nature Communications* (2018)) we find that locations within the OoC, close to the outer hair cells, can show larger displacements and a higher compressive nonlinearity than the BM near the best frequency (BF). Moreover, unlike the BM, sites within the OoC exhibit a compressive nonlinearity at frequencies well below the BF at the longitudinal location. The results suggest that each longitudinal location in the cochlea can operate with a compressive nonlinearity over a wider frequency range than previously believed. The nonlinear compression is enhanced when the ear is stimulated with the broad-band Zwuis complex relative to pure tones.

PS 169

Two-tone Suppression and Distortion Production on the Reticular Lamina at the Base of the Gerbil Cochlea

Wenxuan He; **Tianying Ren**
Oregon Health and Science University

Background

When two tones at frequencies f_1 and f_2 ($f_1 < f_2$) are presented to the ear, a listener with normal hearing can hear sounds not only at f_1 and f_2 but also at frequencies, which do not exist in the stimuli, such as $2f_1 - f_2$. When f_1 is close to f_2 , f_1 tone can also suppress perception of f_2 tone. Although two-tone distortion and suppression have been previously demonstrated in basilar membrane vibrations, auditory nerve responses, and hair cells activities, they have not been measured from the reticular lamina.

Methods

Young Mongolian gerbils of either sex with normal hearing were used in this preliminary study. Reticular lamina and basilar membrane responses to two tones were measured from the base of the gerbil cochlea through the round window using a heterodyne low-coherence interferometer. When f_2 was kept constant at the best frequency of the measured location, f_1 was varied and the reticular lamina and basilar membrane vibration were measured at different f_2/f_1 ratios. Distortion of the reticular lamina and basilar membrane vibration was estimated by the vibration magnitude at distortion product frequencies, and suppression was quantified by the f_1 -induced magnitude decrease of f_2 responses.

Results

Like single tone-induced responses, two tone-evoked reticular lamina vibration at f_1 increased with frequency and reached the maximum when f_1 was close to f_2 . Despite constant f_2 frequency and level, the reticular lamina vibration at f_2 decreased with f_1 frequency, and the maximum decrease occurred when f_1 was close to f_2 . This f_1 tone-induced reduction of f_2 response increased with the sound level. In contrast, two-tone suppression on the basilar membrane was observed in a narrower frequency range and with smaller magnitude. Reticular lamina distortion products at $2f_1 - f_2$ were significantly greater than those of the basilar membrane, and strongly correlated with suppression magnitude.

Conclusion

The strong correlation between suppression and distortion production suggests that the two phenomena share a similar cochlear mechanism. Since the apical ends of outer hair cells are part of the reticular lamina, the current results also indicate that outer hair cells from a broad cochlear region are responsible for distortion product generation.

Funding

Supported by NIH-NIDCD grant R01 DC004554.

PS 170

Mechanical Properties of the Organ of Corti Complex

Sultan Sabha; Apoorva Khadilkar; Selena Khoury; Jong-Hoon Nam
University of Rochester

The geometrical and mechanical properties of the organ of Corti (OoC) complex, often represented by the basilar membrane, vary monotonically along the length of the cochlea. There has been substantial effort to correlate the mechanical properties of the OoC complex with cochlear functions. However, data regarding fundamental cochlear mechanics are still insufficient. For example, the data from the middle turn of the cochlea are rare as compared the data from the basal or apical turn. Stiffness measurements using microprobes suffer ambiguity in interpreting results due to high nonlinearity in force-displacement relationship. Dissipating properties have been much less explored as compared to stiffness properties.

We used a microfluidic chamber system to apply static and dynamic pressures to excised cochlear turns isolated from young gerbils, 18-21 old. Deformations of the OoC complex due to the applied pressures were measured and analyzed. By analyzing optical coherence tomography images, the deforming patterns of the OoC due static and dynamic pressures were obtained. The pressure-displacement relationship was highly linear within physiological pressure ranges (< 2 Pa). Unlike the OoC in situ, the excised preparation showed little sign of traveling waves because of its compromised mechanical boundaries. Instead, it responded like a second-order vibration system. Both in static and dynamic responses, the basilar membrane was displaced in the transverse direction, and its peak displacement occurs near the outer pillar cells. From dynamic responses, the inertial and dissipating properties of the OoC complex were obtained. To analyze the measurement results further, we used a 3-D finite element model. Using the model, the responses of intact cochlea were simulated.

[Supported by NIH NIDCD R01 DC014685]

PS 171

Modeling Cochlear Nonlinearity in the Transmission-line Framework

Alessandro Altoè¹; Renata Sisto²; Arturo Moleti³; Christopher A. Shera⁴

¹Caruso Department of Otolaryngology, University of South California; ²INAIL Research; ³Università di Roma Tor Vergata; ⁴University of Southern California

The cochlea can be thought as a waveguide; as such it can be approximately described by a cascade of mechanical elements coupled together by the cochlear fluids and/or by other structures in the organ of Corti. By necessity, the formulation of cochlear models based on this idea depends on simplifying (and, one hopes, clarifying) assumptions about cochlear mechanics.

A popular family of cochlear models follows from the assumption that the fluid flow in the scalae is predominantly one-dimensional, leading one to describe the motion of the cochlear partition and its basilar membrane (BM) using transmission-line (TL) equations. In particular, TL models represent the cochlea as a cascade of two-port networks consisting of longitudinal impedances (representing coupling via fluids) and shunt admittances (representing the phenomenological mechanics of the organ of Corti).

Transcending the details of different implementations, TL models can be broadly categorized into two families based on the formulation of their cochlear shunt admittance. In the first family of models, such as that of Zweig (1991), the frequency-dependent relationship between BM displacement and the pressure across the partition is represented using an “all-pole” transfer function. In the second family, models such as that of Neely and Kim (1986) employ a transfer function incorporating both poles and zeros. Linear systems theory ensures that linear TL models from the two families are functionally equivalent when they produce similar BM transfer functions.

However, nothing guarantees that nonlinear extensions of the two types of models need behave similarly when their parameters change dynamically to mimic the compressive nonlinearities observed in BM motion. In particular, one expects that moving either the poles or the zeros of the admittance in order to mimic compression at a specific frequency will manifest differently in the time and frequency domains. Hence, nonlinear all-pole models, where only the poles of the BM admittance can vary with level, may behave differently than zero-pole models, in which both zeros and poles can change.

In order to identify the most realistic strategy for modeling cochlear nonlinearities in the TL framework, we study the responses of a nonlinear version of the all-pole model by Zweig (1991) and compare and contrast them with the responses of its zero-pole approximation, where either the zeros or the poles of the shunt admittance are allowed to vary.

PS 172

A nonlinear transmission line cochlear model based on two degrees of freedom micromechanical elements

Renata Sisto¹; Alessandro Altoè²; Christopher A. SHERA³; Arturo Moleti⁴

¹*INAIL Research*; ²*Caruso Department of Otolaryngology, University of South California*;

³*University of Southern California*; ⁴*Università di Roma Tor Vergata*

One-dimensional transmission line cochlear models are able to capture important features of the basilar membrane (BM) dynamics. In the linear approximation, a successful approach consists in fitting the BM transfer function (TF) in terms of its zeros and poles. Although for a nonlinear system the TF is not well-defined, one can still measure the impulse response and find its frequency domain representation in terms of poles and zeros. This way, the system nonlinear dynamics is somehow characterized by the trajectory of the zeros and poles in the complex s-plane, as a function of the stimulus level.

On the other hand, the physical model associated to a particular zeros and poles structure is not completely determined. In other words, given the poles and zeros position, it is not possible to determine the system in terms of the parameters of a lumped elements circuit. In Elliott (2017) the BM response TF is analyzed finding that the best fitting function in the case of 1-d fluid coupling is a two-pole TF. The natural physical system underlying a two-pole TF is a two degrees of freedom mechanical element transmission line. The purpose of this study is finding a plausible nonlinear physical model with two degrees of freedom micromechanics that is able to reproduce the main symmetries of the cochlear response. The linear model by Neely and Kim (1986) is based on two mechanical oscillators that are suitably coupled to reproduce a realistic BM excitement profile, without invoking time-delayed (delayed-stiffness) or spatially-shifted (feed-forward) interactions. In the present study, we propose a nonlinear model in which the action–reaction principle is respected, and the nonlinear coupling between the two masses is tuned (by calculating the eigenvalues of the normal modes of the system at different stimulus levels) to get a nonlinear dynamics in which the resonance frequencies remain approximately unchanged whilst the damping increases significantly, at least in a low stimulus level range. The poles trajectory is approximately horizontal in the s-plane, and the zero-crossing invariance is only weakly violated. These preliminary results are quite promising, as they show that most experimental features of the nonlinear cochlear response can be reproduced by a simple two oscillators coupling, exploiting several hints provided by the coupled linear oscillator theory.

Comparison of Nonlinear Behavior of Extracellular Potentials and Displacements of Outer Hair Cells

Elika Fallah; C. Elliott Strimbu; Lisa Olson
Columbia University

Mechanical displacements of the basilar membrane (BM) and the electrophysiological responses of the auditory outer hair cells (OHCs) are key components of the frequency tuning and cochlear amplification in the living mammalian cochlea. In the work presented here, we measured the responses of (1) the extracellular potentials generated by outer hair cells (OHCs) and (2) displacements of different layers in the organ of Corti complex (OCC) to a multi-tone stimulus, and to pure tones. Using optical coherence tomography (OCT), we were able to measure displacements of different layers in the organ of Corti complex (OCC) simultaneously, at a basal region of gerbil's cochlea.

We compared the nonlinear behavior of the electrical potentials and displacements of the BM and a layer including OHCs in two frequency regions: at frequencies well below the best frequency (BF) and in the BF region. In the sub-BF region: (i) the BM's motion had linear growth for both stimulus types. (ii) The motions of the OHCs was mildly nonlinear for single tones, and relatively strongly nonlinear for multi-tones. (iii) The nonlinear characteristics of the OHC-generated potentials were very similar to that of the OHC-region displacement. By entering the BF region, the BM's motion became nonlinear, and the degree of nonlinearity of the extracellular potentials and the displacements of the OHCs became larger.

To explore the basis for the compression seen in the potentials and displacements of the OHCs in the sub-BF region, a basic nonlinear analytical model was employed. The compression of the OHC extracellular potentials to multi-tone stimulus matched with the analytical predictions when we accounted for the frequency tuning of the multi-tone response.

Ringling in Basilar-Membrane Responses to Clicks - Effect on the Tonotopic Map

Karolina K. Charaziak¹; Alessandro Altoè²; Wei Dong³; Christopher A. Shera¹

¹University of Southern California; ²Caruso Department of Otolaryngology, University of South California; ³VA Loma Linda Health Care System and Otolaryngology, Loma Linda University

The envelope of basilar-membrane (BM) responses to acoustic clicks often exhibit striking temporal structures, including multiple sequential bursts or lobes (i.e., ringling). This temporal structure of the BM response envelope has been hypothesized to arise through a global interference pattern as a consequence of multiple internal reflections of the waves traveling within the cochlea. These internal reflections occur in cochlear models incorporating so called "roughness" that scatters the forward traveling wave. The scattered wavelets combine coherently within the peak region of the BM response giving rise to a backward traveling wave, that is partially reflected again towards the cochlea upon reaching the stapes. It has been hypothesized that the multiple reflections modify the tonotopic map of the cochlea by slightly altering the local best frequency (BF). The change in local BF arises due to a prolonged ringling of the BM response to clicks that translates to spectral ripples in the BM sensitivity around its peak. Consequently, the tonotopic map remains exponential on the largest scales but manifests a local, staircase-like structure consisting of plateaus of nearly constant BF alternating with sudden jumps. Here we test whether the cochlear map is altered by the presence of the ringling in the BM responses to clicks when measured at multiple locations along the cochlear length in gerbils. Small reflective beads were placed on the BM (at least four) and their vibration was measured in response to acoustic clicks with a laser doppler vibrometer. The BF of each bead was estimated from its peak sensitivity before and after removing the ringling from the response with various signal processing strategies. The relative distances between beads (i.e., cochlear location) were estimated from microscope pictures. We demonstrate that, although globally the BF changed exponentially with cochlear distance, the removal of the later lobes from the BM response results in smoother tonotopic maps. Although our recordings are too spatially sparse to unequivocally identify the predicted staircase-like tonotopic map, the fact that local BF is modulated by the ringling in the BM envelope to acoustic clicks agrees with theoretical predictions.

Multilocation Analysis of Mechanoelectrical Signal Envelope Processing in the Guinea Pig and Human Cochlea

Alfred Nuttall¹; Anthony J. Ricci²; George Burwood³; James M. Harte⁴; Stefan Stenfelt⁵; Per Cayé-Thomasen⁶; Tianying Ren¹; Sripriya Ramamoorthy⁷; Yuan Zhang⁸; Teresa Wilson⁸; Thomas Lunner⁵; Brian C.J. Moore⁹; Anders Fridberger¹⁰

¹OHSU; ²Stanford University; ³Oregon Hearing Research Center; ⁴Interacoustics Research Unit; ⁵Linköping University; ⁶Rigshospitalet; ⁷Indian Institute of Technology Bombay; ⁸Oregon Health & Science University; ⁹University of Cambridge; ¹⁰Linköping University

Signal envelopes contain valuable temporal information which aids the interpretation of vocal communication. Human hearing is adapted to extract this temporal information. We previously demonstrated that organ of Corti mechanics could respond to dynamic changes in envelope amplitude, at the apex of the guinea pig cochlea. Thus, envelope processing likely occurs at all levels of the auditory system. Here, we extend the report to investigate dynamic envelope induced mechanical responses at multiple locations within the guinea pig cochlea *in vivo*, electrical responses of hair cells *in vitro* and of the human cochlea *in vivo*.

We demonstrated that isolated hair cells may respond to dynamic envelope signals, and did not find evidence of envelope responses at the basilar membrane of the guinea pig at the 18 kHz location using laser doppler vibrometry. The addition of TTX did not abolish simultaneously measured electrical dynamic envelope responses. We then sought to confirm the presence of envelope responses at the reticular lamina and their absence at the basilar membrane, by measuring mechanical responses at the hook region of the guinea pig cochlea, visible through the round window. Optical Coherence Tomography vibrometry revealed the presence of such envelope signals on the reticular lamina at a characteristic frequency of approximately 30 kHz. Importantly, basilar membrane responses at the hook region also showed no envelope entrainment, despite comparable noise floors, in the presence of a large electrical envelope signal measured by a round window wire electrode. Electrical envelope responses could be recorded at relatively low sound pressure levels, whilst simultaneously recorded mechanical envelope responses were not visible until high levels were used.

Finally, we demonstrated the presence of similar dynamic envelope signals in the electrical responses of humans, measured using a promontory electrode.

These results taken together suggest a dominant role for mechanoelectrical envelope processing throughout the cochlea. The level discrepancy between the mechanical and electrical outputs, and measurements in guinea pig in the presence of TTX, may imply that inner hair cell responses dominate envelope processing. Such a mechanoelectrical mechanism is also validated via mathematical modelling.

This work was supported by grants from the National Institutes of Health NIDCD R01 DC000141.

PS 176

Following furosemide, a shift in the OHC transducer operating point causes cochlear amplification to recover more slowly than EP

Yi Wang; Elika Fallah; Lisa Olson
Columbia University

Endocochlear potential (EP) provides the voltage drop needed to drive outer hair cell (OHC) transducer current, which leads to OHC electromechanical force and cochlear amplification. Earlier studies used furosemide to reduce EP and showed that cochlear amplification was temporarily abolished. Lacking a measurement of EP, it is unknown whether the EP and cochlear amplification recovered simultaneously. In this study, using IV injection of furosemide to reduce EP, the extracellular OHC transducer current, which we term local cochlear microphonic (LCM), was measured simultaneously with EP. We observed that the cochlear amplifier and EP recovered with different time courses: cochlear amplification just started to recover after the EP was nearly fully recovered and stabilized. Using a Boltzmann model and the 2nd harmonic of the LCM to estimate the transducer operating point, we found that this non-simultaneous recovery of cochlear amplification resulted from a shift in the operating point.

PS 177

Locations of Distortion Product Generation Within a Cochlear Model

Thomas Bowling¹; Haiqi Wen¹; Julien Meaud²
¹G.W.W. School of Mechanical Engineering, Georgia Institute of Technology; ²G.W.W. School of Mechanical Engineering and Petit Institute for Bioengineering and Bioscience, Georgia Institute of Technology

Distortion product otoacoustic emissions (DPOAEs) are sounds generated by the cochlea in response to two primary tones (f1 and f2) that can be measured in the ear canal. Although DPOAEs are used both clinically and in research to test for hearing functionality and hearing

loss, questions remain on exactly where distortion products (DPs) are generated. The theory of coherent reflection predicts that distortion products are produced by two distinct mechanisms: (1) by a distortion source due to nonlinear interaction between the two primary tones and (2) a reflection source caused by impedance mismatches along the cochlear partition. DPs are expected to be generated by the distortion source over a broad region around the primary best places where the envelopes overlap and the outer hair cells response to both frequencies. The reflection source DPOAE is expected to be generated in the region around the distortion product best place. Multiple factors, such as stimulus frequencies and levels, are known to affect where distortion products are generated. The exact basal extent of the distortion source is still debated; researchers have found conflicting results, with some finding evidence for the existence of basal generation and others finding no such evidence. Determining the exact locations of DP generation is crucial for DPOAE measurements from locally damaged cochleae to be correctly interpreted.

The present work uses a physiologically-based nonlinear computational model of the gerbil ear cochlea to study the locations of DP generation. The model includes a two-duct three-dimensional model of the intracochlear fluid and is formulated in the time domain. To determine the locations of DP generation, model parameters directly related to DP generation are selectively turned off for different positions along the cochlear partition. By turning off certain generation sites, the relative contributions of different locations to the overall DPOAE measured in the ear canal (or at the stapes) can be determined. Several model parameters directly affect DP generation and the benefits and issues with varying each parameter are discussed. By using a model, the distortion and reflection sources can be studied independently, and the generation sites of each source determined.

Noise Injury I

PS 178

Therapeutic Hypothermia: A Potential Therapy to Protect and Preserve Residual Hearing

Rachele Sangaletti¹; Samantha Rincon²; Jayanti Singh³; Elizabeth Dugan⁴; Nina Latorre³; John N. Barret⁵; Fred F. Telischi⁶; W. Dalton Dietrich⁷; Curtis King⁸; Abhishek Prasad⁴; Michael Hoffer⁹; **Suhru M. Rajguru**¹⁰

¹Department of Otolaryngology, University of Miami;

²Department of Biomedical Engineering, University of Miami; ³Department of Otolaryngology, University of Miami; ⁴Department of Biomedical Engineering, University of Miami; ⁵Department of Physiology and

Biophysics, University of Miami; ⁶University of Miami Miller School of Medicine; ⁷Department of Neurological Surgery, University of Miami; ⁸Lucent Technologies; ⁹Department of Otolaryngology and Neurological Surgery, University of Miami; ¹⁰Department of Biomedical Engineering and Otolaryngology, University of Miami

Introduction. Localized mild to moderate therapeutic hypothermia has been widely studied for neuroprotection against secondary injuries due to brain trauma, strokes, and spinal cord injuries. Multiple studies have considered the effects of temperature of the cochlea and its influences on auditory responses and a protective role of hypothermia in the inner ear has been suggested. In a preclinical model, we have recently shown that acute and localized application of mild hypothermia reduced the trauma associated with cochlear implantation and preserved residual hearing. Here, we review the evidence highlighting therapeutic efficacy and translational potential of hypothermia and investigate the mechanisms underlying its protective effects in the inner ear.

Methods. The University of Miami Institutional Animal Care and Use Committee approved all procedures. Two different models of traumatic injury were used in the preclinical in vivo rodent model: surgical cochlear implantation and noise-induced trauma. Residual function was measured using auditory brainstem responses and distortion product otoacoustic emissions. An in vitro model was also developed to test the efficacy of hypothermia against oxidative stress and hydrogen peroxide mediated cellular impairment and apoptosis. RNA-seq, Western Blot and rt-qPCR were performed at multiple time points to quantify gene and protein level expression of selected factors in control, euthermic and hypothermia-treated conditions. Additionally, a quantification of immune cells with the use of flow cytometry technique was performed. Finally, cadaveric temporal bone and mathematical stimulations were developed to study translational potential of such approach.

Results. Functional measurements suggested that mild hypothermia provided during cochlear implantation surgery or following noise application significantly reduced threshold shifts post trauma. Mild therapeutic hypothermia reduced inflammation and oxidative stress and increased activity of anti-apoptotic pathways, while increasing cell viability and reducing cell death. Moreover, flow cytometric analysis shows that hypothermia treatment significantly reduces the number of activated microglia, macrophages and lymphocytes/leukocytes recruited at the site of the injury (between 5 to 10-fold reduction) when compared with euthermic conditions.

Conclusions. Multiple cellular processes including inflammatory reactions, oxidative stress mechanisms, apoptosis and necroptosis mediate the death or survival of hair cells and neurons. Understanding the mechanisms underlying protective effects of hypothermia will guide its translational potential and lead to identification of potential targets for combinatorial therapeutic modalities.

Supported by NIH 1UL1TR000460, 1R21DC014324, 1R01DC013798, Wallace H Coulter Center for Translational Research and Cochlear grants to SMR.

PS 179

A Role of the Guanylyl Cyclase GC-A in Auditory Function

Lukas Rüttiger¹; Dorit Möhrle¹; Markus Wolters¹; Philipp Eckert¹; Philine Marchetta¹; Steffen Wolter¹; Katrin Reimann¹; Michaela Kuhn²; Marlies Knipper¹
¹University of Tübingen; ²University of Würzburg

Background: In the inner ear, the cGMP signaling pathway has been described to facilitate both protective and harmful processes in response to traumatic events. The aim of this study was to investigate the otoprotective role of the particulate cGMP generator guanylyl cyclase type A (GC-A) and its ligands atrial and B-type natriuretic peptides (ANP, BNP) for auditory function.

Methods: Transgenic mice knockout (KO) for GC-A were tested for hearing function and for auditory recovery from noise injury. We studied GC-A, ANP and BNP expression in the hearing organ in the cochlea of the inner ear. Hearing function was monitored with auditory brainstem responses (ABRs). Integrity of the cochlear amplifier was assessed with distortion product otoacoustic emissions (DPOAEs) that depend on the electromotile activity of cochlear outer hair cells (OHCs).

Results: Our results show that GC-A is expressed in OHCs, while ANP and BNP are expressed in OHCs and sensory inner hair cells (IHCs). We analyzed the hearing function of GD-A-KO animals pre- and post acoustic trauma.

Conclusion: The role of cGMP within the ANP and BNP/GC-A/cGMP signaling pathway in the inner ear will be discussed and scanned for protective prospects for age and noise induced hearing loss.

This work was supported by grants from the Deutsche Forschungsgemeinschaft (FOR 2060 project FE 438/6-1, RU 713/3-2, DFG-Kni-316-10-1, SPP 1608 RU 316/12-1, and SPP 1608 KN 316/12-1).

PS 180

Pathophysiological differences of hearing impairment between two types of blast induced hearing loss

Eiko Kimura¹; Kunio Mizutani¹; Katsuki Niwa¹; Yasushi Satoh²; Shun-ichi Sato³; Akihiro Shiotani¹

¹Department of Otolaryngology, Head and Neck Surgery, National Defense Medical College;

²Department of Pharmacology, National Defense Medical College; ³Division of Bioinformation and Therapeutic Systems, National Defense Medical College

Background

Blast induced hearing loss has been researched because ear is the most fragile organ for blast. Although several blast models have been established, the detailed pathophysiology on blast induced hearing loss has not been revealed. The most critical etiology of blast-induced hearing loss is cochlear permanent injury. However, measurement of detailed cochlear function after blast exposure is difficult, because most blast models cause tympanic membrane perforation (TMP) following conducting hearing loss. We have established two types of blast induced hearing loss models, which have pure sensorineural hearing loss without TMP. In this study, we analyzed these two models; one is induced by air-conducting shock wave generated from an air-compressed shock tube, the other is induced by bone-conducting shock wave generated by laser chamber (laser-induced shock wave: LISW).

Methods

Shock tube: SUS-tubing inflated compressed nitrogen gas was used. Shock wave propagates to low-pressure part by breaking the membrane. The peak pressure was set to 25 kPa, and irradiated to the mouse from diagonally upward.

LISW: Shock wave was generated by 532-nm Nd: YAG laser. YAG laser irradiated to posterior ear of mice through PET seat rubber. Shock wave energy was set to 2.0 J/cm².

Auditory brainstem response (ABR) and distortion product otoacoustic emissions (DPOAE) were used to cochlear function measurement. Cochlear immunohistochemistry was performed 28 days after shock wave exposure, using Myosin VIIA, CtBP2, and GluR2.

Results

In shock tube and LISW groups, permanent ABR threshold shift about 10 - 20 dB was observed. Interestingly, DPOAE threshold in the shock tube group was elevated at higher frequencies, whereas no elevation was observed in LISW group.

Loss of the inner and outer hair cells was not observed in both shock tube and LISW groups. Moreover, the number of synapses was reduced, and orphan synapse degeneration was also appeared mainly at the basal turn in both groups. However, these changes were observed more frequent in LISW group.

Discussion

It is suggested that pathophysiological differences between shock tube induced shock wave and LISW would be caused by shock wave property. Characteristic of cochlear damage induced by air-conducting shock wave generated by shock tube would be similar to that of noise induced hearing impairment, which is mainly observed in the lower turn. Alternatively, LISW affected all turns via bone-conduction, whereas a gradient pattern of severity of damage was observed.

PS 181

Mitochondrial Quality Control in Auditory Hair Cells

Teresa Wilson¹; Sarah Foster¹; Sean Elkins¹; Alfred Nuttall²

¹Oregon Health & Science University; ²OHSU

Background: Mitochondrial dysfunction is believed to be a major underlying cause of hearing loss. Cellular stress, such as that induced by loud sound exposure, can result in mitochondrial dysfunction resulting in increased mitochondrial fragmentation, production of excessive oxidative free radicals, and cell death. The maintenance of mitochondrial integrity occurs through the coordinated activities of mitochondrial biogenesis, dynamics, and mitophagy. The goal of this study was to examine the regulation of mitochondrial quality control mechanisms in response to increased energy needs of outer hair cells (OHCs) that occurs with loud sound exposure.

Methods and Results: PhAMfloxed mice were crossed with prestin-CreERT2 mice to generate mice that express a mitochondrial-specific version of the Dendra2 fluorescent protein. These mice were exposed to either permanent or temporary threshold shift-inducing loud sound levels, and the cochlea were harvested at various times following noise exposure. High resolution imaging revealed primarily punctate mitochondria in the OHCs of control animals. Following loud sound exposure, alterations in mitochondrial morphology were observed primarily in the apical region of the basal OHCs. Depending on the intensity of the loud sound exposure, two different observations were made: 1) following exposure to a highly damaging level of loud sound, the mitochondria became smaller and more punctate; and

2) following exposure to a mildly damaging level of loud sound, the mitochondria became significantly elongated indicating the induction of pro-survival pathways.

Conclusions: Deregulation of mitochondrial quality control mechanisms has long been recognized as the underlying cause of many pathological conditions including hearing loss. The morphological state of mitochondria is believed to be directly related to mitochondrial function and health, and therefore, to cell viability. The observed presence of elongated mitochondria following loud sound exposure suggests that stress induced mitochondrial fusion activity is involved in maintenance of mitochondrial integrity and OHC survival.

Funding: Supported by grants 5R01DC000105, P30DC005983, and W81XWH-15-1-0560.

PS 182

Examination of Transcriptional Changes in Cochlear Hair Cells and Supporting Cells Following Blast Exposure in Adult Mice

Beatrice Mao¹; Tara Balasubramanian¹; Scott Haraczy¹; Ying Wang²; Rodrigo Urioste²; Donna Wilder²; Keri Richards³; Robert J. Morell³; Joseph B. Long²; Matthew Kelley⁴

¹Laboratory of Cochlear Development, National Institute on Deafness and Other Communication Disorders, National Institutes of Health; ²Blast-Induced Neurotrauma Branch, Center for Military Psychiatry and Neuroscience, Walter Reed Army Institute of Research; ³Genomics and Computational Biology Core, National Institute on Deafness and Other Communication Disorders, National Institutes of Health; ⁴NIDCD

Exposure to concussive blasts is increasingly common among active duty military personnel and is associated with subsequent hearing and balance problems. Recent studies have shown that blast exposure induces physical changes in the anatomy of the cochlea, but its effect on gene expression has not previously been investigated. To explore this, anesthetized adult mice expressing GFP in hair cells or supporting cells were placed inside a blast simulator and exposed to three successive blasts. Control animals were held outside the chamber. As a result they were exposed to the sound generated by the blast chamber but were not in the direct path of the pressure wave. Twenty-four hours after exposure, the inner ears were collected, the vestibular portion was removed, and the remaining cochlear tissue was dissociated and FACS sorted to capture either hair cells or supporting cells. Total RNA was collected from the resulting pooled populations of cells and changes in gene expression

were determined using RNA sequencing. Changes in specific injury-related pathways, such as apoptosis and stress response, will be analyzed. The results will provide a basis for the development of interventions that may ameliorate inner ear damage after blast exposure.

PS 183

Involvement of Neutrophils in Cochlear Responses to Acoustic Trauma in B6.129P-Cx3cr1^{tm1Litt}/J Mice

Celia Zhang¹; Mitchell D. Frye²; Juliana Riordan¹; Ashu Sharma³; Wei Sun⁴; Bo Hua Hu¹

¹Center for Hearing and Deafness, State University of New York at Buffalo; ²Callier Center for Communication Disorders, University of Texas at Dallas; ³Department of Oral Biology, State University of New York at Buffalo; ⁴State University of New York at Buffalo

Background

Massive recruitment of circulating monocytes into the cochlea has been documented after acute cochlear stress. Neutrophils are an essential effector of inflammation. While these cells have been identified in many non-cochlear tissues after acute inflammation, their involvement in cochlear responses to acoustic trauma remains unclear. Here, we report the recruitment of neutrophils to the cochlea after acoustic overstimulation in B6.129P-Cx3cr1^{tm1Litt}/J mice.

Methods

Young B6.129P-Cx3cr1^{tm1Litt}/J mice (GFP/GFP and +/- GFP) and wild-type mice were exposed to a broadband noise at either 117, 120 or 125 dB SPL for 1 hour. ABR measurements were performed to assess hearing sensitivity. Cochleae were collected at various time points (6 hours, 1, 2 and 4 days) after acoustic overstimulation. Sensory cell loss was quantified using DAPI nuclear staining. Cochlear inflammation was assessed by examining neutrophils and macrophages. Neutrophils were identified with two Ly6G antibodies recognizing either RB6-8C5 or NIMP R-14 epitope and by their morphology. Monocytes/macrophages were identified based on their GFP fluorescence and were confirmed by Iba1 and F4/80 immunoreactivity. These immune cells were analyzed in multiple cochlear partitions including the scala tympani, the lateral wall and the neural region of the osseous spiral lamina.

Results

Normal cochleae without acoustic overstimulation displayed GFP-positive cells in multiple cochlear partitions. However, only a few Ly6G^{high} cells (~2-5 per

cochlea) were present. After acoustic overstimulation, cochleae exhibited a significant elevation in ABR thresholds and sensory cell degeneration. Accumulation of Ly6G^{high} cells was found in cochleae of CX3CR1-GFP mice exposed to 120-dB or 125-dB noise. These cells lacked GFP fluorescence and were Iba1-negative. They were small in size with lobed nuclei, which is consistent with the phenotypes of a neutrophil. Ly6G-positive cells were identified in both CX3CR1^{GFP/GFP} and CX3CR1^{+/-GFP} mice. These cells were found at 1 day after noise exposure and the majority of them resided in the lateral wall. Quantitative analysis revealed that the number of Ly6G-positive cells was positively correlated with the number of cochlear macrophages, which in turn was correlated with the level of acoustic overstimulation. Ly6G-positive cells were also found in wild-type mice. However, they were present in only a portion of the cochleae that sustained 125 dB-noise and displayed significantly greater sensory cell damage.

Conclusions

CX3CR1 deficiency promotes the recruitment of the neutrophils into the cochlea after acoustic overstimulation and the recruitment is associated with the level of acoustic injury.

PS 184

Circadian Regulation of Inflammation in Noise-Induced Hearing Loss

Heela Sarlus; Christopher Cederroth; Evangelia Tserga; Jacopo Fontana; Barbara Canlon
Karolinska Institutet

Introduction

Inflammatory processes, known to be under strict circadian control, are emerging as important contributors to noise-induced hearing loss. We have shown that the cochlea exhibits greater vulnerability to noise trauma at night compared to day. Depletion of circulating glucocorticoids (GCs) through surgical removal of adrenal glands (adrenalectomy) allowed mice to completely recover from night noise trauma. Our working hypothesis is that GCs regulate an exaggerated inflammatory response after night noise trauma that drives the differences between day and night noise, and contributes to the permanent hearing loss.

Aims

To study the contribution of GCs to inflammation in the circadian regulation of noise-induced hearing loss.

Methods

Sham operated or adrenalectomized mice were exposed

to a free field broadband noise at 6 -12 kHz at intensity of 100 dB SPL for 1 hr during day ZT3 (09.00 am) or night ZT15 (21.00 pm). Two hours post noise exposure, the cochleae were dissected out and prepared for RNAseq. The RNAseq data was analyzed using WGCNA.

Results

The RNAseq data from mice exposed to noise regardless of time showed an increase in a number of genes involved in acute inflammation and stress such as Jun, Fos, Ccl2 and Ccl7. However, the expression of some inflammatory genes increased only after exposure to noise at night in a GC-dependent manner such as Ccl5, IL20rb, Tnfrsf1a, IL15ra, Ptgs2. The day-night differences after noise exposure in these genes were diminished upon adrenalectomy. We also observed an overall reduction in the gene products of T cells whereas an increase in those of B cells in mice subjected to adrenalectomy.

Conclusion

Our data show that noise elicits an inflammatory response which may involve different immune components depending on day or night. These circadian differences in immune responses are partly driven by GCs. Nighttime noise exposure appears to involve greater inflammatory processes than daytime noise exposure.

PS 185

Circadian Regulation of Sensitivity to Noise Trauma in Different Mouse Strains

Jacopo Fontana; Christopher Cederroth; Barbara Canlon
Karolinska Institutet

Noise-induced hearing loss (NIHL) is common in our society resulting from prolonged exposure to high levels of noise. Recent findings demonstrated that CBA/Sca mice (Scanbur) exposed to noise in the day recovered to normal hearing thresholds compared to the night-exposed animals. However, this differential vulnerability to noise was not evident in CBA/JRj mice (Janvier), or in CBA/CaJ (Jackson), likely due to the lack of a prominent circadian corticosterone (CORT) profile in the blood, which we have found to contribute to the circadian vulnerability to noise trauma in CBA/Sca. CBA/JRj mice animals exposed to 100 dB SPL or 105 dB SPL showed no obvious difference in hearing threshold shifts after day or night noise exposure, while CBA/CaJ showed a trend, but which did not reach significance. Blood CORT collected around the clock revealed that CBA/JRj display a flat profile, while CBA/CaJ mice have a less ample peak that occurs at an earlier time than the CBA/Sca. Accordingly, we exposed CBA/CaJ mice to 100 dB SPL at 7am and 5am (in comparison to 9am). We found

that mice exposed at 7am recovered from their noise trauma, while at 5am there was partial recovery. We tested locomotor activity which is a reliable behavioral output of circadian clocks and found differences in the activity between the CBA/Sca and CBA/CaJ strains. These findings suggest that the CORT profile in different strains could influence the circadian activity rhythms and thus help reveal mechanisms underlying the day/night differences to noise trauma.

PS 186

Subjective Reports of Temporary Hearing Changes as a Predictor of Auditory Impairment in Military Personnel

Douglas S. Brungart

Walter Reed National Military Medical Center

Background:

Shifts in auditory thresholds that eventually return to baseline have historically been viewed as an expected and acceptable consequence of exposure to occupationally-acceptable levels of noise. However, recent animal data has suggested that substantial cochlear damage can occur from noise exposures that produce purely temporary shifts in absolute threshold. Many subsequent studies have attempted to find evidence of systematic hearing damage in human listeners who have normal hearing thresholds but report a history of noise exposure. However, the results of these studies have been mixed. One question that has not consistently been asked as part of these noise surveys is the extent to which noise-exposed listeners have experienced temporary changes in their hearing, and the length of time these changes have taken to resolve. The purpose of this study was to survey the self-reported noises exposures and temporary hearing changes of service members and determine the extent to which these reports correlated with subjective measures of hearing impairment and tinnitus.

Methods:

A total of 2324 Service Members were recruited to participate in the study as part of their annual audiometric screening in one of six different hearing conservation clinics. Each participant completed a noise history and hearing symptom assessment consisting of up to 29 questions. The responses to these questions were recorded along with information on age, gender, and pure-tone audiometric thresholds.

The hearing symptom portion of the assessment consisted of four items from the Tinnitus and Hearing

Survey, six items from the Spatial and Sound Qualities questionnaire, and a question on sensitivity to loud sounds. A factor analysis was used to reduce these 13 questions down to seven factors.

These seven factors, plus an additional question on perceptual tinnitus, were subjected to a correlational analysis with 13 questions related to deployment history, exposure to continuous, small-arms, and heavy weapons noise, blast exposure, TBI history, hearing protection use, and the frequency and duration of temporary changes in hearing.

Results and Conclusions:

Self-reports of temporary hearing changes were more strongly correlated with self-reports of hearing impairment and tinnitus than other self-reports of noise exposure. This suggests that discrete and memorable episodes of intense noise exposure that result in noticeable hearing changes may cause more damage than long-term exposures to noisy environments.

Disclaimer:

The views expressed in this abstract are those of the authors and do not reflect the official policy of the Department of Army/Navy/Air Force, Department of Defense, or U.S. Government.

PS 187

Type II Cochlear Afferents Express CGRP within 1 day of Noise Trauma

Megan B. Wood¹; Adrian Jimenez²; Paul A. Fuchs¹
¹*Johns Hopkins University School of Medicine*; ²*Johns Hopkins University*

Research Background Type II afferents are thought to respond to cochlear trauma. It has been documented that these neurons are activated by ATP which may be released after acoustic trauma. Type II afferents are similar both in morphology and their expression of Cgrp C-type fibers in the somatosensory system. Therefore, Type II neurons are thought to be the nociceptors of the cochlea. Studying the function of Type II afferents will further our understanding of their role in auditory sensation and may shed light on ways in which they could respond to inflammation.

Methods CGRP α -EGFP (Tg(Calca-EGFP)FG104Gsat/Mmucd; RRID:MMRRC_011187-UCD) mice were exposed to broadband (4kHz to 40 kHz) noise for 2 hours at 110 dB SPL. Cochleae of exposed and unexposed mice were analyzed for reporter expression and CGRP

protein expression at 1, 7 and 14 days following acoustic trauma. Auditory brainstem response thresholds were recorded at 14 days after trauma to verify that noise exposure caused permanent damage. Ctbp2 staining was analyzed to show that all turns of the cochlea were affected by noise damage.

Results and Conclusions Broadband noise exposure produces threshold shifts of 10 dB and higher at 8, 16, and 32 kHz 14 days after noise exposure indicating permanent hearing loss. At lower frequencies in the apical turn, Ctbp2 staining indicates damage to synapses of the inner and outer hair cells at 7 and 14 days after noise. CGRP immunolabel shows that the protein is expressed in Type II afferent fibers 1 day after noise damage in the base of the cochlea. The protein is punctate much like that seen in the fibers of efferent neurons. In control cochleae not exposed to noise, CGRP immunolabeling is not found in type II afferents, but is present in efferent fibers. By 7 days after noise damage, CGRP protein is no longer observed in Type II afferents. In the CGRP reporter, GFP marks Type II afferents in a basal to apical gradient. Therefore, it is possible that apical neurons may not express CGRP or may require trauma resulting in permanent threshold shifts at lower frequencies to express CGRP protein. CGRP can be released from somatosensory C-fibers and act on local immune cells to alter inflammation. Further study will be required to elucidate whether Type II afferents release CGRP at early timepoints after noise damage.

PS 188

Changes of Auditory Brainstem Responses and Electrocochleography in Miniature Pigs After Impulse Noise Exposure

Xu Liangwei¹; Yuan Shuolong¹; Shi-ming Yang²
¹*Chinese PLA General Hospital*; ²*PLA General Hospital*

[Objective] To investigate the changes of auditory brainstem responses (ABRs) and electrocochleography in miniature pigs after impulse noise exposure.

[Methods] Healthy miniature pigs were exposed to impulse noise 80 times (pressure peak was 145dB SPL, and pulse duration was 0.25ms, interval time 10s). ABR and electrocochleography were tested before and after exposed immediately, 1, 2,4 and 8 weeks after exposure.

[Results] Similar to human beings, five typical peaks can be recognized in ABR waves of healthy miniature pigs, in which wave II and wave V are shown more frequently. The mean threshold of click-ABRs was 26.88 \pm 6.09 dB SPL. After 80 times high intensity impulse noise exposure, the click-ABR threshold and tone burst ABR

thresholds at 1, 2, 4, 8, 16 and 24 kHz were significantly increased. Thresholds of Each group are all higher than 80 dB SPL, and that of 8, 16, 24 kHz are damaged the most severely immediately after exposure. Various degrees of click-ABR thresholds recovery were detected at 1 to 4 weeks, the fastest speed is at 1 week after exposure. While we found that the thresholds got worse at 8 week. Recovery of tone burst ABR thresholds at 1, 2, 4kHz were similar to that of click-ABR within 8 weeks, while that of high frequency such as 8, 16, 24 kHz were not recovered distinctly within 2 weeks. The thresholds of 8 and 16kHz reduced during 2 and 4 weeks, while they increased at 8 week. Furthermore, the thresholds of 24kHz remained at around 90dB SPL after exposure, and no obvious restoration were detected, with poorly differentiated ABR waves. After 80 times high intensity impulse noise exposure, the nonlinear properties of Input/ Output (I/O) of CM were significantly lost, and the amplitude of CM decreased. The nonlinear properties of CM gradually recovered after noise exposure within 8 weeks.

[Conclusions] Compared with the rodents, the ABR waves of miniature pigs are more similar to that of human beings. And the pigs are more sensitive to impulsive noise exposure than the rodents. The miniature pigs provide an ideal large mammal model for auditory research, especially for noise-induced hearing loss and protection research.

PS 189

Blast-Induced Trauma To The Ear And Brain: Implications For Developing Endolymphatic Hydrops

Anthony T. Cacace¹; E. Mark Haacke²; Robert Hong²
¹Wayne State University; ²Wayne State University School of Medicine

Blast-related injuries of returning veterans deployed in the Middle East (Operation Enduring Freedom, Operation Iraqi Freedom, and New Dawn), have resulted in pervasive and debilitating morbidities to the ear and brain. Improvised explosive devices were the weapons-of-choice used by insurgents (roadside bombs, rocket-propelled grenades, mortars, C4 and TNT explosives). Hearing loss, tinnitus, vascular injury, and cognitive impairments were among the most frequently occurring injuries. Developing valid animal models to help understand the pathophysiology and mechanisms underlying these conditions are crucial to formulate useful treatments and guide rehabilitation. Herein, our interest focuses on understanding how exposure to blasts can produce endolymphatic hydrops (EH) of the inner ear.

A recent shock-tube based rodent model suggests that primary acoustic blast injury results in decoupling of outer hair cell stereocilia from the tectorial membrane which is the first step in a complex pathophysiological process of symptom progression. Subsequently, this trauma-initiated cascade impairs sensory transduction, reduces K⁺ bias currents, leads to hair-cell loss, and is correlated with increased endolymph volume, producing EH within the inner ear.

However, exposure to blasts is a complex phenomenon and it is well known that shock waves affect the ear and brain simultaneously. Inertial forces that cause rapid brain motion also produce a compression wave in the brain resulting in shear-wave injuries. Moreover, high impact forces may produce rotation effects and cause brain injury due to stress forces at grey/white matter interfaces and/or between cerebral hemispheres and the brainstem. Relative motion between brain and skull caused by rotation/translation acceleration can also result in subdural hematomas through the tearing of bridging veins and intracerebral hematomas can occur due to parenchymal blood vessel-rupture during brain-skull collisions.

As part of this blast-related process, the vascular system can also be involved. Therefore, another potential consideration holds that chronic cerebrospinal venous insufficiency (CCVI) may be involved in EH following exposure to blasts. CCVI could result in anatomical and functional alterations at the level of the inner ear; particularly with respect to the stria vascularis. In Meniere's disease for example, at least one of the unknown causes of cellular toxicity could be venous stasis (venous thrombosis) whereby cellular damage to the stria vascularis could alter metabolism, endolymphatic homeostasis, and lead to the development of EH.

Accordingly, our intent in this presentation is to develop a dialogue among researchers and clinicians to consider various hypotheses for developing EH following blast injury and consider treatment options.

PS 190

Dexamethasone Regulation of Neuroinflammatory Process after Traumatic Noise Exposure in the Central Auditory Pathway

Ana H Kim; **Hunki Paek**
Columbia University Medical Center

Dexamethasone (Dex) therapy, the only available steroid treatment of noise induced hearing loss (NIHL), can target many different levels of apoptotic/necrotic and neuroinflammatory pathways. However, cellular

mechanism underlying the Dex treatment on the auditory pathway including eighth nerve (8n), cochlear nucleus (CN), and the superior olivary complex (SOC) is largely unknown.

Microglia has a critical role in neuroinflammation through the expression of surface proteins, and secretion of pro-inflammatory cytokines. In this study, we wanted to investigate the cellular alteration of microglia and astrocytes to noise trauma by accessing in vivo cellular distribution, morphological changes, and examining the effects of Dex treatment on the reactivity of these cell types. Noise induced hearing loss CBA mice were treated with either saline or Dex via intra-tympanic (IT) injection. Hearing threshold assessed by auditory brainstem response (ABR) after NIHL showed threshold recovery with Dex treatment but not with saline. Neuroinflammatory characteristics accessed by IBA1, GFAP and TSPO staining showed activation of microglia cells and astrocytes in the CN, SOC after noise exposure in NIHL group compared to the NIHL-Dex treated group. Our results suggest a novel mechanism of neuroprotection against NIHL by Dex via counteracting neuroinflammation caused in the retrocochlear auditory centers.

PS 191

FOXO3's Role in Hearing Recovery from TTS Challenge

Holly J. Beaulac; Patricia White
University of Rochester Medical Center

Introduction: Inflammation's role during recovery from a temporary threshold shift (TTS) challenge remains understudied. The forkhead transcription factor FOXO3 regulates an array of cellular processes including apoptosis and oxidative stress & inflammation reduction. However, the balance between its pro-apoptotic and pro-survival activity depends on mechanisms not yet fully understood. Foxo3a motif analysis shows that IL-10, IL-12b, and TNF have Foxo3a binding sites on their proximal promoters and Foxo3a-KO macrophages produce significantly less IL-12 and TNF but more IL-10 following insult (Joseph et al., 2016). Using Foxo3-KO mice, we have shown that FOXO3 is required for auditory function and OHC preservation following noise exposure and as mice age. **I hypothesize that FOXO3 deletion leads to decreased proinflammatory signaling and cytokine production within the cochlea after noise.** We will perform spatiotemporal macrophage analysis and quantify cytokine production within the Foxo3-KO cochlea before and after TTS. Amoeboid-shaped macrophages are predicted to reflect a more active, inflamed state while those that are ramified with more processes may be surveilling for perturbations.

Methods: Foxo3-KO mice and their wild-type littermates were noise exposed (105 dB at 8-16 kHz for 0.5 hours) at P60, with 2-3 mice per genotype sacrificed at 0.5-hours post-noise (HPN), 1 HPN, and 4 HPN. 2-3 non-exposed mice of each genotype were used as controls. One cochlea per mouse was microdissected, whole mounted, and stained for confocal imaging with MYO7 for hair cells, CD45 for pan-leukocytes, and Iba-1 for macrophages. Total macrophage numbers, mean volume, and morphology were assessed using Amira 6.5 3D-rendering. The other cochlea was homogenized and its lysate used for ELISAs. Pro- and anti-inflammatory cytokines including IL-1 β , TNF, IL-6, IL-12b, and IL-10 along with MHCII were probed.

Results: Following a mild noise exposure, OHC loss occurs basal to the noise band in Foxo3-KO mice as early as 0.5 HPN. Normally, macrophages are round and become more ramified moving from the base to the apex, suggesting that the base may be in a constant state of inflammation (Frye et al., 2016). Analyses of macrophage morphology and inflammatory cytokine levels are currently underway.

Discussion: With altered cytokine signaling, resident macrophages may remain in a ramified, surveillance state within the Foxo3-KO cochlea. This could mean a delayed response to stress, leaving the organ of Corti vulnerable to greater damage during noise, possibly incurred by supporting cells. Investigating whether FOXO3 regulates cochlear inflammation will help us characterize the genetic regulatory network underlying noise susceptibility.

PS 192

Dose-Dependent Strial Macrophage Morphology with Noise Exposure

Weiwei He¹; Alisa Hetrick¹; Liana Sargsyan¹; Yu Sun²; Hongzhe Li¹

¹VA Loma Linda Healthcare System; ²Wuhan Union Hospital, Tongji Medical College, Huazhong University of Science and Technology

Background Substantial cellular immune responses occur in the cochlea upon acoustic overstimulation, which include an orchestra of tissue damage, repair and reconstruction. The macrophage, either residential or recruited, plays a crucial role in mediating these cellular events. The active morphological change of macrophages in the stria vascularis after noise exposure is considered a part of the cochlear immune response that also contributes to the physical dysfunction of the blood-labyrinth barrier. To date, limited studies have focused on the distinction of strial macrophages in

reversible or partially reversible noise-induced cochlear damage, by varying sound levels. We consider this is a viable approach to understand the correlation between the degree of cochlear inflammation and the noise-induced cochlear damage, and consequently, hearing loss.

Methods C57BL/6J mice of 6-8 weeks were divided into four groups including an untreated control group, and exposed to octave-band noise (8–16 kHz) at 100, 106, and 112 dB SPL for 2 hours. Seven days after exposure, immunofluorescence labeling was performed using anti-Iba1 rabbit IgG to identify strial macrophages. Iba1, the abbreviation of ionized calcium binding adapter molecule 1, is a specific protein expressed in monocytic lineages, and a cell marker for macrophages. Here, Iba1-positive strial macrophages were analyzed morphologically and numerically in each animal groups. In addition, the level of cytokines including IL-6 and MCP-1/CCL2 was also evaluated in the cochlea.

Results The localization of strial macrophages was confirmed by Iba1 labeling in adult mice. The macrophages are typically distributed along the stria capillaries, either with or without noise exposure. In the stria vascularis of the control group, most Iba1-positive cells exhibit branched morphology, contacting with and often attaching to the external capillary wall. In the groups with moderate noise exposure (100 and 106 dB SPL), negligible change was observed in cell number or morphology of the macrophages, regardless of their relevant cochlear location. With the highest exposed sound level, 112 dB SPL, a slight increase in the count of macrophages was observed, and a subpopulation of the Iba1-positive cells become more spherical, presenting shorter processes, compared to the control group.

Conclusions In the mouse cochlea, Iba1-positive cells are distributed surrounding the strial capillaries, and identified as macrophages. Acoustic trauma encouraged morphological change in the strial macrophage after a sufficient dosage of noise exposure. Thus, progressively increased macrophage-dependent immune activity occurs with increasing noise exposure in the stria vascularis, implicating a gradually elevated severity of cochlear inflammation.

Ototoxicity I

PS 193

Hospital Gentamicin - Ototoxic and antimicrobial assessment of ten individual components

Mary E. O'Sullivan; Adela Perez; Randy Lin; Robert Greenhouse; Alan G. Cheng; Anthony J. Ricci
Stanford University

Introduction: Aminoglycosides are broad-spectrum antibiotics with ototoxic side effects. Hospital Gentamicin is a mixture of chemically related compounds - Gentamicin C1, C1a, C2, C2a, C2b, A, X, B, Geneticin and Sisomicin. We determined the ototoxicity and antimicrobial potency of these compounds. We ask whether the breadth of antimicrobial activity comes from having a mixture and if there is a less ototoxic compound to use as starting material for future drug development.

Method: Using a novel method we purified gentamicin C1, C2, C2a, C2b, and C1a in gram quantities, other compounds were sourced from commercial vendors. In vitro antimicrobial activity was examined using 40 strains of bacteria - ten strains from *E. coli*, *K. pneumoniae*, *P. aeruginosa*, and *S. aureus*. Minimum 50% inhibitory concentrations (MIC50) were established using an 11-dose log₂ drug-dilution series. Ototoxicity was examined using a novel 3-D P5 rat cochlear culture method validated for MET-channel activity using Gentamicin-Texas-Red. Following a 1hr-drug incubation, cochleae were cultured for 48 hrs, after which MyoVIIa, Dapi, and Phalloidin were used to visualize outer hair cells in the mid-apical turn for counting. Ototoxicity EC₅₀±SD values were established from ≥6-point dose-response curves and fitted with non-linear regression fits.

Results: Hospital gentamicin has an EC₅₀ value of 675±68µM. Geneticin, Sisomicin, and GentC2 are more ototoxic than the hospital mixture. GentC1, C1a, and C2a are comparable to the hospital gentamicin. GentC2b is >40% less ototoxic (EC₅₀ = 1200±180µM), with GentB and GentA having the lowest EC₅₀ values (EC₅₀ >2000µM). Antimicrobial analysis shows that hospital gentamicin is effective against 35/40 strains with a geometric mean MIC₅₀ of 1.11µg/ml. Sisomicin is the most antimicrobial (35/40, 0.66µg/ml). GentC1a, C2, C2a, C2b, and C1 have comparable antimicrobial activity (31-35/40, 0.89-1.77µg/ml). Geneticin, GentA, and GentX show decreased antimicrobial activity (>9µg/ml). Using mass spectrometry, we quantified hospital gentamicin constituents and calculated the predicted versus the experimental ototoxicity and antimicrobial activity values. The predicted ototoxicity value was higher than the experimental value, the antimicrobial activity values were comparable.

Conclusion: We present two key observations. First, GentC2b has comparable antimicrobial activity but is less ototoxic than hospital gentamicin, opening the door to the usage of a single gentamicin compound rather than a mixture. Second, since the experimental ototoxicity value is lower for hospital gentamicin than the scaled sum of the major components, we propose that the impurities may be increasing the ototoxicity of the hospital mixture, and thus should be removed.

Acknowledgements: M.T. at the Clinical Microbiology Institute prepared the antimicrobial panels, L.B. at the Stanford OHNS core facility assisted with imaging automation. The Stanford OHNS core facilities are supported by the Stanford Initiative to Cure Hearing Loss through the Bill and Susan Oberndorf foundation. This work is supported by the NIH R01DC014720.

PS 194

Serial Tomographic Reconstruction of a Damage Repair Process in Aminoglycoside-Treated Hair Cells

Richard T. Osgood; Guy Richardson
University of Sussex

Background

Sensory hair cells of the inner ear are susceptible to damage and death as a result of exposure to aminoglycoside antibiotics. As the hair cells of the mammalian cochlea cannot be regenerated, the ototoxic side effects of these drugs can cause permanent sensorineural hearing loss. When cochlear cultures from early postnatal mice are exposed to a high dose of neomycin, rapid externalization of phosphatidylserine and extensive membrane blebbing occurs at the apical pole of hair cells. Remarkably, following aminoglycoside washout hair cells rapidly repair this damage; within 15 minutes the blebs are no longer observed and membrane lipid asymmetry is restored. Blebs as large as 5 µm in diameter occur as a result of neomycin treatment and are not obviously shed during the recovery process. Recovery therefore involves the retrieval of large areas of membrane.

Methods

A combination of live imaging and transmission electron microscopy (TEM) tomography were used to characterize the process of membrane internalization during this repair process. The nature and time course of bleb retrieval at the apical surface were determined by live DIC imaging. The fate of this membrane was tracked in the cell by live confocal microscopy of the outer leaflet of the neomycin-induced membrane blebs labeled with fluorescently conjugated annexin V. The internalization process was characterized at the ultrastructural level using serial section TEM tomography. Following bleb formation the apical surface of the damaged hair cells was pulse-labelled at 40°C with electron-dense cationized ferritin, and the cells were allowed to recover at 37°C. The cultures were then fixed for TEM at successive time points during recovery.

Results

Live DIC imaging reveals large blebs located in the vicinity of the kinocilium rapidly decrease in size and are resorbed into the cell within the first 15 minutes of

recovery. Large fluorescent densities are observed, by live confocal microscopy, just below the apical surface during this time, and subsequently break up into smaller structures that become dispersed within the cell. Serial electron tomography indicates this bulk endocytic process involves the formation of large multi-laminated structures consisting of multiple concentric membrane folds.

Conclusions

Neomycin-induced blebs are removed from the apical surface of sensory hair cells by the rapid internalization of large areas of membrane using a previously undescribed macro-endocytic process. Sensory hair cells have an astonishing capacity for membrane internalisation and maintenance of the integrity of their apical surface.

PS 195

Cisplatin Induced Oxidative Stress Down-regulates Strial Na⁺/K⁺-ATPase Expression

Sandeep Sheth¹; Raheem Al Aameri¹; Vikrant Borse²; Asmita Dhukhwa¹; Michelle Lowy¹; Debashree Mukherjee¹; Leonard P. Rybak¹; Vickram Ramkumar¹
¹*Southern Illinois University School of Medicine;*
²*Washington University in Saint Louis*

Background: Cisplatin is a chemotherapeutic agent which produces a serious side effect of hearing loss which is bilateral and irreversible. Na⁺/K⁺-ATPase pump is an ATP-dependent transmembrane enzyme which is highly expressed in the marginal cells of the stria vascularis (SVA) and type II fibrocytes in spiral ligament (SL). Na⁺/K⁺-ATPase maintains the ionic gradient of Na⁺ and K⁺ in the endolymph which is crucial for osmotic balance, cell volume regulation and maintenance of endocochlear potential (EP). Preliminary studies from our lab suggests that cisplatin induces down-regulation of Na⁺/K⁺-ATPase in the SVA along with SL. However, the exact molecular mechanism pertaining to this decrease in Na⁺/K⁺-ATPase has not yet been identified. The generation of reactive oxygen species (ROS) by cisplatin has been considered a critical event which initiates damage to the outer hair cells (OHC), SV and spiral ganglion cells (SGC), leading to hearing loss. Based on these observations, we hypothesize that cisplatin-induced decrease in Na⁺/K⁺-ATPase expression is mediated through the production of ROS in the cochlea.

Methods: To inhibit ROS production we used siRNA against NOX3 to knockdown the expression of NOX3 RNA. Auditory brainstem responses (ABRs) in naïve male Wistar rats were recorded prior and 3-days after trans-tympanic delivery of NOX3 siRNA (0.9 µg) and i.p. cisplatin (11mg/kg) to assess hearing loss. Cochleae were then isolated and immunohistochemistry was

performed on mid-modiolar sections to determine Na⁺/K⁺-ATPase α 1 immunoreactivity. Whole mount preparation were used to check for the loss of OHCs using myosin VIIa staining and ribbon synapses using antibodies against CtBP2 and glutamate receptor-2.

Results: Cisplatin-induced hearing loss was abrogated by trans-tympanic administration of NOX3 siRNA at 16 and 32 kHz frequencies, as determined by ABR. Real-time RT-PCR studies indicated that NOX3 siRNA not only reduced NOX3 expression as compared to scrambled siRNA but also inhibited cisplatin-induced NOX3 expression in the cochlea. Immunohistological examination revealed that cisplatin clearly down-regulated the immunostaining of Na⁺/K⁺-ATPase α 1 in SVA and SL in the basal turn of cochlea which is reversed by NOX3 siRNA. Moreover, NOX3 siRNA reduced cisplatin-induced OHC damage and loss of inner hair cell ribbon synapses. These findings were confirmed by administration of epigallocatechin gallate (EGCG), natural scavenger of ROS, which also restored cisplatin-induced suppression of Na⁺/K⁺-ATPase expression.

Conclusion: This study provides a novel insight in the regulation of strial Na⁺/K⁺-ATPase by ROS, thereby highlighting novel targets for the otoprotective agents such as EGCG in the treatment of cisplatin-induced hearing loss.

PS 196

Intracochlear Perfusion of Tumor Necrosis Factor-Alpha Induces Sensorineural Hearing Loss and Synaptic Degeneration in Guinea Pigs

Mehmet¹. Sahin¹; Rebecca M. Lewis²; **Sachiyo Katsumi**²; Janani S. Iyer³; Lukas Landegger²; Konstantina M. Stankovic⁴

¹*Erciyes University Faculty of Medicine*; ²*Eaton-Peabody Laboratories, Massachusetts Eye and Ear; Dept. of Otolaryngology, Harvard Medical School*;

³*Program in Speech and Hearing Bioscience and Technology, Harvard University*; *Eaton-Peabody Laboratories, Massachusetts Eye and Ear*; *Dept. of Otolaryngology, Harvard Medical School*; ⁴*Eaton-Peabody Laboratories, Massachusetts Eye and Ear & Department of Otolaryngology, Massachusetts Eye and Ear and Harvard Medical School & Speech and Hearing Bioscience and Technology Program*

An important cause of sensorineural hearing loss (SNHL) is vestibular schwannoma (VS), a progressive disease characterized by the slow growth of a benign tumor in the brain's cerebellopontine angle. The conventional hypothesis regarding the mechanism underlying VS-induced SNHL is that the tumor

compresses the vestibulocochlear nerve, preventing hearing and balance information from reaching the brain; however, prior work suggests that associations between a) tumor size and proximity to the cochlea and b) hearing ability and intracochlear damage are weak, and that SNHL can worsen over time in VS patients without evidence of corresponding tumor growth. These reports motivate the hypothesis that there are biological factors that distinguish SNHL-inducing VS tumors from those that spare hearing function. Focusing specifically on VS secretions that could alter cochlear function via passage through the internal auditory canal, our group has previously reported significant associations between levels of secreted tumor necrosis factor-alpha (TNF- α) and degree of SNHL in VS patients, in addition to demonstrating significant ototoxicity induced through application of TNF- α and VS secretions to cochlear explants. Here, we further investigate the ototoxic effects of TNF- α by assessing the physiologic and morphologic consequences of intracochlear perfusion of TNF- α in vivo in guinea pigs. Animals were randomly assigned to one of three groups: control, TNF- α , and prevention. The round window region was surgically exposed to facilitate subsequent perfusion of artificial perilymph (control group), TNF- α (TNF- α group), or a TNF- α inhibitor (etanercept) followed by TNF- α (prevention group) into scala tympani. Compound action potential (CAP) and distortion product otoacoustic emission (DPOAE) amplitudes and thresholds were measured prior to and post-TNF- α perfusion, and cochleae were dissected for morphologic investigation at the termination of each experiment. Results reveal significant differences in CAP amplitudes between the control and TNF- α groups and the TNF- α and prevention groups, providing evidence for a) TNF- α 's ototoxic effect, and b) etanercept's ability to protect against TNF- α -induced ototoxicity. Morphologic assessment revealed significant and marginally-significant differences between control and TNF- α and prevention and TNF- α groups, respectively, in number of orphaned synaptic ribbons, suggesting TNF- α -induced synaptic degeneration. No significant differences were observed across groups in CAP or DPOAE thresholds, or in hair cell counts, suggesting a pathologic profile similar to that observed in auditory neuropathy. Findings motivate further investigation into the specific mechanisms by which TNF- α exerts its ototoxic effects, and the extent to which TNF- α -blockers may protect against SNHL in patients suffering from VS.

Exploring Parameters of a Cell Growth Inhibition Assay to Probe the Intracellular Penetration of Novel Aminoglycosides in Gram-Negative Bacteria

Randy Lin; Mary E. O'Sullivan; Alan G. Cheng;
Anthony J. Ricci
Stanford University

Aminoglycosides are broad-spectrum antibiotics used to treat gram-negative bacterial infections, in spite of a progressive and dose-dependent ototoxic side effect. The recent drug design strategy led to the synthesis of novel, less ototoxic analogs of sisomicin (Huth et al., 2015). However, several analogs unexpectedly lost antimicrobial activity, prompting us to develop a method to validate whether drug uptake was responsible for loss of antimicrobial activity and to determine optimal conditions for drug uptake.

Antimicrobial data was first obtained from the Clinical Microbiology Institute (CMI) where minimum inhibitory concentration (MIC) of both aminoglycosides and analogs against *E. coli* and *P. aeruginosa* were obtained using a low density, low volume and long exposure time assay. We compared MIC differences between drugs using cell growth assays for *E. coli* with growth measured by optical density at 600 nm (O.D.600). Dose response curves were generated for each drug. Parameters such as sample volume, starting bacteria density and antibiotic exposure time were tested to optimize uptake conditions, using bacterial growth as a proxy for uptake.

Sisomicin, gentamicin, dihydrostreptomycin, geneticin and two analogs, 1-N-Methylsulfonyl sisomicin (N1MS) and 1-N-Trifluoromethylsulfonyl sisomicin (N1TFMS) were tested against *E. coli* ATCC 25922 and *E. coli* ATCC 35218. CMI antimicrobial data reveals a four-fold difference in MIC between sisomicin and N1MS (0.25 µg/ml and 1 µg/ml), and between gentamicin subtypes C1 and C1a (1 µg/ml and 0.25 µg/ml), against *E. coli* ATCC 35218. We used a low-volume (1 mL) or high-volume (10 mL) growth assay format to elucidate the concentration-dependent effect of aminoglycosides on growth. Surprisingly, we observed little growth inhibition at CMI MIC for sisomicin and N1MS, and we were not able to reproduce the same separation in MIC as CMI. Similarly, high volume and high cell density growth assays were also unable to delineate MIC differences for gentamicin C1 and C1a as compared to CMI data. We further probed these disparate data by altering initial bacteria density and treatment duration. A starting O.D.600 between 0.1 and 2.0 showed a density-dependent decrease in antimicrobial efficacy. When treatment duration was extended, the time response growth plots showed six hours to be sufficient in allowing complete growth inhibition.

Aminoglycoside antibacterial activity is highly dependent on growth assay parameters. Volume, cell density and exposure duration each influence the apparent MIC value measured. Our data indicates the importance of the ratio of drug molecules to bacteria number in establishing MIC values.

PS 198

Differentiating Mechanisms of Aminoglycoside Toxicity In Mammalian Cochlear Hair Cells

Esra D. Camci¹; Patricia Wu¹; Julian Simon²; David W. Raible¹; Edwin Rubel¹
¹University of Washington; ²Fred Hutchinson Cancer Research Center

Hearing loss due to cochlear hair cell death is a significant concern for patients treated with aminoglycoside antibiotics (AG). In the zebrafish lateral line (LL), different AGs have been found to elicit different temporal patterns of hair cell death. In fish treated with neomycin, the majority of cell death occurs within one hour of treatment. In contrast, gentamicin toxicity is only observed after an extended post-exposure incubation period and continues after the exposure period, following a process of delayed toxicity. We investigated the conservation of these patterns in neonatal mouse organ of Corti cultures. Similarities and differences to responses in the zebrafish were found. Consistent with its observed effect on LL hair cell survival, neomycin treatment resulted in rapid dose-dependent outer hair cell death. Gentamicin toxicity was found to be much slower. In contrast to findings in zebrafish, delayed toxicity was observed in both gentamicin- and neomycin-treated cochlear cultures. These observations support the ideas that there are at least two separable patterns of AG-induced hair cell death that can be differentially activated by different AGs and in different model systems. These observations may help us identify the intercellular targets and downstream mechanisms activated by these and other ototoxic drugs.

PS 199

Gene expression and pathway analysis of cisplatin-treated cochlear cells

Pezhman Salehi¹; Zhuo Li¹; Yan Zhang¹; Tal Teitz²; Jian Zuo¹
¹Department of Biomedical Sciences, Creighton University, School of Medicine; ²Department of Pharmacology, Creighton University, School of Medicine

Objectives: Cisplatin is one of the most effective drugs in cancer chemotherapy; but cisplatin chemotherapy has a major dose limiting side effect of ototoxicity.

Clinical research data showing permanent hearing loss in approximately 60% to 80% of the cisplatin treated patients suggest genetic susceptibility to cisplatin-induced hearing loss. This study investigates altered gene expression level and the genetic architecture underlying degenerative changes in cochlear cells caused by cisplatin.

Methods: Cultured mouse cochlear cells (HEI-OC1) were exposed to various concentrations of cisplatin and total RNA was isolated from drug treated and control cells. Sequencing libraries were generated using NextUltr RNA Library Prep for Illumina, and the library preparations were sequenced on an Illumina Hiseq 2000 platform. The genes significantly altered in drug treated cells were carefully studied and the candidates with known effects on cellular apoptosis were selected for further analysis. Knock out HEI-OC1 cell lines will be generated using CRISPR technique and then cisplatin sensitivity of these cell lines will be compared with that of parental cells. Single-cell RNA seq was performed using 10X Genomics technologies in mature mouse cochlear cells treated with cisplatin at various doses and at various post-treatment time points. Protocols were followed as described previously (Yamashita et al., PLoS Genetics 2018). Gene expression profiles were analyzed in hair cells, supporting cells, spiral ganglia, and stria cells.

Results: Over 800 candidate genes ($p < 0.01$) were found altered in cisplatin treated HEI-OC1 cells when compared to the none-treated controls. The major pathways involved in cisplatin treated HEI-OC1 cells, including immune and apoptotic pathways were identified. Validation of the selected genes using knock out cell lines will show altered sensitivity of the cells to cisplatin treatment.

Conclusion: This study identifies altered genes and major pathways involved in HEI-OC1 cells and in mature mouse cochleae in vivo, thus providing therapeutic targets for clinical prevention of cisplatin ototoxicity.

Supported in part by NIHR01DC015010, NIHR01DC015444, ONR-N00014-18-1-2507, USAMRMC-RH170030, and LB692/Creighton.

PS 200

Reciprocal Interaction Between Regulator of G-protein Signaling 17 and Cannabinoid Receptor 2 in Cochlea.

Asmita Dhukhwa¹; Kelly Sheehan²; Sandeep Sheth¹; Leonard P. Rybak¹; Debashree Mukherjea¹; Vickram Ramkumar¹

¹*Southern Illinois University School of Medicine*; ²*St. Johns HSHS Memorial Hospital*

Regulators of G-protein signaling (RGS) catalyze hydrolysis of GTP bound to G proteins (GTPase activity) and terminate the actions of the associated G-protein coupled receptor (GPCR). RGS17, a member of RGS-RZ subfamily, commonly targets GTP bound Gaz, Gai and Gao for hydrolysis and signal termination. Recent data from our laboratory have implicated the GPCR, cannabinoid receptor 2 (CB2), in mediating otoprotection against cisplatin-induced hearing loss. In addition, analysis of whole cochlea transcriptome data revealed higher level of RGS17 in cochlea after cisplatin treatment. These data highlights a novel cellular mechanism of cisplatin ototoxicity, namely regulating RGS17 (and possibly other RGS proteins) to limit the otoprotective actions of endogenous GPCRs.

Auditory brain response (ABR) was recorded from Male Wistar rats prior to treatments. Adenoviral vector (Adv) over-expressing RGS17 (3.9×10^8 p.f.u) was administered trans-tympanically into the rats and post ABRs were taken after 5 days. Similarly, rats were treated with trans-tympanic siRNA (0.9 μ g) for 48h prior to cisplatin (11mg/kg, i.p) administration. Post ABRs were assessed after 72h of cisplatin treatment. Cochleae were collected and processed for either RNA isolation or immunofluorescence. Gene expression studies were determined by quantitative PCR. Apoptosis was determined by TUNEL, Annexin V/PI and MTS assays. RGS17 was increased in cochlea after cisplatin treatment at both mRNA and protein levels. Administration of Adv overexpressing RGS17 also increased ABR threshold shifts and significantly decreased Wave I amplitude following cisplatin treatment. Conversely, knock down of RGS17 (by siRGS17) reduced cisplatin-induced elevations in ABR thresholds. siRGS17 treated cochlea showed fewer TUNEL-positive cells than cisplatin administered animals. Moreover, overexpression of RGS17 in immortalized organ of Corti (UB/OC1) cells increased the ratio of pSTAT1/pSTAT3. Pretreatment of siRGS17 decreased mRNA level of oxidative and inflammatory stress markers such as NOX3 and iNOS, whereas the level of antioxidant genes such as Nrf2 and SOD2 were increased. Additionally, pretreatment of JWH-015 (a CB2 agonist) prior to cisplatin administration significantly reduced RGS17 level in cochlea while elevated level of RGS17 was observed in cochleae where CB2 was knocked down. Celastrol, a RGS17 inhibitor, increased cell viability against cisplatin in vitro.

Our findings suggest that elevation in the levels of RGS17 by cisplatin could represent one mechanism by which it increases oxidative stress, inflammation and hair cell apoptosis, leading to hearing loss. Activation of CB2 tonically suppresses RGS17 expression and antagonizes its effects. These data indicates a tonic inhibitory reciprocal action between RGS17 and CB2

mediated through regulation of G protein signaling. Therefore, RGS17 inhibitors could represent novel therapies for treating hearing loss.

PS 201

Investigating the role of Hsp70 during stress granule formation in cochlear cells

Ana Claudia Goncalves¹; Emily Towers¹; Lisa L Cunningham²; Sally J Dawson³; Jonathan E Gale¹

¹*UCL Ear Institute, University College London;*

²*National Institute on Deafness and Other Communication Disorders, NIH;* ³*UCL Ear Institute, University College London.*

Both Hsp70 induction and stress granule formation are pro-survival mechanisms which have been independently implicated in response to different forms of cochlear stress. Stress granules (SGs) are cytoplasmic aggregates of mRNAs and RNA-binding proteins that regulate posttranscriptional gene expression during cellular stress. SGs optimise the translation of stress-responsive genes, through selective exclusion of RNAs for immediate translation during stress. We have previously shown that SG-induction during aminoglycoside treatment protects outer hair cells from death, indicating their potential importance during cochlear stress. In the inner ear, Hsp70 can mediate protection of hair cells from aminoglycoside-induced death (1,2). Recent studies in HeLa cells show that Hsp70 participates in the SG-clearance after stress (3), suggesting an association between Hsp70 and SGs. Here, we aim to investigate the relationship between Hsp70 and SGs in cochlear cells.

First, we used heat shock and arsenite stresses to generate SG-formation and study Hsp70-expression. Immunocytochemistry shows that UB/OC-2 cells assemble SGs after 1 hour of either heat shock or arsenite exposure. During a subsequent recovery period of 4 hours, the number of SGs decreases; qPCR and immunocytochemistry show that Hsp70 expression increases during recovery from heat shock stress ($p < 0.05$), correlating with SG-clearance. Hsp70 mRNA levels peak after 2 hours of recovery from heat shock (>411-fold activation compared to untreated cells). In comparison, arsenite stress results in a slower and much reduced Hsp70 activation (>28-fold compared to untreated cells), indicating that there is stress-specific activation of Hsp70 in UB/OC-2 cells.

Secondly, we used RNA-immuno-fluorescence in situ hybridisation to locate Hsp70 mRNA in relation to SGs. High resolution microscopy indicates that Hsp70 mRNA is excluded from SGs during both types of stress,

suggesting its preferential translation, consistent with data in other cell types. Furthermore, overexpression of Hsp70, using an adenovirus-mediated construct (Ad-Hsp70), decreases heat shock-induced SG-formation ($p < 0.005$), indicating that there is a causative link between Hsp70-expression and a reduction in the number of SGs during heat shock. Interestingly, Hsp70-overexpression prior to arsenite stress does not affect SG-assembly, suggesting stress-specific interactions between Hsp70 and SGs.

Our data suggest that the protective effect of Hsp70 in the auditory system may involve interactions with the SG-pathway. Given the growing evidence that SGs are involved in cell survival upon stress and the known implications of Hsp70 in hair cell protection, a better understanding of their relationship may contribute to the development of novel therapeutic strategies to avoid cell death during cochlear stress conditions.

References:

- [1] Taleb, M. et al., 2008. Hsp70 inhibits aminoglycoside-induced hair cell death and is necessary for the protective effect of heat shock. *JARO*, 9(3), pp.277-289.
- [2] Taleb, M. et al., 2009. Hsp70 inhibits aminoglycoside-induced hearing loss and cochlear hair cell death. *Cell Stress and Chaperones*, 14(4), pp.427-437.
- [3] Mateju, D. et al., 2017. An aberrant phase transition of stress granules triggered by misfolded protein and prevented by chaperone function. *EMBO J.*, 36(12), pp.1669-1687.

PS 202

Ototoxicity Following Cyclic Administration of Platinum-Based Chemotherapeutic Agents in Mice

Benjamin K. Gersten; Katharine Fernandez; Lisa Cunningham

National Institute on Deafness and Other Communication Disorders

Introduction: While cisplatin is a widely used chemotherapeutic agent that targets a variety of cancers, it is highly ototoxic and causes hearing loss in many patients. Oxaliplatin and carboplatin are generally considered less ototoxic than cisplatin (Hellberg, 2009; Fetoni, 2016), even though all three of these drugs are structured around a core platinum atom. The reasons for the differential effects of these platinum-based drugs remain unknown. Our lab recently developed an in vivo cisplatin administration protocol that is similar to clinical cisplatin administration in that it utilizes multiple cycles of drug administration. Using this protocol, we recently showed that cisplatin accumulates in the stria vascularis and remains there indefinitely (Breglio, 2017). Here

we administered cisplatin, carboplatin, and oxaliplatin to mice using a modified version of this three-cycle protocol with the goals of determining 1) if oxaliplatin and carboplatin are ototoxic in this context, and 2) if carboplatin and oxaliplatin are retained in the stria vascularis in a manner similar to cisplatin.

Methods: 40 CBA/CaJ mice were used for this study. Auditory sensitivity was assessed before drug administration by measuring the auditory brain stem response (8-40 kHz) and distortion product otoacoustic emissions ($f_2 = 4-40$ kHz). Cisplatin, carboplatin, or oxaliplatin was delivered via IP injection over three 4-day cycles of drug administration. Each cycle was followed by a 10-day recovery period. Auditory testing was repeated after the final cycle of drug administration. Mouse cochleae were collected for histology to assess patterns of inner ear damage.

Results: Our data demonstrate a significant hearing loss across all frequencies for cisplatin treated mice with increased severity in the higher frequencies. We observed minimal ototoxicity in mice treated with carboplatin or oxaliplatin. Thus, our three-cycle drug protocol yields data that are similar to what is reported clinically. Cochlear samples will be submitted for inductively coupled mass spectrometry (ICP-MS) analysis of platinum uptake of all three drugs.

Discussion: It is important to understand why cisplatin is particularly ototoxic among cancer drugs so that potential therapies to reduce this effect might be developed. Additionally, examining the platinum uptake by the inner ear will be useful to see if the differential ototoxicity of these drugs is related to the differential uptake of platinum by the cochlea.

This work was supported by the NIDCD Division of Intramural Research.

PS 203

Fate of Cochlear Cells Following DT Injection in the DTR Mouse

Takaomi Kurioka¹; Min Young Lee²; Lisa A. Beyer³; Donald L. Swiderski³; **Yehoash Raphael³**

¹*Department of Otolaryngology-Head-and Neck Surgery, Kitasato University School of Medicine,;*

²*Department of Otorhinolaryngology-Head & Neck Surgery, College of Medicine, Dankook University;*

³*Kresge Hearing Research Institute, Department of Otolaryngology-Head and Neck Surgery, University of Michigan*

Background:

The organ of Corti (OC) is a highly organized epithelium that contains hair cells (HCs) and supporting cells (SCs). Following the loss of HCs due to overstimulation or ototoxic drugs, SCs typically seal the reticular lamina and reorganize the epithelial surface. This scarring process is important for maintaining the separation between endolymph and perilymph after HC death, avoiding secondary cell death and preserving spiral ganglion neurons (SGNs). We and others have shown that selective HC loss in adult mice has no significant impact on SGN survival for at least 2 months (Golub et al. 2012, Kurioka et al. 2016). However, it is unclear whether selective HC ablation without primary damage to SCs is sufficient to induce typical processes of epithelial repair and whether SGNs can survive in the long-term without HCs. Here we investigated the changes in the sensory epithelium and the long-term fate of SGNs elimination of HCs in the diphtheria toxin receptor (DTR) mouse.

Materials and Methods:

DTR mice (from Ed Rubel, University of Washington) were given a single systemic injection of DT (15 ng/g) at 3 weeks of age and allowed to survive 3, 7, 12 days and 2, or 4 months after injection. Cochleae were examined either as whole-mounts stained for prestin (outer HC marker), sox2 (supporting cell nuclei marker), ZO-1 (tight junction maker), and actin (to view adherens junctions in the reticular lamina), or plastic cross-sections.

Results:

DTR mice exhibited near-complete HC loss 1 week after DT injection. SCs remained in the auditory epithelium even at the latest time point (4 months). The reticular lamina of the OC exhibited scar formation and apical junction reorganization as seen after HC loss due to other insults, without holes, at all time-points examined. Prestin-positive clusters were detected in SCs that replaced lost outer HCs. While SGN density remained unchanged at the 2-month time point, neuron depletion was noted 4 months after DT injection.

Conclusions:

Finding of typical scar formation upon HC loss, with outer HC debris in the cytoplasm of SCs add validity to the DTR mouse as a model mimicking HC loss in human ears. However, loss of neurons at 4 months despite survival of SCs provides preliminary indication that the time window for regenerative work is limited. Further work is needed to determine why neurons start to degenerate 2 months after HCs are depleted.

Supported by NIH-NIDCD grants R01-DC014832 and P30-DC005188.

Analysis of hearing function in a mouse model of reactive oxygen species overproduction

Shigefumi Morioka¹; Hirofumi Sakaguchi¹; Taro Yamaguchi²; Takashi Nakamura¹; Yuzuru Ninoyu¹; Hiroaki Mohri¹; Kiyokazu Ogita²; Naoaki Saito³; Takehiko Ueyama³

¹Department of Otolaryngology-Head and Neck Surgery, Kyoto Prefectural University of Medicine; ²Laboratory of Pharmacology, Faculty of Pharmaceutical Sciences, Setsunan University; ³Laboratory of Molecular Pharmacology, Biosignal Research Center, Kobe University

Background

Previous studies have convincingly argued that reactive oxygen species (ROS) contribute to the development of several major types of sensorineural hearing loss, such as noise-induced hearing loss, drug-induced hearing loss, and age-related hearing loss. However, the underlying molecular mechanisms induced by ROS in these pathologies remain unclear. To resolve this issue, we established an in vivo model of ROS overproduction and examined the hearing function of this model.

Methods

To establish a mouse model with overproduction of ROS in the cochlea, we focused on NADPH oxidase 4 (NOX4) which is a constitutively active ROS producing enzyme without stimulation or an activator. We generated transgenic mouse line systemically overexpressing Nox4 (NOX4-TG mice), and confirmed that NOX4-TG mice worked as ROS-overproduction model. We examined hearing function of NOX4-TG mice by auditory brainstem response and morphology of hair cells under baseline conditions and after intense noise exposure. Furthermore, we explored a novel hearing-protective molecule against ROS stimulation.

Results

Nox4-TG mice had no abnormal phenotype without hearing. Overproduction of ROS was detected at the cochlea of the inner ear in NOX4-TG mice, but they showed normal hearing function under baseline conditions. Next, we exposed mice to intense noise at 110dB for 1 hour. Just after noise exposure (NE), hearing level of NOX4-TG mice and control mice were worsened to same level. Their hearing level recovered in time-course but hearing recovery of NOX4-TG mice at high-frequency was significantly less than control mice. And loss of cochlear outer hair cells (OHCs) at basal turn was significantly increased in NOX4-TG mice. The vulnerability to loss of hearing function and OHCs was rescued by treatment with the antioxidant Tempol. Additionally, we identified heat shock protein 47

(HSP47) as potential hearing protective molecule. We found increased protein levels of HSP47 with oxidative stress including H₂O₂ treatment and overexpression of NOX4. Furthermore, the up-regulated levels of Hsp47 were observed in both the cochlea and heart of NOX4-TG mice.

Conclusion

NOX4-TG mice are revealed that their hearing is normal under chronic ROS stimulation, but they have hearing vulnerability under acute stress including NE. And Hsp47 may be an endogenous antioxidant factor, compensating for the chronic ROS overexposure in vivo. We consider that NOX4-TG mice is valuable for investigation of hearing vulnerability related to ROS.

PS 205

Characterization of in-vivo rodent models of cisplatin-induced hearing loss - Acute and chronic administration paradigms

Natalia Tsivkovskaia; Rayne Fernandez; Claudia Fernandez; **Fabrice Piu**
¹Otonomy, Inc.

Background: Cisplatin is a potent chemotherapeutic agent that is widely used to treat a variety of cancers. In the U.S. alone, over 500,000 patients each year receive platinum-based chemotherapy. However, the administration of cisplatin is commonly associated with severe adverse effects including nephrotoxicity, peripheral neuropathy and ototoxicity. Cisplatin-induced ototoxicity, commonly referred to as cisplatin-induced hearing loss (CIHL), has a high prevalence manifesting as sensorineural hearing loss and tinnitus. The hearing loss is progressive, bilateral and irreversible. Importantly, in children, CIHL can severely affect speech, language development and socialization. The degree of hearing loss following cisplatin administration is largely a function of the dose and the clinical regimen. Simplistically, the larger the (cumulative) dose, the more severe the hearing loss. In an effort to address different clinical cisplatin treatment regimens, in-vivo rat models of acute and chronic cisplatin administration were developed.

Methods: Adult rats (Sprague-Dawley) served as subjects in these experiments.

Acute paradigm: animals received a single intraperitoneal infusion (over 30 min) of cisplatin at doses ranging from 9 to 15 mg/kg, and were monitored for up to 7 days

Chronic paradigm: animals received two different treatment regimens: a cycle of 4-6 injections of cisplatin at 5 mg/kg given over the course of 3 weeks, or a cycle of 6 injections of cisplatin at 3 mg/kg given over the course

of 3 weeks, followed by a 5-day recovery.

During the course of the studies, animal health, body weight and mortality were monitored and recorded. Hearing function was measured using ABR (auditory brainstem response) at various frequencies for the duration of the studies. Hair cell integrity was determined at termination via cytochrome c oxidase II (COX II) immunohistochemistry.

Results: Optimal doses of cisplatin were identified for both the acute and chronic administration paradigms. The ideal dosing regimen represented a balance between the preservation of the animal's health (minimal mortality, adequate health status) and the presence of significant hearing threshold shifts in the order of 50 dB at high frequencies. The observed hearing loss was associated with cochlear hair cell loss.

Conclusions: Reliable rat models of acute and chronic cisplatin-induced hearing loss were developed. These paradigms adequately reflect the various cisplatin chemotherapy regimens used in clinical settings. Studies are ongoing to determine the relative otoprotective effects of various therapeutic strategies in these models to address the potential clinical role for cisplatin otoprotection.

Outer & Middle Ear: Biology

PS 206

Establishment of Humanized Mouse Models for Studying Otitis Media

Kwang Pak¹; Chenliang Deng²; Kyung Wook Heo²; Arwa Kurabi¹

¹Department of Surgery / Otolaryngology, University of California, San Diego; San Diego VA Medical Center; ²UCSD;

Background: Otitis media (OM) is one of the largest public health problems in young children, and can have devastating impacts in developing countries. The substantial medical and human costs involved have led to research aimed at understanding this disease and improving treatment. Animal models of OM, long been used in research, have revealed substantial information about the basic immune, inflammatory and genetic mechanisms of OM. However, it is important to link animal studies to human immune and inflammatory responses. In recent years, "humanized" mice have become a valuable tool with which to study the human immune system in an animal model. Here we describe and evaluate their first use to model OM.

Methods: OM was induced by inoculation of nontypeable *Haemophilus influenzae* (NTHi) into the

middle ears (MEs) of NOD-Scid-IL2R_γ^{null}(NSG) mice that have previously been transplanted with human hematopoietic CD34⁺ cells. Blood and ear tissue were collected at different time points after OM induction. The human inflammatory cell mobilization was analyzed by flow cytometer, immunohistochemistry and RNA profile.

Results: The ME inflammatory response, leukocyte infiltration, tissue hyperplasia, bacterial clearance and OM recovery were comparable between humanized NSG (huNSG) and WT mice. At 10 days, all MEs of WT and huNSGs with >30% engraftment were culture-negative, indicating normal recovery from OM. In contrast, animals with

Conclusions: We demonstrate that huNSG mice with a sufficient degree of engraftment recapitulate a normal ME inflammatory response, including the recruitment of human immune cells, and exhibit normal recovery. Moreover, the ME mRNA profile of these animals showed the regulated expression of human-specific immune and inflammatory genes. This preclinical model will have a number of potential uses in OM research, including using hematopoietic stem cells from OM patients with differing degrees of OM susceptibility to understand the role of human immune responses in proneness to this disease.

PS 207

Middle Ear Cellular Responses to Infection

Allen F Ryan¹; Kwang Pak²; Nicholas J. Webster³; Arwa Kurabi¹

¹UCSD Surgery/Otolaryngology; ²Department of Surgery / Otolaryngology, University of California, San Diego; San Diego VA Medical Center; ³UCSD Medicine/Endocrinology

Background: During otitis media (OM), while the expression of thousands of genes is regulated in the middle ear (ME), much less is known about the transcriptional contributions of individual cell types.

Methods: To explore cellular responses during OM, we performed single-cell RNA-Seq of the ME before and after induction of bacterial OM. The 10X Chromium System generated single-cell transcriptomes of more than 20,000 ME cells. PCA-generated cell clusters were classified based on marker genes, and expression of genes known to be important in OM pathogenesis and recovery was assessed.

Results: In the normal ME, three independent samples resulted in 7-11 cell clusters/sample. Epithelial cells (expressing cytokeratins 18 and 19 and epcam) formed up to five different clusters. One expressed cytokeratin

14, a marker of basal epithelial cells. A second expressed ciliary as well as secretory genes. Other, closely-related epithelial clusters preferentially expressed muc1 and muc16. Up to three different stromal cell populations (expressing col1a2), differentially expressed the metalloproteinase genes adam33 or mmp13, or parathyroid hormone-like hormone (pHh). Up to three clusters of endothelial cells differentially expressed the TGF β receptor component Endoglin (eng), the hypoxia-induced regulator of G-protein signaling (rgs5) or the endothelial cell junction protein Cadherin 5 (cdh5). Two leukocyte clusters expressed the monocyte markers csf1r or the lymphocyte marker cd3d. A final cluster expressed the melanocyte gene mlana. At various time points after ME infection, in addition to the above cell types, large numbers of leukocytes were identified, including up to four classes of neutrophils and an additional class of monocytes. A small number of red blood cells were also present. Some ME cell types did not result in separate clusters. Macrophages, identified by itgam expression, and dendritic cells (itgax) were scattered through clusters of neutrophils and monocytes.

Conclusions: ME cells, previously recognized based on morphological criteria, were found to display considerable molecular heterogeneity that identifies previously unrecognized cell types. Genes defining differences in naïve ME cells offer new insights into ME homeostasis. Differences in transcriptional responses to infection identify unexpected cell contributions to the pathogenesis and resolution of OM. For example, the only ME cells expressing beta-defensin are cytokeratin 14-positive basal epithelial cells, with no expression in surface epithelial cells. The growth suppressor gene ecr4, often active in epithelia, is expressed primarily by stromal cells. Also, while the cytokine il1b is highly expressed by leukocytes during OM, il6 mRNA is produced only by stromal and endothelial cells.

PS 208

Evaluation of YAP Nuclear Translocation in a Rat Tympanic Membrane Under a Continuous Negative Pressure Load and in Human Middle Ear Cholesteatoma

Naotaro Akiyama¹; Tomomi Yamamoto-fukuda²; Masahiro Takahashi²; Mamoru Yoshiakwa³; Hiromi Kojima²

¹Department of Otorhinolaryngology, Toho University School of Medicine; Department of Otorhinolaryngology, Jikei University School of Medicine; ²Department of Otorhinolaryngology, Jikei University School of Medicine; ³Department of Otorhinolaryngology, Toho University School of Medicine

Background

Negative pressure in the middle ear is thought to be an important factor related in the acquired middle ear cholesteatoma formation. However, the correlation between negative pressure and the mechanism of cholesteatoma formation remains unclear. Yes-associated protein (YAP) is a primary sensor of mechanotransduction to induce cell proliferation, and we previously revealed the increase of YAP nuclear translocation in the rat thickened tympanic membrane (TM) under a negative-pressure load. Recently, it was found that cytoskeletal remodeling through integrin-linked kinase (ILK) activation induced YAP nuclear translocation. In this study, we investigated ILK and YAP expression patterns in the TM of the rat model and in the human middle ear cholesteatoma tissues immunohistochemically.

Methods

Four male adult rats were used and negative pressure in the middle ear was given through the supply route of a micro infusion pump continuously for five days. Animal care and experimental procedures were performed in accordance with the Guidelines for Animal Experimentation of Nagasaki University with the approval of the Institute of Animal Care and Use Committee (approval number is 1304301058). The study subjects of human samples were 20 ears with acquired Pars flaccida (PF)-type cholesteatoma, 5 ears with acquired Pars tensa (PT)-type cholesteatoma and 20 ears with congenital cholesteatoma. All patients were treated surgically at the Department of Otorhinolaryngology, Jikei University Hospital and the study protocol was approved by the Human Ethics Review Committee of Jikei University School of Medicine, and signed informed consent was obtained from all the patients for this study (approval number is 27-344 8229). An immunohistochemical analysis was performed using anti-ILK and anti-YAP antibodies.

Results

ILK overexpression and increase of YAP nuclear translocation were observed in epithelial cells in the thickened TM under a negative-pressure load and in the human acquired cholesteatoma tissues. Interestingly, YAP nuclear translocation was increased without ILK overexpression in the mesenchyme of those tissues. Neither ILK overexpression nor increase of YAP nuclear translocation was observed in the congenital cholesteatoma tissues.

Discussions and conclusions

In this study, it was suggested that mechanotransduction

might play an important role in the acquired cholesteatoma formation. However, YAP nuclear translocation in the mesenchyme was induced without ILK activation and it was also suggested that some other factors might be important in the mesenchyme. On the other hand, YAP nuclear translocation was not increased in the congenital cholesteatoma tissues. In conclusion, YAP could be a therapeutic target for the acquired middle ear cholesteatoma.

PS 209

Regulator of middle ear cholesteatoma formation: Neural crest derived cell under KGF initiation.

Tomomi Yamamoto-fukuda¹; Norifumi Tatsumi²; Naotaro Akiyama¹; Masataka Okabe²; Hiromi Kojima¹
¹Department of Otorhinolaryngology, Jikei University School of Medicine; ²Department of Anatomy, The Jikei University School of Medicine

Research background: Middle ear cholesteatoma is a gradually expanding destructive epithelial lesion within the middle ear, which leads to extensive tissue destruction in the temporal bone. □The expression of cellular and inflammatory pathways cytokines, keratinocyte growth factor, are important in the growth of middle ear cholesteatoma. In the previous study, we indicated that NC cell is an origin of middle ear cholesteatoma by using adult mouse genetics, Wnt1-Cre/Floxed-EGFP mice, that is conditionally expressing EGFP in the neural crest lineages. To analyze cell kinetics of neural crest lineages is need for establishing new therapy. Here we show for the first time the presence of a novel stem cell-like cell population in our animal model of middle ear cholesteatoma.

Methods: All experiments were performed in accordance with the guidelines of the local ethics committee of the Jikei University School of Medicine. Wnt1-Cre/Floxed-EGFP mice (Shimada K et al. 2012) were used in this study. Based on the role of KGF in the development of cholesteatoma, Flag-hKGF cDNA driven by CMV14 promoter was transfected through electroporation into the right ear 5 times on every fourth day (Yamamoto-fukuda T et al. 2015). Left ears transfected with empty vector were used as controls. After cholesteatoma formation was evaluated by otoendoscopy, Mu p75-saporin (SAP) or PBS was injected. At 7 days after mu p75-saporin injection, mice were sacrificed and temporal bones were removed en bloc. The paraffin sections of middle ear were used for H&E and immunohistochemical analysis.

Results: In the adult middle ear, the neural crest lineages construct almost all mesenchymal cells and a part of epithelial cells in middle ear. The MAPK cascade in KGF

signaling reprogrammed normal neural crest lineages express the neural crest marker p75 and become multipotent. Multipotent-neural crest lineages in middle ear expanded to form middle ear diseases, so called middle ear cholesteatoma. Injections of the immunotoxin Mu p75-saporin (SAP) induced depletion of p75 positive neural crest cells as results middle ear cholesteatoma were diminished in vivo.

Conclusions: These findings indicated that NC cell is an origin of middle ear cholesteatoma. The MAPK cascade in KGF signaling might be reprogrammed normal neural crest lineages express the neural crest marker p75 and become multipotent. To control p75 signaling synergizes with alternative pathways in promoting proliferation of neural crest cell may represent a new therapeutic target for middle ear diseases.

This study was supported by MEXT KAKENHI Grant Number JP16K11186.

PS 210

Downregulation of E-cadherin contributes to epithelial-mesenchymal transition and papillary invasion of epithelial cells in middle ear cholesteatoma.

Masahiro Takahashi¹; Tomomi Yamamoto-fukuda¹; Naotaro Akiyama²; Hiromi Kojima¹
¹Department of Otorhinolaryngology, Jikei University School of Medicine; ²Department of Otorhinolaryngology, Toho University School of Medicine; Department of Otorhinolaryngology, Jikei University School of Medicine

Introduction: Epithelial mesenchymal transition (EMT) is a process in which epithelial cells lose their cell polarity and intercellular adhesion and change into mesenchymal cells by obtaining migration and invasion ability. It is thought to have emerged in wound healing, tissue fibrosis, cancer invasion, metastasis and the like. So we hypothesized that EMT may be one of the key factors on the proliferation activities of epithelial cells in middle ear cholesteatoma. In this study, we compared the expression E-cadherin, and N-cadherin (EMT marker), claudin-1, claudin-4, occludin between acquired cholesteatoma, congenital cholesteatoma and normal skin.

Methods: The cholesteatoma specimens and used in this study were excised during surgeries on 112 patients and the normal skins were excised during surgeries on 30 patients in our department. All tissues were excised surgically at the Department of Otorhinolaryngology, Jikei University Hospital and the study protocol was

approved by the Human Ethics Review Committee of Jikei University School of Medicine, and signed informed consent was obtained from all the patients for this study (approval number is 27-344 8229). Immunohistochemical analyses of E-cadherin, N-cadherin, claudin-1, claudin-4 and occludin were performed.

Results: The expression of E-cadherin was positive in normal skin but negative or suppression in acquired and congenital cholesteatoma. The expression of N-cadherin was unclear in any group. The expression of claudin-1, claudin-4, occludin was not significant difference between acquired cholesteatoma, congenital cholesteatoma and normal skin.

Conclusion: In this study, the expression of E-cadherin was decreased in the basal and upper layer of middle ear cholesteatoma but the expression patterns of claudin-1, claudin-4, occludin were normal. These results indicated that during the epithelial growth process EMT was occurred at first and after normal differentiation might be induced in middle ear cholesteatoma. The downregulation of E-cadherin might be an important molecule in pathogenesis of middle ear cholesteatoma.

PS 211

Lacking BMP5 weaken BMP-induced Chondrogenesis Differentiation of Human Adipose-Derived Mesenchymal Stem Cells in Microtia

Huasong Zhang; Suijun Chen; Yiqing Zhen
Sun Yat-Sen Memorial Hospital of Sun Yat-Sen University

Background/Aims: The aim of this study was to investigate the expression level of bone morphogenetic protein (BMP) superfamily related proteins in residual auricle cartilage and the influence of BMP5 lacking mediated small mothers against decapentaplegic homolog (Smad) signaling pathways in Human adipose-derived mesenchymal stem cells (ADSCs) chondrogenic differentiation regulation. **Methods:** Immunohistochemical were employed to detect protein expressions of target genes in cartilage. ADSCs were cultured and assigned into 3 groups for transfection with BMP5-specificity siRNA. Quantitative real-time polymerase chain reaction (qRT-PCR), Western blotting and immunofluorescence were employed to detect mRNA and protein expressions of target genes. The condition of cartilage was measured by a series of staining methods. **Results:** BMP5, Smad1, Smad4 and collagen type II (Col2) protein expression was observed in the NP group. Col2 expression was observed in MP group, but significantly less than the NP group. However, BMP5, Smad1 and Smad4 were unobservable in

MP group. After induced differentiation, compared to the SI group, the corresponding target mRNAs were overexpressed in the ID groups, and overexpression of Smad1, Smad4, Col2 and aggrecan (ACAN) at the mRNA and protein expression was observed in the SI and ID groups. The mRNA expressions of ACAN and Col2, the glycosaminoglycan content of the extracellular matrix and the expression of ACAN and Col2 were higher in the ID groups than in the SI group. Cell Morphology tests demonstrated evident cartilage differentiation ability in the ID group. In comparison, the SI groups exhibited weaker cartilage differentiation abilities. **Conclusion:** BMP5 lacking weaken BMP-induced chondrogenesis differentiation of ADSCs, which provide a new possible mechanism for the development of microtia.

PS 212

Otopathologic analysis reveals structure changes of the lamina propria of human tympanic membranes with chronic perforations

Danielle R. Trakimas¹; Dhrumi Gandhi²; Erica Christenson³; Iman Ghanad⁴; Jeffrey T. Cheng⁵; Elliott D. Kozin²; Aaron K. Remenschneider⁶

¹*University of Massachusetts Medical School; Massachusetts Eye and Ear Infirmary; Department of Otolaryngology, Harvard Medical School;*

²*Massachusetts Eye and Ear Infirmary; Department of Otolaryngology, Harvard Medical School;* ³*University of Massachusetts Medical School;* ⁴*Mass Eye and Ear, Harvard Medical School;* ⁵*Eaton Peabody Laboratory, Massachusetts Eye and Ear Infirmary; Department of Otolaryngology, Harvard Medical School;* ⁶*Department of Otolaryngology, University of Massachusetts Medical School; Massachusetts Eye and Ear Infirmary; Department of Otolaryngology, Harvard Medical School*

Background: Thin radial and circular collagen fibers comprise the bilayer structure of the tympanic membrane (TM) lamina propria (LP) and impart important structural and acoustic properties. Studies have elucidated a distinct pattern of collagen fibers within the LP of healthy human TMs, with a majority of type II collagen within the outer radial layer and a majority of type III collagen within the inner circular layer. Little is known; however, of how chronic perforations influence the collagen fiber type and arrangement within and overall structure of the remnant TM. We hypothesize perforated TMs will show loss of native LP architecture.

Methods: TMs with chronic perforations were removed en-bloc during total TM replacement surgery. Healthy TMs taken as part of translabyrinthine surgery served as controls. TMs were embedded in paraffin and stained

with haematoxylin-eosin or processed for collagen type II and III immunostaining. All slides were analyzed by light microscopy to assess LP structure and thickness, degree of inflammation, and relative ratio and arrangement of collagen types.

Results: Four patients with chronic perforations (>2yrs) from inactive otitis media (OM) were identified. Two were male and mean age at surgery was 52±10 yr. The TM LP was identified in all perforated cases and showed areas with loss of the bilayer structure (n=4), intralaminar tympanosclerosis (n=2) and mucosal metaplasia (n=1). An increased quantity of loose collagen fibers was qualitatively observed (n=4). All cases showed significant thickening of the LP (on serial section measurements) compared to control (532±281µm vs 90±29µm, p<0.001). Chronic inflammation as identified by lymphocytic infiltration was seen in all perforated specimens, but was absent in the controls.

Conclusions: Chronically perforated TMs from OM demonstrate thickening and structural loss of the bilayer LP, as well as chronic inflammation. These specimens also demonstrated distinct collagen fiber arrangement in comparison to control TMs. Results have implications for pathophysiology of failed tympanoplasty procedures.

PS 213

Lineage Tracing and Time-lapse Imaging Reveal Dynamics of Murine Tympanic Membrane Keratinocytes

Stacey Frumm¹; Joseph Chang¹; Jordan Briscoe²; Aaron Tward¹

¹UCSF Department of Otolaryngology-Head and Neck Surgery; ²UCSF Biological Imaging Development Center

Background: The tympanic membrane (TM) transmits sound from the external auditory canal (EAC) to the middle ear. Its lateral layer is epidermis continuous with that of the EAC. Previous work described behaviors of TM keratinocytes: they proliferate in anatomically restricted regions proximal to the malleus and annulus and migrate outward to join the EAC epidermis. It is not until the outer cartilaginous canal that keratinocytes slough off and mix with glandular secretions to form cerumen. The migration over the TM and canal cleans the outer ear of cellular and exogenous debris. The studies herein aimed to increase understanding of the behavior of TM keratinocytes in mice.

Methods: Three primary techniques were utilized. First, mice were exposed to EdU for three weeks to study tissue turnover, followed by a four-week chase to look for label-

retaining cells. Second, the murine Cre-reporter line R26R-Confetti, which includes four fluorescent proteins (RFP, YFP, CFP, GFP), was crossed with two Cre-driver lines, K5-CreERT2 and Ki67-CreERT2, to assess clonal architecture. The majority of TM keratinocytes express keratin 5 (K5), while Ki67 is restricted to proliferating cells. So, the emergence of general clonal architecture in densely labeled TMs was assessed in K5-CreERT2;confetti mice, and independent clones were observed with sparse labeling in Ki67-CreERT2;confetti mice. Third, keratinocyte migration was evaluated with time-lapse imaging of fluorescent TMs maintained in ex vivo culture for up to 24 hours.

Results: The EdU studies corroborated previous reports of proliferation restricted to areas near the malleus and annulus. Further, all TM keratinocytes incorporated the EdU in approximately three weeks, and no label retention was observed proximal to the malleus following a four-week chase. In the lineage tracing studies, radial streaks of color were hypothesized based on prior work describing radial migration of keratinocytes, but this architecture was not observed. In K5-CreERT2;confetti mice, large blocks of keratinocytes of a single color developed over two to six months, likely due to neutral drift. In Ki67-CreERT2;confetti mice, cells were not contiguous in single clones observed at one to four weeks. Lastly, in the time-lapse imaging studies, pars tensa cells had greater displacement than pars flaccida cells. On the pars tensa, the general direction of movement was from the malleus to the annulus, with a large contribution of superior-to-inferior migration.

Conclusions: Overall, these studies describe the basic dynamics of murine TM keratinocytes and lay the foundation for future studies of TM homeostasis and pathology.

PS 214

Expression of Metalloproteinases in otitis media with effusion in children with atrophy of the eardrum

Lylou Casteil Baume^{1,2,3}, Corentin Affortit^{1,2}, Jean-Luc Puel^{1,2}, Frederic Venail^{1,2,3}, Jing Wang^{1,2} and Michel Mondain^{1,2,3}

¹INSERM - UMR 1051, Institut des Neurosciences de Montpellier; ²Université de Montpellier; ³CHRU Montpellier - Centre Hospitalier Régional Universitaire

Background - Introduction

Otitis media with effusion (OME) is a common childhood disease defined as the presence of liquid in the middle ear without signs or symptoms of acute ear infection. It has been reported that OME can lead to tympanosclerosis or tympanic membrane (TM) atrophy. Metalloproteinases

(MMPs) are a family of zinc-dependent endopeptidases. Their main role is degradation of the extracellular matrix such as collagen included in the TM. The aim of this study was to determine the relationship between activity of MMPs and TM atrophy.

Methods

30 middle ear effusions were collected from patients aged 15 months to 10 years with atrophic TM (11) or non atrophic TM (19). Effusions were collected after tympanotomy during insertion of ventilation tube, and divided into the different groups (mucous, serous and hemorrhagic) according to color and viscosity. ELISA tests have been performed to measure the concentration of MMPs and TIMP-2. Student t-test have been used for statistical analysis.

Results

We found that the average concentration of MMP-2 in effusions with atrophy of the TM was higher than in those without TM atrophy (0.6 ng/mg and 0.5 ng/mg of total protein in effusions with TM atrophy and without TM atrophy, respectively). In addition, the ratio of MMP-2/TIMP-2 was significantly higher in subjects with atrophy ($p=0.034$). Finally, significant higher level of MMPs and TIMP-2 was observed in thick effusion ($p=0.025$).

Conclusion

Our results suggests that activity of MMP-2 could play an important role in the destruction of the eardrum in OME.'

PS 215

Histomorphometric Observations Suggesting the Development of Mastoid Sclerosis

Simona Padurariu¹; Christof Röösl²; Rasmus Røge³; Mogens Vyberg³; Allan Stensballe⁴; Alex Huber²; Michael Gaihede⁵

¹Department of Otolaryngology, Head & Neck Surgery, Aalborg University Hospital (1), and Department of Clinical Medicine, The Faculty of Medicine, Aalborg University (2), Denmark; ²Department of Otorhinolaryngology Head & Neck Surgery, University Hospital Zürich, University of Zurich, Switzerland; ³Institute of Pathology, Aalborg University Hospital (1), and Department of Clinical Medicine, The Faculty of Medicine, Aalborg University (2), Denmark; ⁴Department of Health Science and Technology, Aalborg University, Denmark; ⁵Department of Otolaryngology, Head & Neck Surgery and Audiology, Aalborg University Hospital, Aalborg (1); Department of Clinical Medicine, The Faculty of Medicine, Aalborg University, Aalborg (2), Denmark

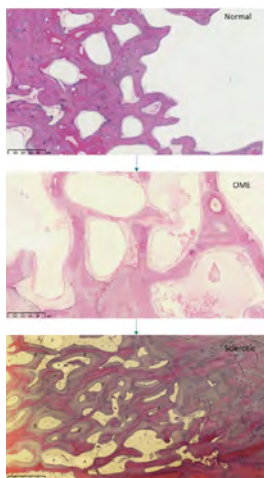
Background. Mastoid pneumatization describes the

normal development of the middle ear (ME) into a series of multiple connected air filled cells behind the tympanum and external ear canal. This structural arrangement increases both the air volume as well as mucosal surface area of the entire ME, and it may bear important functional properties related to its pressure regulation. In cases with chronic otitis media, the mastoid can be subject to a decreasing pneumatization leading to sclerosis, where the normal air cells disappear. While the events behind this process are unknown, it may have important functional implications. We present here a series of morphological observations in human ME's that may represent stages towards mastoid sclerosis.

Materials and methods. The study comprised of a temporal bone archive material with histological preparations of whole-mount ME's. The study group included two normal ME's, eight cases with focal remnants of otitis media with effusion (OME group), and two cases with pronounced sclerosis (sclerosis group). Histological characteristics were described for each group as well as an automatic image analysis was applied for quantitative assessment of the area ratio of air space, bone, and mucosa.

Results. The histological changes included occasional fluid in the air cells, mucosal hypertrophy, soft tissue invasion of the air cells, polyps and granulation tissue as well as mucosal adhesions. Together with these inflammatory changes we also found areas of new bone formation. The average area ratio of air space, bone and mucosa in the normal group were 52%, 39%, and 9% laterally, and 52% 36%, and 12% medially; in the OME group 50%, 31%, and 20% laterally, and 50%, 33%, and 18% medially. In the sclerosis group the air space was almost entirely replaced by connective or fat tissue and an increased bone content; the bone ratios were 75% laterally and 59% medially (Figure).

Conclusions. Distinct focal inflammatory changes were found in the mastoid accompanied by areas of new bone formation. In the OME group, mucosa including soft tissue expansions and adhesions increased, while in the sclerosis group the mucosa and air space disappeared completely replaced by increasing amounts of connective tissue, fat and bone; the bone ratio doubled in the sclerotic group, and the lateral mastoid was found more sclerotic than the medial. Thus, mastoid sclerosis seems to be linked to inflammatory changes, which may result in extensive structural degeneration including loss of its normal pneumatization and its functional properties.



PS 216

Laser-induced Collagen Remodeling within the Tympanic Membrane

Sophie A. L. Schacht; Patricia Stahn; Marius Hinsberger; Bernhard Schick; Gentiana I. Wenzel
University of Saarland

Repeated pathologies of the tympanic membrane (TM) can permanently decrease its tension inducing conductive hearing loss and adhesive processes up to cholesteatoma. The current main therapy is its surgical reconstruction. Even though lasers have been proposed to tighten atrophic TM's already by Kurokawa and Goode (1995), details of this effect, especially histological analysis are missing.

We therefore used laser pulses to induce TM-collagen remodeling in an animal model and be able to compare the histological and electrophysiological effects of different applied laser intensities before entering clinical studies. We irradiated Fuchsin-stained areas of the TM in anesthetized mice with 532nm laser-pulses of 10mW, 25mW or 50mW monitoring hearing with auditory brainstem responses (ABR). The mice were sacrificed after 2-8 weeks and histologically analyzed.

An increase in the tympanic membrane thickness within the defined, stained and irradiated areas could be observed after 4 weeks. Polarized light microscopy and transmission electron microscopy demonstrated the tissue volume increase majorly due to new collagen-fibrils. Directly after irradiation ABR-thresholds did not increase.

We herein demonstrate that a controlled laser-induced collagen remodeling within defined areas of the TM is possible. This novel method might be a prophylactic solution for chronic inflammatory ear pathologies related to decreased TM-tension.

PS 217

Extended Release Cipro-Dex Hydrogel for Middle Ear Infection

Erik Pierstorff; Matthew Ku; William Slattery
O-Ray Pharma

Otitis media (OM) is one of the most common diseases of childhood. OM and associated otorrhea is a common complication of myringotomy with tympanostomy tube (ear tube, TT) insertion, the most common operation performed on children in the United States. Prevention or treatment of otorrhea in the postoperative period is important to improve the child's hearing and to treat/prevent persistent drainage. Strategies to reduce the occurrence of early postoperative otorrhea include the use of topical antibiotic (drops or gels) or antibiotic/steroid drops during surgery or during the early postoperative period. Antibiotics (i.e. ciprofloxacin) have been shown to reduce early OM/otorrhea in trials when compared to no treatment and the use of an antibiotic/anti-inflammatory combination product (i.e. ciprofloxacin/dexamethasone drops) was shown to be even more effective than antibiotics alone. Both cure rates and elimination of infection were significantly higher and fewer treatment failures were observed in the ciprofloxacin/dexamethasone group. Unfortunately, the administration of drops into the middle ear of children can be very difficult and patient compliance can be a challenge. A ciprofloxacin/dexamethasone hydrogel formulation is being developed here as an enhancement on hydrogels containing ciprofloxacin alone. In this study, a novel combination drug/hydrogel formulation was developed for the treatment of OM/otorrhea. This hydrogel releases both ciprofloxacin and dexamethasone over a 2-3 week period. Initial characterization and safety of the formulation was tested. Drug release was monitored in vitro to validate release over the desired timeframe. The activity of both drugs was monitored through the duration of release to confirm retention of full activity over the release period. The activity of eluted ciprofloxacin was tested using the Broth Microdilution Method for susceptibility testing against *Haemophilus influenzae* according to NCCLS guidelines. The activity of eluted dexamethasone was tested by monitoring its suppression of lipopolysaccharide mediated inflammation of RAW 264.7 cells via real time PCR. Lastly, the safety of the combination hydrogel and its inactive components was assessed via in vivo otic toxicity studies in guinea pigs, including hearing tests, gross microscopy and cytochrome analysis. These studies lay the groundwork for extended release middle ear hydrogel formulations that are capable to safely release combinations of active pharmaceutical agents over a desired duration. The Cipro-Dex formulation developed here should offer significant advantages over current treatments of OM/otorrhea that are in use in the clinic.

Grant Support from the National Institute on Deafness and Other Communication Disorders #R44DC014416

The Role of Neutrophils in *Pseudomonas aeruginosa* Chronic Suppurative Otitis Media

Kelly Khomtchouk; Ali Kouhi; Anping Xia; Peter Santa Maria
Stanford University School of Medicine

Chronic suppurative otitis media is a persistently discharging tympanic membrane perforation in the middle ear, producing hearing loss in more than 50% of cases. According to the World Health Organization, up to 330 million individuals suffer from associated hearing loss due to this infection, making this the most common cause of permanent hearing loss among children in developing countries. Recent work in our lab currently led to the creation of the first murine model for chronic suppurative otitis media (CSOM) to study the pathogenesis of this disease.

Chronic suppurative otitis media is largely due to biofilm-forming bacteria, of which *Pseudomonas aeruginosa* is a common pathogen. Neutrophils are well-known to have various contributions in both promoting and restricting bacterial growth in other biofilm-mediated diseases, as they are the first cells recruited to sites of infection. Herein we propose that 1) fluorescent *P. aeruginosa* develop into biofilms and form chronic infections in the middle ear of a mouse model of Eustachian tube obstruction and acute tympanic membrane wounds; 2) this biofilm reduces functional capacity and recruitment of professional phagocytes; 3) biofilm initiates apoptosis of responding neutrophils; and 4) neutrophils drive disease post-inoculation. We also determine neutrophil subsets with a leading role in the establishment of bacterial biofilm-mediated disease, and test the capacity of polymorphonuclear leukocytes to suppress initial infection.

Neutrophil function is quantified as a measure of phagocytosis and the production of extracellular traps; we also measure cell survival and clearance via efferocytosis to determine host-mediated barriers to this recalcitrant infection. Using novel methods in flow cytometry coupled with fluorescent-tagged *P. aeruginosa*, we are able to assess middle ear effusion post-inoculation and develop a timeline of response to acute and chronic infection in our CSOM model.

Importantly, this study establishes a model system for further translational studies, including testing of topical therapeutics. The results of this work will also inform potential efforts of neutrophils as predictors for disease exacerbation and guide additional therapeutic development for an illness affecting millions of children globally.

Positive and negative signalling pathways and new therapeutic targets in the pathogenesis of otitis media

Jian-Dong Li

Institute for Biomedical Sciences, Georgia State University

Uncontrolled inflammatory and immune response is a hallmark of otitis media (OM). Although appropriate inflammation and immune response is critical for eradicating pathogens, excessive inflammation often results in middle ear immunopathology and conductive hearing loss. Thus, inflammation and immune response must be tightly controlled. However, how inflammation is tightly regulated in OM remains largely unknown. There is currently an urgent need for understanding the molecular mechanisms underlying tight regulation of inflammation and immune response in OM pathogenesis and identifying novel therapeutic targets. Among various mechanisms underlying tight regulation of inflammation, both positive and negative feedback regulators are thought to play a critical role in controlling overactive innate immune and inflammatory response. Using multiple experimental approaches including knock-out (KO) mice, we have identified deubiquitinase CYLD (cylindromatosis) as a key negative feedback regulator for inflammation induced by nontypeable *Haemophilus influenzae* (NTHi), a major bacterial pathogen for OM. In particular, CYLD negatively regulates NTHi-induced inflammation by specifically suppressing lysine K63-linked non-proteolytic ubiquitination of MyD88. In addition, IL-1 receptor-associated kinase M (IRAK-M) also plays an important role in negatively regulating NTHi-induced inflammation. Moreover, we found that MyD88 short (MyD88s) also acts as a negative regulator for NTHi-induced inflammation. Finally, we further explored the therapeutic potential of up-regulating the expression of negative regulators using pharmacological approaches. Interestingly, phosphodiesterase 4 (PDE4) inhibitor Roflumilast, a recently approved drug for COPD, suppresses NTHi-induced inflammation in a CYLD-dependent manner. In addition, host innate immune defense response has also been found to be dysregulated in otitis media. Together, our studies bring new insights into our understanding on tight regulation of inflammation and innate immune response and may help identify novel therapeutic targets for treating otitis media.

PS 220

Height of the Jugular Bulb is Unrelated to Mastoid Size

N. Wendell Todd

Emory

Background: Height of the jugular bulb is quite variable, and contributes to clinical challenges.

Objective: Describe the height of the jugular bulb relative the tympanic annulus, the inferior most portion of the basal turn of the cochlea, and the confluence with the sigmoid sinus. Prior reports have not involved exact positioning.

Methods: Ten clinically ear-normal crania underwent computed tomography in a custom non-metallic positioning device that referenced the Frankfort horizontal plane. The crania, from a series of 41, were the five with the largest mastoids, and the five with the smallest mastoids, as assessed by plain lateral radiograph.

Results: Most apices of jugular bulbs were above the level of the tympanic annulus. The jugular bulb was typically higher in right than left ears. Mastoid size did not associate with height of jugular bulbs.

Conclusion: Regardless of how height of the jugular bulb was expressed, mastoid size did not correlate.

Psychoacoustics: Some Current Trends

PS 221

Absolute Pitch Perception for Challenging Notes Relates to Cognitive, Linguistic, and Musical Factors

Stephen C. Van Hedger¹; Howard C. Nusbaum²

¹Brain and Mind Institute, Western University;

²Department of Psychology, The University of Chicago

Background: Individuals with absolute pitch (AP) can categorize an isolated musical note with near perfect accuracy without an external reference note. This definition implies a uniformity of performance across people; however, AP may only appear uniform because it is generally tested with familiar instruments and octave ranges. In the present study, we assess whether AP possessors'; accuracy for identifying isolated notes is more distributed when judging challenging instrumental timbres and octaves, as well as whether variability in note categorization could be explained by individual differences in musical expertise, language background, or working memory.

Method: Thirty-seven self-identified AP possessors completed the study. Participants first completed a standard test of AP ability - consisting of piano and guitar notes - in which an isolated note had to be classified into one of twelve Western note categories. Following this standard AP test, participants were presented with instrumental timbres that were hypothesized to pose a perceptual challenge to classification. These included sine wave notes, timpani notes, bell notes, and thumb piano notes. No feedback was provided at any time. Participants also completed an auditory n-back task as a measure of working memory and an extensive musical questionnaire.

Results: In the standard test of AP, all participants performed virtually perfectly. When tested on the challenging notes, performance was normally distributed. In exploratory analyses, we found (1) lower accuracy among participants who speak a tonal language, (2) less musical expertise among tonal language participants, and (3) a positive relationship between working memory and note performance among tonal language participants that was not present for non-tonal language participants.

Conclusion: Although individual differences in AP possessors has been observed for some time, there is a tendency to treat AP listeners as homogeneous largely due to ceiling effects on standard measures of note identification. The present results suggest that these differences in note categorization, even among AP possessors, are informative about the basic cognitive and perceptual mechanisms that support absolute pitch representations. The observation that working memory may be important in AP categorization under challenging listening conditions is consistent with recent theoretical accounts of how working memory and expertise relate to auditory recognition in other domains, such as speech.

PS 222

The biological and cultural basis of rhythmic representations: a global survey of rhythm priors

Nori Jacoby¹; Josh H. McDermott²

¹Columbia University; ²Massachusetts Institute of Technology

Recent cross-cultural comparative work has made various claims about the universality of aspects of music, aesthetic preferences, and emotion (Fritz 2009, Brown & Jordania 2013, Savage et al. 2015). However, recent experimental work suggests that features that were previously regarded as universal—such as consonance / dissonance, or rhythm perception— may in fact be strongly influenced by culture (McDermott et al. 2016; Jacoby & McDermott 2017). To more comprehensively

explore these influences we initiated the Global Survey of Rhythm Representation, a multicultural collaborative project that aims to measure cross-cultural variation in the perception of simple rhythms. In previous work (Jacoby & McDermott 2017) we developed a method to estimate priors for simple rhythms via iterated reproduction of random temporal sequences. Listeners were asked to reproduce random “seed” rhythms; their reproductions were fed back as the stimulus and over time became dominated by internal biases, such that the prior could be estimated from the distribution of reproductions. Priors in US participants measured in this way show peaks at rhythms with simple integer ratios, consistent with the importance of these rhythms in Western music. Because the paradigm requires little verbal description, it can be applied irrespective of the participant’s musical or cultural background. We ran the paradigm in a large set of cultures spanning a wide range of geographic and demographic conditions as well as linguistic and musical traditions. Using a network of over 30 collaborators, data has thus far been collected from over 700 participants hailing from Botswana, Bolivia, Brazil, Bulgaria, China, India, Japan, Mali, Turkey, Uruguay, South Korea, the United Kingdom, and the United States. All tested groups showed priors that significantly overlap with integer ratio rhythms, supporting the idea that integer ratios are universal. However three groups in Mali and Uruguay showed prominent peaks in relatively complex integer ratios (ratio that are described with large numbers such as 2:3:7 or 3:4:9) challenging previous explanations for rhythm perception based on neural resonance. In addition, the magnitude and relative importance of the different integer ratio categories varied significantly from culture to culture, driven mainly by passive musical exposure rather than language or demography. The results illustrate the biological and cultural factors that determine the perception and production of rhythm.

PS 223

Physiological and Psychoacoustical Measures of Two Different Auditory Efferent Systems

William B. Salloom¹; Hari Bharadwaj²; Elizabeth A. Strickland¹

¹*Speech, Language, and Hearing Sciences, Purdue University*; ²*Speech, Language, & Hearing Sciences, and Weldon School of Biomedical Engineering, Purdue University*

Background:

The human auditory pathway has two efferent systems that can dynamically adjust our ears to incoming sound at the periphery. One system, known as the medial olivocochlear reflex (MOCR), can decrease amplification

of sound by the outer hair cells in the cochlea. A second system, known as the middle-ear muscle reflex (MEMR), causes contraction of the muscles in the middle-ear in response to loud sound, and decreases transmission of energy to the cochlea. Because both efferent systems are activated by sound, separating MOCR effects from MEMR effects is important to understand their effects on perception and on physiological measures such as otoacoustic emissions. The MOCR seems to affect multiple frequencies and turn down the gain in the system at lower sound levels, whereas the MEMR has been thought to activate at higher sound levels and be biased towards low frequencies. However, it hasn’t been carefully considered that the MEMR may be activated at lower sound levels, and affect higher frequencies. This may have important implications for auditory perception, especially as both systems may be active at the same time. In the current study, characterization of the strength, laterality, and frequency specificity of MOCR and MEMR is measured both physiologically and behaviorally in normal-hearing humans.

Methods:

The effects of a pink broadband noise precursor on wideband acoustic immittance, transient-evoked otoacoustic emissions (TEOAEs), and behavioral measures were made as a function of precursor level and laterality (ipsilateral, contralateral, or bilateral) in normal-hearing humans. Wideband acoustic immittance measurements were used to measure MEMR activation across the frequency range (0.2 - 8 kHz). TEOAEs were also measured to estimate MOCR and MEMR strength across the frequency range (0.2 – 5 kHz). Lastly, a psychoacoustic forward-masking paradigm was used to measure the effects of the precursor on masking by on- and off-frequency maskers at 1, 2, and 4 kHz. Gain reduction is thought to be indicated by a relatively larger shift for the off-frequency masked threshold than for the on-frequency one.

Results/conclusions:

The effects of the precursor on behavioral thresholds, TEOAEs, and wideband acoustic immittance tasks will be compared as a function of precursor level. The goal is to determine what frequency ranges are affected by each reflex, at what elicitor levels, and how this is reflected in perception.

Acknowledgements:

Research supported by funding from NIH(NIDCD) RO1 DC008327

Effects of listener response bias and temporal uncertainty for observer-based threshold estimation

Lori Leibold¹; Emily Buss²

¹Boys Town National Research Hospital; ²University of North Carolina at Chapel Hill

Introduction: Several observer-based procedures have been developed to assess auditory behavior in infants using efficient adaptive tracking algorithms. These procedures are feasible and reliable, but the influence of procedural modifications made to accommodate infant testing is not fully understood. For example, while the observer sitting outside the booth receives real-time information regarding the timing of observation intervals, those intervals are undefined for the listener inside the booth. Thus, listener response bias and/or signal-temporal uncertainty may influence threshold estimates obtained using these procedures. The purpose of the present study was to evaluate the effect of both factors by comparing threshold estimates obtained from adults using single-interval, yes/no (Y/N) and two-interval, forced-choice (2IFC) procedures. Trials were initiated and judged by the observer (observer-response), or by the listener (listener-response).

Methods: Listeners were 11 adults (19-34 years) with normal hearing. Detection thresholds corresponding to 71% correct were estimated adaptively for two stimuli: a 1000-Hz FM tone presented in quiet and a spondee word (playground) presented in continuous, 60-dB-SPL two-talker speech. There were four test procedures: (1) observer-response Y/N; (2) listener-response Y/N; (3) observer-response 2IFC; and (4) listener-response 2IFC. For all four test procedures, the level of target was adaptively varied to estimate the detection threshold. Listening intervals were temporally uncertain from the perspective of the listener in both observer-response procedures.

Results: Overall, thresholds were higher for the observer-response than the corresponding listener-response procedures. For FM tone detection in quiet, thresholds differed by 5.7 dB (Y/N) and 6.3 dB (2IFC). For word detection in a two-talker masker, those differences were 10.2 dB (Y/N) and 7.7 dB (2IFC).

Conclusions: The current results provide evidence that both response bias and signal-temporal uncertainty influence estimates of auditory sensitivity obtained using observer-based procedures. Further, the magnitude of these effects is stimulus dependent.

Learning Interference from Sequential but Not Interleaved Training on Two Perceptual Tasks: Evidence That Anterograde Learning Interference Arises from an Interaction of Tasks in Different Learning Stages

Ruijing Ning; Beverly A. Wright

Northwestern University

Perceptual skills improve with practice, providing a means to treat perceptual disorders and to enhance normal perceptual abilities. However, learning on one perceptual task can be disrupted by training on another. A greater understanding of this interference could lead to more optimal training strategies. We recently observed that training on interaural-time-difference (ITD) discrimination disrupted improvement on interaural-level-difference (ILD) discrimination in the anterograde [ITD-ILD] but not retrograde [ILD-ITD] direction. The specificity of this interference to the anterograde case suggests that the interference occurs during the earliest stage of learning on ILD, the encoding stage. Here, we tested the hypothesis that such anterograde interference occurs because an influence of training on the first task lingers in the encoding stage, altering the encoding of the second task. If anterograde interference occurs simply because of a non-beneficial mixture of the two tasks in the encoding stage, then alternating training between the two tasks, while both are still clearly being encoded, should also disrupt the learning. To test this prediction, we examined learning on ILD (two-interval-forced-choice; standard: 4 kHz, 0 dB ILD) between a training session and a testing session the next day. Four groups of young, normal-hearing adults were trained with different regimens: 1) 300 trials of ILD, 2) 300 trials of ILD preceded by 300 trials of an interaural-time-difference discrimination task (ITD) (standard: 0.5 kHz, 0 microsecond ITD), and 3) 300 trials of ILD and 300 trials of ITD alternating every 60 trials. Practicing only ILD generated learning on ILD. This learning was disrupted when practice on ITD was completed before practicing ILD (anterograde interference), but not when practice alternated between ILD and ITD every 60 trials. These results suggest that the anterograde interference of training on ITD on learning of ILD does not occur simply because the influence of the ITD training lingers in the encoding stage. Rather, it appears that the training on ITD must enter a different learning stage, namely consolidation, by sufficient training, before it becomes disruptive to the encoding of ILD. The implication is that the initially encoded form of ITD learning is modified during consolidation into another form and it is this consolidated form that is disruptive to learning on ILD.

Relationship Among Selective Inner Hair Cell Loss, Auditory Brainstem Response Amplitudes, Distortion Product Otoacoustic Emissions and Gap Detection in Carboplatin Treated Chinchillas

Celia Escabi; Eliza Granade; Christina Campbell; Edward Lobarinas
University of Texas at Dallas

Abstract: In previous experiments we showed that moderate to severe selective inner hair cell (IHC) loss had minimal effect on hearing thresholds but increased thresholds in competing background noise. In follow-up experiments we evaluated gap detection to evaluate whether this task was more sensitive to IHC loss. Gap detection has been used as an indirect index of auditory temporal resolution. Our earlier results showed a significant increase in gap detection thresholds using a broadband noise carrier (40-70 dB). Here we sought to evaluate whether these deficits were frequency specific and whether a higher intensity carrier had any effect on gap detection thresholds. Our hypothesis was that if poorer gap thresholds were found at specific frequencies, this could suggest the presence of tinnitus whereas poorer gap detection at multiple frequencies were likely to represent an overall deficit in performing the task. Auditory brainstem responses (ABRs) and distortion product otoacoustic emissions (DPOAEs) were evaluated to assay the status of normal cochlear nonlinearity and to provide an objective measure of overall hearing thresholds.

Methods: Free feeding, young adult chinchillas (1-3 years-of-age), housed in an enriched environment, were trained on a shock avoidance task described in previous publications as part of a larger study aimed at assessing a variety of functional hearing changes associated with selective IHC loss. Gap detection thresholds were assessed with narrowband noise carriers centered at 1, 2, 4, 8, and 12 kHz with an overall intensity of 60 or 80 dB SPL. Pre and post ABR and DPOAE measures were obtained using a commercially available clinical system. Following baseline measures, animals were treated with a single dose of 75 mg/kg of carboplatin (i.p.), a dose reliably shown to produce 50-80% IHC loss with no outer hair cell (OHC) loss. Post-carboplatin assessments were performed three weeks post-treatment.

Results and Conclusions: Carboplatin treatment had no effect on DPOAEs, suggesting both survival and function of OHCs. ABRs were characterized by relatively low thresholds, reduced wave I amplitudes and poorer morphology. Gap detection thresholds showed significant increases post-carboplatin, particularly at the higher 80 dB SPL presentation. The overall findings suggest that a

gap detection task may be substantially more sensitive to IHC loss, even when the presentation level is high. The observed results demonstrate substantial suprathreshold deficits even in the presence of near normal thresholds and normal cochlear non-linearity. The overall findings highlight the importance of suprathreshold testing in assessing cochlear status.

PS 227

Objective Quantification of Musical Features: A Python Algorithm for the Analysis of Music

Lucas Hahn¹; Charles J. Limb²

¹Columbia University; ²Dept of Otolaryngology-Head and Neck Surgery, University of California, San Francisco

Although the experience of listening to music is subjective, objective features in musical stimuli constitute the basis for this subjective experience. Ultimately, characterization of these objective differences may provide an important basis with which to quantify musical material such that comparisons may be made that do not rest entirely on individual subjectivity. In this study, we used the Python programming language to design an analysis tool that quantitatively examines music through the framework of music theory. We hypothesized that this analysis would reveal measurable differences between musical performances by expert/novice musicians, and also by genre. We developed algorithms to parse "musicxml" files and perform a wide array of rhythmic, pitch, and harmonic analysis. We compared pieces of music from jazz (performed by experts), to commercial pop music (genre analysis) and to novice musicians (expertise analysis). Jazz and popular music selections were chosen based on popularity and diversity of style within their genre; beginner improvisations were randomly selected among available performances on YouTube. Our analysis examined rhythmic features (rest percentage, note duration distribution, dissonant note distribution), pitch features (number of each pitch, interval jumps, chromatic range, interval distribution), and harmony features (scale degree distribution, non-tonic note percentage, number of dissonant notes, dissonant note percentage). Our results showed significant differences by T-Test for the genre and expertise analyses. Significant differences in the genre analysis were in rest percentage (23.4% jazz vs. 6.9% pop, $p=0.001$), dissonant note percentage (14.1% jazz vs. 2.5% pop, $p=0.014$), non-tonic percentage (83.7% jazz vs. 69.1% pop, $p=0.027$), and dissonant note scale degree (3.47 SD jazz vs. 1.92 SD pop, $p=0.001$). No significant pitch differences were observable, indicating homogeneity between the genres in that category. Expert musicians showed significant

differences in comparison to novice musicians, particularly for dissonant note duration (0.245 SD expert vs. 0.100 SD novice, $p=0.047$), note duration (0.306 SD expert vs. 0.475 SD novice, $p=0.034$), dissonant scale degree (347 SD expert vs. 2.20 SD novice, $p=0.010$), and chromatic range (32.2 semitones expert vs. 15.5 semitones novice, $p=0.032$). These results demonstrate the potential utility of objective characterization of musical features to provide insight into subjective appraisal of music, identify differences in musical skill or style between musicians, or even differentiate between multiple performances by a single musician. This quantitative approach may help answer the elusive question as to why one piece of music or musical performance may be regarded as “better” than another.

PS 228

Individual Differences and Cross-cultural Variation in Pitch Perception Revealed by Sung Reproduction

Nori Jacoby¹; Eduardo Undurraga²; Malinda J. McPherson³; Joachin Valdez⁴; Tomas Ossandon⁴; Josh H. McDermott⁵

¹Columbia University; ²School of Government, Pontificia Universidad Católica de Chile; ³Harvard Medical School; ⁴Facultad de Medicina, Pontificia Universidad Católica de Chile; ⁵Massachusetts Institute of Technology

Musical pitch perception is argued to result from nonmusical biological constraints, and thus to have similar characteristics across cultures, but its universality has yet to be tested. One feature that has long been regarded as universal is octave equivalence. While Western music typically regards pitches an octave apart as musically equivalent, experimental evidence for octave equivalence in non-musicians is weak. We developed a novel paradigm to probe octave equivalence in non-musicians based on sung reproduction of short melodies presented in different frequency ranges. Most participants accurately replicated heard melodic intervals on a logarithmic scale, even for tones outside the singing range. However, only some participants reproduced the position of heard tones within the octave with the “correct” note chroma (A, B, etc.), suggesting substantial individual differences in octave equivalence. These individual differences were present for both pure and complex artificial tones as well as naturally sung stimuli. Moreover, they remained when participants received explicit feedback, suggesting that the failure of some participants to chroma match was not due to differences in the interpretation of the task. Furthermore, when we probed pitch representations in native Amazonians who live in relative isolation from Western culture (the

Tsimane’); we found octave equivalence as measured by our singing task to be largely absent. The results suggest that octave equivalence is culturally contingent, plausibly dependent on individual experience and engagement with particular musical systems.

PS 229

Discrimination of Temporal Envelope Statistics as a Biomarker of Dysfunction in the Inner Hair Cell Pathway

Rebecca E. Millman; Michael A. Stone
Manchester Centre for Audiology and Deafness, NIHR Manchester Biomedical Research Centre

Exposure to high levels of noise may alter the functioning of multiple sites along the inner hair cell (IHC) pathway, such as damage to cochlear IHCs, loss of synapses and degeneration of primary auditory neurons. Dysfunction in the IHC pathway (IHCd) leads to multiple perceptual changes. A hearing aid provides limited compensation for the deficits caused by IHCd. Early detection of IHCd is desirable to identify susceptible individuals in order to counsel behavioural change.

IHCd appears likely to result in reduced fidelity of coding of acoustic information in humans (Stone et al., 2008; Vinay & Moore, 2010; Stone & Moore, 2014) and consequently impairs the ability to discriminate sounds based on their statistical properties. Here we present an objective behavioural measure, the “ELEVEN test”, designed to be sensitive to the effects of IHCd. The ELEVEN test measures discrimination thresholds for sounds based on changes in temporal envelope statistics. The ELEVEN test restricts stimulus-evoked excitation to a small extent of the cochlea through the use of narrowband noise and presentation at low sensation levels (SL). Background noise is used to limit off-frequency listening.

Profiles of exposure to primarily high-noise events (> 95 dBA, Stone & Moore, 2014) were obtained from young (18-25 years) normal-hearing listeners. Absolute thresholds were measured for frequencies of 0.5, 1, 3 and 6 kHz. These thresholds were used to set presentation levels of 15 and 25 dB SL. The detection threshold for a tone in Gaussian-statistic broadband noise (the TEN(SPL) test; Moore et al., 2000) and, in the ELEVEN test, a discrimination threshold of a tone in a narrowband low-noise noise (Pumplin, 1985), were measured for each test frequency.

Performance was poorer on both the TEN(SPL) and the ELEVEN tests at the lowest SL in some listeners, consistent with the definition of a “dead region” (Moore

et al. 2000) and hence suggesting IHCd. For some listeners, performance on the TEN(SPL) test was “normal” but thresholds for the ELEVEN test were elevated, suggesting subtle IHC pathway damage that was not identified by the TEN(SPL) test. The ELEVEN test has the potential to identify the detrimental effects of subtle IHCd on the coding of the temporal envelope of sounds.

References:

Moore, B.C.J., Huss, M., Vickers, D.A., Glasberg B.R. and Alcántara, J. (2000). *Brit. J. Audiol.* 34: 205–224.

Pumplin, J. (1985). *J. Acoust. Soc. Am.* 78: 100-104.

Stone, M.A., Moore, B.C.J. and Greenish, H. (2008). *Int. J. Audiol.* 47: 737-750.

Stone, M.A. & Moore, B.C.J. (2014). *Hear. Res.* 317: 50-62.

Vinay & Moore B.C.J. (2010). *J. Acoust. Soc. Am.* 128: 3634-3641.

PS 230

Effects of acoustic overstimulation on hearing loss in C57BL/6.CAST mice missing the glutathione peroxidase

Katja Bleckmann¹; Sonja J. Pyott²; Georg M. Klump¹

¹*Custer of Excellence Hearing4all, Department of Neuroscience, Carl von Ossietzky University;*

²*University of Groningen, University Medical Center Groningen Department of Otorhinolaryngology and Head/Neck Surgery*

Background

Elevated levels of reactive oxygen species and oxidative stress have been implicated in cochlea injury after acoustic overstimulation. Ohlemiller et al. (2000, *JARO* 1: 243-254) successfully knocked out the glutathione peroxidase (Gpx1) in C57BL/6 mice showing that a genetic modification impairing antioxidant defense increases cochlea injury after a noise exposure. Since C57BL/6 mice also suffer from age-related hearing loss which may interfere with noise-induced hearing loss, we re-evaluated the effect of acoustic trauma in Gpx1 knock-out mice in the C57BL/6.CAST-Cdh23Ahl+ strain that suffers less from age-related hearing loss than C57BL/6.

Methods

To demonstrate the effects of noise-induced hearing

loss (NIHL) we compared absolute auditory thresholds in quiet and masked threshold in background noise (spectrum level 20 dB/Hz, frequency range 2-50 kHz) before and two weeks after acoustic overstimulation. Absolute and masked thresholds were assessed applying a reward-based Go/NoGo procedure. Based on hit and false alarm rates, thresholds were obtained for a sensitivity value d' ; of 1.8.

To elicit temporary threshold shifts by acoustic trauma, ketamine-anesthetized animals were exposed to an octave band of noise (8-16 kHz) for 2 h at 98 dB SPL (Liberman & Liberman 2015, *JARO* 16: 205-219). Auditory brainstem response (ABR) thresholds were measured before, 48 h after the noise exposure and at the end of behavioral experiments under ketamine anesthesia using pure tones of 5, 10 and 20 kHz (0.5 ms) and clicks (20 μ s). The amplitude of ABR wave 1 was evaluated. Following acoustic trauma, hair cell and afferent synapse loss were quantified at defined tonotopic regions in isolated organs of Corti (Braude et al. 2015, *Hear Res* 321: 52-64).

Results and Conclusions

Results from the ongoing study demonstrate that pre-trauma ABR thresholds for Gpx1 knock-out (KO) are similar to those in C57BL/6.CAST-Cdh23Ahl+ (WT) mice. However, behavioral pre-trauma thresholds in silence in KO mice are considerably higher than in WT mice while masked thresholds of both groups are more similar. After trauma, the thresholds in silence of WT mice are unchanged while those of KO mice are elevated (10 – 20 dB). Masked thresholds in WT mice appear unchanged after trauma. Currently, we are assessing ABR and behavioral thresholds in Gpx1 KO mice after trauma and correlating these measures to sensorineural pathology. Our results suggest that Gpx1 KO mice with a C57BL/6.CAST-Cdh23Ahl+ background are more vulnerable than WT mice to background noise exposure in the breeding facility and to acoustic trauma.

Funded by the DFG, EXC 1077

PS 231

Neural Networks Trained to Estimate F0 from Natural Sounds Replicate Properties of Human Pitch Perception

Mark R. Saddler; Ray Gonzalez; Josh H. McDermott
Massachusetts Institute of Technology

Despite a wealth of psychophysical data, developing computational models that account for pitch perception has proven challenging. In human listeners, the pitch of a sound depends on both spectral and temporal

information available in the auditory periphery, but the relative contribution of the various cues and the reasons for their varying importance remain poorly understood. We investigated whether the properties of human pitch perception would emerge simply from optimizing a general-purpose architecture to estimate fundamental frequency (F0) from cochlear representations of natural sounds. We trained a convolutional neural network to classify simulated auditory nerve representations of speech and instrument sounds according to their F0. An established model of the auditory periphery (Bruce et al. 2018) was used to simulate the instantaneous firing rate responses of 50 auditory nerve fibers. Once trained, we simulated psychophysical experiments on the network. Pitch discrimination thresholds measured from the trained neural network replicated many of the known dependencies of human pitch discrimination on stimulus parameters such as harmonic composition and relative phase. Discrimination thresholds were best for stimuli containing low-numbered harmonics that were resolved by the cochlear filters and increased for stimuli containing only higher-numbered, unresolved harmonics. Randomizing the relative phase of harmonic components worsened pitch discrimination performance only when harmonics were unresolved, indicating the network learned to use temporal cues for pitch extraction when spectral cues were unavailable. Furthermore, the trained network qualitatively replicated human pitch judgments on a number of classic psychoacoustic manipulations (pitch-shifted inharmonic complexes, mistuned harmonics, transposed tones, alternating-phase harmonic complexes). We also simulated neurophysiological experiments on the trained network and found units in the later convolutional layers that exhibited pitch-tuning and selectivity for either resolved or unresolved harmonics. To better understand how the dependencies of pitch perception arise from either constraints of the peripheral auditory system or from statistics of sounds in the world, we independently manipulated parameters of the peripheral model and the training corpus, and found that each altered the network's performance characteristics. The results collectively suggest that human pitch perception can be understood as having been optimized to estimate the fundamental frequency of natural sounds heard through a human cochlea.

PS 232

Effect of stimulus duration, bandwidth, and background noise on loudness growth in rats

Kelly Radziwon¹; Anika French²; Li Li²; Richard Salvi³
¹State University of New York at Buffalo; ²Center for Hearing and Deafness, SUNY at Buffalo; ³University at Buffalo

Previous studies have demonstrated that auditory reaction time (RT) is a reliable surrogate of loudness perception in humans and several animal species. Reaction time-intensity (RT-I) functions faithfully recapitulate equal loudness contours, but RT measurements are easier to obtain than equal loudness judgments, especially in animals. In humans, sounds are perceived as louder as stimulus duration increases up to about 300 ms. Loudness also increases as stimulus bandwidth increases beyond the critical bandwidth. Finally, background noise mimics loudness recruitment; loudness growth is rapid near threshold, but growth becomes normal at suprathreshold levels. Therefore, to evaluate whether RT-I functions are a reliable measure of loudness growth in rats, we obtained auditory RTs across a range of stimulus intensities, durations, and bandwidths, in both quiet and in the presence of background noise.

Six Sprague-Dawley rats were trained to detect broadband noisebursts (BBN), narrowband noisebursts (NBN; 16-20 kHz), and tonebursts (4 and 16 kHz) in a go/no-go operant conditioning procedure. RTs were taken from the onset of the noise/tone burst to the time the rat made a response. To determine the effect of stimulus duration on loudness growth, RT-I functions were collected for BBN across four stimulus durations (20, 50, 100, and 300 ms). To evaluate the effect of stimulus bandwidth on loudness growth, RT-I functions were compared for BBN, NBN, and 4 and 16 kHz pure tones (300 ms). Finally, to determine the effect of background noise on loudness growth, RT-I functions for BBN and tonebursts were collected in quiet and in the presence of a 40 dB SPL BBN masker.

As in previous human studies, the rats had faster RTs with increasing stimulus duration and bandwidth, suggesting that longer and wider-band stimuli were perceived as louder. In contrast, the rats demonstrated recruitment-like behavior in the presence of background noise. The rats had slower than normal RTs for lower level stimuli but normal RTs for high level stimuli in the noise conditions, strongly suggesting that the rats were experiencing a recruitment-like percept when a noise masker was present.

Ultimately, the results of these three studies suggest that RT is a reliable surrogate of loudness perception in rats as it is for humans. Using auditory RT as a measure of loudness perception will allow us to accurately measure loudness growth in rats following both drug and noise exposure while reliably assessing the rats for hearing loss, loudness recruitment, and hyperacusis.

Representation of Dissonance Is Culturally Invariant Even Though Aesthetic Responses to Dissonance Are Not

Malinda J. McPherson¹; Sophia Dolan²; Tomas Ossandon³; Joachin Valdez³; Eduardo Undurraga⁴; Nori Jacoby⁵; Ricardo Godoy⁶; Josh H. McDermott²

¹Harvard Medical School; ²Massachusetts Institute of Technology; ³Facultad de Medicina, Pontificia Universidad Católica de Chile; ⁴School of Government, Pontificia Universidad Católica de Chile; ⁵Columbia University; ⁶The Heller School for Social Policy and Management, Brandeis University

Music from around the world tends to use pitch intervals approximated by simple integer ratios. How can this regularity be reconciled with recent evidence that preferences for canonically consonant (simple integer ratio) pitch intervals vary cross-culturally? We evaluated the hypothesis that pitch combinations vary perceptually by their similarity to the harmonic series, independent of aesthetic preferences for the same combinations. We measured the extent to which concurrent pitches were misperceived as a single sound ('fused';) by members of a remote Amazonian society, as well as Western listeners. We also measured preferences for the same pitch intervals in the same listeners. Although Amazonian listeners were aesthetically indifferent to consonant and dissonant musical intervals, replicating previous findings, their fusion judgments closely resembled those of American listeners – both groups were more likely to hear consonant intervals as a single sound. These cross-cultural results indicate that perceptual mechanisms for representing music can be largely independent of musical experience and culture, but that the resulting perceptual equivalences develop culture-specific aesthetic associations.

PS 234

Assessing Pitch Perception Using Sung Responses

Malinda J. McPherson¹; Nori Jacoby²; Josh H. McDermott³

¹Harvard Medical School; ²Columbia University; ³Massachusetts Institute of Technology

Pitch perception is generally studied using explicit judgments about stimuli, for instance when a participant listens to two tones and decides which is higher. However, pitch perception in everyday listening often bypasses explicit judgments. Instead, the pitch someone hears can be translated into a spoken or sung response, as when matching prosodic contours in speech or repeating a sung melody. We investigated whether singing could be used to study pitch perception,

and whether sung responses align with traditional psychophysical measurements. Our preliminary results indicate that sung responses replicate some effects from the traditional psychophysical literature. Sung responses are intuitive and natural, and are potentially useful for studying populations where traditional psychophysical judgments may be difficult to elicit (e.g. young children or remote cultures without formal educational systems). Symptoms of Age-Related Hearing Loss in Humans

PS 235

Evidence for Age-related Cochlear Synaptopathy Unconnected to Auditory Temporal Processing Deficits in Humans

Enrique A. Lopez-Poveda; Peter T. Johannesen; Byanka C. Buzo
University of Salamanca

In humans, ageing is associated with auditory temporal processing deficits as well as with cochlear synaptopathy, and several studies suggest that synaptopathy degrades the neural coding of temporal sound features. Here, we investigate if synaptopathy may underlie age-related temporal processing deficits. For each of 62 listeners (aged 12 to 68 years) with normal hearing (thresholds < 20 dB HL), we measured the slope of threshold-duration functions (TDSs), gap detection thresholds (GDTs), frequency modulation detection thresholds (FMDTs), lifetime noise exposure, and the slope of the ABR wave-I magnitude-level function (in units of microVolts/dB). Based on animal research, we assumed that the shallower the slope of ABR wave-I, the higher the risk of suffering from synaptopathy. TDSs were inferred from absolute detection thresholds for pure tones (0.5 to 8 kHz) with durations from 2 to 20 ms and TDSs were corrected for the effects of long tone (500 ms) thresholds. GDTs were measured as the shortest detectable silent gap between two marker tones (2 kHz, 80 dB SPL) with 5 or 50 ms durations. FMDTs were measured for 30 and 60 dB SL carrier tones at 1.5 kHz modulated at 2 Hz. ABR wave I slope decreased with increasing age but was not correlated with noise exposure, consistent with age-related but not noise-related synaptopathy. TDSs, GDTs and FMDTs were not correlated with noise exposure. GDTs and FMDTs increased significantly with increasing age (consistent with previous studies) but TDSs were not correlated with age. TDS and FMDT were not correlated with wave I slope. GDTs increased with decreasing wave I slope, but the correlation became not significant after correcting GDTs and wave-I slopes for the effect of absolute threshold. Altogether, the data suggest that synaptopathy is not the cause of age-related deficits in gap and frequency modulation detection. In addition, the data undermine

the notion that synaptopathy impairs the detection of brief sounds (Marmel et al., 2014, *Front. Aging Neurosci.* 7:63). [We thank James M. Harte, Niels H. Pontoppidan and Filip Rønne for useful discussions. Work supported by the Oticon Foundation (ref. 15-3571), Junta de Castilla y León (ref. SAP023P17), MINECO (ref. BFU2015-65376-P), and the European Regional Development Fund].

PS 236

Mutual Information Analysis of Neural Representations of Speech in Noise in the Aging Midbrain

Peng Zan¹; Alessandro Presacco²; Samira Anderson³; Jonathan Z. Simon⁴

¹*Department of Electrical and Computer Engineering, University of Maryland, College Park*; ²*Institute for Systems Research, University of Maryland, College Park*; ³*Department of Hearing and Speech Sciences, University of Maryland; Neuroscience and Cognitive Science Program, University of Maryland*; ⁴*Department of Electrical and Computer Engineering, Institute for Systems Research & Department of Biology, University of Maryland, College Park*

Younger adults with normal hearing can typically understand speech in the presence of a competing speaker without much effort. However, the ability to understand speech in challenging conditions deteriorates with age. Older adults, even with clinically normal hearing, typically have problems understanding speech in noise. Earlier auditory studies using the frequency following response (FFR), dominantly generated by the midbrain, have demonstrated age-related neural deficits when analyzed using traditional measures. Here we analyze speech-driven FFR, for speech masked by competing speech, using a mutual information paradigm, by estimating the amount of stimulus information contained in the FFR. Our results show first a wide-band informational loss in both amplitude and phase of FFR associated with aging. Second, the loss of information is more severe in higher frequency bands (several hundred Hz) in older listeners. Third, the information decreases as noise level increases for both age groups, but older adults benefit when the background speech is changed from meaningful (talker speaking a language that they can comprehend, such as English) to meaningless (talker speaking a language that they cannot comprehend, such as Dutch), while younger do not. The results reveal a clear foreground informational loss in midbrain associated with aging, which is more severe when the background noise is meaningful to them than when it is meaningless.

This research was funded by grants from the National Institutes of Health, R01-DC014085 and P01-AG055365.

PS 237

The Effects of Cadmium and Lead Exposure on Incidence of Olfactory Impairment and Decline in a Cohort of Middle-aged Adults

Adam J. Paulsen; Carla R. Schubert; Dayna S. Dalton; Mary E. Fischer; Alex Pinto; Karen J. Cruickshanks
University of Wisconsin Madison

Background: Cadmium (Cd) and lead (Pb) are neurotoxic heavy metals with common sources of exposure in the general U.S. population. The potential effect of these neurotoxins on olfactory function is not well known. This study aims to quantify the risk of incident olfactory impairment and decline associated with Cd and Pb exposure.

Methods: The Beaver Dam Offspring Study (BOSS) is an ongoing longitudinal cohort study of aging in the adult children of the population-based Epidemiology of Hearing Loss Study. BOSS participants were aged 21-84 years at baseline examinations (2005-2008) and follow-up examinations were conducted every 5 years (2010-2013, 2015-2017). Olfactory function was measured at each examination using the San Diego Odor Identification Test (SDOIT). Olfactory impairment (OI) was defined as a score of fewer than 6 of 8 correctly identified odorants after two trials. Olfactory decline (OD) was defined as a decrease of 2 or more in SDOIT score between baseline and follow-up. Cd and Pb were measured in whole blood samples collected at baseline and stored at -80°C until assayed in 2017. The associations between Cd and Pb exposures and olfactory function were examined by comparing those in the highest quintile (Q5) of exposure to all others (Q1-4) and by the effect of doubling of exposure. Hazard Ratios (HR) and 95% confidence intervals (CI) were estimated using Cox-proportional hazards models.

Results: There were 2312 participants, mean age of 49 years (SD=9.7) and 55% women, at risk of OI at baseline. The 10-year cumulative incidence of OI was 3.9%, and was higher in older age groups (21-34y: 0.7%, 35-44y: 1.1%, 45-54y: 2.9%, 55-64y: 6.6%, 65-84y: 18.5%, p-value<0.0001). Out of 2374 participants at risk for decline, 7.2% had OD in the 10-year follow-up. In multivariable models controlling for age, sex, carotid artery plaque, hypertension, alcohol consumption, history of head injury and history of deviated septum, those in Q5 of Cd exposure were more likely to develop impairment or decline, HR=1.93 (95% CI=1.15, 3.22) and HR=1.70 (95% CI=1.15, 2.51), respectively. Doubling of Cd exposure carried an increased risk in similarly controlled models (OI: HR=1.22, 95% CI=1.01, 1.47; OD: HR=1.16, 95% CI=1.01, 1.33). Pb levels were not associated with increased risk of OI or OD.

Conclusions: Cadmium, but not lead, exposure was associated with increased risk of olfactory impairment and decline in olfactory function in this cohort study of middle-aged adults. Reduction in exposure to Cd may help to reduce the overall burden of olfactory dysfunction.

PS 238

Techniques for Assessing Fractional Hair Cell Survival in Archival Human Temporal Bones: New Insights from Old Specimens

Peizhe Wu¹; Alicia Quesnel²; Jennifer T. O'Malley¹; M. Charles Liberman³

¹*Dept. of Otolaryngology, Mass. Eye and Ear*; ²*Dept. of Otolaryngology, Harvard Medical School*; ³*Mass. Eye and Ear Infirmary*

Human otopathology is typically studied in specimens serially sectioned at 20 microns, and a cytochleogram is created by rating hair cells as either present or absent in each row, based on light-microscopic evaluation of the organ of Corti (Schuknecht's Pathology of the Ear, Third Edition). Such a binary analysis will underestimate the loss of hair cells, given that a single 20-micron section typically contains at least 2 - 3 hair cells in each row, and that most cochlear regions of most ears show fractional hair cell loss of varying degrees when viewed as immunostained whole mounts (Wu et al. 2018, Neuroscience Epub ahead of print). Furthermore, reliance on nuclear and cellular morphology in post-mortem material to distinguish hair cells from supporting cells under light microscopy can be difficult. Here, we present an enhanced technique for analysis of archival human temporal bones that enables accurate assessment of fractional hair cell survival, even in cases with severe post-mortem autolysis.

Selected cases from the MEEI collection were reanalyzed, observer blinded to case history, using differential interference contrast (DIC) microscopy, with a high-N.A. (1.3) objective, to enable complete optical sectioning of each slide. Rather than count nuclei, we assessed cuticular plates and hair bundles, because they are 1) easily seen with DIC, 2) more resistant to post-mortem autolysis, 3) rigidly fixed by the actin-dense reticular lamina and 4) virtually impossible to confuse with supporting cells. Some sections were also imaged with a confocal, using the eosin fluorescence of hair cells to create 3-D virtual displays of the entire section thickness. As a further cross-check, some sections were immunostained with Myosin VI and VIIa. Reproducibility of results was assessed across two observers.

Included in our reanalysis were archival cases of

"Conductive Prebycusis", which prior study concluded were not "explained" by hair cell loss, stria atrophy or spiral ganglion cell loss (Ramadan & Schuknecht 1989, Otolaryngol Head & Neck Surg 100:30). In contrast, our analysis showed a clear apical-basal gradient of fractional hair cell loss that correlated well with the descending audiograms, thus obviating the need to ascribe this "4th type" of presbycusis to unseen changes in cochlear mechanical stiffness. It is likely that re-analysis of fractional hair cell survival will suggest important modifications to our views on the functionally important structural changes in all four types of human presbycusis, as classically defined.

Research supported by a grant from the NIDCD (P50 DC015857)

PS 239

Effects of Age and Native Language on Discrimination of Rhythmic Tonal Sequences

Peter Fitzgibbons; Rebecca Bieber; Sandra Gordon-Salant
University of Maryland

Overview

Previous research has shown that older listeners exhibit significantly poorer sensitivity to increments of a target inter-onset interval embedded within tone sequences compared to younger listeners (Fitzgibbons & Gordon-Salant, 2015). Age-related differences in temporal sensitivity were notably large for sequences featuring variable rhythmic grouping compared to control sequences featuring uniform timing.

One issue that has not been examined previously is the influence of a listener's native language on the ability to process timing information in non-speech signals. It is likely that people of different native language experiences process the timing characteristics of acoustic signals (both speech and non-speech) differently. For example, experience with a native language that has a syllable-timing pattern (e.g., Spanish) may result in different temporal discrimination abilities than experience with a native language that has a stress-timing pattern (e.g., English). Moreover, listener age is known to have a strong influence on auditory temporal processing abilities for simple and complex stimuli. The current experiment compares the abilities of younger and older listeners whose native language is either English or Spanish on their sensitivity to durational characteristics of temporal intervals embedded within tonal sequences designed with different temporal grouping characteristics.

Methods

There were 4 groups of participants (n = 15 participants/group): Young normal-hearing native English listeners (YNH-NE), older normal-hearing native English listeners (ONH-NE), young normal-hearing native Spanish listeners (YNH-NS), and older normal hearing native Spanish listeners (ONH-NS).

Stimuli were 6-tone sequences. Each tone in the sequence was 1kHz and 50 ms in duration. The inter-onset-interval (IOI) is the time between the onset of one tone and the next in the sequences. There were 11 different sequences comprised of different groupings of short (200 ms) and long (400 ms) IOIs, in addition to time-compressed (50%) versions of many of these sequences. One sequence IOI was designated as a target interval, and the experiment measured a duration DL for that target interval across listeners.

Results

The findings show that older listeners demonstrated significantly poorer temporal sensitivity to the rhythmic sequences than younger listeners, and native Spanish listeners demonstrated poorer sensitivity to the sequences than native English speakers. Moreover, performance of the native Spanish listeners was generally poorest for the time-compressed sequences. The effects of age and native language appear to be independent.

Conclusions

Native language appears to affect listeners'; temporal sensitivity to non-speech tonal sequences with different timing characteristics.

Research supported by NIA/NIH, grant#R01AG0009191.

PS 240

Detection and Recognition of Asynchronous Audiovisual Sentences by Younger and Older Adults

Kelsey Oppler; Maya Freund; Sandra Gordon-Salant
University of Maryland

Introduction: Speech recognition performance by both younger and older adults generally improves when the listener has access to both auditory (A) and visual (V) information. When AV speech is temporally asynchronous, younger listeners are able to integrate the AV information and perceive the speech as synchronous over a 200 ms window of asynchrony. Additionally, younger listeners maintain speech recognition performance over a range

of AV asynchronies. In older adults, AV integration may be more difficult due to slowed auditory temporal processing, possibly resulting in poorer AV asynchronous speech recognition performance, especially when there are other temporal alterations in the speech signal, such as those accompanying foreign-accented speech. The present study investigates younger and older listeners'; detection and recognition of AV asynchronous speech over a wide range of asynchronies using unaccented and accented AV sentence materials in noise.

Method: Three listener groups participated in the AV asynchrony detection and recognition experiments: younger normal hearing, older normal hearing, and older hearing impaired. In both experiments, IEEE sentences spoken by unaccented and Spanish-accented talkers were presented to participants at an individualized SNR targeting 71% performance. In the detection experiment, sentences were presented over a range of asynchronies (-450 ms to +450 ms) and participants indicated if they perceived the stimuli as synchronous or asynchronous. In the speech recognition experiment, sentences were presented at different asynchronies (ranging from -300 ms to +400 ms) and listeners repeated the sentence presented.

Results: The results generally indicate that age affects listeners'; detection of asynchronous speech, but does not influence their recognition of asynchronous speech stimuli. The findings also reveal different windows of AV integration for unaccented and accented speech, with a slightly larger window of AV integration observed for the unaccented stimuli. However, the resulting windows of AV integration observed for each accent do not correspond to participants'; recognition performance. Maximum speech recognition performance for both unaccented and accented stimuli is maintained over a wider temporal window than the AV window of integration (based on detection) for participants of all three listener groups.

Conclusions: Despite slowed auditory temporal processing, older adults perform similarly to younger adults at recognizing asynchronous speech. Findings also reveal that while talker accent does influence the window of AV integration, detection judgments for both accents are not related to the range of asynchronies over which listeners maintain maximum recognition performance.

Research Supported by NIH/NIA: R01AG0009191

Redefining Survival of the Fittest - Redux 2019**Robert J. Ruben***Albert Einstein College of Medicine*

Redefining survival of the fittest: communication disorders in the 21st century was published in 2000. This article analyzed the effects of communication disorders on the evolving economy, characterized by a decrease in manual labor and an increase in communication dependent employment. It showed that for the 21st century, the United States needed its workers to have optimal communications skills, and that most people with hearing, voice, speech and language disorders were did not have optimal communication skills. During the past 19 years there have been three interrelated developments that will be substantial factors in determining the economic, and concomitant social, conditions of nations in 2050. The first is that employment needs for communication skills world-wide will have vastly increased over those for manual skills by 2050. The second is that the dependency ratios -

$$\text{Dependency ratio (DR)} = \frac{\text{Number of Children (0-15)} + \text{number of Pensioners (> 65)}}{\text{Number of Working age 16-65}}$$

for most countries will be substantially increased by 2050. The consequence of this increase is that fewer workers will be available to support a greater number of the population. For example, Japan will have 39 % (DR increased to 96 from 57) fewer workers in 2050 than in 2010 to support their population. Thus, each Japanese worker in 2050 must be 39% more productive in 2050 to support their economy at the same level as in 2010. The third is that in the context of the projected increased dependency ratio, if the prevalence of communications disorders remains in the range of 10%, that 10% will have an even greater effect on pressure on the productive population. The 10% prevalence of communication disorders, unless diminished, will exacerbate the growing dependency ratio and consequently increase the need for economic output of every worker in the labor force to maintain economic stability. In order to optimize the growing dependency ratios, the prevalence of communication disorders must be reduced so as to preserve and grow the economic and social wellbeing of each nation. This is a critical public health concern of the 21st century. In a world of increasing dependency ratios, optimal communication skills are the generating mechanisms of survival of the fittest.

A Longitudinal Study of Hearing Loss and Risk of Subjective Cognitive Function Decline in Men**Sharon Curhan¹**; Walter Willett²; Francine Grodstein³; Gary Curhan¹¹*Brigham and Women's Hospital/Harvard Medical School*; ²*Harvard TH Chan School of Public Health*;³*Brigham and Women's Hospital*

BACKGROUND: Hearing loss may be a risk factor for accelerated cognitive decline. Worsening subjective cognitive function (SCF) is a strong predictor of future dementia, yet information on the relation between hearing loss and SCF is scarce. Therefore, we examined the relation of self-reported hearing loss and risk of subsequent SCF decline and whether this risk was attenuated by hearing aid use.

METHODS: We conducted a longitudinal study of 10,107 men aged 62 years in the Health Professionals Follow-up Study, who had no cognitive concerns at baseline (SCF=0) and were followed for 8 years. SCF score was assessed by a 6-item questionnaire administered at baseline and years 4 and 8. SCF decline was defined as new onset of at least one cognitive concern during follow-up.

RESULTS: After 52,752 person-years of follow-up, there were 2,771 cases of incident SCF decline (SCF>1). Self-reported hearing loss was associated with higher risk of SCF decline, and the magnitude of the risk was greater with increasing severity of hearing loss (Table 1). Compared with no hearing loss, the multivariable-adjusted relative risk (95%CI) of incident subjective cognitive decline was 1.30 (1.18,1.42) for mild hearing loss, 1.42 (1.26,1.61) for moderate hearing loss, and 1.54 (1.22,1.96) among men with severe hearing loss who did not use hearing aids (p-trend<0.001). Among men with severe hearing loss who used hearing aids, the magnitude was somewhat attenuated [1.37(1.18,1.60)], but was not statistically significantly different from the risk among men with severe hearing loss who did not use hearing aids. In analyses examining risk of more pronounced cognitive decline (SCF2), the magnitudes of the associations were greater among those with mild or moderate hearing loss. In sensitivity analyses that removed questions that could potentially be related to hearing ability from the SCF score, hearing loss remained associated with higher risk of SCF decline, with a greater risk among those with more severe hearing loss (p-trend<0.001); however, the magnitudes of the point estimates were attenuated (Table 2).

CONCLUSIONS: Hearing loss was associated with higher risk of subjective cognitive decline in men, and

the magnitude of the risk was greater with increasing severity of hearing loss. Among those with severe hearing loss, there was a suggestion that hearing aid use may moderate the risk. Further, measures of cognition typically used in cognitive research may be sensitive to hearing ability; thus, hearing status could be an important consideration in studies of cognitive decline and dementia.

Table 1: Self-Reported Hearing Loss and Risk of Incident Subjective Cognitive Decline* in the Health Professionals Follow-up Study

Hearing Status	SCF Score ≥ 1		SCF Score ≥ 2	
	Cases	Multivariate-adjusted RR† (95% CI)	Cases	Multivariate-adjusted RR† (95% CI)
No difficulty	1250	1.00 (ref)	438	1.00 (ref)
Mild hearing loss	645	1.30 (1.18, 1.42)	335	1.45 (1.26, 1.68)
Moderate hearing loss	378	1.42 (1.26, 1.61)	140	1.51 (1.24, 1.84)
Severe, no hearing aid	77	1.54 (1.22, 1.96)	23	1.33 (0.86, 2.04)
Severe, use a hearing aid	221	1.37 (1.18, 1.60)	86	1.40 (1.09, 1.80)

*Incident subjective cognitive decline defined as Subjective Cognitive Function Score (SCF) ≥ 1 or ≥ 2 at follow-up

†Adjusted for: Age, race, occupation, body mass index, waist circumference, smoking (past/current), physical activity, hypertension, diabetes, hypercholesterolemia, depression, aspirin use, ibuprofen use, acetaminophen use, and Alternate Mediterranean diet (AMED) adherence score.

Abbreviations:
RR: relative risk
CI: confidence interval

Table 2: Self-Reported Hearing Loss and Risk of Incident Subjective Cognitive Decline* in the Health Professionals Follow-up Study (after excluding two questions that potentially could be influenced by hearing status)

Hearing Status	Person-years	Cases	Multivariate-adjusted RR† (95% CI)
No difficulty	28623	1208	1.00 (ref)
Mild hearing loss	14638	790	1.26 (1.15, 1.38)
Moderate hearing loss	5438	326	1.29 (1.13, 1.46)
Severe, no hearing aid	986	65	1.37 (1.06, 1.77)
Severe, use a hearing aid	3068	179	1.18 (1.00, 1.39)

*Incident subjective cognitive decline defined as Subjective Cognitive Function Score (SCF) ≥ 1 . Score does not include questions on "difficulty in understanding or following spoken instructions" or "trouble following a group conversation or plot in a TV program."

†Adjusted for: Age, race, occupation, body mass index, waist circumference, smoking (past/current), physical activity, hypertension, diabetes, hypercholesterolemia, depression, aspirin use, ibuprofen use, acetaminophen use, and Alternate Mediterranean diet (AMED) adherence score.

Abbreviations:
RR: relative risk
CI: confidence interval

PS 243

Apathy In Presbycusis Is Related With Brain Atrophy And Functional Loss

Chama Belkhiria¹; Melissa Martínez²; Simon San Martín¹; Alexis Leiva¹; Maricarmen Andrade²; Paul H. Delano²; Carolina Delgado²

¹Audition and Cognition Center. Faculty of Medicine. University of Chile; ²Faculty of Medicine.

Background: Presbycusis is associated with cognitive decline (CD) in the elderly and is recognized as one of the principal modifiable risk factors for dementia. Late onset neuropsychiatric symptoms (NPS) are also associated with dementia and apathy is the most prevalent NPS.

We hypothesized that presbycusis and apathy would have an additive negative effect on the aging brain and would be related to brain volume loss and cognitive and functional decline.

Objectives: Study the interrelations between presbycusis and apathy on brain structure, cognitive and functional performance

Methods: The ANDES (Auditory and Dementia study) is a prospective cohort of healthy Chilean hispano-mestizo elders ≥ 65 years, "cognitively" normal (MMSE >24) with different levels of hearing loss without hearing aids. Patients were evaluated with comprehensive neuropsychological assessment, neuropsychiatric evaluation using the neuropsychiatry inventory questioner (NPI-Q) and apathy evaluation scale (AES), functionality in activities of daily living (ADL) and pure tone average (PTA).

Results: 110 subjects were recruited; mean age and education were 74 ± 5.5 and 9.5 ± 4.2 years, mean PTA= 26 ± 12 . 56 subjects had normal auditory thresholds (controls) (PTA= 17 ± 5) and 54 had presbycusis: 35 mild (PTA= 30 ± 4) and 19 moderate (PTA= 47 ± 8). Presbycusis patients were significantly older than controls, without differences in cognitive, neuropsychiatric or functional assessment. Once adjusted by age and education, the PTA was correlated with apathy, sleep disorders and functional impairment but not with cognitive measurements. Presbycusis patients but not controls, had significant positive correlations between apathy and impairment in ADL and brain volume loss in several brain regions: accumbens, cingulate cortex, orbitofrontal cortex, insular cortex, amygdala, precuneus, superior temporal and total grey matter.

Conclusions: Presbycusis patients had more NPS and functional impairment than controls, which is related with volume loss in frontal/subcortical, limbic and temporal regions. Hearing loss and apathy interaction are predisposing functional loss and neurodegeneration that precedes dementia.

Funded by Proyecto Anillo ACT1403 and Fondecyt 1161155.

PS 244

Role of the Auditory Periphery in Self-Assessment of Hearing Ability in Younger and Older Adults

Alanna Schloss¹; Logan Fraser²; Samira Anderson³
¹Department of Hearing and Speech Sciences, University of Maryland; ²University of Maryland; ³Department of Hearing and Speech Sciences, University of Maryland;

Objective: Older adults often report that speech is audible but unclear, and this lack of clarity may arise from peripheral deficits that are not revealed during standard clinical audiometric procedures. Recent evidence suggests that aging can be associated with a loss of auditory nerve synapses despite normal hearing thresholds and outer hair cell function. However, there is a lack of evidence supporting a role of synaptopathy in human perceptual deficits. This study investigates the role of threshold and supra-threshold measures of peripheral auditory function in self-assessment of hearing ability.

Method: Participants included thirty young normal-hearing adults (YNH, ages 18-24) and thirty older normal-hearing adults (ONH, ages 56-76) who had normal audiometric thresholds (≤ 20 dB HL, 0.125–4 Hz; ≤ 30 dB HL, 6–8 Hz) and passed a screening test for mild cognitive impairment (Montreal Cognitive Assessment, ≥ 26). The Speech, Spatial and Qualities of Hearing Scale (SSQ) was used to provide a self-assessment of hearing difficulty in a variety of listening situations. Threshold measures included high-frequency (HF) audiometric thresholds (8–12.5 Hz) and HF distortion-product otoacoustic emission (DPOAE) thresholds (7.4–12.5 Hz). Suprathreshold measures included Wave I, Wave V/I ratio, and Wave V latency quiet-to-noise slope obtained from auditory brainstem responses (ABRs).

Results: HF audiometric and DPOAE thresholds were significantly higher in older adults than in younger adults. Wave I amplitude was lower in older adults than in younger adults, but the Wave V/I ratio and Wave V latency quiet-to-noise slope were equivalent between groups. In younger adults, Wave I amplitude significantly contributed to the variance in the SSQ, but in older adults, the HF pure-tone average significantly contributed to SSQ variance. DPOAE thresholds did not predict SSQ variance in either group.

Conclusions: Older adults; perception of hearing difficulties appears to be affected by decreases in hearing thresholds at frequencies that are higher than those that are considered clinically important for understanding speech. In contrast, young adults; perception of hearing difficulties appears to be affected by decreased Wave I amplitudes, a putative measure of synaptopathy. The next step in this study is to analyze noise exposure histories to determine if extent of noise exposure relates to suprathreshold measures of peripheral function.

Research supported by NIH/NIDCD grant R21 DC015843

Cortical Over-representation of Speech in Older Listeners Correlates with a Reduction in both Behavioral Inhibition and Speech Intelligibility

Peng Zan¹; Alessandro Presacco²; Samira Anderson³; Jonathan Z. Simon⁴

¹Department of Electrical and Computer Engineering, University of Maryland, College Park; ²Institute for Systems Research, University of Maryland, College Park; ³Department of Hearing and Speech Sciences, University of Maryland; Neuroscience and Cognitive Science Program, University of Maryland; ⁴Department of Electrical and Computer Engineering, Institute for Systems Research & Department of Biology, University of Maryland, College Park

The ability to segregate speech from noise deteriorates with aging. Aging is also associated with an exaggerated representation of the speech envelope in auditory cortex. However, the relation between this cortical over-representation and intelligibility of speech in noise in older listeners remains an open question. Here we develop a robust and novel approach based on information theory to investigate the cortical response phase-locked to speech envelopes of both attended and unattended speakers, using mutual information between the neural responses and the speech stimuli. The responses were recorded by magnetoencephalography (MEG). The results show an over-representation of mutual information of both unattended and attended speakers; speech in older listeners above and beyond the cortical over-representation previously reported. In particular the relative enhancement of mutual information for attended over unattended speech decreases with decreasing SNR, in older listeners for the late response component (~250 ms latency). In contrast, younger listeners show an increasing trend, as might be expected with increasing attention. In older listeners, the mutual information in this same late response to attended speech negatively correlates with behavioral inhibition, as measured by performance in a visual Flanker task, and also negatively correlates with speech intelligibility in noise, as measured by QuickSIN score. Neural source space analysis shows that this late response in older listeners is lateralized to right hemisphere auditory cortical regions. The results suggest that the over-representation of speech in the late response in the aging auditory cortex may be due to the same neural mechanism responsible for decreasing behavioral inhibition, and deterioration of speech intelligibility, in older listeners. From a broader view, this research demonstrates a powerful tool for analyzing phase-locked cortical responses and their relationship to relevant behavioral measures.

This research was funded by grants from the National Institutes of Health, R01-DC014085 and P01-AG055365.

PS 246

Afferent-Efferent Connectivity Between Auditory Brainstem and Cortex Accounts For Poorer Speech-In-Noise Comprehension In Older Adults

Caitlin Price¹; Gavin Bidelman¹; Dawei Shen²; Steve Arnott²; Claude Alain²

¹University of Memphis; ²Rotman Research Institute, Toronto

Senescent changes in audition (e.g., hearing loss) impact auditory skills, leading to reduced speech-in-noise (SIN) comprehension in the elderly. SIN deficits in older adults have been linked to declines in auditory neural coding at both subcortical and cortical levels of the brain. Yet, it remains unclear whether older adults' difficulty understanding SIN relates solely to reduced neural output of brainstem-cortical structures or rather, an imbalance in signal transmission (i.e., functional connectivity) between brainstem and auditory cortices. We measured neuroelectric brain responses in older adults with and without mild hearing loss (HL) while they actively identified speech in background noise. Source imaging parsed region-specific contributions of brainstem (BS) and primary auditory cortex (PAC) activity to speech perception. At the cortical level, noise weakened responses in both groups, but HL listeners showed a stark rightward PAC asymmetry not observed in the bilateral activations of normal-hearing listeners, suggesting a hemispheric reweighting in speech processing. Contrastively, BS responses showed little hearing-related changes. Functional connectivity, indexing directed (causal) neural signaling between BS and PAC, showed that afferent (BS→PAC) but not efferent (PAC→BS) transmission weakened with increasing hearing loss and predicted listeners' behavioral SIN performance. Our findings suggest that in older adults (i) mild hearing loss differentially reduces neural output at several stages of auditory processing (PAC>BS), (ii) subcortical-cortical connectivity is more sensitive to hearing insult than top-down (cortical-subcortical) control, and (iii) reduced functional connectivity in afferent auditory pathways plays a significant role in SIN comprehension problems.

PS 247

High-frequency masking reveals peripheral deficits in normal-hearing listeners with poor speech recognition

Anita M. Mevani¹; Sarah Kirk¹; Kenneth E. Hancock²;

Kelsie J. Grant¹; M. Charles Liberman³; **Stéphane F. Maison**⁴

¹Eaton-Peabody Laboratory, Massachusetts Eye & Ear Infirmary, Boston MA; ²Eaton-Peabody Laboratories, Massachusetts Eye and Ear; Dept. of Otolaryngology, Harvard Medical School; ³Mass. Eye and Ear Infirmary; ⁴Eaton-Peabody Laboratory, Massachusetts Eye & Ear Infirmary and Department of Otolaryngology, Harvard Medical School, Boston MA

Animal studies show that noise-induced or age-related hair cell loss is often preceded by loss of cochlear synapses, and a recent temporal bone study shows that many surviving inner hair cells in aging humans are partially de-afferented (Wu et al., 2018). Silencing auditory nerve fibers, especially those with high thresholds and low spontaneous rates, degrades auditory processing and may contribute to difficulties understanding speech in noise. Although cochlear synaptopathy can be diagnosed in animals by measuring auditory-nerve suprathreshold responses, its diagnosis in humans remains a challenge.

We recruited 125 normal-hearing subjects (≤ 25 dB HL from 0.25 – 8 kHz) from 18 – 63 yrs, with no history of ear or hearing problems, no history of neurologic disorders and unremarkable otoscopic examinations. All subjects were native English speakers and passed the Montreal Cognitive Assessment. Word recognition was assessed at 55 dB HL in quiet and in difficult listening situations using the NU-6 corpus (with competing white noise at 0 SNR or with a 45% or 65% compression with 0.3 sec reverberation). Performance on a modified QuickSIN was also measured. Outer hair cell function was assessed using DPOAEs from 0.5 kHz to 16 kHz, while cochlear nerve function was assessed by electrocochleography (ECochG) in response to 100-ms clicks (9.1 / sec) delivered in alternate polarity at 125 dB pSPL, in the absence or presence of a 90-msec forward masker (8-16 kHz noise) at 15 dB SL (n=125) or 35 dB SL (n=86). Lastly, an unmasked click-evoked EcochG was obtained using a 40.1 Hz repetition rate. The total noise dose for all ECochG measurements was well within OSHA and NIOSH standards.

Results show that the SP/AP ratio is correlated with word-recognition scores, whereas DPOAE amplitudes are not, consistent with selective neural loss. Furthermore, forward masking suppresses SP and AP amplitudes to a greater extent in subjects with the poorest word scores when compared to those who did best. These results support the idea that some of the differences in word recognition scores among listeners with normal audiometric threshold arise from cochlear neuropathy.

Research supported by a grant from the NIDCD (P50 DC015857)

Factors Associated to the Efficiency of Hearing Aids on Presbycusis Patients

Xu Wu; Qixuan Wang; Zhiwu Huang; Hao Wu
Clinical Audiology

Objective: To investigate the satisfaction of presbycusis patients with individual, accurate and precise fitting work which is priority for bilateral hearing aids, exploring the related influencing factors and their role in predicting the efficiency of hearing aids.

Methods: 73 cases of presbycusis patients aged 60-95 years old underwent pure tone audiometry and speech recognition ability examination to obtain the pure tone average hearing threshold of the better ear (BPTA) and maximum speech recognition rate of the better ear (BSRR) in quiet environment. Our fitting process gave preference to bilateral, individual and accurate hearing aids intervention and modulation. Audiologists evaluated the efficiency and satisfaction of participants according to International Outcome Inventory of Hearing Aids (IOI-HA) questionnaire scores by face-to-face or telephone investigations after using the hearing aids at least 3 months. Correlation analysis was performed among Age, Gender, First fitting age, Unilateral /bilateral hearing aids, BPTA, BSRR, Score of the factor 1, Score of the factor 2, Total score of the IOI-HA questionnaire, Score of each item and each Hearing threshold of the 0.5,1,2,4KHz.

Results: Among those participants with over 3 months using of hearing aids, total satisfaction percentage according to IOI-HA scores was 86.3%. There was no significant correlation between Age, First fitting age, unilateral or bilateral hearing aids, BPTA and IOI-HA total score. BSRR was strongly correlated to total IOI-HA scores ($r = 0.768$). According to the multiple linear regression analysis, BPTA and BSRR both had a statistically significant effect on the total IOA-HA scores after hearing aid intervention.

Conclusion: Presbycusis patients with accurate hearing aid fitting could get high satisfaction, and bilateral hearing aids is better than unilateral. Age and First fitting age are not meaningful influencing factor on the satisfaction of hearing aid in presbycusis patients. A higher maximum speech recognition rate before fitting could predict the better efficiency and satisfaction of the hearing aids. Therefore, completing speech recognition ability examination before fitting could make a great contribution to predict the efficiency of patients after hearing aids, as well as help the presbycusis patients to establish available expectation.

Blocked Training, but not Randomized Training, Leads to Improvement in Temporal Rate Discrimination and Increased Energy in Auditory Steady State Responses

Samira Anderson¹; Matthew Goupell²; Alyson Schapira³; Rachel Robinson³; Reynier Hernandez³; Sandra Gordon-Salant²

¹*Department of Hearing and Speech Sciences, University of Maryland; Neuroscience and Cognitive Science Program, University of Maryland;* ²*University of Maryland;* ³*Department of Hearing and Speech Sciences, University of Maryland, College Park*

Objective: Age-related decreases in temporal processing affect many aspects of hearing, including perception of rapid acoustic events and speech perception in noise. These aging deficits have been demonstrated in behavioral and electrophysiological studies using simple and complex stimuli. This study's aim is to determine the extent to which training on perceptual rate discrimination improves perceptual performance and neural encoding in younger and older adults.

Methods: The stimuli were band-limited pulse trains with a duration of 300 ms presented at 75 dB SPL at rates of 100, 200, 300, and 400 pulses per second (pps). At the pre-test session, frequency difference limens were obtained for the four rates in young normal-hearing (YNH), older normal-hearing (ONH), and older hearing-impaired (OHI) adults. Auditory steady-state responses (ASSRs) were recorded to the same stimuli. Preliminary data were then obtained using two different training paradigms conducted over nine sessions. The first paradigm trained five participants (3 YNH and 2 ONH) on pulse-rate discrimination using all four rates, with the presentation of any specific rate randomly varying from trial to trial, for a total of 180 trials per rate. The second paradigm trained eight participants (2 YNH, 3 ONH, and 3 OHI) on pulse-rate discrimination using just two rates, 100 and 300 pps, that were presented in blocks for a total of 240 trials per rate. The same pre-test measures were obtained at the post-test session.

Results: The participants who received randomized training did not demonstrate consistent improvement in perceptual performance or neural responses. The participants who received blocked training demonstrated overall improvement in perceptual and neural performance, but the changes differed by group. The ONH participants showed a more consistent pattern of improvement across rates than the YNH or OHI participants. Furthermore, generalization was noted to the untrained rates (200 and 400 pps). In neural responses, ASSR energy increased at 100 pps, and the

effect was seen in the ONH and YNH, but not the OHI participants. The increase in ASSR energy at 100 pps correlated with improvement in pulse-rate discrimination for the same 100-pps rate.

Conclusion: Perceptual training on pulse-rate discrimination can lead to improvement in perceptual performance and neural representation, especially in older adults, but the effects depend on the type of training used – randomized vs. blocked training. This investigation will continue to consider the training parameters that achieve the greatest efficacy.

Research supported by NIH/NIA grant P01 AG055365

PS 250

Age-Related Degradation is more Evident for Speech Stimuli with Longer than with Shorter Consonant Transitions

Samira Anderson¹; **Abigail Anne Poe**²; Roque Lindsey²; Caitlin Le²; Hanin Karawani³

¹*Department of Hearing and Speech Sciences, University of Maryland; Neuroscience and Cognitive Science Program, University of Maryland;* ²*Department of Hearing and Speech Sciences, University of Maryland, College Park;* ³*Department of Hearing and Speech Sciences, University of Maryland; Department of Communication Sciences and Disorders, University of Haifa; Department of Otorhinolaryngology-Head and Neck Surgery, Rambam Health Care Campus*

Objective: Speech understanding in older adults may be reduced by deficits in the neural representation of consonant transitions in speech stimuli. Behavioral studies demonstrate that older adults require longer consonant transition durations to discriminate between words that differ on this temporal dimension (e.g., “beat” vs. “wheat”). Studies that have recorded frequency-following responses (FFRs) to a consonant-vowel syllable have found that aging effects are more pronounced for the steady-state rather than for consonant-transition regions. The stop consonant burst and rapidly changing formants in a consonant transition are more likely to generate the synchronous firing of auditory nerve fibers necessary to produce a robust response, compared to a steady-state vowel. Because of a decrease in auditory nerve fibers, older adults’ responses may be more degraded when presented with stimuli that are less effective in generating synchronous firing. Here, we tested the following hypotheses: 1) older adults require a longer consonant transition duration to identify a glide vs. a stop consonant, and 2) aging effects on phase locking and response amplitude in the FFR are most evident for stimulus regions containing longer rather

than shorter transition durations.

Method: The planned enrollment is 30 younger normal-hearing (YNH) and 30 older normal-hearing (ONH) participants. Current enrollment includes 16 YNH (ages 18-28) and 8 ONH (ages 56-70) participants who meet the criteria of normal audiometric thresholds (≤ 20 dB HL, 0.125 – 4 kHz; ≤ 30 dB HL, 6 – 8 kHz) and a passing score of ≥ 26 on the Montreal Cognitive Assessment. Perceptual identification functions were obtained for the words “beat” and “wheat” on a 7-step continuum of consonant-transition duration. FFRs were recorded to the endpoints of the beat-wheat continuum. Phase-locking factor and response amplitudes were calculated for the response regions corresponding to the consonant transition and vowel regions for each word.

Results and conclusion: Older adults required longer transition durations to identify “wheat” vs. “beat” compared to younger listeners. There was a main effect of aging on phase locking, both to the envelope and to the fine structure. Phase locking was lower in older than in younger adults, and this reduction in phase locking was more pronounced for the word “wheat”, containing the longer consonant transition, than for “beat”. Overall results suggest that decreases in neural representation for sustained stimuli may contribute to perceptual deficits in the identification of words based on consonant transition.

Research was supported by NIH-NIDCD, R21 DC015843-01

PS 251

The Dietary Approaches to Stop Hypertension (DASH) Diet and Risk of Hearing Threshold Decline

Sharon Curhan; Gary Curhan

Brigham and Women’s Hospital/Harvard Medical School

BACKGROUND: Greater adherence to healthful dietary patterns was associated with lower risk of self-reported hearing loss, but the association with risk of audiometric hearing threshold decline has not been evaluated. We examined the association between adherence to the Dietary Approaches to Stop Hypertension (DASH) diet and longitudinal changes in air conduction hearing thresholds among a large cohort of women across the US in the Nurses’; Health Study II (NHS II) substudy, the Conservation of Hearing Study (CHEARS).

METHODS: Longitudinal cohort study among 3,749 women (mean age 56.6 (SD 4.4) years) who were

participants in the CHEARS Audiology Assessment Arm and who reported their hearing was excellent, very good, or they had a little trouble hearing at baseline. Usual diet was assessed using food frequency questionnaires administered in 1991 and every 4 years thereafter, from which we calculated DASH adherence scores. We established 19 geographically diverse Testing Sites that followed our rigorous research protocol and completed baseline testing on 3749 participants and 3-year follow-up testing on 3136 participants (84%). Characteristics of participants did not differ appreciably from the full NHS II cohort. Pure-tone audiometry measuring air and bone conduction thresholds was performed for each ear for standard frequencies (500 Hz to 8000 Hz), using sound booths and equipment calibrated to meet current ANSI standards. Baseline and updated covariate information obtained from validated biennial questionnaires was used in Cox proportional hazards regression models to examine the independent associations between cumulative average DASH scores and risk of ≥ 5 dB decline in mid-frequency (PTA(3,4 kHz)) or high-frequency (PTA(6,8 kHz)) hearing thresholds.

RESULTS: At 3-year follow-up, 1197 cases of mid-frequency and 1537 cases of high-frequency PTA decline were identified. Higher DASH scores were inversely associated with risk of hearing decline (see Table). For women with scores in the highest quintile of DASH score compared with lowest quintile, the multivariable-adjusted relative risk (MVRR) of mid-frequency PTA decline ≥ 5 dB was 0.76 (95% CI 0.60,0.97)(p-trend 0.01) and of high-frequency PTA decline ≥ 5 dB was 0.81 (95% CI 0.64,1.02)(p-trend 0.07).

CONCLUSION: In this large longitudinal geographically diverse study among women, a substantial proportion of participants demonstrated 3-year decline in hearing sensitivities. Greater adherence to the DASH diet was significantly and independently associated with lower risk of mid-frequency hearing loss and marginally associated with lower risk of high-frequency hearing loss. Consuming a healthy diet may be helpful in reducing the risk of acquired hearing loss.

DASH Score and Risk of 3-year Mid- and High-frequency PTA Decline¹ ≥ 5 dB Among Women in the Nurses' Health Study II

DASH Score	Quintile 1	Quintile 2	Quintile 3	Quintile 4	Quintile 5	p-trend
Mid-frequency PTA (3,4 kHz)						
Cases	263	245	263	233	213	
Age-adjusted RR (95% CI)	(REF)	0.96 (0.77, 1.21)	1.02 (0.81, 1.28)	0.82 (0.65, 1.03)	0.76 (0.61, 0.96)	0.008
MVRR ² (95% CI)	(REF)	0.96 (0.76, 1.20)	1.02 (0.81, 1.29)	0.84 (0.66, 1.06)	0.76 (0.60, 0.97)	0.01
High-frequency PTA (6,8 kHz)						
Cases	310	318	292	324	284	
Age-adjusted RR (95% CI)	(REF)	1.02 (0.81, 1.27)	0.96 (0.68, 1.07)	0.94 (0.76, 1.18)	0.80 (0.64, 1.00)	0.04
MVRR ² (95% CI)	(REF)	1.02 (0.81, 1.28)	0.87 (0.68, 1.09)	0.96 (0.77, 1.20)	0.81 (0.64, 1.02)	0.07

DASH: Dietary Approaches to Stop Hypertension
PTA: Pure-tone-average

¹Defined as ≥ 5 dB or greater worsening of mid-frequency (PTA (3,4 kHz)) and high-frequency (PTA (6,8 kHz)) hearing thresholds

²MVRR: Multivariate relative risk, adjusted for age, body mass index, waist circumference, physical activity, hypertension, diabetes, baseline PTA, and use of aspirin, ibuprofen, and acetaminophen.

PS 252

Software Application Development and Acoustic Validation of a Sound Field Hearing Screening Tool

Pooja Nair¹; Jamie Shade¹; Anne Feliciano²; Nicholas Reed³; James West¹; J. Tilak Ratnanather¹

¹Johns Hopkins University; ²University of Miami; ³Johns Hopkins Cochlear Center for Hearing and Public Health

Introduction: In the United States, 26.7 million adults over age 50 have a clinically meaningful hearing loss (Chien & Lin, 2012). Hearing loss is associated with communication difficulties, poorer quality of life, and cognitive decline. The American Speech-Language-Hearing Association recommends that adults undergo hearing screenings once per decade prior to the age of 50, and every 3 years thereafter (Moyer, 2012). There is currently no systematic approach for adult hearing screening in the United States. Hospitals represent a potential location for adult hearing screenings. Among the current barriers to universal adult hearing screenings in hospitals is the lack of adequate screening technology. Current hearing screening tools are non-intuitive to use, requiring significant training time. Furthermore, they make contact with patients' skin, resulting in a need for frequent sterilization. Current screening tools also fail to control for ambient noise, which in the hospital environment is variable and often at a considerable volume. Therefore, there is a need for a fast, intuitive, low-contact tool for hearing screening that can be integrated easily into clinical workflow and that accounts for ambient noise.

Methods: A hearing screener prototype, consisting of an Android software application and Bluetooth headphones, was developed. The software application functions as a warble tone generator, as current literature suggests that in comparison with pure tones, warble tones have reduced energy loss over distances (Morgan et al., 1979). In order to determine the optimal warble tone parameters for sound field hearing screenings, the degree to which sound energy was dissipated over a fixed distance for both pure tones and warble tones constructed with different parameters was measured. **Results:** The optimal modulation rate for warble tones was 2/second, as this modulation rate resulted in the least error in base frequency and the greatest decibel level within the relevant modulation range. The modulation range had a relatively insignificant effect on decibel level. In comparison with pure tones, warble tones had significantly less decibel drop-off over distances.

Conclusion: The findings regarding modulation range are inconsistent with existing literature, which suggests that modulation range should significantly impact

decibel drop-off over distances. Warble tones had less decibel drop-off over distances than pure tones, which is consistent with previous findings. In the near future, the use of an ergonomic screener including a software application will enable effective hearing screenings in sound field.

PS 253

Aging Effects on the Auditory Evoked Cortical Potentials in Cochlear-Implant Users: The Role of Stimulus Presentation Rate

Zilong Xie¹; Olga A. Stakhovskaya¹; Matthew Goupell²; Samira Anderson³

¹*Department of Hearing and Speech Sciences, University of Maryland, College Park;* ²*University of Maryland;* ³*Department of Hearing and Speech Sciences, University of Maryland; Neuroscience and Cognitive Science Program, University of Maryland*

Introduction

Cochlear-implant (CI) usage is increasing among the aging population. Aging is associated with degraded cortical processing of time-varying speech cues. The extent to which aging affects cortical temporal processing in CI users, however, remains understudied. Prior work suggests that aging effects on cortical temporal processing may depend on the rate of stimulus presentation, such that the age-related deficit in cortical temporal processing may only occur at fast stimulus presentation rates. Therefore, the current study aims to examine aging effects on the cortical processing of speech signals in CI users, and the extent to which such aging effects are influenced by stimulus presentation rate.

Methods

A 510-ms speech syllable /da/ and a 510-ms, 1000-Hz pure tone were used to elicit cortical evoked potentials in younger CI (YCI) and older CI (OCI) users. To manipulate stimulus presentation rates, each stimulus was presented in randomized blocks with interstimulus intervals (ISI) of 500, 1000, 2000, 3000, or 4000 ms (fast to slow presentation rate). The stimuli were presented to the self-reported better ear via direct audio input to the sound processor at a comfortable listening level. The evoked responses were acquired using a Biosemi 32-channel recording system and referenced off-line to the earlobe contralateral to the stimulation ear. The direct-current (DC) artifact produced by the CI was removed using multivariate regression analysis.

Results

Preliminary results from one YCI and three OCI participants revealed a salient P1-N1-P2 complex for both stimuli following removal of the DC artifact. The

amplitudes of cortical peaks (e.g., N1 and P2) increased with slower stimulus presentation rates (i.e., longer ISIs). The latencies of cortical peaks (e.g., N1 and P2) in responses to the speech syllable /da/ were delayed in comparison to the responses to the pure tone across stimulus presentation rates. We plan to collect data from fifteen YCI and fifteen OCI participants to determine if there is an interaction between the effects of aging and stimulus presentation rate on the auditory cortical responses in CI users.

Discussion

Human CIs provide a unique approach to investigate aging effects on cortical temporal processing by minimizing some of the confounding effects from factors related to age-related changes in the auditory periphery. Critically, findings from this study may inform future CIs studies concerning age-related differences in cortical responses to avoid the confound of stimulus presentation rate effects.

[Research supported by NIH/NIA grant R01 AG051603.]

Temporal Bone Pathology & Histology

PS 254

Comparisons of Methods to Improve Immunofluorescence Staining of Human Temporal Bone Samples

Sumana Ghosh; Mark Lewis; Bradley J. Walters
UMMC

To increase confidence in the translational relevance of functional studies in rodents and other animal models, it is important to verify patterns of gene and protein expression in human samples. Human cochleae reside in thick temporal bones which impose a significant challenge for accessing the delicate sensory tissue for immunohistochemical studies. In the current study we compared two methods of decalcification of human temporal bones. We used hydrochloric acid-based solution RDO and traditional EDTA mediated decalcification in formalin fixed samples. The primary aim of the study was to investigate if there was any difference in immune labelling between these methods. We also examined the effects of different signal enhancers to mask the background and improve signal to noise ratio in the samples exposed to fixative for prolonged times. Cadavers were embalmed with a mixture of formalin and glutaraldehyde and stored at 4 degrees Celsius and then immersed in formalin in anatomy tables and maintained at ~20 degrees Celsius for use in medical anatomy education. Following completion of a course (~3 - 6 months), temporal bones were collected. The tissue samples were then

decalcified using either (1) immersion in RDO for two days followed by removal of extraneous bone to reveal the otic capsule, followed by 0.5M EDTA for 3-5 additional days, or (2) decalcification by 0.5MEDTA only for 4- 6 weeks at room temperature, where extraneous bone was dissected away each week and EDTA solution was replaced twice weekly. Cryosections of decalcified cochleae were subjected to various additional treatment steps such as antigen retrieval by low pH citrate buffer, increasing concentrations of triton-X, tissue sonication, treatment with 0.3% hydrogen peroxide, incubation in 0.3M glycine, and/or treatment with Image-It FX signal enhancer. Sections were covered with primary antibodies overnight at 4 degrees Celsius, washed several times and then Alexa fluor conjugated secondary antibodies were then added for 2-3hrs at room temperature. Tissue sections were imaged using a Nikon C2 confocal microscope. We found that RDO significantly accelerates the decalcification process compared to use of EDTA alone. Moreover, our preliminary data also indicate that there is no significant difference in the immunolabelling of cytoplasmic or membrane bound proteins (e.g. oncomodulin and prestin) between these two methods. Treatment of tissue samples with Image-iT FX signal enhancer noticeably increased the signal to background ratio while hydrogen peroxide and permeabilization by sonication modestly improved the labeling of nuclear proteins such as GATA3.

PS 255

Changes to the Vestibular Peripheral System Following Head Injury: A Human Otopathologic Study

Renata M. Knoll¹; Reuven Ishai²; Danielle R. Trakimas³; David Jung⁴; Joseph B. Nadol⁵; Aaron K. Remenschneider⁶; Elliott D. Kozin⁷

¹Department of Otolaryngology, Harvard Medical School/Massachusetts Eye and Ear; ²Otopathology Laboratory, Department of Otolaryngology, Massachusetts Eye and Ear; ³University of Massachusetts Medical School; Massachusetts Eye and Ear Infirmary; Department of Otolaryngology, Harvard Medical School; ⁴Department of Otolaryngology, Harvard Medical School/ Massachusetts Eye and Ear; ⁵Massachusetts Eye and Ear Infirmary / Harvard Medical School; ⁶Department of Otolaryngology, University of Massachusetts Medical School; Massachusetts Eye and Ear Infirmary; Department of Otolaryngology, Harvard Medical School; ⁷Massachusetts Eye and Ear Infirmary; Department of Otolaryngology, Harvard Medical School

Background: Head injury is a major public health concern. It is estimated that more than 5.3 million individuals in the United States live with a head injury-

related disability. Vestibular dysfunction has long been recognized as one of the possible sequelae of head injury. However, while the clinical findings of dizziness, disequilibrium, and vertigo after head injury are well described, less is known about the pathophysiology of vestibular dysfunction. Herein, we aim to use human otopathologic techniques to analyze the histopathology of the peripheral vestibular system in patients with a history of head injury.

Methods: Specimens from the National Temporal Bone Pathology Registry with history of head injury with or without temporal bone fracture (TBF) were included. Cases were categorized into TBF (Group A), and no evidence of fracture (Group B). Specimens were evaluated for qualitative and quantitative characteristics, such as number of Scarpa ganglion cells (ScGC) in the superior and inferior vestibular nerves, vestibular hair cells (HC) and/or dendrites degeneration in vestibular end organs, presence of vestibular hydrops and obstruction of the endolymphatic duct. Cases were compared to age-matched controls (Group C) without history of head injury.

Results: Fourteen temporal bones (TBs) corresponding to 10 cases were identified. Five TBs had evidence of TBF (Group A) while 9 TBs had no evidence of fracture (Group B). Group A demonstrated severe degeneration of the vestibular membranous labyrinth in the semicircular canals (60%, n= 3TB), and mild to severe degeneration of the maculae utriculi and sacculi (60%, n= 3TB). Group B showed moderate to severe degeneration of the vestibular membranous labyrinth in the semicircular canals (44%, n= 4TB), and moderate to severe degeneration of the maculae utriculi and sacculi (22%, n= 2TB). Vestibular hydrops was present in Group A (40%, n= 2TB) and Group B (22%, n= 2TB). Blockage of the endolymphatic duct was identified in Group A (60%, n= 3TB) and Group B (11%, n= 1TB). There were a 52.6% and 40.3% in the mean total ScGC count compared to age-matched controls (n=7) for Group A and B, respectively (p=0.036, and p=0.001).

Conclusions: This is the first histopathological study of human temporal bones to examine the vestibular system in patients with a history of head injury with and without temporal bone fractures. Otopathological analysis in patients with history of head injury demonstrated distinct peripheral vestibular pathology, including reduction of ScGC even in cases without TBF.

Otopathologic Changes in the Cochlea Following Head Injury with and without Temporal Bone Fracture

Reuven Ishai¹; Renata M. Knoll²; Danielle R. Trakimas³; David Jung⁴; Joseph B. Nadol⁵; Aaron K. Remenschneider⁶; Elliott D. Kozin⁷

¹Otopathology Laboratory, Department of Otolaryngology, Massachusetts Eye and Ear, Boston, Massachusetts, USA; ²Department of Otolaryngology, Harvard Medical School/Massachusetts Eye and Ear ³University of Massachusetts Medical School; Massachusetts Eye and Ear Infirmary; Department of Otolaryngology, Harvard Medical School; ⁴Department of Otolaryngology, Harvard Medical School/ Massachusetts Eye and Ear; ⁵Massachusetts Eye and Ear Infirmary / Harvard Medical School; ⁶Department of Otolaryngology, University of Massachusetts Medical School; Massachusetts Eye and Ear Infirmary; Department of Otolaryngology, Harvard Medical School; ⁷Massachusetts Eye and Ear Infirmary; Department of Otolaryngology, Harvard Medical School

Background: Head injury is a major worldwide cause of death and disability. In the United States, around 2.5 million Americans sustain head injury every year, resulting in 235,000 hospitalizations and 2.8 million visits to the emergency room. Auditory disturbance has long been recognized as one of the possible consequences of head injury. The prevalence of audiovestibular problems following head injury is estimated to occur in up to 80% of patients. The terms “labyrinthine concussion”, “inner ear concussion”, “commotion labyrinthitis”, have been used in the literature since the era of Politzer. Pathologic understanding of “inner ear concussions”, however, is limited. Herein, we aim to evaluate the inner ear of patients who sustained head trauma to better understand the associated histopathology that may give rise to auditory dysfunction.

Methods: Subjects from the National Temporal Bone Pathology Registry with history of temporal bone fracture (TBF) (Group A) and without TBF (Group B) were included. Cases with history of other otologic disorders and/or ear surgery, which may result in hearing loss were excluded. The cochleae were evaluated by light microscopy including count of spiral ganglion cells (SGC), hair cells (HC), health of stria vascularis (SV) and the presence of endolymphatic hydrops(EH) was evaluated. SGC counts were compared to age-matched controls.

Results: Twelve TBs corresponding to nine cases met inclusion criteria. Four TBs had evidence of TBF (Group A) while eight TBs had no evidence of fracture (Group

B). All cases had evidence of inner ear pathology, and nine of the twelve (75%) cases had decreased number of SGC. In Group A and B, the mean SGC loss was 69.6% (range 39.8 to 87.0%) and 59.0% (range 33.8 to 77.3%) compared to age-matched controls ($p=0.007$ and $p=0.002$, respectively). Group A demonstrated severe degeneration of HC in all four (100%) cases, and Group B demonstrated severe degeneration in two (25%) cases and moderate degeneration in six (75%) cases. Group A cases presented with moderate-severe to severe atrophy of SV in 75% cases, compared to 62% cases in Group B. Group A had cochlear EH in three (75%) cases compared to 38% in Group B.

Conclusions: Otopathological analysis in patients with a history of head injury illustrate significant cochlear pathology, even in the absence of TBF. These findings have implications for understanding the mechanisms of hearing loss and unrecognized auditory pathology in patients following head injury.

PS 257

Congenital Middle Ear Cholesteatoma Associated with Isolated Congenital Ossicular Anomalies

Meng Zhao; Jing Yu; Xin-Wei Wang; Xiao-Qing Qian; Ya-Sheng Yuan; Fang-Lu Chi; **Dong-Dong Ren** Affiliated Eye and ENT Hospital, Fudan University

Objective: The present study is aimed to document and analyze the clinical features of congenital middle ear cholesteatoma that is associated with isolated congenital ossicular anomalies.

Methods: The clinical data of ten patients (10 ears) with non-syndromic hearing loss were reviewed retrospectively. All ten patients were diagnosed congenital middle ear cholesteatomas associated with isolated congenital ossicular anomalies. The clinical data included sex, age, symptoms, signs, audiological results, electro-otoscopy, temporal bone computed tomography scan, intraoperative findings, management, pathological findings and follow-up results.

Results: In all ten cases, the cholesteatoma was resided in the postero-superior tympanum. The ossicular anomalies were mainly incus and/or stapes anomalies; seven of them were categorized to Teunissen class IIIa and the other three to Teunissen class IIa. The high-resolution computed tomography (HRCT) revealed seven cases of cholesteatoma and ten cases of ossicular anomalies. In all ten cases, the ossicular chain was reconstructed after removal of the cholesteatoma. In eight of the ten cases, the postoperative hearing function showed improvement. The other two cases missed follow-up contact.

Conclusions: Congenital middle ear cholesteatomas associated with isolated congenital ossicular anomalies is considerably rare. To conduct the reconstruction of the ossicular chain and the removal of the cholesteatoma at the same time is an appropriate surgical approach to resolve the pathological situation.

Key Words: Congenital cholesteatoma; congenital ossicular anomalies; ossicular chain reconstructed; surgical treatment.

PS 258

Characterizing Chemotherapy-induced Dysgeusia in a Mouse Model

Carlos Green¹; Stephen Roper²

¹University of Miami Department of Otolaryngology;

²University of Miami Department of Physiology and Biophysics

Platinum-based chemotherapeutic agents such as cisplatin are commonly used as part of the primary treatment regimen for many cancers including gastric, testicular, lung and head and neck cancers. However, these agents cause the under-appreciated side effect of dysgeusia resulting in reduced appetite, reduced nutritional intake, and poor quality of life. Here, we aim to characterize the acute and chronic effects of cisplatin on taste in mice—specifically sweet and bitter—in order to develop an animal model to test therapies to prevent or reduce chemotherapy-induced dysgeusia. We hypothesize that cisplatin treatment will produce acute and chronic changes in taste behavior and in taste buds in mice and that the mouse will be an effective animal model for chemotherapy-induced taste dysfunction. To test our hypothesis, we are employing brief access taste tests using apparatus that controls the presentation of taste stimuli and monitors the licking responses of mice. We measure the threshold and concentration-response relations for licking behavior elicited by a prototypical sweet (sucrose) or bitter (quinine hydrochloride) stimulus, before and after injecting mice with cisplatin or saline (sham control). Moving forward, we will further characterize the effects of cisplatin at the level of the taste bud using immunohistochemistry to quantify and qualify changes in the cells that are responsible for detecting sweet and bitter taste, namely type 2 taste cells. Additionally, we will employ in vivo confocal Ca²⁺ imaging to record neuronal activity in the geniculate ganglion of transgenic mice that express GCaMP3 in sensory neurons. This will allow us to characterize the effects of cisplatin at the level of the geniculate ganglion in response to sweet and bitter stimuli applied via oral lavage. Here, we present the animal model and validated

methods for studying taste changes that may be applied to various therapies and procedures, and thus helpful in elucidating mechanisms and therapeutic interventions for chemotherapy-induced dysgeusia.

PS 259

The Prevalence of Hearing Loss Among Infants with In Utero Zika Virus Exposure

Megan Ballard; Xue Z. Liu

University of Miami

Zika virus (ZIKV) has been an evolving global public health crisis since 2015. In adults, ZIKV most often is an innocuous viral illness, symptomatically manifesting as mild flu-like symptoms; however, for the developing fetus, the teratogenic effects are devastating. Intrauterine ZIKV exposure is much more detrimental to the developing fetus, resulting in a wide spectrum of neurologic deficits known as Congenital Zika Virus Syndrome. Given the unknown severity of hearing loss or long-term behavior of the virus, we sought out to determine the incidence and characteristics of congenital hearing loss associated with ZIKV. We hypothesized that both symptomatic and asymptomatic Zika exposed infants are at increased risk of hearing loss compared to healthy infants. Our research design was a prospective longitudinal study. We combined our Miami population of ZIKV exposed infants with the Brazilian groups of Universidade de Federal de Pernambuco and the Federal University of Rio Grande do Norte. Pregnant mothers and their babies after delivery underwent ZIKV laboratory testing for enrollment. All infants had screening auditory brainstem response testing and then continued testing at 6 month intervals. We found that the incidence of sensorineural hearing loss among infants with in utero Zika Virus exposure was much higher than the general population. The combined prevalence of hearing loss at the University of Miami, Hospital Agamenon Magalhaes and Hospital of Rio Grande do Norte was 5.1% (6.3%, 5%, 4.2% respectively) compared to the known incidence of 0.1% reported in the general population. We conclude that in utero zika virus exposure does increase the risk of hearing loss among infants. So that we may provide proper assistance to affected infants, further studies are needed for characterization of the effects of the virus on the developing auditory system as well as its patterns throughout development.

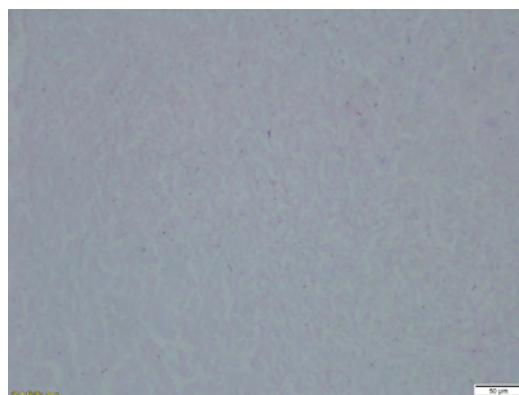
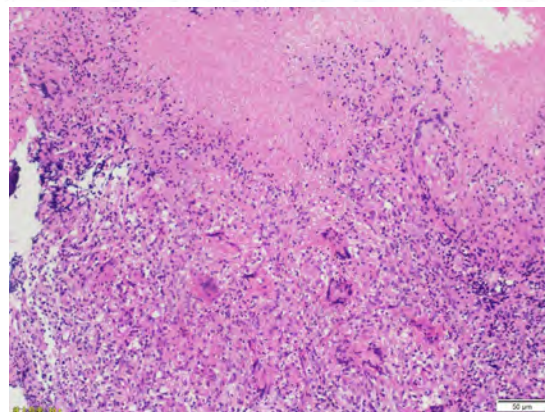
Tuberculous otitis media and mastoiditis without lung involvement in a 3-month-old baby girl-A case Report

Feng Bo¹; Liao Ka-xi¹; Dai Pu¹; Wang Guo-Jian¹; Shi-ming Yang²; Peng Tao³; Feng Hui-Qiong³
¹Department of Otolaryngology-Head and Neck Surgery & Institute of Otolaryngology, Chinese PLA General Hospital; ²PLA General Hospital; ³Department of Otolaryngology-Head and Neck Surgery, Nanchong Central Hospital, The second affiliated hospital of North Sichuan Medical College.

Introduction: Tuberculous otitis media (TOM)/mastoiditis is an uncommon disease, which usually encountered in the pediatric age group. Its main manifestation is chronic ear drainage and generally it occurs unilaterally. The infection often disseminates directly through adjacent organs via the Eustachian tube (i.e. the lungs, larynx, pharynx and nose), or through haematogenous spread from other primary sites. TOM is polymorphic, insidious condition. Due to the entity of signs and symptoms are difficult to differentiate from nontuberculous chronic otitis media, it is frequently delayed and misdiagnosed. Delay of recognition and treatment of TOM may result in serious damage and complications, including hearing loss, facial palsy, intracranial infection and postaural fistula formation. We herein present an infant with otorrhea and a lump in front of the antilobium, who was confirmed to have TOM and mastoiditis.

Case report: A 3-month-old baby girl showed unilateral TOM. Her mother infected with pulmonary tuberculosis during pregnancy and was not treated effectively. The baby girl had suffered from chronic intermittent otorrhea in the right ear since 27 days after birth, refractory to conventional medical therapy. And two weeks before admission, she was found to have a lump in front of the right antilobium. Otoscopic examination revealed small perforation of the tympanic membrane and swollen mucosa with purulent discharge, and normal left ear. In addition, there was nothing be found in her chest X-ray while CT scan of the temporal bone demonstrated middle ear cavity and mastoid cavity along with soft tissue attenuation, also defect of the right temporal bone. The baby girl underwent radical mastoidectomy subsequently, which showed purulent secretion and inflammatory granulation tissue in the right mastoid cavity. The pathologic findings revealed necrotic debris and granuloma formation, acid-fast stain (+) and PAS(-), which was considered as tuberculosis. She is now receiving antituberculous chemotherapy (rifampicin, isoniazid and pyrazinamide-after operation). The symptoms of her right ear were obviously relieved and the wound healed well in the recent follow-ups.

Conclusion: Infants with tuberculosis generally have no typical history, so it is necessary to exclude whether their parents have past histories related to tuberculosis infection or not. In this case, the baby girl with TOM was secondary to her mother's pulmonary tuberculosis infection during pregnancy. Patients of TOM can classically be presented with multiple perforations of the tympanic membrane, massive purulent secretion. If a patient manifests with otitis media or otorrhea that does not respond to conventional therapy, TOM should be considered. Pathologic evidences are increasingly taking an important place in the diagnosis since biomolecular techniques are now available to diagnose tuberculosis as early as possible to avoid unnecessary treatment and sequelae. Treatments consist of effective systemic antitubercular therapy and early surgical intervention have dramatically improved the prognosis.



Evaluation of Rapid Decalcification Methods for Histological Assessment of Rodent Temporal Bones

Anne Harrop-Jones; Jeremy Barden; Fabrice Piu;

Bonnie Jacques

¹*Otonomy, Inc.*

Background: Histological assessment of inner and middle ear tissues requires extensive decalcification in order to sufficiently soften the dense bone for histological assessment. Traditional methods for decalcifying rodent temporal bones can take from 2 to 12 weeks, depending on the species, to be soft enough for fine sectioning. The recent growing interest in therapeutic development for ear-related disorders as well as basic otolaryngological research has created the need for more rapid histopathological and morphological assessment. Here we evaluated several different methods of temporal bone decalcification to identify an optimized protocol that minimizes processing time without compromising the quality of the histological evaluation.

Methods: Temporal bones from adult female Sprague-Dawley rats (200-350 g) were used for all experiments. Deeply anesthetized rats were perfused with PBS and 4% PFA; isolated temporal bones were then post fixed for up to 3 days. Temporal bones were placed into 10% disodium EDTA or 10% tetrasodium EDTA at room temperature or in a Pelco Biowave system. Surgipath Decalcifier I and RapidCal were both evaluated at room temperature for 72 hours or 24-48 hours, respectively. The time required for sufficient decalcification to enable paraffin sectioning was determined for each decalcification method. Sections from various regions of the inner, middle and outer ear from each of the decalcification protocols were then analyzed by H&E staining and fluorescent immunohistochemistry for tissue quality and antigenicity.

Results: Commonly used 10% disodium EDTA required about 2-3 weeks for decalcification of rat temporal bones when used in conjunction with a microwave system. In contrast, tetrasodium EDTA sufficiently decalcified rat temporal bones in 2 weeks at room temperature; however, the use of a Biowave did not substantially reduce this time. Among the acidic decalcifying agents that were tested at room temperature, incubation in Surgipath Decalcifier I for 72 hours did not result in sufficient decalcification for sectioning, whereas RapidCal had the shortest processing time of 24-48 hours for complete decalcification of rat temporal bones. Tissues processed with RapidCal retained all histological structures and produced sections of good quality, and both H&E and fluorescent immunostaining appeared normal. However, fluorescent nuclear counter-stains were quenched and

could not be evaluated due to the highly acidic treatment.

Conclusions: RapidCal is the fastest method for safely decalcifying temporal bone tissue while retaining antigenicity, tissue quality and the ability to perform histopathological assessments. Non-acidic decalcifying agents should be used if nuclear counter-stains are required.

PS 262

Cellular Consequences of Zika Virus Infection on the Cochlea in a Mouse Model

Kathleen T. Yee¹; Biswas Neupane²; Amber M. Paul²; Fengwei Bai²; Douglas E. Vetter¹

¹*Dept. of Neurobiology and Anatomical Sciences, University of Mississippi Medical Center;* ²*Dept. of Cell and Molecular Biology, University of Southern Mississippi*

Introduction: An emerging and significant concern for human health in the United States is that Zika virus (ZIKV)-carrying mosquitoes have been detected in various southern states. Prenatal ZIKV infection is a well-known risk factor for developmental defects, including microcephaly. Emerging evidence indicates that both prenatal and postnatal ZIKV infection can alter hearing, and ZIKV infection in adults has been reported to produce transient hearing loss. However, little is known about the underlying etiology leading to ZIKV caused hearing dysfunction. There is no data on the effects of ZIKV infection on the cochlea at the cellular level. We report here the morphological consequences to the cochlea following pre- and postnatal ZIKV infection.

Methods: Two ZIKV infection paradigms were employed: 1) Prenatal infection- pregnant dams (C57BL/6j) were infected with ZIKV (embryonic day 8), and pups survived for 3 months, 2) Postnatal infection- 5-6 week old mice (INFAR1-/- on a C57BL/6j background) were infected and survived for 9 days. Mice were perfused (4% paraformaldehyde), temporal bones were isolated and prepared for wholmount processing or cryostat sectioning. Wholmount preparations were immunostained for afferent presynaptic ribbons (CtBP2) and postsynaptic receptors (GluA2). Cryostat sectioned material was stained with hematoxylin and eosin (H&E) or immunostained with primary antibodies 4G2, AQP1, S100b, F4/80 or endothelial nitric oxide synthase (eNos). Immunofluorescence was visualized using confocal microscopy.

Results: Prenatal infection- Regions of the spiral ligament were H&E stain-sparse. Immunostaining revealed more

unpaired hair cell ribbons and glutamate A receptors compared to controls.

Postnatal infection- At 9 days following infection, the ZIKV envelope protein, revealed by 4G2 antibody, was detected in support cells indicating presence of virus at this time point. S100b, a damage associated molecular pattern molecule is upregulated in support cells and the spiral ligament. The aquaporin 1 (AQP1) water channel is upregulated in the spiral ligament and stria vascularis. A molecule, eNOS, highly expressed in degenerative states is upregulated in blood vessels, the spiral ligament, spiral ganglion and auditory nerve. The macrophage marker F4/80 is upregulated by cells in a region previously shown to harbor immune system cells following cochlear insult.

Conclusions: ZIKV infects the cochlea. Infection alters expression levels of AQP1 in the lateral wall, damage-associated molecules in the cochlea and lateral wall, and immune markers for macrophages. These findings indicate that cochlear function is likely compromised following both prenatal and postnatal ZIKV infection. Future experiments will address this notion.

Support: R21DC015124 (DEV), P30GM103328 (Confocal Imaging Core, UMMC)

PS 263

Osteoclastic activity in the human temporal bone - Possible relevance to dehiscence of the superior semicircular canal (SSCD)

Takefumi Kamakura¹; Joseph B. Nadol²
¹*Otemae Hospital*; ²*Massachusetts Eye and Ear Infirmary / Harvard Medical School*

Backgrounds: Bone remodeling within the otic capsule has been reported to be inhibited especially at or near the cochlea, except under some pathological conditions such as otosclerosis, Paget's disease, or mastoiditis. Microcavitations found in periosteal and endosteal layers of human temporal bone specimens without otosclerosis, Paget's disease, or inflammation as reported in the current study are consistent with osteoclastic bone resorption.

Materials and Methods: Thirty-three temporal bones from thirty-three patients were prepared for light microscopy, and classified into four groups: three temporal bones with histologically proven dehiscence of the superior semicircular canal (SSCD) (Group 1); ten with an age of 20 years or younger (Group 2); ten with an age of 90 years or older and with otosclerosis (Group 3); ten with an age of 90 years or older without

otosclerosis (Group 4). The degree of microcavitation at the endosteal and periosteal surfaces of the temporal bone at nine anatomic locations were assessed using a semiquantitative grading system.

Results: Various degrees of microcavitation were seen at nine anatomic locations in the temporal bone in all four groups. The average score of Group 1 tended to be higher than that of the other three groups for the total scores across all nine locations, for the middle fossa cranial base, and for the three semicircular canals, but did not reach statistical significance.

Conclusions: Microcavitation within the temporal bone is likely due to osteoclastic activity, and is seen in both young and old patients, especially in cases with SSCD. Osteoclastic resorption of the bone at the middle fossa base and in the superior semicircular canals may play a role in the development of SSCD.

PS 264

Expression of advanced glycation end-product in the cultured utricles

Kazuma Sugahara; Yoshinobu Hirose; Makoto Hashimoto; Shunsuke Tarumoto; Hiroshi Yamashita
Department of Otolaryngology, Yamaguchi University Graduate School of Medicine

Introduction

It is known that the prevalence of hearing loss is high in the patients with diabetes. In the last meeting, we presented that the model mice of metabolic syndrome showed the progressive hearing loss with an obesity and hyperlipidemia, high blood pressure. Advanced glycation end products (AGEs) are proteins or lipids that become glycated after exposure to sugars. AGEs are prevalent in the diabetic vasculature and contribute to the development of atherosclerosis. We have shown that the formation of AGEs in the inner ear plays an important role in the progressive hearing loss with diabetes.

In the present study, we tried the formation of AGEs in the inner ear tissue with in vitro model.

Materials and Methods

Cultured utricles of CBA/N mice were used. The utricles were divided to 2 groups (Control group, High glucose group). In the high glucose group, utricles were cultured with glucose (60 mM). Five days after exposure to glucose, the cultured tissues were fixed with 4% paraformaldehyde. To evaluate the expression of AGEs, immunohistochemistry was performed using anti-AGEs antibody. In addition, the immunohistochemistry with anti-calmodulin antibody could label the hair cells. The signal intensity was evaluated with the fluorescence microscope.

Results

The signal intensity of immunohistochemistry against AGEs were stronger in the high glucose group than in the control group. The formation of AGEs was observed in the whole cultured utricles, not hair cell specific. The hair cell degeneration was not observed in both groups.

Discussion

The results suggested that the inner ear tissues exposed to high concentration glucose accumulate AGEs. This phenomenon has not been reported in the past. AGE is closely related to the tissue damage in the patients with diabetes. The relationship between inner ear damage and AGE formation have been unknown. However, I would like to clarify the role of AGE in inner ear disorders.

PS 265

Degeneration of the neuroepithelium of the cristae ampullares and a thickened subepithelial extracellular deposit in the human.

Tadao Okayasu¹; Jennifer T. O'Malley²; Joseph B. Nadol¹

¹Massachusetts Eye and Ear Infirmary / Harvard Medical School; ²Dept. of Otolaryngology, Mass. Eye and Ear

Background: Recently, we reported a unique pattern of degeneration of the neuroepithelium of the cristae ampullares with a thickened subepithelial extracellular deposit in three human subjects. However, the cause of the unique pattern of degeneration of the neuroepithelium with a thickened subepithelial extracellular deposit is not known. Because a thickened deposit was present bilaterally in all three cristae, age was considered as a possible causative factor. Therefore, we compared the thickness of the subepithelial extracellular deposits in age-matched controls.

Objective: The purpose of this otopathologic study was to characterize the vestibular degeneration, to measure the thickness of the subepithelial deposits, and to evaluate the effect of age.

Methods: The subepithelial deposits of the vestibular end organs of the three subjects cases were studied using H&E, PAS and Gomori trichrome staining. Immunostaining for anti-collagen 4a1 was also done. The thickness of deposit as measured by light microscopy was compared to that of age-matched controls. In addition, the correlation of thickness of deposits with age from 0-100 years in 111 humans was investigated.

Results: Thickened subepithelial deposits were found in all three cristae of the three study cases. Immunostaining

demonstrated that the basement membrane was distinguishable from the subepithelial deposit and fragmented in the area near the summit of the crista. The thickness of the subepithelial deposits in the three cristae of the three study cases was significantly greater than that of age-matched controls. In the three cristae of normal controls, the thickness of deposits demonstrated a positive correlation with age.

Conclusion: Our results demonstrated that age may be associated with the thickness of the subepithelial deposits in this unique pattern of degeneration.



Tinnitus & Hearing Loss: Clinical Studies

PS 266

No Evidence for Anti-Retroviral Drug Effects on Audiometric Thresholds or Otoacoustic Emissions in HIV Positive Individuals

Abigail Fellows¹; Albert Magohe²; Jiang Gui³; Enica Massawe⁴; Ndeserua Moshi⁴; Jay Buckey¹

¹Space Medicine Innovations Laboratory; ²Dar Dar Health Study, Muhimbili University of Health And Allied Sciences; ³Biomedical Data Science; ⁴Otorhinolaryngology

Background: Human immunodeficiency virus positive (HIV+) individuals complain of hearing problems. In our previous cross-sectional study in Tanzania, we demonstrated lower average distortion product otoacoustic emission (DPOAE) levels in HIV+ adults on anti-retroviral therapy (ART) compared to an HIV-group. These findings could reflect an effect of ART on the cochlea, or could be due to other factors, such as inadequate matching between the HIV- and HIV+ groups or greater disease severity in those individuals where ART was started. To assess the effects of ART on

DPOAE amplitude and audiometric thresholds we have been following a cohort of HIV+ subjects in Tanzania longitudinally. If ART were affecting the cochlea we expected to see reduced DPOAE amplitudes and worsening audiometric thresholds after starting ART.

Methods: As part of an overall study following HIV+ patients and a HIV- control group longitudinally, HIV+ individuals had an auditory evaluation including audiometric thresholds and DPOAEs at each visit. Visits were scheduled for 6-month intervals, but the number and spacing of follow up visits varied. In the group that started ART while in the study, 214 HIV+ individuals had longitudinal audiometric thresholds and 202 had longitudinal DPOAE measurements suitable for analysis. The repeated measurements were analyzed with a linear mixed model with time and starting ART as fixed effects and individual subject repeated measures as random effects.

Results: The slope of the DPOAE amplitude/time relationship was negative and significantly different from zero ($p < 0.001$) indicating that DPOAE amplitudes decreased significantly over time. The slope of this relationship changed significantly ($p < 0.001$), but direction was toward a less negative slope (i.e. a slowing of the gradual reduction of DPOAE amplitude over time). The slope of the audiometric threshold/time relationship was not significantly different from zero, and there was no significant interaction between starting ART and changes in audiometric thresholds.

Conclusions: Longitudinal data show no evidence for an effect of starting ART on either DPOAE amplitudes or audiometric thresholds suggesting common ART drugs are not major ototoxins. Other results from the study show effects on central auditory processing, suggesting the origin of the hearing complaints may be in the central auditory system.

PS 267

Sound Exposure and Hearing Problems in Non-Classical Musicians

Agnete T. Hoffmann-Petersen¹; Helene M. Paarup²; Jesper Baelum³; Søren Möller⁴; Jesper Hvass Schmidt⁵

¹Department of ORL Head and Neck Surgery and Audiology, Odense University Hospital. Institute of Clinical Research, University of Southern Denmark. Odense Patient data Explorative Network (OPEN), Odense University Hospital; ²Department of Clinical Immunology, Odense University Hospital; ³Institute of Clinical Research, University of Southern Denmark. Department of Occupational and Environmental

Medicine, Odense University Hospital; ⁴Institute of Clinical Research, University of Southern Denmark. Odense Patient data Explorative Network (OPEN), Odense University Hospital; ⁵Dept. of Otolaryngology, Head and Neck Surgery and Audiology, Odense University Hospital, Denmark. Dept. of Clinical Research, University of Southern Denmark, Odense, Denmark. Odense Patient data Explorative Network (OPEN), Region of Southern Denmark

Background: Existing literature on sound exposure and hearing in non-classical musicians is sparse compared to the amount of studies concerning classical musicians. This study aims to investigate the association between sound exposure and hearing problems in professional rock, pop and jazz musicians. Additionally, Distortion Product Otoacoustic Emissions (DPOAE) and Transient-Evoked Otoacoustic Emissions (TEOAE) are assessed as early detection tools for noise induced hearing loss in non-classical musicians.

Methods: In this cross-sectional study, measurements on 82 professional non-classical musicians were carried out at venues and rehearsal rooms in Denmark. Binaural sound level measurements, DPOAE and TEOAE were conducted during solitary practice, band practice and concerts, and differences in hearing before and after exposure to music was evaluated. Additionally, questionnaires from 645 musicians in total were collected in order to estimate lifetime sound exposure and hearing problem prevalence.

Results: All musicians were exposed to sound levels, Leq > 90.3 dBA, which was influenced by instrument type, genre, type of event and band size. The highest Leq of 103.5 dBA and Lpeakmax of 130.6 dBC was found among drummers and percussionists. The lowest Leq of 90.3 dBA and Lpeakmax of 119.7 dBC was found among acoustic strings. Rock musicians were exposed to an Leq of 105.2 dBA, which was 10.3 dB higher than jazz musicians. The sound at concerts was 7.8 dB louder than at solitary practice. Regarding DPOAE, the SNR at 3000 Hz, 4000 Hz and 6000 Hz, especially, was reduced binaurally after music exposure. TEOAE did not show reduced otoacoustic emissions after music exposure. High prevalences of hearing disorders (hearing loss 40%, tinnitus 46.3%, hyperacusis 26.2% and distortion 5.6%) were found.

Conclusion: Non-classical professional musicians are exposed to sound levels > 90.3 dBA considered to be hearing damaging. Whereas TEOAE did not show reduced otoacoustic emissions after music exposure, DPOAE showed affected hearing at 3000 Hz, 4000 Hz and an absence of otoacoustic emissions at 6000 Hz. A high prevalence of hearing problems was reported.

The prevalence and related factors of bilateral audiometric notches in 11070 Chinese workers

Qixuan Wang; Xu Wu; Lu Yang; Xueling Wang; Zhiwu Huang; Hao Wu
Clinical Audiology

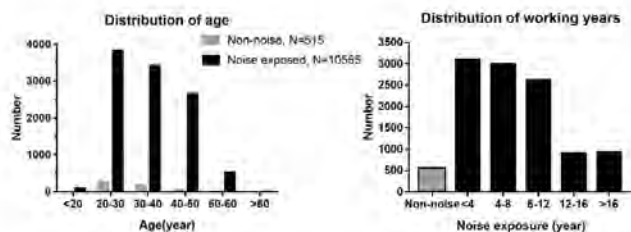
Objective: Noise induced hearing loss(NIHL) is one of the primary occupational diseases around the world, while there is no large epidemiological survey in China. The purpose of this study was to investigate the noise exposure and hearing situations of a large number of Chinese workers, identify the prevalence of bilateral audiometric notches in relation to influencing factors.

Method: This cross-sectional survey was carried out from 2017 to 2018, a total of 11070 workers aged 18-69 years old from the eastern and southern China were included. A face-to-face interview was conducted to collect the following information: general personal information, occupational noise exposure history, history of hearing protector use, personal life habits, and overall health conditions. Pure-tone audiometric testing at frequencies 0.25, 0.5, 1, 2, 3, 4, 6, and 8 kHz was performed in an isolated acoustic room, at least 16 hours after the subject's last occupational noise exposure. Audiograms were analyzed using the algorithm defined by Hoffman et.al to identify bilateral high-frequency audiometric notches, related to gender, age and noise exposure. Statistical analysis was done using SPSS 24.0 version.

Results:10,555 workers (average working year 7.79 ± 0.06 years, average age 34.18 ± 0.09 years old) exposed to 80 – 95 dB(A) occupational noise, and 515 workers without occupational noise exposure (average age 30.82 ± 0.34 years old) were included in this study. The prevalence of bilateral audiometric notch among noise-exposed workers was 34.1% in 9471 males, 12.9% in 1084 females, while 8.7%, 15.7%, 33.7%, 49.6% and 53.8% in aged <20, 20-29, 30-39, 40-49 and 50-59 year-old groups respectively. Among non-noise control workers, the prevalence of bilateral audiometric notch was 4.7% in 379 males, 0.7% in 136 females, while 2.6%, 2.9%, 10% and 8.3% in aged 20-29, 30-39, 40-49 and 50-59 years old group respectively. The differences between groups were statistically significant (p<0.05).

Conclusion: No matter whether exposed to occupational noise or not, the prevalence of bilateral high-frequency audiometric notches was significantly higher in males than females, which increased with age as well. Compared to non-noise exposed workers, the prevalence of bilateral notches in noise exposed workers was considerably higher at any age group, suggesting that the bilateral high-frequency audiometric notches

might be a vital sign of NIHL in China workers, especially in young population. Other potential risk factors of NIHL still need to be studied.



Age group (yrs)	Binaural high frequency auditory notch, %			
	Non-noise		Noise exposed	
	NHANES N=2,360	This study N=515	NHANES N=1,223	This study N=10,555
17-19	/	0.0	/	8.7
20-29	3.6	2.6	5.7	15.7
30-39	3.4	2.9	6.9	33.7
40-49	7.9	10.0	7.4	49.6
50-59	6.1	8.3	11.8	53.8
60-69	/	/	/	60.0
χ ²	/	8.707	/	998.701
P	/	0.069	/	<0.001**

PS 269

Refining the Audiologic Test Battery: Speech-In-Noise Testing Better Predicts Self-perceived Patient Performance

Steven Gianakas; Steven Losorelli; Austin Swanson; Jason Qian; Matthew Fitzgerald
Stanford University

Ideally, the standard audiologic test battery should be sensitive to auditory pathology and address both patient concerns and real-world performance. The conventional audiologic test battery is focused predominately on identification of auditory pathology, and site-of-lesion testing. However, the routine test battery does not address real-world communication abilities, as audiologists do not consistently assess measures of perceived communication ability, or the ability to understand speech in noise (SIN). Thus, there is a disconnect between many patient concerns and routine audiologic testing. Many of these issues could be alleviated if SIN abilities were routinely obtained in audiologic assessment instead of traditional measures of word-recognition in quiet (WRQ). Recent work from our lab indicates that SIN abilities can be used to predict whether a patient has excellent or poor WRQ scores. Here, we explore whether SIN testing is a better predictor of self-perceived patient performance

in comparison to audiometry thresholds and traditional WRQ scores.

Here we report data on over 2000 patients who as part of their audiologic assessment completed pure-tone audiometry, WRQ, the QuickSIN, and the SSQ12. PTA and WRQ are staples of the standard audiologic test battery. The QuickSIN determines the signal-to-noise ratio needed to repeat 50% of key words in low-context sentences. The abbreviated Speech, Spatial and Qualities of Hearing scale (SSQ12) was administered to gauge patient self-perceived ability to communicate in the real-world. The questionnaire contains 12 questions relating to three main subcategories: Speech hearing, Speech Quality, and Localization. Patient self-perceived handicap (SSQ12) was compared with QuickSIN, WRQ, and audiometry thresholds. In addition, we examined the effect of asymmetries in hearing threshold and other demographic variable such as age on SSQ12 scores.

Results demonstrate that most patients have excellent ability to understand speech in quiet but still perceive having difficulty communicating with others according to the SSQ12. In contrast, individuals with deficits understanding speech in noise are likely to have self-reported communication deficits on the SSQ12. It is worth noting that the relationship between SIN performance and SSQ12 was not linear, suggesting that other patient-specific factors such as lifestyle demands may influence perceived handicap. Taken together, these data provide further evidence supporting the addition of self-reported handicap and SIN measures to routine audiologic testing. Making this subtle, but fundamental change to audiologic testing may better equip audiologists with the tools to provide improved patient-centered hearing health care to individuals with hearing loss.

PS 270

Audiological Predictors of Tinnitus in Patients at Massachusetts Eye and Ear

Rebecca M. Lewis¹; Aravindakshan Parthasarathy²; Daniel B. Polley¹

¹*Eaton-Peabody Laboratories, Massachusetts Eye and Ear; Dept. of Otolaryngology, Harvard Medical School;*

²*Department of Otolaryngology, Harvard Medical School; Eaton-Peabody Laboratories, Mass. Eye and Ear Infirmary*

Approximately one in five adults perceives a continuous phantom sound. Chronic subjective tinnitus remains a common reason for visits to the audiology clinic, even though the co-morbidity with hearing loss is heterogeneous and treatment options are limited. To better understand the clinical predictors of tinnitus, we have characterized

the audiograms and clinical presentation of over 20,000 individuals who report tinnitus as the primary reason for their visit to the Mass. Eye and Ear over the last 25 years. Audiometric threshold configurations of these individuals were analyzed, as well as age- and gender-specific incidence rates in this clinical population. We searched for common audiometric configurations: (1) thresholds within normal clinical limits for both ears; (2) flat hearing loss across all thresholds for both ears; (3) hearing loss in the high frequencies alone for both ears; (4) notched configuration, with a point of poorest hearing that is worse than both adjacent frequencies for both ears; (5) unilateral hearing loss, with normal hearing in one ear and hearing loss in the other; and (6) asymmetric hearing loss, with unequal hearing loss in both ears. Our results show that certain audiometric profiles are more common than others in the tinnitus patient population; significantly fewer individuals with tinnitus present with flat or unilateral hearing loss than other audiometric profiles. Tinnitus incidence increases with age until the 5th decade of life, after which age incidence of tinnitus as a primary complaint appears to diminish. While relatively more females report clinically significant tinnitus in their 70s compared to males, males consistently demonstrate greater incidence of tinnitus than females through the late 50s. Clinicians will continue to consider audiometric configuration for each patient with tinnitus to guide clinical recommendations for tinnitus management; stage of life may also be an additional factor to consider. In the future, we aim to better understand the heterogeneity of the tinnitus patient population through detailed physiological and behavioral testing after first taking into account the differences in age and audiometric configurations reported here.

PS 271

Recreational Noise Exposure in Young Adults

Prashant Angara; Hillary Snapp

University of Miami Department of Otolaryngology

Background:

Overexposure to loud sounds can result in permanent hearing damage. Noise-induced hearing loss (NIHL) often presents in the form of high frequency sensorineural hearing loss and tinnitus. Because of the dangers of excessive sound exposure, the National Institute of Occupational Safety and Health has set standards for daily noise exposure based on decibel levels, with louder sound levels assigned more rigorous limits for safe exposure. Research has shown that young adults, defined here onwards as 18 to 30 years of age, are being exposed to dangerous levels of sound as a consequence of their use of personal media devices, and their attendance at concerts, nightclubs and bars

(Gilliver 2013) and a 2017 CDC report found 25% of adults had audiometric profiles suggestive of high-frequency NIHL (Carroll 2017). The purpose of this study was to investigate recreational noise exposure in young adults to determine relative risk for noise induced hearing loss.

Methods

Noise exposure in young adults was investigated using an anonymous survey to undergraduate and medical students at the University of Miami. The survey consisted of 13 questions on recreational noise exposure and common activities that may result exposure to sound doses higher than the accepted annual workplace limit in recreational settings. The most commonly reported recreational settings in the study include nightclubs, bars/pubs, restaurants, fitness classes, and movie theaters. Subjects were also queried on their risk perception of loud sounds, and exposure to loud sounds in their reported recreational activities. Survey data was correlated to objective sound level measurements conducted in the field at representative environments of noise exposure reported by the study population, regional to the survey. Measurements were taken over a 10 minute period.

Results:

115 adults aged 18 to 29 completed the survey. Preliminary data shows 74% of participants experience muffled hearing after visiting a night club or bars. When queried about knowledge of "at risk" exposure, 79% of participants were could not correctly identify the decibel threshold for damage as defined by NIOSH. The majority of participants reported being naïve listeners, as demonstrated by no prior knowledge of NIHL.

PS 272

Pure Tone Audiometry Threshold Changes for 10 Years in the Same Individuals: a Retrospective Cohort Study

Hun Yi Park

Dept. of Otolaryngology, Ajou University School of Medicine

Purpose: The objectives of this study were to measure the changes of the hearing thresholds during 10 years in the same individuals and to suggest a clinical reference for the age-related hearing threshold changes.

Methods: In this retrospective cohort study, we used regular health check-up data including two pure tone audiometries with 10-year interval in the same individuals from 1,288 subjects. The subjects'; data including demographics, smoking habit, and the diagnosis of chronic diseases were used.

Results: Age, male, smoking, and osteoporosis were identified as variables affecting age-related hearing loss. The actual effect of aging on ARHL for 10 years according to age groups and genders were 1.4 dB in 20's, 4.0 in 30's, 5.0 in 40's, 8.2 in 50's, and 11.2 in 60's of males and 2.3 in 20's, 2.9 in 30's, 5.1 in 40's, 6.5 in 50's, and 9.4 in 60's of females.

Conclusions: We could demonstrate the actual effect of aging on age-related hearing loss, and it might be used as a clinical reference. The hearing ability decreased more in male, and the velocity of the aggravation increased not constantly but exponentially along with age in both male and female.

PS 273

Unbiased classification of audiometric phenotypes in the NHANES database

Golbarg Mehraei; Erik Larsen

Decibel Therapeutics

Compact and meaningful descriptions of phenotypic data are helpful for exploratory, descriptive and association studies, especially when dealing with large datasets. The most widely available phenotypic data on hearing function are pure tone thresholds (audiograms), but these are not particularly efficient descriptions. Large-scale studies therefore often extract a small number of features from audiograms, e.g. pure tone average, or presence and type of notches.

In an effort to find more complete ways to analyze hearing data, we conducted an unbiased cluster analysis on audiograms from 11,420 participants using the National Health and Nutrition Examination Survey (NHANES) data from 1999-2012. Our clustering method matches audiograms to one of several prototype shapes. Absolute hearing level and vertical scale are free parameters, adjusted for each audiogram to achieve the best match. This results in each audiogram being classified by the prototype shape identifier.

This process was able to match 94% of audiograms to one of the following five prototype shapes (prevalence % in parentheses):

1. Flat profile (25%)
2. Gradual sloping profile above 2 kHz (31%)
3. Abrupt sloping profile above 4 kHz (22%)
4. Notched profile (11%)
5. Rising low-frequency profile (10%)

Other findings were:

1. Only about 50% of participants have the same

- audiogram prototype shape in both ears
2. Prevalence of prototype shape varies by gender and age
 3. Mean hearing level as a function of age depends strongly on prototype shape

Whether the specific prototype shapes identified here are truly representative will have to be confirmed by independent validation studies. However, this analysis serves as proof of concept that hearing function in a large, representative population sample can be summarized by a relatively small number of parameters, greatly facilitating descriptive and association-type analysis of hearing function and probable etiology. This should benefit both public health and biomedical research applications.

PS 274

Audiometric Characteristics of Blast and Non-blast Patients with Chronic Subjective Tinnitus

Jenny X. Chen¹; Jonathon Whitton²; Aravindakshan Parthasarathy³; Kenneth E. Hancock⁴; Daniel B. Polley⁴
¹Massachusetts Eye and Ear, Harvard Medical School; ²Decibel Therapeutics; ³Department of Otolaryngology, Harvard Medical School; Eaton-Peabody Laboratories, Mass. Eye and Ear Infirmary; ⁴Eaton-Peabody Laboratories, Massachusetts Eye and Ear; Dept. of Otolaryngology, Harvard Medical School

Patients with tinnitus typically undergo a limited battery of audiometric tests that do not fully capture the scope of their symptoms. The sparse and inconsistent characterization of hearing status and tinnitus metrics impede progress towards homing in on the etiology and clinical treatment options for chronic, subjective tinnitus. In this study, we performed a broad range of audiometric testing in patients with blast and non-blast related chronic tinnitus and identified correlations between measured tinnitus characteristics and participant reported severity and handicap on standard clinical questionnaires. We tested 25 participants, among whom 12 were female and 13 were victims of blast injury from the 2013 Boston Marathon bombing. All participants reported tinnitus lasting longer than 1 year. Using custom software programmed for a tablet interface, subjects completed a series of medical and handicap questionnaires (Tinnitus Handicap Questionnaire [THI], Tinnitus Reaction Questionnaire [TRQ], Patient Health Questionnaire-9 [PHQ-9]) and underwent 2 weeks of serial audiometric tests, all from home. Automated audiometric testing included a validated self-administered audiogram, subjective measurements of tinnitus loudness (visual analogue scales [VAS], minimum tinnitus masking levels [MML]), psychophysical matching of tinnitus percept

across 4 acoustic dimensions, loudness discomfort estimates and several different approaches to measure speech intelligibility in fluctuant background noise. Our ongoing work explores the correlations between tinnitus questionnaires and subjective estimates of phantom percept intensity. We further correlate subjective estimates of tinnitus severity against objective measures of pure tone threshold shift, loudness discomfort levels, tinnitus masking levels and tinnitus pitch. To address the hypothesis that tinnitus and speech-in-noise processing are outcomes that might both reflect a shared underlying central auditory pathophysiology, we closely compare the audiometric estimates above against measures of speech in noise intelligibility. Collectively, our work is aimed at identifying associations between tinnitus health questionnaires, hearing status and self-reported tinnitus characteristics and documents any systematic differences between tinnitus arising from sudden blast injury versus typically developing tinnitus.

PS 275

Distortion Product Otoacoustic Emissions in Blast-Exposed Veterans

Frederick J. Gallun¹; Elizabeth Haley²; Lindsey Jorgensen³; Linmin Kang²; Leslie Zhen²; David Jedlicka²; Serena Dann⁴; Sheila Pratt²

¹VA Portland RR&D National Center for Rehabilitative Auditory Research and OHSU; ²VA Pittsburgh and University of Pittsburgh; ³VA Sioux Falls and University of South Dakota; ⁴VA Portland RR&D National Center for Rehabilitative Auditory Research

Many Veterans present with normal or near-normal peripheral hearing on standard audiometric tests, yet report a wide variety of listening complaints, particularly with challenging listening environments. These problems are frequently evident in those who have suffered from exposure to one or more high-velocity blasts and subsequent mild traumatic brain injury (Elder & Cristian, 2009). A standard audiometric test battery may not be sensitive to these listening problems, which warrants additional study into other measures that may elucidate hearing/listening problems in this population.

This poster will describe preliminary data from an ongoing large multisite study being conducted at three VA Health Care System sites – Pittsburgh, PA, Portland, OR and Sioux Falls, SD. The poster will focus on distortion product otoacoustic emissions (DPOAE), a frequency-specific measure of outer hair cell function, measured in Veterans with and without blast exposure. Comparisons also will be made between individuals that report tinnitus and those that do not.

The presence of DPOAEs is predictive of normal/near normal pure-tone hearing thresholds; however, absent and/or abnormal OAEs have been observed in people with normal pure-tone hearing thresholds in a number of populations, including those with tinnitus, ototoxic medication exposure, and excessive noise exposure (Ceranic et al., 1998; Karch et al, 2016). In such instances, DPOAEs may be more sensitive to abnormal outer hair cell function than pure-tone hearing tests. Social/emotional complaints related to hearing difficulties and self-reported tinnitus and/or abnormal auditory perception also will be discussed.

DPOAEs in Veterans who have been exposed to blasts have not been found to be abnormal (Gallun et al., 2012). However, this study had limited control of related factors such as age and noise exposure. In contrast, a recent animal study reported a reduction in DPOAEs after blast exposure (Race et al., 2017).

Preliminary analyses of data from 108 participants suggested differences in between the blast-exposed (n=48) and non-blast exposed (n=60) groups, such that those with a blast history tended to have lower mean DPOAE signal-to-noise ratios (SNRs) than those with no blast history. The presence of tinnitus also was related to lower mean DPOAE SNRs. As this is an ongoing study, data will be re-analyzed prior to completion of the final poster presentation. These early results support, in a new sample drawn from across the United States, the previously observed relationship between blast exposure and auditory dysfunction (Race et al., 2017).

Works Cited

Ceranic, B. J., Prasher, D. K., Raglan, E., & Luxon, L. M. (1998). Tinnitus after head injury: evidence from otoacoustic emissions. *Journal of Neurology, Neurosurgery & Psychiatry*, 65(4), 523-529.

Elder, G. A., & Cristian, A. (2009). Blast-related mild traumatic brain injury: mechanisms of injury and impact on clinical care. *Mount Sinai Journal of Medicine: A Journal of Translational and Personalized Medicine*, 76(2), 111-118.

Gallun, F. J., Diedesch, A. C., Kubli, L. R., Walden, T. C., Folmer, R. L., Lewis, S., McDermott, D. & Leek, M. R. (2012). Performance on tests of central auditory processing by individuals exposed to high-intensity blasts. *Journal of Rehabilitation Research & Development*, 49(7).

Race, N., Lai, J., Shi, R. & Barlett, E.L. (2017). Differences in postinjury auditory system pathophysiology after mild blast and nonblast acute acoustic trauma. *Journal of*

Neurophysiology, 118, 782-99.

PS 276

Effects of Age, Hearing Loss, and Tinnitus on Auditory Brainstem and Perceptual Responses

Katie Turner¹; Omid Moshtaghi²; Neil Saez³; Matthew L. Richardson⁴; Fan-Gang Zeng⁴; Harrison Lin⁴
¹UC Irvine; ²UC San Diego; ³University of Virginia; ⁴University of California, Irvine

Background

Tinnitus is characterized by the perception of sound without an external source of the sound. Tinnitus often co-occurs with hearing loss after noise exposure and may arise as a result of neurodegeneration in the peripheral auditory system and subsequent overcompensation by the brain. Tinnitus is often perceived as relatively high-pitched, and in animal models, noise exposure produces greater neurodegeneration at points corresponding to processing of higher frequencies. We investigated here whether tinnitus modulates measures of auditory function in human listeners in a frequency-specific way.

Methods

We performed objective and behavioral auditory measures in listeners with tinnitus along with control listeners who did not have tinnitus but had similar average age and audiometric thresholds, additionally grouping our listeners by age and hearing loss status. We recorded auditory brainstem responses (ABR) to clicks as well as 1000, 4000, and 8000 Hz tone bursts, presented at 30, 50, and 70 dB nHL. We measured the amplitude and latency of waves I and V. We also measured temporal modulation detection thresholds and speech reception thresholds in noise. Modulation detection was measured using 250, 2000, and 8000 Hz carrier pure tones modulated at 4, 41, and 80 Hz. Speech reception in noise was measured using English sentences spoken by a male talker, masked separately with speech-spectrum-shaped noise, a female talker, and a male talker.

Results and Conclusions

Results showed smaller wave I and V amplitudes, and longer wave V latencies, with age and hearing loss, as expected. No significant differences in ABR measures were seen between listeners with and without tinnitus. Listeners with tinnitus were actually better at detecting 4 Hz modulation at all carrier frequencies; no difference was seen in detection of 41 or 80 Hz modulation, and no difference in modulation detection was seen with age or hearing loss. Our results suggest that, unlike changes produced with age and hearing loss, changes produced with tinnitus are subtle and difficult to detect using conventional auditory brainstem responses and perceptual tasks in human listeners.

Funding

This work was supported by National Institutes of Health, Hearing Health Foundation, and American Academy of Otolaryngology – Head and Neck Surgery

PS 277

Evaluation of Noise Attenuating Headphones for Audiometric Threshold Testing Outside the Sound Booth

Odile Clavier¹; Jesse Norris¹; Claire Healy-Leavitt¹; Sigfrid Soli²; William Hal Martin³; Lee Shi Yuan³; Erik Larsen⁴; Tera Quigley⁴; Golbarg Mehraei⁴; Douglas S. Brungart⁵; Jaclyn Schurman⁶

¹Creare LLC; ²House Clinic; ³National University of Singapore; ⁴Decibel Therapeutics; ⁵Walter Reed National Military Medical Center; ⁶University of Maryland, College Park

Background. Worldwide, increasing access to hearing health care will require enabling currently available commodities (Internet, smartphones) to conduct surveillance of hearing loss beyond traditional clinical environments. To address this need, a prototype for a noise attenuating mobile audiometric headset was developed. To evaluate its accuracy as compared to existing devices, the first step was to obtain the reference equivalent threshold sound pressure levels (RETSPL) to provide the equivalence for hearing levels as compared to a normative sample. Typically, this process is accomplished by following the ISO 389-9:2009 standard, which describes how to recruit a normative sample.

Methods. Two separate studies were conducted following the specific requirements of the standard, each with a cohort of otologically normal subjects. The first cohort was recruited in Los Angeles, CA (N=35 ears, mean age of 22.3 +/- 2.2 years) and the second was recruited in Singapore (N=47 ears, mean age of 21.3 +/- 2.3 years). In both cases, subjects were deemed to have normal hearing based on a questionnaire. Thresholds were obtained on all subjects using an automated algorithm with the new headset. Thresholds were also obtained manually using a commercially available system (different systems at each location) and with two different audiologists.

Results. The RETSPL values of the new headset were computed as the median threshold value in SPL in each studies and were in excellent agreement: ± 5 dB at all frequencies between 125Hz and 16 kHz, except for 750 Hz and 10 kHz where the differences were 10 and -15 dB respectively. Considering the accepted ± 5 dB test-retest inter-subject variability for behavioral thresholds,

these discrepancies are clinically insignificant (except at 10 kHz). However, thresholds measured with commercial devices revealed that both populations had average thresholds that were 5 to 10 dB above zero at most frequencies below 6 kHz. As a result, using the RETSPLs as computed according ISO 389-9 leads thresholds that are consistently lower with the new headset than with commercial devices. This discrepancy persisted across two other studies that compared thresholds obtained with the new headset and commercial systems using standard headphones.

Conclusions. The high degree of variability across populations used for RETSPL studies can yield RETSPL values that lead to inconsistencies in thresholds measured across multiple systems and headphones. Some revisions to the standard could help narrow down the variability to ensure newer headphones can be used in the clinic alongside other devices.

PS 278

Synaptopathy May Precede Hearing Loss in Mice and Humans Post Congenital Cytomegalovirus Infection.

Ali Almishaal¹; **Pranav D. Mathur**²; Lesley Franklin¹; Aleksandra Martinovic¹; Kayla Sivas¹; Jun Yang¹; Matthew Firpo¹; Albert Park¹

¹University of Utah; ²Otonomy, Inc.;

Introduction: Cytomegalovirus (CMV) infection is the leading infectious cause of pediatric sensorineural hearing loss (SNHL), and yet its pathogenesis remains unclear. SNHL is absent in majority of the CMV-infected kids at birth, but appears within first two years of life, which then progresses. Furthermore, several CMV-infected kids do not develop SNHL. Loss of the synapses (synaptopathy) between the inner hair cells and the spiral ganglion neurons (SGNs) without hearing threshold elevation or outer hair cells loss was observed previously in various animal models of hearing loss. The goal of this study was to determine whether synaptopathy is a precursor to subsequent SNHL in CMV-infected animals, and whether a similar effect of CMV-infection is observed in humans.

Methods: C57BL/6 mice were intracerebrally inoculated with murine cytomegalovirus (mCMV) on postnatal day 3. DPOAEs and ABR wave I were measured from control and CMV-infected C57BL/6 mice at 4, 6, 8 weeks of age. Cochleae from these animals were then harvested and immunostained for synaptic ribbons (Ctbp2) and hair cell markers. Synapses and hair cells were counted across different frequency regions in uninfected and CMV-infected cochleas. A blinded

retrospective data analysis was performed using ABR results from 44 children between the ages of 14 days and 17 years who obtained ABRs at Primary Children's Hospital between 2014-2018. ABR waveforms were analyzed for raw amplitude, wave I:V amplitude ratio, absolute latency, and interpeak latency, with reference to the normal hearing group. Amplitude measures were log transformed to distribution skew, so that the effects represent permanent (%) difference from controls.

Results: At 4 and 6 weeks, CMV-infected mice exhibited comparable cochleograms, ABR and DPOAE thresholds, but significantly reduced wave I amplitude compared to uninfected mice. This was associated with reduced synaptic counts across the cochlear length. The loss of synaptic ribbons progressed up to 8 weeks of age when hearing threshold elevation and hair cell loss are first observed. The human subjects were categorized (age and gender matched) into four groups: cCMV-infected (with or without SNHL) and non-CMV-infected (with or without HL). The wave I:V amplitude in both the cCMV-infected groups was reduced in both ears with statistical significance for the left ear under click stimulus.

Conclusion: This is the first ever study suggesting cochlear synaptopathy in response to CMV-infection preceding the loss of hair cells and elevation in hearing thresholds in both mice and humans. Therapeutically targeting synaptopathy may prevent CMV-induced SNHL.

PS 279

Relating Physiological Measures of Cochlear Synaptopathy to Speech Perception in Individuals with Noise-Induced Tinnitus

Chhayakanta Patro; Alix Klang; Magdalena Wojtczak
University of Minnesota

Background:

Previous work from our lab has shown that individuals with noise-induced tinnitus and normal or near-normal hearing exhibit reduced strength of the middle-ear-muscle reflex (MEMR) compared to the age-matched and gender-matched controls without tinnitus. The difference in MEMR strength could not be explained by differences in hearing sensitivity for frequencies above the audiometric range. The finding is consistent with the idea that tinnitus in the absence of audiometric hearing loss may originate from loss of synaptic connections between inner hair cells in the cochlea and auditory-nerve fibers termed cochlear synaptopathy. In this study, we explored the relationship between MEMR strength and two other measures thought to be affected by cochlear synaptopathy: the envelope following response

(EFR) to a high-rate amplitude modulation (AM), and the spatial release from masking for speech presented in a two-talker background.

Methods:

Individuals with noise-induced tinnitus and no-tinnitus controls with normal hearing or with mild hearing loss were recruited to participate in this study. Normal hearing was defined as hearing thresholds of 20 dB hearing level (HL) or better. A mild hearing loss was defined as normal thresholds for frequencies up to 2 kHz and a hearing loss ≤ 40 dB HL at higher audiometric frequencies. A wideband measure of the MEMR was used to evaluate the reflex strength. EFRs were measured for 2- and 4-kHz tones modulated at 91.4 Hz and presented in broadband noise. Speech recognition was measured for IEEE sentences presented with a two-talker babble in a simulated reverberant room. The background speakers were either collocated (0-deg azimuth) or non-collocated (± 15 -deg azimuth) with the target and the pitch of their voices was either the same as that of the target or differed from the target by three semitones. Speech stimuli were amplified at higher frequencies for listeners with mild hearing loss.

Results:

Preliminary results show that MEMR strength is significantly weaker in individuals with tinnitus than in age-matched controls, consistent with our previous findings. Spatial release from masking in speech recognition was significantly less for the tinnitus than the control group. Correlations between EFRs, the MEMR, and the spatial release from masking will be investigated.

Conclusion:

The weaker MEMR and the reduced spatial release from masking in speech recognition in the tinnitus group provide further support for the hypothesis that tinnitus in the absence of hearing loss may result from the lack of peripheral input due to cochlear synaptopathy. [Supported by NIH grant R01 DC015987].

PS 280

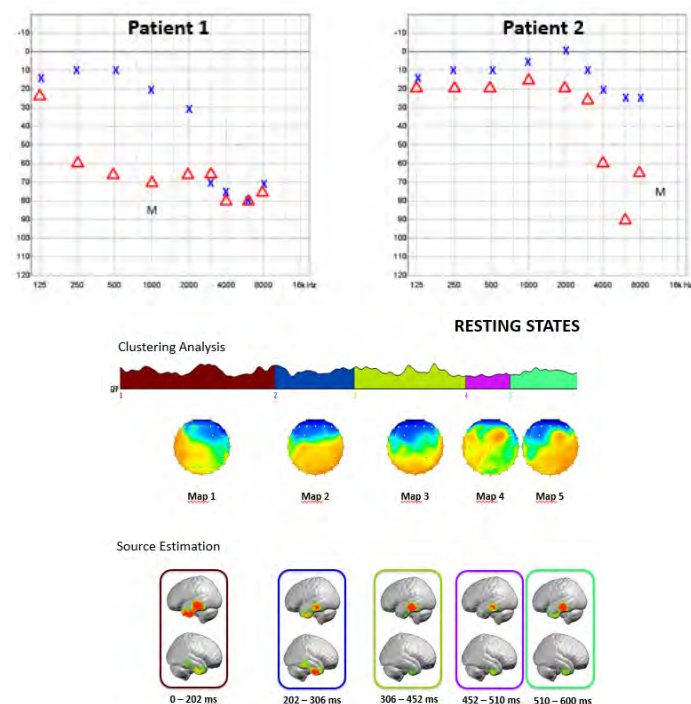
Multichannel EEG to Study Large-Scale Neuronal Networks in Patients with Unilateral Tinnitus

Gérard Loquet¹; Ranjeeta Ambett²

¹*Department of Clinical Medicine, Aalborg University, Aalborg, Denmark.* ²*Department of Electronic Systems, Aalborg University; Department of Otolaryngology and Head and Neck surgery and Audiology, Aalborg University Hospital*

Background: The subjective nature of tinnitus and its association with hyperacusis makes it a diagnostic challenge. Traditional electroencephalogram (EEG)

used waveform morphology at selected electrodes as an outcome measure. However there has been no clear correlation between tinnitus and frequency band power. This study is based on spatial EEG analyses that measures changes in the global field potential, therefore allowing characterization of large-scale neuronal networks at rest, in response to stimuli or in the presence of pathology. Method: This initial study involved 2 subjects who were previously normal hearing individuals and presented with unilateral sudden onset tinnitus following baro trauma and acoustic trauma respectively. Pure tone audiometry and tinnitus frequency and loudness matching were performed. EEG (65 electrodes) was recorded in resting states, and in the presence of a pure tone stimulus corresponding to the frequency of tinnitus. Analyses of the data was performed using CARTOOL software. Results: The multicentric origin of tinnitus was revealed with a continuous response at the contralateral auditory cortex in resting states. In the presence of an auditory stimulus in the affected ear (simulating masking or distraction techniques of treatment) the response recorded in the contralateral auditory cortex was more intense and diffused than the “tinnitus alone” response. With an auditory stimulus in the normal ear a response was recorded in the respective contralateral cortex with no response in the ipsilateral cortex proving that there were no permanent cortical changes that had occurred in the auditory cortex due to the auditory trauma. In conclusion spatial EEG analyses is a valid investigative tool and has potential for use in detecting biomarkers for tinnitus. The information gathered has relevance in diagnosing tinnitus and its severity with the intention of designing treatment options.



PS 281

Is 'Hidden Hearing Loss' prevalent in Professionals exposed to Music?

Aikaterini Vardonikolaki¹; Athanasios Bimpas¹; Adriana Razou²; George Chrysovitsiotis²; Dimitris Kikidis¹

¹National & Kapodistrian University of Athens;

²Hippokrateion Hospital

Objectives: Hidden hearing loss (HHL) is an ambiguous clinical entity where patients experience difficulty in hearing (especially in noisy environments), without any evidence of abnormality in classical pure tone audiometry. The aim of the study is an attempt to identify hidden hearing loss among professional musicians using Auditory Brain Response (ABR) and Acoustic Reflex Thresholds (ART).

Study design: This is a prospective cross-sectional study.

Methods: The study included two groups of professionals musicians and sound engineers with normal pure tone audiograms. The study group (N=29, Male=18) reported one or more auditory symptoms (tinnitus, hyperacusis, diplacusis or sound distortion) and the control group was asymptomatic (N=14, Male=11). Subjects from both groups underwent a full audiological investigation, including ABRs (50ms clicks at 90 dB SPL, rate of 11 clicks/s,) and ARTs. Both wave amplitude and latency were measured, as well as amplitude ratios. Ipsilateral and contralateral. ARTs were measured using tones (0.5,1,2,4 kHz) as well as broadband stimulus.

Results: No differences were found for age, gender, ARTs except right broadband contralateral reflex and thresholds in pure tone audiogram between groups and between right and left ears. Between group comparison revealed, that both wave V amplitude (0.46 μ V vs 0.26 μ V, p=0.014) and a wave V/I amplitude ratio (median 2.1 vs 1.5, p=. 015, Mann-Whitney U) were found significantly higher in the left, but not in the right ears of the study group compared to controls.

Conclusions: Although lateralization of findings in ABR/ARTs is identified in our subjects, further studies are needed in order to establish the prevalence of hidden hearing loss in musicians.

Inner Ear Efferents: Form and Function

Chairs: Amanda Lauer & Soroush Sadeghi

SYMP 01

Efferent Modulation of Afferent Activity in the Inner Ear: An Overview of Underlying Cellular Mechanisms

Elisabeth Glowatzki

Johns Hopkins University

Efferent modulation of afferent activity in the inner ear is an important mechanism to modulate dynamic range of afferent inputs and to protect inner ear structures from harm due to overstimulation. This overview presentation will provide a comparative summary of cellular mechanisms that mediate efferent function in the cochlea (including lateral and medial efferent function) and in the vestibular system. Advances as well as roadblocks in methodology for investigating efferent function in the inner ear will be discussed.

SYMP 02

Hair Cell Efferent Synapse Formation

Isabelle Roux

National Institute on Deafness and Other Communication Disorders

In the mammalian cochlea, both inner and outer hair cells receive efferent inputs from the brainstem which modulate their activity. Only present transiently during the development on the inner hair cells, these inputs persist through life on the outer hair cells. Combining mouse genetics, electrophysiology and fluorescent toxin labeling, we tested several hypotheses regarding the molecular mechanisms involved in the formation of these cholinergic synapses, which have the particularity to be inhibitory due to the interplay between $\alpha 9$ nicotinic acetylcholine receptors and closely associated calcium-dependent potassium channels. We will discuss our results showing that these mechanisms are different than expected.

SYMP 03

Vestibular Efferent Inputs are Required for Normal Activity of Vestibular Nerve Afferents

Soroush Sadeghi

Center for Hearing and Deafness, Dept. of Communicative Disorders and Sciences, State University of New York at Buffalo, Buffalo, NY

Stimulation of the vestibular efferent pathway, which carries signals from the brainstem to the inner ear

increases the resting discharge and decreases the sensitivity of afferent fibers, specially those with irregular resting discharge and phasic response properties. Efferents are also required for normal function of the vestibular system, as shown by the defective development and adaptation of the vestibulo-ocular reflex in mice lacking $\alpha 9$ cholinergic receptors. In mammals, both cholinergic and GABAergic efferents innervate the vestibular periphery. However, the functional roles of different efferent neurotransmitters and the receptors mediating their effects on the two kinds of afferents (i.e., irregular/phasic and regular/tonic afferents) are largely unknown. Calyx afferent terminals contain voltage sensitive potassium channels that are open at resting membrane potentials. As a result, calyces (specially, those in central areas of the neuroepithelium) do not readily depolarize, show little spontaneous activity, and have strong spike frequency adaptation. Our recent in vitro patch clamp recordings from calyces in the cristae of 2-3 week old rats provide evidence that activation of muscarinic acetylcholine receptors (mAChR) as well as metabotropic GABA-B receptors increase the speed and sensitivity of responses of calyx terminals. These effects are mediated through changes in the activity of different potassium channels: mAChRs decrease the activity of KCNQ channels and GABA-B receptors inactivate calcium channels and in turn, calcium-activated potassium channels. This suggests that efferents can modulate the contribution of calyx inputs to dimorphic afferent fibers and probably set the irregularity of discharge and response properties (phasic vs. tonic) of afferent fibers. Next, our in vivo extracellular single unit recordings from afferent fibers in anesthetized C57BL/6 mice suggest that efferent inputs are required for the normal activity of irregular afferent fibers. We show that heat - applied through either 460 nm LED-coupled fiber optics or by temperature-controlled local saline perfusion - could selectively inhibit the activity of irregular afferent fibers by 40-100%. Similar results were observed when the fiber optic was positioned over the midline brain stem (i.e., crossing efferent fibers), suggesting that this effect is mediated through an inhibition of unmyelinated or lightly myelinated efferent fibers. Together, these findings suggest that lack of activity of efferents could result in inhibition of irregular afferents and that cholinergic and GABAergic efferent inputs are required for sensitive and fast responses by irregular afferents.

Funded by NIH-NIDCD grant 5R03DC015091 and a research grant from the American Otological Society (AOS)

SYMP 04

Evidence for Dopaminergic Forebrain Efferents as Modulators of Seasonal Peripheral Auditory Sensitivity in a Vocal Fish

Paul Forlano

Dept. of Biology, Brooklyn College, City University of New York, Brooklyn, NY USA ; Programs in Ecology, Evolution, and Behavior ; Neuroscience ; and Behavioral and Cognitive Neuroscience, The Graduate Center, City University of New York, New York

The function of dopaminergic efferent modulation in the peripheral auditory system is poorly understood, especially in the context of natural behaviors. Accumulating evidence from the plainfin midshipman fish (*Porichthys notatus*) suggests peripheral dopamine is important for auditory processing related to social communication and reproduction. During the summer breeding season, males produce long duration vocalizations at night to attract females. Females undergo a steroid-dependent enhancement of peripheral auditory sensitivity that facilitates mate localization. We identified forebrain dopaminergic neurons that directly innervate both the saccule of the inner ear, the main end organ of hearing, and the cholinergic auditory efferent (AE) nucleus in the hindbrain. Electron microscopic analysis of the saccule revealed that dopamine terminals do not form traditional synapses but contain vesicles in proximity to hair cells, suggesting paracrine release and the potential for dopamine to modulate hair cells directly. In contrast, dopaminergic terminals form synapses on both the soma and dendrites of AE neurons. Dopaminergic terminals also make axo-axonic synapses onto unlabeled, inhibitory-like terminals on AE neurons. Seasonal neuroanatomical investigations have demonstrated that dopaminergic innervation of the AE is higher in the summer vs. non-reproductive winter, but importantly, dopaminergic innervation of the saccule is reduced in the summer while cholinergic input is seasonally unchanged. Based on the seasonal, reproductive-related changes in dopamine innervation, we hypothesized an inhibitory effect of dopamine on the peripheral auditory system. We confirmed this with pharmacological manipulations in the saccule combined with sound-evoked extracellular recordings from hair cells. Dopamine increased thresholds in both summer and winter fish, and therefore appears to have an inhibitory effect on sound-evoked hair cell activity. Furthermore, a D2 receptor agonist mimicked the inhibitory effect of dopamine and D2a receptor expression in the saccule is reduced in the summer. Our results suggest that seasonal reduction of dopamine in the saccule serves as a release of inhibition to improve female hearing sensitivity. We propose that a novel biological function for dopamine in the peripheral auditory system is to facilitate

detection of social-acoustic signals, a function which may be conserved in other vocal vertebrate species.

Grant support from NIH SC2DA034996 and NSF IOS-1456743

SYMP 05

The Efferent Vestibular System in Context: Input vs Output

Aaron Camp

Sensory Systems & Integration, Sydney Medical School; Bosch Institute; University of Sydney Sydney, NSW 2006

Sensory modalities adopt efferent circuitry to modulate peripheral targets. Unlike other modalities, the function of the efferent vestibular system (EVS) remains elusive. Our recent work investigates the central context within which the EVS is activated by using monosynaptic rabies tracing to determine the direct inputs to efferent neurons in mice. We show direct inputs from diverse regions throughout the brainstem, cerebellum, and forebrain including from telencephalon and diencephalon structures. This information may allow the manipulation of efferent neurons, or their inputs, via electrical, chemical or optogenetic methods and provide a means to systematically explore the context-dependent modulation of vestibular function.

SYMP 06

The Role of Medial Olivocochlear Transmission during Selective Attention to Visual Stimuli with Auditory Distractors

Paul H. Delano

University of Chile

The mammalian auditory efferent system is a unique neural network that originates in the auditory cortex and projects to the cochlear receptor through the olivocochlear bundle. It has been proposed to function as a top-down filter of peripheral auditory responses during selective attention to cross-modal stimuli. In the last years, we have been studying the role of olivocochlear transmission in animal models, including chinchillas and the α -9 nicotinic receptor subunit knock-out mice. Experiments performed in chinchillas show that selective attention to visual stimuli reduces auditory-nerve responses to auditory distractors, while cochlear microphonic responses are enhanced. These findings suggest that the medial olivocochlear fibers are activated during selective attention to visual stimuli. Next, we show that selective attention to visual stimuli with auditory distractors is altered in α -9 nicotinic receptor knock-out (KO) mice, as they made less correct

responses and made more omissions than wild type (WT) mice in presence of auditory distractors. Moreover, we evaluated the effects of contralateral noise on auditory nerve responses in alpha-9 KO and WT mice by measuring the amplitude of wave I from auditory brainstem responses with and without contralateral broadband noise. We found that alpha-9 KO mice have a reduced olivocochlear reflex strength, and that the individual magnitude of the olivocochlear reflex correlates with the number of correct responses made by WT and KO mice. Taken together, our results, demonstrate that an intact medial olivocochlear transmission aids in ignoring auditory distractors during selective attention to visual stimuli, probably by suppressing auditory-nerve responses through medial olivocochlear activation.

SYMP 07

Efferents in Aging and Inner Ear Pathology

Amanda Lauer

Johns Hopkins University

In the auditory system, olivocochlear efferent activation modifies neural pathway development, protects against damage, enhances afferent neural representation of acoustic transients in noise, and enhances auditory selective attention. Dysfunction of efferent feedback pathways projecting from the brainstem to the ear may contribute to developmental sensory processing disorders, impaired compensation for peripheral damage with age, and increased vulnerability to damage from high-level sensory stimulation. We will discuss recent work aimed at understanding how olivocochlear efferent neurons contribute to and change with aging and sensory pathology, affecting the brain's capacity to protect against peripheral damage and modulate incoming sensory input. Confocal and electron microscopic analysis reveals that anatomical organization of olivocochlear efferent neurons is plastic under conditions of peripheral sensory decline and environmental noise exposure. Even seemingly innocuous environmental sounds such as vivarium noise result in olivocochlear plasticity. Changes in these pathways have important implications for the way sounds are processed and perceived in quiet and in the presence of competing sensory stimulation. Ongoing experiments aimed at understanding olivocochlear specializations in species with different natural auditory processing abilities and how these specializations might be leveraged to increase resistance to hearing loss will be discussed.

Mechanisms of Auditory Hypersensitivity in Fragile X Syndrome

Chairs: Yuan Wang & Elizabeth McCullagh

SYMP 08

Interactions of the Fragile X Mental Retardation Protein (FMRP) with Ion Channels in Auditory Neurons

Leonard Kaczmarek

Yale University

Patients with Fragile X Syndrome are hypersensitive to auditory stimuli. This condition is caused by loss of FMRP, an RNA-binding protein. The mRNAs for several ion channels highly expressed in auditory brainstem nuclei bind FMRP. These include the Kv3.1 and Kv3.3 potassium channels, which are required for neurons to fire at high rates, as also channels such as Kv1.2 and KNa1.1, required for accurate phase-locking. Some of these channels also bind FMRP directly and, their activity can directly alter mRNA translation. Accordingly, the firing patterns of neurons and the tonotopic distribution of channels are substantially altered in animals lacking FMRP.

SYMP 09

Enhanced Excitatory Connectivity and Increased Firing in the Lateral Superior Olive of Fragile X Mice

Ursula Koch

Freie Universität Berlin

People with Fragile X syndrome (FXS) exhibit profound hypersensitivity to sounds. These symptoms are recapitulated in a mouse model of FXS, a genetic knock-out of the Fmr1 Protein (FMRP), which is highly expressed in the auditory brainstem. Using this mouse model we explored whether a deletion of FMRP causes maladaptive connections in the lateral superior olive (LSO), a binaural brainstem nucleus. Electrophysiological recordings in acute brain slices show that excitatory inputs to LSO neurons are enhanced in FXS mice, whereas inhibitory inputs are unaltered. Concomitantly, these neurons exhibit increased firing rate and broadened frequency tuning in response to sound stimulation.

SYMP 10

Sound Localization Impairments in a Mouse Model of Fragile X Syndrome

Elizabeth A. McCullagh¹; Sarah Rotschafer²; Achim Klug¹; Karina S. Cramer³

¹University of Colorado Anschutz; ²Mercer University School of Medicine; ³University of California Irvine, Dept. of Neurobiology and Behavior

Individuals with Fragile X Syndrome often experience hyperacusis and increased sound sensitivity. Our

research groups have explored the possibility that this phenotype arises, at least in part, at the level of the brainstem. Fmr1 protein is expressed in the auditory brainstem nuclei and its deletion is associated with abnormalities in these nuclei. We quantified the levels of several presynaptic excitatory and inhibitory synaptic proteins in several nuclei in a mouse model, the Fmr1 KO mouse. The most significant effects were seen in the medial nucleus of the trapezoid body (MNTB), a sign-inverting relay nucleus. These effects are evident at early developmental stages. Here, we present a synthesis of the data from our labs and speculate on how changes in synaptic proteins may lead to altered auditory excitability.

SYMP 11

Multiple functions of FMRP in establishing auditory brainstem circuits

Yuan Wang

Florida State University

A global loss of the fragile X mental retardation protein (FMRP; encoded by the Fmr1 gene) leads to synaptic deficits and sensory dysfunction in human and animal species. Our lab aims to determine the key cellular locations and critical timing of aberrant synaptic development resulted from FMRP deficiency. Using temporally controlled genetic manipulations, we determine how the periphery input from the ear, cochlear bushy neurons, and local astrocytes contribute differentially to delayed maturation of excitatory Endbulb synapses. Through examinations of normally developed brains, we have also identified a novel post-transcriptional regulation mechanism which actively suppresses FMRP expression during specific synaptic developmental windows.

SYMP 12

FMRP in the Human Auditory Hindbrain: Correlations to Fragile X Syndrome

Randy J. Kulesza

Anatomy

To explore possible roles of FMRP in hearing, we examined the distribution of this protein in human auditory brainstem centers. Using immunohistochemistry, we found that FMRP was widely expressed in the cochlear nuclei and superior olivary complex. Specifically, we found the vast majority of octopus cells, bushy cells and neurons in the medial superior olive (MSO) were FMRP+. Additionally, we identified drastic neuronal dysmorphology in the MSO of a subject with Fragile X syndrome. Together, these results suggest that FMRP

expression is abundant in auditory brainstem centers and that this protein plays an important role in development of the MSO.

SYMP 13

Auditory Hypersensitivity and Circuit Disruptions in a Rat Model of Fragile X Syndrome

Benjamin D. Auerbach¹; Kelly Radziwon¹; Richard Salvi²

¹*State University of New York at Buffalo*; ²*University at Buffalo*

Abnormal sensory processing is a hallmark of Fragile X syndrome (FXS), most notably manifesting as extreme sensitivity to sound (i.e. hyperacusis). We have combined two novel behavioral assays with high-density in vivo electrophysiological recordings from multiple points along the auditory pathway to identify the pathophysiological changes associated with auditory hypersensitivity in a newly developed Fmr1 KO rat model of FXS. This novel symptoms-to-circuit approach has the potential to: (1) uncover fundamental neural disruptions at the core of FXS pathophysiology; (2) provide a clinically translatable platform for screening therapies; and (3) offer insight into the mechanisms underlying hyperacusis of diverse etiology.

SYMP 14

Auditory cortex specific deficits in the Fmr1 knockout mice

Jonathan W. Lovelace¹; Devin Binder¹; Iryna Ethell¹; Khaleel A. Razak²

¹*University of California Riverside*; ²*UC, Riverside*

Auditory hypersensitivity is a common symptom in humans with FXS and the Fmr1KO mouse model. Using EEG recordings in awake, freely moving mice, we have identified a number of phenotypes in the Fmr1 KO mice that provide insights into hypersensitivity and abnormal auditory processing in FXS. These phenotypes include increased resting gamma power, larger N1 amplitude of ERPs and reduced inter-trial phase synchrony to sound stimulus. The EEG phenotypes in mice are remarkably similar to those observed in humans with FXS. We also used region specific removal of FMRP to identify sources of EEG deficits. In the Nex1-Fmr1 KO mice, FMRP is removed from forebrain excitatory neurons. EEGs from these mice show that the auditory cortex deficits are the same as full Fmr1 KO mice, but the frontal cortex is similar to WT mice. This suggests that the high gamma deficits observed arise through independent mechanisms in frontal and auditory cortices. In the auditory cortex, high gamma is due to loss of FMRP in excitatory neurons present locally. We

have also tested the effects of Minocycline on EEG phenotypes in full Fmr1 KO mice and report that frontal cortex gamma phenotype is absent after treatment, but partial auditory cortex gamma effects remain. Together, these data suggest that enhanced gamma in frontal and auditory cortices is driven through different mechanisms and responds differently to drug administration.

Auditory Cortex: From Sensation to Perception

Stephen David & David Yi Zhou

PD 01

Transient hyperconnectivity to L2/3 neurons during the critical period in the mouse auditory cortex

Xiangying Meng¹; Bingham Xue²; Joseph P. Y. Kao³; Patrick O. Kanold²

¹Department of Biology, University of Maryland, College Park; ²Department of Biology, University of Maryland, College Park; ³Center for Biomedical Engineering and Technology, and Department of Physiology, University of Maryland School of Medicine

Auditory information is transmitted from the ear to the auditory cortex via the ascending auditory pathways. It enters layer 4 (L4) and is further processed by supragranular layer 2/3 (L2/3) neurons. In the adult auditory cortex L2/3 contains a heterogeneous group of cells with distinct sublaminal differences in their functional intracortical circuits (Meng, Winkowski, et al. 2017). Sensory maps in A1 change during development, but the development of the functional heterogeneity of the intralaminar and interlaminar circuits is unknown.

To address this question we performed Laser-scanning photo stimulation (LSPS) combined with whole-cell patch clamp recoding of L2/3 neurons in thalamocortical slices from P5 to P28 mice and measured the spatial pattern of excitatory and inhibitory connections. We found that during development the excitatory connection from both L2/3 and L4 inputs to L2/3 neurons increased after P5 and reached the peak between P9-P16, whereas the excitatory connection from L5/6 increased after P5 but reached its peak at P12-P16. Thus, there is a transient period of hyperconnectivity, esp. from deep layers, which coincides with the critical period revealed by the susceptibility to sensory manipulations. Moreover, we observed that the functional circuit diversity in L2/3 emerged after P18-P20 and that this diversity reaches its maximum after P28.

Together, our results revealed distinct laminar changes in the intracortical connections over development. Our prior two-photon imaging data on anesthetized mice (Solerana et al. Abstract SFN 51.17; 2016) showed that L2/3 cells have highest pairwise signal correlation and maximal responsiveness to auditory stimuli at P15-16. Our results here suggest that these high signal correlations are due to the transient hyperconnectivity we observe and that this period of hyperconnectivity underlies the capacity for plasticity during the critical period.

PD 02

Neuronal Plasticity in Primary Auditory Cortex of Adult Monkeys Trained to Discriminate Temporally Modulated Signals

Ralph E. Beitel¹; Christoph E. Schreiner¹; Maike Vollmer²

¹Department of Otolaryngology-HNS, University of California, San Francisco, USA; ²Department of Otorhinolaryngology-HNS, University Hospital Magdeburg, Germany; Leibniz Institute for Neurobiology, Magdeburg, Germany

The spectral-temporal diversity and complexity of environmental sounds confront animals with a challenging problem in selective listening. Against a “noisy” environmental background, animals must discriminate sounds that are behaviorally relevant, and their sound processing strategies change as a function of their experience. Many studies have shown that behavioral training can significantly alter spectral and temporal information coding in the primary auditory cortex (A1).

The current study used a go/no go temporal discrimination paradigm to train adult owl monkeys to identify a change in the modulation frequency of a sinusoidally amplitude-modulated (SAM) 1 kHz tonal carrier. A monkey's task was to compare a standard temporal modulation frequency (4 Hz or 10 Hz) with higher modulation frequencies. The task required extensive training before novel SAM tonal carriers (range: 0.5-5 kHz) could be tested. Successful discrimination performance of the monkeys was limited to SAM tonal carriers between 0.5 kHz and 1.67 kHz. We hypothesized, therefore, that redundant overtraining with a low frequency carrier (1 kHz) remodeled neuronal spectral receptive fields (SRFs) and temporal processing in A1.

When compared to naïve, untrained monkeys, extracellular recordings in A1 indicated that behavioral overtraining significantly narrowed SRFs of neurons with characteristic frequencies within one-octave bands

centered at 1 or 2 kHz. As a result, the proportions of neurons activated by the trained 1 kHz carrier frequency were clearly reduced. Modulation transfer functions of neurons in trained animals revealed increased phase-locking to higher SAM frequencies. This improvement in temporal processing occurred for carrier frequencies ranging between 0.5 and 2 kHz.

The physiological results in this study demonstrate that temporal discrimination training in adult primates can induce large-scale alterations in spectral and temporal information processing of A1 neurons. Remodeled SRFs in cortical field A1 may account for the limited ability of the trained monkeys to generalize the learned task to higher carrier frequencies. However, spectrally broad changes in A1 temporal processing suggest that decision-making stations other than A1 may contribute to the poor SAM discrimination performance for higher carrier frequencies observed in the trained monkeys.

Supported by RO1-DC-02260 and DFG VO 640/2-2.

PD 03

Investigating the temporal window of sensory representation in the auditory cortex

Monzilur Rahman¹; Crystal Y. C. Leung¹; Andrew J. King¹; Nicol S. Harper²

¹*Department of Physiology, Anatomy and Genetics, University of Oxford*; ²*Dr*

In this study, we investigated the temporal window represented by the neural population in auditory cortex; how far into the past does the population represent auditory information, and how far into the future can it predict, and what kind of mechanisms might be involved in this representation. We played 20 natural sound clips, each of 5 s duration, to 6 anaesthetized ferrets and recorded single-unit responses in primary auditory cortical areas A1 and AAF, providing a neural population response for 73 neurons. We then processed the sound clips through a simple cochlear model to provide a time-dependent frequency decomposition (a 'cochleagram');. Then, using linear decoding, we estimated the past and future cochleagram from a 5 ms window of neural population response at the present. We could reconstruct about 0.7 s into the past, and predict about 0.3 s into the future, with at least some fidelity. We also performed the same analysis for a neural population response in the inferior colliculus (30 neurons). For the inferior colliculus, we could reconstruct only 0.1 s into the past and predict 0.15 s into the future. We investigated if the capacity for prediction and reconstruction could be explained by the linear spectrotemporal response properties of auditory neurons plus a static nonlinearity, i.e. a linear-

nonlinear-Poisson (LNP) model. For both the cortical and collicular datasets, neuronal activity estimated low frequency spectral components of future sounds more faithfully than the LNP model, but estimated past sounds and high frequencies in future sounds with less accuracy. This suggests nonlinear mechanisms that increase some capacities for prediction may be involved in auditory processing, potentially at the expense of representation of the past. However, it should be noted that both datasets were dominated by high frequency tuned neurons, and the natural sound clips tended to have most power at low frequencies, which are points to consider in interpretation. We also examined decoding using different time windows of neural response (spans of 1, 5, and 10 time bins of 5 ms duration each). Longer time windows tended to improve the LNP model's capacity to estimate the past relative to that of the real neural responses, but had little effect on prediction of the future.

PD 04

Cholinergic Modulation of Stimulus Specific Adaptation in the Rat Auditory Cortex

Cristian Aedo-Sanchez; David Perez-Gonzalez; Manuel S. Malmierca

University of Salamanca

Introduction. One of the main characteristics of sensory systems is their ability to detect novel stimuli in the environment. In the auditory cortex, as well as in other subcortical auditory areas, there are neurons that specifically decrease their response to repetitive sounds (standard tones) but that increase their firing rate against novel stimuli (deviant), and the difference of both responses is known as stimulus specific adaptation or SSA. It is still unclear how SSA is generated or modulated. This study describes the cholinergic modulation of SSA in rat auditory cortical areas.

Methods. We measured SSA levels in single neurons of primary and secondary auditory cortical areas, in response to oddball auditory paradigms, before, during and after the microiontophoretic application of acetylcholine (Ach). As a control, in a subset of neurons we also applied cholinergic antagonists of muscarinic (scopolamine) and nicotinic (mecamylamine) receptors.

Results. In the majority of isolated single units, the SSA levels (SSA index) increased 25% on average after the injection of Ach. These changes were mediated mainly by an increment in the neuronal firing rate in response to the deviant tones (27% increase on average). On the

other hand, the cholinergic antagonists decreased the SSA index, mainly the muscarinic type (15% decrease on average). In contrast, the effect of blocking the nicotinic receptors was not statistically significant. Ach injection decreased the acoustic threshold at the characteristic frequency and also decreased the sharpening of the tuning curve in the frequency response area (FRAs) of the isolated single neurons. These effects have a duration between 60-90 minutes approximately. The cholinergic antagonists reverse these effects.

Conclusions. The results suggest that cholinergic modulation in the auditory cortex increases SSA values mainly by increasing the neuronal firing rate in response to the deviant tones and this modulation would be mediated mainly by muscarinic receptors. The cholinergic modulation also affects the threshold and bandwidth of the response areas.

Financial support was provided by the Spanish MINECO (Grant # SAF2016-75803-P)

PD 05

Experience Dependent Coding of Intonations by Offsets in Mouse Core and Secondary Auditory Cortex

Kelly K. Chong; Alex G. Dunlap; Dakshitha B. Anandakumar; **Robert C. Liu**
Wallace H. Coulter Department of Biomedical Engineering, Georgia Institute of Technology and Emory University

Frequency modulations are an inherent feature of many behaviorally relevant sounds, including vocalizations and music. Changing trajectories in a sound's frequency often convey meaningful information, which can be used for differentiating sound categories, such as in the case of intonations in tonal languages. However, how frequency modulations are encoded within the auditory system is still an open question. In particular, it is not clear what features of the neural responses in what parts of the auditory pathway (e.g. primary or secondary auditory cortex) might be more important for conveying information about behaviorally relevant frequency modulations, and how these responses may change with experience. Our work utilizes a natural paradigm in which mouse mothers learn the behavioral significance of pup ultrasonic vocalizations during maternal experience to study how mice use frequency trajectory to discriminate vocalization categories. We model the whistle-like mouse vocalizations using a parameterized sinusoidally frequency modulated (sFM) tone such that the vocalization's entire frequency trajectory is captured

by a set of six parameters. We employed a combination of in-vivo head-fixed awake single unit electrophysiology and modeling of the natural mouse vocalization repertoire to explore neural sensitivity in frequency trajectory parameter space. We obtained recordings across core (A1, AAF, UF) and secondary auditory (A2) regions, from animals with and without maternal experience. We found that neurons across the entire hearing range can show tuning to sFM parameters such as amplitude and frequency of frequency modulation, and that spiking occurring after the end of stimulus playback (Offset responses; $n=18/40$) were more likely to prefer sFM stimuli over pure tones compared to firing during stimuli (On responses; $n=9/41$, $p<0.05$). In addition, we found an increased prevalence of Offset responses accompanied by a decreased prevalence and strength of On responses to natural vocalizations after maternal experience in A2 ($p<0.001$), while no changes are seen on population average in A1/AAF/UF. Moreover, in maternal A2 units, there is a bias in both On and Offset responses that favors vocalizations that have pup-typical sFM parameters ($p<0.05$), as defined by a nominal logistic regression model. This bias can be explained by a shift in the tuning of maternal A2 neurons towards parameter values that are more characteristic of the pup vocalization category ($p<0.05$). This work furthers our understanding of how auditory cortex attunes to features in acoustic space, demonstrating that offset tuning to frequency trajectory in secondary auditory cortex plays a role in natural sound category learning.

PD 06

Sound and behavioral meaning encoding in a tertiary area of the ferret auditory cortex

Diego Elgueda¹; Daniel Duque¹; Susanne Radtke-Schuller¹; Pingbo Yin¹; Stephen V. David²; Shihab A. Shamma³; Jonathan B. Fritz³

¹*Institute for Systems Research, University of Maryland*; ²*Oregon Health & Science University*;

³*Neural Systems Laboratory, Institute for Systems Research, University of Maryland*

The mechanisms by which the brain integrates acoustic feature information with internal representations (such as behavioral goals, expectations and memories of previous sound-meaning associations) and links them with appropriate audio-motor responses is currently unknown. In order to better understand how the brain performs this task, we recorded auditory responses in a newly described tertiary area, the Rostral-Ventral Posterior field (VPr) of the Posterior Ectosylvian Gyrus (PEG) from four ferrets performing auditory discrimination tasks. We have previously shown that neurons in primary auditory cortex (A1) of the ferret undergo rapid

task-related plasticity of spectrotemporal receptive fields (STRFs) in order to enhance their ability to encode task-relevant sounds during performance of auditory tasks requiring discrimination between stimuli belonging to different behavioral categories. We have also shown that the representation contrast between task-relevant sounds is further increased in non-primary auditory cortical areas in the dorsal PEG (dPEG). Our previous findings in the dorsolateral Frontal Cortex (dlFC) are consistent with a model in which top-down signals from the frontal lobe coding for abstract stimulus meaning can modulate auditory cortex plasticity. However, it is currently unknown how and where in the brain veridical acoustical information integrates with top-down abstract information. Our results reveal that neurons in VPr, while being responsive to auditory stimuli, can greatly enhance the contrast between sound representations belonging to different behavioral categories, similar to dlFC neurons. Furthermore, VPr shows increased responses during passive listening to behaviorally-relevant target stimuli in trained compared to task-naïve animals, which suggests long-term learning. This selective enhancement to target stimuli is further amplified during active performance of auditory discrimination tasks. VPr neurons also show long sustained short-term memory activity after target stimulus offset, correlated with task response timing and action - a type of persistent response we previously reported in dlFC neurons. These rapid task-related changes in activity and filter properties enable VPr neurons to quickly and nimbly switch between different responses to the same acoustic stimuli in different behavioral contexts, reflecting either the timing or spectrotemporal properties or behavioral meaning of the sound. Furthermore, they demonstrate an interaction between the dynamics of long-term learning and short-term attention as incoming sound is selectively attended, recognized and translated into action.

Funding: NIH/NIDCD-R01-DC00577, R00-DC010439, CONICYT/Becas-Chile postdoctorado 74170109.

PD 07

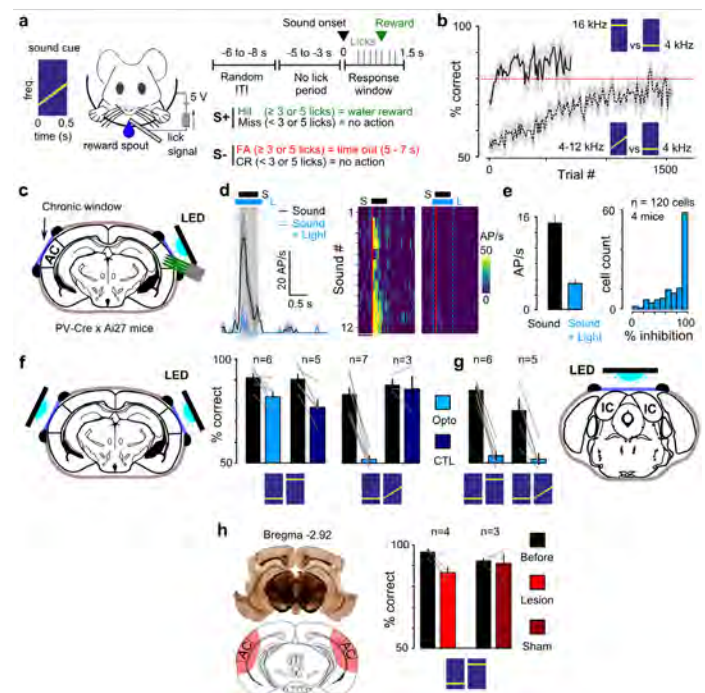
A Slow Cortical Pathway Drives Decisions in a Challenging Sound Discrimination

Sebastian Ceballo¹; Zuzanna Piwowska¹; Jacques Bourg¹; Aurélie Daret¹; Brice Bathellier²
¹CNRS UNIC; ²CNRS - UNIC

While auditory cortex (AC) is often seen as the output stage of the auditory system, it is not always required for sound-driven behaviors, as classically illustrated by unperturbed fear responses after AC inactivation in simple auditory fear conditioning protocols. This lack of

necessity also exists for the popular appetitive sound discrimination tasks, for which claims of AC dependence are still controversial, with different results arising from the use of varied sound pairs, species and inactivation protocols. However, because no study has yet shown both necessity and sufficiency of AC in appetitive tasks, it remains unknown whether inactivation effects uncover a permissive role, by gating or modulating other structures, or a driving role, by providing information that triggers behavioral decisions. Despite a few examples indicating that AC activity can modulate discrimination performance, it remains unclear why AC impacts behavior in certain cases but not others. Here, using well-controlled optogenetics strategies to silence and focally activate AC, we show that, when AC is necessary and sufficient for the execution of a Go/NoGo discrimination task, either involving a challenging sound pair or optogenetically-driven cortical patterns, discrimination occurs with a long (>300ms) delay. In contrast, discrimination of dissimilar pure tones occurs within only ~100ms and does not require AC for execution. Hence, AC participates in a “reflective” pathway with a surprisingly long integration time, which is systematically bypassed by faster, coarser subcortical circuits unless particular complexities in the structure of the discriminated sound pair prevent fast discrimination and entail the slower cortical loop.

Figure Arial 12
 Figure Arial 10
 r Arial 10



Phasic Arousal Optimizes Auditory Evidence Accumulation

Jan Willem de Gee¹; Konstantinos Tsetsos²; David McCormick³; Tobias Donner²; Matthew McGinley¹
¹Baylor College of Medicine; ²University Medical Center Hamburg-Eppendorf; ³University of Oregon

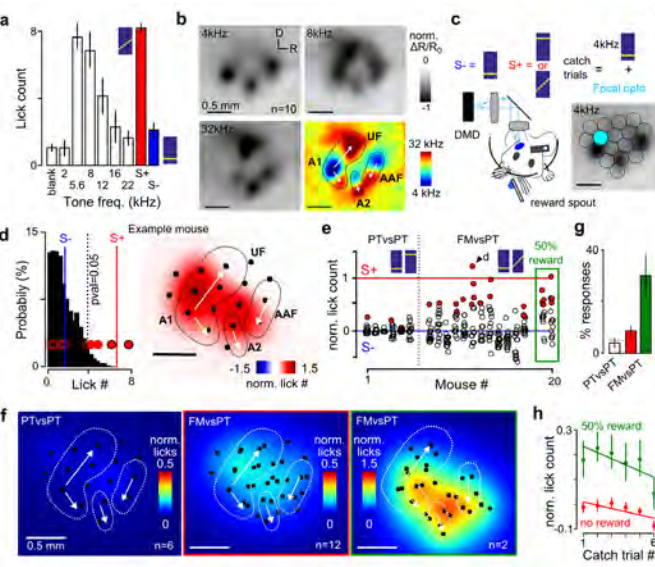
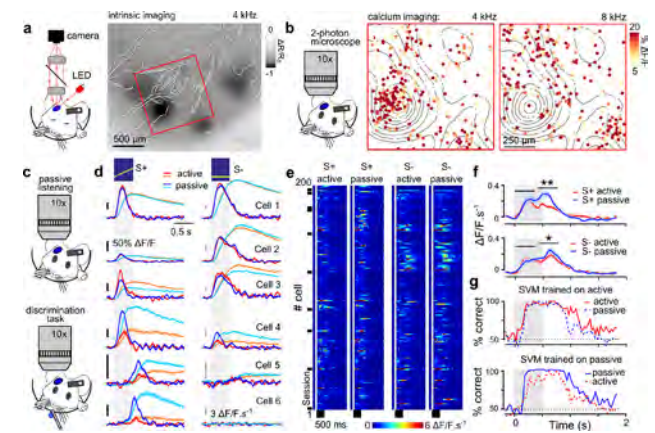
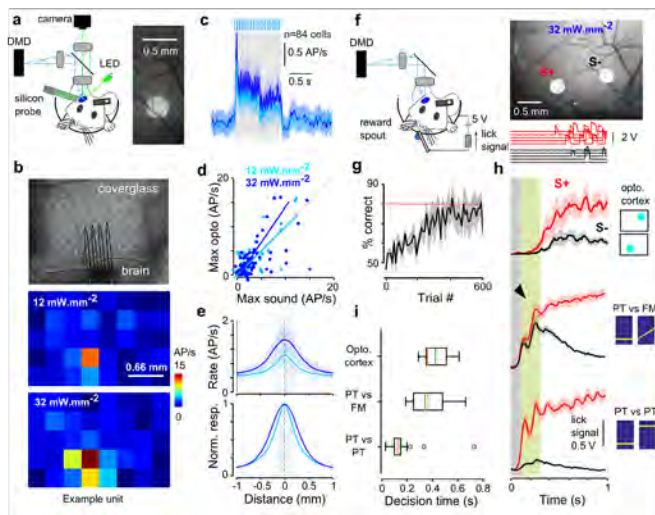
Aim. Neuromodulatory brainstem systems controlling the global arousal state of the brain are phasically recruited during cognitive tasks, such as challenging listening paradigms. The function of such task-evoked neuromodulatory signals in general, including during the processing of sound information, is debated. Here, we uncovered a general principle of their function, across species and behavioral tasks: optimizing sensory evidence accumulation.

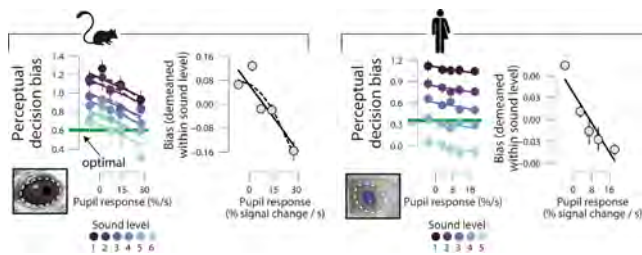
Methods. We exploited that neuromodulatory brainstem responses are mirrored in rapid dilations of the pupil. We thus recorded the pupil diameter of 20 humans and 5 mice during a difficult auditory go/no-go detection task. Humans responded with a button press, mice by licking for sugar water reward. In both species, stimulus difficulty was manipulated by varying signal volume. To test for generalization, and to control for contamination of pupil signals by movements, we additionally tested humans in a forced choice version of the same auditory task.

Results. In both species, task-evoked pupil responses predicted a reduction in a suboptimal conservative bias but no change in perceptual sensitivity. In humans, the same bias reduction effect was present in the auditory forced-choice task. Fitting the behavior with accumulator models of decision-making revealed that the bias reduction was due to a selective modulation of the evidence accumulation process.

Conclusions. Pupil-linked, phasic arousal suppresses suboptimal biases in humans and mice during perceptually challenging auditory decisions. Taken together, our results indicate that phasic changes in arousal state shape decision formation. Thereby, phasic arousal accounts for a significant component of the trial-to-trial variability in overt choice behavior, which would appear as random 'noise'; without tracking arousal.

Outlook. We are currently investigating how the motivational state of an animal drives neuromodulatory systems to exert control of brain state, perception, and behavior. We approach this question with a range of high-tech tools including simultaneous two-photon microscopy and pupillometry in mice during behavior that is under tight stimulus control. We hope to determine the role of phasic arousal in adapting behavior to fluctuating auditory stimulus value.





Adaptive Coding for Efficient Behavioral Performance in the Auditory System

Chairs: Manuel Malmierca & Jose Pena

SYMP 15

Cortical circuits for dynamic auditory adaptation

Maria N. Geffen

Departments of Otorhinolaryngology & Neuroscience, University of Pennsylvania, Philadelphia.

In the auditory cortex, excitatory neurons serve the dominant function in transmitting information about the sensory world within and across brain areas, whereas inhibitory interneurons carry a range of modulatory functions. The mammalian auditory cortex contains a large number of different inhibitory neuronal types. We recently found that a specific class of inhibitory neurons, somatostatin- positive interneurons (SOMs), regulate adaptation to frequent sounds, in a stimulus-specific fashion. SOMs selectively reduce excitatory responses to frequent tones, whereas another type of interneurons, parvalbumin-positive neurons, amplify adaptation by non-specific inhibition. The role of SOMs extends to other forms of adaptation to temporal regularities. These results expand our understanding of how specific cortical circuits contribute to auditory perception.

SYMP 16

Auditory Midbrain Coding of Temporally Sparse Context-Sound Associations

Livia de Hoz

Charité - Universitätsmedizin Berlin

Statistical learning of patterns in the sensory world is essential for selective attention and predictive coding. Statistical learning of relatively fast (seconds to tens of seconds) ongoing changes in a constant stimulus stream are known to occur through sensory adaptation of neuronal response-gain. Little is known, however, about statistical learning of temporally sparse patterns (across minutes/hours). I will describe how neurons in the auditory midbrain can encode temporally sparse context-sound associations through changes in

response gain and signal-to-noise ratio throughout the structure that are partially independent from corticofugal input. Parallel changes in behavioural outcomes suggest a role in decision making.

SYMP 17

Is Neural Sensory Processing Optimized for Prediction of Future Input?

Nicol S. Harper

University Research Lecturer

What determines the form of neural receptive fields? We posit that neuronal selectivity is optimized to represent features in sensory input that best predict immediate future inputs. This may help find underlying variables, discard irrelevant information, and better enable future actions (Bialek et al., 2001). We trained simple feedforward neural networks to efficiently predict the next few moments of video or audio input for clips of natural scenes (Singer et al., 2018). These temporal prediction networks developed receptive fields that matched those of cortical neurons, including the oriented spatial tuning of primary visual cortex, the frequency selectivity of primary auditory cortex and, notably, their temporal tuning properties. The better a network predicted future inputs the more closely its receptive fields resembled those in the brain.

This principle of temporal prediction may have general applicability beyond primary sensory cortex. When we applied temporal prediction networks to unprocessed audio or video, the networks' receptive fields resembled those found in the cochlea or retina. Furthermore, these networks can be extended hierarchically or made recurrent. When we extended them in this manner the networks' units developed tuning properties consistent with various more complex features of neural tuning found in primary sensory cortical areas and also higher non-primary sensory cortical areas. These results together suggest that many aspects of sensory processing are optimized to extract those features with the most capacity to efficiently predict future input.

Bialek W, Nemenman I, Tishby N (2001) Predictability, complexity, and learning. *Neural Computation* 13: 2409-2463.

Singer Y, Teramoto Y, Willmore BDB, Schnupp JWH, King AJ, Harper NS (2018) Sensory cortex is optimised for prediction of future input. *eLife* 7: e31557.

SYMP 18

Neurons Along the Auditory Neuroaxis Exhibit a Hierarchical Organization of Prediction Error

Manuel S. Malmierca

¹Auditory Neuroscience Laboratory, Institute of Neuroscience of Castilla y León, University of Salamanca, Salamanca 37007, Spain

Stimulus-specific adaptation (SSA) is the reduction in the responses to a common sound relative to the same sound when rare. It was originally described in the primary auditory cortex (A1) as the neuronal correlate of the mismatch negativity (MMN), an important component of the auditory event-related potentials that is elicited by changes in the auditory environment. However, the relationship between SSA and the MMN is still a subject of debate. The MMN is a mid-late potential (~150-200 ms in humans), and its neural sources have been located mainly within non-primary auditory cortex in humans and animal models. Moreover, SSA is also present as early as in the auditory midbrain and thalamus (IC and MGB).

In this talk, I will show our recent findings on recordings from single neurons in the IC, MGB and auditory cortex (AC) of anaesthetized rats and awake mouse to an oddball paradigm similar to that used for MMN studies. Our data demonstrate that most neurons in the non-lemnical divisions of the auditory brain show strong SSA and that there is a hierarchical emergence of prediction error signals along the central auditory system. Recordings from prefrontal cortex show that neurons exhibit the highest degree of prediction error along the hierarchy. We have also observed that acetylcholine seems to play a role in shaping SSA by differently affecting the response to the standard or deviant tones sounds only in IC or AC, respectively.

Taken together our results unify three coexisting views of perceptual deviance detection at different levels of description: neuronal physiology, cognitive neuroscience and the theoretical predictive coding framework.

Financial support was provided by the Spanish MINECO (Grant # SAF2016-75803-P), Junta de Castilla y León (Grant # SA023P17) and the European Union's Horizon 2020 research and innovation programme under the Marie Skłodowska-Curie grant agreement No 72209 to MSM.

SYMP 19

Emergence of an adaptive behavioral command for sound localization: converging strategies in owls and humans

Jose L. Pena

Albert Einstein College of Medicine

The brain can be viewed as a probabilistic estimator, where sensory statistics bias judgments. We examined this topic in the neural pathway supporting the owl's sound localization. We found that in the owl's auditory midbrain sensory evidence on sound direction is weighted by its reliability to generate an adaptive motor command for head-orientation. We found that this coding can be explained by convergence of projections from a map of space onto premotor neurons that control behavior. We further show that manipulating the sensory input yields changes in both premotor responses and behavior in a manner predicted by statistical inference. Thus, the topographic sensory representation of auditory space can be read out to adjust behavioral responses by statistics of the sensory input. These experimental results indicate that sensory statistics are both represented and anticipated in the owl's brain, and built into premotor signals. We tested whether human sound lateralization was consistent with the ability to anticipate sensory statistics, as observed in owls. Experimental results on human subjects yielded consistent results, providing evidence towards convergent coding strategies underlying orienting responses across species.

Development II

PD 09

Sox2 and Beta-catenin Compete During Hair Cell Differentiation from Lgr5-positive Cochlear Progenitors

Danielle R. Lenz¹; Albert Edge²

¹Harvard Medical School, Eaton-Peabody Laboratories, Massachusetts Eye and Ear; ²Department of Otolaryngology, Harvard Medical School

Sox2 and β -catenin are important transcription factors in the regulation of proliferation and differentiation of stem cells during development and regeneration, and their interplay has been shown to be highly significant in various systems, such as retina, bone, lung, gut and brain. Interactions of Sox2 and β -catenin with binding partners determine the biological role of these transcription factors. Sox2 and β -catenin have been demonstrated to be essential for specification of the prosensory domain in the inner ear and for differentiation into hair cells during development. Specifically, both transcription factors bind at overlapping sites of the Atoh1 3'-enhancer and activate it. Lgr5-positive cochlear progenitors (LCPs)

have been demonstrated as a powerful tool, since they can be expanded and differentiated into hair cells in large numbers. Initial analysis of Sox2 and β -catenin interaction at the Atoh1 3';-enhancer using luciferase assay revealed a complex competitive mechanism that depends on Sox2 and β -catenin expression levels and favors high levels of β -catenin. Subsequent examination of LCPs from WT mice, as well as from several transgenic mice that mis-express Sox2 and β -catenin, was performed using quantitative real-time PCR, chromatin immune-precipitation and flow cytometry. Sox2 absence resulted in inhibition of early differentiation but had a milder effect after differentiation initiation. β -catenin stabilization using a genetic model was able to drive differentiation, while β -catenin knock-out inhibited differentiation. We hypothesize that Sox2 is required to initiate differentiation through binding to the Atoh1 3';-enhancer. As its levels increase, β -catenin appears to replace Sox2 at the enhancer in order to drive differentiation forward. The interplay between Sox2 and β -catenin is essential for Atoh1 regulation during development.

PD 10

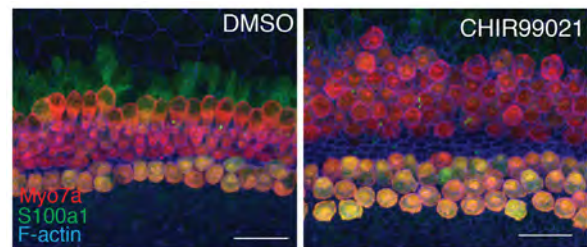
GSK3 Regulates Medial-Lateral Cell Fate in the Developing Organ of Corti

Kathryn Ellis¹; Elizabeth C. Driver²; Takayuki Okano³; Matthew Kelley⁴

¹Decibel Therapeutics; ²Laboratory of Cochlear Development, National Institute on Deafness and Other Communication Disorders, National Institutes of Health; ³Department of Otolaryngology-Head and Neck surgery, Graduate School of Medicine, Kyoto University; ⁴NIDCD

The sensory epithelium of the mammalian cochlea (the organ of Corti, OC) comprises two types of innervated mechanosensory hair cells – the medial inner hair cells (IHCs) and the lateral outer hair cells (OHCs) and at least six types of supporting cells. IHCs and OHCs, and their associated supporting cells, differ structurally and functionally, and are physically separated by a single row of inner pillar cells. The overall structure is an exquisitely patterned mosaic of cells whose proper differentiation and organization is critical for hearing. While many of the molecular mechanisms required for development of the prosensory domain that will give rise to the hair cells and supporting cells have been identified, little is known about how the prosensory domain is split into functionally distinct medial and lateral domains. Glycogen synthase kinase 3 (GSK3), a serine/threonine protein kinase, has been shown to play important roles in many pathways including Hedgehog, Notch, GPCRs, and, most commonly, canonical Wnt signaling, in which it acts

indirectly as an antagonist. To determine whether GSK3 plays a role in medial-lateral patterning within the OC, the effects of multiple GSK3 inhibitors were determined using in vitro cochlear explants. Results indicate a dramatic increase in the size of the medial domain and a proportional decrease in the size of the lateral domain in response to GSK3 inhibition. Fate mapping reveals that this shift occurs as a result of lateral cells adopting a medial cell fate. This phenotype is quite different from the significant increase in numbers of both hair cell types in response to direct activation of canonical Wnt signaling. The differing results suggested that the effects of GSK3 inhibition were not mediated through activation of the Wnt pathway. To confirm this, explants were treated with both the GSK3 inhibitor CHIR99021 and the Wnt antagonist FH535. Phenotypic changes in double-treated explants included a consistent lateral-to-medial shift in HC fate, while qPCR results indicated a decrease, rather than an increase, in the expression of the canonical Wnt targets Axin2, Ccnd1, and Lgr5. In contrast, Bmp4, which is known to play a role in cellular patterning along the cochlear medial-lateral axis, is down regulated in the presence of CHIR99021, and treatment with BMP4 partially rescues the shift in lateral-to-medial cell fate. These results suggest that GSK3 regulates medial-lateral patterning in the cochlea, at least in part, through regulation of Bmp4 expression.



(L) DMSO-treated control explant. Hair cells are labeled with Myo7a (red), IHCs and Deiters' cells labeled with S100a1 (green), and actin labeled with phalloidin (blue). (R) GSK3 inhibition with CHIR99021 results in an increase in medial hair cells labeled with S100a1, indicating they are specified as IHCs.

PD 11

Bmp4-Id signaling regulates medial-lateral axis formation in developing cochlear epithelium

Susumu Sakamoto¹; Tomoko Tateya²; Koichi Omori²; Ryoichiro Kageyama¹

¹Institute for Frontier Life and Medical Sciences, Kyoto University; ²Department of Otolaryngology-Head and Neck Surgery, Graduate School of Medicine, Kyoto University

Inhibitor of differentiation and DNA-binding (Id) proteins, including Id1 to Id4, function as transcriptional regulators known to inhibit DNA binding of other basic HLH proteins. Ids have been reported to play important roles in development of various organs and to function

as downstream factors of Bmp4 signaling; however, the roles and regulation of Id genes in embryonic cochleae are not fully elucidated. The purpose of this study is to clarify the roles of Bmp4-Id signaling in the development of cochlear sensory epithelium. We verified that Id1, Id2 and Id3 are the downstream genes of Bmp4 in developing cochlear epithelium by quantitative RT-PCR using embryonic cochlear explants cultured with a serially-diluted BMP4 protein or BMP4 inhibitor. We produced Id1/2/3 triple conditional knockout (CKO) mice, and the cochlear duct of Id triple CKO mice was short, randomly kinked but not coiled. The lateral cochlear compartment (outer hair and adjacent supporting cells) was amorphic or hypomorphic. Bmp4 expression lateral to the prosensory domain was downregulated as well. The phenotypes of Id triple CKO mimicked by embryonic cochlear explants cultured with a BMP4 inhibitor. These results suggested that Bmp4-Id signaling regulates medial-lateral axis formation in developing cochlear epithelium, and both normal coiling of cochlear duct and lateral compartment formation need the medial-lateral axis in cochlear epithelium. RNA-Seq was performed using Id triple CKO and control cochlear epithelium. The results of RNA-Seq were compatible with the phenotypes of Id triple CKO cochlear epithelium, and moreover revealed that Bmp4 antagonist Grem1 was upregulated in Id triple CKO cochlear epithelium. Administration of Grem1 protein to the explants of embryonic cochlear epithelium resulted in downregulation of Bmp4. It indicates that Grem1 is a potential antagonist of Bmp4 in developing cochlear epithelium to inhibit the medial-lateral axis formation regulated by Bmp4-Id signaling.

PD 12

Establishing the Tonotopic Organization of the Mammalian Cochlea

Heiyeun Koo¹; Min-A Kim²; Hyehyun Min¹; Jae Yeon Hwang³; Jeong-Oh Shin¹; Ji-Hyun Ma¹; Harinarayana Ankamreddy¹; Meenakshi Prajapati-DiNubila⁴; Martin Matzuk⁵; Juwon Park³; Angelika Doetzlhofer⁶; Un-Kyung Kim²; Jinwoong Bok¹

¹Yonsei University College of Medicine; ²Kyungpook National University; ³University of Louisville; ⁴The Solomon H. Snyder Department of Neuroscience and Center for Sensory Biology, Johns Hopkins University School of Medicine; ⁵Baylor College of Medicine; ⁶Johns Hopkins Medical Institution

Background

The vertebrate cochlea is tonotopically organized, such that hair cells in the base are tuned to high frequency sounds and their counterparts towards the apex progressively tuned to lower frequencies. Recent studies suggest that the tonotopic organization

is established by a temporal signaling cascade that is initiated by an increasing base-to-apex gradient of Sonic hedgehog (SHH) signaling both in birds and mammals. In the chicken basilar papilla, Bmp7 is shown to be a key downstream target of SHH in mediating the tonotopic organization. However, the downstream mediators of SHH have been elusive in the mammalian cochlea. It has been shown that expression of Follistatin (Fst), an antagonist for Bmp/TGF β pathway, is activated by SHH and exhibits a similar graded pattern in the developing mouse cochlea.

Methods

To test whether Fst plays a role in mediating SHH signaling to facilitate the tonotopic organization of the mammalian cochlea, we analyzed the cochlear structures and function of Fst knockout (KO) and inner ear-specific conditional knockout (Pax2-Cre; Fst^{lox/lox}; cKO) mice.

Results

The inner ear morphology of Fst KO embryos was generally normal, yet the cochlear duct was slightly shorter with an extra row of outer hair cells in the apex. Importantly, apical cochlear markers that are positively regulated by SHH and preferentially expressed in the apical cochlea, were specifically abolished or downregulated in Fst KO cochlea. These abnormal patterning of the apical cochlea did not appear to be due to disrupted SHH signaling. Since Fst KO mutants were embryonic lethal, we generated inner ear-specific Fst cKO mice, which were viable and closely recapitulated the Fst KO phenotypes. Tonotopic characteristics of the hair cells such as gradual changes of stereocilia lengths and angles appeared to be shifted toward the base in 4-week Fst cKO mice. RNA-seq analysis along the cochlear duct suggest that global gene expression profile of the apical cochlea became similar to that of the middle cochlea. Furthermore, Fst cKO mice showed a significant increase in ABR thresholds and decrease in DPOAE amplitudes specifically in the low-frequency range. These results show that morphology, gene expression, and function of the apical cochlea are compromised in the absence of Fst in mice.

Conclusion

Taken together, these results suggest that Fst plays an essential role in the tonotopic organization in the mammalian cochlea by promoting the apical cochlear identity.

Supported by the BK 21 PLUS Project for Medical Science, Yonsei University

The Notch Ligand Jagged1 is Required for the Survival of Supporting Cells in the Mouse Cochlea

Elena Chrysostomou¹; Angelika Doetzlhofer²

¹The Solomon H. Snyder Department of Neuroscience and Center for Sensory Biology, Johns Hopkins University School of Medicine; ²Johns Hopkins Medical Institution

Notch-mediated lateral inhibition during embryonic development, is the mechanism that regulates the highly organized, mosaic pattern of hair cells (HCs) and supporting cells (SCs) in the mammalian cochlea. Progenitor cells destined to become HCs express Notch ligands which bind to the Notch receptor expressed on neighboring cells to inhibit a HC fate and promote a SC fate. In addition to this HC repressive function, a recent study by Campbell et al., suggests that Notch signaling plays an instructive role in SC differentiation and survival. A potential candidate for mediating this function is the Notch ligand, Jagged 1 (Jag1). In the differentiating cochlea, Jag1 is expressed by SCs. While other Notch ligands are downregulated during the first postnatal week, SC-specific Jag1 expression continues throughout adulthood where its function is unknown. To investigate the role of Jag1 in differentiating SCs, we generated Sox2-CreER/+::Jag1loxP/loxP mice, which received tamoxifen at embryonic day (E) 14.5 and were analyzed at E18.5. Controls included Cre-negative littermates, as well as Sox2-CreER/+::Jag1loxP/loxP mice that did not receive tamoxifen to control for Sox2 haploinsufficiency. In the absence of Jag1, we found that the density of SCs, particularly the Deiters' cells and their neighboring Hensen's cells (HeCs), was significantly reduced compared to controls. A similar ~50% reduction in the number of HeCs was also observed in the postnatal cochlea at P7, when Jag1 was deleted at stages (P) 0 and P1. Embryonic as well as postnatal ablation of Jag1 did not alter HC density, suggesting that the reduction in HeCs was not due to HeC-to-HC conversion, but most likely due to degeneration of HeCs. To identify pathways/genes that may be deregulated in the absence of Jag1, we conducted a series of microarray experiments. These experiments revealed that the expression of genes linked to mitochondrial function and oxidative stress response are significantly reduced in the absence of Jag1. Ongoing experiments are examining the link between Jag1 and the mitochondrial function of SCs and the underlying mechanism of HeC cell death. In summary, our findings demonstrate that Jag1 mediated Notch signaling plays a critical role in the differentiation and maturation of HeCs.

Funding: NIH/NIDCD R01DC011571 (AD and EC)

Trans-Differentiation of Outer Hair Cells into Inner Hair Cells in the Absence of INSM1

Jaime Garcia-Anoveros; Teerawat Wiwatpanit; Sarah M. Lorenzen; Jorge A. Cantu; Chuan Zhi Foo; John C. Clancy; Mary Ann Cheatham; Anne Duggan
Northwestern University

The mammalian cochlea contains two types of mechanosensory hair cells that play different and critical roles in hearing. Inner hair cells (IHCs), with an elaborate presynaptic apparatus, signal to cochlear neurons and communicate sound information to the brain. Outer hair cells (OHCs), equipped for electromotility, mechanically amplify sound-induced vibrations, enabling enhanced sensitivity to sound and sharp tuning. Cochlear hair cells are solely generated during development and their death, most often of OHCs, is the main cause of deafness. Hence, attempts to revert many cases of hearing loss should aim at generating OHCs. OHCs and IHCs, together with supporting cells, originate embryonically from the prosensory region of the otocyst, but how hair cells differentiate into two different types is unknown. Here we show that *Insm1*, which encodes a zinc finger protein transiently expressed in nascent OHCs, consolidates their fate by preventing trans-differentiation into IHCs (1). In the absence of INSM1 many hair cells born embryonically as OHCs switch fates towards late embryogenesis (~E17) and proceed to differentiate into mature IHCs. The OHC to IHC conversion was more frequent in the neural than abneural rows, suggesting an IHC-inducing gradient in cochlear development to which OHCs are normally unresponsive, but become responsive in the absence of INSM1. In order to identify the genetic mechanisms by which *Insm1* operates, we compared transcriptomes of immature IHCs vs OHCs, as well as OHCs with and without INSM1. We find that OHCs lacking INSM1 upregulate a set of genes, most of which are normally preferentially expressed by IHCs. The homeotic cell transformation of OHCs without INSM1 into IHCs reveals for the first time a mechanism by which these neighboring mechanosensory cells begin to differ: INSM1 represses a core set of early IHC-enriched genes in embryonic OHCs, so that they proceed to mature as OHCs. Without INSM1, many of the OHCs upregulating these few IHC-enriched transcripts trans-differentiate into IHCs. Because the misexpression of these IHC-enriched genes in early OHCs underlies their trans-differentiation into IHCs, these genes likely include the regulators driving IHC-specific differentiation.

(1) Wiwatpanit, T., Lorenzen, S. M., Cantú, J. A., Foo, C. Z., Hogan, A. K., Márquez, F., Clancy, J. C., Schipma, M. J., Cheatham, M., Duggan, A., and García-Añoveros,

J. (2018) Trans-Differentiation of Outer Hair Cells into Inner Hair Cells in the Absence of INSM1. *Nature* (In Press).

PD 15

Beta-Catenin is required for pillar cell fate determination

Sung-Ho Huh; Michael Huh

University of Nebraska Medical Center

Introduction

Inner and outer pillar cells are specialized cell-types which make tunnel of Corti in higher vertebrates including mouse and human. In addition, recent study identified that inner pillar would serve as a postnatal progenitor population. Despite of importance of pillar cells in the organ of Corti, understanding generation and maintenance of pillar cells remain elusive. The aim of this work is to understand role of beta-Catenin during pillar cell development.

Methods

beta-Catenin gene was deleted using two Cre lines including *Fgf20^{Cre}* which is active in the prosensory domain of the cochlea beginning E10.5 and *Lgr5^{CreERT2}* which deletes beta-catenin at the time of prosensory cell differentiation. We used *beta-Catenin^{flox(Ex2-6)}* for complete deletion of the gene, *beta-Catenin^{dm}* for canonical Wnt pathway deletion, and *beta-Catenin^{fl(Ex3)}* for canonical Wnt pathway activation. We also used *Rosa^{TdTomato}* for lineage tracing. Morphology, number, and lineage of the cells in the organ of Corti was analyzed.

Results

Deleting *beta-Catenin^{flox(Ex2-6)}* allele in the prosensory domain resulted in cell alignment defects but in *beta-Catenin^{dm}* allele. Number of hair cells was not changed in both *beta-Catenin^{flox(Ex2-6)}* and *beta-Catenin^{dm}* allele. Number of inner pillar cells was decreased and number of outer pillar cells was increased in both *beta-Catenin^{flox(Ex2-6)}* and *beta-Catenin^{dm}* allele. Number of inner pillar cells was increased and number of outer pillar cells was decreased in *beta-Catenin^{fl(Ex3)}* allele. Lineage tracing of *beta-Catenin^{dm}* with *Rosa^{TdTomato}* identified that inner pillar cells changed their faith to outer pillar cells in *beta-Catenin^{dm}* allele.

Conclusion

This work identifies canonical Wnt/beta-Catenin is necessary and sufficient to maintain inner pillar cells against outer pillar cell. Considering importance of inner

pillar cells as a postnatal progenitor cells, this information may guide us to ectopically generate progenitor cell for regeneration.

PD 16

Dorso-Ventral Specification of Human Inner Ear Organoids in Response to Sonic Hedgehog Pathway Modulation

Emma Longworth-Mills; Jing Nie; Jade Harkin; Edward Srour; Eri Hashino

Indiana University School of Medicine

During inner ear development, the otic vesicle is patterned along a dorso-ventral axis in response to graded signaling molecules, including Sonic Hedgehog (SHH). SHH loss-of-function studies in mice revealed disrupted formation of cochlear structures associated with loss of ventral marker expression, strongly suggesting an essential role for SHH signaling in ventral specification of the inner ear. The inner ear phenotype observed in SHH KO mice resembles the cellular composition in human embryonic stem cell (ESC)-derived inner ear organoids, in which all derived hair cells bear morphological and functional properties of native vestibular hair cells with a lack of cochlear cells types. We reasoned that commitment to a vestibular fate in this model may be due to a lack of sufficient ventralization signals and that timed activation of SHH signaling may promote ventralization, leading to the induction of cochlear tissue. To test this hypothesis, we first generated a human *PAX2-2A-nGFP* ESC line to monitor and isolate otic progenitors arising in culture. These *PAX2-2A-nGFP* ESCs were differentiated into inner ear organoids, with the SHH pathway agonist purmorphamine added on day 12 of culture. Purmorphamine-treated aggregates consistently became larger in size than untreated controls due to increased cell proliferation as evidenced by a larger number of KI67+ cells. All *PAX2+* cells in purmorphamine-treated organoids also express *PAX8*, indicative of an otic identity. Since *PAX2* is not only an otic progenitor marker, but also a well-established marker for the ventral region of the otic vesicle, we evaluated its expression in treated and untreated cultures. qRT-PCR analysis revealed a higher expression level of *PAX2* in purmorphamine-treated aggregates compared to controls. FACS analysis confirmed this with an increased percentage of *PAX2-nGFP+* cells in purmorphamine-treated aggregates compared to untreated aggregates. Additionally, we found a larger number of cells expressing the ventral marker *OTX2* in *PAX2+* vesicles of purmorphamine-treated aggregates. In contrast, the number of cells expressing the dorsal marker *DLX3* within the *PAX2+* otic vesicles of treated aggregates was smaller than in controls. These results strongly suggest that augmentation of SHH signaling

with purmorphamine promotes cell proliferation and expression of ventral otic markers in human inner ear organoids, consistent with known SHH functions as a mitogen and ventralizer. Single-cell RNA-sequencing analysis is currently underway to further evaluate the effects of SHH pathway modulation on global gene expression patterns.

This study was supported by NIH R01DC013294 and F31DC015968.

Middle-Ear Mechanics

PD 17

Development of the Ear and Hearing in Bearded Dragons (*Pogona vitticeps*)

Helene Krogh Mogensen; **Jakob Christensen-Dalsgaard**

Department of Biology, University of Southern Denmark

The tympanic middle ear with one or three middle ear ossicles is an important adaptation to hearing in the tetrapods (the terrestrial vertebrates). However, the tympanic ears in the five major tetrapod groups (frogs, lizards, turtles, crocodiles and birds, and mammals) probably originated independently and rather late in evolutionary history - around 120 million years after the origin of the tetrapods. Much of the evidence for middle ear evolution naturally is based on the fossil record, where the transitional stages unfortunately are rare. However, changes to the middle ear during evolutionary history most likely occurred as changes to the developmental pathways of the organism. Development of the lizard middle ear has not been studied in any detail previously, but is therefore highly relevant to understand the independent evolution of lizard tympanic hearing, especially how different the development is to the closest diapsid relatives (birds and crocodiles).

In this study the development of the middle ear was examined on an anatomical and functional level during growth of the central bearded dragon, *Pogona vitticeps*. Three methods were used; micro computed tomography scanning, auditory brainstem response and laser vibrometry. The CT scanning show increased length, density and bone volume to total volume ratio for the middle ear bone columella with age. We found an onset of columellar development between day 51 and 54 embryos, with an almost full-length columella developed in day 64 embryos. It was clear, however, that the columellar density was higher in post-hatch animals. ABR responses could be recorded from one day post-hatch, but we failed to record any responses in the embryos, even when stimulating by vibrations. Maximal sensitivity of the audiogram increased with age, by 20-

30 dB within the first 200 days post-hatch. However, the most sensitive frequency decreased by approximately 1 kHz. This change is correlated with changes in middle ear function, as shown by laser vibrometry measurements, where the frequency at peak sensitivity of the eardrum decreases by 2.5 kHz, but may also depend on changes in the auditory papilla.

PD 18

Human Tympanic-Membrane Shape and Middle-Ear Delay Changes Due to Mechanically Pulling the Tensor-Tympani Muscle

Nam-Hyun Cho¹; Michael E. Ravicz²; Xiyang Guan¹; Sunil Puria³

1Harvard Medical School; 2Eaton-Peabody Lab, Mass. Eye & Ear; 3Eaton-Peabody Laboratories

Introduction: The three-bone flexible ossicular chain may allow controlled alterations of middle-ear sound transmission via its two attached muscles. The stapedius (ST) muscle attached to the stapes posterior crus is known to stiffen the stapes annular ligament and reduce sound transmission below 1.5 kHz. The tensor-tympani (TT) muscle attached to the malleus neck is thought to increase tension of the tympanic membrane (TM). However, the effects of human TT muscle activity on middle-ear sound transmission are not known. Could TT activation change the shape and stiffness of the TM and therefore influence sound transmission through the middle ear?

Methods: Unfixed thawed human-cadaver temporal bones were used for this study. The middle-ear cavity and facial recess were opened to access the TT and stapes. Forceps were attached to the TT muscles near the bony tunnel near the malleus to apply known amounts of TT pull in their natural direction (0 to 3 mm, in 1 mm steps) with a micromanipulator. A Thorlabs Ganymede-III-HR 905-nm optical coherence tomography (OCT) system, along with custom VibOCT software, measured both TM shape and motion. Sound generated by a loudspeaker was delivered to a glass-covered ear-canal coupler with a calibrated microphone to measure pressure. TM surface displacement (through the glass using VibOCT) at the umbo and 6 other locations, and stapes velocity (using a PolyTec HLV-1000), were evaluated in the 0.1- to 10-kHz range.

Results and Discussion: Static pulls of the TT produced TM shape changes that increased with increasing TT pull in a nonlinear fashion. Below about 1 kHz, a static TT pull produced a reduction of sound-driven umbo displacement and an increase in phase. These changes were transmitted to the stapes, resulting in a reduction of middle-ear transmission by a factor of ~6 and a reduction in middle-ear delay of ~200 μ s (for an example

2-mm pull). These are the first results to demonstrate that the delay through the human ME is altered by TM-shape changes caused by TT-tendon pulls that mimic muscle activation. The ~200- μ s decrease in delay is about 25% of the maximum interaural time difference across the human head. This suggests that a role for TT muscle activity might be to modify sound-localization cues. [Work supported by grant R01-DC005960 from the NIDCD of the NIH.]

PD 19

Middle-ear Muscle Contractions Should Not Be Included in Damage-Risk Criteria

Heath Jones¹; Stephen Tasko²; Gregory Flamme³; Kara McGregor²; Madeline Smith²; Kristy Deiters³; William Murphy⁴; Nathaniel T. Greene⁵; William Ahroon¹

¹U.S. Army Aeromedical Research Laboratory;

²Western Michigan University; ³Stephenson and Stephenson Research Consulting; ⁴The National Institute for Occupational Safety and Health;

⁵University of Colorado School of Medicine Department of Otolaryngology

Middle-ear muscle contractions (MEMCs) involve activation of the stapedius and/or tensor tympani muscles. MEMCs can be elicited by acoustic and non-acoustic stimuli, and can sometimes be engaged voluntarily. Responses typically increase the middle-ear impedance for low frequencies (95% confidence of > 95% prevalence) within the population, and are of sufficient strength and duration to serve as a protective mechanism. These assumptions were addressed by determining (1) the prevalence of acoustic reflexes using clinical protocols, (2) the likelihood of observing an MEMC for short-duration acoustic and non-acoustic stimuli among people with clinically-measured acoustic reflexes, and (3) attempts to condition or train an anticipatory MEMC in laboratory environments. Studies varied in size from 26 to 15,106 participants. The largest study examined the prevalence of clinically-measured acoustic reflexes drawn from the U.S. National Health and Nutrition Examination Survey. The laboratory studies included 220 healthy adults with excellent hearing ($n=194$) or slight/mild hearing impairment ($n=26$). Reflexive MEMCs to short-duration acoustic and non-acoustic stimuli were assessed in all laboratory studies. Additionally, the presence of conditioned MEMCs was investigated using five different training tasks administered to subgroups chosen at random. No participant group exhibited pervasive MEMCs, which obviated the need for assessment of whether the observed responses had sufficient strength or duration. Results indicated the likelihood of observing an MEMC for short-duration acoustic stimuli was much lower

than for non-acoustic stimuli and that voluntary eye closure produced the greatest likelihood of an MEMC. Conditioned MEMC responses were well below the 0.95 criterion necessary to consider the responses pervasive. Interestingly, participant attention greatly influenced the likelihood of observing an early, conditioned MEMC. Although clinical acoustic reflexes are often observed in a normal hearing population, clinical observations do not generalize to the stimuli and contexts relevant to DRC. Collectively, these studies indicate MEMCs should not be included as a protective factor in DRC for impulsive noises.

PD 20

Stapes Displacement in Response to Low-Frequency, High-Intensity Sounds: A Cross Species Study

John Peacock¹; Mohamed Alhussaini²; Nathaniel T. Greene³; Daniel J. Tollin⁴

¹University of Colorado School of Medicine, Department of Physiology and Biophysics; ²Assiut university Egypt; ³University of Colorado School of Medicine Department of Otolaryngology; ⁴Department of Physiology & Biophysics, and Department of Otolaryngology, University of Colorado School of Medicine

Stapes displacement increases linearly with increasing ear canal sound pressure until it reaches its maximum, at which point it will act to attenuate the amount of energy entering the cochlea. If stapes displacement were to saturate at a lower applied sound pressure level, this could help to limit damage to the inner ear from exposure to high intensity sounds. Alternatively, if the stapes displacement were to saturate at a higher applied sound pressure level, this could make it easier for high intensity sounds to cause damage.

Stapes displacement will vary between species, and thus the potential for inner ear trauma due to blast exposure will also vary between species. Different animals will require exposure to different sound intensities before damage can occur. Some studies have suggested a peak to peak stapes displacement in rabbits and cats of around 30 μ m, which is much smaller than the ~150 μ m displacement that has been measured in humans.

The middle ear transfer function also varies between species. Different animals ears are tuned to different frequency ranges, thus the transfer function will vary across frequency. Blast energy is mostly concentrated at the lower frequencies, and thus different species may be more or less susceptible to hearing trauma, depending on how easily energy at lower frequencies is transmitted through the ear. These species differences are important

to consider when choosing an animal model to study trauma from blast.

To better understand how high intensity sounds are transmitted through the middle ear in common animal models used for blast studies, we made measurements of stapes displacement in response to high intensity, low frequency sounds in humans, cats, chinchillas, guinea pigs, gerbils, rats and mice. A custom-built sound concentrating horn was used to expose cadavers to a series of single frequency tones of varying pressure levels, while a laser Doppler vibrometer was directed at the stapes footplate to record velocity. We then calculate (following numerical integration) peak displacement in each species.

Humans had the highest stapes displacements, while mice, rats and gerbils had the lowest. The species which was closest to humans was the chinchilla.

PD 21

Finite-element modelling of middle-ear vibrations under pressurization

Dongfang Qian¹; W. Robert J. Funnell²
¹*Dept. BioMedical Engineering, McGill University, Canada;* ²*Depts. BioMedical Engineering and Otolaryngology - Head & Neck Surgery, McGill University, Canada*

Early identification of hearing loss is important because if untreated it can lead to delayed language development and other difficulties. Current newborn hearing-screening tools are subject to excessively high false-positive rates. Tympanometry is a promising tool for improving screening tests by evaluating the condition of the middle ear, but it is poorly understood in newborns. Tympanometry involves large deformations, non-linear responses, viscoelastic (time-dependent) effects, and complex dynamic responses, which make it hard to model. A previous gerbil finite-element model developed in our lab (Choukir, 2017) was the first numerical simulation of tympanometry involving the simultaneous application of large quasi-static pressures and small sound pressures, and it succeeded in replicating some features of tympanometry. However, the model involved over-simplified anatomical details of the ossicles to reduce the computational cost. The goal of this study is to improve the model by adding a representation of the incudostapedial joint (ISJ). Upon verification and validation of the ISJ insertion, we can also investigate the effects of the ISJ in tympanometry.

The model employs a quasi-linear visco-hyperelastic model with several time constants in a Prony series.

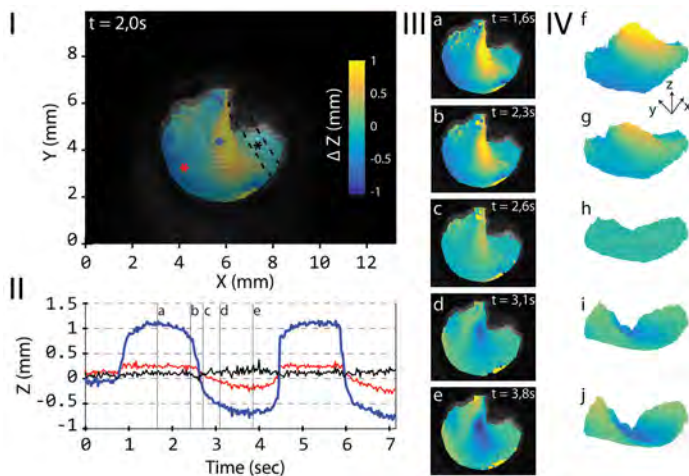
Material properties are taken from previous models and publications. The tympanic membrane is assumed to be homogeneous and nearly incompressible. The loads, combining high quasi-static pressures with low-amplitude sound pressures, reflect the conditions in tympanometry. The model can be verified against our previous linear model (Maftoon et al., 2015) and can be validated against our gerbil laser vibrometry data (Kose, 2019). This numerical model will help us gain insight into how the middle ear responds to different stimuli and thus open up new approaches to the interpretation of tympanometric measurements.

PD 22

Otoscopic Profilometry: Measuring Eardrum Deformation in 3D and in Real-time

Sam Van Der Jeught; Joris Dirckx
Universiteit Antwerpen

An otoscopic profilometry device based on real-time structured light triangulation is presented. A clinical otoscope head is mounted onto a custom-handheld unit containing both a small digital light projector and a high-speed digital camera. Digital fringe patterns are projected onto the eardrum surface and are recorded at a rate of 60-120 unique frames per second. The relative angle between projection and camera axes causes the projected patterns to appear deformed by the eardrum shape, allowing its full-field three-dimensional (3-D) surface map to be reconstructed. By combining hardware triggering between projector and camera with a dedicated parallel processing pipeline, the proposed system is capable of acquiring a live stream of point clouds of over 300,000 data points per frame at a rate of 30-40 Hz. Real-time eardrum profilometry adds an additional dimension of depth to the standard two-dimensional otoscopic image and provides a noninvasive tool to enhance the qualitative depth perception of the clinical operator with quantitative 3-D data. Visualization of the eardrum from different perspectives can improve the diagnosis of existing and the detection of impending middle ear pathology. The capability of the handheld device to detect small middle ear pressure changes by monitoring eardrum deformation in real time is demonstrated. Full-field height maps of the tympanic membrane can be recorded at 40 frames per second with a measurement precision varying between 10 and 100 μm , depending on local surface reflection parameters and total object depth span. The device has a form factor similar to existing otoscopes, is easy to use, and provides a first step toward implementation of quantitative tympano-topography in the clinical ENT office.



were first trained and optimized with a “cross-validation” dataset (n = 137). We used a 10-fold cross validation procedure for training and validation. We found that important features to train the algorithm were at four frequencies over a wide bandwidth between 400 Hz – 5000 Hz. We also used parameters extracted from the previously developed classifier (notch detector) as features in our analysis. Our preliminary results show that using a repeated 10-fold cross-validation procedure, a Random Forest (RF) classifier produced the best results, with an average ROC value of 0.82.

We then evaluated the optimized classification methods on a separate test dataset (n = 34). The sensitivity and specificity of the optimal RF classifier on the test set was 0.90 and 0.93, respectively. We are currently finding new features and exploring other machine learning algorithms to improve classification.

Conclusion: WAI shows promise as a stand-alone measurement to detect SCD if appropriate analyses and classification methods are used. Here we show promising preliminary results with common machine learning techniques. We plan to investigate other classification methods that have great potential in efficient and accurate diagnoses of SCD as well as other mechanical pathologies of the middle and inner ear.

Supported by: NIH/NIDCD R01DC004798, T32DC000038, F31DC016761

PD 24

Refining Absorbance Measurements in Newborns: Probe-Fit and Intra-Subject Variability

Hammam AIMakadma¹; Beth Prieve²
¹University of Louisville; ²Syracuse University

Background: Absorbance is one of the measures under the umbrella of wideband acoustic immittance (WAI). It indicates the proportion of acoustic power absorbed by the auditory conductive pathway. Assessment of the conductive pathway concurrently with the newborn hearing screening can mitigate consequences of the high referral rate of non-permanent, typically conductive, hearing loss. One obstacle is the large absorbance variability from ears with normal conductive pathways, which in newborns is exacerbated by poor probe fitting. The current project addresses intra-subject factors that contribute variability in absorbance. The objectives were to: 1) develop WAI-based criteria to indicate absorbance changes associated with poor fits (2) characterize the variability due to poor fits, and 3) evaluate test-retest variability with probe-reinsertions, given good probe-fit.

Methods: Repeated measurements were recorded in 50 newborns (98 ears) who passed TEOAE screenings. One

PD 23

Application of Machine Learning Techniques to Detect Superior Canal Dehiscence (SCD) using Wideband Acoustic Immittance

Salwa F. Masud¹; Daniel J. Lee²; Inge M. Knudson³; Hideko H. Nakajima¹

¹Eaton-Peabody Laboratories, Massachusetts Eye and Ear; Graduate Program in Speech and Hearing and Bioscience and Technology, Harvard Medical School; ²Department of Otolaryngology, Massachusetts Eye and Ear; ³Eaton-Peabody Laboratories, Massachusetts Eye and Ear

Objective: Patients with superior canal dehiscence (SCD) have a distinct wideband acoustic immittance (WAI) pattern and we hypothesize that detection of this pattern can help distinguish SCD ears from Normal ears. The main goals of this study are to 1) develop a machine learning algorithm based on WAI measurements that can accurately distinguish SCD from Normal ears and 2) evaluate the ability of this technique to classify ears as normal or with SCD.

Methods & Results: Power reflectance was analyzed from WAI measurements in 100 SCD ears that were symptomatic and diagnosed with SCD by high-resolution computed tomography (CT), and 71 Normal ears. A previously developed power reflectance diagnostic algorithm to detect a narrow-band pattern (notch detector) for SCD (Merchant et al., *Otology and Neurotology*, 2015) was tested on the whole dataset—this classifier produced an area under the Receiver Operating Characteristic (ROC) curve of 0.71, and an accuracy rate of 71%. To improve classification, we utilize more information from the power reflectance measurements and new classification techniques.

We investigated modern machine learning techniques to develop a novel approach for diagnostic procedures for power reflectance. Multiple classification models

absorbance measurement was chosen as the baseline that served as a best-fit reference in each ear. 'Probe-fit differences'; were calculated relative to the baselines. To determine which WAI measures predicted poor fits, correlations between the probe-fit differences and multiple WAI measures were tested, and probe-fit criteria were derived. The criteria identified the measurements affected by poor fits. Absorbance changes due to poor fits was characterized. Once poor fits were eliminated, test-retest was analyzed as 'probe-reinsertion differences'; Variability was assessed using the standard deviations (SD) associated with absorbance changes in poor fits, test-retest, and absorbance.

Results: Two WAI-based probe-fit criteria were derived based on the analysis of twelve moderate-strong correlations: 1) impedance phase-based criterion [500-1000 Hz] > -0.11 cycles, and 2) absorbance-based criterion [250-1000 Hz] > 0.58. The magnitude of absorbance change in the criteria-identified poor fits was 0.08 and significant 1000-6000 Hz, and up to 0.4 at < 1000 Hz. The SDs associated with these changes were greatest and similar to absorbance SD in the low frequencies. Probe reinsertion differences were 0.02, and were significant 500- 5000 Hz. Their SDs were also greatest and similar to absorbance SD in the low frequencies.

Conclusions: Controlling for poor fits reduced absorbance variability across a wide range of frequencies that extended to the diagnostically important mid-frequencies. The finding that the greatest increase in absorbance in poor fits was in the low frequencies is consistent with controlled experiments on acoustic leaks in adults. Test-retest with probe reinsertion was generally small in magnitude. Nevertheless, it contributed significantly to absorbance variability in the low frequencies, consistent with reports in adults.

Hearing Science History

Chairs: Stefan Raufer & Christopher Shera

SYMP 20

Physicists, Physiologists, and the Standardization of Musical Performance and Musicians' Bodies

Myles W. Jackson

Institute for Advanced Study, Princeton University

Throughout the nineteenth and twentieth century, natural scientists and physicians collaborated with musicians and music pedagogues to elucidate the physics, anatomy, and physiology of playing the piano and bowed instruments with a view to improve technique. Many hoped that the mechanical principles of the natural sciences could somehow assist musical pedagogy. A

number of music pedagogues turned to acousticians, physiologists, and physicians during the first half of the nineteenth century to see if they could uncover certain attributes of virtuosi, such as Niccolò Paganini and Franz Liszt. Natural scientists and physicians were given the charge of ferreting out the virtuoso's skilled manipulations, some of which were enviously guarded secrets. Other pedagogues found the exaggerated techniques of the virtuosi repulsive, arguing that that teachers needed to assist students to play with a style quite different from the virtuosi's. Playing difficult passages with lightning speed was antithetical to the true purpose of music. Natural scientists and physicians in this case were called upon to assist in eliminating wasted movement and correcting technique by drawing upon the principles of the biological and physical sciences. Often these instructors sought assistance in eliminating wasted movement and correcting technique. Other pedagogues still balked at the idea of having the natural sciences explain their idiosyncratic craft via depersonalized, rational knowledge.

Perhaps the critical question was: could the performer's touch be reduced to mechanical principles? If so, how did this affect teaching the requisite techniques? If music teachers focused on the mechanical principle of playing, then perhaps one could standardize both practice and the body. Did such standardization detract from the individual styles of performance? A number of music instructors insisted counterintuitively that standardized musical treatises based on scientific investigations enabled students to enhance their own styles of play. In this case, by drawing upon the universal principles of natural science, the individual could cultivate her/his own technique. The story that unfolds in this paper touches on an interesting historical theme, namely how other forms of contemporary culture- in this instance, music, perceived the roles of physics, anatomy, physiology, and (later) neurophysiology in pedagogy.

SYMP 21

Hearing Loss in Children and Older Adults: Disparities in Policy, Screening, Intervention, and Outcomes

Dillan Villavisanis¹; Jeremy A. Greene²; Frank R. Lin³; Jennifer A. Deal⁴

¹Department of Medicine, Science, & the Humanities, Johns Hopkins University Krieger School of Arts & Sciences, Baltimore, MD, USA; ²Department of the History of Medicine, Johns Hopkins School of Medicine, Baltimore, MD, USA; ³Department of Otolaryngology - Head & Neck Surgery, Johns Hopkins School of Medicine, Baltimore, MD, USA; ⁴Department of Epidemiology, Johns Hopkins Bloomberg School of Public Health, Baltimore, MD, USA

Hearing loss is a public health concern which affects patients of all ages. Hearing loss in children affects speech ability and language acquisition, whereas hearing loss in older adults has been demonstrated to have associations with cognitive decline and increased risk of mortality. Our aim was to quantify research on hearing loss in children and older adults and determine if disparities were reflected in policy, screening, intervention, and outcomes between the groups. To quantify research items on hearing loss in children and older adults, we used an advanced search in the PubMed databases. To specify literature in children we used the terms “children,” “pediatrics,” and “adolescents,” and to specify literature in older adults we used the terms “older adults,” “geriatrics,” and “elderly,” in addition to each categorical term specified, such as “policy,” “cochlear implants,” or “hearing aids.” The PubMed literature search query demonstrated that over five-times as many literature items have been written on children with hearing loss (9743) compared to that of older adults (1880), and that this magnitude of difference has only decreased slightly in recent years. The magnitude of difference is largest for topics on cochlear implants (22.4) and language (15.0) and smallest for hearing aids (2.5) and cognition (1.3). Our findings identified substantial disparities in the medical literature surrounding hearing loss comparing older adults to children. Given the prevalence of hearing loss is about two in three for older adults over age 70 and one in seven for children, it is intriguing that research efforts and prevalence are not proportional. The deficiency of research on older adults is exemplified by disparity in existing screening methods and policies, lack of knowledge and efficacy of interventions, and lagging outcomes. Additional research in older adults, particularly on cochlear implantation, language, and screening, is needed in order to provide the evidence base for policy and clinical care.

SYMP 22

Integrating the Role of History, Research, and Technology in the Rehabilitation of Deafness

James Naples

Department of Otorhinolaryngology-Head and Neck Surgery, University of Pennsylvania

The history of rehabilitating deafness is complex and controversial. The common goal in rehabilitating deafness is to provide early language acquisition. Unfortunately, early generations did not have the advantage of technology to offer subjects. Thus, rehabilitation options were largely limited to learning oral or manualist language techniques. There was significant philosophical divide regarding which rehabilitation option was best, and physicians and hearing scientists

played a limited role in the process during this early history. These limited options were the mainstay of the rehabilitation process until after the middle of the 20th century. The evolution in rehabilitation options occurred with concomitant advancements in the application of research to the study of language acquisition and hearing assistive technologies such as hearing aids and cochlear implantation. The mechanism by which history, research, and technology have been integrated to provide current management options for rehabilitating deafness and the evolving role of the physicians and hearing scientists will be discussed.

SYMP 23

Three Pianos: Musical instruments in Hugo Riemann, Hermann Helmholtz, and Ernst Mach's science of sound

Alexandra Hui

Department of History, Mississippi State University

What can the personal pianos of Hugo Riemann, Hermann Helmholtz, and Ernst Mach tell us about their respective theories of sound sensation? This presentation juxtaposes the material culture — the instruments, both scientific and musical — of the sound sensation studies of against the aesthetic and epistemic priorities of the scientists' respective psychophysical worldviews. At times their scientific values were in tension with their individual musical aesthetics but other times they were not. This prompts a more general discussion of the role of cultural context of the sensing scientist's practice, both in the past and presently.

SYMP 24

David M. Green and the Theory of Auditory Profile Analysis

Christopher Conroy

Department of Speech, Language & Hearing Sciences, Boston University

In a series of articles and a book-length review written during the mid-1980s and early-1990s, David M. Green and colleagues outlined a new theory of auditory intensity discrimination termed “profile analysis” (Green, 1983, 1988). Predicated as it was on the notion that in processing broadband signals observers rely on a simultaneous, across-frequency analysis of “spectral-shape” (Kidd, Mason, & Green, 1986), profile analysis marked a sharp theoretical departure from the critical-band energy detector model that had dominated psychoacoustics for the previous half-century (e.g. Fletcher, 1940; Zwicker et al., 1957; Scharf, 1961). By exploiting novel experimental techniques, rigorously controlled stimuli, and an ever-growing arsenal of custom-built electronics, Green and colleagues showed

that, under certain experimental conditions, masker energy in multiple, spectrally-remote auditory filters could have a significant influence—either positive or negative, depending on the stimulus—on observer performance on perhaps the most fundamental of all psychoacoustic tasks: the discrimination of a difference in intensity between two successively presented sinusoids. For instance, early profile analysis experiments revealed that Weber fractions for an intensity increment added to a sinusoidal target actually improved with the addition of a relatively small number of flanking sinusoidal “maskers” widely-spaced in frequency and remote from the signal’s critical-band (Green & Mason, 1985). Conversely, observer uncertainty regarding the number and pattern of the flanking signals had a negative effect that far surpassed what would have been predicted based on traditional masking theory (Spiegel, Picardi, & Green, 1981; Neff & Green, 1987). Accordingly, profile analysis became part of a broader movement within psychoacoustics in which ‘old-school’ theory and methods began to explicitly incorporate concepts such as memory and attention, uncertainty and similarity, and other non-peripheral factors in complex sound processing. By focusing on the reflections of the scientists involved in its development, this talk will trace the theoretical and methodological antecedents to profile analysis and the subsequent research programs that found root in its empirical findings. Interwoven with this discussion will be a relatively informal portrait of Green the scientist—as told by his students, colleagues, and himself—presented for the benefit of the current/emerging generation of psychoacousticians and auditory scientists who may not be familiar with the details of his illustrious and highly influential career.

SYMP 25

Electroencephalography: an old technique with new potentials

Lindsey N. Van Yper

Department of Linguistics, The Australian Hearing Hub, Macquarie University, Sydney, Australia

Electroencephalography (EEG) has become increasingly important in auditory neuroscience. While the field has long been dominated by the peripheral auditory evoked potentials (AEPs), there is a renewed interest in cortical responses. In this talk, I will provide a historical overview of EEG-techniques, starting with the first human recordings by Hans Berger in the 1920s. The early efforts to record AEPs and subsequent technological advances will be discussed. Based on these historical events, I will review how this remarkable technique impacted and continues to impact auditory neuroscience, as well as clinical practice.

Inner-Ear Therapeutics

PD 25

Sodium Thiosulfate as otoprotectant to reduce Cisplatin induced hearing loss in Children with Liver Cancer.

Kaukab Rajput; Penelope Brock; Rudolf Maibach; Edward Neuwelte; Margaret Childs
Primary investigator and Oncologist

Bilateral high-frequency hearing loss is a serious permanent side-effect of cisplatin (Cis) therapy; particularly debilitating when occurring in young children. Sodium Thiosulphate (STS) has been shown to reduce Cis-induced hearing loss. SIOPEL 6 is a phase III randomised trial to assess the efficacy of STS in reducing ototoxicity in young children treated with Cis for the most common form of primary liver cancer in children namely hepatoblastoma.

Newly diagnosed patients were randomised to Cis or Cis+STS for 4 preoperative and 2 postoperative courses. Cis 80mg/m² was administered over 6 hours, STS 20g/m² was administered intravenously over 15 minutes exactly 6 hours after stopping Cis. Tumour response was assessed after 2 and 4 preoperative cycles with serum alphafoeto-protein (AFP) and liver imaging. . The primary endpoint was centrally reviewed absolute hearing threshold, at the age of ≥3.5 years by pure tone audiometry. The Brock grading scale (0-4) was used to compare hearing loss between groups<./p>

Absolute hearing threshold was assessed in 101 evaluable patients, hearing loss of Brock grade 1-4 occurred in 29/46 = 63.0% under Cis and in 18/55 = 33.0% under Cis+STS, showing a 48% reduction in the incidence of hearing loss (RR: 0.52, p = 0.002; 95% CI: 0.33-0.81).

Conclusion: This randomised phase III trial of cisplatin versus cisplatin plus sodium thiosulfate in localised hepatoblastoma showed that the addition of sodium thiosulfate significantly reduced the incidence of cisplatin-induced hearing loss without any evidence of tumour protection. These results support the use of the platinum otoprotectant STS in localised disease.

PD 26

Development of Small Molecule Protein Kinase Inhibitors for Hearing Protection

Matthew A. Ingersoll¹; Joe DiGuseppi²; Lauryn E. Caster³; Zhenhang Xu⁴; Duane Currier⁵; Jaeki Min⁵; Taosheng Chen⁵; Jian Zuo⁴; Tal Teitz⁶

¹Pharmacology Department, Medical School, Creighton University; ²Biomedical Sciences Department, Medical School, Creighton University; ³Pharmacology Department, Medical School, Creighton University; ⁴Department of Biomedical Sciences, Creighton University, School of Medicine; ⁵Department of Chemical Biology and Therapeutics, St Jude Children's Research Hospital; ⁶Department of Pharmacology, Creighton University, School of Medicine

Hearing loss caused by chemotherapy, various drugs, noise and aging is a major medical problem in our society, affecting over 360 million people worldwide (World Health Organization, 2017). Cisplatin chemotherapy causes permanent hearing loss in 40-60% of treated patients. To date, no drugs have been approved by the FDA for protection from cisplatin-, noise-, or age-related hearing loss. Protein kinases are particularly attractive therapeutic targets as they regulate critical cellular functions and many kinase inhibitors have been approved by the FDA for effective cancer therapy. We recently conducted high-throughput screens (HTS) of highly-specific kinase inhibitor compound libraries in dose response mode in an inner ear cell line (HEI-OC1) and identified two kinase inhibitor families with therapeutic potential: aurora kinase inhibitors and platelet-derived growth factor receptor (PDGFR) inhibitors. The screen identified multiple compound hits from each of these two kinase families and the top hit in both groups (compounds SNS314 and crenolanib, respectively) have cisplatin EC50 of 2-4 μ M in the inner ear cell line and in an ex-vivo mouse cochlear explant assay in which they conferred full protection against cisplatin-induced hair cell death. The most potent cisplatin-protective compounds in the cochlear explants will be tested in tumor cell lines and neurospheres to confirm their lack of interference with cisplatin's tumor killing activity. The top compound/s will subsequently be evaluated in vivo for cisplatin ototoxicity protection in rats by local and/or systemic delivery. We will perform absorption, distribution, metabolism, and excretion (ADMET) studies of these top compounds. If the top compound(s) do not confer complete protection in animals against cisplatin after optimizing its concentration and formulation, we will perform structure-activity relationship (SAR) studies to chemically modify the lead compounds to improve efficacy and lower toxicity. Genetic mouse models in which the targeted kinase is tissue-specific and conditionally deleted will be generated to validate the role of this specific kinase in cisplatin-induced hearing loss. Finally, the activity of the top protective compounds will be tested in combination with specific inhibitors of cyclin-dependent kinase 2 (CDK2) that we have recently identified as protective compounds against cisplatin- and noise- induced hearing loss (Teitz et al, JEM 2018; Hazlitt et al, JMC 2018) for potential synergistic effects.

The long-term goal of this work is to develop optimized pre-clinical and clinical compounds that can be tested in humans for protection against cisplatin-induced hearing loss.

PD 27

Human Otic Progenitors Derived from Induced Pluripotent Stem Cells Survive and Differentiate upon Transplantation into a Guinea Pig Model of Ototoxicity

Alejandra Lopez-Juarez¹; Hannae Lahlou²; Yves Cazals³; Christian Chabbert³; Said Assou⁴; Quan Wang²; Albert Edge⁵; **Azel Zine**⁶

¹CNRS UMR 7260 Aix-Marseille Université, France & Universidad de Guanajuato, Mexico; ²Harvard Medical School, Eaton-Peabody laboratories, Massachusetts Eye and Ear; ³CNRS UMR 7260 Aix-Marseille Université, France; ⁴INSERM U1051 University of Montpellier, France; ⁵Department of Otolaryngology, Harvard Medical School; ⁶UFR Pharmacie, University of Montpellier, France

Background: Human induced pluripotent stem cells (hiPSCs) technology holds great expectations for drug discovery and clinical applications such as cell transplantation. Along this line, progresses have been made in applying hiPSC technology to a variety of organ systems such as the retina, the cardiovascular system as well as the peripheral and central nervous systems. Noteworthy, the inner ear represents another system of interest for drug discovery and cell therapy applications relying on the use of hiPSCs. Recently, our group has been able to derive molecularly characterized human otic progenitor cells (hOPCs) from differentiation of hiPSCs in adherent monolayer cultures (Lahlou et al., 2018). The further *vitro* differentiation of these hOPCs generated cells that upregulated a subset of embryonic hair cell-associated markers (ATOH1, POU4F3, MYO7A). The primary objective of this study is attempted to explore the capacity of hOPCs to migrate, survive and differentiate within cochlear sensory epithelia upon engraftment into a guinea pig model of ototoxicity. **Methods:** We initially generated hOPCs from the induction of hiPSCs in a monolayer culture system, and subsequently examined the *in vivo* engraftment of these partially differentiated hOPCs in our established guinea pig model of ototoxicity. Prior to cell engraftment, hOPCs were pre-labeled with the lipophilic dye Vybrant-Dil cell labeling solution and transplanted through a lateral wall cochleostomy in amikacin-damaged cochleae. **Results:** Using hiPSCs differentiated in a monolayer guidance culture protocol, we generated a large number of hOPCs that express a comprehensive panel of otic lineage markers. Transplanted vybrant Dil-positive hOPCs migrated at different turns

along the entire cochlear duct of ototoxin-damaged cochleae at least until 14 days post-grafting. Cell fate analyses revealed that a subset of hOPCs survived and differentiated within ototoxin-damaged cochlear epithelia into cells expressing initial hair and supporting cell markers for up to four weeks post-graft. **Conclusions:** Our findings indicate that hiPSC otic derivatives can be used as a source of transplants for successful engraftments in an animal model of ototoxicity. This study represents a significant step toward developing stem cell-based cell therapy for balance and hearing deficits.

Acknowledgements: This work is supported by EC FP7-Health-2013-Innovation, No. 603029-1.

PD 28

Protection from Gentamicin Ototoxicity in Cochlear Cultures by Carvedilol Derivatives that Block the Mechano-Electrical Transducer Channel

Corné J. Kros; Molly O'Reilly; Nerissa K. Kirkwood; Simon E. Ward; Guy Richardson; Marco Derudas
University of Sussex

Background

Aminoglycosides (AGs) are broad-spectrum antibiotics used to treat serious bacterial infections. Ototoxicity is a major side effect of these drugs. Because aminoglycosides enter hair cells mainly through their mechano-electrical transducer (MET) channels (Marcotti et al 2005 *J Physiol* 567:505; Alharazneh et al 2011 *PLoS ONE* 6:e22347), we search for compounds that compete with AGs by binding to the MET channel. Carvedilol is a nonselective α 1- and β -adrenergic blocker used for the treatment of hypertension and heart failure. It protects zebrafish lateral line hair cells from AG toxicity and hinders their uptake of Texas Red labelled gentamicin (GTTR) (Ou et al 2009 *JARO* 10:191), suggesting MET channel block as a protective mechanism. We tested whether this applied to mammalian cochlear hair cells and evaluated carvedilol and a series of newly-synthesized analogues.

Methods

Carvedilol analogues were synthesized by modifying the carbazole moiety, the anisole ring or the β -hydroxyl amino group. Cochlear cultures from P2 mouse pups were exposed to 5 μ M gentamicin for 48 h, and/or carvedilol or analogues. Survival of outer cells (OHCs) in the high-frequency basal coil was quantified. Loading of GTTR (0.2 μ M for 10 min) into OHCs without or without compounds was evaluated by fluorescence intensity. MET currents were recorded from OHCs to assess block by the compounds.

Results

Carvedilol (10 and 20 μ M) fully protected hair cells in cochlear cultures against 5 μ M gentamicin, but proved toxic at ≥ 30 μ M. Carvedilol blocked OHC MET currents in a voltage-dependent manner. Block was maximal at +16 mV with a K_D of 0.1 μ M and was relieved at both negative (K_D at -164 mV 6.3 μ M) and more positive (K_D at +96 mV 1.5 μ M) membrane potentials, identifying carvedilol as a permeant blocker of the MET channel. One of the analogues had a higher affinity to the MET channel at the biologically relevant membrane potential of -164 mV (K_D 4.6 μ M) and offered greater protection at lower concentrations than carvedilol itself. Both compounds reduced GTTR uptake into OHCs. Other blockers of adrenergic receptors were not otoprotective.

Conclusions

Carvedilol protected OHCs in mouse cochlear cultures from gentamicin toxicity, likely by competing for entry through the MET channel. One analogue had a higher affinity for the MET channel and offered enhanced protection, possibly because it is more basic than carvedilol itself, resulting in a stronger interaction with negative charges in the MET channel pore.

Funding

Supported by MRC Programme Grant MR/K005561/1

PD 29

The Protective Role of ATP-Gated P2X7 Receptors in the Noise-Induced Cochlear Ribbon Synapse Degeneration

Hong-Bo Zhao; Yan Zhu; Shu Fang
Dept. of Otolaryngology, University of Kentucky Medical Center, Lexington, KY 40536

Background: Recent studies in our laboratory and other laboratories reveal that ATP-purinergic signaling has important roles in many aspects of cochlear hearing function, including regulation of sound transduction, outer hair cell electromotility, gap junctional coupling, K^+ -sinking and recycling, and endocochlear potential (EP) generation, by activation of ATP-gated P2X receptors. Moreover, it has been found that P2X2 mutations can lead to hearing loss (DFNA41) and increase susceptibility to noise. Similar to P2X2, P2X7 also predominantly expresses in the cochlea, including hair cells, supporting cells, and auditory nerves. Our previous study demonstrated that deficiency of P2X7 can also increase susceptibility to noise stress. In this study, we further explored the function of P2X7 receptors in the cochlear ribbon synapses and noise-induced ribbon synapse degeneration.

Methods: P2X7 knockout (KO) mice were used, and exposed to noise to examine the susceptibility to noise-stress. ABR threshold, DPOAE, and cochlear microphonics (CM) were recorded to assess cochlear and hearing function. The ribbon synapse degeneration was examined by immunofluorescent staining for CtBP2.

Results: Under normal condition, hearing function in P2X7 KO mice measured as ABR threshold showed no significant difference in comparison with wild-type (WT) mice. After being exposed to white noise (~ 95 dB SPL, 2 hr), both WT and P2X7 KO mice had similar initial temporary threshold shift (TTS). However, P2X7 KO mice showed less recovery than WT mice. Consistently, immunofluorescent staining shows that ribbon synapses in P2X7 KO mice and WT mice had no significant difference. After noise exposure, P2X7 KO mice had more significant reduction of ribbon synapses than that in WT mice.

Conclusions: These new data suggest that P2X7 deficiency can exacerbate the cochlear ribbon synapse degeneration in noise exposure, revealing a protective role of ATP-gated P2X7 receptors in the cochlear ribbon synapses to noise stress.

Supported by NIH R56 DC 016585 and R01 DC 017025

PD 30

Honokiol Protects Against Cisplatin Ototoxicity Without Compromising its Antitumor Effects

Xiaodong Tan¹; Yingyue Xu¹; Yingjie Zhou²; Katherine Shi¹; Nicolette Zielinski Mozny¹; Aditi Agarwal¹; Jing Zheng¹; Claus-Peter Richter³

¹Northwestern University; ²Northwestern University;

³Department of Otolaryngology; Department of Biomedical Engineering; Knowles Hearing Center; Northwestern University

Background

Cisplatin is frequently used as a compound for chemotherapy. One of its sequelae is hearing loss in up to 90-100% of the patients. The ototoxicity of cisplatin is related to outer hair cell (OHC) death caused by the accumulation of reactive oxygen species (ROS). To prevent hearing loss, antioxidants have been proposed to detoxify ROS. However, those compounds also protect tumor cells and require the local delivery through transtympanic injection. We have shown in the pilot study that systemic delivery of honokiol (HNK) protects hearing during cisplatin treatment through direct activation of sirtuin3 (SIRT3), a deacetylase exclusively expressed in mitochondria. HNK also protects the heart, brain, liver, and kidney, against oxidative stress. In this study, we tested additional cancer cell lines to verify that HNK does not protect cancer cells.

Methods

Different cancer cell lines (prostate, cervical and colon cancers) and cochlear explants from P3-5 C57BL/6 mice were cultured with the co-application of cisplatin (50 or 100 μ M, respectively) and HNK (0, 5, 10, 25 μ M, respectively). Cancer cell survival was determined by counting cell number with a hemocytometer. OHC survival was determined by immunostaining. For in vivo studies, HNK (20 mg/kg) was injected intraperitoneally 1 hour prior to cisplatin injections (20 mg/kg) in adult C57BL/6J mice. Auditory brainstem responses (ABR) were measured pre- and post-treatment up to 14 days to examine changes in the hearing threshold. After euthanasia and fixation, immunostaining and confocal microscopy of cochlear whole mounts were performed to examine the OHC survival and morphological changes. Tumor growth will be induced by injecting murine squamous cell carcinoma (SCC) into the flank of FVB mice. Cisplatin chemotherapy for cancer treatment and HNK for hearing protection will be studied following standard procedure (4 mg/kg/day each for 5 days).

Results

1) HNK application did not increase the survival of different cancer cell lines. 2) Cisplatin treatment (20 mg/kg) induced an elevation of ABR thresholds up to 40 dB in C57BL/6J mice. 3) Pre-treatment with honokiol significantly reduced the threshold elevation and improved animals' health. 4) Confocal imaging also showed that honokiol increased OHC survival compared to mice receiving cisplatin only.

Conclusions

Honokiol protects against cisplatin-induced ototoxicity in mice while showed no protection to cancer cells in cultures. Further results on tumor-bearing mice will be obtained to verify these findings in cisplatin chemotherapy.

Funding

Work supported by the Hearing Health Foundation through a 2017 Emerging Research Grants Award to XT.

PD 31

STOP OTOTOXICITY: Phase 1/2 Clinical Trial of SPI-1005 in Cystic Fibrosis

Jonathan Kil¹; Maria Tupayachi Ortiz²; Daniel Dorgan³; Raksha Jain⁴; Patrick Flume⁵

¹Sound Pharmaceuticals, Inc; ²University of Miami Health System; ³University of Pennsylvania; ⁴UT Southwestern; ⁵Medical University of South Carolina

Background: The incidence of tobramycin induced hearing loss, tinnitus, vertigo or dizziness (ototoxicity) varies widely in the CF population. Reasons for this include a lack of consistent patient selection, dosing,

audiometric methods, and applied ototoxic criteria. SPI-3005-501 is a Phase 1/2 clinical trial involving ebselen (SPI-1005) to prevent and treat tobramycin induced ototoxicity. Here we report the incidence of tobramycin induced ototoxicity (observational) and tobramycin levels before/after oral SPI-1005 (Sentinel PK).

Methods: Twenty CF adults were enrolled on standard treatment including IV tobramycin (10-21 days) for acute pulmonary exacerbation. Audiometric changes from baseline were calculated at 2 and 4 weeks post-treatment and ASHA cochleotoxic criteria were applied. Audiologic methods included pure tone audiometry (PTA) in both conventional and extended high frequencies in the sensitive range for ototoxicity (SRO), the words-in-noise test (WINT), and distortion product otoacoustic emissions (DPOAEs). The Tinnitus Functional Index (TFI) and Vertigo Symptom Scale (VSS), validated patient reported outcome (PRO) measures, were also tested. For Sentinel PK, serum tobramycin levels (mg/L) were analyzed from 0-12 hrs post-infusion on Day 1-3 after three oral doses of SPI-1005.

Results: The observational study enrolled 20 adult CF females/males average age of 31 yrs (18-59) at 4 US sites. At 2 and 4 weeks post-treatment, the incidence of cochleotoxic change from baseline was 69% and 70%, respectively. For DPOAE, the incidence of a ≥ 5 dB shift was 81% and 50%. For WINT, the incidence of a $\geq 10\%$ increase was 15% and 0%. For TFI, the incidence of a ≥ 10 pt increase was 25% and 20%, and for VSS, the incidence of a ≥ 6 pt increase was 0% and 13%. In the Sentinel PK study, 6 adult CF females/males average age of 32 yrs (20-51) were enrolled after starting IV tobramycin qd (10 mg/kg). On Day 1, no SPI-1005 was given. On Day 2, an am/pm SPI-1005 dose and on Day 3, an am dose of SPI-1005 were given. The Day 1 avg Cmax (27) and Cmin (0.7) were compared to the Day 2 or 3 avg Cmax (30 or 25) and Cmin (1.4).

Conclusion: In this CF population, a standard course of IV tobramycin was sufficient to cause hearing loss and other ototoxic symptoms. Conventional PTA, SRO, DPOAE were more sensitive than TFI and VSS in identifying ototoxic change. Patient age and duration of tobramycin treatment were not obvious factors for predicting ototoxicity. SPI-1005 did not alter serum tobramycin levels.

Supported by the CFFT.

PD 32

mGluR7 Negative Allosteric Modulation, a Novel Approach for Sensorineural Hearing Loss: Preclinical Evidence from a Noise Exposure Model in CBA mice

Reza Amanipour¹; Xiaoxia Zhu²; Guillaume Duvey³; Sylvain Celanire³; Joseph P. Walton⁴; Robert D. Frisina²

¹Medical Engineering Department, Global Center for Hearing & Speech Research, University of South Florida; ²Medical Engineering Dept., Global Center for Hearing & Speech Research, University of South Florida; ³Pragma Therapeutics; ⁴Communication Sciences & Disorders Dept., Medical Engineering Dept., Global Center for Hearing & Speech Research, University of South Florida

Introduction: Acoustic overstimulation causes cochlear damage, resulting in hearing loss. The main excitatory neurotransmitter in the inner ear and central auditory systems is glutamate. Excessive release of glutamate results in excitotoxicity, contributing to hearing impairment through degeneration of synaptic contacts between hair cells and spiral ganglion neurons. Here, we study the effects of PGT117, a negative allosteric modulator (NAM) of the metabotropic glutamate receptor subtype 7 (mGluR7) to prevent and reduce hearing loss following acute noise-exposures in mice.

Methods: Male CBA/CaJ mice with normal hearing (age 3-6 months) were utilized. The mice were randomly placed in control and treatment groups (N=8/group). Auditory brainstem responses (ABRs) and distortion product otoacoustic emissions (DPOAEs) were used to measure hearing at four time points: pre-noise exposure (baseline), 24 hours, 2 and 4 weeks post-trauma. PGT117 was administered orally (treated group) at 1 hour pre-exposure and immediately following the exposure. Awake mice were exposed to an octave-band noise at 110 dB SPL for 45 minutes. ABRs and DPOAE amplitudes and thresholds were measured at each time point, following our previously published procedures.

Results: ABR and DPOAE threshold elevations as well as reductions in DPOAE amplitudes occurred at every tested frequency within the untreated mouse group. However the treated group showed smaller threshold elevations or sometimes no threshold shifts. In fact, the differences in temporary threshold shifts between the two groups were highly significant when measured 24 hours post-exposure (e.g., $F(1,14) = 28.79$, $P < 0.0001$). At 2 and 4 weeks post-exposure permanent threshold shifts were much larger in the control group. However, the treated group showed almost complete recovery. Following noise exposure, DPOAE amplitude

levels were reduced in both groups, but this outer hair cell damage was significantly greater in the controls; i.e., the differences in amplitude levels were statistically significant for the low frequency range (6-12 kHz) when measured 24 hours post-exposure ($F(1,14) = 16.07, P = 0.0013$).

Conclusion: These results indicate that negative modulation of mGluR7 provides noteworthy otoprotection from glutamate excitotoxicity that occurs in the cochlea following acoustic trauma. This novel drug is unique in that it targets the mGlu7 receptor which implication, until now, has not investigated for preventing noise induced hearing loss (NIHL). Therefore, medical options to prevent or reduce NIHL have been advanced.

Support: TRIH T05 Grant from UK Action on Hearing Loss, Pragma Therapeutics.

Tinnitus

PD 33

Tinnitus-related Changes in Intrinsic Neural Networks

Somayeh Shahsavarani; Sara Schmidt; Yihsin Tai; Rafay Khan; Fatima Husain
University of Illinois at Urbana-Champaign

Studies from our lab and other centers using functional magnetic resonance imaging (fMRI) have shown that tinnitus alters functional connectivity in resting-state networks. Specifically, changes in the default mode network (DMN), the dorsal attention network (DAN), and the auditory network have been reported. However, there is no consensus on the extent and type of these tinnitus-related changes, possibly due to the heterogeneity of the patient population and small sample sizes. Our goal in the present study was to examine the replicability of previous findings using a large sample. We obtained resting-state EPI data from 44 participants with tinnitus (18 females, mean = 53.20 years, TFI: mean (SD) = 23.63±18.7) and 24 participants without tinnitus (13 females, mean = 47.04 years) while they were at "rest" with eyes open for 10 minutes. Statistical Parametric Mapping software (SPM12) was used to preprocess the fMRI data. Using the Functional Connectivity Toolbox (Conn), seed-based analysis was conducted to compute resting-state functional connectivity (rs-fc) where the DMN, DAN, and auditory network were represented with multiple seeds (or regions of interest). In the DMN, significant increased connectivity was found in the bilateral insular cortex in people with tinnitus compared with the controls. Further, significant changes in correlation between precuneus and DMN were identified within each group, with decreases seen in the tinnitus condition. This finding of decreased connectivity between precuneus and DMN

within the tinnitus group is in line with DMN-precuneus decoupling suggested previously by our group (Schmidt et al. 2017, NeuroImage: Clinical). In the DAN, no significant differences were found between the groups. However, further analysis revealed a large variability in the correlation between precuneus and DAN within the tinnitus group, pointing to the influence of heterogeneity in this group. Such variability can be related to tinnitus severity or duration (Schmidt et al., 2017, NeuroImage: Clinical). In the auditory network, significant increased connectivity was observed in the right superior frontal gyrus, left posterior inferior temporal gyrus, and posterior cingulate gyrus in the tinnitus group compared with the control group. Consistent with previous findings, our current results highlight tinnitus-related variability in rs-fc and further provide evidence for the role of precuneus as an objective biomarker of tinnitus. This is an ongoing study; additional data, with further analyses accounting for participants' hearing sensitivity and heterogeneity of the patient population, are required to corroborate previously identified invariant resting-state tinnitus-related neural correlates or even to identify new neural networks.

PD 34

Subjective Pulsatile Tinnitus [if Somatosensory]: (A) Does Not Require Imaging and (B) Can Be Abolished

Robert Levine
Tel Aviv Medical Center

Pulsatile, cardiac synchronous tinnitus [PT] can be subjective or objective and can have several causes. Some are related to (a) abnormalities of intracranial or cervical blood flow, (b) defects in the barrier isolating acoustically the cochlea from intracranial blood flow, or (c) aberrant blood flow in the middle ear or cochlea capsule. In all these case an acoustic source, a somatosound, is responsible for the PT. It is nearly always unilateral and can often be heard and/or recorded. Other cases of PT are subjective: they have no recordable or identifiable [via imaging, blood work, or physical exam] acoustic source. We report our experience with 46 such patients seen over the past 10 years. One group of such patients can suppress their pulsations with intense activation of their head and/or neck muscles; this syndrome has been termed the somatosensory pulsatile tinnitus syndrome [SSPT]. As first described, SSPT is constant and can be lateralized or non-lateralized. In addition to constant SSPT [cSSPT], as was originally described, two types of intermittent SSPT [iSSPT] have been observed: (a) iSSPT only and (b) constant non-pulsatile tinnitus intermixed with iSSPT [cT+iSSPT]. All 13 subjects with iSSPT or cT+iSSPT, who had PT at the time of testing, could totally suppress their tinnitus. Nine of the iSSPT

subjects had no pulsations at the time of testing; but when tested with intense activation of their head and/or neck muscles, 2 of these 9 developed PT.

All 28 subjects with cSSPT could totally suppress their pulsations with intense activation of their head and/or neck muscles; of these 28, 19 could totally suppress their tinnitus.

Another 5 subjects could not suppress their pulsations despite constant pulsatile tinnitus with no identifiable somatosound. In four of the five patients their tinnitus was non-lateralized.

Additional support for the somatic nature of cSSPT, iSSPT, and cT+iSSPT comes from the 4 subjects [2 with cSSPT, 1 with iSSPT, and 1 with cT+iSSPT] whose tinnitus resolved with either needling of trigger points or pinna electrical stimulation.

In conclusion, if cardiac synchronous pulsatile tinnitus can be suppressed somatically, (a) imaging is not necessary and (b) needling of trigger points or pinna electrical stimulation may abolish the pulsatile tinnitus.

PD 35

Effect of Tinnitus on Reaction Time and Short-Term Memory

LaGuinn P. Sherlock¹; Douglas S. Brungart²
¹Army Public Health Center / Walter Reed National Military Medical Center; ²Walter Reed National Military Medical Center

Tinnitus is the perception of sound in the absence of an external sound source and can interfere with concentration. This may explain why those with bothersome tinnitus often perform more poorly on tests that require concentration and memory than those without tinnitus. There is no objective measure of the presence of tinnitus so the primary evaluation of tinnitus is accomplished using subjective questionnaires. An objective measure of the functional impact of tinnitus on concentration could potentially facilitate appropriate focus of tinnitus management and serve as a measure of management efficacy. Additionally, there has not been a systematic evaluation of the impact of task-irrelevant background noise on visual tests of attention and memory performance for those with bothersome tinnitus. Low-level noise-like maskers appear to provide some relief for individuals with tinnitus, and irrelevant speech-like sounds are known to interfere with memory tasks for listeners without tinnitus. In this study, individuals with bothersome tinnitus and age- and hearing-matched controls performed a selective attention task, where they identified the direction of an arrow while ignoring the direction of the flanking arrows, and a spatial location

task where they recalled the location of letters in a 4x4 grid. These tasks were completed in three auditory conditions: 1) quiet, 2) low-level white noise, and 3) irrelevant speech signal to determine the impact, if any, of task-irrelevant background sound on performance. The results indicate that those with bothersome tinnitus have longer reaction times and reduced memory span, and that performance is better in the presence of irrelevant sound than in quiet for both the tinnitus and control groups.

PD 36

An Experimental Study of Stress Induced Tinnitus in a Dual Stress Rat Model

Jung Mee Park¹; Min Jung Kim¹; So Young Park¹; Ilyong Park²; Hyo Jeong Yu¹; Shi Nae Park¹
¹Department of Otorhinolaryngology-Head and Neck Surgery, College of Medicine, The Catholic University of Korea; ²Department of Biomedical Engineering, College of Medicine, Dankook University

Background: The proper function of neurons in many brain areas depends on the physiological homeostasis maintained and regulated by glutamate and GABA, main neurotransmitters which create opposite excitatory/inhibitory forces in the brain. The mechanism behind tinnitus generation due to stress can be explained by the disrupted balance of these neurotransmitters in the auditory pathway. This animal study has been performed to evaluate the association between stress and tinnitus in non-auditory pathway of the brain in rat models of dual stress.

Methods: Male Wistar rats aged 1 month were used and subgrouped according to the single or double stimuli of noise and stress. Noise-induced tinnitus (NIT) was induced by 110 dB SPL, 16 kHz narrow band noise for 1 hr and restraint-induced acute stress (RIAS) was induced by restraining rats with taped plastic film envelopes for 1 hr. ABR thresholds and DPOAEs were recorded before and after the induction of noise and stress. Tinnitus was assessed by gap-prepulse inhibition of the acoustic startle reflex (GPIAS) by obtaining GN ratios. Stress hormones and relevant neurotransmitter receptors, NMDA and GABA receptors (NMDAR and GABAR) were observed in the cochlea and the brain hippocampal tissues.

Results: Increased ABR thresholds and decreased DPOAE responses were observed after 1 hr noise stimuli in NIT groups. RIAS only group, without changes in hearing level, showed increased GN ratio compared to the control group ($P < 0.05$), which indicated that stress alone can cause tinnitus. Dual stimuli of noise and stress showed more significantly increased GN ratios regardless of their induction order. In western blot of whole hippocampus,

GABA_A receptors were significantly decreased in RIAS +NIT group ($P < 0.05$). Immunofluorescence staining of CA3 area of hippocampus showed increased expression of NMDAR in the experimental groups and decreased expression of GABA_A receptors compared to the control group ($P < 0.05$).

Conclusion: This study is first known animal study that shows tinnitus can be induced by stress alone. Reduced GABA_A receptors in the hippocampus seems to be related to the relevant mechanisms on tinnitus development and its association with stress. This novel animal study results support the strong association among noise, stress, and tinnitus.

PD 37

Safety and Long-Term Efficacy of a New Bimodal Sensory Neuromodulation Treatment for Tinnitus Evaluated Through a Randomized Clinical Trial in 326 Patients

Hubert Lim¹; Caroline Hamilton²; Stephen Hughes²; Martin Schecklmann³; Sven Vanneste⁴; Deborah Hall⁵; Berthold Langguth³; Brendan Conlon⁶

¹University of Minnesota, and Neuromod Devices Limited; ²Neuromod Devices Limited; ³University of Regensburg; ⁴The University of Texas at Dallas; ⁵University of Nottingham, and NIHR Nottingham BRC; ⁶St. James's Hospital - Trinity College Dublin, and Neuromod Devices Limited

Background: Tinnitus is a major health issue in our society. Unfortunately, there is limited evidence for the efficacy of different tinnitus treatments with few confirmatory randomized clinical trials. Recent animal research and pilot human studies have demonstrated the ability to drive extensive auditory plasticity and potentially treat tinnitus by pairing sound with trigeminal or somatosensory nerve activation, such as with tongue stimulation. Therefore, we conducted a blinded and randomized clinical trial in 326 tinnitus patients to evaluate the safety and efficacy of a new home-use bimodal neuromodulation device, consisting of auditory and somatosensory (tongue) stimulation.

Methods: Three stimulation algorithms (PS1, PS2, PS3) consisting of different acoustic and tongue activation patterns were tested. Treatment was delivered for 12 weeks with a take-home device (recommended for one-hour usage per day). The patients were randomized across two clinical sites (in Ireland and Germany) to the three treatment arms and the patients, investigators and statisticians were blinded to treatment assignment. Pre-specified outcome measures included the Tinnitus Handicap Inventory (THI) and Tinnitus Functional Index (TFI) that were measured at the start, interim and end of the 12-week treatment as well as several post-

treatment time points up to 12 months. Protocols and analyses were pre-specified in a published protocol paper (*D'Arcy et al., BMJ Open 7(10):e018465, 2017*) and on clinicaltrials.gov (NCT02669069).

Results: All three stimulation algorithms resulted in statistically significant improvements in tinnitus during treatment for both THI ($p < 0.0001$) and TFI ($p < 0.0001$) that were also clinically significant (> 7 THI points, > 13 TFI points). Large improvements in tinnitus occurred within the first 6 weeks with further improvement in the second 6 weeks of treatment. Post-treatment, PS1 resulted in persistent long-term improvements lasting 12 months after treatment ceased that clinically outperformed the other stimulation algorithms. The treatment was safe and well-tolerated with a high compliance rate (84%; > 36 hours of usage). Furthermore, analyses in several pre-specified subtypes of tinnitus patients revealed that PS1 exhibits larger therapeutic effects in tinnitus patients who have greater hypersensitivity to sounds, which was not observed for PS2 or PS3.

Conclusions: These findings demonstrate that bimodal neuromodulation with sound and tongue stimulation can safely provide fast-acting tinnitus treatment with long-lasting therapeutic effects post-treatment that has been shown in one of the largest randomized clinical trials for tinnitus. We will continue to conduct large-scale randomized clinical trials to further identify optimal stimulation settings for different subtypes of tinnitus patients.

PD 38

NHPN-1010, a Phase II-ready Oral Drug Demonstrates Excellent Pre-clinical Effectiveness in Treating Blast- and Noise-induced Tinnitus.

Richard D. Kopke¹; Jianzhong Lu²; Xiaoping Du²; Qunfeng Cai²; Matthew B. West²; Don Nakmali³; Wei Li²; Weihua Cheng²; Xiangping Huang²; Elaine E. Hamm⁴; Richard E. Gammans⁴; Donald L. Ewert²
¹Hough Ear Institute; Oklahoma Medical Research Foundation; Departments of Physiology and Otolaryngology, University of Oklahoma Health Sciences Center; Otologic Pharmaceuticals, Inc.; ²Hough Ear Institute; ³Hough Ear Institute; ⁴Otologic Pharmaceuticals, Inc.

Tinnitus, the phantom perception of sound, is a frequent neuropathological consequence of noise- or blast-induced cochlear injury. This disorder occurs in 14-20% of the population and is one of the most prevalent service-related disabilities among military personnel, which represents an especially high-risk demographic for cochlear traumas and comorbidities. In some individuals, the tinnitus percept can become sufficiently debilitating that it leads to psychological

distress and loss of situational awareness, negatively impacting health, interpersonal relationships, and job performance. Despite the inherent urgency to develop a pharmacological therapy to address this auditory disorder, no such FDA-approved therapeutic is currently available.

From a mechanistic vantagepoint, unifying theories regarding the pathophysiological origins of chronic tinnitus involve compensatory hyperactivity and hyper-neurosynchrony in the central auditory system (brain) that develop to compensate for reduced peripheral cochlear signaling. Objective characteristics of tinnitus have, thus, been reported to include synaptopathy among sound-transducing hair cells (HCs) in the cochlea, reduced auditory brainstem response (ABR) wave I amplitudes (i.e. reduced peripheral input), increased ABR wave V amplitudes (i.e. compensatory central gain), and pathological changes in the expression levels of key signal gating factors associated with hyperactivity in auditory centers of the brain. Consistent with these reported observations, we reproducibly induced behavioral evidence of tinnitus percept in rats that directly correlated with elevated ABR wave V/I amplitude ratios and ribbon synapse loss across broad tonotopic ranges, using a shock tube model of blast exposure. These blast-induced sequelae coincided with chronic, tinnitus-related histopathological changes in central and peripheral biomarker levels, including reduced Arc/Arg3.1 mobilization in the central auditory pathway.

While developing NHPN-1010, an FDA Phase II-ready oral combination drug consisting of *N*-acetylcysteine and 2,4-disulfonyl α -phenyl tertiary butyl nitron, as a therapeutic for preventing hearing loss, we discovered that its administration significantly reduced behavioral evidence of tinnitus in rat models of both steady-state noise- and blast-induced cochlear injury. In our shock tube blast injury model, NHPN-1010 treatment significantly reduced both behavioral and neuropathological evidence of tinnitus, including normalization of ABR wave V/I amplitude ratios, ribbon synapse densities, and expression patterns of Arc/Arg3.1 and other tinnitus-related biomarkers in the auditory pathway. Moreover, our recent work has revealed that NHPN-1010 treatment induces neuritogenesis *in vitro* and post-traumatic cochlear synaptogenesis *in vivo*, promoting re-innervation of de-afferented inner HCs even after a significant interventional delay. Based on these expanded therapeutic attributes, NHPN-1010 represents an exciting candidate for mitigating, and potentially reversing, tinnitus.

PD 39

Tinnitus Treatment Using Non-invasive and Minimally-invasive Electric Stimulation

Fan-Gang Zeng; Matthew L. Richardson; Phillip Tran; Harrison Lin; Hamid Djalilian
University of California, Irvine

Non-invasive transcranial or minimally-invasive transtympanic electric stimulation may offer a desirable treatment option for tinnitus because it can activate the deafferented auditory nerve fibers while posing little to no risk to hearing. Here we built a flexible research interface to generate and control accurately charge-balanced current stimulation as well as a head-mounted instrument capable of holding a transtympanic electrode steady for hours. We then investigated the short-term effect of a limited set of electric stimulation parameters on tinnitus in 10 adults with chronic tinnitus. The preliminary results showed that 60% of conditions of electric stimulation produced some degree of tinnitus reduction, with total disappearance of tinnitus in 4 subjects in response to at least one condition. The present study also found significant side effects such as white flashes, tactile and even pain sensations during electric stimulation. In addition to masking and residual inhibition, neuroplasticity is likely involved in the observed tinnitus reduction. To translate the present electric stimulation into a safe and effective tinnitus treatment option, we need to optimize stimulation parameters that activate the deafferented auditory nerve fibers and reliably suppress tinnitus, with minimal side effects and tolerable sensations. Non-invasive or minimally-invasive electric stimulation can be integrated with sound therapy, invasive cochlear implants or other forms of coordinated stimulation to provide a system-oriented, analytic strategy for tinnitus treatment or even a cure.

PD 40

Mechanisms Underlying Cochlear Electrical Stimulation-Induced Tinnitus Suppression

Jinsheng Zhang¹; Hao Luo¹; Ethan Firestone¹; Edward Pace¹; Bin Liu¹; Syed Ahsan²; Eric Kim¹; Zhiguo Zhao¹; Yong Xu¹

¹Wayne State University; ²Kaiser Permanente Hospital

Cochlear electrical stimulation (CES), used to restore hearing, can also significantly suppress clinical manifestation of tinnitus. However, little is known about the underlying mechanisms leading to this phenomenon. Utilizing our established rat model of CES, we subjected animals to intense noise exposure (8-16 kHz, 115 dB SPL, 2 hrs) and subsequently performed unilateral cochlear implantation in both acoustic-trauma and control groups. We then conducted

behavioral testing for tinnitus and electrophysiological recordings from the auditory cortex (AC) before, during, and after CES. We found that 30-minute stimulation of the basal turn (mid-high frequency region) of the cochlea significantly suppressed behavioral evidence of middle-frequency range tinnitus in acoustically traumatized rats. This result was accompanied by decreased spontaneous firing rate, bursting, and neurosynchrony in the mid-high frequency regions of the AC, and at the local field potential level, by decreased coherence and phase locking index: especially in the gamma-band. For control rats, we found that cochlear implantation alone induced low-frequency tinnitus, which did not benefit from CES. Electrophysiologically in these control rats, CES elevated spontaneous firing rate, bursting, neurosynchrony, coherence, except for phase-lock index, in the AC. Taken together, since the behavior results from animals with acoustic trauma-induced tinnitus are in line with published clinical data, these experiments confirmed the validity of our rat model as an appropriate means for studying the mechanisms underlying CES-induced tinnitus modulation. Consequently, the electrophysiological data indicate that down-regulation of spontaneous firing rate, bursting, and neural connectivity in the AC are important for generating tinnitus suppression.

Auditory Brainstem II

PS 282

Developmental Regulation of Cholinergic Signaling in the Gerbil MNTB

Sonia Weimann; R. Michael Burger
Lehigh University

The ionotropic $\alpha 7$ nicotinic acetylcholine receptor (nAChR) has broad distribution throughout the mammalian brain (Morley et al. 1977). The role of this receptor can vary based on its cellular location and the timing of its peak expression. Presynaptic expression of $\alpha 7$ nAChRs is known to facilitate neurotransmitter release (Albuquerque et al. 1997; McGehee et al 1995) while postsynaptic expression can have broad effects including the regulation of gene expression and the mediation of excitatory currents. Happe and Morley (2004) showed that the $\alpha 7$ nAChR is expressed in the superior olivary complex (SOC), with peak expression just prior to hearing onset in neurons specialized to compute sound location. However, physiological function within these nuclei has not been demonstrated.

In addition to nAChRs, other molecules are indicative of cholinergic synaptic activity. One key presynaptic marker,

vesicular acetylcholine transferase (VAcHT), was examined within the medial nucleus of the trapezoid body (MNTB). Tissue was labeled prior to, during, and after hearing onset in gerbils aged p9-p30. VAcHT was positively stained in the calyx of Held terminals upon MNTB neurons and exhibited peak expression just prior to hearing onset. Labeling was most prominent in the lateral (low frequency) MNTB. Furthermore, localization of VAcHT expression to Calyx synapses was confirmed by colabeling VAcHT positive synapses with fluorescent dextran tracer orthogradely labeled from cochlear nucleus injections. Dye delivery was facilitated by pulses of electroporation (Burger et al. 2005).

The physiological function of nAChRs in MNTB was investigated using in vitro whole-cell patch clamp on brain stem slices obtained from gerbils age P9-20. Effects of nAChRs on cell excitability were assayed by evaluating discharges in response to depolarizing current injection in 50 pA steps before and during bath application of nicotine and/or nAChR antagonists. In the presence of nicotine, MNTB neurons increased discharges to current steps ranging from 261% to 2650%. This effect was fully suppressed by preapplication of nicotinic antagonists or partially reversed by antagonist application.

Our results demonstrate that cholinergic function is prominent in MNTB and occurs both before and after hearing onset cholinergic signaling via nAChRs. These data combined demonstrate the presence of functional nAChRs within the MNTB and that cholinergic signaling may contribute to the development of the sound localization circuitry or mediate information processing in this crucial node in the sound localization pathway.

PS 283

Afferent Regulation of the Fragile X Mental Retardation Protein in the Chicken Cochlear Nucleus

Xiaoyan Yu¹; Hitomi Sakano²; Yuan Wang¹
¹*Florida State University;* ²*Department of Biochemistry and Biophysics, School of Medicine and Dentistry, University of Rochester*

Fragile X syndrome (FXS) is the most common inherited cause of autism and intellectual disability, resulting from a loss or dysfunction of the fragile X mental retardation protein (FMRP). Normally, FMRP regulates synaptic plasticity and neuronal excitability by controlling local translation of a large number of RNAs. The importance of FMRP in experience-dependent brain plasticity has been well documented across sensory modalities, however, how afferent activity regulates FMRP itself in sensory neurons is not fully understood.

Here, we used immunocytochemical method to characterize the time course of FMRP changes in the chick nucleus magnocellularis (NM) following unilateral afferent deprivation by removing one cochlea. NM is homologous to the mammalian anteroventral cochlear nucleus (AVCN). It is known that this manipulation leads to neuronal cell loss in NM and AVCN within 48 hours.

After cochlea removal, we identified two subpopulations of NM neurons with dramatic changes in the intensity and pattern of FMRP immunostaining. For the first group, FMRP rapidly aggregated into distinct puncta within the cytoplasm. The average immunoreactivity intensity per cell significantly increased at 4-6 hours, followed by a decrease at 12-24 hours. These neurons eventually lost their cytoplasmic Nissl substance and Y10B immunostaining, a ribosome marker, by 24 hours, indicating their fate to death. For the second group, FMRP intensity reduced at 12-24 hours without aggregation. Although their Y10B immunoreactivity was lower than control neurons, they exhibited normal Nissl staining. For remaining neurons, FMRP intensity and pattern was largely unchanged in response to afferent deprivation. Interestingly, survived NM neurons at 48-96 hours exhibited an enhanced heterogeneity of FMRP immunoreactivity, as compared to the intact NM on the other side of the brain. We are exploring the biological relevance of this heterogeneity to synaptic organization.

These findings indicate that the level and subcellular distribution of FMRP in the cochlear nucleus is regulated by the afferent input from the ear, and this regulation may play a role in determining cell fate following hearing loss.

PS 284

Bilateral Hearing Loss Alters Intrinsic Excitability of Medial Superior Olive Neurons Through Changes in Action Potential Mechanisms.

David Haimes; Nace L. Golding
University of Texas at Austin

The Medial Superior Olive (MSO) is a mammalian brainstem nucleus that computes cues used for azimuthal sound localization. MSO neurons exhibit strong developmental changes in hyperpolarization-activated cation channels (HCN) and low voltage-gated potassium channels to confer fast processing capabilities, especially after the onset of hearing (~P12 in gerbils). These findings raise the possibility that early auditory experience at least in part drives changes in intrinsic excitability.

To address this question, we performed either bilateral

cochlear ablations (CA) or sham surgeries (CTL) in Mongolian gerbils at P10, before hearing onset, and then made whole-cell current clamp patch recordings in coronal slices at P23-61. Hearing was evaluated in both sets of animals via auditory brainstem evoked responses (ABRs) and given ≥ 1 day for recovery prior to slice recordings. In a separate set of experiments, we quantified axon initial segment (AIS) morphology in CTL and CA animals through immunolabeling of MSO slices with antibodies to AnkyrinG, a scaffolding protein specific to the AIS, and HCN1, a voltage-gated ion channel that effectively outlines the soma and dendrites, demarcating the MSO.

In slice experiments we characterized the intrinsic electrophysiological properties of ventral (high-frequency) MSO neurons (CTL, $n=100$; CA, $n=54$). Compared to controls, we found that in CA animals, the amplitude of action potentials (AP) from rest was significantly larger (CTL, 29.7 ± 2.20 mV; CA, 46.6 ± 2.33 mV; $p=1.83E-6$) and exhibited faster rates of rise (CTL, 152.22 ± 17.71 mV/s; CA, 264.43 ± 20.49 mV/s; $p=2.61E-05$). The resting potential remained constant (CTL, -49 ± 0.75 mV; CA, -49 ± 0.58 mV; $p=0.96$). Interestingly, despite little differences in peak input resistance across the populations (CTL, 8.30 ± 0.64 M Ω ; CA, 14.17 ± 1.65 M Ω , $p=6.7E-4$), the required threshold current was dramatically reduced (CTL, 2740 ± 183 pA; CA, 1020 ± 97 pA; $p=5.26E-12$). At the same time the absolute voltage thresholds were higher in neurons from CA gerbils (CTL, -35.62 ± 1.50 mV; CA, -28.89 ± 1.14 mV; $p=9.25E-4$). Parallel results from AIS immunolabeling experiments revealed that CA gerbils exhibited a small, $\sim 10\%$ increase in AIS length (CTL, 17.8 ± 0.10 μ m; CA, 20.0 ± 0.35 μ m; $p=2.39E-5$), more closely resembling AIS length in pre-hearing (P9) gerbils (22.7 ± 0.38 μ m).

Taken together, the robust effects of CA on the amplitude and rate of rise of action potentials suggest that early auditory experience impacts the expression and/or physiology of voltage-gated sodium channels. The increase in the voltage threshold of spiking in the face of a reduction in required current may reflect differential changes in the density, subunit specificity or modulatory state of voltage-gated sodium channels in the axon vs. the soma and dendrites.

PS 285

Comparison of Direct Injection vs. Silk Fibroin Scaffolds for Viral Vector-mediated Expression of Opsins in the Auditory Brainstem

Angela Zhu¹; Stephen McInturff²; Ariel E. Hight³; Elliott D. Kozin⁴; M. Christian Brown⁵; Daniel J. Lee⁶

¹Massachusetts Eye and Ear Infirmary; ²Eaton-

Peabody Laboratories, Massachusetts Eye and Ear, Harvard Program in Speech and Hearing Bioscience and Technology; ³Eaton-Peabody Laboratories, Massachusetts Eye and Ear; Program in SHBT, Division of Medical Sciences, Harvard Medical School; ⁴Massachusetts Eye and Ear Infirmary; Department of Otolaryngology, Harvard Medical School; ⁵Eaton-Peabody Laboratories, Massachusetts Eye and Ear, Harvard Medical School, Harvard Program in Speech and Hearing Bioscience and Technology; ⁶Department of Otolaryngology, Harvard Medical School

Introduction

An optogenetics-based auditory brainstem implant (ABI) may enhance spectral resolution by increasing the number of independent auditory channels compared to electrical stimulation. Photosensitization of cochlear nucleus (CN) neurons, however, requires gene therapy approaches using viral vectors to enable expression of opsin protein in non-transgenic models. Direct inoculation (via microinjection) is effective but requires visualization of target tissues and is invasive, preventing translation to the clinic. Silk fibroin films have been shown to enhance adeno-associated virus (AAV)-opsin expression in the motor cortex and dorsal brain surface by enabling more uniform AAV expression and better anatomical alignment with a light source (Jackman, S L, et al. (2018) *Cell Reports*. 22: 3351-3361). In this study, we hypothesize that a novel silk fibroin/AAV scaffold placed on the surface of the brainstem can enable efficient opsin expression in CN neurons.

Methods

Following craniotomy in CBA/CAJ mice, AAV constructs containing Chronos (blue light sensitive opsin) and GFP reporter were delivered to CN via 1) direct pressure injections or 2) AAV-coated or silk fibroin/AAV-coated silicone discs placed on the surface of dorsal subdivision of the CN (DCN). Optically-evoked ABRs (oABRs) and multiunit activity in inferior colliculus (IC) were recorded following 3-4 week incubation. Post-experiment histology was performed for mice who underwent direct injection.

Results

In mice directly injected with AAV, we observed Chronos expression in the CN in both neuronal and non-neuronal populations (Hight, AE et al. (2015) *Hear. Res.* 322: 235-241). In response to light pulses to the surface of the DCN, there was optically evoked auditory brainstem response and evoked neural activity in the IC. Ongoing studies will characterize differential expression levels of opsins in the CN neurons when comparing direct injection, AAV-coated or silk fibroin/AAV-coated discs.

Conclusion

This is the first study to use a novel silk fibroin scaffold in the auditory system for vector delivery. Non-invasive transduction of CN neurons could hasten clinical translation of optogenetics for a new-generation ABI based on optogenetics.

PS 286

Exposure to male advertisement call alters dopamine synthesis in the hindbrain auditory efferent nucleus of female plainfin midshipman fish

Kelsey N. Hom¹; Jonathan Perelmuter²; Brooke Vetter³; Joseph Sisneros³; Paul Forlano⁴

¹The Graduate Center, CUNY; ²CUNY Brooklyn College; ³University of Washington; ⁴Dept. of Biology, Brooklyn College, City University of New York; Programs in Ecology, Evolution, and Behavior ; Neuroscience ; and Behavioral and Cognitive Neuroscience, The Graduate Center, City University of New York

Dopamine is important for mediating the salience of environmental and social stimuli. Dopaminergic modulation of auditory processing has been investigated throughout the brain, but few studies have examined coordinated dopamine release across multiple levels of the auditory system. The plainfin midshipman (*Porichthys notatus*) is a great model for understanding neural mechanisms of social-acoustic behaviors because reproductive females use the advertisement call of territorial males to locate a potential mate. Furthermore, the auditory system and its connectivity with social behavior network nuclei and innervation by multiple neuromodulators is well-delineated. Diencephalic dopamine neurons project widely throughout the brain, including multiple levels of the auditory system, from the inner ear to the forebrain. Dopamine fiber innervation in certain auditory brain regions changes seasonally with reproductive state and playbacks of male advertisement calls activate dopaminergic neurons in the diencephalon of males and behaviorally attentive females. However, it is unclear to what degree local dopamine release is altered by socially salient signals. Therefore, we tested the hypothesis that dopamine synthesis in auditory brain regions changes in response to social-acoustic signals. We exposed 22 female midshipman to one of three playback conditions: hum (the male advertisement call), brown noise, or ambient sound for 15 minutes and used immunohistochemistry to measure phosphorylated tyrosine hydroxylase (pTH), a marker for active dopamine synthesis in neurons and fibers and a proxy for dopamine release. We found that there was significantly less pTH in the hum condition in comparison to ambient and brown noise groups within dopaminergic neurons of the forebrain and dopaminergic fibers innervating

the cholinergic hindbrain auditory efferent nucleus. We did not see significant differences between groups in thalamic and hypothalamic auditory regions. Synthesis and/or release of dopamine in these regions may require behavioral engagement. Since cholinergic hindbrain efferent neurons can directly inhibit hair cells in the inner ear, we propose that a reduction of dopamine synthesis and release reduces activation of these efferent neurons, indirectly increasing hair cell responses to the hum. Modulation of the peripheral auditory system to enhance the detection and evaluation of social-acoustic signals may be a conserved feature of the dopaminergic system in other vocal vertebrates.

PS 287

Impaired Auditory Processing in The Inferior Colliculus of the Fragile X Mouse Model

Jeremie Sibille¹; Ursula Koch²

¹Charite Universitätsmedizin; ²Freie Universität Berlin

Background: After Down's syndrome, Fragile X Syndrome (FXS) is the most common inherited cause of intellectual disability. Affecting approximately 1 in 4000 males and 1 in 6000 females, the individuals suffer from an over-expansion of the CGG triplet repeat within the Fragile X Mental Retardation 1 gene (FMR1) resulting in an impaired development of neuronal networks. The Fmr1 KO mouse model mimics many of the patient's symptoms, including auditory hypersensitivity and reduced habituation^{1,2,3}. Consequently, neurons in the auditory brainstem and auditory cortex of Fmr1 KO mice show an altered balance of excitation and inhibition, a broadening of frequency tuning and an increased spike rate in response to monaural and binaural stimuli^{4,5}. The present study aims to find out to what extent auditory processing in the inferior colliculus (IC), a central auditory structure that interconnects -almost exclusively- lower auditory nuclei with higher cortical structures, is affected by the loss of FMRP.

Methods: Single-cell recordings were obtained from neurons of ketamine/xylazine anesthetized mice aged two to four months. Most neurons were located in the dorsal and external cortices of the IC. A battery of monaural and binaural stimulus were presented via earphones where responses were compared between Fmr1 WT and Fmr1 KO mice. Neurons are first grouped according to their spiking pattern in response to pure tone stimulation, then their response to diverse monaural and binaural stimulation are analysed using locally written MATLAB scripts.

Results: The majority of IC neurons of both genotypes responded with a primary like response pattern. IC

neurons (from the dorsal and external cortices) of Fmr1 KO mice showed broader frequency tuning, a slightly earlier and stronger onset response coupled to an enhanced rebound spiking. In addition, the tonotopic gradient seemed to be partially degraded in Fmr1 KO mice compared to their WT relatives. We also analyzed habituation using a stimulus specific adaptation (SSA) response paradigm. Surprisingly, lesser neurons than expected in both genotypes exhibited SSA-mediated plasticity.

Conclusion: Together the higher responses observed in the Fmr1 KO mice throughout our protocols point toward weaker-delayed inhibitory regulations. Our results confirm that the Fmr1 KO mice IC exhibits an hypersensitive auditory processing as broadly characterized in the patient.

- 1- Ciaccio et al. 2017,
- 2- Turner et al, 1996,
- 3- Chen and Todt 2001,
- 4- Garcia-Pino et al. 2017,
5. Rotschafer and Razak 2001,

PS 288

Oligodendroglial BDNF Regulates Presynaptic Properties and Neurotransmission in The Auditory Brainstem

Eun Jung Kim; Miae Jang; Elizabeth Gould; Jun Hee Kim
University of Texas Health Science Center

Neuron–glia communication contributes to the precise control of synaptic functions. Oligodendrocytes near synapses detect and respond to neuronal activity, but their role in synapse development and plasticity remains largely unexplored. Here we show that oligodendrocytes modulate neurotransmitter release at presynaptic terminals through secretion of brain derived neurotrophic factor (BDNF), an activity-dependent signal. Oligodendrocyte-derived BDNF functions via presynaptic tropomyosin receptor kinase B (TrkB) to ensure fast, reliable neurotransmitter release and auditory transmission in the developing brain. In auditory brainstem slices from Bdnf+/- mice, reduction in endogenous BDNF significantly decreased vesicular glutamate release by reducing the readily releasable pool of glutamate vesicles, without altering presynaptic Ca²⁺ channel activation or release probability. Using conditional knockout mice, cell-specific ablation of BDNF in oligodendrocytes largely recapitulated this effect, which was recovered by BDNF or TrkB agonist application. This study highlights a novel function for oligodendrocytes in synaptic transmission and their potential role in activity-dependent refinement of presynaptic properties.

Vibration Threshold of the Western Ratsnake (*Pantherophis obsoletus*)

Dawei Han; Catherine Carr
University of Maryland College Park

Although snakes lack tympanic ears, which hinders their ability to detect sound pressure, studies on ball pythons and rattlesnakes have shown acute sensitivity to substrate vibration. Both species are considered dormant ambush predators, which means that they spend extended periods of time with their head either directly or indirectly in contact with the substrate. This allows for detection of vibration in their environment via the lower jaw, which is connected to the inner ear by the quadrate. In contrast, active predators rarely exhibit such behavior, and how they compare to dormant animals in hearing sensitivity is unknown. Here, we quantified vibration thresholds in the western ratsnake (*Pantherophis obsoletus*), a more active and visually-oriented animal, by measuring the brainstem evoked potential. Their hearing is most sensitive to low frequency vibrations (100 Hz) with a threshold of -37 dB re 1 m/s², which deteriorates at higher frequencies. Across all frequencies tested, the western ratsnake has a vibration threshold 5-40 dB higher than that of ball pythons and rattlesnakes. Thus the western ratsnake is less sensitive to vibration than ball pythons and rattlesnakes, consistent with the difference in their lifestyle. Note however that possible phylogenetic effects require further comparative studies.

PS 290

Differential Expression of Isoforms of the Synaptic Calcium Sensor Synaptotagmin in the Avian Auditory Brain Stem

Katrina MacLeod¹; Sangeeta Pandya²
¹*Univ Maryland*; ²*University of Maryland*

In the avian auditory brain stem, acoustic timing and intensity cues are processed in separate ascending pathways, yet all information arises from the same set of 8th nerve fibers. Synaptic properties of the connections between the auditory nerve and its neuronal targets in the cochlear nuclei contribute to differences in what information is extracted, processed and transmitted further. Previously research has shown such differences in these properties of excitatory and inhibitory synaptic inputs to the two anatomical distinct cochlear nuclei, nucleus angularis (NA) and nucleus magnocellularis (NM), as well as the third order nucleus laminaris (NL). For example, short-term synaptic plasticity differs between presumptive nerve inputs to NA and NM which in turn depends on significant differences in average release probability. How release probability is

differentially regulated is not well understood, but may depend on differences in the molecular components of the presynaptic transmission. Synaptotagmins are a family of C2-domain-containing Ca²⁺-binding proteins, and two main isoforms, Syt1 and Syt2, are thought to be the major calcium sensors for exocytosis. To begin to determine the molecular components of release in the avian auditory nuclei, we investigated the distribution of Syt1 and Syt2 via immunohistochemistry, immunofluorescence and Western blot in the hatchling (postnatal day 1) chick brain stem (*Gallus gallus*). In this study, we found that antibodies against the Syt2 protein strongly labeled the avian auditory pathway in a way consistent with glutamatergic transmission. In the timing pathway, anti-Syt2 label appeared to resemble the calyx terminals in NM and labeled many terminals in the cell body layer and dendritic field of NL, highly reminiscent of VGlut2 labeling. Antibodies against the Syt1 protein only very weakly labeled NL, except in the most caudolateral extreme. In NM, anti-Syt1 showed weaker intensity and was more punctate than anti-Syt2. In NA, however, Syt1 and Syt2 were expressed more similarly in intensity and throughout the nucleus with no gradient, while anti-Syt1 label was more patchy. These results suggest that the two major synaptotagmins may be differentially and complementarily expressed in the auditory brain stem inputs, but whether they control distinct neurotransmitter systems remains to be determined.

PS 291

Presynaptic FMRP Regulates Axonal Targeting and Synaptogenesis in the Developing Cochlear Nucleus

Xiaoyu Wang; Diego A.R. Zorio; Yuan Wang
Florida State University

Fragile X mental retardation protein (FMRP) is a mRNA-binding protein that regulates local protein translation. Reduced FMRP levels lead to synaptic alterations in the fragile X syndrome (FXS), which is characterized by intellectual disability and auditory dysfunction. In this study, we aimed to determine the autonomous function of presynaptic FMRP in circuit formation and synaptogenesis in the chicken nucleus magnocellularis (NM), the avian analogue of spherical bushy cells (SBCs) in the mammalian anteroventral cochlear nucleus (AVCN). NM and SBC neurons are innervated by the central processes of spiral ganglion (SG) neurons, also known as auditory nerve fibers (ANFs), via the endbulb of Held, a well-conserved synaptic structure among vertebrate species.

We first characterized the developmental profile of FMRP expression in SG neurons during critical periods

of synaptogenesis and endbulb maturation from embryonic (E) day 2 to E19. Both immunohistochemistry and western blot revealed consistently high levels of FMRP throughout this developmental window. Interestingly, we observed a significant reduction of FMRP level at posthatch (P) day 6, when the auditory system is considered mature-like. To determine the role of strong FMRP expression in SG neurons in endbulb development, we next knocked down FMRP levels selectively in SG neurons without interfering FMRP expression in postsynaptic NM neurons. Drug-inducible constructs expressing Fmr1-shRNAs were introduced into cochleovestibular ganglion precursors via in ovo electroporation at E2, leading to transfection of a subset, but not all, SG neurons. When examined at E9, the transfected ANFs are capable of reaching towards the NM region normally. In the next a few days, however, a considerable number of ANFs failed to show obvious terminals on NM neurons. Instead, these fibers continued to grow, passing through the NM ventrally, indicating defective axonal targeting and/or terminal maintenance. A small number of ANFs did terminate on NM neurons with endbulb-like endings, however, these endings were significantly smaller than those created by neighboring non-transfected ANFs.

Taken together, these data demonstrate that normal levels of FMRP in the spiral ganglion are required for endbulb formation and growth. Ongoing studies are investigating potential biophysical and functional consequences of the axonal and synaptic alterations as induced by FMRP deficiency.

PS 292

Targeted Genetic Labelling Reveals Dynamic Subcellular Localization of FMRP in the Developing Cochlear Nucleus

Xiaoyu Wang¹; Ayelet Kohl²; Diego A.R. Zorio¹; Dalit Sela-Donenfeld²; Yuan Wang¹

¹Florida State University; ²The Hebrew University of Jerusalem

The cochlear nucleus is a critical gateway for auditory activity entering the brain. How this cell group develops during early embryonic stages and how its neurons establish characterized axonal projections for binaural processing have not been fully understood. In this study, we characterize the development of the chicken nucleus magnocellularis (NM) using targeted genetic labeling, which allows selective visualization of NM neurons and their axon projection to the nucleus laminaris (NL), during the entire development. NM and NL are analogue to the mammalian anteroventral cochlear nucleus (AVCN) and medial superior olive (MSO), respectively.

Previous fate map studies demonstrate that the progenitor dA1 cells located along the dorsal-most region of the caudal rhombic lip express a basic helix-loop-helix transcription factor atonal homolog 1 (Atoh1) and give rise to the excitatory neurons in cochlear nuclei. We generated Atoh1 promoter-driven myristoylated-EGFP and introduced the constructs into a subset of dA1 cells located at rhombomeres 5 and 6, where NM precursors are located, via in ovo electroporation at embryonic day 2 (E2). When examined at later stages upon the completion of neuronal migration, the majority of, if not all, EGFP-labeled cells are located in NM, thus providing a powerful tool for studying developmental events specific to NM precursors/neurons.

We next examined the development of the fragile X mental retardation protein (FMRP), a mRNA binding protein with critical roles in neuronal development. Recent studies from our lab found that FMRP deficiency results in a number of morphological and physiological alterations in NM neurons. In this study, we co-transfected NM precursors with Atoh1-EGFP and FMRP-mCherry. We identified strong expression and intense axonal localization of FMRP in NM precursors as early as E4. At later stages, FMRP puncta were identified in NM dendrites and often accumulated at branch points, implying a role of FMRP in dendritic branching. Multi-photon imaging further identified two types of FMRP puncta in cell bodies and dendrites: small-size puncta that are highly mobile and large stable puncta. Interestingly, FMRP puncta are also abundantly distributed in NM axons projecting to NL at E9 which were largely diminished at E15. We are currently determining the biological significance of the dynamic patterns of subcellular localization of FMRP.

Taken together, these data demonstrate that (1) Atoh1 enhancer is a useful tool for studying the development of cochlear nucleus, and (2) subcellular localization of FMRP is highly dynamic in developing neurons, implicating important roles in morphogenesis and circuit establishment.

PS 293

Synaptic Maintenance in the Absence of Synaptic Activity in the Auditory Brainstem

Christoph Körber¹; Lena Ebberts²; Simone Hoppe¹; Hans Gerd Nothwang²

¹Heidelberg University, Institute of Anatomy und Cell Biology; ²Carl von Ossietzky University Oldenburg, Department of Neuroscience, Excellence Cluster Hearing4all

The maintenance and integrity of synapses are thought to rely on the presence of neuronal activity.

This includes the release of synaptic vesicles (SVs) at presynaptic active zones (AZs), either in response to an action potential or spontaneously. SV release is inhibited by bacterial neurotoxins which cleave neuronal SNARE proteins thereby preventing the assembly of the crucial SNARE complex. One of these neurotoxins is tetanus toxin (TeNT), which cleaves the SNARE protein synaptobrevin/VAMP2.

We expressed TeNT in the bushy cells of the ventral cochlear nucleus (VCN) in the auditory brainstem using a specific Cre-driver mouse line (Math5). The globular bushy cells of the VCN give rise to the calyx of Held in the contralateral medial nucleus of the trapezoid body (MNTB), a giant axo-somatic synapse that comprises 300-700 individual AZs. The expression of TeNT at this specific synapse led to a gradual decrease of SV release with the virtual absence of neurotransmission by P15. However, we did not observe any alterations in the MNTB, neither on the number and size of the MNTB principal cells, nor on the morphology of calyx of Held synapse. Moreover, TeNT expression did not lead to a reduction in AZ number or a loss of SVs from AZs, albeit the number of “docked” SVs close to the plasma membrane was strongly reduced.

PS 294

Uncovering the Role of Presynaptic GIT Proteins for Fast Auditory Signaling

Christian Keine¹; Samuel M. Young, Jr.²

¹Carver College of Medicine, Department of Anatomy and Cell Biology, University of Iowa; ²Department of Otolaryngology, Iowa Neuroscience Institute, Aging Mind Brain Initiative, University of Iowa

To encode sounds, the auditory system relies on temporally precise action potentials (AP) and rapid changes in AP firing rates in the auditory brainstem. However, the timing and efficacy of AP firing critically depends on the tight regulation of neurotransmitter release at the presynaptic terminal, from a limited number of fusion competent synaptic vesicles (SVs), the readily releasable pool (RRP). Therefore, to understand how sound is encoded it is imperative to determine the molecular mechanisms that control SV release dynamics. A critical synapse for the first stages of binaural sound processing is the calyx of Held/MNTB synapse located in the auditory brainstem. The calyx of Held/MNTB synapse has extraordinary fidelity and reliability of synaptic transmission up to kilohertz firing rates which provides fast synaptic inhibition to several auditory nuclei involved in sound localization. Recently, we identified at the calyx of Held that the G protein-coupled receptor kinase-interacting proteins (GITs) control synaptic strength by regulating SV release probability. However,

the GIT proteins' role in enabling temporally precise and sustained auditory signaling is unknown. To elucidate their roles, we used Cre recombinase expressing viral vectors in conjunction with a GIT1fl/fl GIT2^{-/-} mouse line to ablate both GIT isoforms in the calyx of Held right after birth. To mimic in vivo conditions, we performed all experiments at 37C with in vivo like release probability on functionally adult synapses (P20-P25). Using afferent fiber stimulation frequencies similar to sound-evoked firing rates (300 Hz and 500 Hz), we found that ablation of both GIT isoforms resulted in a two-fold increase in initial release probability with no change in RRP size and slightly slower rate of RRP recovery. Importantly, this effect was developmentally independent, as GIT ablation after hearing onset exhibited a similar phenotype. Despite the robust change in the initial SV release probability, however, the reliability and temporal precision of AP spiking in MNTB neurons was not affected. These results suggest that the late steps in SV life cycle controlling initial release probability are not critical for information transfer at the calyx of Held-MNTB synapse.

PS 295

Toward Optogenetics in Barn Owls: Promising AAV-mediated Opsin Expression

Nadine Thiele¹; Meike Rogalla¹; Jannis Hildebrandt¹; Christine Köppl²

¹Cluster of Excellence “Hearing4all”; ²Department of Neuroscience, School of Medicine and Health Sciences, Carl von Ossietzky University Oldenburg

Background

Optogenetics is a tool for manipulating neuronal activity with light sensitive proteins. Adeno-associated virus (AAV) vectors are commonly used in mice for delivering optogenetic constructs into cells of interest. However, different AAV serotypes vary in transduction efficiency, depending on the targeted species and cell type. As a first step towards establishing optogenetic manipulation in barn owls, we tested three AAV vectors with different serotypes to identify the most promising one for future experiments on Nucleus laminaris (NL), a large nucleus of the auditory brainstem involved in binaural processing of interaural time differences.

Methods

Virus injections were carried out in 6 adult barn owls (*Tyto alba*), anesthetized with ketamine/xylazine and monitored by EKG recordings. To identify the target site, a tungsten recording electrode was first lowered through the cerebellum into the brainstem. Stimuli were noise and tone bursts delivered through a closed, calibrated sound system. Subsequently, 1 to 2 µl of the virus solution was injected at the desired stereotaxic coordinates.

Three virus vectors were tested, of different AAV serotypes (AAV2/1, AAV2/9 and AAV5) and with different fluorescent tags (GFP or TdTomato); with a neuronal (CAG) promoter and ArchT opsin in all cases. Both hemispheres were injected, in some cases with different vectors, with one week recovery time between treatments. After one to five weeks expression time, the owls were euthanized and the brains analyzed for ArchT expression patterns, labeled by the expression of the fluorescence protein tag.

Results

The two serotypes AAV2/1 and AAV5 resulted in clear expression three to four weeks after injection, whereas AAV2/9 did not work in our hands within 3 weeks. The expression pattern suggested possible retrograde transport of the vector, with expression in neurons projecting to the injection site.

Conclusions/Outlook

Our preliminary results suggest that commercially available AAV vectors are suitable to drive virus-mediated expression of target genes in the barn owl brain. However, whereas in another bird species, the zebra finch (Roberts et al., 2012, *Nature Neurosci* 15:1454-1459), serotype 2/9 was most successful, this serotype did not work in the owl. Our next steps will be to improve the targeting of the expression to NL, and establish light stimulation for optogenetic manipulation of neural activity.

Supported by the Bundesministerium für Bildung und Forschung (BMBF) grant 01GQ1505B, as part of the German-US-American Collaboration in Computational Neuroscience "Field Potentials in the Auditory System"

PS 296

In Vivo Physiological and Histological Investigation of Cholinergic Modulation in the MNTB of the Adult Gerbil

Chao Zhang¹; Nichole L. Beebe²; Michael Pecka³; Brett R. Schofield²; R. Michael Burger¹

¹Lehigh University; ²Northeast Ohio Medical University;

³Biocenter, Section of Neurobiology, Department Biology II, Ludwig Maximilian University of Munich

The superior olivary complex (SOC) is a vital component of auditory circuitry devoted to localization of sound sources. Within SOC, principal neurons of the medial nucleus of the trapezoid body (MNTB) reliably convert contralaterally derived monaural excitation to inhibition that is distributed to several postsynaptic targets, thus conveying precisely timed inhibition to nuclei involved in computation of sound location. Secure synaptic

transmission is essential to maintain temporal precision for accurate sound localization. The Calyx of Held synapse in MNTB appears specialized for reliable transmission. However, this reliability is challenged in some species when confronted by intense stimulation (Kopp-Scheinflug et al., 2003a; Hermann et al., 2007). Maintaining computational stability requires MNTB neurons to employ adaptive mechanisms that dynamically modulate neurons'; responses, however, the underlying modulatory mechanisms have yet to be illuminated. One candidate mechanism is the cholinergic system, which influences neural signaling throughout the brain. Happe and Morley (1998) first demonstrated intense labeling of acetylcholine receptors (nAChRs) in SOC, suggesting a role for cholinergic modulation. Despite this evidence, no physiological investigation of cholinergic function has been reported for MNTB neurons. Further, the source of putative cholinergic input to MNTB is not known, but two sources are strong candidates. First, the pontomesencephalic tegmentum (PMT) projects cholinergic inputs to multiple auditory nuclei (Schofield et al., 2011). Second, ventral nucleus of trapezoid body (VNTB) has a projection to MNTB and is known to contain cholinergic cells (Gomez-Nieto et al., 2008). However, no study to date has investigated whether these areas project cholinergic input to MNTB.

In order to investigate the role of endogenous cholinergic input to the MNTB, we made *in vivo* extracellular recordings from anesthetized gerbil MNTB, using piggyback multi-barrel electrodes which allowed us to pharmacologically block cholinergic inputs with iontophoresis antagonists of nAChRs. Application of the nAChRs antagonist revealed cholinergic modulation of acoustically driven MNTB responses. To establish sources of cholinergic input, we injected fluorescent tracers (FluoroGold and latex retro-beads) in SOC to retrogradely label neurons that project to SOC. This tissue was then immunolabeled for choline acetyltransferase (ChAT) which identifies cholinergic neurons. Colocalization of retrograde tracer and ChAT was found in PMT and VNTB. These data are the first, to our knowledge, confirming that PMT and VNTB provide cholinergic inputs to the SOC. Further we show ACh potently modulates MNTBs'; responses to acoustic input.

PS 297

Knockout of MicroRNA-96 Impacts Auditory Brainstem Morphology and Synaptic Integrity

Constanze Krohs¹; Tina Schlüter¹; Christoph Körber²; Haydn M. Prosser³; Hans Gerd Nothwang⁴

¹Carl von Ossietzky University Oldenburg, Department of Neuroscience; ²Heidelberg University, Institute of Anatomy and Cell Biology; ³Wellcome Trust Sanger Institute; ⁴Carl von Ossietzky University Oldenburg,

MicroRNAs (miRs) play a crucial role in posttranscriptional gene regulation via sequence-specific binding to mRNA, resulting in downregulation of the expression of targeted genes. miR-96 is a member of the highly conserved microRNA-183 cluster which consists of miR-183, -96 and -182. Point mutations in the seed region of miR-96 were linked to nonsyndromic progressive hearing loss in men and mice. Analysis of the *Diminuendo* (*Dmdo*) mouse, harboring a point mutation in the seed region of miR-96, revealed degeneration of auditory hair cells as well as anatomical, morphological, physiological and molecular changes in the auditory brainstem. Importantly, these changes were not observed in the *Claudin14* knockout mouse, a peripheral deafness mouse model, suggesting an on-site effect of the miR-96 mutation in the central auditory pathway. However, it remains unclear whether the identified changes in the *Dmdo* mouse reflect a gain of function of mutated miR-96 due to newly recognized mRNA targets or a loss of function due to original mRNA targets that are not recognized anymore. To answer this fundamental question, a constitutive miR-183-96-/- mouse model was analyzed on the anatomical, electrophysiological and molecular level.

Similar to *Dmdo* mice, anatomical analysis revealed a volume reduction of several auditory hindbrain nuclei (VCN, LSO and MNTB) in young-adult miR-183-96-/- mice. This volume reduction was due to decreased cell number and cell size. Electrophysiological recordings at the calyx of Held synapse identified severely enlarged excitatory postsynaptic currents. This was accompanied by an altered clustering of the AMPA receptor subunit GluR-1, as demonstrated by quantitative confocal microscopy. Other biophysical parameters and the abundance of the synaptic marker protein SV2 were unchanged, as was the expression of voltage gated potassium channels. The latter observation contrasts our previous findings in *Dmdo* mice, which show reduced expression of KV1.6 and BK β 2.

In summary, our data substantiates the essential role of the miR-183, -96, -182 cluster in the gene regulatory network underlying development of the auditory hindbrain. Furthermore, the observed shared and distinct phenotypes between miR-183-96-/- mice and *Dmdo* mice demonstrate that both gain and loss of function of mutated miR-96 contributes to the *Dmdo* phenotype in the central auditory system.

PS 298

Relating Human Envelope-ITD Sensitivity to LSO Membrane Filters

Andrew Brughera¹; Jessica J.M. Monaghan²; Jason Mikiel-Hunter³; David McAlpine²

¹*Boston University*; ²*Macquarie University, Department of Linguistics*; ³*Macquarie University*

Neurons of the lateral superior olive (LSO) are sensitive to interaural time difference (ITD) in the envelopes of acoustic sinusoidally amplitude-modulated high-frequency carriers (SAM tones). For ipsilateral SAM tones, spike rates in some LSO neurons vary with modulation frequency as a lowpass function with a resonance-peak at a modulation frequency from 80 to 500 Hz; this response was successfully modeled previously as via low-threshold potassium (KLT) channels, activating with membrane depolarization to produce a counteractive outward current now associated with a second-order resonance. Human listeners can typically discriminate envelope-ITD in a 4-kHz carrier for amplitude modulation rates up to 256 Hz (with upper limits of 512 to 800 Hz for some listeners). This upper modulation frequency (and sensitivity in general) decreases as carrier frequency increases to 10 kHz, despite better passing of modulation side bands by peripheral auditory filters which increase in bandwidth with characteristic frequency (CF).

We hypothesize that this decreasing performance as carrier frequency increases from 4 to 10 kHz originates in lowpass LSO membrane impedances, well characterized previously as low-CF membranes where KLT-channels and resonances from 80 to 400 Hz are common, transitioning to high-CF membranes with cutoff frequencies below 80 Hz, with no KLT channels and no resonances. The present study will leverage these observations, tuning an existing model LSO neuron for CF, and quantifying the resulting models' envelope-ITD sensitivity as Fisher information. Existing models from auditory nerve to cochlear nucleus bushy cells will drive ipsilateral excitatory inputs and contralateral inhibitory inputs to model LSO neurons. SAM tone stimuli at 2 and 4 kHz will test whether broader peripheral filters at higher CFs increase envelope-ITD sensitivity in identical model LSO neurons. Transposed tones (a high-frequency carrier modulated by a half-wave rectified low-frequency sinusoid) at carriers from 4 to 10 kHz, with modulation rates from 32 to 800 Hz, will be applied to compare envelope-ITD sensitivity of model LSO neurons with available human envelope-ITD discrimination thresholds. The membrane filter of each model LSO neuron will act on inputs phase-locked to the sound envelope; and as carrier frequency increases above 4 kHz, particularly from 6 to 10 kHz, we expect the

higher-CF model LSO membranes with their lower cutoff frequencies will attenuate high modulation frequencies, outweighing the effect of broader peripheral filters, and decreasing envelope-ITD sensitivity.

PS 299

Preferential Myelination of Active Axons within a Fiber Tract of Mixed Active and Non-Active Axons

Mihai Stancu; Ezhilarasan Rajaram; Conny Kopp-Scheinflug
LMU Munich

Myelin plasticity represents a mechanism to fine-tune the flow of information along axons, which is of particular importance in the auditory system where the rate of action potential generation and conduction speed operate at the upper limits observed in the mammalian CNS. We previously showed that in the auditory system, more active axons are correlated to thicker myelin and faster conduction speed compared to less active axons following binaural sensory deprivation in both young and adult animals (Sinclair et al., *J. Neurosci.* 2017). Literature suggests that activity-dependent release of soluble factors from active axons stimulate oligodendrocytes to enhance myelination.

However, such a communication would fail in a monaural deprivation paradigm if (like in the trapezoid body, TB), active axons and axons leaving the deprived ear are located in close proximity so that individual oligodendrocytes might myelinate fibers going in either direction. In that case a soluble factor will not be specific enough to adapt myelination in axons leaving the control or the deprived ear only.

Monaural sensory deprivation was induced by raising mice of both sexes with earplugs between P10-20, a period normally associated with significant increase in firing rates, myelin thickness and conduction speed in the auditory brainstem. Axon caliber and myelin thickness were measured in TB fibers by using immunolabeling for neurofilament and myelin basic protein. Physiological measures of activity-dependent control of myelination were taken from auditory brainstem recording (ABR) in vivo and patch-clamp recording in vitro.

At the end of the ear plugging period, auditory thresholds were compared between control ear (22 ± 2 dB SPL) and the deprived ear, after ear plug removal (47 ± 2 dB SPL). Sound-evoked latencies were measured for ABR waves I-IV at similar dB above thresholds. DIV-I latencies were significantly slower when stimulating the deprived ear (3.01 ± 0.14 ms) compared to the control (2.79 ± 0.07 ms), suggesting slower conduction speed in

the pathway leaving the deprived ear. TB axons leaving the deprived ear were traced via biocytin injections and their diameter and myelin thickness compared to axons leaving the control ear, revealing a significant reduction in myelin exclusively in the axons associated with the deprived ear.

These results suggest that changes in axonal activity within the mixed TB fiber tract might be communicated to the myelinating oligodendrocytes on a local, single axon level. Voltage-clamp recordings of oligodendrocytes within the TB before and after axonal stimulation support such local axon-oligodendrocyte communication.

PS 300

Required Input Number for Action Potential Generation in Auditory Brainstem Nuclei

Nikolaos Kladisios; Linda Fischer; Felix Felmy
Tierärztliche Hochschule Hannover

The number of input fibers required to generate supra-threshold excitation varies between auditory brainstem nuclei. Furthermore, during developmental circuit refinement the input size of a single fiber is changed. The number of individual fibers that generate supra-threshold excitation is therefore highly specific for each nucleus. In relay nuclei, like the medial nucleus of the trapezoid body (MNTB) or the ventral nucleus of the lateral lemniscus (VNLL), between one and two inputs are present and generate supra-threshold excitation even during ongoing activity with only a limited number of failures. In structures that perform integration of spatial cues, like the medial superior olive (MSO) or the dorsal nucleus of the lateral lemniscus (DNLL), a larger convergence is observed. The number of inputs that are minimally required to drive these neurons supra-threshold during ongoing activity is not fully clarified.

To estimate the number of required inputs that evoke supra-threshold excitation we recorded in current-, voltage- and dynamic-clamp in acute brain slices from neurons of the MNTB, VNLL, MSO and DNLL from juvenile (postnatal day 9/10) and mature (postnatal day 26-90) Mongolian gerbils. Towards our aim we first determined strength-duration relationships to estimate the stimulation time dependence of action potential current thresholds. Next, we measured unitary EPSC IV-relationships to quantify the time course and size of the AMPAR and the voltage-dependent NMDAR components. Using the EPSC time course we estimated from the strength-duration relationship the fiber numbers required for supra-threshold excitation. As synaptic transmission is history dependent, we determined the synaptic depression in 1.2 mM extracellular $[Ca^{2+}]$. From the amount of depression, we inferred the required

input number for ongoing supra-threshold activity. We found that in juvenile VNLL neurons two to three and in adult one input were sufficient to generate ongoing supra-threshold excitation. For MNTB neurons our estimate yielded no failures in juvenile and the emerging of failures in adult neurons with a single input. MSO neurons required between 10 and 25 and between 5 and 10 inputs in juvenile and adult animals respectively. DNLL neurons were surprisingly excitable, with only four to eight and two to four inputs required to sustain ongoing activity in juvenile and adult animals respectively.

In the next step we aim to verify the estimated number of inputs by using dynamic-clamp and to further untangle the contribution of NMDAR and AMPAR currents and post-synaptic adaptations on ongoing supra-threshold excitation.

PS 301

Urocortin 3 Increases Excitatory Postsynaptic Currents at the MNTB Synapse

Sara Pagella; Conny Kopp-Scheinpflug
LMU Munich

Background

In the medial nucleus of the trapezoid body (MNTB) high sound frequencies are represented medially and low sound frequencies laterally. There is increasing evidence that other gradients are superimposed on this tonotopic axis: for example the expression of potassium channels, somatic cell size, axonal conduction speed or timing of synaptic transmission. Here we report about Urocortin 3 (UCN3), an orthologue of corticotropin releasing factor (CRF) which is expressed exclusively in the very lateral (low-frequency) calyces. UCN3 binds with high affinity to the CRF receptor type 2 (CRFR2) and can act independently of the hypothalamus-pituitary (HPA) axis. While its role in many different circuits in the nervous system has been described to be protective against stress and crucial for mouse social behavior, its presence in nuclei of the auditory system is not understood. We previously found that UCN3 acts via presynaptic mechanisms to potentiate the transmission at the calyx of Held-MNTB synapse. However, the underlying cellular mechanism of action is still unclear.

Methods

Anatomical description of the localization of UCN3 expressing cells and axons was accomplished with the use of UCN3 TdTom mouse model. Whole-cell patch clamp experiments were carried out on wild-type C57BL6 mice aged P14 to P22 in the lateral MNTB. Excitatory postsynaptic currents (EPSCs) were evoked using a bipolar electrode placed at the midline over the trapezoid body fibers. 10 μ M SR95531 and 1 μ M

Strychnine were added to the aCSF to inhibit IPSCs. Baseline data was acquired before the addition in the aCSF of UCN3 (600nM/300nM/200nM/100nM) or a CRFR2-specific inhibitor, K41498 (200nM), and after 10 minutes of drug wash out. Calyceal currents were identified as EPSC with an amplitude >1nA. mEPSCs were recorded with additional 1mM TTX. Spontaneous activity and intrinsic properties of recorded cells were studied in current-clamp mode.

Results

600nM UCN3 significantly increased the amplitude of EPSCs (48.5% $p < 0.0001$) as well as the frequency of mEPSCs. Conversely, K41489 caused a decrease (25.5% $p = 0.0003$) in the amplitude of EPSCs and in the frequency of mEPSCs. Intrinsic properties of recorded cells were unaffected by both drugs.

Conclusions

The proof of the presence of both a receptor and a ligand of the CRF pathway at the Calyx of Held offers the possibility to thoroughly study the release characteristics of this neuropeptide from presynaptic terminals and its effects on synaptic transmission. Our preliminary data suggests that UCN3 causes a larger number of miniature synaptic events and increased evoked postsynaptic currents. Together the changes in these parameters are well suited to impact synaptic strength and reliability of the Calyx of Held.

PS 302

Properties of Distal and Small-Caliber Dendrites of MSO and LSO Neurons Studied Using 2-Photon-Guided Dendritic Patch-Clamp Recordings

Bradley D. Winters¹; Nace L. Golding²

¹*Department of Neuroscience and Center for Learning and Memory*; ²*The University of Texas at Austin*

Neurons of the MSO and LSO extract location-related cues from the relative timing and intensity of sounds to the two ears, processing that depends heavily on dendritic cable properties. Previous data from our laboratory revealed effective and rapid propagation from the dendrites to the soma of MSO neurons. However, the bias of these recordings to larger, primary dendrites raises the question of whether these features generalize across dendrites of differing morphologies. The dendrites of LSO neurons differ in size and branching pattern from MSO dendrites, but their properties are unknown. To address these issues, we have begun to make dual somatic/dendritic current-clamp recordings at 35°C in acute brain slices from Mongolian gerbils (P16-40). Somatic patch pipettes included Alexa 594 fluorescent dye and two-photon imaging at 830 nm was used to visualize and approach dendrites with a second pipette.

In MSO neurons, recordings from distal dendrites 115-154 μm from the soma revealed cable properties that were diverse ($n=4$). Action potential (AP) backpropagation from the soma to the dendrite was variable with one cell at 115 μm exhibiting lower attenuation than expected (d/s ratio 0.56) while another at 154 μm exhibited virtually complete attenuation. Forward propagating simulated EPSCs (sEPSC) were attenuated more than backpropagating ones—as expected. However, the degree of attenuation was also variable. Despite large local sEPSC amplitudes in the dendrites with current injections up to 8 nA, it was not possible to elicit AP firing at the soma. This suggests relative electrical isolation of distal dendritic compartments in the MSO.

We also report the first dendritic recordings from LSO neurons. One cell in the high frequency limb of the LSO had a complex bipolar dendritic arbor with 2 branch points between the soma and a narrow recorded dendrite 72 μm away (diameter 1.4 μm). This cell fired repetitively with large APs. Attenuation of backpropagating APs (d/s ratio 0.53) was similar to MSO neurons at this age and distance despite anatomical and intrinsic membrane property differences. Conversely, a cell from an intermediate frequency region had a simple bipolar arbor where the diameter was 2.5 μm at the 59 μm recording location. This cell exhibited small APs (~ 15 mV) and would only fire transiently. Despite being very MSO-like in morphology and somatic response properties, the amount of attenuation in this cell was less than would be expected (d/s ratio 0.68 vs MSO 0.46) suggesting considerable ion channel composition differences.

Auditory Cortex: Anatomy & Physiology II

PS 303

Neural Variability Limits Adolescent Skill Learning

Melissa Caras; Dan H. Sanes
New York University

Skill learning is fundamental to the acquisition of many complex behaviors that emerge during development. For example, years of practice give rise to perceptual improvements that contribute to mature speech and language skills. Behavioral studies show that sensory and learning capabilities continue to develop through childhood and adolescence, suggesting that the neural mechanisms supporting perceptual learning are slow to mature. However, to date, the neural mechanisms of perceptual learning have been explored only in adults. To address this issue, we first compared the rate and magnitude of perceptual learning in young, adolescent, and adult gerbils, as they trained on an auditory task. Adolescents displayed slower rates of perceptual learning compared to their young and

mature counterparts. We then recorded auditory cortical neuron activity from adolescent and adult gerbils as they underwent perceptual training. While training enhanced the sensitivity of most adult units, the sensitivity of many adolescent units was unchanged, or even declined, across training days. Therefore, the average rate of cortical improvement was significantly slower in adolescents as compared to adults. Both smaller differences between sound-evoked response magnitudes and greater trial-by-trial response fluctuations contributed to the poorer sensitivity of individual adolescent units. Together, these findings suggest that heightened sensory neural variability limits adolescent skill learning.

PS 304

An Interhemispheric Comparison of Projections to Temporal Auditory Cortex in Normal Hearing and Early Deaf Cats

Blake E. Butler¹; Stephen G. Lomber²

¹*Department of Psychology, University of Western Ontario*; ²*Department of Physiology & Pharmacology and Department of Psychology, University of Western Ontario*

Early-onset hearing loss initiates changes within and between sensory brain regions that can be measured electrophysiologically and behaviorally. However, the nature of the anatomical changes underlying these differences remains poorly understood. In a recent study, Lomber and colleagues observed that deaf cats learn to discriminate between conspecific and human faces faster than normal hearing animals. Reversible deactivation of auditory cortex via cooling revealed that this behavioural advantage is mediated by the temporal auditory cortex (area T); moreover, this effect was shown to be lateralized to the left hemisphere – a region that contributes to the processing of conspecific vocalizations in normal hearing animals. Here, we assess the connectivity to this presumptive auditory cortical region by injecting the retrograde anatomical tracer BDA into either the left or right hemisphere of normal hearing animals, and cats ototoxically deafened at the onset of hearing. Coronal sections were taken at regular intervals and neurons showing a positive retrograde labeling were counted, and assigned to functional cortical areas according to published criteria. We provide a detailed quantification of the thalamocortical and corticocortical projections to area T, comparing across hearing conditions and hemisphere to determine whether behavioural advantages are mediated by an increase in the proportion of projections arising from visual cortex. Differences in these labeling profiles will be discussed in the context of crossmodal plasticity in sensory systems responsible for conspecific identification.

PS 305

Rats in a Complex Auditory Environment: Behavior and Responses in Auditory Cortex

Ana Polterovich¹; Maciej M Jankowski¹; Alexander Kazakov¹; Israel Nelken²

¹*Edmond and Lily Safra Center for Brain Sciences, Hebrew University*; ²*Edmond and Lily Safra Center for Brain Sciences and Department of Neurobiology, Silberman Institute of Life Sciences, Hebrew University*

In the real world, animals face a complex auditory environment. Animals are capable of extracting relevant information from the environment and plan their actions appropriately.

We developed a complex behavioral environment, the Rat Interactive Fantasy Facility (RIFF). The RIFF consists of a large arena (diameter: 160 cm) with 6 interaction areas (each consisting of a water port and a food port), activated by nose pokes into the ports. We use the RIFF to implement general Markov Decision Processes (MDP). An MDP consists of 'states'; (that define mappings between rat actions and their consequences – sound presentations and the administration of rewards and punishments) as well as transitions between states that depend on the current state and on the rat action. The states are made known to the rat by using sounds – each state is either associated with the presentation of a sound, or follows deterministically such a state. Importantly, the MDPs we use have optimal policies (maximizing reward acquisition) so that it is possible to check the optimality of rat behavior in the RIFF. Rat behavior is followed online using video tracking and nose-poke identification. Neural responses are recorded using telemetry (a 64-channel TBSI transmitter integrated in an Alpha-Omega SNR data acquisition system).

As an initial test of the concept, we show here data on a multiple arbitrary association task. We used auditory cues consisting of a set of 12 modified human words. The words were generated using the Festival text-to-speech software. The frequency content of all words was stretched up to 30 kHz with the help of the STRAIGHT vocoder. When a rat approached an interaction area, it heard either a reward cue (in which case nose pokes were rewarded by food and water) or a neutral cue (in which case nose pokes were unrewarded, but not punished). These cues were different in each area. We present an analysis of rat behavior and of the neural responses recorded while rats were exploring this environment.

PS 306

Motor Preparatory Signals Activate Auditory Corticothalamic Neurons

Kameron K. Clayton¹; Ross S. Williamson²; Kenneth E. Hancock²; Daniel B. Polley²

¹*Eaton-Peabody Laboratories, Massachusetts Eye and Ear; SHBT Program, Division of Medical Sciences, Harvard Medical School*; ²*Eaton-Peabody Laboratories, Massachusetts Eye and Ear; Dept. of Otolaryngology, Harvard Medical School*

Auditory cortex (ACtx) pyramidal neurons are suppressed during movement, which reduces sound-evoked activity and behavioral awareness of faint sounds. Movement-related suppression predominantly reflects an intra-telencephalic circuit wherein motor planning signals from the basal forebrain and motor cortex engage local GABA circuits within the ACtx to suppress spiking in pyramidal neurons. The precise connectivity between long-range motor planning inputs and local GABA neurons is not fully understood. While some fraction of pyramidal neuron suppression reflects monosynaptic connections from motor inputs onto GABA neurons, it is also possible that translaminar ACtx suppression may reflect a local intermediary that regulates sensory gain across the cortical column. Ntsr1-expressing layer 6 corticothalamic (L6 CT) neurons exactly fit this profile. L6 CTs powerfully modulate excitability throughout all layers of cortex by activating specialized networks of fast-spiking inhibitory neurons. Here we test the hypothesis that L6 CTs are an additional node in the motor suppression circuit, interposed between the preparatory motor signal and local GABA neurons. We used 2-photon calcium imaging to measure activity from hundreds of L6 CT neurons, parvalbumin-expressing GABA neurons or pyramidal neurons while mice performed a simple behavioral task that allowed us to isolate the contribution of movement inputs, sensory inputs, and reward-related inputs. We confirmed earlier reports that self-generated movements such as licking or running suppressed spontaneous and sound-evoked activity in pyramidal neurons. By contrast, L6 CTs were strongly activated prior to (and during) movement onset, such that sound-evoked responses were enhanced rather than suppressed during movement. Moreover, their activation precedes movement onset by hundreds of milliseconds. Because L6 corticothalamic neurons regulate columnar excitability through their connections with local GABA networks, we propose that they are a critical intermediary between long-range neuromodulatory inputs and local circuits for cortical excitability. Further work using single unit recordings from functionally identified cell types will define a sequence of local circuit activation that modify spontaneous and sound-evoked excitability prior to – and throughout – self-generated movement.

PS 307

Interactions between Auditory and Frontal Cortices during Vocal Production in Marmoset Monkeys

Joji Tsunada; Steven Eliades

University of Pennsylvania Perelman School of Medicine

The control of vocal or speech production requires the calculation of error between intended vocal output and the resulting auditory feedback. Recent evidence has demonstrated neural correlates of this calculation in the auditory cortex. Activity in the auditory cortex is suppressed shortly before and during vocal production, yet is still sensitive to the difference between vocal output and altered auditory feedback. The auditory cortex has thus been hypothesized to receive information about the intended vocal output, an efference copy signal, originating from motor or frontal cortical areas. However, whether or not such areas provide the efferent signal to the auditory cortex during vocalization is unknown. Here, we simultaneously recorded neural activity from both auditory and frontal cortices of marmoset monkeys while they produced self-initiated vocalizations. We found modulations of neural activity in both brain areas immediately before and during vocal production. Theta-band activity, thought to be involved in coordinating neural activities between brain regions, increased in both areas immediately prior to the onset of vocal production. We further found a subset of recording sites with temporally covarying activities, including frontal activation preceding auditory just prior to vocal production. These results suggest that the frontal cortex communicates with the auditory cortex, with frontal-temporal pre-vocal signals that may reflect the transmission of an efference copy signal. This interaction between auditory and frontal cortices may underlie mechanisms to calculate error between intended and actual vocal outputs during vocal communication.

PS 308

Cortical mechanisms supporting complex sound processing

Pilar Montes-Lourido; Shi Tong Liu; Srivatsun Sadagopan
University of Pittsburgh

We recognize complex sounds such as speech accurately, reliably, and in real-time, despite the widely varying listening conditions in which we encounter these sounds. We aim to determine the algorithms and neuronal mechanisms underlying rapid and accurate sound recognition in real-world conditions. We focus on the categorization of vocalizations in the face of two sources of real-world variability: 1) production variability, which is the within- and between-subject

variability with which sounds are produced, and 2) environment variability, which encompasses the noise, reverberations, and other sounds added by the acoustic environment. We use Guinea pig (GP) vocalizations as an experimental model to address these questions in naturalistic settings. We first show using an information theoretic model that calls can be categorized while generalizing across production variability by detecting smaller, optimal features. These model features predict some nonlinear cortical response properties at the single-neuron level, and population transformations between auditory processing stages. Consistent with this model, we find critical transformations to sound representation that occur between layer 4 (L4) and layer 2/3 (L2/3) of primary auditory cortex (A1). To understand the mechanisms underlying environment invariance, we first used pupillometry to determine the threshold of call detection in noise. In electrophysiological experiments, we found that at these signal-to-noise ratios, environment-invariance also increases between thalamus and A1 L2/3. These results suggest that a dense, non-invariant representation of complex sounds in thalamus and A1 L4 is transformed into an invariant and sparse representation in A1 L2/3. Ongoing experiments using novel optogenetic methods to address the mechanisms underlying this transformation will be discussed.

Funding: NIDCD R01DC017141, Pennsylvania Lions Hearing Research Foundation, Samuel and Emma Winters Foundation.

PS 309

Resistance to noise in the auditory system: where does it come from ? An electrophysiological study from cochlear nucleus to primary auditory cortex.

Samira Souffi¹; Christian Lorenzi²; Chloé Huetz¹; Jean-Marc Edeline¹

¹*NeuroPSI UMR CNRS 9197*; ²*Laboratoire des systèmes perceptifs, Ecole Normale Supérieure (UMR 8248)*

It is known that human subjects can discriminate speech in quite challenging situations such as the presence of important background noise. Many electrophysiological studies, especially performed at the cortical level, have described the way neuronal responses are altered by noisy conditions and have tried to relate response degradation at the neuronal level and behavioral performance. However, very few of these studies have compared the way neuronal responses are impacted at the different levels of the auditory system. Here, we compare the abilities of neurons recorded from primary auditory cortex down to cochlear nucleus to discriminate between spectrally similar communication calls.

Four utterances of a guinea pig whistle were presented in quiet and in two types of frozen noise (a stationary noise and a chorus noise) at 3 SNR levels (+10dB, 0 and -10dB). The vocalizations were presented while recording evoked responses in primary auditory cortex (AI, n=354), the ventral division of auditory thalamus (MGv, n=262), the central nucleus of inferior colliculus (CNIC, n=386) and cochlear nucleus (CN, n=499). Both in stationary and in chorus noise, neuronal responses were degraded but in each structure there was a large diversity of effects from responses already largely attenuated as early as the SNR value of +10dB, up to detectable responses at SNR value of 0dB. In all structures, the stationary noise strongly attenuated the mean evoked firing rate, the trial-to-trial reliability of neuronal responses and the neuronal discriminative abilities indexed by computing Mutual Information (MI). Based on the group data, the best discriminative abilities were observed in the CNIC with a non-significant decrease in MI mean value up to SNR level of 0dB. In the chorus noise, the evoked firing rate, the trial-to-trial reliability of neuronal responses were also decreased in all structures, but the average MI value was only slightly decreased due to the presence of spectro-temporal cues in the frozen chorus noise. Despite this, the subcortical neurons were, on average, better in discriminating the four target whistles than the cortical ones.

These data indicate that the discrimination between spectrally similar vocalizations can be achieved in noisy conditions at all levels of the auditory system but seems more prominent in the CNIC.

PS 310

Neurophysiological Coding of Temporal Fine Structure in the Auditory Forebrain of the Zebra Finch

Adam R. Fishbein¹; Kai Lu²; William J. Idsardi³; Shihab A. Shamma⁴; Jonathan B. Fritz⁴; Robert J. Dooling⁵

¹*Department of Psychology, Neuroscience and Cognitive Science Program, University of Maryland;*

²*Neural Systems Lab, Institute for Systems Research, University of Maryland;* ³*Department of Linguistics, University of Maryland;*

⁴*Neural Systems Laboratory, Institute for Systems Research, University of Maryland;*

⁵*Department of Psychology, University of Maryland*

Research Background: A critical component of human speech perception is the ability to perceive the temporal fine structure (TFS) in the acoustic waveform of speech. The TFS of a signal – rapid changes in frequency and amplitude within the envelope – provides information important to word recognition and hearing speech in noise. Songbirds, such as zebra finches (*Taeniopygia guttata*), are excellent models for studying TFS

processing because their learned vocal communication system relies on complex auditory perception. Past behavioral work with zebra finches using natural harmonic vocalizations and a synthetic version of these sounds, called Schroeder harmonic complexes, has shown that the birds can hear TFS at a level that far surpasses humans and other mammals. Schroeder waveforms are useful stimuli because they can be manipulated so that long term spectra, envelopes, and harmonic amplitudes are held constant while the TFS is changed – by monotonically increasing (positive Schroeder) or decreasing (negative Schroeder) the phase of the harmonics. Here, we use Schroeder harmonic complexes for the first time to investigate neuronal coding of TFS in the zebra finch.

Methods: Zebra finches were implanted with head posts in sterile surgery under anesthesia, and after 2-3 days of recovery, a small craniotomy was made, and electrodes were inserted into the auditory forebrain, enabling neurophysiological recordings of TFS from field L, NCM, and CMM. Following recordings, sites were labeled with fluorescent dye, for subsequent neuroanatomical confirmation.

Results: We present preliminary results of the responses of >100 neurons in field L, the primary nucleus in the zebra finch central auditory system, to positive and negative Schroeder complexes of different fundamental frequencies. We found differential spike rates in response to negative and positive Schroeder complexes.

Conclusions: We show that Schroeder waveforms can be successfully used to probe the coding of TFS in the central nervous system. The synthetic nature of these stimuli also enables us to probe the coding of acoustic sequences in addition to TFS, providing an avenue for deeper understanding of complex auditory perception.

PS 311

Neural encoding of auditory stimulus value during a patch-based foraging task in acoustic virtual reality

James Webb¹; Jack Shi¹; Anton Banta¹; Zakir Mridha¹; Wenhao Zhang¹; Daeyeol Lee²; Caleb Kemere³; Matthew McGinley¹

¹*Baylor College of Medicine;* ²*Yale University;* ³*Rice University*

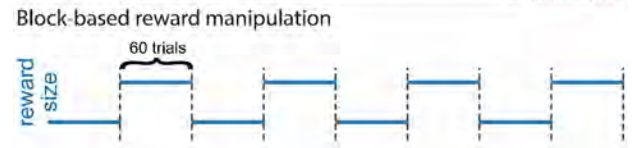
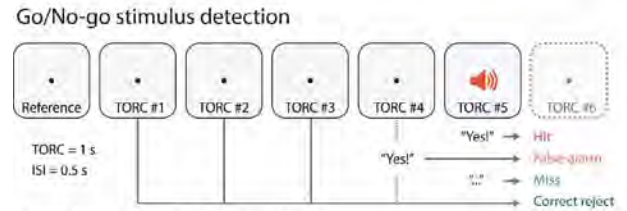
Animals, including humans, adjust their behavioral response to an auditory stimulus according to the learned meaning of the stimulus. For example, when sounds are associated with rewards or punishments, auditory cortex reorganizes to selectively alter its response based on

stimulus value. This receptive field plasticity is thought to be a critical function of the auditory cortex in optimizing behavior. Current experimental designs typically shift the value of the stimulus either arbitrarily in blocks, or across sessions or animals. In addition, the core decision made by the animal typically reflects only sensory identification of single target stimuli (e.g. Go/No-Go), or of multiple targets simultaneously (e.g. two-alternative choice).

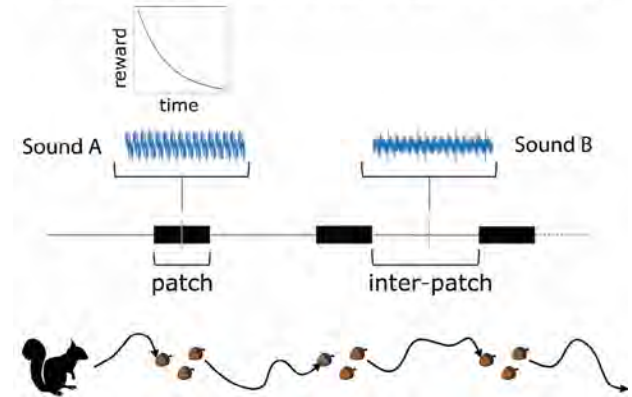
While such designs have led to a great deal of knowledge about brain areas involved in certain aspects of value-based decisions, the unnaturally simplistic stimulus-reward association lacks construct validity. Specifically, in natural conditions, animals evolved to assess stimulus value through foraging. Foraging-type decisions differ from the above-mentioned block-based approaches, by exhibiting the following features: 1) rewarded stimuli are confined in space to 'patches'; 2) Stimulus value decreases with utilization as the animal harvests reward in a patch; and 3) the core decision related to stimulus value is whether to stay in, or leave, each patch. Indeed, a robust set of behavioral and analysis approaches for these patch-based foraging tasks exists in the behavioral ecology literature.

Here, we have developed a patch-based foraging task that adapts standard behavioral ecology approaches to mice head-fixed on a cylindrical treadmill, implementing an acoustic virtual space. The space is defined by patches and inter-patch regions. Within each patch, the animal performs an auditory detection task, "harvesting" sucrose reward on correct trials. The reward volume decreases on each subsequent trial, mimicking natural patch depletion. The animal must travel a specified distance on the wheel to enter the next patch, which is replenished to a high initial reward volume. To date, we have implemented the virtual reality patch-based foraging system in a custom-designed, LabVIEW-based, hardware and software system. We have found several signs that mice can successfully learn this task: 1) successful foraging within patches; 2) intermittent walking and standing in virtual space; and 3) increasing harvest rate across sessions. We are currently manipulating spatial, acoustic, and reward-related parameters to optimize the task. Physiology experiments will seek to reveal how acoustic information is routed to decision-related structures such as the frontal cortex and hippocampus during virtual patch-based foraging.

Conventional value-based decision making:



Patch-foraging value-based decision making:



PS 312

Influence of Early-onset Maternal Hypothyroidism on Distribution and Function of Layer 5 Corticocollicular Neurons in Mouse Auditory Cortex

Minzi Chang; Takahiro Nagayama; Makoto Nakanishi; Hideki Kawai
Soka University

Maternal thyroid hormone is essential for normal development of the central auditory system in the fetus during pregnancy. It was reported that the lack of maternal thyroid hormone in rodents affected radial and tangential migration of cortical neurons. While contralaterally projecting corticocortical neurons were reportedly mismigrated in auditory cortex, little is known about whether corticocollicular (CC) neurons were affected. It was also reported that c-Fos mRNA was elevated in inferior colliculus (IC) neurons but not in auditory cortex. In the previous study, cell type specificity has not been clearly defined, and therefore whether CC neurons were affected is unclear. Here, we examine whether and how the distribution and function of CC neurons in layer 5 of primary auditory cortex (A1) were affected by early-onset (embryonic day (E) 10) maternal hypothyroidism in mice.

To induce hypothyroidism, 0.02% methiamazole was given in drinking water from E10 until sacrifice at postnatal day (P) 5, 10, 15, 20 and in the adult (P60-P70). We performed immunofluorochemistry by targeting cells expressing COUP-TF interacting protein 2 (Ctip2), a transcription factor expressed by ~90% of CC neurons in layer 5 of A1 and examined their distribution as well as the protein expression of c-Fos, an activity-dependent immediate early gene. We also examined the electrophysiological properties of retrogradely-identified CC neurons in both control and hypothyroid animals.

The distribution of Ctip2-immunopositive (Ctip2+) cells in layer 5 was apparently altered from P10 onwards, while there were no significant differences in the density of Ctip2+ cells at all ages examined. The largest difference in the cell distribution was detected in the adult, where Ctip2+ cells were distributed much closer to the border of layer 5 and layer 6 in hypothyroid mice compared to control mice. In the adult, there were less c-Fos-expressing Ctip2+ cells in the upper part of layer 5 in hypothyroid mice. In addition, an electrophysiological analysis of retrogradely-labeled CC neurons showed an elevated resting membrane potential, a decreased amplitude to spike threshold, and increased amplitude and frequency of spontaneous excitatory postsynaptic synaptic currents. These data indicate that maternal thyroid hormones are required for the proper distribution and function of CC neurons in layer 5 of A1 in the adult mice.

PS 313

Tone Exposure During the Critical Period Impairs Frequency Representation and Network Characteristics in Primary Auditory Cortex.

Kevin Armengol¹; Alireza Sheikhattar²; Behtash Babadi³; Patrick O. Kanold⁴

¹*Neuroscience and Cognitive Science Program, University of Maryland, College Park*; ²*Department of Electrical and Computer Engineering, University of Maryland, College Park*; ³*Institute for Systems Research, University of Maryland, College Park*;

⁴*Department of Biology, University of Maryland, College Park*

The sensory environment during development can influence brain function and circuits. Repetitive, single-frequency tone exposure during early auditory critical periods in rodents has been shown to result in cortical overrepresentation of that frequency in layer IV of the primary auditory cortex (A1). Notably, these studies have relied on multiunit electrode characterization of neuronal threshold sensitivity in anesthetized animals. Little is known about the effects of these exposure paradigms on suprathreshold frequency representation

in single-cells as well as the broader effects on network activity in the awake animal and across cortical layers. Using in vivo widefield and two-photon calcium imaging in awake, adult mice (P45-60), we find that early single-frequency tone exposure (P10-P21) results in cortical underrepresentation of the exposure frequency in excitatory neurons at moderate sound levels in layers IV and II/III of A1. These results are largely consistent with studies in cats (Noreña et al., 2006) and with habituation effects on A1 responses seen with prolonged exposures in adults (Pienkowski et al., 2011). We analyze the functional networks in layer II/III of A1 using Granger Causality (GC) analysis (Francis et al., 2018; Sheikhattar et al., 2018) and graph theory. Preliminary results suggest several network level effects of early tone exposure such as decreased inhibitory connection strength at the exposure frequency and a decrease of the spatial distance of GC linked neurons. These changes in A1 may reflect a compensatory response to increase the reliability of information transmission through the network. Thus, tone exposure during early critical periods of auditory cortical development may have more complex neural effects than previously noted.

PS 314

Nonlinear Coding of Naturalistic Sound Streams in Marmoset Auditory Cortex

Luke A. Shaheen¹; Stephen V. David²

¹*Oregon Health and Science University*; ²*Oregon Health & Science University*

The human auditory system is adept at isolating and comprehending a single sound out of multiple sources (auditory streaming). The early auditory system encodes sound across a population of neurons, each sensitive to distinct low-level features, such as spectral frequency, spatial location, and modulation frequency. Because natural sound sources can contain overlapping features, the activity of individual neurons at early stages reflects a mixture of multiple sources. As signals pass through the auditory hierarchy, they undergo a series of nonlinear transformations which have been proposed to support emergent stream segregation. Evidence for streaming effects is well-documented for static, synthetic stimuli in auditory cortex (ACTx). How these mechanisms extend to natural, dynamic stimuli such as human speech is unknown.

To study streaming of naturalistic sounds at the single-neuron level, we recorded ACTx activity in passively-listening marmosets during presentation of a two-“voice” stimulus that retained the temporal dynamics of speech but had static spectra. Each voice consisted of a harmonic complex tone (HCT) with a unique fundamental frequency, modulated by a temporal

envelope drawn from human speech. The envelope could be the same for both voices (coherent) or different (incoherent). Coherent voices were perceived as originating from a single source, and incoherent voices as two sources.

Responses to two dynamic HCTs were poorly predicted by responses to static HCTs or by the sum of responses to each voice in isolation. Responses were mostly suppressed relative to the sum of the isolated responses, but periods of nonlinear enhancement were also observed. Nonlinear interactions varied with the degree of coherence between streams. Incoherent stimuli evoked more frequent periods of suppression and poorer correlation with responses to each voice in isolation, possibly reflecting differences in streaming between conditions. A linear-nonlinear (LN) encoding model incorporating a spectro-temporal filter followed by a static nonlinearity was able to predict some nonlinear interactions (ex. saturation), but most neurons remained poorly predicted. Ongoing efforts will determine if a model incorporating nonlinear adaptation and/or multiple LN units is sufficient to predict responses across streaming conditions.

PS 315

Context Dependent Encoding of Ultrasonic Vocalization Sequences in the Mouse Auditory Cortex

Swapna Agarwalla¹; Sharba Bandyopadhyay²

¹Indian Institute of Technology, Kharagpur; ²Indian Institute of Technology Kharagpur

Ultrasonic vocalisations (USVs) of mouse are of communicative significance. Adult male mice USVs were recorded under different social contexts and using information theoretic measures we show that syllable sequences in bouts of USVs has structure in them which undergoes modulation with social context. Neurons in the auditory cortex are known to be selective to species specific vocalizations, however cortical encoding of structured sequences of vocalizations has not been studied. Since male mouse vocalizations have specific sequential structure in order of syllables that change under different social contexts involving female mice we ask whether single neurons in the auditory cortex (ACX) female mice show selectivity to natural structure in syllable sequences emitted by male mice. We designed a set of stimuli with mouse USV syllable sequences having the same probability of occurrence of each syllable type as in the natural sequences but with random ordering of syllables. The second set of stimuli was natural sequences of syllables which are produced naturally by male mice. We use 12 random order sequences (SR) and 8 natural sequences (SN). Single

unit electrophysiological recordings were performed from the ACX of female mice under anesthesia and also from awake, passively listening female mice chronically. Responses to syllables in recorded spike trains of single units, as well as the local field potential (LFP), were characterized using various response measures (namely, spike rate and root mean square value of LFPs). Neurons in the ACX showed significantly higher selectivity to the same syllables occurring in SN compared to that in SR, in passively listening mice and not under anesthesia. However, LFPs showed similar stronger selectivity for syllables in SN compared to SR both in awake and anaesthetized conditions. In order to understand the effect of context, responses to transitions of one syllable to another (successive) in the sequences were analyzed. LFPs did not show selectivity to transitions in SN over SR, however rate responses in spikes showed stronger responses to the same transitions occurring in SN over those SR. Thus our study indicates that under awake conditions transitions in natural sequences cause stronger responses. Further, selectivity for transitions for natural sequences over random sequences is emergent in the ACX.

PS 316

Evaluation of Auditory Biomarkers in Patients with Schizophrenia: A Phase Ib Clinical Trial with AUT00206

Victoria Sanchez¹; John Hutchison²; Anil Sajjala²; Alice Sharman²; Charles Large²

¹University of South Florida; ²Autifony Therapeutics Limited

Patients currently treated with antipsychotics for Schizophrenia receive relief from positive symptoms (e.g., hallucinations, delusions), but still often complain of cognitive and negative symptoms including sensory processing impairments. There is an urgent need for novel therapies with improved efficacy across all symptom domains, and which have a better safety profile compared to existing drugs. AUT00206 is a novel and selective small molecule modulator of Kv3.1 and Kv3.2 voltage-gated potassium channels. There is reduced expression of Kv3 channels in the cortex of patients with schizophrenia and pre-clinical results in relevant animal models suggest that AUT00206 could be an effective oral treatment for cognitive and sensory symptoms of schizophrenia by increasing the neural synchrony that underpin attention, sensory processing, and cognition. Furthermore, patients with schizophrenia also show an impairment in central auditory processing, which we speculate is linked to reduced Kv3 channel function. AUT00206 is currently being evaluated in a randomized, double-blind, placebo-controlled Phase Ib clinical trial (clinicaltrials.gov ID# NCT03164876) to assess the

pharmacokinetics, safety and tolerability of repeated doses of AUT00206, for 28 days, as adjunctive therapy in male patients with a diagnosis of schizophrenia within the last 5 years and already taking stable doses of 1 or 2 antipsychotic drugs. The secondary and exploratory objectives selected to evaluate the effects of AUT00206 include the auditory-evoked Mismatch Negativity (MMN) and several hearing-related outcomes. Typically, the auditory-evoked MMN is reduced in patients with Schizophrenia, but it is not known if the reduction in cortical activity starts lower at the brainstem or even within the peripheral auditory system. Therefore, the hearing tests selected for this trial are known to be sensitive at detecting abnormalities at the level of the cortex (dichotic digits), brainstem (masking level difference), and the peripheral structures and functions (pure-tone audiometry, speech-in-noise, and contra-lateral suppression otoacoustic emission). In addition to reporting the trial design, methodology and the rationale behind the selected outcome measures, the purpose of this presentation is to present the baseline data collected so far (n=15), and demonstrate the observed deficits in these outcomes compared to normative data. The observed deficits provide confirmation of a therapeutic target and introduce a discussion of the potential of these hearing-related outcome measures as biomarkers for the present and future pharmaceutical studies.

PS 317

Ensemble Modeling of Auditory Stream Segregation Reveals Potential Sources of Perceptual Bistability Throughout the Ascending Auditory Pathway

David F. Little¹; Joel S. Snyder²; Mounya Elhilali¹
¹Johns Hopkins University; ²University of Nevada, Las Vegas

Introduction

Auditory bistability—spontaneous fluctuations in perception between two interpretations of an acoustic stimulus—can occur while listening to ambiguous acoustic scenes. Understanding this phenomenon is likely to shed light on general mechanisms of auditory perception, including both stimulus-driven and perception-related processes. For instance, bistability may reflect ongoing processes that select the current conscious percept from a range of possible interpretations that are simultaneously competing at an unconscious level of processing. The present work evaluates an ensemble of models that all include three analysis stages: the first stage models the auditory periphery (early feature-level), the second models cortical responses to different spectral shapes (late feature-level), and the third models the generation

of multiple interpretations of an auditory scene and selection of a single interpretation (object-level).

Methods

We evaluated each model in the ensemble using an auditory scene composed of two repeating tones (A and B). The scene was either unambiguous—perceived by human listeners as consistently one stream or two streams—or ambiguous—perceived in a bistable fashion, with fluctuations between one and two streams. Each model computed, from an acoustic waveform, the number of streams perceived, which we compared to existing human data. We considered three classes of model, with bistability in only one of the three analysis stages, respectively. For each of the three model classes, we injected one of 5 possible levels of inhibition and 5 levels of adaptation in a factorial fashion for a total of 25 model variants per class, and 75 models in total.

Results

Each of the three classes considered—with bistability in either the early feature-level, late feature-level or object-level—included some model variants that were capable of generating a form of perceptual bistability. However, there were more object-level variants, compared to the two feature-level variants, for which the distribution of perceptual switches in time were consistent with that of human listeners.

Conclusions

The more limited number of model variants capable of generating a plausible form of bistability at earlier stages of analysis suggests that bistability may more readily and frequently arise from object-level processing than feature-level processing. Nevertheless, it appears that bistability can arise within each of the proposed stages of auditory scene analysis simply by introducing an appropriate amount of adaptation and inhibition, dynamics that are pervasive throughout the nervous system.

PS 318

Revising the Organization of the Corticocollicular System: a Comparison of Long-range Contributions of Layer 5 and Deep Layer 6.

Georgiy Yuditsev; Daniel Llano
University of Illinois at Urbana-Champaign

Processing of sensory information, particularly in the auditory modality, often relies on centrally-generated cues in higher brain regions that are sent to subcortical

nuclei. The auditory cortex is an important part of the hierarchy, sending long-range projections to virtually all subcortical structures important for audition. One such projection - the corticocollicular (CC) projection - recently garnered much attention due to its potential to alter response properties in the inferior colliculus (IC). Although multiple studies focused on understanding of the CC system through characterization of its component originating from cortical layer 5, more recent evidence suggests a significant contribution from deep layer 6 projection neurons, constituting roughly 25 % of the CC neurons in mouse. Currently, the relative contributions of layer 5 vs. layer 6 projections to the IC are poorly understood. We show that layer 5 and deep layer 6 CC neurons differ in their cortical areas of origin and that these regions differ in their responses to sound and patterns of thalamic input, as well as termination patterns within the three subdivision of the IC, with layer 5 projecting to all three subdivisions, while deep layer 6 was found to project only to the dorsal and external cortical components of the IC. These findings suggest differential functionality for layer 5 and deep layer 6 CC neurons, and provide a more detailed neuroanatomical foundation for further consideration of the CC system functions in healthy and impaired hearing.

PS 319

Planum Temporale: Morphological Taxonomy of the Posterior Superior Temporal Plane

Aaron Whiteley¹; Barrett St George²; Frank Musiek¹
¹University of Arizona; ²The University of Arizona

Background: Planum Temporale (PT) is a crucial neuroauditory structure located in the dorsal superior temporal plane (STP) posterior to Heschl's gyrus (HG). The PT has been implicated in complex auditory function and is well known for its preponderance of leftward asymmetry in normal brains and classic "pie" shaped morphology. While a majority of cases have easily identifiable PT and HG, there exist some cases in which distinguishability of these two structures is difficult due to morphological variation. The goal of this study is to create a taxonomy of PT morphological features in order to improve the sometimes difficult identification and differentiation of PT from surrounding structures.

Methods: A total of 50 (100 hemispheres) healthy intact, high-resolution T1- weighted brain MRIs were included in this retrospective study. There were 28 women and 22 men, all right-handed; Ages ranged from 18-57 (mean=26.44) years. A 3D cortical surface mesh (grey matter) for each brain was generated using FreeSurfer and manipulated to view the STP using BrainVISA Anatomist neuroimaging software. The PT was isolated from surrounding structures based on pre-

defined anatomical criteria and subsequent surface area measurements, linear measurements and qualitative measures were made using a custom PYTHON script.

Results: A total of four PT configurations were identified:

- 1) Pie-shaped [45%]
- 2) Trapezoid-shaped [27%]
- 3) Rectangular-shaped [19%]
- 4) None [9%]

Mean surface areas of measurable PT configurations were: 508.82 mm² for "Pie-shaped" (n=45), 540.44 mm² for "Trapezoid-shaped" (n=27) and 477.68 mm² for "Rectangular-shaped" (n=19). The fourth category, "None" (n=9), was not calculable. There were significantly more "Trapezoid" PTs in females ($X^2(1, N=27) = 6.26, p=0.01, \phi=0.48$). The right hemisphere was demonstrated to have significantly more "None" PT classifications ($X^2(1, N=9) = 5.44, p=0.02, \phi=0.78$). The left hemisphere demonstrated significantly greater surface area for "Pie-shaped" PTs ($F(1) = 6.92, p=0.012$). With regards to the "None" classification, it is suspected that in these cases, portions extend with the Posterior Sylvian Fissure and is continuous with Planum Parietale. This is consistent with cytoarchitectonic studies that have demonstrated that parakoniocortex, or auditory association cortex, extrudes onto the posterior wall of the Posterior Sylvian Fissure and ultimately disrupts the classical criteria of PT's posterior boundary.

Conclusion: We believe that the proposed classifications is the first step in creating a comprehensive taxonomy of the STP. This will aid neuroanatomists, clinicians and students in terms of differentiation of sometimes complex topography of the STP.

PS 320

Encoding of Aperiodic Amplitude Modulations in Gerbil Auditory Cortex

Kristina B. Penikis; Dan H. Sanes
New York University

Temporal regularity in sounds can entrain neural activity and is associated with perceptual benefits in humans. While natural acoustic signals often contain some temporal predictability, the amplitude modulations (AM) are rarely periodic. However, our understanding of AM encoding is largely based on periodic stimuli. To assess whether auditory cortex AM coding is influenced by temporal regularity, we recorded single neuron

responses to sinusoidal AM stimuli, in which the AM rate was switched every few seconds. Trials were either periodically (P) modulated at rates of 2-32 Hz, or aperiodically (AP) modulated: quasi-random sequences of individual periods drawn from the same set. During recordings, gerbils performed an aversive Go-Nogo detection task in which all modulated stimuli were safe, and unmodulated noise served as the warn signal that predicted a brief electrical shock. The average firing rates during P stimuli were strongly predictive of the average responses to AP stimuli, indicating no broad impact of temporal regularity. We also compared responses to individual shape- and time-matched periods across P and AP contexts. Again, there was no effect across the population in any of several different response metrics. Sparse coding models suggest that only a subset of cortical neurons optimally represent a given stimulus. Along these lines, when we restricted stimulus-evoked responses to periods corresponding to the best modulation frequency of each neuron, a difference between P and AP contexts emerged. In this case, the firing rate during the P context was higher than in the AP context. These observations leave open the possibility that temporal regularity may emerge as a stronger response feature in regions downstream of A1. Currently, we are gathering data on a larger scale to assess whether a population code more reliably represents AM and whether an influence of temporal regularity can be observed at this level.

Auditory Pathways: Midbrain

PS 321

Neural Coding of Concurrent Harmonic Complex Tones in the Auditory Midbrain of Unanesthetized Rabbits

Oded Barzelay¹; Bertrand Delgutte²

¹*Harvard Medical School / Mass Eye and Ear*; ²*Dept. of Otolaryngology, Harvard Medical School; Eaton-Peabody Lab, Mass. Eye and Ear*

Background

Everyday auditory scenes often contain mixtures of harmonic complex sounds such as speech and musical sounds that each evoke a pitch at their fundamental frequency (F0). The auditory system exploits pitch differences between harmonic sounds to parse the scene into separate perceptual objects. Previous studies of the auditory nerve and auditory cortex have shown that the neural patterns of activity evoked by pairs of concurrent harmonic complex tones (HCT) with different F0s contain sufficient cues for identifying both F0s. Less is known about the coding of concurrent HCTs in the inferior colliculus (IC), where a major transformation from a temporal code to a rate code takes place. Here we

measured responses of IC neurons to pairs of concurrent HCTs in unanesthetized rabbits to test whether the F0s can be represented by a rate-place code.

Method

We recorded from single units in the IC of unanesthetized rabbits in response to both single HCTs and pairs of concurrent HCTs with varying F0s. All stimuli had equal-amplitude harmonics in cosine phase and were presented at 20-60 dB SPL. For each neuron, the F0 range was chosen so that low-order harmonics likely to be resolved varied around the pure-tone best frequency (BF). For concurrent HCTs, both F0s co-varied with their ratio held at 2 or 4 semitones.

Results

In response to single HCTs, 35% of the neurons showed peaks in firing rate when a low-order (1-6) harmonic aligned with the neuron's BF. Such rate-place coding of resolved harmonics was most prominent for neurons with BFs above 6 kHz. In response to concurrent HCTs, we rarely observed distinct firing rate peaks when a harmonic of either tone aligned with the BF. Instead, the peaks in firing rate encompassed two neighboring harmonics, one from each HCT. These peaks were broader than those produced by harmonics of single HCTs, thereby providing cues to the presence of concurrent HCTs. A linear filter model with bandwidths matching those of rabbit auditory-nerve fibers generally predicted the locations of the firing-rate peaks in response to both single and double HCTs.

Conclusion

While rate-place profiles of rabbit IC neurons contain information for distinguishing a single HCT from concurrent HCTs with neighboring F0s, the information is only available for low-order harmonics (1-3), suggesting the identification of the F0s from rate-place profiles would be challenging. Supported by NIH Grant DC002258.

PS 322

Characterizing Midbrain Selectivity for Direction and Velocity of Frequency Sweeps

Paul Mitchell; Kenneth S. Henry; Laurel H. Carney
University of Rochester

Neurons in the inferior colliculus (IC) are selective for direction and velocity of frequency sweeps in Schroeder-phase harmonic complexes (Carney & Klump, ARO 2018). The goal of this study was to ask whether these neurons are tuned for the direction and/or velocity of instantaneous-frequency (IF) sweeps. We developed a stimulus with a randomly varying IF and recorded

responses in the IC of the awake rabbit using tetrodes. The IF of the stimulus was varied with respect to the characteristic frequency of the neuron using a band-limited gaussian noise. The range of frequencies in the stimulus was controlled by the amplitude of the gaussian noise, and the range of velocities was controlled by the noise bandwidth. The distribution of IF velocities included those in frequency sweeps in Schroeder stimuli for which sensitivity is typically observed.

To determine whether specific frequency sweep(s) preceded IC responses, a reverse-correlation (revcor) analysis was used based on the random IF of the stimulus. Several repetitions of each long-duration stimulus were used to allow both revcor analysis and predictions of the post-stimulus time histograms (PSTH) of the responses.

IF revcor functions were well-defined, containing fast upward and downward frequency sweeps that preceded responses at different times within the function. The steepest slopes in the IF revcor functions were comparable to the velocities of frequency sweeps in Schroeder stimuli for which IC neurons are often selective.

Predictions of the IC response PSTHs were computed using either the entire revcor function or specific features, such as upward vs. downward IF slopes or high vs. low frequency regions. The ultimate goal is to refine this strategy for characterizing the strong selectivity of IC neurons for frequency sweeps. These results will guide efforts to incorporate this property into a model for IC neurons that currently lacks direction selectivity for frequency sweeps. These models should improve our understanding of midbrain responses to natural stimuli, such as voiced speech sounds that have fast sweeps within each pitch period due to the phase configuration of harmonics.

Supported by NIH-R01-DC001641.

PS 323

Neural Correlates of Behavioral Tone-in-Noise Detection in the Avian Inferior Colliculus

Yingxuan Wang; Kristina S. Abrams; Laurel H. Carney;
Kenneth S. Henry
University of Rochester

Communication under everyday listening conditions requires signal detection in competing noise. The mechanisms that support signal detection in noise are not well understood. Whereas a temporal code is generally thought to support signal detection at the level

of the auditory nerve, mechanisms are less clear for central processing nuclei where the upper frequency limit of neural response synchrony is lower. We used matched behavioral operant conditioning experiments and neural recordings from the inferior colliculus (IC; midbrain) to explore the central mechanisms underlying behavioral tone-in-noise (TIN) detection. Experiments were conducted in the budgerigar (*Melopsittacus undulatus*), an avian vocal mimic with human-like behavioral sensitivity to many simple and complex sounds. Tone frequency ranged from 0.5-4 kHz. Noise was one third octave in bandwidth, centered on the tone. TIN thresholds in budgerigars were remarkably similar to human thresholds tested using the same stimuli, and relatively constant across frequencies and across sound levels from 45-85 dB SPL. Notably, thresholds were not impacted by introduction of a roving level paradigm in which stimulus level varied from trial to trial within test sessions. Thus, signal detection could not be explained based on energy output from a single auditory filter. Extracellular neural recordings from the IC revealed both an average rate code and a temporal code for TIN detection. Average rate decreased with increasing tone level in most IC neurons. This pattern is consistent with the fact that the TIN envelope flattens with increasing tone level, and that most cells showed band-pass modulation tuning (i.e., fluctuating inputs evoke a stronger response). For the temporal TIN code, the relative strength of low-frequency response fluctuations (<500 Hz) also decreased with increasing tone level. Neural thresholds based on average rate and temporal response fluctuations are compared to behavioral TIN thresholds across frequency to gain insight in the neural mechanisms that support signal detection in noisy listening environments. This research was supported by grants R01-DC001641 and R00-DC013792 from NIDCD.

PS 324

Neural Coding of Binaural Cues between Acoustic and Electrical Stimulation in an Animal Model of Single-Sided Deafness

Yoojin Chung; Bertrand Delgutte
*Dept. of Otolaryngology, Harvard Medical School;
Eaton-Peabody Lab, Mass. Eye and Ear*

Background

Cochlear implant (CI) users increasingly have significant acoustic hearing in the non-implanted ear and continue to use a hearing aid (HA) in the non-implanted ear. In addition, CIs have become a treatment option for people with single-sided deafness (SSD). These populations of CI users can potentially enjoy the benefits of binaural hearing such as improved sound localization and

speech reception in noise by utilizing binaural cues present between the two modes of stimulation. Here, we investigated the sensitivity of midbrain auditory neurons to interaural time differences (ITD) with bimodal stimulation to understand how the binaural cues are represented in the central auditory pathway and identify the most effective stimulation parameters for delivering these cues.

Method

Single-unit recordings were made from the inferior colliculus (IC) of an unanesthetized Dutch-belted rabbit that was deafened and implanted in one ear and had normal hearing in the non-implanted ear. Periodic trains of acoustic clicks and electric pulses at low repetition rate (20-80 Hz) were used to characterize bimodal ITD sensitivity of the IC neurons.

Results

In many neurons, the temporal discharge pattern showed strong responses to both stimuli for large ITDs, either acoustic leading or electric leading. The acoustic response latency was longer than the electric latency reflecting the additional biological delay of the sound traveling through the external, middle and inner ear. For smaller delays near zero-ITD after adjusting for the difference in response latencies, IC neurons showed clear binaural interaction to the bimodal stimuli in that the firing rate could be either increased or decreased relative to the rate for stimulation in either mode. We observed similar shapes of ITD tuning curves such as peak and trough types as previously observed in response to pairs of acoustic clicks or electrical pulses. Neural ITD discrimination thresholds were in the similar range as thresholds observed in IC neurons of bilaterally deafened and implanted animals.

Conclusion

The results show that neurons in the auditory midbrain can be sensitive to binaural cues in combined acoustic and electric stimulation and suggest that binaural benefits with bimodal hearing could be improved by providing better access to binaural cues in SSD/CI users and HA-CI users.

Funding: NIH grant R01 DC005775.

PS 325

The contribution of stimulus driven and noise correlations for neural decoding and identification of texture sounds

Xiu Zhai¹; Fatemeh Khatami²; Mina Sadeghi³; Heather Read³; Ian Stevenson³; **Monty Escabi**⁴

¹University of Connecticut; ²Univ. of Cal San Francisco; ³Univ of Conn; ⁴Univ of Connecticut

The amount of information conveyed by neural ensemble about a sensory stimulus is critically dependent on the correlation structure of its neural activity. On the one hand, stimulus driven correlations between neurons are often thought of as form of redundant encoding with limited encoding capacity and reduced efficiency. Alternately noise correlations, i.e. correlated firing due to network activity unrelated to the sensory stimulus, are thought of as a form of noise that limit the classification accuracy of neural population codes. Using multi-channel neural recording arrays to record neural responses to natural sound textures in unanesthetized rabbits we demonstrate that correlated firing between frequency organized neural ensembles in the auditory midbrain (inferior colliculus) can be used to recognize sounds. To explore the contribution of stimulus driven and noise correlations for decoding the sound texture identity, we developed a noiseless and single-trial classifier. The noiseless classifier excludes the noise correlations and thus sets an upper bound on the classification accuracy provided by the stimulus driven correlation structure. The single trial classifier, by comparison, requires that both the noise and stimulus driven correlations be taken into account. Unlike noise correlations, which are mostly unstructured (diagonalized) and vary little with the sound, stimulus driven correlations are highly stimulus dependent and their time-frequency structure was quite diverse and informative for the classification task. The noiseless classifier approached near perfect identification accuracy (average 90%) using stimulus-driven correlations only and sets an upper bound on the classification accuracy. Although the average single-trial classification performance was on average lower (70%), individual penetrations were found that approached near perfect accuracy (90%). The reduction in the classification accuracy was accurately accounted for by the noise correlations. First, when noise correlations are not included as part of the single-trial classifier model, single trial performance drops to near chance (20%) indicating that noise correlations are necessary to make accurate predictions of single trial activity. Furthermore, performance was highly correlated with the signal-to-noise ratio (SNR) of the neural correlations: classifier performance was higher for recording locations with higher SNR. Thus, unlike previous studies which have proposed that correlated firing is generally detrimental,

these findings suggest that stimulus-driven correlations can be quite informative for sound identification. By comparison, noise correlations need to be accounted for making accurate predictions, yet they ultimately limit the classification performance (supported by NIDCD R01DC015138).

PS 326

Peripheral and mid-level auditory filters enhance temporal representations of natural sounds

Fengrong He; Monty Escabi
University of Connecticut

Efficient coding theories for natural sound processing propose that auditory system is optimized to take into account statistical regularities in natural environments. One widely observed statistical regularity is the 1/f modulation spectrum of natural sounds where the power of amplitude modulations drops off with increasing frequency. Both physiology and modeling studies have suggested that receptive fields across multiple levels of the auditory pathway are consistent with efficient sparse codes that enable efficient transfer of information and equitable use of neural resources. Despite the implications for optimality, how acoustic information is sequentially transformed by such coding schemes is not well understood. Using a small database of background and vocalized sounds including human speech, we explore the transformations of spectro-temporal modulations across peripheral and mid-level (midbrain) models of the auditory pathway and compare the resulting representations to Fourier based signal representations. For both the peripheral cochlear model filters and mid-level modulation filters, bandwidths scaled with the filter frequency, mirroring physiological observed trends. Comparing, Fourier based and physiological based filters, dramatic differences are observed. The Fourier based decomposition produce high spectral resolution at the expense of limiting the amount of temporal information. The modulation power spectrum (MPS) obtained using commonly used Fourier based decomposition, had limited temporal resolution, with temporal modulations limited to ~25 Hz. By comparison, the cochlear model representation sacrifices spectral information while still capable of encoding temporal modulations exceeding 500 Hz, as observed physiologically. Upon processing by the mid-level modulation filterbank, the bandwidth scaling properties of the modulation filters whiten and further enhance the temporal modulation content of natural sounds which has a 1/f structure at the cochlear stage. Thus, unlike Fourier based representations, which have little temporal information, the results suggest that combined cochlear filtering and modulation filtering transformations across the auditory pathway equalize and whiten the power of natural sound modulations

allowing for an enhanced temporal representation (supported by NIDCD R01DC015138).

PS 327

Manipulating Levels of Endogenous Serotonin Affects How Social Vocalizations are Represented in the Brain's Social Behavior Network

Christopher L. Petersen; Sarah E.D. Davis; Bhumi Patel; Laura M. Hurley
Indiana University - Bloomington

Vocalization is an important aspect of rodent social behavior. It is therefore surprising that relatively few studies have investigated how vocalizations are represented in the brain's social behavior circuitry. Mouse vocalizations are categorized as ultrasonic vocalizations (USVs), which are emitted more by males in sexual contexts, and broadband vocalizations (BBVs) or "squeaks" which are primarily emitted by females in this context. While USVs are generally thought to be prosocial, the function of BBVs remains somewhat ambiguous as they are produced during both mounting and rejection-like behavior. One way in which different contexts are represented in the brain is via the release of neuromodulators. For example, levels of serotonin (5-hydroxytryptamine; 5-HT) increase within the auditory midbrain (inferior colliculus) of male mice when they are interacting with females, but are negatively related to the amount of rejection-like behaviors males receive. Likewise, serotonin levels increase in some socially integrative brain regions during sexual activity. Therefore, we tested the hypothesis that manipulating levels of endogenous serotonin in male mice would affect neural activity (as assayed by immediate early gene induction) in the brain's core social behavior network following presentation of female BBVs. Male CBA/J mice (*Mus musculus*; Jackson) were played 60-minute bouts of female BBVs; prior to playback, mice were injected with saline, fenfluramine (a serotonin releaser and reuptake inhibitor), or para-chlorophenylalanine (PCPA; which blocks the production of serotonin by inhibiting tryptophan hydroxylase). After playback, brains were collected and processed for fluorescent immunohistochemistry. We labeled the immediate early gene product c-Fos as a putative marker for neural activation within the social behavior network (SBN). The SBN is an interconnected suite of nuclei within the basal forebrain, hypothalamus, and midbrain that is essential for the appropriate production of social behaviors. c-Fos immunoreactivity (-ir) was quantified within 8 nodes of the SBN including the lateral septum (LS), medial bed nucleus of the stria terminalis (BNST), medial preoptic area (mPOA), as well as the paraventricular nucleus (PVN), anterior nucleus (AH) and ventral medial nucleus (VMH) in the hypothalamus, and the midbrain ventral

tegmental area (VTA) and periaqueductal gray (PAG). We find that fenfluramine increased c-Fos-ir neurons within LS relative to saline and pCPA injected animals. Continued analysis will determine to what extent the presence or absence of serotonin affects auditory processing in other nuclei within the SBN, as well as the circuit as a whole.

PS 328

Functional Organization of Excitatory and Inhibitory Neurons in the Mouse Dorsal Inferior Colliculus

Aaron B. Wong; J. Gerard G. Borst
Erasmus Medical Center

The inferior colliculus (IC) is an auditory hub, which receives inputs from most brainstem auditory nuclei. The non-lemniscal regions of the IC, the dorsal cortex (DCIC) and lateral cortex (LCIC), are major targets for feedback projections from the cerebral cortex. Although the corticocollicular projections are glutamatergic in nature, direct stimulation of auditory cortex can have inhibitory effects on the IC, suggesting an important role for inhibitory neurons within the IC in the descending feedback. An abnormal excitation-inhibition balance has been implicated in pathological condition such as tinnitus and hyperacusis.

Relatively little is known about the functional organization of inhibitory and excitatory neurons within the DCIC and LCIC. In the mouse, large parts of the DCIC and LCIC lie superficially, making it a favorable structure for long-term *in vivo* two-photon imaging. We measured tone-evoked Ca²⁺ transients in mouse lines that specifically label either GABAergic or non-GABAergic neurons with the genetically encoded calcium indicator GCaMP6s, up to a period of several months. Frequency response areas of neurons were generally stable for B6CBAF1/J mice. To gain a better understanding of the spatial organization of frequency tuning, we aligned recorded neurons from multiple animals to a common coordinate system based on anatomical landmarks. We found a general rostromedial-caudolateral gradient of characteristic frequencies, even when analysis was restricted for neurons within 80 μm from the pial surface.

We performed simultaneous Ca²⁺ imaging and juxtacellular recording in both mouse lines to link the four observed types of tone-evoked fluorescent responses in IC cells (onset, sustained, inhibited and offset) to response types defined electrophysiologically. We observed that onset type fluorescence responses can include both onset and (quickly-) adapting firing patterns, and sustained fluorescence responses correspond to sustained, buildup or (slowly-) adapting

firing patterns. Inhibited and offset fluorescence correspond to inhibited and offset firing, respectively. In conclusion, long term Ca²⁺ imaging allows a spatial characterization of neurons in the dorsal IC, and provides a platform to study age- or trauma-induced changes in neural tuning.

PS 329

The Effect of Choline Alphoscerate on Cognitive Behavioral Function of Chronic Noise and Restraint Stress Rat Models

Hyo Jeong Yu¹; Dong Won Yang²; Min Jung Kim¹; Jung Mee Park¹; So Young Park¹; Shi Nae Park¹
¹*Department of Otorhinolaryngology-Head and Neck Surgery, College of Medicine, The Catholic University of Korea;* ²*Department of Neurology, College of Medicine, The Catholic University of Korea*

Purpose: Noise exposure has been well characterized as an environmental stressor with auditory and non-auditory effects. Restraint stress induces negative outcomes on feeding behavior conditions as well as neurogenesis in rats due to physiological changes. Choline Alphoscerate (α-GPC) is a common choline compound and acetylcholine precursor in the brain, which has been shown to be effective in the treating of neuronal injury and to increase Brain-derived neurotrophic factor (BDNF) that enhances memory and cognitive function. The purpose of this study was to establish chronic dual stress rat models using noise and restraint, and to investigate the effect of α-GPC on cognitive function after dual stress.

Methods: Wistar rats were divided into four age-matched groups: control group (C), drug-treated group (CD), experimental group exposed to dual stress of noise and restraint (NS), and experimental dual stress group with treated drug treatment group (NSD). The two experimental groups were exposed to double stress stimuli of noise and restraint which involved 110dB SPL white band noise for 3 hours every day up to 7 days and restraint in cylindrical plastic films, DecapiCones, with rubber bands fixed at the tails at the same time. While C and NS group received saline, other 2 groups received α-GPC orally after stress exposure. Hearing tests of ABR and DPOAE were performed before and after stress exposure. Behavior assessment was also performed by novel object recognition (NOR) test. BDNF expressions in the hippocampus, morphologic changes in organ of Corti, changes in body weight, and corticosterone concentration in plasma were also investigated.

Results: Cognitive function measured by NOR test significantly decreased in the NS group compared to the other groups (p<0.05), but increased in NSD group compared to NS group (p<0.05). Experimental groups showed significantly decreased hearing levels and the

body weights after the dual stress ($p < 0.05$). collapsed organ of Corti and increased corticosterone concentration in plasma were found in experimental groups. BDNF expression in brain of NS group was significantly decreased compared to C group ($p < 0.05$). Although BDNF was increased in NSD groups compared NS group ($p < 0.05$), it was not as high as the control C group. **Conclusion:** Dual stress in rat models caused cognitive dysfunction as well as significant decrease in BDNF protein expression. α -GPC may boost BDNF expression and enhance memory and cognitive function. The study investigating the role of BDNF relevant receptor, TrkB, in the hippocampus is ongoing in our laboratory.

PS 330

The Density of Perineuronal Nets in the Inferior Colliculus of Fischer Brown Norway Rats Increases with Age.

Amir Mafi; Lindsay Hofer; Jeffrey Mellott
Northeast Ohio Medical University

A prominent feature of the aging inferior colliculus (IC) is the downregulation of inhibition. Throughout the IC are perineuronal nets (PNs), aggregates of extracellular matrix, that are routinely associated with GABAergic neurotransmission, synaptic stabilization and inhibiting plasticity. Previous reports in sensory cortex have shown that aging alters the presence of PNs. We sought to determine if PNs in the IC are also altered with age. We assessed Fischer Brown Norway rats in four age groups: "young adult-early" (2-3 months); "young adult-late" (4-7 months); "middle-aged" (19-22 months); "aged" (28-30 months). Brain sections (40 μ m), perfused with 4% paraformaldehyde, were immunostained for GAD67 (Millipore; MAB5406), Wisteria Floribunda Lectin (WFA; Vector; B-1355) and NeuroTrace (Molecular Probes; N-21480). Cell bodies were classified as PN-positive if ~75% of the perimeter was covered by WFA. A total of 16,236 PNs were quantified across 29 sections of IC.

Our main finding is that the density of PNs in the IC increased with age. We found a 45.7% increase of PN density in the aged IC when compared to the young adult IC (764 PNs/mm³ vs. 524.5 PNs/mm³). PN densities increased in each of three major subdivisions between the aged and young adult groups; IC central, IC lateral cortex, and IC dorsal cortex; 38.3%, 39.6% and 56.8%, respectively. There was also a 27.6% increase in PN density in the aged IC when compared to the middle-aged IC (764 PNs/mm³ vs. 598.75 PNs/mm³).

We determined that the age-related increase of PNs was not specific to either GABAergic or glutamatergic cells. In the young adult groups 68.4% of PNs were

associated with GAD-immunonegative cells and 31.6% with GAD-immunopositive cells. While in the aged group 69.9% and 30.1% of the PNs were associated with GAD-immunonegative cells and GAD-immunopositive cells, respectively.

Our data lead to two main conclusions regarding the expression of PNs in the aged IC. First, we find that the density of PNs is significantly increased in the aged group. PNs can serve to stabilize synapses, it is possible that the upregulation of PNs is a compensatory mechanism to help maintain temporal precision as the age-related loss of inhibitory inputs in the IC occurs. Second, age-related increases of PN density occurs on both GABAergic or glutamatergic cells in the aged group. This implies, given that PNs inhibit plasticity, inhibitory and excitatory circuits in the IC become less plastic in old age.

PS 331

Intrinsic Physiology of Several Molecularly Defined Neuron Classes in the Inferior Colliculus Varies Along the Tonotopic Axis

Alexander P. George; David Goyer; Marina A. Silveira; Michael T. Roberts
University of Michigan

Located in the midbrain, the inferior colliculus (IC) is a major site of convergence for ascending and descending auditory information. Like most nuclei in the ascending auditory pathway, the central nucleus of the IC (ICc) is tonotopically organized, such that neurons respond best to narrow bands of the sound spectrum according to their physical location along a dorsolateral to ventromedial axis. In the auditory brainstem, the physiological properties of neurons often vary along the tonotopic axis. These variations in intrinsic physiology generally improve the ability of neurons to respond to the temporal components of their preferred sound frequencies. However, it is not known whether the physiological properties of defined neuron classes in the IC also vary along the tonotopic axis. To address this question, we targeted whole cell recordings to several molecularly defined neuron types in the IC and compared the intrinsic physiology of individual neurons to their location along the tonotopic axis. Recordings were targeted to neurons labeled in three Cre-driver mouse lines that we have recently identified as labeling distinct populations of IC neurons: vasoactive intestinal peptide-Cre (VIP-Cre), somatostatin-Cre (SST-Cre), and neuropeptide Y-Cre (NPY-Cre). Each of these mouse lines was crossed with Ai14 mice to drive expression of tdTomato in Cre-expressing neurons. In coronal slices of the IC, we assessed the intrinsic physiology of fluorescent neurons

by measuring input resistance, hyperpolarization-activated cation current, and membrane time constant. Neurons were filled with biocytin via the recording pipette, and coordinates for the location of each neuron were subsequently recovered using biocytin-streptavidin histochemistry and confocal imaging. Our results show a significant variation in membrane time constant along the tonotopic axis for all three neuron types, with lower frequency regions of the ICc having lower membrane time constants and thus faster membrane properties. In VIP and SST neurons, we also observed a significant variation in steady state input resistance, again with lower input resistances present in lower-frequency regions. In addition, in VIP neurons we observed that hyperpolarization-activated cation current was highest in low frequency regions of the ICc. Combined, these results suggest that the intrinsic physiology of several distinct classes of IC neurons systematically varies along the tonotopic axis of the ICc. We hypothesize that these variations reflect an increased requirement for temporal precision and therefore faster membrane properties in the lower frequency regions of the ICc.

PS 332

Temporal Processing in the Inferior Colliculus is Impaired in Mice Lacking the Extracellular Matrix Protein Brevican

Mira Türknetz; Jutta Engel; Simone Kurt
Saarland University, Dept. Biophysics and CIPMM, Hearing Research

The proteoglycan brevican is a major component of the extracellular matrix of perineuronal nets and is highly enriched in the perisynaptic space suggesting a role for synaptic transmission. Brevican is part of perineuronal nets at various stages of the auditory pathway, e.g. at inner hair cells synapses and at the somata of bushy cells, octopus cells in the cochlear nuclear complex, medial nucleus of the trapezoid body (MNTB) neurons, medial superior olive (MSO) and lateral superior olive (LSO) neurons, neurons of the dorsal nucleus of the lateral lemniscus (DNLL) and some neurons of the inferior colliculus (IC) and the auditory cortex (AC). Here we study the impact of brevican on dynamics and reliability of temporal processing of neuronal response properties of IC neurons. To this aim, we performed in vivo electrophysiological recordings from neurons of the IC from systemic brevican knockout (*brevican^{-/-}*) mice and their wildtype littermates. The responses of those neurons to pure tones and amplitude-modulated (AM) tones were characterized to examine the role of brevican for spectral and temporal coding.

Neurons of the IC in *brevican^{-/-}* mice showed no differences in response properties to pure tones and

frequency tuning compared to wildtypes. In contrast, evoked rates in response to AM tone stimulation were increased in *brevican^{-/-}* mice. Further, we found an increased upper cut-off frequency of phase locking at the expense of a reduced temporal precision in *brevican^{-/-}* mice in response to stimulation with AM tones.

Taken together, our results demonstrate that lack of the extracellular matrix protein brevican impairs auditory processing of AM tones. Because brevican is present at various stages of the ascending auditory pathway, the observed phenotype could result from an additive effect but could also be the result from a deficit at a specific location. This question can only be answered by a conditional, region-specific knockout mouse.

This study was supported by DFG PP1608/2

PS 333

Rate-Place Coding of Harmonic and Inharmonic Complex Tones in the Inferior Colliculus of Unanesthetized Rabbits

Yaqing Su¹; Bertrand Delgutte²

¹Dept. of Biomedical Engineering, Boston University; Eaton-Peabody Lab, Mass. Eye & Ear; ²Dept. of Otolaryngology, Harvard Medical School; Eaton-Peabody Lab, Mass. Eye and Ear

Harmonic complex tones (HCT) with resolved harmonics evoke a strong pitch percept at their fundamental frequency (F₀). When the component frequencies of an HCT are all shifted by the same amount, the pitch of the resulting inharmonic tone changes although the envelope repetition rate remains the same. Previously, we identified a rate-place code for resolved harmonics in the rabbit inferior colliculus (IC) that was relatively robust across sound levels. Here we further characterize this code using harmonic and inharmonic tones to test whether IC neurons are sensitive to harmonicity as some neurons in auditory cortex (Feng and Wang, PNAS 114(5): E840-8).

We recorded responses of 162 IC neurons to HCTs with equal-amplitude harmonics and varying F₀ from four unanesthetized rabbits. In some neurons, we also measured responses to inharmonic tones in which all harmonics were shifted by a constant fraction of F₀. HCTs were usually presented at 30, 45 and 60 dB SPL per component, and inharmonic tones at 30 dB SPL per component.

Among the 162 neurons, 63 showed peaks in firing rate in response to HCTs when a low-order harmonic aligned with the neuron's best frequency (BF), demonstrating

rate-place coding of resolved harmonics. The number of harmonics resolved in the firing rate ranged from 2 to 11. Rate profiles of the 13 neurons tested with inharmonic tones showed peaks when a low-order component aligned with the BF, regardless of harmonicity. Both the number and the strength of the resolved peaks were similar for different amounts of frequency shift, suggesting the neurons are not sensitive to harmonicity.

To further test whether rate-place coding by IC neurons is sensitive to harmonicity, we compared the ability of two filter models to predict the firing rates from the stimulus spectrum: a Gaussian filter and a difference of Gaussians (DoG) function with symmetrical inhibitory sidebands. For a majority of neurons, the DoG model fit the rate profiles better, suggesting a role of lateral inhibition in enhancing rate-place coding. Responses to inharmonic tones could be predicted from the DoG model fit to the HCT responses with comparable goodness-of-fit, further indicating that IC neurons are not sensitive to harmonicity.

In conclusion, rate-place coding of resolved harmonics was identified in many IC neurons. This code likely arises in the periphery but appears to be sharpened by lateral inhibition. Neither physiology nor model results gave any evidence for harmonic template neurons.

Supported by NIH grant R01 DC002258

PS 334

Extramodular Ephrin-B3 Expression in the Lateral Cortex of the Inferior Colliculus in Neonatal Mice

Mark L. Gabriele; Isabel D. Lamb-Echegaray
James Madison University

Background

The lateral cortex of the inferior colliculus (LCIC) is a multimodal center which receives major inputs of somatosensory and auditory origin. The LCIC exhibits characteristics in keeping with a discrete neural map, whereby somatosensory modular compartments are surrounded by extramodular auditory zones. Eph-ephrin guidance mechanisms have been implicated in instructing similar arrangements in other central structures, including the striatum and olfactory bulb. Previous studies in our lab have shown patchy EphA4 and ephrin-B2 expression during the early postnatal period that overlaps developing GAD-positive modules, and is complementary to calretinin-defined extramodular zones. The present experiments examine another member of the Eph-ephrin signaling family, ephrin-B3, and correlate its early postnatal expression with developing LCIC compartments.

Methods

Fluorescent immunocytochemical approaches were used in a developmental series of GAD67-GFP mice (P0-P12). This knock-in line specifically labels GABAergic neurons, facilitating easy visualization of developing LCIC modules. Free-floating sections were reacted for ephrin-B3 (1:200, R&D Systems) and visualized using a biotinylated streptavidin signal amplification (DyLight 549, 1:200, Vector Laboratories). Double-labeling experiments included processing for calretinin (1:250, Swant) with a direct conjugate AlexaFluor 350 secondary antibody (1:25, Thermo Fisher Scientific). A Nikon C1si TE2000 microscope was used for all microscopy (widefield and confocal) applications and image acquisition.

Results

LCIC ephrin-B3 expression was strong at birth and throughout the first postnatal week. Ephrin-B3 labeling was most concentrated in mid-rostrocaudal LCIC regions, exhibiting a pattern that was complementary to GAD-positive modules. Furthermore, ephrin-B3 patterning aligned with that of the extramodular marker, calretinin. By P12, once a clear modular-extramodular framework is readily apparent, ephrin-B3 expression appears downregulated.

Conclusion

The present study reveals that ephrin-B3 is present during the critical period of the establishment of LCIC modular-extramodular zones. Its extramodular expression appears to complement that of previously described modular EphA4 and ephrin-B2 patterns. Taken together, these findings suggest a potential role for Eph-ephrin signaling in segregating developing multimodal LCIC compartments and their respective connections.

PS 335

Orthogonal Populations of Tectothalamic Neurons in the Gerbil Inferior Colliculus Targeted by Intersectional Adeno-associated Viruses

Lauren J. Kreeger; Catherine J. Connelly; Preeti Mehta; Boris V. Zemelman; Nace L. Golding
The University of Texas at Austin

Neurons in the central nucleus of the inferior colliculus (ICC) exhibit diverse morphologies, electrophysiological properties, and projection targets. Two major anatomical classes of ICC neurons, disk-shaped and stellate, can be distinguished by the orientation of their dendritic branching relative to tonotopic lamina. Disk-shaped and stellate neurons have dendritic trees that are parallel and perpendicular to the lamina, respectively. The opposing orientation of the dendritic morphologies suggests that

disk-shaped and stellate neurons may play different roles in auditory processing. To understand whether the two anatomical classes of ICC neurons can be further subdivided, we targeted neurons with interdependent adeno-associated viruses (AAVs) and evaluated their anatomy, physiology, and neurochemical markers. This technique allowed us to target, then optogenetically activate distinct groups of excitatory and inhibitory neurons of both anatomical classes.

Interdependent AAVs were injected into the ICC of gerbils. Infected neurons were later visualized in an acute slice preparation for targeted whole-cell current clamp recordings in gerbils aged P35-50. Voltage responses to current steps were analyzed according to firing pattern, spike shape, and passive membrane properties. ChR2 was also expressed in neuron classes to find synaptic connections within the local ICC circuit or ascending targets. We also made in vivo extracellular recordings of neuron classes identified with viral-mediated ChR2 expression. The specificity of viral expression was verified using multiplexed in situ hybridization.

Using these viral vectors, we targeted and characterized subpopulations within both the disk-shaped and stellate anatomical classes for in vitro whole-cell current clamp recordings. The genetically-targeted subset of disk-shaped neurons have an adapting discharge pattern, while the genetically-targeted subset of stellate neurons have a sustained discharge pattern. Anatomical reconstructions of the two subgroups show axonal projections within the ICC and projections to the ventral division of the medial geniculate body (vMGB). Synaptic terminals in the vMGB from both groups are highly branched, consisting of both small boutons with en passant swellings, and medium to large axons with large complex endings. Preliminary in vivo recordings of disk-shaped neurons reveal V-shaped receptive fields and sustained discharge patterns.

Together our results suggest that while disk-shaped and stellate neurons have contrasting intrinsic firing features, they appear to have similar terminal morphologies and spatial domains in the ventral division of the medial geniculate nucleus. Ongoing experiments will continue to investigate potential interactions between these two ascending pathways in both the ICC and thalamus and assess their functional roles.

PS 336

Early Targeting of Lateral Cortex of the Inferior Colliculus Modular Fields by Descending Somatosensory Cortical Projections

Erin K. Kavusak; Jeremiah PC. Stinson; Isabel D. Lamb-Echegaray; Sean M. Gay; Mark L. Gabriele
James Madison University

ARO Abstracts

Background

The lateral cortex of the inferior colliculus (LCIC) receives various multimodal inputs including somatosensory afferents from the spinal trigeminal nuclei (Sp5), dorsal column nuclei, and somatosensory cortex, as well as auditory inputs originating from auditory cortex and the IC itself. During the postnatal period, the modular-extramodular LCIC arrangement emerges and can be visualized with a variety of neurochemical stains. Among these, glutamic acid decarboxylase (GAD) is a reliable marker of modular zones, while calretinin (CR) highlights surrounding extramodular domains. In the adult mouse, inputs of somatosensory origin specifically target LCIC modules. The current study focuses on the development and shaping of descending corticocollicular projections that arise in the ipsilateral somatosensory cortex and target developing LCIC modules.

Methods

Anterograde tract-tracing using biocytin in living slice preparations was performed in a developmental series (P0 to P20) of GAD67-GFP mice. Crystals were localized in layers 5 and 6 of somatosensory cortex prior to blocking the brain in such a manner that minimized slice thickness, while also preserving the corticocollicular pathway. Slices were then bubbled overnight at room temperature in artificial cerebrospinal fluid (95% O₂, 5% CO₂). Following postfixation and cryoprotection, sections were cut at 50 μm on a sliding freezing microtome. Streptavidin Dylight 549 (Vector Laboratories) was used for visualization of biocytin labeling and slides were coverslipped with Prolong Diamond. A Nikon C1si TE2000 microscope was used for all image capturing.

Results

Biocytin placements in somatosensory cortex labeled descending corticocollicular projections that reliably targeted the developing LCIC. Axonal terminal arborizations were robust ipsilaterally, ending in a series of patches along LCIC layer 2 that overlapped GAD-positive modules. Such projection patterns were evident during the early postnatal period, with discrete terminal distributions that aligned precisely with the developing neurochemical modularity. This early projection specificity became increasingly distinct with age, with highly refined adult-like modular terminal fields readily apparent by postnatal day 12.

Conclusions

The present study provides evidence that descending somatosensory inputs exhibit an early projection alignment with developing LCIC modular zones. Ongoing studies aim to determine the developmental mechanisms that influence the segregation of multimodal LCIC afferent-efferent streams into its modular-extramodular framework.

Microglial and CX3CL1 Patterning with Respect to the Developing Modular-Extramodular Framework in the Lateral Cortex of the Inferior Colliculus

Cooper A. Brett; Mark L. Gabriele
James Madison University

Background

Microglial cells (MGCs) are highly versatile and have been implicated in shaping discrete neural maps in a variety of systems. MGCs respond to numerous cues in their microenvironment, among them the neuronally-expressed chemokine, CX3CL1 (fractalkine). The present study examines MGC and CX3CL1 patterns with regard to the emerging modular-extramodular framework within the lateral cortex of the inferior colliculus (LCIC). A host of reliable modular markers, including acetylcholinesterase (AChE), cytochrome oxidase (CO), glutamic acid decarboxylase (GAD), and nicotinamide adenine dinucleotide phosphate-diaphorase (NADPH-d), together with an extramodular marker, calretinin (CR), enable visualization of modular-extramodular domains in the nascent mouse LCIC. Major multimodal afferent and efferent systems of the LCIC appear to interface with its neurochemically-defined patch-matrix-like organization. Here we utilize Iba-1 (a microglial marker) and CX3CL1 labeling to explore the potential involvement of MGCs and fractalkine signaling in establishing LCIC functional compartments.

Methods

A developmental series of postnatal C57BL/6J and GAD67-GFP mice were utilized. GABAergic neurons are specifically labeled in the GAD67-GFP knock-in line, thereby highlighting LCIC modular fields. Brains were sectioned at 50µm on a sliding freezing microtome prior to immunocytochemistry protocols for Iba-1 (1:1000, Wako Chemicals) and/or CX3CL1 (1:100, R&D Systems). Appropriate biotinylated secondary antibodies and streptavidin fluorescent conjugates were utilized to visualize the developing LCIC framework with respect to MGC and CX3CL1 expression. A Nikon C1si TE2000 microscope was used for all widefield and confocal image acquisition.

Results

GAD-positive LCIC modules emerge shortly after birth and further sharpen over the first two postnatal weeks. Iba-1 staining confirms MGCs are present in the LCIC and that their spatial organization and morphological appearance changes over the course of the period that the modular-extramodular framework is shaped. At the earliest postnatal stages, MGCs are present in the IC, albeit sparse and with no clear distribution or pattern.

By P8 and up to hearing onset (P12), MGCs are more prevalent in the LCIC, with most residing at modular-extramodular borders. Labeling for CX3CL1 is strong at P12 and clearly modular, in keeping with the notion of fractalkine signaling of resident MGCs.

Conclusion

The present study provides developmental data of MGC and CX3CL1 patterns with respect to neurochemically-defined LCIC modular-extramodular zones. Ongoing studies utilizing transgenic lines with compromised fractalkine signaling aim to determine the precise role of MGCs in synaptic pruning events and the shaping of multimodal LCIC compartments.

PS 338

Distribution and Projections of VIP-Expressing Cells in the Inferior Colliculus in Mice

Nichole L. Beebe¹; Ryan M Edelbrock¹; David Goyer²; Marina A. Silveira²; Michael T. Roberts²; Brett R. Schofield¹

¹Northeast Ohio Medical University; ²University of Michigan

A challenge to understanding the processing of sound in the inferior colliculus (IC) is that neuronal populations are heterogeneous, and markers that have been determined to be associated with a single subtype of neuron are few. Here, we investigated the expression of vasoactive intestinal polypeptide (VIP, a neuropeptide) in the IC, to determine whether VIP can be used as a marker for a specific subtype of IC neuron. As a first step, we examined the distribution of VIP+ neurons within the IC, and determined which of the IC output pathways VIP+ neurons participate in.

To examine the distribution of VIP+ neurons, we crossed VIP-Cre transgenic mice with Ai14 reporter mice, leading to expression of a red fluorescent protein in VIP-expressing neurons in the F1 offspring. Additionally, some of the F1 offspring of this cross received a unilateral, stereotaxic injection of an adeno-associated viral vector carrying a Cre-dependent green fluorescent protein gene. This allowed us to examine the projections of VIP+ neurons originating in the IC across the mouse brainstem and thalamus.

VIP+ cells are prominent in caudal parts of the IC, where they inhabit all three subdivisions (central nucleus, lateral and dorsal cortices), with the greatest number in IC dorsal cortex. VIP+ neurons are rare in the rostral IC, including the rostral pole and intercollicular tegmentum. In animals that had received AAV injections, VIP+ projections could be traced in several major projections

made by IC neurons. Labeled VIP+ boutons originating from the IC were found in the medial geniculate body, the nucleus of the brachium of the IC, the contralateral IC, the superior olivary complex, and within the ipsilateral IC. Labeled VIP+ boutons were also observed in non-auditory areas that are known to receive projections from the IC, including the superior colliculus and the periaqueductal gray.

The presence of VIP+ neurons in most of the major output pathways of the IC implicates them in a wide range of functions, from processing of ascending input to top-down modulation to orientation and defensive behaviors. In companion studies, we are characterizing the neurotransmitter phenotype and intrinsic physiological properties of these neurons to better understand the functional roles of this subtype of IC neuron.

PS 339

Cholinergic Projections to GABAergic and Glutamatergic Neurons in the Rostral Inferior Colliculus (IC) and Nucleus of the Brachium of the IC

William A. Noftz; Nichole L. Beebe; Brett R. Schofield
Kent State University; Northeast Ohio Medical University

Acetylcholine modulates sound processing in the inferior colliculus (IC). The majority of cholinergic inputs to the IC originate from the pedunculo-pontine tegmental nucleus (PPT), which projects bilaterally to the IC with an ipsilateral dominance. These cholinergic axons contact GABAergic and non-GABAergic neurons in the central nucleus, lateral cortex and dorsal cortex. More rostral subdivisions of the IC have different patterns of connections (compared to the caudal subdivisions) and serve different functions. The rostral pole receives inputs similar to central IC, but has more GABAergic cells and substantial projections to the superior colliculus. The intercollicular tegmentum is the main source of IC projections to pontine reticular formation. Finally, the nucleus of the brachium of the IC lies in the fiber bundle between the IC and the thalamus. This nucleus is multimodal and has projections to the thalamus, superior colliculus and the IC. Here, we ask whether the GABAergic and/or the glutamatergic cells that constitute the nucleus of the brachium of the IC and the rostral divisions of the IC receive direct input from cholinergic PPT axons. We injected an adeno-associated viral vector (rAAV/EF1a-DIO-EYFP or rAAV/EF1a-DIO-mCherry; UNC Vector Core) into transgenic rats (LE tg (ChAT-Cre) 5.1 Deis; RRRC) to label cholinergic PPT cells and their axons. Sections were stained with antibodies to glutamic acid decarboxylase (GAD) to label GABAergic

neurons and counterstained with antibodies to NeuN or a Nissl stain (Neurotrace).

All three auditory regions – nucleus of the brachium of the IC, intercollicular tegmentum and the rostral pole of the IC – received cholinergic inputs from the PPT. The cholinergic projections were bilateral with ipsilateral predominance. PPT contacts in the rostral pole and intercollicular tegmentum were present uniformly throughout the nuclei. Cholinergic contacts in the nucleus of the brachium of the IC were less uniform with a greater density of contacts in the medial portion. In all three regions, cholinergic PPT axons contacted GAD-negative (i.e., glutamatergic) neurons and, less often, GAD+ (i.e., GABAergic) neurons.

We conclude that cholinergic PPT axons contact neurons throughout the intercollicular tegmentum, rostral pole of the IC and the nucleus of the brachium of the IC. Cholinergic effects are likely mediated through synaptic contacts on both excitatory and inhibitory neurons. In combination with our earlier studies, the data suggest that cholinergic axons from the PPT likely modulate activity throughout the auditory midbrain, and thus affect many aspects of auditory perception and behavior.

PS 340

In vivo Characterization of an Identified Excitatory Cell Type in the Inferior Colliculus using Intersectional Viruses

Catherine J. Connelly; Lauren J. Kreeger; Boris V. Zemelman; Nace L. Golding
The University of Texas at Austin

The central nucleus of the inferior colliculus (ICC) mediates the convergence of numerous ascending and descending pathways, but our understanding of its function has been limited by the lack of correlation between intrinsic firing types, dendritic morphology, and in vivo receptive fields. To better delineate functional circuits within the ICC, we are using recombinant adeno-associated viruses (rAAVs) intersectionally to target unique populations of cells in the Mongolian gerbil.

We developed an rAAV that targets a population of cells that is both excitatory and expresses cholecystokinin (CCKE neurons). These cells represent ~30% of the excitatory neurons in the ICC. In patch-clamp recordings from slices of the ICC cut parallel to the isofrequency laminae, CCKE neurons exhibit only an adapting firing phenotype, and anatomical analyses have revealed that these neurons project both locally within the ICC, as well as to the ventral division of the medial geniculate nucleus.

To understand the auditory information conveyed by CCKE neurons *in vivo*, we performed single unit recordings in ketamine/xylazine-anesthetized gerbils (2 to 3 months old) two weeks after an injection of a ChR2-expressing CCKE-specific virus. During recordings, we identified CCKE neurons via their light-evoked spiking produced by a 473 nm laser coupled to an independent fiber optic. Identified CCKE neurons were then characterized *in vivo* via their receptive fields and temporal firing patterns in response to 4 Hz, 100 ms pure tone presentations. Recording sites were marked with a small lesion or tracer dye injection to confirm post hoc that recordings were both within the ICC and the rAAV injection site.

Preliminary data show that CCKE disc-shaped neurons consistently exhibit V-shaped receptive fields and fire sustained action potentials to best frequency stimulation, in contrast to the high diversity of these parameters in the general population of ICC neurons. This general population displays a variety of receptive field shapes including the classic I-, V- and O-shaped receptive fields, and we have noted both onset and sustained firing patterns to best frequency stimulation.

Taken together with data with *in vitro* and anatomical data, these *in vivo* results suggest that an intersectional viral approach can circumscribe a neuron population that shares intrinsic electrical properties, axon projection patterns, and *in vivo* function. Ongoing experiments seek to further classify whether or not this excitatory route to the thalamus carries specific types of auditory information.

PS 341

Puncta of neuronal nitric oxide synthase (nNOS) mediate NMDA-receptor signalling in the auditory midbrain

Bas MJ. Olthof¹; Sarah E. Gartside¹; Adrian Rees²

¹*Institute of Neuroscience, Newcastle University;*

²*Newcastle University*

Nitric oxide (NO) is a gaseous molecule synthesised in the brain by neuronal nitric oxide synthase (nNOS). Although the expression of nNOS in the inferior colliculus (IC) is well documented in neurons in the dorsal and lateral cortices of the IC (Coote & Rees, 2008), the functional relevance of NO in the IC *in vivo* remains elusive.

Using fluorescent immunohistochemistry against NMDA-R1, nNOS, sGC(α 2) and PSD95, and confocal imaging on 40 μ m coronal sections obtained from adult pigmented guinea pigs, transcardially perfused with

0.1M PBS followed by 4% PFA, we show that nNOS occurs in two distinct cellular distributions.

We confirm that a subset of neurons in the cortices of the IC, express nNOS throughout their cytoplasm, while in the central nucleus (ICc) such nNOS filled neurons are absent. However, we observe that, all neurons in the ICc do express nNOS in the form of discrete puncta at the cell membrane.

Our multi-labelling studies reveal that nNOS puncta form multi-protein complexes with NMDA receptors, soluble guanylyl cyclase (sGC), and PSD95. These complexes are found directly opposed to glutamatergic terminals indicative of synaptic function. Interestingly, these glutamatergic terminals express both vesicular glutamate transporter 1 and 2 denoting a specific source of brainstem inputs.

To investigate the functional role of these multi protein complexes in the ICc, we combined microdialysis with *in vivo* electrophysiological recordings of multiunit activity in the guinea pig ICc. Pigmented guinea pigs were anesthetized with urethane (1g/kg), fentanyl (0.3mg/kg) and midazolam (5mg/kg). Pure-tone sound stimuli were delivered using closed field presentation. Drugs targeting NO signalling were applied by reverse dialysis via a microdialysis probe inserted in the IC. Neurons across the frequency laminae of the central nucleus were recorded using a 32 channel single shank electrode inserted rostral to the dialysis probe.

We found that local application of NMDA enhances sound-driven activity in a concentration-dependent and reversible fashion. This response is abolished by blockade of nNOS with L methyl arginine or sGC with ODQ indicating that the NMDA effect is mediated solely via the NO and cGMP signalling pathway.

This discovery of a ubiquitous, but highly localised expression, of nNOS throughout the ICc and demonstration of the major influence of the NMDA activated NO pathway on sound-driven neuronal activity, imply a key role for NO signalling in auditory processing.

Acknowledgements

Supported by BBSRC Project Grant BH154379

References

Coote EJ & Rees A. (2008) *Neuroscience* 154, 218-225.

Auditory Pathways: Midbrain, Thalamus & Cortex

PS 342

Auditory Processing Deficits Correspond to Secondary Injuries along the Auditory Pathway Following Mild Blast Induced Trauma

Emily X. Han¹; Joseph Fernandez²; Riyi Shi²; Edward Bartlett³

¹*Purdue Institute for Integrative Neuroscience, Weldon School of Biomedical Engineering, Department of Biological Sciences;* ²*Purdue Institute for Integrative Neuroscience, Weldon School of Biomedical Engineering, Department of Basic Medical Sciences;* ³*Depts of Biology and Biomedical Engineering, Purdue University*

Background

Blast-induced hearing difficulties affect thousands of veterans and civilians each year. The long-term impact of blast exposure on the central auditory system (CAS) can last months, even years, without major external injury, and is hypothesized to contribute to many behavioral complaints associated with mild blast traumatic brain injury (bTBI). Our group has previously documented the short-term (two-weeks) and longer-term (one month) effects of acute blast and non-blast acoustic impulse trauma on click/tone pip and sinusoidally amplitude modulated (AM) carriers in adult rats. However, the mechanisms that underlie these long-term impairments are still poorly understood. Examining the acute time course and pattern of neurophysiological impairment (within the first two weeks), as well as the underlying molecular and anatomical post-injury environment, is therefore critical to understanding the mechanisms that lead to long-term CAS impairments.

Although initial mechanical injury likely plays a role in central auditory damage, many measures of auditory function, including thresholds and DPOAEs either recover or exhibit subclinical deficits. A secondary molecular mechanism of damage likely results in the chronic auditory deficits following mild bTBI. Oxidative stress, along with inflammation, have been suggested as key players in secondary molecular damage in other models of CNS injury, including other TBIs, and may underlie functional auditory deficits in mild bTBI as well.

Methods

Here, we recorded the changes in auditory brainstem response (ABR) and auditory evoked potential (AEP) response to amplitude modulation (AM) and speech-like stimuli (iterated rippled noise pitch contours) in blast-exposed and control rats over the course of two months. Single-Unit (SU) recordings in the Inferior Colliculus

are made on key time points (post-blast day 7 and 2-months) in comparison with unexposed young rats of the same strain. We stained the auditory brainstem, midbrain, and thalamus for tetramethylrhodamine (TMR) and used immunohistochemistry to label GAD67, and acrolein to test for axonal damage, changes in inhibition, and oxidative stress, respectively. Preliminary results suggest axonal damage in the trapezoid body, increased GAD67 in IC, and increased acrolein in IC 48 hours post-blast.

Conclusion

Our results suggest that a cascade of (axonal) membrane damage, oxidative stress, and excitatory/inhibitory imbalance contributes to blast-induced subcortical CAS impairments. Ultimately this research can inform improved diagnostic and therapeutic strategies for bTBI related deficits.

PS 343

Where are in the auditory system the most resistant discriminative abilities when removing of spectro-temporal acoustic details? A study from cochlear nucleus to primary auditory cortex using vocoded vocalizations.

Samira Souffi¹; Christian Lorenzi²; Jean-Marc Edeline¹; Chloé Huetz¹

¹*NeuroPSI UMR CNRS 9197;* ²*Laboratoire des systèmes perceptifs, Ecole Normale Supérieure (UMR 8248)*

For more than two decades (Shannon et al. 1995), it is known that human subjects can discriminate speech when removing the temporal fine structure (TFS) with vocoded stimuli. A vast literature describes the human perceptive abilities to identify speech as a function of the number of frequency bands used by the vocoder. Very few electrophysiological studies have determined to what extent auditory neurons can still discriminate communication sounds when processed via a vocoder. More importantly, it is unknown whether there is a level in the auditory system discriminative abilities are preserved. Here, we compare for the first time the abilities of neurons recorded from primary auditory cortex down to cochlear nucleus to discriminate between spectrally similar communication calls.

Four utterances of a guinea pig whistle (original stimuli) were processed by a tone vocoder using several levels of spectral resolution (38, 20 and 10 frequency bands). Original and vocoded vocalizations were presented while recording evoked responses in primary auditory cortex (AI, n=354), the ventral division of auditory thalamus

(MGv, n=262), the central nucleus of inferior colliculus (CNIC, n=386) and cochlear nucleus (CN, n=499). In all the auditory structures, robust evoked responses were observed at presentation of the original and vocoded stimuli. With the original vocalizations, the strength of evoked responses was stronger in subcortical structures than at the cortical level. There was also a higher trial-to-trial reliability of evoked discharges in subcortical structures (especially in CNIC and MGv) than at the cortical level. Discriminative performance was quantified by computing Mutual Information (MI) using a large range of temporal resolution. In all structures, there was a diversity of discriminative abilities, ranging from a perfect discrimination to almost no discrimination at all whatever the temporal resolution, but on average MI was significantly higher in subcortical structures (especially at the MGv level) than at the cortical level. As the spectral resolution was decreased (by reducing the number of frequency bands from 38 to 20 and 10) the MI values decreased in all structures. Despite these decreases, the hierarchy between structures observed in terms of MI values was preserved in all vocoding conditions: the subcortical neurons, especially in the MGv, were always better in discriminating vocoded stimuli than the cortical neurons. These data indicate that a robust discrimination between vocoded vocalizations is present at all levels of the auditory system and is prominent in MGv.

PS 344

A Feedforward Inhibitory Circuit that Limits EPSP Duration in the Inferior Colliculus of Mice

David Goyer¹; Marina A. Silveira¹; Alexander P. George¹; Nichole L. Beebe²; Brett R. Schofield²; Michael T. Roberts³
¹University of Michigan; ²Northeast Ohio Medical University; ³Kresge hearing research - University of Michigan

The central nucleus of the inferior colliculus (ICC) is the hub of the ascending auditory system. Numerous studies have shown that feedforward inhibition (FFI) critically shapes how ICC neurons respond to sounds and that the strength and spread of inhibition in the IC change following hearing loss or acoustic trauma. However, because we lack an understanding of the fundamental classes of neurons that make up the ICC, the circuits that give rise to FFI and how they are regulated remain largely unknown. To address this problem, we recently identified a novel class of glutamatergic principal neurons in the IC that are labeled in Vasoactive Intestinal Peptide (VIP)-IRES-Cre mice. VIP neurons in the ICC have a sustained firing pattern (182 out of n=199), their intrinsic physiology differs significantly from the general neuronal population in the IC, they have a stellate morphology, and 94% have spiny dendrites. Via axonal tract tracing studies, we found that VIP neurons project to auditory

thalamus and to some auditory brainstem nuclei. Using Channelrhodopsin assisted circuit mapping, we have found that VIP neurons receive input from the contralateral IC (n=12) and the contralateral DCN (n=6). Commissural inputs were either excitatory (EPSPs: 1.15 ± 0.28 mV, halfwidth: 12.9 ± 7.2 ms, risetime: 4.28 ± 1.18 ms, decay tau: 47.59 ± 54.62 ms) or inhibitory (IPSPs: -2.61 ± 0.65 mV, halfwidth: 36.44 ± 11.23 ms, risetime: 7.53 ± 1.16 ms, decay tau: 87.07 ± 64.92 ms). The NMDA receptor antagonist AP5 slightly reduced the halfwidth and decay time constant of EPSPs, revealing a small, yet significant NMDA receptor contribution. NBQX, an AMPA receptor blocker, completely abolished EPSPs. Commissural IPSPs were completely blocked by the GABAA receptor antagonist GABazine, consistent with studies showing that inhibitory neurons in the IC are GABAergic. EPSPs evoked by optical stimulation of DCN afferents were excitatory, surprisingly slow (2.39 ± 0.52 mV, halfwidth: 15.8 ± 9.8 ms, risetime: 2.22 ± 0.42 ms, decay tau: 18.1 ± 6.9 ms) and had no NMDA receptor contribution. In some cases, activation of DCN afferents also elicited feedforward inhibition (FFI), which limited EPSP duration. This FFI was TTX sensitive, confirming its disynaptic transmission. We are now working to identify how inputs from the DCN and contralateral IC combine with FFI to shape the output of VIP neurons.

PS 345

Subcortical Origins of the Frequency-following Response: Evidence from Two Case Studies

Travis White-Schwoch¹; Samira Anderson²; Jennifer Krizman¹; Trent Nicol¹; Nina Kraus¹

¹Northwestern University; ²Department of Hearing and Speech Sciences, University of Maryland; Neuroscience and Cognitive Science Program, University of Maryland

The auditory frequency-following response (FFR) reflects synchronized, phase-locked activity along the auditory pathway in response to sound. While historically this activity has been thought to be predominantly subcortical, recent evidence suggests an auditory cortex contribution as well. This finding has complicated the interpretation of studies using scalp-recorded FFRs as outcome measures.

To provide clarity to the origins of the scalp-recorded FFR we conducted a dual case study. Specifically, we conducted an electrophysiological test battery in two patients who provide rare opportunities to test multiple hypotheses about the origins of the FFR.

The first case, NR, is an adult male who developed bilateral auditory cortex lesions following chemotherapy

as a young adult. He is cortically deaf: he has inconsistent sound awareness, cannot discriminate between speech and non-speech sounds, and relies on written communication. Although NR could not complete an audiogram, OAEs were normal and click-ABRs were reliable (albeit slightly delayed). Neuroimaging confirmed bilateral auditory cortex lesions, as did absent auditory cortical evoked potentials (P1/N1). Despite his cortical lesions, NR had robust and highly replicable FFRs that were similar to normative data with respect to timing, amplitude, and morphology. The FFR to the fundamental frequency—which has been specifically attributed to auditory cortex—was also normal. We measured FFRs to multiple speech-like sounds and his responses faithfully reflected acoustic contrasts between stimuli. Thus, auditory cortex is not necessary to generate a scalp-recorded FFR.

The second case, IT, is an adult woman with auditory neuropathy—she has no auditory brainstem response despite a normal audiogram and OAEs. While she has excellent speech perception in quiet, she struggles significantly to understand speech in adverse listening conditions such as noise and accents. Neuroimaging studies and cortical potentials were normal, suggesting no cortical involvement in her difficulty with sound processing. Despite having robust and highly replicable cortical evoked potentials, IT has no FFR. Multiple stimuli and rates were attempted, but responses were dominated by cochlear microphonic. Thus, subcortical neural synchrony is necessary to generate an FFR.

This is not to gainsay potential cortical contributions to healthy patients'; FFRs, nor to undermine the strong, long-term influence of cortical processing on subcortical auditory function. Nevertheless, when considered in tandem, these case studies provide strong evidence that accurate and synchronous encoding of the auditory midbrain, but not auditory cortex, is necessary and sufficient to generate an FFR.

Supported by the Knowles Hearing Center.

PS 346

Impact of Hearing Impairment on Cognitive Function and Alzheimer's Disease

Munyoung Choi¹; Dami Kim²; Alphonse Umugire²; Manikandan Samidurai²; Jihoon Jo²; Sungsu Lee³; Hyong-Ho Cho¹

¹Hearing and Neurotology lab, Department of Otolaryngology-Head and Neck Surgery, Chonnam National University Hospital; ²Department of Biomedical Science, College of Medicine, Chonnam National University Graduate School, BK21 PLUS Center for Creative Biomedical Scientists at Chonnam National

University; ³Kresge Hearing Research Institute, Department of Otolaryngology - Head and Neck Surgery, Michigan Medicine

Introduction

Relationship of hearing loss (HL) with cognitive decline and Alzheimer's disease (AD) has been reported clinically. Animal models can enhance elucidating the underlying mechanism of their relationship. Herein, we tested the effect of HL on cognitive function by mouse models.

Methods

Several transgenic mice that over-expressed amyloid precursor protein and presenillin have been used as Alzheimer model (Tg2576, 5xFAD, 3xAD). To induce deafness, kanamycin (900mg/kg) and furosemide (200mg/kg) were administrated to 4 week mouse. Then, one day after injection, the tympanic membrane was removed. The combination of the injection and surgery resulted in profound HL. ABR and middle latency response (MLR) were checked to evaluate hearing level and auditory pathway. Behavioral tests conducted were as follows; novel object, Y-maze, radial water maze, elevated plus maze. Long term potentiation (LTP) was measured with brain slices to assess the synaptic plasticity. micro PET-CT was taken to evaluate the activity of the brain. Conductive HL (CHL) model was made by occluding the external auditory canal with silicone/fibrin glue.

Results

Novel object and Y-maze test showed decreased activities in AD mouse which were more lowered in HL group. Radial water maze revealed that HL group spent longer time to complete the task. In elevated plus maze, AD stayed more on the open arm, and HL group extended this time. These results revealed that HL aggravates cognitive impairment in an animal model. LTP was decreased in AD group compared to the wild type control. This LTP was more down-regulated in the HL group. Moreover, HL deteriorated LTP in the wild type mouse. We refined the method for MLR recording and the AD group demonstrated Na-Pa interlatency elongation and interamplitude decrement. Brain activity checked in 5xFAD by FDG PET-CT showed attenuated metabolism in the AD group, further accelerated by HL. CHL model also showed decreased LTP compared to the control group.

Conclusion

Cognitive impairment and AD were aggravated by HL. AD HL mouse models are useful for studying the effects of hearing on the progression of AD. Hearing preservation or recovery may reduce the severity of AD.

Support: This research was supported by Basic Science Research Program through the National Research Foundation of Korea (NRF-2016R1D1A1A02937094) and Chonnam National University Hospital Biomedical Research Institute Grant (CRI 18095–1).

PS 347

Stimulus Specific Adaptation to Simple and Complex Sounds in the Ascending Auditory System: Dense Recordings using Neuropixels Probes

Mor Harpaz¹; Maciej M Jankowski¹; Leila Khouri¹; Israel Nelken²

¹Edmond and Lily Safra Center for Brain Sciences, Hebrew University; ²Edmond and Lily Safra Center for Brain Sciences and Department of Neurobiology, Silberman Institute of Life Sciences, Hebrew University

Stimulus-specific adaptation (SSA) is the reduction in the responses of a neuron to a common sound (standard) which does not generalize to other, rare sounds (deviants). SSA has been demonstrated in multiple stations of the auditory pathway, including inferior colliculus (IC), medial geniculate body (MGB) and auditory cortex. The simplest model for SSA consists of activity-dependent Adaptation in multiple Narrow Frequency Channels that are integrated by the recorded neuron (ANFC). We test here one specific prediction of ANFC in IC, MGB and auditory cortex. We measured SSA to tone clouds - broad band stimuli designed to generate approximately the same level of adaptation in all frequency channels within a wide range of frequencies (1-64 kHz). Clearly, ANFC models predict no SSA in response to tone clouds. Using Neuropixels probes, we recorded responses in IC, MGB and auditory cortex of anesthetized rats to pure tones and to tone clouds. We recorded activity of 2076 units (104/2076 well-separated units) with significant auditory responses in IC of 5 rats, 2243 auditory units (282/2243 well-separated units) in MGB of 5 rats and 2078 units (185/2078 well-separated units) in the auditory cortex of 5 rats. SSA to pure tones was evident in all three stations. However, while SSA to tone clouds was strong in auditory cortex (5218/8383, 62.24%, cases with responses to deviant > responses to standard), in IC and MGB SSA to tone clouds was much weaker (MGB: 8727/17394, 50.17%; IC: 10444/20578, 50.75%). Thus, auditory cortex clearly violates the prediction of ANFC models. The extent to which the minor SSA to tone clouds in IC and MGB contributes to the large effects in auditory cortex remains to be determined.

PS 348

Restricted Tinnitus-related Changes of Neuronal Nicotinic Neurotransmission in Auditory Thalamus

Rui Cai¹; Lynne Ling¹; Donald M. Caspary²

¹Department of Pharmacology, Southern Illinois University School of Medicine; ²Department of Pharmacology and Department of Surgery, Division of Otolaryngology, Southern Illinois University School of Medicine

Background:

Neural nicotinic acetylcholine receptors (nAChRs) play a fundamental role in the attentional circuitry throughout the mammalian central nervous system. Auditory information projecting through auditory thalamus (medial geniculate body, MGB) is regulated, in part, by cholinergic projections from the pontomesencephalic tegmentum (PPTg). Tinnitus patients perform poorly on selective attention tasks seemingly having attentional resources partially coopted by their tinnitus. The MGB is known to show functional tinnitus-related changes and nAChRs are present on a subset of pre- and post-synaptic sites. However, how tinnitus impacts nAChRs mediated attention in auditory thalamus has not been examined. nAChRs in MGB may be involved in tinnitus pathology via altering the relative gain of ascending/descending acoustic signals.

Methods:

The present study used in vitro whole cell recordings from MGB neurons to compare post-synaptic responses to ACh in sound-exposed/tinnitus rats with control Long Evans rats. Sound-exposed animals were evaluated using a gap-prepulse inhibition behavioral test and given a tinnitus score (TIN); compared with unexposed age-matched controls (CON). Saturation receptor binding analysis was used to investigate nAChR number and affinity changes between groups.

Results:

In the presence of muscarinic receptor antagonist (atropine), exogenous application of ACh evoked dose-dependent post-synaptic currents were significantly larger in MGB neurons from CON rats than in neurons from TIN rats ($p < 0.01$). The ability of selective $\alpha 4\beta 2$ nAChR antagonist (DH β E) or DH β E together with mecamylamine (Mec) to inhibit ACh evoked post-synaptic currents showed no statistical differences between groups. Saturation analysis using [3H] epibatidine receptor binding showed no statistical differences between TIN and CON rats'; MGB.

Conclusions:

Results suggest that tinnitus-related changes in the

magnitude of post-synaptic nAChR responses to ACh were not explained by changes in receptor binding in MGB. In addition, the lack of differential blockade effects between selective and nonselective $\beta 2$ nAChR antagonists also does not directly support a tinnitus-related subunit change. Limited nAChR changes, not detected by our saturation binding assay, remains a possibility for the inconsistency between physiology and receptor binding. Other possibilities not tested including calcium homeostasis, tinnitus-related changes in sodium and/or potassium channel distribution and/or neuronal functional changes resulting in a diminished response to ACh in MGB of the tinnitus rats.

PS 349

Apoptosis-related Neurodegeneration in the Mouse Ascending Auditory Pathway after Repeated Noise Trauma

Moritz Gröschel; Sebastian Jansen; Tanyo Manchev; Felix Fröhlich; Ira Strübing; Arne Ernst; Dietmar Basta
Department of Otolaryngology at ukb, University of Berlin, Charité Medical School, Germany

Several studies have shown an impact on the peripheral and central auditory pathway either by acoustic deprivation or acoustic overstimulation. Our group has described a significant loss of cells in several structures of the ascending auditory pathway after a single noise trauma. Moreover, we were able to detect apoptotic cell death mechanisms after traumatizing single noise exposure, particularly in the auditory brainstem, which started immediately postexposure and lasted for several days. The present study describes neurodegeneration and cell death mechanisms after repeated noise trauma in the pre-damaged peripheral and central auditory system using histological and immunohistochemical techniques. Normal hearing mice (NMRI strain) were exposed twice to a broadband noise (5-20 kHz) at a sound pressure level of 115 dB for 3 hours, whereby the second exposure was applied one week after the initial trauma. After another 7 days, cell densities were measured in brain slices after hemalum eosin (HE) staining. Further, cell death mechanisms were visualized via TUNEL-staining (terminal deoxynucleotidyl transferase dUTP nick-end labelling). Data from our earlier studies have shown a strong decrease in cell densities as well as a significant increase of TUNEL-positive cells particularly in subcortical auditory structures and only to a lesser extent in cortical areas after a single noise trauma compared to normal hearing controls. In contrast, the present experiments indicate a much stronger impact on higher auditory brain structures in response to a second noise trauma compared to a single exposure, whereas the lower pathway seems to be less affected. Interestingly, only a slight additional shift in auditory

thresholds has been reported. Possibly, afferent inhibitory projections from hierarchically lower auditory areas protect higher structures from a direct acute noise impact during the first exposure. However, the effects after a second trauma could be due to a reduction of protective mechanisms as a result of pre-existing damage as well as deprivation-induced neurodegeneration. In conclusion, neurodegeneration in higher brain areas after repeated noise exposure might represent an anatomical correlate to several psychoacoustic symptoms (tinnitus, hyperacusis, reduced speech perception), which might remain unidentified during objective clinical measurements (e.g. ABR recordings). Despite the effects on higher central processing of complex sound features and accompanying hearing disorders, the observed pathophysiologies might also play a role during high power hearing aid supply in hearing loss patients.

The present work was supported by the Deutsche Forschungsgemeinschaft DFG (grant number: GR 3519/3-1).

Auditory Prosthesis II: Applications & Novel Technologies

PS 350

Optical transmission properties of tissues in the mid-infrared

Kyle Feliciano¹; Yingyue Xu¹; Xiaodong Tan¹; **Claus-Peter Richter**²

¹Northwestern University; ²Department of Otolaryngology; Department of Biomedical Engineering; Knowles Hearing Center; Northwestern University

Background: Pulsed optical radiation can be used to stimulate neural activity in vivo. Little data are available on the tissue optical properties at relevant wavelengths. Here, we have measured the effect that various tissues have on the transmitted beam width at wavelengths in the visible range, 453nm, 532nm, 680nm, and for selected wavelengths in the near infrared, 1375nm, 1465nm, 1550nm, 1850nm, and 1860nm. The bulk transmission and the angle of spread have been quantified for skin, fatty tissue, muscle and different types of bone.

Method: A 600 μ m core diameter optical fiber (Ocean Optics) was coupled to the light source. The distal tip of the optical fiber was mounted to a three dimensional-micromanipulator (MMW-203, Narishige) and oriented vertically above a large plastic Petri dish with a thin glass window. A razor blade was mounted to a second micromanipulator and was positioned below the dish, parallel to the glass window. The Petri dish

was placed above an energy sensor. For the visible light measurements, the sensor was a photodiode. For the mid-infrared wavelengths, the sensor was a J50LP-1A energy sensor (Coherent-Moletron). Mid-infrared diode laser modules were from SemiNex, Peabody, MA emitting at 1375nm, 1460nm, and at 1550nm. The diode laser modules were driven by a high power precision current source (LDX-32420, ILX Lightwave, Bozeman, MO). Diode lasers emitting at 1850nm and at 1860nm were from Lockheed Martin Aculight. The lasers were operated at 100 μ s and a pulse repetition rate of 10 Hz. Several tissue types were tested, including rat and pig skin, pig muscle, calcified and decalcified bone of the guinea pig bulla, and calcified bone of the chinchilla bulla. Human cochleae were received from Northwestern University Feinberg School of Medicine through the anatomical gift act.

Results: The results show that biological tissues, such as muscle, fat, skin, and bone, attenuate radiation to different degrees and also cause different degrees of spread to the incoming light. From these data, we see that the attenuation for the wavelength in the visible comes from broadening of the light beam, whereas in the infrared the attenuation of the incident light is mostly due to absorption by the tissue.

Funding: This work was supported by the NIH, R01-DC011855 and the Hugh Knowles Center at Northwestern University.

PS 351

Infrared neural stimulation at different wavelengths

Yingyue Xu¹; Mario Magnuson¹; Xiaodong Tan¹; Claus-Peter Richter²

¹Northwestern University; ²Department of Otolaryngology; Department of Biomedical Engineering; Knowles Hearing Center; Northwestern University

Background:

Infrared neural stimulation (INS) has been proposed for the next generation of cochlear implants (CIs). More restricted activation of spiral ganglion neuron (SGN) populations was shown with INS, suggesting a higher spatial selectivity and a larger number of independent channels are achievable. Infrared lasers at different wavelengths have different properties on laser-tissue interaction, such as the absorption rate and penetration depth. INS with wavelengths around 1860 nm has been commonly used in existing literature due to its penetration depth in water. Other wavelengths in the infrared range that share similar penetration depth are around the wavelength for communication, i.e., wavelengths ranging from 1260 to 1675 nm. The

technology is more mature for these wavelengths, yielding higher wall-plug efficiency. Thus, infrared laser with a wavelength between 1260 to 1675 nm might serve as a superior alternative compared with wavelength at 1860 nm. In this study, we have compared the efficiency for INS at four different wavelengths.

Method:

Compound action potentials (CAPs) were acquired in guinea pigs in response to both acoustic stimuli and INS with different wavelengths: 1860, 1550, 1460, 1375 nm. Cochlear function was determined by recording acoustically evoked CAPs before and after the cochleostomy surgery. A 200 μ m optical fiber was coupled to the four lasers respectively and was inserted into the cochleostomy for INS. The lasers were operated with a 100 μ s pulse width and 4 Hz repetition rate. The input radiant energy increased from 0 to ~100 μ J/pulse. The CAP amplitudes evoked by INS were recorded. CAP amplitudes were plotted versus the input radiation energies for all four lasers.

Results:

We compared the averaged CAP responses evoked by INS at the four wavelengths to examine the INS efficiency dependency on wavelengths. The data showed the INS at 1375 nm generated the largest CAPs among the four tested wavelengths. CAPs from the 1460 nm laser had the smallest amplitude. The responses from the 1550 nm laser and the 1860 nm laser had similar amplitudes.

Conclusion:

Our data showed that the efficiency of INS is the highest at 1375 nm compared with 1460, 1550, and 1860 nm. Future studies will focus on adopting this wavelength for the development of optical cochlear implant electrodes.

Acknowledgment:

Funded with federal funds from the NIDCD, R01 DC011855 and by the Hugh Knowles Center for Clinical and Basic Science in Hearing and its Disorders at Northwestern University.

PS 352

Design and Manufacture of Novel Partial Ossicular Prostheses

Brandon Kamrava¹; Jonathan Gerstenhaber²; Yah-el Har-el³; Pamela C. Roehm¹

¹Department of Otolaryngology, Temple University School of Medicine; ²Department of Bioengineering, Temple School of Engineering, Temple University; ³Department of Bioengineering, Temple University School of Engineering

Introduction: Although popular, partial ossicular replacement prostheses (PORPs) do not provide ideal long-term results for patients, with extrusion and displacement of the prosthesis cited as most common causes of poor hearing results. Our team has previously developed a 3-dimensional (#D) adjustable model of the incus in order to generate custom prostheses for patients who would normally require a PORP. Current 3D printing technology is inadequate to manufacture prostheses in a biocompatible material to scale required for this application. In this study, we have explored the use of silicon molding and casting using a 3D printed model with otologic bone cement to manufacture a custom PORP.

Methods: To verify the production methodology, three variations of the prosthesis were developed: one with normal anatomical proportions, and two with exaggerated morphologies. Using a 3D printer, each model variant was produced at scale in a plastic proprietary to the printer. From these prints, molds were created under centrifugation for removal of microscopic air bubbles. Molds were cast with OtoMimix® Bone Cement (Olympus America, Center Valley, PA) to produce hydroxyapatite prostheses. Manufactured prostheses were then assessed for mass and morphological measurements. Additionally, the maximal force for breakage of the incus long process was recorded. Four incuses were extracted from cadaveric temporal bones and were similarly assessed to provide control data regarding maximal force for breakage.

Results: Four prostheses of each variant were produced through casting, providing a total of 12 manufactured prostheses (Figure 1). Morphological measurements on average differed by 0.037% (S.D. 2.70%). The average mass of all manufactured prostheses was 26.67mg (S.D. 5.85mg). The average force for breakage was 0.54N (0.16N). For comparison, the mass of cadaveric incuses on average was 30.71 mg and average force of breakage was greater than 4.85 N.

Conclusions: From the results, our team has concluded that the novel manufacturing methods we have developed allow for the accurate morphological production of middle ear prostheses. OtoMimix® bone cement was used for this testing due to its qualities of setting very rapidly with minimal processing requirements. Ultimately, the durability of manufactured prostheses may require adjustment to increase the strength of breakage of the casted prostheses. Additional studies into the integration of collagen or other materials into the prosthesis may increase the force required to break the casted prostheses.

Figure 1. Novel PORPs were generated from 3D printed models, molded in silicon, and casted using OtoMimix® cement. Left panel displays the normal model while the middle and right panel display the two variants. Ruler, mm.



PS 353

Estimation of the Hearing Ability by the Novel Hearing Device Accompanying Fine Electrical Current on the Skin

Ichiro Furuta¹; Hideaki Ogita²; Fukuichiro Iguchi³; Takayuki Okano⁴; Kohei Yamahara⁵; Tatsuya Namatsu⁶; Shinsuke Shichi⁶; Kazuya Nakatera⁶; Yoshihiro Iwasaki⁶; Shuichi Kawata⁶; Koichi Omori¹; Norio Yamamoto¹

¹Department of Otolaryngology-Head and Neck Surgery, Graduate School of Medicine, Kyoto University; ²Shiga Medical Center Research Institute;

³Department of Otolaryngology-Head and Neck Surgery, Graduate School of Medicine, Kyoto University; ⁴Department of Otolaryngology-Head and Neck surgery, Graduate School of Medicine, Kyoto University; ⁵Dep. Otolaryngology, Head and Neck Surgery, Shizuoka City Shizuoka Hospital; ⁶Murata Manufacturing Co., Ltd.

Recently, many kinds of hearing prostheses have been developed. However, a conventional bone conduction hearing aid is still widely used for the treatment of conductive hearing loss including the atresia of the external auditory canal. Although conventional bone conduction hearing aids are a very effective method to support the hearing ability of patients with conductive hearing impairment, they require the hard contact of the transducer against the head skin, resulting in the erosion of the skin and causing pain on the head.

To overcome this weak point of conventional bone conduction hearing aids, we have been developing a novel hearing prosthesis that utilizes a special piezoelectric diaphragm. Piezoelectric diaphragms are usually composed of one piezoelectric material and two electrodes that add voltage to the piezoelectric materials to vibrate. Our special piezoelectric diaphragm has only one electrode and the other electrode

attaches to the skin, causing sound perceived with a human ear. To transmit the sound to the materials attached to the piezoelectric materials, acoustic boundary layers are basically required. However, our new piezoelectric diaphragm may transmit sound to its attached target material without them. Moreover, and most intriguingly, hard contact to the target is unnecessary for the new piezoelectric diaphragm.

To evaluate the volume and transmission mode (whether it is bone or air conduction) of the sound caused by our special piezoelectric diaphragm, animal models are necessary. The most popular method to evaluate the hearing in animals is auditory brainstem response (ABR) that records the electrical activity using electrodes attached to the skin.

We tried to record ABR response from guinea pigs that hear sound delivered from the novel piezoelectric diaphragm. However, the big noise was observed by the micro-current in the skin related to the electrode of the novel piezoelectric diaphragm and the detection of the signal turned out to be impossible. Thus, ABR is not suitable to evaluate the ability of our novel piezoelectric diaphragm as a hearing prosthesis. As a next step, we used compound action potential (CAP) that records the electrical activity of the cochlear nerve using electrodes located near the cochlea and subcutaneous layer of the head. In CAP, the signal was much larger than the noise caused by electrodes of the novel piezoelectric diaphragm.

In this study, we found that CAP is useful to evaluate the sound signal delivered from the hearing prosthesis accompanying fine electrical current through the skin.

PS 354

Evaluating the Effect of Implanting an Artificial Auditory Epithelium in the Guinea Pig Cochlea

Hideaki Ogita¹; Koji Nishimura²; Takayuki Nakagawa²; Juichi Ito¹; Tetsuro Tsuji³; Satoyuki Kawano³; Hidetoshi Kotera⁴; Takeshi Nizuka⁵; Masanori Enrin⁵

¹Shiga Medical Center Research Institute; ²Department of Otolaryngology-Head and Neck Surgery, Graduate School of Medicine, Kyoto University; ³Graduate School of Engineering Science, Osaka University; ⁴Institute of Physical and Chemical Research (RIKEN); ⁵Kyocera Corporation

Hearing impairment is the most frequent sensory deficit in human populations, affecting more than 250 million people in the world. In profound hearing loss and deafness, current treatment is based on cochlear implant placement. We are developing a new hearing prosthesis which mimics auditory epithelium, which we called 'an artificial auditory epithelium'. This device consists of a 40-micrometer-thick piezoelectric material fixed in a

trapezoid-shape. This device can be implanted in the inner ear. We previously showed that this device can imitate the function of the cochlear sensory epithelia and transform vibrations into electric signals with frequency characteristics. We also showed that the electrical potentials generated by this device in response to sound stimuli can induce auditory brain stem responses (ABRs) in deafened guinea pigs, indicating its capacity to mimic basilar membrane function.

In the present study, we evaluated the degree of surgical trauma after insertion of the device into the cochlea and evaluated its potential for recovery of hearing. Male Hartley guinea pigs were partially deafened by subcutaneous injection of kanamycin (100 - 150 mg/kg) followed by intravenous injection of furosemide (100 mg/kg). One week after the deafening, the device was implanted into the scala tympani of the basal cochlea. To minimize the surgical invasion, we developed the implantation procedure using a robot. The robot consists of UR3 robot arm and a homemade manipulator which holds tweezers. ABRs were measured every week after implantation for five weeks. After ABRs were measured, animals were sacrificed and histological investigation was proceeded. We will show the potential of the artificial auditory epithelium for the treatment of hearing impaired patients.

PS 355

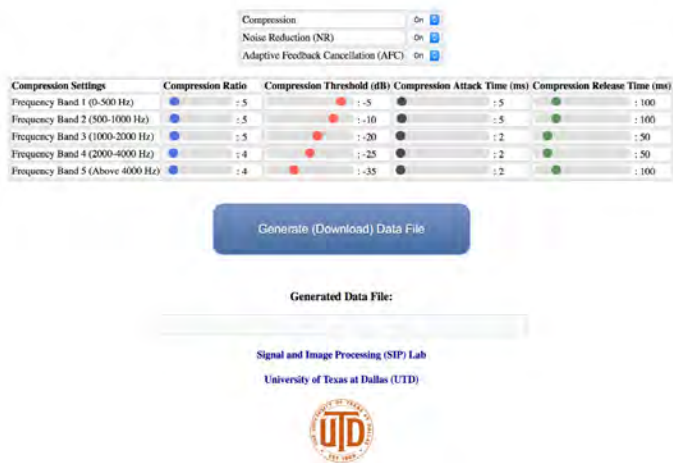
Making Hearing Aid Open Source Platforms Easy-to-use for Clinical Studies

Nasser Kehtarnavaz; Nasim Alamdari
University of Texas at Dallas

The lack of an open-source, programmable, and portable platform has hindered the deployment of existing or new hearing improvement signal processing algorithms in the field to be conducted seamlessly with ease for clinical studies. The NIH-NIDCD has taken steps towards the development of such open platforms by offering and guiding the Open Design Tools for Speech Signal Processing funding opportunity. A major concern associated with the open platforms that are being developed is that specialized information technology (IT) skill set is required in order to easily use these platforms in clinical environments. Most audiologists and hearing science researchers do not possess the IT skill set for dealing with the steps that need to be taken in order to run signal processing algorithms on the embedded processors of these open platforms. In this presentation, it is shown how to make such hearing aid open platforms easily usable by audiologists and hearing science researchers without requiring them to have any engineering or programming knowledge of these platforms. The solution to be presented involves

the development of an easy-to-use interactive website accessible from any device capable of running an internet browser. Such an approach allows decoupling the technical know-how that goes into running signal processing codes on the hearing aid open platforms from clinical utilization of these platforms, thus enabling non-IT users to easily use them without requiring the engineering background needed for their utilization. A demo of the solution proposed will be shown indicating how such platforms can be used with ease without knowing the software tools and the IT knowledge that go into using them.

Web-based Fitting of Hearing Aid Open Source Platforms



PS 356

Multiscale Modelling Approaches and Advanced Manufacturing Techniques for a New Generation of Biocompatible Middle Ear Prostheses

Mario Milazzo¹; Serena Danti²; Markus J. Buehler¹; Cesare Stefanini³

¹Massachusetts Institute of Technology; ²University of Pisa; ³The BioRobotics Institute

Conductive hearing loss, due to traumas or pathologies of the middle ear structure, affects more than 5% of the population worldwide and more than 15% of the elderly. Current middle ear prostheses, needed to restore the mechanical sound transmission after surgery for pathologies or traumas, are based on synthetic or biological materials, such as titanium and hydroxyapatite (HA) or homo/allografts, for their better biocompatibility in this anatomic setting. Although the good success of these state-of-the-art prostheses, some disadvantages still occur (e.g. significant rate of extrusion in the mid/long term of titanium prostheses and sub-optimal acoustic behavior especially for the highest frequencies). This work provided a new methodology to overcome

these issues by exploiting a synergic approach involving both multiscale modeling and advanced manufacturing techniques, aimed at designing and producing a new generation of biocompatible middle ear micro-prostheses made of Collagen Type I (COL1) and HA. This biocomposite, selected for the purpose of the work, owns the two main components of the bone tissue, thus gathering the compliance of the natural polymer with the stiffness of the ceramic. Moreover, this approach does not suffer from any transplanted tissue issues (Figure 1A). In this study, a multiscale modeling approach is used to study the mechanical behavior of the composite from the atomistic to macro-scale point of view, namely, modelling COL1 with different percentages of mineralized HA in order to understand the roles of both the components in transmitting pressure waves (e.g. acoustic impedance, energy loss) (Figure 1B). Based on the results achieved by simulations, a bioinspired optimization of the topology of the micro-prostheses is carried out to improve the acoustic behavior of the prostheses with respect to the commercially available devices (Figure 1C). Advanced manufacturing technologies have been finely reviewed in order to select the best solution to 3D print the acoustic prostheses with the requested precision. Micro-extrusion 3D printing, based on a high-pressurized pneumatic nozzle, is currently the technology which, better than other available techniques, can cope with high-viscous biomaterials and might represent the best approach for the fabrication of a new generation of oto-compatible prostheses through a continuous material slurry (Figure 1D). This project has received funding from the European Union's Horizon 2020 research and innovation programme under the Marie Skłodowska-Curie grant agreement COLLHEAR No 794614.

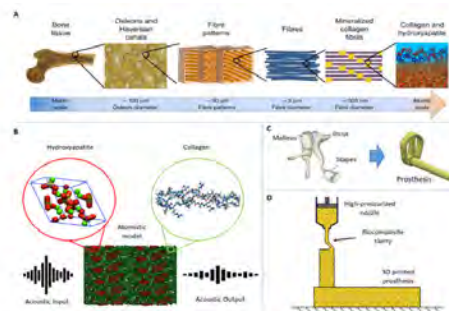


Figure 1. A. Bone structure and model development taken from Arun et al., 2012. B. Atomistic model to evaluate the acoustic properties of the Collagen Type I – Hydroxyapatite. Modified from Arun et al., 2012. C. Bioinspired optimized design of a middle ear prosthesis. D. Manufacturing of the middle ear prosthesis via micro-extrusion 3D printing technique.

Modelling Piezoelectric Electrospun Fiber Meshes for Cochlear Implants

Mario Milazzo¹; Luca Sagresti²; Stefano Berrettini³; Zhao Qin¹; Serena Danti²; Markus J. Buehler¹

¹Massachusetts Institute of Technology; ²University of Pisa; ³Dept. Of Surgical, Medical, Molecular Pathology and Emergency Medicine

Sensorineural hearing loss is due to damaged or dead sensory cells inside the organ of Corti in the cochlea, which is devoted to transduction of the acoustic into electric signals and the former transmitted by the middle ear, thus enabling cochlear spiral ganglion neuron depolarization. Recent experimental studies have demonstrated that polymer-based piezoelectric films could play a key role in restoring the impaired sensory functionalities by exploiting the tonotopy of the basilar membrane. However, the results achieved so far have demonstrated only the proof of principle, but they have been not fully satisfying, due to a lack of sensitivity in the order of 10⁴. Modeling the electro-mechanical behavior of piezoelectric biomaterials within the cochlea could be the key to demonstrate the effective feasibility of this approach. Ultrafine fiber meshes obtained via electrospinning were selected for this study as they provide nanostructured features potentially suitable for neuronal interaction.

This study described a mesoscale model of different meshes of electrospun fibers, performed through a combination of softwares (i.e. MATLAB and LAMMPS), able to investigate the mechanical behavior of the piezoelectric material stressed by uniaxial loading strain focusing also on how crosslinking can affect the results.

Starting from the behavior of a single fiber, two different baseline models were analyzed: array of horizontal non-cross-linked fibers and random fibers. In the first model, the sensitivity analysis was carried out by increasing progressively the number of transverse fibers cross-linked to the basic array whilst, whereas in the second, different percentages of crosslinks were analyzed (Figure 1). Therefore, the outcomes were used to develop an analytical model to study the electrical behavior of the material through the equivalent circuits associated to the samples. By assuming in first instance each fiber as serial multiple batteries, the main challenge was the modeling of the cross-links: by considering neglectable the inductive effect, as widely demonstrated in literature, the resistance and capacitance effects were taken into account by modeling each couple of fibers as two conductors that share charge and mechanical contact (Figure 2).

Further steps will consider not only a specific

orientation degree of the electrospun fibers, obtainable during manufacturing, but also an integrated coarse-grained model of the piezoelectric fiber meshes including both mechanical and electrical effects. MIT-UNIFI project NANO-SPARKS (MISTI funds) 2017 is gratefully acknowledged.

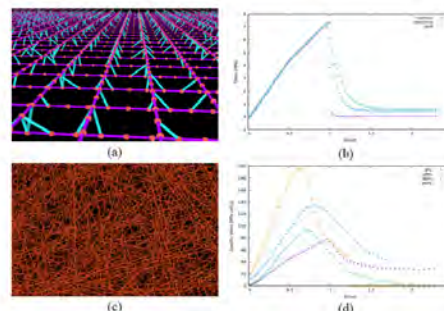


Figure 1. Meso-scale model of piezoelectric fiber meshes. (a) grid of ordered cross-linked fibers. (b) Mechanics of the horizontally aligned fibers with/without crosslinks with other ordered fibers. (c) random cross-linked fibers. (d) Sensitivity analysis on the effect of crosslinking on a random fiber mesh.

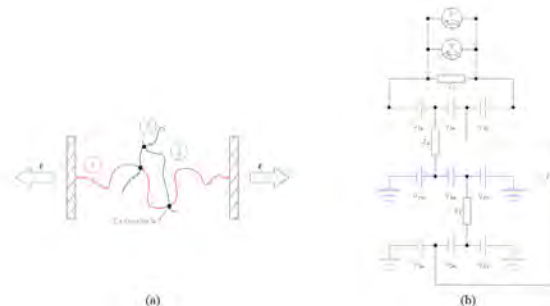


Figure 2. Analytical model for estimating the electrical behavior of a mesh composed of three cross-linked fibers under uniaxial strain loading. (a) Sample model. (b) Equivalent electrical circuit.

PS 358

Ultra Hearing: Effects of Body-Coupled Amplitude-Modulated Ultrasound Stimulation for a New Hearing Technology

Gerardo Rodriguez¹; John Basile¹; Hongsun Guo¹; Cory Gloeckner¹; Hubert Lim²

¹University of Minnesota- Twin Cities; ²University of Minnesota, and Neuromod Devices Limited

Background: Recently, our lab has shown that ultrasound applied to the head activates the auditory system likely via vibration of cerebrospinal and cochlear fluids (Guo et al., Neuron, 2018). This discovery of transcranial ultrasound activation of the peripheral auditory pathway opens up the possibility for a new type of hearing technology, which can bypass damaged outer and middle ear regions and can avoid acoustic feedback issues. We are investigating the neural selectivity of ultrasound activation of the auditory system via amplitude-modulated ultrasound

pulses. We are also investigating the safety of different ultrasound parameters that are relevant for hearing applications.

Materials and Methods: We positioned electrode arrays in the central nucleus of the inferior colliculus (ICC) of ketamine-anesthetized guinea pigs. We collected frequency response maps (1-40 kHz, 10-400 kPa) in response to amplitude-modulated ultrasound (carrier: 220 kHz) pulses presented on the skull and exposed brain, coupled with degassed agarose. The transducer was also decoupled from the animal to confirm there were no air-conducted sound effects. To investigate safety and functional stability of stimulation, thresholds and best frequencies per electrode site were assessed over time. Additionally, we presented ultrasound to isoflurane-anesthetized guinea pigs for 5 hours each day over a period of 5 days with different pressures (100-800kPa), duty cycles (5-80%), and sonication durations (.05-9.6 s) in continuous mode. We then performed histological analysis to characterize any brain tissue damage.

Results: Initial results demonstrate that the auditory midbrain can be selectively activated in a tonotopic pattern with different modulation frequencies, and higher stimulation intensities elicit broader activation across ICC. Increased pressures also lead to increased neural activity as occurs with acoustic stimulation. Threshold shifts have been noted with some parameters involving longer stimulation durations but need further investigation. Histological analysis of the brain suggests that the tested ultrasound parameters are safe.

Conclusions: Ultrasound applied to the head appears to achieve safe and frequency-specific activation of the auditory system at very low ultrasound intensity levels. Future studies will evaluate if complex sound signals such as speech can be sufficiently transmitted to the cochlea and auditory system with ultrasound and if there are optimal locations on the head for an ultrasound-based hearing device. Further experiments also need to be performed to characterize the safety limits of ultrasound pressure, duty cycle, and duration interactions.

Funding: This work was supported by the NSF, NIH, and Institute for Engineering in Medicine at University of Minnesota.

PS 359

Cochlear Implantation in Postlingually Deaf Adults is Time-sensitive Towards Positive Outcome: Prediction using Advanced Machine Learning

Techniques

Min Young Kwak; Hong Ju Park
Seoul Asan Medical Center;

Given our aging society and the prevalence of age-related hearing loss that often develops during adulthood, hearing loss is a common public health issue affecting almost all older adults. Moderate-to-moderately severe hearing loss can usually be corrected with hearing aids; however, severe-to-profound hearing loss often requires a cochlear implant (CI). However, post-operative CI results vary, and the performance of the previous prediction models is limited, indicating that a new approach is needed. For postlingually deaf adults (n=120) who received CI with full insert, we predicted CI outcomes using a Random-Forest Regression (RFR) model and investigated the effect of preoperative factors on CI outcomes. Postoperative word recognition scores (WRS) served as the dependent variable to predict. Predictors included duration of deafness (DoD), age at CI operation (ageCI), duration of hearing-aid use (DoHA), preoperative hearing threshold and sentence recognition score. Prediction accuracy was evaluated using mean absolute error (MAE) and Pearson's correlation coefficient r between the true WRS and predicted WRS. The fitting using a linear model resulted in prediction of WRS with $r=0.7$ and $MAE=15.6\pm 9$. RFR outperformed the linear model ($r=0.96$, $MAE=6.1\pm 4.7$, $pr=0.91$, $MAE=9.6\pm 5.2$). The contribution of DoD to prediction was the highest (MAE increase when omitted: 14.8), followed by ageCI (8.9) and DoHA (7.5). After CI, patients with DoD Machine learning demonstrated a robust prediction performance for CI outcomes in postlingually deaf adults across different institutes, providing a reference value for counseling patients considering CI. Health care providers should be aware that the patients with severe-to-profound hearing loss who cannot have benefit from hearing aids need to proceed with CI as soon as possible and should continue using hearing aids until after CI operation.

PS 360

Audiologic outcome of middle ear implant in young adults with sensorineural hearing loss

Jeong-Hoon Oh; K-Hong Chang; Su Bin Kim
St. Paul's Hospital, The Catholic University of Korea

Objectives: The aim of this study was to assess the surgical and audiological outcome of the middle ear implant Vibrant Soundbridge (VSB) in the patients younger than 40 years old with moderate sensorineural hearing.

Method: A retrospective, case-series study (n=3) was performed. The mean age at implantation was 32 years (min. = 19, max. = 39). Audiological outcome and speech intelligibility were assessed before and after the Incus short process vibroplasty.

Results: Bone conduction (BC) thresholds were preserved after the implantation and a functional gain of 20-30 dB was achieved in all frequencies including 250 and 500 Hz. All patients reported better sound quality and more natural voice perception.

Conclusion: The authors report that the residual hearing of the young patients with sensorineural hearing loss can be preserved with incus short process vibroplasty with remarkable functional gain.

Auditory Prostheses III: Animal Models, Trauma & Survival

PS 361

Cochlear Lesions targeting Primary Afferents or Spiral Ganglion Neurons Differentially Affect Electric Responses

Peter Baumhoff¹; Wiebke S. Konerding²; Julie G. Arenberg³; Andrej Kral⁴

¹ Department of Experimental Otolology, Hannover Medical School; ²1 Department of Experimental Otolology, Hannover Medical School, 2 Cluster of Excellence 'Hearing for All', DFG Exc. 1077; ³3 Department of Speech & Hearing Sciences, University of Washington Seattle, 4 Massachusetts Eye and Ear Infirmary, Harvard Medical School; ⁴Institute of AudioNeuroTechnology & Dept. of Experimental Otolology, ENT Clinics, Hannover Medical University, Germany

The exact place of spike initiation with electric stimulation using cochlear implants (CI) has not been clarified yet. This information might explain a part of the outcome variance with CIs and the impact of patchy degenerative processes on evoked activation patterns. Here we investigate how focal, micro-lesions targeting either primary afferents or spiral ganglion neuron cell bodies (SGNs) within Rosenthal's canal differently affect the response properties to electrical stimulation.

The experiments were performed in normal hearing Dunkin-Hartley guinea pigs (N=7; cochleae N=12). We used a micro-electrode to lesion either primary afferents or SGN in the basal cochlear turn. The penetration was performed under visual control through a surgical microscope. The cochleotopic position of the lesion was identified by audiograms measured with the compound action potential (CAP). After lesioning, the cochleae

were pharmacologically deafened by an intra scalar perfusion with Neomycin-sulfate solution. The deafened cochleae were electrically stimulated through custom 6-contact CIs (MedEl, Innsbruck) and electrically-evoked CAPs and auditory brainstem responses (eABRs) were recorded. The lesions were histologically identified via μ CT imaging (N=8) and 3D autofluorescence confocal microscopy of optically cleared cochleae (N=6).

So far, 5 cases were identified as primarily lesions of SGNs and 4 mainly along the primary afferents. The micro-lesions resulted in focal CAP threshold shifts for frequencies above 8 kHz. The damage was heterogeneous among cases and dependent on the exact lesion site as well as on the extent of the lesion. In general, lesions of SGNs led to more pronounced damage than lesions along the primary afferents. Electric stimulation in bipolar configuration led to eCAP threshold elevations for stimulations close to the SGN lesion site as compared to more apical stimulation. Lesions of the peripheral afferents led to a reduction in eCAP dynamic range for stimulation sites apical to the lesion. No significant difference was observed between eCAP thresholds elicited by cathodic- and anodic-leading stimulation.

We established a method for focal micro-lesioning, targeting primary afferents or SGNs in the guinea pig cochlea. Results reveal distinct changes in electrical excitability depending on the lesion site. This approach will allow us to further study spike initiation during electric stimulation.

This project was supported by the DFG within the Cluster of Excellence "Hearing4All" (DFG Exc. 1077) and MedEl Company (Innsbruck).

PS 362

The Threshold of Electrophonic Response Correlates with Residual Hearing

Mika Sato¹; Peter Baumhoff²; Jochen Tillein³; Andrej Kral¹

¹Institute of AudioNeuroTechnology & Dept. of Experimental Otolology, ENT Clinics, Hannover Medical University; ²1 Department of Experimental Otolology, Hannover Medical School; ³MED-EL Germany GmbH

Electrophonic response (EP) in cochlear implant (CI) stimulation is mediated by hair-cells. Its threshold is lowest at the dominant frequency component of the time function of the electrical stimulus (Sato et al., 2016, J Neurosci). The response to direct neural stimulation (electroneural response, EN) is strongest at the cochlear location of the active electrode.

We investigated whether also at the dominant EN position hair cells are electrically activated. Normal hearing guinea pigs were implanted with a CI through a cochleostomy, keeping most of the hearing intact. A Neuronexus double-shank 32-channel electrode array was stereotactically placed within the inferior colliculus parallel to the tonotopic axis. The electrical stimuli were single, charge-balanced biphasic electric pulses (100µs/phase). Threshold, firing rate and onset latency were computed from local field potential and multiunit activity in the midbrain. The cochlea was subsequently deafened with CI left in place and the stimulation was repeated.

The thresholds for multiunit activity to electrical stimulation through CI were compared at the characteristic frequency (CF) of dominant EP (near 5 kHz) and at the CF of dominant EN (near 9.5 kHz) before and after deafening. The threshold of EP (threshold before deafening, mean 45.2±2.6 dB att.re 10 mA pp) was significantly lower than the threshold of EN (threshold after deafening, 30.5±5.1 dB). Differences of the electric threshold before and after deafening within the same channels (CF~5kHz or ~9kHz) were computed and this difference correlated the acoustic threshold of the corresponding channels recorded before the electrical stimulation (i.e. post-implantation) ($r=-0.63$, $p<0.05$ [JT1]).

The mean onset latency at the threshold before deafening (at the threshold EP) at the CF~5kHz was 6.6±1.5 ms and at the CF~9.5kHz was 5.8±1.5 ms. These are significantly longer than latencies at the threshold after deafening (at the threshold EN) (5.2±0.4 ms at CF~5kHz and 4.6±0.6 ms at CF~9.5kHz). At the current levels higher than the threshold EN, the difference in responses to the same current level between hearing and deafened conditions was indiscernible both in the onset latency and in maximal firing rate. This similarity in responses suggests that EN dominates at high stimulation levels in hearing condition.

The correlation of the electrical threshold differences (hearing vs. deafened condition) with the acoustic threshold of post-implantation suggests that the amount of residual hearing at the corresponding frequency is one factor that determines a characteristic of electrophonic response.

Supported by Deutsche Forschungsgemeinschaft (Exc 1077)

PS 363

Relationship of Intrascalar Neoplastic Tissue Density and Nerve Survival to Cochlear Implant Function

Donald L. Swiderski; Aaron P. Hughes; Deborah J. Colesa; Kara C. Schwartz-Leyzac; Yehoash Raphael; Bryan E. Pflugst
Kresge Hearing Research Institute, Department of Otolaryngology-Head and Neck Surgery, University of Michigan

Among guinea pigs with cochlear implants (CIs), roughly 50% of the variance in several measures of implant function can be explained by variance in spiral ganglion neuron (SGN) survival, raising the possibility that other factors are also important. Neoplastic tissue is often seen in scala tympani after CI insertion in humans and animals, varying from loose connective tissue to bone. We investigated the relationship between it and measures of implant function, examining 47 guinea pigs with variation in SGN densities produced by implanting CIs in hearing ears, ears deafened with neomycin, or neomycin-deafened ears treated with neurotrophin. Measures of implant function were obtained over a period averaging nine months, then animals were euthanized and assessed histologically. Psychophysical measures included thresholds for single pulses, 200 msec trains of short-phase-duration pulses (25 microsec/phase) and 100 Hz sinusoids, and multipulse integration (MPI) functions. Electrophysiological measures included electrically-evoked compound action potential amplitude growth functions and the effect of interphase gap (IPG) duration on those functions. Density of healthy-appearing SGNs (cells/mm²) was evaluated near the stimulating electrode and at 180° and 360° more apically. Neoplastic tissue between implant and modiolus was scored as low density (LD) or high density (HD - cartilage or bone present). Mean SGN density was lower in the HD group. SGN density and neoplastic tissue score were correlated with treatment. Procedures enhancing SGN survival were associated with less neoplastic tissue, especially less HD tissue. When all animals were analyzed as a single group, all functional measures except single pulse thresholds were correlated with SGN density. Thresholds for trains of 25 microsec/phase pulses were negatively correlated with SGN density but thresholds for 100 Hz sinusoids were positively correlated. When LD and HD groups were separated, MPI slope and detection thresholds for the trains of short-phase-duration pulses were correlated with SGN density only in the LD group. Correlations of other measures with SGN density did not differ significantly between the tissue density groups. In the HD group, MPI slope and detection thresholds for trains of short-phase-duration pulses varied little across subjects and were not correlated with variation in SGN

density. In the LD group, there was more across-subject variation in those measures, and although correlations with SGN density were significant, much of that variation was independent of SGN density, raising the possibility that properties of the fibrous neoplastic tissue influence CI function.

Supported by NIH/NIDCD R01DC015809 and P30 DC005188.

PS 364

Chronic Intracochlear Electrical Stimulation at High Charge Densities Results in Pt Dissolution but not Neural Loss in vivo

Robert Shepherd¹; Paul Carter²; Ya Lang Enke²; Andrew Wise³; **James Fallon**¹

¹Bionics Institute; ²Cochlear Ltd; ³1. Bionics Institute 2. University of Melbourne, Department of Medical Bionics

Background: Although there are useful guidelines defining the boundary between damaging and non-damaging electrical stimulation (Shannon, IEEE Trans Biomed Eng, 39: 424-6, 1992), they were derived from acute stimulation studies using large surface area Pt electrodes in direct contact with cortical neurons and stimulated at 50 pulses per second (pps). These parameters are a small subset of the parameters used by neural stimulators. We sought to establish the response of the cochlea to chronic electrical stimulation over a range of charge densities including levels considered to be beyond those regarded as safe in Shannon (1992).

Materials and Methods: Eighteen pigmented guinea pigs were used in this study. Each animal was systemically deafened and 2 weeks later implanted with an 8 platinum (Pt) contact intracochlear electrode array. Each electrode array had exposed Pt contact areas of 0.05, 0.075 or 0.2 mm². Animals were stimulated continuously for 28 days using charge balanced biphasic current pulses of 0.2 mC/ Φ at 200 pps, generating charge densities of 400, 267 or 100 mC/cm²/ Φ . Charge-balance was achieved using electrode shorting. Electrically-evoked auditory brainstem responses (EABRs) were recorded to monitor neural function. At completion of the stimulation program the electrode arrays were examined using scanning electron microscopy and cochleae prepared for histology. Finally, trace analysis of Pt in cochleae tissue was measured using inductively coupled plasma mass spectrometry (ICP-MS).

Results: Chronic electrical stimulation at 267 or 400 mC/cm²/ Φ resulted in significant Pt corrosion from the electrode surface compared to 100 mC/cm²/ Φ (P2/ Φ exhibited an extensive tissue response including an "amorphous" zone located adjacent to the Pt electrodes

that appeared to consist of cellular debris. Chronic stimulation at 100 mC/cm²/ Φ evoked a mild tissue response without evidence of an amorphous zone. Despite chronic stimulation at charge densities well above the Shannon limit there was no loss of auditory neurons in stimulated cochleae compared with their contralateral control cochleae. Moreover, these animals showed no statistically significant increase in EABR thresholds over the course of the chronic stimulation program.

Conclusions: Chronic electrical stimulation of Pt electrodes at 400 or 267 mC/cm²/ Φ evoked a vigorous tissue response and produced Pt corrosion products that were located close to the electrode. Despite these changes at the electrode/tissue interface there was no evidence of neural loss or a reduction in neural function over the 28 day electrical stimulation program.

Funding: This work was supported by NIDCD (R01DC015031). The Bionics Institute acknowledges support of the Victorian Government through OISP.

PS 365

Persistent Expression of Functional Proteins in the Human Spiral Ganglia Neurons in the Implanted Cochlea

Akira Ishiyama¹; Gail Ishiyama²; Dora Acuna³; Ivan A. Lopez⁴

¹Department of Head and Neck Surgery, David Geffen School of Medicine; ²Neurology Department, David Geffen School of Medicine; ³Department of Neurology, UCLA School of Medicine; ⁴3Department of Head and Neck Surgery, David Geffen School of Medicine

Background: Human spiral ganglia neurons (SGNs) persist in the human cochlea after hair cell loss, in contrast to SGNs in the cochlea of animal models. These suggest that the hair cell-primary afferent interaction is differential among different species, and the differential expression of neurotrophic factors is determinant for the survival of either the organ of Corti and SGNs in different inner ear pathologies. The otoprotective role of the neurotrophin brain derived neurotrophic factor (BDNF), has been extensively in the inner ear of animal models. We hypothesize that the human cochlea post-implanted is not only benefited by a proper selection and surgical implantation but also benefits by the chronic electrical stimulation by preserving and stimulating remaining spiral ganglia neurons and cells of the organ of Corti. In this study, we investigated the presence of neurofilaments (NF) and acetylated tubulin (AT) and BDNF in the SGNs in patients who have undergone cochlear implantation using immunohistochemistry.

Methods: Temporal bones from 15 patients (age: 8-89 years; n=5 normal hearing, and 10 received cochlear implants (CI) and their contralateral side) were used in the present study. Celloidin-embedded cochleas were immunoreacted with mouse monoclonal antibodies against pan-neurofilaments, acetylated-tubulin, and brain derived neurotrophic factor BDNF. Detailed immunohistochemical analysis was performed in mid-modiolar sections.

Results: NF and AT were present in the SGNs of all temporal bones examined i.e. normal cochleas, and were persistent in both implanted and non-implanted ears despite the loss of hair cells. NF and AT were detected in the cytoplasm of the SGNs and fibers. NF and AT distribution were similar throughout the basal, middle, and apical turns of the cochlea including the organ of Corti. BDNF was expressed in a minimum basal level in the normal cochlea in the SGNs, but upregulated in SGNs and satellite cells of the CI side.

Conclusions: The persistence of immunostaining of these three proteins in the SGNs including implanted versus non-implanted ears suggests that they may be functional despite the absence of hair cells, supporting an important role in inner ear function. NF, AT and BDNF immunoreactivity persisted in remaining spiral ganglia and neurons despite cochlear implantation. SGN degree of survival was not clearly predictable from implanted versus non-implanted ears. The consistent and reliable detection of these neural markers in human temporal bone specimens allows to investigate normal inner ear cytoarchitecture, and their changes with age, disease and CI.

Support: NIDCD grant 1U24DC015910-01

PS 366

Effect of Electrical Stimulation on Inner Ear in a Guinea pig Model of Cochlear Implantation

Adrien A. Eshraghi; Mario M. Perdomo; Rahul Mittal; Jorge Bohorquez; Carolyn Garnham; Hannah Marwede; Frederick Barhydt; Jeenu Mittal
University of Miami Miller School of Medicine

Introduction: We described previously, the pattern of hearing loss post cochlear implantation (CI) and electrode insertion trauma (EIT) in animal models. This loss of hearing post CI has both an acute component (direct trauma) and an early post-operative component (cellular and molecular damage) that develops over the period of at least a week following the initial trauma event. However, the effect of the electrical field generated by the implant has not been investigated to date. Some

recent data suggests that the electrical stimulation can have a negative effect on the auditory system. However, the role of such stimulation on hearing ability in vivo is not well established. The objective of this study was to determine the effect of electrical stimulation on auditory system employing in vivo model.

Materials and Methods: The adult guinea pigs were implanted with a cochlear implant and subjected to electrical stimulation via constant activation of the implant. Unoperated contra-lateral ears or unstimulated animals subjected to EIT or naïve animals were used as controls. Stimulation was applied with varying parameters to determine the effects of the stimulation on the survival of hair cells. Auditory brainstem recordings (ABR), electrical auditory brainstem recordings (eABR) and Distortion Product Otoacoustic Emissions (DPOAEs) were performed to determine hearing thresholds in the guinea pig model. Hearing tests were performed at day 1, 7, 14, 30, 90 post surgery. Oxidative stress levels were determined at different time periods post-implantation.

Result: Spiral ganglion neurons and number of hair cells were decreased in guinea pigs subjected to EIT and electrical stimulation compared to control and EIT alone. There were high levels of oxidative stress in EIT + electrical stimulation compared to control and EIT alone. We observed a increase in ABR threshold shifts and DPOAE amplitudes in the electrical stimulated CI group compared to unstimulated implanted animals at all frequencies and time-periods

Conclusion: The results of this study suggest that electrical stimulation has an adverse effect on Spiral ganglion neurons that can predict CI outcome. Oxidative stress plays an important role in hearing loss following EIT and electrical stimulation. This in vivo model can be used to assess the long term effects of electrical stimulation on the cochlea following CI. In addition, this guinea pig model of electrical stimulation can serve as a powerful tool to determine the efficacy of future therapeutic interventions for the preservation of residual hearing post CI.

PS 367

Changes of Electrocochleographic Responses During Insertion in Cochlear Implant Recipients

Adrian Dalbert¹; Alex Huber²; Dorothe Veraguth¹; Christof Rössli²; Flurin Pfiffner¹

¹*ENT department, University Hospital of Zurich;*

²*Department of Otorhinolaryngology Head & Neck Surgery, University Hospital Zürich, University of Zurich*

Background: In human cochlear implant (CI) recipients,

electrocochleographic (ECoG) responses have been recorded from extra- and intracochlear sites. Especially intracochlear ECoG recordings using the CI as recording electrode have great potential to become a clinically widely used tool to monitor cochlear function during cochlear implantation.

Objective: The aim of this study was to monitor extra- and intracochlear ECoG responses during cochlear implantation and correlate ECoG changes with postoperative hearing preservation.

Material and Methods: ECoG responses to 250, 500, 750 or 1000 Hz tone bursts or acoustic click stimuli were recorded during insertion of the CI electrode array. For extracochlear ECoG, a recording electrode was placed on the promontory. For intracochlear ECoG recordings, the most apical contact of the CI electrode array was used as recording electrode. Changes of ECoG recordings were correlated with pure-tone audiometric findings 4 weeks after surgery.

Results: Mean hearing loss in subjects without decrease or loss of extracochlear ECoG signals was 12 dB, compared to a mean hearing loss of 22 dB in subjects with a detectable decrease or a loss of ECoG signals ($p = 0.0058$, $n = 51$). In extracochlear ECoG recordings, a mean increase of the ECoG signal of 4.4 dB occurred after opening the cochlea and a mean decrease of 2.5 dB until the end of insertion. In ECoG recordings from an extracochlear site, permanent decreases were detectable in approximately 50% of the cases and occurred mainly during the second half of the insertion. No temporary decreases appeared in extracochlear recordings. Amplitude changes in intracochlear ECoG recordings were detectable during all stages of the insertion and could be permanent or temporary. Abrupt amplitude changes were more likely to occur during the last 5mm of insertion. Intracochlear ECoG recordings showed continuous phase changes during insertion in all cases, amplitude changes could be accompanied by abrupt changes of phase or not. In extracochlear ECoG recordings, phase changes were accompanied by amplitude changes in all cases.

Conclusion: ECoG recordings allow detection of electrophysiological changes in the cochlea during cochlear implantation. Some of these changes seem to be associated with loss of residual acoustic hearing. Extra- and intracochlear ECoG recordings show different characteristics. Especially intracochlear ECoG signals are challenging to interpret. The correlation of extra- and intracochlear ECoG responses could help to elucidate the implications of intracochlear ECoG findings.

PS 368

Reduced Threshold Shift and Hair Cell Loss after Cochlear Implantation Following Pre-Treatment by Near-Infrared-Light

Dietmar Basta¹; Ira Strübing¹; Dan Jiang²; Patrick Boyle³; Moritz Gröschel¹; Arne Ernst¹

¹Department of Otolaryngology at ukb, University of Berlin, Charité Medical School; ²Department of Otolaryngology at St Thomas' Hospital, University of London; ³Advanced Bionics European Research Center

The protection of residual hearing is becoming increasingly important in cochlear implant (CI) surgery. Various approaches have been investigated for the prevention of cochlear functional damage. One effective option without side effects could be the application of near-infrared light (NIR) perioperatively. Specific wavelengths within the NIR-spectrum are known to influence cytochrome-c-oxidase activity which leads in turn to a decrease of apoptotic mechanisms. It has been shown previously that NIR can decrease the cochlear hair cell loss significantly if applied daily after noise exposure. Recently, studies by our group indicated that even a single NIR-pre-treatment has the ability to reduce auditory threshold shifts and rescue cochlear sensory tissue when applied immediately before loud sound exposure. The present study investigated the efficacy of a single NIR pre-treatment before cochlear implantation in an animal model. During a cochlear implant surgery, normal hearing adult guinea pigs had one cochlea pre-treated with NIR-light for 15 minutes. Immediately after light exposure, a CI electrode array, specifically designed for guinea pigs, was inserted through a cochleostomy into the scala tympani of the first cochlear turn. The contralateral ear received a similar treatment (insertion) but was sham-exposed only.

Four weeks after implantation, hair cell loss was determined in histological cochlear samples and data were compared between the two ears (with or without NIR pre-treatment) in each animal. The data demonstrate that outer hair cell loss was significantly reduced in NIR-pre-treated ears compared to the contralateral side (implanted only). Moreover, the hearing threshold shift (based on ABR-measures) was significantly reduced on the pre-treated side.

Our results suggest that a very effective protection of cochlear structures is possible during cochlear implantation by a single NIR pre-treatment.

This study was supported by Advanced Bionics GmbH, Hannover, Germany.

Chronic Mouse Cochlear Implant Model Demonstrates Similarity to Guinea Pig Models Albeit High Variability and Fragility

Jenna Devare; Deborah J. Colesa; Bryan E. Pfingst; Yehoash Raphael
Kresge Hearing Research Institute, Department of Otolaryngology-Head and Neck Surgery, University of Michigan

Background

Chronic animal cochlear implant (CI) models have been limited because the condition of the auditory nerve (AN) is closely tied to hair cell (HC) survival in deafened animals. The deafened diphtheria toxin receptor (DTR) mouse (Golub et al., 2012) presents a unique opportunity to preserve AN cells while completely eliminating HCs, as well as to establish the mouse as a chronic animal CI model.

Methods

Nondeafened wild-type mice, nondeafened DTR mice, and DT-deafened DTR mice were implanted with a single platinum/iridium ball electrode in the scala tympani. Mice were implanted at 14 weeks of age on average and survived 40 days post-implantation on average, up to 108 days in the longest-surviving mouse. Electrically-evoked auditory brainstem responses (EABRs) were recorded under anesthesia weekly to assess the stability and trajectory of responses following implantation. Additionally, ensemble spontaneous activity levels were tested in each population to assess differences in neural activity. Cochlear sections were performed, and spiral ganglion neuron (SGN) densities and HC counts were compared to functional responses. Results were compared to those in stable long-term guinea pig CI models.

Results

A majority of CIs remained functional for at least 1 month following implant surgery, with few instances of implant failure over time. Animal survival was dependent on tolerance to repeated anesthetics. Vestibular side effects in some mice appeared after electrical stimulation. EABR neural response thresholds increased initially following implantation and decreased in the subsequent weeks, similar to results seen in guinea pigs. Slopes of EABR amplitude growth functions (AGFs) demonstrated variable results across subjects. The animal with lowest SGN cell density also had the shallowest EABR AGF slopes, consistent with results in guinea pigs. Histology confirmed complete HC loss in DT-deafened DTR mice. In a subset of both nondeafened and deafened mice, SGN loss was observed in the region of the implant, likely related to implant insertion trauma.

Conclusions

A long-term chronic mouse CI model was successfully created and demonstrated results similar to those seen in stable long-term chronic guinea pig models. Further manipulation of the AN and HCs, as well as implantation in mouse models of hereditary deafness, will allow for a better understanding of how cochlear health impacts CI function.

Acknowledgements

We thank Lisa Beyer for technical assistance. Support: NIH/NIDCD grants R01 DC015809, R01 DC14832, P30 DC005188, T32 DC005356 and AAO-HNSF Resident Research Award.

PS 370

Characterizing Mechanisms of Intracochlear Pressure Transients During Cochlear Implantation via Simultaneous Cochlear Fluoroscopy and Intracochlear Pressure Measurements

Nathaniel T. Greene¹; Renee M. Banakis Hartl²; John Peacock³; Stephen P. Cass¹

¹*University of Colorado School of Medicine, Department of Otolaryngology;* ²*University of Colorado School of Medicine Department of Otolaryngology;*

³*University of Colorado School of Medicine, Department of Physiology and Biophysics*

Cochlear implantation has been an effective treatment for the profoundly deaf for decades, and is increasingly being offered to patients with some residual (usually low frequency) acoustic hearing. This functional residual hearing allows for combined electrical-acoustical stimulation (EAS), which allows access to temporal and binaural information unavailable to standard Cochlear Implant (CI) users, and correlates with improved hearing outcomes. Unfortunately, a subset of patients lose this residual hearing either immediately or some time after CI implantation, thus eliminating the potential benefits of EAS.

Several mechanisms may contribute to the loss of residual hearing, including mechanical trauma and changes to inner-ear mechanics. Another possible mechanism is the generation of high amplitude pressure transients in the inner ear during CI insertion, which have been reported in several studies. Exposure to these transients may compromise residual hearing by inducing a noise-induced hearing loss. However, while these prior studies identified the existence of these transients, they did not indicate their source; thus limiting our ability to develop mitigation strategies.

To begin to fill this gap we made simultaneous measurements of intracochlear pressures with

fluoroscopic imaging during CI electrode insertion through the round window. Cadaveric human heads were surgically prepared for CI insertion with an extended facial recess. Fiber-optic pressure sensors were inserted into the scala vestibuli and scala tympani near the oval and round windows to measure intracochlear pressures. Three CI electrode models (including both straight and perimodiolar styles) from a single manufacturer were inserted via a round window approach under time-synced fluoroscopy.

CI electrode insertions produced pressure transients in the cochlea up to 160-170 dB SPL equivalent, consistent with results from previous studies. The electrode position within the cochlea (particularly electrode contact with either the medial or lateral walls), design-related electrode dynamics, and poor surgical technique, were associated with increased rates of pressure transient generation.

These results provide baseline data that elucidate the risk of generating injurious pressure transients during CI electrode insertion. Knowledge of these results may help reduce damage to residual hearing by helping CI manufacturers improve electrode designs, and by helping surgeons improve “soft” surgical techniques.

PS 371

Chirp-evoked CAP in a Guinea Pig Model of Cochlear Implantation

Youssef Adel¹; Jochen Tillein²; Tobias Weissgerber¹; Uwe Baumann¹

¹*Audiological Acoustics, Department of Otorhinolaryngology, University Hospital Frankfurt;*

²*MED-EL Germany GmbH*

Background: Patients with severely impaired high-frequency hearing and sufficient residual low-frequency hearing can be provided with cochlear implants (CIs), thereby facilitating ipsilateral electric and acoustic stimulation (EAS) with well-established advantages over electric stimulation alone. Still, residual hearing is often only partially preserved due to, inter alia, acute mechanical trauma during implantation. Possibilities of intraoperative monitoring using electrocochleography (ECoChG) have been extensively studied in CI patients, primarily using the ongoing outer hair cell response to low-frequency tone bursts, i.e. cochlear microphonics. In contrast, neural phase-locking to the ongoing response as well as the neural transient response, i.e. compound action potential (CAP), were generally less prominent or sometimes absent, thus falling short of providing useful contribution to ECoChG analysis. In this study, we investigate using chirps to better synchronize the neural response from the apex and provide more robust CAP in a guinea pig model of cochlear implantation.

Methods: In experiment 1, ECoChG was measured in 9 normal-hearing guinea pigs (Dunkin Hartley) via gold-wire electrode placed at the round window niche. We compared input-output (IO) functions and derived-band responses using high-pass noise masking to infer apical contribution to the CAP. Stimuli were constructed by adding a harmonic series either with zero phase delay (band-limited click) or by adjusting the phase delay according to a model of basilar membrane group delay (chirp) with 3 different parameters in order to examine level-specific changes in the delay model. The amplitude spectrum was thus identical between stimuli with differences only in phase. In experiment 2, guinea pigs were implanted with MED-EL custom-built CI electrode carrier using a motorized micromanipulator. ECoChG was measured at each insertion step for the following stimuli: broadband click, band-limited click, chirp (3 parameters), and 10-ms tone bursts at frequencies 1, 2, 4, and 8 kHz. Insertion depths ranged between 4 and 5 mm.

Results: Preliminary analysis shows lower thresholds and steeper slopes at the inflection point of sigmoid-fitted IO functions for chirps when compared with band-limited click. Derived-band analysis suggests that chirp-evoked CAP has more apical contribution than click-evoked responses. Finally, intraoperative monitoring shows differences between stimuli in relative amplitude change over insertion depth. Further analysis of collected data will be presented.

Conclusion: The chirp could constitute an effective stimulus to synchronize neural response from the apex and therefore be used to achieve a more holistic assessment of residual hearing.

PS 372

Multichannel Implants in Chronically Implanted Mice: Challenges and Opportunities

Deborah J. Colesa; Jenna Devare; Bryan E. Pfungst; Yehoash Raphael

Kresge Hearing Research Institute, Department of Otolaryngology-Head and Neck Surgery, University of Michigan

Introduction

Mice are an important model for chronic cochlear implant (CI) studies due to their ability to be genetically modified to represent many auditory conditions that are effectively treated with cochlear implantation. Some research in cochlear implanted mice to date has utilized short-term studies, but longer term studies are needed to evaluate function under stable conditions. Because mice can be difficult to implant and test frequently under anesthesia due to their size and sensitivity to frequent manipulation, a chronic CI model that can be tested in the awake condition with multiple electrodes is desirable.

In this study, we look at changes and/or stability of functional measures over time after implanting mice with multichannel implants and assess the relationship of these measures to the condition of the cochlea.

Methods

Non-deafened normal hearing mice were implanted in the scala tympani with a multichannel cochlear implant comprised of 3 platinum/iridium electrodes. Electrically-evoked compound action potentials (ECAPs) were obtained in the awake condition and electrically-evoked auditory brainstem responses (EABRs) and ensemble spontaneous activity (ESA) levels were recorded under anesthesia. These data were obtained to assess differences in evoked neural activity and changes over time after implantation, and the longevity of the implants for chronic studies. We compared these results to long-term stable chronic CI guinea pig data to determine if the chronic CI mouse model would have similar trends to those in the well-established guinea pig model.

Results

The reliability and stability of the multichannel implants in the mice implanted to date has been very poor with the period of implant functionality lasting from 9 - 29 days post-implantation. For data that were collected, ECAP and EABR amplitude growth functions (neural response magnitude vs stimulus current level) and ESA levels were within the range reported for CI guinea pigs. Histology at the end point of the last functioning electrode will determine the condition of the cochlea and its relation to the electrophysiological results.

Conclusions

While CI work in mice is possible and important, the technique is challenging and the outcomes can be variable. Further research is needed to improve the long-term reliability of these implants and to determine the relationships between long-term stable function and various cochlear conditions.

Acknowledgements

We thank Lisa Beyer for technical assistance. Support: NIH/NIDCD grants R01-DC015809, R01-DC14832, P30-DC005188, and T32-DC005356.

PS 373

Endocochlear Potential and Stria Vascularis Changes Associated with Cochlear Implantation

Joseph H. McClellan; Wenxuan He; Joseline Raja; Peter S. Steyger; Tianying Ren; Lina Reiss
Oregon Health and Science University

Background: The cause of hearing loss following implantation in electroacoustically stimulated (EAS)

cochlear implant patients remains poorly understood. Recent work shows a correlation between vascular changes in the cochlear lateral wall and post-implantation hearing loss (Tanaka et al., 2014), suggesting a possible role of the stria vascularis and the endocochlear potential (EP). The goals of this study were to 1) evaluate whether cochlear implantation altered the EP, 2) assess the correlation between any changes in EP and hearing loss, and 3) assess whether EP and hearing changes correlated with changes in vascular morphology within the stria vascularis.

Methods: Thirteen normal-hearing guinea pigs received cochlear implants, using either: a cochleostomy approach (n=8), or an extended round window approach (n=5). Hearing was assessed via auditory brainstem responses (ABRs) obtained pre- and post-operatively. Three weeks after implantation, EP measurements were obtained via an opening in the bony lateral wall and stria vascularis. Then, cochleae were fixed and decalcified, allowing for whole mount dissection and histological staining. Twelve control animals underwent ABR and EP measurements without cochlear implantation.

Results: The implanted group experienced significant postoperative threshold shifts at 8-24 kHz (mean threshold shift 9.1 +/- 1.1 dB SPL). Higher threshold shifts occurred in the RW subgroup (13.7 +/- 1.6 dB SPL) compared with the cochleostomy subgroup (4.2 +/- 3.6 dB SPL). Implanted animals had a significant decrease in EP in the first turn (81.4 +/- 5.1 mV) compared with controls (87.9 +/- 6.1 mV). No differences were seen in the second turn (87.9 +/- 6.1 mV for implanted animals compared to 76.5 +/- 7.0 mV for controls). There was no correlation between EP measurements and turn-specific threshold shifts or stria blood vessel density. There were no group differences in inner or outer hair cell counts.

Conclusions: Hearing loss after implantation is not explained by changes in stria vascular density or reductions in EP. However, there was only mild hearing loss in the implanted group, and correlations may not be detectable at these small threshold shifts. The extended round window approach caused more hearing loss than the cochleostomy approach, and may represent a more suitable approach for future studies utilizing this hearing loss model.

PS 374

Post-Cochlear Implantation Macrophage Response in CX3CR1-GFP Mice

Rene Vielman Quevedo¹; Alexander D. Claussen¹; Brian J. Mostaert¹; Jonathon R. Kirk²; Marlan R. Hansen¹

Introduction: Cochlear implants (CI) are increasingly used to treat hearing loss, especially with recent advances that extend the candidate population to include patients with residual hearing. It is becoming more pertinent to address issues that hamper their efficacy, including loss of residual hearing after CI (Kopelovich et al., 2014; Kamakura & Nadol, 2016). Post-implantation intracochlear inflammation and ossification may play a role in post-implantation loss of residual hearing and also affect post-implantation hearing outcomes in traditional cochlear implantation (Quesnel, et al. 2016). This work studied the inflammatory response to cochlear implantation and stimulation at different time points up to 14 days post op using a mouse model.

Method: Normal hearing CX3CR1-GFP; Thy1-YFP/C57Bl6 adult (10-12 week old) mice were divided into three groups. These included an implanted, electrically stimulated group; an implanted, non-stimulated group; and an acute insertion group. Subjects in the stimulated and non-stimulated groups were unilaterally implanted with a percutaneously connected 3-channel CI electrode array (Cochlear, Australia). Subjects in the acute insertion group had the electrode array removed following insertion. The non-stimulated group did not receive electrical stimulation. Subjects in the electrically stimulated group received 4 hrs of monopolar stimulation per day via an implant emulator (Cochlear, Australia) coupled to a custom tethered setup from post-op day 7 (switch-on). Device programming was based on neural response telemetry (NRT) and device integrity was monitored using regular impedance measurements (Custom Sound EP 4.2, Cochlear, Australia). Non-stimulated and acute insertion subjects were sacrificed at post-op day 1, 3, 7, 8, 11 and 14 (n=3 per time-point). Chronic stimulated subjects were sacrificed at 4 hrs, 1, 4 and 7 days post switch-on. Unimplanted contralateral ears served as untreated controls. Cochleae were harvested at each time-point and prepared for immunohistochemistry with confocal imaging. The images were analyzed (Imaris, Bitplane, USA) to obtain CX3CR1-GRP+ macrophage and Thy1-YFP+ neuron cell density.

Results: All implants maintained functional NRT and impedance measures during the entire experiment. An inflammatory response was observed near the insertion site in both chronically implanted groups and the acute insertion group. A robust inflammatory response was observed in implanted groups as early as 7 days post-operative. This included a consistent tissue response in the region of the implant and macrophage infiltration within the scala tympani. An increase in cochlear

macrophage density was seen in all groups, present in the lateral wall, implant-associated tissue response and Rosenthal's Canal.

Conclusion: In the mouse model, cochlear implantation with and without electric stimulation is associated with a heightened inflammatory response with associated macrophage infiltration throughout the cochlea. This may suggest a role for both surgical trauma and foreign body response in post-implantation intracochlear inflammation. Our model provides an opportunity for testing strategies to reduce this post-implantation response.

PS 375 now PD 160

PS 376

Monitoring Phase and Amplitude of the Response to Low Frequency Tones during Cochlear Implant Insertion Using an Extracochlear Electrode.

Douglas C. Fitzpatrick; Christopher K. Giardina; Kendall A. Hutson; Harold C. Pillsbury; Kevin D. Brown
University of North Carolina at Chapel Hill

Electrocochleography (ECochG) is increasingly being assessed as an intraoperative monitor of cochlear function during cochlear implantation (CI). Typically, the target measure is magnitude of the ongoing, or steady-state, response to a loud, low frequency tone (e.g., 500 Hz at 90 dB nHL), and the expectation is that a reduction in response may be related to trauma from the insertion. The ongoing response includes the cochlear microphonic (CM), derived from hair cells spread across a greater or lesser spatial extent in different subjects, and a variable degree of neural input from the auditory nerve neurophonic (ANN). Thus, interactions and distortions between different cochlear locations and different sources can be expected to produce complex patterns of response changes, confusing a simple equation between response loss and trauma. Here, we examined the responses to 500 Hz, 90 dB nHL tones during implant insertions in terms of phase, magnitude, and contributions of neural sources. An extracochlear site was used so that any changes would indicate interaction between the array and cochlear tissues, rather than due to movement of the array, as is possible when recording intracochlearly from the apical contact. Results showed that magnitude could be stable even while the phase and/or neural contribution was changing or could even increase with such changes. Since any change indicates interaction between the array and cochlear tissue, steady magnitudes or increases are not clearly benign. In some cases, reductions in response magnitude were accompanied by phase changes, but in other cases they were not. Because of these complex

interactions, it is not yet possible to associate response changes with degrees of surgical trauma.

PS 377

Evaluation of Cochlear Trauma following Micromechanical Insertion of Electrode Arrays

Allan Henslee¹; Christopher Kaufmann¹; Marlan R. Hansen²

¹*iotaMotion, Inc.*; ²*University of Iowa Department of Otolaryngology Head and Neck Surgery*

BACKGROUND

Hearing preservation cochlear implants (CIs) and techniques provide significant benefits to patients with residual hearing. However, additional functional acoustic hearing loss following surgery has been reported in some patients, often attributed to intracochlear trauma sustained during the electrode insertion. We have developed a micromechanical CI insertion system which aims to reduce this electrode insertion trauma. In this study, we evaluated the ability of the insertion system to reduce the electrode insertion forces as well as the intracochlear trauma in a cadaveric model.

METHODS

The custom insertion system was utilized to insert lateral wall electrodes from 4 manufacturers into cadaveric cochleae at an insertion rate of 0.5 mm/sec. Device insertions were characterized with respect to the maximum insertion force (mN) and force variation (mN/sec) using a single axis force transducer and compared to manual insertions by hand. To evaluate trauma, a high-resolution Xradia 3D X-ray system was used to image cochleae and subsequently score the trauma of intracochlear tissue via the Eshraghi scale.

RESULTS

At an insertion velocity of 0.5 mm/sec into cadaveric cochleae, results showed the system significantly reduced the average maximum insertion force from 92.4 ± 18.4 to 63.6 ± 8.7 mN and the force variation from 474.3 ± 131.0 to 64.6 ± 17.8 mN/sec, when compared to manual insertions respectively. Average Eshraghi scale trauma scores for the insertion system trended towards less than scores obtained via manual by-hand insertions across all electrodes, although not significantly in every case. Typical trauma included basilar membrane elevation or electrode translocation into scala vestibule.

CONCLUSIONS

The micromechanical insertion system reduces maximum insertion forces and force variations compared to manual electrode insertions for four different electrode manufacturers. Intracochlear trauma scoring also suggests that slow and controlled insertion leads to

reduced incidence of electrode translocation and resultant trauma to the cochlea. The micromechanical insertion system has the potential to improve hearing preservation CI surgery by facilitating atraumatic electrode insertion.

Binaural Hearing: Real & Simulated Impairments

PS 378

Relationships Between the Neural Coding of IPD Cues and Binaural Perception in Aging Listeners

Tess Koerner¹; Leslie Grush¹; Jay Vachhani¹; Melissa Papesch¹; Frederick J. Gallun²; Curtis J. Billings¹

¹*VA RR&D NCRAR*; ²*VA Portland RR&D National Center for Rehabilitative Auditory Research and OHSU*

Binaural hearing and the ability to use interaural phase differences (IPDs) are important for understanding speech in adverse listening environments. There is growing interest in the use of electroencephalography (EEG) measures as objective tools for assessing the neural coding of IPD cues, as these non-invasive measures do not require any overt behavioral responses on the part of the participant and appear to be related to behavioral performance on tasks involving IPD discrimination and binaural hearing. The interaural phase modulation following response (IPM-FR) is one EEG measure that has previously been used to assess the neural coding of IPD cues. Previous results suggest that the IPM-FR can reflect the effects of various participant factors on the neural coding of IPD cues, including effects due to aging. The IPM-FR is evoked in response to a dichotic stimulus in which the phase of the signals in the right and left ears are shifted in relation to one another. The current study used the IPM-FR to further assess and confirm the effects of aging on the neural coding of IPD cues and to explore whether these neural responses are predictive of performance on additional behavioral measures that assess binaural hearing abilities. Neural responses were measured in a group of adults that varied in age using an amplitude modulated 500 Hz carrier signal that alternated between a diotic and a dichotic presentation. The dichotic portion of the stimulus had a phase reversal rate of 6.8 Hz at an IPM depth of $\pm 90^\circ$. The IPM-FR was measured as the steady-state response to the 6.8 Hz phase reversal rate during the dichotic presentations. Behavioral measures included a binaural frequency modulation detection task and a speech perception task that measured spatial release from masking. Analyses included an examination of the effects of age on the IPM-FR. In addition, relationships between the neural coding of the IPD cue and performance on the behavioral tasks were also explored. This work has important implications regarding the use of the IPM-FR as a tool for assessing

binaural temporal processing in clinical populations. [Work supported by R01 DC015240 (CJB)]

PS 379

Sound Localization Behavior of Normal Hearing Plugged Listeners Fitted with the ADHEAR Bone-Conduction Device

Hillary Snapp¹; Katharina Vogt²; Martijn Agterberg²
¹University of Miami Department of Otolaryngology;
²Radboud University

BACKGROUND:

Bone conduction devices are a common treatment option for individuals with conductive hearing loss. Recent reports suggest high rates of non-use with percutaneous bone-conduction devices (BCD) in patients with unilateral conductive hearing loss (UCHL) (Nelissen et al., 2015). In children, consistent and unambiguous input to the auditory system is expected to play an important role in auditory development and learning. Several studies demonstrated that sound localization with one normal hearing ear can be surprisingly accurate for both listeners with UCHL (Agterberg et al., 2012), and SSD (Agterberg et al., 2018), while qualitative studies suggest some listeners learn to cope with unilateral hearing. In patients with bilateral conductive hearing loss (BCHL) it has been demonstrated that bilateral amplification by BCDs result in a clear advantage over the unilateral hearing condition. Still, a minority of patients with BCHL are bilaterally aided with BCDs.

This study addresses the potential advantages of BCDs in unilateral and bilateral plugged normal hearing listeners. This study aimed to investigate the potential binaural benefits provided by bone conduction in conductive hearing loss when listening with the non-invasive ADHEAR BCD.

METHODS:

Localization performance of 15 normal hearing adults and 5 children was evaluated in the normal hearing condition. Listeners were then tested under simulated unilateral and bilateral conductive hearing loss conditions, where binaural hearing was disrupted. Stimuli consisted of broadband, high-pass, and low-pass noise bursts, 150-ms in duration, and presented at sound levels of 45, 55 or 65 dB SPL. (for details see Vogt et al., 2018).

RESULTS:

In the simulated bilateral conductive hearing loss condition, mean absolute error (MAE) deviated significantly from normal hearing; however, MAE approximated true localization behavior with a relatively low degree of error (~ 25) for moderate and loud stimuli. Soft stimuli were largely undetected, and bilateral ADHEAR devices restored access to this signal with

comparable localization abilities to the bilateral plugged condition (~25). In the unilateral plugged condition, the bone conduction stimulation with the ADHEAR device had minimal effect on sound localization abilities.

CONCLUSION:

Sound localization abilities are disrupted by asymmetric hearing. Best aided benefit is observed in BCHL conditions for stimuli presented at the lowest sound level. The limited benefit of a BCD in the unilateral plugged listening condition might be related to the reported non-use of a significant proportion of the population of patients with congenital UCHL.

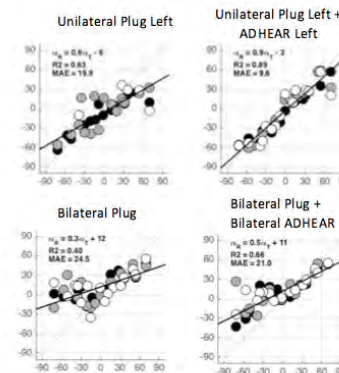


Figure 1:

Target response plots for a single subject in the bilateral plug condition (A), bilateral plug + bilateral ADHEAR condition (B), unilateral plug left condition (C), and unilateral plug left + ADHEAR left condition (D). Performance is indicated by level (white 45 dB SPL, grey 55 dB SPL, dark 65 dB SPL). Overall MAE is reported.

PS 380

Effects of Contralateral Routing of Signal on Monaural Localization Performance

Hillary Snapp¹; Seba Ausili²; Ad Snik³

¹University of Miami Department of Otolaryngology;
²Radboud University; ³Radboudumc

Contralateral Routing of Signal (CROS) hearing aids are increasing in adoption and acceptance in individuals with severe-profound unilateral sensorineural hearing loss. Although binaural hearing, specifically localization performance, remains largely impaired. Some monaural listeners are able to use level and spectral cues to achieve near-normal horizontal localization ability (Slattery and Middlebrooks, 1994; Van Wanrooji & Van Opstal, 2007) in the unaided condition. It is possible that those who can reliably use monaural spectral cues to facilitate localization, experience a disruption of these remapped (Keating et al., 2015) auditory cues with use of the CROS. The purpose of this study was to evaluate localization performance with CROS hearing aids under simulated unilateral hearing loss conditions.

Methods:

Localization performance of 12 normal hearing subjects was evaluated in a simulated unilateral hearing loss condition with and without CROS hearing aids. Subjects were plugged and muffed to provide maximum attenuation. Stimuli consisted of 150 ms High-Pass noise bursts (3kHz to 20kHz) presented at random at 45, 55, 65 dB SPL in a darkened sound attenuated room. Stimuli were presented at +/-75° azimuth and +/- 30° elevation. Listening conditions included normal hearing, normal hearing +unilateral plug and muff, and normal hearing + unilateral plug and muff CROS aided. Responses were recorded using a custom headtracker to measure the head rotation of the subject in response to the stimuli.

Results:

Preliminary findings demonstrate a decrease in performance in elevation with the CROS hearing device on, suggesting a disruption of monaural spectral cues. Performance in azimuth is also significantly reduced for CROS aided localization performance compared to the simulated unilateral hearing loss condition. Preliminary results demonstrate that deviations for CROS aided performance from the simulated unilateral hearing loss condition are greater than that of the simulated unilateral hearing loss condition from normal hearing. Delays in reaction times are also observed to be greater in the CROS aided condition over the simulated unilateral hearing loss condition as compared to the normal hearing responses. Preliminary results suggest that despite the recent advances in design, CROS hearing aids disrupt monaural spectral cues. For those monaural listeners who successfully adapt to use such cues, this may contribute to failure to adopt CROS technology.

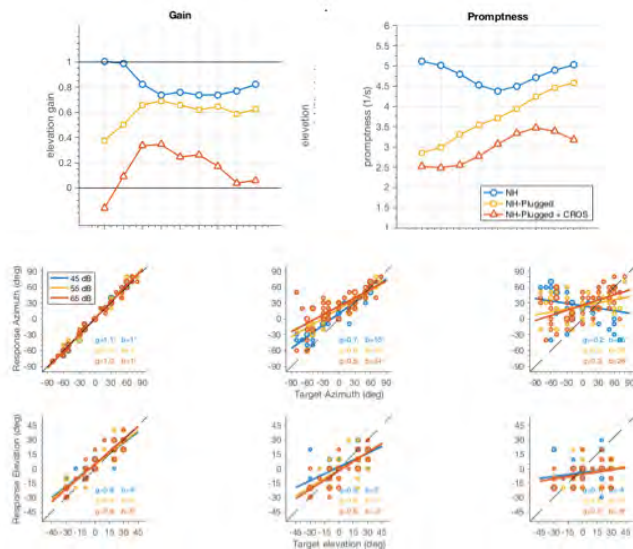


Figure 1) Target response plots demonstrating decreased localization performance from the 1) normal hearing condition to the 2) unilateral plugged condition to the 3) CROS aided condition.

PS 381

Relating Spatial Hearing Benefits to Binaural Cue Sensitivity in Combined Electric and Acoustic Stimulation (EAS)

Rebekah Funkhouser¹; G. Christopher Stecker²; René Gifford²

¹University of Mary Washington; ²Vanderbilt University Medical Center

Cochlear implant (CI) users with preserved acoustic hearing in the CI ear demonstrate significant benefit from combined electric and acoustic stimulation (EAS) for speech recognition in complex listening environments (diffuse noise and reverberation) and horizontal plane localization. It is thought that such benefits arise primarily through access to interaural time differences (ITDs) in the low-frequency audible acoustic range. To date, all investigations of EAS spatial hearing have focused on ITD sensitivity and its impact on spatial hearing with static sources. No studies have quantified sensitivity to interaural level differences (ILDs), which are present at low frequencies and may also be responsible for EAS benefit, particularly in dynamic conditions (e.g. moving sound sources) in which access to binaural cues should prove beneficial. The purpose of this study was to describe the ITD and ILD sensitivity of EAS listeners and relate that sensitivity to spatial hearing in dynamic conditions, e.g. the minimum audible movement angle (MAMA) task. ITD, ILD, and MAMA thresholds were obtained for 17 adult EAS listeners. ITD and ILD thresholds for acoustic hearing were assessed via insert earphones for low-frequency noise (100-800 Hz) at 90 dB SPL. MAMA thresholds for a single stimulus velocity (20 deg/sec) were obtained in the bimodal [CI + Contralateral hearing aid (HA), CI+CHA] condition as well as the everyday listening condition (CI + Bilateral HA, CI+BHA) for three stimulus types presented at 70 dB SPL: low-frequency noise (100-800 Hz), high-frequency noise (2000-8000 Hz), and broadband noise (100-8000 Hz). As compared to bimodal hearing (CI+CHA), the everyday listening condition (CI+BHA) yielded significantly lower MAMA thresholds for low-frequency noise ($p = 0.045$), but no significant benefit for high-pass noise ($p = 0.123$) or broadband noise ($p = 0.739$). MAMA thresholds for low-frequency noise were significantly correlated to ITD thresholds, ILD thresholds, and degree of interaural asymmetry in low-frequency audiometric thresholds. There was no correlation between MAMA and low-frequency audiometric thresholds in the CI ear alone. These results demonstrate that preserved acoustic hearing in the CI ear provides significant benefit to spatial hearing in dynamic conditions and that this benefit is related to both ITD and ILD sensitivity. Sensitivity to binaural cues for EAS users is likely driven by greater interaural symmetry in acoustic hearing suggesting that

CI users with better rates of hearing preservation are most likely to derive EAS benefit.

PS 382

Speech Evoked Auditory Brainstem Response to Assess Binaural Processing in Children with Early Onset Hearing Loss.

Robel Z. Alemu¹; Jonah Gorodensky¹; Simrat S. Gill¹; Blake C. Papsin²; Sharon Cushing¹; Karen Gordon²

¹The Hospital for Sick Children, The University of Toronto; ²Hospital for Sick Children

Objectives: 1) To assess temporal and spectral characteristics of speech and their integration in the bilateral auditory pathways and 2) to identify abnormalities in this processing of speech in children with hearing loss.

Background & Rationale: Speech is received at each ear but integrated in the bilateral auditory pathways to create perception of one “fused” image coming from a particular direction in space. Our previous work in children using bilateral cochlear implants suggests that binaural hearing is impaired by deafness and inaccuracies in binaural input generated by auditory prostheses such as cochlear implants and hearing devices. In the present study, we examined binaural processing of speech using the Frequency-Following Response (FFR) which is an electrophysiological response to a speech stimulus. We hypothesized that temporal and spectral peaks of the FFR normally increase in amplitude during bilateral listening compared to unilateral listening but that this bilateral advantage is impaired in children with bilateral hearing loss who use two hearing aids.

Methods: A single syllable speech stimulus (/da/) was presented to each ear individually and then bilaterally at balanced levels. Participants were 9 children with normal hearing (mean = 12.1 ± 2.5 years of age) and 6 children with bilateral hearing loss (mean = 14.0 ± 2.6 years of age) who were bilateral hearing aids users. The FFR was obtained and peaks were extracted over time and frequency. Peak amplitude and latency differences were compared between listening conditions and groups.

Results: Amplitudes of both temporal and spectral peaks in FFR responses were larger in bilateral than unilateral listening conditions in children with normal hearing. These measures of bilateral advantage were reduced in the group of children with bilateral hearing loss.

Conclusion: These findings indicate a normal binaural advantage of temporal and spectral processing as measured by FFR responses to a speech

sound. Deterioration of this binaural advantage was found in children with hearing loss and suggests that their access to sound through bilateral hearing aids, as fit presently, does not correct for this deficit.

PS 383

Effect of Long Term Exposure to ITD Cues on Processing of Binaural Cochlear Implant Input

Alexander Thompson¹; Dexter Irvine¹; Samuel Irving¹; Aasha Riordan¹; Nathan Bordonaro¹; Andrew Wise²; James Fallon¹

¹Bionics Institute; ²University of Melbourne, Department of Medical Bionics

Introduction: Although performance with bilateral cochlear implants is superior to that with a unilateral implant, bilateral implantees have poor performance in sound localisation and in speech discrimination in noise compared to normal hearing subjects. Studies of the processing of sound localisation cues have shown that long-term deafness from a young age degrades processing of interaural time differences (ITDs) and that use of conventional clinical implants does not prevent degradation of ITD processing. It has been speculated this poor processing is due to the fact that current clinical devices do not provide fine ITD information, and that delivery of this information might reverse the degradation. To test if long-term exposure to relevant ITDs would improve ITD processing, we developed a custom sound processor to deliver high fidelity ITDs for chronic stimulation in an animal model.

Method: Four groups of cats were used: normal hearing controls (NH, n=2), neonatally profoundly deafened unstimulated cats (NDUS, n=2), two groups of neonatally profoundly deafened cats that received approximately 6 months of bilateral intra-cochlear electrical stimulation from clinical cochlear implants and speech processors (NDS, n=6) or from our custom sound processor and stimulator (NDITDS, n=1). One NH, two NDS and one NDITDS cats were trained on an automated go/no-go food reward sound localisation task. Single-unit responses (n= 110, 60, 137, 9 for the NH, NDUS, NDS and NDITDS groups respectively) to electric binaural stimulation with a range of ITDs and ILDs were recorded from the central nucleus of the inferior colliculus bilaterally, using 32-channel silicon arrays (NeuroNexus).

Results: On the sound localisation task, the NH animal was readily able to discriminate between two tones played from one speaker or moving between two speakers positioned 50 cm apart, reaching a D’ score of 2 by 26 days, while the NDS and NDITDS cats were unable to perform the task even after 60 days. Neuronal sensitivity to ITDs was significantly poorer in all the neonatally

deafened groups compared to the normal hearing animals (Kruskal-Wallis test, $p < 0.05$), and there was no difference between the NDS and NDTDS groups ($p > 0.05$).

Conclusion: Our strategy to deliver physiologically relevant ITDs from bilateral clinical cochlear implants did not prevent/reverse the degradation in ITD processing that occurs following long-term deafness from a young age.

This work was funded by the NHMRC. The Bionics Institute acknowledges the support it receives from the Victorian Government through its Operational Infrastructure Support Program.

PS 384

Spatial Hearing as a Function of Presentation Level in Moderate-to-Severe Unilateral Conductive Hearing Loss

Michael Canfarotta; Nicholas Thompson; Stacey Kane; Corbin Nicole; Emily Buss
University of North Carolina at Chapel Hill

Background: Spatial hearing is essential in everyday tasks such as listening to speech in noisy environments and localizing sound in a three-dimensional setting. Patients with unilateral conductive hearing loss (UCHL) are known to have poorer spatial hearing due to decreased access to binaural difference cues. In children, unilateral hearing loss has been shown to negatively impact language abilities, speech and psychosocial development, and academic performance despite normal hearing in the contralateral ear.

Objective: The objective of this study was to investigate whether children and adults with moderate-to-severe UCHL have improved spatial hearing ability when stimuli are presented at a high enough level to provide some audibility in the affected ear.

Methods: Listeners were 12 patients with moderate-to-severe UCHL, most due to atresia, and 12 age-matched controls with normal hearing bilaterally. All completed two spatial hearing tasks: (1) spatial release from speech-in-speech masking (SRM), and (2) sound source localization. For assessment of SRM, target speech was Pediatric AzBio sentences, presented at 0o. The masker was two-talker speech, either co-located with the target (0o) or spatially separated from the target (symmetrical, at +90o and -90o). Localization ability in the horizontal plane was assessed in a 180-degree arc of eleven evenly-spaced loudspeakers. The stimulus was a 200-ms burst of pink noise, bandpass filtered 126-6000 Hz (48-dB/octave), gated using 20-ms raised-cosine ramps. These two tasks were completed at 50 and 75 dB SPL.

Results: Both children and adults with UCHL performed more poorly than controls when recognizing speech in a spatially separated masker or localizing sound. However, this group difference was larger at 50 than 75 dB SPL. Increases in both SRM and localization accuracy at the higher presentation level are consistent with the idea that patients with UCHL can use binaural cues when they are audible.

Conclusion: The finding of better spatial hearing at the higher presentation level in the UCHL group suggests that the auditory deprivation associated with a moderate-to-severe UCHL does not preclude exposure to -- or use of -- binaural difference cues. Implications for audiologic/otologic management of UCHL and our understanding of the underlying binaural system will be discussed.

PS 385

Binaural Intelligibility Level Difference with a Simulation of a Mixed-rate Strategy for Bilateral Cochlear Implants

Thibaud Leclère¹; Seamus Doyle¹; Alan Kan²; Ruth Litovsky²

¹*Waisman Center, University of Wisconsin-Madison;*

²*University of Wisconsin - Madison*

In noisy situations, bilateral cochlear implant (BiCI) listeners demonstrate poorer spatial release from masking compared to normal hearing (NH) listeners, likely due to the limited access to interaural time differences (ITDs). Clinical processors typically convey speech information by modulating a pulsatile high-rate (~1000 Hz) carrier by the speech envelope, and discard temporal fine structure (TFS), leading to good speech recognition in quiet. But such processing is not optimal for conveying TFS ITD cues, because they are not encoded. BiCI listeners are not sensitive to ITDs at high pulse rates, however, previous psychophysical data showed that using low pulse rates (Towards the goal of introducing ITD cues without disrupting speech understanding, we propose a mixed-rate strategy. Both high and low pulse rates occur across the electrode array, to preserve both well-sampled speech envelopes and ITD sensitivity, respectively. While previous work on mixed rates studied speech understanding and ITD sensitivity separately, the present study investigates whether such a mixed-rate strategy will allow listeners to access and process both cues, and enable binaural unmasking. Binaural Intelligibility Level Differences (BILD) were measured over headphones in NH listeners using a 16-channel mixed-rate tone vocoder, where the envelopes of low-rate channels were down-sampled to simulate low pulse rates. Five mixed-rate configurations were tested: All High, All Low, Apical high (high rates towards apex), Basal high (high rates towards base) and Interleaved (high and low rates alternate across the channels). The

masker was speech-shaped noise presented with a 0- μ s ITD, and the target had either a 0 or 800- μ s ITD applied only to the low-rate channels to simulate a co-located or spatially-separated condition, respectively. Three groups of listeners were each tested on the two spatial conditions and at six signal-to-noise ratios (from -15 to 10 dB) in three out of the five mixed-rate configurations. For most participants, in the presence of co-located noise, All High and All Low conditions led to the highest and lowest scores, respectively, and intermediate scores were observed for mixed-rate configurations, which is in agreement with previous work done in quiet. In separated conditions, BILDs were often larger with an Interleaved configuration compared to All Low, although it depended on the participant and SNR, suggesting that introducing high-rate channels did not entirely disrupted binaural unmasking for CI simulations.

Work supported by NIH-NIDCD (R01-DC003083 and 1R01DC016839 to RYL, R03-DC015321 to AK), and NIH-NICHHD (U54HD090256 to Waisman Center).

PS 386

Effect of Simulated Interaural Frequency Mismatch on Interaural Time Difference Lateralization and the Relationship to the Amplitude of the Binaural Interaction Component

Iona McLean¹; Matthew Goupell²; Samira Anderson³; Olga A. Stakhovskaya⁴

¹University of Maryland, College Park; ²University of Maryland; ³Department of Hearing and Speech Sciences, University of Maryland; Neuroscience and Cognitive Science Program, University of Maryland; ⁴Department of Hearing and Speech Sciences, University of Maryland, College Park

Introduction:

Differences in cochlear-implant (CI) insertion depths, which produce interaural frequency mismatch, may partially account for binaural-hearing deficits experienced by CI users. Two parallel experiments simulated interaural frequency mismatch in normal-hearing (NH) listeners. The experiments evaluated binaural hearing by measuring (1) lateralization of interaural time differences (ITDs) and (2) the amplitude of the binaural interaction component (BIC). The BIC is a putative measure of binaural processing that compares Auditory Brainstem Responses (ABRs) obtained in monaural and binaural presentation. We hypothesized that the range of ITD lateralization curves and the magnitude of the BIC amplitude would decrease with increasing interaural frequency mismatch.

Methods:

In the first experiment, ITD lateralization was measured in 13 NH listeners. Interaural frequency mismatches were created by presenting acoustic pulse trains (PTs) at different center frequencies (CFs) (1663, 2593, 4000, 6128, and 9350 Hz) across ears, resulting in mismatches of 0, 3, 6, 9, and 12 mm of basilar membrane length. PTs had a rate of 21.6 pulses/sec and a bandwidth of 1.5 mm, which simulated electrical current spread from a single electrode. The range of the ITD lateralization curves were measured.

In the second experiment, the ABRs of listeners from the first experiment were recorded during presentation of PTs at 4000 Hz and at interaural frequency mismatches of 0, 3, and 6 mm. The BIC amplitude was defined as the difference in ABR Wave V amplitude between the summed monaural and the binaural responses.

Results:

As the absolute value of the interaural frequency mismatches increased, the range of ITD lateralization curves decreased, suggesting that larger frequency mismatches diminish binaural processing. In the second experiment, the magnitude of the BIC amplitude decreased with greater mismatch for most subjects. Future analyses will attempt to observe a correlation between behavioral and electrophysiological findings.

Discussion:

Greater interaural mismatch produces binaural hearing deficits, both in behavior and electrophysiology. This provides support for attempting to remove interaural frequency mismatch in CI users with binaural electrophysiological measures like the BIC. [Research supported by NIH/NIDCD grant R01 DC015798.]

Clinical Vestibular Applications

PS 387

Combination Therapy Targeting mTOR- and EPH Receptor-Mediated Signaling as a Novel Therapeutic Strategy for Vestibular Schwannoma

Jessica E. Sagers¹; Yanling Zhang²; Roberta L. Beauchamp²; Lei Xu²; Vijaya Ramesh²; Konstantina M. Stankovic³

¹Harvard Medical School and Massachusetts Eye and Ear; ²Massachusetts General Hospital and Harvard Medical School; ³Eaton-Peabody Laboratories, Massachusetts Eye and Ear & Department of Otolaryngology, Massachusetts Eye and Ear and Harvard Medical School & Speech and Hearing Bioscience and Technology Program

Background: mTORC1 and mTORC2-specific serum/glucocorticoid-regulated kinase 1 (SGK1) are highly expressed and activated in meningiomas with loss of

the NF2 gene. Additionally, a recent high-throughput kinome screen in NF2-null human arachnoidal and meningioma cells revealed activation of EPH RTKs, c-KIT, and SFK members independent of mTORC1/2 activation. Combination therapy with the dual mTORC1/2 inhibitor AZD2014 and the tyrosine kinase inhibitor dasatinib was recently shown to be effective in NF2-deficient meningiomas. Therefore, we investigated mTORC1/2 and EPH receptor-mediated signaling in sporadic and NF2-associated vestibular schwannoma (VS), the fourth most common intracranial tumor and an important cause of sensorineural hearing loss.

Methods: Using primary human VS cells and a mouse xenograft model of schwannoma, we evaluated the effect of the dual mTORC1/2 inhibitor AZD2014 and the tyrosine kinase inhibitor dasatinib as monotherapies and in combination in order to slow or halt the growth of tumor cells. This study has been conducted in strict compliance with all ethical standards and applicable regulations regarding animal use and human subjects.

Results: Escalating dose-response experiments on primary VS cells grown from 15 human tumors show that combination therapy with AZD2014 and dasatinib is more effective at reducing metabolic activity than either drug alone and exhibits a therapeutically promising effect at a physiologically reasonable concentration (100 nM). In vivo, though AZD2014 and dasatinib each inhibit tumor growth when administered alone, the effect of combination therapy exceeds that of either drug.

Conclusions: Co-targeting the mTOR and EPH receptor pathways with these or similar compounds may constitute a novel therapeutic strategy for VS, a condition for which there is no FDA-approved pharmacotherapy.

PS 388

Clinical Imaging-Based Endotyping in Meniere's Disease

David Bächinger¹; Catrin Brühlmann²; Tim Honegger²; Joseph B. Nadol³; Steven D. Rauch⁴; Joe Adams⁵;

Andreas Eckhard²

¹Department of Otorhinolaryngology, Head and Neck Surgery, University Hospital Zurich; ²Department of Otorhinolaryngology - Head and Neck Surgery, University Hospital Zurich; ³Massachusetts Eye and Ear Infirmary / Harvard Medical School; ⁴Massachusetts Eye and Ear Infirmary, Harvard Medical School; ⁵Otopathology Laboratory, Massachusetts Eye and Ear Infirmary

Introduction: Meniere's disease (MD) presents a broad clinical spectrum with regard to the frequency and severity of clinical symptoms, the long-term

course of the disease, and the responsiveness to different therapies. The existence of multiple clinical "phenotypes" and distinct etiologies (endotypes) was proposed in order to explain this clinical heterogeneity. However, such distinct phenotype-endotype correlations have not been demonstrated so far. Own previous post mortem temporal bone studies revealed at least two different pathologies in the endolymphatic sac (ES) in MD, i.e. epithelial degeneration (dgES) and developmental hypoplasia (hpES).

Materials and methods: Retrospective study: 1) Gadolinium-enhanced magnetic resonance imaging (Gd-MRI, 3T) data of temporal bones from MD patients (n=76) was used. Relative loss of T1 signal intensity (3D FLAIR sequence) in unilateral MD cases was used as a marker for dgES pathology. The angular trajectory ($b > 140^\circ$) of the vestibular aqueduct (VA) in the axial plane was used to identify hpES pathology, 2) Chart review and collection of audiological/vestibular data from MD patients, 3) Statistical patient subgroup comparisons.

Results: Based on the established Gd-MRI criteria, four MD patient subgroups with either unilateral dgES (74% of patients, n = 54) or hpES pathology (12%, n = 9), or bilateral dgES (12%, n = 9) or hpES pathologies (4%, n = 4) were identified. MD patient subgroups with dgES and hpES pathology revealed significant differences with regard to (I) sex prevalence, (II) prevalence of radiographic semicircular canal dehiscence, (III) prevalence of headache types, (IV) vestibular function of the affected ear, and (V) the frequency of vertigo attacks.

Conclusion: A total of four MD patient subgroups with distinct pathomorphological and clinical traits were identified. Our results indicate that 1) Gd-MRI can be applied to identify dgES and hpES pathologies in clinical MD patients, 2) different ES pathologies are associated with distinct disease phenotypes, and 3) these new diagnostic criteria have the potential to enable a more specific clinical diagnosis and allow to prognosticate crucial features in the course of MD for individual patients.

PS 389

Clinical imaging of the vestibular aqueduct in patients with early and late onset Meniere's disease

Ngoc-Nhi Luu¹; Judith S. Kempfle²; Andreas Eckhard³; David Bächinger⁴; Hugh Curtin⁵; Steven D. Rauch⁶

¹University Department of Otolaryngology, Head and Neck Surgery; ²Massachusetts Eye and Ear Infirmary, Eaton-Peabody Laboratories; ³Department of Otorhinolaryngology - Head and Neck Surgery, University Hospital Zurich; ⁴Department of

Otorhinolaryngology, Head and Neck Surgery, University Hospital Zurich; ⁵Massachusetts Eye and Ear Infirmary; ⁶Massachusetts Eye and Ear Infirmary, Harvard Medical School

Background:

Meniere's disease (MD) is a chronic inner ear condition that presents with intermittent symptoms of vertigo, fluctuating hearing loss, tinnitus, and aural fullness.

Heterogeneous presentation of auditory and vestibular symptoms makes clinical diagnosis of MD difficult. Prior studies have suggested an involvement of the endolymphatic sac (ES) in disease manifestation. Two distinct ES pathologies, degeneration or hypoplasia of the sac may be associated with different clinical phenotypes of the disease. In order to further investigate this hypothesis, the trajectory and angle of the vestibular aqueduct in early and late onset MD patients was analyzed.

Methods: Prospective clinical study enrolling early (50 years) subjects with unilateral or bilateral MD. Patients underwent high resolution cone beam CT scan of the temporal bone, and angle and trajectory of the vestibular aqueduct were analyzed using OsiriX imaging software.

Results: Preliminary results suggest a significantly stronger angled vestibular aqueduct in the late onset MD group ($\alpha \sim 90\text{-}100^\circ$), correlating with the degenerative-type ES pathology, whereas the early onset MD group demonstrated less angled vestibular aqueducts ($\alpha \sim 150^\circ$), which is more consistent with possible hypoplastic-type ES pathology.

Conclusion:

We demonstrate preliminary cone beam CT imaging data of early and late onset MD patients that suggests different trajectory and angle of the vestibular aqueduct consistent with previously described distinct endolymphatic sac pathology for early versus late onset groups.

PS 390

Vestibular Aqueduct Morphology Correlates with Endolymphatic Sac Pathologies - a Clinical Method to Identify Subgroups in Meniere's Disease

David Bächinger¹; Ngoc-Nhi Luu²; Judith S. Kempfle³; Daniel Zürrer⁴; Daniel J. Lee⁵; Hugh D. Curtin⁶; Steven D. Rauch⁷; Joseph B. Nadol⁸; Joe C. Adams⁹; Andreas H. Eckhard¹

¹Department of Otorhinolaryngology, Head and

Neck Surgery, University Hospital Zurich; ²University Department of Otolaryngology, Head and Neck Surgery; ³Massachusetts Eye and Ear Infirmary, Eaton-Peabody Laboratories; ⁴Independent Researcher; ⁵Department of Otolaryngology, Harvard Medical School; ⁶Department of Radiology, Massachusetts Eye and Ear Infirmary; ⁷Massachusetts Eye and Ear Infirmary, Harvard Medical School; ⁸Massachusetts Eye and Ear Infirmary / Harvard Medical School; ⁹Otopathology Laboratory, Department of Otolaryngology, Massachusetts Eye and Ear Infirmary

Background: Patients with Meniere's disease (MD) demonstrate a high degree of interindividual variability in the presentation of audiovestibular symptoms. This variability has previously raised the questions of whether distinct disease endotypes exist among patients. Recently, we demonstrated two etiologically different inner ear pathologies that both affect the endolymphatic sac (ES) and that are ubiquitously present among MD patients: degenerative changes in the ES and developmental hypoplasia of the ES. Here, we investigated whether different angular trajectories of the vestibular aqueduct (ATVAs) in the temporal bone are associated with different ES pathologies (degeneration vs. hypoplasia). Thereby, we aimed to establish a radiographic criterion that allows to distinguish subgroups of MD patients based on the ATVA.

Methods: First, we determined age-dependent normative data for the ATVA based on histological temporal bone sections from normal adults and fetuses. We then used these data to validate ATVA measurements from normative CT imaging data. Second, ATVA was assessed in histological materials and CT imaging data from MD patients. **Results:** Among the control cases, ATVA showed only little inter-individual variation. However, in MD patients ($n = 35$), using the ATVA, in particular its axial trajectory in the opercular region (angle α_{exit}), patients could be grouped according to ES pathology, i.e. degenerative ES pathology ($\alpha_{\text{exit}} < 120^\circ$) and hypoplastic ES pathology ($\alpha_{\text{exit}} > 140^\circ$). Furthermore, a strong correlation was found between ATVA measurements in histological sections and CT imaging ($r = 0.78$, $p < 0.001$).

Conclusions: In summary, we have established a new strategy that allows to isolate distinct subgroups of MD patients with clinical imaging. Further studies will show whether these two subgroups of MD patients in fact differ significantly in the course of their disease.

The Development of the Benign Paroxysmal Positional Vertigo (BPPV) Symptom Impact Questionnaire (BSIQ)

Faith W. Akin¹; Sherri L. Smith²; Courtney D. Hall¹; Kristal M. Riska²; Annabelle Larkin³

¹James H. Quillen VA Medical Center; ²Duke University;

³East Tennessee State University

Background: The BPPV Symptom Impact Questionnaire alpha version (BSIQ-a) was developed as a disease-specific quality-of-life outcome measure for BPPV. Fourteen vestibular experts provided feedback on relevance, clarity, simplicity, and ambiguity for each of the 15 items on BSIQ-a. Based on expert feedback, the BSIQ-a was revised to improve clarity and remove redundancy in an 11-item beta version (BSIQ-b; see Figure). The purpose of this study was to determine initial psychometric properties of the BSIQ-b.

Methods: Veterans who had BPPV within the previous year completed the BSIQ-b based on their experience when they were symptomatic. To explore the subscale structure of the BSIQ-b, a factor analysis was performed using principal components analysis (PCA). Cronbach's α was used to determine internal consistency reliability. Inter-item correlations were evaluated to determine item redundancy.

Results: Before the factor analysis, one item (related to falls) was removed because most Veterans (80%) responded with 0% (never). A Kaiser-Meyer-Olkin test was performed and resulted in a value of 0.725, which confirmed that the sample size ($n = 30$) was 'good'; for conducting a factor analysis (Kaiser, 1970, 1974; Hutcheson & Sofroniou, 1999). The subscale structure was explored using a PCA analysis with varimax rotation. Only factors with eigenvalues greater than 1.0 and that explained at least 5% of the variance were extracted. Only items with factor loading values 0.50 or greater were considered. A scree plot test confirmed a two-factor solution. Factor 1, Triggers and Symptoms, consisted of 7 items primarily related to head positions that provoke vertigo (43.6% variance explained). Factor 2, Impacts and Quality of Life, consisted of 3 items related to avoiding provoking symptoms and quality of life (25.1% variance explained). Overall, the factor loading values were high (mean = 0.76, range 0.62 – 0.88), suggesting that the items are highly related to each other. The internal consistency reliability, Cronbach's α , was 0.90. Reliability was also assessed by evaluating inter-item correlations and ranged from fair to moderate suggesting that the items are related but not overlapping in content.

Conclusions: Preliminary results suggest that the BSIQ-b has strong construct validity and good internal consistency reliability. Future studies will confirm the psychometric properties of the BSIQ-b in a prospective sample and expand upon the current evidence by evaluating criterion validity and test-retest reliability. These psychometric are required before implementing the BSIQ as a disease-specific outcome measure in the clinical care of patients with BPPV.

Benign Paroxysmal Positional Vertigo Symptoms Impact Questionnaire

Check UP TO TWO of the symptoms that best describe your **sensation of dizziness**.

<input type="checkbox"/> No dizziness	<input type="checkbox"/> About to faint or pass out
<input type="checkbox"/> Spinning	<input type="checkbox"/> Nausea
<input type="checkbox"/> Unsteady/off-balance	<input type="checkbox"/> Light-headed
<input type="checkbox"/> Pulsed to one side	<input type="checkbox"/> Sensations other than those listed above. Please describe: _____

Instructions: For each question below, circle the best answer for how you have felt in the past week. Notice that each choice includes a percentage to help you decide on your answer.

1) In the past week, how often did you feel dizzy?	Never 0%	Occasionally 25%	Half the Time 50%	Most of the Time 75%	Always 100%
2) In the past week, how often did you feel dizzy when you looked up?	Never 0%	Occasionally 25%	Half the Time 50%	Most of the Time 75%	Always 100%
3) In the past week, how often did you feel dizzy when you bent over (e.g. tying your shoes)?	Never 0%	Occasionally 25%	Half the Time 50%	Most of the Time 75%	Always 100%
4) In the past week, how often did you feel dizzy when you turned your head left or right?	Never 0%	Occasionally 25%	Half the Time 50%	Most of the Time 75%	Always 100%
5) In the past week, how often did you feel dizzy after you rolled over in bed?	Never 0%	Occasionally 25%	Half the Time 50%	Most of the Time 75%	Always 100%
6) In the past week, how often did you feel dizzy when you moved from sitting up to lying down?	Never 0%	Occasionally 25%	Half the Time 50%	Most of the Time 75%	Always 100%
7) In the past week, how often did you feel dizzy when you got up from lying down?	Never 0%	Occasionally 25%	Half the Time 50%	Most of the Time 75%	Always 100%
8) In the past week, how often did your dizziness cause you to fall?	Never 0%	Occasionally 25%	Half the Time 50%	Most of the Time 75%	Always 100%
9) In the past week, how often did you avoid putting your head in a certain position so you would not feel dizzy?	Never 0%	Occasionally 25%	Half the Time 50%	Most of the Time 75%	Always 100%
10) In the past week, how often did you avoid doing certain activities so you would not feel dizzy?	Never 0%	Occasionally 25%	Half the Time 50%	Most of the Time 75%	Always 100%
11) In the past week, how often did your dizziness impact your quality of life?	Never 0%	Occasionally 25%	Half the Time 50%	Most of the Time 75%	Always 100%

Impact of Otolith Dysfunction on Postural Stability and Quality of Life: A Chronic Effects of Neurotrauma Consortium Study

Courtney D. Hall¹; Faith W. Akin¹; Owen D. Murnane²; Jennifer R. Sears²; Richard B. Atlee²; Barry S. Eggleston³; Elizabeth V. Fogleman³

¹James H. Quillen VA Medical Center; ²James H. Quillen VAMC; ³RTI International

Background: Until recently, clinical vestibular function assessment was limited to measurement of horizontal semicircular canal pathways. Vestibular evoked myogenic potentials are becoming more widely used to supplement the vestibular test battery by providing information about the otolith organs and their pathways; yet, the clinical significance of otolith organ dysfunction is unclear. The purpose of this study was to determine the functional consequences of otolith organ dysfunction on postural stability and quality of life.

Methods: A prospective case-control study of Veterans ($n=130$) was completed. Comprehensive vestibular site-of-lesion testing was performed and participants were grouped according to patterns of vestibular test

findings. Three vestibular groups included individuals complaining of dizziness/imbalance with: (1) otolith organ dysfunction only (Otolith Only, n=21), (2) otolith organ and semicircular canal dysfunction (Otolith+Canal, n=19), and (3) semicircular dysfunction only (Canal Only, n=12). Two control groups included individuals with normal vestibular function and (1) complaining of dizziness/imbalance (Dizzy Control, n=52) or (2) with no complaints of dizziness/imbalance (Healthy Control, n=26). Self-report questionnaires and physical performance measures of balance and gait assessed postural stability and quality of life. MANOVAs were performed to determine significant group differences ($p < 0.05$) for balance and gait and quality of life outcome measures. As appropriate, post hoc analyses of covariance and pairwise comparisons were performed to identify specific group differences ($p < 0.05$).

Results: There were no significant group differences for age, race, ethnicity, gender or occupational status. MANOVAs indicated significant group differences for both gait and balance and quality of life measures (see Table). The Otolith+Canal group performed significantly worse than both control groups and the Otolith Only and Canal Only groups on the Sensory Organization Test. The Otolith+Canal group also performed significantly worse than both control groups on the Functional Gait Assessment.

The Otolith Only group performed significantly worse than the Healthy Control group on a measure of the impact on activities, the Activities-specific Balance Confidence scale (ABC), and the Dizziness Handicap Inventory (DHI). The Otolith+Canal group performed significantly worse than the Healthy Control on a measure of the impact on activities, the ABC, DHI, and Vestibular Activities and Participation measure.

Conclusions: Otolith organ dysfunction negatively impacts quality of life, and in conjunction with semicircular canal dysfunction, negatively impacts balance and gait. The findings of this study have important implications for developing effective clinical protocols for the diagnosis and management of individuals with dizziness related to otolith organ dysfunction.

Table. Descriptive statistics (mean \pm SD) for gait, balance and quality of life measures by study group.

	Study Group				
	Vestibular			Control	
	Otolith Only (N=21)	Canal + Otolith (N=19)	Canal Only (N=12)	Dizzy (N=52)	Non-Dizzy (N=26)
Sensory Organization Test (/100)	68.4 \pm 14.6	45.6 \pm 19.5	65.8 \pm 11.9	70.9 \pm 13.7	75.5 \pm 9.5
Functional Gait Assessment (/30)	22.8 \pm 5.3	17.4 \pm 5.0	21.0 \pm 5.0	23.6 \pm 5.1	25.6 \pm 3.9
Activities-specific Balance Confidence scale (%)	66.9 \pm 27.9	60.2 \pm 24.1	68.8 \pm 20.3	72.3 \pm 24.5	96.2 \pm 4.1
Dizziness Handicap Inventory (/100)	30.5 \pm 20.8	41.8 \pm 22.1	37.0 \pm 24.0	33.5 \pm 22.1	1.1 \pm 2.1
Vestibular Activities and Participation measure (/136)	25.1 \pm 16.0	39.1 \pm 25.7	30.8 \pm 20.9	28.6 \pm 22.6	2.6 \pm 4.2

PS 393

Objective Measures to optimize the Utility of the Functional Gait Assessment in Identifying Impairments in Vestibular Schwannoma Patients Before and After Surgical Treatment

Omid Zobeiri¹; Gavin Mischler¹; Susan King²; Richard Lewis²; Kathleen E. Cullen¹

¹Johns Hopkins University; ²Harvard University

A wide range of functions, from basic reflexes to high-level behaviors, depend on the vestibular system. By sensing head motion and then generating the appropriate reflexes, the vestibular system is vital for maintaining balance and stabilizing gaze. Using clinical measures, it has been shown that following unilateral vestibular loss, patients experience dizziness, headache, and impaired balance, postural, and gaze control. However, to date, much less is known about the effects of vestibular loss on voluntary behavior. Here, we assessed whether changes in locomotive behavior can predict clinical measures in a group of patients with a diagnosis of vestibular schwannoma (VS) before and after primary surgical resection of their tumor via suboccipital craniotomy and retrosigmoid approach with sectioning of the vestibular nerve. Head movements were recorded during Functional Gait Assessment (FGA), which include 10 gait tasks, using a six-dimensional motion sensor (3-axis linear acceleration and 3-axis gyroscope) in (1) healthy volunteers and (2) acute patients before and six weeks after surgery (3) chronic unilateral vestibular patients. We computed measures of gait speed, asymmetry, and variability during FGA and then compared these with multiple clinical outcome measures including; dizziness handicap inventory (DHI), activities-specific balance confidence (ABC), Beck anxiety inventory (BA), FGA score, postural sway, and vestibulo-ocular reflex gain. First, comparison of patients prior to surgery with controls revealed similar gait measures during standard walking, however patients showed significant differences for more dynamic gait tasks such as those that required changes in walking speed or claiming stairs. Next, comparison of patients before and six weeks after the surgery, revealed a reduction in head movements variability during standard surface-level walking following the unilateral vestibular loss. Interestingly, this reduced variability was correlated with multiple clinical measures. Most notably, patients with more reduced variability had lower anxiety and dizziness scores. Taken together, these results show that variability during standard gait test can identify changes following unilateral vestibular loss in vestibular schwannoma patients. Moreover, testing using more challenging gait tests can be used prior to surgery to identify vestibular impairment in schwannoma patients relative to healthy controls.

PS 394

Prediction of Functional Limitations in Balance after Tests of Tandem Walking and Standing Balance

Helen S. Cohen¹; Susan P Williams¹; Haleh Sangi-Haghpeykar¹; Ajitkumar P Mulavara²; Jacob J Bloomberg³

¹Baylor College of Medicine; ²KBRwyle; ³NASA/Johnson Space Center

Geriatricians have no good tests with which to predict decreased balance skill in aging patients. Subjects with no apparent balance problems were tested in the Geriatric Medicine clinic on Tandem Walking (eyes closed) and three conditions of Romberg on foam with eyes closed: head stationary, head moving in yaw, head moving in pitch, and retested 1.5 to 2 years later. The hypothesis was that some pre-test results would predict subsequent functional balance or reports of dizziness or vertigo. The analyses showed slight but significant decrements in Romberg tests over time, but no relationship to reports of falls, vertigo, lightheadedness or use of a cane/ hip surgery. Tandem walking did not change significantly over time but was moderately related to use of a cane/ having had hip surgery. It was not related to vertigo or lightheadedness. These data suggest that tandem walking results may help the physician to determine which patients are most at risk for clinically significant changes in their gait status.

Supported by NIH grant 2R01 DC009031.

PS 395

Adaptation of Vestibular Heading Perception in Normal Subjects

Raul Rodriguez; Benjamin T. Crane
University of Rochester

After unilateral vestibular lesions patients often have persistent dizziness symptoms. This perceptual problem can be addressed with rehabilitation techniques. But, previous work has shown that these patients have persisting biases in heading perception which may be the source of symptoms. Establishing a method of adaptation of these heading biases could assist in dealing with long-term vestibular symptoms. This study explores the potential for heading adaptation in normal subjects.

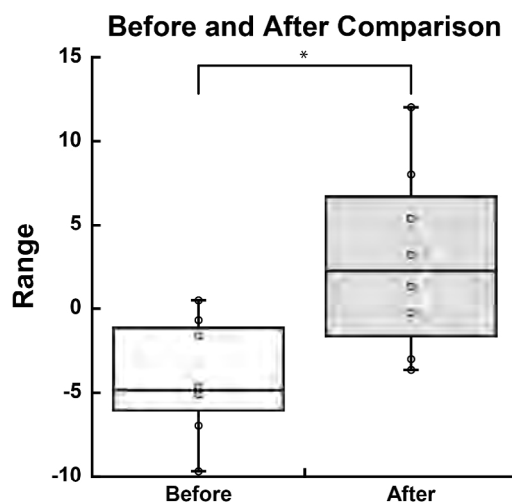
Subjects were asked to report inertial heading direction using a forced choice task in which they reported headings as left or right of midline, until the point of subjective equality was reached (as previously published) to

establish a baseline heading perception. They were then placed in a virtual reality environment which consists of white dots on a black spherical background (i.e. "star-field"). The sphere has a radius of 50 virtual meters. The star-field consists of 500 dots randomly placed along the spherical surface. Every frame 10% of the stars in the star-field randomly change their location, giving a 90% visual coherence and eliminating the potential to identify patterns as landmarks. The stars are 6 pixel diameter circles on a 1080×1200 screen. The sphere has a 40°/sec angular rotation, in the horizontal plane, either clockwise or counter-clockwise. Direction of star-field rotation was alternated between experiments to prevent possible long-term adaptation. In the virtual environment, subjects were encouraged to move their heads by presenting a figure that followed the sphere's rotation. After the subjects fixated on the figure it would disappear and a new figure would spawn at a random location after 1 sec. Subjects were in the virtual environment for 10 minutes; afterwards the subjects'; post VR inertial heading perception was measured, as before.

Prior to adaptation subjects had an average heading perception of $4.1 \pm 3.4^\circ$ (mean \pm SD) leftward. Post adaptation heading perception was $2.9 \pm 5.4^\circ$ to the right and was significantly (p

Exposure to a rotating virtual environment can significantly alter a subject's perception of heading direction. This raises the possibility that applying an adaptation to patients with long-term unilateral vestibular lesions would help alleviate perceptual difficulties they may have.

Support: R01-DC013580



Influence of Heading Separation on Visual and Vestibular Direction Perception and Common Causation

Benjamin T. Crane; Raul Rodriguez

University of Rochester

During movement through a fixed environment, both visual and vestibular (inertial) cues are relevant to direction determination. Visual cues can represent either self or environmental motion. However, with environment motion, such as in a crowd, visual may be offset from vestibular cues. In a fixed environment visual and inertial cues have a common causation and should be integrated. In a moving environment, visual and inertial cues no longer have common causation and should be perceived independently. Directionally offset visual and inertial cues were used to study common causation for heading perception. Both inertial and visual stimuli consisted of 2s of motion with a similar motion profile. The visual stimulus consisted of a star field with coherence reduced to 70% to make reliability similar to inertial motion. Trial blocks included 12 possible visual and inertial headings which covered the full 360° range in the horizontal plane in 30° increments. Every heading combination was presented in random order with 144 stimuli in each block. During each block a mechanical dial was used to report the perceived direction of the visual (V_p) or inertial (I_p) heading (Fig. 1A), and buttons to report if the headings were the same or different. Six trial blocks were performed in each subject, in 3 blocks inertial heading was reported and in the other 3 visual heading was reported. In all 6 blocks subjects reported if headings were the same or different. With a 0° offset subjects reported they were the same in 64% of trials, with a 30° offset in 46%, and 60° offset in 14%, and less than 4% for larger offsets (Fig. 1B). Visual heading perception was not influenced by the inertial heading (Fig. 1C), even with small offsets in 2 subjects (T-test, $p > 0.1$), but there was a small offset towards the inertial heading in 1 subject (green in Fig. 1C, $p=0.02$). Inertial headings were biased towards the visual heading with offsets of 30-120° (Fig. 1C) (T-test $p < 0.01$, for each subject). Over this range, the amount of bias did not depend on the offset and averaged $11.6 \pm 2.7^\circ$ (mean \pm SD). Thus, visual motion influences inertial heading perception even when headings are displaced beyond the range in which they are perceived to have common causation. These experiments demonstrate that integration of visual and inertial cues are independent of common causation perception making it different from other types of multisensory integration.

Support: R01 DC013580

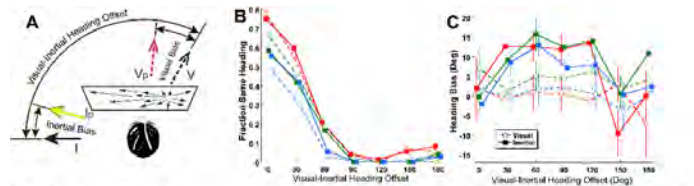


Figure 1. Subjects experienced visual and inertial headings. Visual headings are represented by dashed lines and inertial or vestibular headings by solid lines. Panel A: Experimental setup. Subjects viewed a visual screen and experienced platform motion while separating visual (pink) or inertial (yellow) direction and if these stimuli were in the same direction or not. In the example shown they are separated by 120°. Visual and inertial bias were defined as positive if they were towards the other stimulus. In cases of 0 and 180° offsets, positive was towards the right. Panel B: Fraction of stimulus presentations where headings were reported to be the same by offset. Each of the 3 subjects is shown as a different color. Panel C: Heading bias by offset. Offsets in opposite directions have been combined. Error bars represent standard error.

PS 397

Vestibular Hypofunction Alters the Statistics of the Vestibular Input Experienced during Natural Self-Motion

Omid Zobeiri¹; Benjamin Ostrander¹; Jessica Roat¹; Yuri Agrawal²; Kathleen E. Cullen¹

¹Johns Hopkins University; ²Division of Otolaryngology, Neurology, and Skull Base Surgery, Department of Otolaryngology-Head and Neck Surgery, Johns Hopkins University

It is widely believed that sensory systems are adapted to the statistical structure of natural stimuli, thereby optimizing neural coding. Recent evidence (Carriot et al., 2014, 2017) suggests that this is also the case for the vestibular system, which senses self-motion and in turn contributes to essential brain functions ranging from the most automatic reflexes to spatial perception and motor coordination. However, little is known about how the statistics of self-motion stimuli actually experienced during everyday life change when the vestibular system is damaged by disease or injury. Accordingly, we examined whether and how the statistics of the naturalistic movements are altered in patients with vestibular hypofunction. We quantified the natural self-motion signals experienced by eleven vestibular hypofunction patients and five age-matched healthy controls as they performed the standardized Functional Gait Assessment (FGA) as well as a series of dynamic self-paced activities, which were designed to mimic natural movements during daily life. MEMS-based inertial sensors were attached to each subject's head, waist, and ankles, which enabled quantification of motion in six dimensions via three-axis accelerometers (fore-aft, interaural, and vertical acceleration) and three-axis gyroscopes (pitch, roll, and yaw rotations). Rotational data recorded from the head sensor were projected onto the vestibular semicircular canal planes (anterior, posterior, and horizontal). Statistical analysis revealed that probability distributions for all six dimensions of motion (three rotations, three translations) in both patients and age-matched controls deviated from normality due to heavy tails evaluated by the kurtosis significantly higher than three (7.6 ± 3.2 , 7.8 ± 2.1). Second, comparison of power spectra across

the two groups revealed that healthy controls achieved higher frequency movements ($p < 0.05$) during natural behaviors compared to patients, suggesting a reduced dynamic range in patients. Third, healthy controls achieved higher frequency ankle movements ($p < 0.05$) than patients during standard FGA testing, while their head motion was as stable as patients. Taken together, our results suggest evaluating patient performance during more naturalistic activities provides insight into how the absence of vestibular input alters behavior, and that such testing can potentially help inform diagnosis and rehabilitation.

PS 398

Gaze stability post unilateral vestibular deafferentation surgery is still impaired after 5 weeks of vestibular rehabilitation.

Jennifer Millar¹; Yoav Gimmon²; Dale Roberts³; Michael C. Schubert²

¹Johns Hopkins Medical Institutions; ²Johns Hopkins University Department of Otolaryngology; ³Johns Hopkins University

Purpose: To compare behavioral and physiological measures of gaze stability following 5 weeks of progressive gaze and postural stability exercises.

Hypothesis: We hypothesized that ipsi and contralesional head rotation would show improved behavioral measures (Dynamic Visual Acuity, DVA) of gaze stability but not improved physiological measures (Video Head Impulse Test, VHIT)

Materials/Methods: 12 patients (6 Right, 6 Left UVD) completed the exercise protocol. The DVA Test1 included custom software developed by the JHU LVNA Lab integrated with a Windows 10a tablet and a single inertia measurement unit (XSENS Technologies, Enschede, Netherlands) mounted on a headband. We also collected DVA data in aged-matched healthy control subjects. All DVA (static, right, left) testing was completed at 200 cm. A minimum of $> 120^\circ/\text{second}$ active head rotation was required to generate the random optotype presentation. We used the Otometrics ICS System (Natus Medical Incorporated, Denmark) to measure the vestibular ocular reflex (VOR) gains (eye/head velocity). Subjective measures of balance confidence and dizziness handicap were also collected.

Results: The average time between UVD surgery and initial DVA/VHIT testing was 51 (± 54) days. Baseline yaw DVA scores were significantly impaired for both ipsi and contralesional head rotation. VOR gains were reduced only for ipsilesional head rotations; contra-

lesional VOR yaw gains were normal. After a 5 week intervention, 50% showed improvement in DVA; 11/12 and 12/12 subjects reported positive change in their Activities Balance Confidence (ABC) and Dizziness Handicap Inventory (DHI) respectively; 6 reported MCID (> 18 point change) in DHI scores, including subjects who did not show change in DVA or VOR gain measures.

Conclusion: Our data suggest patients with UVD have bilaterally impaired DVA even though contralesional VOR gains are preserved.

Clinical relevance: Patients are reporting improved functional outcomes, despite not always showing improvements in DVA or VOR gains after a 5 week vestibular rehabilitation program.

References:

1 Herdman SJ, Tusa RJ, Suzuki A, Venuto PJ, Roberts D. Computerized dynamic visual acuity test in the assessment of vestibular deficits. *Am J Otol.* 1998 Nov; 19 (6) 790-6.

2 Herdman SJ, Schubert MC, Das VE, Tusa RJ. Recovery of dynamic visual acuity in unilateral vestibular hypofunction. *Arch Otolaryngol Head Neck Surg.* 2003 Aug; 129(8):819-24.

This work is supported by Department of Defense grant, W81XWH-15-1-0442.

PS 399

Sports Related Concussion is Associated with Impaired Perception of Torsional Alignment

Thuy Tien Cao. Le¹; Michael C. Schubert²; Jorge Manuel. Serrador¹

¹Rutgers School of Graduate Studies; ²Johns Hopkins University Department of Otolaryngology

Sports related concussion is an increasing concern for both professional and recreational sports. It is estimated that as many as 1.6-3.8 million concussions occur in the US per year, which is likely an underestimate since many players with concussions do not seek treatment and therefore are not reported. Recent data has suggested that vestibular impairment may be an objective measure of concussion. We have developed a non-invasive, behavioral measure of ocular alignment using computer tablets, colored lenses and touch screen software that provides a rapid on field assessment of vestibular function. The goal of this study was to determine if there is a difference between healthy controls from players with an acute mild traumatic brain injury (concussion). In the vertical alignment nulling test (VAN), subjects adjusted

a horizontal line that was initially positioned above or below a stationary horizontal line. In the torsional alignment nulling test (TAN), subjects adjusted a line that was initially offset in torsion (i.e. clockwise or counter-clockwise) to match a stationary horizontal line. The final amount by which the lines are separated, vertically or torsionally, relative to the stationary line provides a perceptual measure of vertical and torsional ocular alignment. We measured VAN and TAN in 21 healthy rugby players and 8 concussed rugby players directly on the field of a Rugby Tournament. All subjects participated in at least one game on the day of testing; concussed subjects were tested in the first few hours following injury. Subjects with concussion had worse scores than controls on TAN (1.00 ± 0.79 vs 0.55 ± 0.45 , $p < 0.06$), but no differences for VAN scores compared to controls (0.06 ± 0.04 vs. 0.07 ± 0.06 , $p=0.62$). These preliminary results suggest perception of torsional alignment is acutely impaired in concussed rugby players. This may reflect damage to the utriculo-ocular pathways. These findings suggest that on-field assessment of vestibular function may provide an objective measure of concussion in sports related injuries.

PS 400

HoloBalance: Motivation and Monitoring of Vestibular Rehabilitation with use of Holograms in Augmented Reality.

Doris-Eva Bamiou¹; Dimitris Kikidis²; Marousa Pavlou³; Xristos Nikitas²; Dimitris Gatsios⁴; Themis Exarchos⁵; Dimitris Fotiadis⁴; **Athanasios Bimpas²**

¹*UCL Ear Institute & NIHR BRC Deafness and Hearing Problems*; ²*National & Kapodistrian University of Athens*; ³*King's College London*; ⁴*University of Ioannina*; ⁵*Ionian University, Greece*

Introduction: Balance disorders increase the risk of falls, resulting in a very high socio-economic burden. Vestibular rehabilitation is treatment of choice according to the guidelines for patients with chronic dizziness and instability. However, lack of compliance has been reported as high as 50% and this significantly decreases overall efficacy. The use of advanced technology (augmented reality) is one of the suggested solutions to overcome the mentioned difficulties.

Objectives: Objective of the HOLOBALACE project (funded by the European Commission – H2020-SC1-2016-2017) is to deliver a cost effective virtual coach consisting of a hologram balance physiotherapist, an augmented reality cognitive game, including an auditory exercises tool, and a physical activity planner. HoloBalance platform will provide real time monitoring via wearable and ambient sensors, personalized guidance

and multilevel motivation promoting independence and empowerment of the users in patients with chronic unsteadiness and/or at risk of fall.

Methods: A platform consisting of smart glasses, sensors and laptop will be created. The patients will be able to see a human-like hologram who will motivate them and guide them to properly and safely perform the programmed set of exercises, demonstrating movements and giving real time feedback to the patients. Exercise plan will be provided by the physiotherapists during initial assessment, whereas a technical team will install the platform in patients' homes. Proof of concept validation trial will be implemented as a multicenter cross-sectional, parallel group study in 4 different clinical sites (UCL, KCL, NKUA, UKLFR). Participants ($n=160$ in total, 40 participants in each center) will be randomized in two groups. The intervention group will use the virtual coach platform at home in daily basis and the control group will follow the standard care. Outcome measures, including questionnaires and functional tests for the balance, cognitive, physical activity and social participation assessment will be evaluated at baseline, at a follow-up session after 4 weeks and at the end of the trial after 10 weeks. For the statistical analysis, appropriate test for between-group and in group correlations and a general linear model analysis of variance for the primary outcomes will be completed as well as an impact assessment and a socio-economic analysis.

Conclusions: HoloBalance virtual-coach platform in addition to real time monitoring will provide objective measurements about exercise compliance, feedback to healthcare experts, will enhance continuous communication between stakeholders and will make possible personalization of care.

PS 401

Patients Presenting to the Otologic Clinic with Dizziness Have Visual Dependence and Visual-Vestibular Mismatch

Doaa Al-Sharif¹; Logan Lindemann²; Emily Keshner¹; Pamela C. Roehm²

¹*Department of Physical Therapy, College of Public Health, Temple University*; ²*Department of Otolaryngology, Temple University School of Medicine*

Background: Dizziness affects 20-30% of the general population. A subgroup of dizzy patients with chronic migraine suffer vertigo, gaze instability, and sensitivity to visual and head motion. This disorder has been termed vestibular migraine or migrainous vertigo. Vestibular migraine remains a diagnosis of exclusion

based on history, and many patients only receive a partial alleviation of symptoms with medication. Recent evidence suggests that dizziness and instability generated by complex visual environments (e.g., the grocery store) or with wide-field of view visual motion (e.g., movie screen) results from inability to correctly process or adapt to conflicting visual and vestibular signals.

Hypothesis: We hypothesized that individuals with VM would also exhibit increased weighting of visual information, which has been shown to correlate with a positive result for visual sensitivity on the rod-and-frame test (Isableu).

Methods: A convenience sample of patients presenting to the otologic clinic with a variety of vestibular complaints and diagnoses underwent visual dependence and rod-and-frame testing. Individuals lacking vestibular complaints or a history of vestibular disorders were used as controls. Visual-vestibular mismatch (VVM) was measured using a modified VVM questionnaire (Longridge et al., 2002). Visual error to subjective visual vertical and horizontal was measured using a computerized rod-and-frame test (Virtualis, France) projected as a 3D virtual reality image on a head-mounted display (Oculus Rift).

Results: Of the 74 men and women (M:F 22% v. 52%; average age 56.2 years; range 23-82 years) who presented to the Otolaryngology clinic with complaints of dizziness, 42 (56.8%) tested positive for VVM. 68.9% of patients with headache tested positive for VVM. Of 68 healthy controls (M:F 55.9% v. 44.1%; average age 26.3 years; range 21-59 years), 0 tested positive for VVM.

33 patients and 60 controls were tested for visual error. Of those tested, 41.5% of patients and 0% of controls were found to have visual dominance. 22.2% of patient with headache had visual dominance.

Conclusion: Patients with complaints of dizziness showed far higher rates of VVM and visual dominance than healthy controls. This suggests that reweighting of sensory stimuli occurs for patients with dizziness in general. VVM occurs at even greater rates for patients with migraine, and provides future directions for novel therapy for these patients. Limitations of this study include lower average age of controls than patients. Further studies will focus on comparison of age-matched controls with patients to further establish this correlation.

PS 402

Linking Vestibular Function and Cortical and Sub-Cortical Alterations in an Aging Population

Athira Jacob¹; Daniel Tward¹; Sarah Flaherty²; Susan Resnick³; Tilak Ratnanather¹; Yuri Agrawal⁴

¹Johns Hopkins University; ²Loyola University; ³National Institute on Aging; ⁴Division of Otology, Neurotology, and Skull Base Surgery, Department of Otolaryngology-Head and Neck Surgery, Johns Hopkins University, Baltimore, MD, USA

BACKGROUND: While it is well known that the vestibular system is responsible for maintaining balance, posture and coordination, there is increasing evidence that it also plays an important role in cognition. Moreover, vestibular loss has been increasingly implicated with cognitive loss in the elderly. While there are many epidemiological studies that demonstrate a relation between vestibular dysfunction and cognitive deficits in the elderly, the exact pathways through which vestibular loss affects cognition is unknown. In this cross-sectional study, we seek to identify relationships between vestibular function, and morphometric changes in brain structures from neuroimages.

METHODS: We use a subset of participants from the Baltimore Longitudinal Study of Aging (BLSA), who had both brain MRI and vestibular physiological data taken at the same visit. Vestibular function was evaluated through the cervical vestibular-evoked myogenic potential (cVEMP). For these subjects, we analyze the hippocampus, amygdala, thalamus, caudate nucleus, putamen, insula, entorhinal cortex (ERC), trans-entorhinal cortex (TEC) and the perirhinal cortex (PRC), as these structures comprise the putative “vestibular cortex” in literature. We model the volume and shape of these structures with the vestibular variable.

RESULTS: We find a positive correlation between volume of left ERC and cVEMP. In fact, with 1 μ V amplitude increase of cVEMP, there was a significant increase of 56.8 mm³ ($p = 0.03$) in left ERC volume. In case of shape, we see positive correlation locally with left caudate nucleus (10.5% increase in surface area locally, with every 1 μ V increase in cVEMP, $p = 0.002$), left putamen (6% increase, $p = 0.02$), right thalamus (6.4% increase, $p = 0.008$), right insula (6% increase, $p = 0.03$) and negative correlation with left hippocampus (an average of 13% decrease in surface area locally in posterior hippocampus, with every 1 μ V increase in cVEMP, $p =$), left amygdala (5.5% decrease, $p = 0.01$), left ERC (10.3% decrease, $p = 0.01$) and left ERC-TEC complex (collateral sulcus) (15.8% decrease, $p = 0.008$).

CONCLUSIONS: We observed significant relationships of vestibular function with volume of ERC, as well as with regional shapes of other investigated structures. This could potentially allow us to understand pathways through which vestibular loss contributes to cognitive loss, raising the possibility of vestibular sensory therapy as a viable treatment option to mitigate effects of cognitive loss due to vestibular dysfunction.

PS 403

Self-Reported Sense of Direction and Vestibular Function in the Baltimore Longitudinal Study of Aging (BLSA)

Priyal Gandhi¹; Yuri Agrawal²

¹Johns Hopkins University School of Medicine;

²Division of Otolology, Neurotology, and Skull Base Surgery, Department of Otolaryngology-Head and Neck Surgery, Johns Hopkins University

Background

Age-related vestibular loss has been linked to impaired spatial cognition. Spatial cognition involves spatial memory and navigation, which represent the brain's ability to generate a mental map and navigate through a given environment. Several animal and human studies have shown that vestibular input is necessary for accurate spatial orientation. However, these studies do not account for individual differences in intrinsic navigational ability. Numeric scales of self-reported sense of direction have been found to correlate well with objective measures of navigational ability. In this study, we evaluated age and sex-related variation in self-reported sense of direction. We will also determine how vestibular function in aging adults is associated with sense of direction. We hypothesize that vestibular function will be related to self-reported sense of direction in healthy older adults.

Methods

Participants for this cross-sectional study were recruited from the Baltimore Longitudinal Study of Aging (BLSA), a long-running cohort study of healthy aging. Eligible participants were administered both vestibular physiological testing and a modified version of the Santa Barbara Sense-of-Direction Scale at the same visit. Participants rated statements about spatial and navigational abilities from a scale of 1 (strongly agree) to 7 (strongly disagree), with the average score corresponding to self-reported sense of direction. Vestibular function testing consisted of the cervical vestibular-evoked myogenic potential (cVEMP) to assess saccular function, the ocular VEMP (oVEMP) to assess utricular function, and the video head-impulse test (VHIT) to assess semicircular canal function based

on vestibular ocular reflex (VOR). Multivariate linear regression will be used to investigate the relationship between vestibular function and self-reported sense of direction.

Results

The preliminary study sample included 21 participants with mean(\pm SD) age of 73.4(\pm 13.9) years and mean(\pm SD) Sense-of-Direction Scale score of 5.43(\pm 1.53). The average Sense-of-Direction Scale score for female participants was 5.1(\pm 1.66) while the average for male participants was 5.73(\pm 1.42); this difference was not statistically significant. Participants under the age of 60 reported an average Sense-of-Direction Scale score of 6.67(\pm 0.58), while participants between the ages of 60-80 reported an average score of 5.75(\pm 1.83) and participants older than 80 reported an average score of 4.8(\pm 1.23), with a significant difference observed between participants under age 60 and over age 80.

Conclusions

In our preliminary sample, we observed differences in self-reported sense of direction between age groups that is consistent with previous work on age-related variation in sense of direction. We will continue to explore the associations between self-reported sense of direction and measures of vestibular function.

PS 404

Saccular Function is associated with both Angular and Distance Errors on the Triangle Completion Test

Dara Bakar¹; Eric Anson²; Matthew Ehrenburg³; Eric Wei³; Eleanor Simonsick⁴; Yuri Agrawal⁵

¹The Warren Alpert Medical School of Brown University, Department of Otolaryngology-Head and Neck Surgery, Johns Hopkins University; ²Department of Otolaryngology-Head and Neck Surgery, Johns Hopkins University, Department of Otolaryngology, University of Rochester; ³Department of Otolaryngology - Head & Neck Surgery, Johns Hopkins University School of Medicine; ⁴Longitudinal Studies Section, National Institute on Aging; ⁵Division of Otolology, Neurotology, and Skull Base Surgery, Department of Otolaryngology-Head and Neck Surgery, Johns Hopkins University

Objective: The present study was designed to determine whether healthy older adults with age-related vestibular loss have deficits in spatial navigation.

Methods: 154 adults participating in the Baltimore Longitudinal Study on Aging were tested for semicircular canal, saccular, and utricular function and spatial navigation ability using the blindfolded Triangle Completion Test (TCT). Multiple linear regression was

used to investigate the relationships between each measure of vestibular function and performance on the TCT (angular error, end point error, and distance walked) while controlling for age and sex.

Results: Individuals with abnormal saccular function made larger angular errors ($\beta = 4.2$ degrees, $p < 0.05$) and larger end point errors ($\beta = 13.6$ cm, $p < 0.05$). Independent of vestibular function, older age was associated with larger angular (β 's= 2.2 - 2.8 degrees, p 's< 0.005) and end point errors (β 's= 7.5 - 9.0 cm, p 's< 0.005) for each decade increment in age.

Conclusions: Saccular function appears to play a prominent role in accurate spatial navigation during a blindfolded navigation task.

Significance: We hypothesize that gravitational cues detected by the saccule may be integrated into estimation of place as well as heading direction.

Genetics of Hearing Loss

PS 405

Susceptibility to Cisplatin Induced Hearing Loss in Mice within the Hybrid Mouse Diversity Panel

Danielle M. Gillard¹; Ely Cheikh Boussaty²; Juemei Wang³; Jaana Hartiala⁴; Hooman Allayee⁴; Rick A. Friedman²

¹University of California San Diego, School of Medicine;

²Division of Otolaryngology, Head and Neck Surgery, Department of Surgery, University of California, San Diego;

³USC-Tina and Rick Caruso Department of Otolaryngology-Head & Neck Surgery, Zilkha Neurogenetic Institute, USC Keck School of Medicine, University of Southern California; ⁴Keck School of Medicine of University of Southern California

Cisplatin chemotherapy for solid tumors is associated with progressive, permanent bilateral hearing loss that has been seen in up to 80% of children and young adults after treatment. Although several Genome-Wide Association Studies (GWAS) of cisplatin induced hearing loss (CIHL) have been performed in humans, they are limited by genetic heterogeneity, which requires costly sample sizes to reveal moderate effect-size variants. Inbred mouse panel GWAS allows for a carefully controlled environment and replication of measurements in genetically identical animals so a greater proportion of heritability can be captured. We have chosen to use the Hybrid Mouse Diversity Panel (HMDP), a collection of classical inbred and recombinant strains whose genomes have been sequenced and/or genotyped at a high resolution to study the genetic susceptibility of CIHL. Power calculations have shown that this panel is

capable of detecting loci responsible for 5% of overall variance. The HMDP has been used to study complex traits including age-related hearing loss, noise induced hearing loss and vestibular dysfunction. Currently, we have determined the cisplatin susceptibility in 27 of the roughly 100 strains in the HMDP. A total of 136 mice were used (4-5mice/strain). All mice underwent Auditory Brainstem Response testing before and after administration of 15mg/kg intraperitoneal cisplatin. Threshold shifts were determined at 4, 8, 12, 16, 24 and 32 kHz. Efficient Mixed-Model Association (EMMA) algorithm was applied to each phenotype separately to identify genetic associations for each frequency. Adjusted association p-values were calculated for 108,064 SNPs with minor allele frequency of >5% ($p < 6$, $-\log_{10}P = 5.39$). We observed phenotypic variation in susceptibility to CIHL at each frequency. Four associations with genome-wide significance were identified at chromosome 7, including at 8kHz (rs13479174; $p = 4.74 \times 10^{-8}$). Two SNPs from the same haplotype block on chromosome 7 were identified at 12kHz; rs46420051 ($p = 4.83 \times 10^{-12}$) and 16kHz; rs48373903 ($p = 1.37 \times 10^{-12}$). The same SNP (rs48373903) was also identified at 24 kHz ($p = 5.57 \times 10^{-11}$). Five significant associations were detected on chromosome 17 including, rs48653865 (8 kHz; $p = 4.08 \times 10^{-9}$), rs3145424 (12 kHz; $p = 7.00 \times 10^{-10}$) and rs29504535 (32 kHz; $p = 1.62 \times 10^{-6}$). The SNP rs45973976 was identified at both 16kHz and 24kHz ($p = 6.19 \times 10^{-11}$ and 1.26×10^{-9}). Our results provide the first large scale phenotypic data on cisplatin-sensitivity in mice. We demonstrate clear strain variation in sensitivity, highlighting the potential genetic component of CIHL, and provide a potential resource for the study of specific genes that may be associated with CIHL.

PS 406

A mouse model of a human DFNA22 variant demonstrated semi-dominant inheritance pattern

Jinghan Wang¹; Jun Shen²; Cheng Cheng³; Luo Guo¹; Renjie Chai⁴; Yilai Shu¹; Huawei Li¹

¹ENT Institute and Otorhinolaryngology Department, Affiliated Eye and ENT Hospital, State Key Laboratory of Medical Neurobiology, Fudan University. 2

NHC Key Laboratory of Hearing Medicine (Fudan University), Shanghai, 200031, China; ²Department of Pathology, Brigham and Women's Hospital, Harvard Medical School. 4.Laboratory for Molecular Medicine, Partners Personalized Medicine; ³Key Laboratory for Developmental Genes and Human Disease, Ministry of Education, Institute of Life Sciences, Southeast University anjing, China; ⁴Key Laboratory for Developmental Genes and Human Disease, Ministry of Education, Institute of Life Sciences, Southeast University.

In human, myosin VI (MYO6) gene is located on chromosome 6q13, encoding the actin-associated molecular motor that is vital for auditory and vestibular function. Deficiencies of MYO6 gene lead to either dominant or recessive forms of hearing loss. Given the high homology of this gene between mammals, we previously established a mouse strain to copy the C442Y missense mutation of MYO6 gene, which renders autosomal semi-dominant nonsyndromic hearing loss that resembled DFNA22 variant in human. Here we found that in comparison to wild type mice, both homozygous C442Y mice Myo6A/A-C442Y and heterozygous C442Y mice Myo6A/G-C442Y showed progressive hearing loss beginning from 3 weeks after birth. And the time elapse severely aggravated this hearing impairment as profound deafness appeared on these mutant mice around their 6 to 9 weeks of age. Simultaneously, the degeneration of hair cells in organ of Corti and disorganised hair bundles with irregular morphological features could be seen by scanning electron microscopy and immunohistochemistry tests. Additionally, phenotypes of Myo6A/A-C442Y mice deteriorate more drastically than those in Myo6A/G-C442Y mice during the time course of research. This novel Myo6-C442Y mutant mouse strain, whose auditory performances resemble the progressive postlingual sensorineural deafness in corresponding human kindred very much, provides a useful model for elucidating the role myosin VI plays in the mammalian auditory system. Meanwhile, the late-onset hearing loss of this mouse strain may provide a therapeutic window for the emerging gene therapy, a promising strategy to treat certain forms of genetic deafness.

PS 407

Two Different Sequencing Platforms Identified an Additional Phenotype Caused by a HOXA2 Variant in a Family with Mixed Hearing Loss and Middle Ear Anomaly without Microtia

Yoshihiro Noguchi¹; Shin-ya Nishio²; Shin-ichi Usami³

¹Department of Otorhinolaryngology-Head and Neck Surgery, International University of Health and Welfare School of Medicine; ²Department of Hearing Implant Sciences, Shinshu University School of Medicine;

³Department of Otorhinolaryngology, Shinshu University School of Medicine

Two different platforms for Whole Exome Sequencing (WES) are commonly used for genetic analysis: (1) super-multiplex PCR based enrichment like Ion AmpliSeq with IonProton sequencer, and (2) hybrid capture based enrichment like SureSelect with illumine HiSeq sequencer. These two types of WES have quite different enrichment strategies; therefore, variants identified in both platforms are considered appropriate

for validated status. In this study, two types of WES analysis by using both Ion AmpliSeq Exome/Ion Proton and Agilent SureSelect/illumine HiSeq platforms and the combined data analysis were performed for a Japanese family with autosomal dominant nonsyndromic mixed hearing loss and middle ear anomaly without apparent microtia. In addition, screening for a candidate gene variant were performed for 18 individuals with middle ear anomaly or microtia. Two platform analysis detected four potential causative variants, including a duplication variant in HOXA2, a deletion variant in MYCT1, and two non-synonymous missense variants. Direct sequencing confirmed that all the four variants were segregated with hearing loss. However, the two missense variants were predicted as “tolerated” in bioinformatics tools. Furthermore, MYCT1 was not likely to be a candidate causative gene, because it is thought to be a candidate tumor suppressor gene. Therefore, we considered HOXA2 to be the most potential candidate causative gene. Direct sequencing analysis detected no pathogenic or likely pathogenic variant in HOXA2 for the 18 patients with middle ear anomaly or microtia. Previous publications reported that HOXA2 variants were responsible for autosomal recessive or dominant microtia with or without hearing loss in three unrelated families. The findings of this study suggested that a novel HOXA2 variant could be responsible for an additional phenotype to HOXA2-related disorders in terms of the absence of microtia. Furthermore, the combination analysis of two different WES strategies was powerful tool to reduce false positive and/or sequencing errors identified through only each technic.

PS 408

Genetic Basis of Auditory Pathology in the Belgian Waterslager Canary

Farrah N. Madison¹; Matthew A. Conte²; Gregory F. Ball¹; Jane A. Brown¹; Ronna Hertzano³; Karen L. Carleton²; Robert J. Dooling⁴

¹Department of Psychology; ²Department of Biology;

³University of Maryland Baltimore-School of Medicine;

⁴Department of Psychology, University of Maryland

Canaries have been bred for several hundred years for song quality or plumage and it is possible that other phenotypic traits may have also been changed as a result of this artificial selection. For example, it has long been known that Belgian Waterslager (BW) canaries have damaged and missing hair cells in the apical end of the basilar papilla resulting in poor high frequency hearing. Tests on cross-bred and back-crossed birds indicates a factor linked to the Z chromosome is responsible for this pathology. We sought to investigate further the genetic basis for this frequency hearing loss in BW canaries by characterizing the putative Z chromosome factor causing

this auditory pathology. We conducted whole-genome Illumina sequencing in three canary strains: Border (male, n=5), American Singer (male, n=5), and BW (male=3, female=2). Individual genomes were aligned to a modified canary reference anchored to chromosomes using zebra finch. SNP and indel calls were filtered using SnpEff for high-impact variants that were unique to BW males. Hearing thresholds were also measured in these birds both physiologically (auditory brainstem responses) and behaviorally (psychophysics). All Border canaries had normal hearing and all BW canaries had a high-frequency hearing loss. Interestingly, all American Singer canaries also showed varying degrees of impaired hearing. A total of 20 BW-male specific high-impact variants were identified. Several of these mutations occurred within genes previously identified in mammalian hair cell abnormalities and hearing loss disorders, including two on the Z chromosome. These candidate gene mutations present a first step in the investigation of the molecular mechanism(s) of high-frequency hearing loss in the BW canary. And it is worth considering the possibility that breeders, in artificially selecting for certain song characteristics, may have also selected for an auditory pathology.

PS 409

Characterization of Usher syndrome Natural History in Pcdh15KI/KI mice

Saamil Sethna¹; Arnaud P.J. Giese²; Saima Riazuddin³; Zubair M. Ahmed³

¹University of Maryland Baltimore; ²University of Maryland School of Medicine; ³University of Maryland, School of Medicine

Usher syndrome (USH), is a neurosensory disorder characterized by partial or total hearing loss (HL), balance problem, and vision loss due to retinitis pigmentosa (RP) that worsens over time. Almost all of the known variants in PCDH15 (USH1F) are private mutations, except p.Arg245*, which has a carrier frequency of approximately 2% in the Ashkenazi Jewish population. Using CRISPR/Cas9 technique we generated Pcdh15 p.Arg250* (orthologue of human p.Arg245* allele - Pcdh15KI) mice. Here we report natural history of vision, hearing, balance loss, and associated physiopathology in Pcdh15KI/KI mice. At P16-P30, control Pcdh15KI/+ mice have normal auditory brainstem response (ABR) waveforms and thresholds. However, Pcdh15KI/KI homozygotes do not respond to click or tone pip stimuli of 100 dB SPL, indicating that they are profoundly deaf. By P60, outer hair cells (OHCs) of Pcdh15KI/KI mutant mice were degenerated in the mid-basal part of the cochlea, while, inner hair cells (IHCs) remained largely intact. Similarly, Pcdh15KI/KI mice showed repetitive circling and severe head bobbing behaviors. To quantify

the vestibular dysfunction, we performed tail-suspension, and swimming tests, at P16. The swimming test showed that Pcdh15KI/KI mice were not able to swim at all, and the tail hang test revealed that the vestibular function was drastically impaired. Contrary to the organ of Corti, the vestibular hair cells were mostly preserved at P60 but have highly disorganized and thin stereocilia bundles at their apical surface. Finally, retinal functional testing using electroretinograms (ERGs) revealed significant attenuation of both a- and b-waves in Pcdh15KI/KI mice as compared to littermate controls at P30, while, in vivo, non-invasive imaging of the retinal layers revealed no gross retinal dysmorphology at this age. Taken together our Pcdh15KI mice faithfully recapitulates all three human USH1 phenotypes. Currently, we are using this valuable mammalian model to identify and study the safety and efficacy of therapeutic options, like nonsense read-through, gene delivery and genome editing techniques.

Support: This work was supported by the Usher 1F Collaborative (Z.M.A.).

PS 410

Investigating the Role of Tricellulin Interactors in the Tricellular Junctions of the Inner Ear.

Adam R. Chambers¹; Dimitria Gomes¹; Arnaud P.J. Giese²; Zubair M. Ahmed¹; Saima Riazuddin¹

¹University of Maryland, School of Medicine; ²University of Maryland School of Medicine

Mutations in tricellulin (TRIC) —the first known transmembrane protein specific to tricellular tight junctions (tTJs)—have been implicated in moderate to profound deafness in humans and mice (Riazuddin et al., 2006; Nayak et al., 2013). Previous studies have presented evidence that this phenotype is due to a loss of barrier function in the reticular lamina of the organ of Corti, strongly suggesting a critical role in maintaining the ion composition of the fluid compartments of the inner ear (Nayak et al., 2013).

TRIC is known to interact with angulin family proteins (LSR, ILDR1 and ILDR2), which are also localized to tTJs. Interestingly, mutations in the angulin family coding genes also cause nonsyndromic deafness (Higashi T, et al., 2013). To further characterize TRIC molecular network in the inner ear, and to elucidate the intracellular pathways required to maintain tricellular junctions and prevent hair cell death in the cochlea, we performed a yeast two-hybrid screen using the cytosolic domain of TRIC as a bait, and a cochlear cDNA prey library. Our study identified several known (e.g. LSR and TUBA) as well as novel potential interactors. To validate these

intracellular interactions, co-immunoprecipitations, nano Scale Pull Down, as well as co-localization assays have been performed. The potential cytosolic interactors investigated in this study are essential for signaling and apoptotic pathways, ubiquitination and endocytosis of junctional proteins. Their immunocolocalization was analyzed in the inner ear of tricellulin mutant mice. These preliminary results increase our understanding of the molecular composition and assembly of tTJs in the inner ear and suggest that TRIC may have a unique role in the cell, mediated by a cytoplasmic domain not shared by other proteins of its type.

Grant support information: R56DC011803 (SR).

PS 411 - WITHDRAWN

PS 412

Genotype-Phenotype Studies are Fundamental to the Introduction of Inner Ear Therapies

Ronald Pennings; Jeroen Smits; Mieke Wesdorp; Cris P. Lanting; Wouter Koole; Ilse Feenstra; Helger Yntema; Hannie Kremer
Radboud University Medical Center

Research background

Over the past decades, many genes have been identified to cause hereditary hearing impairment (HI). More recently, the attention is also shifting towards the development of inner ear molecular therapies. The first clinical trials to treat sensorineural HI have already started. The pathogenic mechanisms underlying HI in the inner ear are, however, complex and in order to be successful, we believe that all future inner ear therapies should include genotype-phenotype evaluations. This study presents an overview of the results from genotype and phenotype evaluations in a large Dutch cohort of patients with HI seen over the past six years.

Methods

Since 2015, whole exome sequencing (WES) targeting a panel of (100-140) HI-related genes, has been implemented in ENT and Genetics out-patient clinics of all university medical centers in the Netherlands. All genetic tests are reimbursed by national health insurance companies. Since 2015, WES has been performed for approximately 900 index patients, mostly of Dutch origin with presumed hereditary HI. Hearing impairment was assessed by pure tone and speech audiometry. On indication, a more extensive phenotypic evaluation was performed by imaging, psychoacoustic, vestibular and

other measures. Genotype evaluation consisted of WES or targeted single gene testing guided by phenotype analyses. The results for single gene testing in a cohort of patients with HI seen in 2013 and 2014 are used as a reference.

Results

Causative variants underlying HI were identified in ~35% of patients. The diagnostic yield for HI using WES targeting a HI gene panel is higher than targeted sequencing of single genes. Heterogeneity of hereditary HI was confirmed and the leading causes in our patient cohort were causative variants in GJB2, USH2A, MYO15A, STRC, MYO6 and COCH. Analyses of the whole exome data (beyond the gene panel for HI) revealed four novel human deafness genes, including MPZL2 and LMX1A, and related audiovestibular impairment is evaluated and presented.

Conclusions

The diagnostic yield for HI using WES targeting a HI gene panel is higher than targeted sequencing of single genes. Using WES also enables us to screen for novel deafness genes by performing an exome-wide analysis. Segregation analysis is important to evaluate variants of uncertain significance and further increases the diagnostic yield of WES. A practical workflow for genetic testing of hereditary HI for screening in the out-patient clinic will be presented. In-depth genotype and phenotype evaluations should be part of future inner ear therapies.

PS 413

Establishment and preliminary results of a hereditary SSD Bama Miniature pig model

Hui Zhao; Wei Ren; Cong Xu; Weiwei Guo; Shi-ming Yang
PLA General Hospital

Background

Single side deafness (SSD) becomes a clinical concern in recent years with a high incidence of nearly 1/1000 in infants. SSD can negatively affect life quality because of cognitive and social developmental delay. However, etiology of UHL remains unknown, it can be inherited as part of a syndrome, e.g. Waardenburg syndrome, or it can also be induced by environmental factors such as prematurity, trauma, or meningitis. Moreover, patients benefit little from the limited treatments, including cochlear implant. In 2015, we discovered a spontaneous SSD Bama miniature pig, after a four-generation breeding scheme, we finally obtained a SSD porcine model with a high penetrance of 40%.

Methods

Auditory Brainstem Response (ABR) (TDT RZ6), both click and tone burst, was used to assess the auditory electrophysiology at P1, P7, P14, P30, P180, age of 1, 2, 3 and 4. Celloidin embedding and H&E staining (CE-HE) were used to assess the morphology of inner ear. Scanning electron microscopy (SEM) and transmission electron microscopy (TEM) were used to examine the morphology of hair cells and stria vascularis.

Results

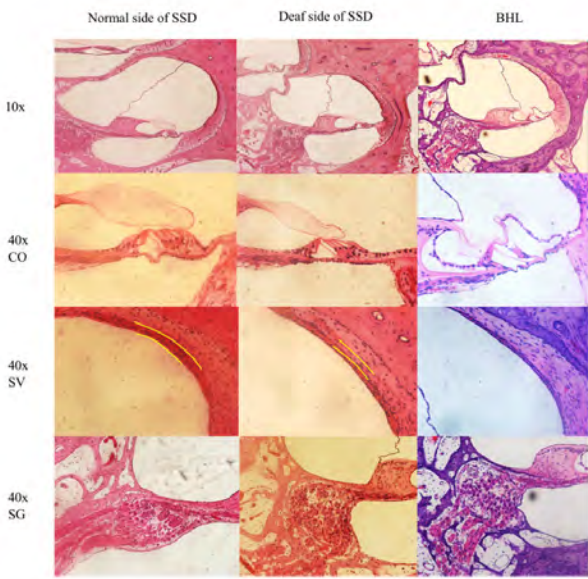
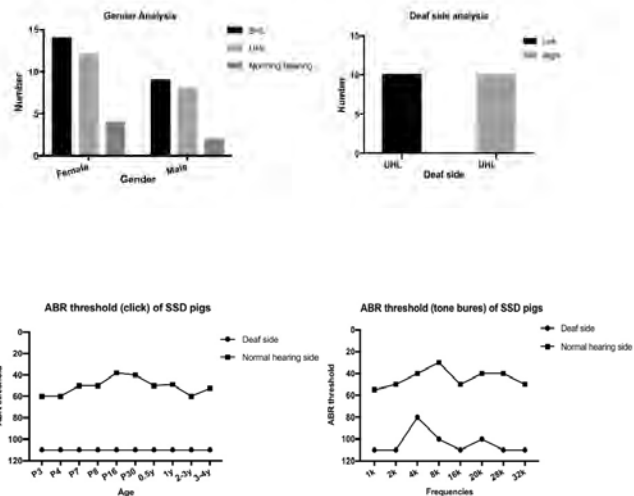
We successfully found and established a four-generation Bama miniature model with SSD. A total of 30 pigs with SSD were obtained in this pedigree. 50 pigs were obtained in the 4th generation, among them 20 exhibited unilateral deafness (penetrance=40%), 23 exhibited bilateral deafness, 5 exhibited bilateral normal hearing, 1 exhibited asymmetric hearing loss and 1 died during delivery. (Figure 1)

No auditory response was evoked at 100 dB SPL by both click and tone burst at frequencies of 1k, 2k, 4k, 8k, 16k, 20k, 32k in all SSD pigs'; deaf side while responses were all successfully evoked in the normal side. Auditory thresholds of all offspring remained unchanged through ages. (Figure 2)

CE-HE showed thinner stria vascularis in SSD deaf side than both its normal side and control cochlea without other significant changes. BHL presented much thinner stria vascularis and disruption of supporting cells compared to SSD deaf side. (Figure 3)

Conclusion

These results firstly indicated that SSD might be a congenital and hereditary disease. This porcine model might provide us as a tool to further explore the mechanism and causative gene of UHL in the future.

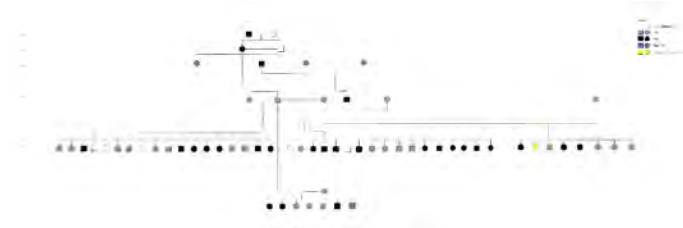


PS 414

Inducible Conditional Deletion of Gjb2 Leads to Reduction of Endocochlear Potential and Elevation of ABR Thresholds Without Loss of Hair Cells or Neurons

Donna M. Martin¹; Jennifer M. Skidmore²; Xiaobo Ma³; Jelka Cimerman⁴; Lisa A. Beyer³; Donald L. Swiderski³; Yehoash Raphael³

¹Depts. Pediatrics and Human Genetics, University of Michigan; ²Dept. Pediatrics, University of Michigan; ³Kresge Hearing Research Institute, Department of Otolaryngology-Head and Neck Surgery, University of Michigan; ⁴Department of Pediatrics, University of Michigan



Mutations in GJB2, encoding connexin26 (Cx26), are the most common cause of autosomal recessive hereditary deafness. Despite high prevalence, specific pathogenic mechanisms leading to GJB2-related hearing loss are not understood, and there are no cures. Individuals with GJB2-related hearing loss exhibit normal organ of Corti morphology and spiral ganglion neurons (SGNs), suggesting the mechanisms of hearing loss do not involve major disruptions in morphology of auditory epithelia or nerves. In contrast, mice with conditional loss of Gjb2 in supporting cells (Sox10Cre;Gjb2flox/flox) exhibit profound loss of hair cells and SGNs. To provide a better model which more closely resembles human patients with GJB2 mutations, we generated mice with inducible Sox10iCre -mediated loss of Gjb2. To delete Gjb2, tamoxifen was injected intragastrically in Sox10iCreERT2;Gjb2flox/flox animals and Gjb2flox/flox littermates at postnatal day 1 (P1) or intraperitoneally at P14. Mice injected at P1 were allowed to mature until P21 to determine if Cx26 is required for the onset of hearing, and mice injected at P14 were allowed to mature until P21 or P35 to determine if Cx26 is required for the maintenance of hearing. Hearing was analyzed using ABR audiometry and ears were collected from the same animals and analyzed histologically. Deletion of Gjb2 was confirmed by reduced anti-Cx26 staining in ears from mice injected at P1 and P14. Gjb2 deletion at P1 led to severe hearing loss, and no major changes in hair cell organization. Similarly, Gjb2 deletion at P14 resulted in no changes in hair cell organization and progressively decreased hearing ability with prolonged Gjb2 loss (analysis at P35 vs P21). In mice with prolonged Gjb2 loss, endocochlear potential was reduced significantly. As a first step for testing phenotypic rescue by gene replacement therapy in these mice, we confirmed that injecting AAV2.GFP into the cochlea of young pups leads to gene expression in supporting cells. These studies demonstrate important roles for Cx26 in development and maintenance of hearing.

Supported by NIH-NIDCD grants R01-DC014832, R01-DC010412, R01-DC009410, R01-DC014456 and P30-DC005188, The Donita B. Sullivan M.D. Research Professorship in Pediatrics and Communicable Diseases (DMM) and The R. Jamison and Betty Williams Professorship (YR). We thank Leda Dimou for the Sox10iCreERT2 mice and Xi Lin for the AAV vectors.

PS 415

Variant Identification in Whole Exome Sequencing of Patients with Adult Onset Hearing Loss

Morag A. Lewis¹; Lisa S. Nolan²; Barbara Cadge²; Sally J Dawson³; Lois J. Matthews⁴; Bradley A. Schulte⁵; Judy R. Dubno⁴; Karen P. Steel⁶

¹King's College London; ²UCL Ear Institute; ³UCL Ear Institute, University College London.; ⁴The Medical University of South Carolina; ⁵Medical University of South Carolina; ⁶King's College London and Wellcome Trust Sanger Institut

Hearing loss is one of the most common sensory deficits in the human population, and it has a strong genetic component. However, although to date more than 140 loci relating to human hearing loss have been mapped, and over 100 genes identified, the majority of genes involved in hearing remain unknown. It is also unclear whether adult-onset hearing loss results from rare Mendelian gene variants with large effect size or multiple variants each making a small contribution to hearing loss. Several genome-wide association studies have been carried out, but only five loci have been associated with hearing status at the genome-wide significance level.

We have therefore chosen to carry out whole exome sequencing to explore the landscape of variation associated with adult-onset hearing loss. However, pathogenic variant identification is a challenge in common complex diseases. In our pilot study of 30 exomes from people with hearing loss, we found each individual bore predicted pathogenic variants in multiple deafness genes, and the same was true of exomes from the 1000 Genomes project (for which there was no phenotypic data). This was an unexpected finding, and has significant implications for current diagnostic sequencing in deafness as well as for gene discovery research.

We are proceeding with exome sequencing analysis on a further 532 exomes, including 78 from older people with normal hearing, which is a more appropriate control population. We have identified several interesting mutations from our work, and are following up on candidate novel deafness genes.

This work was supported by NIH/NIDCD.

PS 416

High Throughput Deafness Gene and Drug Screening System Using Acoustic Startle Response of Zebrafish

Jinming Yang; Weitao Jiang; Meide Du; Ling Zheng;
Fangyi Chen
Southern University of Science & Technology

Background

Clinical treatment of sensorineural deafness is an important field in hearing research. FDA has not approved any drugs that could be used for the treatment or protection of sensorineural deafness. In this situation, there is a need of developing an efficient drug screening system to test the effect of the drug to the inner ear system.

Zebrafish is an immersing animal model in auditory system study. Zebrafish has high comparability to humans, good accessibility to the hearing organ and high throughput capacity. By evaluating auditory function of zebrafish, we can study the deafness gene and drug effect to the inner ear.

To develop a efficient deafness gene and drug screening system, we designed an automatic high throughput startle response testing system. The system could evaluate the auditory function and measure the hearing threshold of zebrafish larvae.

Methods

Experiments were approved by the Institutional Animal Care and Use Committees at Southern University of Science and Technology. The subjects were zebrafish larvae. The fish were contained in 10 petri dishes (20 fish in each dish). A mechanical vibrator was used to generate acoustic stimulation. Pre-pulse inhibition was used to detect hearing threshold, which is much higher than the threshold of the startle response. Then the movements evoked by the stimulus were recorded by a camera. The camera was fixed on a moving stage. The moving stage enables the camera to record the startle response from ten dishes in sequence. By analyzing the captured video, the velocity and distance of the movement of each fish were calculated to quantify the startle response. The hearing threshold was achieved by analyzing the startle response.

Result

Stronger stimulus resulted larger startle response. The startle of gentamicin treated zebrafish larvae was

significantly smaller than the control group. Histological analysis highlighted hair cell damage in zebra fish larvae inner ear.

Conclusions

The startle response to vibration stimulus compared well with previous observations. This system could measure 200 samples in a run. This high throughput behavior testing system provides a potential new method for drug and deafness gene screening.

Supported by

the National Natural Science Foundation of China (8177188 and 81470701 to FC) and 2018 Shenzhen Basic Research Fund (JCYJ20170817111912585 to FC)

PS 417

Kinesin light chain 2 mutation causes age-related progressive hearing loss in mice

Elisa Martelletti¹; Neil J. Ingham¹; Chi Chung Lam¹;
Felix D. Weiss¹; Jing Chen²; Karen P. Steel²
¹King's College London; ²King's College London and
Wellcome Trust Sanger Institute;

Kinesin light chain 2 (Klc2) together with kinesin heavy chains (Kif5) forms the kinesin-1 motor complex, which is involved in the microtubule-associated anterograde transport of organelles and macromolecules. In humans, a gain-of-function KLC2 mutation (216bp deletion upstream of the coding region) was described leading to increased KLC2 expression and a neurodegenerative disorder involving progressive axonal neuropathy (Melo et al., 2015).

Klc2 mutant mice (Klc2tm1e(EUCOMM)Wtsi) mutant mice were generated as part of the Sanger Institute Mouse Genetics Project and exhibited progressive hearing loss starting at low frequencies at 2 weeks old. The ABR thresholds were gradually increased at all frequencies by 6 months old. At this age, the distortion product otoacoustic emissions (DPOAEs) were also severely impaired, whereas the endocochlear potential was maintained at a normal level, but the anoxia potential in scala media was significantly less negative in the Klc2 mutants. X-gal staining on wax sections, using a LacZ reporter in the allele, revealed that Klc2 is widely expressed in the cochlear duct, especially in the spiral ganglion. Klc2 mutant mice showed no major abnormalities in the overall structure of the middle and inner ear. In contrast, within the inner ear at one-month old there was extensive loss of outer hair cell (OHC) hair bundles, DAPI-stained OHC nuclei and CtBP2-

labelled presynaptic ribbons of OHCs in the region that normally responds best to 12kHz, corresponding to the worst ABR thresholds. There were few signs of inner hair cell (IHC) degeneration. *Klc2* is involved in the anterograde transport of GluR1/2-containing vesicles to axon terminals, but we found no abnormality in GluR2-labelled postsynaptic densities below mutant IHCs suggesting other transport systems must move this AMPA receptor to the membrane. As it has been reported that *Klc2* interacts with *Kcnma1*, a calcium-activated potassium channel in hair cells, we investigate the labelling of *Kcnma1* in IHCs and we found that at 4 weeks old it was less extensive in mutants compared with littermate controls at 12kHz.

Overall, *Klc2* mutant mice show age-related progressive hearing loss revealed by increased ABR thresholds associated with impaired DPOAEs, suggesting that the OHCs contribute to the phenotype. As the increase in ABR threshold is larger than would be expected if only OHCs are affected, we can suggest that IHCs have also impaired function which might be partly linked to the reduction in *Kcnma1* expression.

PS 418

Clarin-2 is Required for Maintenance of Mechanotransducing Stereocilia and Essential for Hearing

Lucy Dunbar¹; Pranav Patni²; Carlos Aguilar¹; Philomena Mburu¹; Laura Corns³; Helena RR. Wells⁴; Sedigheh Delmaghani²; Andrew Parker¹; Stuart Johnson³; Lauren Chessum¹; Andrea Lelli²; Gemma Codner¹; Sara Wells⁵; Frances MK. Williams⁴; Christine Petit²; Sally J Dawson⁶; Steve Brown¹; Walter Marcotti⁷; Aziz El-Amraoui²; Michael Bowl¹

¹*Mammalian Genetics Unit, MRC Harwell Institute;* ²*Génétique et Physiologie de l'Audition, Institut Pasteur;* ³*Department of Biomedical Science, University of Sheffield;* ⁴*Department of Twin Research & Genetic Epidemiology, King's College London.;* ⁵*Mary Lyon Centre, MRC Harwell Institute;* ⁶*UCL Ear Institute, University College London.;* ⁷*The University of Sheffield*

Background

Inner and outer hair cells (IHCs and OHCs) convert sound wave-induced mechanical stimuli into neuronal signals. They detect these stimuli via hair bundles protruding from their apical surface. These bundles consist of a highly organised array of actin-filled stereocilia arranged in a 'staircase' pattern, which when deflected leads to opening of mechanically-gated cation channels in the shorter 'mechanotransducing' stereocilia. While we know some of the genes and processes involved in hair

cell development, we currently do not understand all the molecular mechanisms underlying bundle formation, maintenance, or mechanotransduction.

Aim

Characterize *clarin2*, a novel ENU-induced mouse model of early-onset hearing loss, which has identified *Clarin-2* as critical for hearing.

Methods

We have undertaken a comprehensive characterization of the *clarin2* mouse mutant including: a complementation test to confirm that the *Clarin-2* gene, *Clrn2*, underlies the *clarin2* phenotype; auditory, vestibular, and retinal phenotyping studies to investigate the requirement of *Clarin-2* for hearing, balance and vision (*Clrn2* is a paralogue of the Usher syndrome 3a gene, *Clrn1*); scanning electron microscopy to ascertain hair cell stereocilia bundle architecture; cochlear RT-PCR and immunolabelling to determine the expression of *Clrn2* and localization of proteins critical for hearing; and, electrophysiological studies to assess the function and maturation of cochlear sensory hair cells.

Results

clarin2 mutants exhibit a severe, early onset, progressing hearing loss and reduced otoacoustic emissions, suggesting dysfunction of both IHCs and OHCs. However, they have normal retinal responses and do not show overt balance deficits. Ultrastructural analyses show that hair cell bundles develop normally during the early postnatal period, thereafter the shorter row stereocilia begin to regress, with the shortest row OHC stereocilia almost completely absent by 16 days of age. Consistently, we found that IHCs and OHCs both display significantly reduced mechano-electrical transducer (MET) channel currents.

Conclusion

Our studies of *clarin2* mice show that *Clarin-2* is essential for hearing, but dispensable for vision and balance. *Clarin-2* is critical for the maintenance of the hair cell bundle staircase. While the hair bundles are patterned correctly and begin to develop normally, the shorter 'mechanotransducing' stereocilia later progressively regress at terminal differentiation stages. Consistent with these data, IHC and OHC maximal MET channel currents are reduced in *clarin2* mice. Finally, utilizing the UK Biobank data, *CLARIN2* has independently been identified as a gene highly associated with human adult hearing, indicating the role of *Clarin-2* in mammalian hearing is likely conserved between mouse and human.

PS 419

A Human Variant of PCDH15 affects Hearing in the Mouse.

Neil J. Ingham¹; Alberto Capurro¹; Michal Szpak²; Chris Tyler-Smith²; Karen P. Steel³

¹King's College London; ²Wellcome Trust Sanger Institute; ³King's College London and Wellcome Trust Sanger Institut

Following the out-of-Africa expansion, humans have adapted to a diverse range of new environments and selective pressures. Scanning genomes for genetic signatures of such adaptations in populations yields lists of thousands of genetic candidates. Their functional validation and investigation of their biological consequences is a roadblock in the field and modelling of non-pathological human variation has received limited attention to date. Linking mouse phenotype to fitness in humans is complex; nevertheless, animal models provide one of the few ways to test hypotheses regarding recent human evolution.

Using a tool for pinpointing and prioritisation of candidate selected variants for functional follow-up studies (FineMAV; Szpak et al. 2018), a list of ~100 high-priority candidates across different continental populations was compiled. This included Protocadherin-15, a crucial gene for hearing function. A PCDH15 allele is highly selected in East Asia (Grossman et al. 2010). We have used CRISPR/Cas9 technology to knock this variant into the mouse; an A>C SNP confers a change from Aspartate, D, to Alanine, A, (GAC>GCC), producing a D-allele and an A-allele. This D435A polymorphism is predicted to have no affect on the structure or dynamics of Pcdh15 protein (Powers et al. 2017).

We used auditory brainstem response (ABR) recordings in the mouse to assess auditory function from 4 weeks old to 1 year old. We noted an unexpected difference in auditory phenotype between mice carrying the D-allele or the A-allele. From as young as 4 weeks old, mice homozygous for the A-allele demonstrated mild-moderate elevations of ABR threshold for tone pips of 24kHz and higher compared to mice homozygous for the D-allele. These elevations became progressively more pronounced as the mice aged and extended as low as 12kHz in older mice.

To further investigate functional differences between the two alleles, we measured supra-threshold features of the ABR, including wave 1 growth functions in response to different tone stimuli, frequency tuning curves measured at 12kHz and 24kHz, and responses to forward masking stimuli to allow estimations of the depth of adaptation of

wave 1 at short stimulus intervals and the time course of recovery from adaptation.

There is no reported difference in auditory function in humans carrying the two different alleles, but this requires further investigation.

References.

Grossman et al. (2010). *Science* 327: 883-886. doi: 10.1126/science.1183863

Powers et al. (2017). *Structure* 25: 1-14. doi : 10.1016/j.str.2017.01.014

Szpak et al. (2018). *Genome Biology* 19:5. doi: 10.1186/s13059-017-1380-2

PS 420

The Pathological Mechanism of Sensorineural Hearing Loss Caused by KCNQ4 Mutations

Koichiro Wasano¹; Satoe Takahashi²; Kazuaki Homma²

¹National Institute of Sensory Organs, National Hospital Organization Tokyo medical Center; ²Northwestern University Feinberg School of Medicine

Background

Kv7.4 (KCNQ4) is a tetrameric potassium ion channel abundantly expressed in the outer hair cells (OHCs). OHC dysfunction and subsequent degeneration of the cell underlie progressive sensorineural hearing loss caused by Kv7.4 mutations. The severity of hearing loss and the rate of progression vary depending on the kind of Kv7.4 mutations the patients carry, and haploinsufficiency and dominant negative effects are considered as the basis for understanding the various disease severity. However, these concepts do not readily account for: (i) the severe hearing loss associated with the c.725G>A mutation that truncates the Kv7.4 protein at the beginning of the S5 helix (Hildebrand et al., 2008), (ii) the recessive inheritance of the c.1044_1051del8 mutation that truncates the Kv7.4 protein before the C-terminal multimerization domains (Wasano et al., 2015), and (iii) the absence of hearing phenotype in heterozygous Kv7.4-KO mice (Kharkovets et al., 2006). In this study, we characterized three truncated human Kv7.4 proteins due to the c.211delC (p.Q71fs), c.725G>A (p.W242X), and c.1044_1051del8 (p.A349fs) mutations in a heterologous expression system in order to explore pathological mechanisms not based on haploinsufficiency or dominant negative effects.

Methods

HEK293T-based stable cell lines that heterologously express human Kv7.4 with c.211delC, c.725G>A, or c.1044_1051del8, with or without co-expressing wild-type (WT) Kv7.4, were generated. The electrophysiological properties of these cell lines were determined by the whole-cell patch-clamp technique. The effects of the Kv7.4 mutants on cell viability were determined using the RealTime-Glo MT Cell Viability Assay kit (Promega, Madison, WI).

Results

None of the three Kv7.4 mutants showed the potassium ion channel activity when singly expressed. Neither c.211delC-Kv7.4 nor c.1044_1051del8-Kv7.4 affected the potassium ion channel activity of co-expressed WT-Kv7.4. However, c.725G>A-Kv7.4 significantly inhibited WT-Kv7.4. All three Kv7.4 mutants, but not WT-Kv7.4, significantly impaired cell viability.

Conclusions

Assessing cytotoxic effect would be the key to fully appreciating both dominantly and recessively inherited mutations found in Kv7.4 (KCNQ4) and other KCNQ family of potassium ion channels.

PS 421

Hearing Impairment Due to Mir96 Mutations Suggests Both Loss and Gain of Function Effects

Morag A. Lewis¹; Francesca Di Domenico¹; Haydn M. Prosser²; Miguel A. Moreno-Pelayo³; Karen P. Steel⁴

¹King's College London; ²Wellcome Trust Sanger Institute; ³Hospital Universitario Ramon y Cajal; ⁴King's College London and Wellcome Trust Sanger Institut

miR-96 is a master regulator of hair cell maturation, coordinating the physiological and structural development of the hair cells. Mutations in the seed region of Mir96, which is critical for correct targeting, result in dominant progressive hearing loss in humans and in mice, but different mutations result in different auditory phenotypes. The mouse Mir96Dmdo mutation leads to early-onset hearing loss, but the two human mutations, MIR96s403 and MIR96s1334, lead to dominant progressive hearing loss after a decade or more of normal hearing.

We have previously shown that many genes are dysregulated as a result of the Mir96Dmdo mutation, indicating that miR-96 controls a complex network of genes in the inner ear. Some of the most downregulated genes, such as Ocm, Slc26a5 (prestin) and Ptprq, appear

to contribute to specific features of the Mir96Dmdo mutant phenotype. However, the Mir96Dmdo mutation causes both the loss of the normal targets of miR-96 and a gain of novel targets due to the new seed region, and it is not clear how much each contributes to the phenotype.

Here we present data from a mouse carrying a null allele of Mir96/183, and from mice carrying two of the mutations seen in humans, Mir96s1334 and Mir96s403. While homozygotes from all four Mir96 mutant lines exhibit profound deafness from the earliest age tested, the auditory phenotype of heterozygotes is much more variable; Mir96/183 and Mir96s403 heterozygotes have normal hearing, while Mir96s1334 heterozygotes develop progressive hearing loss at higher thresholds, and Mir96Dmdo heterozygotes exhibit early-onset, rapidly progressive hearing loss. Hair cell degeneration at young ages is seen only in Mir96Dmdo homozygotes, but abnormal stereocilia bundles are visible in all mutant mice except for Mir96s403 heterozygotes. RNA-seq analysis of RNA from the organ of Corti at P4 shows fewer genes are affected in Mir96/183 homozygotes than in Mir96Dmdo homozygotes, which corresponds to the auditory and structural phenotype.

Our finding of milder effects of a knockout allele compared with point mutations in Mir96 suggest that the gain of novel targets can play an important role in the phenotype caused by a microRNA mutation. All known Mir96 mutations cause hearing loss, so identifying regulatory interactions common to all four will allow us to focus on pathways critical for hearing. The genes involved in mediating the effect of a regulator such as miR-96 are candidate therapeutic targets.

PS 422

Alteration in FH2 domain of DIAPH1 causes late-onset human deafness via cell toxicity by loss-of-function mechanism

Bong Jik Kim¹; Shin-ichiro Kitajiri²; Takushi Miyoshi³; Seungmin Lee⁴; Jin Hee Han⁴; Hye-Rim Park⁴; Ah Reum Kim⁴; Jayoung Oh⁴; Min Young Kim⁴; Doo Yi Oh⁴; Takehiko Ueyama⁵; Byung Yoon Choi⁴

¹Chungnam National University College of Medicine;

²Shinshu University School of Medicine; ³Graduate School of Medicine, Kyoto University; ⁴Seoul National University Bundang Hospital; ⁵Laboratory of Molecular Pharmacology, Biosignal Research Center, Kobe University

Objectives:

DIAPH1 is the first gene reported to cause autosomal dominant nonsyndromic hearing loss primarily affecting

low frequencies. DIAPH1 gene encodes Dia1 protein (Diaphanous-related formins 1), which has several domains such as the GTPase binding domain (GBD), Dia Inhibitory Domain (DID), Dia Autoregulatory Domain (DAD), and formin homology domains (FH1 and FH2). Previously, p.R1049X of DIAPH1 residing in FH2 domain was suggested to be associated with very severe, early-onset phenotypes including microcephaly, blindness, and seizures in an autosomal recessive inheritance pattern. However, their audiologic phenotype was not thoroughly studied. Here we report that the same variant also could cause non-syndromic human deafness in a different inheritance pattern.

Methods:

A 72-year-old female (SB70-122) and her mother complained of progressive hearing loss that became prominent in their fifties. Targeted exome sequencing of 80 genes and bioinformatics analysis was performed to detect a candidate variant of hearing loss in this family. Functional studies were done to prove the pathogenic potential of the identified variant.

Results:

Genetic study revealed a nonsense variant of DIAPH1 (c.C3145T: p.R1049X) to be the candidate variant of hearing loss in SB70.

To examine the pathogenic potential of DIA1R1049X (Mutant), we made plasmids expressing AcGFP-tagged DIA1, and transfected them into HeLa cells. Expression levels of mutant evaluated by immunoblotting was surprisingly low compared with AcGFP-DIA1WT (Wild-type, WT). Mutant showed markedly low fluorescence intensity compared with WT. WT showed cytoplasmic localization, while mutant exhibited the plasma membrane localization, which was previously associated with pathogenic potential of the variants in DAD. Interestingly, it was almost impossible to find cells with high green fluorescence in the mutant-transfected dishes, and cells with relatively high green fluorescence showed round shape, suggesting that high expression of mutant may cause dysfunction of cells, thereby inducing cell death. R1049X-expressing cell were not positive to active caspase-3, indicating that the cell death was at least not through the apoptosis.

We also evaluated stress fiber and microvilli in AcGFP DIA1R1049X-expressing HeLa cells. While enhanced stress fiber formation and elongated microvilli were observed in AcGFP DIA1R1213X-expressing HeLa cells, showing constitutive activation in the previous study, these phenotypes were not observed in

AcGFP DIA1R1049X-expressing or AcGFP DIA1WT-expressing HeLa cells. These results could suggest that DIA1R1049X is not a constitutively active mutant, further possibly revealing that p.R1049X may exert a pathogenic potential of inducing cell death, not via constitutive activation proposed by the variant residing in DAD.

In single-molecule speckle microscopy (SiMS) study, most of R1049X XTC cells died, which seemed to be due to necrosis because the nuclei were left without fragmentation.

Conclusion:

Taken together, we report that p.R1049X of DIAPH1 could cause late-onset human deafness in a semi-dominant inheritance pattern for the first time, which is backed by genetic study and molecular cell biology study.

PS 423

Influence of SLC26A4 Haplotype upon Phenotype in Patients with Enlargement of the Vestibular Aqueduct

Janet Chao¹; Parna Chattaraj²; Tina Munjal³; Keiji Honda⁴; Kelly King²; Christopher Zalewski²; Wade W. Chien⁵; Carmen Brewer²; Andrew Griffith²
¹NIDCD, Yale University; ²NIDCD; ³NIDCD, Stanford University; ⁴NIDCD, Tokyo Medical and Dental University; ⁵NIDCD, Johns Hopkins University

Background: Recessive mutations of coding regions and splice sites of the SLC26A4 gene cause hearing loss with enlargement of the vestibular aqueduct (EVA). Some patients also have a thyroid iodination defect that can lead to multinodular goiter as part of Pendred syndrome. We previously reported a haplotype of variants upstream of SLC26A4, called CEVA, that acts as a pathogenic allele in trans to a mutation affecting the coding regions, including adjacent splice sites, of SLC26A4 (Chattaraj et al., *Journal of Medical Genetics*, 2017). In the current study, we hypothesized that CEVA, acting as a recessive mutant allele, is correlated with a less severe phenotype than mutations affecting the coding regions of SLC26A4. We also hypothesized that CEVA, acting as a genetic modifier, is correlated with a more severe phenotype in patients with mutations affecting the coding regions of both alleles of SLC26A4 or in patients with EVA caused by other factors.

Methods: This was a prospective cohort study of 114 individuals and 202 ears with EVA ascertained at the National Institutes of Health Clinical Center. To test our

first hypothesis, we compared the thyroid and auditory phenotypes of subjects with mutations affecting coding regions of both alleles of SLC26A4 with those of subjects carrying CEVA in trans to mutations affecting the coding regions. To test our second hypothesis, we compared the phenotypes associated with the presence versus absence of CEVA among subjects with no coding region mutations, as well as among subjects with mutations affecting coding regions of both alleles.

Results: Subjects carrying CEVA in trans to a mutation of SLC26A4 have a normal thyroid phenotype and less severe hearing loss in comparison to individuals with mutations affecting coding regions of both alleles of SLC26A4 (Fig. 1). Hearing loss in ears of subjects with no mutant alleles of SLC26A4 was more severe in subjects who were heterozygous or homozygous for CEVA. There was no correlation of CEVA with the phenotype of subjects with mutations affecting coding regions of both alleles.

Conclusions: We conclude that CEVA, acting as a pathogenic recessive allele, is associated with a less severe phenotype than alleles with a mutation affecting the coding regions or splice sites of SLC26A4. This is consistent with our previous observation that CEVA is a mildly pathogenic allele and homozygosity for CEVA is not sufficient to cause EVA. CEVA may act as a genetic modifier in patients with EVA caused by other factors.

Influence of SLC26A4 Haplotype upon Phenotype in Patients with Enlargement of the Vestibular Aqueduct

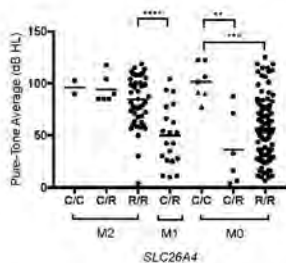


Figure 1. Four-frequency (0.5/1/2/4 KHz) pure-tone threshold averages for ears with enlargement of the vestibular aqueduct. Each data point represents one ear displayed according to SLC26A4 genotype status (M0, M1 or M2) and haplotype status (C, Caucasian enlarged vestibular aqueduct or CEVA, R, reference (most common haplotype)) **p<0.01, ***p<0.001, ****p<0.0001, Mann-Whitney Rank Test. M0 data points shown as a triangle (▲) correspond to CEVA homozygotes with one allele in cis with p.M775T, a hypofunctional variant thought to be pathogenic only in trans with a mutation affecting the coding region or splice sites.

PS 424

Correlation of Micro CT and Histopathology in SLC26A4-Null Mice Unveils the Cochlear Pathogenesis of Incomplete Partition Type II

Taku Ito¹; Taro Fujikawa¹; Ayane Makabe¹; Keiji Honda²; Yoshiyuki Kawashima¹; Takeshi Tsutsumi¹; Andrew Griffith³

¹Dept. of Otorhinolaryngology, Tokyo Medical and Dental University; ²NIDCD, Tokyo Medical and Dental University; ³NIDCD

Background: Incomplete partition type II (IP-II) is a cochlear anomaly associated with sensorineural hearing loss. IP-II was first described in 1791 as Mondini dysplasia, which was accompanied by an enlarged vestibular aqueduct and a dilated vestibule. While a normal cochlea has two and one-half turns, a cochlea with IP-II is generally thought to have one and one-half turns; the basal turns being normally formed with a dilated or cystic apical turn. Patients with IP-II are sometimes affected with Pendred syndrome, which is caused by SLC26A4 mutations.

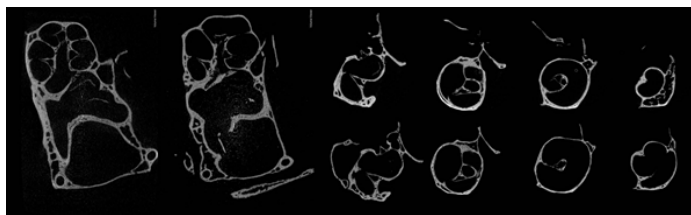
Goal: To reveal the pathogenesis of IP-II, Slc26a4-null mice were used as an animal model of cochlear anomaly.

Methods: The otic capsules of Slc26a4Δ/+ and Slc26a4Δ/Δ mice at 1, 8 days and 1 and 3 months of age were dissected out and fixed in 4% PFA for one week. The samples were imaged with micro CT, inspeXio SMX-100CT, at 10-micron resolution. A multiplanar reconstructed view was used to calculate the cochlear duct lengths, the angles of cochlear turns and apical heights from basal to apical end. Membranes and myelinated nerve fibers were identified by Osmium tetroxide (OsO₄) staining, if required. Next, the membranous labyrinth was carefully microdissected and immunostained with anti-MYO6 antibodies to count the number of inner hair cells and measure the length of the cochlear duct in a whole-mount preparation. Numeric data are presented as average ± SD.

Results: The otic capsules at 1 day of age were obscure because ossification was not complete. After 8 days of age, the ossicles, osseous labyrinth and otoconia were clearly visualized. Mid-modiolar planes revealed four cross-sections of cochlear duct separated by bony septa in Slc26a4Δ/+mice but only three cross-sections, at most, in Slc26a4Δ/Δmice. Apical turns looked cystic with severe endolymphatic expansion, which seemed to correspond to incomplete partition type II in humans. On the other hand, planes vertical to the modiolus revealed turns from the ductus reunion to the apical end, about 720 degrees in total, in both Slc26a4Δ/Δand

Slc26a4 Δ /+mice. The angles were nearly unchanged with age. Whole-mount preparations showed that the mean cochlear duct length in Slc26a4 Δ /+mice was 6.16 ± 0.06 mm while that in Slc26a4 Δ / Δ mice was 5.76 ± 0.18 mm at 1 day of age. There was a significant difference between the two groups ($p < 0.05$). At 8 days of age, mean cochlear duct lengths increased to 6.86 ± 0.01 and 6.36 ± 0.24 in Slc26a4 Δ /+ and Slc26a4 Δ / Δ mice, respectively, and a significant difference was still observed ($p < 0.05$). The average number of inner hair cells was 691.0 ± 14.7 in Slc26a4 Δ /+ while that was 657.7 ± 19.9 in Slc26a4 Δ / Δ . There was also a significant difference between the two groups ($p < 0.01$).

Conclusions: Micro CT analysis of Slc26a4-null mice suggested that incomplete partition type II seen on conventional CT reflects loss or deossification of bony septum due to congenital severe endolymphatic expansion. However, the membranous labyrinth is slightly smaller in IP-II. Further investigation is required to delineate how and when endolymphatic expansion leads to loss or deossification of bony septum.



PS 425

Deep Phenotyping and Computational Modeling of Highly Diverse Forms of Hearing Loss Due to Specific Gene Mutations Identified in Families from Newfoundland, Canada

Ian C. Bruce¹; Michael R. Wirtzfeld¹; Anne Griffin²; Amanda K. Morgan³; Matthew B. Lucas³; Jill Lowther²; Terry-Lynn Young²; Susan G. Stanton³

¹McMaster University; ²Memorial University Newfoundland; ³Western University

Many diverse genetic disorders have been molecularly characterized from the genetically isolated human population of Newfoundland, Canada. In some of these disorders, unrelated patients have been found to carry the exact same underlying genetic mutation due to a recent shared ancestor, the result of natural population expansion from a limited number of English and Irish settlers in the late 1700s. Among these, four distinct forms of genetic hearing loss have been recently reported: a CLDN14 autosomal recessive mutation, affecting the protein Claudin14 that regulates the formation of tight cellular junctions, produces precipitous

mid/high frequency hearing loss at around 4–6 years of age; a FOXL1 autosomal dominant mutation affecting the signaling protein FOXL1 gives rise to otosclerosis; a KCNQ4 autosomal dominant mutation affecting the Kv7.4 ion channel leads to progressive high frequency hearing loss; and a WFS1 autosomal dominant mutation, affecting the protein Wolframin that is involved in intracellular Ca²⁺ regulation, gives rise to a nonsyndromic low-frequency hearing loss.

The long-term goal of this project is to characterize the pathophysiology and resulting perceptual deficits experienced by affected family members. Computational models incorporating this pathology will then be utilized to develop improved hearing aid amplification strategies. The first stage of this project focuses on deep phenotyping of affected members of the KCNQ4 and WFS1 families, including the acquisition of advanced electrophysiological recordings (ABR and ECochG), word perception in quiet and noise, psychophysical tuning curves, and DPOAE growth functions, in addition to routine audiometric measures. The data from these recordings is being used, along with available animal models of the gene mutations, to inform the incorporation of appropriate pathology into the Bruce et al. (Hear. Res. 2018) model of the auditory periphery. Quantitative predictions of the electrophysiological and speech intelligibility data will be used for model validation. In this presentation, we will report on the analysis of deep phenotyping data collected from several members of each family and on computational models fit to those data. The impaired models will subsequently be used to optimize hearing aid amplification strategies to compensate for specific deficits caused by these genetic mutations, along with other individuals with similar patterns of pathophysiology.

[Supported by ACOA Innovative Communities Fund Project # 204210 and Business Development Program Project # 205595, the Government of Newfoundland and Labrador Regional Development Fund Ref # 30-11044-003, Excite Corporation, and NSERC Discovery Grant 261736.]

PS 426

First Independent Confirmation of TBC1D24 as an Autosomal Dominant Hearing Loss Gene and Audiological Characteristics of Affected Individuals

Dominika Ozieblo¹; Marcin Leja¹; Anna Sarosiak¹; Grazyna Tacikowska²; Krzysztof Kochanek³; Henryk Skarzynski⁴; **Monika Oldak**⁵

¹Department of Genetics, Institute of Physiology and Pathology of Hearing; Postgraduate School of Molecular Medicine, Medical University of Warsaw;

²Department of Otoneurology, Institute of Physiology

and Pathology of Hearing; ³Department of Experimental Audiology, Institute of Physiology and Pathology of Hearing; ⁴Oto-Rhino-Laryngology Surgery Clinic, Institute of Physiology and Pathology of Hearing; ⁵Department of Genetics, Institute of Physiology and Pathology of Hearing

Background

To date different genetic variants in TBC1D24 gene were causally involved in the development of neurological syndromes and profound prelingual hearing loss (HL) inherited in a recessive manner (DFNB86). In 2014 the first and so far only TBC1D24 pathogenic variant has been linked with postlingual autosomal dominant HL (DFNA65).

Material and methods

Five-generation Polish family participated in the study. Clinical exome sequencing on the proband's DNA and family segregation analysis of the identified variants were performed. Audiological assessment included pure tone audiometry (PTA), impedance audiometry, transient evoked otoacoustic emissions (TEOAE) and auditory brainstem responses (ABRs). Vestibular system function was evaluated using ocular and cervical vestibular evoked myogenic potentials (oVEMP, cVEMP). Temporal bone computed tomography was also performed.

Results

Genetic testing revealed a novel probably pathogenic c.553G>A (p.Asp185Asn) TBC1D24 variant, which fully segregated with HL in the studied family. Clinically, progressive HL involving mainly high frequencies was observed. No TEOAE were recorded in the study subjects and no or increased threshold of the stapedial muscle reflex was found. Function of the vestibulocochlear nerve measured by ABR was normal. No vestibular dysfunction and anatomical abnormalities of cochleovestibular system were detected.

Conclusions

Our results represent the first independent confirmation of TBC1D24 involvement in the development of autosomal dominant HL and the first thorough clinical characteristics of TBC1D24-induced autosomal dominant HL. The identified TBC1D24 variant affects the cochlear component of the auditory system and results in a high frequency HL usually observed in the third decade of life.

Supported by: 2016/22/E/NZ5/00470

PS 427

Evidence for Causative Role of PTPRQ in Autosomal Dominant Hearing Loss Development

Dominika Ozieblo¹; Anna Sarosiak¹; Marcin Leja¹; Henryk Skarzynski²; **Monika Oldak**³

¹Department of Genetics, Institute of Physiology and Pathology of Hearing ; Postgraduate School of Molecular Medicine, Medical University of Warsaw ; ²Oto-Rhino-Laryngology Surgery Clinic, Institute of Physiology and Pathology of Hearing; ³Department of Genetics, Institute of Physiology and Pathology of Hearing

Background

Hearing loss (HL) is the most common birth defect affecting about 1-6/1000 births and the most common disability of human senses. Genetic factors play an important role in the development of HL. The PTPRQ gene has been previously reported in the context of autosomal recessive HL and in 2017 for the first time in the development of autosomal dominant HL.

Material and methods

A five-generation Polish family with progressive, high frequency autosomal dominant HL was recruited for the study. Genomic DNA was isolated from peripheral blood samples or buccal swabs of available family members. Clinical exome sequencing was conducted in the proband's DNA sample. Family segregation analysis of the identified variants was performed using Sanger sequencing.

Results

Molecular genetic testing showed the presence of probably pathogenic c.6881G>A (p.Trp2294*) variant in the PTPRQ gene, which fully segregated with HL observed in the family. The identified variant is located in the last coding exon of the PTPRQ gene and introduces a premature stop codon. The c.6881G>A transition has not been reported in population databases. To date, the PTPRQ variant has been described in one family worldwide and is the only PTPRQ genetic variant causally involved in autosomal dominant HL.

Conclusions

Identification of the c.6881G>A variant provides an independent confirmation of the PTPRQ involvement in autosomal dominant HL, which is progressive, affects high frequencies and is usually diagnosed in the first decade of life.

Supported by: 2016/22/E/NZ5/00470

Exome Sequencing Reveals Novel Variants and Unique Allelic Spectrum for Hearing Impairment in Filipino Cochlear Implantees

Brittany Truong¹; Talitha Karisse Yarza²; Tori Bootpetch Roberts¹; Seema Lalani³; Karen Mohlke⁴; Nanette Lee⁵; Eva Maria Cutiongco-de la Paz⁶; Ma. Rina Reyes-Quintos⁷; **Regie Santos-Cortez**¹; Charlotte Chiong⁷

¹University of Colorado School of Medicine; ²Philippine National Ear Institute; ³Baylor College of Medicine; ⁴University of North Carolina; ⁵University of San Carlos; ⁶University of the Philippines Manila-National Institutes of Health; ⁷Philippine National Ear Institute

Worldwide cochlear implantation is a rehabilitation option for congenital hearing impairment in order for children to develop language and speech skills during the early years of development. However in poor countries where in general the burden of health care costs are carried by the patient, cochlear implantation may be restricted to patients who can afford the high cost of surgical, audiological and speech-language services out-of-pocket. For these patients, the study of factors that may impact cochlear implant outcomes is therefore beneficial. There are hundreds of genes identified for hearing impairment, and prevalence of genetic variants varies by population. In general, in patients of Asian descent, variants within GJB2 are the most common, followed by SLC26A4, MYO15A and CDH23 variants. Exome sequencing performed in a cohort of 30 Filipino cochlear implantees revealed a unique allelic spectrum that is different from other populations. Fifteen patients had pathogenic or likely pathogenic variants in known hearing impairment genes, of which eight are novel. A previously reported SLC26A4 c.706C>G (p.Leu236Val) remains the most common cause (13.3%) of hearing impairment in Filipinos. Rare, damaging novel variants identified for hearing impairment lie within the following genes: MYO15A, OTOA, DFNA5, EYA4, WFS1, COL4A3, MYH14 and CHD7. In addition, known variants were identified within GJB2, CDH23 and KCNQ4. Except for SLC26A4, all other variants were identified in a single patient. For each patient clinical correlations helped in determining the hearing loss-causal variant. Patients with genetic variants had significantly higher pre-surgical audiometric thresholds compared to patients in which no likely pathogenic variants were identified. There was no association between genetic variant and age at implantation, duration of implant use, and post-surgical audiometric thresholds. This suggests that although etiology may affect the severity of hearing loss at birth, in general carriage of the genetic variants identified in this study does not determine the outcome of cochlear implantation. Therefore cochlear implantation for individuals with the variants and genes identified in this report remains an excellent option for rehabilitation.

FUT2 Variants Confer Susceptibility to Familial Otitis Media

Regie Santos-Cortez¹; Charlotte Chiong²; Daniel Frank¹; Allen F Ryan³; Arnaud P.J. Giese⁴; Wasyl Szeremeta⁵; Harold Pine⁵; Melissa Scholes⁶; Norman Friedman⁶; Todd Wine⁶; Samuel Gubbels⁷; Stephen P. Cass⁸; Jeremy Prager⁶; Saima Riazuddin⁹; Patricia Yoon⁶; Sven-Olrik Streubel⁶; Herman Jenkins¹; Kenny Chan⁶; Tasnee Chonmaitree⁵; Zubair M. Ahmed⁹

¹University of Colorado School of Medicine; ²Philippine National Ear Institute; ³UCSD Surgery/Otolaryngology; ⁴University of Maryland School of Medicine; ⁵University of Texas Medical Branch; ⁶Children's Hospital Colorado; ⁷University of Colorado Anschutz Medical Campus; ⁸University of Colorado School of Medicine, Department of Otolaryngology; ⁹University of Maryland, School of Medicine

Non-secretor status due to homozygosity for the common FUT2 variant c.461G>A (p.Trp154*) is associated with either risk for autoimmune diseases or protection against viral diarrhea and HIV. We determined the role of FUT2 in otitis media susceptibility by obtaining DNA samples from 609 multi-ethnic families and sporadic individuals with otitis media. Exome and Sanger sequencing, linkage analysis, Fisher exact and transmission disequilibrium tests (TDT) were performed. The common FUT2 c.604C>T (p.Arg202*) variant co-segregates with otitis media in a Filipino pedigree (LOD=4.0). Additionally a rare variant c.412C>T (p.Arg138Cys) is associated with recurrent/chronic otitis media in European-American children (p=1.2x10⁻⁵) and US trios (TDT p=0.01). The c.461G>A (p.Trp154*) variant was also over-transmitted in US trios (TDT p=0.01) and was associated with shifts in middle ear microbiota composition (PERMANOVA p<10⁻⁷) and increased biodiversity. When all missense and nonsense variants identified in multi-ethnic US trios with CADD>20 were combined, FUT2 variants were over-transmitted in trios (TDT p=0.001). Fut2 is transiently upregulated in mouse middle ear after inoculation with non-typeable Haemophilus influenzae. Four FUT2 variants namely p.Ala104Val, p.Arg138Cys, p.Trp154* and p.Arg202* reduced A antigen in mutant-transfected COS-7 cells, while the nonsense variants also reduced FUT2 protein levels. Common and rare FUT2 variants confer susceptibility to otitis media, likely by modifying the middle ear microbiome through regulation of A antigen levels in epithelial cells. Our families demonstrate marked intra-familial genetic heterogeneity, suggesting that multiple combinations of common and rare variants plus environmental factors influence the individual otitis media phenotype as a complex trait.

DNA Methylation Dynamics in the Mouse Inner Ear Sensory Epithelium

Tom Ben-Dov¹; Ofer Yizhar-Barnea¹; Cristina Valensisi²; Naresh Doni Jayavelu²; Kishore Kamal³; Colin Andrus²; Tal Koffler-Brill¹; Kathy Ushakov¹; Kobi Perl¹; Yael Noy¹; Yoni Bhonker¹; Mattia Pelizzola³; R. David Hawkins²

¹Tel Aviv University; ²University of Washington;

³Fondazione Istituto Italiano di Tecnologia

DNA methylation, an epigenetic modification, is critical for regulating underlying genetic information. To evaluate global methylation at single-base resolution in the mouse inner ear, we performed whole genome bisulfite sequencing on sensory epithelium at key developmental stages: embryonic day 16.5 and postnatal days 0 and 22. To assess DNA methylation in both the CpG (mCG) and non-CpG (mCH) contexts, we generated 1.3 billion unique mapped reads, combining two biological replicates per each time point and with an average genomic coverage ranging from 11X to 19.5X. At P22, we observed a prevalence of mCH methylation in both CHG and CHH, similar to what has been found previously in neurons and the brain. To identify putative regulatory elements, we defined unmethylated and low-methylated regions (UMR/LMRs). As LMRs are representative of distal regulatory elements, we examined their overlap with known DNase I Hypersensitive Sites (DHS) in the mouse genome, which are indicative of transcription factor binding. We were able to assign a number of distal LMRs to functionally relevant genes with known roles in mouse inner ear development and deafness. We converted our mouse (mm10) LMR coordinates to human (hg19) coordinates using the UCSC LiftOver tool. We determined differentially methylated regions (DMRs), where there was at least a 30% loss or gain in methylation across the developmental and maturation transitions. Constructing in silico regulatory networks around sites of DMRs enabled us to link key inner ear regulators, such as *Atoh1* and *Stat3*, to pathways responsible for cell lineage determination and maturation, such as the Notch pathway. Finally, we further validated one of the LMRs found in the GJB2-GJB6 locus. Using the CRISPR-on system targeting this putative regulatory element, we showed expression modulation of both GJB6 and a non-coding RNA, suggesting the LMR can operate as a gene enhancer. These results represent the development of the sensory epithelium tissue as a whole and allow us to concentrate on the DNA methylation and epigenetic regulation of specific pathways and cellular populations of the inner ear.

Precision Medicine in Cochlear Implant Recipients: A Genomics-oriented Approach

Barbara Vona¹; Saskia Dofek¹; Saskia Biskup²; Sarah Fehr³; Marcus Müller⁴; Hubert Löwenheim⁵; Anke Tropitzsch¹

¹Hearing Research Center, Department of Otorhinolaryngology, Head & Neck Surgery, University of Tübingen Medical Center; ²Center for Genomics and Transcriptomics (CeGaT) GmbH and Practice for Human Genetics.; ³Center for Genomics and Transcriptomics (CeGaT) GmbH and Practice for Human Genetics; ⁴Hearing Research Center, Department of Otolaryngology - Head & Neck Surgery, University of Tübingen Medical Center; ⁵University of Tübingen

Precision medicine is the selection of patient treatment based on the genetics of patients. It is an emerging area in medicine that is fueled by the development and widespread availability of low cost sequencing technologies. Precision medicine for cochlear implant candidates is of high interest to develop optimized clinical algorithms based on molecular genetic outcomes. The “spiral ganglion hypothesis” proposes that cochlear implant recipients with genetic variants expressed in the neural partition of the cochlea have poorer outcomes than patients with genetic variants expressed in the sensory partition.

High-throughput sequencing gene panel diagnostics was performed in 284 patients that included 95 cochlear implant users. The most commonly affected genes in cochlear implant users were identified as GJB2, MYO7A, MYO15A, TECTA, and MYO6. Cochlear implant outcome was determined through a series of audiological tests before and after implantation. These tests included pure-tone, free field, and speech audiometry, as well as the Freiburger single syllable speech intelligibility tests routinely used in clinical practice. Patients with variants in genes expressed in the sensory partition of the cochlea, such as ACTG1, KCNQ4, and GJB2 scored with 80% speech intelligibility in the Freiburger test. Notably, five patients with variants in *TMPRSS3* were identified who scored with 10% speech intelligibility. This gene is expressed in the neural partition of the cochlea. Patients with variants in genes with overlapping neural and sensory partition-expressed genes such as *GIPC3* and *PAX3* scored with 70% to 80% speech intelligibility. Our results suggest that further research is required to understand the effects of variants that are expressed in the neural and sensory partitions of the cochlea and its impact on cochlear implant outcome.

PS 432

Cochlear Processing and Genetic Hearing Impairment: Site-of-Lesion Testing Beyond the Audiogram

Cris P. Lanting¹; Joop Leijendeckers²; Arjan Bosman¹; Ad Snik¹; Ronald Pennings³
¹Radboudumc; ²Pento; ³Radboud University Medical Center

Research background
The relation between the degree of hearing loss and the subsequent speech recognition scores is not straightforward. Impaired cochlear processing of sound due to genetic mutations may cause the same degree of hearing loss according to the audiogram but may result in very different speech recognition scores.

Methods

We studied nine different groups of patients with a genetic hearing loss (DFNA 8/12, DFNA10, DFNA13, DFNA22, DFNA18B/48B, Usher 2a, Muckle Wells, Non-ocular Stickler, HDR-syndrome) and we related speech recognition to cochlear processing as assessed by psychophysical measurements (loudness perception test, temporal and spectral processing tests). We further developed objective methods (based on DPOAEs, ECoChG- and ABR-measurements) aimed at assessing the cochlear site-of-lesion with new candidate genes where the mechanisms and site-of-lesion of sensorineural hearing loss are unclear.

Results

The results indicate that differences in speech perception between patient groups could be explained by psychophysical variables such as the loudness growth function and the frequency resolution. Different types of cochlear impairments and its underlying site-of-lesion could be identified and distinguished. Speech understanding was primarily related to malfunction of various parts of the cochlea due to genetic mutations, and not to the degree of hearing loss.

Conclusions

This work shows that the combination of psychophysics and objective methods can be used to assess the exact site of lesion in the cochlea in a range of genetic mutations leading to different types of cochlear impairments and thus different speech recognition scores. These insights will be further used to guide rehabilitation with hearing aids.

Hair Cells: Mechanotransduction

PS 433

Top-Connector Mediated Cooperativity of Hair Bundle Mechano-Electrical Transduction Channels Detected by Atomic Force Microscopy

Alexander Cartagena-Rivera¹; Elisabeth Verpy²; Paul Avan³; Christine Petit⁴; Richard Chadwick⁵
¹National Institute on Deafness and Other Communications Disorders; ²Institut Pasteur; ³University of Auvergne; ⁴G n tique et Physiologie de l'Audition, Institut Pasteur; ⁵National Institute on Deafness and Other Communication Disorders

Coordinated mechanical opening of mechano-electrical transduction (MET) channels, required for optimal hearing sensitivity, is thought to be related to coherent bundle motion. Stereocilin-deficient (*Strc*^{-/-}) mice lack horizontal top connectors in outer hair cell (OHC) stereocilia bundles causing loss of hair bundle cohesion and progressive hearing loss. Avan, B ki, and Petit (2013) hypothesized that the loss of top connectors leads to non-cooperative opening of MET channels [1]. To test this, we used contact mode atomic force microscopy (AFM) to measure the cantilever deflection as it gently deflects mature hair bundles from postnatal day P13-P15 stereocilin-null mice with detached tectorial membrane (*Strc*^{-/-}/*Tecta*^{-/-}) and compared with heterozygous littermate controls (*Strc*^{+/-}/*Tecta*^{-/-}). OHC bundles from *Strc*^{+/-}/*Tecta*^{-/-} showed cooperative MET channels opening in the form of a single well-defined 100-150 nm jump in the force-displacement curves. *Strc*^{-/-}/*Tecta*^{-/-} OHC bundles showed multiple random smaller ~50-60 nm jumps or no detectable jumps. Also, *Strc*^{-/-}/*Tecta*^{-/-} OHC bundles have a significantly reduced apparent bundle stiffness compared to *Strc*^{+/-}/*Tecta*^{-/-}, consistent with previous work using noncontact frequency-modulated AFM. Altogether, the presence of horizontal top connectors maintains the bundle cohesiveness and coherent motion enhancing the cooperativity and probability of opening MET channels during bundle deflection which is critical for optimal OHC mechanotransduction.

[1] P. Avan, B. B ki, C. Petit, Auditory distortions: origins and functions. *Physiological Reviews* 93, 1563 (2013).

PS 434

Contribution of TMC1 to Mechanotransduction Channels in Cochlear Hair Cells

Runjia Cui¹; Maryline Beurg²; Adam Goldring³; Seham Ebrahim⁴; Bechara Kachar¹; **Robert Fettiplace**²
¹National Institute on Deafness and Other Communication Disorders; ²University of Wisconsin-

Functional mechanoelectrical transduction (MET) channels of cochlear hair cells require the presence of transmembrane channel-like protein isoforms TMC1 or TMC2, and channel properties depend on which TMC isoform is present. However, during post-natal development, TMC2 is progressively down-regulated, and in older animals, only TMC1 occurs in hair bundles of both outer hair cells (OHCs) and inner hair cells (IHCs). TMC1- and TMC2-dependent channels differ in their properties, including calcium permeability and fast adaptation, but it is unclear what advantage to hearing is conferred by TMC1. To address this question, whole-cell recordings were made from OHCs and IHCs in cochleas of TMC mutant mice (E18 - P12), and single MET-channel measurements were made after brief treatment with sub-micromolar calcium. Mice expressing TMC1-mCherry and TMC2-AcGFP were used to localize these TMCs in fixed tissue using spinning disk confocal fluorescence microscopy.

Here we show that in OHCs, only TMC1-dependent channels support a tonotopic apex-to-base gradient in single-channel, and hence macroscopic, MET conductance. This gradient is absent in inner hair cells (IHCs). Several methods of analysis suggested that each MET channel complex possesses up to five conductance states in ~50 pS increments, basal MET channels in OHCs having more large-conductance levels. Using mice expressing fluorescently-tagged TMCs, we found a three-fold increase in the number of TMC1 molecules per stereociliary tip from cochlear apex to base in OHCs, but not in IHCs. These changes in expression mirror the channel conductance gradient in the two types of hair cell. Single-molecule photobleaching indicated that the number of TMC1 molecules per MET complex changes from about 8 at the apex to 20 at base. The results are consistent with TMC1 being a component of the MET channel pore. Moreover, they suggest there are varying numbers of channels per MET complex, each requiring multiple TMC1 molecules, which together operate in a coordinated or cooperative manner.

PS 435

Localization of TMC1 and TMHS in Auditory Hair Cells in Neonatal and Adult Mice

Xiaofen Li¹; Xiaojie Yu¹; Xibing Chen¹; Zhengzhao Liu¹; Guangqin Wang²; Chao Li²; Elaine Y.M. Wong³; Mai Har Sham⁴; Jie Tang⁵; Jufang He⁶; Wei Xiong⁷; Zhiyong Liu²; Pingbo Huang¹

¹Hong Kong University of Science and Technology;

²Institute of Neuroscience, CAS Center for Excellence in Brain Science and Intelligence Technology, Shanghai

The channel that governs mechanotransduction (MT) by hair cells in the inner ear has been investigated intensively for 4 decades, but its molecular identity remains enigmatic. Transmembrane channel like protein 1 (TMC1) was recently suggested to be a promising MT-channel candidate, and TMHS (tetraspan membrane protein of hair cell stereocilia) is considered to be part of the MT complex and to functionally couple the tip link to the MT channel. As a candidate channel or component of the MT complex, TMC1 and TMHS are expected to localize, exclusively or otherwise, at the lower end of the tip link in hair cells, a notion generally supported by previous studies on neonatal mice. However, the localization of these two proteins, particularly in the hair cells of adult mice, remains incompletely elucidated.

Because determination of TMC1 and TMHS localization at distinct developmental stages is essential for understanding their function and regulation, we used several approaches here to examine the localization of these proteins in neonatal and adult hair cells in the mouse. We report several notable findings: (1) TMC1 and TMHS predominantly localize at the lower end of the tip link in neonatal hair cells, which largely verifies the previously published findings in neonatal hair cells; (2) TMHS persists in the hair bundle of hair cells after P7, which clarifies the unexpected absence of TMHS after P7 reported previously and supports the view that TMHS is a permanent component in the MT complex; and (3) TMC1 and TMHS remain at the lower end of the tip link in adult outer hair cells, and, interestingly, TMC1 is uniformly distributed in both the tallest and the shorter rows of stereocilia whereas TMHS is uniformly distributed in the shorter rows of stereocilia in adult inner hair cells; this raises intriguing questions regarding the turnover rate, regulation, additional functions, and functional interaction of TMC1 and TMHS. Our study confirms the previous findings in neonatal hair cells and reveals several previously unidentified aspects of TMC1 and TMHS localization in more mature hair cells.

The work was supported by Hong Kong RGC GRF16111616 and in part by the Innovation and Technology Commission (ITCPD/17-9).

PS 436

Mechano-electrical Transduction in Mature OHCs from α - and β -tectorin Knockout Mice

Jing-Yi Jeng¹; Lukas Rüttiger²; Richard Goodyear³; Csaba Harasztosi²; Kevin Legan²; Stuart Johnson⁴; Laura Corns⁴; Marlies Knipper²; Guy Richardson³; Walter Marcotti¹

Background

The transduction of sound stimuli into neural signals relies on mechano-electrical transduction in hair cells. However, mechano-electrical transducer (MET) current is normally recorded during pre-hearing stages of development (<P12), especially when measured from OHCs, which limits our ability to investigate biophysical properties of the MET channel in hearing animals. This is most likely due to the fact that the tips of the stereocilia of outer hair cells (OHCs) are attached to the tectorial membrane, which has to be removed in order to displace the hair bundle and record the MET current, a procedure that damages the hair bundle. In order to address this technical issue we have investigated the constitutive TectA/TectB knockout mice, which do not express α -tectorin and β -tectorin, two non-collagenous proteins required for the formation of the tectorial membrane (reviewed by Goodyear and Richardson et al. 2018 *Curr Top Dev Biol* 130:217-244).

Methods

We performed in vivo and in vitro electrophysiological recordings and morphological studies in the above knockout adult mouse (TectA/B). MET currents were elicited by stimulating the bundle of apical coil OHCs with a piezoelectric driven fluid jet. For confocal and scanning electron microscopy, cochleae were perfused with fixatives and the organs of Corti were dissected and stained accordingly. DPOAEs were measured as cubic distortion products at the frequency $2f_1$ - f_2 , where f_2 was 11.3 kHz.

Results

In TectA/B knockout mice the stereocilia of OHCs were not attached to the tectorial membrane, but retain a normal structure. Despite the decreased DPOAEs in adult mice, the biophysical properties of OHCs from TectA/B knockout mice develop normally, including prestin expression and electromotile activity. We were also able to record large and adapting MET currents in mature OHCs.

Conclusions

Our results showed that the TectA/B knockout mice are an ideal model to study mechano-electrical transduction in OHCs after the onset of hearing. The loss of both α -tectorin and β -tectorin did not affect the morphology and function of OHCs.

PS 437

Structural Relationship Between the Putative Hair Cell Mechanotransduction Channel TMC1 and TMEM16 Proteins

Angela Ballesteros¹; Cristina Fenollar-Ferrer²; Kenton J. Swartz¹

¹National Institute of Neurological Disorders and Stroke; ²National Institute of Deafness and Other Communication Disorders and National Institute of Mental Health

Our senses of touch, hearing, balance, and proprioception depend on mechanically gated ion channels, which transduce mechanical energy into electrical signals that are transmitted to the brain. Previous studies on the mechanisms of hearing have elucidated the biophysical properties of the mechanotransduction (MET) channel essential for hearing, yet its molecular identity and structure remain elusive. The transmembrane channel-like (TMC) protein 1 localizes to the site of the MET channel, interacts with the tip-link responsible for mechanical gating, and genetic alterations in TMC1 alter MET channel properties and cause deafness, supporting the hypothesis that TMC1 forms the MET channel. We generated a structural model of TMC1 based on the X-ray and cryo-EM structures of the TMEM16 proteins, revealing the presence of a large cavity near the protein-lipid interface that also harbors the two TMC1 mutations (p.M418K and p.D572N/H) that cause autosomal dominant hearing loss (DFNA36), suggesting that it could function as a permeation pathway. We also find that hair cells are permeable to 3 kDa dextran labeled with Texas Red, and that dextran permeation requires TMC1/2 proteins and functional MET channels, supporting the presence of a large permeation pathway and the hypothesis that TMC1 is a pore-forming subunit of the MET channel complex.

PS 438

Voltage and Calcium Modulate Stereocilia Membrane Fluidity: Implications Regarding Hair Cell Mechanotransduction

Shefin S. George; Charles Steele; Anthony J. Ricci
Stanford University

Cochlear hair cells are specialized mechanoreceptors that detect sound. Hair cells have specialized organelle called the hair bundle, composed of an array of actin-filled microvillae, termed stereocilia that increase in height in a staircase-like manner. Hair bundle deflection exerts force onto the tip link (proteinaceous link between adjacent rows of stereocilia) that is translated to mechanically-gated (MET) ion channels located at the tops of the shorter stereocilia. Recent

data suggest that the lipid membrane can modulate MET channel open probability (Popen) in mammalian cochlear hair cells through membrane potential and external and internal calcium (Peng, A. et al. 2016).

As the first step toward understanding how manipulating membrane potential and calcium affect the membrane mechanics and MET channel gating, we combined whole-cell patch-clamp with two-photon FRAP (fluorescence recovery after photobleaching) in rat inner hair cells. FRAP provides an estimate of lateral diffusion of dye molecules within the membrane. Diffusivity was determined by fitting the fluorescent recovery time course to a diffusion model of the cylindrical stereocilia.

Two-photon FRAP confined photo-bleaching to within 3 μm of the stereocilia tip. Similar half-recovery times ($t_{1/2}$) were calculated within the stereocilia using two different membrane dyes, Di-3-ANEPPDHQ and RH795, validating that FRAP technique is dye independent. Prolonged depolarization resulted in faster diffusivity in 24 out of 30 cells ($\Delta t_{1/2}$ (-80mV to +80mV) = $0.29 \pm 0.06\text{s}$ and $0.26 \pm 0.08\text{s}$ for 1st and 2nd row stereocilia respectively), suggesting that the gradual decrease in resting Popen during prolonged depolarization could be through a lipid-based mechanism which reduces the force applied to MET channels.

Lowering extracellular calcium resulted in an immediate increase in resting Popen without a significant change in membrane diffusivity, suggesting a local mechanism to change force applied to MET channels. Lowering intracellular calcium resulted in slower diffusivity ($t_{1/2}$ for 0.1CsBAPTA = $1.14 \pm 0.2\text{s}$ and $0.88 \pm 0.13\text{s}$ for 1st and 2nd row stereocilia respectively, and $t_{1/2}$ for 10CsBAPTA = $1.56 \pm 0.17\text{s}$ and $1.19 \pm 0.14\text{s}$ for 1st and 2nd row respectively) and an increase in resting Popen, suggesting a mechanism in which Popen modulation occurs through the membrane lipid. Our data support the hypothesis that the lipid bilayer modulates force transfer to MET channels.

This work is supported by NIDCD RO1 DC003896 and NIDCD RO1 DC014658 to AJR.

PS 439

LOXHD1, a Sub-Membranous Stereociliary Protein, is Required for Mechanotransduction in Mature Inner Hair Cells

Alix Trouillet; Shefin S. George; Katharine Miller; Noor-E-Seher Ali; Charles Steele; Anthony J. Ricci; **Nicolas Grillet**

Stanford University

Background

The stereocilia bundle is the mechanoreceptor organelle of hair cells that detect sound and gravity in the inner ear. Stereocilia are organized in rows of increasing heights and interconnected at their top by tip-links. Tip links convey the mechanical force received by the taller stereocilia to the mechanotransduction (MET) channel complex, localized at the lower part of the tip link, at the top of the lower stereocilia. In mice the cochlear hair cells acquire mechanosensitivity at birth and the MET channel complex matures molecularly after the first postnatal week.

Here we investigated the molecular function of the LOXHD1 gene that we previously linked to an autosomal-recessive form of hearing loss in mice and human (Grillet N., AJHG, 2009). LOXHD1 encodes a protein made of 15 PLAT (Polycystin/Lipoxygenase/Alpha-Toxin) domains, known in other protein to bind lipid and proteins. LOXHD1 is expressed by hair cells only after the first postnatal week. The LOXHD1 protein is then found in the stereocilia, at the junction between membrane and the actin-cytoskeleton. The molecular function of LOXHD1 is unknown, and our goal is to determine it. We hypothesize that LOXHD1 is necessary for the hair bundle functionality by forming a physical link between the membrane and the actin-core of the stereocilia.

Methods

To test this hypothesis, we studied two mouse strains carrying mutations in the LOXHD1-PLAT10. We analyzed the auditory phenotype (ABR, DPOAE, CM), the stereocilia structure (SEM, TEM), the IHC mechanosensitivity (patch-clamp) and their stereocilia membrane dynamics (two-photon FRAP).

Results

We found that, while IHC MET of *Loxhd1*-mutants animals is normal at P6, the amplitude of the MET current is drastically reduced by P11. Despite this strong MET phenotype, the hair bundle organization is not affected, and the number of tip-links not decreased. As LOXHD1 localizes below the stereocilia surface, we asked if the stereocilia membrane dynamics were affected by LOXHD1 expression. For this purpose, we measured lipid diffusivity in single stereocilia. We discovered that in WT animals, the lipid diffusivity of stereocilia naturally decreases between P7 and P11, and is LOXHD1-dependent.

Conclusions

We conclude that in mature IHCs, the sub-membranous protein LOXHD1 can regulate mechanotransduction while not concentrated at the tip of transducing

stereocilia. LOXHD1 influences also the stereocilia membrane dynamics. We propose that LOXHD1 acts as a linker between the actin-cytoskeleton and the membrane, necessary for the force-translation between stereocilia and the gating of the mature MET complex.

PS 440

Single-molecule Nanomechanics of the Tip-link Protein Protocadherin 15

Tobias F. Bartsch¹; Felicitas E. Hengel¹; Aaron Oswald¹; Gilman Dionne²; Iris V. Chipendo¹; Simranjit S. Mangat¹; Muhammad El Shatanofy¹; Ulrich Müller³; Lawrence Shapiro²; A.J. Hudspeth⁴

¹The Rockefeller University; ²Columbia University;

³Johns Hopkins University School of Medicine;

⁴Rockefeller University

The mechanically sensitive hair bundles of vertebrate hair cells are stereotyped in structure. Each of the constituent stereocilia is connected to its tallest neighbor by a filamentous tip link, a dimer of dimers of atypical cadherins, whose lower third consists of protocadherin 15 (PCHD15) and upper two-thirds of cadherin 23 (CDH23). The lower end of the tip link is thought to be connected to the gates of a few mechanosensitive ion channels. Deflection of a hair bundle increases the tension in the links, opens the channels, allows the influx of K⁺ and Ca²⁺ into a cell, and thus initiates electrical signaling.

Progressively greater hair-bundle deflections must lead to gradually increasing open probabilities of the ion channels. This behavior is thought to be mediated by a mechanical element called the “gating spring,” which converts bundle displacement into a force capable of opening the channels. The tip link itself is a strong candidate for this spring: its elasticity could result from the compliance of individual extracellular cadherin domains, from the rearrangement of the domains relative to each other, or from the Ca²⁺-dependent unfolding and refolding of the domains. Although the behavior of fragments consisting of a few cadherin domains from protocadherin 15 and cadherin 23 have been simulated by molecular dynamics, the mechanical properties of the full-length proteins remain unknown.

Using high-precision optical tweezers, we have measured the force-extension relation of the full extracellular domain of protocadherin 15 at subnanometer resolution and with physiologically relevant forces. Our data reveal that the stiffness of the folded protein is largely of entropic origin and increases with applied tension from 0.5 mN/m to 9 mN/m. We identify three classes of reversible, stepwise unfolding events that protocadherin 15 can undergo under physiological force, elongating the

protein by about 3 nm, 15 nm, and 30 nm. Extensions in steps of 30 nm, which are strongly dependent on the Ca²⁺ concentration, suggest the unraveling of entire cadherin domains. The unfolded polypeptide chains act as additional entropic springs that further diminish the molecule's stiffness. Such elongations might provide stress relief to protect the integrity of the tip link during loud sounds. Finally, we show that a point mutation associated with hearing loss compromises the mechanical stability of the protein.

PS 441

Both LHFPL5 and the Novel Protein LHFPL4 are Located at the Site of Mechanotransduction in Cochlear Hair Cells and Both Interact with TMC1 and PCDH15

K. Domenica Karavitaki¹; Panos I. Tamvakologos²; Eric M. Mulhall¹; Duan-Sun Zhang¹; Artur A. Indzhukulian³; Bence György⁴; David P. Corey²

¹Department of Neurobiology, Harvard Medical School;

²Harvard Medical School, Department of Neurobiology;

³Department of Otolaryngology, Massachusetts Eye and Ear, Harvard Medical School; ⁴Department of

Neurobiology, Harvard Medical School, Massachusetts General Hospital

Identification of deafness genes has revealed many essential proteins of the mechanotransduction complex of hair cells, including TMC1, PCDH15, TMIE, CIB2 and LHFPL5. Other proteins, not encoded by known deafness genes, might also play an important role. We have used data from a comprehensive transcriptome study (SHIELD database) to identify mouse genes preferentially expressed in cochlear and vestibular hair cells. We identified Lhfp14, a close homolog of Lhfp15, which has a similarly selective expression in hair cells with increased expression during the first postnatal week. Both LHFPL4 and LHFPL5 are small proteins (220-250 aa) with four predicted transmembrane domains, a five-strand extracellular beta sheet and intracellular N- and C-termini. Recent work on the structure of the PCHD15-LHFPL5 complex (Ge et al., 2018) shows extensive interactions within the transmembrane regions of these proteins. Other than a short characterization of Lhfp14 gene expression in zebrafish (Cox et al., 2011), little has been published on LHFPL4. Could LHFPL4 have an essential role in hair cells, similar to that of LHFPL5?

We optimized an in vitro electroporation method to deliver plasmids encoding LHFPL4 and LHFPL5 to P2-P5 mouse cochlear hair cells. To label LHFPLs, we used a novel tandem GCN epitope and a cognate engineered antibody with picomolar affinity and high specificity. Placement of these epitopes in extracellular

domains, with normal function confirmed by rescue of knockout mice, allowed both live-cell fluorescence imaging and immunogold electron microscopic localization of LHFPLs. We confirmed localization of LHFPL5 near the tips of the stereocilia, especially the shorter rows. Antibody labeling of native LHFPL4 also showed localization near the tips of the stereocilia. This was confirmed with electroporation of tagged LHFPL4 in wild type mice as well as in mice lacking LHFPL5, TMC1 or TMC2, suggesting that LHFPL4 localization is independent of these proteins in P2-P5 mice. Immunogold SEM further localized LHFPL4 near the tips of all stereocilia.

We also assessed the binding of LHFPLs to known transduction proteins and to control proteins such as N-cadherin. Based on co-immunoprecipitation following co-expression in HEK cells, LHFPL5 interacts with all isoforms of PCDH15 but not with N-cadherin. Contrary to previous reports, the co-IP suggested binding between LHFPL5 and TMC1. We also observed co-IP of LHFPL4 with TMC1 but not with N-cadherin. Based on the localization of LHFPL4 near the tips of stereocilia and its likely binding to TMC1, we suggest that LHFPL4 participates in the mature transduction complex.

PS 442

cAMP Signaling Modulates Mechanotransduction Channel Set Point and Operating Range in Rat Outer Hair Cells

Andrew Mecca¹; Anthony Peng²

¹University of Colorado Denver; ²University of Colorado Anschutz Medical Campus

Auditory hair cells of the inner ear are highly specialized mechanoreceptors that transduce mechanical forces arising from sound waves into an electrical potential through a process termed mechanotransduction (MET). MET is necessary for normal hearing, and processes that modulate outer hair cell (OHC) MET are hypothesized to underlie the wide dynamic range and frequency selectivity of the mammalian cochlea. However, the molecular mechanisms which regulate MET in mammalian OHCs are still unclear. In this study, we explored the novel hypothesis that cAMP signaling in OHCs serves a physiologically protective role in hair cell function by desensitizing the MET channel, potentially in response to periods of high channel activity. The intracellular cAMP pathway is an evolutionarily-conserved and ubiquitous signaling mechanism that has shown to be important for hearing in humans, zebrafish, and turtles^{1,2}. In humans, mutations in adenylate cyclase 1 (ADCY1) have been linked to hearing loss via an unknown mechanism, but a comparable mutation in zebrafish hair cells produced

defects in MET as measured by FM1-43 dye uptake¹. Importantly, ADCY1, and cyclic nucleotide-sensitive channels are expressed in hair cell stereocilia of mouse and rat cochlea and vestibular organs, where they have unknown functions^{1,3,4}. One study demonstrated that the cyclic nucleotide-sensitive channel family HCN1-4 is not required for MET⁴, but this work did not address possible changes to the MET activation curve, which provides a readout of channel operating range and sensitivity. Coincidentally, data from turtle hair cells indicates that pharmacological upregulation of cAMP signaling produces a rightward shift of the activation curve, desensitizing the MET channel². Together, this evidence points to the possible involvement of cAMP in mammalian MET regulation, but more detailed MET studies are needed. Here, we used pharmacology, patch-clamp electrophysiology, force-controlled fluid jet bundle stimulation, and high-speed imaging to interrogate the role of cAMP in MET mechanisms and hair bundle mechanics in outer hair cells of the rat cochlea. We find that pharmacological stimulation of the cAMP pathway modulates the sensitivity and operating range of the MET channel in OHCs, providing evidence for a potentially new mechanism of mammalian MET regulation.

1. Santos-Cortez et al., Human Molecular Genetics 2014
2. Ricci & Fettkoppe, The Journal of Physiology 1997
3. Selvakumar et al., Biochemical Journal 2012
4. Horwitz et al., PLoS One 2010

PS 443

Cis-regulatory divergence of lipoma HMGIC fusion partner-like 5 (lhfp15) paralogs in zebrafish.

Timothy Erickson¹; Itallia V. Pacentine²; **Alexandra Venuto**³; Teresa Nicolson²

¹East Carolina University; ²Oregon Hearing Research Center and Vollum Institute, Oregon Health & Science University; ³Department of Biology, East Carolina University

One possible fate of duplicated genes is cis-regulatory divergence, where paralogous genes take on unique roles due to divergence of their mRNA expression patterns. In mice and humans, a single lipoma HMGIC fusion partner-like 5 (LHFPL5 / TMHS) gene is required for proper functioning of the mechano-electrical transduction (MET) complex in auditory and vestibular hair cells. Zebrafish have two lhfp15 genes (lhfp15a and lhfp15b), but their contributions to sensory hair cell function have not been fully described.

Here, we show that teleost fishes possess paralogous lhfp15a and lhfp15b genes, likely originating with the teleost-specific whole-genome duplication event. In zebrafish, these paralogs are expressed in discrete

populations of hair cells: *lhfp15a* expression is restricted to auditory and vestibular hair cells, while *lhfp15b* expression is specific to hair cells of the lateral line neuromasts. Consequently, *lhfp15a* mutants exhibit defects in auditory and vestibular function, while disruption of *lhfp15b* affects hair cells of the lateral line only. This work highlights an evolutionarily conserved role for *Lhfp15* in MET complex function, and demonstrates the subfunctionalization of zebrafish *lhfp15a* and *lhfp15b* paralogs through cis-regulatory divergence.

PS 444

Different Effects of Prolonged Depolarization and Channel Closure on the Resting Mechanotransducer Current in Mammalian Auditory Hair Cells

Abbey Dragich; A. Catalina Vélez-Ortega; Gregory I. Frolenkov
Department of Physiology, University of Kentucky

The exquisite mechanosensitivity of the inner ear hair cells at the threshold of hearing depends on the resting tension in the mechano-electrical transduction (MET) machinery. This tension results in a constitutive influx of positive ions, including Ca^{2+} , through the MET channels that are partially open at rest. According to the classical model that is largely based on the data from non-mammalian hair cells or mammalian vestibular hair cells, Ca^{2+} -dependent myosin motors set the resting tension in the MET apparatus through the process that is known as MET adaptation. The model postulates that a decreased Ca^{2+} influx through MET channels, either during cell depolarization or after MET channel closure by a negative bundle deflection, causes myosin-dependent re-tensioning of the MET machinery. However, mammalian auditory hair cells exhibit an order of magnitude faster adaptation that is unrelated to the much slower regulation of the MET machinery during cell depolarization (Peng et al., *J. Neurosci.*, 2016). In addition, our recent data revealed that blockage of Ca^{2+} influx through MET channels causes selective retraction of transducing stereocilia in the mammalian auditory hair cell bundles that could also result in re-tensioning of the MET apparatus but on a much slower time scale compared to myosin-dependent motors (Velez-Ortega et al., *eLife.*, 2017; Velez-Ortega et al., *Hear J.*, 2017). Therefore, using conventional whole cell recordings of the MET current evoked by fluid-jet stimulation, we compared the effects of prolonged (1s or more) depolarization and negative bundle deflection on the resting open probability of the MET channels (Popen) in the same young postnatal mouse cochlear outer hair cells. Consistent with the previous report (Peng et al., *J. Neurosci.*, 2016), cell depolarization resulted in an increase of Popen that develops and recovers on a time scale of hundreds of milliseconds. However,

we did not observe any statistically significant changes of Popen after prolonged negative bundle deflections. Our data suggest that in mammalian auditory hair cells: (i) the mechanisms of Popen regulation during cell depolarization and negative bundle deflection are different; and (ii) the potential re-tensioning of the MET machinery during prolonged negative bundle deflections is either extremely slow or requires more physiological conditions.

Supported by NIDCD/NIH R01DC014658 (to G.I.F.)

PS 445

Silencing Beethoven: Allele-Specific Deafness Gene Disruption by *S. aureus* Cas9-KKH Prevents Progressive Hearing Loss in Mice after AAV-Mediated Gene Delivery

Bence György¹; Carl Nist-Lund²; Bifeng Pan²; Yukako Asai³; Benjamin Kleinstiver⁴; Sara Garcia⁴; Mikolaj Zaborowski⁴; K. Domenica Karavitaki⁵; J. Keith Joung⁴; Jeffrey R. Holt⁶; **David P. Corey**⁷

¹*Department of Neurobiology, Harvard Medical School, Massachusetts General Hospital*; ²*Boston Children's Hospital, Harvard Medical School*; ³*Boston Children's Hospital, Harvard Medical School*; ⁴*Massachusetts General Hospital*; ⁵*Department of Neurobiology, Harvard Medical School*; ⁶*Boston Children's Hospital & Harvard Medical School*; ⁷*Harvard Medical School, Department of Neurobiology*

Single nucleotide changes in over 30 genes can cause dominant forms of hereditary hearing loss. Strategies such as siRNA, miRNA or genome editing can inactivate the disease-causing allele. However, distinguishing mutant from wild-type alleles remains challenging. Here, we explored strategies to inactivate a dominant M412K mutation in *Tmc1* using the Beethoven (Bth) mouse model, characterized by progressive hair cell degeneration and deafness.

We transfected fibroblast lines from *Tmc1*^{Bth/+} and *Tmc1*^{+/+} animals with *S. pyogenes* and *S. aureus* CRISPR/Cas9 systems to target the mutation using four strategies: (1) changing the position of the protospacer-adjacent motif (PAM), (2) truncating gRNAs, (3) using a novel *S. aureus* Cas9 (SaCas9-KKH), (4) using SaCas9-KKH and truncating gRNAs. We selected a Cas9-KKH with a PAM site specific for the Bth mutation. In fibroblasts, deep sequencing of the *Tmc1* gene revealed that none of the *S. pyogenes* Cas9-gRNA designs targeted the Bth mutation with high specificity, as we observed genome editing on both the mutant and the wild-type *Tmc1* alleles. With standard *S. pyogenes*

Cas9, a truncated gRNA produced the highest Bth/WT relative specificity ratio but it was only moderately specific (81.9%). In striking contrast, the *S. aureus* Cas9-KKH with a truncated gRNA yielded essentially no WT allele cutting, but led to insertion and deletion (indel) formation on the *Tmc1*Bth allele (relative specificity ratio of 99.8%).

Unlike SpCas9, SaCas9-KKH fits in AAV, so we next injected AAVAnc80 carrying CMV-Cas9-KKH-U6-gRNABth into inner ears of heterozygous neonatal Bth mice. With sequencing, we analyzed allele-specific genome editing seven days later. Sequencing from injected cochleas revealed allele-specific indel formation in the *Tmc1* gene, disrupting the reading frame. We tested hearing with ABR recordings at 4-12 weeks post-injection, and quantified surviving hair cells at 12 weeks using myosin-VIIa staining. Heterozygous Bth mice normally show severe-to-profound hearing loss. However injection of AAVAnc80-CMV-Cas9-KKH-U6-gRNABth led to robust improvement of hearing thresholds, with some animals exhibiting near normal hearing sensitivity. Hearing sensitivity was stable out to 12 weeks, the latest time tested.

We conclude that AAV delivery of SaCas9-KKH can disrupt an allele bearing a point mutation, with high specificity and efficiency based on PAM site recognition, preventing hair-cell degeneration and arresting progressive hearing loss. AAV-mediated in vivo genome editing holds promise for DFNA36 and other dominant progressive hearing loss. Indeed, we calculate that appropriate gRNAs and SaCas9-KKH with an allele-specific PAM site could potentially disrupt ~22% of all dominantly inherited genetic diseases.

PS 446

Ion Permeation in Molecular Dynamics Simulations of TMEM16-based TMC1 Homology Models

Sanket Walujkar; Lahiru N. Wimalasena; Jeffrey M. Lotthammer; **Marcos Sotomayor**
The Ohio State University

Mechanical stimuli from sound and head movements are converted into electrical signals in the inner ear during a process known as mechanotransduction. The molecular identity of the cation channel involved in inner-ear mechanotransduction has been unclear for years, although four transmembrane proteins (PCDH15, TMIE, TMHS, and TMC1/2) have been shown to be part of the mechanotransduction complex. Recent studies suggest that TMC1 is the pore-forming subunit of the mechanotransduction complex and that it assembles as a dimer (Pan et al., *Neuron* 2018), yet the structure

of TMC1 and the mechanisms of ion conduction and activation remain to be elucidated. Bioinformatic analyses suggest that TMC1 is related to the dimeric TMEM16 family of membrane proteins, including anion channels and lipid scramblases for which high-resolution structures have been recently reported. Here we present molecular dynamics simulations of TMC1 homology models based on the mouse Ca²⁺-activated chloride channel TMEM16A and the fungal Ca²⁺-activated lipid scramblase TMEM16. Unlike most ion channels, these templates, and consequently the TMC1 homology models, do not show a central ion conduction pore. Instead, the ion conduction pore and lipid-scrambling region are located on the periphery of the proteins, facing the lipids. Simulations of TMC1 homology models show that the putative pore is hydrated and supports cation permeation. Results from further simulations performed in the absence and presence of applied membrane potentials and tension will be discussed.

PS 447

Structure and Elasticity of a Complete Protocadherin-15 Dimer

Deepanshu Choudhary¹; Yoshie Narui¹; Brandon L. Neel¹; Lahiru N. Wimalasena¹; Carissa F. Klanseck¹; Conghui Chen¹; Pedro De-la-Torre¹; Raul Araya-Secchi²; Elakkiya Tamilselvan¹; **Marcos Sotomayor**¹
¹*The Ohio State University*; ²*University of Copenhagen*

Protocadherin-15 (PCDH15), an atypical member of the cadherin superfamily, is essential for vertebrate hearing and its dysfunction has been associated with deafness and progressive blindness. The ectodomain of PCDH15, composed of 11 extracellular cadherin (EC1-11) repeats and a membrane adjacent domain, assembles as a parallel homodimer that interacts with cadherin-23 (CDH23) to form the tip link, a fine filament necessary for inner-ear mechanotransduction. Here we report ten X-ray crystal structures of overlapping PCDH15 fragments that show all of PCDH15's EC repeats, all its EC linkers, and also its membrane adjacent domain (MAD12). These structures, along with molecular dynamics (MD) simulations, allowed us to assemble a complete high-resolution model of the monomeric extracellular domain of PCDH15, to suggest models of trans and cis PCDH15 homodimers, and to build a model of the heterotetrameric PCDH15 and CDH23 tip-link bond. Steered MD simulations of these models predict their strength and calcium-dependent elasticity, and suggest conditions in which tip-link bond rupture precedes unfolding and vice versa. These results provide a detailed view of PCDH15's structure and insights into the first molecular steps of inner-ear sensory perception.

Hair Cells: Stereocilia

PS 448

The Short Isoform of Myosin-XVa is Required not only for Staircase Architecture but also for Gradation of Stereocilia Diameters in the Auditory Hair Cells

Shadan Hadi; Andrew J. Alexander; A. Catalina Vélez-Ortega; Gregory I. Frolenkov
Department of Physiology, University of Kentucky

The postnatal development of hair cell stereocilia bundles involves three stages: elongation, thickening, and supernumerary stereocilia retraction. Although myosin-XVa is known to be essential for stereocilia elongation and staircase bundle formation, its role in stereocilia retraction and stereocilia thickening remains unknown. We used scanning electron microscopy (SEM) to image inner (IHCs) and outer (OHCs) hair cells in the middle of the mouse cochlea from postnatal days 0 through 21. We quantified stereocilia numbers and diameters in shaker-2 mice (*Myo15sh2*) that have deficiencies in both the “long” and “short” isoforms of myosin-XVa, and in mice lacking only the “long” myosin-XVa isoform (*Myo15ΔN*) (Fang et al., *eLife*, 2015). Our data showed that myosin-XVa is largely not involved in the developmental retraction of supernumerary stereocilia in either IHCs or OHCs. In contrast, we observed that myosin-XVa is, indeed, a key regulator for stereocilia thickness within the rows of auditory hair bundles. In the normal development of IHCs and OHCs, the diameters of the first (tallest) and second row stereocilia within a bundle are nearly equal and grow simultaneously. The diameter of the third row stereocilia increases together with that of taller stereocilia until P1-2 and then either decreases almost two-fold in IHCs or stays the same in OHCs, resulting in a prominent diameter gradation in IHCs and less prominent in OHCs. In spite of subtle residual diameter differences, the *sh2* mutation does disrupt stereocilia thickness gradation given that stereocilia of all rows grow in diameter nearly equally in *Myo15sh2/sh2*IHCs and OHCs. In contrast, the ΔN mutation does not affect normal developmental stereocilia diameter gradation until ~P10 and leads to stereocilia thinning only afterward, as previously observed by Fang et al., *eLife*, 2015. Therefore, we conclude that the myosin-XVa “short” isoform is essential for the developmental thinning of third row stereocilia, which causes the diameter gradation within a hair bundle.

Supported by NIH/NIDCD (R01DC014658).

PS 449

A Photoreceptor-like, Rhodopsin-linked cGMP Pathway in Inner Ear Hair Cells

Marian J. Drescher; Dennis G. Drescher
Wayne State University

Background: The cone phototransduction cyclic nucleotide channel alpha subunit CNGA3 and rod phototransduction beta subunit CNGB1 were previously identified in purified saccular hair cells (IEB Abstr. 52:011, 2015). Direct protein-protein interaction analysis by competitive pull-down assays and SPR indicated CNGA3 tightly interacts with myosin VIIA in competition with tip-link-protein cadherin 23 (Selvakumar et al., *J. Biol. Chem.* 288:7215-7229, 2013). The photoreceptor-like membrane guanylyl cyclase pathway proteins for synthesizing cGMP, required to gate this CNG channel that couples to rhodopsin and its regulatory proteins, are being identified as well as their PPI in both teleost vestibular and mammalian cochlear hair cells.

Methods: PCR carried out with degenerate primers on teleost saccular hair cell cDNA produced hair cell specific transcripts representing rod/cone photoreceptor transduction proteins. Hair cell transcripts (crossing introns) were submitted to NCBI GenBank for consideration of publication with GenBank Accession number assignment. Rhodopsin, CNGB1, and peripherin 2 have been immunolocalized in the mammalian cochlear hair cells.

Results: Coding sequence for hair cell expressed rhodopsin-linked rod phototransduction pathway proteins has been published by NCBI with assignment of GenBank Accession numbers. Phosphorylation of rhodopsin in hair cells at its C-terminus by rhodopsin kinase (GRK1) (GenBank Accession No. **MH191403**) is followed by binding of visual S-antigen form of arrestin (SAG) (GenBank Accession No. **MH094034**). CNGB1-binding partners include the tetraspan flippase ABCA4 (GenBank Accession No. **MH311980**), previously described as “expressed exclusively in retina photoreceptor cells,” mediating transport of **11-cis-retinylidene** phosphoethanolamine (PE) photoisomerized to all-trans configuration in phototransduction. CNGB1-binding photoreceptor-specific tetraspanin peripherin-2 (RDS), putatively generating disk-disk tethering, is also expressed (GenBank Accession No. **MH311980**). Recoverin-1b (RCVRN-1b) blocking GRK1 phosphorylation of rhodopsin has now been identified in hair cells (GenBank Accession No. **MH341531**). Rhodopsin and peripherin 2 have been immunolocalized to subcuticular plate sites in mammalian cochlear hair cells and rhodopsin along

with CNGB1 localized to mammalian cochlear hair cell stereocilia.

Conclusions: A membrane guanylyl cyclase pathway with highest similarity to the rod phototransduction pathway has been identified in saccular hair cells. Expression of GC-F and GC-E, activating proteins GCAP1 and GCAP2, transducins GNAT1 and GNAT2, coupling rhodopsin to PDE6, cone PDE6C degrading cGMP, GRK1, SAG, ABCA4, and RDS has been verified and rhodopsin, CNGA3, CNGB1, and PDE6C immunolocalized to mammalian cochlear hair cell stereocilia. Yeast-two hybrid results indicate that CNGA3 directly interacts with FKBP9 and FKBP2, which couple to stereociliary ezrin and FKBP12, respectively, the latter binding to a ryanodine receptor, now immunolocalized to stereocilia.

PS 450

Dynamic Fascin-2 Crosslinks Stabilize the Mammalian Stereocilia Actin Core

Pallabi Roy; Benjamin Perrin
Indiana University-Purdue University Indianapolis

Stereocilia are mechanosensitive protrusions on the surface of sensory hair cells in the inner ear that detect sound, gravity, and head movement. Their cores are comprised of parallel actin filaments that are cross-linked and stabilized by several actin-binding proteins, including fascin-2, plastin-1, espin, and XIRP2. The actin filaments are the most stable known, with actin turnover primarily occurring at stereocilia tips. While stereocilia actin dynamics has been well studied, little is known about the behavior of the actin crosslinking proteins, which are the most abundant type of protein in stereocilia after actin and are critical for stereocilia morphogenesis and maintenance. Here, we developed a novel transgenic mouse to monitor EGFP-fascin-2 incorporation. In contrast to actin, EGFP-fascin-2 readily enters the stereocilia core. We also compared the effect of EGFP-fascin-2 expression on developing and mature stereocilia. Whether expression was initiated during development or in mature hair cells, EGFP-fascin-2 displaced both espin and plastin-1 from stereocilia. Altering the actin crosslinker composition might affect actin stability and potentially allow for repair or replacement of the stereocilia core. To address this question, we measured actin-EGFP incorporation in hair cells expressing mutant fascin-2 R109H, which has reduced actin crosslinking ability. As observed previously, in control mice actin-EGFP incorporation was restricted to the stereocilia tips. In contrast, in fascin-2 R109H mice actin-EGFP was frequently incorporated along the length of apical IHC stereocilia. These data

suggest that dynamic fascin-2 crosslinks stabilize the stereocilia actin core.

PS 451

XIRP2 May Facilitate the Repair of Stereocilia F-Actin Core Damage

Elizabeth Wagner; Tingting Du; Maura Nakahata
University of Virginia

The exquisite sensitivity of sensory hair cells makes them especially vulnerable to overstimulation. This weakness is exacerbated in mammals due to the inability of mammalian hair cells to regenerate. However, hair cells are capable of repairing some types of minor damage, avoiding the necessity of regeneration, such as in the case of tip link breakage. Additionally, damage to the stereocilia F-actin core may also be repaired. This damage can be visualized as phalloidin-negative "gaps" in F-actin staining, which appear after noise trauma. We also observe an increase in the number of gaps found in wild type stereocilia as the mice age, suggesting that this damage accumulates over time and possibly contributes to age-related hearing loss. The enrichment of gamma-actin and other F-actin remodeling factors have been reported at these sites, suggesting that the damage can be repaired.

Here we report that XIRP2 (Xin actin binding repeat containing 2), a hair bundle-enriched protein that colocalizes with F-actin, is also enriched at gaps. In addition, Xirp2-null mice, which develop progressive hearing loss, have an abundance of gaps in both vestibular and auditory hair cell stereocilia without overstimulation. Further supporting a role for XIRP2 in gap repair, we see an enrichment of XIRP2 in gaps in a genetic model of stereocilia damage (Ptprq-null mice), and, in double knockout mice (Ptprq^{-/-}/Xirp2^{-/-}), we see an increased number of gaps and more severe hearing loss than in the single knockouts alone. Based on these data, we hypothesize that XIRP2 may facilitate the repair of stereocilia F-actin damage.

PS 452

Myosin VIIa Isoforms are Differentially Expressed in Auditory Inner and Outer Hair Cells and Control the Resting Open Probability of the Mechanotransduction Channel

Sihan Li¹; Andrew Mecca²; Elizabeth Wagner¹; Tingting Du¹; Jeewoo Kim¹; Runjia Cui³; Bechara Kachar³; Anthony Peng⁴; Jung-Bum Shin¹

¹University of Virginia; ²University of Colorado Denver; ³National Institute on Deafness and Other Communication Disorders; ⁴University of Colorado Anschutz Medical Campus

Mutations in Myosin VIIA (MYO7A) are the most common cause for Usher syndrome type I, leading to combined deafness and blindness. Myosin VIIA was proposed to function as a molecular motor to establish tension on the hair cell mechanotransduction (MET) complex, but conclusive evidence is lacking. Here we report that the cochlea expresses two MYO7A isoforms, generated by alternative transcription start sites. In a genetically engineered mouse model in which the longer isoform (Myo7a-L) is specifically deleted (Myo7a-ΔL mouse), hearing performance is only mildly affected initially, but worsens over time, culminating in profound hearing loss by 9 weeks of age. Distortion product otoacoustic emissions (DPOAEs), a measure for outer hair cell (OHC) function, were not affected. Consistent with this inner hair cell (IHC)-specific hearing loss phenotype, MYO7A expression in Myo7a-ΔL mice was severely diminished in IHCs, but only mildly affected in OHCs, suggesting that MYO7A-L is preferentially expressed in IHCs, while the shorter isoform (MYO7A-S) is predominantly expressed in OHCs. Ultrastructural and immunohistological analyses suggest that IHCs in Myo7a-ΔL mice, despite a ~80% reduction in MYO7A levels, undergo normal development. Electrophysiological analysis of MET currents demonstrated that mutant IHCs have normal peak currents, but exhibit markedly reduced resting open probability, consistent with a role of MYO7A in establishing tip link tension. Mirroring a gradual decline in MET and hearing function, the transducing rows of IHC stereocilia degenerate over time, as shown by ultrastructural analysis. Taken together, we provide evidence for a distinct expression of MYO7A isoforms in inner and outer hair cells, with potential implications for MYO7A's role in specifying MET physiology in inner and outer cochlear hair cells.

PS 453

Whirlin binds to protocadherin-15 and anchors links to the actin cytoskeleton of stereocilia in cochlear hair cells

Vincent Michel¹; Elise Pepermans¹; Isabelle Perfettini¹; Asadollah Aghaie¹; Patrick England²; Jacques Boutet de Monvel³; Christine Petit⁴; Amel Bahloul¹

¹INSERM UMRS1120-Pasteur Institut; ²Director of PF Biophysique de Macromolécules et de leurs Interactions - Institut Pasteur; ³INSERM UMRS 1120; ⁴Génétique et Physiologie de l'Audition, Institut Pasteur

In vertebrates the auditory sensory cells harbor apical microvilli-like structure forming the hair bundle, a mechanosensitive antenna that operates the mechano-electrical transduction (MET) function. Two cadherin-related (cdhr) proteins, cdhr23 and cdhr15, play critical roles in the hair bundle, where they form tip links that gate the MET channels, as well as transient lateral

interstereocilia links that are required for hair bundle morphogenesis. While the proteins harmonin, sans, and myosin VIIa are known to bind cdhr23 and to link it to the F-actin cytoskeleton, the binding partners responsible for the anchoring of cdhr15 to actin have not yet been described. Here, we characterize the distribution of the long isoform of whirlin (L-whirlin) in cochlear hair cells. We show that it localizes to the ankle-links and to the apices of all the stereocilia during hair bundle maturation, and persists at the apex of the longer row of stereocilia only in adults. We further show that L-whirlin binds to all cdhr15 isoforms and that its localization to the ankle-links requires cdhr15. These observations provide evidence that L-whirlin bridges cdhr15 and F-actin in stereocilia.

PS 454

Auditory Pathology in Kihl18 Mutant Mice

Navid Banafshe¹; Neil J. Ingham¹; Morag A. Lewis¹; Karen P. Steel²

¹King's College London; ²King's College London and Wellcome Trust Sanger Institut

Following a large-scale screen of new mouse mutants using Auditory Brainstem Response (ABR) recording, we discovered an allele of the Kihl18 gene, Kihl18lowf, with progressive hearing loss predominantly affecting low frequencies. Kihl18lowf was a spontaneous missense mutation of Kihl18 (9:110455454 C>A; V55F), predicted to have a damaging effect on protein structure. Mutants had normal ABR thresholds at 3 weeks old but showed progressive increase in ABR thresholds from 4 weeks onwards affecting low frequencies first. DPOAE recordings up to 14 weeks old revealed normal thresholds.

Our aims here were (1) to investigate potential cochlear pathologies that could be associated with the impairment and (2) to analyse suprathreshold responses to characterise temporal processing capacity in mutants and controls. Comparisons were made between cochlear regions where threshold was normal (24kHz) and where thresholds were raised (6-12kHz).

We used confocal microscopy to assess numbers of synapses (marked by Ribeye for the presynaptic ribbon and GluR2 for the postsynaptic density). Our results revealed no significant difference in the number of synapses in 6 week old Kihl18lowf homozygotes at the 12 kHz and 24 kHz cochlear regions compared with controls. Stereocilia of four week old Kihl18lowf were imaged using Scanning Electron Microscopy. We observed abnormal morphology of inner hair cell stereocilia which were tapered towards the tip in homozygous mutants at

the 6 and 12 kHz region when compared to wildtypes. A less pronounced structural defect was observed in heterozygous mutants.

To characterise temporal processing, we used three different test conditions involving varying repetition rates, varying rise/fall times and forward masking in four week old Kih18lowf homozygotes and wildtypes. Homozygous mutants responded with reduced ABR wave I amplitudes to clicks and tones across all repetition rates and rise/fall times, respectively. Heterozygotes have an intermediate phenotype. In the forward masking paradigm, a similar proportion of amplitude reduction at shorter gaps and a similar recovery profile was observed in mutants when compared to controls. For the 12 kHz tone differences in the ABR wave I amplitude slopes were observed at 1 ms rise/fall times. At high sound intensities dB SPL, rate of growth is higher in homozygous mutants when compared to controls.

The underlying low frequency hearing impairment and the observed ABR wave I amplitude reductions in mutant Kih18lowf are associated with an abnormality of stereocilia morphology and intermediate phenotypes are found in heterozygous mutants in both electrophysiology and structure.

Inner-Ear Therapeutics I

PS 455

Gene Therapy Rescues the Audiovestibular Phenotypes in Pjvk-Defected Mice

Ying-Chang Lu¹; Chin-Ju Hu¹; Chen-Chi Wu¹; Yen-Fu Cheng²; Chuan-Jen Hsu³

¹National Taiwan University Hospital; ²Taipei Veterans General Hospital; ³Taichung Tzu Chi Hospital

Background: Cochlear implantation is currently the treatment of choice for patients with profound sensorineural hearing impairment. However, the outcomes with cochlear implants (CIs) vary significantly among recipients. In our previous study, we identified that mutations in PJKV and PCDH15 were associated with unfavorable CI performance. To explore the molecular mechanisms and therapeutic strategies, we then used the CRISPR/Cas9 technology to generate transgenic mouse models with these mutations, including the common PJKV p.G292R mutation in the Han Taiwanese. The Pjvk p.G292R mice showed significantly higher hearing thresholds and impaired balance. In this study, we further explore the feasibility of gene therapy in this animal model using the Anc80L65 vector, a novel AAV vector which can target the sensory cells and neurons of the inner ear with high efficiency.

Methods: The Anc80L65 vector was constructed and obtained from the Gene Transfer Vector Core at the Massachusetts Eye and Ear Infirmary. The Anc80L65 vector contained the predominant longest isoform of Pjvk cDNA (NCBI accession no. 001080711.2) and was driven by a cytomegalovirus promoter. The carrying capacity of this vector was estimated to be about 4,500 bp. The predominant longest isoform of Pjvk cDNA is 1,059 bp and could fit within the Anc80L65 vector. Surgery was performed only on the left ear of each animal at P0-P3. A total of 0.7 μ l Anc80L65.CMV.Pjvk was injected into round window membrane. Sham surgeries were performed as above with Anc80L65-GFP as a negative control virus. Mice were then subjected to a battery of audiologic assessments, vestibular evaluations, and histological studies.

Results: Gene therapy using the novel Anc80L65 vector was able to improve hearing and restore balance function in Pjvk p.G292R mice for at least 3 months. Auditory brainstem responses measured at 6 weeks showed improved hearing thresholds in the treated ears than the controls ears, especially at high frequencies. Rotarod tests at 3 m showed normal vestibular performance in the treated mice compatible to those in the wild-type mice. Histological studies showed increased number of spiral ganglion neurons in the treated ears than in the control ears.

Conclusions: Our data indicate that gene therapy is likely to become a treatment option for hereditary hearing impairment, as well as a possible armamentarium that can augment the function of CIs. These findings also suggest that biological therapies to treat deafness may be suitable for translation to humans with genetic inner ear disorders.

PS 456

Otoprotection by the Small-Molecule UPR Modulator ISRIB Across a Broad Range of Noise Exposures

Stephanie L. Rouse; Ian R. Matthews; Dylan K. Chan
University of California, San Francisco

Background: Acoustic overstimulation causes a spectrum of hearing loss, ranging from permanent threshold shifts to suprathreshold ABR Wave I amplitude reduction related to cochlear synaptopathy, in which loss of inner hair cell-spiral ganglion neuron synapses can manifest as central auditory processing deficits including speech-in-noise difficulties, tinnitus, and hyperacusis. Recent work by our group implicates the unfolded protein response (UPR) pathway in noise-induced hearing loss (NIHL). We found that the UPR and endoplasmic reticulum (ER) stress modulator ISRIB (Integrated

Stress Response Inhibitor), which activates eIF2B and leads to decreased synthesis of the pro-apoptotic UPR protein Chop (C/EBP-homologous protein) provides partial protection against permanent threshold shifts and hair-cell loss after 106 dB SPL noise exposure. In this study, we sought to investigate whether the protective effects of ISRIB extend to lower sound levels, including those associated with cochlear synaptopathy.

Methods: 8 week-old WT CBA/J mice were pretreated 3 hours prior to noise exposure with a single intraperitoneal injection of ISRIB (10 mg/kg) or vehicle. Acoustic trauma consisted of exposure to 8-16 kHz octave-band noise for 2 hours at 106, 97.7, 96.6, 95.5, 94 and 92 dB SPL. ABR thresholds and intensity functions (10-90 dB SPL) were recorded at baseline as well as post noise exposure (PNE) days 1, 7, 14, 21 using pure-tone bursts at 4, 8, 16, 24, 32, 40 kHz. Amplitude and latency of suprathreshold ABR wave I peaks were analyzed both by an individual blinded to experimental conditions and a custom peak detection program.

Results: Noise exposures produced temporary shifts in ABR thresholds ranging from 30-60 dB SPL immediately after NE with variable recovery 3 weeks post NE that correlated with the NE level. Suprathreshold Wave I ABR amplitudes were also decreased in a frequency- and noise level-dependent manner. Across all noise exposure paradigms, a single pre-exposure dose of ISRIB reduced noise-induced changes in permanent ABR thresholds and Wave-I amplitudes, without affecting temporary threshold shifts.

Conclusions: Our data show a protective effect of ISRIB across a broad range of noise exposure levels, both in terms of permanent ABR threshold shifts as well as suprathreshold Wave-I amplitudes. Future work will directly examine synapse counts and examine effects of ISRIB on noise-induced UPR pathway activation across this range of exposure levels. Overall, this work suggests that the UPR is a promising pathway to target for development of future treatment options across a range of noise-induced hearing loss paradigms.

PS 457

HDAC Inhibitor Rescues the Hearing in a Model of Alport Syndrome

Dami Kim¹; Munyoung Choi²; Alphonse Umugire¹; Hyong-Ho Cho²; Sungsu Lee³

¹Department of Biomedical Science, College of Medicine, Chonnam National University Graduate School, BK21 PLUS Center for Creative Biomedical Scientists at Chonnam National University,; ²Hearing and Neurotology lab, Department of Otolaryngology-

Head and Neck Surgery, Chonnam National University Hospital; ³Kresge Hearing Research Institute, Department of Otolaryngology - Head and Neck Surgery, Michigan Medicine

Introduction

Genetic hearing loss is one of the most prevalent sensory disorders. Potential future treatments include in utero gene transfer and postnatal gene delivery by adeno-associated virus or anti-sense oligonucleotide administration. Alport syndrome (AS) is caused by mutations in collagen type IV, one of the major protein in the basement membrane. Kidney and cochlea are frequently involved causing glomerulonephritis and hearing loss. Hearing in AS is usually normal at birth, progressively deteriorating thereafter. To assess the influence of epigenetic changes on disease progression, we tested the effects of HDAC inhibitor on hearing in an AS model.

Methods

Knockout (KO) mouse of type IV collagen alpha 3 chain were used for AS model (Jackson lab, Col4a3tm1Dec/J). For the treatment group, a HDAC inhibitor CG200745 (CrystalGenomics, Inc.) was given orally with drinking water starting from the age of 3 weeks. Hearing levels were measured by auditory brain stem response audiometry (ABR) starting from age 4 weeks through 10 weeks when the homozygote KO began to die due to the end-stage renal failure. Cochleae were harvested at 10 weeks, decalcified in EDTA, embedded in paraffin, sectioned and stained with H&E or immunocytochemistry for ICAM2 and Collagen type IV.

Results

Beginning from week 3, hearing thresholds were gradually elevated in AS mice reaching a plateau at 60 dB at the age of 5 weeks. Col4a3 KO showed dispersed and enlarged lateral wall especially in the stria vascularis. Spiral ganglion neurons and hair cells in organ of Corti appeared to be normal. With ICAM2 and Collagen type IV staining, cochlear vessels were visualized. Vascular lumens of the stria vascularis were markedly enlarged in the KO group. HDAC inhibitor treated KO group had better ABR thresholds of 40 dB whereas untreated group was 70 dB at age 7 weeks in AS mouse. Histology of the stria vascularis vessel was preserved in the HDAC inhibitor treated group and the organ of Corti remained unchanged.

Conclusion

Vascular function seems to be related to the hearing loss in AS. HDAC inhibitor prevented the vascular change in the stria vascularis and the outcome was associated with preserved hearing threshold in AS mouse model. The underlying mechanism is yet to be established.

Support: This research was supported by Chonnam National University Grant (2017-2824), Chonnam National University Hospital Biomedical Research Institute Grant (CRI 18035–1) and National Research Foundation of Korea (NRF-2016R1D1A1A02937094)

PS 458

Antioxidants Attenuate Noise-Induced Hearing Loss in the Lateral Line of Larval Zebrafish

Abigail Jiang¹; Dyana Novicio¹; Beija Villalpando¹; Maria Sokolova¹; Phillip Uribe²; Allison B. Coffin¹
¹Washington State University Vancouver; ²Otonomy, Inc.;

Damage to hair cells in humans and other mammals is permanent due to the inability to regenerate hair cells, resulting in hearing loss. In the U.S., hair cell death due to excessive noise from either occupational or recreational sources is a common cause of sensorineural hearing loss, with significant socioeconomic consequences. However, studies suggest that limiting the accumulation of reactive oxygen species (ROS) production by reducing oxidative stress can attenuate hair cell apoptosis. The present study expands on this previous work to further understand the onset and progression of noise-induced hearing loss (NIHL) and the protective benefits of antioxidant therapy. In a recently published study, we developed a novel acoustic trauma device capable of causing hair cell-specific damage to the lateral line in larval zebrafish (*Danio rerio*). The device creates an oscillation of microbubbles underwater which then implode, producing broadband shockwaves that damage the lateral line in a consistent manner. We have demonstrated the reproducibility of key features of NIHL in the lateral line, analogous to noise trauma seen in the mammalian cochlea. Here, we employed our model to conduct a high throughput redox drug screen and identified six antioxidants – D-alpha-tocopheryl quinone, D-alpha-tocopheryl succinate, resveratrol, 2-oxo-4-thiazolidinecarboxylic acid, ferulic acid ethyl ester, and picetannol – that protect hair cells from acoustic trauma. These aromatic compounds effectively reduce hair cell death when administered for 48 hours after noise exposure. Dose-response experiments are underway to establish the optimally protective concentration of each antioxidant. The efficacy of these compounds will then be further evaluated through a fluorescence-based ROS assay. Our data suggest that NIHL can be mitigated with

a post-noise treatment using these aromatic compounds to reduce hair cell damage. Future studies will further examine the optimal therapeutic window for antioxidant application and the efficacy of these compounds in a mammalian model of NIHL.

PS 459

Mitigation of Auditory Damage after Blast Exposure with Glucagon-like Peptide-1 (GLP-1) - A Study in Chinchilla

Rong Gan; Kyle Smith; Tao Chen; Shangyuan Jiang
University of Oklahoma

Introduction: Human auditory system is vulnerable to both peripheral and central damages from blast exposure. Repeated exposures, even at low overpressure level (below mTBI) without rupture of the eardrum, frequently result in permanent hearing damage in Service members. Recent studies have assessed Incretin glucagon-like peptide-1 (GLP-1) receptor agonist (Liraglutide) as a potential treatment strategy for TBI [1, 2]. However, there is no report about the therapeutic function of GLP-1 for blast-induced progressive hearing damage. This paper reports our preliminary study in chinchillas to examine possible function of Liraglutide to mitigate the process of auditory damage after blast exposure.

Methods: Young adult chinchillas were used in this study and divided into three groups: Exp. Groups 1 and 2 and Control Group. Liraglutide was delivered to animals with subcutaneous injection at 48 hours before (“pre-treatment”) or 2 hours after blast exposure (“post-treatment”) within 7 consecutive days in Exp. Groups 1 and 2, respectively. On Day 1, six consecutive blast exposures with 10 minutes interval between exposures at blast overpressure below 5 psi or 35 kPa were conducted to chinchillas in Exp. groups. ABR for hearing threshold, DPOAE for cochlear response, and middle latency responses (MLRs) for central auditory cortex function were measured on Days 1, 4, 7, and 14 for each animal. On the final day, the animal was euthanized, and the brain and cochlea were harvested for immunohistochemistry or immunofluorescence study to determine the therapeutic function of Liraglutide in post-blast apoptosis process in auditory cortex and cochlea.

Results: An initial study to verify the GLP-1R expression in auditory system of chinchilla using immunohistochemistry technology on the cochlea of a control animal showed that GLP-1R was widely expressed in chinchilla’s cochlea, especially in the spiral ganglion neurons. We then explored that GLP-1R expression was found in the central auditory system. The function

tests in Exp. Groups showed the hearing restoration in both pre- and post-treatment animals.

Conclusions: Preliminary study on therapeutic function of Liraglutide for hearing restoration after blast exposure suggests that the repeated exposure-induced hearing damage can be mitigated gradually through 7-14 days of post-blast. However, more future studies on effects of GLP-1 on hearing restoration over longer time course following blast exposure are needed.

Acknowledgements: This work was supported by DOD W81XWH-14-1-0228.

References:

[1] Y. Li et al. *J. Neurochemistry*, Vol. 135(6): 1203-1217, 2015.

[2] D. Tweedie et al. *Alzheimer's & Dementia*, Vol. 12(1): 34-48, 2016.

PS 460

mGluR7 Negative Allosteric Modulation Protects the Auditory System Following Acute Noise Trauma: Biomarker Analyses

Reza Amanipour¹; Bo Ding²; Xiaoxia Zhu³; Guillaume Duvey⁴; Sylvain Celanire⁴; Joseph P. Walton⁵; Robert D. Frisina³

¹*Medical Engineering Department, Global Center for Hearing & Speech Research, University of South Florida;* ²*Communications Sciences and Disorders Dept., Global Center for Hearing & Speech Research, University of South Florida;* ³*Medical Engineering Dept., Global Center for Hearing & Speech Research, University of South Florida;* ⁴*Pragma Therapeutics;* ⁵*Communication Sciences & Disorders Dept., Medical Engineering Dept., Global Center for Hearing & Speech Research, University of South Florida*

Background: Noise-induced hearing loss (NIHL) affects millions of people worldwide, resulting in damage to cochlear receptor cells, and is coupled with increased hearing thresholds. Depending on the duration and level of acoustic trauma, NIHL is linked to loss of inner and outer hair cells, as well as spiral ganglion neurons (SGNs). Histological observations suggest that SGNs cell density and volume of the cochlear nucleus will reduce after noise-exposure. Nuclear factor κ B (NF κ B) is a transcription factor that regulates immune responses, and is an important element of neural excitotoxicity following noise-exposure. NF- κ B is an induced-dependent cytokine and AKT is a

downstream target of NF- κ B. Here, we investigated the biological mechanisms of the otoprotectant PGT117, a negative allosteric modulator (NAM) of the metabotropic glutamate receptor subtype 7 (mGluR7) to prevent or reduce hearing loss following acute noise-exposure in CBA/CaJ mice.

Methods: Male CBA/CaJ mice, normal hearing at age 3-6 months were utilized. The mice were randomly placed in control and treated groups (N=8/group). Their pre-exposure condition served as the baseline. PGT117 was administered orally for treated mice 1 hour pre-exposure and immediately following the exposure. All mice were exposed to an octave-band of noise (110 dB SPL, 45 minutes). Five months post-exposure subjects were sacrificed, and one of the cochleae and brain were dissected, fixed in 4% paraformaldehyde in PBS, decalcification in 10% EDTA in PBS, and placed in cryoprotection solution. The cochlea and brain were embedded and degassed in OCT, then frozen. Cryosectioning was performed at 5 μ m/section and stained with H&E and DAB (brain: 10 μ m/section, cresylviolet). Stria vascularis (SV) tissue was also examined for NF- κ B and AKT. qPCR was performed to observe regulation of both pro- and anti-inflammatory cytokines. Cochlear nuclei (CN) cells are counted using MetaMorph.

Results: Higher SGN cell density was observed in the treated group relative to controls. Differences between the groups were significant when measured from the basal, middle, and apical turns, respectively. NF- κ B and AKT gene levels for controls were higher than for treated group across all three tonotopic regions, suggesting that transcriptional factors, NF κ B and AKT decrease due to the treatment.

Conclusion: Further investigation will determine if changes in cell density occur in CN sections after noise-exposure. In addition, the cross-talk via modulation of mGluR7 for NF- κ B and the PI3-Kinase/AKT pathways might be part of a potential treatment approach for NIHL.

Support: TRIH T05 Grant from UK Action on Hearing Loss, Pragma Therapeutics.

PS 461

Inhibition of MIF Protein Promotes Mouse Cochlear Hair Cell Survival After Neomycin Damage

Liman Liu¹; Yan Chen²; Mo Chen³; Yi Wei¹; Weiping Wen¹

¹*The First Affiliated Hospital of Sun Yat-sen University;* ²*ENT Institute and Otorhinolaryngology Department*

of Affiliated Eye and ENT Hospital, State Key Laboratory of Medical Neurobiology, Fudan University; ³Department of Otolaryngology, Harvard Medical School and Eaton-Peabody Laboratories, Mass Eye and Ear

Adult mammalian inner ear hair cells do not have regenerative capacity after hair injury, hair cell damage can lead to permanent hearing loss, so the study of cochlear hair cell protection is essential for the maintenance of hearing function. It has been reported that cochlear hair cell damage was accompanied by the occurrence of inflammation, and there are emerging papers to state the role of inflammation during the cochlear hair cells loss suggesting that the inner ear inflammatory response is not an ignored factor of hair cells survival. Nevertheless, the mechanism of inflammatory factors on hair cell survival after damaged is unclear. MIF is a multifunctional cytokine regulatory factor involved in the regulation of innate immune processes and affecting tissue function, and literature has reported that Mif gene defect could affect the development of the inner ear, however, the role of MIF in cochlear hair cells survival remains unclear.

In the experiment, we found that MIF was highly expressed in the sensory epithelium during the process of hair cell damage. By inhibiting the MIF factor, we found that the expression level of pro-inflammatory factors was lower than control group after neomycin damage, hair cell apoptosis was reduced, and hearing loss was blocked suggesting that MIF factor is an important factor for hair cells survival during injury. In this study, we will use of small molecule compounds to study the hidden mechanism how MIF impacts inner ear hair cell survival during neomycin injury, this is an important supplementary study for interpreting the effect of inner ear inflammatory response on sensory cells survival and cochlear function, and it also has an important guiding significance for clinical application.

PS 462

Hydrogen treatment after continuous noise-exposure

Anette Fransson¹; Penilla Videhult Pierre²; Göran FE. Laurell³

¹Department of Neuroscience, Karolinska Institutet; ²Dept of Clinical Science, Intervention, and Technology, Karolinska Institutet; ³Department of Otolaryngology, Uppsala university hospital

Background

Despite successful prevention strategies to reduce

work-related noise exposure to an acceptable level, many people still suffer from occupational hearing loss due to continuous and/or impulse noise. Some earlier studies have reported that experimental animals drinking aqueous molecular hydrogen (H₂) achieve protection against noise-induced hearing loss via a reduction of oxidative stress. Noise-induced hearing loss is a condition where the window of therapeutic opportunity is most probably critical. We tested the hypothesis that inhalation of H₂ directly after exposure to continuous noise can rescue the hearing.

Materials & Methods

Fortyeight guinea pigs were placed in a soundproof box and exposed awake to broadband noise at 2-20 kHz dB SPL for two hours. Immediately after termination of noise exposure, the animals were anesthetized and were subjected to inhalation of H₂ for one hour (Noise+H₂ groups) or room air (Noise groups). Frequency specific auditory brainstem response (ABR) was recorded at 3.15, 6.3, 12.5 and 20 kHz before noise exposure and two hours, one week or two weeks after the noise exposure. After the final ABR measurement the animal was deeply anesthetized and decapitated, and both cochleae were fixed and dissected for morphological analysis. The left cochlea was used for hair cell counting, while the right cochlea was used for immunohistochemistry to assess progression of synapse degeneration and inflammation.

Results

Two hours after noise exposure, ABR measurement showed severe threshold shifts in both the Noise and Noise+H₂ groups, while almost no hair cell loss was observed. At one week and two weeks outer hair cell (OHC) loss was demonstrated in all groups. ABR threshold assessment and OHC counting revealed significant differences between the Noise and Noise+H₂ groups, with better preserved ABR thresholds and less loss of OHCs in the Noise+H₂ group. However, the ABR thresholds at one week indicated a significant recovery in both groups. The results of the immunohistochemical analyses will be presented at the meeting.

Conclusion

Since oxidative stress plays an important role in noise-induced hearing loss, a number of different antioxidants have earlier been used to rescue the hearing function after deleterious noise-exposure. In the present in vivo study inhalation of H₂ immediately after continuous noise trauma demonstrated a partial therapeutic effect. The results indicate that inhalation of H₂ positively affects pathological redox-related processes in the cochlea. As a hearing rescue treatment, H₂ has the advantage to be easily administered after a noise trauma.

PS 463

Non-invasive Localized Induction of Therapeutic Hypothermia Mitigates Noise Induced Hearing Loss

Samantha Rincon¹; Rachele Sangaletti²; Ilmar Tamames¹; Anne Feliciano³; Michael Hoffer⁴; Curtis King⁵; Suhrud M. Rajguru⁶

¹Department of Biomedical Engineering, University of Miami; ²Department of Otolaryngology, University of Miami; ³University of Miami; ⁴Department of Otolaryngology and Neurological Surgery, University of Miami; ⁵Lucent Technologies; ⁶Department of Biomedical Engineering and Otolaryngology, University of Miami

Background:

Noise-induced hearing loss (NIHL) remains one of the leading sensorineural diseases, with an estimated 1.1 billion people at risk of NIHL due to occupational and recreational exposure to hazardous sounds (>85 dB SPL). In the present study, we assessed the therapeutic benefit and mechanisms of localized therapeutic hypothermia in the mitigation of cochlear injury from NIHL in a rat model.

Methods:

Juvenile Brown Norway rats were randomly separated into three groups: normothermic NIHL, hypothermia-treated NIHL, and non-NIHL control. Auditory brainstem responses and distortion product otoacoustic emissions were performed to quantify changes in hearing threshold in anesthetized rats prior to NIHL and up to 28 days following trauma. Animals with normal hearing and aged 15-20 weeks were subjected, under isoflurane anesthesia, to two hours of continuous 4-8 kHz noise at intensities of 105 or 120 dB SPL. Mild hypothermia (31-33 °C) was induced in cochleae of hypothermia-treated NIHL rats at 15 minutes post-exposure for a two-hour period. At 28 days post-exposure in female rats, cochleae were harvested for immunolabeling and counting of inner and outer hair cells. In a separate set of animals, cochleae were harvested up to 3 days post-exposure for labeling and counting of hair cells and ribbon synapses. To study the mechanisms of NIHL and therapeutic hypothermia, changes in apoptotic-related genes were measured using RT-PCR at 1 or 7 days post-exposure in male rats.

Results:

Hypothermia-treated rats receiving 105 dB noise had significantly lower temporary threshold shifts at

1-7 days post-exposure. There was no significant difference in hair cell counts between groups at 28 days post-exposure. The normothermic group elicited significantly lower wave I amplitudes at day 1 and day 3 when compared with hypothermia-treated group. After exposure to 120dB noise, significant loss of outer hair cells was observed, resulting in permanent threshold shifts for both NIHL groups. However, ABR threshold shifts were lower for hypothermia-treated animals. Results of RT-PCR show that at 1 day post-exposure, hypothermia prevents additional damages by inhibiting the activation of caspase 3 and 8, thus interrupting the extrinsic apoptotic pathway.

Conclusions:

Early neural response may suggest neuronal loss in high frequency regions under the normothermic conditions. Mild therapeutic hypothermia reduced inflammation, increased activity of anti-apoptotic pathways, and reduced oxidative stress. Overall, non-invasive induction of localized therapeutic hypothermia may be an efficacious and safe approach to preserve residual hearing following noise over-exposure.

Supported by 1R01DC013798 and Wallace H Coulter Center for Translational Research.

PS 464

The effects Cannabidiol (CBD and Dexanabinol (HU-211) as a countermeasure for hearing loss after blast injury in the small rodent model

Roberta Allgayer de Moraes¹; Dan Lan²; Jackson R Rossborough³; Faran Ahmad⁴; Jinahong Liu¹; Laura Gomezllanos⁵; Curtis King⁶; Carey Balaban⁷; Suhrud M. Rajguru⁸; Michael Hoffer⁹

¹Department of Otolaryngology, University of Miami; ²Department of Otolaryngology, University of Miami; ³Department of Biomedical Engineering, University of Miami; ⁴Department of Biomedical Engineering, University of Miami; ⁵Department of Otolaryngology, University of Miami; ⁶Lucent Technologies; ⁷Department of Otolaryngology, Neurobiology, Communication Sciences & Disorders, and Biogengineering, University of Pittsburgh; ⁸Department of Biomedical Engineering and Otolaryngology, University of Miami; ⁹Department of Otolaryngology and Neurological Surgery, University of Miami

Background

Mild traumatic brain injury (mTBI) secondary to blast and blunt head trauma is an increasingly recognized injury

pattern with known acute and chronic sequelae. Despite significant study in this area there remains a need for pharmaceutical countermeasures that impact both acute and long-term sequelae after mTBI. Cannabinoids have been described to have positive effects on a variety of neurological disorders through an array of protective mechanisms. In this work we describe the impact of both cannabidiol (CBD) and dexanabinol (HU-211) on hearing outcomes on rats given one or both of the agents one hour after the blast exposure.

Methods

The tube design has been previously described (Courtney 2012, Rossborough 2018) Anesthetized animals were subjected to blast injury in the mild to moderate range 10-18 psi and then were treated with CBD (1mg/kg), HU-211 (0.1 mg/kg), a combination of both agents, or a vehicle beginning immediately after the blast exposure and then performed once a day for a total of seven doses via an intraperitoneal method. The animals then underwent hearing testing at defined intervals over a 28-day period using auditory brainstem testing (IHS, Inc., Miami, Florida).

Results

The animals had normal baseline hearing results over the frequencies tested. At 24 hours all of the post-blast the animals in each of the treatment groups showed a profound hearing loss which slowly corrected over time. By the 14-day time point all of the groups showed significant hearing improvement over baseline. This improvement was significantly greater for the three treatment groups (CBD alone, CBD plus HU-211 and HU-211 alone) when compared to the vehicle treated animals at 12K and 22K. . The hearing results for one representative frequency are shown in figure 1.

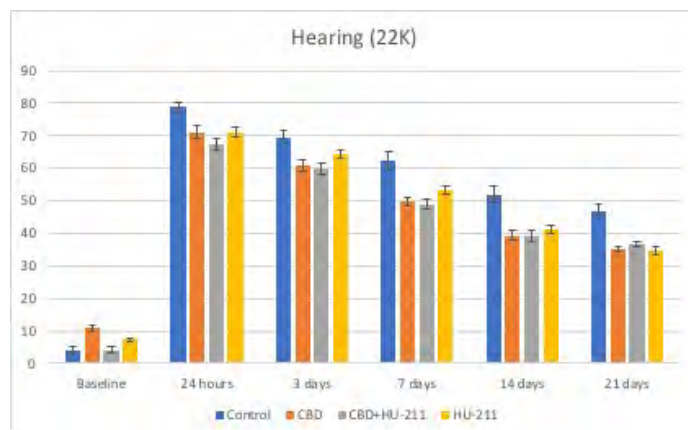
Conclusion

CBD, HU-211, and CBD plus HU-211 has a positive impact on hearing improvement in a small rodent model after blast injury. Our lab is in the process of exploring the mechanisms whereby this effect as seen as well as the impact of different doses on animals with head injury.

References

- 1) Courtney et al. Rev Sci Instrum. 2012 Apr; 83(4):045111
- 2) Rossborough, et al, Ecological Validity of a rodent blast tube, Presented at the 41st Annual Midwinter ARO Meeting, February 10-14. 2018, San Diego, CA.

Figure 1 – Audiometry results over time at 22 K



PS 465

Ebselen Mediated Otoprotection from Noise-Induced Hearing Loss: Once vs Twice Daily Dosing

Ryan Longenecker; Jennifer Homan; Rende Gu; Jonathan Kil
Sound Pharmaceuticals, Inc

Background

Noise-induced hearing loss (NIHL) is the leading occupational disease in the United States, especially in military populations. Previous works by several labs have shown that ebselen prevents NIHL in mice, rats and guinea pigs, in both acute and chronic periods. To further develop ebselen as an otoprotectant, the acoustic startle reflex (ASR) mouse model was used to advance our understandings at a behavioral level. Following noise exposure, mice were examined with auditory brainstem responses (ABR), various ASR assays (including prepulse inhibition and gap detection), and cochlear histology. We hypothesize that ebselen will effectively prevent and treat behavioral evidence of hearing loss as well as noise-induced tinnitus. In addition, we will determine if a single daily dose of ebselen can achieve the same level of otoprotection as twice daily dosing.

Methods

Three groups (n=8/per group) of Swiss Webster mice were noise exposed to an octave band noise centered at 12 kHz, presented for 4 hours at 113 dB SPL. Prior to noise, Group 1 received ebselen once po (10 mg/kg/qd), and Group 2 received ebselen twice po (5 mg/kg/bid). The control groups received the saline/dmsol (vehicle). Hearing assessments included ABRs, prepulse inhibition, and gap detection assays. These assays were collected before, 1 day, and 1 month after

noise exposure. The ABRs and prepulse tests used pure tones of 6, 12, 16, and 24 kHz for evidence of hearing loss, while the gap detection test used a broadband noise and varied the gap duration (0-50 ms). Following hearing assessments, mice cochleae were prepared for hair cell and spiral ganglion analyses.

Results

Following noise exposure, the vehicle group (controls) demonstrated dramatic ABR threshold shifts, decreased prepulse inhibition, and decreased gap detection abilities compared to the ebselen treated groups. Cochlear histology also demonstrated a difference between ebselen treated and vehicle treated mice.

Conclusions

Results of this study indicate that ebselen can be administered less frequently while providing the same level of otoprotection. This dosing strategy will be tested in future clinical trials for ebselen as a treatment for noise-induced hearing loss

PS 466

Molecular Dynamics Simulations of CDK2 Inhibitors that Prevent Ototoxicity Effect of Cisplatin

Zhuo Li¹; Sandor Lovas¹; Tal Teitz²; Jian Zuo¹
¹Department of Biomedical Sciences, Creighton University, School of Medicine; ²Department of Pharmacology, Creighton University, School of Medicine

Cisplatin is a widely used chemotherapeutic agent to treat various cancers. Unfortunately, around 40 – 80 % adults and over 50 % children are suffering permanent hearing loss caused by cisplatin-based chemotherapy. There are currently no FDA-approved compounds for treating any kind of hearing loss. Recently, in a high throughput screening of over 4000 diverse compounds, Teitz et al. (JEM 2018) have identified ten compounds that can protect hair cell damage caused by cisplatin. Among these hit compounds, three are cyclin-dependent kinase 2 (CDK2) inhibitors. Mice devoid of CDK2 protein were shown to be resistant to cisplatin-induced hearing loss. While the CDK family has been extensively studied as a cancer treatment target, the role of CDK2 in the post-mitotic hair cells is not clear. In a more recent screening on a focused library of 192 CDK2 inhibitors (Hazlitt et al., JMC 2018), 38 compounds have been identified with EC₅₀ more potent than 7 mM in HEI-OC1 cells. Subsequently, 36 analogs of AT7519 (EC₅₀ = 0.38 mM) were synthesized and found that analog 7 (EC₅₀

=0.013 mM) exhibited the better therapeutic index than the parent molecule. However, analogs 6 and 8, which share the most similar structure with analog 7, namely only the hexanyl hydroxyl group being replaced either by a hydrogen atom or by an amine group, respectively, are at least 2000-fold less potent in HEI-OC1 cells while the CDK2 inhibition of these three analogs are comparable. In current study, we employed micro-second scale molecular dynamics simulations to explore the structural perturbation induced by different AT7519 analogs to reveal the mechanism of the CDK2 inhibition in the hearing protection at the atomic level. We compared the trajectories of various CDK2 states, namely with and without cyclin binding, wild-type and phosphorylated Thr160, Thr14 and/or Tyr15, with and without these AT7519 analogs. Our analysis of the trajectories focused on the known functional motifs of CDK2, such as the T-loop, the G-loop, the DFG motif and the ATP binding pocket. Knowing the unique molecular features of the effective perturbation of CDK2 structure will enable the employment of the virtual screening to identify drug candidates more effectively. Also, as inhibition of CDK2 activity will prevent cancer cell from proliferating, this group of compounds will be promising drug candidates to protect cisplatin induced hearing loss without conflicting with the cancer treatment.

Supported in part by NIHR01DC015010, NIHR01DC015444, ONR-N00014-18-1-2507, USAMRMC-RH170030, and LB692/Creighton.

Teitz, T., Fang, J., Goktug, A. N., Bonga, J. D., Diao, S., Hazlitt, R. A., Iconaru, L., Morfouace, M., Currier, D., Zhou, Y. et al. 2018. CDK2 inhibitors as candidate therapeutics for cisplatin- and noise-induced hearing loss. *J. Exp. Med.* 215:1187-1203.

Hazlitt, R. A., Teitz, T., Bonga, J. D., Fang, J., Diao, S., Iconaru, L., Yang, L., Goktug, A. N., Currier, D., Chen, T. et al. 2018. Development of second-generation CDK2 inhibitors for the prevention of cisplatin-induced hearing loss. *J. Med. Chem.* 61:7700-7709.

PS 467

In vivo evaluation of GSK3077978A compound, a CD38 inhibitor, on age-related hearing loss in SAMP8 mice

Rick Cousins¹; Sergio Gonzalez-Gonzalez²; Gaëlle Naert²; Susanna Malmström²; Sylvie Cosnier-Pucheu²; James Ellis¹; Nienke Fishwick¹; Joanne Storey¹; Christine Rozier¹; Rakesh Nagilla¹; Tanya Mullaney¹
¹GSK; ²Cilcare

Introduction: Age-related hearing loss (ARHL) is the most common sensory disorder in the elderly population. The senescence-accelerated prone strain 8 (SAMP8) mouse model presents accelerated senescence and has been identified as a model of gerontological research. SAMP8 displays sequential degeneration of cochlear hair cells, spiral ganglion neuron and stria vascularis which mimic human ARHL. The molecular mechanisms associated with SAMP8 senescence involve oxidative stress and altered levels of antioxidant enzymes leading to chronic inflammation and apoptosis. Nicotinamide Adenine Dinucleotide (NAD) levels decrease during aging and are involved in age-related metabolic decline. The CD38 enzyme metabolizes NAD and may be involved in the age-related NAD decline and mitochondrial dysfunction. The objective of this study was to assess the effect of GSK3077978A compound, a CD38 inhibitor, on the progression of age-related hearing loss in SAMP8 mice.

Material & Methods: Firstly a PK study was performed to measure the concentration of compound GSK3077978A after oral administration to SAMP8 mice, in the tympanic bulla and in plasma, and to compare single and repeated dosing regimens. Secondly, to study the effect of GSK3077978A in age-related hearing loss, the compound was administered orally in female SAMP8 mice, one month of age, once a day for 14 weeks, at a dose of 30 mg/kg, and the auditory brainstem response (ABR) was measured along with the distortion product otoacoustic emissions (DPOAEs), two auditory parameters, every two week during the study.

Results: The PK study indicated the compound concentration in the tympanic bulla was sufficient for treatment in the ARHL model. The concentration declined at 8h in both dose regimens suggesting a daily treatment was necessary. GSK3077978A treatment of SAMP8 mice prevented the onset of auditory declines after 2, 4 and 6 weeks of treatment. ABR thresholds were statistically decreased at all frequencies and DPOAE amplitudes were statistically increased at high frequencies in treated SAMP8 mice compared to control SAMP8 mice.

Conclusion: These results showed that GSK3077978A delayed the senescence process by slowing down the age-related hearing loss, protecting the auditory function, suggesting that the CD38 enzyme could be a potential pharmacological target for age-related hearing loss.

All animal studies were ethically reviewed and carried

out in accordance with European Directive 2010/63/EEC and the GSK Policy on the Care, Welfare and Treatment of Animals.

PS 468

Calpain Inhibitor Prevents Noise-induced Hair Cell Loss through Upregulation of p-Akt Signaling

Ruoshan Lai¹; Qiaojun Fang¹; Song Pan¹; Guangyong Tuan²; Su-Hua Sha¹

¹Medical University of South Carolina; ²the Third Affiliated Hospital of Southern Medical University

Background: Noise-induced calcium influx in sensory hair cells has been well-documented in the pathogenesis of noise-induced hearing loss (NIHL). Calcium influx activates calpains, a family of calcium-dependent cysteine proteases. Overactivation of calpains is associated with the pathogenesis of a wide variety of neurodegenerative diseases and therefore could serve as a potential therapeutic target. Here, we tested calpain inhibitor MDL28170 in prevention of noise-induced hair cell loss and hearing loss.

Methods: CBA/J mice at the age of 12 weeks were exposed to broadband noise (BBN) with a frequency spectrum from 2–20 kHz for 2 h at 101 dB sound pressure level (SPL) to induce permanent threshold shifts (PTS) with loss of inner hair cell synaptic ribbons and outer hair cells (OHCs) when assessed 2 weeks after the exposure. Auditory thresholds were measured by auditory brainstem response (ABR). OHC losses were counted from DAB-stained and myosin-VIIa-labeled surface preparations. Synaptic ribbons were counted from Z projections on surface preparations of immunolabeled CtBP2. Cochlear surface preparations and OC-1 cells were utilized to elucidate cellular mechanisms responsible for noise-induced losses of hair cells and synaptic ribbons and NIHL.

Results: Ionomycin-treated OC-1 cells showed increased levels of a-fordrin by immunoblots initially and apoptotic cell death at a later time points by flow cytometry analysis. Noise-induced loss of OHCs and auditory threshold shifts were reduced by treatment with the calpain inhibitor MDL28170. Unfortunately, noise-induced losses of synaptic ribbons were not attenuated. Furthermore, noise-decreased immunolabeling for p-Akt in OHCs was prevented by MDL28170 treatment.

Conclusions: These results indicate that treatment with calpain inhibitor MDL28170 could prevent noise-induced hair cell loss and hearing loss suggesting calpain as therapeutic target for treatment of NIHL.

Acknowledgements: The research project described was supported by the grant R01 DC009222 from the National Institute on Deafness and Other Communication Disorders, National Institutes of Health.

PS 469

In Vitro Characterization of Different AAV-Ntf3s for Proof of Concept In Vivo Studies

Changsuk Moon¹; Ryan C. McCarthy¹; Martin Schwander¹; Yong Ren¹; Guo-Peng Wang²; David Kohrman³; Gabriel Corfas⁴; Janeta V. Popovici-Muller¹; Inmaculada Silos-Santiago¹

¹*Decibel Therapeutics*; ²*Kresge Hearing Research Institute, Dept. of Otolaryngology Head and Neck Surgery, University of Michigan*; ³*Kresge Hearing Research Institute, Dept. of Otolaryngology Head and Neck Surgery, University of Michigan*; ⁴*Dept. of Otolaryngology Head and Neck Surgery, University of Michigan*

Introduction:

Delivery of consistent levels of proteins for prolonged period of time to the inner ear is important for proof of concept studies for drug development. Adeno-associated virus (AAV) can be an ideal gene delivery tool for in vivo applications because of its low immunogenicity and ability to provide constitutive gene expression in non-dividing cells. Different types of AAV-Ntf3 were designed and the pharmacological properties of the recombinant Ntf3 produced by these AAV-Ntf3 transduced in HEK293 cells were characterized.

Similar to native NT3, the AAV-Ntf3 was expressed, secreted and activated neurotrophin receptor tyrosine kinase C (TrkC) in cell lines resulting in receptor autophosphorylation and rapid generation of phosphorylated docking sites for downstream target cytoplasmic proteins. In addition, the secreted protein activates NT3/trkC pathways in murine spiral ganglion neurons (SGNs) in culture inducing neurite outgrowth and neuronal survival.

Methods:

2 AAV-Ntf3 were transduced in HEK293 cells. Cell pellets and cell culture supernatants containing secreted NT3 protein were collected from 2 days culture of transduced cell. ELISA, Western blot and qPCR were performed to quantitatively and qualitatively evaluate the expression and secretion of recombinant NT3.

Cellsensor assay using TrkC-overexpressing ChoK1 cells exposed to secreted NT3 from cell culture supernatant

was performed to assess the pharmacological activity of recombinant NT3. Western blots were also used to demonstrate target engagement (Trk phosphorylation) and activation of downstream signaling pathways (ERK phosphorylation).

The physiological effects of secreted NT3 was tested in a neurite outgrowth assay using neonate mouse dissociated SGN, in addition to newly developed adult mouse modiolus culture assay.

Conclusions:

AAV-Ntf3s transduced into HEK293 cells express and secrete active NT3 protein. Secreted NT3 activates TrkC-receptor as determined by Cellsensor assay, phosphorylation of TrkC and downstream target, ERK. Moreover, secreted NT3 induces neurite outgrowth in neonate and adult mouse primary SGNs.

Peripheral Vestibular System

PS 470

Hair cells turnover widely exists in mammalian vestibular organs

Dan You¹; Wenyan Li²; Huawei Li²

¹*ENT Institute and Otorhinolaryngology Department, Affiliated Eye and ENT Hospital, State Key Laboratory of Medical Neurobiology, Fudan University*; ²*1 ENT Institute and Otorhinolaryngology Department, Affiliated Eye and ENT Hospital, State Key Laboratory of Medical Neurobiology, Fudan University. 2 NHC Key Laboratory of Hearing Medicine (Fudan University)*,

Inner ear hair cells (HC) undergo turnover (cell death and replacement) throughout life in non-mammalian vertebrates. In contrast, spontaneous hair cell regeneration in adult mammalian vestibular is limited. To quantitatively study the phenomenon of hair cell turnover, we generated a novel strain of reporter mice; in which tamoxifen administration induces supporting cells (SCs) expressing SRY-related high mobility group-box gene9 (Sox9) express red fluorescent protein (tdTomato) at the same time. Fortunately, Sox9 specifically expressed in vestibular SCs. Then, we undertook comprehensive observation in murine utricles at different ages. We demonstrated that vestibular SCs in utricle persist differentiate to HCs in all ages, but the efficiency gradually decreased as the age increased. Both SCs in striolar and extrastriolar region can differentiate into HC, but the amount of HC derived from the differentiation of SC is higher in extrastriolar region three weeks after birth. To assess the cell division, we gave mice an injection of EdU at different ages. We found that a large

number of SCs proliferated in three days after birth and such proliferation continued for two weeks after birth. A part of the proliferated SCs differentiate into HC. Only type II hair cells turnover were detected. This project provides an efficient vestibular support cell transgenic mice and expand our understanding of hair cell turnover in mammalian vestibular organs.

PS 471

Mechanosensation-Mediated Yap1 Nuclear Localization in Supporting Cells of the Mouse Utricle.

Vikrant Borse¹; Tejbeer Kaur²; Angela Schrader¹; Mark E. Warchol¹

¹Washington University in Saint Louis; ²WASHINGTON UNIVERSITY SCHOOL OF MEDICINE

Background:

The Yap1 transcriptional coactivator regulates cell proliferation, differentiation and survival. Yap1 normally resides in the cytoplasm but can translocate into the nucleus in response to various biochemical signals as well as certain mechanical stimuli (e.g., cell-cell contact and cell attachment to the extracellular matrix). Once in the nucleus, Yap1 interacts with several transcriptional regulators to modulate gene expression. Loss of hair cells (HC) in the cochlea and vestibular organs has been shown to cause nuclear translocation of Yap1. The present study examined the effect of mechanosensation stimulated by surface attachment of the mouse utricle in Yap1 nuclear translocation in the SCs in vitro. This study also investigated Yap1 localization in response to DT-mediated HC lesion in the Pou4f3-huDTR knock-in mouse model.

Methods:

Utricles were explanted from mice, placed in Matrigel-coated dishes, and cultured for various time points as either surface-attached or free-floating samples. Some cultures were also treated with 1mM neomycin, to characterize the effect of ototoxic injury on Yap1 localization. The Pou4f3-huDTR knock-in mouse model was used to study the effect of HC damage on Yap1 nuclear translocation in vivo. Immunolabeling for Yap1, Myosin VIIa (HC marker) and Sox2 (SC and Type II HC marker) was used to determine YAP1 expression patterns and cellular distribution in the experimental and control groups.

Results:

Yap1 expression in the utricles of newborn and the adult mice was mainly confined to supporting cell cytoplasm. In cultures prepared from P15 mice, nuclear translocation of Yap1 was observed after 2, 6 and 12hr

in vitro, but not after 48 and 72hr in vitro. In 2, 6 and 12hr culture utricles, more than 75% SCs nuclei were positive for Yap1 immunostaining, however, in 48 and 72hr culture utricles, Yap1 nuclear labeling was absent in the SCs. Similar effects were observed in cultured utricles taken from mice at different ages (P2, P5, P10 and 1-2-month-old animals). In contrast, neomycin treatment did not evoke significant Yap1 nuclear translocation in supporting cells. There was also no nuclear Yap1 observed in the supporting cells after DT treatment in Pou4f3DTR Het and wild type newborns and adults in vivo. Some Yap1 immunoreactivity was also observed in hair cell cytoplasm after ototoxic injury.

Conclusion:

This study suggests that the removal of the mouse utricle from the mechanical constraints of its in vivo environment can promote transitory Yap1 nuclear translocation in SCs. However, hair cell injury leads to no nuclear translocation of Yap1.

PS 472

Loss of Sestrin2 (SESN2) Potentiates Noise-Induced Vestibular Deficits

Tianwen Chen¹; Youguo Xu¹; Yang Ou¹; Nathan Yin¹; Phoebe Xu¹; Yiji Tu¹; Jun Huang¹; Alberto Arteaga¹; David Sandlin¹; Douglas E. Vetter²; Kathleen T. Yee²; Ji Li³; Wu Zhou¹; **Hong Zhu¹**

¹Department of Otolaryngology University of Mississippi Medical Center; ²Dept. of Neurobiology and Anatomical Sciences, University of Mississippi Medical Center;

³Department of Physiology University of Mississippi Medical Center

Introduction: Noise exposure not only causes hearing loss but also causes vestibular deficits. Our early studies have demonstrated that high intensity noise exposure induces peripheral vestibular damage in rats (Stewart et al., 2016). The mechanisms underlying the noise-induced vestibular deficits, however, remain to be elucidated. Sestrin2 (SESN2) is a stress-responsive protein that provides cytoprotection against various noxious stimuli. Loss of SESN2 has been shown to potentiate the early onset of age-related sensory cell degeneration in the cochlea (Hu et al., 2017). The goal of the present study was to examine the role of SESN2 in noise-induced vestibular dysfunction by measuring the vestibulo-ocular reflex (VOR) responses before and after noise exposure.

Methods: Eight adult male SESN2 KO mice and 11 wild type mice (C57BL/6J) were involved in the study. The animals were unrestrained within a subdivided wire mesh cage on a rotatory platform directly below the horn of a calibrated speaker in a reverberant

chamber. Broadband noise (200Hz-20kHz) at 103 dB SPL was delivered for 2 hours. VOR responses to sinusoidal head rotation (0.2~4Hz) and linear translation (0.2-2Hz) were recorded using an infrared eye tracking system before and after the noise exposure. **Results:** There was no significant difference in VOR gains to head rotations and linear translations between the wild type mice and the SESN2 KO mice before noise exposure. Twenty-four hours following the noise exposure, significant decreases in VOR gains to head rotation at 0.2 and 4 Hz were observed in the wild type mice. Their VOR gains returned to baseline 7 days following the noise exposure. However, the SESN2 KO mice exhibited more severe loss of gain to head rotations at all frequencies 24 hours following the noise exposure and did not recover for 8 weeks. Neither wild type nor SESN2 KO mice showed changes in VOR sensitivity to linear translations following noise exposure. **Conclusions:** Our results suggest that SESN2 plays a role in protection of noise-induced vestibular deficits. Ongoing studies will further study the underlying mechanisms. Support by R01DC012060 (HZ), R21 DC017293 (HZ), R01DC014930 (WZ), R21EY025550 (WZ), R21DC015124 (DEV), R01AG049835 (JL) and R01GM124108 (JL).

PS 473

Transient and persistent effects of intense noise on the peripheral vestibular system

Courtney E. Stewart¹; David Bauer¹; Megan Battersby²; Samantha Katz¹; Ariane Kanicki¹; Tarana Joshi¹; Halima Haque¹; Richard Altschuler¹; W. Michael King¹

¹University of Michigan, Kresge Hearing Research Institute; ²College of Wooster; University of Michigan, Kresge Hearing Research Institute

Introduction: The vestibular system plays a critical role in detection of head movements and is essential for normal postural control and balance. Because of their anatomical proximity to the cochlea, the otolith organs are vulnerable to sound pressure and at risk for noise-overstimulation. Although clinical reports suggest a link between noise-induced hearing loss and balance problems, the physiology underlying this linkage is not well understood. It is known, however, that irregularly discharging vestibular afferents are the most sound-sensitive (Murofushi & Curthoys, 1997) and this population of afferents plays a critical role in descending vestibular reflexes (Bilotto et al., 1982). The vestibular short-latency evoked potential (VsEP) is generated by irregularly firing afferents (Jones et al., 2011). Our previous study demonstrated noise-induced loss of

VsEP responses (Stewart et al., 2018). The goal of the current study is to correlate changes in VsEP waveform amplitudes and the jerk thresholds for evoking VsEPs with changes in rats'; ability to cross a narrow balance beam. Results of this work will link noise-induced changes in VsEP with changes in motor performance in a vestibular-dependent task.

Methods: Adult Long-Evans rats (400-450g) were exposed to either 120 dB pSPL (0.5-4kHz) noise or sham conditions for six hours on a single day. Changes in auditory function were evaluated by measuring auditory brainstem response (ABR) before and after noise exposure. Before and across time points up to 28 days after noise exposure, the VsEP was evaluated. Balance beam crossings were analyzed for overall crossing time, foot slip errors, and falls. Additionally, fast Fourier transforms of head acceleration and velocity were used to identify the dominant frequency components of head movements during beam crossing.

Results: Following noise exposure, the VsEP P1N1 waveform (reflecting vestibular nerve activity) was abolished or severely attenuated in response to weak (<0.5/ms) jerk stimuli, and the attenuation persisted for up to four weeks in some animals. However, the P2N2 waveform (reflecting activity in secondary vestibular neurons) partially recovered. For larger jerk stimuli, VsEP amplitudes were initially reduced, but later recovered. Preliminary analysis suggests that beam crossing times may increase in noise-exposed rats.

Conclusions: Presence of P2N2 in the absence of P1N1 for smaller jerk stimuli may be associated with an adaptive central amplification of surviving peripheral nerve activity. These results suggest that noise may produce transient and persistent deficits in VsEP responses and these changes may produce impaired vestibulo-spinal reflexes.

PS 474

Calbindin Distribution in Otoferlin-null Vestibular Epithelia

Terry J. Prins; Johnny J. Saldate; **Larry Hoffman**
Geffen School of Medicine at UCLA

The vestibular sensory epithelia represent an exquisite organization of cellular characteristics that collectively encode head kinematics and orientation relative to the Earth's gravity vector. While there are far more questions than answers concerning specific functional contributions of these characteristics, we are beginning to understand the salient features that support stimulus coding. One

approach to understanding the association between the cellular organization of vestibular epithelia and head movement coding is to test hypotheses concerning the cellular modifications that result from alterations in sensory input. To this end, the otoferlin-null (*Otof*^{-/-}) mouse represents a valuable model, since striolar type I hair cells of these mice do not exhibit stimulus-evoked exocytosis, while striolar type II hair cells exhibit stimulus-evoked exocytosis with modified kinetics (Dulon et al. 2009). This model has thus allowed us to explore which features of the utricular striola are labile to stimulus evoked modulation, which revealed a markedly attenuated expression of calretinin in the vestibular afferents of *Otof*^{-/-} mice. These epithelia exhibited no discernable change in the hair cell expression of oncomodulin, consistent with the conclusion that alterations in postsynaptic calretinin was associated with attenuated sensory input (Prins et al. 2018) and not a more general disorganization secondary to the genetic modification. In the present study, we further explored the expression of calbindin in afferent neurons to test whether the expression of other postsynaptic calcium-binding proteins is compromised by sensory alterations in vestibular epithelia.

Immunofluorescent stains for calbindin in wild type (WT) vestibular epithelia initially revealed a high level of colocalization between the expression of calbindin and calretinin in postsynaptic vestibular afferents. However, the presence of calbindin positive afferents encompassed a larger area than calretinin and extended to regions of the utricle lateral to the line of polarity reversal (LPR). This distribution, despite significant sequence homology between calbindin and calretinin, appeared to more closely resemble our previous observations with the hair cell calcium binding protein oncomodulin. Additionally, our calbindin results to date mirror our previous findings of oncomodulin expression, in which the distribution of calbindin positive afferents appear to be similar between the epithelia of WT, heterozygotes (*Otof*^{+/-}), and *Otof*^{-/-} mice. These data imply that calbindin expression, within vestibular afferents of the inner ear, are not dependent upon stimulus evoked exocytosis from type I hair cells and are likely driven by factors that are at least partially independent of those responsible for the expression of calretinin.

PS 475

Topographic Distribution of Efferent Projections in Murine Vestibular Epithelia

Johnny J. Saldate; Sarah Jobbins; Zach Myers; Felix Schweizer; Larry Hoffman
Geffen School of Medicine at UCLA

Sensory epithelia of the vestibular labyrinth receive projections from efferent vestibular neurons, which are thought to provide centrifugal feedback. Vestibular efferent neurons are well-characterized with respect to their principal mode of neurotransmission (i.e. cholinergic), laterality (both ipsi- and bi-lateral projections have been identified), and effects on afferent discharge. While the predominant receptor types mediating cholinergic feedback to inner ear sensory epithelia are nicotinic, recent evidence indicates that muscarinic neurotransmission also makes important contributions to vestibular efferent modulation (Holt et al. 2016; Lee et al. 2017). These data support the notion that this feedback component alters the dynamic coding capabilities by attenuating the influence of Kv7.4 (aka KCNQ4) channels within the inner face of the dendritic calyces. These channels exhibit a unique topographic distribution within the vestibular epithelia, where calyces exhibiting heaviest expression are found in a region extending beyond the utricular striola and crista central zone (Spitzmaul et al. 2012). The present investigation tested the hypothesis that efferent terminals within vestibular epithelia exhibit a similarly heterogeneous distribution, supporting a consequential role of muscarinic-driven efferent modulation. Sensory epithelia from adult mouse labyrinths were harvested and immunohistochemically processed using methods previously described (Hoffman et al. 2018). Anti-vesicular choline transporter (VChT) was used to identify efferent terminals within whole mounts of utricular and crista epithelia. The specificity of VChT immunolabeling was verified through experiments examining colocalization with choline acetyltransferase (ChAT). Notably, anti-KCNQ4 immunolabeling elucidated epithelial regions exhibiting the heaviest expression in afferent calyces. Fluorescence emission was quantified across the topography of each epithelia, within which efferent terminal density was also quantified. Furthermore, we found that efferent terminal density was not homogeneous across utricular and crista topography; the region of highest density VChT-positive terminals expanded beyond the utricular striola or crista central zone. This finding indicates that the heterogeneous distribution of efferent terminals is not specifically confined by factors related to these specialized regions. However, the region of greatest efferent terminal density was coincident with the regions of epithelia that harbored calyces exhibiting high KCNQ4 expression. These data infer that centrifugal modulation by efferent neurons may result from muscarinic tuning of the dendritic generator potential by modifying the “m” current through KCNQ4.

Cholinergic Eminentia Cruciatum Associated Cells Discovered in Mice

Holly A. Holman¹; Lauren A. Poppi²; Yong Wan³; Micah Frerck¹; Richard D. Rabbitt¹

¹University of Utah; ²University of Newcastle and Hunter Medical Research Institute; ³Scientific Institute of Computing

Background

One of the most pronounced differences in the semicircular canals beyond their spatial orthogonal positions is a phylogenetic divergent anatomical structure bisecting the central zone of sensory epithelia in vertical cristae, referred to as the eminentia cruciatum (EC). A version of the EC is present in reptiles, birds, bats, and although relatively smaller also in lower vertebrates, but has not been detected in higher vertebrates to date. More than half a century after identifying the EC, its physiological function and cellular composition remain largely unknown. With the aid of a newly developed transgenic mouse, we provide evidence that the mouse EC has a robust cholinergic signaling component in a unique set of cells.

Methods

Transgenic mice from a Gad2-IRES-Cre driver line crossed with the GCaMP5G-tdTomato (tdT) reporter line provided a calcium indicator with a constitutively active tdT reporter for identifying transgene expression. Microdissected labyrinths exposing the apical surfaces of sensory neuroepithelia of the posterior and anterior cristae were performed according to the University of Utah IACUC. Within 20 min tissues were transferred to an imaging chamber and continuously perfused under an upright swept field confocal microscope (Bruker; LUMPLFN60XW). Confocal images were collected using a 35µm slit aperture in linear galvanometer mode. Image sequences consisted of 600-1000 frames collected at 10 frames per second. Each xy image was smoothed in (x,y) space with a 3-pixel Gaussian filter (WaveMetrics, Igor).

Results

Here we report strong evidence for newly identified cells of the EC in the mouse based on morphology, physiology, and immunohistochemistry. These specialized eminentia cruciatum associated (ECA) cells are present from embryonic day 20, the earliest time examined, and include a predominant cell, named clino herein. ECA cells develop complex basolateral processes throughout the lifetime of the animal. ACh evoked [Ca²⁺]_i transients in clino and adjacent ECA cells were reversibly blocked by the muscarinic acetylcholine receptor antagonist, atropine, and by the inositol triphosphate (IP₃) receptor antagonist 2-aminoethoxydihenyl borate (2-APB).

Conclusions

ECA cells express the transgene tdT reporter embryonically and in adulthood, suggesting a transcriptional role for the Gad2 machinery not only during early stages of development but throughout the lifetime in the mouse. Unexpectedly, ECA cells show robust excitatory [Ca²⁺]_i transients evoked by the efferent neurotransmitter ACh. Further examination of these cells may provide new insight for the role of cholinergic signaling and a functional aspect of the eminentia cruciatum in the crista.

PS 477

Developmental Calcium Transients in Mammalian Utricular Macula: From Spontaneous to Cholinergic

Holly A. Holman¹; Lauren A. Poppi²; Micah Frerck¹; Richard D. Rabbitt¹

¹University of Utah; ²University of Newcastle and Hunter Medical Research Institute

Background

During early postnatal development, spontaneous afferent neural activity occurs in the absence of gravito-inertial stimulation and transmits inputs to vestibular pathways in the central nervous system. How this spontaneous neural activity is generated during early postnatal development and what role it might play in establishing mature vestibular function is unknown. Cochlear spiral ganglion neurons in lower vertebrates exhibit spontaneous calcium events at birth. This spontaneous activity involves interplay between calcium transients in supporting cells (SCs) and hair cells (HCs) and is essential to the onset of hearing (1-3). In the present work, we examined the hypothesis that spontaneous calcium transients are also present during a similar developmental time course in utricular macula and are intricately linked to establishing utricle function.

Methods

Transgenic mice from a Gad2-IRES-Cre driver line (4) crossed with the GCaMP5G-tdTomato (tdT; 5) reporter line provided a calcium indicator with a constitutively active tdT reporter for identifying transgene expression. Within 20 min post microdissection the apical surface of utricular sensory neuroepithelia tissue was transferred to an imaging chamber and continuously perfused under an upright swept field confocal microscope (Bruker; LUMPLFN60XW). Images were collected using a 35µm slit aperture in linear galvanometer mode. Spontaneous GCaMP5 (ΔF/F) fluorescence was recorded at a 100ms frame rate over successive optical sections. Each xy image was smoothed in (x,y) space with a 3-pixel Gaussian filter (WaveMetrics, Igor).

Results

Spontaneous intracellular calcium transients $[Ca^{2+}]_i$ in HCs, SCs, and neuronal calyces in the early postnatal developing mouse utricle were observed. Spontaneous calcium activity is present at birth in HCs, followed by increased numbers of spontaneous calcium transients in SCs. Spontaneous calcium transients in both HCs and SCs largely subside at the end of the first postnatal week. We further demonstrate that $[Ca^{2+}]_i$ transients in the utricular macula can be modulated by the efferent neurotransmitter ACh, as soon as postnatal day 3, suggesting the presence of a feedback loop to and from the CNS that may be involved in coordinating development of vestibular synaptic connections and pathways during this early postnatal period.

Conclusion

Results confirm the hypothesis that spontaneous calcium transients are present in developing utricular HCs and juxtaposed SCs. The distinct temporal sequence of activity further suggests that spontaneous calcium transients in HCs and partner SCs likely modulates activity in di-morphic vestibular afferents during the first postnatal week and that this may play a key role in the maturation of vestibular neural circuits.

References

1. N. X. Tritsch et al., *Nature* 450, 50-55 (2007).
2. S. L. Johnson et al., *Proc Natl Acad Sci U S A* 110, 8720-8725 (2013).
3. D. H. Sanes, V. Siverls, *J Neurobiol* 22, 837-854 (1991).
4. H. Taniguchi et al., *Neuron* 71, 995-1013 (2011).
5. J. M. Gee et al., *Neuron* 83, 1058-1072 (2014).

PS 478

Otopettrin Immunolocalization in the Human Macula Utricle

Ivan A. Lopez¹; Gail Ishiyama²; Dora Acuna³; Akira Ishiyama⁴

¹*Department of Head and Neck Surgery, David Geffen School of Medicine;* ²*Neurology Department, David Geffen School of Medicine;* ³*Department of Neurology, UCLA School of Medicine;* ⁴*Department of Head and Neck Surgery, David Geffen School of Medicine*

Background: Benign paroxysmal positional vertigo (BPPV) is the single most common cause of vertigo seen in the otoneurologic clinic. It has been suggested that BPPV is caused by a lesion of the otolith organs

and cupulolithiasis. A variety of damages to the inner ear (trauma, infection, ischemia) could lead to dislodging of the calcium carbonate crystals from the otolith. Vestibular drops attacks (VDA) also known as Tumarkin falls are sudden violent falls are present in a small subset of patients with endolymphatic hydrops. BPPV and VDA has been associated with Meniere's disease (MD). The proteins present in formation of otoconia has been fair well characterized in the otolithic organs of mouse models but not in the human. Recently otopettrin a protein involved the otoconia metabolism has been shown to be a proton channel. In the present study we begin to characterize the expression of otopettrin in the human macula utricle.

Methods: Macula utricle were acquired at surgery from patients who required transmastoid labyrinthectomy for intractable vertigo (MD)(3) and/or VDA (n=2), and patients who required a translabyrinthine approach for acoustic neuroma (AN) resection (surgical "controls", N=3). Microdissected vestibular endorgans were obtained from temporal bones acquired at autopsy from individuals with no auditory or balance disorders (n=3). Immunofluorescence staining was made in cryostat sections or whole microdissected utricle (for flat mount preparations). The otopettrin-2 (rabbit affinity purified polyclonal antibody) and GFAP mouse monoclonal antibody (used to identify the supporting cells) were simultaneously incubated. Secondary antibodies against rabbit (Alexa 488) and mouse (Alexa 594) were used for the identification of both proteins. Digital images were obtained using a Leica (SP8) laser confocal microscope.

Results: Using cryostat sections or flat mount preparations otopettrin and GFAP were detected in the supporting cell cytoplasm immunofluorescence. In cryostat sections otopettrin was seen as punctated signal throughout the supporting cells cytoplasm. Using flat mount preparation of the macula utricle otopettrin was concentrated in the apical portion of supporting cells cytoplasm. The distribution of otopettrin-2 was similar in the macula utricle obtained from MD, AN or autopsy normative patients.

Conclusions: Otopettrin-2 was localized in supporting cells in a similar fashion that otopettrin previously reported in the mouse macula utricle. The differential expression of otopettrin-2 in the supporting cells suggest and important role in the otoliths homeostasis.

Acknowledgements: Supported by a NIDCD grant # 1U24DC015910-01.

Pericytes populations identified by Immunofluorescence in the Human Macula Utricle

Gail Ishiyama¹; Akira Ishiyama²; Dora Acuna³; Ivan A. Lopez⁴

¹Neurology Department, David Geffen School of Medicine; ²Department of Head and Neck Surgery, David Geffen School of Medicine; ³Department of Neurology, UCLA School of Medicine; ⁴Department of Head and Neck Surgery, David Geffen School of Medicine

Background: The integrity of the blood labyrinthine barrier (BLB) in the inner ear is important to control the passage of fluids, molecules and ions. Ultrastructural and cellular biological in the human BLB of the macula utricule from Meniere's disease (MD) patients showed pathological damage in the vascular endothelial cells (VEC) (Ishiyama et al., 2017), in addition the effect of oxidative stress in the VEC and pericytes of the human macula utricule have recently been identified (Ishiyama et al., 2018). In the present study we begin to identify the cellular biological changes in the pericytes that surround the VEC in the human macula utricule.

Methods: Macula utricule were acquired at surgery from patients diagnosed with MD that required transmastoid labyrinthectomy for intractable vertigo (n=4), patients who required a translabyrinthine approach for acoustic neuroma resection (N=3). Microdissected vestibular endorgans were obtained from temporal bones acquired at autopsy from individuals with no auditory or balance disorders(n=3). Immunofluorescence staining was made in whole utricule. VECs were identified using glucose transporter-1 (GLUT-1) and isolectin IB4, pericytes were identified using alpha-SMA, PDGFR, desmin and phalloidin. Secondary antibodies against rabbit (Alexa 488) and mouse (Alexa 594) were used for the identification of both proteins. Digital images were obtained using a Leica (SP8) laser confocal microscope.

Results: Using flat mount preparation and double and triple labeling immunolocalization VEC were identified using GLUT-1 throughout the macula utricule vasculature located stroma underneath the sensory epithelia in all type of specimens. This preparation allows to follow the trajectory of the microvessel which were of thick diameter in the periphery to intermediate to thin size to the central portion of the stroma sensory epithelia. IB4 was almost absent in MD specimens. Alpha-SMA was present in pericytes located in thick vessels (50 um), medium (25 um) and thin vessels (10 um) with varied morphology, PDGFR was present in pericytes

around thick and medium size vessels. Desmin was present mainly in pericytes of thin vessels. Phalloidin in pericytes was uniformly distributed in all size blood vessels. These markers showed a similar distribution in all types of specimens immunostained.

Conclusions: VECs showed uniform expression of GLUT-1 and IB4 in non-MD specimens. The phenotypical identification of pericytes in the human macula utricule add to the complex dynamics of the BLB in the human macula utricule.

Acknowledgements: Supported by a Hearing Health Foundation grant 21180673 (GI) and NIDCD grant # 1U24DC015910-01 (AI).

PS 480

Expanding the Chick Embryo Model into Biomedical Research on Congenital Vestibular Disorders

Hayley E. Seal¹; Sigmund J. Lilian²; Anastas Popratiloff³; June C. Hirsch³; Kenna D. Peusner³
¹George Washington University; ²Temple University School of Medicine; ³George Washington University School of Medicine

The chick has a long and distinguished history in biomedical research as a model for understanding human inner ear development and central nervous system diseases. In congenital disorders of the vestibular inner ear, children show a wide range of postural and behavioral deficits, including problems with balance and delayed motor development. The most common inner ear pathology is a sac-like inner ear with truncated or missing semicircular canals. The outcome of this vestibular inner ear pathology on central vestibular system development has not been studied due to lack of a suitable animal model. To address this question, our lab designed and implemented a chick embryo model with the otocyst surgically rotated 180° in ovo in two-day-old chick embryos. Paint-fills of the inner ear show that the Anterior-posterior axis Rotated Otocyst chick, or ARO chick, forms a sac-like inner ear in 85% of cases, making the model highly reproducible. Furthermore, the inner ear pathology of the ARO chick is isolated from abnormalities in related systems which occur in mutant mouse models. ARO hatchlings display vestibular symptoms similar to humans, including stumbling while walking, frequently closed eyes, and head nystagmus. In Nissl-stained serial tissue sections, the ARO sac contains three cristae and maculae utriculi and sacculi, which have type I hair cells surrounded by calycine endings. The superior crista and utricule are decreased in anterior-posterior extent, and the superior

crista is disoriented. Using tubulin and phalloidin immunolabeling with confocal imaging, the vestibular ganglion in E4 ARO chicks connects to the otocyst, but the posterior nerve branch deviates from its normal course. In ARO chicks, some vestibular ganglion cells form connections with principal cells of the tangential nucleus, a major avian vestibular nucleus. However, the tangential nucleus contains 66% fewer principal cells on the rotated side, indicating that the central vestibular neural circuitry is adversely affected by sac formation. The high reproducibility of the ARO chick model provides an unparalleled opportunity to characterize development of the central vestibular system in subjects with sac-like inner ears, which may lead to new clinical treatments to address causes of the disorders, rather than only treating symptoms.

PS 481

Generation of a Mouse Model of Unilateral Vestibular Dysfunction

Koji Nishimura¹; Hideaki Ogita²; Steven Meas³; Akiko Taura²; Juichi Ito²

¹*Department of Otolaryngology-Head and Neck Surgery, Graduate School of Medicine, Kyoto University;*

²*Shiga Medical Center Research Institute;*

³*Department of Laboratory Medicine and Pathobiology, University of Toronto*

Vestibular dysfunction is a significant clinical problem with limited regenerative therapeutic options. Hence, new therapeutic strategies for the recovery of vestibular function need to be investigated. However, there are a lack of animal models demonstrating vestibular dysfunction. A model of unilateral vestibular dysfunction, as opposed to the bilateral form, is useful for the investigation of functional recovery. Equilibrium is dependent on the vestibular inputs from both ears. Therefore, when both ears are damaged, it is difficult to interpret which ear(s) is the primary cause of dysfunction and/or recovery. Additionally, it is sometimes the case that vestibular inputs from the healthy ear are not able to compensate for the dysfunctional inputs from the affected ear, resulting in a state of persistent disequilibrium. Genetic causes of vestibular dysfunction typically affect both ears, however it is possible to generate a model of unilateral vestibular dysfunction through local application of an ototoxic drug or injection of a virus. The aim of this project is to generate a mouse model of unilateral vestibular dysfunction that can be used for developing cell-based or gene therapy methods to treat vestibular disturbances caused by loss of vestibular hair cells and neurons. The following two different experimental conditions were generated using eight-week-old male C57BL/6N mice. (1) Vestibular hair cells were ablated by

injecting 1 µl of gentamicin (360 mg/ml) via the posterior semicircular canal (modified Kawamoto et al., *Hear Res* 247: 17-26, 2008). (2) Vestibular neurons were ablated by injecting 1 ul of ouabain (5 mM) via the posterior semicircular canal. Histology indicated that gentamicin and ouabain preferentially ablated either vestibular hair cells or neurons, respectively. Functional analysis as determined by the vestibular ocular reflex (VOR) demonstrated that both models (i.e. hair cell loss, and neuronal loss) showed reduced VOR gain in the affected ear. Therefore, we have demonstrated the production of a model of unilateral vestibular neurosensory degeneration that can be a useful tool to investigate functional regeneration of the vestibular system.

PS 482

Hypergravity Stimulation Deteriorates Vestibular Function With Hair Cell Degeneration In The Mouse With Selective P2RX2 Deficit

Hansol Hong¹; Michelle Suh²; Jinsei Jung¹; Jae Young Choi¹; Gyu Cheol Han³; Sung Huhn Kim¹

¹*Yonsei University College of Medicine;* ²*Jeju National University College of Medicine;* ³*Gacheon University College of Medicine*

P2RX2 was reported to contribute cochlear hair cell protection against severe mechanical stimulation by the stimulation of paracrine ATP. This study was designed to investigate if P2RX2 have similar function in the vestibular system. ATP secretion in the vestibular system was investigated after mechanical stimulation by luciferin-luciferase assay. P2RX2 expression in P2RX2 KO, hetero, and wild type mice by immunocytochemistry and western blot analysis. The cation transport function of P2RX2 via vestibular transitional cell in those mice were investigated by scanning vibrating probe technique. Mechanical stimulation was given to the mice using mouse centrifugation system (4G – 6G for 4 hours – 48 hours). Vestibulo-ocular reflex and histology of vestibular epithelia of those mice were analyzed with animal rotator after hyper-gravity acceleration stimulation (4G for 4 hour). ATP secretion was detected in the vestibular system with the order of ampulla > utricle > common crus > saccule. P2RX2 receptor was expressed and functioned in the supporting cell and transitional cell of the vestibular labyrinth with dose dependent manner in KO, hetero, and wild type P2RX2 mice. After the hypergravity stimulation, VOR gain was more decreased in P2RX2 hetero and KO mice than that of wild type (p=0.001). Vestibular hair cells around striolar were revealed to be damaged in the mice with reduced VOR after hypergravity stimulation. It seems that P2RX2 contributes protection of vestibular hair cell in the situation of severe acceleration stimulation by

providing cation shunt through extra-sensory epithelial cells near hair cells.

PS 483

The Properties of Synaptic Transmission in Adult Mammalian Vestibular Hair Cells Differs Between Type I and Type II Cells

Paolo Spaiardi¹; Walter Marcotti²; Sergio Masetto¹; **Stuart Johnson³**

¹*Department of Brain and Behavioural Sciences, University of Pavia;* ²*The University of Sheffield;*

³*Department of Biomedical Science, University of Sheffield*

Inner ear sensory synapses faithfully transduce information over a wide range of stimulus intensities for prolonged periods of time. The efficiency of such demanding and stringent exocytotic activity depends on the presence of specialised presynaptic ribbons in the sensory hair cells. Ribbons are electron dense structures able to tether a large number of releasable vesicles at the synaptic active zone and can maintain high rates of vesicle release. Calcium entry through CaV1.3 (L-type) Ca²⁺ channels in response to cell depolarization causes local increases in Ca²⁺ at the ribbon synapses, which is detected by the exocytotic Ca²⁺ sensors. At ribbon synapses of mature vestibular hair cells (VHCs), the coupling between Ca²⁺ channels and the exocytotic Ca²⁺ sensor remains unclear. We studied the Ca²⁺ dependence of exocytosis and the release kinetics of different vesicle pool populations in mature synaptotagmin-4 (Syt-4) mouse VHCs using patch-clamp capacitance measurements under physiological recording conditions. Exocytosis in adult Type II VHCs showed a high order dependence on Ca²⁺ entry, which contrasts with the linear Ca²⁺ dependence observed in adult mammalian auditory inner hair cells (IHCs). The synaptic properties of mature Type II VHCs, including the characteristics of the Ca²⁺ current and dynamics of vesicle release, were not affected by an absence of Syt-4. By contrast, the release of synaptic vesicles from Type I VHCs was very small in both Syt-4 control and KO cells, even for long voltage steps, which prevented us from uncovering the Ca²⁺ dependence of release. Our findings show that the coupling between Ca²⁺ influx and neurotransmitter release at VHC ribbon synapses at Type II VHCs is described by a non-linear relation that is likely to be more appropriate for the faithful encoding of low frequency vestibular information, consistent with that observed in very low frequency mammalian IHCs. On the other hand synaptic vesicle release at mature Type I VHCs was very small suggesting that these cells favour faster non-quantal transmission in order to drive the most rapid reflex in the body, the vestibular-ocular reflex.

PS 484

Nav1.6-mediated Currents in Early Postnatal and Mature Vestibular Calyx Afferent Terminals

Frances Meredith; Alex Arne; Karen Dockstader; Katherine Rennie
University of Colorado School of Medicine

Introduction

Voltage-gated Na⁺ channels typically produce fast, transient currents (INa) mediating the rising phase of the action potential (AP), but can also produce atypical currents. A small persistent current continues to flow after the transient current decays and can enhance excitability by boosting membrane depolarization at subthreshold potentials. A resurgent current, produced during the falling phase of an AP, can contribute to repetitive AP firing. Nav1.6 channels have been implicated in autonomous pacemaker firing and the production of resurgent and persistent currents in several systems. Here we investigated their contribution to Na⁺ currents in calyx terminals from central zones (CZ) and peripheral zones (PZ) of immature and mature cristae.

Methods

We made whole cell patch clamp recordings from calyx terminals of gerbil cristae in two age groups: immature (postnatal day (P)5 to P14) and mature (P24 to P44). Transverse crista slices (100 µm) were cut and placed in solutions formulated to minimize K⁺ currents. Voltage protocols were designed to elicit transient, resurgent and persistent Na⁺ currents. APs were elicited in current clamp with brief hyperpolarizing steps and averaged. 4,9-ah-tetrodotoxin (4,9-ah-TTX) was used to selectively inhibit Nav1.6 channels. ATX-II, a sea-anemone toxin that slows down the inactivation of Na⁺ channels, was used to enhance persistent currents. In some experiments fluorescent dye fills were used to identify calyx-only and dimorphic afferents. Immunohistochemistry was performed using an antibody to target Nav1.6 channels.

Results

4,9-ah-TTX reduced peak INa on average by 20 % in immature calyces, by 37 % in mature dimorphic PZ calyces, but by only 13 % in mature CZ calyx-only terminals. This suggests that dimorphic terminals in mature crista have the greatest expression of Nav1.6 channels. Immunohistochemistry showed nodal and terminal staining for Nav1.6 in mature cristae. In mature PZ calyces, 4,9-ah-TTX significantly reduced the height and increased the width of APs implicating a role for Nav1.6 channels in firing in dimorphic afferents. A

resurgent current was noted in a subset of mature calyces under control conditions and a small persistent current was seen in ~50 % of mature calyces. ATX-II slowed down the inactivation of INa and boosted persistent currents in all immature and mature calyces tested, but 4,9-ah-TTX reduced the enhanced Na⁺ current in mature calyces only. Nav1.6 channels therefore underlie a component of the persistent current in mature calyces. The identity of Nav subunits contributing to persistent current at immature ages is not yet known.

PS 485

Assessment of Utricular Nerve, Hair Cell, and Mechanical Function, In Vivo

Christopher Pastras; Ian S. Curthoys; Daniel J. Brown
The University of Sydney

OBJECTIVE: Reflex tests are commonly used to diagnose vestibular loss. Unfortunately, there is no way to determine if this loss is either due to mechanical, hair cell, or neural dysfunction. This study aimed to develop measures of the mechanical, hair cell, and nerve response of the utricle, to enable differential diagnosis of utricular dysfunction, in vivo.

METHODS: Experiments were performed in anaesthetized guinea pigs, placed in an ear-bar setup. The cochlea was surgically removed allowing full access to the utricular macula. A reflective micro-bead was placed on the macula and a Laser Doppler Vibrometer (LDV) was used to record the velocity of the bead. A wire electrode was placed in the facial nerve canal to record the Vestibular short-latency Evoked Potential (VsEP), and a glass micropipette was placed on the basal epithelial surface of the macula to measure the Utricular Microphonic (UM). Responses were evoked by Bone Conducted Vibration (BCV) or Air Conducted Sound (ACS), via transducers attached to the ear-bars.

RESULTS: Continuous BCV and ACS stimuli evoked cyclic UM and macular velocity responses that distorted at high intensities. The UM was the most sensitive to stimuli between 100-300Hz. Relative to the phase of the macular vibration, the UM phase differed between BCV and ACS stimulation, suggesting a different macromechanical receptor activation. One caveat to our utricular vibration measurements is that we could only measure the velocity of the macula in one direction, and this woefully underestimates the mechanical drive to the utricle, which is stimulated by a differential shearing between the epithelium and the overlying otoconia, and in 3 dimensions.

CONCLUSION: This is the first-time hair cell and mechanical responses have been recorded from the mammalian utricle, in vivo. Experimental manipulations selectively altered utricular nerve, hair cell or mechanical function and provide the means to differentially diagnose peripheral utricular function.

PS 486

A Computational Model of Vestibular Fluid Response to Human Body Motion

Marie Baronette-Okeke; Sonya T. Smith; Werner Graf
Howard University

The vestibular system is the balance center of the body, responsible for sensing both linear and angular accelerations, as well as gravity. This motion information is transmitted to the brain, where it is used to generate compensatory eye and body movements that stabilize gaze and maintain balance. Due to its position, studying the response within the vestibular system is difficult while the head is in motion. Animals models have been used to understand much of the physiology of the vestibular system. Current research is focused on understanding the dynamic response of human vestibular systems, primarily using computational models.

This computational study focuses on the fluid response within the vestibular system by developing a computational model that relates body movement to eye movement and endolymph displacement within the vestibular system. It is capable of modeling vestibular response under conditions experienced in day-to-day motion. The resulting mathematical model provides a link between the internal and external function of the vestibular system, developing a more complete approximation of the system.

Our model incorporates existing numerical approximations to relate head velocity to endolymph displacement. Eye velocity and head velocity were then related using a novel transfer function, based on the observed response of the vestibulo-ocular reflex (VOR). Though the relation between these two parameters has been observed experimentally, our model links them numerically.

Endolymph displacement during head motion is the cause of the deflection of vestibular hair bundles. This model defines endolymph displacement as a function of eye velocity. Endolymph displacement cannot be easily measured during head motion, so an accurate computational representation of endolymph displacement is crucial to understanding the dynamics of this function of the vestibular system. By quantifying this displacement, we can determine the applied force causing the deflection of said bundles which is important in mechanotransduction.

Computational models, particular in biological studies,

have been invaluable in advancing vestibular system research. This model is an important contribution to the field as it both accurately represents the portions of the vestibular system that can be measured and predicts the response of portions of the system that cannot be measured.

PS 487

Single Unit Recording Studies of Vestibular Afferents in Mice Lacking *Tmc1* and *Tmc2*

Hong Zhu¹; Tianwen Chen¹; Jun Huang¹; Youguo Xu¹; Yang Ou¹; Yiji Tu¹; David Sandlin¹; Alberto Arteaga¹; Gwenaelle S. Geleoc²; Jeffrey R. Holt²; **Wu Zhou**¹
¹*Department of Otolaryngology University of Mississippi Medical Center*; ²*Boston Children's Hospital, Harvard Medical School*

Introduction: Vestibular hair cells convert the mechanical stimuli of gravity and head accelerations into electrical signals. This mechano-transduction process is initiated by opening of cation channels near the tips of hair cell stereocilia. Compelling evidence suggests *Tmc1* and *Tmc2* encode pore-forming subunits of mechanosensory transduction channels in vestibular hair cells (Pan et al., 2018). Recent behavioral studies found that mice lacking *Tmc1* and *Tmc2* exhibited zero-gain VOR responses to head rotation (Asai et al., 2018). In the present study, we employed a single unit recording approach to characterize the vestibular afferents in mice lacking *Tmc1* and *Tmc2*.
Methods: Single unit recordings of vestibular afferents of the mice with *Tmc1* and *Tmc2* deletions (C57BL/6J background, *Tmc1* Δ/Δ ; *Tmc2* Δ/Δ) and wild type mice (C57BL/6J, Jackson Laboratories) were performed under ketamine/xylazine anesthesia as described before (Zhu et al., 2011, 2014). The afferent populations were from both the superior and inferior branches of the vestibular nerve.
Results: We recorded 180 vestibular afferents from three mutant mice and five WT mice and measured their mean spontaneous firing rates and coefficients of variation (CV). Preliminary analysis revealed two findings. First, the mutant mouse afferents exhibited less spontaneous discharge activity; their mean firing rates were about 50% of that in WT mice. Second, the mutant mice had fewer regular units (CV < 0.1) than the WT mice.
Conclusions: The results suggest mutations in *Tmc1* and *Tmc2* lead to lower spontaneous discharge activity in vestibular afferents as well as a decrease in the proportion of regular afferents. Ongoing studies will further characterize vestibular afferents in the two groups of mice. Because vestibular afferent neurons provide the final output from the peripheral vestibular system, recordings from vestibular afferents provide important insights into the roles of *Tmc1* and *Tmc2* in mediating vestibular functions in normal and diseased conditions.

R01DC012060 (HZ), R21 DC017293 (HZ), R01DC014930 (WZ), R21EY025550 (WZ), R01 DC013521 (JRH) and R01 DC008853 (GSG)

PS 488

Modification of Vestibular Afferent Discharge Properties by 4-Aminopyridine and Galvanic Stimulation in the *Xenopus laevis* Tadpole

Kathrin Gensberger¹; Julia Dlugaiczyk²; Hans Straka¹
¹*Department Biology II, Ludwig-Maximilians University Munich*; ²*German Center for Vertigo and Balance Disorders*

Background: A major principle of vestibulo-motor processing is the encoding of head motion in frequency-tuned channels. The different thresholds, sensitivities and spike time regularities of individual vestibular nerve afferents determine the signal content and the respective contribution during particular motion dynamics. Here, we studied the functional organization of vestibular nerve afferent fibers in *Xenopus laevis* tadpoles at mid-larval stages and the effect of 4-aminopyridine (4-AP) and galvanic noise on their discharge pattern.

Methods: Whole-head in vitro preparations of *Xenopus laevis* tadpoles (larval stages: 52–55) were used for extracellular recordings from single horizontal canal (HC) afferent nerve fibers and immunofluorescence staining of Kv1.1.-channels in vestibular afferents. Rotational stimulation on a two-axis turntable helped characterising and identifying afferent cell types. The contribution of Kv1.1.-channels on the spike time regularity of individual afferents was studied by bath application of 4-AP (10 μ M). For electrical stimulation, a band-limited noise was applied through galvanic electrodes that were placed unilaterally on the otic capsule to specifically stimulate the horizontal canal.

Results: Kv1.1.-immunopositive vestibular neurons in Scarpa's ganglion showed particularly large somatic and axonal diameters and terminated mainly on hair cells in the central zone of the HC crista. Extracellular recordings from different single vestibular afferent nerve fibers (n=102) displayed a broad range of coefficients of variation (CVs) (0.1 – 1.5) and inter-spike intervals (ISIs, 30 – 10.000 msec) with a positive correlation between CV and ISI. Afferents with a high CV were more sensitive to rotational stimuli than fibers with a low CV. Washing in of 4-AP to the bath solution resulted in a decrease of the mean CV (from 0.7 to 0.3) and the mean ISI (from 200 to 70 msec) of HC vestibular nerve afferents. When an intermediate level of electrical noise was applied during sub-threshold rotational stimulation of the preparation, vestibular afferent fibers show a stochastic resonance

effect (that is more pronounced in regular units.)

Conclusions: Tadpole HC afferents display a high variability of spike time regularity. The effects of 4-AP on the CV and ISI of vestibular nerve afferents indicate a crucial role of Kv1.1.-channels for phasic response properties. Thus, 4-AP offers a powerful tool for further analysing phasic and tonic discharge patterns of vestibular afferents. Furthermore, the whole-head in vitro preparation of tadpoles can be used as an animal model for deciphering the effects of stochastic electrical noise on vestibular afferent activity.

PS 489

Guinea Pig Irregular Primary Otolithic Afferents Have More Precise Phase Locking to Sound and Vibration Than Cochlear Primary Afferents

Ian S. Curthoys; Ann M. Burgess
The University of Sydney

Introduction. Some guinea pig primary vestibular afferents with irregular resting discharge originating mainly from the striola of the utricular and saccular maculae are activated by and phase-lock to sinusoidal sound and vibration up to frequencies above 2000Hz (Curthoys et al., 2016). This study reports the precision of that phase locking and compares it to the evidence of phase locking of auditory afferents in guinea pigs (Palmer and Russell, 1986).

Methods. Single primary vestibular neurons were recorded extracellularly using glass microelectrodes filled with 2% neurobiotin in 2M NaCl with impedances of 2-15 megohms. Vibration stimulation up to 2g peak-to-peak was delivered by a Radioear B-71 bone oscillator cemented to the skull. Sound stimulation of up to 140dB SPL was delivered by a TDH-49 headphone via a speculum.

Results. Many otolithic neurons had spontaneous activity, but a sizable number were silent at rest and were only detected because of repeated search stimulation during the electrode advance. Most otolith irregular neurons had a vigorous response to sound or vibration.

Different irregular neurons showed phase locking to different phase angles at the reference frequency of 500Hz. When tested with high frequencies (250-2000Hz) it was found that some guinea pig primary otolithic neurons have, on average, significantly higher precision of phase locking as measured by asymptotic vector strength compared to the asymptotic vector strength of guinea pig auditory afferents (data from Palmer and Russell 1986). Furthermore the phase-locking of these

otolithic afferents extends to higher frequencies than is the case for auditory afferents.

Discussion and Conclusion One difference between otolithic and cochlear afferents is their very different synapses on receptors: irregular otolithic afferents make calyx synapses on type I receptors at the striola whereas cochlear afferents make bouton terminations on inner hair cells. We suggest (following Alan Brichta) that the high precision phase-locking of irregular otolithic afferents may be due to the release of potassium by the type I receptor into the calyx cleft and that potassium functions as an "ionic neurotransmitter" (Lim et al., 2011; Contini et al., 2017). We suggest that the high precision of phase locking implies that type I otolithic receptors function as jerk detectors.

References

- Contini, D. et al. *J Physiology-London* 2017: 595(3): 777-803
Curthoys, I. S et al. *Hearing Research* 2016: 331: 131-143
Lim, R., et al. *Experimental Brain Research* 210(3-4): 607-621.
Palmer, A. R. & Russell, I. J. (1986). *Hearing Research* 24(1): 1-15.

PS 490

A Novel Technique for Rapid and Innocuous Drug Delivery to Vestibular End Organs via Intracochlear Injection

Vishal Raghu¹; Soroush Sadeghi²
¹*State University of New York At Buffalo*; ²*Center for Hearing and Deafness, Dept. of Communicative Disorders and Sciences, State University of New York at Buffalo*

The vestibular periphery is a complex ecosystem of hair cells, afferent synapses and efferent terminals comprising of many neuromodulators. Local drug injection techniques are important for exploring this complex interplay. Injection of drugs into the inner ear has been used for delivering drugs or viruses to the cochlea. Here, we propose a novel technique for rapid delivery of drugs in adolescent mice targeting the vestibular epithelia via the round window, such that it preserves the normal functioning of the cells. The injection was made via a metal tube passing through the external ear canal, which was inserted into the round window (RW) under direct visualization after ablating the tympanic membrane and the middle ear ossicles. A craniotomy was also made in the parietal portion of the skull and part of the cerebellum suctioned out to allow

direct visualization of the ampulae of the horizontal and superior canals. A hole was made in the superior canal providing an exit path for the perilymph. To visually test the reach of the drug in the labyrinth, colored artificial perilymph (AP) was injected through the RW at different rates and durations. We found that the optimal infusion rate was 0.3 ul/min for 30 s, followed by a 5 min wait for the AP to diffuse to the cristae as observed under the surgical microscope. Next, we recorded from afferents before, during and after injection of AP (similar to that used for in vitro patch clamp recordings). With the above protocol, all recorded afferents retained sustained and unperturbed firing rates during and after injection. Fluid displacement during injection was confirmed by observing the leakage of fluid through the superior canal fenestra. These findings suggest that the faster rate of injection with the AP as the vehicle along with fenestration of the superior canal could be used for rapid delivery of solutions and drugs to vestibular end organs without artificial effects on the vestibular neuroepithelia.

PS 491

Changes in cardiovascular function and heart rate variability during infrared stimulation of vestibular endorgans

Darrian L. Rice¹; Gay R. Holstein²; Giorgio P. Martinelli³; Suhrud M. Rajguru⁴

¹University of Miami; ²Icahn School of Medicine Mount Sinai; ³Icahn School of Medicine at Mount Sinai; ⁴Department of Biomedical Engineering and Otolaryngology, University of Miami

Background

Applications of sinusoidal galvanic vestibular stimulation (GVS) and head tilts are known to evoke significant changes in the blood pressure (BP) and heart rate (HR) via the activation of vestibulo-sympathetic reflex (VSR). To investigate the contribution of individual endorgans to the VSR, we have developed the application of pulsed infrared radiation (IR) to activate the posterior semicircular canal or utricle receptors in a rodent model.

Methods

The University of Miami Institutional Animal Care and Use Committee approved all procedures. Changes in HR and BP were studied in adult male Long-Evans rats weighing 300-500g, anesthetized with ketamine (44mg/kg) and xylazine (5mg/kg). A head post cemented to the skull of each rat and attached to a custom-designed stereotaxic frame restricted head movement during stimulation. Frequency modulated IR pulses (1863nm,

200us, 250pps, varied radiant exposure) were delivered at 0.05Hz either to the posterior canal (PC) crista or utricular macula via a 200 or 400 mm optical fiber. Mean BP and HR were measured via a small animal single pressure implantable device (DSI pressure sensing technologies, HD-S10) inserted into the femoral artery prior to stimulation). Eye movements simultaneously recorded using a custom-modified video-oculography system (ISCAN Inc.) and post-mortem micro computed-tomography confirmed the site of stimulation. In three rats, the vestibular system was activated with electrical stimulation (biphasic bipolar, 200Hz pulse rate, 0.05Hz modulation to mimic IR stimulation parameters) and results were compared to changes evoked by focused IR stimulation.

Results

Sinusoidal IR (0.05 Hz) delivered to PC induced an initial drop in both BP (4.44 ± 2.96 mmHg) and HR (17.45 ± 13.07 bpm) followed by sinusoidal modulation. The responses ceased following IR stimulation. Corresponding eye movements and post-mortem microCT confirmed the PC ampullary region to be the primary target of stimulation. Results of electrical activation of peripheral vestibular system matched those from IR stimulation. In at least half of the animals, the high to low frequency ratio of heart rate variability (HRV) increased during IR stimulation over baseline resting condition.

Conclusions

PC receptor activation evoked robust changes in BP and HR and the responses were confirmed with electrical stimulation. HRV analysis indicates sympathetic activation during PC stimulation. Results are further suggestive of selective activation of the vestibular system by focused IR, which can be used to detail the VSR pathways and contributions of individual end organs.

Funding NIH NIDCD 1R01DC008846 (GRH) and 1R01DC013798 (SMR)

Psychophysical Characterization of Normal & Impaired Ears

PS 492

Hearing the Ending: Psychophysical Measures of Sound-Offset Sensitivity

Fatima Ali¹; Doris-Eva Bamiou²; Jennifer F. Linden¹

¹UCL Ear Institute; ²UCL Ear Institute & NIHR BRC Deafness and Hearing Problems

Auditory processing problems such as difficulty perceiving speech in noise are common symptoms of developmental or language disorders (Dawes and Bishop, 2010, *Arch Dis Child*; Ferguson et al., 2011, *J Speech Lang Hear Res*) and often occur without any apparent loss of peripheral hearing sensitivity. These perceptual difficulties are therefore thought to be caused by abnormalities in the brain. However, there is no gold standard for the screening or testing of central auditory processing disorders; clinical evaluations are usually based on subjective symptoms. The nature of the deficits has therefore remained controversial.

Recent studies in a mouse model of developmental disorder reported an auditory brain abnormality specific to the processing of sound offsets (Anderson & Linden, 2016, *J Neurosci*). If similar brain abnormalities occur in humans with developmental disorders, the consequences could include difficult-to-diagnose problems with perception of speech in noisy environments. Sound offsets play a valuable role in recognising, distinguishing and grouping sounds, and are likely to be essential for perceiving consonants that lie in the troughs of amplitude fluctuations in speech. However, standard audiometric tests do not assess sensitivity to sound offsets.

Here we report on the development of a psychophysical test battery which could be used to quantify sound-offset sensitivity in human subjects, including patient populations. Core tasks include detection of a click following noise, and discrimination of the duration of 'filled'; versus 'empty'; intervals (i.e. time elapsed between onset and offset of a noise or between two successive clicks). A further task involved discrimination of vowel-consonant-vowel (VCV) stimuli using 16 consonants in 3 vowel environments and 5 varying levels of background multi-talker babble noise. We used mathematical modelling to predict how a deficit in sound-offset sensitivity could influence the discrimination of particular VCV stimuli in noise.

Analysing performance of normal adult subjects, we validated model predictions for discrimination of VCV pairs with high or low relative offset salience. We also corroborated previous reports (Rammsayer and Lima, 1991, *Percept Psychophys*) that duration discrimination thresholds are lower for filled than empty intervals. In ongoing work, we are testing the hypothesis that click-following-noise detection thresholds and filled/empty duration discrimination thresholds can be used as individual measures of sound-offset sensitivity, and investigating the relationship between these measures, gap-in-noise detection thresholds, and speech-in-noise perception. We are also using our test battery to study sound-offset sensitivity in a group of patients clinically diagnosed with central auditory processing disorder.

Supported by EPSRC (1644123), MRC (MR/P006221/1), AoHL (G77) and NIHR UCLH BRC.

PS 493

The Effects of Duration and Level on Spectral Modulation Perception

Sittiprapa Isarangura; Ann Eddins; Erol Ozmeral;
David A. Eddins
University of South Florida

Spectral envelope perception is often characterized using a spectral modulation detection task in which spectral modulation that is a sinusoidal function on a log₂ frequency axis and a log₁₀ (dB) amplitude scale is superimposed on a broadband carrier. Representation of modulation detection thresholds as a function of modulation frequency (cycles/octave) results in a spectral modulation transfer function (SMTF). To minimize the possibility of using local (audio-frequency specific) level cues across intervals in a multi-interval, forced-choice task, the modulation phase is randomized, resulting in peaks and valleys in the modulated spectrum at unpredictable audio frequencies. Analyses of investigations of across-interval level discrimination reveal systematic changes in discrimination with changing duration and changing level. On the contrary, investigations of auditory profile analysis indicate increased thresholds for durations less than 100 ms and little change with level. Assuming that spectral modulation detection reflects spectral envelope perception, it is expected that the influence of duration and level should parallel those reported for spectral profile analysis. Spectral modulation detection was measured for frequencies of 0.25, 0.5, 1, 2, 4, and 8 cycles/octave superimposed on noise carriers. To investigate the potential influence of stimulus duration, stimulus durations were 50, 100, 200, or 400 ms and the noise carrier was six octaves wide (200 to 12800 Hz). To investigate the potential effects of presentation level, sensation levels were either 10, 20, 30, 40, or 60 dB relative to noise band detection thresholds for three-octave (400 to 3200 Hz) and six-octave (200 to 12800 Hz) carriers. The results indicated no significant differences in spectral modulation detection for stimulus durations of 400 and 200 ms. As the duration decreased to 100 ms, detection thresholds were slightly higher but significant and were markedly high for the 50-ms duration with a larger variation across listeners. In terms of presentation level, spectral modulation detection did not differ between 20, 30 and 60 dB sensation level but were markedly higher for the 10 dB sensational level conditions with a larger variation across listeners. These results are consistent with the detection of changes in simultaneous, across-frequency level variations and are not consistent with the detection of sequential, across-interval level comparisons. In sum, the duration and level dependences illustrated here should be considered in the context of models of auditory perception, when

interpreting data, and/or design of spectral envelope perception tasks.

PS 494

Binaural Psychoacoustic Protocols to Explore Phase Locking in Human

Antoine Lorenzi¹; Frederic Venail²; Jean-Luc Puel³;

Jean-Charles Ceccato³

¹Otology and Neurotology unit - CHRU Montpellier - Centre Hospitalier Régional Universitaire - Montpellier, France; ²Otology and Neurotology unit - CHRU Montpellier - Centre Hospitalier Régional Universitaire, Montpellier, France - INM, Inserm, Univ Montpellier;

³INM, Inserm, Univ Montpellier

Background: Recently, the understanding of neural phase locking role in coding sounds has greatly improved. The various structure involved run all along the auditory pathway to improve phase locking and allow segregation of sound sources. This temporal coding is of crucial importance to the perception of low frequency sounds, even more in noise and is also a key point of many binaural interactions. To explore those interactions focusing on phase locking we used binaural protocols where temporal comparison of signal is essential. The first is binaural masking release using variable intercorrelation of binaural noise. The temporal coherence of noises vary randomly over all frequencies, decreasing the usability of phase locking to compare and extract signals. The second one is an auditory illusion called Huggins pitch based on the perception of a sound created by an interaural phase-shift of a narrow frequency band in a broadband noise. The difference between noises is only present in the phase of some frequencies making phase locking necessary to the perception of the pitch.

Methods: The various explorations were spread on 126 normal hearing young people (18-35 years) using forced choice adaptive tests. In binaural masking release protocol we were looking for critical signal to noise ratio allowing perception of a pure tone burst in a white noise. Different tests were made varying the position of the tone and of the noise (monaural or binaural), the frequency (500, 1000, 2000, 4000 Hz) and the interaural noise correlation (-1, 0, 0.2, 0.4, 0.6, 0.8, 1). In Huggins pitch protocol we were looking for critical level of perception varying the frequency (500, 1000, 1414, 2000, 2520, 3175 and 4000 Hz) of the narrow band phase shift.

Results: We found that binaural masking release is the sum of two effects, the first is antimasking and seems to be the consequence of the suppression effects of contralateral outer hair cells through the medial

olivocochlear complex and is independent of frequency but very slight and effective mainly with very-transient sound. The second is the main release and its effect decrease with frequency and with temporal coherence of binaural noises. With Huggins pitch we found that the perception of interaural phase shift decrease with frequency and disappear around 3.5 kHz.

Conclusion: Consistently with limits found on phase locking in auditory nerve fibers and brainstem auditory cells, binaural interaction based on temporal comparison fades with increasing frequency and disappear after 3.5 kHz.

PS 495

Can Listeners Hear the “Missing Fundamental” Pitch by Combining Groups of Unresolved Harmonics of Different Constituent Pitches?

John M. Deeks; Hedwig Gockel; Robert P. Carlyon
MRC Cognition & Brain Sciences Unit

Contemporary pitch theories state that listeners can derive the missing fundamental (F0) of a complex tone by combining phase-locking information from auditory nerve responses to each of its low-numbered harmonics. However, two studies reported that listeners could not derive a missing F0 by combining information from the envelopes of three transposed tones or from the repetition rates of three bandpass-filtered pulse trains with different rates (Oxenham et al, 2004; Deeks et al, 2009). Hence, there is no evidence that listeners can combine purely temporal information, in the absence of place-of-excitation cues, to hear the missing F0. A caveat is that those studies used stimuli in very high frequency regions where the pitch of the individual transposed tones and bandpass pulse trains was quite weak.

We revisited this issue using stimuli where at least some components had low-to-moderate frequencies, and with a simple task that probed whether participants listened analytically or synthetically to a given sound. In one condition of experiment 1, each trial consisted of two pure-tone dyads with frequencies 80+160 Hz and 106.7+160 Hz. If the latter stimulus is perceived as the 2nd and 3rd harmonics of 53.3 Hz (synthetic listening) it should be judged as lower than the 80+160 Hz dyad. Conversely, analytic listening should result in it being judged as higher. Trials in this condition were mixed with another condition that presented two groups of unresolved harmonics. The lower group had components between 640-1280 Hz and an F0 of either 40 or 53.3 Hz. The components were summed in alternating phase leading to a pulse rate (and expected pitch) of 80 or 106.7 Hz - the same as the lower component of the pure-tone dyads. The upper

group contained components of a 160-Hz F0, ranging from 1680-2560 Hz, summed in sine phase. All stimuli were presented in a noise background. Results showed that all 7 participants listened synthetically to the pure-tone dyads. Results for the pulse-train condition were more mixed and may have been influenced by context effects from, for example, listening to a pulse-train trial immediately after a pure-tone-dyad trial. Nevertheless, participants seem more likely to listen synthetically to pairs of pure tones than to pairs of pulse trains. We will present the results of experiment 2 which controls for possible context effects by presenting the two conditions in separate blocks, and which varies the pitch strength of the upper group by varying its bandwidth.

PS 496

Individual Differences in Spatial Hearing may arise from Monaural Factors

Agudemu Borjigan¹; Hari Bharadwaj²

¹Weldon School of Biomedical Engineering, Purdue University; ²Speech, Language, & Hearing Sciences, and Weldon School of Biomedical Engineering, Purdue University

In challenging environments with multiple sound sources, successful listening relies on precise encoding and use of fine-grained spectrotemporal sound features. Indeed, human listeners with normal audiograms can derive substantial release from masking when there are discrepancies in the pitch or spatial location between the target and masking sounds. While the temporal fine-structure (TFS) in low-frequency sounds can convey information about both of these aspects of sound, a long-standing and nuanced debate exists in the literature about the role of TFS cues in masking release in complex environments. Understanding the role of TFS in complex listening environments is important for optimizing the design of assistive devices such as cochlear implants. The long-term goal of the present study is to leverage individual differences across normal-hearing listeners to address this question.

As a first step, TFS and spatial-hearing sensitivity were measured from a large cohort of “normal-hearing” human subjects via both psychophysical and electroencephalography (EEG) approaches. Individual TFS sensitivity was quantified as thresholds for detecting slow (2 Hz) frequency-modulations (FM) applied to a 500 Hz tone. Spatial hearing sensitivity was quantified using interaural time difference (ITD) thresholds at 500 Hz. Preliminary data show large variance across subjects in both the FM and ITD detection performance. Moreover, we observe a significant positive correlation between the monaural FM and binaural ITD detection

thresholds, with the mean of the TFS thresholds in two ears being a good predictor of ITD thresholds. This result suggests that monaural TFS coding can be the primary bottleneck determining binaural sensitivity. Further, we measured EEG responses to a transient change in the ITD of a 500 Hz tone. We find that the magnitude of the EEG response increases monotonically with the magnitude of the ITD change, suggesting that this may be useful as an objective measure of ITD sensitivity, and by correlation, TFS sensitivity. These results parallel previous findings that individual differences in sensitivity to ITDs in the temporal envelope (ENV) of high-frequency sounds are also driven by monaural ENV coding variations and are predicted by EEG responses tracking the ENV (Bharadwaj et al., *J Neurosci*, 2015). Follow-up experiments will compare individual differences in these TFS-coding measures to speech-in-noise perception with complex maskers in co-located and spatially separated configurations, and EEG-measures of spatial selective attention.

This work was supported by NIH R01DC015989 and institutional startup funds from Purdue University.

PS 497

Masking and Suppression of Infrasound Tones by Higher Frequency Tones

Torsten Marquardt

UCL Ear Institute

Environmental infrasound is a growing concern and related occurrences of complaints are notoriously difficult to predict. Consequently, the perceptual mechanism needs to be better understood.

Detection threshold of 4, 8, 16, 32 and 64 Hz tones were measured without and in the presence of 140 Hz and 500 Hz tones of 85 dB SPL using a standard 2I-2AFC, 3-down-1-up procedure. All stimuli were delivered monaurally using an acoustically closed system (sealing ear plug). Low and high frequency tones were generated by separate speakers to avoid hardware inter modulation.

The presence of the 140-Hz tone elevated the threshold of all target tones; the two higher tones by approx. 20 dB, the infrasound tones by approx. 10 dB. The 140-Hz tone did here likely act as a classic masker, i.e., it activated auditory nerve fibres that also serve the detection of the target tones. Nevertheless, it is remarkable that the travelling wave (TW) of a masker tone as high as 140 Hz reaches the most apical region of the basilar membrane (BM), where the target tones are thought to be detected. These results support studies indicating that the lowest

tone frequency that causes a clear TW peak on the human BM is well above 50 Hz [1]. It is likely that the 140-Hz TW has not fully decayed at this characteristic place.

In contrast, the presence of the 500-Hz tone elevated only the threshold of the two infrasound tones. Their thresholds increased by approx. 10 dB. Because the threshold of the other three target tones remained within 3 dB of their absolute threshold, classic masking cannot be the explanation here. But, infrasound generates large cochlear potentials, presumably enhanced by the phase-synchronised displacement of the outer hair cells (OHC's) stereocilia. These have been shown to be very effectively suppressed by a moderate 500-Hz tone [2]. Because inner hair cells (IHCs) are velocity-sensitive and velocity drops sharply with decreasing frequency, it was suggested that below 10 Hz excitation of IHCs might be dominated by these OHC-generated electrical potential [3]. This mechanism does not only explain the observed infrasound-specific suppression by the 500-Hz tone, but also the flattening of the detection threshold curve for tones below 15 Hz [4].

1. Jurado et al., *J. Acoust. Soc. Am.* 129(5), 2011.
2. Salt et al., *J. Acoust. Soc. Am.* 133(3), 2013.
3. Cheatham and Dallos, *Hear. Res.* 108(1-2), 1997.
4. Møller and Pedersen, *Noise Health* 6, 2004.

PS 498

Physiological Model Simulations of Comodulation Masking Release for Listeners with Normal Hearing and Hearing Loss

Langchen Fan¹; Paolo A. Mesiano²; Torsten Dau³; Laurel H. Carney¹

¹University of Rochester; ²Technical University of Denmark; ³Hearing Systems Group, Department of Electrical Engineering, Technical University of Denmark

Comodulation masking release (CMR) refers to the reduced thresholds in tone-in-noise detection when the noise masker is modulated (i.e. multiplied) by a low-frequency noise. Listeners with sensorineural hearing loss (SNHL) benefit less from the modulated masker (i.e. show a reduced CMR), but the amount of CMR varies, even for those with similar audiograms (see companion study by Mesiano et al., this conference). In this study, we modeled CMR for both normal-hearing (NH) and SNHL listeners. Previous studies of CMR have focused on the envelope statistics of the stimuli; we include the transformation of envelope cues that

occurs in the peripheral system (e.g. due to inner-hair-cell transduction and cochlear compression). In general, neural fluctuations in the responses of auditory-nerve (AN) responses differ from the stimulus envelope and are affected by hearing loss.

We used a phenomenological AN model followed by a band-pass modulation filter as a simple model for inferior colliculus (IC) neurons with band-pass modulation transfer functions. Measured thresholds for NH and SNHL listeners were taken from a companion study (Mesiano et al.). The model decision variable was the difference between the average rate of the model IC response of each stimulus interval (in each 3-interval trial) and the average rate across 21 noise-alone responses. The stimulus interval with the largest decision variable was determined to be the tone-plus-noise interval. The percentage of correct responses was calculated for each tone level and interpolation was used to find the threshold tone level corresponding to 79% correct. For simulations of SNHL listeners, the AN model was impaired based on the individual listener's audiogram. Different proportions of hearing loss associated with outer hair cell (OHC) function were simulated to investigate differences across listeners.

Our results showed that a single AN channel at the tone frequency followed by a model IC cell with 100-Hz best modulation frequency described the general trends in detection thresholds as a function of the masker bandwidth, both for NH and SNHL listeners. Model results were explained by neural fluctuation statistics of AN responses. For simulations of CMR in listeners with SNHL, varying the amount of loss due to OHC impairment affected thresholds for some tone frequencies. Modeling individual results with different amounts of OHC impairment may provide a better understanding of differences in thresholds and CMRs for listeners with similar audiograms.

The study was supported by NIH DC-010813 and the Oticon foundation.

PS 499

Spectral Integration in Normal Hearing Listeners

Rebekah Havens¹; Marelina Gutierrez¹; You-Ree Shin²; Yang Soo Yoon³

¹Texas Tech University Health Sciences Center; ²Soree Ear Clinic; ³Baylor University

Background

The auditory system integrates complementary information, redundant information, or a combination of these two speech-acoustic cues detected and processed

by each ear. In this study, conducted with normal hearing (NH) listeners, we aimed to determine whether the integration process is optimal when complementary spectral information of consonants is presented.

Methods

Ten NH adult listeners participated in the study. The most frequently used 14 consonants (/b/, /d/, /g/, /p/, /t/, /k/, /m/, /n/, /f/, /s/, /ʃ/, /v/, /dʒ/, & /z/) were produced by one female talker. They were presented in the consonant-/a/ context. Consonant recognition was measured in a dichotic manner, in quiet, using the 14-alternative forced-choice paradigm. We measured the spectral integration with three signal processing conditions: (1) unprocessed consonants, (2) processed consonants by 3DDS, a new signal processing tool, with conflicting cues, and (3) processed consonants by 3DDS, but without conflicting cues removed by 3DDS. To create complementary spectral information, each consonant was low-pass filtered in the left ear, with one of four cutoffs: 250Hz, 500Hz, 750Hz, and 1000Hz. The same consonant presented to the left ear was presented to the right ear, but was high-pass filtered with an initial cutoff of 5000Hz. When a subject's response was incorrect, the cutoff of the high-pass filter decreased by 250Hz (i.e., from 5000Hz to 4750Hz). The threshold of the complementary integration was determined when the target was selected three times in a row.

Results

Mean consonant recognition processed by 3DDS requires narrower spectral ranges ($\leq 250\text{Hz}$ in the left ear plus $\geq 3500\text{Hz}$ in the right ear) as compared to the performance with unprocessed consonants ($\leq 250\text{Hz}$ + $\geq 3100\text{Hz}$). The two 3DDS conditions require a similar spectral range. The spectral ranges required for consonant recognition increased approximately linearly with the increasing low-pass filter cutoff values for all three stimuli conditions. However, the spectral ranges needed for consonant recognition greatly differ across all 14 consonants.

Conclusions

The results in this study suggest that 3DDS processing makes acoustic cues more prominent for consonant perception and requires a narrower range of spectral information, when in comparison to the unprocessed condition. The results also imply that the enhancement of complementary spectral integration across both ears may lead to improved speech perception.

PS 500

Temporal Integration in Normal Hearing Individuals

Marelna Gutierrez¹; Rebekah Havens¹; You-Ree

Shin²; Yang Soo Yoon³

¹Texas Tech University Health Sciences Center; ²Soree Ear Clinic; ³Baylor University

Background

Our pilot data confirmed that three-dimensional deep search (3DDS), a new signal processing tool, enhanced the consonant perception in normal hearing (NH) listeners. Due to these findings it is possible 3DDS can facilitate the integration process on spectral and temporal cues, when processed across ears. True motivation for this study came from our interest in bimodal hearing, which consists of a cochlear implant in one ear and a hearing aid in the contralateral ear. Bimodal patients must detect and integrate temporal and spectral cues processed independently by a hearing aid ear and a cochlear implant ear. As a control study, we measured temporal integration ability of NH listeners on consonant perceptions, prior to measuring bimodal hearing listeners.

Methods

Ten NH adult listeners participated in the study. The most frequently used 14 consonants (/b/, /d/, /g/, /p/, /t/, /k/, /m/, /n/, /f/, /s/, /ʃ/, /v/, /dʒ/, & /z/) were produced by one female talker and presented in the consonant-/a/ context. Consonant recognition was measured in a dichotic manner in quiet in the 14-alternative forced-choice paradigm. For the left ear, each of the consonants were presented with 10%, 15%, and 20% of their original length from the onset. For the right ear, the same consonants were presented from the previous left ear test but were truncated at 70% from the onset. When a subject's response was incorrect, the amount of truncation decreased by 10% from the previous amount of truncation (i.e., from 70% truncation to 63% truncation). The threshold of the percent truncation was determined when the subjects correctly chose the target from the screen three times in a row. We measured the temporal integration with three signal processing conditions: (1) unprocessed consonants, (2) processed consonants by 3DDS with conflicting cues, and (3) processed consonants by 3DDS, but without conflicting cues removed by 3DDS. Each consonant was presented 10 times in random order at each listening condition and at each SNR.

Results

Consonant perception can be achieved with the large segment of the consonant truncated. 3DDS processing provides a listening condition that requires a less complete length of consonants presented for the perception. The relationship between the amount of not-truncated portion presented in the left ear and of the truncated portion presented in the right ear is linear: the longer not-truncated portion presented, therefore, longer truncation allowed for the perception.

Conclusions

Consonant perception does not require the total length of consonant presentation. 3DDS can provide additional auditory information so that temporal integration can be done for listeners who suffer combining temporal cues across ears.

PS 501

Internal noise for AM and FM detection: Effects of modulation rate and age

Sarah Attia¹; Andrew King¹; Léo Varnet²; Christian Lorenzi³

¹Laboratoire des systèmes perceptifs (LSP), Ecole normale supérieure (UMR 8248); ²Laboratoire des systèmes perceptifs, Ecole Normale Supérieure, Paris; ³Laboratoire des systèmes perceptifs, Ecole Normale Supérieure (UMR 8248)

Auditory perception of amplitude modulation (AM) and frequency modulation (FM) has attracted substantial attention over the last decades. Still, questions remain as to i) how FM is processed (in comparison to AM) by the normal auditory system and ii) the effects of ageing on AM and FM processing. Surprisingly, little effort has been devoted to the characterization of perceptual inefficiencies and more specifically “internal noise” (i.e., sources of variability such as the stochastic nature of neuronal firing, the internal state of the listener, or fluctuations in attention) in AM and FM detection.

The purpose of this research was to assess internal noise for AM and FM detection by measuring double-pass consistency in 15 young (NH_y) and 15 older (NH_o) normal-hearing listeners for detection of sine AM and FM at two rates (2 and 20 Hz) using a low-frequency (500 Hz) sine carrier presented at a level of 70 dB SPL.

The psychophysical measures were performed using a 2-interval, 2-alternative forced choice detection task and a constant-stimuli paradigm. A bandpass (0.5-80 Hz) modulation noise with a fixed (low or high) standard deviation was applied to all stimuli. The sine AM or FM targets were presented at a sensitivity (d') of 0.5, 1 or 1.5, estimated for each listener using an adaptive task in a preliminary experiment. All stimuli used during the first session (the first “pass”) were stored and presented again in a different order during a second session (the second “pass”) after about 5 min. Percent agreement (PA) between responses to corresponding trials in the first and second pass was calculated and used as a measure of internal noise for AM and FM detection.

Statistical analyses carried out on the PA data showed that the main effect of group (NH_y versus NH_o) was not

significant. The analyses also showed a significant main effect of d' ; level (0.5, 1 or 1.5) and a significant interaction between factors modulation type (AM versus FM) and modulation rate (2 versus 20 Hz). Post-hoc analyses revealed significant differences in PA measured using rates of 2 versus 20 Hz in the FM condition only. These results suggest that different sources of internal noise constrain slow-AM and FM processing, consistent with the existence of separate mechanisms for slow (< 10 Hz) AM and FM detection when the carrier is low (< 1-4 kHz). However, the results do not show any effect of ageing on the efficiency in modulation processing.

PS 502

Characterizing the Role of Hearing Loss in Comodulation Masking Release: Behavioral Measurements and Computational Model Predictions

Paolo A. Mesiano¹; Johannes Zaar¹; Borys Kowalewski¹; Langchen Fan²; Laurel H. Carney²; Torsten Dau³

¹Technical University of Denmark; ²University of Rochester; ³Hearing Systems Group, Department of Electrical Engineering, Technical University of Denmark

The detection of pure tones embedded in noise can be facilitated if amplitude modulations are imposed on the noise masker by multiplying it by low-frequency noise (i.e., modulated noise). This phenomenon is known as comodulation masking release (CMR). It can be quantified by measuring the reduction in the masked threshold observed when the masker is modulated, compared to a masker with the same spectrum and level but with an unmodulated envelope (i.e., unmodulated noise).

CMR in normal-hearing (NH) listeners has been observed through several experimental paradigms. Nevertheless, the perceptual mechanisms responsible for it are still unclear. In the studies investigating CMR in listeners with sensori-neural hearing loss (SNHL), an overall reduction in the amount of masking release was observed. Loss of sensitivity and reduced frequency selectivity were found to be linked to the reduction in CMR. However, the deficits in auditory processing directly responsible for the reduced CMR have not been precisely identified.

The aim of this study is to extend the investigation of CMR in relation to SNHL including other aspects of hearing. CMR was measured in a group of listeners with sloping, mild-to-severe SNHL. Large differences in the CMR across participants were observed, some showing normal CMR, others exhibiting reduced or absent CMR.

The amount of CMR was related to several aspects of auditory processing, assessed by means of behavioral experiments. These included measurements of absolute thresholds, estimates of auditory filter width, cochlear compression and sensitivity to temporal fine structure. A statistical analysis of the results indicated a significant effect of frequency selectivity and sensitivity on the amount of CMR in HI listeners, in line with previous studies. No significant effect of the estimated cochlear compression ratio or temporal fine structure was observed. Additionally, simulations have been conducted with a computational model of auditory perception that has been shown to account for several aspects of hearing impairment. The model failed to predict the experimental results, even when the individual elevation of absolute thresholds, increased auditory filter bandwidth and loss of cochlear compression were included in the model front end. This suggests that other deficits in the auditory system, such as the processing of the temporal envelope of the stimulus, might be related to the CMR in listeners with SNHL (see companion study by Fan et al., this conference).

The study was supported by NIH DC-010813, the Oticon foundation, and the Centre for Applied Hearing Research (CAHR).

PS 503

Neural Fluctuation Profiles: Yet Another Model for Pitch

Laurel H. Carney¹; Adrian B. Go¹; Cecilia Esterman²; Braden Maxwell¹

¹University of Rochester; ²Massachusetts Institute of Technology

Recent studies have focused on the profile of low-frequency fluctuations in response amplitudes across auditory-nerve (AN) frequency channels as a code for detection of tones in noise, identification of spectral peaks in speech, etc. The profile of fluctuation amplitudes across the population of AN responses is of interest because it results in an average rate profile across midbrain neurons that are sensitive to amplitude fluctuations. In this study, we focused on fluctuation profiles in response to stimuli that elicit pitch percepts. The amplitudes of fluctuations in AN responses are strongly influenced by the capture of AN responses by single harmonics in tone complexes. Fluctuation profiles across the population are further influenced by the effects of suppression on frequency channels near spectral edges of stimuli. In response to bands of noise, which lack discrete tonal components, fluctuation amplitude profiles are primarily affected by suppression. Fluctuation profiles in AN responses are strongly determined by the responses of inner hair cells,

and thus they occur for all types of AN fibers. Here, we focus on responses of high-spontaneous-rate AN fibers, for which average rates are saturated at the sound levels typically used in pitch experiments.

A recent study by Bianchi et al. (ARO, 2018) showed that discrimination limens for the pitch of harmonic tone complexes were well predicted for different sets of components, several phase conditions, and for listeners with both normal hearing and sensorineural hearing loss. Here, we extended the model by surveying several classic pitch percepts. Illustrations of neural fluctuation profiles were generated using computational models for populations of AN fibers and midbrain neurons. Stimuli explored include the edge pitch associated with low-pass or high-pass noise, edge pitch associated with a harmonic tone complex, the pitch associated with a narrowband noise, pitches of stationary and time-varying Shepard tones, and pitches of spoken vowels. In each case, minima in the rate profiles of model midbrain neurons with bandpass modulation tuning were used to specify perceived pitches.

Neural fluctuations are influenced by several peripheral nonlinearities, including “capture”, compression, suppression, and synaptic saturation and adaptation. Thus, the physiological state of the auditory periphery contributes to the pitches perceived in response to various complex stimuli. We hypothesize that some of the across-listener differences in these pitch-related percepts (e.g. in edge pitches) may be due to differences in inner-ear nonlinearities.

Supported by R01-DC010813.

PS 504

Effects of Gap Position on Perceptual Gap Detection Across Development

Jennifer Gay¹; Merri J. Rosen²; Julia Huyck³
¹Northeast Ohio Medical University; ²Hearing Research Group, Dept. Anatomy & Neurobiology, Northeast Ohio Medical University; ³Kent State University

The ability to detect a silent gap within a sound, i.e. gap detection, is critical for accurate speech perception. In certain conditions, the detectability of the gap changes as the temporal placement of the gap within the signal is changed, where gaps close to signal onset are harder to detect. Gap detection has an extended developmental trajectory both in human and animal models, and early gap detection abilities in children can predict later speech and language skills. Early in development, when temporal processing is immature, the challenge of detecting

gaps shortly after signal onset may be exaggerated. The present study aims to explore the developmental timeline of gap detection abilities, specifically when the temporal placement of the gap is varied.

Normal hearing subjects aged 8-19 years were asked to indicate, on each trial, which of three broadband noises contained a silent gap (a 3-alternative forced choice task). The onset of the gap varied between 10 to 50 ms, and the duration of the gap was adjusted using a 3-down 1-up adaptive rule, with threshold defined as the gap duration that subjects could detect on 79.4% of trials. Subjects completed two testing blocks per day over the course of two consecutive days. Preliminary data shows a strong effect of age, with younger (8-10 and 11-13 years) listeners showing higher (poorer) gap detection thresholds for all gap onset times. Further, all age groups showed increased thresholds for gaps with short delays, with better thresholds for longer delays between signal onset and gap onset. There was no interaction between age and gap position: younger groups did not have differentially more trouble with short gap onset times than older groups. The older groups (11-13, 14-16, and 17-19 years) did not improve their thresholds within a single day, but demonstrated learning between days. The youngest age group tested (8-10 years) did not demonstrate learning between days, and further showed within-day worsening, with higher thresholds for the second block on each day. This work supports earlier studies showing that gaps are harder to detect near stimulus onset, and confirms that gap detection abilities continue to mature into adolescence. It also suggests that younger listeners may have different requirements for perceptual learning of gap detection than older children and adults.

PS 505

Spectral Weighting for Sound Localization in the Free Field

Monica L. Folkerts¹; G. Christopher Stecker²

¹Vanderbilt University; ²Vanderbilt University Medical Center

The localization of sounds in azimuth is known to rely primarily on binaural cues (interaural time [ITD] and level [ILD] differences) which—in complex tones—are distributed across stimulus frequency. According to the duplex theory of sound localization [Strutt 1907, *Philos Mag* 13:214-32; Macpherson & Middlebrooks 2002, *J Acoust Soc Am* 111:2219-36] low-frequency tones are localized on the basis of ITD and high-frequency tones primarily on the basis of ILD. That view has been extended to show the overall dominance of low-frequency ITD cues even in broadband sounds [Wightman & Kistler 1992, *J Acoust Soc Am* 91:1648-61] but no studies have systematically quantified the relative contribution of spatial cues across

the frequency spectrum. The current study adapted the temporal-weighting-function (TWF) approach of Stecker [2001, *ARO Abs* 24:258] to measure spectral weighting functions (SWF) that directly quantify spatial-cue weights across frequency. Briefly, listeners judged the spatial positions of 100-ms complex tones containing seven components (harmonics of a 200 or 800 Hz fundamental, or octaves from 100 to 6400 Hz) or 100-ms noise bursts divided into seven adjacent sub-bands (1-octave bands spanning 70-9000 Hz or 1/3-octave bands spanning 180-900 Hz). Stimuli were presented from an array of loudspeakers with azimuthal spacing 5.625° and 2-m radius in the Vanderbilt Anechoic Chamber Lab. Each trial presented a single stimulus at a “base” azimuth selected from the range ±56.25°. The azimuth of each individual component or sub-band deviated—randomly and independently—from the base azimuth by 0°, ±5.625°, or ±11.25° (i.e. 0, 1, or 2 loudspeakers to the left or right). Procedural and analytical methods closely followed those of Stecker and Moore [2018, *J Acoust Soc Am* 143:786-93]: Listeners used a touch-sensitive display to indicate the perceived location on each trial. Localization weights were estimated by multiple linear regression of rank-transformed response azimuths onto per-component azimuths across trials. The resulting set of seven weights comprises the SWF and quantifies the relative potency of spatial cues carried by each frequency component or sub-band. Preliminary results in all conditions exhibited a stereotypical pattern of elevated weights around 800 Hz. Thus, SWF shapes appear inconsistent with an overall dominance of low-frequency cues, but align closely with Bilsen & Raatgever's [1973, *Acustica* 28:131-132] proposed “dominance region” for binaural processing around 600-700 Hz. Supported by NIH-NIDCD R01 DC016643.

PS 506

Investigating the Parameters of Temporal Integration in Pitch

Anahita H. Mehta¹; Andrew J. Oxenham²

¹University of Minnesota; ²Department of Psychology, University of Minnesota

Background

Auditory perception requires the integration of information over time. For pitch in particular, given that it is most closely associated with repetition rate or frequency, a valid estimate is contingent upon its integration over time. Our current understanding of pitch perception and models for harmonic and inharmonic complex tones only consider the length of the stimulus as the factor for temporal integration, where all frequency components of the complex tone are simultaneously presented. However, it is known that the pitch of the fundamental frequency (F0) can also be elicited by a

sequence of short consecutive tones when presented in a background of noise. In this study, we conducted a series of experiments to determine the spectro-temporal properties under which this virtual pitch from non-simultaneous harmonics can be perceived.

Methods

Fundamental frequency difference limens (F0DLs) were measured for different F0s in 15 normal-hearing participants. The DLs were measured for sequentially presented components that were harmonic, inharmonic, resolved, and unresolved conditions as a function of inter-tone interval (ITI) within the sequence. The tones were presented in background noise to facilitate the perception of the virtual F0 pitch. The measured F0DLs in the various sequential conditions were compared with F0DLs using complex tones with synchronous components.

Results

The preliminary results for the resolved harmonic complexes broadly replicate the original findings with non-simultaneous complex tones. However, different limits of temporal integration (in terms of the ITI) were found for different F0s. Preliminary data suggest that the percept becomes weaker or absent when only high-numbered harmonics (> 10) are presented. This outcome suggests that low-numbered harmonics, which are normally spectrally resolved, are required to elicit the illusion of F0 in the absence of simultaneously presented components, and that higher-numbered harmonics, which normally elicit pitch via temporal-envelope cues, do not elicit a pitch when presented sequentially.

Conclusions

These results provide a more detailed understanding of the largely overlooked property of sequential temporal integration in pitch perception using an illusory stimulus that highlights important properties of pitch perception and helps us to further understand the role of harmonic resolvability in complex pitch perception.

[Supported by NIH grant R01DC005216.]

PS 507

Investigating the Role of Dynamic Range Adaptation to Level Statistics in Detection of Amplitude Modulation Using Fixed-level and Roved-level Tones in Noise

Juraj Mesik¹; Nathan Torunsky¹; Magdalena Wojtczak²

¹Department of Psychology, University of Minnesota;

²University of Minnesota

Background

Recent studies on detection of amplitude modulation

(AM) of tones presented in a simultaneous masking noise reported that AM detection thresholds are lower (better) when measured with than without a noise precursor. Previous work from our lab, using stimulus-frequency otoacoustic emissions, ruled out the possibility that the precursor improved AM detectability via medial olivocochlear efferent activation. An alternative explanation invoked adaptation of neural rate-level functions to level statistics during the precursor. Such dynamic range adaptation has been shown in animal physiological studies at all levels in the auditory pathway. In this study, detection of AM was measured with and without a precursor using a fixed-level and a roved-level paradigm. The hypothesis was that AM detection should be adversely affected by a wide-range level rove without a precursor, when the response to the noise with a tonal carrier is unadapted to masker level statistics. In contrast, the rove should have little effect on AM detection measured with a precursor due to neural adaptation to the noise level during the precursor.

Methods

The listeners' task was to detect a 20-Hz AM of a tonal carrier (1 and 4 kHz) embedded in a two-octave noise band centered on the carrier frequency. The level of the tone was fixed at 55 dB SPL in one condition and randomly roved across observation intervals over a range from 30 to 85 dB SPL while keeping the signal-to-noise ratio fixed, in another condition. Both fixed- and roved-level conditions were run with and without a noise precursor. The precursor level was equal to that of the simultaneous masking noise.

Results

AM detection thresholds were remarkably robust to the wide-range level rove independent of whether or not a precursor was present. In both fixed- and roved-level conditions, AM detection thresholds were lower with than without a precursor at comparable levels.

Conclusions

Preliminary data suggest that a precursor acts to facilitate detection of AM at any fixed level but does not provide an additional benefit when the stimulus level is varied over a wide range across observation intervals. The results do not provide compelling support for the hypothesis that neural dynamic range adaptation is needed for robust coding of level changes across a wide range of levels. [Supported by NIH grant R01DC015462].

PS 508

Within-Subject Average Performance and Performance Consistency Across Years of Musical Training for Frequency and Temporal-Interval Discrimination Tasks

Alex E. Clain¹; David F. Little²; Huanping Dai³; Beverly A. Wright⁴

¹Northwestern University Department of Communication Sciences and Disorders; ²Johns Hopkins University; ³University of Arizona Department of Speech, Language, and Hearing Sciences; ⁴Northwestern University

Introduction

Musicians have been reported to have lower (better) thresholds than non-musicians for frequency and temporal-interval discrimination tasks. The thresholds used in these studies are computed as the within-subject average of multiple threshold estimates. However, it is not known whether in addition to better average thresholds musicians also show better consistency in their performance on these tasks.

Methods

To begin to address this issue, we examined the within-subject mean and standard deviation of frequency and temporal-interval discrimination threshold estimates for listeners with 0-22 years of musical training. For each discrimination task, we tested three stimulus conditions: 1 kHz 50 ms, 1 kHz 100 ms, 4 kHz 100 ms (N = 117 - 156 per condition). For each condition, we obtained five threshold estimates per listener (two-interval forced-choice 3-down/1-up adaptive tracking, 60 trials per estimate). We then computed the within-subject geometric mean (average performance) and within-subject standard deviation (consistency) of the five threshold estimates, and submitted these means and standard deviations to linear regressions with respect to years of musical training.

Results

For all six conditions, within-subject mean thresholds decreased (improved) with increasing years of musical training. For the frequency-discrimination task, within-subject standard deviations decreased (improved) for the 1-kHz, 100-ms condition, showed a trend of a decrease for the 4-kHz, 100-ms condition, and showed no systematic change for the 1-kHz, 50-ms condition. In contrast, for the temporal-interval discrimination task, within-subject standard deviations showed no systematic change over years of musical training for any of the three conditions.

Conclusions

Thus, it appears that there can be a musician advantage for performance consistency (within-subject standard deviation) as well as for average performance (within-subject mean threshold) as in two of the three frequency conditions. However, this musician advantage can also be restricted to average performance with no advantage for performance consistency, as in one of the three frequency conditions and all three temporal-interval conditions. More broadly, this result demonstrates that average performance and performance consistency are separable, and therefore may be tapping into distinct perceptual mechanisms.

PS 509

Spectral Ripple Discrimination in Normal Hearing Infants Using Static and Dynamic Spectral Resolution Testing

Anisha R. Noble¹; Mariette S. Broncheau²; Jay T. Rubinstein²; Lynne A. Werner²; David L. Horn¹

¹University of Washington Department of Otolaryngology; ²University of Washington

Background: Spectral ripple discrimination (SRD) is a potentially useful test to evaluate device efficacy in young cochlear implant users too young for speech perception testing. However, spectral ripple discrimination matures gradually through school-ages. Inattention accounts for some of the immaturity across psychoacoustic tasks in infants. It was hypothesized that infants would pay more attention on a dynamic (where spectral peaks vary in frequency over time) than static (where spectral peaks are fixed in frequency) SRD task. To test this hypothesis, we compared threshold yield, mean threshold, effect of ripple depth on threshold and psychometric function (PMF) shape obtained from infants tested with spectrally static versus dynamic SRD tasks.

Methods: Participants were 6-month-old and adult normal hearing listeners. For experiment 1, stimuli were 2s broadband multitone noises with amplitude modulated, or "rippled", spectral envelope of particular ripple density and depth. Listeners were trained to respond when the second 1s spectral envelope was shifted 90° in phase from the first 1s. For experiment 2, stimuli were 1s broadband multitone noises with rippled spectral envelopes where ripple peaks moved in frequency at a 5kHz rate. Listeners were trained to respond when the ripple density of the stimulus was lower than 20 ripples per octave. In both studies, an observer-based psychoacoustic procedure was used to measure listener performance as a function of ripple depth. Threshold was defined as the 0.7 correct point on the PMF. Stimuli were presented at 65-70dB SPL and

thresholds were measured for each listener at two ripple depths (10dB, 20dB) in counterbalanced order.

Results: Two thresholds were obtained from 51% of infants in study 1 compared to 88% of infants from study 2. In addition, mean infant SRD threshold was poorer in study 1 compared to study 2. Mean infant SRD was significantly better at 20dB than 10dB depth in study 2 but the effect of depth did not reach significance for infants in study 1. Finally, mean upper asymptote of the PMF for infants was significantly lower in study 1 compared to study 2.

Conclusion: Although methodological differences between studies exist, the results suggest that dynamic SRD testing produces better threshold yield, higher thresholds, and may be more sensitive than static SRD for measuring effect of ripple depth on task performance in normal hearing infants. Differences in mean threshold and PMF asymptotes between the two tasks support the hypothesis that infants are more attentive to dynamic versus static SRD stimuli.

PS 510

Pitch Perception of Concurrent High-frequency Complex Tones

Daniel R. Guest; Andrew J. Oxenham
Department of Psychology, University of Minnesota

Recent studies have shown that accurate pitch perception is possible for harmonic complex tones with fundamental frequencies (F0s) in the musical range (1.4 kHz) but with all of their harmonics beyond the putative limits of phase locking (i.e., above 8 kHz). The findings are consistent with a place code for pitch at these high frequencies. However, it is unknown whether such a code can facilitate pitch perception in more complex situations, such as with concurrent complex tones. To address this question, we studied pitch perception using mixtures of complex tones with low F0s (around 280 Hz) and mixtures of complex tones with high F0s (around 1400 Hz), comprising a target complex tone and one or more masker complex tones. The target tones contained only harmonics 6-10 of their F0s to ensure that in the high-frequency case only harmonics beyond the limits of phase locking were present. The task involved discriminating whether the final target tone had a higher or lower F0 than the preceding reference tones. Three masker conditions were tested: ISO, in which the target tone was presented without a masker; GEOM, in which the target tone was presented with a masker whose F0 was geometrically centered between the reference and target F0s; and DBL, in which the target tone was flanked by one masker with a higher F0 and

one masker with a lower F0. Notably, place code cues to pitch were preserved in the GEOM masker condition but severely limited in the DBL masker condition. The ISO and GEOM conditions were tested with an adaptive procedure, while the DBL condition was tested with a constant interval based on each listener's performance in the ISO condition. Although pitch perception was generally poorer for the high-frequency tones (mean F0DL = 3%) than for the low F0 tones (mean F0DL = 1%) in the ISO condition, the effect of adding the GEOM masker was equivalent for the low F0 and high F0 tones (an elevation of F0DLs by a factor of 3). In contrast, good performance (~70% correct) was retained for the low F0 tones, but not the high F0 tones (~50% correct), in the presence of the DBL masker. These findings may indicate that different mechanisms underlie the perception of combinations of complex tones at low and high frequencies. [Grant support: R01 DC005216 and NSF NRT-UtB1734815]

PS 511

Discrimination of Periodicity and Pitch Effects in Musicians and Non-musicians

Devin Inabinet; Gabriella Musacchia
University of the Pacific

Pitch perception is related to sound periodicity and provides important information for musical and vocal communication. Numerous studies show musical training and expertise are associated with better pitch processing, suggesting that internal representation of pitch is plastic. However, sound periodicity can be established in many ways and mechanisms of complex encoding are distributed across numerous auditory nuclei in brainstem and cortical regions. This makes it difficult to determine whether specific neural mechanisms are impacted or simply a general tuning of the auditory system occurs as a result of musical training. The current study employs the diversity of periodic acoustics to probe whether different types of pitch computations are plastic with auditory (musical) training. Based on previous data, our initial hypothesis was that musicians would perform better when pitch perception was evoked primarily by temporal or interaural cues, compared to percepts relying on tonotopic frequency selectivity. A traditional approach for determining how accurately listeners can perceive pitch involves measuring frequency difference limens (DLFs) for the fundamental frequency (F0). Here, we measured DLFs with a 3-alternative-forced-choice task in four stimulus conditions: 1) pure sinusoidal tones (PT), 2) interaurally correlated broadband noise ("Huggins" pitch, HP), 3) complex tones (CT) and 4) iterated rippled noise (IRN). In addition, we tested musical ability according to the International Laboratory for Brain Music and Sound Research

(BRAMS) online test. According to our hypothesis, we predicted the biggest differences between musicians and nonmusicians would be observed in HP and IRN conditions. Initial results show BRAMS measures of musicality positively correlate to DLFs in all conditions, suggesting that either several pitch processing mechanisms are employed during music perception judgements or that more sensitive measures may need to be employed. Regarding pitch, musicians appear to have at least ~50% smaller DLFs than nonmusicians in the HP condition, and ~15% smaller DLFs in the PT condition but do not differ from nonmusicians in the CT or IRN conditions. These preliminary data suggest that interaural computation of pitch periodicity at the cortical level is most impacted by auditory training with music. We speculate this may be due in part to the increased flexibility of cortical computation, compared to pitch processing mechanisms that rely on more hard-wired frequency selective tonotopicity or phase-locked timing.

PS 512

The effects of duration on monaural and binaural temporal fine structure coding

Katherine N. Palandrani¹; Eric C. Hoover²; Frederick J. Gallun³; David A. Eddins¹

¹University of South Florida; ²University of Maryland;

³VA Portland RR&D National Center for Rehabilitative Auditory Research and OHSU

Detection of frequency modulation (FM) can be used as a tool to evaluate monaural or binaural temporal fine structure (TFS) processing. Measures of FM detection often include relatively long-stimulus durations (e.g., 1250 ms) with a low modulation depth (e.g., 2 Hz) and a low-frequency carrier (e.g., 500 Hz). Previous studies have reported the clinical efficiency of such a task despite requiring a long stimulus duration. The goal of the current study is to determine if the efficiency of this common measure of TFS perception can be improved by using a shorter stimulus duration. Additionally, two different modulation starting phases were used to evaluate the relative contribution of the maximum deviation of instantaneous frequency and the total modulation cycles completed to FM detection. A total of 16 conditions were tested including four stimulus durations of 500, 750, 1000, and 1250 ms and two modulation starting phases, sin and -cos, tested both monaurally and dichotically. The carrier frequency was randomly selected for each interval ranging from 460 to 540 Hz to minimize the use of place cues. The presentation level was 65 dB SPL. Detection thresholds were obtained from ten young participants with normal hearing using a four-interval, two-alternative forced-choice method with 3-down, 1-up tracking. Monaural FM detection thresholds increased gradually and monotonically as duration decreased

from 1250 ms to 500 ms. Thresholds were significantly different across different stimulus durations in the monaural condition for both starting phases, consistent with an integration of TFS over time. There was no significant difference in threshold with duration in the binaural condition, consistent with the use of different cues for the detection of binaural compared to monaural TFS. There were no significant differences in threshold with starting phase for monaural or binaural conditions. Consistent measurement error was observed across all phase and duration conditions for both monaural and binaural tasks, confirming the potential utility of short duration stimuli in the efficient evaluation of TFS perception in a clinical battery.

PS 513

Effect of Auditory Spectral Degradation on Shape of Spectral Modulation Transfer Function in Normal Hearing Adults

Anisha R. Noble¹; Mariette S. Broncheau²; Jay T. Rubinstein²; Lynne A. Werner²; David L. Horn¹

¹University of Washington Department of Otolaryngology; ²University of Washington

Background: Cochlear implants provide spectrally-degraded auditory information for prelingually deaf children and post-lingually deaf adults. Tests of spectral shape discrimination, such as spectral ripple discrimination (SRD), are known to be strongly correlated with speech recognition and discrimination in CI users. According to the model of Supin et al. (1999), SRD depends on both frequency resolution (FR) and sensitivity to across-channel intensity modulation (SMS). The relationship between these two independent factors can be described using the spectral modulation transfer function (SMTF). We hypothesized that spectral degradation with a vocoder would affect FR (reflected by SMTF slope) but not SMS (reflected by SMTF x-intercept).

Methods: SRD was measured in NH adult listeners with a three-alternative forced choice task. Stimuli were spectro-temporally modulated 500ms broadband multitone noises with rippled spectral envelopes from 1 to 20 ripples per octave (RPO) and peak temporal modulation rate of 5Hz (Aronoff & Landsberger, 2013). On each trial, two 20 RPO reference signals and one target signal at a lower ripple density were presented. Presentation level was 70dB SPL in soundfield and temporal starting phase was randomized each trial. Listener response was used to adaptively modulate signal RPO to obtain a threshold defined as highest RPO of target stimulus at which 50% discrimination was achieved. Each listener was tested, in counterbalanced order, at multiple ripple

depth (5 to 20dB) and spectral resolution (unprocessed and 8 channel noise vocoded) conditions for a 4X2 repeated measures design. For each subject and spectral resolution condition, logarithmic functions were fit to derive SMTF slope and x-intercept.

Results: SRD was better in the unprocessed condition compared to the vocoded condition. SMTF slope was significantly flatter in the vocoded condition. Preliminary data suggests no significant difference in x-intercept between the two conditions.

Conclusion: Spectral degradation with a vocoder is associated with flatter SMTF slope on an SRD task. This pattern suggests that poor SRD with spectral degradation is due primarily to poor frequency resolution. These data indicate that SMTF slope could be used in young CI patients – who are known to have immature SRD – to assess efficacy of device modifications aimed at improving frequency resolution.

Speech Perception: Intelligibility

PS 514

Neurophysiological Validation of Envelope-based Models of Speech Intelligibility

Vibha Viswanathan¹; Hari Bharadwaj²; Barbara Shinn-Cunningham³; Michael Heinz²

¹*Weldon School of Biomedical Engineering, Purdue University*; ²*Speech, Language, & Hearing Sciences, and Weldon School of Biomedical Engineering, Purdue University*; ³*Carnegie Mellon University*

Models of speech intelligibility that accurately reflect human listening performance across a broad range of background noise conditions are important both clinically (e.g., for deriving hearing-aid prescriptions, and optimizing cochlear-implant signal processing), and for evaluating speech-processing algorithms in technological applications (e.g., in mobile phones). Envelope-coding based models of speech intelligibility in noise have been widely successful (e.g., Jørgensen & Dau, JASA 2011; 2013). However, these acoustic models have not been validated neurophysiologically. Here, using electroencephalography (EEG), we derived a neural metric of envelope coding (ENVneural) of speech in noise to evaluate whether neural envelope coding can predict speech intelligibility. A crucial test of envelope-based models is whether a mapping between ENVneural and perceptual intelligibility derived from one type of background noise can be used to predict intelligibility from just the ENVneural metric for other novel background-noise conditions and linear and non-linear distortions applied to the input sounds.

Subjects performed a speech-identification task using sentences in the IEEE Harvard corpus in a background of speech-shaped (stationary) noise (SSN) presented at different signal-to-noise ratios (SNRs). The SNRs were varied to span the full range of speech intelligibility (i.e., 0 - 100%). Simultaneously, thirty-two-channel EEG data were collected. The spectral phase-locking value (PLV) was calculated between the EEG data and the speech envelopes at the output of ten gammatone filters simulating cochlear frequency selectivity. The PLV values from different EEG channels and across different cochlear gammatone filters were thresholded and combined to yield a single ENVneural value for each listening condition. Preliminary results show a robust monotonic relationship between ENVneural and intelligibility for different SNRs of the SSN background condition, allowing a mapping to be created between ENVneural and intelligibility. To test whether ENVneural can be used with this mapping to predict intelligibility in novel but realistic listening conditions, subjects also performed speech-identification tasks: (1) in a background of 4-talker babble, (2) with babble and extensive room reverberation (linear distortion), and (3) with babble denoised through a binary-masking-based procedure (a nonlinear strategy often used in technological applications). Preliminary data show that intelligibility varies across these novel conditions. Whether these perceptual variations in speech intelligibility can be predicted from ENVneural using the mapping from the stationary noise condition will be evaluated and discussed.

Funding provided by an International Project Grant from Action on Hearing Loss (Heinz), NIH R01DC009838 (Heinz), and NIH F31DC017381 (Viswanathan).

PS 515

Integration of Speech Information (or not) across Multiple Cochlear Implants and/or Acoustic Modes of Hearing.

Bob McMurray

Department of Psychology and Brain Sciences, The University of Iowa

Approaches to hearing remediation increasingly combine disparate types of inputs. Many people use two cochlear implants (bilateral CIs), or combine a CI and hearing aid (A+E listeners, including both bimodal and hybrid configurations). Others use a CI despite preserved unaided hearing on the contralateral ear (single side of deafness, SSD). Such configurations yield improved speech perception (particularly in noise), over a single standard CI. However, it is not well understood if this benefit derives from a truly integrated percept, or if CI users are benefitting from redundancy afforded by two inputs or from other factors (e.g. localization).

We examined this in a duplex perception experiment. Listeners heard the four cardinal vowels from six talkers. Formants were split between modes (e.g., the first formant was presented to the CI, and the second to the other CI or hearing aid), or presented to both modes simultaneously. Here, each formant individually should be insufficient for accurate perception, however, if listeners can fuse inputs across ears or devices they can achieve robust perception. In normal hearing listeners (N=14), accuracy under duplex presentation (each formant presented to different ears; M=.80) did not differ from combined presentation (both formants were presented to both ears, M=.76, $p=.14$). However, performance dropped to near chance when isolated formants were presented to both ears (M=.40, $p<.001$), validating that fusion was necessary for accurate perception. In contrast, CI users (Bilateral: N=8; A+E: N=11; SSD: N=9) performed as well in combined presentation as NH listeners (Bilateral: M=.75, A+E: M=.70, SSD: M=.81), and similarly poorly with isolated formants (Bilateral: M=.42, Bimodal: M=.40, SSD: M=.45). However, unlike NH listeners, performance under duplex presentation was significantly poorer than combined in all hearing impaired groups (Bilateral: M=.57 [vs. .75], $p=.0024$; A+E: M=.50 [vs. .70], $p<.001$; SSD: M=.52 [vs. .81], $p<.001$), though it was better than with isolated formants ($p<.05$). In A+E listeners, this decrement was significant regardless of which formant was sent to the CI or hearing aid ($p<.05$). Thus CI users—even those with NH in one ear—may not fuse inputs well at an auditory level. This suggests that CI users do not fuse input into a single auditory object and then identify speech sounds; rather, they conduct speech perception on each mode (ear or input) independently and fuse the results. Thus, the benefits of acoustic+electric hearing or bilateral implantation may derive from redundancy and not true auditory integration.

PS 516

Lexical Access in the Face of Degraded Speech: Dealing with Uncertainty Through Cognitive Adaptation

Francis X. Smith; Bob McMurray

Department of Psychology and Brain Sciences, The University of Iowa

Speech unfolds over time. As a result, listeners must deal with the fact that at early portions of a word, there are many potential lexical items that match the current input. For example, when hearing the bee-in-beet, the input is consistent with not only beet but also competitors like beak and bean. Normal hearing listeners cope with this temporary ambiguity by activating multiple lexical candidates which compete with one another for recognition (McClelland & Elman,

1986). There is evidence competition dynamics change when processing degraded speech input (Brouwer & Bradlow, 2016; McMurray, Farris-Trimble, & Rigler, 2017; McQueen & Huettig, 2012) but it is unclear whether this reflects natural consequences of processing degraded input, or functional adaptation to cope with the increased uncertainty inherent to degraded speech. We set out to isolate a potential central contribution to this using two visual world paradigm experiments in which normal hearing listeners heard different levels of degraded (noise-vocoded) speech and matched the auditory input to pictures of the target word and its competitors (e.g., beet and beak). Here, eye-movements to each picture over the course of the trial can reveal the strength by which that interpretation is competing at any moment. Experiment 1 manipulated degradation level such that some participants heard only one of the two levels of degradation (4- or 15-channel vocoding) while other participants heard both randomly interleaved across trials. As seen previously, highly degraded speech led to reduced peak looks to onset competitors consistent with a “wait and see” approach (McMurray, Farris-Trimble, & Rigler, 2017). However, interleaving led to processing delays beyond that of degradation alone and there were switch-costs when degradation level differed between trials. This suggests differences in lexical dynamics are not solely due to degradation level but may also reflect cognitive demands. In Experiment 2, all participants heard interleaved levels of degradation, but a visual cue indicated the degradation level before each trial. This reduced the delay and switch costs, suggesting listeners were able to adapt before the input was heard. These experiments support a role for central processing in dealing with degraded speech and suggest that listeners may be actively forming expectations about the level of degradation they will encounter and that these can shape the dynamics of lexical access.

PS 517

Neurophysiological, Linguistic, and Cognitive Predictors of Children’s Ability to Perceive Speech in Noise

Elaine Thompson; Jennifer Krizman; Travis White-Schwoch; Trent Nicol; Ryne Estabrook; Nina Kraus
Northwestern University

To learn in a bustling classroom, children must effectively perceive speech in noise. Hearing in noise is a complicated task that relies upon attention, memory, and linguistic knowledge, in addition to precise auditory-neurophysiological processing of sound. Accumulating evidence suggests these mechanisms vary depending on the speech-in-noise task demands. For instance, when speech and noise are co-located, this demands a large cognitive load and recruits working memory,

while spatially separating the speech and noise diminishes this load and draws on alternative skills. However, research has focused on the mechanisms underlying hearing in noise in isolation; no study to date has considered how they interact during critical developmental years. This project sought to identify the neurophysiological, cognitive, and linguistic processes supporting speech-in-noise perception in young children under various masking conditions (i.e., co-located, spatially separated). Structural equation modeling was used to examine these processes as latent constructs and determine their unique contributions in predicting speech in noise. Results reveal neural processing of sound contributes to speech-in-noise perception overall and differentially: while F0 processing predicts of speech in noise under both masking conditions, transition timing is important for spatially separated, but not co-located, perception. In addition, cognitive and language skills are tightly linked, and when combined into one latent construct, predict speech-in-noise perception across both masking conditions. Taken together these findings suggest co-located and spatially separated speech-in-noise perception draw on similar cognitive/linguistic skills, but differential neural mechanisms in early childhood. Finally, through a retrospective analysis of longitudinal data, we see that neural and cognitive/language factors, when measured at ~age 3, predict speech-in-noise perception later in development at ~age 6, suggesting these foundational skills are integral for functional listening throughout early childhood.

PS 518

Hidden Intelligibility: Interaction between Independent Acoustic Dimensions and Word Predictability

Somayeh Shahsavarani¹; Thomas Carrell²

¹University of Illinois at Urbana-Champaign; ²University of Nebraska-Lincoln

Words are nearly always embedded in the context of daily life. Contextual information is known to facilitate speech recognition, especially under adverse listening conditions. Different adverse conditions such as speech signal degradation or listener hearing impairment deteriorate different aspects of the acoustic representation of speech. For example, the distance between speaker and listener can affect the amplitude envelope of speech signals yet leave spectral information relatively intact. Or, listeners with cochlear implants receive speech signals that are represented poorly in the spectral domain while the amplitude envelope is preserved relatively well. Do these different representations of acoustic information interact with contextual information to affect intelligibility? To approach this question, we investigated

how word predictability interacts with two orthogonal acoustic dimensions: amplitude envelope and spectral resolution. Word predictability was manipulated using the Speech Perception in Noise (SPIN) test. Noise-vocoding techniques were employed to systematically manipulate the amplitude and spectral parameters. Participants were 27 normal-hearing listeners with bilateral pure-tone thresholds ≤ 20 dB HL measured at 1, 2, 4, and 6 kHz. Their task was to write the final word of each sentence. Word intelligibility was the dependent measure and all listeners were exposed to all stimulus types in a repeated-measures design. To evaluate the participants' performance, we measured the percentage of the final words correctly identified. Further, we measured the phonemic distance between target and answer final words using the Levenshtein Algorithm. Performance gain was used to quantify the context effect. Our results showed that increasing amplitude information did not improve the intelligibility of low-predictability (LP) sentences whereas it improved the intelligibility of high-predictability (HP) sentences. This suggests that although increasing amplitude information introduced additional acoustic information to both LP and HP sentences, this information was not sufficient to improve the intelligibility of LP sentences. In other words, the effect of increasing amplitude information on intelligibility remained hidden until more contextual information became available. Additionally, using repeated measure ANOVA, our results revealed a significant ($p < 0.05$) interaction effect between amplitude envelope, frequency, and context in both word recognition and phonemic distance measures. Our findings point to the importance of considering different aspects of acoustic representation of speech and their interactions with contextual information while evaluating the effect of adverse listening conditions on speech intelligibility. In future work, different experimental settings (than noise-vocoded speech and word predictability) will be needed to better understand the interaction of context with amplitude envelope and spectral resolution.

PS 519

Speech Understanding in Real-World Environments: Comparison of Monaural and Binaural Listening

Calli Yancey¹; Mary Barrett¹; Douglas S. Brungart²; Sandra Gordon-Salant¹

¹University of Maryland; ²Walter Reed National Military Medical Center

Background:

Laboratory studies of speech understanding in noise may not accurately reflect listener performance in real world noise environments, because they do

not capture the effects of fluctuating noise levels and visual cues and distractions. In laboratory settings, speech understanding is usually tested monaurally under earphones, but in the real-world, people listen binaurally with the exception of individuals with single-sided deafness. Little is known about the performance of individuals who listen monaurally in real-world settings, which often incorporate complex spatial cues that are difficult to accurately replicate in the laboratory. The purpose of this study is to assess monaural and binaural listening performance in real-world listening environments.

Method:

Normal hearing adults were recruited into four-person groups who participated in the experiment at a noisy local restaurant. Each participant was provided with a touch-sensitive tablet computer. At the start of each trial, one participant was prompted to say an item from the Modified Rhyme Test. Then each of the other participants identified the spoken word from a closed set of six choices. Two experimental conditions were tested: a binaural condition, where the listeners had access to signals from both ears, and a monaural condition, where a sound-isolating earphone playing speech-shaped noise was inserted into either the left or right ear. Subjective measures of difficulty were collected for each block of trials, and visual cues were assessed both by instructing the participants to look at either the target talker or the tablet on some trials and by equipping one participant with an eye tracking device. A personal dosimeter was used to record overall noise level during each trial.

Results:

The data were analyzed to evaluate both the percentage of correct responses and the average response time in conditions with all combinations of monaural and binaural talkers and listeners. Preliminary results indicate that participants have significantly better speech understanding scores in the binaural listening conditions compared to the monaural listening conditions, and that monaural masking may decrease the intelligibility of talkers in noisy environments. This latter result is presumably caused by a lowering of the talker's speaking level in the monaural conditions due to some combination of occlusion and the Lombard effect.

Conclusions:

Performance in real-world noisy settings indicates that listeners' speech understanding performance improves with binaural listening compared to monaural listening, and that access to binaural cues may increase the intelligibility of talkers in noisy environments as well.

PS 520

Cochlear implant-induced changes of speech-in-noise processes in single-sided deafness

Kyung-Joong Kim¹; Nicholas Giuliani²; Subong Kim³; **Caroline Emory**³; Ruth Litovsky⁴; Camille Dunn²; Bruce J. Gantz²; Inyong Choi⁵

¹Medical Research Institute, School of Medicine, Sungkyunkwan University; Hearing Research Lab., Samsung Medical Center; Department of Communication Sciences and Disorders, University of Iowa; ²Department of Otolaryngology - Head and Neck Surgery, University of Iowa Hospitals and Clinics; ³Department of Communication Sciences and Disorders, University of Iowa; ⁴University of Wisconsin - Madison; ⁵University of Iowa

Listeners with single-sided deafness (SSD) experience significant difficulties in understanding speech in background noise. It is a still question whether cochlear implant (CI) in the deafened ear, an only way of restoring of binaural hearing in SSD listeners, provides benefits for such difficulty. This study aimed to investigate the CI effect in performance and listening effort during a speech-in-noise task, measured by electroencephalographic (EEG) and pupillometry responses. We hypothesized that CI would improve speech-in-noise performance by providing binaural release from energetic masking. However, an alternative hypothesis was available about the CI benefit on reducing listening effort; additional cognitive resources might have to be engaged to resolve the sound quality disparity between the normal and CI ears. In our speech-in-noise test, listeners heard a target word in stationary noise, followed by a 4AFC recognition task. The noise started 2 seconds before the target arises from one of three directions (-30°, 0°, and 30° azimuth: L, C, and R). A target word from California Consonant Test was presented at +3 dB SNR, always arising at 0° azimuth. Subjects completed 150 trials (50 at each noise direction, presented randomly). We examined accuracy, reaction time, and the distribution of errors. We also analyzed cortical evoked responses and pupil dilation time courses following speech and noise onsets. Our results demonstrate that CI improves the accuracy of responses, although CI increased reaction time, induced delays in cortical evoked responses, and enlarged pupil dilation. These results may imply that CI provides extra information that is helpful to understand a target speech in background noise, although the extra information demands increase cognitive processing. To confirm the benefit of CI in SSD listeners, a longitudinal study will be performed to see if the accuracy improvement is maintained while listening effort is reduced over time through better integration of CI inputs in central processes for speech-in-noise understanding.

PS 521

Effect of Harmonic Structure on Speech-in-Speech Recognition in 5- to 7-year-olds and Adults

Margaret Miller¹; Lori Leibold¹; Emily Buss²

¹Boys Town National Research Hospital; ²University of North Carolina at Chapel Hill

Introduction: The present study evaluated effects of target and masker harmonicity on speech-in-speech recognition in children and adults. We predicted that children would perform more poorly than adults in all target/masker conditions, but that both age groups would show better performance when the target and masker were natural. This prediction was based on published data from adults (reviewed by Darwin, 2008). It was also predicted that SRTs would be lower when whispered speech targets were presented in a natural speech masker than vice versa. This prediction was based on the hypothesis that harmonic cancellation of masker speech is more effective than harmonic enhancement of target speech (de Cheveigné et al. 1995).

Methods: Listeners were school-aged children (5-7 years) and adults (19-40 years). Word recognition was assessed using a 3AFC procedure with a picture-pointing response. Target stimuli were 30 monosyllabic words which lent themselves to illustration. The masker was continuous two- talker speech. All stimuli were produced by female talkers in two styles: (1) natural and (2) whispered. The overall level of the signal-plus-masker was 60 dB SPL throughout testing, and SNR was adjusted adaptively to estimate the speech reception threshold (SRT).

Results: SRTs were significantly lower for adults than for children. The average child/adult difference was substantial for all conditions, but was smallest when both the target and masker were whispered (10.9 dB). While the average SRT for adults was 8.2-dB higher using naturally produced target and masker speech than using whispered target and masker speech, this difference was only 2.6 dB for children. The smaller effect of speaking style in children could reflect a reduced reliance on the harmonic structure of natural speech. SRTs were significantly lower for natural targets in a whispered masker than for whispered targets in a natural masker for both children (average difference = 4.8 dB) and adults (average difference = 3.7 dB).

Conclusions: As previously observed, children were more susceptible to speech-in-speech masking than adults in all target/masker conditions. While lower SRTs were observed for naturally produced target and masker speech than for whispered target and masker

speech, harmonic structure appeared to benefit children to a lesser extent than adults. Results for conditions in which the target and masker speech were mismatched in speaking style were inconsistent with the harmonic cancellation hypothesis.

PS 522

Speech Predictability Hinders Sentence Recognition in Difficult Listening Conditions

Miriam I. Marrufo-Pérez; Almudena Eustaquio-Martin; Enrique A. Lopez-Poveda
University of Salamanca

The auditory system adapts progressively to the background noise, and this adaptation improves the recognition of isolated words embedded in noise over time. On the other hand, listeners are continually making predictions during language comprehension, and correct predictions can facilitate the recognition of upcoming words in running speech. These two mechanisms should make it more likely to recognize the later than the earlier words in congruent, spoken sentences. We tested this hypothesis by presenting normal-hearing listeners (N = 100) with sentences in quiet or in noise at individualized levels where they had 50% probability of recognizing a full sentence. Word recognition was measured as a function of word position in the sentence. Contrary to expectations, recognition gradually deteriorated with increasing word position along the sentence. The worsening in recognition was unlikely due to differences in word audibility or word type, and was not correlated with age or working memory capacity. In fact, results revealed that the recognition of a word was significantly biased by the recognition of the preceding word. We developed a probabilistic model of word recognition based on the assumption that our perception of a word in a sentence can bias our perception of the upcoming word. Using the model, we show that the worsening in word recognition along a sentence occurs because misunderstandings generate inaccurate predictions that outweigh the benefits from accurate predictions. Analyses also revealed that noise adaptation was insufficient to compensate for this harmful effect. We conclude that although speech predictability can facilitate sentence recognition, it also causes word recognition to decrease along a sentence. [Work supported by the University of Salamanca, Banco Santander, and MINECO (BFU2015-65376-P), and the European Regional Development Fund].

Selective Attention Training Enhances Speech-in-Noise Recognition

Subong Kim¹; Caroline Emory¹; Adam Schwalje²; Inyong Choi²

¹Department of Communication Sciences and Disorders, University of Iowa; ²University of Iowa

Speech recognition in noise is challenging even for normal hearing listeners. One useful strategy is directing top-down attention to the target sound while suppressing background noises. Attention modulates neural responses; the strength of cortical auditory evoked responses to target sounds are enhanced when they are attended but lessened when ignored. Our question was whether specific training can enhance listeners' selective attention and whether the effects of the training can be transferred to speech-in-noise recognition performance. Recent studies showed that good performers on speech-in-noise recognition tasks more efficiently utilized selective attention compared to the others. We hypothesized that the neurofeedback training using attention-driven brain-computer interface could enhance listeners'; selective attention and that this would result in better speech-in-noise recognition performance. Two competing stimuli, five "up"s in a straight rhythm spoken by a female speaker and four straight "down"s spoken by a male speaker, were given simultaneously, and the participants were asked to attend to one of those two auditory streams. The difference in the stimulus rhythm enabled electroencephalographic (EEG) responses to be entrained to the attended auditory stream. For the experimental group, each single-trial EEG response was classified using a template-matching method based on pre-defined patterns of cortical auditory responses elicited by either "up" or "down" stream. Visual feedback was given to the participants assigned to the experimental group for each trial by moving a cursor at the center on a screen up or down. On the other hand, a control (placebo) group completed the same selective attention task, but feedback was given only based on behavioral accuracy. All listeners performed pre- and post-training speech-in-noise recognition tests that used a hundred monosyllabic words where the target words started 1-second after the noise onset. After four weeks of training, we found consistent improvement in speech-in-noise recognition performance only in the experimental group. A training effect was also evident in EEG responses only in the experimental group; the amplitude of auditory evoked responses to target word increased while evoked responses to noise decreased. These results indicate that the strength of attentional modulation is reinforced by the neurofeedback training, and the training effect transfers to speech-in-noise performance. To the best of our knowledge, this is the first report of selective attention training enhancing speech recognition in noise performance.

Comparisons in Consonant Recognition Enhancement with and without Conflicting Acoustic Cues

You-Ree Shin¹; Marelina Gutierrez²; Rebekah Havens²; YANG SOO Yoon³

¹Soree Ear Clinic; ²Texas Tech University Health Sciences Center; ³Baylor University

Background

Li and Allen (2010) showed that their novel signal processing tool, three-dimensional deep search or 3DDS, has been effective to extract acoustic cues critical for consonant recognition in normal hearing (NH) populations. However, the effect of 3DDS signal processing on consonant perception was measured in less consistent manner; it is difficult to quantify the benefit of the signal processing. The purpose of this study is to compare consonant recognition with and without 3DDS processing in NH listeners.

Methods

Ten NH adult listeners participated in the study. The most frequently used 14 consonants (/b/, /d/, /g/, /p/, /t/, /k/, /m/, /n/, /f/, /s/, /ʃ/, /v/, /dʒ/, & /z/) were produced by one female talker and presented in the consonant-/a/ context. Consonant recognition was measured unilaterally and bilaterally in noise at -10, -20, and -30 dB signal-to-noise ratio (SNR) under three signal processing conditions: (1) unprocessed consonants, (2) processed consonants by 3DDS with conflicting cues, and (3) processed consonants by 3DDS, but without conflicting cues removed by 3DDS. Each consonant was presented 10 times in random order at each listening condition and at each SNR.

Results

Performance is the highest for "without conflicting cues" condition, and the lowest performance for the unprocessed condition. Unilateral scores are not significantly different, but binaural performance is improved after 3DDS processing. Integration efficiency is improved after 3DDS processing with conflicting cues relative to the unprocessed condition due to improved voicing and place, but integration is not further improved when conflicting cues were removed.

Conclusions

The results suggest that 3DDS is an effective tool to enhance the perception of specific spectral and temporal acoustic cues in NH listeners, resulting in improved consonant perception. 3DDS also can contribute to identify and remove conflicting cues, leading to further improved integration efficiency.

PS 525

Tasks, Talkers and the Perceptual Learning of Time-Compressed Speech

Maram Tarabehi- Ghanayim¹; Yizhar Lavner²; Karen Banai¹

¹University of Haifa; ²Tel-Hai College

Background: Many auditory skills (e.g., the recognition of perceptually difficult speech) improve with practice, but the generalization of this learning to untrained materials is limited. **Methods:** Here, we asked whether the type of practice (semantic or accent judgment) and the number of different talkers encountered during practice (2 or 6) influenced the perceptual learning of time-compressed speech and its generalization to unpracticed materials. Five groups of participants (n = 14-16 per group) were tested twice on the recognition of time-compressed speech (a baseline assessment and 5 test conditions). One group was an untrained control group. The other groups completed 45 minutes of practice between the two tests. Each of the four practice groups completed a single practice type/talkers combination. The semantic judgement groups had to determine whether sentences presented by either 2 or 6 talkers were semantically valid; the accent judgement groups had to determine whether sentences were presented by native or non-native speakers of Hebrew with either 2 or 6 talkers. The test conditions included a learning test in which a subset of the sentences from the practice phase was presented by one of the talkers encountered by the trained groups during practice. The remaining conditions included tests of generalization to (1) new sentences presented by one of the talkers encountered in training, (2) new sentences presented by a novel talker, (3) sentences taken from the practice phase but presented by a new native Hebrew speaker, and (4) sentences taken from the practice phase but presented by a new non-native Hebrew speaker. **Results:** Across groups, training led to substantial learning of the trained tokens and to generalization across talkers (compared to the untrained control group). However, neither type of training had any effect on the recognition of tokens not encountered in training. Semantic training yielded more learning and better retention of learning over a 2 weeks interval than accent training. The number of talkers had only marginal effects. **Conclusions:** These results suggest that learning of time-compressed speech is robust and only partially task specific, but its generalization to untrained tokens following brief practice is limited. In contrast to other types of speech training, here talker variability had no influence on the transfer of learning to new materials.

PS 526

Can Energetic Masking of Competing Talkers Increase Informational Masking?

Virginia Best¹; Christopher Conroy²; Gerald Kidd¹
¹Boston University; ²Department of Speech, Language & Hearing Sciences, Boston University

In many everyday environments, speech understanding may be hindered both by the presence of loud sounds that obscure parts of the speech of interest (“energetic masking”, EM) and by the presence of competing talkers which may cause not only EM but also “informational masking” (IM). These two kinds of interference have been studied extensively, but usually separately, and so the many ways that they could interact are not well described. Anecdotally, we have noticed that even low-level background noise (e.g., in a pub or restaurant) can make the task of ignoring competing voices even harder than it is without background noise. One possible explanation we examined here was that background noise reduces the available information about the target talker, but also about the competing talkers, making segregation of the sources more difficult. We sought to untangle the effects of EM and IM when background noise was added to a competing-talker mixture using a glimpsing approach. The mixture consisted of two equal-level talkers (one target and one masker), which were presented either in quiet or in increasing levels of speech-shaped noise (speech-to-noise ratios of +6, +3, 0, -3, -6 dB). Intelligibility was measured for this “natural” mixture as well as for a “glimpsed target” condition (which quantified the energetic effect of the noise on the target). The difference between these conditions provided an estimate of the IM. A novel “glimpsed target+masker” condition enabled us to examine the segregation of the two talkers while taking into account energetic effects of noise on them both. Control conditions were included to help attribute the impact of the noise to the reduced number of target and masker glimpses vs. the reduced quality of the retained glimpses. The results suggested that the addition of background noise, at certain levels, increased the strength of IM in the mixture. This increase was driven by a disruption to the segregation of the competing talkers, which could be explained primarily by a reduction in the number, but also in the quality, of the target and masker glimpses.

PS 527

The Importance of High-Frequency Information for Understanding “Glimpsed” Speech

Virginia Best; Elin Roverud; Lucas Baltzell; Jan Rannies; Gerald Kidd
Boston University

When speech is interrupted by other talkers, listeners must not only segregate the voices but also recreate the target message from the available time-frequency “glimpses”. Here we tested the hypothesis that high-frequency audibility is more important for sparser representations of speech than for intact speech. This question may be relevant for understanding the impact of high-frequency hearing loss on everyday speech communication. Listeners with normal hearing were presented with sentences that were either intact, or progressively glimpsed according to a competing two-talker masker presented at various levels (target-to-masker ratios of 0, -10, -20 dB). This was achieved using an ideal binary mask to exclude time-frequency units in the target that would be dominated by the masker in a natural mixture. In each glimpsed condition, speech intelligibility was measured for a range of low-pass conditions (cutoff frequencies from 500-8000 Hz). Intelligibility was poorer for sparser speech, as expected. In addition, the bandwidth required for optimal intelligibility increased with the sparseness of the speech. The patterns of performance are compared with predictions based on overall target energy retained, and on the coherence-based speech intelligibility index.

PS 528

Contribution of Stimulus Variability to Word Recognition in Noise vs. Two-talker Speech for School-age Children and Adults

Emily Buss¹; Diana Regalado¹; Lauren Calandruccio²; Jacob Oleson³; Lori Leibold⁴

¹University of North Carolina at Chapel Hill; ²Case Western Reserve University; ³University of Iowa; ⁴Boys Town National Research Hospital

Background: Test-retest reliability is often poorer for masked word recognition when the masker is composed of speech compared to steady noise. This could be due to listener factors, such as trial-by-trial variability in auditory stream segregation or selective attention. It could also be related to stimulus variability, with some speech-in-speech samples posing more of a challenge than others. The purpose of this experiment was to test two hypotheses: 1) that stimulus variability is a dominant factor in adults’; word recognition in a two-talker speech masker, and 2) that stimulus variability plays a smaller role in children’s performance due to relatively greater contributions of listener factors.

Methods: Listeners were normal-hearing children (5-10 yrs) and adults. Target speech was a corpus of 30 disyllabic words, each associated with an unambiguous illustration. The masker was 30 samples of either two-talker speech or speech-shaped noise. The task was

a four-alternative forced choice. Adaptive threshold estimation was used to determine a signal-to-noise ratio associated with approximately 65% correct for each listener and masker. Two 30-word blocks of fixed-level testing were then completed in each of two conditions: 1) with the target-masker pairs randomly assigned prior to each block, and 2) with frozen target-masker pairs.

Results: Thresholds were higher for adults than children, particularly for the two-talker speech masker. Listener responses in fixed-level testing were evaluated for consistency across replicate blocks within a listener and across listeners. The target sample was the best predictor of performance in the speech-shaped noise masker for both the random and frozen conditions. In contrast, the target-masker pair was the best predictor of performance in the frozen, two-talker masker condition; neither target nor masker alone was a good predictor in the random condition. The pattern of results was broadly similar for children and adults.

Conclusions: Word recognition in noise differed consistently across target words for both children and adults. In contrast, recognition in a two-talker speech masker depended on the target-masker pairing. This outcome supports the idea that stimulus variability has a detrimental effect on test-retest reliability in both maskers, although the details of these effects differ across maskers. There is no evidence of differential effects in school-age children and adults.

PS 529

A Task for Inducing Reliability Expectations for Speech Comprehension Under Noisy Conditions

Adrian Cho¹; Gerald Kidd²

¹Graduate Program in Speech and Hearing Bioscience and Technology, Harvard Medical School; ²Boston University

Human listeners frequently are confronted with the task of following the flow of speech between multiple participants in conversation in noisy communication situations. Normally, a variety of acoustic features combine to form low-level perceptual cues that support segregation of target speech from background noise (“noise” means any unwanted source of sound, including competing speech). It also is known that contextual information may greatly facilitate the understanding of speech in noise by tapping cognitive resources including memory and selective attention. For example, listeners may rely on their prior knowledge of the talkers themselves to enhance identification of a message in adverse listening situations [cf. Johnsrude et al., 2013, *Psychological Science*, 24(10)].

In this study, we investigated whether listeners were able to formulate and make use of expectations regarding the likelihood of individual talkers (called “respondents”) correctly answering questions during conversation under noisy conditions. To accomplish this, we used a novel question-and-answer paradigm developed by Best et al. [cf. Best et al., 2016, *Trends in Hearing*, 20] in which the observer judges whether the answer to a question was correct or incorrect. In order to facilitate learning the reliability of the specific respondents answering questions, the observer first learned to identify the voices of the respondents and then listened to repeated Q&A exchanges so as to foster the development of expectations about the likelihood of a respondent answering questions correctly. In these Q&A exchanges, a questioner was masked at four target-to-masker ratios (TMRs) and two respondents were assigned either a low or high a priori probability of answering the question correctly. The observers were asked to determine whether the questions were answered correctly before and after they were informed that the respondents had different a priori probabilities of providing the correct response. The observer response patterns were analyzed within the framework of Signal Detection Theory and estimates of sensitivity and bias were obtained for all conditions. Preliminary results indicated that the observers were able to make use of expectations about talker reliability - especially at low TMRs - to enhance performance in speech-in-noise conditions.

PS 530

Electrophysiological and Behavioral Measures of Some Speech Contrasts in Attention Conditions and Noise

David Morris; John Tøndering
University of Copenhagen

The gain theory of attention, with complementary up and down regulation of neuronal populations according to their sensitivity to a target, is essentially a form of noise reduction. We probe the veracity of this by investigating the salience of speech contrasts in noise, in relation to how listening attention affects scalp-recorded cortical responses. The contrasts that were examined with consonant-vowel syllables, were place of articulation, vowel length and voice-onset time (VOT) and our analysis focuses on the correspondence between the effect of attention on the electrophysiology and the decrement in behavioral results when noise was added to the stimuli. Normal-hearing subjects (n=20) performed closed-set syllable identification in no noise, 0, 4 and 8 dB signal-noise ratio (SNR). Behavioral results showed that place of articulation was markedly affected by the introduction of noise while vowel length and VOT were not. The same syllables were

used in two electrophysiology conditions, where subjects attended to the stimuli, and also while their attention was diverted to a visual discrimination task. Differences in global field power between the attention conditions calculated for each contrast showed that the effect of attention was negligible for place of articulation, they implied offset encoding of vowel length and they were early (starting at 117 ms), and of high amplitude (>3 mV) for VOT. There were significant correlations between the difference in syllable identification in no noise and 0 dB SNR and electrophysiology results between attention conditions from the VOT contrast. Comparison of the two attention conditions with microstate analysis showed a significant difference in the duration of microstate class D. These results show differential integration of attention and syllable processing according to speech contrast and they suggest that there is an inverse correspondence between the salience of a contrast in noise and the effect of attention on the evoked electrical response.

PS 531

Effects of Listener Age, Masker Type and Cognitive Function on Discourse Comprehension and Intelligibility Performance

Jaclyn Schurman¹; Douglas S. Brungart²; Sandra Gordon-Salant³

¹*University of Maryland, College Park*; ²*Walter Reed National Military Medical Center*; ³*University of Maryland*

Background: Most auditory research is focused on measuring intelligibility in noisy environments, but the ability to comprehend a message is more relevant to daily communication. Listening comprehension is difficult to measure because it typically requires long trial times. However, preliminary results from our laboratory suggest that methods of self-selection where participants adjust parameters of spoken stimuli until they are just able to understand the meaning may allow for rapid evaluation of comprehension. This could make it more feasible to study comprehension, which is a complex process that requires listeners to interpret the meaning of an incoming message and integrate this message into memory. In a previous experiment, participants were asked to adjust the time-compression ratio of stories from the Discourse Comprehension Test (DCT) to the fastest rate at which they could still understand and answer questions. The results showed that both older and younger listeners naturally selected rates that differed across individuals, but resulted in consistent average comprehension scores near 80%. The current study expanded this paradigm to use signal-to-noise ratio (SNR) rather than speed to examine the effects of listener age, masker type and cognitive function on comprehension and intelligibility performance.

Methods: DCT stories were presented to older and younger listeners in the presence of speech shaped noise, cafeteria noise, or a single-talker masker and listeners self-selected an SNR for two stories in each masker condition. A comprehension score was measured for each story, and then intelligibility performance was measured at the selected SNR. Intelligibility stimuli were high-context and anomalous SPIN sentences and the Modified Rhyme Test (MRT). Cognitive domains of interest included working memory (RSPAN), speed of processing (Trail Making task), and attention (Flanker task).

Results: The results show that both age groups achieved similar performance levels on the comprehension task, however older listeners self-selected a higher SNR compared to younger listeners for all masker types. Results also suggest a relationship between cognitive function and self-selected SNR, implying that additional factors beyond age-related auditory declines may contribute to comprehension performance. The Trail Making task and the RSPAN showed the strongest relationship with the SNR required for comprehension, implying that working memory and speed of processing may influence listening comprehension.

Conclusions: The self-adjusted SNR outcome measure may be useful for evaluating performance in realistic listening scenarios where a listener's task requires the use of multiple cognitive resources to process speech beyond the level of intelligibility.

PS 532

Speech-In-Noise Recognition Is Predicted By Subcortical Envelope Representations In Younger And Older Adults

Carolyn M. McClaskey¹; James W. Dias¹; Kelly C. Harris²

¹Medical University of South Carolina; ²Medical University of South Carolina-Dept of Otolaryngology-Head & Neck Surgery

Accurate temporal processing is crucial for speech recognition, particularly in complex environments that require listeners to maintain robust representations of subtle envelope fluctuations. Such temporal representations depend on synchronous neural firing, and individual variation in neural synchrony is therefore thought to partially underlie individual differences in speech in noise perception. Temporal envelope processing can be assessed by measuring physiological responses to the modulation frequency of amplitude modulated sounds. Listeners with better temporal envelope processing have a more robust representation of the envelope and stronger neural synchrony even at shallow modulation depths. We hypothesize that the strength and synchrony

of subcortical temporal coding is predictive of listeners'; speech-in-noise perception.

Subcortical temporal coding was assessed by measuring envelope following responses (EFRs) elicited in response to amplitude modulated (AM) tones with modulation frequencies of 80 Hz and carrier frequencies of 3000 Hz. Stimuli had modulation depths of -8 dB, -4 dB, and 0 dB, measured as 20 log(m). Participants were 35 older (age 56-90+) and 22 younger (age 18-30) adults with clinically normal hearing to 3000 Hz. EFRs were analyzed in three ways. Autocorrelation coefficients quantified temporal regularity in the time domain, spectral power measured the strength of the response at the modulation frequency, and inter-trial phase coherence, or phase-locking value (PLV), indicated the consistency of the response phase across trials. Speech-in-noise perception was assessed using the QuickSIN speech tests. Regression analyses evaluated whether EFR metrics predicted speech-in-noise performance at low SNRs.

All EFR metrics decreased with decreasing modulation depth and QuickSIN scores decreased with decreasing SNR. Consistent with previous studies, there were no age group differences. EFR PLV at all three modulation depths predicted QuickSIN scores at 0 dB SNR. Autocorrelation coefficients and spectral power at the lowest modulation depth (-8 dB) predicted QuickSIN scores at SNR = 0 dB. These results indicate that EFR response strength and synchronicity in younger and older adults predicts speech-in-noise perception for low SNR conditions.

Here we show that individuals with better subcortical representations of envelope periodicity also exhibit better speech-in-noise perception. Previous research has suggested that the perception of amplitude modulated stimuli at high sound levels and shallow modulation depths, like those used here, reflects the contribution of high-threshold auditory nerve fibers that are important for speech-in-noise perception, and our results support this view.

Synaptopathy & Hidden Hearing Loss

PS 533

ROCK inhibitor Y-27632 accelerates auditory nerve fiber growth and synapse formation after excitotoxic trauma in organotypic culture of cochlea

Yutaka Koizumi; Tsukasa Ito; Seiji Kakehata
Yamagata University

Background

Sensorineural hearing loss (SNHL) has been shown to be caused by damage to inner ear hair cells which

causes auditory nerve degeneration. However, evidence is growing that SNHL may sometimes be the result of damage to auditory nerve fibers resulting in no neural pathways between the auditory nerve and hair cells. Thus SNHL could be caused by the breakdown of the synaptic pathways between the auditory nerve fibers and hair cells. The serine-threonine protein kinase, ROCK, has been reported to suppress nerve fiber elongation throughout the brain while ROCK inhibitors have been reported to promote blood flow, have a neuroprotective effect and regenerate synaptic pathways. Moreover, ROCK inhibitors have been reported to promote auditory nerve fiber elongation. We thus created an auditory nerve fiber damage model of the cochlea by using the glutamate agonists, NMDA and kainic acid, to induce in vitro excitotoxic trauma. The resulting culture was used to examine how the ROCK inhibitor, Y-27632, affected auditory nerve fiber and related synaptic pathway regeneration.

Methods

Cochlear tissues were isolated from newborn mice to investigate the effects of the ROCK inhibitor on the excitotoxic cochlea. Tissue samples were divided into three groups: a control group; a NMDA/kainic acid (NK) treatment group; and a ROCK inhibition group. The control group was cultured in a normal culture medium. The NK treatment group was incubated in a NMDA 0.5 mM + kainic acid 0.5 mM solution for 2 hours to impair the synapse between auditory nerve fibers and hair cells, followed by washing and culturing the samples in a normal culture medium. The ROCK inhibition group was incubated in the same NMDA/kainic acid solution, washed and then cultured in the same medium with the addition of 10 μ M Y-27632. The number of auditory nerve fibers and synapses were determined immunohistochemically for all three groups at 24- and 72-hours post-treatment.

Results

The ROCK inhibition group had a significantly higher number of both auditory nerve fibers projecting to hair cells and synapses between auditory nerve fibers and hair cells compared to the NK group.

Conclusions

The ROCK inhibitor Y-27632 appears to protect against auditory neuropathy and can be used to further investigate whether damage to auditory nerve fibers and their synaptic pathways can result in SNHL in the absence of or prior to damage to hair cells.

Funding

This work was supported by JSPS KAKENHI Grant Numbers JP17K16887, JP17K19713 and JP26861356.

PS 534

Experimental Study of Animal Model and Protection of Hidden Hearing Loss

Guowei Qi¹; Ning Yu²; Chi Zhang³; Yi-yong Hu³; Mian Zu⁴; Shi-ming Yang¹

¹PLA General Hospital; ²General hospital of Chinese PLA; ³General Hospital of Chinese PLA; ⁴Chinese PLA General Hospital

To explore the method of establishing animal model for hidden hearing loss, we use guinea pig as the experimental animal and impulse noise is adopted as the noise resource. Guinea pigs were exposed to 30 and 15 times of impulse noise and the auditory changes were analyzed to explore a suitable condition for hidden hearing loss animal model. At the same time, hydrogen was given to explore its preventive effect on hidden hearing loss.

Sixteen guinea pigs with normal ABR threshold were randomly divided into 4 groups: control group, impulse noise 30 times group, impulse noise 15 times group, hydrogen + impulse noise 15 times group. The peak of the impulse noise is 163 dB SPL, the pulse width is 0.25ms, and the interval is 6.5s. The auditory brainstem response was measured before and 24h after the impulse noise exposure.

Through statistical analysis, 24 hours after 30 times of impulse noise exposure, guinea pig's ABR threshold and the Tone Burst 16 kHz 70 dB I amplitude changed significantly. All of the auditory results of the 15 times groups occurred significant changes. The ABR threshold and the Tone Burst 16 kHz 70 dB I amplitude of the hydrogen group were statistically different from the 15 times group.

In this study, 30 times and 15 times of impulse noise exposures all had caused significant effects on guinea pigs' hearing. The auditory results of 15 times group accorded with the auditory characteristics of hidden hearing loss. 15 times of Impulsive noise exposure was a suitable condition for establishing an animal model of hidden hearing loss. In addition, the auditory results of hydrogen protection group is significantly different from the 15 times group, which indicating that hydrogen has a preventive effect on hidden hearing loss, and this provides a direct experimental basis for further molecular mechanism research.

PS 535

Detecting Metaplasticity after Cochlear Synaptopathy

Grace Szatkowski¹; Bethany Dade¹; John Hawks²; Christina Palomo¹; Jianxin Bao¹

¹Northeast Ohio Medical University; ²Gateway Biotechnology Inc.

Background

Recent studies have suggested that the cochlear synapse between inner hair cells and spiral ganglion neurons is the most sensitive structure to age-related or noise-induced damage. Although one type of cochlear synaptopathy, or hidden hearing loss (HHL), has been clearly demonstrated in various animal models, there are no conclusive data to prove its presence on humans. One critical obstacle is the lack of sensitivity and reliability of current electrophysiological methods for longitudinal human studies. In order to address this urgent issue, we have studied electrophysiological profiles specific for HHL in a mouse model. Identified profiles are then used to detect human HHL.

Methods

CBA/CaJ mice at 4 months old were randomly assigned to either control group (no noise) or noise-exposed group [96 dB sound pressure level (SPL), 8-16 kHz, 2 hours]. Auditory brainstem response (ABR) and distortion product otoacoustic emission (DPOAE) assays were performed before and two weeks after the noise exposure. Paired-click data were collected under two conditions: 1) a different level pair (DLP), 70 dB SPL (1st click) and 90 dB SPL (2nd click), and 2) the same level pair at 70 or 90 dB SPL. Similar paired clicks were performed for human electrocochleography (ECochG) analysis in order to detect age-related or noise-induced human cochlear synaptopathy.

Results

HHL was verified by a significant reduction in wave I amplitude at 20 and 40 kHz in the noise-exposed group. A detailed analysis of amplitude, latency, and inter-wave interval (IWI) for ABR waves I-III was subsequently performed. Analysis of variance (ANOVA) revealed a significant two-way interaction (group x day) of DLP responses from the noise-exposed group. Specifically, for the first click, our analyses showed significant longer latencies of wave I ($p=0.018$) and IWI of waves II-III ($p=0.043$), and a significant reduction in amplitude of wave II ($p=0.047$). For the second click, the amplitudes of waves II and III were significantly reduced ($p=0.001$, $p=0.003$, respectively), and the IWI of waves II-III also was significantly longer ($p=0.047$).

Conclusion

We have identified new electrophysiological profiles sensitive to cochlear synaptopathy with a well-established HHL animal model. These profiles provide new ways to analyze ECochG data, which can be more sensitive and reliable to detect HHL in human participants.

PS 536

Modified versions of NT-3 enable enhanced activation of TrkB and TrkC responses in ex vivo models relevant to cochlear synaptopathy

Stephanie Szobota¹; Pranav D. Mathur¹; Sairey Siegel¹; Fouad Brahimi²; H. Uri Saragovi²; Alan C. Foster¹

¹Otonomy, Inc.; ²Lady Davis Institute-Jewish General Hospital, McGill University

Background: Several forms of hearing loss are attributed to the destruction of spiral ganglion neurons or their synaptic connections to the hair cells of the inner ear. In particular, cochlear synaptopathy can contribute to “speech-in-noise” difficulties that may underlie hidden hearing loss in humans. Animal studies have suggested that treatment with the neurotrophins BDNF and NT-3 can reverse this damage through selective activation of their cognate receptors, TrkB and TrkC. NT-3 is known to also activate TrkB, but with lower potency than BDNF. The goal of this research effort was to explore “multifunctional” versions of NT-3 that have been mutated to enhance agonist activity at TrkB receptors as well as diminish activation of p75.

Methods: The binding characteristics of NT-3 and several modified versions of NT-3 (mNT-3s) were evaluated by FACS using an indirect competition assay to biotinylated NT-3. Functional activity was assessed by measuring several downstream effectors, including phosphorylated ERK and AKT, using Western Blot, AlphaLISA, and qPCR in stable cell lines that express Trk receptors. The ability of the mNT-3s to stimulate survival was tested by MTT assays, and the ability to drive differentiation was assessed with PC12/nnr5 cells expressing TrkC and p75. The effectiveness of mNT-3s to activate native cochlear TrkB and TrkC was evaluated in several ex vivo cochlear cultures obtained from postnatal Sprague Dawley rats, and included measures of SGN survival, neurite outgrowth, and synaptogenesis.

Results: The mNT-3s had enhanced binding and activation of TrkB and TrkC, with greater potency than wild-type NT-3. A reduction in binding to p75 for certain mNT-3s was confirmed. The mutants promoted proliferation and differentiation of PC12/nnr5 cells that express TrkC and p75 to a greater degree than wild-type NT-3. Treatment with mNT-3s improved survival of dissociated spiral ganglion neuron cultures and induced neurite outgrowth and synaptogenesis in ex vivo cochlear cultures.

Conclusions: The multifunctional versions of NT-3 evaluated are potent activators of TrkB and TrkC

signaling in cell-based assays and are effective in ex vivo models relevant to cochlear synaptopathy. These molecules warrant further investigation to assess their potential effects in animal models of hidden hearing loss.

PS 537

Hidden Hearing Loss in Human Temporal Bones: Deafferentation of Surviving Inner Hair Cells in the Aging Ear

Peizhe Wu¹; Leslie Liberman¹; Jennifer T. O'Malley¹; M. Charles Liberman²

¹Dept. of Otolaryngology, Mass. Eye and Ear; ²Mass. Eye and Ear Infirmary

In noise-damaged or aging animal ears, synapses between inner hair cells (IHCs) and auditory-nerve fibers (ANFs) are lost before hair cells degenerate. This cochlear synaptopathy does not elevate thresholds, but likely impairs performance on complex listening tasks. In animals, the phenomenon can be quantified via post-mortem synaptic counts, and can be diagnosed via suprathreshold ABR amplitudes, so long as the thresholds remain normal. In humans, the prevalence of cochlear synaptopathy is controversial, as some studies find association between electrophysiology and hearing, while others don't.

Here, we assess primary neural degeneration in aging or noise-exposed humans by counting hair cells and ANF peripheral axons in cochlear wholemounts from autopsy specimens or in sections from the Mass. Eye and Ear archive. We analyzed wholemounts from 22 normal-aging cases (0 - 86 yrs) and retrieved sections from 61 archival cases including 31 with a noise-exposure history and 30 age-matched controls (50 - 96 yrs) with audiometric thresholds within age-adjusted limits. For wholemounts, the temporal bone was drilled decalcified, microdissected and immunostained for 1) myosin VI/VIIa (hair cells), 2) CtBP2 (synaptic ribbons), 3) NF-H (nerve fibers) and stained with Cellmask® to highlight myelin. Hair cells and nerve fibers were counted at 14 log-frequency spaced locations. For archival material, we selected tangential sections through the IHCs and adjacent osseous spiral lamina from each half turn, and used a combination of H&E, Cellmask and/or Myosin VI/VIIa to count hair cells and peripheral axons. Cytocochleograms were also derived from the full archival section set in each case.

Loss of IHCs and OHCs in normal aging showed slopes of 3% and 4% per decade, respectively, similar to age-related loss of spiral ganglion cells (SGCs) seen in a prior human study (Makary et al. 2011, JARO 12:711). In contrast, loss of ANF peripheral axons was 2 - 3 times

steeper. Thus, by 60 yrs, ~50% of surviving SGCs were disconnected from their IHC targets. Cases with an acoustic trauma diagnosis showed even greater primary neural degeneration. In the archival material, hair cell losses were correlated with audiometric threshold, and word-recognition scores were correlated with ANF survival.

Thus, the primary neural degeneration seen in animal studies is also significant in humans. However, most of the older subjects studied here had measurable threshold shift, thus the extent of deafferentation of surviving IHCs in humans with normal audiograms remains unknown.

Research supported by the NIDCD (P50 DC015857).

PS 538

Virally-mediated NT3 Overexpression Minimizes Noise-induced Cochlear Synaptopathy

Ken Hashimoto¹; Tyler Hickman²; Lingchao Ji³; Gabriel Corfas⁴; M. Charles Liberman⁵

¹Dept. of Otolaryngology, Harvard Medical School;

²Dept. of Otolaryngology, Mass. Eye and Ear; ³Dept. of Otolaryngology, Head and Neck Surgery, University of Michigan; ⁴Dept. of Otolaryngology Head and Neck Surgery, University of Michigan; ⁵Mass. Eye and Ear Infirmary

Noise exposures causing only temporary threshold shifts can cause permanent loss of auditory-nerve synaptic connections without loss of inner or outer hair cells, and synapses are lost before hair cells in the aging ear. Standard threshold measures are insensitive to this cochlear synaptopathy, but loss of synapses must impair more complex hearing tasks. Here, we asked whether forced overexpression of NT3 via local virus delivery can minimize noise-induced synaptopathy.

CBA/CaJ mice at 6 wks were injected unilaterally via the posterior semicircular canal, 3 wks prior to noise exposure (8-16 kHz, 99 dB, 2 hrs), with an Anc80 adeno-associated virus containing either the NT3 or GFP gene, with a CMV promoter. Controls included exposed animals receiving vehicle-only injections, as well as unexposed animals receiving NT3- or GFP-expressing virus. 2-5 wks post exposure, ABR and DPOAE thresholds were measured, and cochleas were harvested for histological analysis of hair cell loss and synaptopathy via confocal analysis of wholemounts immunostained for myosin, NFH, CtBP2 and GluA2. In a separate set of virus-injected animals, cochleas were extracted for qRT-PCR analysis of NT3 expression.

Results with the GFP reporter showed that AAV virus transduced virtually all inner hair cells (IHCs) throughout

the cochlea, and many outer hair cells (OHCs), especially in the apical cochlea. qRT-PCR results with the NT3-containing virus showed significant overexpression of NT3 (mean increases from 3-6 fold), at sampling times from 1 - 21 days post-injection, with expression levels remaining 2-fold above baseline at 40 days post-injection. Injection of the NT3 virus produced a dose-dependent reduction of synaptopathy, with the highest injection volume (1000 nL) providing almost complete protection at some cochlear locations. There was no evidence of ectopic neurite extension in any of the virally transduced ears, and, in unexposed ears, cochlear thresholds were unaffected by the AAV-NT3 injections. However, forced GFP overexpression led to significant IHC loss in all unexposed ears when examined 5 wks post-injection, and forced NT3 overexpression led to significantly higher (>20 dB) noise-induced permanent threshold shifts in more than half of the injected ears.

Thus, although overexpression of neurotrophins can be beneficial in protecting the afferent synapses, or in stimulating their recovery, from noise, the forced overexpression of gene products may be harmful to hair cells during subsequent cochlear stresses.

Research supported by grants from NIDCD (R01 DC000188 and R01 DC004820) and the Lauer Tinnitus Center.

PS 539

Effects of Noise Exposure on Young Adults with Normal Audiometric Thresholds

Hannah Guest¹; Garreth Prendergast¹; Samuel Couth¹; Rebecca Dewey²; Karolina Kluk¹; Rebecca E. Millman³; Kevin Munro⁴; Deborah Hall⁵; Susan Francis²; Christopher J. Plack¹

¹Manchester Centre for Audiology and Deafness; ²Sir Peter Mansfield Imaging Centre; ³Manchester Centre for Audiology and Deafness, NIHR Manchester Biomedical Research Centre; ⁴The University of Manchester; ⁵University of Nottingham, and NIHR Nottingham BRC

Background

Noise exposure can destroy synapses between inner hair cells and auditory nerve (AN) fibres, without widespread loss of hair cells or elevation of cochlear thresholds (Kujawa and Liberman, 2009). Termed 'cochlear synaptopathy', this pathophysiology has been observed in a variety of animal models and has been suggested as a possible cause of listening difficulties and tinnitus (Kujawa and Liberman, 2015). Here, we summarise the results of five research projects designed to investigate

possible physiological and perceptual consequences of noise exposure in humans with normal audiograms.

Methods

All five projects recruited audiometrically normal adults aged between 18 and 40. Each involved a detailed self-report estimate of lifetime noise exposure (to activities with estimated sound level >80 dBA) and a measure of AN function: the amplitude of wave I of the auditory brainstem response. Other measures included envelope-following-response amplitude (used in two projects), middle-ear-muscle-reflex thresholds (one project), a measure of spatial speech perception in noise (three projects), a wide range of psychoacoustic measures (one project), and functional magnetic resonance imaging (fMRI; one project).

Results

Across all studies, no significant relations were observed between lifetime noise exposure and physiological measures of auditory nerve function, despite a wide range of exposures. Nor did lifetime noise exposure relate to behavioural measures, nor to changes in the central auditory pathways, as assessed via fMRI. Presence of tinnitus was, however, significantly associated with lifetime noise exposure, despite close audiometric matching between participants with tinnitus and controls.

Conclusion

The summarised research reveals no evidence for noise-induced cochlear synaptopathy in young humans with normal audiograms. Potential explanations, which are not mutually exclusive, include the possibility that all outcome measures are insufficiently sensitive to synaptopathy (results of animal models notwithstanding), that human cochlear synapses are far more resilient than those of animals, and that synaptopathy is prevalent in humans only in combination with audiometric hearing loss. It does appear that noise has the capacity to induce 'hidden'; auditory changes leading to tinnitus in individuals with entirely normal audiograms, but we find no evidence to suggest that cochlear synaptopathy is one of them.

Acknowledgements

This research was funded by the Medical Research Council UK (MR/L003589/1) and supported by the NIHR Manchester Biomedical Research Centre.

References

Kujawa, S.G. & Liberman, M.C. (2009). *Journal of Neuroscience*, 29, 14077–14085.

Kujawa, S.G. & Liberman, M.C. (2015). *Hearing Research*, 330, 191–199.

PS 540

Mapk14 deletion reduces noise-induced hearing loss

Lourdes Rodríguez-de la Rosa¹; Silvia Murillo-Cuesta¹; Ángela García-Mato²; **Isabel Varela-Nieto¹**
¹IIBM CSIC-UAM, CIBERER, IDIPAZ; ²IIBM CSIC-UAM

P38 mitogen-activated protein (MAP) kinases p38 α , β , γ and δ are codified by Mapk14, 11, 12 and 13 genes, respectively. P38 kinases are activated by phosphorylation in response to a variety of extracellular stress stimuli that transduce to the nuclei. The MAPK14 (p38a) isoform is ubiquitously expressed and is critical for mammalian embryonic development. MAPK14 participates in the cochlear response to stressors like cisplatin, UV radiation or noise exposure (1-3). MAPK14 expression and activity also increase as a consequence of Igf1 deletion in mice in association with hearing loss and cellular apoptosis (4).

We have studied the expression pattern of the four p38 isoforms along ageing in wild type and knock out Igf1 null mice, to show that they are age- and IGF-1- regulated.

To further explore the role of Mapk14 in the cochlea, we have studied the Mapk14lox/loxRERTnERT/ERT conditional knock out mouse (5) and cell lines derived from embryonic fibroblasts. Mapk14 knock out mice auditory brainstem responses (ABR) recording showed that ABR thresholds do not vary upon Mapk14 deletion induced by tamoxifen treatment. RT-qPCR gene expression studies of the p38 isoforms indicated that other isoforms are induced and maybe taking over MAPK14 cochlear functions. P38 isoforms relative expression levels also varied in Mapk14-knock out fibroblasts, as well as the transcripts for MEF2, FoxM1 and FoxG1, which are also altered in the cochlea of Igf1-null mice (4).

Finally, we assessed the response to noise-induced injury in Cre/loxP Mapk14 knock out mice before and after noise exposure. Interestingly, mice with total or partial deletion of Mapk14 exposed to violet noise at an intensity of 105 dB SPL during 30 minutes showed a better recovery of hearing thresholds than wild type mice.

These data suggest that MAPK14 plays a central role in the progression of cochlear damage after noise exposure.

Research was supported by Spanish MINECO/FEDER-SAF2017-86107-R and EU FP7-PEOPLE-TARGEAR grants to IV-N. LRR and SMC hold CIBERER contracts. AGM holds a MECDFPU fellowship. We warmly thank Drs. Ana Cuenda (CNB, CSIC), M. Carmen Guerrero (CIC, CSIC) and Almudena Porras (UCM) for their support and comments.

References 1: Kaur T et al. *J Neurosci*. 2016;36(14):3962-77. 2: Shin YS et al. *Neurotoxicology*. 2014;40:111-22. 3: Maeda Y et al. *PLoS One*. 2013;8(3):e58775; 4: Sanchez-Calderon H et al. *PLoS One*. 2010;5(1):e8699; 5: Ventura JJ et al. *Nat Genet*. 2007 Jun;39(6):750-8.

PS 541

Protection of Noise-induced Cochlear Synaptopathy by Systemic Administration of a Selective CP-AMPR Antagonist

Ning Hu; Steven H. Green
The University of Iowa

Research background

Animal experiments have shown that moderate noise exposure, even at levels too low to destroy hair cells, can damage cochlear synapses. In these animal models, such noise-induced cochlear synaptopathy (NICS) can be noninvasively detected by auditory brainstem response (ABR), as a decline in wave I amplitude, and histologically measured by counting synapses on inner hair cells (IHCs). We have shown that NICS is a consequence of excessive glutamate release from overstimulated IHCs (“excitotoxicity”) and Ca²⁺ influx into the postsynaptic bouton largely via Ca²⁺ permeable AMPA receptors (CP-AMPRs) (Hu et al, ARO-2013), and can be mitigated in mice by intracochlear perfusion of IEM-1460, a CP-AMPR blocker (Hu et al, ARO-2015). Here we ask whether systemic administration of IEM-1460 can protect NICS.

Methods

The maximum safe dose of IEM-1460 was determined at ~12 mg/kg. IEM-1460 in saline was injected intraperitoneally into male and female CBA/CaJ mice. Time-lapse ABRs were measured for 1-2 hours after IEM-1460 injection to determine whether it affects normal hearing. To determine effects on NICS, 12-14 week-old mice were exposed to 100 dB SPL 8-16 kHz octave band noise for 2-hrs. Two doses of IEM-

1460 (12 mg/Kg/dose) were given: 10-min prior to and 1-hr after noise onset. Controls received saline injections. ABRs were measured at 8, 16, and 32 kHz prior to noise, one day postnoise (PND1) and PND14 to obtain measures of baseline, temporary threshold shift (TTS), and threshold recovery in a within-subject design, respectively. Postsynaptic densities, presynaptic ribbons, and HCs were visualized, respectively, with anti-PSD95, anti-Ribeye/CTBP2, and anti-myosin antibodies for quantitation of synapses/IHC by PND14 in organ of Corti wholemounts at 8, 16 and 32 kHz locations.

Results

IEM-1460 administration itself did not cause changes in ABR threshold and wave I amplitude. IEM-treated mice did show reduced TTS and smaller reduction of ABR wave I amplitude on PND1. By PND14, ABR amplitude in IEM-treated recovered nearly to prenoise levels. Correspondingly, cochlear synapse counts in IEM-treated mice are close to those in non-noise-exposed control mice and significantly greater than in saline-injected noise-exposed mice. Consistent with our report that NICS in females is influenced by the estrous cycle (Hu et al, ARO-2017), the protective effect of IEM-1460 was constant in males but varied in females.

Conclusions

Systemic administration of IEM-1460 to selectively block CP-AMPA in cochlear synapse does not affect the normal peripheral hearing, but can protect against NICS. This suggests CP-AMPA blockade is an effective therapeutic to protect NICS.

PS 542

Round-window delivery of lithium chloride using P407 regenerates cochlear synapses after acoustic overexposure

Nathaniel Carpena¹; Jae-Hun Lee²; So-Young Chang²; Min Young Lee¹; Jae Yun Jung¹; Ji Eun Choi¹

¹Department of Otorhinolaryngology-Head & Neck Surgery, College of Medicine, Dankook University;

²Beckman Laser Institute Korea, College of Medicine, Dankook University,

Background:

Hearing loss in humans is often caused by acoustic overexposure from loud noises or ototoxicity from certain drugs and is usually reflected as an elevated hearing threshold. However, a certain degree of acoustic overexposure can cause hearing problems without the permanent change of hearing threshold. Cochlear

synaptopathy happens when the communication between the sensory inner ear hair cells and cochlear nerve fibers are permanently interrupted which manifests as difficulty in speech perception in noise and temporal processing. Meanwhile, recent studies show that lithium exerts a neuroprotective effect from diverse insults via multiple signaling pathways. Two key factors to this effect of lithium involves the; inhibition of GSK-3 reducing cell death due to excitatory neurotransmission; and the downregulation of NMDA receptor reducing oxidative stress and protecting against glutamate induced excitotoxicity. Thus, the aim of this study was to evaluate the therapeutic effect of lithium on noise-induced neurodegeneration.

Materials and Methods:

In this study, we showed the round-window delivery of low and high-doses of lithium chloride using P407 in noise-exposed rats and compared to confirmed transient threshold shift (TTS) model as well as sham OP. Tone-burst ABR was done for baseline and 3, 7 and 14 days after noise exposure. Cochleae from rats at 7 and 14 days after noise exposure were also harvested and examined as whole-mounts stained for MyosinVIIa and CtBp2.

Results:

Results showed faster recovery in hearing threshold in both low and high dose of lithium chloride treated rats compared to the sham OP group. This functional recovery is also seen in the suprathreshold amplitude of auditory brainstem response Wave 1. Immunostaining showed the regeneration of synapses at the hair cell / cochlear nerve interface.

Conclusions:

Cochlear delivery of lithium chloride demonstrated in the present study may play an important beneficial role in its therapeutic actions in acquired hearing loss due to noise exposure. Further work is needed to determine the specific pathway responsible for this effect of lithium in hearing recovery.

Acknowledgment:

This study was supported by a grant from the Basic Science Research Program through the National Research Foundation (NRF) of Korea funded by the Ministry of Science, ICT, & Future Planning (NRF-2015R1C1A1A01052624), and supported by Leading Foreign Research Institute Recruitment Program through the National Research Foundation of Korea (NRF) funded by the Ministry of Science and ICT (MSIT) (NRF-2018K1A4A3A02060572). The program had no further role in the study design, collection, analysis, or interpretation of data; in the writing of the report; or in the decision to submit the paper for publication.

PS 543

AC102 in the Treatment of Functional Hearing Loss and Synaptopathy in a Guinea Pig Model of Noise-Induced Hearing Loss

Hans Rommelspacher¹; Florian Theden¹; Rachael E. Ward¹; Tomasz Zygmunt¹; Reimar Schlingensiepen²
¹AudioCure Pharma GmbH; ²AudioCure GmbH

Background

Over recent years it has become increasingly evident that sensorineural hearing loss (SNHL) involves both the loss of intact synapses between the sensory inner hair cells (IHCs) and the auditory pathway as well as the apoptotic loss of outer hair cells (OHCs). AC102 is a small, lipophilic molecule developed to address these pathophysiological mechanisms underlying SNHL.

Methods

All in vivoproof of principle studies were performed in a well-established guinea pig model of noise-induced hearing loss (NIHL: 118dB, quarter octave band centered at 8kHz for 1h). 10 μ L of AC102 formulated in a thermosensitive hydrogel were administered to the round window niche 1, 24, 48 or 72h after acoustic trauma. Permanent threshold shifts (PTS) were assessed by BERA 14 days following trauma. Cochleae were processed for visualization of OHCs and ribbon synapses. In pharmacokinetic studies, apical perilymph was sampled after i.t. AC102 administration and analyzed by fluorescence HPLC.

Results

Treatment 1 h after the trauma with i.t. AC102 resulted in a significant reduction in PTS compared to vehicle-treated controls. In these animals, AC102 also significantly protected against the noise-induced loss of OHCs throughout the cochlea observed at 14 days after trauma. Importantly, AC102 improved ABR thresholds when dosed up to 48h after acoustic trauma while significantly enhanced ribbon synapse survival was observed when treatment was delayed until 72h. Following i.t. administration, AC102 shows rapid entry into the perilymph (t_{max}0.5h) and was detected within the inner ear for at least 24h after dosing.

Conclusions

Taken together, these findings demonstrate the functional efficacy of AC102 in an animal model of NIHL resulting in a clinically relevant improvement in ABR threshold. This functional effect is likely to be linked to the protective effect of AC102 on OHCs. Moreover, the ability of AC102 to reverse synaptopathy suggests that

AC102 protects against hidden hearing loss (HHL) which is of great importance for speech perception. Finally, the wide treatment window (\leq 72h) for AC102 in this model indicates these effects may be successfully translatable into the clinical environment. Based on proof of principle and safety studies, clinical trial planning and regulatory interactions are underway for First in Human clinical trials in sudden SNHL (SSNHL).

PS 544

Inner Hair Cell Synaptic Changes upon Noise Exposure

Mattia Nova¹; Ursula Stalman²; Philippe Jean¹; Nicola Strenzke²; **Tina Pangrsic**¹

¹Institute for Auditory Neuroscience, University Medical School Goettingen; ²University Medical School Goettingen, Dept. for Otolaryngology

Recent studies in animal models exposed to moderate levels of noise described a form of hearing loss with only temporary increase in the auditory thresholds, but permanently reduced suprathreshold amplitudes of the compound action potential of the spiral ganglion. The mechanisms underlying this form of hearing impairment include a loss of synaptic contacts between the inner hair cells (IHCs) and the auditory nerve fibers with both, pre- and postsynaptic damage, followed by late degeneration of auditory nerve fibers. While work has been done to describe the functional manifestations of this cochlear synaptopathy, the underlying mechanisms are not yet well understood. We employed systems physiology, patch-clamp recordings, and immunohistochemistry to investigate changes in the IHC presynaptic structure and function. In agreement with previous studies, immunohistochemistry, as well as direct labeling of synaptic ribbons, revealed a partial loss that persisted after noise exposure. In the absence of otoferlin, required for IHC synaptic transmission, no noise-induced loss of ribbons was detected. Immunostaining of calcium channels and patch-clamp recordings revealed noise-evoked changes in the brightness of immunofluorescent spots and whole-cell calcium currents, indicating an alteration in the presynaptic calcium channel clusters. Patch-clamp recordings further showed changes in IHC exocytosis.

PS 545

Cochlear Synaptic Loss after Gaussian and Non-Gaussian Noise Exposure

Dan Guo¹; Mo Chen²; Wei Qiu³; Sharon G. Kujawa⁴

¹Department of Medicine and Scientific Research, Henan Medical College (current); ²Department of Otolaryngology, Harvard Medical School and Eaton-

Peabody Laboratories, Mass Eye and Ear; ³Auditory Research Laboratory, State University of New York at Plattsburgh; ⁴Department of Otolaryngology, Harvard Medical School and Eaton-Peabody Laboratories, Massachusetts Eye & Ear Infirmary

Background: Prior work shows that noise exposures with non-Gaussian energy distributions can yield greater threshold sensitivity and hair cell losses than energy-equivalent Gaussian noise (Hamernik and Qiu, 2001). Although these are important metrics of noise injury, recent work has shown that widespread cochlear afferent synapse loss can be present with or without persistent noise-induced threshold shifts or hair cell loss (Kujawa and Liberman, 2009). To date, cochlear synaptopathy has been studied most extensively using a noise exposure model with Gaussian noise-induced injury. As human noise exposures are often non-Gaussian in nature, we extend our consideration of cochlear physiologic and histologic consequences of noise by quantifying cochlear synapses in Gaussian and non-Gaussian noise-exposed animals with and without permanent threshold shifts (PTS).

Methods: Adult CBA/CaJ mice were exposed to Gaussian or non-Gaussian noise (8-16kHz, 2hr, 100 or 106dB). Non-Gaussian noises were created with impulses embedded in the noise signal and these differed in the degree of kurtosis ($k=25-75$) this produced. A Gaussian noise was created and delivered at equal overall energy. Animals were held, with unexposed controls, for 24h or 2wks after exposure. DPOAE and ABR thresholds and amplitudes were then quantified and hair cell and synaptic counts were made in immunostained cochlear whole mounts at log-spaced frequencies, 5.6-64kHz.

Results: Gaussian noise (100dB) produced ~45dB threshold elevations at 24h, with no PTS at 2wks, and a ~50% synapse loss in the 20-30kHz region, without hair cell loss. Acute threshold shifts for energy-matched, non-Gaussian noise varied with the level of kurtosis and at 2wks, small PTS remained for high-kurtosis exposure. Synaptic losses were small compared to those for Gaussian exposure.

For the higher-level exposure (106dB), threshold shifts at 24h were large in all animals; they extended across a broader range of frequencies and were largest for non-Gaussian noise with higher kurtosis. All 106dB exposures resulted in PTS without significant hair cell loss. Patterns of synaptic loss differed for Gaussian and non-Gaussian exposures, with Gaussian noise producing the largely basal turn lesion seen at 100dB, and the equal-energy non-Gaussian exposures producing kurtosis-graded synaptic loss over an extended frequency range.

Conclusions: Noise damage in humans may take many forms, and consequences may differ for exposures with varying temporal properties. Results suggest that the kurtosis of noise exposure is a significant variable influencing noise risk.

Work supported by the Department of Defense, the Department of Medicine, Henan Medical College and the Office of China Postdoctoral Council.

PS 546

Noise-Induced Cochlear Synaptopathy in Inbred Strains of Mice

Anbuselvan Dharmarajan¹; Ulysse Puel²; Sharon G. Kujawa¹

¹Department of Otolaryngology, Harvard Medical School and Eaton-Peabody Laboratories, Massachusetts Eye & Ear Infirmary; ²School of Medicine, Montpellier University

Background. Large differences in the vulnerability of individuals to noise-induced hearing loss have been reported within various outbred species, including human (Kujawa, 2016). In contrast, individual differences in noise vulnerability within inbred strains of mice are small, but can be large between inbred strains. These robust phenotypes have been exploited in studies aiming to reveal mechanisms and inform future treatments. In our previous work, characterization of these noise vulnerability phenotypes focused on the magnitude of the acute and chronic threshold shifts resulting from exposure. This work has not considered a recently described consequence of noise, the loss of synapses between inner hair cells (IHCs) and cochlear neurons (Kujawa & Liberman, 2009). Here, we studied synaptopathic consequences of noise exposure in several inbred strains of mice with varying noise vulnerabilities.

Methods. Mice from a noise-resistant inbred strain (MOLF/EiJ) and from 2 comparatively noise-vulnerable strains (CBA/CaJ, C57BL/6J) were noise exposed (8-16kHz, 2hr, 97dB SPL) at 6 weeks, when baseline threshold differences are small and restricted to highest frequencies. Animals were then held with unexposed, age-matched controls for 24h or 2wk. At the relevant post-exposure time, cochlear function was characterized via distortion product otoacoustic emission (DPOAE) and auditory brainstem response (ABR) thresholds and suprathreshold growth. Immunostained cochlear whole mounts from the same animals were studied to quantify hair cells (MyoVIIa), pre-synaptic ribbons (CtBP2) and post-synaptic glutamate receptor patches (GluA2) across a broad range of cochlear frequencies (5.6-64

kHz).

Results. At baseline, threshold sensitivity and suprathreshold response magnitude differences among the strains were minor and restricted to C57BL/6J response declines at frequencies >32kHz. After exposure, vulnerability differences among these strains were seen as differences in the magnitude, and to some extent the pattern, of threshold shifts and suprathreshold amplitude declines at 24h and the degree to which they recovered by 2wk. There was no IHC loss, but C57BL/6J showed OHC losses in both unexposed and exposed animals at basal turn frequencies. Differences in synapse counts among control groups were small and losses after exposure (~50% in the base) did not emerge as an important variable for this exposure to young mice.

Conclusions. Differences in genetic makeup are presumed to play a role shaping individual differences in noise vulnerability. Large inter-strain differences in threshold sensitivity and hair cell losses with apparently small differences in synapse losses have important implications for diagnosis and treatment of noise-induced hearing loss.

Supported by Office of Naval Research Grant N00014-16-1-2867.

PS 547

Enhanced Resilience to Noise-Induced Hearing Loss in Mice Lacking the Vesicular Zinc Transporter ZnT3

Brandon Bizup¹; Amantha Thathiah²; Thanos Tzounopoulos¹

¹Pittsburgh Hearing Research Center, Department of Otolaryngology, University of Pittsburgh; ²University of Pittsburgh, Department of Neurobiology and Pittsburgh Hearing Research Center, Department of Otolaryngology, University of Pittsburgh

Exposure to loud noise results in a degenerative cascade in the peripheral auditory nervous system, with damage ranging from synaptic loss and delayed ganglion neuron degeneration to death of hair cells and damage to sensory membranes, depending on the severity of the noise insult. While our understanding of these processes has continued to improve, treatment strategies to restore hearing after noise-induced hearing loss (NIHL) have remained few and insufficient.

Zinc has been implicated in neurodegeneration, yet little is known regarding its role in NIHL in the cochlea. ZnT3-dependent (synaptic zinc) is mobilized to trigger diverse

signaling pathways in cases of excitotoxicity and other types of nervous system damage. ZnT3 is expressed in the cochlea, particularly in spiral ganglion cells. To test whether ZnT3 is important in normal hearing, resilience and recovery from NIHL, we evoked auditory brainstem responses (ABRs) to measure ABR thresholds and wave 1 amplitudes in ZnT3 knockout (KO) and wild-type (WT) mice before and after noise exposure. Whereas before noise exposure ABR thresholds and wave 1 amplitudes were not different between WT and KO mice, after noise exposure, ZnT3 KO mice displayed less elevated ABR thresholds and larger wave 1 amplitudes compared to WT mice. Additionally, ZnT3 KO mice recovered to baseline ABR thresholds sooner than WT mice after noise exposure and maintained baseline wave 1 amplitudes following noise exposure. These results suggest that ZnT3, possibly via zinc signaling, contributes to vulnerability to NIHL.

PS 548

Distribution of Ribbon Synapses Correlated with Hearing Decline after a Single Dose of Ototoxic Injury

Liana Sargsyan; Alisa Hetrick; Weiwei He; Glen K. Martin; Hongzhe Li
VA Loma Linda Healthcare System

Background: It is established that a correlation exists between the wave-I ABR amplitude and the count of ribbon synapses in age-related and/or noise-induced hearing loss. Here, we studied the dose dependent effect of gentamicin and furosemide in combination, to 1) characterize the residual hearing function, 2) distinguish the morphology of outer and inner hair cells (IHCs), and ribbon synapses at various cochlear locations, and 3) determine whether there is change of the number, or the distribution, of synaptic ribbons.

Methods: Mice were intraperitoneally injected with either a low dose (25, 50 and 100 mg/kg) or a high dose (200, 400 mg/kg) of gentamicin followed by furosemide (200 mg/kg) after 30 minutes. All the mice underwent distortion product otoacoustic emissions (DPOAE) and auditory brainstem response (ABR) tests prior to and at several post-treatment time points. Seven days after the treatment, cochleae were micro-dissected, immunolabelled with anti-CtBP2 antibodies and phalloidin. Cochlear segments were observed at 8, 12 and 16 kHz locations by confocal microscopy.

Results: Compared to the pre-exposure level, combined single dose treatment temporarily produced mild elevation of ABR thresholds on the 3rd day and

recovered by the 7th day. The ototoxic treatment also resulted in a reduction of the ABR wave-I amplitude at 8 and 12 kHz. Normal DPOAE amplitudes were observed post-exposure, suggesting functional OHCs. CtBP2 antibodies immunolabelled the nuclei and synaptic ribbons of hair cells. No loss of IHCs was observed, and the number of ribbons remained unchanged in the treatment group. Instead, the confocal analyses indicated larger ribbon size, with marked integral density at 8 and 12 kHz frequency locations, while immunofluorescence signal intensity was equivalent at these locations compared to the control group. At the 16 kHz frequency location, treated cochleae presented weaker immunofluorescence signal and neither ribbon area size nor integral density were altered. Remarkably, the distribution of ribbons that were referenced axially to the IHC nuclei, was gentamicin dosage dependent which was confirmed by histogram displays.

Conclusions: Preliminary results suggested morphological alterations of synaptic ribbons in terms of ribbon size and fluorescence signal, and a correlation between the wave-I ABR amplitude and the distribution of ribbon synapses one week after medication exposure. These observations in total indicated that the reduction of wave-I ABR amplitude does not necessarily imply a reduction of the number of synaptic ribbons, as suggested in noise-induced and/or age-related hidden hearing loss.

Age-Related Hearing Loss and Cognitive Decline

Chairs: Paul Delano & Anu Sharma

SYMP 26

Hearing Loss, Cognition, & Dementia - Insights from Epidemiology

Frank R. Lin

*Department of Otolaryngology - Head & Neck Surgery,
Johns Hopkins School of Medicine, Baltimore, MD,
USA*

Age-related hearing loss in older adults is often perceived as being an unfortunate but relatively inconsequential part of aging. However, the broader implications of hearing loss for the health and functioning of older adults are now beginning to surface in epidemiologic studies. I will discuss recent epidemiologic research demonstrating

that hearing loss is independently associated with accelerated cognitive decline, incident dementia, and brain aging. Current studies to investigate the impact of hearing rehabilitative interventions on reducing cognitive decline and the risk of dementia in older adults will be discussed.

SYMP 27

Cortical Neuroplasticity in Age-Related Hearing Loss

Anu Sharma

University of Colorado at Boulder

A basic tenet of neuroplasticity is that the brain will re-organize following sensory deprivation. Compensation for the deleterious effects of hearing loss include alterations in cortical functional dynamics such as engagement of additional or alternative cortical networks to for listening to degraded auditory input. Our high-density EEG experiments suggest that age-related hearing loss results in significant changes in neural resource allocation, reflecting patterns of increased listening effort which may be associated with increased cognitive load in age-related hearing loss. Cross-modal plasticity is another form of cortical re-organization associated with hearing loss. Cross-modal plasticity occurs when an intact sensory modality recruits and repurposes cortical resources from a deprived sensory modality. Deaf animals show recruitment of higher-order auditory cortical areas, by visual and somatosensory modalities resulting in enhanced processing capabilities for the recruiting modality. Our experiments in human subjects show evidence of recruitment of higher-order auditory cortical areas by visual and somatosensory modalities in age-related hearing loss. Cross-modal cortical re-organization is evident as early as mild-moderate hearing loss and is related to difficulty understanding speech in noise, suggesting that recruitment by other sensory modalities may influence the variability in outcomes in adults with hearing loss. Finally we will explore the relationship between cortical re-organization and cognitive decline in patients with untreated hearing loss and those who are fitted with amplification and/or electrical stimulation. A better understanding of the cortical re-organization that accompanies hearing loss may allow us to incorporate improvements in the design of prostheses to allow them to better accommodate altered cortical processing. Overall, our results suggest that compensatory cortical plasticity in hearing loss may influence behavioral outcomes in age-related hearing loss.

Supported by the National Institutes of Health and Hearing Research Consortium

SYMP 28

Age-related effects on the auditory system

Gregg Recanzone

University of California at Davis

Age-related hearing deficits are a major health concern, affecting over half of the geriatric population. While some patients have clear peripheral hearing loss, many have what is considered normal detection thresholds yet still have spatial and/or temporal processing deficits. Studies in sub-cortical regions, primarily in rodents but also our own work in monkeys, suggests that aging causes an imbalance in the excitatory and inhibitory networks. We have recently investigated the responses of auditory cortical neurons in aged macaque monkeys that have normal hearing audiograms. In these studies we have found that there is an increase in spontaneous activity, with a corresponding increase in driven activity to broadband noise stimuli, amplitude modulated noise stimuli, and tone-pip and noise-burst sequences, consistent with the hypothesis of the altered excitatory/inhibitory imbalance. These findings were furthered by changes in spatial, temporal, and intensity processing ability in aged cortical neurons compared to younger ones. In the spatial domain, spatial receptive fields are slightly larger in A1 of aged compared to young animals. However, in the higher-order cortical area, the caudolateral field (CL), spatial tuning is sharpened in younger animals, but not in aged animals. With respect to temporal processing, for A1 neurons there was no difference in the percentages of neurons that were sensitive to the envelope of amplitude modulated noise in young and aged animals. However, the percentage of neurons that were sensitive by their overall firing rate was increased in aged animals at the expense of neurons that were sensitive by their temporal responses as measured by the vector strength to the envelope. This indicates that a different encoding strategy was employed by the aged neurons, shifting from primarily a temporal code in the young animals to a firing rate based code in the aged animals. These studies were furthered by results from the tone-pip and noise-burst sequences, where the selectivity of the responses to different presentation rates was compromised in the aged animals compared to the younger animals. Finally, intensity tuning was also broadened in aged animals compared to younger ones. These results indicate that there are dramatic changes in the firing rates of aged neurons, with a corresponding decrease in sensitivity and selectivity of spatial and temporal parameters. These changes could underlie the age-related hearing deficits noted in human patients.

SYMP 29

Cochlear and auditory-nerve functions are associated to cognitive decline in elders

Paul H. Delano

University of Chile

Epidemiological evidence shows an association between age-related hearing loss and cognitive decline in elderly people. Presbycusis subjects with audiometric hearing thresholds (PTA) worse than 40 dB are more likely to develop dementia. The mechanisms that connect this epidemiological association are unknown. Here we propose that the amplitude of auditory-nerve responses at supra-thresholds levels (80-90 dB), which has been used as a proxy of the loss of synapses between inner hair cells and auditory nerve neurons, is an important factor linking presbycusis and cognitive decline. Methods: The ANDES (Auditory and Dementia study) project is a prospective cohort of Chilean hispano-mestizo elders ≥ 65 years, "cognitively" normal (MMSE >24) with different levels of age-related hearing impairment. A total of 112 people have been evaluated with comprehensive neuropsychological and audiological evaluations, including: audiometric thresholds (0.25 to 8 kHz), amplitudes and latencies of auditory brainstem responses (ABR) waves I and V obtained at 80-90 dB nHL, distortion product otoacoustic emissions (DPOAEs). Results: 99 participants (60 women) complied with the inclusion criteria, with a mean age of 73.9 ± 5.2 years, and a mean education of 9.4 ± 4.1 years. The mean pure tone average (PTA) for the right ear was 29.3 ± 12.1 dB HL. Mean HHIE-S was 7.00 ± 7.3 points, while average MMSE was 28.1 ± 1.3 (range between 24 and 30 points). In the group of normal hearing subjects, the amplitude of the left ABR wave I and of the left amplitude ratio between wave I and V correlated with the Trail Making Test A (TMT-A) time (Spearman test, $r=-0.45$, $p=0.04$; $r=-0.52$, $p=0.02$ respectively), while there was no correlation in the amplitude of DPOAEs and in the contralateral noise effects on DPOAEs from the left ear. In addition, the amplitude of the right ABR wave I and the right wave I/V ratio correlated with the Frontal Assessment Battery (FAB) score (Spearman test, $r=-0.471$, $p=0.03$; $r=-0.541$, $p=0.01$), while there were non-significant correlations between the amplitude of DPOAEs and the contralateral noise effects in the right DPOAEs with the FAB score. Conclusions: These results suggest that hidden hearing loss is associated to slower processing speed and diminished frontal functions in elderly humans. Funded by Anillo ACT1403, Fondecyt 1161155 and ICM P09-015F.

SYMP 30

Depression and social isolation in hearing loss.

Sergi Costafreda

University College London

Age related hearing loss ARHL is being recognized as an independent risk factor in the development of dementia. One of the causal pathways which could account for the risk increase is through the adverse effects of ARHL on social function and mental health. I will present recent evidence on the association between ARHL, social isolation, depression and other psychopathology, including auditory hallucinations and suicidal ideation, and their potential links to cognitive health and dementia.

Beyond the Basilar Membrane: Measuring Cochlear Micromechanics

Chairs: Marcel van der Heijden & Tianying Ren

SYMP 31

Cochlear Mechanics in the Apex

John S. Oghalai

USC Caruso Department of Otolaryngology - Head and Neck Surgery

The exquisite sensitivity and frequency discrimination of mammalian hearing derive from forces generated by outer hair cells (OHCs) within the auditory portion of the inner ear, the cochlea. These forces amplify the sound-induced vibrations within the tissues of the cochlea to enhance quiet sounds and sharpen frequency tuning. Our group using optical coherence tomography to measure sound-induced vibrations within the mammalian cochlea without opening the bone that surrounds it, thus minimizing artifacts. Furthermore, we study transgenic mice with targeted mutations that affect different biomechanical aspects of the cochlea to localize the underlying processes necessary for normal hearing. The goal of this work is to understand the fundamental biomechanical processes involved in normal and impaired hearing.

SYMP 32

Drilling Further in the Cochlear Base with Displacement and Extracellular Voltage Measurements

Lisa Olson; Clark Elliott Strimbu; Nathan C. Lin; Elika Fallah

Columbia University

Coupled measurements of intracochlear responses are particularly helpful for understanding cochlear processing. For example, the correlation between basal auditory nerve tuning and basilar membrane motion showed that

cochlear traveling wave tuning underlaid the sharp tip of auditory nerve tuning. Recent measurements of basilar membrane motion and extracellular voltage revealed a phase shift of voltage that seemed to activate traveling wave amplification. The new OCT-based displacement measurements allow us to peer into the organ of Corti. Coupling these with extracellular voltage measurements allow us to further probe the basis of cochlear traveling wave amplification.

SYMP 33

The Hidden Mechanics of the Organ of Corti

Nigel P. Cooper; Anna Vavakou; Marcel van der Heijden

Erasmus MC

Basilar membrane (BM) vibrations introduce tonotopy, level dependent tuning, and frequency dependent nonlinearities that are fundamentally important to the auditory system. How the BM achieves this feat remains mysterious. Here we investigate the hidden mechanics of the organ of Corti which we believe 'control' the BM's motion. We report a previously unobserved motion hotspot deep within the body of the organ of Corti. The hotspot is physiologically vulnerable, but has none of the other hallmarks that might be expected of a cochlear amplifier. It looks more like a part of a mechanical gain control system.

SYMP 34

Comparison of Apical and Basal organ of Corti Vibration to Tone and Tone Complexes

Alfred Nuttall¹; George Burwood²; Anders Fridberger³; Riukang Wang⁴

¹OHSU; ²Oregon Hearing Research Center;

³Linskooping University; ⁴University of Washington-Seattle

The mammalian cochlea produces mechanical responses to tones that have local and propagated components. Detection of frequency complexes is tonotopic while non-linear processing of the complex can generate propagating distortion, e.g. otoacoustic emissions. One distortion subtype permits the extraction of tonal complex envelopes, potentially contributing to the perception of speech and music. Therefore, envelope encoding may first occur mechanically in the auditory periphery. Here, Optical Coherence Tomography vibration measurements in the apical and basal turns of the guinea pig cochlea investigate the location and function of peripheral envelope processing mechanisms. Our observations indicate that envelope information is produced by non-linear mechanosensory pathways. The resulting nonlinearities could then feasibly permit envelope information to be transduced by the auditory nerve, enabling the interpretation of complex acoustic signals.

SYMP 35

Non-invasive and Non-destructive Imaging and Vibrometry of Organ of Corti Structures in the Gerbil Cochlear Apex

Sunil Puria

Eaton-Peabody Laboratories

We use a commercial OCT system driven by custom software (VibOCT) that facilitates near real-time frequency response measurements. The 905-nm wavelength laser and high-speed (100 kHz) camera provide higher axial resolution (3 μm in air) than previous studies and a sub-nanometer noise floor. We have made in-vivo scans and on our way towards making point vibrometry measurements at multiple locations of the organ of Corti. This system can provide valuable information on cochlear anatomy and function useful for the development of detailed cochlear models of the passive and active gerbil apex.

SYMP 36

Heterodyne Low-coherence Interferometry of Cochlear Partition Vibrations in Sensitive Living Cochleae

Tianying Ren¹; Wenxuan He¹; David Kemp²
¹OHSU; ²UCL

A heterodyne low-coherence interferometer was developed to measure the cochlear partition vibrations in mice and gerbils. Responses to tones and clicks show that the reticular lamina vibrates earlier than the basilar membrane, with a larger magnitude and stronger nonlinearity. The phase of the reticular lamina vibration leads the basilar membrane phase by up to 180 degrees at low frequencies, and this phase lead decreases with frequency, approaching zero near the best frequency. The current results suggest a new micromechanical mechanism responsible for cochlear sensitivity, tuning, and dynamic range.

Intracochlear Drug Delivery & Biomarkers

PD 41

Delivery of Bone-Binding Brain-Derived Neurotrophic Factor (BDNF) Analogue Ris-DHF Supports Hearing Recovery After Noise Damage In Vivo

Judith S. Kempfle¹; Christine Hamadani²; Kim Nguyen³; Boris Kashemirov³; Andrea Zhang²; Albert Edge⁴; Charles McKenna³; **David Jung**⁵
¹Massachusetts Eye and Ear Infirmary, Eaton-Peabody Laboratories; ²Massachusetts Eye and Ear Infirmary; ³University of Southern California; ⁴Department of Otolaryngology, Harvard Medical School; ⁵Department of Otolaryngology, Harvard Medical School/

Massachusetts Eye and Ear

Background:

Sensorineural hearing loss has classically been associated with degeneration of cochlear hair cells (HCs), spiral ganglion neurons (SGNs), or the stria vascularis. However, recent work has identified primary synaptopathy as another, “hidden” cause for sensorineural hearing loss: noise exposure results in a loss of ribbon synapses between intact HCs and SGNs and SGN neurite retraction, while cell bodies of SGNs and HCs persist. Recent regenerative approaches with exogenous neurotrophins (NTs) have been successful in promoting neurite outgrowth and re-forming of ribbon synapses to reverse synaptopathy and improve hearing. Brain-derived neurotrophic factor (BDNF) is one of two major neurotrophins of the inner ear and promotes proper neuronal wiring during development and neuronal survival in adulthood. We have previously explored a hybrid small molecule approach to cochlear drug delivery by linking a bone-binding bisphosphonate, Risedronate (Ris), to 7-8 dihydroxyflavone (DHF), a small molecule analogue of BDNF. In an *in vitro* model of cochlear synaptopathy, we demonstrated that Ris-DHF improved neurite outgrowth and cochlear synaptogenesis, with preserved activity following binding to bone matrix.

We now show that surgical application of Ris-DHF leads to significant functional recovery of hearing after synaptopathic noise damage.

Methods:

Adult 6-week old CBA mice underwent synaptopathic noise damage at 8-16 kHz for 2 hours at 98 dB. Auditory brainstem response (ABR) testing was performed to evaluate for a temporary threshold shift (TTS). 24 hours after noise exposure, DHF, Ris-DHF, or artificial perilymph carrier was applied to the round window via a surgical bullotomy. Four weeks after surgery, ABRs were re-measured and whole mount preparations of the organ of Corti were evaluated.

Results:

Following noise exposure, we observed a TTS. After recovery of the TTS, suprathreshold Wave 1 amplitudes at 32 kHz remained decreased in untreated animals and animals treated with artificial perilymph alone. Surgical application of Ris-DHF resulted in substantial recovery of ABR suprathreshold wave 1 at 32 kHz 4 weeks after noise damage. Animals treated with unconjugated DHF showed minimal improvement. Evaluation of synapses in cochlear whole mounts is underway.

Conclusion:

Small hybrid molecule Ris-DHF promoted significant recovery after synaptopathic noise damage in vivo, while

unconjugated DHF supported minimal recovery. These findings suggest that bisphosphonate conjugation may provide a generalizable, non-cochlear invasive method for drug delivery.

PD 42

Vgf Expression Is a Biomarker of NTF3 Target Engagement in Mouse Spiral Ganglion Neurons in Vitro and in Vivo

Tian Yang¹; Changsuk Moon¹; Matthew Nguyen¹; Guo-Peng Wang²; Kathy S. So¹; Gabriela Pregonig¹; Trang Nguyen¹; Joseph Manna¹; Ryan C. McCarthy¹; Noah Druckenbrod¹; David Kohrman³; Adam T. Palermo¹; Gabriel Corfas⁴; Janeta V. Popovici-Muller¹; Inmaculada Silos-Santiago¹; Joseph C. Burns¹

¹Decibel Therapeutics; ²Kresge Hearing Research Institute, Dept. of Otolaryngology Head and Neck Surgery. University of Michigan; ³Kresge Hearing Research Institute, Dept. of Otolaryngology Head and Neck Surgery. University of Michigan; ⁴Dept. of Otolaryngology Head and Neck Surgery. University of Michigan

The neurotrophins NTF3 and BDNF regulate development and survival of cochlear spiral ganglion neurons (SGNs). In damage models, local delivery of neurotrophins is reported to promote SGN survival and outgrowth, as well as synaptic reconnection with hair cells. While various histological and physiological outcomes have been used to assess these effects, engagement of target receptors on SGNs has not been reported. A validated biomarker of neurotrophin target engagement would be valuable given the difficulties and variability of consistently delivering small volumes to the inner ear.

To circumvent the challenges of measuring neurotrophin receptor binding in vivo, we sought to identify downstream changes in gene expression that could serve as a proxy readout of target engagement. For this, we delivered AAV8-*Ntf3* to the cochlea of mice and simultaneously assessed exogenous *Ntf3* levels and associated transcriptional changes with RNA-Seq. Bulk profiling confirmed a significant increase in *Ntf3* expression in 5 AAV8-*Ntf3*-treated ears compared to 5 AAV8-GFP and 5 naïve controls. *Ntf3* levels were positively correlated with the levels of 191 other genes. Interestingly, *Vgf*, which is specifically upregulated by neurotrophin family members in the CNS, showed one of the strongest correlations.

To test whether *Vgf* induction was specific to SGNs, we performed single-cell RNA-Seq on cochleae from AAV8-*Ntf3*-treated and naïve mice. Minimal *Ntf3* transcripts were detected in the naïve ears; however, *Ntf3* transgene was elevated in a variety of cell types after AAV delivery, including SGNs. *Vgf* transcripts demonstrated a

corresponding increase but were highly restricted to SGNs, despite broader viral tropism. *In situ* labeling of transcripts with RNAScope confirmed the strikingly specific upregulation of *Vgf* in SGNs.

Since AAV8-*Ntf3* appeared to robustly target SGNs, additional experiments were conducted to confirm that *Vgf* upregulation resulted from extracellular NTF3 protein binding to its cell surface receptors. To assess this more directly, we confirmed that *Vgf* expression increased in response to treatment with NTF3 protein in primary cultures of SGNs. In addition, we established an ELISA-based method for detecting NTF3 protein levels in perilymph sampled from the intact cochlea and found that AAV8-*Ntf3* gene delivery was able to produce detectable levels of secreted NTF3.

Combined, the data indicate that *Vgf* is a downstream component of the NTF3 signaling pathway in SGNs. Furthermore, ELISA and RNAScope should be convenient methods for assessing successful delivery of NTF3 protein and concomitant *Vgf* upregulation in therapeutic applications.

PD 43

Dual AAV Vectors for Delivery of Large Genes

Theresa Abell; Jonathon Whitton; Adam T. Palermo; Kathryn Ellis

Decibel Therapeutics

Hearing loss affects 1 in 500 newborns in the United States. In developed countries, roughly 80% of congenital hearing loss is due to genetic causes. Importantly, the majority of these cases are non-syndromic and recessive, making these cases ideal targets for a gene replacement strategy. Hearing loss is an especially attractive indication for gene therapy as local delivery of virus to the inner ear circumvents the need for high titer or large volumes of virus as well as the possibility of negative systemic effects.

However, the inner ear has a disproportionately high number of large genes that exceed the 4.7 kb carrying capacity of standard adeno-associated viruses (AAV). One approach to large gene delivery is to use a dual AAV vector approach in which a gene is divided in half and each half is packaged separately in two viruses. When cells are infected with both of the viruses, the halves will recombine creating an intact gene capable of generating a full-length, functional protein. Three dual vector strategies have been used to deliver large genes in discovery efforts and one is currently in use in clinical trials: 1. Overlapping dual vectors make use of homology arms to recombine each half of the gene, 2. Trans-splicing dual vectors use splice donor and

acceptor sequences to splice together the transcript, and 3. Dual hybrid dual vectors which use a combination of both homologous recombination and splice donor/acceptor sequences.

We have developed *in vitro* and *ex vivo* assays for comparing the efficiency of recombination for several dual vector strategies in cochlear tissues. These assays are critical for iteratively identifying the optimal configuration of the dual AAV for each gene with a reasonable throughput. Here we demonstrate recombination of two halves of a reporter gene *in vitro* using PCR and Sanger sequencing, we show full length functional protein using immunofluorescence *in vitro*, we demonstrate dual vector recombination efficiency in hair cells of the cochlea using cochlear explants *ex vivo*, and we show recombination of dual vectors *in vivo*. Using these assays we can compare recombination efficiencies of various recombination strategies and permutations of dual vector constructs.

PD 44

Gene Transfer with AAV9-PHP.B Rescues Hearing in a Mouse Model of Usher Syndrome 3A and Transduces Hair Cells in a Non-Human Primate

Maryna V. Ivanchenko¹; Bence György²; Elise J. Meijer¹; Kelly Tenneson³; Frederick Emond³; Killian S. Hanlon¹; Artur A. Indzhukulian⁴; Adrienn Volak⁵; K. Domenica Karavitaki⁶; Panos I. Tamvakologos¹; Mark Vezina³; Vladimir Berezovskii¹; Richard Born¹; Maureen O'Brien³; Jean-François Lafond³; Yvan Arsenijevic⁷; Margaret Kenna⁸; Casey A. Maguire⁵; David P. Corey¹

¹Harvard Medical School, Department of Neurobiology;

²Department of Neurobiology, Harvard Medical School, Massachusetts General Hospital; ³Charles River Laboratories; ⁴Department of Otolaryngology, Massachusetts Eye and Ear, Harvard Medical School;

⁵Molecular Neurogenetics Unit, Massachusetts General Hospital, Harvard Medical School; ⁶Harvard Medical School; ⁷Unit of Retinal Degeneration and Regeneration, Department of Ophthalmology, University of Lausanne, Jules-Gonin Eye Hospital;

⁸Boston Children's Hospital, Harvard Medical School

Hearing loss occurs in approximately 1/1,000 births, with roughly half having a genetic cause. Many of the known deafness genes affect hair cells (HCs) so gene delivery to hair cells is a promising treatment strategy. Adeno-associated virus (AAV) serotype 1 has been used for viral transduction of hair cells; however, it only transduces inner hair cells (IHCs) and not the equally important outer hair cells (OHCs).

Recently our group and others demonstrated efficient

gene delivery to IHCs and OHCs in neonatal mice using new AAV-based systems. However, significant challenges remain for clinical translation of AAV-based gene therapy for deafness. First, gene transfer to the cochlea has been performed almost exclusively in mice, with no reports in non-human primates, so the translational potential of various AAVs for cochlear gene therapy in humans is unknown. Second, in many human hereditary deafnesses, the hair cells are thought to degenerate before birth so postnatal gene therapy interventions would have no target. Thus, studies showing rescue of hearing in neonatal mice models may not apply to humans.

To identify a vector for effective gene therapy to all cochlear HCs, we tested the recently described AAV9-PHP.B capsid variant. AAV9-PHP.B encoding GFP injected through the round window membrane (RWM) of P1 mice resulted in viral transduction of 70-100% IHCs and 50-80% OHCs. We also observed robust IHC and OHC GFP expression in neonatal Sprague Dawley rats. In adult Cynomolgus monkeys, AAV9-PHP.B encoding GFP was injected through the RWM following a transmastoid surgical approach. AAV9-PHP.B transduced nearly 100% of both IHCs and OHCs, from base to apex.

To explore gene therapy in a relevant mouse model, we used a mouse lacking functional CLRN1. In humans, variants in the *CLRN1* gene can cause Usher syndrome type 3A, an autosomal recessive deafness and blindness. The hearing loss is not profound at birth but is progressive, providing a reasonable window for AAV-mediated gene therapy. In the mouse model at P1, we injected AAV9-PHP.B encoding HA-tagged CLRN1. We observed tagged protein in the hair bundles and cuticular plates of both inner and outer hair cells (~90% of IHC and ~40% of OHC). To assess hearing restoration, we tested ABR at 4 weeks post-injection and observed rescue of hearing at lower frequencies. Together, these data support a feasible path towards clinical development of gene therapy for a hereditary hearing loss.

PD 45

Restoration of Hearing in Tmc1-Deficient Mice Depends on Early and Well-Regulated Gene Delivery

Xichun Zhang; Nancy Paz; Ning Pan; Kathryn Ellis; Martin Schwander; Joseph C. Burns; Jonathon Whitton;

Adam T. Palermo

Decibel Therapeutics

Tmc1 is believed to be the primary ion channel responsible for hair cell depolarization in response to mechanical stimulation. Functional Tmc1 is necessary for hearing,

and both humans and mice without Tmc1 fail to develop hearing. Previous work has shown that restoration of functional Tmc1 to Tmc1-deficient mice can partially rescue hearing when delivered neonatally via AAV containing a ubiquitous promoter. We explore here the effect of mouse age at delivery and promoter specificity on hearing rescue and on preservation of cochlear hair cells.

We delivered Anc80-CMV-Tmc1 at P2-P3 to Tmc1 knock out (KO) mice. Consistent with previous reports, we observed partial rescue of ABR thresholds (~70 dB SPL) in Tmc1 KO mice that were treated with AAV-based gene therapy. By contrast, no ABR response could be measured at equipment limits in untreated controls. We also observed preservation of cochlear hair cells in treated Tmc1 KO mice as compared to untreated animals. In contrast, when we delivered the same gene therapy vector to Tmc1 KO mice after P17, we observed minimal benefit, with ABR thresholds between 80 and 105 dB SPL. Interestingly, the observed onset of outer hair cell (OHC) loss in Tmc1-deficient animals is around P17 in our hands, suggesting that most hair cells are present at the time of delivery, but cannot be rescued with the Anc80-CMV-Tmc1 vector.

We also used DPOAE to assess outer hair cell function in the animals rescued at P2-P3. By this measure, we observed almost complete rescue of response for F2 frequencies at and below 16 kHz, suggesting better recovery of outer hair cell function than implied by the ABR threshold responses alone. We hypothesized that non-optimal levels of transgene expression, either in inner hair cells or in another cell type, may have limited ABR threshold recovery.

To test this hypothesis, we delivered an Anc80-Tmc1 vector driven by a hair cell-specific promoter to P2-P3 TMC1 KO mice. When ABRs were assessed in these animals, we observed normalization of thresholds to within 20 dB of heterozygous controls for low and mid frequency sounds. We conclude that both age of delivery and specificity of expression are tightly linked to functional rescue in Tmc1-deficient mice.

PD 46

Optimization of Surgical Approach and Vector Delivery for Highly Efficient Gene Transfer to Inner Hair Cells in Rhesus Macaque

Eva Andres-Mateos¹; Lukas D. Landegger²; Carmen Unzu³; Jeanne Phillips⁴; Brian Lin⁴; Nicholas Dewyer⁴; Julio Sanmiguel¹; Fotini Nicolaou¹; Michelle Valero⁵; Kathrin Bourdeu⁶; William Sewell⁵; Rudolph Beiler⁷; Michael McKenna⁸; Konstantina M. Stankovic⁹; Luk Vandenberghe¹⁰

¹Grousbeck Gene Therapy Center, Schepens Eye Research Institute and Massachusetts Eye and Ear Infirmary & Ocular Genomics Institute, Department of Ophthalmology, Harvard Medical School; ²Massachusetts Eye and Ear and Harvard Medical School; ³Grousbeck Gene Therapy Center, Schepens Eye Research Institute and Massachusetts Eye and Ear Infirmary & Ocular Genomics Institute, Department of Ophthalmology, Harvard Medical School; ⁴Department of Otolaryngology, Massachusetts Eye and Ear and Harvard Medical School; ⁵Eaton Peabody Laboratories, Massachusetts Eye and Ear & Department of Otolaryngology, Massachusetts Eye and Ear and Harvard Medical School; ⁶Department of Anesthesia, Massachusetts Eye and Ear, Harvard Medical School; ⁷Animal Science Center⁸Eaton Peabody Laboratories, Massachusetts Eye and Ear & Department of Otolaryngology, Massachusetts Eye and Ear and Harvard Medical School & Otopathology Laboratory, Massachusetts Eye and Ear & Speech; ⁹Eaton-Peabody Laboratories, Massachusetts Eye and Ear & Department of Otolaryngology, Massachusetts Eye and Ear and Harvard Medical School & Speech and Hearing Bioscience and Technology Program; ¹⁰Grousbeck Gene Therapy Center, Schepens Eye Research Institute and Massachusetts Eye and Ear Infirmary & Ocular Genomics Institute, Department of Ophthalmology, Harvard Medical School & Harvard Stem Cell Institute, H

Cochlear and vestibular gene transfer holds significant potential to alleviate hearing and balance disorders. Previously, Adeno-associated viral vector (AAV) systems have been shown to partially rescue of hearing and balance in murine disease models. The efficiency and targeting of the gene transfer is largely determined by the AAV serotype. Our data in newborn mice established the benefits of Anc80L55 in targeting primarily inner and outer hair cells following round window membrane injection (RWM) (Landegger et al., Nature Biotech, 2017).

Here, we aimed to establish the feasibility and efficiency of the surgical approach and vector delivery in a large non-human primate model to control for scaling, species translation, host response, and pharmacokinetics within the fluid-filled cochlea. AAV1 (n=2) or Anc80L65 (n=3) expressing eGFP was injected in rhesus macaques through the round window membrane following a small fenestration in the oval window for pressure release. The procedure and vector injection was well tolerated with no clinical signs of discomfort or focal neurologic or systemic signs. Cochlear transduction was evaluated 7 to 14 days following injection. All animals except one showed significant cochlear eGFP expression with up to 90% of inner hair cells transduced with Anc80L65. AAV1

was markedly less efficient at equal dose. Transduction pattern for both vectors declined from apex to base in the absence of vector-induced damage or toxicity at the base. Several other cochlear and vestibular cell types were also transduced at variable rates. Blood cell counts and chemistries were within normal range. AAV neutralizing antibodies were detected in serum but not in CSF following, but not prior to injection in all animals.

These data from non-human primates demonstrate that Anc80L65 allows both safe and efficient gene transfer to the inner ear via round window membrane injection. Our results motivate future translational studies in large animal models of auditory and vestibular dysfunction affecting hair cells, prior to human clinical trials.

PD 47

Cytokine Levels in Perilymph of Young and Aged Mice as Molecular Biomarkers of Noise-Induced Hearing Loss

Lukas D. Landegger¹; Takeshi Fujita¹; Sasa Vasilijic¹; Vitor Y. Soares¹; Lei Xu²; Konstantina M. Stankovic³

¹Massachusetts Eye and Ear and Harvard Medical School; ²Massachusetts General Hospital and Harvard Medical School; ³Eaton-Peabody Laboratories, Massachusetts Eye and Ear & Department of Otolaryngology, Massachusetts Eye and Ear and Harvard Medical School & Speech and Hearing Bioscience and Technology Program

BACKGROUND: Sensorineural hearing loss (SNHL) is the most common sensory disability globally and it typically originates from the inner ear. While SNHL is commonly caused by harmful noise exposure, robust molecular biomarkers of acoustic trauma do not yet exist. Perilymph, a proximal fluid of the inner ear, bathes nearly all cells vital to sound transduction. Consequently, any protein secreted or released by a noise-damaged cell will be found in perilymph at higher concentrations than in other bodily fluids such as cerebrospinal fluid (CSF) or blood. Here we test the hypothesis that the levels of pro-inflammatory cytokines are elevated in perilymph after acoustic trauma that causes permanent threshold shifts in auditory brainstem response and distortion product otoacoustic emissions.

METHODS: Four groups of six-week-old CBA/CAJ mice were used: 1) 30 mice exposed to neuropathic noise that causes temporary threshold shift, TTS (8-16 kHz noise at 97 dB SPL for two hours); 2) 30 mice exposed to non-neuropathic noise that causes TTS (8-16 kHz noise at 94 dB SPL for two hours); 3) 30 mice exposed to noise that causes permanent threshold shift (8-16 kHz noise at 103 dB SPL for two hours), 4) 30 unexposed control mice. For each group, we collected cochlear and vestibular perilymph and CSF (via the

posterior semicircular canalostomy) and CSF (via cisterna magna) six hours (10 animals), two weeks (10 animals) or two years (10 animals) after noise exposure. The levels of ten pro-inflammatory cytokines were measured in these samples using multiplex arrays based on electrochemiluminescence.

RESULTS: Noise trauma causing permanent threshold shift resulted in statistically significant elevation of interleukin 6, tumor necrosis factor alpha and chemokine (C-X-C Motif) ligand (CXCL1) levels in perilymph 6 hours after noise exposure. These differences were not detectable after longer post-exposure times or different noise levels. Because cellular expression of CXCL1 had not been described in the inner ear before, we report immunohistochemical localization of CXCL1 in pillar cells.

CONCLUSIONS: This study provides the first direct measurements of cytokines in perilymph after noise trauma, and suggests molecular biomarkers of acute acoustic injury. Our pre-clinical findings pave the way for a future clinical “liquid biopsy” of the inner ear based on diagnostic sampling of a microliter of perilymph via a minimally-invasive, transcanal approach. Establishing robust and reliable molecular biomarkers of acoustic trauma has a potential to provide therapeutic targets, promote hearing protection, and guide response to emerging restorative therapies for SNHL.

PD 48

Preliminary Characterization of Extracellular Vesicles from Auditory HEI-OC1 Cells

Gilda M. Kalinec¹; Whitaker Cohn¹; Julian P. Whitelegge¹; Kym F. Faull¹; **Federico Kalinec²**
¹UCLA; ²Department of Head and Neck Surgery, David Geffen School of Medicine at UCLA

Extracellular vesicles (EVs) are small structures (30-1000-nm) of endosomal origin consisting of lipids, proteins, mRNAs, and DNA enclosed by a membrane. EVs have the capacity to transfer material from the secreting cells to other cells in sites remote to the vesicular origin. This ability confers on them the power to alter simultaneously multiple signaling pathways in the target cells by the concurrent delivery of numerous different molecular messengers. More importantly, EVs can be loaded with specific molecules and/or pharmacological agents using simple procedures, stored for extended periods, and then used—without any processing prior to administration—to deliver their tailored cargo via many different routes, including oral administration and intranasal spray, making them more advantageous than many traditional pharmaceutical approaches.

EVs are believed to be secreted by most types of

cells, but in different numbers and with different cargo. Therefore, we decided to investigate whether auditory HEI-OC1 cells produce them and whether they naturally express biomolecules associated to the function and protection of the hearing organ. We found that, indeed, HEI-OC1 cells continuously produce abundant EVs that can be easily isolated and characterized. High-purity EVs-containing fractions from auditory HEI-OC1 cells grown in culture were obtained using the commercially available isolation kit ExoEasy™ (Qiagen, USA). EVs size and concentration were characterized by nanoparticle tracking with a NanoSight™ NS300 (Malvern Instr., USA). Although EVs's size and concentration varied among samples, typical values were in the ranges 100-600 nm and 9×10^8 - 3×10^9 /mL, respectively. Quantitative proteomics of EVs, either freshly obtained or stored for up to 4 month at -30°C , was performed by LC-ESI-MS/MS using deuterium-labeled standards. We found that EVs from HEI-OC1 naturally expressed abundant copies of molecular mediators that promote the resolution of inflammatory process. Comparison with the proteomic profile of whole HEI-OC1 cells indicated, as expected, that EVs concentrate some proteins while others were below the limit of detection. We also found that HEI-OC1 EVs were easily loaded with drugs by simple co-incubation at room temperature for 1 hour, and that the loading could be further improved with 5 minutes sonication. No significant differences between fresh and stored EVs were detected either in protein profile or drug loading capacity.

Whereas the significance of these results is still under investigation, our preliminary data suggest that EVs from HEI-OC1 cells could be advantageously used as nanocarriers for the delivery of specific molecules and drugs into the inner ear.

Benefits of Extended High Frequency Hearing

Chairs: Lisa Hunter, Brian Monson & Dave Moore

SYMP 37

Benefits of Extended High-Frequency Hearing

Brian B. Monson

University of Illinois at Urbana-Champaign

A fundamental principle of neuroscience is that each species' and individual's sensory systems are tailored to meet the demands placed upon them by their environments and experiences. Why has the human auditory system retained sensitivity to acoustical energy produced beyond 8 kHz? Although this sensitivity is believed to be useful for some auditory tasks (e.g., judgements of sound source elevation or front/back distinctions for sound source localization), an additional possibility is that extended high-frequency (EHF)

hearing is advantageous for detection and perception of conspecific vocalizations (i.e., speech). Here we provide an overview of EHF hearing and report on a series of studies revealing the utility of EHF hearing for speech perception. Historically, speech energy beyond 8 kHz was deemed unnecessary for applications of interest (i.e., telephony), and has often been neglected by tradition. We find, however, that EHF energy in speech is audible up to approximately 13 kHz for healthy young adult listeners. Furthermore, access to EHF improves some speech perception tasks. The ability of listeners to make judgements of a talker's head orientation was improved with access to EHF. This improvement is likely due to the directional nature of EHF energy radiation from the mouth. Listeners performed above chance in vowel and consonant identification tasks utilizing only EHF cues, suggesting EHF speech energy provides phonetic information per se. Our results suggest EHF energy produced in speech is audible and provides useful information regarding the speech signal. These findings suggest the preservation of sensitivity to EHF for humans may be, in part, to improve detection and perception of communication by conspecifics.

SYMP 38

Frequency Discrimination in the Extended High-Frequency Range: Implications for Theories of Pitch

Andrew J. Oxenham

University of Minnesota

Pitch is a fundamental auditory percept that is crucial for many aspects of speech and music perception. Exploring the pitch elicited by harmonic complex tones in the extended high-frequency range (above 8 kHz) provides an opportunity to test theories of pitch that rely on neural phase-locking to the temporal fine structure of stimuli, as it is widely believed that such phase-locking is not available at these frequencies. Earlier results from our lab have shown that pitch can be extracted from harmonic complex tones with all components above 8 kHz, even when cues based on the temporal-envelope repetition rate and distortion products are eliminated, suggesting that phase-locking is not necessary for the perception of complex pitch. More recent results have suggested that the accuracy of pitch perception in the extended high-frequency range may not be limited by phase-locking but is instead constrained by more central processes. Overall the results suggest that harmonics in the high-frequency range can be used to convey pitch, but that such pitch sensitivity does not extend to fundamental frequencies in that range. These outcomes suggest that exposure and experience, rather than peripheral physiological limitations, explain the upper limit of musical pitch.

Grant support: NIH grant R01 DC005216.

SYMP 39

Extended High Frequency Hearing Contributes to Speech Perception in Noise

Lina Motlagh Zadeh¹; David R. Moore²

¹*Cincinnati Children Hospital Medical Center;*

²*Cincinnati Children's Hospital and the University of Cincinnati*

Young healthy adults can hear tones up to at least 20 kHz. However, clinical audiometry, by which hearing loss is diagnosed, is limited at high frequencies to 8 kHz. Evidence suggests there is salient information at extended high frequencies (EHF; 9-20 kHz) that may influence speech intelligibility, but whether that information is used in challenging listening remains unknown. Difficulty understanding speech in challenging environments is the most common concern people have about hearing and usually the first sign of age-related hearing loss. Digits-in-noise (DIN), a widely used test of speech perception in noise, can be sensitized for detection of early high frequency hearing loss by low-pass filtering the normally broadband masking noise. In the present study, we used successively higher cutoff frequency filters (2-8 kHz) in a DIN test, standard and EHF audiometry, and self-report to investigate contributions of EHF hearing to speech-in-noise perception. Three surprising results were found. First, 53/76 'normally hearing' adult listeners had at least some, mostly bilateral hearing loss at frequencies above 8 kHz. Second, EHF hearing loss correlated with self-reported difficulty hearing in noise. Finally, even with the broadest filtered noise (≤ 8 kHz), DIN thresholds were significantly better ($p < 0.0001$) than those using broadband noise. Sound energy above 8 kHz thus contributes to speech perception in noise. People with 'normal hearing' frequently report difficulty hearing in challenging environments. Our results suggest that one contribution to this difficulty is an EHF hearing loss.

SYMP 40

EHF Hearing and Speech Perception in Children

Lisa L. Hunter

Cincinnati Children's Hospital and the University of Cincinnati

Children and teens have exceptionally sensitive hearing in the extended high frequency (EHF) region in comparison to adults, but EHF insensitivity happens early and is progressive. By the second decade of life, significant decreases in sensitivity have occurred, and continue to progress in a basal to apical pattern. EHF hearing is highly susceptible to genetic variance, ototoxic drugs, chronic otitis media with effusion and noise. There has been debate about the importance of EHF sensitivity to speech perception, and this factor has been implicated as a possible explanation for poorer

speech understanding, especially in noise. Recent studies point to EHF hearing as a highly sensitive method to study speech perception deficits in children and teens. One such example is in Auditory Processing Disorder (APD) or particular difficulty understanding speech in noisy environments, such as in classrooms. We recently reported poorer extended high frequency hearing in children with normal standard pure-tone threshold sensitivity, who had defined listening difficulties on a standardized questionnaire. In children with listening difficulties compared with age-matched typically developing children, poor speech-in-noise performance on a spatial listening task (low cue subtest of the Listening in Spatialized Noise or LiSN-S test) was related both to poorer EHF hearing and to a history of otitis media treated with tubes, but not specifically to defined listening difficulties (Hunter et al., ARO, 2017). A second line of evidence for EHF hearing contribution to speech perception in children is in ototoxicity. Aminoglycoside (AG) drugs (tobramycin, amikacin) are frequently used to treat drug-resistant chronic lung infections in patients such as those with cystic fibrosis, but unfortunately cause hearing loss due to ototoxicity starting first in the basal cochlea. In a sample of children and teens aged 6 to 18 years, speech in noise performance (BKB-SIN) showed poorer thresholds for CF patients exposed to aminoglycosides compared to age-matched controls. A high proportion of CF cases (40%) had hearing loss in the EHF range and also had mild to moderate threshold elevation in one or both ears on the BKB-SIN test relative to age-related norms and the normal control group. Discussion of the relationship between EHF hearing and speech perception measures in both groups will be included. The functional impact of SIN difficulty is relevant for environments that teens and adults listen and learn in, such as in the classroom, the workplace and in social settings.

SYMP 41

Extended High Frequency Hearing in Adults with Difficulty Hearing in Noise but 'Normal' Audiograms

Beverly A. Wright; Rohima Badri; Jonathan H. Siegel
Northwestern University

Some adults complain of difficulties hearing speech in the presence of background noise despite having clinically normal audiograms. Though these individuals do not display any significant hearing loss in the standard audiometric range, there are reports of hearing loss in the extended high frequency range, impaired frequency resolution, and reduced distortion product otoacoustic emissions (DPOAEs) in this population. We examined the relationships among these three factors across listeners who reported difficulty hearing in noise, and who performed more poorly than controls

on a sentence-in-noise perception test, and controls. We measured: (1) absolute thresholds at standard audiometric frequencies (0.5 to 8 kHz) as well as at extended high frequencies (10, 12.5, and 14 kHz) using a Békésy tracking procedure and methods designed to minimize calibration errors; (2) auditory filter shapes at 2 kHz using notched-noise maskers and three fixed signal levels (30, 40, or 50 dB SPL); and (3) DPOAEs at 2, 4, and 8 kHz using a fixed f1 level and f2 levels ranging from 0 to 60 dB SPL. Compared to controls (n=10), listeners with hearing difficulties (n=14) had normal absolute thresholds at the standard audiometric frequencies, but elevated thresholds at 12.5 and 14 kHz, wider auditory filters because of shallower-than-normal filter slopes on the high-frequency side at all three signal levels, and smaller DPOAEs at all three frequencies. Across all listeners, the average absolute thresholds computed over the three extended high frequencies were correlated with the speech-perception scores, with the DPOAE magnitudes, and with the slope of the high-frequency side of the filter for the 40-dB SPL signal level. The strongest correlation was between the slopes of the high-frequency side of the filter and the speech-perception scores. These data strengthen the idea that people who complain of speech recognition difficulties in noise despite having clinically normal audiograms have hearing deficits that go undetected by standard audiometry. They also add to the evidence that measuring absolute thresholds over the full frequency range of hearing provides a more sensitive assay of impaired hearing capabilities than conventional audiometry and suggest that elevated absolute thresholds in the extended high-frequency range may be an indicator of other hearing abnormalities at lower frequencies.

SYMP 42

Modern Calibration and Common Measures of Auditory Function

Sumit Dhar
Northwestern University

Work conducted by several groups has recently converged to allow accurate calibration of test signals and recording of otoacoustic emissions at extended high-frequencies (> 8 kHz), while avoiding contamination by multiple reflections in the ear canal. We utilize these developments to examine hearing thresholds and otoacoustic emissions from a large sample of normal-hearing human ears (N ~ 1000). Our results provide a glimpse of the earliest age-related changes in the human cochlea. Comparison of these data with those previously reported in the literature makes clear that differences in ear canal acoustics critically influence findings even at frequencies below 8 kHz.

SYMP 43

Clinical Application of EHF Audiometry

Kevin Munro
The University of Manchester

Pure tone audiometry has long been regarded as the audiology workhorse. It involves measuring detection thresholds in quiet of pure tones at different frequencies, typically between 0.25 and 8 kHz. Instead of slavish reliance on conventional test frequencies, hearing professionals could re-tool the clinic to include EHF audiometry. Potential benefits of EHF audiometry include early warning of ototoxicity or noise exposure, and understanding unexplained hearing difficulties. EHF audiometry does not need to increase test time e.g., inclusion of air-conduction at 12 kHz can be offset by omission of bone-conduction at 4 kHz, the latter often of limited value.

Kölliker's Organ: BigGERer Roles for an Overlooked Organ

Chairs: Matthew Kelley & Jonathan Gale

SYMP 44

Exploring Cellular Diversity in Kolliker's Organ Using Single Cell RNAseq

Matthew Kelley
NIDCD

Kolliker's organ (KO) comprises a population of epithelial cells that are morphologically homogenous. However, recent results have revealed a number of unique and varied roles for KO during cochlear development. To understand the cells that mediate these effects, we used single cell RNAseq to characterize cellular transcriptomes within KO. Results indicate a striking degree of heterogeneity with multiple cell clusters present at different developmental time points. This presentation will describe the transcriptomic profiles of the different types of cells within the organ and attempt to relate their identities to the growing roles of KO in development and regeneration.

SYMP 45

Supporting Cell Regulation of Hair Cell Excitability in the Developing Cochlea

Dwight E. Bergles
JHMI

The columnar epithelial cells that form Kolliker's organ play an important role in triggering spontaneous activity in the auditory system prior to hearing onset. Pharmacological and genetic knockout studies indicate that activation of a metabotropic autoreceptor, P2ry1,

initiates a sequence of events leading to stimulation of inner hair cells through focal elevation of K⁺. Conversely, our recent studies show that sustained inhibition of P2ry1 results in the tonic firing of inner hair cells through elevation of extracellular K⁺. These results suggest that purinergic signaling through P2ry1 has bimodal effects on the excitability of hair cells during development.

SYMP 46

Fgf10 in Kölliker's Organ

Suzanne Mansour
University of Utah

Fibroblast growth factor 10 (Fgf10) is required for otic placode induction, otic epithelial morphogenesis and Reissner's membrane specification. During development, cochlear epithelial expression of Fgf10 becomes increasingly restricted to the lateral side of Kölliker's organ, but its specific role in that tissue is unclear. Taking conditional and timed approaches to interfere with Fgf10 expression or function, we have evidence suggesting that together with other cochlear Fgfs, Fgf10 is required for supporting cell differentiation, development of the third row of outer hair cells and auditory function. Progress in defining these roles will be presented.

SYMP 47

Development of the Tectorial Membrane

Guy Richardson
University of Sussex

The tectorial membrane is an acellular structure essential for normal hearing. Composed of precisely-oriented collagen fibrils imbedded in a matrix of glycoproteins that are only expressed at high levels in the inner ear, the tectorial membrane develops in intimate association with the greater and lesser epithelial ridges. Quite how such a structure forms during development remains to be resolved. Recent studies, however, suggest molecular crowding/confinement of collagens within a narrow space defined by a primordial, tectorin-based matrix, and signals linked to the expression patterns of PCP proteins in the underlying epithelium, play a significant role in determining collagen-fibril organization.

SYMP 48

The Sensory Competence of Kölliker's Organ

Angelika Doetzlhofer
Johns Hopkins Medical Institution

Previous studies found that non-sensory epithelial cells

of the Kölliker's organ have the capacity to generate sensory hair cells. The Kölliker's organ is a transient epithelial structure, located medial to the cochlear sensory domain. The sensory competence of Kölliker's cells is thought to be restricted by the Notch signaling pathway. Similar to supporting cells, Kölliker's cells express high levels of Hey1, Heyl and Hes1, which are known Notch effectors and hair cell fate repressors. Here, we will highlight the similarities and differences in how Notch signaling functions in Kölliker's cells and supporting cells and how it may limit their capacity for hair cell generation/regeneration.

SYMP 49

Injury Evoked Supporting Cell Activity in the Organ of Corti

Jonathan Gale
University College London

The organ of Corti is constantly subjected to cellular stress, be it mechanical, metabolic or excitotoxic. Hair cells are essential for the sensory capacity of the organ but it is the supporting cells, the cochlea's glial-equivalent cells, that minimise and prevent damage to the sensory epithelium. In response to damage, supporting cells maintain the barrier function of the epithelium, clear damaged cells by phagocytosis and minimise excitotoxicity by removing excess glutamate. The cellular and molecular mechanisms underlying these critical functions will be described and discussed.

SYMP 50

Thyroid Hormone, Cochlear Remodeling and the Development of Hearing

Douglas Forrest
National Institute of Health

Thyroid hormone (T3) promotes the development of hearing and disrupted T3 signaling is associated with hearing loss. In rodent models, T3 receptors coordinate the morphological and functional maturation of diverse cell types in the cochlea, including a prominent role in the remodeling of the sensory epithelium and the adjacent greater epithelial ridge. Within the cochlea, Dio2 and Dio3 deiodinase enzymes amplify or deplete levels of active hormone to control the rate of remodeling. Delayed or accelerated remodeling are both associated with deafness, suggesting that T3 determines critical developmental timing of cochlear remodeling to facilitate the appropriate onset of hearing.

Inferior Colliculus: Function, Connections & Plasticity

PD 49

Decoding Sound Texture Identity via Statistics of Neuron Ensembles

Xiu Zhai¹; Fatemeh Khatami²; Mina Sadeghi¹; Heather Read¹; Ian Stevenson¹; Monty Escabi¹

¹University of Connecticut; ²Univ. of Cal San Francisco

Although pure tones and noise stimuli have been used extensively in auditory neuroscience, there is growing evidence that the higher-order sound statistics, such as the correlations between frequency channels or the sound modulation spectrum, play a key role in sound recognition and perception. How the brain encodes such sound statistics and utilizes them for sound identification is largely unknown. Here we examine the responses of neuron ensembles in the auditory midbrain (inferior colliculus) of unanesthetized rabbits listening to natural sound textures using 16 and 32 channel neural recording arrays. Sound textures, such as running water, fire, wind, and speech babble have complex, but homogeneous, higher-order statistics, and are perceptually salient. We use texture synthesis (McDermott & Simoncelli 2011) to manipulate the different statistics of natural sound textures and explore their neural representation. Five texture sounds (running water, bird chorus, crackling fire, rattling snake and crowd noise) were manipulated by progressively incorporating statistical structure from the power spectrum, amplitude marginals, modulation spectrum, and the sound correlation structure. We demonstrate that correlated firing between frequency organized recording sites are modulated by each of the tested sound statistics and that these neural correlations can be used to decode and identify sound textures. Specifically, stimulus-driven spectro-temporal correlations were measured across the frequency organized recording array and a minimum distance classifier was applied to the ensemble correlation activity to identify the delivered sounds. For the original texture sounds, the classifier was able to decode and identify the original sound approaching near perfect accuracy (~90%). Spectral correlations between recording locations had slightly higher performance and were somewhat more informative than temporal correlations alone. The performance of the classifier improved as additional statistics were added to the synthetic variants and approached the performance for the original sounds when the full set of statistics was included (~80% accuracy). Finally, the decoding accuracy improved with sound duration with evidence accumulation times in the order of approximately 1 sec, mirroring human trends. These findings suggest that coordinated firing in auditory midbrain ensembles provide a statistical signature that may contribute to perception and recognition of texture sounds (supported by NIDCD R01DC015138).

PD 50

Decoding Complex Sounds from Activity Patterns

Typhaine Dupont¹; Richard Felix II²; Olivier Postal³; Christine Petit⁴; Nicolas Michalski⁵; **Boris Gourevitch**⁶
¹INSERM; ²Washington State University; ³Pasteur Institute; ⁴Génétique et Physiologie de l'Audition, Institut Pasteur; ⁵Institut Pasteur; ⁶CNRS

Neurons from the auditory system have long been characterized through their SpectroTemporal Receptive Field (STRF), which is basically a linear approximation of the spectrogram having evoked a spike. This method, while useful for neuron features assessment, has been shown to perform poorly in predicting neural activity from acoustically complex sounds (coding) or reconstructing sounds from spike trains (decoding). This may be due to the specific neural code in the auditory system, and especially in the auditory cortex, which is based on very precise spike timing. Insofar as this is the case, coincident spiking and temporal patterns of spikes support most of the information about acoustic cues, and these features are largely ignored by STRFs. In this preliminary study, we present a simple and intuitive jackknife-like decoding method to predict stimulus information from multiple spike trains, here applied to auditory processing. We show that temporal patterns of spikes allow for the accurate reconstruction of complex acoustic cues based on the activity of small numbers of neurons. We then compare reconstruction performance of acoustic stimulus between neurons from the inferior colliculus, the thalamus and the primary auditory cortex of mice. This very generic decoding method can also be reversed to perform a completely non-parametric prediction of evoked neural firing rate.

PD 51

Two novel classes of inferior colliculus neurons, one glutamatergic and one GABAergic, labeled in Neuropeptide Y-Cre mice

Marina A. Silveira¹; Alexander P. George¹; Justin Anair¹; Michael T. Roberts²

¹University of Michigan; ²Kresge hearing research - University of Michigan

Located in the midbrain, the central nucleus of the inferior colliculus (ICC) integrates information from numerous auditory nuclei and is an important hub for sound processing. Despite its importance, little is known about how defined neuron types in the ICC function within the auditory pathway. We are applying a multi-faceted approach to understand how specific classes of neurons labeled by defined molecular markers function within neural circuits in the ICC. We have identified that both Neuropeptide Y (NPY) and Neuropeptide Y Receptor 1 (NPY Y₁) are expressed in the IC. NPY is

a 36 amino-acid neuropeptide that is essential for the modulation of excitability in the central nervous system. In order to better understand how NPY functions in the IC, we are working with two mouse lines: NPY-hrGFP and NPY-IRES-Cre x Ai14. In both animals, we found that NPY neurons are distributed along the rostral-caudal axis of the IC. Immunohistochemical staining against GAD67 suggested that NPY neurons labeled in the NPY-Cre x Ai14 mouse can be divided into GABAergic and glutamatergic subclasses. Immunoreactivity for NPY demonstrated that only the GABAergic population synthesizes NPY in adult mice. In agreement with that, in the NPY-hrGFP mouse, GFP-expressing neurons are exclusively GABAergic. To examine the physiology of NPY neurons, we targeted whole cell patch clamp recordings to tdTomato or hrGFP-expressing neurons in acute brain slices. These recordings demonstrated that NPY-tdTomato neurons exhibited both adapting (41.7%) and sustained (58.3%) firing patterns. NPY-hrGFP neurons exclusively exhibited a sustained firing pattern. Post hoc reconstruction of the morphology of recorded neurons using biocytin-streptavidin histochemistry suggests that both GABAergic and glutamatergic NPY neurons are subtypes of stellate cells. In NPY-Cre x Ai14 mice, we used a Cre-dependent virus to drive GFP expression in the axons of Cre-expressing neurons. This showed that NPY neurons project to both contralateral IC and auditory thalamus. Next, using channelrhodopsin-assisted circuit mapping in NPY-Cre x Ai14 mice, we found that NPY neurons receive both excitatory and inhibitory input from the contralateral IC. Combined, our results suggest that GABAergic and glutamatergic NPY neurons represent two novel classes of ICC stellate neurons, at least one of which projects to the auditory thalamus. We are currently working to more fully identify and differentiate the postsynaptic targets of GABAergic and glutamatergic NPY neurons and to determine the sources of input to these neurons. Future experiments will be aimed at determining how NPY modulates excitability in the IC.

PD 52

Non-auditory projections to the inferior colliculus

Bas MJ. Olthof; Sarah E. Gartside; Adrian Rees
Institute of Neuroscience, Newcastle University

The inferior colliculus (IC), the principal midbrain nucleus in the auditory pathway, processes and integrates virtually all ascending auditory information. In addition, the IC receives extensive descending connections from the auditory cortex modulating sound processing in the IC. These cortico-collicular connections play an important role in auditory processing, and may sub-serve auditory predictive coding. Although cortico-collicular projections are well established, little is known about the

extent to which the IC receives inputs from non-auditory structures. Here we aimed to map all the non-auditory projections to the IC in the rat using retrograde and anterograde tracers.

Six Lister hooded male rats (250-300g) were anaesthetised and received injections of retro beads (Lumafluor®) into the IC. Animals were allowed to recover and, 72 hours later, were transcardially perfused with heparinized 0.1 M PBS and 4% PFA. Brains were harvested, post fixed, and cryoprotected in 30% sucrose. Coronal sections (40 µm) through the whole brain were cut using a cryostat. The sections were collected on slides, air dried, dipped in DAPI to label the nuclei and stored at -20 C. All sections were visually inspected for the presence of retro beads using a wide field microscope with appropriate filters. The presence of beads was recorded, and mosaic images were obtained at high power using a wide field microscope.

As expected, pyramidal cells, principally in layer V, of the auditory cortex showed a high density of retro beads. Cells were labelled in the ipsi- and contralateral cortex with a higher proportion ipsilateral to the injection. We also observed labelling from many non-auditory regions including, but not limited to, prefrontal, somatosensory (S1 and S2 but not barrel field), motor (M1, M2), and visual (V1, V2) cortices, nucleus accumbens, amygdala, hypothalamic areas, superior colliculus and the dorsal raphe nucleus. To confirm these projections, we injected fluorescently labelled dextran anterograde tracers into auditory, prefrontal, somatosensory, and visual cortices in eight rats. The presence of fluorescent labelling in the IC confirmed the conclusion of the retrograde experiments. Moreover, these studies highlighted that different regions of the IC receive varying densities of projections from auditory and non-auditory cortical regions.

These results demonstrate that the IC receives descending projections from many structures outside the auditory pathway. These non-auditory projections to the IC suggest that the processing of sound information is influenced by sensory, cognitive, and executive inputs at a much earlier stage than previously believed.

Acknowledgements

Supported by BBSRC PG BH154379

PD 53

Sex Differences in Subcortical Timing and Frequency Encoding Emerge at Different Rates Across Development

Jennifer Krizman; Silvia Bonacina; Sebastian Otto-Meyer; Nina Kraus

Human subcortical auditory processing is sexually dimorphic. Relative to males, females have earlier latencies in their auditory brainstem response (ABR) to clicks and tones and frequency-following response (FFR) to speech syllables. Additionally, female FFRs show more robust encoding of frequencies above the fundamental. Because of differences in length and stiffness of the basilar membrane between males and females, the cochlea has been a presumed origin for these processing differences.

To test whether the cochlea is the source of sex differences in subcortical auditory processing, we analyzed suprathreshold click-ABRs and FFRs to 'd'; in 516 participants (250 female) across three age groups: 3-5 year olds, 14-15 year olds, and 22-26 year olds. Specifically, we compared click-ABR latencies, FFR latencies, FFR frequency encoding, and non-stimulus activity, a measure not previously analyzed for sex differences but known to show a developmental effect. The cochlea is structurally and functionally adult-like at birth, thus, if sex differences in auditory processing stem solely from cochlear differences, then we should observe sex differences in auditory processing that are constant across these three age groups.

Instead we find that sex differences in peak timing and frequency encoding emerge across development. In the youngest age group, some peak latencies, including ABR click I latency, did not show sex differences, though these peaks did differ between adolescent and young adult males and females. High frequency encoding also did not differ between the 3-5 year old males and females. Remarkably, with increasing age, both latency and high-frequency encoding became more distinct between the sexes. These differences were driven by later latencies and smaller frequency encoding in males. Sex differences in auditory processing were not driven by changes in non-stimulus activity, as this measure only showed a decline between early childhood and adolescence that did not differ between the sexes.

In conclusion, sex differences in subcortical auditory processing emerge over different developmental time courses. Thus, sex differences cannot be attributed solely to the cochlea but may be the result of continued maturation of central auditory structure and function. Given the differing effects of sex and age on latency, frequency encoding, and non-stimulus activity, these measures likely reflect different aspects of auditory processing.

Supported by the Knowles Hearing Center and NIH R01 HD069414.

PD 54

Activation of Cortical Kainate Receptors Modulates Subcortical Balance of Excitation and Inhibition

Jeff Lin; Jeongyoon Lee; **Guangying Wu**
The George Washington University

Cortical activities are characterized by different levels of synchronized oscillations. Activation of kainate receptors induces gamma oscillations in the neocortex. It remains obscure whether and how these cortical oscillations could affect subcortical sensory processing via extensive descending projections. To address the neural circuitry mechanisms behind it, we developed a new strategy to silence or alter cortical oscillations when paired with *in vivo* whole-cell recordings from auditory midbrain neurons of mice. Dual recordings revealed that the local field potentials of the auditory midbrain and the primary auditory cortex were more coherent when the cortex was characterized by increased oscillations in beta and low gamma ranges. The spectrotemporal balance between excitatory and inhibitory synaptic inputs in the midbrain was dynamic and can be associated with the levels of cortical oscillations within this range. These results point to the power of top-down control by the descending excitatory circuit, which could dynamically modulate local neural circuits to adjust the stimulus sensitivity and selectivity.

PD 55

Prenatal Exposure to Valproic Acid Disrupts Morphology and Ascending Projections to the Central Nucleus of the Inferior Colliculus

Yusra Mansour¹; Ryan Zimmerman¹; Tatiana Fech¹;
Randy J. Kulesza²

¹Lake Erie College of Osteopathic Medicine; ²Anatomy

Prenatal exposure to the antiepileptic valproic acid (VPA) is associated with an increased risk of autism spectrum disorder (ASD) in humans and is a validated and biologically relevant animal model of ASD. The majority of human subjects with ASD have some degree of auditory dysfunction and rats exposed to VPA in utero have abnormal neuronal responses to sound and mapping of sound frequency in the cerebral cortex and hyperactivation in the central nucleus of the inferior colliculus (CNIC) after auditory stimulation. Additionally, VPA exposure results in significantly fewer neurons in the cochlear nuclei (CN) and superior olivary complex (SOC) and surviving neurons demonstrate marked dysmorphology. Furthermore, VPA exposure results in reduced immunolabeling for the calcium binding proteins calretinin and calbindin in the CN and SOC. Herein we used a combination of morphometric techniques, histochemistry, immunofluorescence, and retrograde tract tracing to examine the impact of

prenatal VPA exposure on neurons in the CNIC and their ascending inputs. Our results indicate that prenatal VPA exposure resulted in significantly fewer neurons in the CNIC but surviving neurons had significantly larger somata. VPA exposure resulted in significantly fewer dopaminergic terminals in the CNIC but had no impact on the proportions of CNIC neurons associated with perineuronal nets. Finally, deposits of the retrograde tract tracer Fast Blue in the CNIC resulted in significantly lower proportions of labeled neurons in the nuclei of the lateral lemniscus, SOC and CN. Together, these results indicate that in utero VPA exposure significantly impacts structure and function of the entire auditory brainstem and had a preferential impact on neurons providing long-range ascending inhibitory input to the CNIC.

PD 56

Chronic Bilateral Stimulation through Cochlear Implants during Development Can Reverse the Effect of Early-Onset Deafness on Neural ITD Sensitivity

Woongsang Sunwoo¹; Bertrand Delgutte²; Yoojin Chung²

¹Dept. of Otolaryngology, Harvard Medical School; Eaton-Peabody Lab, Mass. Eye and Ear; Dept. of Otolaryngology, Gachon University Gil Medical Center, S. Korea; ²Dept. of Otolaryngology, Harvard Medical School; Eaton-Peabody Lab, Mass. Eye and Ear

Background

Bilateral cochlear implant (CI) users with a pre-lingual onset of hearing loss show poor sensitivity to interaural time differences (ITD) compared to those with post-lingual hearing loss. Similarly, neural ITD sensitivity in the inferior colliculus (IC) of rabbits that are deafened as neonates is degraded compared to animals deafened as adults. Here we investigated whether chronic bilateral CI stimulation during development can reverse the effect of early-onset deafness on ITD sensitivity.

Methods

Four Dutch-belted rabbits were deafened as neonates with daily injection of neomycin and then bilaterally implanted at 2 months of age. Starting just after implantation, they received daily environmental stimulation (5 hrs/day) with wearable sound processors programmed with the "Fundamental Asynchronous Stimulus Timing" (FAST) strategy designed to deliver ITD information effectively with bilateral CI. Single-unit recording from the IC using an unanesthetized preparation commenced at 5 months of age. Stimuli were periodic trains of biphasic electric pulses with varying pulse rates (20 - 640 pps) and ITDs (-2000 to +2000 μ s). The results are compared to measurements from adult-deafened rabbits (Chung et

al., J Neurosci. 36:5520) and early-deafened rabbits that did not receive daily stimulation.

Results

More IC neurons in the stimulated rabbits showed significant ITD sensitivity in their overall firing rate (77%) compared to unstimulated animals (62%). The difference in prevalence of ITD sensitivity was most prominent at high pulse rates (>200 pps). ITD sensitivity measured by the ITD signal-to-variance ratio (STVR) and neural ITD discrimination thresholds also showed improvements in the stimulated animals compared to unstimulated animals, with the largest effect found at high pulse rates. The fraction of ITD sensitive neurons, and ITD STVRs and thresholds in the stimulated animals were comparable to those from adult-deafened animals at high pulse rates.

Conclusions

Chronic bilateral cochlear implant stimulation during development can partly reverse the degradation in neural ITD sensitivity resulting from early-onset deafness. The effect is most pronounced in response to high-rate stimulation.

Funding: NIH grant R01 DC005775.

Spontaneous Otoacoustic Emissions and Active Amplification in the Inner Ear

Chairs: Pim van Dijk & Dáibhid Ó Maoiléidigh

SYMP 51

Making an Effort to Listen: Mechanical Amplification by Ion Channels and Myosin Molecules in Hair Cells of the Inner Ear

AJ Hudspeth

The Rockefeller University

Hearing is enhanced by an active process that amplifies the ear's mechanical inputs several hundredfold, sharpens frequency discrimination to 0.2 %, and compresses a millionfold range of acoustic input into a hundredfold range of output. Spontaneous otoacoustic emissions emerge from ears when the active process becomes so exuberant as to foster instability. Cooperativity between mechano-electrical-transduction channels confers negative stiffness on the hair bundle, which together with adaptation motors elicits a dynamical instability that underlies the active process. Experiments on hair bundles indicate that their operation near this instability, a Hopf bifurcation, accounts for the four characteristics of the active process.

SYMP 52

Whistling While it Works: Spontaneous Otoacoustic Emissions and the Cochlear Amplifier

Christopher Shera

Departments of Otolaryngology and Physics & Astronomy, University of Southern California

Spontaneous otoacoustic emissions (SOAEs) are commonly thought to arise through a mechanism first proposed by Gold (1948). In the language of dynamical-systems theory, Gold's local-oscillator model supposes that cochlear hair cells operate near a "critical point" (e.g., a "Hopf bifurcation") where spontaneous oscillation sets in. SOAEs occur when the control mechanisms needed to hold a hair cell close to the critical point break down. An alternative model, first proposed by Kemp (1979), proposes that SOAEs are continuously self-evoking stimulus-frequency emissions, a global collective phenomenon in which SOAE frequencies are determined not by local cellular properties, such as hair-bundle adaptation or transduction kinetics, but by non-local characteristics such as round-trip traveling-wave phase shifts and the impedance mismatch at the cochlear boundary with the middle ear. This presentation introduces these two models, reviews the evidence that supports them, and discusses their relationship to one another and to possible mechanisms of cochlear amplification.

SYMP 53

Amplification by Noisy Oscillators

Dáibhid Ó Maoiléidigh

Department of Otolaryngology - Head & Neck Surgery, Stanford University School of Medicine

The hair bundles of many auditory and vestibular systems are active oscillators — hair bundles have been observed to oscillate spontaneously and to amplify their responses to weak periodic stimuli. In the mammalian cochlea, somatic motility, mechanotransduction channels, and electrochemical gradients may also form an active oscillatory module, which can be coupled to mechanically active hair-bundles. I will describe how spontaneous oscillations and amplification can be suppressed or enhanced by an oscillator's environmental conditions and intrinsic noisy fluctuations. The ear's ability to distinguish low-level sounds from noise is likely determined by the operating points of active hair-cell oscillators within the cochlea.

SYMP 54

Spontaneous Otoacoustic Emissions and Near-Threshold Tone Detection

Pim Van Dijk¹; Glenis R. Long²

¹Dept. of Otorhinolaryngology, University Medical Center Groningen; ²The Graduate Center, City University of New York

In the ear, internal noise in the cochlear amplifier is presumably responsible for instabilities of spontaneous otoacoustic emissions. In principle, this noise could define our threshold of hearing. However, we will show that during a tone-detection task, the SOAE exhibits a nearly deterministic response to an external stimulus at the SOAE frequency, suggesting that under these circumstances internal noise in the cochlear amplifier plays no limiting role. A consequence of this finding is that subsequent noise sources (e.g. at the inner hair cell) must define the threshold of hearing. In other words, noise in the cochlear amplifier is subthreshold.

SYMP 55

Lizard SOAE Reflect an Active Process in the Hair-Cell Bundles

Geoffrey A. Manley; Christine Köppl

Department of Neuroscience, School of Medicine and Health Sciences, Carl von Ossietzky University Oldenburg

Despite their variable body temperatures and very low endocochlear potentials, many lizard audiograms are only a few dB less sensitive than those of most mammals and birds. The question arises as to how lizards achieve this and whether the mechanisms underlying their sensitivities are the same. Furthermore, the basilar membranes of lizards are not locally, sharply tuned to frequency (Peak and Ling, 1980, *J Acoust Soc Amer* 67:1736-1745). Instead, early observations of hair-bundle movements in isolated papillae indicated the hair-cell bundles are the tuned elements (Frishkopf and DeRosier, 1983, *Hear Res* 12:393-404 and Holton and Hudspeth, 1983, *Science* 222:508-510).

Among land vertebrates, lizards are the most robust producers of SOAE and the spectral patterns of a given species to some extent reflect papillar anatomy. The characteristics of lizard SOAE (e.g. their sensitivity to changes in temperature and calcium concentrations) are essentially identical to those observed in vitro using amphibian sacculus hair cells. In lizards, SOAE have centre frequencies above 1 kHz and the corresponding papillar area(s) always contain hair cells whose stereovillar bundles show two opposing orientations. This feature, which is unique among amniotes, made it possible to design a unique test for the origin of

otoacoustic emissions from these hair cells. Otoacoustic emissions were electrically evoked at frequencies in the kHz range, while simultaneously biasing hair-cell transduction by low-frequency acoustic stimulation. This revealed the separate contributions from each of the oppositely oriented hair-cell populations to the high-frequency, electrically-evoked otoacoustic emissions. If emissions originated from a prestin-based membrane motor as in mammals, the phases of emissions emitted from the two hair-cell populations due to the electrical stimulation should be the same. In fact, they were 180° out-of-phase, indicating that the active element in lizards is located in the bundles (Manley et al. 2001, Proc. Nat. Acad. Sci. USA. 98:2826-2831. In addition, emissions emitted by only one polarity population were much larger than emissions generated in the absence of acoustic biasing, consistent with mutual cancellation of the electrically evoked emissions generated by the two populations. Thus, in lizards, a hair-cell-bundle-based, active mechanism boosts sensitivity. This mechanism may be further enhanced by having oppositely-oriented bundles that reciprocally contribute to oscillations.

SYMP 56

How Does Sound Vibrate Inner Ear Tissues in Different Species?

John S. Oghalai

USC Caruso Department of Otolaryngology - Head and Neck Surgery

Traditionally, frequency tuning within the auditory papilla of most non-mammalian species is thought to derive primarily from the ion channel resonances and/or bundle mechanics within each individual sensory hair cell. In contrast, tuning within the mammalian cochlea is thought to derive primarily from the passive and active mechanics that create and amplify the basilar membrane traveling wave. Our group uses optical coherence tomography to measure sound-induced vibrations within the inner ear of different species to understand these differences. Furthermore, we study multiple locations within the inner ear in an effort to localize the processes underlying frequency tuning and amplification. Our ultimate goal is to understand the fundamental biomechanical processes involved in normal and impaired hearing.

SYMP 57

Spontaneous Emissions as Biomarkers for Tectorial Membrane Defects in Mice

Mary Ann Cheatham

Northwestern University

Although spontaneous otoacoustic emissions (SOAE)

are common in humans, most laboratory animals are rarely emitters. It is, therefore, provocative that these behaviors can be duplicated in mice but primarily in animals with abnormal tectorial membranes (TM) due to genetic manipulations. Our work on mutant mice indicates that structural changes to the TM increase the incidence of SOAEs. Because a surprising number of human mutations affect genes targeted to the TM, and because SOAEs reflect the feedback process associated with normal outer hair cell function, TM mutants can be used to enhance our understanding of the processes associated with cochlear amplification.

Auditory Cortex: Human Studies

PD 57

Auditory Texture Models Derived from Task-Optimized Deep Neural Network Representations

Jenelle Feather; Josh H. McDermott

Massachusetts Institute of Technology

Textures are distinguished from other sound signals by homogeneity in time. The brain is believed to take advantage of this homogeneity by representing textures with statistics that average information across time. Models of texture perception are based on such statistics, and are commonly evaluated by synthesizing stimuli that produce the same representation in the model as a natural stimulus. Such synthetic sounds should evoke the same texture percept as the natural sound if the model replicates the representations underlying texture perception. Prior auditory (and visual) texture models produce textures that resemble natural textures, but use ad hoc statistics derived through trial and error. Further, traditional texture models rely on statistics measured from multiple stages of the underlying sensory cascade (for instance, statistics from cochlear filters as well as subsequent stages of modulation filters), but it is arguably implausible that perceptual decisions could be based directly on the output from the cochlea. We explored whether a single, simple class of statistic measured at a single stage of an auditory model could replicate the multistage, multi-statistic representation of traditional texture models. We compared textures generated from three different sets of statistics: (1) the power from each of the first-layer filters from a task-optimized convolutional neural network, (2) the power from each of a set of spectrotemporal filters commonly used as a model of primary auditory cortex, and (3) statistics in the the McDermott and Simoncelli (2011) texture model (consisting of power and other marginal statistics measured from cochlear and temporal modulation filters, as well as correlations between filters). When cochlear statistics were included in the synthesis constraints, the learned filters and the spectrotemporal filters both produced textures that were as realistic and recognizable as those from the McDermott and

Simoncelli model. However, when cochlear statistics were omitted, only textures generated from the learned filters maintained a high level of realism and recognizability – textures generated from the spectrotemporal filters became less realistic and recognizable when not explicitly constrained by cochlear statistics. These results held across convolutional networks trained on three different tasks: word identification, speaker identification, and genre classification. The results suggest that the learned filters incorporate peripheral information that matters for a task and that matters for perception, and that texture information could be represented at a single stage of cortical representation.

PD 58

Functional organization of human perisylvian cortex in response to speech

Bahar Khalighinejad¹; Sam Norman-Haignere²; Jose Herrero³; Ashesh Mehta⁴; Nima Mesgarani⁵

¹*Columbia University*; ²*HHMI Postdoctoral Fellow of the Life Sciences Research Foundation*; ³*Feinstein Institute for Medical Research*; ⁴*The Feinstein Institute for Medical research*; ⁵*Zuckerman Institute for Brain Research, Columbia University, Program in Neurobiology and Behavior, Columbia University, Department of Electrical Engineering, Columbia University*

Auditory cortex is thought to be organized into different cortical fields, each of which encodes multiple acoustic properties. Functional characterization of human cortical fields has largely depended on non-invasive brain imaging techniques such as fMRI. However, because fMRI indirectly measures neural responses via hemodynamic activity, it has limited temporal resolution, making it difficult to study the neural encoding of speech features which vary on the timescale of milliseconds. Thus, here we used direct intracranial recordings from 12 human subjects that were implanted with depth and grid electrodes.

We recorded neural data in response to 40 minutes of natural speech and other commonly heard sounds. Using 350 electrodes in primary and secondary auditory cortices, we created seven cortical maps based on tuning for each of seven different acoustic features: frequency, latency, temporal modulation, spectral modulation, phonetic features, speaker features, and speech-specificity. The frequency and latency preferences were calculated from spectro-temporal receptive fields (STRF), estimated from each electrode. The temporal and spectral modulation maps were calculated by filtering the acoustic spectrograms through different cochlear filters and then by selecting the cochlear filters that best represent the temporal modulation preference

and spectral modulation preference of the neural data.

Consistent with prior fMRI studies, we found that topographic maps of frequency preference, latency, temporal modulation, and spectral modulation were dependent on two axes of medial-lateral and posterior-anterior direction in human auditory cortex. But contrary to prior fMRI studies, we did not find any specialized region for analyzing phonetic features, meaning that all of the four regions of medial Heschl's gyrus (HG), lateral Heschl's gyrus, planum temporale, and superior temporal gyrus (STG) encode the distinctive acoustic features of phonemes, and there was not a significant difference between their preferred phonetic feature. In addition, we found that information about speaker identity was better encoded in early auditory areas such as HG in comparison with secondary areas such as STG. Finally, we found that electrodes in STG selectively responded more to human speech compared to nonspeech sounds, such as animal vocalization, tones and music, confirming prior reports of speech-selectivity based on fMRI.

Together, these findings advance our knowledge of the representational and functional organization of human auditory cortex and pave the way toward more complete models of cortical speech processing in the human brain.

PD 59

Neural Substrates of Auditory Sequence Processing and Language Skill in Early-to-mid Adolescence

Manon Grube¹; Faye Smith¹; Sukhbinder Kumar¹; Heather Slater¹; Timothy D. Griffiths²

¹*Newcastle Auditory Group*; ²*Wellcome Centre for Human Neuroimaging, University College London; Institute of Neuroscience, Newcastle University*

This work seeks the neural substrates of auditory sequence processing and language skill in the adolescent brain. First findings from 42 early adolescents suggested a correlation between grey matter density in the left intra-parietal sulcus (IPS) and composite measures (first principal components) of auditory as well as language skills (Grube et al., Society for Neuroscience 2011: XX27 509.10). The current work assesses correlations between grey matter density and a systematic battery of tests of melodic and rhythmic sequence processing over the course of adolescent development.

The study is part of a large initiative at a local high school (St. Thomas More Catholic School), where we carry out extensive behavioral testing to assess auditory and language skills on whole-year group cohorts (see PMID 22951739 for initial report). This study was carried out on subgroups from the larger assessments of approximately n = 240 each. Auditory sequence

processing and language skill and their structural correlates were measured in two sub-groups of two whole-year groups with a mean age 12 (n = 20) and 14 (n = 24), respectively. Structural MRI scans were T1 weighted images, acquired using high-resolution sequence (resolution, 1x1x1 mm; TR, 8.278 ms) in a Philips 3T whole-body scanner and voxel-based morphometry (VBM) implemented in SPM 8 is applied to seek correlations between grey matter density and auditory and language skill, taking into account the effect of non-verbal intelligence.

We previously developed the idea that there is a change in the behavioral link between auditory sequencing and language skill from early to mid-adolescence toward a stronger correlation between language skills and higher-order complexity in the older group (Grube et al., Society for Neuroscience 2016: HHH3 85.07). This work examines whether this altered behavioral relationship is accompanied by altered correlations between the grey matter density and sequence measures in IPS.

PD 60

Evidence for Linear but not Helical Automatic Representation of Pitch in the Human Auditory System

Tamar I. Regev¹; Israel Nelken²; Leon Y. Deouell³
¹*Edmond and Lily Safra Center for Brain science, Hebrew University;* ²*Edmond and Lily Safra Center for Brain Sciences and Department of Neurobiology, Silberman Institute of Life Sciences, Hebrew University;* ³*Edmond and Lily Safra Center for Brain Sciences and Department of Psychology, Hebrew University*

The perceptual organization of pitch is frequently described as helical - with a monotonic dimension of pitch-height and a circular dimension of pitch-chroma (pitch class). However, it is not clear whether the pitch-helix model describes automatic, preattentive processes in the human auditory system. We addressed this question using EEG in response to unattended tone sequences. We provide evidence that it is height, rather than chroma, that is processed preattentively; furthermore, height is encoded in the activity of frequency channels whose width is substantially wider than the critical band. Musicians, who were able to classify pitch-chroma across octaves, were presented with sequences of five tones distributed across four octaves, while attending to a silent film. In a control condition, these five tones had five different chromas, whereas in the experimental condition four tones were of the same chroma and the middle tone of a different chroma. To test whether the mismatch negativity (MMN) is elicited in response to a chroma change, implying automatic processing of pitch-chroma, we compared the ERPs elicited by the middle

tone in the two conditions. No MMN was elicited to a chroma change in the unattended sequences, even for participants who could perfectly detect the chroma change while attending to it. In another control sequence, a change in pitch-height robustly elicited the MMN in the same performers. This finding suggests that height is processed pre-attentively whereas chroma requires higher cognitive processes. Importantly, in all unattended sequences, ERPs were sensitive to the distribution of heights, on various timescales. N1 was sensitive to the distance between the current tone and the global mean height of the sequence. P2 was sensitive to the distance between the current tone and the previous one. We propose a biophysical model of adapting neuronal populations with wide tuning curves (about one octave) and different time constants of recovery from adaptation to account for these results.

PD 61

Investigating the Cortical Tracking of Melodic Expectation during Naturalistic Music Listening

Giovanni di Liberto¹; Claire Pelofi²; Roberta Bianco³; Alain de Cheveigné⁴; Shihab A. Shamma⁵
¹*École Normale Supérieure;* ²*Institut de Neurosciences des Systèmes;* ³*UCL Ear Institute;* ⁴*École Normale Supérieure; UCL Ear Institute;* ⁵*Neural Systems Laboratory, Institute for Systems Research, 2Sensory Perception Laboratory, Ecole Normale Supérieure*

Research in speech perception has demonstrated that cortical signals track changes in acoustic and linguistic properties, ranging from low-level features such as the acoustic envelope (Ding and Simon, 2014) to higher-level linguistic properties such as phonemes (Di Liberto et al., 2015). Moreover, this cortical tracking is modulated by high-order cognitive factors, such as attention and intelligibility. Similar to speech, music is another highly structured acoustical signal whose cortical processes have seldom been explored in naturalistic music listening conditions. Here, we investigate the tracking of melodic expectation and how it is affected by musical expertise. Electroencephalographic (EEG) data were recorded while participants, ten musicians and ten non-musicians, listened to two-minute long pieces of monophonic classical music for about an hour. Each piece was presented in random order and repeated three times over the course the experiment to assess for possible effects of prior exposure. Familiarity ratings were collected for each trial and showed an increase in familiarity to the piece with repetition for both musicians and non-musicians. A statistical model of melodic structure (Pearce, 2005) was used to estimate the likelihood of musical notes, likely reflecting their subjectively perceived expectedness. Linear system identification methods (temporal response function –

TRF; canonical correlation analysis – CCA) were used to assess whether and how strongly the EEG signals reflect the changes in note-likelihood, thus providing us with a measure of cortical tracking of melodic expectation in both musicians and non-musicians. Our results indicate that low-frequency EEG signals track melodic expectation. This phenomenon was strongest when using a model of melodic expectation that took into account stimulus repetition. Furthermore, musical expertise modulated the cortical tracking of melodic expectation both in magnitude and latency. By providing evidence of cortical tracking of high-level musical features, this work opens a new avenue in the exploration of music cognition in naturalistic listening conditions.

PD 62

Extended Frontal Networks For Auditory Cognition

Abigail Noyce¹; Rebecca Lefco¹; James Brissenden¹; Sean Tobyne¹; David Somers¹; Barbara Shinn-Cunningham²

¹*Boston University*; ²*Carnegie Mellon University*

The prefrontal cortex is often thought to serve as a general-purpose processing center for difficult or abstract cognitive computations. However, discrete bilateral auditory attention structures have been identified in human caudolateral frontal cortex, as have frontal elements of a speech and language network. The transverse gyrus bridging precentral sulcus (tgPCS) and caudal inferior frontal sulcus (cIFS) are consistently more strongly recruited during auditory attention and working memory (regardless of linguistic content) than during corresponding visual tasks (Michalka et al 2015, Noyce et al 2017). Analyses of fMRI resting-state functional connectivity between posterior sensory cortex and LFC suggested additional sensory-biased regions extending rostrally along the inferior frontal sulcus and frontal operculum (Tohyne et al 2017). We collected fMRI while subjects (n=15) performed auditory and visual 2-back working memory (stimuli were animal vocalizations and human face photographs, respectively). Directly contrasting auditory 2-back with visual 2-back revealed additional bilateral auditory-biased structures in the frontal operculum, as well as additional bilateral visual-biased structures. Resting-state functional connectivity analyses confirm that auditory-biased frontal regions and visual-biased frontal regions consistently assort into two discrete networks, grouping with posterior auditory and visual attention regions respectively. Further analysis of whole-brain functional connectivity from each auditory-biased frontal structure shows that different sub-regions of temporal cortex are preferentially connected to tgPCS versus cIFS versus FO. This differential connectivity has implications for functional specialization of auditory-biased frontal regions. These functional specializations

may include directing attention, subvocal rehearsal, linguistic processing, and fine perceptual discrimination. Frontal lobe structures play a key role in auditory attention and working memory.

PD 63

Examining the Effects of Noise Exposure on the Auditory System Using Evoked Potentials

Christopher Niemczak¹; Sean Kampel²; Curtis J. Billings²; Naomi Bramhall²

¹*Syracuse University*; ²*VA RR&D NCRAR*

Background

In animal models, noise-induced loss of cochlear synapses is associated with decreased suprathreshold auditory brainstem response (ABR) wave 1 amplitudes. We have previously demonstrated decreased ABR wave I amplitude in young Veterans with high levels of noise exposure during their military service and non-Veterans with a history of firearm use, suggesting that noise-induced synaptopathy may occur in humans. To investigate how noise-induced reductions in ABR wave I amplitude impact the central auditory system, we measured the ABR, the middle latency response (MLR), and the cortical auditory evoked potential (CAEP) in young Veterans and non-Veterans with normal audiograms and varying levels of noise exposure.

Methods

ABR, MLR, and CAEP measures were obtained in military Veterans and non-Veteran controls aged 19-35 years (40+ participants). ABR stimuli consisted of 90, 100, and 110 dB p-pe SPL tonebursts (4 and 6 kHz). The MLR and CAEP were obtained simultaneously in response to a 100 μ s click at four intensity levels (75, 85, 95, 105 p-pe SPL). Pure tone stimuli (4 and 6 kHz) at four intensity levels (50, 60, 70, 80 dB SPL) were also used to elicit the CAEP alone. ABR wave I amplitude was measured from the peak to the following trough. Rectified area measures with fixed latency cutoffs were calculated for the entire complex of both the MLR (4-80 ms) and the CAEP (30-330 ms). Self-reported noise exposure was assessed using the Lifetime Exposure to Noise and Solvents Questionnaire (LENS-Q). Participants also completed a questionnaire that asked if they experienced frequent or constant tinnitus.

Results

In response to a click stimulus, participants with tinnitus showed a reduction in MLR area compared to those without tinnitus, but an increase in CAEP area. Both low ABR wave I amplitude and high reported noise exposure history were associated with decreased MLR area and with decreased CAEP area among participants without tinnitus.

Conclusions

Reduced MLR and CAEP area in individuals with low ABR wave I amplitudes suggests that subclinical peripheral deficits in auditory nerve input may be associated with impaired processing at higher levels of the auditory system. In contrast, among participants with tinnitus, reduced MLR, but increased CAEP area suggests central compensation. This is consistent with the central gain hypothesis that in response to reduced peripheral input, individuals with tinnitus experience hyperactivity or loss of inhibition in the central auditory system that leads to the tinnitus percept.

PD 64

Complete or partial loss of hearing in humans caused by lesions of bilateral auditory cortex or auditory radiations

Ryohei Akiyoshi; Mitsuko Shindo; Kimitaka Kaga
National Institute of Sensory Organs, National Tokyo Medical Center

Complete or partial loss of hearing due to lesions of bilateral auditory cortex or auditory radiations is a particular defective function of perceiving and understanding various sounds in a human life. For instance, people with such disorders cannot recognize sounds of speech or conversation, environmental sounds such as rain and thunder, birds singing, ambulance sirens, and sounds of music or automobiles and other machinery. Pure-tone audiometry often reveals bilateral progressive sensorineural hearing loss despite mild threshold elevations in the early stage. These hearing problems are often caused by bilateral cerebrovascular events in the temporal lobe or subcortical area in the basal ganglia. Auditory impairment due to these bilateral lesions is considered to represent information deficits in auditory processing. However, much remains unknown regarding the pathophysiological mechanisms of central auditory information processing underlying complete or partial loss of hearing in humans caused by lesions of bilateral auditory cortex or auditory radiations.

Such disorders are divided into two groups: auditory agnosia and cortical deafness. Patients with auditory agnosia have residual hearing, whereas those with cortical deafness have complete bilateral hearing loss. Here, we evaluated patients with auditory agnosia or cortical deafness. Our aim was to reveal the role of the central auditory information processing mechanism in humans by examining the patients manifesting auditory agnosia and cortical deafness. We focused on the functional and morphological characteristics of the central auditory pathway, extending from the medial geniculate body via the auditory radiation to the primary auditory cortex.

We examined 5 patients with auditory agnosia and 3 with cortical deafness. Brain CT and/or MRI in the

former group revealed localized partial lesions of the bilateral auditory cortex or auditory radiations. However, in the latter group, MRI revealed lesions with complete damage in the bilateral auditory radiations. Moreover, pathological evaluation of one patient with auditory agnosia showed the disappearance and degeneration of neuronal cells in the medial geniculate body, which might have resulted in retrograde degeneration in the form of bilateral auditory cortex or auditory radiation lesions. Therefore, we suggest that complete or partial loss of hearing caused by lesions of bilateral auditory cortex or auditory radiations can result from a defective change or reorganization of neuronal networks in the central auditory neuronal pathway after the onset of patient's cerebrovascular accidents. These findings are important for understanding the human central auditory system through the pathologic representation following after lesions of auditory cortex or auditory radiations.

Regeneration I

PD 65

Epigenetic Regulation of Supporting Cell Fate, and Transdifferentiation Potential, in the Perinatal Organ of Corti: a Role for "Bivalency" and H3K27ac.

Litao Tao¹; Haoze (Vincent) Yu²; Talon Trecek³; Juan Llamas²; Zltaka Stojanova⁴; Neil Segil⁵

¹*Department of Stem Cell Biology and Regenerative Medicine, Caruso Department of Otolaryngology, Keck School of Medicine, University of Southern California;* ²*Department of Stem Cell Biology and Regenerative Medicine, Keck School of Medicine, University of Southern California;* ³*Caruso Department of Otolaryngology, Keck School of Medicine, University of Southern California;* ⁴*Department of Stem Cell Biology and Regenerative Medicine, Keck School of Medicine, University of Southern California;* ⁵*Department of Stem Cell Biology and Regenerative Medicine, Keck School of Medicine, University of Southern California;* ⁵*Department of Stem Cell Biology and Regenerative Medicine, and Caruso Department of Otolaryngology - Head and Neck Surgery, Keck School of Medicine, University of Southern California*

Background: Overcoming the failure of sensory hair cell regeneration in the mammalian organ of Corti remains a significant goal for researchers seeking a cure for the permanent hearing loss that occurs when hair cells die. In neonatal mouse cochlea, supporting cells retain a latent transdifferentiation potential, however, this potential is lost within the first week of postnatal development. We have previously shown that Atoh1 is maintained in a "bivalent" state in postnatal day 1 supporting cells. Here we expand this analysis genome-wide, and analyze

the underlying epigenetic mechanisms responsible for maintaining supporting cell fate, and the changing transdifferentiation potential during the perinatal period.

Method: We profiled the transcriptome (RNAseq), chromatin accessibility (μ ATACseq) and histone modifications (H3K27Ac and H3K27M3) (ATM-ChIPseq) in FACS-purified subpopulations of supporting cells. Using lineage markers specific to hair cells and supporting cells, we were able to characterize DAPT-responsive and -nonresponsive supporting cells independently, enabling an investigation of the epigenetic changes in supporting cells based on their developmental stage and latent transdifferentiation ability.

Result: We confirm that supporting cells lose transdifferentiation potential in both an age-dependent and spatially-dependent (base-to-apex) manner. As we have previously described at the *Atoh1* locus, these changes correlate with genome-wide changes in epigenetic and chromatin structure, consistent with a role for regulated histone acetylation, and promoter bivalency responsible for maintaining the silence of the hair cell gene regulatory network in supporting cells. Inhibitor studies indicate a mechanistic role for PRC2 and HDAC-containing nucleosome-modifying machinery in both the maintenance of supporting cell fate, and changing transdifferentiation potential.

Conclusions: Our genome-wide studies strongly indicate a role for epigenetic regulation of cell fate and transdifferentiation potential of supporting cells in the maturing mouse organ of Corti. We hypothesize that these changes underlie the changing potential for transdifferentiation of supporting cells during the early perinatal period, leading to the failure of regeneration in the adult organ of Corti.

PD 66

Improved Hearing Recovery After Noise Damage Following ERBB2 Activation in Genetically Modified Mice

Jingyuan Zhang¹; Kenneth S. Henry²; Patricia White³
¹Department of Neuroscience, University of Rochester School of Medicine; ²University of Rochester; ³University of Rochester Medical Center

Introduction: Hearing loss after noise damage afflicts combat veterans and industrial workers world-wide. Such permanent threshold shifts do not improve with time, and no biological treatments are available to promote recovery. Here we report significantly improved auditory thresholds in mice after a noise exposure that induced permanent threshold shifts. This improvement followed the activation of ERBB2 signaling in cochlear supporting cells.

Methods: We generated mice that can be induced to express a constitutively active rat ERBB2 ("CA-ERBB2") receptor in cochlear supporting cells upon injection of doxycycline. We bred this Tet-On CA-ERBB2 transgenic mouse line to one harboring the *Fgfr3-iCre* knock-in. Double-positive progeny from that cross were then bred to a homozygous floxed ROSA-rtTA knock-in line, where expression of the TA transcription factor, co-expressed with GFP, may be induced after CRE recombination of the flanking lox-P sites. The strain of the resulting cross was CBA/CaJ X B6. The inducible CRE protein was activated by two injections of tamoxifen at P28. Noise damage, consisting of an 8-16 kHz band, was presented at 110 dB for two hours. This exposure drove temporary thresholds shifts of an average of 30 dB and permanent threshold shifts of 25 dB across all frequencies. The CA-ERBB2 transgene was induced three days after noise damage through the injection of doxycycline, followed by the injection of furosemide. Mice also received doxycycline-containing food for two days, spanning the injections. Hearing thresholds and hearing loss were determined using auditory brainstem response (ABR) and scored by an individual blinded to genotype and time point. Histological analysis was performed using staining for hair cells on cryosections and in whole mount preparations, including cochleograms.

Results: Hearing recovery in mice with all three genetic modifications averaged 13.3 ± 4.6 dB compared to controls with -1.0 ± 2.4 dB ($n=19$ total mice, $p=0.016$, ANOVA). This effect was only seen at 8 kHz. We primarily detected GFP in apical sections of CA-ERBB2, consistent with the idea that the CA-ERBB2 induction occurred in the cochlear regions where improvement was observed. Hair cell counts are ongoing and will be reported.

Conclusions: Early reports investigated EGF family ligands for potential roles in promoting regeneration. We report that the expression of a constitutively active receptor, ERBB2, involved in this signaling pathway correlates with improved hearing after noise damage. The underlying mechanisms for this improvement will be the focus of future study.

PD 67

Lgr5+ Cochlear Progenitor Cell Proliferation is Driven by the Combined Activation of the Wnt, Non-Canonical Notch, and PI3K Pathways

Megan Harrison; Sara Strecker; Melissa Hill-Drzewi;
Will McLean
Frequency Therapeutics

Loss of cochlear hair cells, which do not spontaneously regenerate in mammals, is a leading cause of hearing

loss. Previous work by McLean et al. 2017 showed that 3D organoid culture of Lgr5+ hair cell progenitors is a useful tool to study how various small molecules affect the ability of Lgr5+ cells to proliferate. In addition, 3D organoid culture can be a useful *in vitro* system for investigating the underlying biological pathways involved in progenitor cell regulation and plasticity. Enrichment for Lgr5+ cells can be achieved by treatment with molecules including the GSK3 inhibitor CHIR99021 (CHIR) and valproic acid (VPA). While CHIR is considered to promote proliferation by driving the Wnt pathway, the molecular mechanism by which VPA enhances CHIR-driven proliferation of Lgr5+ progenitor cells is not fully understood.

Here, organoid cultures were treated with CHIR and VPA individually as well as in combination, and the effects on gene modulation, total protein, and phosphorylated protein were assessed to elucidate the mechanism of synergistic Lgr5+ cell expansion. It was originally hypothesized that VPA functions by upregulating the Notch pathway. However, we find that VPA does not appear to lead to global gene or protein changes within the canonical Notch pathway, such as increased Hes and Hey expression. Exceptionally, Jagged1, a shared Wnt and Notch ligand, is upregulated by treatment with CHIR alone and is further upregulated upon dual treatment with CHIR and VPA, which correlates with the synergistic effects of these molecules in eliciting Lgr5+ cell proliferation. Engagement of Notch receptors by the addition of a peptide corresponding to the Jagged1 extracellular domain recapitulates the activity of VPA in Lgr5+ cell proliferation. Interestingly, inhibition of γ -secretase, the enzyme that cleaves Notch receptors, does not affect Jagged1 induction level, signifying that Jagged1 induction may be γ -secretase independent.

Together, these findings indicate that VPA may activate a non-canonical, γ -secretase independent Notch pathway mechanism. One route of γ -secretase-independent Notch signaling entails activation of the PI3K pathway. Indeed, we find that VPA activates the PI3K pathway in cultured Lgr5+ organoids as judged by increased levels of phosphorylated Akt. Further, a PTEN inhibitor, which activates the PI3K pathway, can substitute for VPA to enhance Lgr5+ cell proliferation and Jagged1 induction without inhibiting HDAC. Taken together, these findings indicate that combined activation of the Wnt, non-canonical Notch, and PI3K pathways elicits synergistic proliferation of Lgr5+ cochlear progenitor cells in culture.

PD 68

Evidence for stem/progenitor cells in the human postmortem adult inner ear

Hubert Löwenheim¹; Hasan Avci²; Aurelie Dos

Santos²; Megan Ealy³; Mohamed Bassiouni²; Marcus Müller¹; Andreas Wagner⁴; Bernhard Hirt⁴; Stefan Heller⁵

¹Hearing Research Center, Department of Otolaryngology - Head & Neck Surgery, University of Tübingen Medical Center, Tübingen Germany;

²Hearing Research Center, Department of Otorhinolaryngology, Head & Neck Surgery, University of Tübingen Medical Center, Tübingen, Germany;

³Stanford School of Medicine; ⁴Institute of Clinical Anatomy and Cell Analysis, Eberhard Karls University Tübingen; ⁵Stanford University, School of Medicine, Department of Otolaryngology-HNS

The mammalian auditory sensory epithelium is considered to be a quiescent organ that undergoes terminal mitosis during embryonic development. It is generally accepted that lost hair cells are not replaced in adult mammals due to lack of intrinsic regenerative capacity and results in permanent hearing loss. In contrast, lost hair cells of adult mammalian vestibular epithelia regenerate, albeit in limited number. In the vestibular macula of mice resident adult stem cells capable of generating newly differentiated hair cells were discovered.

Here we demonstrate that human postmortem inner ear tissues harbor cells, which can be maintained in culture, propagated and differentiated into sensory cells *in vitro*.

Human inner ear sensory epithelia obtained from body donors were dissociated into single cells in a proliferative environment supplemented with growth factors. Within the first week in culture, cells formed spheres by mitosis, as EdU incorporation was observed in some cells. These newly generated cells expressed stem/progenitor cell markers like Nestin, SOX2, PAX2 and PAX8. We compared the proliferation characteristics and gene expression of the vestibular and cochlear spheres. Comprehensive gene expression profiling of spheres, differentiated cells and native tissue revealed that progenitor markers are transiently upregulated in spheres. Upon differentiation, the otic progenitor spheres displayed a general trend to upregulate mature marker genes for hair cells, accompanied by downregulation of developmental genes. Finally, based on immunocytochemical analysis we assessed the differentiation potential of newly generated sphere cells into supporting cell-like (EdU⁺ and SOX2⁺) and sensory hair cell-like cells (EdU⁺ and MYO7A⁺).

These findings indicate that the adult human vestibular and cochlear sensory epithelia harbor stem/progenitor cells capable to generate new sensory cells, which opens new opportunities for hair cell regeneration therapies in humans.

The research leading to these results has received

funding from the European Research Council under the European Union's Seventh Framework Programme (FP7 grant agreement No. 603029 - Project OTOSTEM).

PD 69

Combinatory application of p27Kip1 antagonists and Pou4f3 agonists in promoting hair cell regeneration in adult mice in vivo

Hao Feng¹; Cassidy Nguyen²; Jian Zuo¹

¹Department of Biomedical Sciences, Creighton University, School of Medicine; ²Department of Neuroscience, College of Arts and Sciences, Creighton University

Objectives To date, no FDA-approved drugs are available to treat hearing loss induced by genetic mutations, cisplatin, antibiotics, noise, or aging. A clinical trial with ATOH1 gene therapy is ongoing for regeneration of sensory hair cells as treatment of deafness in humans; however, its outcome is uncertain. Recently we have demonstrated that combinatory genetic manipulation of Atoh1, Pou4f3 and p27Kip1 (p27) led to hair cell regeneration in mature mouse cochleae (Walters et al., Cell Reports 2017). Based on these results in mouse models, we performed large scale screens for agonists of Pou4f3 and antagonists of p27 (Walters et al., PLoS One 2015; Diao et al., ARO 2018). Alsterpaullone, 2-Cyanoethyl (A2CE) was identified as an antagonist of p27, both at the level of mRNA transcription and protein expression. Significantly, local delivery of A2CE transtympanically causes 60% mRNA reduction of p27 in murine Corti's Organ. We also identified three agonists for Pou4f3 in transient and stable cell lines that exhibited Pou4f3 and/or Atoh1 agonist activities. Here we hypothesize that combinations of p27 antagonists and Pou4f3 agonists promote hair cell regeneration in mature mice.

Methods Transtympanic injection of A2CE (5 mM, 5 μ l) or DMSO was performed in the Fgfr3-iCreER; Atoh1-HA; p27^{fllox/+} adult genetic mouse model after tamoxifen induction. Newly regenerated hair cells were examined three weeks post-A2CE treatment that expressed both Atoh1-HA and Myosin 6, as described previously (Walters et al., Cell Reports 2017). Similarly, transtympanic injection of Pou4f3 agonists at various doses were performed in wildtype FVB adult mice. Finally, combination of A2CE and Pou4f3 agonists were injected transtympanically in wildtype FVB or Fgfr3-iCreER; p27^{fllox/+} mice. New hair cells were examined subsequently.

Results We obtained ~50 new hair cells per cochlea in A2CE-treated Fgfr3-iCreER; Atoh1-HA; p27^{fllox/+} mice compared to ~5 new hair cells in DMSO-treated control littermates. The effects of Pou4f3 and their combinations

with A2CE will be examined.

Conclusion We demonstrated that A2CE is an effective compound that induce new hair cell formation in a genetic mouse model in adult age. We are hopeful that Pou4f3 agonists and their combinations with p27 antagonists will enhance the mature cochlea's ability to regenerate hair cells. Future optimization of A2CE and Pou4f3 agonists will be necessary in terms of delivery and toxicity and pharmacology before clinical use.

Supported in part by NIHR01DC015010, NIHR01DC015444, ONR-N00014-18-1-2507, USAMRMC-RH170030, and LB692/Creighton.

PD 70

YAP-Activating Small Molecules for Inner Ear Regeneration

Nathaniel Kastan; A.J. Hudspeth
Rockefeller University

Because hair cells of the mammalian inner ear do not regenerate, damage accumulates across a lifetime, often culminating in disabling hearing loss and vestibular dysfunction. Because there is no effective medicinal treatment for hearing loss, treatment focuses on preventative measures, coping strategies, and hearing aids, a cumbersome and often insufficient response to the problem. The goal of this investigation is to identify small molecules that induce proliferation of supporting cells, thus mimicking a key step of the hair cell regeneration observed in non-mammalian vertebrates.

The sensory epithelia of all hearing and vestibular organs share two cell types: supporting cells, which play a homeostatic and architectural role, and mechanosensitive hair cells. In birds the regenerative process involves two phases. Supporting cells adjacent to a site of damage undergo proliferation, yielding daughter cells that can either differentiate into hair cells or remain supporting cells. In the adult mammalian utricle, it has been shown that a modest number of hair cells regenerate after total ablation. However, the new hair cells are predominantly the result of trans-differentiation, and it is unclear whether there is any significant functional recovery. Although this is a meager response, it lies in stark contrast to the total inability of the mammalian cochlea to yield any regenerative response.

Given this backdrop, many researchers have turned to investigating potential avenues of first inducing a proliferative response. Our group identified YAP signaling as requisite for delimiting the size of the developing utricle. This pathway is active during, and necessary for, proliferative regeneration in the neonatal

utricle. We therefore performed a drug screen of over 80,000 chemicals to identify those that activate YAP. Having identified and validated six drugs in this system, we have explored these drugs' potentials to induce supporting cell proliferation and subsequent hair cell regeneration in the murine utricle and cochlea. One compound has shown promising results, and we are exploring its mechanism of YAP activation. These drugs may serve as broadly applicable tools with which to perturb and thus further elucidate this signaling pathway or as a basis of therapeutic intervention. Finally, because there are several tissues – such as cardiomyocytes – in which YAP activation induces regeneration, we aim to survey these other non-proliferative tissues as potential therapeutic targets.

PD 71

Trial for Improvement of Hair Cell Induction Method from Human Induced Pluripotent Stem Cell

Hiroe Ohnishi¹; Desislava Skerleva¹; Hideaki Okuyama¹; Tatsuo Miyamoto²; Shinya Matsuura²; Kosuke Kirino³; Norio Yamamoto¹; Juichi Ito⁴; Koichi Omori¹; Megumu Saito⁵; Kayoko Tsukita⁶; Haruhisa Inoue⁶; Takayuki Nakagawa¹

¹Department of Otolaryngology-Head and Neck Surgery, Graduate School of Medicine, Kyoto University; ²Department of Genetics and Cell Biology, Research Institute for Radiation Biology and Medicine, Hiroshima University; ³Department of Pediatric Surgery, Graduate School of Medical Science, Kyushu University AND Department of Clinical Application, Center for iPS Cell Research and Application; ⁴Shiga Medical Center Research Institute; ⁵Department of Clinical Application, Center for iPS Cell Research and Application, Kyoto University; ⁶Department of Cell Growth and Differentiation, Center for iPS Cell Research and Application, Kyoto University AND iPSC-based Drug Discovery and Development Team, RIKEN BioResource Research Center

Background: Deafness has many causes including drug side effects, infectious and hereditary diseases, and noise exposure. However, effective drugs against deafness have not been developed yet. Mammalian inner ear hair cells lose proliferative potency after completing their development so that we cannot use tissue culture or primary culture for drug screening. Additionally, no appropriate cell lines with characteristics of hair cells are available. For these reasons, the development of drugs against deafness is far behind other diseases. Recently human induced pluripotent stem cell (hiPSC)-derived cells, which has the potential to differentiate into any types of cells within a whole body, are used for drug screening. Although we reported hair cell induction method from hiPSC in 2D culture using stepwise method

(Ohnishi et al., 2015), the efficiency of this method was unsatisfactory. Therefore, in this study, we aimed to improve our hair cell induction method.

Methods: Previously, we induced hair cells from hiPSCs. At this time, we examined the conditions of differentiation method for otic placode from hiPSC-derived preplacodal ectoderm with a reference to Ealy et al. in 2016. In this method, we treated the cells with growth factors and small molecules. To confirm the proper otic placode induction, we performed immunocytochemistry and RT-PCR analyses of the cells. Then, we incubated the cells in a serum-free medium containing Matrigel for hair cell induction. The hair cell induction was examined by immunocytochemistry and scanning electron microscopy. Moreover, we generated ATOH1-eGFP hiPSC line using CRISPR/Cas9 to easily confirm the appropriate induction of hair cells.

Results: After treatment of hiPSCs with some growth factors and small molecules, induction rate of otic placode marker PAX2-positive cells increased more than hundredfold. Additionally, the cells after otic induction showed expression of otic placode marker genes. The hair cell-like cells, which we induced from the cells after otic induction by culture in serum-free medium, showed expression of a hair cell marker and stereocilia bundle-like structures on their apical surface. In the experiments using ATOH1-eGFP hiPSCs, GFP positive cells were observed after hair cell induction, indicating that these cells are useful in the hair-cell induction experiments.

Conclusion: In this study, we achieved two important things for the improvement of our hair cell induction method. One is increasing in the induction rate of otic placode-like cells which is a crucial step in hair-cell induction. Second is generating ATOH1-eGFP hiPSCs which is an important tool for establishing hair cell induction method.

PD 72

Medial and Lateral Supporting Cells Preferentially Adopt IHC and OHC Fate Respectively

Craig Hanna¹; Danielle R. Lenz²; Albert Edge³; David Kaplan⁴

¹Tufts University School of Medicine, Tufts University Sackler School of Graduate Biomedical Sciences,; ²Harvard Medical School, Eaton-Peabody Laboratories, Massachusetts Eye and Ear; ³Department of Otolaryngology, Harvard Medical School; ⁴Tufts University Department of Biomedical Engineering, Tufts University Sackler School of Graduate Biomedical Sciences

Introduction: Sensorineural hearing loss (SNHL) commonly involves damage to cochlear hair cells (HCs), and since mammalian HCs are incapable of regeneration,

PS 549

Arousal-dependent Variability of Correlated Neural Activity in Primary Auditory Cortex

Charles R. Heller; Zachary P. Schwartz; Daniela Saderi; Stephen V. David
Oregon Health & Science University

Sensory responses of auditory cortical neurons vary across repeated presentations of identical stimuli. These trial to trial fluctuations are often correlated across neurons. Theoretical work has argued that these correlations must impair sensory coding, as shared variability across the population cannot be averaged away. In support of this hypothesis, correlations have been shown to decrease during epochs when faithful sensory encoding is important, such as task-engagement, selective attention, and during periods of high global arousal. However, relatively little is currently known about the origin of these correlations. To better characterize the origin of cortical variability and its dependence on behavioral state, we recorded activity from primary auditory cortex (A1) of awake, head-fixed ferrets using 64-channel multi-electrode arrays. Simultaneously, we measured the animal's level of arousal via pupillometry. The linear array provided access to several (5-20) closely spaced single units within a single cortical column. We classified recorded units as putative fast-spiking (FS) or regular-spiking (RS) based on their mean waveform shape. Before addressing the question of shared cortical variability, we first asked to what extent we could explain variability in single cell auditory responses with pupil-indexed arousal. Using a standard linear model, we found that approximately 18 percent of recorded units exhibited significant variability in their responses that can be explained by changes in arousal. Interestingly, FS units were affected at higher rate (~25 percent of all FS units versus ~10 percent of all RS units). Because the activity of many units depends on pupil-indexed arousal, we hypothesized that subtracting the model prediction from the response of each neuron would remove a substantial amount of shared variability in the population. Indeed, this caused the number of correlated pairs to decrease significantly, changing from approximately 45 percent of the population to 35 percent. Thus, some shared cortical variability is due to a common arousal signal. Finally, we asked how the magnitude of shared variability depends on pupil-indexed arousal, i.e., are correlations stronger or weaker in a high arousal state? Overall, we found that correlations decreased in high arousal states. This effect was robust amongst FS/FS pairs, but RS/RS pairs were equally likely to increase or decrease correlation strength

most forms of SNHL are permanent. Recent work has demonstrated the ability to isolate, expand, and differentiate neonatal murine Lgr5+ cochlear progenitors (LCPs) in high yield. These Lgr5+ cells are found in both the medial (MC) and lateral (LC) compartments of the cochlea, surrounding inner hair cells (IHCs) and outer hair cells (OHCs), yet, it currently is not known what drives LCPs toward IHC or OHC fate.

Methods: Sensory epithelial tissue from P3-P5 FgfR3-iCreER;tdTomato (LC expression) and Glast-CreER;tdTomato (MC expression) transgenic mouse pups was harvested, expanded in 3D culture, and differentiated for 10 or 15 days. LCP organoids were fixed and stained for myosin 7a, prestin, and vGlut3. vGlut3/myo7a (marking IHCs) or prestin/myo7a (marking OHCs) double positive organoids co-expressing the reporter from each mouse line were imaged and quantified. To confirm quantification findings, qPCR analysis was used to determine *prestin* and *vGlut3* expression in sorted reporter positive and negative cells obtained from both mouse lines.

Results: Following differentiation, most prestin/myo7a double positive organoids from the FgfR3-tdTomato mouse line co-expressed tdTomato while vGlut3/myo7a double positive organoids did not. Similarly, qPCR analysis demonstrated that reporter positive cells expressed significantly higher levels of *prestin* than *vGlut3*. While most vGlut3/myo7a double positive organoids from the Glast-tdTomato mouse line co-expressed the reporter, approximately half of the observed prestin/myo7a double positive organoids did as well. Interestingly, tdTomato expression was not uniform across all cells within these organoids, suggesting that some of these organoids were not clonal. Despite this observation, qPCR demonstrated a trend with reporter positive cells expressing higher levels of *vGlut3* than *prestin*.

Future Directions: Using the LCP model system, we have demonstrated that MC and LC origin limits the capacity of supporting cells to transdifferentiate towards IHC and OHC fate respectively. Future work will focus on better understanding this limited plasticity with respect to time and flexibility by exploring methods of driving these cells towards IHC or OHC fate regardless of compartmental origin.

in a high-arousal state. Thus, our results indicate that arousal impacts correlated activity of neurons in A1, both through modulation of common inputs and through cell type specific modulation of coupling between neuronal pairs.

PS 550

Effects of Vagus Nerve Stimulation on Auditory Learning and Activity in Auditory Cortex

Jesyin Lai¹; Stephen V. David²

¹Oregon Hearing Research Center; ²Oregon Health & Science University

Individuals with learning disabilities or hearing loss often have difficulty with language learning, taking longer to learn than normal-hearing listeners. Moreover, as age increases, the speed of language learning slows down, even without disability. Recently, extended pairing of vagus nerve stimulation (VNS) with speech sound presentation (300 times/day for 20 days) was shown to strengthen tuning of stimulus-specific neural responses in auditory cortex. This finding led us to hypothesize that VNS can increase the rate of sound category learning by promoting stimulus-specific cortical plasticity. To test this hypothesis, we implanted cuff electrodes onto the vagus nerve of ferrets and trained them by classical conditioning to associate one specific target sound (T1) with a reward and another target sound (T2) with no reward. T1 and T2 frequencies were about 2-2.5 octaves away and were changed every 400-500 trials, typically after learning their reward associations. Rates of learning the association reward increased when T1 and T2 were paired with VNS (1 s duration, 30 Hz, 100 us biphasic pulses, 1.5-2 mA, VNS onset 100 ms before T1/T2 onset). In contrast, animals' learning rates were lower when VNS occurred randomly during the silence after T1 or T2 presentation (non-paired condition). As VNS is suspected to relate to arousal, and pupil dilation is an indicator of arousal, pupil size was measured during VNS. Pupil dilation was observed at 0.5-1 s after VNS and could last for several seconds, indicating an increase in arousal, which may associate with greater learning efficiency. To measure effects of VNS on cortical activity, we recorded neurophysiological single- and multi-unit activity in primary auditory cortex of passively listening animals. Three conditions were tested: (1) tones at neurons' best-frequencies (BFs) paired with VNS; (2) tones at 2-2.5 octaves away from BF paired with VNS; (3) VNS at 6 s after BF tone presentation (non-paired). The data showed reduced tone-evoked responses in the condition of BF tone paired with VNS. This outcome contrasted with previous findings, which reported enhancement of stimulus-specific responses after VNS. This difference may reflect the fact that the

timescale of VNS was shorter (20 times per stimulus) in our study. Overall, the results of this study support a role for VNS in auditory learning and help establish VNS as a tool to speed up language learning in humans.

PS 551

Hippocampal Encoding of Space During Navigation of an Acoustically Defined Virtual Reality

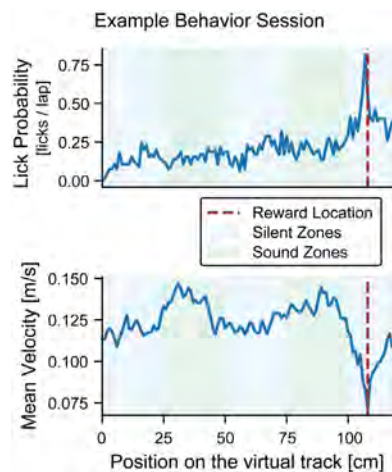
Sibo Gao¹; Anton Banta²; Jack Shi²; Zakir Mridha²; Wenhao Zhang²; Caleb Kemere¹; Matthew McGinley²

¹Rice University; ²Baylor College of Medicine

Auditory cues play an important role in navigation, especially in darkness when the visual system cannot detect objects or prey. Decades of work in many labs has led to a deep understanding of how spatial cues in sound stimuli are extracted and encoded in the auditory brainstem, and represented in cortex, almost entirely in immobilized animals. However, little is known about how these spatial acoustic cues are used by the brain to aid in navigation. Parallel work in rodents has shown that spatial representations in rodent hippocampus are thought to underlie memory-guided navigation. Herein, the hippocampus generates a 'place map'; of the environment within which the animal is currently navigating. More specifically, a large fraction of neurons in CA1 of dorsal hippocampus are 'place cells'; meaning that individual neurons selectively fire action potentials within a single location, called a 'place field.';

Here, we seek to test the hypothesis that the hippocampus generates a place map of the animal's environment even when spatial information about the environment is provided purely by acoustic landmarks. To do so, we developed a new behavioral paradigm for head-fixed mice on a cylindrical treadmill that implements an acoustic virtual reality. As mice walk on the treadmill, they are presented with a repeating sequence of three sounds, separated by three silent zones, simulating a large (150 cm) virtual circular track. The mice are rewarded for licking when their virtual location is within the middle half of one of the silent zones, referred to as the 'reward zone.'; In addition, the magnitude of the reward is inversely proportional to the walking velocity at the time of licking. This encourages the mice to slow down in the reward zone in order to receive maximum reward. We find that mice, on average, show increased licking, and slowed walking, preceding entry to the reward zone on each lap. This provides behavioral evidence that they have learned the sound sequence and the location of the reward zone in the virtual space. In ongoing experiments, we are performing high-channel count (128 channel) silicon array recording in the pyramidal cell layer of CA1, in order to determine if neurons, there, exhibit place fields in the acoustically

defined virtual space. These experiments are a first step in understanding how spatial features of sounds extracted by the auditory system are used by the brain to execute behaviors that require memory-guided navigation using sound cues.



PS 552

Effect of Linguistic Information of Maskers on Cortical Auditory Responses

Anoop Basavanahalli Jagadeesh; Ajith Kumar
All India Institute of Speech and Hearing

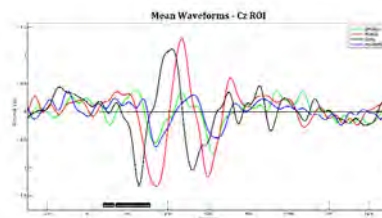
Introduction: Informational masking(IM) refers to the additional amount of masking caused over and above energetic masking. Typically, IM is elicited using speech or speech-like maskers (time-reversed speech). Effect of IM can be evaluated through behavioral or electrophysiological measures (Billings et al., 2015; Niemczak & Vander Werff, 2018). In this paper, we used cortical auditory evoked potentials (CAEPs) observe the effects of maskers with varying linguistic information.

Method: CAEPs were recorded in four background conditions – quiet, speech-noise (SN), 4-speaker babble (SB) and its time-reversed version (RB). While the SN caused only energetic masking, the RB and SB caused additional informational masking at phonetic and semantic levels respectively. Target sound was presented 70 times at 70 dB SPL in all four background conditions. SNRs of the masked conditions were maintained at +10 dB. Preliminary data on 8 normal-hearing native speakers of Kannada was subjected to basic preprocessing (down-sampling, filtering, bad data rejection, and re-referencing). Peak latencies of N1 and P2 components were recorded for averaged waveforms of 5 electrodes around Cz channel, for all four conditions.

Results: One-way repeated measures ANOVAs for the peak latencies (N1 and P2) showed that all masked conditions caused significantly delayed peaks compared to the quiet condition. However, there were

no differences in the peak latencies between the three masked conditions. The individual waveforms across the four conditions were also compared using permutation-based statistics. Statistics revealed a significant main effect in amplitudes across the four conditions in the latencies between 85 ms and 304 ms post-stimulus. These latencies correspond to the dominant P1-N1-P2 complex. However, post-hoc paired comparisons (FDR correction for multiple comparisons) yielded no significant differences in the amplitudes for any of the comparisons. Nevertheless, mean peak amplitudes of the both babbles (regular and reversed) were visualized to be lower than both quiet and noise backgrounds.

Discussion: Similar latency delays for both noise and babbles indicate that the masking effect was predominantly energetic in nature, as the spectral and intensity composition of both types of backgrounds were nearly identical. The role of informational (linguistic) masking appears to be driven predominantly by the SNR of the listening situation. The SNR of +10 dB ensured that there was clear audibility of the target word, and hence, there appears to be minimal 'informational'; confusion. However, increasing the number of subjects and/or changing the SNRs could reveal more significant effects of informational masking, particularly on the amplitudes.



PS 553

Neural Circuits and Pupil Readouts of Motivated Shifts in Attentional (Listening) Effort

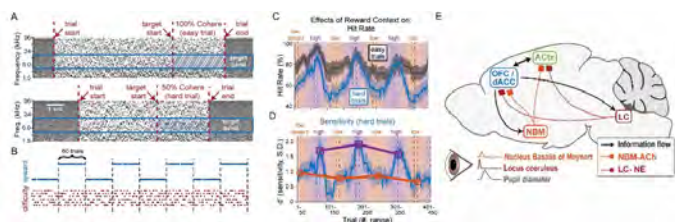
Zakir Mridha; Jack Shi; Anton Banta; Jan Willem de Gee; Wenhao Zhang; **Matthew McGinley**
Baylor College of Medicine

Attending to a speaker in a noisy environment, such as a cocktail party, can be a pleasantly immersive experience for individuals with normal hearing and cognitive function. However, for individuals with hearing loss, this 'listening effort'; is their primary complaint, and can be a severe source of stress and fatigue. Unlike an audiogram, which can be measured objectively, listening effort is a subjective, cognitive process that eludes quantification. Pupillometry (measuring the size of the pupil of the eye) has proven extremely useful as a physiological readout of listening effort. However, we have very little understanding of what the pupil actually

indicates about activity in the brain during listening tasks, including about the neural circuits underlying listening effort. Therefore, analysis approaches to human data are unclear and rather arbitrary.

In previous work, we extensively characterized the physiological correlates in the auditory system of several pupillometry metrics during a simple auditory behavior. The combined results led us to the following two hypotheses: 1) pupil metrics of listening effort track release of norepinephrine and acetylcholine into the auditory cortex, on fast and slow timescales, respectively; and 2) efficacious listening effort (motivated, high d' ;) is associated with improved extraction of task-relevant acoustic information by the auditory cortex. In addition, human fMRI work consistently finds that frontal cortex structures known to combine task performance and motivation contribute to listening effort. We hypothesize that activity in frontal areas may be tracked by the pupil during listening effort.

To test these hypotheses, we have developed a behavioral approach to motivated listening effort in mice. Mice report detection of temporal coherence in a cloud of tones by licking for sugar reward. We parametrically vary the difficulty on each trial, and manipulate listening effort by changing reward volume in blocks of trials. We find that mice better detect weak temporal coherence during blocks with large reward. Specifically, we dissociate effects on task engagement from detection ability (d'), and find large increases (~ 1 S.D.) in d' ; on hard trials during high reward blocks. In ongoing work, we are electrically recording from neurons in the auditory cortex and two-photon imaging interactions with neuromodulatory systems or frontal cortex, while doing pupillometry during our task. Our results will reveal the contributions of neuromodulatory and frontal cortex inputs to auditory cortex to motivated shifts in temporal coherence detection, and will directly relate multiple pupillometry metrics and statistical modeling approaches to these circuit mechanisms.



PS 554

Pupil Dilation and Other Eye Movements as Readouts of Vagus Nerve Engagement for Closed-Loop Enhancement of Auditory Learning

Zakir Mridha¹; Jack Shi¹; Rayan Alkashgari²; Wenhao Zhang¹; Matt Ward³; Aaron Suminski²; Justin Williams²; Matthew McGinley¹

¹Baylor College of Medicine; ²University of Wisconsin, Madison; ³Purdue University

The state of the brain fluctuates continuously and rapidly during wakefulness. Only a subset of waking states is optimal for performing a particular task, such as learning a new language. Release of neuromodulators is a large contributor to these state changes. We have previously shown that the size of the pupil tracks neuromodulatory state and its influence on auditory task performance (McGinley et al., 2015; Reimer et al., 2016). In parallel work, vagus nerve stimulation (VNS) was found to enhance auditory learning, probably resulting from recruitment of the same neuromodulators (Engineer et al., 2015). A major challenge in the use of VNS, to enhance learning or for various therapeutic purposes, is that there is no known readout of nerve engagement. As a result, stimulation parameters are chosen, and optimized, only through trial-and-error and/or feedback from patients about symptoms and side effects.

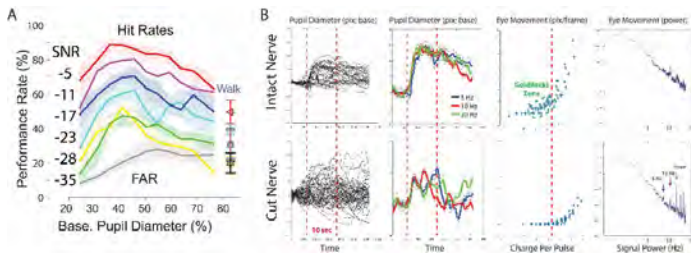
Here, we test the hypothesis that pupil dilation can serve as a readout of efficacious nerve engagement. We developed a chronic VNS preparation for awake, head-fixed mice using an implanted cuff design based on prior work in rats (Ward et al., 2015). While monitoring pupil size and other eye and facial movements, we explored a VNS parameter space (pulse width, pulse amplitude, stimulation rate). We found consistent dilation of the pupil. In addition, small eye movements phase locked to the stimulus were observed, and their magnitude was strongly correlate to the charge-per-pulse, irrespective of stimulation train rate. In control experiments with severed nerve, we found that pupil dilations and eye movements still occurred, but were smaller, and recruited at higher shock strengths, revealing a 'goldilocks zone'; of stimulation parameters. We conclude that pupil dilation and small eye movements track nerve engagement, and that careful parameter titration is necessary to avoid off-target effects. Our results will allow carefully controlled VNS for the enhancement of auditory learning, and other applications, including with closed-loop feedback based on current brain state.

McGinley et al. (2015). Cortical membrane potential signature of optimal states for sensory signal detection. *Neuron*, 87.

Reimer, McGinley, et. al. (2016). Pupil fluctuations track rapid changes in adrenergic and cholinergic activity in cortex. *Nature communications*, 7.

Engineer et al. (2015). Pairing speech sounds with vagus nerve stimulation drives stimulus-specific cortical plasticity. *Brain Stimulation*, 8.

Ward et al. (2015). A flexible platform for biofeedback-driven control and personalization of electrical nerve stimulation therapy. *IEEE Trans Neural Syst Rehabil Eng*, 23.



PS 555

Multiplexed encoding of auditory and aversive reinforcement cues in the cholinergic basal forebrain supports associative learning and cortical plasticity

Blaise Robert¹; Wei Guo²; Daniel B. Polley³

¹*SGBT Program, Division of Medical Sciences, Harvard Medical School*; ²*Eaton-Peabody Laboratories, Massachusetts Eye and Ear Infirmary*; ³*Eaton-Peabody Laboratories, Massachusetts Eye and Ear, Dept. of Otolaryngology, Harvard Medical School*

The rodent basal forebrain is studded with dense clusters of cholinergic neurons. Artificial stimulation of these areas can produce striking plasticity in sensory cortex, but an organizing schema for understanding the natural activators of cholinergic basal forebrain units has proven elusive due to the technical difficulty of recording from genetically defined cell types across this distributed deep brain network in behaving animals. Here, we describe an optogenetic antidromic phototagging approach to isolate single cholinergic units in Nucleus Basalis (NB) that project to the auditory cortex (ACx) and characterize their response properties and learning-related plasticity in awake, head-fixed mice.

We found that phototagged cholinergic NB --> ACx units (ChACx) and neighboring non-cholinergic NB units (NChACx) had robust, short-latency responses to meaningless, unconditioned auditory stimuli such as tones or noise bursts. ChACx and NChACx units also showed robust responses to unpleasant stimuli, such as

air puffs directed at the face. Because NB unit spike trains multiplex neutral sensory stimuli and unconditioned behavioral reinforcers, we reasoned that they could play a critical role in linking conditioned stimuli with temporally delayed (i.e., distal) reinforcement cues. We tested this by pairing pure tone stimuli (CS+) followed by air puffs (US) 5s later and confirmed behavioral evidence of associative trace learning. We observed a rapid tone-specific plasticity in the frequency receptive fields of ACx units and ChACx units, but not NChACx units. Paired recordings from ACx and NB over the course of conditioning revealed a strong increase in gamma band coherence that parallels a selective potentiation of spike-evoked L2/3 local network activity from ChACx units during the initial CS and US pairings.

These findings identify a new role for sound processing in cholinergic units in the caudolateral extreme of the Globus Pallidus. Nucleus Basalis units were strongly activated during learning to support associative plasticity of sensory conditioned stimuli and distal, temporally delayed reinforcement cues. Our ongoing studies utilize deep-brain imaging methods to identify regional differences among cholinergic basal forebrain neurons to sensory stimuli, behavioral reinforcement valence, and the encoding of sensory and reinforcement error signals. By discerning underlying rules for activating these distributed deep brain neuromodulatory neurons, we hope to develop new approaches to efficiently transform neocortical sensory representations.

PS 556

Multisensory Integration of Auditory and Visual Cues in Awake Non-Human Primates

Alexandra Kokanovic¹; Sophie Robert-Grandpierre²; Véronique Moret³; Ranjeeta Ambett⁴; Eric Michel Rouiller³; **Gérard Loquet⁵**

¹*Institute of Oncology Research IOR*; ²*University of Lausanne*; ³*Department of Medicine, University of Fribourg*; ⁴*Department of Otolaryngology and Head and Neck surgery and Audiology, Aalborg University Hospital*; ⁵*Department of Clinical Medicine, Aalborg University, Department of Electronic Systems, Aalborg University*,

Sensory processing research has classically investigated one modality at a time assuming that the different senses were operating independently from each other. Although it has led to important discoveries regarding brain functioning, it has become clearer over the last two decades that such an approach was unable to explain how we truly perceive environment unified. With the advent of the bimodal neuron in the 90s, real evidence of multisensory integration began to come out from high-order association cortices then from primary

cortical areas and finally at lower processing levels. Audiovisual experience like in speech perception is typically triggering numerous multisensory interactions, but the underlying neural mechanisms are still poorly understood. To investigate these mechanisms, we used simple behavioral tasks in non-human primates while characterizing large-scale neuronal networks with spatial EEG analysis. This way we tested the hypothesis that neural processes engaged during socio-cognitive situations rely on multisensory integrative phenomena. In the present study, we built a paradigm formed by unisensory and multisensory conditions around two common primate calls: one long and non-specific (“coo”-sound), and another short and more intimate (“grunt”-sound). Those two vocalizations have been presented to the auditory system (A-condition) then to the visual system (V-condition) and finally to both simultaneously (audiovisual condition or AV). Averaged reordered waveforms show that “coo” A, V and “grunt” V stimuli produce a similar two step response differing from the others obtained in different conditions, hypothesizing an unisensory processing pattern. The single step “grunt” A response happening later may reflect processing of the shortest auditory vocalization. Single step “coo” AV response and fragmented “grunt” AV responses may correspond to some multisensory processing. Topographic scalp maps show strong lateralized activities in all “coo” conditions, differing from all “grunt” conditions and second “coo” responses, which exhibit less strong bilateral activity. Distributed source estimations show stronger activities in the anterior lobe for “coo” A against the posterior lobe for “grunt” A. More specifically, “coo” V and AV induce an early activation around what could correspond to the superior temporal sulcus area whereas “grunt” V and AV stimuli clearly implicate regions in the prefrontal cortex. In conclusion, we suggest that such patterns represent an electrophysiological signature of each vocalization. Eventually, the present study allowed us to provide whole brain mapping of face/voice integration with the perspective to address later specific micro-networks, approach not feasible in humans.

PS 557

Processing of spectrotemporally complex sound patterns (speech) in an animal model

Joseph Sollini; Jennifer Bizley
UCL Ear Institute

Speech processing is one of the most complex tasks the auditory system performs. It requires the simultaneous analysis of a range of different acoustical (e.g. pitch, location, frequency and amplitude modulation) and cognitive (e.g. attention, semantics) features. While animals make a poor model to study human language they could prove useful for understanding non-linguistic

elements of speech processing (e.g. complex acoustical and attentional processing). We aimed to use an animal model (the ferret) to study the segregation and discrimination of spectrotemporally complex sound patterns (i.e. speech in speech or noise) while recording from auditory cortical neurons.

Training was split into 4 stages: initial shaping, single word discrimination (target vs non-target word), target in sentence discrimination (respond to the target in a stream of distractor words) and target/sentence in noise discrimination (track target stream in noise and respond to the target word). After initial shaping animals were trained to discriminate a target word from other non-target words using a go-no go paradigm. Discrimination performance was found to be highly accurate (>85% correct) where even phonetically similar words could be accurately discriminated. Next animals were trained to discriminate the target word within a sentence, performance was significantly above chance in all animals (p, Monte Carlo, chance = ~32% correct, average = ~62%, n =7). Subsequent testing revealed animal's performance was largely invariant to changes in talker, suggesting animals were able to generalise across features such as pitch and rate. Follow-up investigation demonstrated that manipulation of these features in isolation (using STRAIGHT) did not affect performance, demonstrating invariance to each. Finally, animals were trained to attend to speech streams in the presence of noise or other talkers (at present n = 2). Addition of a distracting speech stream significantly increased false alarms but performance remained significantly above chance (second stream -10dB SNR at present, p

We have successfully trained animals (ferrets) to perform a range of speech related tasks. Performance is invariant to changes in a number of features including pitch and rate, as in humans. Efforts are underway to understand the role of primary and secondary auditory cortex in selectively attending to a given speech stream in the presence of distracting sound sources (other talkers or noise backgrounds).

PS 558

Formation and Retrieval of Sound Categories in Auditory and Frontal Cortex

Pingbo Yin¹; Dana Strait²; Susanne Radtke-Schuller¹; Jonathan B. Fritz³; Shihab A. Shamma³

¹*Institute for Systems Research, University of Maryland*; ²*Neural Systems Laboratory, Institute for Systems Research, University of Maryland*; ³*Neural Systems Laboratory, Institute for Systems Research, University of Maryland*

Background: Categorization can arise by natural grouping of sensory stimuli sharing perceptual similarity or as a result of behavioral training, in which sensory stimuli are assigned to behaviorally relevant, defined classes associated with learned responses. Neuronal category representations of visual images have been previously identified in prefrontal, inferotemporal and parietal cortices, but there are many fewer studies of auditory category representation.

Method: Ferrets were trained to classify auditory stimuli distributed along continuous feature dimensions (e.g. frequency or amplitude modulation) into classes based on behavioral meaning (Go or No-Go). Single-unit activity was recorded from different fields of ferret auditory cortex (A1 and secondary areas in dPEG) and dorsolateral frontal cortex (dlFC) when animals were passively listening to sounds or actively engaged in task performance with the same set of sounds. A categorical index (CI) was defined to evaluate the categorical effects, which were computed from the grand difference between the mean distance between stimuli from different categories, and mean distance between stimuli from same category - based on evoked neuronal activities. Population analysis was also applied after PCA reduction to reveal the categorical boundary effect.

Results: Categorical information (Go versus No-Go) was observed in all three regions during task performance. Neurons exhibited rapid modulations of responses during the classification reflecting a mix of the sensory attributes of the stimuli (in A1 and dPEG) and their categorical labels (Go vs NoGo), with the balance shifting gradually towards the categorical in higher areas. The task-driven response modulations became greater in higher auditory cortical areas, and appeared earlier in the dlFC, then dPEG, and lastly in A1. We also found a subpopulation of cells in A1 and dPEG, in which the categorical responses to task stimuli were independent of task performance and had short latencies. This subpopulation was associated with cells that were relatively narrowly tuned to sensory features (frequency or AM rate).

Conclusion: These results are consistent with findings on the neural basis for visual categorization and provide insight into how the primary and secondary auditory cortices and frontal cortex are differentially involved in the Formation and Retrieval of sound categories.

PS 559

Are auditory cortex neurons better in discriminating communication sounds in mother vs. in virgin mice ? An electrophysiological study in C57BL/6 mice.

Juliette Royer; Florian Occelli; Chloé Huetz; Jean-Marc Edeline; José-Manuel Cancela
NeuroPSI UMR CNRS 9197

The responses of auditory cortex (ACx) neurons to communication sounds are influenced by many physiological factors such as the neuromodulators and neurohormones which can control the strength and temporal reliability of cortical responses. During parturition and motherhood, many physiological changes occur and can influence cortical responses to behaviorally significant stimuli. Ultrasonic vocalizations emitted by pups prompt the mother to search and retrieve the pup to the nest. Over the last decade, studies have compared the responses to communication sounds recorded in virgin and mother mice. Some studies reported that ACx neurons in mothers discriminate pup calls better than in virgins (Liu and Schreiner 2007), whereas others found that low frequency neurons displayed suppressed responses at presentations of high frequency sounds (Shepard et al. 2016). Most studies were performed in CBA mice, whereas the most commonly strain used in behavioral studies is the C57BL/6 mice. Here, we compared the receptive field parameters and the responses to communication sounds obtained from ACx neurons in virgins and in lactating mothers at 9 days after parturition.

The day of the experiment, the ABR of each mouse (2-6months old) was tested and a threshold <45dB to clicks was required to be included in our study. On average, the ABR thresholds were similar in virgins and mothers. Responses from primary ACx neurons were tested under Ketamine/Xylazine anesthesia using adult and pup calls and also heterospecific vocalizations (guinea pig whistles). When tested with pure tones (4-80 kHz at 75dB), the distribution of Best Frequencies did not significantly differ but the receptive fields of ACx neurons differed: The response latency, the spectral bandwidth and the response duration were smaller in mothers than in virgins. The spontaneous and evoked firing rates triggered in ACx by pure tones were also lower in mothers than in virgins, but the responses at the BF were unchanged.

When tested with communication sounds, the firing rate evoked by pup and adult vocalizations was lower in mothers than in virgins. The responses trial-to-trial reliability, indexed by the CorrCoef index, were similar in mother and virgin mice. Finally, the neurons

discriminative ability, indexed by mutual information, did not significantly differ between mothers and virgins, but ACx neurons responded to more pup and adult calls in mothers than in virgins. These results suggest that despite a reduced firing rate, the processing of communication sounds can potentially be more efficient in mothers than in virgins.

PS 560

Novelty Responses in the Rat Medial Prefrontal Cortex

Lorena Casado-Román; Manuel S. Malmierca
University of Salamanca

To survive in an ever-changing acoustic environment, our brain needs to react to novel, and significant stimuli while ignoring predictable ones. Mismatch negativity (MMN) is one of the most studied manifestations of novelty or deviance detection in the auditory system. MMN is a memory-based response to discriminable changes in a stream of auditory stimulation that can be recorded from the human scalp during the presentation of the oddball paradigm (Näätänen et al., 1978). Stimulus-specific adaptation (SSA) has been proposed to be the neuronal correlate of MMN (Parras et al., 2017). Under the predictive coding account, SSA and MMN are made of two main processes: repetition suppression (RS) and prediction error (PE). When an incoming input is repeated, it generates a regularity such that forthcoming inputs are predicted but if a new, different stimulus arrives, it violates the rule and will generate a PE (Friston, 2005). A previous study in our lab (Parras et al., 2017), has empirically disentangled the role of RS and PE at the auditory cortex (AC) and their hierarchical organization. It is understood that MMN has two main generators at the AC and the prefrontal cortices. However, the contribution of RS and PE at the level of the prefrontal cortex is currently unknown.

Here, we systematically recorded MUA and LFP in the medial PFC (mPFC: medial agranular cortex, anterior cingulate cortex, prelimbic and infralimbic cortices), under the oddball paradigm in urethane-anesthetised rats. Furthermore, we also used two control sequences, many-standard and cascade sequences, which make possible to differentiate between RS and PE (Ruhnau et al., 2012)).

Results show significantly stronger evoked responses after the presentation of deviant tones compared to both, standard and control conditions while control sequences and standard tones were not significantly different from each other. Notably, we systematically observed that neurons only show PE responses and lack RS. These neurons are located at the highest level of the auditory

hierarchy and thus, are especially suited to code for contextual changes in the auditory scene, rather than the physical properties of the sounds. Moreover, the fact that this novelty mechanism is present even in the absence of behavioural needs or conscious attention suggests that it is a fundamental property of the mPFC.

Financial support was provided by the Spanish MINECO (Grant # SAF2016-75803-P) and the European Union's Horizon 2020 research and innovation programme under the Marie Skłodowska-Curie grant agreement No 722098 to MSM.

PS 561

Auditory Cortical Detection of Deviant Temporal Modulations in Sequences of Amplitude Modulated Sounds

Tanmayika Saha¹; Amrita Mukherjee²; Muneshwar Mehra³; Sharba Bandyopadhyay⁴

¹*School of Bioscience, IIT Kharagpur*; ²*Dept of E&ECE, IIT Kharagpur*; ³*ATDC, IIT Kharagpur*; ⁴*Indian Institute of Technology Kharagpur*

Low probability stimuli, especially in the auditory system, are usually salient and important for carrying meaningful information about the external world. Further, amplitude modulations (AM) are known to play an instrumental role in identification and discrimination of many natural sounds and vocalizations. In this study we examine the selectivity of low probability, oddball sinusoidally amplitude modulated (SAM) noise or tone in the mouse auditory cortex (ACX). It has been shown that there is modulation frequency (MF) specific adaptation using a preceding SAM tone masker of a particular MF followed by a SAM tone of a different MF. The above result suggests presence of parallel modulation frequency channels. If multiple such parallel modulation frequency channels get integrated in single neurons of the ACX, then we hypothesize to observe stronger responses to a low probability or an oddball MF SAM sound (deviant, DMF) embedded in a stream of an MF SAM sounds (standard, SMF). The above expectation is based on results of similar stimulus specific adaptation (SSA), long been observed in the auditory pathway, using a low probability deviant tone token of a particular frequency embedded in a stream of a standard tone tokens of a different frequency. We primarily used SMF/DMF pairs of 8 and 16 Hz SAM tones and broadband noise and recorded single unit and LFP activity from the mouse ACX in response to such streams of SAM tones or noise tokens. Responses to the DMF tokens were compared to the immediately preceding SMF tokens and no selectivity to the deviant was found in spiking rate responses or vector strength. However there were strong rate responses during the inter-token silence immediately following the DMF token, significantly higher

than rates in the previous SMF or following it, showing detection of the DMF. Such selectivity was compared to that in LFPs to show aspects of the DMF selectivity emergent in the ACX. Population distribution of selectivity index, normalized for a neuron's inherent selectivity to different MFs show a significant positive median value. To further investigate mechanisms of DMF selectivity we performed 2-photon Ca(2+) imaging experiments with the same stimuli using syn-GCamp6s expressed in single neurons in the ACX, with an inhibitory neuron subclass in them expressing td-Tomato, to identify specific inhibitory neurons. We show that, subclass of inhibitory neurons (INNs), specifically somatostatin positive (SOM+), were more selective to the deviant. Further, both in single unit electrophysiology and Ca(2+) imaging we observe that DMF selectivity was present primarily when DMF was higher than SMF. Our study thus provides the first evidence of temporal modulation deviant selectivity in the ACX and proposes hypotheses about integration of different modulation frequencies which may be useful in auditory object formation aiding acoustic scene analysis.

PS 562

Auditory and Visual Stimulus Interactions in the Orbitofrontal Cortex of the Mouse

Sudha Sharma; Abhrajyoti Chakrabarti; Sharba Bandyopadhyay

Indian Institute of Technology Kharagpur

In a dynamic environment where contingencies change rapidly, flexible behaviour is important. The orbitofrontal cortex (OFC) is known for its role in flexible behaviour, decision making and in the coding of stimulus value. However, sensory responses in OFC and their interaction along the various nodes of information transfer are poorly understood. A comparison of early cortical (auditory cortex, ACX) and higher order frontal cortical regions (OFC) in their ability to integrate simultaneous events, involving different modalities will give an insight into the evolution of temporal window of integration along the hierarchy of information processing. Here, we investigate response properties of single neurons in the mouse OFC in their ability to integrate simultaneous or near simultaneous events, in this case, auditory (Tone) and visual (LED) stimuli. We first characterized the basic response properties for unisensory stimuli, auditory and visual, in OFC which differed in latency and duration of response. We then presented the animal with varying onset asynchronies between auditory and visual stimuli. We found an increase in responses as compared to unisensory condition when the two stimuli come within 200ms proximity of each other and decrease subsequently on further increasing the difference between the onsets, suggesting the presence of a temporal window of integration. Further we find that most neurons in the OFC are multisensory in nature

responding to both auditory as well as visual stimuli. Further, with sufficient difference in onset of auditory and visual stimuli, we observed suppression in response to an auditory stimulus when a visual stimulus precedes the auditory stimulus while the responses to both stimuli are intact when auditory precedes the visual stimulus. This differential response to auditory and visual stimuli and their interaction might explain the differential effects of association of auditory and visual stimulus on auditory responses compared to visual responses. Based on the above results we propose a model of OFC that integrates auditory and visual information which can affect the computation of stimulus value in a dynamic multisensory environment.

PS 563

Prevalence of Front-Back Confused Responses in the Marmoset Auditory Cortex

Yi Zhou

Arizona State University

Front-back confusions (FBCs), a common error in sound localization, occur when a sound source is localized with the correct lateral angular displacement, but to the wrong front-back hemifield. Unlike non-systematic errors related to noisy neural processing, FBCs arise because binaural cues do not specify a unique location in space, but rather a range of locations called "cones of confusion." The rate of FBCs depends on the spectral content of a stimulus and its duration. Low-mid frequency (< 4kHz) and short-duration stimuli evoke the most FBC errors. While behavioral manifestations of FBCs are well documented, our understanding of FBCs at the neural level, in terms of the effects of stimulus frequency and stimulus duration, remains limited. In this study, we investigated the spatial selectivity of neurons in the marmoset auditory cortex over the full 360° azimuthal plane. The spatial functions of neurons were evaluated based on their responses to best-frequency tones and broadband noises (100-500 msec duration). We found that cortical neurons show diverse spatial selectivity with respect to the peak direction and width of their spatial tuning. Neural FBC responses were identified, but they were less frequently observed than frontal and contralateral preferences. We found that pure-tone responses were sometimes highly spatially tuned, as often found for broadband noises. This contrasts with human behavioral data, where pure tones are localized less accurately than broadband noise. Furthermore, spatial selectivity was not limited to the beginning of a stimulus. The onset, ongoing and offset portions of neural responses all encode the spatial location of a sound. Finally, neural spatial selectivity was evidenced by both excitatory and inhibitory responses, where the inhibitory tuning could be either spatially

restricted or broad. These results suggest that spatial selectivity in the auditory cortex might not directly correlate with behavioral outcomes found in humans and the excitatory-inhibitory spatial tuning might reflect the overall role of auditory cortex in sound source segregation. [Supported by NSF-BCS-1539376.]

Auditory Nerve II

PS 564

Assessment of Auditory Nerve Function Using Electrically Evoked Auditory Potential With Multi-Site Stimulation

Doo Hee Kim¹; Ji Yeon Bae²; Woojin Ahn³; Hoseung Lee³; Jin Won Kim³; Kyou Sik Min³; Seung-Ha Oh²
¹Seoul National University; ²Seoul National University Hospital; ³TODOC LLC.

The rehabilitation results after cochlear implantation are relevant to the amount of the auditory spiral ganglion cells to encode the electrical sound stimulation. Clinically, the electrically evoked auditory potentials, such as electrically evoked auditory brainstem response (EABR) are used for the functional estimation of the auditory periphery intraoperatively and postoperatively via implanted intra-cochlear electrodes. Their properties are relevant to the number of auditory ganglion cell. However, a limited population of auditory ganglion cells could be involved by single site stimulation.

In this study, we analyzed the peak waves of the electrically evoked auditory potentials following stimulation via surface type electrode of normal hearing and hearing loss group. The surface-type electrode with multi-channel was attached on the promontory of the inner ear of the animals. The correlation between evoked potential and the auditory ganglion cell population were observed.

The eV amplitude of EABR in the deaf group is smaller than that of the normal group. There was a positive correlation between the eV amplitude of the EABR and the population of the ganglion cell. The slopes of the negative to the positive peak of eV between channels were different. It may mean that more redundant and reliable functional assessment of the auditory nerve function could be possible via multi-site stimulation.

PS 565

Kainic Acid-Induced Synaptopathy in Gerbils

Artem V. Diuba¹; Jérôme Bourien¹; Martin Nédélec¹; Gilles Desmadryl¹; Chantal Ripoll¹; Sharon G. Kujawa²; Jean-Luc Puel³
¹INM, Inserm, Univ Montpellier; ²Department of

Otolaryngology, Harvard Medical School and Eaton-Peabody Laboratories, Massachusetts Eye & Ear Infirmary; ³INM, Inserm, Univ Montpellier,

Background. Since intracochlear perfusion of glutamate agonists and acoustic trauma induce similar damage at the level of inner hair cell (IHC) synapses with auditory nerve fibers (ANF), it has been postulated that excitotoxicity may play an instigating role in the de-afferentation observed after noise. However, noise acts both at pre- and post-synaptic levels, whereas the exogenously-applied glutamate agonists selectively act post-synaptically (see Puel, 1995 for review). Therefore, to clarify a possible role for glutamate-like excitotoxicity in noise trauma, the consequences of the agonist vs. noise exposures need to be carefully examined. The present work is part of a larger set of experiments aiming to study the similarities and differences between the two types of injury by examining the time course of the damage, the involvement of pre- and post-synaptic structures and the potential for recovery. Here we quantified how the glutamate agonist kainate affects auditory nerve and outer hair cell (OHC) function and IHC synapses with their ANF targets.

Methods. A platinum wire was placed onto the round window membrane in young adult Mongolian gerbils to measure the compound action potential (CAP) of the auditory nerve and the cochlear microphonic (CM). Artificial perilymph alone (AP control) or containing kainic acid (KA, 25 mM) was infused into the round window niche for 1 hour. Distortion-product otoacoustic emission (DPOAE), CAP of the auditory nerve and CM were measured before and 1, 3, 7 and 14 days after control and KA infusion. Following final assessments of function, the cochleae were removed and immunostained with CtBP2 and anti-GluA2 to count synapses.

Results. KA did not affect OHC function as assayed by DPOAE and CM. In contrast, one day after KA infusion, CAP thresholds were elevated by 20 to 40 dB and CAP amplitudes were reduced by 75 to 90% compared to the control animals at all tested frequencies (i.e. from 2 to 32 kHz). Two weeks after KA infusion, CAP thresholds recovered whereas CAP amplitudes were still reduced by 40 to 60%. The number of synapses in KA-perfused cochleae was reduced by 50 to 75% as compared to AP-perfused cochleae, throughout the tonotopic axis.

Conclusion. Two weeks after KA infusion, the CAP amplitude and the number of synapses did not fully recover. Ongoing experiments will assess structure and function at longer post-drug times and will provide additional pharmacologic characterization of the agonist-induced synaptopathy.

Supported by Office of Naval Research Grant N00014-16-1-2867

Combined BDNF and NT-3 Treatment of the Auditory Nerve in Deafened Guinea Pigs

Henk A. Vink; Huib Versnel; Hans G.X.M. Thomeer; Dyan Ramekers
University Medical Center Utrecht

Numerous studies have shown that treatment with neurotrophic factors prevents degeneration of the auditory nerve in deafened animals. This is relevant for clinical application in deaf patients receiving a cochlear implant. Two neurotrophic factors that are often studied, and that yield comparable results in terms of neural survival, are the structurally homologous neurotrophins brain-derived neurotrophic factor (BDNF) and neurotrophin-3 (NT-3). Interestingly, *in vitro* these neurotrophins induce different temporal response patterns of spiral ganglion cells (SGCs): BDNF-treated neurons show phasic firing patterns and NT-3-treated neurons show tonic firing patterns (Adamson et al., 2002, *J Neurosci* 22:1385-1396). Since both are present in the healthy cochlea, treatment with both BDNF and NT-3 is arguably preferable over either neurotrophin separately. Using electrically evoked compound action potentials (eCAPs) we therefore compare *in vivo* responsiveness of the auditory nerve in deafened guinea pigs with BDNF, NT-3, or BDNF+NT-3 treatment.

Guinea pigs were deafened by systemic administration of kanamycin and furosemide. After two weeks, gelfoam soaked in neurotrophin solution was placed on the punctured round window membrane, which is a clinically feasible delivery method, enabling the neurotrophins to protect the SGCs in the basal turn (Havenith et al., 2015, *Otol Neurotol* 36:705-713). Various advanced stimulation paradigms of eCAP recordings were applied which measure temporal response characteristics, including varying the inter-phase gap (IPG) of single pulses, and varying inter-pulse intervals in double-pulse or pulse train stimuli (Ramekers et al., 2015, *J Neurosci* 35:12331-12345).

Histological quantification showed that in the basal turn SGC degeneration was equally prevented in BDNF-treated, NT-3-treated and BDNF+NT-3-treated animals. The combination of BDNF and NT-3 appeared to only slightly enhance SGC survival further up to the middle turn. Varying the IPG did not yield clear differences among treatment groups, although all treatments appeared to moderately counter functional decline after deafening. Recovery characteristics derived from double-pulse responses showed slightly more normal-like recovery for BDNF-treated than for the other two treatment groups. Pulse train measures showed all treated groups to behave in between the normal-hearing and untreated controls, without a clear inclination toward either.

In summary, all treated groups showed improved cell survival and nerve functionality when compared to the untreated group, although the latter improvement was only small. There was, moreover, no clear difference among treatment groups.

PS 567

A mouse model of Charcot-Marie-Tooth disease 1A (CMT1A) provides evidence that myelin disorders can cause hidden hearing loss

Luis Cassinotti¹; Lingchao Ji²; Adam T. Palermo³; Joseph C. Burns³; Gabriel Corfas²

¹University of Michigan; ²Dept. of Otolaryngology, Head and Neck Surgery, University of Michigan; ³Decibel Therapeutics

Hidden hearing loss (HHL) is a recently described auditory neuropathy characterized by normal hearing thresholds but reduced suprathreshold amplitude of the sound-evoked auditory nerve compound action potential. It has been proposed that HHL leads to speech discrimination and intelligibility deficits in people with normal audiological tests, particularly in noisy environments. Early studies in animal models indicated that HHL can be caused by moderate noise exposures or aging, and that loss of inner hair cell synapses could be its cause.

However, Wan and Corfas (*Nat. Comm.* 2017) provided evidence that transient loss of cochlear Schwann cells also causes HHL in mice. HHL caused by this novel mechanism, which occurs in the absence of synapse loss, is evident early in the demyelination process and persists for the animal's lifespan, even after Schwann cells regenerate and axons remyelinate. It was found that the transient demyelination leads to a permanent disruption of the first heminode at the auditory nerve peripheral terminals. Recently, Choi et al. (*Sci. Reports* 2018) showed that patients with a subtype of Charcot-Marie-Tooth disease (CMT1A) present symptoms of HHL, supporting the hypothesis that defective myelin is another mechanism for HHL. CMT is a hereditary demyelinating motor and sensory neuropathy that affects 1 in 2500 people in United States. CMT1A, which results from a duplication of PMP22 gene, is the predominant subtype (50% of cases of CMT).

In the present study, we tested a CMT1A mouse model to determine if this mutation results in HHL. We assessed auditory brainstem responses (ABRs) and distortion product of otoacoustic emissions (DPOAEs) on CMT1A and wildtype littermates at different ages. CMT1A mice have normal ABR and DPOAE thresholds, but reduced amplitude of the first peak of the ABR waveform. The reduction in peak 1 amplitude is evident by one month

and becomes greater with age. These results provide further evidence that myelin defects can cause HHL. They also provide support for the findings in CMT1A patients and suggest that patients suffering from other peripheral myelin disorders are likely to have HHL. CMT mouse models are useful tools to define the cellular and molecular mechanisms of HHL related to demyelination.

This research was supported by funding from Decibel Therapeutics, Inc., a company in which Dr. Corfas holds an equity interest and serves as a consultant.

PS 568

The Study of Cochlear Synaptopathy in Humans Associated with Industrial Noise Exposure

Wei Qiu¹; Meibian Zhang²; Adrian Fuente³; Wulan Zhao⁴

¹*Auditory Research Laboratory, State University of New York at Plattsburgh*; ²*Zhejiang Provincial Center for Disease Control and Prevention*; ³*Ecole d'orthophonie et d'audiologie, Faculte de medecine, Universite de Montreal*; ⁴*Zhejiang Chinese Medial University*

Recent animal studies have revealed that moderate noise exposure could cause extensive loss of synaptic connections between cochlear inner hair cells and auditory nerve terminals. This study was conducted to evaluate whether cochlear synaptopathy occurs in workers who are exposed to various industrial noises. Noise-exposed workers (N=35) and non-exposed (control) young people (N=35), all having normal hearing thresholds (250-8000 Hz) were recruited for this study. A test battery including electrocochleography (EcochG), speech-evoked auditory brainstem response (s-ABR) and speech-in-noise (SIN) test were conducted in better ear of all subjects. The differences between noise-exposed and control groups for the results of all above-mentioned tests were analyzed. The results show that 1) in EcochG, the amplitude ratio of SP/AP of noise-exposed group was significantly higher than that of the control group at stimulus intensity of 96, and 90 dBnHL; 2) In s-ABR, the latencies of waves A, D, and O obtained from the noise-exposed group were significantly longer than the control group; 3) The noise-exposed group showed significantly poorer performance on speech recognition in noise. These results suggest that cochlear synaptopathy may occur in noise-exposed workers, and the clinical measures such as EcochG, s-ABR and SIN may be useful in detecting noise-induced cochlear synaptopathy.

PS 569

Using the Middle Ear Muscle Reflex to Assess the Impact of Noise Exposure on Auditory Nerve Function in Humans

Naomi Bramhall; Patrick Feeney; Sean Kempel
VA RR&D NCRAR

Background

Wave I amplitude of the auditory brainstem response (ABR) has been the focus of many human studies of synaptopathy because reduction in wave 1 amplitude is associated with synaptopathy in animal studies. However, human studies investigating the relationship between noise exposure and ABR wave I amplitude in young people with normal audiograms have yielded mixed results. One possible explanation for the differing results is that ABR wave I amplitude can be impacted by factors unrelated to synaptic/neuronal function such as sex and outer hair cell (OHC) dysfunction. More recent animal studies have suggested that the middle ear muscle reflex (MEMR) is even more sensitive to synaptopathy than ABR wave 1 amplitude. The MEMR is relatively insensitive to pure tone threshold elevation and does not appear to be impacted by sex differences. Therefore, the MEMR may be a more reliable indicator of synaptic/neuronal function in humans than ABR wave I amplitude.

Methods

In young Veterans and non-Veterans with normal audiograms and a range of noise exposure histories, we measured suprathreshold ABR wave I amplitude in response to a 4 kHz toneburst and contralateral wideband MEMR for broadband and 4 kHz elicitors. Self-reported noise exposure was assessed using the Lifetime Exposure to Noise and Solvents Questionnaire (LENS-Q). Participants also completed a questionnaire that asked if they experienced frequent or constant tinnitus.

Results

Lower ABR wave I amplitudes, higher levels of reported noise exposure, and report of tinnitus were all associated with weaker MEMRs when using a broadband elicitor.

Conclusions

A positive relationship between ABR wave I amplitude and MEMR strength in this sample suggests that despite measurement error due to factors such as subclinical variability in middle ear function, subclinical OHC dysfunction, electrode impedance, and sex, both types of measurements are providing similar information about synaptic/neuronal function in humans. The negative relationship between reported noise exposure and MEMR strength in the context of a normal audiogram is

consistent with animal models of noise-induced cochlear synaptopathy. This suggests that MEMR measurements may be informative in human studies of synaptopathy. In addition, the observed reduction in MEMR strength among individuals reporting tinnitus confirms previous findings and adds support to the hypothesis that some forms of tinnitus may be a perceptual consequence of cochlear synaptopathy.

PS 570

The Auditory Nerve Overlapped Waveform (ANOW) as a Detector of Early-Onset, Chronic Endolymphatic Hydrops

Choongheon Lee¹; Carla Valenzuela¹; Keiko Hirose¹; Shawn Goodman²; Craig Buchman¹; Jeffery Lichtenhan¹

¹Washington University in St Louis; ²University of Iowa

Background

Low-frequency sensorineural hearing loss is a hallmark symptom of endolymphatic hydrops. However, the relationship between hearing loss and hydrops is not understood, as human temporal bones with endolymphatic hydrops rarely have sensory cell loss in the cochlear apex. Conventional objective measurements like otoacoustic emissions (OAEs) and compound action potentials (CAPs) perform poorly at low frequencies below ~1 kHz, thus limiting the use of animal models of endolymphatic hydrops to provide insight into this relationship. We recently overcame this long-standing obstacle by developing an objective measure of low-frequency hearing: the Auditory Nerve Overlapped Waveform (ANOW). The ANOW is a neural measure that originates in the apical half of the cochlear spiral (Lichtenhan et al. 2013, 2014). Previously we found that the ANOW technique can detect acute endolymphatic hydrops when conventional measurements are normal (Lichtenhan et al. 2017). Since patients present to the clinic with chronic conditions, not acute, here we address the hypothesis that ANOW can detect early stages of chronic hydrops before the pathology progresses and damages higher-frequency cochlear regions that can be measured with conventional physiologic measures. Conventional treatments that should work in theory, but generally perform poorly in patients with a substantial history of complaints, may work when hydrops is detected early.

Methods

We created endolymphatic hydrops by using a posterior craniotomy and an intradural approach to surgically expunge the osseous portion of the endolymphatic sac of the right ear in guinea pigs. Measurements of auditory function – stimulus-frequency and distortion-product OAEs, CAPs, and ANOWs – were made at post-

surgery days 1, 2, 4, and 30. Immediately after auditory function measurements were made, ears were fixed, decalcified, and embedded in plastic for histological analysis. The length of the Reissner's membrane and the cross-sectional area of the endolymphatic space were measured.

Results & Conclusions

Surgical expungement of the endolymphatic sac increased ANOW thresholds (at ≤ 1 kHz) in most 1, 2, 4, and 30-day post-surgery ears. In contrast, conventional measures (at ≥ 1 kHz) were not markedly different in most post-surgery ears compared to controls. Four and 30-day post-surgery ears can have increased ANOW amplitudes from moderate level sounds. The length of Reissner's membrane and the cross-sectional area of scala media were larger for the 30-day post-surgery group only. These results suggest that, as chronic endolymphatic hydrops develops, changes in low-frequency electrophysiology can detect endolymphatic hydrops before conventional, histological or high-frequency electrophysiological measures.

PS 571

Time to Face the Music: Analysis of Baseline Data from a Longitudinal Study of Musicians' Hearing Health and Use of Hearing Protection

Samuel Couth¹; Michael Loughran²; Hannah Guest¹; Garreth Prendergast¹; Rebecca E. Millman³; Kevin Munro⁴; Christopher J. Armitage⁵; Christopher J. Plack¹; David R. Moore⁶; Jane Ginsborg⁷; Piers Dawes⁸

¹Manchester Centre for Audiology and Deafness; ²Division of Human Communication, Development & Hearing; ³Manchester Centre for Audiology and Deafness, NIHR Manchester Biomedical Research Centre; ⁴The University of Manchester; ⁵Division of Psychology & Mental Health; ⁶Cincinnati Children's Hospital and the University of Cincinnati; ⁷Royal Northern College of Music; ⁸Manchester Centre for Audiology and Deafness, The University of Manchester.

Background

Professional musicians are at greater risk of hearing problems due to regular and prolonged exposure to loud sounds, but only 6% of musicians use hearing protection devices (HPDs) on a regular basis. Recent evidence from animal models suggests that auditory nerve synapses may be particularly susceptible to noise damage (cochlear synaptopathy). Therefore, it may be important to monitor hearing health in "at risk" individuals using measures sensitive to neural damage, and to promote the use of HPDs. The aims of the current research are to: i) assess hearing health of early career musicians over the course of three years, and ii) formally determine the reasons for non-use of HPDs from a

behavioural science perspective. Here we report the baseline findings of this longitudinal study.

Methods

Eighty-four early career musicians (female $n = 42$, mean age = 20.3 years) and 51 non-musicians (female $n = 28$, mean age = 21.5 years) were recruited. Participants completed a battery of standard audiological measures, click-evoked auditory brainstem responses, and a speech-in-noise (SiN) test. Lifetime noise exposure was estimated by structured interview. These tests are to be repeated every 12 months for up to 3 years. Musicians' opinions on the use of HPDs were gathered at baseline using semi-structured interviews. Qualitative data were analysed using deductive thematic analysis using the Capability, Opportunity, Motivation – Behaviour (COM-B) model as a framework for understanding reasons for non-use of HPDs.

Results

There were no significant differences between musicians and non-musicians for any of the audiological, electrophysiological, or SiN measures, and no significant effects of noise exposure. Forty percent of musicians reported using HPDs at least once a week. The majority of reasons for non-use of HPDs were categorised according to 'Capability'; and 'Motivation'; components of the COM-B model, such as lack of knowledge/awareness of hearing problems (Capability), and the belief that HPDs are superfluous for certain ensembles (Motivation). However, there were also a small number of relevant themes categorised according to 'Opportunity';, such as the perceived stigma attached to wearing HPDs.

Conclusions

At baseline, there was no evidence for noise-induced hearing loss in musicians, including cochlear synaptopathy, and no evidence for perceptual deficits related to noise exposure. We will continue to monitor the effects of prolonged noise exposure on hearing abilities. Based on the reasons for non-use of HPDs, interventions to encourage HPD use may be best targeted at developing capabilities and increasing motivation.

PS 572

Considering Cognition in the Search for Hidden Hearing Loss

Aryn Kamerer; Judy Kopun; Sara Fultz; Stephen Neely; Daniel Rasetshwane
Boys Town National Research Hospital

Background

In the search for the indicators of suprathreshold

auditory deficits in humans (often referred to as hidden hearing loss), researchers are using a number of physiologic and behavioral measures to gain insight into cochlear pathologies and their resultant experiential manifestations. Studies that attempt to isolate suprathreshold deficits view aging as either a confounding factor that should be removed, or a catalyst of hidden hearing loss that must be included. Negative effects of age on physiologic (e.g. otoacoustic emissions) and behavioral (e.g. word recognition) measures of hearing, independent from audiometric thresholds, are well-documented. The negative effect of age on cognition is also well-established, however, cognitive ability, independent of age, could have effects on both the physiologic and behavioral markers of hidden hearing loss. This study examined the relationships between age-adjusted cognitive ability and several hearing measures: speech, frequency modulation (FM) detection threshold, middle ear muscle reflex (MEMR), and both tone-burst and speech-evoked auditory brainstem responses (ABR).

Methods

Pure tone and FM detection thresholds were obtained using an adaptive alternative-forced-choice task to avoid confounds of age-related response bias. Time-compressed speech recognition and speech recognition in noise were measured using NU-6 word lists. The MEMR was calculated from responses to a click probe before and after eliciting the reflex with broadband noise. Waves I and V of ABRs to 1.5 and 4 kHz tone-bursts were identified. The speech ABR was elicited using a 170-ms /da/ stimulus. The Montreal Cognitive Assessment (MoCA) scored cognitive ability which was adjusted for age. All variables were regressed with pure tone thresholds and the resulting residuals were used to observe relationships between cognition and markers of hidden hearing loss. The residuals served as a proxy for hidden hearing loss, as they represent the portion of each measure that cannot be explained by pure tone threshold.

Results

Significant relationships were observed between age-adjusted MoCA scores and time-compressed word recognition, FM detection threshold, and speech ABR.

Conclusions

Cognition unrelated to age may partially account for apparent temporal-processing deficits. Even slight cognitive impairment may contribute to deficits in both behavioral and physiologic measures of hearing. Cognitive decline may be evidence of a more global neural pathology that also cultivates hidden hearing loss. Hence, cognitive ability should be considered in

the quest to find hidden hearing loss in humans.
Funding: This study was funded by grants from NIH NIDCD.

PS 573

Altered AMPAR Subunit Expression and Sex-Specific Vulnerability to Noise-Induced Synapse Loss and Deafness in GluA3 KO Mice

Samantha N. Skobel¹; Hou-Ming Cai¹; Mark A. Rutherford²; **Maria E. Rubio**³

¹University of Pittsburgh; ²Washington University in St. Louis; ³University of Pittsburgh School of Medicine

Rapidly gating AMPA-type glutamate receptors (AMPA; GluA2, GluA3 and GluA4 subunits) mediate synaptic transmission at the mature synapse between the inner hair cells (IHC) and the afferent fibers of the cochlear nerve (IHC synapse). However, the contribution of each type of AMPAR subunit to overall glutamatergic receptor function and afferent transmission/sensitivity in the cochlea is poorly understood. Understanding this process is important because glutamate excitotoxicity through AMPAR has been implicated in the pathogenesis of hearing loss caused by noise, ischemia, and aging. Humans show sex differences in the vulnerability to hearing loss, e.g. the male humans show greater prevalence of high-frequency hearing loss (Agrawal et al., 2008), however, the contributing biological factors are unknown. We therefore began investigating the contribution of AMPAR subunits to cochlear function, and assessed sex-specific differences in AMPAR subunits that may contribute to sex differences in excitotoxic vulnerability of IHC synapses. Our functional (Auditory Brain Stem Responses, ABRs) and ultrastructural data (Electron Microscopy) show that GluA3 AMPAR subunits have a critical role in the sexually dimorphic vulnerability to hearing loss. With confocal microscopy and quantitative immunofluorescence analysis, we show that spiral ganglion neurons and IHC synapses of GluA3 knockout (KO) mice, contain less GluA2 but more GluA4. Tone-pip ABR thresholds show that GluA3-KO mice have hearing loss across all frequencies. Intriguingly, we find that female GluA3-KO mice show more hypersensitivity to sound-induced cochlear damage than male littermates. Our goal is to define mechanistically how GluA3 contributes to the structural and molecular components of IHC synapses and to sex differences that underlie the hypersensitivity to sound-induced cochlear damage.

PS 574

The Glutamate Receptor Antagonist Kynurenate Protects Against Kanamycin-induced Synaptopathy in vitro

Benjamin M. Gansemer; Steven H. Green
The University of Iowa

Background: Spiral ganglion neurons (SGNs) transmit information about acoustic stimuli from cochlear hair cells to the central nervous system. SGNs degenerate gradually following hair cell loss induced by aminoglycosides such as kanamycin (KM), but the reason for this degeneration is unclear. Similarly, SGNs degenerate gradually after noise-induced synaptopathy (Kujawa & Liberman, 2009), which, in turn, is due to excitotoxic trauma to synapses. Here we ask whether KM exposure causes excitotoxic trauma to cochlear synapses, trauma that may contribute to subsequent long-term loss of SGNs. To this end, we exposed organotypic cochlear explant cultures to KM in the presence of glutamate receptor antagonists and counted surviving synapses.

Methods: Organotypic cochlear explants were prepared from the middle turn of the cochlea from P4-P6 rat pups as described in Wang & Green, 2011. This preparation maintains the synaptic interactions between the hair cells in the organ of Corti and the SGNs. To assess whether KM induces synapse loss before hair cell death, cultures were incubated with 1.5 mM or 5 mM KM for 4, 8, 12, or 20 hours. Cultures were then labeled with anti-CtBP2, anti-PSD95, anti-myosinVI/VIIa, and anti-NF200 to visualize presynaptic ribbons, post-synaptic densities, hair cells, and SGN fibers, respectively. Synapses, defined as colocalized CtBP2 and PSD95 puncta, were quantified and compared between KM-treated and untreated control cultures. To test whether KM-induced synaptopathy is caused by excitotoxicity, cultures were treated with 1.5 mM KM for 4 hours \pm 1 mM kynurenate (KynA), a nonselective glutamate receptor blocker. Following the incubation period, cultures were labeled, and synapses quantified as described above. Synapse numbers were compared among untreated controls, KM-treated, and KM+KynA-treated cultures.

Results: Exposure to 5 mM KM for \geq 4 hours or to 1.5 mM KM for 20 hours resulted in reduced synapse number, relative to untreated controls, but also in inner hair cell damage and death. Exposure to 1.5 mM KM for \leq 12 hours resulted in a \sim 50% reduction in the number of synapses with no detectable hair cell loss. Cotreatment with KynA significantly reduced synapse loss.

Conclusions: Aminoglycosides induce synapse damage and loss prior to and independent of hair cell loss. Protection of synapse loss by a glutamate receptor antagonist implies that the synapse damage is due, at least in part, to excitotoxicity, possibly because of pathological release of glutamate from damaged hair cells. These findings raise the possibility that excitotoxic synapse damage leads to SGN degeneration.

PS 575

Combined BDNF and NT-3 Neurotrophin Cocktail Stimulates Neurite Outgrowth in an In Vitro Mouse Spiral Ganglion Explant Model

Fink Stefan¹; Marcus Müller¹; Hubert Löwenheim²

¹Hearing Research Center, Department of Otolaryngology - Head & Neck Surgery, University of Tübingen Medical Center; ²University of Tübingen

Auditory function in patients with severe hearing loss or deafness can partially be restored by electrical stimulation with a Cochlea implant (CI). Despite over 30 years of CI technology, a limiting factor in CI performance is still the anatomical gap between the electrode array in scala tympani and the stimulated regions of the auditory nerve in Rosenthal's canal. Due to this gap, only a limited number of information channels within the auditory nerve can be activated by the CI electrodes. Thus, at present, the electric stimulation by a CI is still inferior to normal hearing. To overcome this problem, we set out to improve the nerve-electrode interactions by stimulating spiral ganglion neuron outgrowth towards and onto the CI electrodes.

In the cochlear spiral ganglion, an opposing neurotrophin gradient of neurotrophin 3 (NT-3) and brain derived neurotrophic factor (BDNF) was described, also a reversal of these gradients during maturation. We therefore tested neuronal outgrowth in an murine in vitro spiral ganglion explant model applying combinations of the neurotrophins in varying concentrations. To account for the switch in the neurotrophin gradient and for better comparison to the adult situation, we established an in vitro organotypic culture model of postnatal (P7) mouse spiral ganglion explant in 96 well plates. Neurite outgrowth was analyzed using micrographs quantified with a custom adapted Sholl analysis. Effective stimulation of neurite outgrowth was quantified after application of BDNF and NT-3 alone with increasing concentrations as well as of both neurotrophins in varying combinations.

In common organotypic culture models of early postnatal (P0-P4) spiral ganglion explants outgrowth under control conditions is very limited and can be increased in a dose-dependent manner with addition of individual

neurotrophins. In contrast, in the later postnatal (P7) spiral ganglion explants substantial outgrowth even under control conditions was observed. Upon culture medium supplementation with BDNF or NT-3 the neurite outgrowth could further be increased, similarly to common models. Interestingly, a BDNF and NT-3 cocktail with both growth factors in combination seems to improve neurite outgrowth when compared to the individual compounds. The presented new organotypic culture model of late postnatal stage (P7) spiral ganglion explants is suitable for the evaluation of single neurotrophins, their combinations or even other compounds affecting the neurite outgrowth of the explants.

PS 576

The Effects of the Interphase Gap on Neural Response of the Electrically-Stimulated Auditory Nerve in Children with Cochlear Nerve Deficiency and Children with Normal-Size Cochlear Nerves

Shuman He¹; Angela Pellitteri¹; Fuh-Cherng Jeng²; Xiuhua Chao³; Lei Xu³; Jianfen Luo³; Ruijie Wang³

¹The Ohio State University Wexner Medical Center;

²Ohio University; ³Shandong Provincial Hospital affiliated to Shandong University

Background: The sensitivity of neural response generated by the electrically stimulated auditory nerve (i.e. the electrically evoked compound action potential, eCAP) to changes in the inter-phase gap (IPG) provides an indication for cochlear nerve (CN) neural survival in guinea pigs (Prado-Guitierrez et al., 2006; Ramekers et al., 2014). However, studies investigating the effects of the (IPG) on eCAP results in human CI users have shown conflicting findings (Hughes et al., 2018; Schwartz-Leyzac and Pfingst, 2016, 2018), presumably due to the unpredictable CN neural survival pattern in individual patients. Compared to children with normal-sized CNs, children with cochlear nerve deficiency (CND) have fewer CN fibers (i.e., poorer CN neural survival) and a unique CN neural survival pattern (He et al., 2018b). Therefore, comparing the eCAP sensitivity to changes in the IPG between these two subject groups provides an extremely valuable opportunity to confirm these important animal research findings.

Methods: To date, 10 children with CND and 10 children normal-size CNs have been recruited and tested for this study. All study participants used a Cochlear® Nucleus™ cochlear implant (CI) in the tested ear. The eCAP to a biphasic, charge-balanced pulse was recorded in each participant at three electrode locations that extended to the most apical electrode location where an eCAP was recorded and had a relatively equal separation between testing electrodes. IPGs tested in this study ranged from 7 to 42 ms. Slopes of eCAP Input/Output (I/O)

function were estimated using statistical modeling with a sigmoidal regression function. Dependent variables (DV) of interest included eCAP thresholds, slopes of eCAP I/O functions, and eCAP amplitudes measured at the common maximum comfortable level (C level) at all IPGs. Effects of study group, IPG and electrode location on each DV were evaluated using Generalized Linear effect Mixed Models.

Results: Results of our preliminary data analysis indicated that children with CN had flatter slopes of I/O functions, higher eCAP thresholds and smaller eCAP amplitude at the C level than children with normal-sized CNs. More importantly, children with CN demonstrated reduced eCAP sensitivity to changes in IPGs, with greater reduction observed at more apical electrode locations.

Conclusion: Our preliminary results indicate that the eCAP sensitivity to changes in the IPG is associated with CN neural survival.

PS 577

Role of Complement in Neurodegeneration in Kanamycin deafened Rats

Muhammad T. Rahman¹; Jack H. Parker²; Steven H. Green³

¹Interdisciplinary Graduate Program in Human Toxicology, The University of Iowa; ²Department of Biology, The University of Iowa; ³The University of Iowa

Spiral ganglion neurons (SGNs) gradually die after destruction of hair cells, their sole afferent input. However, unmyelinated type II SGNs die more slowly than myelinated type I SGNs. In our experiments, Sprague Dawley rats were deafened by daily intraperitoneal injection of kanamycin, postnatal day 8 (P8)-P16. Loss of hair cells was confirmed histologically but rats showing detectable ABR for clicks <95 dB SPL were excluded. During SGN degeneration post-deafening, markers of inflammation, cellular and humoral, are upregulated. Correspondingly, immunosuppressive drugs are protective to type I SGNs. Complement proteins are a group of proteins involved in inflammation. When activated, the early components (C1-C5) of the complement system, which are synthesized at the site of inflammation, can opsonize cells (foreign or native) to facilitate phagocytosis and also serve to recruit inflammatory cells. The late components (C6-C9) are synthesized in the liver, recruited by the early components, and form the membrane attack complex (MAC) to lyse cells. Our gene expression profiling demonstrated that, in deafened rats, expression of the early complement components is upregulated in spiral ganglion. Here we used immunofluorescence imaging to

determine the spatial relationship between complement components and the cells of the spiral ganglion. Rats deafened as above were euthanized at P70 by which time <50% of the SGNs remain. The cochleae were fixed and cryosectioned (6 μ m) parallel to the midmodiolar plane. Hair cells were labeled with antibodies to myosin 6/7; neurons with TuJ1; type II SGNs selectively with anti-peripherin; Schwann cells with anti-S100. To identify cells opsonized by complement, we used anti-C3 antibody and we used C5b-9 antibody to detect MAC formation. Image analysis was done using the FIJI ImageJ package with custom-written macros. In deafened but not in control spiral ganglia, C3 immunofluorescence was seen only on type I SGNs, which were viable at that time as assessed by nuclear morphology. In contrast, type II SGNs and Schwann cells showed no C3 immunofluorescence. No cells in the ganglion showed the presence of a MAC. We conclude that neuroinflammation postdeafening involves opsonization of live type I SGNs by complement component C3 that may facilitate their phagocytosis by phagocytic cells (e.g., macrophages). However, direct complement mediated lysis of cells in spiral ganglion after deafening is unlikely given the absence of MAC formation. These studies present the complement system as a promising new target for therapeutic intervention to prevent SGN degeneration in deaf patients.

PS 578

Gap Junction Gene Cx30 Deficiency can Induce Cochlear Synaptopathy

Yan Zhu; Shu Fang; Hong-Bo Zhao
Dept. of Otolaryngology, University of Kentucky Medical Center

Background: Gap junction (GJ) channels play an important part in hearing function. GJ connexin gene mutations induce high incidence of nonsyndromic hearing loss. Most of the previous studies focused on their roles in homeostasis of inner ear through gap junctional intercellular communication (GJIC). Connexin30 (Cx30, JGB6) is one of the predominant gap junctional isoforms in the cochlea and its mutations can also lead to hearing loss. Here, we investigate whether the connexin gene Cx30 deficiency can affect the cochlear synapse degeneration.

Methods: Cx30 knockout (KO) mice and littermate wild-type (WT) mice were used. ABR threshold, DPOAE, and cochlear microphonics (CM) were recorded to assess cochlear and hearing function. The ribbon which is the structural hallmark of cochlear inner hair cell (IHC) afferent synapses was examined by immunofluorescent staining for CtBP2.

Results: Cx30 KO mice showed hearing loss in comparison with WT mice. Immunofluorescent staining shows that ribbon synapses in Cx30 KO mice were significantly reduced in numbers compared to those in WT mice. Ribbon synapses in Cx30 KO mice also demonstrated a specific, “deer-hoof-print” like distribution that WT mice do not possess.

Conclusions: These data indicate that gap junction gene Cx30 deficiency can induce the cochlear ribbon synapse degeneration, revealing a novel role of gap junctions in the neural development in the cochlea.

Supported by NIH R01 DC 017025

PS 579

Progesterone Promotes Cochlear Synapse Regeneration After Excitotoxic Trauma

Seband Bafti¹; Ning Hu; Steven H. Green

¹*University of Iowa*

Animal experiments have shown that moderate noise exposure, even at levels too low to destroy hair cells, can destroy synapses between inner hair cells (IHCs) and spiral ganglion neurons (SGNs). This noise-induced cochlear “synaptopathy” (NICS) is a consequence of excitotoxic trauma to the postsynaptic bouton due to excessive release of glutamate from IHCs. Some studies have suggested that NICS can impair speech comprehension in noise or cause tinnitus. Synaptopathy can be mimicked in vitro by adding the glutamatergic agonist kainic acid (KA) to organotypic cochlear explant cultures that possess intact synaptic connections between hair cells and SGNs (Wang & Green, 2011). A synapse is defined as colocalized CtBP2/Ribeye (ribbon) and PSD95 immunofluorescent puncta. Using this model system we have investigated means to regenerate lost synapses and here focus on promotion of synapse regeneration by steroid sex hormone progesterone. Cochlear explant cultures from postnatal day 5 rat pups were exposed to KA (0.5 mM) for 2 hrs, which resulted in loss of >80% of synapses on IHCs. Addition of progesterone (20 ng/ml) to the culture medium after KA exposure induced regeneration of >90% of synapses within 16 hrs. NT-3 is an endogenous neurotrophic factor in the organ of Corti, previously shown to promote regeneration of synapses on IHCs. We asked whether endogenous NT-3 is necessary for promotion of synapse regeneration. As previously (Wang & Green, 2011), NT-3 signaling was blocked by adding TrkC-IgG, which specifically binds NT-3 with high affinity, to the culture medium. Sequestering NT-3 effectively prevented synapse regeneration induced by progesterone. In conclusion, our data show that progesterone effectively promotes synapse regeneration

in vitro, and that this ability requires concomitant NT-3 produced by the organ of Corti. These studies are aimed at determining the molecular and cellular mechanisms of cochlear synapse regeneration that could provide insights for future therapeutic interventions for hearing impairments due to NICS.

PS 580

Dynamic Range Adaptation in the ECochG of the Mongolian gerbil

Gilberto D. Graña; Kendall A. Hutson; Brendan T. Lutz; Douglas C. Fitzpatrick

University of North Carolina at Chapel Hill

The auditory system is faced with a large range of sound pressure levels and needs to maintain sensitivity across this range. Previous studies have shown that both midbrain auditory neurons and auditory nerve fibers can adapt to the distribution of sound levels from a dynamic, continuous stimulus by shifting their rate-level functions to place the most frequently-occurring sound levels near the midpoint (Wen et al., 2009; Dean et al., 2005). In our study, we sought to determine whether this dynamic range adaptation at the peripheral level is primarily a cochlear or neural phenomenon.

Anesthetized animals were presented with continuous, 4-kHz tonal stimuli where the intensity was randomly changed between 16-90 dB SPL in 1-2 dB steps. A baseline condition was presented with no high probability range of intensities, followed by conditions where 80% of the intensities were in different 10 dB high-probability ranges (HPRs) centered around 48, 72, or 84 dB SPL, followed by a repeat of the baseline condition. We then analyzed input/output functions of the cochlear microphonic (CM) and compound action potential (CAP) to each condition to see if changes occurred as a function of the HPR used. The study was performed both in normal hearing animals and in animals with the OHCs removed by a combination of furosemide and kanamycin (FK).

The results were that the input/output functions of the CAP, but not the CM, shifted with the HPR, and that the shifts were similar whether starting from baseline and then increasing to the HPR or presenting the stimuli in the opposite direction. The same result was observed in both normal-hearing and FK animals. These results indicate that the site for dynamic range adaptation is most likely at the site of the auditory nerve synapse rather than involving cochlear effects such as the MOC reflex.

PS 581

Effects of Noise-Induced Hearing Loss on Speech-In-Noise Envelope Coding

Satyabrata Parida¹; Michael Heinz²

¹Weldon School of Biomedical Engineering, Purdue University; ²Speech, Language, & Hearing Sciences, and Weldon School of Biomedical Engineering, Purdue University

Speech-intelligibility (SI) models aim to predict human perceptual performance when speech is subjected to a range of acoustic manipulations. SI models not only test our understanding of how the brain processes speech, but can also assess hearing-aid and cochlear-implant signal-processing strategies. To date, a single SI model that can explain all of the normal-hearing effects of the wide range of tested manipulations remains elusive. Furthermore, even state-of-the-art strategies for hearing aids continue to struggle in adverse backgrounds. These problems highlight two key gaps. Firstly, most SI models are implemented in the audio domain and rely on numerous assumptions. Unfortunately, there is a scarcity of published neural data to evaluate these model assumptions. Secondly, it's not straightforward for audio-domain SI models to predict the effects of hearing impairment (beyond audibility). This gap is primarily due to our limited understanding of the variety of effects of cochlear hearing impairment on speech (especially speech-in-noise) coding. For example, two subjects with similar audiograms can have very different speech-understanding ability. Animal models of cochlear hearing impairment provide a useful opportunity to collect data to directly address these SI-model gaps. Here, we collected spike trains from auditory-nerve fibers in anesthetized chinchillas in response to speech, spectrally-matched stationary-noise, and noisy-speech mixtures at perceptually relevant SNRs (-10, -5 and 0 dB). Overall speech intensity was fixed at ~65 dB SPL for normal-hearing and ~80 dB SPL for hearing-impaired animals. Peristimulus-time histograms constructed from spike trains were filtered to extract response envelopes in different modulation bands. Preliminary data reveal that the correlation between AN-fiber response envelopes of noisy-speech and noise-alone is increased for hearing-impaired fibers, suggesting a greater potential degree of distraction from inherent envelope fluctuations following cochlear hearing loss. This novel finding is significant given the emphasis recent SI models (e.g., Jørgensen and Dau, JASA 2011) have placed on the importance of inherent envelope fluctuations in predicting noisy-speech perception. In addition, fundamental-periodicity coding of clean speech was enhanced for the hearing-impaired group, at the expense of place-specific formant coding. Preliminary data also show a degradation of burst envelopes of high-frequency fricatives. These results

highlight significant effects of cochlear hearing loss on the strength of inherent noise fluctuations in noisy speech, which are likely to be important in addition to speech-coding fidelity when predicting hearing-impaired SI.

Work supported by an International Project Grant from Action on Hearing Loss (UK).

PS 582

Non-Invasive Assays of Cochlear Synaptopathy in Humans and Chinchillas

Kelsey Dougherty¹; Hannah Ginsberg²; Alexandra Mai¹; Satyabrata Parida²; Jennifer Simpson¹; Michael Heinz³; Hari Bharadwaj³

¹Speech, Language, & Hearing Sciences, Purdue University; ²Weldon School of Biomedical Engineering, Purdue University; ³Speech, Language, & Hearing Sciences, and Weldon School of Biomedical Engineering, Purdue University

Histological studies in multiple species, including post-mortem human studies, have shown that acoustic overexposure and normal aging can lead to the loss of afferent synapses innervating the cochlea. Insidiously, this "cochlear synaptopathy" (CS) can occur without any measurable changes in audiometric thresholds and hence can be "hidden" from standard clinical diagnostics. Hypothetically, CS, while hidden, can lead to speech-understanding deficits in noisy environments, and reduced ability to perceive subtle spectrotemporal features of suprathreshold sounds. To test this hypothesis comprehensively in behaving humans and animals, and to aid in the clinical diagnosis of CS, non-invasive assays of CS need to be established.

Here, through parallel experiments in at-risk humans and noise-exposed chinchillas, we evaluate a common battery consisting of three physiological measures implemented using shared software tools -- auditory brainstem responses (ABR), wideband middle-ear muscle reflexes (WBMEMR), and swept-tone distortion-product otoacoustic emissions (DPOAE).

Each chinchilla will be exposed to moderate-level octave-band noise for two hours to produce CS and a temporary threshold shift (TTS), while not producing appreciable permanent threshold changes. Measurements will be gathered prior to noise exposure, one day after exposure to confirm TTS, and two weeks after exposure to assay for CS. The same physiological measures will be acquired in a cross-sectional design across young humans reporting regular and substantial acoustic exposure, middle-aged individuals, and young "control" subjects with nominal acoustic exposures. Preliminary results in both species suggest that suprathreshold ABR wave-I

amplitudes, MEMR amplitudes, and MEMR thresholds are correlated with CS risk. DPOAE measures help to control for variations in threshold sensitivity.

Future experiments will compare these non-invasive assays to perceptual measures of temporal processing in both species and speech-in-noise measures in humans. Direct measurements of CS using immunohistochemistry will also ultimately be compared to the results from our non-invasive battery in chinchillas.

Funding was provided by NIH R01DC015989 (Bharadwaj) and R01DC009838 (Heinz), as well as the Purdue Summer Undergraduate Research Fellowship Program.

Auditory Perception in Complex Environments

PS 583

Environmental Sound Recognition in Reverberation as Causal Inference

James Traer; Josh H. McDermott
Massachusetts Institute of Technology

Natural audio contains the combined effects of sound sources and environmental reverberation. Reverberation provides information about the environment but distorts source sound signals, posing a challenge for recognition. Humans are known to robustly recognize speech in reverberation, but it is not clear how well this robustness extends to other types of sounds. We investigated human recognition of environmental sounds in the presence of reverberation, evaluating overall robustness and its dependence on source and reverberation characteristics. We presented listeners with recordings of environmental sounds and asked them to identify the source. Some of the trials had reverberation added digitally. Recognition of environmental sounds was fairly robust to naturalistic reverberation but was impaired if the imposed reverberation violated natural reverberation statistics. Recognition in reverberation was also substantially more impaired if the sound source was typically quiet (e.g. a salt-shaker) than if the source was typically loud (e.g. a jackhammer). An additional experiment suggested that this impairment results from the source distance implied by reverberation, potentially because distance implied source intensities that were physically implausible for typically quiet sounds. The results are consistent with the idea that sound sources and reverberation are separated to some extent by the auditory system, but that source recognition is constrained by estimates of source intensity derived using reverberation.

PS 584

Benefit of Ambiguous Visual Stimuli on Auditory Spatial Discrimination Is Modulated by Task Difficulty

Madeline S. Cappelloni; Ross K. Maddox
University of Rochester

Localization of audiovisual objects is largely dominated by the perceived location in the visual modality. This is particularly evident in studies of the ventriloquist effect, which describes a bias of auditory location towards a visual stimulus. The auditory bias decreases when visual stimuli are blurred or otherwise rendered less reliable than the perceived auditory location, indicating that the visual impact is dependent on the relative quality of the auditory evidence. We previously demonstrated that visual influence on the spatial perception of simultaneous auditory stimuli can give rise to a performance benefit in an auditory spatial discrimination task. Here we investigate how this visual benefit changes when the auditory stimuli are manipulated to make the task easier or harder.

Listeners completed a concurrent auditory spatial discrimination task. During each trial, we presented two sounds and two visual stimuli. The two sounds, a pink noise token and a harmonic tone complex, were symmetric about zero degrees azimuth, such that listeners could report whether the tone complex was on the left or right by a button press. Visual stimuli were assigned random shapes and colors for each trial, and either appeared in spatial alignment with the auditory stimuli or in the center of the monitor. To modulate the difficulty of the auditory task, three stimulus durations were tested, 100 ms, 300 ms, and 1 s, with the shortest being the most difficult. We used weighted one up one down adaptive tracks to determine the 75% separation threshold for each duration. The visual benefit was then defined as the decrease in threshold of the spatially aligned condition relative to the central control condition. Preliminary results suggest that the visual benefit decreases as the duration of the auditory stimulus increases and the auditory task becomes easier.

We previously found that uninformative visual stimuli can improve auditory spatial discrimination. Here we replicate that result and expand on it by showing that the effect increases in behavioral importance as the task becomes harder.

PS 585

Intuitive Physics in Auditory Scene Analysis

James Traer; Josh H. McDermott
Massachusetts Institute of Technology

Upon hearing objects collide, humans can estimate many of the underlying physical attributes, such as material and force of impact. Although the physics of sound generation are well established, the inverse problem that listeners must solve – of inferring physical parameters from sound – remains poorly understood. Here we show that humans use implicit knowledge of acoustical physics to constrain auditory inference, allowing disambiguation of distinct object properties from a single impact sound. We presented listeners with recorded sounds of a ball impacting a board and demonstrate that humans can disambiguate the properties of ball and board, even when both are unknown a priori. We present a generative model to make explicit how physical factors affect the impact sound and we show that listeners can disambiguate ball from board only if the sounds are consistent with this model. Listeners presented with visual or auditory cues to one object's material more accurately estimated the mass and impact force of the other object, suggesting that listeners separate the acoustic contributions of different objects using internal physical models. The results demonstrate intuitive physical inference in audition, and suggest that it is inseparable from auditory scene analysis.

PS 586

Fusion and Identification of Dichotic Consonants in Normal-Hearing and Hearing-Impaired Listeners

Nishad Sathé; Alexander Kain; Lina Reiss
Oregon Health & Science University

Hearing-impaired (HI) individuals can exhibit increased fusion of different phonemes across ears, which is associated with poorer speech perception in quiet and noisy environments. Prior studies using tone and vowel stimuli have shown that the fused percept is often a spectral average of the two original stimuli. The goal of the present study was to investigate fusion and identification of dichotic consonant sounds in normal-hearing (NH) and HI listeners who wear hearing aids.

Two experiments were conducted using 1) natural (recorded) and 2) synthesized speech. Synthetic consonants varied in the starting frequency of the second formant. Four stop consonants (/ba/, /pa/, /ga/, /ka/) differing in place of articulation and/or voicing were presented with headphones, with interaural difference in fundamental frequency (ΔF_0) varied. For HI listeners, stimuli were shaped according to NAL-NL2

prescriptive targets. Listeners were asked to identify 1 or 2 consonants heard without being informed that consonants always differed across ears. Options also included /ta/ and /da/, for a total of 6 possible responses, in case of spectral averaging of fused stimuli.

With natural consonants, at $\Delta F_0=0$, both NH and HI subjects exhibited mainly single-item responses (fusion) and performed poorly at identification of both consonants. As ΔF_0 increased, both groups showed decreases in fusion and increases in percent correct identification of both consonants. HI subjects had overall higher fusion rates and poorer identification performance than NH subjects. With synthetic consonants, NH subjects showed similar patterns as with natural consonants, but overall increased fusion and decreased performance, nearing identification performance in HI subjects for natural consonants. HI subjects were unable to discriminate synthetic consonants and thus could not do the synthetic consonant task.

The findings suggest that ΔF_0 is an important cue used by listeners to separate speech streams and prevent fusion of similar acoustic signals. Additionally, greater fusion of synthetic consonants compared with natural consonants implies that natural voice cues provide additional cues for separation of streams. However, the finding that HI listeners could not discriminate the synthetic consonants indicates that HI listeners are unable to use formant transitions for consonant discrimination, and that other cues may be more important for HI listeners. Further research is needed to determine the cues used by HI listeners for consonant discrimination, as well as the cues in natural consonants used for stream segregation. [Supported by NIH-NIDCD grant R01 DC013307]

PS 587

Evaluating Enhanced Auditory Perception Augmentation via Stochastic Resonance

Sage Sherman; Keith Covington; Allison Anderson
University of Colorado Boulder

Noise exposure and age decrease the cochlea's ability to hear sound at low intensities; however, white noise may be able to lower auditory thresholds in humans. Stochastic resonance (SR) is a phenomenon in nonlinear systems where noise can increase the throughput of a signal, periodic or aperiodic. This suggests that SR can improve auditory perception in low signal-to-noise environments by having white noise resonate with subthreshold signals, amplifying them to suprathreshold signals. Past research has focused on modeling this phenomenon within the auditory system (Sumner et al. 2002) and in cochlear implants (Morse & Roper 2000). There have also been animal studies

in gerbils (Henry et al. 1999) and crayfish (Douglass et al. 1993); however, little research has been done with employing SR in human subject testing. This research aims to understand if there is utility to external input SR in terms of enhancing auditory perception. Morse & Roper (2000) has detailed that the optimal level of noise for cochlear implants is equal to the RMS value of the auditory threshold at that frequency. The second aim of this research is to explore if this optimal level of noise translates to the cochlea of normal hearing subjects.

To test these goals, twelve human subjects will participate in audiometry with and without the addition of noise. These subjects will meet strict inclusion criteria to determine if they have normal hearing. The inclusion is determined using questionnaires related to their hearing health, otoscopic exams of the ear canal and tympanic membrane, tympanometry to identify any pathology, and audiometric thresholds ≤ 25 dB HL. Once the subject meets the criteria, we will take their audiometry without noise at frequencies equal to 0.5, 1, 4, 8, and 14 kHz. This will be done within a sound-treated booth to ensure external distractions do not affect near threshold audiometry. The Békésy-style tracking approach to audiometry will be conducted to determine thresholds. Subjects will then find their thresholds with ambient white noise mixed into the signal. To test if the optimal level of noise at a given frequency is equal to the subject's threshold at that frequency without noise, white noise levels will be presented in increments of 5 dB SPL, ranging from -15 dB SPL below threshold to +10 dB SPL above threshold. Pure tone audiometry with and without the addition of noise will be compared. Thresholds taken with varying noise levels will also be compared.

PS 588

Correlation between Performances in Informational Masking and Visual Crowding

Min Zhang¹; Thuy Tien Cao. Le²; Antje Ihlefeld¹

¹New Jersey Institute of Technology; ²Rutgers School of Graduate Studies

Background

In everyday environments, two types of masking, called informational (IM) versus energetic (EM) masking, commonly occur. While EM mechanisms are well characterized, we still do not understand the mechanisms causing IM. A comprehensive literature establishes that IM occurs when competing sources in the auditory scene are perceptually similar or when a listener is uncertain about the features of the target source. Furthermore, a hallmark of IM is that dramatic differences in thresholds exist across listeners. A potentially related phenomenon in vision, called visual crowding, occurs when observers excessively integrate perceptual features in the visual

scene. Here, we compare performance in IM versus Visual Crowding in the same individuals to test the hypothesis that IM and Visual Crowding share a common processing limitation.

Methods

Eight young normal-hearing listeners without formal musical training were tested in three tasks.

Task 1 measured detection of 8-tone melodies in IM, contrasting two notched-masker conditions: a noise masker (Patterson JASA 1976), used to estimate thresholds in EM, versus a melody masker, used to estimate IM thresholds. In each trial, the masker was delivered at a fixed sound level while the target sound level was variable. Melody-IM susceptibility was defined as the detection threshold difference between noise versus melody masker.

Task 2 tested speech intelligibility with a previously established paradigm (Arbogast et al. JASA 2002). Speech utterances from a closed-set corpus were vocoded using 16 bands. On each trial, nine randomly chosen bands were added to create the target. The masker was comprised of the remaining seven bands and consisted of either noise (EM) or speech from a different talker (IM). Percent correct was measured as a function of target-to-masker broadband energy ratio (TMR). Speech-IM susceptibility was defined as the difference in TMR at 50% correct in EM versus IM background.

Task 3 assessed visual crowding using a paradigm developed by Pelli et al. (F1000 Research 2016). Participants were tasked to identify a target letter among distracting letters. The spacing threshold required to identify the target letter, called Critical Spacing, was used to measure visual crowding.

Results

Linear regression fits reveal a significant correlation between Melody-IM- versus Speech-IM-susceptibility ($R^2 = 0.74$, $p = 0.005$). In addition, Critical Spacing correlates strongly with both Melody-IM-susceptibility ($R^2 = 0.6$, $p = 0.02$) and Speech-IM-susceptibility ($R^2 = 0.62$, $p = 0.02$). However, Critical Spacing and absolute thresholds are uncorrelated. Results suggest that a common mechanism limits Visual Crowding and IM.

PS 589

Exploring Auditory Salience in Natural Scenes Using Amazon Mechanical Turk

Nicholas Huang; Sandeep Reddy Kothinti; Mounya Elhilali

Johns Hopkins University

A salient stimulus is one that attracts bottom-up attention in an automatic fashion. Although salience is primarily driven by qualities of the stimulus itself, it can be influenced by task-related goals and other aspects of top-down attention. As a result, dissociating these two attentional components can be difficult, particularly for studies of audition. While visual studies can rely on gaze, no such overt measures of attention exist in the auditory domain. As such, measurements of auditory attention (particularly for natural stimuli) have largely been performed with manual ranking or labeling. These methods can be heavily influenced by top-down attention.

A recent work has presented a salience measurement method using continuous dichotic comparison between pairs of natural scenes. Recording responses continuously better captures the immediate reaction to each instant of the natural scene. However, this method requires collecting a relatively large amount of data so that each scene can be compared to many others, and to reduce the effect of individual differences. In the current study, we examine the effectiveness of this dichotic salience method using data collected through Amazon's Mechanical Turk system. We compare salience judgments obtained through Mechanical Turk with results previously collected in a laboratory setting to verify the consistency of the data. In addition, we explore altering scenes in a controlled manner in order to manipulate the context and semantic information within the scenes.

PS 590

Influence of Binaural Hearing on Speech Intelligibility and Listening Effort

Joseph Roche¹; Ellen Snodgrass¹; Ruth Litovsky²

¹*The University of Wisconsin - Madison School of Medicine and Public Health*; ²*University of Wisconsin - Madison*

Introduction

Binaural hearing can improve speech intelligibility performance when sound sources are spatially separated. Additionally, binaural hearing may reduce the effort required to complete a listening based task. However, the influence of binaural hearing abilities on listening effort remains poorly understood. Pupil dilation can be used to measure listening effort and engagement

during listening tasks. Large pupil sizes indicate high effort during the task, and small pupil sizes indicate low effort. We used pupillometry to investigate the effect of spatially separating target speech from competitors. We hypothesized that pupil dilation will be reduced in conditions where target and competitors are spatially separated compared to the co-located conditions.

Methods

Normal hearing adult subjects participated. During testing participants listened to, and repeated target stimuli (male voiced IEEE sentences) in the presence of competing signals (male voiced AZ-Bio sentences). Pupil size was measured concurrently. Target sentence were presented at 0° azimuth and competing sentences were presented at either 0° azimuth (Co-located) or at to the right and left at 90° azimuth (Symmetric) configurations. The symmetric configuration was selected to maximize use of binaural cues. Target and masker presentation levels were varied to signal-to-noise ratios (SNR) of -12 to +9 in 3 dB steps. The overall sound level was held constant 65dBA. A total of 32 sentences per condition were presented across 2 blocks of 8 sentences during each of 2 sessions. Speech intelligibility was measured as the number of correctly repeated keywords. An Eyelink 1000 infrared camera focused on one eye measured the area of the pupil over time starting 2 seconds prior to stimulus onset and continuing for 7 seconds after the stimulus offset.

Results

Speech intelligibility scores reached approximately 95% correct responses at 0 dB SNR with percent correct scores decreasing with decreasing SNR in both stimulus configurations. Pupillary response waveforms were averaged for each SNR/stimulus configuration and the peak pupil response was determined. Analysis of peak pupil responses indicate that pupil dilation systematically increased when Target SNR decreased, and pupil dilation was greater in Co-located conditions than Symmetric conditions at the same SNRs from -12 to 0 dB.

Conclusions

These preliminary findings provide further evidence regarding the interaction of speech intelligibility and listening effort in normal hearing adults, and the role of binaural hearing.

Funding: Work supported by the UW Department of Surgery, by NIH-NIDCD (grant R01DC003083 to Ruth Litovsky) and a Core grant from NIH-NICHHD U54HD090256 to the Waisman Center.

PS 591

Modeling Auditory Scene Analysis as Bayesian Sound Source Inference

Maddie Cusimano¹; Luke B. Hewitt¹; Joshua B. Tenenbaum¹; Josh H. McDermott²

¹Massachusetts Institute of Technology, Department of Brain and Cognitive Sciences; ²Massachusetts Institute of Technology

Inferring individual sound sources from the mixture of soundwaves that enters our ear is a central problem in auditory perception, termed auditory scene analysis (ASA). Auditory illusions have been used to demonstrate ASA at work in human perception, and have provided evidence for implicit assumptions that listeners make about sound source structure (Bregman, 1990). However, most explanations of these phenomena lack formal models that predict perceived sources from the acoustic waveform, or only account for a narrow class of illusions. Thus, it is unclear whether the diverse set of ASA illusions can be explained by a small set of principles. We present a Bayesian model of ASA which infers representations of simple acoustic sources from audio. Inference is performed via Markov chain Monte Carlo sampling following initialization using a neural network. Given a sound waveform, our system infers the number of sources present, the parameters defining each source, and the sound produced by each source. The model qualitatively accounts for perceptual judgments on a variety of ASA illusions, and can in some cases infer perceptually valid sources from simple naturalistic audio. The results provide a proof-of-concept for how inference in a source-based model of sound generation could account for auditory scene analysis.

PS 592

Illusory Sound Texture Reveals Extended Statistical Completion in Auditory Scene Analysis

Richard McWalter; Josh H. McDermott
Massachusetts Institute of Technology

Auditory scenes often contain multiple sound sources that differ in their temporal variability. Sound textures, as arise from swarming insects or falling rain, lie on one end of this spectrum, having properties that remain relatively constant over a multi-second timescale. Sound textures are well described by statistics measured from early auditory representations [McDermott & Simoncelli, 2011], and are thought to be represented with statistics averaged over a multi-second window [McWalter & McDermott, 2018]. However, little is known about the perception of sound textures when they co-occur with other sound sources in an auditory scene.

We investigated the perception of sound textures under these conditions, asking whether the auditory system infers the texture to continue when it is plausibly masked by another sound. We found that sound textures are perceived to continue when interrupted by up to several seconds of noise, so long as the noise is sufficiently high in intensity to plausibly mask the texture. The effect is analogous to the well-known illusions of continuity that occur for tones or speech interrupted by noise, but differs in that it lasts much longer (~2 seconds for textures vs. ~200 ms for tones or speech), and because the extrapolated sound must be defined statistically due to the stochastic nature of texture.

We next asked whether the representation of illusory texture is similar to that of actual texture. In a second experiment listeners judged which of two textures was most similar to a reference texture. The first texture underwent a change in statistics, while the second texture had fixed statistics. The experiment leveraged the fact that texture judgements are biased by several seconds of the stimulus history [McWalter & McDermott, 2018]. We found that when interrupting noise was inserted prior to the statistic change, texture judgments were biased as if texture was actually present, suggesting that the illusory texture heard during the noise was represented like actual texture. When we inserted a silent gap prior to the noise, disrupting the subjective impression of illusory texture, the bias was eliminated.

The results suggest that illusory sound textures can be heard over several seconds and appear to be represented similarly to actual texture, revealing new aspects of perceptual completion in auditory scenes.

PS 593

Attentional and Peripheral Components of Auditory Context Effects

Jackson Graves¹; Claire Chambers²; Daniel Pressnitzer¹

¹Département d'études cognitives, École normale supérieure, PSL University, CNRS; ²Department of Neuroscience, University of Pennsylvania

The auditory system is frequently required to deal with ambiguous information and to choose between multiple plausible interpretations of an auditory scene. Laboratory stimuli have been designed to probe the underlying decision mechanisms, such as the "tritone paradox", wherein two successive Shepard tones containing only octave-spaced components (Shepard, 1964) are spaced half an octave apart. In this case, the frequency shifts are balanced in terms of upward or downward shifts, but listeners clearly hear one or the other interpretation. It has been recently shown that this percept is strongly

influenced by the preceding context (Chambers et al., 2017). Here, we investigate whether these context effects are implemented at a more peripheral or a more central level of auditory processing. We presented context sequences producing opposite biases to the left and right ears and asked listeners to attend to one ear only. Then, listeners had to judge the shift of an ambiguous Shepard test pair, presented in one ear only. The attended ear and test ear were experimental parameters, counterbalanced across conditions. We used fully ambiguous test pairs with balanced contexts, but also slightly biased test pairs with strong and weak contexts. Overall, we observed significant effects of both tested ear and attended ear, such that responses were more likely to follow the attended context, but were also more likely to follow the context sequence presented to the tested ear—even when that ear was unattended. These findings show that auditory contextual processing includes both a central component related to selective attention and a peripheral component related to ear of entry.

References

Chambers, C., Akram, S., Adam, V., Pelofi, C., Sahani, M., Shamma, S., and Pressnitzer, D. (2017). "Prior context in audition informs binding and shapes simple features," *Nature Communications*, 8, 15027.

Shepard, R. N. (1964). "Circularity in judgments of relative pitch," *J. Acoust. Soc. Am.*, 36, 2346.

PS 594

A Glimpsing Model with a Variable "Tile" Size

Christopher Conroy¹; Todd R. Jennings²; Gerald Kidd²
¹*Department of Speech, Language & Hearing Sciences, Boston University*; ²*Boston University*

Ideal time-frequency segregation (ITFS) has been used previously—and quite successfully—to separate the peripheral and central components of speech-on-speech (SOS) masking [Brungart et al., 2006, *JASA*, 120(6)]. A core assumption underpinning the use of ITFS is that it roughly emulates the effects of the peripheral component of masking under a given stimulus configuration. Thus, the increase in masking observed for unprocessed stimuli relative to ITFS processed ("glimpsed") stimuli can be attributed to the central component of masking. This difference, measured as the dB increase in target-to-masker ratio at threshold for unprocessed stimuli relative to the corresponding threshold for glimpsed stimuli, has been termed "additional masking". Recent unpublished work from our laboratory (Kidd et al., submitted) using ITFS has yielded evidence of greater additional masking in hearing impaired (HI) than in normal hearing (NH)

observers on SOS masking tasks. However, this finding is complicated by the fine time-frequency resolution that was used during ITFS processing (i.e., a relatively "small" analysis "tile") which may be incompatible with the well-established consequences of cochlear pathology (e.g., increased peripheral spread of masking) and thus could affect NH and HI performance differently. In the Kidd et al. study, the ITFS processing used 128 frequency analysis bands ($n=128$), further subdivided into 20 ms time windows ($m=20$). In the present study, n and m were varied systematically during stimulus generation in a manner meant to crudely approximate the degraded peripheral resolution typical of HI observers. Masked speech identification thresholds for both speech and noise maskers were obtained in NH observers for the reference condition ($n=128$, $m=20$). Comparison conditions in which $n=8$, 32 or 128 and $m=20$ or 80 were tested. Lower n yielded significantly higher thresholds for both masker types. An increase in m from 20 to 80 ms at a given n yielded significantly higher thresholds for noise maskers only. Results suggest that part of the greater additional masking in HI relative to NH observers may be attributable to increased peripheral spread of masking, as was modeled in conditions in which $n<128$ and/or $m=80$. Acoustic analyses generally support this interpretation.

PS 595

Temporal Integration Windows for Sound Texture Statistics

Richard McWalter; Josh H. McDermott
Massachusetts Institute of Technology

Sound textures, as arise from falling rain or galloping horses, are sounds defined by their temporal homogeneity. Sound textures are well described by statistics measured from early auditory representations, and, as such, are thought to be represented in the auditory system with time-averaged statistics. Recent work has suggested that texture statistics can be averaged over integration windows as long as several seconds [McWalter and McDermott, 2018]. However, it remains unclear whether all statistics are averaged over the same extent, or whether averaging windows might vary across statistics, potentially adapted to the robustness of the statistic.

In this study, we probed the extent of time-averaging for individual classes of statistics from the auditory texture model of McDermott and Simoncelli (2011): marginal moments (envelope mean, envelope variance, and amplitude modulation power) and pair-wise envelope correlations. In addition, the amplitude modulation power statistic was partitioned into four bands ranging from slow to fast modulations. These statistics differ in the sample

size required for robust estimation, and we hypothesized that the averaging window might mirror these differences.

In the experiment, listeners judged which of two sound textures was most similar to a reference texture [McWalter & McDermott, 2018]. The duration of the two sound textures varied across trials (from 50ms to 5s). The values of the selected class of texture statistic differed between the two stimuli, drawn from a continuum between the statistics of a real-world sound texture (the reference) and Gaussian noise. The experiment leveraged the finding that texture discrimination performance increases with stimulus duration and then asymptotes, presumably when the duration of the sound texture exceeds the time-averaging window used to estimate the statistics [McWalter & McDermott, 2018]. We found that the performance asymptote occurred at different durations for different statistics, ranging from roughly 100 milliseconds for the envelope mean (capturing the spectrum) to several hundred milliseconds for the envelope correlation, to a second for the envelope variance. The performance asymptote for the modulation power depended on the modulation band rate, ranging from several hundred milliseconds for fast modulations to a few seconds for slow modulations.

The results reveal that the extent of time-averaging varies across texture statistics, as might be required to obtain stable statistic estimates of functions differing in intrinsic variability.

PS 596

Entrainment of stream segregation in a dynamic environment

James Rankin¹; Aine Byrne²; John Rinzel²

¹University of Exeter; ²New York University

Background: The auditory streaming paradigm (van Noorden 1975), in which alternating high- A and low-frequency tones B appear in a repeating ABA-pattern, has been shown to be perceptually bistable (Pressnitzer & Hupe 2006) for extended presentations (order of minutes). For a fixed, repeating stimulus, perception spontaneously changes at random times between an integrated interpretation with a galloping rhythm and segregated streams, switching every 2-8s. However, streaming in a natural auditory environment requires segregation of auditory objects with features that evolve over time. With the relatively idealized ABA- triplet paradigm, we begin to explore switching in a non-static environment, by considering slowly and periodically varying stimulus features.

Methods: Participants listened to three-minute long presentations of ABA- triplet stimuli with the difference in frequency DF between the higher A and lower B tones

modulated sinusoidally about 5 semitones. Different periods of modulation were tested, either matching, faster, or slower than the group intrinsic mean percept duration T as measured without modulation; mean durations for the two percepts are equal for DF fixed at 5. Preliminary results using our neuromechanistic model (Rankin, Sussman & Rinzel 2015) helped to set stimulus parameters for the DF modulation.

Results: Exploration of periodically modulated stimuli in the model lead the following predictions: 1) switches into segregated (integrated) occur on the DF upswing (downswing), with most switches occurring before the maximal (minimum) DF values 2) maximal entrainment occurs when the DF modulation rate matches T (has period 2T). Fig 1A shows the DF modulation profile and Fig 1B shows the predicted timing of switches into segregated (red) occurring before the peak in DF and into integrated before the trough. Our experimental data confirm these predictions and show that perceptual switches are entrained to the periodically modulated stimulus. The paradigm is extendable to consider modulation of other stimulus parameters such as location, loudness or presentation rate.

Conclusions: Our results demonstrate perceptual entrainment for slowly varying stimuli, which carries practical implications for future auditory bistability experiments with human listeners and animal models. Knowledge of the likely perceptual state as dependent on instantaneous phase could allow for performance of human participants in other tasks to be measured with a time-locked a priori expectation of their perceptual state. This knowledge could prove useful for animal models where invasive recording is possible, but objective measures of perception are limited (Christison-Lagay & Cohen 2014).

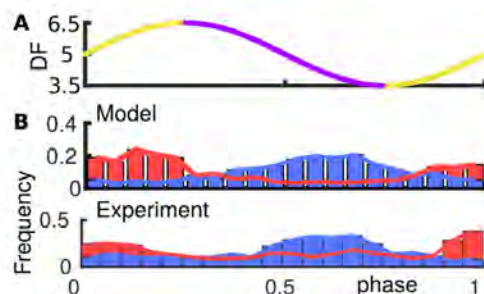


Figure 1: **A:** Shows one cycle of DF-modulation between 3.5 and 6.5 semitones with the phase normalised to the interval [0,1]. Increasing phase is yellow, decreasing purple. Period of modulation was 10s, which is roughly double the intrinsic perceptual duration of 5s with fixed DF=5. **B:** Phase-histogram of times of switches from integrated to segregated (red) and from segregated to integrated (blue) from model and experiment with $N = 7$ participants.

PS 597

Modeling Multi-Feature Regularity Extraction from Dynamic Sounds

Ben Skerritt-Davis¹; Mounya Elhilali²

¹John Hopkins University; ²Johns Hopkins University

To make sense of our auditory surroundings, the brain tracks sound sources as they evolve and move through the scene, collecting and combining information about regularities over time across multiple features to represent each sound source as a single auditory object. The computational mechanisms behind the construction of this multi-feature representation and its use in auditory scene analysis is not well understood. To investigate this process, we employ a previously proposed model for regularity extraction that builds statistical representations of sounds sequentially over time and adapts these representations to changes in the scene. We extend this model to represent sounds across multiple features—both spectral and spatial—and we use the model to simulate psychophysics data collected from humans in a change detection task. We compare alternative computational mechanisms for combining information across features to determine whether regularities are collected jointly in a high-dimensional feature space or if they are collected independently along each feature and combined at a later stage.

PS 598

Comparing Speech Perception in Noise and Speech for Musicians and Non-musicians in More Ecologically Valid Environments

Sara M. K. Madsen¹; Marton Marschall¹; Torsten Dau¹; Andrew J. Oxenham²

¹Hearing Systems Group, Department of Electrical Engineering, Technical University of Denmark;

²Department of Psychology, University of Minnesota

Several studies have measured speech perception in noise and competing speech in non-musicians and highly trained musicians to investigate the effect of musical training, but the results have been inconclusive. Most studies find little or no benefit of musicianship. Nevertheless, two recent studies found a sizeable musician advantage in conditions where the target and two natural speech maskers were separated by $\pm 15^\circ$ in azimuth (Clayton et al., 2016; Swaminathan et al., 2015). These studies used highly similar speech signals from a closed-set matrix test for both the target and masker, did not include reverberation, and used average head-related-transfer functions to simulate spatial separation, which can limit externalisation. It is not clear if the musician advantage observed generalizes to more natural situations.

The present study attempted to replicate the earlier findings and to extend them using more realistic speech material in conditions with and without reverberation. The target and two speech or noise maskers were either colocated or spatially separated by $\pm 15^\circ$ in azimuth. The speech experiments were conducted in a large anechoic chamber using a virtual sound environment with a spherical array of 64 loudspeakers. The study also measured F0 discrimination limens (F0DLs), interaural time difference limens (ITDLs), and attentive tracking (Woods and McDermott, 2015) in a double-walled acoustically shielded booth. Sixty-four young listeners (32 musicians and 32 non-musicians) were tested. The two groups were matched in age, gender, and IQ as measured with Raven's Advanced Progressive Matrices.

The musicians exhibited enhanced F0DLs, ITDLs and better attentive-tracking abilities. However, there was no musician advantage in any of the speech perception tasks, providing no evidence that musicians are better at understanding speech in more ecologically valid situations. It is not clear why it was not possible to replicate the previous results, but the difference may be related to the large within-group variability observed in both the present and previous studies.

Clayton, K. K., Swaminathan, J., Yazdanbakhsh, A., Zuk, J., Patel, A. D., and Kidd, G. (2016). "Executive function, visual attention and the cocktail party problem in musicians and non-musicians," *PLoS One*, 11, 17. doi:10.1371/journal.pone.0157638

Swaminathan, J., Mason, C. R., Streeter, T. M., Best, V., Kidd, G., and Patel, A. D. (2015). "Musical training, individual differences and the cocktail party problem," *Sci Rep*, 5, 1. doi:10.1038/srep14401

Woods, K. J. P., and McDermott, J. H. (2015). "Attentive Tracking of Sound Sources," *Current Biology*, 25, 2238–2246. doi:10.1016/j.cub.2015.07.043

PS 599

The Effect of Temporal Regularity on Immediate Serial Recalls of Synthesized Vowel Sequences

Yi Shen; Anna M. Hopkins

Indiana University Bloomington

Cognitive processes, such as working memory, play important role in the recognition of running speech in noisy backgrounds. Previous studies from our lab have developed an experimental paradigm in which synthesized vowel sequences are presented in noise and the listener is instructed to recall the vowels in the correct order. The primacy and recency effects associated with the immediate serial recall task have

been used as indicators of listeners'; cognitive efforts. The current study aims to investigate the effects of temporal regularity of the vowel sequences on the performance of the same immediate serial recall task. It is hypothesized that greater temporal irregularity will cause an increase in cognitive load, leading to enhanced primacy or recency effects. Sequences of five synthesized vowels were presented in steady-state noise and listeners were instructed to recall the vowel sequences in the correct order. The sequences were either isochronous (in the Regular condition), or anisochronous and randomized across trials (in the Irregular condition). The average rate of the vowel sequence was either 1 or 4 Hz. The vowels were synthesized with the periodicity in the glottal source systematically manipulated, leading to different pitch strengths under different conditions. As the pitch cues in the target vowels were systematically removed, it was expected that the listeners would rely more on the temporal rhythm of the target sequence to segregate it from the background noise. The level of the background noise was adjusted so that an 80-% recognition rate was expected for the synthesized vowels in isolation across all pitch-strength conditions. Results show that even at the Signal-to-Noise Ratio corresponding to 80-% correct performance for isolated vowels, poor performance was observed for the five-vowel sequences for all listeners. In the Regular condition, the average performance was close to 60-% correct and in the Irregular condition, average performance was close to 40-% correct, with some vowels near the center of the sequence recognized only at chance (i.e. 20%). Performance was poorer for the 4-Hz than the 1-Hz vowel rates. A primacy effect was observed and it was more prominent for higher presentation rates, lower pitch strengths, and the Irregular condition. A recency effect was also observed in most listeners, but much less prominent than the primacy effect.

PS 600

Phoneme-based analysis of continuous speech-evoked cortical responses reveals speech intelligibility

Youngmin Na¹; Subong Kim²; Inyong Choi³; Jihwan Woo¹

¹Department of Biomedical Engineering, University of Ulsan; ²Department of Communication Sciences and Disorders, University of Iowa; ³University of Iowa

Background

Speech intelligibility (SI) is an index of the comprehensive level of speech. SI has been used to evaluate the performance of both hearing aids and cochlear implants. SI is typically measured in clinics by scoring dictation tests in a listening task. However, the subjective nature of

this scoring approach can be significantly influenced by task difficulty and subject condition. Recently, changes in electroencephalography (EEG) signals in response to word or tone stimuli have been used to objectively evaluate auditory function. However, the EEG responses to simple stimuli are limited in their ability to predict the SI of natural speech in sentence form. In this study, we aimed to develop a new approach using continuous speech-evoked EEG to predict the SI.

Methods

We recorded 64-channel EEG signals from twelve young, normal-hearing adults in response to ten naturally-spoken sentences and their corresponding vocoded sentences in a passive listening condition. We also used spectrally degraded (8-channel noise vocoded) sentences to mimic degraded SI. Each sentence was repeated one hundred times. The cross-correlation coefficients between the EEG signals and 1) the speech temporal envelope, and 2) the phoneme-onset impulse train were computed. The cross-correlation coefficients in natural- and vocoded-speech conditions were compared at each electrode using paired t-tests.

Results

The cross-correlation coefficients revealed the morphology of P1-N1-P2 components within 70-240 ms after speech onset. The P1-N1-P2 components of the cross-correlation coefficients between EEG signals and the phoneme impulse train were significantly higher in the natural condition than in the vocoded condition. Dominance was observed at left frontal, temporal, and parietal sites. However, the speech envelope-based analysis showed no significant difference between natural and vocoded conditions.

Conclusion

This study developed an objective approach to predict SI using continuous speech-evoked EEG signals. Our results demonstrate that natural continuous speech-evoked EEG responses follow phoneme onsets, rather than temporal envelopes. Our results also show that the cross-correlation between EEG signals and phoneme trains is sensitive to SI.

Supported by National Research Foundation of Korea grants (2017R1E1A1A01078409), NIDCD P50 DC000242 31A1, and Hearing Health Foundation Emerging Research Grant.

Auditory Prostheses IV: Stimulus Coding & Nerve Survival

PS 601

Effect of asymmetric pulses on spatial selectivity in cochlear implants: Computational Model Study

Hyejin Yang¹; Jong Ho Won²; Jihwan Woo³

¹*School of Electrical Engineering, Biomedical Engineering, University of Ulsan;* ²*Division of Ophthalmic and Ear, Nose and Throat Devices, Office of Device Evaluation, Center for Devices and Radiological Health, US Food and Drug Administration;* ³*Department of Biomedical Engineering, University of Ulsan*

Background

Despite the successful restoration of speech perception for cochlear implant (CI) users in a quiet listening environment, the poor spatial selectivity of CIs negatively impacts speech understanding in a noisy environment as well as music perception. To improve the spatial selectivity of CIs, several attempts were made previously including a new electrode design and novel stimulation strategies. Our previous studies indicated that the neural excitation of the auditory nerve is sensitive to pulse shape, polarity, and stimulation rate. In this study, we investigated the effect of asymmetric pulse shapes on the spatial selectivity of CIs using a computational neural model. Moreover, we systematically investigated the extent to which variations in the pulse shapes could influence spectral ripple discrimination performance by CI recipients.

Methods

A charge-balanced biphasic stimulus was used to simulate auditory nerve fiber (ANF) responses. The durations of the first (cathodal) and second (anodal) phases were systematically varied from 25 to 50 ms and from 25 to 50, 100, 200, and 400 ms, respectively. The responses of the spatially distributed ANFs were used to evaluate the spatial selectivity for each of these pulse shapes. The spectral ripple discrimination by CI recipients was evaluated by computing the similarity of two neurograms in response to the spectral ripple stimulation. The pulse trains for spectral ripple stimulation for each channel were generated by the advanced combination encoder (ACE) strategy.

Results

The preliminary results showed that as the duration of the second (anodal) phase increases the threshold and excitation of neighboring ANFs decrease. The

duration of the second phase also influences the neural dynamic range (i.e., relative spread) and jitter, but these depend on electrode-to-fiber distance. We will present parametric data showing how pulse duration influences the spatial selectivity of CIs. We will also present pulse shape parameters that are optimized for the best spectral ripple discrimination.

This work is supported by National Research Foundation of Korea grants (2017R1E1A1A01078409). The views expressed in this paper are those of the authors and do not necessarily reflect the official policy or position of the US Department of Health and Human Services and the US Food and Drug Administration. No official endorsement is intended or should be inferred.

PS 602

Effect of the distance between the stimulation electrodes and auditory nerve fibers on spectral resolution of cochlear implants: Computational model study

Jong Ho Won¹; Hyejin Yang²; Jihwan Woo³

¹*Division of Ophthalmic and Ear, Nose and Throat Devices, Office of Device Evaluation, Center for Devices and Radiological Health, US Food and Drug Administration;* ²*School of Electrical Engineering, Biomedical Engineering, University of Ulsan;* ³*Department of Biomedical Engineering, University of Ulsan*

Background:

Spectral resolution of cochlear implant (CI) users has been widely evaluated using the spectral ripple discrimination (SRD) test, which showed significant correlations with speech perception performance for CI users. Despite the high correlation, the across-subject variability in SRD performance is quite large even among the patients implanted with the same implants, the same sound processors with the same coding strategy. The hypothesis of this study was that the distance between the electrode and auditory nerve fiber (ANF) affects SRD performance for CI users. To test this hypothesis, we evaluated the effects of the electrode positions on SRD performance using a computational neural model and the model predictions were compared to the behavioral SRD data collected from human CI subjects.

Methods:

An ANF model developed by Woo (Woo et al., 2009) was used to predict ANF response to ripple noise stimuli. This model was based on the Hodgkin-Huxley model, and the parameters of this model were set by the geometry of cat. This model was composed of the

peripheral axon with three internodes, cell body, and central axon with 20 internodes. Five different electrode-ANF distances were tested to investigate the effects of the electrode position on SRD performance. The SRD performance was predicted by calculating the similarity of two neurograms in response to standard and inverted ripple stimuli.

Results:

The current study showed that the predicted SRD performance decreased as the ripple density increased, consistent with human CI subjects. More importantly, the SRD performance was predicted to improve with the closely located electrode. The range of the across-subject variability for the SRD performance for human CI subjects was covered by the simulated SRD performance using the five different distance values, suggesting that the effect of the electrode position could be a significant factor to account for the variability of SRD performance for human CI users. The current study suggests that the computational model study combined with the human psychoacoustic experiment may provide a useful tool to understand the underlying factors affecting CI outcomes that cannot be evaluated by the behavioral study alone.

Acknowledgement: Supported by National Research Foundation of Korea grants (2017R1E1A1A01078409). The views expressed in this paper are those of the authors and do not necessarily reflect the official policy or position of the US Department of Health and Human Services and the US Food and Drug Administration. No official endorsement is intended or should be inferred.

PS 603

Polarity Sensitivity in Children and Adults with Cochlear Implants

Kelly N. Jahn¹; Julie G. Arenberg²

¹University of Washington; ²3 Department of Speech & Hearing Sciences, University of Washington Seattle, 4 Massachusetts Eye and Ear Infirmary, Harvard Medical School

The physiological integrity of spiral ganglion neurons likely influences cochlear implant (CI) outcomes. In fact, demographic variables that are implicitly related to neural health, such as duration of deafness and hearing loss etiology, are the most consistent predictors of speech perception scores across CI listeners. These patient-specific variables differ substantially between prelingually deafened children and postlingually deafened adults with CIs, suggesting that neural status might also differ between the two populations. Biophysical modeling studies suggest that sensitivity to stimulus polarity might reflect neural integrity in CI listeners. Specifically, anodic

stimulation is a more effective neural stimulus than cathodic stimulation when the peripheral processes are degenerated or demyelinated. The goal of the present study was to determine whether psychophysical polarity sensitivity at threshold differs as a function of hearing history in children and adults with CIs. A secondary goal was to determine whether polarity sensitivity is related to focused behavioral thresholds, a well-established measure of the quality of the electrode-neuron interface. Electrode-specific thresholds in response to monopolar, triphasic pulses where the central high-amplitude phase was either anodic (CAC) or cathodic (ACA) were measured on four electrodes. Two low-threshold channels and two high-threshold channels were tested, to represent relatively good and poor electrode-neuron interfaces, respectively. The polarity effect was defined as the difference in threshold response to the ACA compared to the CAC stimulus. Based on modeling data, a positive polarity effect is inferred to reflect peripheral degeneration, whereas a negative polarity effect represents good neural health. Site-specific focused behavioral thresholds were also measured. Results indicate that high-threshold channels have a larger polarity effect than low-threshold channels. Furthermore, the average polarity effect does not differ between individuals implanted as children and those implanted as adults. Duration of deafness was correlated with the average polarity effect on high-threshold channels for adults, but not for children. Overall, results indicate that both pediatric and adult CI listeners may experience some degree of peripheral process degeneration. Moreover, peripheral degeneration likely degrades the quality of the electrode-neuron interface in CI listeners. These data could have important clinical implications for developing electrode-specific CI programming interventions for children and adults.

PS 604

Spread of excitation with increasing pulse amplitude or phase duration

Ning Zhou¹; Lixue Dong²; Juliana Mathews¹; John Galvin³

¹East Carolina University; ²East; ³House Ear Institute

Background: In electric hearing, loudness increases with pulse amplitude (PA) or phase duration (PD). For a fixed PD, increasing PA increases both current spread and spread of excitation (SOE). For a fixed PA, increasing PD does not increase current spread but may increase SOE due to greater neural firing probability. It is unclear whether SOE may differ as PA or PD is increased.

Method: Subjects were adult users of Cochlear Corp. cochlear implants (CIs). Forward-masked excitation patterns were measured for maskers that spanned a

range of loudness levels in which the PD was fixed and the PA increased (PA masker), or the PA was fixed and the PD increased (PD masker). All masker stimuli were presented to a middle electrode (11) at 1000 pulses per second. First, the dynamic range (DR) of the maskers was estimated. The PD for the PA masker was fixed at 25 ms, and the PA was increased until achieving threshold and MAL. For the PD masker, PA was fixed at the threshold level and the PD was increased from 25 ms until achieving maximum acceptable loudness (MAL). Loudness growth functions were estimated for the PD and PA maskers on a linear scale. The PA masker was loudness-balanced to the PD masker at 30, 50, and 70% DR. Forward-masked thresholds were measured for probe electrodes 8-14 for the equally loud PA and PD maskers at the three presentation levels.

Results: As a function of %DR, loudness growth functions were shallower for the PA than the PD maskers. After normalizing to the peak, the slopes of the masking pattern (i.e., SOE) were steeper for the PD masker than for the equally-loud PA masker at the low level; SOE was similar for the two maskers at the medium and high levels. SOE for the PA and PD maskers (and the difference in SOE between the maskers) were correlated with speech performance in noise only at the low level.

Discussion: The reduced SOE with the PD maskers suggest that channel interaction may be reduced by using longer phase durations in clinical CI speech processing, especially at the lower end of the DR. The negative correlation between speech performance and the difference in SOE between the PA and PD maskers suggests that longer phase durations may especially benefit poorer-performing CI listeners, who may be more susceptible to increased channel interaction associated with PA intensity coding.

PS 605

Neural Time Constants are Key Determinants of Simulated Electrically Evoked Compound Action Potential Growth Function Shape

Jesse M. Resnick; Jay T. Rubinstein
University of Washington

Electrically evoked compound action potentials (eCAPs) are Intracochlear recordings of cellular responses to implant stimulation that can be obtained in both humans and animal models. In principal these recordings provide an objective measure of neural response to stimulation and a method of bridging findings between the human and animal model literature. Unfortunately, in practice there is enormous eCAP variability between individuals, and even amongst electrodes within a single implant, that cannot be adequately explained and frustrates

interpretation and synthesis of results. Here we have extended a stochastic, biophysical, computational model of electrical stimulation of spiral ganglion fibers to simulate eCAPs in populations differing along multiple dimensions including neural degeneration, demyelination, and electrode placement to explore possible biophysical mechanisms underlying this variability. These simulated eCAPs recapitulate many of the key morphological features of those recorded both in CI recipients and animal models while enabling simultaneous analysis of spiking activity.

Adenis et al. 2018 explored eCAP threshold growth functions in acutely and chronically deafened guinea pigs to stimuli where delivered charge was controlled by varying either pulse amplitude or phase durations. They observed great between-animal heterogeneity of relative growth functions, particularly in chronically deafened animals. eCAP growth functions of normally myelinated simulated populations recapitulate key features of the acutely deafened animal responses. Notably, with high total charge delivery, response amplitudes to phase-duration-based stimuli lagged those to amplitude-based stimuli of equal net charge, reflecting the importance of neural time constants even amongst healthy neurons. Demyelination and degeneration yielded response growth functions that exhibited many of the key dimensions of variability observed by Adenis et al., including alterations in relative slope and peak response amplitudes but that failed to capture others, notably thresholds. Analysis of fibers' strength-duration curves suggests increases in the mean and variance of fiber time constants with demyelination may drive much of this eCAP variability. While eCAP growth functions exhibited a notable effect of demyelination with long pulse widths, spike efficiency functions did not. Analysis of spike latency and eCAP peak width demonstrates that this variable amplitude growth is due to eCAP amplitudes reflecting both fiber recruitment and response synchrony. These results suggest that relatively nuanced changes in neural health, even without loss of spiral ganglion neurons, may significantly alter eCAP properties and that continued attention to temporal integration may unravel these dynamics.

(Supported by NIH/NIDCD grant 1F31DC017349-01 and an American Otological Society Fellowship Grant.)

PS 606

Channel Interactions in Cochlear Implants: Do They Really Increase at High Current Levels?

Quentin Mesnildrey¹; Olivier Macherey¹; Stéphane Roman²

¹Aix-Marseille Univ., Centrale Marseille, CNRS, LMA;

²Department of Pediatric Otolaryngology and Neck Surgery, Aix-Marseille University.

Because of the conductive properties of the cochlea, the neural populations recruited by adjacent electrodes overlap. These channel interactions are thought to alter the transmission of sound information to cochlear implant (CI) listeners. Here we aim to better understand the relationship between these interactions and the stimulation level.

When considering a single electrode, an increase in level enables the recruitment of more distant neurons. One, therefore, often concludes that channel interactions should increase with current level.

However, if we assume that channel interactions relate to the proportion of fibers stimulated by both electrodes relative to the total number of fibers excited, the effect of current level is more difficult to predict.

This question was investigated in a pitch discrimination task with CI users (Cochlear Corporation). On each trial, the subjects heard a reference and a test stimulus, presented in random order and had to indicate which one was higher in pitch. The reference stimulus consisted of two 300-ms duration, 80-pps interleaved pulse trains presented on both electrodes. The delay between the two pulse trains was equal to half a period yielding an "aggregate" temporal pattern of 160-pps pulse rate. This reference was compared to seven different test stimuli with rates ranging from 80 to 210-pps. For all test stimuli, the two electrodes were activated with a very short delay so that the aggregate temporal pattern was identical to the temporal pattern on each electrode. This task was repeated at two levels corresponding to 60%(soft) and 100%(loud) of the dynamic range. In this paradigm, the temporal pitch of the reference stimulus being judged close to 160Hz would suggest that the percept is dominated by neurons responding to the aggregate stimulus. In the opposite, a reference pitch judged close to 80Hz would indicate that the recruited neural populations were more independent.

Preliminary results with two subjects show that the perceived pitch was closer to the aggregate pitch, suggesting that in all conditions, the neural excitation patterns significantly overlapped. For one subject, the perceived pitch for the soft and loud

conditions did not differ. For a second subject, however, the perceived pitch was lower for the loud condition, suggesting that, in this case, the neural population conveying the aggregate temporal pattern was relatively smaller at the loud than at the soft level.

Additional data are being collected with a group of CI users for further investigation.

PS 607

Amplitude Modulation Depth Discrimination by Cochlear Implant Users

Jessica J.M. Monaghan¹; Robert P. Carlyon²; John M. Deeks²

¹Macquarie University, Department of Linguistics; ²MRC Cognition & Brain Sciences Unit

Most cochlear implants (CIs) convey the amplitude envelope of speech by modulating high-rate pulse trains. However, not all of the envelope may be necessary to perceive amplitude modulations (AM); the effective envelope depth may be limited by forward masking from the envelope peak. We studied the effective portion of the dynamic range (DR) contributing to the perception of AM depth (AMD) by CI users, and its dependence on AM rate.

Nine users of the Cochlear device took part. Standard stimuli were 1000-pps 448-ms pulse trains modulated at 100% of DR, presented on electrode 16. Modulation rates were 15.625, 31.25, 62.5, 125 and 250 Hz. Experiment 1 used 3-Interval 2AFC adaptive trials with feedback; subjects indicated the 'different'; (signal) stimulus, which differed from the standard only in its AMD. Peak amplitude for all stimuli was fixed at MCL, and signal AMD was adjusted to determine the threshold (AMDT), defined in terms of %DR in decibels. Subjects could use any cue, including the possibility that the signal was louder than the 100%AMD standard. An rmANOVA revealed a highly significant effect of modulation rate on AMDTs, which were highest (best) at the 31.25-Hz rate. AMDTs dropped at higher rates consistent with the expected influence of forward masking, and at 15.625 Hz, where there were only seven modulation cycles.

Experiment 2 used identical stimuli, but 2-Interval 2AFC adaptive trials where subjects were instructed to ignore loudness cues. To check whether subjects complied, 'catch-trials'; were inserted, with no feedback, in which the less-modulated signal was softer than the standard. These showed that, for about 80% of subject/AM rate combinations, subjects were not using loudness cues. The effect of modulation rate was not significant, but was broadly similar to that in Exp. 1. Overall, AMDTs were significantly lower (worse) than in experiment 1,

and, averaged across rates and subjects, were equal to about 35%. Hence in the absence of loudness cues the lower 65% of the DR does not, on average, contribute to AMD perception for the stimuli used here. We will also report the results of an experiment where the portion of the envelope below a cut-off was modified without changing loudness, and where the cut-off was adjusted to determine the proportion of the modulated waveform over which CI listeners can discriminate changes in envelope shape.

Funded by a Macquarie University Visiting Research Fellowship for JMD and by MRC award MC_UU_00005/3 to RPC.

PS 608

Effect of the Relative Timing Between Same-Polarity Pulses on Thresholds and Loudness in Cochlear Implant Users

François Guérit¹; Jeremy Marozeau²; Bastian Epp²; Robert P. Carlyon³

¹MRC Cognition and Brain Sciences Unit, University of Cambridge; ²Hearing Systems, Technical University of Denmark; ³MRC Cognition & Brain Sciences Unit

Background

Knowledge about the temporal integration of electrical currents by the spiral ganglion neurons is relevant for the clinical fitting of cochlear implants, as it may reveal underlying pathologies. However, the clinical use of biphasic pulses limits such measures, because currents of opposite polarities interact at the level of the neural membrane. Here, we describe a paradigm for studying polarity-specific summation of currents with pulse pairs at short inter-pulse intervals (IPIs).

Methods

We used pairs of pseudo-monophasic (PS) pulses, where a 43- μ s high-amplitude phase of one polarity was followed or preceded by an 8-times-longer and 1/8th-amplitude phase of the opposite polarity. The interphase gap within each pulse was 2 ms. The short-high phases of the two PS pulses within each pair always had the same polarity; one pulse was time-reversed so that the short-high amplitude phases of the two pulses followed each other. We assumed that most of the excitation would stem from these short-high phases.

We created PS pulse pairs having inter-pulse intervals (IPIs) from 0 to 345 μ s, and with the short-high pulses being either anodic or cathodic. Six adult users of an Advanced Bionics cochlear implant balanced the loudness of the pulse pairs with varied IPIs to that of a single pulse having the same polarity. The pulse pairs/single pulses were presented for 400 milliseconds

at a 100-Hz rate. We also measured the detection thresholds of the listeners for all pulse-pair and single-pulse stimuli using an adaptive tracking procedure.

Results

In the loudness matching task, the IPI had a significant effect, with the loudest stimuli being perceived at the shortest IPI. For both polarities, the 0-us-IPI pulse pairs were on average 4 dB louder than the single pulse of same polarity. Furthermore, the effect of IPI interacted with the polarity of the pulse pairs. The loudness difference between single pulses and the pulse pairs at the longest IPI was 2.2 dB when the short-high phases were cathodic, but only 0.9 dB when anodic.

In the detection threshold task, thresholds were overall lower when the short-high phases were anodic than when they were cathodic, but the effect of IPI was not significant and did not interact with polarity.

Conclusions

The effect of IPI on loudness was consistent with a combination of an exponential facilitation at short IPIs and with spiral ganglion neurons that did not fire to the first pulse being given a second chance to do so by the second pulse. Both effects might be polarity-dependant. We will discuss possible peripheral origins of those results, including the absence of an effect of IPI at threshold.

PS 609

Perceptual Changes with Monopolar, Phantom and Pseudomonophasic Electrode Stimulation

Waldo Nogueira¹; Monica Padilla²; Natalia Stupak³; David M. Landsberger⁴

¹Department of Otolaryngology, Hannover Medical School; ²University of Southern California Keck School of Medicine; ³New York University School of Medicine; ⁴NYU School of Medicine

Introduction

In cochlear implants (CIs), there is great interest in extending the range of stimulation towards more apical regions than those provided by the electrode array. Three possible techniques have been explored to lower pitch perception. The first technique is Phantom Electrode (PE) stimulation which is achieved by simultaneously stimulating out-of-phase two adjacent intra-cochlear electrodes with different amplitudes (e.g. Klawitter et al 2017). The ratio between these amplitudes is typically denoted by σ . If the basal electrode stimulates with smaller amplitude than the apical electrode of the pair, the resulting electrical field is pushed away from the basal electrode producing a lower pitch. The second technique uses asymmetric pseudo-monophasic

anodic-first pulses presented in bipolar configuration (PSA; Macherey and Carlyon 2012). The third technique combines the two previous ones (PE+PSA). The aim of this study is to investigate perceptual differences between monopolar (MP), PE, PSA and PE+PSA stimulation. Specifically it examines if a) there is a perceptual qualitative difference between these modes other than place of stimulation and b) examines the relative magnitude of the perceptual shifts for each of these modes. Furthermore, this work investigates if the perceptual changes caused by the three stimulation techniques are dependent on electrode location.

Methods

10 Advanced Bionics users (3 from USC and 3 from NYU in the US and 4 from MHH in Germany) participated in two experiments. The first experiment used a multidimensional scaling procedure (MDS) and the second used a traditional scaling procedure. In the MDS experiment, CI users reported the perceptual distances between 5 single electrode (typically 1, 3, 5, 7, and 9) stimuli in MP, PE, PSA and PE+PSA modes. The PE modes were configured with $\sigma = 0.5$. Subjects were asked to report how perceptually different each pair of stimuli were using any perceived differences except loudness. In the second experiment, each stimulus was presented in isolation and subjects scaled how “high” or how “clean” each stimulus sounded.

Results

Results from the MDS task suggest that perceptual differences between MP, PE, PSA and PE+PSA stimulation can be explained by a single dimension. In general, it seems that the dimension that explains the perceptual differences is dominated by place pitch. However, the analysis of individual data reveals that for some subjects there is relation between how high is the sound and how clean the sound is.

In summary the results demonstrate the potential of these techniques PE, PSA and PE+PSA to lower the pitch perception and show that these stimulation modes can be used for new sound coding strategies in order to extend the pitch range for CI users without perceptual side effects.

Acknowledgements

The authors would like to thank the subjects who have participated in the experiments. This work was supported by the DFG Cluster of Excellence EXC 1077/1 “Hearing4all” and the NIH/NIDCD (R01 DC012152, PI: Landsberger).

PS 610

Psychophysical Tuning Curves, Thresholds, and Vowel Identification in Children and Adults with Cochlear Implants

Julie G. Arenberg¹; Lindsay DeVries²

¹3 Department of Speech & Hearing Sciences, University of Washington Seattle, 4 Massachusetts Eye and Ear Infirmary, Harvard Medical School;

²Department of Hearing and Speech Sciences, University of Maryland, College Park

Although cochlear implants are highly successful for restoring hearing for children and adults with severe to profound hearing loss, the outcomes are highly variable, even in early implanted children. One possible source of variability may be the interface of electrodes to nearby neurons but another source may be the quality and timing of the input to the auditory system during development. Pre-lingually deaf and early implanted children differ from post-lingually deaf adults in this way. Previous studies have demonstrated that focused stimulation may be sensitive to the quality of the electrode-neuron interface at the periphery. In animal models, altered input can lead to central reorganization of the representation of stimulation at the periphery for all sensory systems, including auditory. It is as yet unknown the degree to which this happens in humans implanted early with electrical stimulation of the cochleae. Psychophysical tuning curves (PTCs), although thought to reflect primarily peripheral activation, might be sensitive to central reorganization. In this study, we compare the PTC bandwidth of children with cochlear implants to those of adults. We relate these tuning curve bandwidths to signal detection thresholds obtained using focused stimulation and to speech perception measures. Thirteen unilaterally implanted adults and twelve children, 8 of whom were bilaterally, sequentially implanted with the Advanced Bionics, HiRes90k device participated. A forward masking paradigm was used to measure PTCs for one electrode in the middle of the array. Masker stimuli were presented to electrodes 2–15. Adults used a sweep procedure (modified from Sek and Moore, 2005; Bierer et al., 2015), where the masker was steered across cochlear implant electrodes and the probe was fixed. Children used a 2I2AFC procedure. Steered quadrupolar (focused) stimulation was used for the masker stimulus with sigma of 0.5 and monopolar for the probe stimulus. Masker and probe pulse trains were 500 and 20 ms long, respectively, and presented at 1000 pulses per second. Equivalent rectangular bandwidth and tuning curve slopes were used to quantify the sharpness of tuning. In the children, age of implantation was not related to age of implantation, but was related to focused threshold. As well, individuals with higher thresholds tended to perform more poorly

on a medial vowel identification task. These results may lead to new insights in optimal methods for stimulation individuals with cochlear implants of all ages.

PS 611

Patient Specific Factors that Influence Hearing Preservation Following Cochlear Implantation

Heba Isaac¹; Andrew S. Liu²; Camille Dunn³; Bruce J. Gantz³; Bob McMurray⁴; Marlan R. Hansen⁵

¹Carver College of Medicine, University of Iowa;

²Department of Otolaryngology - Head and Neck Surgery, University of Iowa Hospitals and Clinics;

³Department of Otolaryngology - Head and Neck Surgery, University of Iowa Hospitals and Clinics;

⁴Department of Psychology and Brain Sciences, The University of Iowa; ⁵University of Iowa Department of Otolaryngology Head and Neck Surgery

Introduction: Hearing preservation cochlear implants combine electric stimulation with a hearing aid. This allows listeners to leverage cues derived from both electric hearing in the high frequencies with residual low frequency acoustic hearing to enable better performance in difficult listening situations, such as recognizing speech in a noisy background. Hearing preservation strategies rely on the successful preservation of low frequency hearing in the implanted ear. Recent developments in electrode technology and surgical techniques have led to improved hearing preservation outcomes. However, the role of patient factors on predicting the maintenance or loss of residual acoustic hearing remains to be clarified. In some reports, most users experience hearing loss under < 15 dB HL after hearing preservation cochlear implantation. But a minority of patients experience a larger, clinically significant loss of residual hearing after activation. Our goal is to study how patient-specific medical comorbidities and device characteristics affect loss of residual hearing.

Methods: We obtained longitudinal audiometric data from 189 hearing preservation cochlear implant users (Cochlear L24, S8, S12, SRW, 422/522, Med-EI Flex20/24, and Advanced Bionic SlimJs) who agreed to participate in research with the University of Iowa Cochlear Implant Clinical Research Center. Their comorbid medical conditions were extracted from the electronic medical record. We used random effects mixed models to model the relationship between the CI user's medical comorbidities and their change in residual hearing post-implantation to identify factors that contribute to the preservation of residual hearing.

Results: Overall rates of hearing preservation of functional hearing (low frequency pure tone average >85dB) were excellent and dependent on preoperative

hearing levels and electrode type. These results include 83% for S8 (n=23), 92% for S12 (n=14), 100% for SRW (n=5), 72% for L24 (n=76), 45% for 422/522 (n=47), 88% for Flex 20/24 (n=17), and 100% for SlimJ (n=7). Results of random mixed models are currently being analyzed to identify patient specific factors and co-morbidities that contribute to the preservation of residual hearing.

Conclusions: These results will help us better understand the relationship between patient specific factors including comorbid medical conditions and hearing preservation outcomes. They will help clinicians to more appropriately counsel patients in whether to proceed with hearing preservation cochlear implantation and to guide appropriate device selection.

PS 612

Hearing Preservation in Cochlear Implant Users

Lendra M. Friesen¹; Monita Chatterjee²

¹University of Connecticut; ²Boys Town National Research Hospital

Recent studies have demonstrated that low-frequency hearing preservation is possible with implanted patients using new electrode technology and a soft surgical technique. Studies are beginning to reflect benefit in clinical outcomes. However, the neural mechanisms underlying this benefit are unknown.

In this study, we examined the psychophysical just noticeable difference (jnd), a measure of sensitivity, of stimulus pulse phase durations (400 ms pulse trains) on basal, medial, and apical electrodes using a lower reference range (30-80us) and a higher reference range (345-395 us) of the pulse phase duration and using a 3 down, 1 up alternative-forced choice procedure. We hypothesized that we would see smaller jnds (greater sensitivity) at the apical end than in the basal end and also smaller jnds in individuals with hearing preservation than in those without. We then recorded the N1-P2 (responses at 50-200ms after stimulus onset) and the Acoustic Change Complex (ACC) on basal, medial, and apical electrodes for both the low and high range of phase durations to determine the relationship to the behavioral jnd. An 800 ms pulse train was used, where the first 400 ms was the standard and the second 400 ms of the stimulus was the jnd of the phase duration. We also tested patient's'; sentence recognition in soundfield in quiet and at a +5 S/N to examine the relationship to the jnds and the cortical responses. Results will be discussed.

PS 613

Correlation of Intracochlear Electrocochleography Responses with Cochlear Implant Speech Perception

Carla Valenzuela¹; Jeffery Lichtenhan¹; Kanthaiah Koka²; Craig Buchman¹; Amanda Ortmann¹
¹Washington University in St Louis; ²Advanced Bionics

Background

There is wide variability in speech perception scores among cochlear implant (CI) users. Clinical and surgical factors explain less than 30% of the variance in speech perception scores. A recent study demonstrated that the addition of intra-operative round window electrocochleography (ECoChG) with clinical factors can explain up to 45% of the variance. An innovation has made it possible to advance use of intra-operative use of ECoChG: CI electrodes that are traditionally used for electrical stimulation of the cochlea can also be used as recording electrodes to make measurements of responses to acoustic stimuli. ECoChG measurements can now be made both intra-operatively and at any time post-operatively. The use of intra-cochlear ECoChG measurements made during the post-operative period provide previously unprecedented information on the extent to which ECoChG can be used to understand changes in cochlear health and cochlear physiology that may influence surgical techniques and device design. Thus far, ECoChG measurements have been made within only a few months after implantation. We aim to understand the correlation of intra-cochlear ECoChG measures with speech perception scores obtained at least nine months after implantation.

Methods

Intra-cochlear ECoChG measurements were obtained from the most apical CI electrode in nine adult recipients with some degree of low-frequency acoustic hearing pre-implantation. ECoChG measurements were made in response to 110 dB SPL 50-ms tone bursts at 125 Hz - 2000 Hz. The first and second harmonics at all tone burst frequencies were measured, summed, and converted to dB (re: 1uV) to yield the "total response" (TR). Speech perception testing consisted of word scores (consonant-nucleus-consonant words) and sentence scores in quiet (AzBio) and background noise (AzBio at 10 dB SNR).

Results & Conclusions

Intra-cochlear ECoChG measurements, speech testing, and audiometric thresholds to acoustic sounds were obtained at the time of implantation and at a median of 13 months post-operatively. All patients experienced

some decline in their residual low-frequency audiometric thresholds. The median TR response was 35.23 dB re: 1uV at the time of implantation and 4.41 dB re: 1uV post-operatively. There was a positive correlation between intra-operative ECoChG TR and all speech perception measures, but post-operative ECoChG TR did not correlate with any speech perception measures. Future work should aim to improve the correlations by separating hair cell from neural components in ECoChG measurements, and perhaps use objective measures of the auditory central nervous system, to understand the variability of speech perception scores in CI users.

PS 614

Correlating the number of spiral ganglion cells with speech perception in cochlear implant users

Yew Song Cheng¹; Mario Svirsky²
¹Department of Otolaryngology-Head and Neck Surgery, New York University Medical Center; ²New York University School of Medicine

For successful speech perception after cochlear implantation, the presence of spiral ganglion cells (SGCs) is widely accepted to be a requisite component of the neural conduit between the implant electrode and the auditory cortex. By extension, it is hypothesized that the number of SGCs might influence auditory performance of cochlear implant (CI) users. The most direct test of this hypothesis stems from an impressive body of work from Nadol and colleagues at Massachusetts Eye and Ear (MEE), and Fayad and Linthicum et al. at House Ear institute, who spent decades painstakingly collecting and preparing temporal bones from CI users so SGCs could be counted and correlated with the patients'; last speech perception scores.

We found five studies that used multichannel CI patients, four from MEE (Kamakura et al. 2016, Seyyedi et al. 2014, Li et al. 2007 and Khan et al. 2005) and one from House (Fayad and Linthicum 2006), which provided a total of 56 ears. Mixed results were reported. Seyyedi et al. and Kamakura et al. showed statistically significant positive correlations between the number of SGCs and speech perception scores. However, the other three studies did not find statistically significant correlations, with the Fayad and Linthicum study curiously showing a negative correlation. Considering all data from both centers, the results were not statistically significant ($P=0.7706$). Several confounding factors were explored, including shallow depth of insertions and long durations of deafness, but excluding potentially problematic cases did not affect the general findings from our analysis, which remained inconclusive. Limiting the analysis to data from MEE revealed a statistically significant, but weak positive correlation ($n=46$, $R=0.1637$, $P=0.0032$). However,

in the absence of a principled justification to exclude a particular study, the best estimate of the underlying phenomenon should include all available data.

One caveat is that speech perception data and SGC counts were obtained, by necessity, at different points in time (pre- and post-mortem) and at intervals that varied greatly among patients (ranging from 1 to 93 months between last test and death in the Khan et al. study), which might weaken the hypothesized correlation. It is also possible that a relationship does exist, but only when a certain minimum threshold of SGCs is crossed.

To conclude, although the hypothesized relationship between SCGs and speech perception scores remains logically sound, a detailed analysis of all available data in our study failed to provide support for it.

Auditory Prostheses V: Music Perception & Binaural Hearing

PS 615

A Comparison of hearing aid music-listening programs on perceived sound quality of individual musical instruments by child and adult musicians

Patti M. Johnstone¹; Jeffery Reinbolt²; Jeffery Pappas²; Jennifer Hausladen¹; Marshall Chasin³; Tyler Phillips¹; Kristen Thornton¹; Karen Martin¹

¹University of Tennessee Health Science Center;

²University of Tennessee Knoxville; ³Musicians' Clinics of Canada

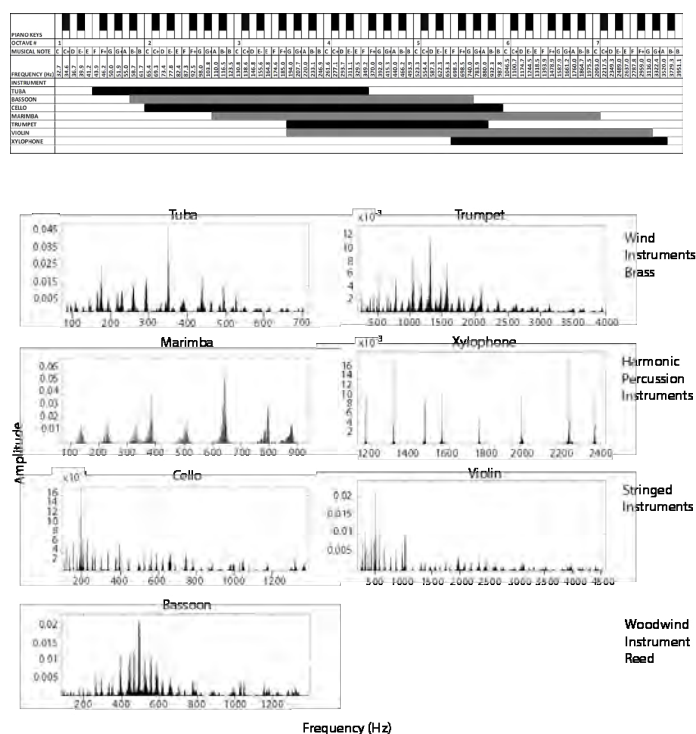
Objectives: Knowledge is limited about how to design hearing aids to optimize music listening for musicians who may spend hours each day playing an individual musical instrument. Some digital hearing aids have dedicated music programs (DMP) designed to enhance music listening. It is unknown if activation of such a DMP improves the subjective quality of amplified music for musicians. Research Aim: determine if child and adult musicians, in blind comparisons, would prefer live music recordings of individual musical instruments from hearing aids with an activated DMP as compared to deactivated.

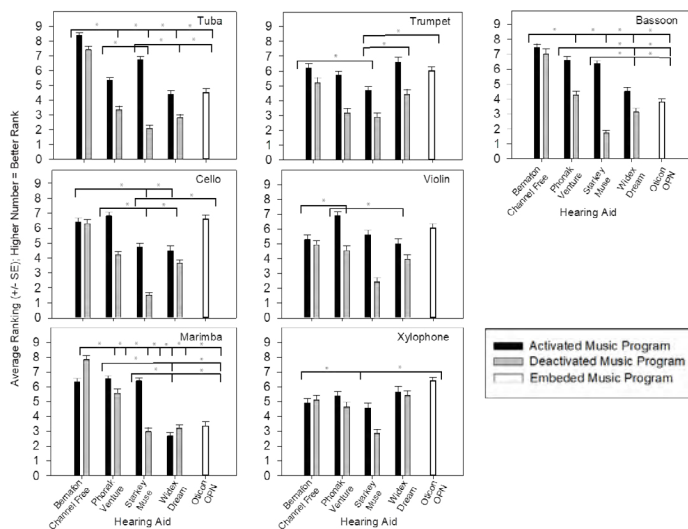
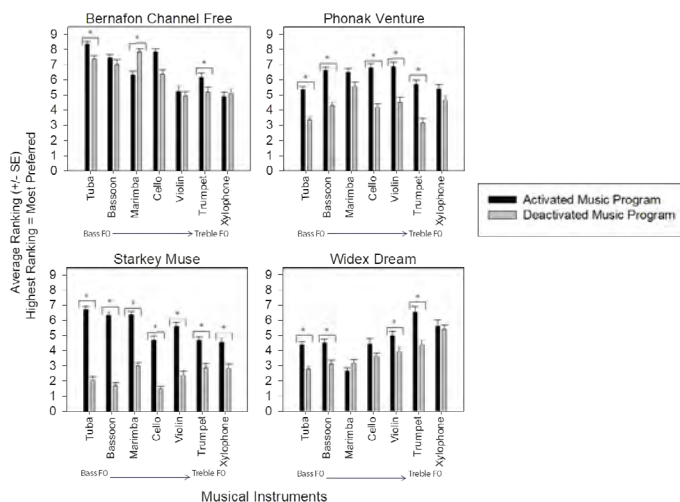
Design: 30 child (8–17 years) and 30 adult (18–50 years) musicians with normal hearing participated. Seven different, single musical instruments were recorded through 5 different hearing aids, each fit to KEMAR® for a flat hearing loss with thresholds at 50 dBHL. Four of the hearing aids had a DMP and one did not. For those devices with DMPs, music recordings were made with the DMP activated and deactivated. On each trial, participants were asked to blindly judge the relative preference of randomly paired-comparisons of

the music recordings. A QuickSort algorithm was used to efficiently sort and rank-order the preferred hearing aid outputs for each participant for each musical instrument. Participants were asked to subjectively rate their highest ranked choice for richness, pitch distortion, fidelity, and noise. Participants were asked to imagine how long they would be willing to wear their top-ranked hearing aid each day.

Results: A significant 3-way interaction between DMP Activation, Hearing Aid Make, and Musical Instrument was found. On average, participants reported that they would be willing to listen with their top-choice hearing aid 1-3 hours a day. However, the willingness to listen with their top-choice hearing aid correlated significantly and negatively with length of reported musical experience (adults), distraction of perceived noise, and/or pitch distortion (children and adults). A significant positive correlation existed between willingness to listen and perceived richness and/or fidelity of their top-choice hearing aid (children and adults).

Conclusions: Child and adult musicians prefer music recorded through a hearing aid with an activated DMP, however, this preference depends on the hearing aid make and musical instrument listened to at the time. For individual musical instruments with bass harmonics, musicians ranked ChannelFree® processing significantly higher than all other processing schemes. Music fidelity, richness, distraction of circuit noise, and pitch distortion are important factors that may influence musicians'; willingness to use a hearing aid.





PS 616

Effects of Music Training on Cochlear Implant Outcomes

Fawen Zhang¹; Chun Liang²; Gabrielle Underwood¹; Kelli McGuire¹; Jing Xiang³; Chelsea Blankenship⁴

¹University of Cincinnati; ²University of Cincinnati, Shenzhen maternity and child healthcare hospital; ³Cincinnati Children's hospital; ⁴University of Cincinnati/Cincinnati Childrens Hospital Medical Center

Background. For most cochlear implant (CI) users, pitch-based speech tasks and music perception are extremely challenging. Evidence has shown that music training enhances auditory perceptual skills such as frequency change detection and cognitive functions that can benefit speech perception. The objective of this project is to examine the effects of a short-term music training protocol on CI hearing outcomes. This study is expected to have important impact on post-implantation intervention and assessment in CI users. **Methods.** Nine post-lingually deafened adult CI users (age range:

31-64 years) who have used their CIs for at least 1 year participated in the study. Participants used Pandora program or similar music programs downloaded on their home computer or smartphone for music training. They were instructed to select music genres of their preference that have an emphasis on the melody. During the training, they were asked to pay attention to the music melody, rather than other musical elements and were encouraged to sing along mentally. Music training occurred during a time when the participant was not distracted. The training schedule was 40 minutes/day x 5 days/week x 4 or 8 weeks. They were required to log the training details. Direct audio input was used to send the training stimuli so that the untrained ears were not involved during training. The pre-training and post-training tests included: a questionnaire (Speech, Spatial and Qualities of Hearing Scale or SSQ), a psychoacoustic test of frequency change detection, speech tests (CNC words, Azbio sentences, and QuickSIN), and electroencephalographic (EEG) recordings. For the EEG and psychoacoustic test, the stimuli were a series of 1-sec 250 Hz pure tones containing different magnitudes of upward frequency changes at 0.5 sec after the tone onset (see method section in Liang et al., 2016). **Results.** Compared to the pre-training results, there was a significant improvement ($p < 0.05$) in the performance on CNC (pre- vs. post-performance: 70.1% vs. 80.7%) and QuickSIN (16.9 vs. 12.4 dB SNR loss), as well as SSQ (4.6 vs. 6.2). The frequency change detection threshold (FCDT) was improved (2.63% vs. 1.33%), but the improvement did not reach statistical level due to the large variability. The ACC showed a larger amplitude for both 5% and 50% change and the percentage of present ACC for the 5% change increased after the training.

PS 617

Automatic Gain Controls Improve Sound Localization in Bilateral Cochlear-Implant Users

Casey Gaskins¹; Chen Chen²; Amy Stein²; Olga A. Stakhovskaya¹; Matthew Goupell³

¹Department of Hearing and Speech Sciences, University of Maryland, College Park; ²Advanced Bionics; ³University of Maryland

Introduction:

Automatic gain controls (AGCs) in hearing-assistive devices limit the output gain to comfortable levels. In most devices used bilaterally, AGCs apply compression and gain independently across the ears, which distorts the natural binaural cues necessary to localize sound. Synchronization of AGCs for bilateral hearing-aid users have demonstrated improved speech intelligibility in the presence of competing noise. However, research on this topic is limited in bilateral cochlear-implant (CI) users. Since bilateral CI users mainly rely on interaural level differences (ILDs) to localize sound, the distortion of ILDs

by independent AGCs may be more detrimental than in hearing aids. We hypothesized that synchronized AGCs would improve localization performance for bilateral CI users, and that larger improvements would be seen for more spectral-temporal dynamic stimuli (e.g., running speech compared to static noise) due to greater ILD distortions.

Methods:

Ten bilateral CI users using Advanced Bionics (AB) Naida Q90 research processors participated in two experiments. Participants were seated in a soundproof booth in the center of a 360°, 24-loudspeaker sound field array. In experiment I, the target stimulus was an 800-ms unmodulated broadband pink noise. The noise was presented nominally at 55 or 75 dB SPL. In experiment II, the stimuli included: broadband noise (BBN), speech-shaped noise (SSN), speech-modulated noise (SMN), and speech tokens (sentences and words). Stimuli were presented nominally at 75 dB SPL. Level was roved over a 10-dB range for both experiments. All stimuli were randomized across speakers with five target presentations per speaker location. Participants were instructed to identify the location of the target stimulus by selecting the corresponding numbered speaker on the touchscreen computer provided to them. The research processors were programmed to measure the effects of AGC (independent vs. synched) and microphone placement (behind-the-ear vs. ear canal).

Results:

Root-mean-square (RMS) error significantly worsened with independent AGC settings, particularly for 75-dB presentation level and for lateral locations (>45°). The ear-canal level microphone also significantly improved RMS error and front-back confusions at lateral locations. In experiment II, AGC improved RMS errors for all stimulus types except SMN.

Conclusions:

Results show synchronized AGCs improve performance in localization tasks for both static and dynamic stimuli, thus better preserving ILDs for sound localization. Understanding the impact of synchronized AGCs and ILD processing on performance is critical for helping bilateral CI users better understand speech in background noise. [Work supported, in part, by Advanced Bionics and NIH R01DC014948 (M.J.G).]

PS 618

Evaluation of a Novel Music Timbre Discrimination Test in Cochlear Implant Users

Melanie Gilbert¹; Lauren Jacobs²; Charlotte Jeppsen³; Grace Williams⁴; Patpong Jiradejvong¹; Charles J. Limb¹

¹Dept of Otolaryngology-Head and Neck Surgery, University of California, San Francisco; ²Washington University School of Medicine; ³Princeton University; ⁴Vanderbilt University

Musical timbre is conveyed by spectrotemporal features beyond fundamental frequency and amplitude that give a particular sound its characteristic tone color. Timbre perception is typically examined using musical instrument identification tasks that generally reveal poor performance in cochlear implant (CI) users. Relatively little is known, however, regarding timbre discrimination—the ability to differentiate between two notes of different timbres—a task which may provide greater insight into CI-mediated listening than whether or not instruments can be correctly identified. We therefore developed a novel timbre discrimination task utilizing acoustic blends of source instruments combined in varying amplitude ratios while maintaining constant overall volume. We hypothesized that normal hearing (NH) listeners would outperform CI recipients and that the within-family instrument blend comparisons would be more difficult than the between-family comparisons. Test paradigm was a three interval, two alternative forced-choice task. We selected two-second samples from six source instruments (clarinet, flute, french horn, tuba, violin, cello), representing three musical families (two each of woodwind, brass, string). These instruments were chosen because they have sustained temporal envelopes and target frequencies (F0 of 200 Hz and 600 Hz, chosen for their fine-structure affordances) that lie within the “normal range” of those instruments. We made six instrument pairings (three within-family and three between-family blends) to provide a range of acoustic contrasts and difficulty. Similar to signal-to-noise ratio (SNR) threshold determination, we identified the threshold of blend ratios of source instruments that a listener can correctly discriminate (with >90% accuracy) using timbre cues. Twenty-five NH and eight MED-EL CI participants have been evaluated to date. Our results revealed that the NH group performed better than the CI group, particularly for more difficult blend comparisons. CI users demonstrated a wide range of discrimination abilities, suggesting that the test can effectively evaluate timbre discrimination among good and poor performers, providing a meaningful metric currently lacking in the field. This test provides a more nuanced idea of CI users’ timbre discrimination abilities, which may be useful for understanding timbre discrimination in other areas, such as speaker identification and speech perception in noise. Future studies include the creation of more difficult blends (created from smaller dB step ratios) to assess a wider range of ability levels and incorporation of adaptive test protocols.

PS 619

The second cochlear implant showed much faster speech perception development and reached a plateau earlier than the first implant in prelingually deaf children with sequential bilateral cochlear implantation

Yehree Kim¹; Min Young Kwak²; Ji Won Seo¹; Hong Ju Park²

¹Asan Medical Center; ²Seoul Asan Medical Center

Objective: We evaluated the growth patterns of speech perception in the first and second cochlear implants (CIs) in children with sequential bilateral CI and the effects of age at CI operation on the growth patterns of speech perception.

Study Design: Retrospective study.

Setting: Tertiary referral center.

Patients: Seventy children without any cochlear anomalies or cognitive deficits who underwent sequential bilateral CI operations.

Main Outcome Measures: Monosyllabic word recognition scores (WRSs) by the Asan-Samsung Korean word recognition test were the main outcomes. The durations of CI use when the mean WRS exceeded 80% or reached a plateau were compared between the groups which were classified by the age at CI operation (G1, ≤ 3.5 ; G2, 3.6-7.0; G3, 7.1-13; G4, > 13 years old).

Results: G1 ears with the 1st CI showed the best WRS (98%) and G4 ears with the 2nd CI showed the worst WRS (65%). For the 1st CI, G1 ears showed shorter durations of CI use (40 ± 19 months) to reach a plateau of WRS than G2 (64 ± 25 months); however, the 2nd CI ears showed much shorter durations (11-17 months) of CI use compared to the 1st CI ears, which were similar to each other regardless of the age at the 2nd CI operation. For the 1st CI, the mean WRSs of G1 ears exceeded 80% after 2 years, but it took 4.5 years for G2 ears. For the 2nd CI, it took 3 months for G2 ears to exceed 80%, and 12 months for G1 and G3 ears, but the WRSs of G4 ears did not exceed 80% even after 3 years of CI use.

Conclusions: Mean word recognition scores of the second CI ears started to be $> 80\%$ at even 3 months postoperatively and reached a plateau before 1.5 years after CI, which were much faster compared to those (2 and 4.5 years, respectively) for the first CI, suggesting that the second CI was working using the auditory pathways which had been already established by the first CI. Though the youngest second CI group did not show the best WRS in the early postoperative period,

they caught up with the other groups in 12 months, suggesting that linguistic ability and the age at the second CI operation significantly influenced the growth patterns of WRS after CI.

PS 620

Perception of Dissonance for Musical Intervals is Similar with Acoustic and Electric Hearing in Unilaterally Deaf Cochlear Implant Patients

Emily R. Spitzer¹; David M. Landsberger¹; David Friedmann¹; John Galvin²

¹NYU School of Medicine; ²House Ear Institute

Background: Musical intervals contribute to the emotional response to music. In normal-hearing (NH) listeners, some simultaneously presented music intervals may sound more dissonant (e.g., minor 2nd, tritone) than others (e.g., major 3rd, perfect 5th). Because of limited spectral resolution, pitch perception is generally poor in cochlear implant (CI) listeners; as such, perception of musical intervals is impaired. However, it is unclear whether CI users are sensitive to the relative dissonance across intervals. In this study, dissonance ratings for musical intervals were measured in 11 unilaterally deaf CI patients, in whom ratings with the CI ear could be anchored to those with the NH ear.

Methods: Dissonance ratings were collected with the NH ear, the CI ear, and with both ears for 13 simultaneously presented musical intervals, separated by 0-12 semitones (i.e., from unison to perfect octave). Ratings for the 13 intervals were collected for two ranges: F3-F4 (~175-350 Hz) and C4-C5 (~262-524 Hz). Another condition was tested in which the intervals were separated by 1 octave (e.g., a major 2nd would be F3+G4). During testing, an interval was presented and subjects were asked to rate pleasantness by clicking on line with extreme anchors "least pleasant" and "most pleasant."

Results: Overall ratings were much poorer with the CI ear than with the NH ear, with little difference between the NH ear and both ears. With the NH ear, the minor 2nd, tritone, and major 7th were rated least pleasant and the unison, major 3rd, perfect 5th and perfect octave were rated most pleasant, consistent with previous studies. While ratings were poorer with the CI, intervals ratings were significantly correlated between the NH ear and the CI ear for all interval conditions. Ratings with the NH ear, CI ear, and both ears were also significantly correlated across the interval conditions.

Discussion: While overall ratings were much poorer with the CI (most likely due to sound quality), ratings across intervals were similar between acoustic and electric

hearing, suggesting that CI listeners may be similarly sensitive to relative dissonance across intervals. Ratings were generally similar when component frequencies were within an octave or separated by an octave; with electric hearing, listeners may have attended more strongly to temporal envelope interactions within or across channels. Contrary to previous studies that showed binaural advantages for sound quality, no binaural advantage was observed over the NH ear alone for dissonance ratings.

PS 621

Listening Effort in Bilateral Cochlear Implant Users with Asymmetric Across-ear Performance in Speech Perception Scores

Emily Burg¹; Tanvi Thakkar²; Shelly Godar¹; Matt Winn³; Ruth Litovsky²

¹Waisman Center, University at Wisconsin-Madison;

²University of Wisconsin - Madison; ³University of Minnesota

Bilateral cochlear implants (BiCIs), as compared to a unilateral cochlear implant, facilitate improved speech intelligibility in noise and sound localization abilities. Nevertheless, individuals with BiCIs frequently demonstrate an asymmetry, with one ear outperforming the other on measures of speech intelligibility. It has yet to be determined how the better- and poorer-ear individually impact the amount of effort experienced by BiCI users. The measure of pupil dilation (pupillometry) can be used to quantify listening effort and task engagement during listening tasks. Large pupil sizes indicate a high amount of effort and engagement in the task, and small pupil sizes indicate low effort and engagement. We used pupillometry to investigate the effect of an across-ear asymmetry in speech intelligibility on listening effort in BiCI users. Participants heard female-talker IEEE sentences presented from a loudspeaker at 0° azimuth in quiet while changes in pupil dilation were measured using an Eyelink 1000 Plus. An experimenter scored verbal responses. The degree of asymmetry in speech intelligibility varied among participants, with two exhibiting large asymmetries (40% and 58%), and two exhibiting smaller asymmetries (10% and 22%). For the two participants with large asymmetries, the effects of the poorer-ear in the bilateral condition differed. One had high intelligibility in the better-ear (95%) and poor intelligibility in the poorer-ear (38%); bilateral listening resulted in similar intelligibility but smaller pupil dilation than the better-ear alone, suggesting that the poorer-ear facilitated a reduction in listening effort. The other participant scored 66% in the better-ear and 20% in the poorer-ear; bilateral listening elicited similar intelligibility and pupil dilation to better-ear listening, suggesting that they may rely solely on their better-ear,

even when listening bilaterally. For both participants with smaller asymmetries, bilateral listening resulted in improved intelligibility compared to better-ear listening (68% to 78% and 90% to 94%), but there was also an increase in pupil dilation. This suggests that the improved intelligibility in the bilateral condition may be due to heightened engagement in the task. In summary, most participants received some kind of advantage in the bilateral compared to the better-ear condition, either in increased intelligibility or decreased listening effort. However, these results differed depending on the amount of asymmetry, and demand further interpretation of whether increased pupil dilation reflects increased effort (negative) or increased engagement (positive). These preliminary results provide new evidence regarding the contributions of each ear to bilateral speech understanding and listening effort in BiCI users.

PS 622

Spatial Speech Perception in Bimodal and Single-Sided Deaf Cochlear Implant Users: Complementary Usage of Information or Better-Ear-Listening?

Ben Williges¹; Nils Schreiber²; Ladan Zamaninezhad²; Tim Jürgens³

¹Medical Physics and Cluster of Excellence

“Hearing4all, University Oldenburg; ²Medical Physics

and Cluster of Excellence “Hearing4all”, University Oldenburg; ³Institute of Acoustics, University of Applied Sciences Lübeck

A growing number of cochlear implant (CI) users consist of usable acoustic hearing supported by a hearing aid (bimodal CI users) or even normal hearing in the contralateral ear (CI-Single-sided deaf, CI-SSD). The combination of electric and acoustic hearing leads to improved speech intelligibility, better localization abilities and an improved quality of life. The underlying mechanism of this acoustic and electric combination is not fully understood, and it is very likely subject-specific and task-dependent. This study investigates possible mechanism of this combination in spatial speech perception using a model-based approach:

An ongoing debate is, how much of the bimodal or CI-SSD users’ performance can be explained by using each listening mode alone and how much of the performance is due to the combination of complementary information across ears. Here we compare measured data from actual CI subjects with data predicted using two different versions of a detailed physiologically-inspired speech intelligibility prediction model based on an automatic speech recognition approach: One model version uses for speech reception thresholds (SRTs) in the combined stimulation mode only the

better of the two monaurally predicted SRTs (better-ear-listening mode). The other model version consists of a concatenation of the acoustic and electric internal representations, thus enabling the speech recognizer to take advantage of both acoustic and electric information, i.e., using of complementary information.

Reference data for simple, but realistic anechoic acoustic scenes were beforehand collected in stationary speech-shaped noise in eight bimodal CI and in eight CI-SSD listeners. This was done for three spatial scenarios (frontal speech and noise either from the front, the left side or the right side). All possible listening modes were measured in all subjects using each (aided) ear alone, and using both ears.

Using the simple better-ear-listening mode, an absolute RMS error of 1.7 dB was achieved with a correlation coefficient of 0.85 compared to the measured data.

Results suggest that complementary information was not particularly needed to explain spatial speech perception of the bimodal CI and CI-SSD users in this scenario. This might be due to the stationary noise employed, which makes it difficult to have a bilateral advantage due to transmission of complementary information. Other maskers might show more benefit and could be employed in the model in the future.

PS 623

Estimation of Interaural Place-of-Stimulation Mismatch for Bilateral Cochlear-Implant Users with Pitch Matching, Interaural-Time-Difference Discrimination, and Computed-Tomography Scans

Olga A. Stakhovskaya¹; Joshua G.W. Bernstein²; Kenneth K. Jensen²; Jack Noble³; Michael Hoa⁴; H. Jeffrey Kim⁵; Matthew Goupell⁶

¹*Department of Hearing and Speech Sciences, University of Maryland, College Park*; ²*Walter Reed National Military Medical Center*; ³*Vanderbilt University*; ⁴*NIDCD/NIH*; ⁵*Dept of Otolaryngology-HNS, Georgetown University Medical Center*; ⁶*University of Maryland*

Introduction:

For bilateral cochlear-implant (BICI) users, interaural frequency mismatch can be detrimental for sound localization and speech understanding in noise. However, it is difficult to estimate the interaural frequency mismatch in this population. This study compared computed-tomography (CT) estimates of electrode location with two perceptual measurements: pitch matching and interaural-time-difference (ITD) discrimination.

Methods:

Single-electrode pitch-match estimates were based on the pitch ranking of all even electrodes in both ears using 300-ms, 1000-pulses-per-second (pps) electrical pulse trains. ITD discrimination just-noticeable differences (JNDs) were measured using loudness-balanced 300-ms, 100-pps electrical pulse trains for five reference electrodes. Five or more comparison electrodes were used in the other ear to obtain an ITD sensitivity tuning curve for each reference. CT scans were used to determine precise intracochlear location of the electrodes.

Results:

The three methods suggested modest mismatches of ≤ 3 electrodes for four out of five BICI participants (out of 15 planned). The best ITD JNDs were observed within two electrodes from the number-matched pair in approximately 80% of electrodes tested and ranged from 40–2090 μ s, although the width of the ITD tuning curves varied considerably across participants and electrodes (range: 1-8 electrodes), which sometimes precluded clear peak estimation. Pitch estimates were more variable and were less consistent with CT or ITD estimates in three out of five participants. CT images showed interaural placement mismatches within 2-3 electrodes for four participants, consistent with the ITD-based estimates. For the fifth participant, CT scans showed a systematic mismatch of 6-7 electrodes across the ears. ITD sensitivity was very poor on three reference electrodes, while the other two suggested interaural mismatches of 4-5 electrodes, in the direction consistent with CT findings. However, pitch-matching estimates for this participant generally suggested less mismatch (0-2 electrodes) than the other two measures.

Discussion:

CT, pitch-matching, and ITD-based interaural place-of-stimulation estimates were within 2-3 electrodes for most participants and electrodes. For the participant where the CT scan showed a larger mismatch, the ITD discrimination task suggested a mismatch of similar magnitude, whereas the pitch-ranking task suggested substantially less mismatch. These preliminary results suggest that ITD discrimination yields estimates of interaural mismatch closer to the estimated electrode position, whereas pitch ranking estimates are more variable. [Research supported by NIH/NIDCD grant R01 DC015798. The views expressed in this article are those of the authors and do not reflect the official policy of the Department of Army/Navy/Air Force, Department of Defense, or U.S. Government.]

PS 624

Sound Localization Bias Induced by Weak Sensory Cues

Rodrigo Pavao¹; Thaís Gonçalves¹; Juliana Gutierrez¹; Jose L. Pena²

¹*Centro de Matemática, Computação e Cognição, Universidade Federal do ABC, SP, Brazil;* ²*Albert Einstein College of Medicine*

Localizing low-frequency sounds in the horizontal plane requires detection of interaural time differences (ITD). For most sound frequencies, ITD varies sinusoidally across azimuth with a steepest slope in the front. Therefore, sound lateralization based on the physical relationship between azimuth and ITD should follow the inverse function (arcsine). However, azimuth estimation displays a sinusoidal relationship with ITD, revealing lack of correspondence between estimated and actual azimuths. This is consistent with low ITD-discriminability in the periphery and frontal bias, previously described. Previous human studies manipulating sound intensity or reverberation levels in ITD-varying stimuli show that quiet or anechoic sounds in the periphery are estimated more frontally than loud or reverberant sounds. We hypothesized that weak sensory evidence underlies this frontal bias. To approach this question, we applied behavioral and computational methods, testing (1) whether weak cues lead to frontal bias and (2) examining the possible benefit of this perceptual bias.

Sounds with varying ITD were presented through headphones. Subjects were instructed to click on the best-matching virtual position and report their confidence. We assessed the effect of the amount of sensory-evidence on performance in two experiments: Exp1) 50-ms tones were presented repeatedly in one or ten-element sequences. Exp2) the stimulus bandwidth was manipulated in tonal (600Hz), narrowband (560-740Hz) and broadband (150-1050Hz) signals. Azimuth estimation across ITD saturated in the periphery. In addition, weak sensory evidence (single-repetition sounds or narrowband stimuli) led to increased frontal bias. Interestingly, estimations of frontal locations were more variable across trials, displayed longer reaction times and yielded lower confidence scores than peripheral locations. These seemingly counterintuitive results may be explained by more stringent estimations in the front, and more automatic and stereotyped (biased) estimations in the periphery, matching ITD-discriminability. The “stringent” strategy is more accurate, less precise (more variable) and therefore more time-consuming than the “biased” strategy, which relies on

stereotyped azimuth estimation.

We developed a computational model which replicated our results, based on: (1) metacognition variable specifying ITD-discriminability; (2) choice threshold for stringent-vs-biased strategy; (3) estimation times; and (4) bias location. After matching parameters by behavioral data, a seek-until-find simulation was implemented. Remarkably, the model switching between stringent and biased strategies localized sound sources faster than a model using only the stringent strategy.

In sum, our results are consistent with the hypothesis that weak sensory evidence induces biased frontal estimation, which is efficient and allows to explain previous experimental results in human subjects and other species.

PS 625

Interaural Correlation Modulates Cortical Oxyhaemoglobin Concentration

Robert Luke¹; Hamish Innes-Brown²; Jaime A. Undurraga³; David McAlpine³

¹*Macquarie University;* ²*Bionic Ear Institute;* ³*Macquarie University, Department of Linguistics*

Background

The extent to which sounds arriving at each ear are similar (the interaural correlation, or IAC) contributes to the spatial qualities of the listening environment, including features such as the spatial width of a sound source. Sounds with a high IAC are usually perceived as having a compact sound image, whereas whilst those with low IAC are perceived as more spatially diffuse. Consequently, IAC likely plays a critical role in distinguishing compact sound sources (‘foreground’;) from the more diffuse ‘background’;, including situations where reverberation reduces IAC.

Previous studies indicate that brain structures within Heschl’sgyrus and the planum temporale play a role in the processing of spatial width [1, 2]. Here, we use functional near-infrared spectroscopy (fNIRS) to investigate how cortical oxyhaemoglobin concentration in auditory cortex varies as a function of the magnitude of the IAC. Changes in oxyhaemoglobin concentration act as a proxy for neural energy demand, and therefore the neural activity of a brain region.

Methods

fNIRS was used to determine the change in oxyhaemoglobin concentration with varying IAC in 10 participants. Stimuli were 6 s segments of bandpass noise (300–700 Hz, centred at 500 Hz), amplitude modulated at 40 Hz. Each stimulus was separated by a

period of silence varying between 15 and 30 seconds. Stimuli were presented binaurally with interaural correlation values of 0.0, 0.25, 0.5, and 1.0, respectively. The change in oxyhaemoglobin concentration relative to the silence baseline was calculated for each condition.

Results

Significant oxyhaemoglobin changes were detected in response to auditory stimuli relative to the silence baseline. The change in oxyhaemoglobin concentration increased monotonically with decreasing IAC. A smaller increase in oxyhaemoglobin concentration was observed in response to stimuli with higher values of IAC (more perceptually compact sounds) compared to lower values of IAC (more perceptually diffuse sounds).

Conclusions

Our data indicate that auditory stimuli with high IAC, and more perceptually compact, are less metabolically demanding to process than more-diffuse auditory stimuli with low IAC. This increase in blood oxygen requirements for sounds with lower IAC is consistent with previous fMRI data showing that the blood-oxygen-level-dependent (BOLD) response in auditory cortex is greater for 500-Hz centred, band-pass noise with long ITDs, and concomitantly lower values of IAC, than it is for short ITDs [3]. This finding has implications for the fundamental understanding of binaural processing in humans, and for the clinical fitting of hearing devices.

1) Budd, T. W., et al. "Binaural specialisation in human auditory cortex: an fMRI investigation of interaural correlation sensitivity." *Neuroimage* 20.3 (2003): 1783-1794.

2) Hall, Deborah A., et al. "Cortical representations of temporal structure in sound." *Journal of neurophysiology* 94.5 (2005): 3181-3191.

3) von Kriegstein, Katharina, et al. "Responses to interaural time delay in human cortex." *Journal of neurophysiology* 100.5 (2008): 2712-2718.

PS 626

A Physiologically Plausible Model for Human Sound Lateralization based on Envelope Interaural Time and Level Differences.

Jonas Klug¹; Lisa Schmors¹; Go Ashida²; Mathias Dietz¹

¹*Universität Oldenburg*; ²*University of Oldenburg*

The human auditory system uses binaural cues to localize sound sources. Sounds originating from off-midline directions are received with an interaural time difference (ITD) and an interaural level difference (ILD). Presenting artificial ILDs and ITDs via headphones

causes a lateralized intracranial percept. Bernstein and Trahiotis (J. Acoust. Soc. Am. 131. 409-415, 2012) psychoacoustically measured the extent of lateralization caused by combinations of envelope ITD and ILD for a variety of different stimuli. They were able to account for 94 % of the variance in their data with a computational model, extracting ITDs by means of a cross-correlation approach that resembles so-called delay lines. However, mammals, including humans, likely extract ITD information without delay lines. Here, we propose an alternative model of sound lateralization, by combining the well-established Zilany et al. (J. Acoust. Soc. Am. 135. 283-286, 2014) model of the auditory periphery with a coincidence counting model of the lateral superior olive (LSO) from Ashida et al. (PLOS Comp. Biol. 12, e1004997, 2016). The latter integrates ipsilateral excitatory signals together with negatively weighted inhibitory signals from the contralateral ear in millisecond short coincidence windows. In its simplest version, the model employs only one left-right pair of simulated LSO neurons, and maps the hemispheric LSO rate difference to an extent of lateralization.

This version of the model holds physiological plausibility and explains the psychoacoustic data with a similar accuracy as the delay line model. Experimental data with temporally asymmetric envelopes, which impose a major challenge for conventional models, can also be qualitatively accounted for with the spiking LSO model. The successful simulation of envelope ITD and ILD lateralization has triggered follow-up studies which have recently started: By adding a model of the medial superior olive, we aim to account for low-frequency fine structure ITD sensitivity. By adding different decision stages, we are setting up the model for detection and discrimination tasks within the same framework.

PS 627

Binaural masking level difference as a function of noise bandwidth and noise delay

Mathias Dietz; Kristin Bracklo; Stephan D. Ewert
Universität Oldenburg

A classic psychoacoustic task is the detection of a tone in noise. The human binaural system can exploit differences of the interaural phase of a noise and target tone to improve detection thresholds. Maximum benefit is obtained for detecting an antiphase tone ($S\pi$) in diotic noise ($N0$), which improves detection thresholds in the order of 12 to 15 dB. It has been shown in several studies that this benefit slowly declines as an interaural time difference (ITD) is applied to the $N0S\pi$ complex. This decline has been attributed to the decorrelation of the noise. The available datasets have also been used to fit models of binaural processing, especially to

fit the length of assumptive delay lines. The approach is tempting, because the compensatory internal delays can effectively be subtracted from the external ITD, and cause an increase in binaural benefit. However, the effective bandwidth of the auditory filter at the target frequency is also unknown and affects the decay of the binaural advantage with ITD. With the existing data it is thus difficult to disambiguate the two effects and to correctly parameterize a binaural model.

Here, we measure detection thresholds of (N0S π)ITD stimuli, with ITDs up to 8 ms, for a noise bandwidth from 25 to 1000 Hz. The target is always a 500 Hz tone. Its level is varied adaptively in a 2-down 1-up fashion within a three alternative forced-choice task.

Results up to this point show that for bandwidths of 150, 200, and 1000 Hz detection thresholds are similar for all ITDs, whereas for 25, 50, and 100 Hz the negative impact of ITD is smaller, i.e. decorrelation progresses slower with increasing ITD. The data can be simulated best with an effective filter bandwidth near 100 Hz. Further data is currently collected to make more accurate predictions about the bandwidth and if the decay rate can be predicted with a model that only uses internal delay compensation of less than 0.4 ms.

PS 628

Binaural Coherence Between Temporal Fine Structure and Envelope Determines Interaural Time Difference Sensitivity

Jessica J.M. Monaghan; Jaime A. Undurraga; Lindsey N. Van Yper; David McAlpine
Macquarie University, Department of Linguistics

Background

When low-frequency sounds arrive at the ears, both the location of a source and the characteristics of a room are conveyed by the temporal fine-structure (TFS) and the envelope (ENV) of the acoustic signal arriving to each ear. In an environment free of reflections, ecological ITDs conveyed by the TFS and the ENV will be coherent; that is, both ITDs will indicate the same direction. However, in a reverberant environment, ITDs conveyed by the TFS and the ENV become incoherent, with conflicting ITD cues. Recently, we have demonstrated that neural responses evoked by abrupt modulations of the ITD—the interaural time modulation following-response (ITM-FR)—where the ITD of a 400-Hz band of noise centered at 500 Hz was modulated within and beyond the ecological range—resulted in an oscillating, damping function, consistent with the trade-off between conflicting envelope and fine structure ITD cues. Here, we investigate whether this damping pattern is reflected in behavioral measures of ITD thresholds.

We hypothesize that ITD sensitivity should be greater when TFS and ENV ITDs are coherent, compared to when they are in conflict.

Methods

ITD sensitivity was assessed in 10 normal-hearing listeners. Stimuli were similar to those used by Undurraga et al. 2018 (ARO). In short, a 400-ms band-limited filtered noise (300-700Hz; centered at 500 Hz) was presented with a given ITD. We used a 4-interval, 2-alternative-forced-choice task, with first and last intervals always identical (with a fixed reference ITD), and one of the two middle intervals different (fixed reference ITD + delta_ ITD). Participants were instructed to select the interval that was different. Delta ITD was adapted using a 2-down 1-up staircase tracking procedure with an initial step of 1.58 and a final step of 1.12. The ITD thresholds were obtained by averaging the last 12 reversals. ITD sensitivity was assessed at several reference points: 0 us; 500 us; 1000 us; 1500us; 2000us; 2500us; 3500 us; 3500 us; and 4000 us.

Results

Consistent with our hypothesis, ITD sensitivity showed an oscillating damping factor which correlates well with our EEG measures. ITD sensitivity was greater when both ENV and TFS were coherent. There was an overall increase of ITD sensitivity

Conclusions

Consistent with our EEG data, the data demonstrate that ITD sensitivity does not decrease monotonically with reference ITD, but that sensitivity appears to reflect a trade-off between TFS and ENV cues.

PS 629

Neural Representation of Interaural Time Differences in the Human Cortex - an MEG Study

Lindsey N. Van Yper¹; Jaime A. Undurraga¹; Blake Johnson²; Jessica J.M. Monaghan¹; David McAlpine¹
¹*Macquarie University, Department of Linguistics*;
²*Macquarie University, Department of Cognitive Science*

Background: Auditory stream segregation refers to the ability of the auditory system to segregate competing sound sources into perceptually distinct auditory objects – a key factor for cocktail party listening (Bergman, 1990). Although the mechanisms underlying auditory stream segregation are poorly understood, temporal coherence between the acoustic features of a sound source has been shown to be critical. In a recent study, we demonstrated that the magnitude of the interaural time modulation following response (ITM-FR; an EEG response to periodic transitions in interaural

time differences or ITDs) depends on the coherence between the ITDs in the temporal envelope and fine-structure of the signal, with larger amplitudes for coherent as opposed to incoherent signals (Undurraga et al., ARO MidWinter Meeting, 2018). Here, we employ MEG to (1) cross-validate these initial results, and (2) determine whether cortical representation are different for coherent versus incoherent sounds.

Methods: MEG recordings will be obtained from ten normal hearing listeners, using a whole-head MEG system with 160 axial gradiometers. Stimuli are 400 Hz-wide band-pass filtered noise with a centre frequency of 500 Hz. ITM-FRs will be elicited by periodically modulating the ITD between -0.5/0.5, -1.0/1.0, -1.5/1.5, -2.0/2.0, -2.5/2.5, -3.0/3.0, -3.5/3.5, and -4/4 ms. Dipole source localization will be used to determine the cortical regions involved in the neural processing of coherent and incoherent ITD cues.

Results: Based on our previous study, we expect a damping function with maximal MEG activity when the envelope and fine-structure of the signal are coherent. Also the results of dipole source locations will be presented.

Conclusions: This study provides further insight into the effects of binaural coherence on neural activity of ITD processing, thereby improving our insight into the neural mechanisms underlying auditory stream segregation.

PS 630

Understanding the Importance of Heterogeneity in the Superior Olivary Complex to the Correct Lateralization of Reverberant Speech Signals

Jason Mikiel-Hunter¹; Andrew Brughera²; Jessica J.M. Monaghan³; Nicholas R. Haywood³; David McAlpine³
¹Macquarie University; ²Boston University; ³Macquarie University, Department of Linguistics

Normal hearing listeners can localize sound sources accurately in a large variety of reverberant, real-world environments. This is despite interaural cues carried by extraneous acoustic reflections potentially confounding a listener's ability to lateralize the signal correctly. Numerous studies have highlighted the importance of processing cues in the stimulus onset to ensure robust spatial localization in reverberation (Devore et al., 2009; Stecker and Brown, 2010); however, when a carrier tone is amplitude-modulated and an interaural time difference (ITD) is introduced into its temporal fine structure, onset dominance appears frequency-dependent: proving effective for a 600-Hz carrier but less so at 200 Hz (Hu et al., 2017). While ITDs are the dominant binaural cue at both carrier frequencies, it is likely that differences/limitations in the underlying neural mechanisms at 200

Hz Vs. 600 Hz help generate their relative lateralization sensitivities to stimulus onset cues.

One possible explanation for this varying stimulus onset sensitivity is that binaural neurons along the tonotopic axis of the Superior Olivary Complex are heterogeneous and receive inputs from Bushy cells of the Cochlear Nucleus (CN) with their own frequency-dependent temporal response profiles. To determine whether such an arrangement indeed affects stimulus onset sensitivity along the tonotopic axis and what implications it might subsequently have on the ability to lateralize reverberant speech signals, we have developed a multi-stage computational model containing a heterogeneous population of coincidence-detecting neurons. The neuron model used for coincidence-detection is linear with membrane properties modelled after principal neurons in the Medial and Lateral Superior Olives (MSO and LSO respectively) (Remme et al., 2014). In addition, a monaural coincidence stage is introduced prior to binaural interaction as observed biologically in the CN. This stage receives simulated Auditory Nerve inputs (Zilany et al., 2014) that adapt and recover with a realistic time course previously applied when reproducing MSO neuronal responses to amplitude-modulated binaural beating stimuli (Wang and Manis, 2008; Dietz et al., 2014; Brughera et al., 2018). A neurometric response is generated for comparison with behavioural results by calculating the rate-difference between two populations of these model neurons that encode left and right azimuthal hemifields (best ITDs shifted $\pm 1/8$ cycles relative to characteristic frequency of each model neuron).

Initial results confirm that heterogeneity in a population of coincidence-detecting neurons that receives adapting inputs can indeed produce frequency-dependent stimulus onset sensitivity. Furthermore, it may offer robust encoding of lateralization for a mixture of speech signals presented in reverberant conditions.

PS 631

Lateralization of Competing Interaural Cues in Envelope-Modulated High-Frequency Tones

Stephen Dennison¹; Alan Kan²; Ruth Litovsky²
¹University of Wisconsin-Madison; ²University of Wisconsin - Madison

Spatial hearing and sound localization depend on interaural level differences (ILDs) and interaural time differences (ITDs). The duplex theory of sound localization suggests that, for temporal fine structures, ILDs dominate perception and ITDs are not utilized at higher frequencies. In addition to fine structure, listeners are sensitive to ITDs in low-frequency envelopes

imposed on high-frequency carriers. For these stimuli, there is evidence for interaction between ILD and ITD cues in high-frequency envelopes in normal hearing listeners. Cochlear implants can encode envelopes cues, and bilateral cochlear implant (BiCI) users appear to use envelope ITDs, but little is known about ITD-ILD cue competition in these listeners. We are ultimately interested in understanding how BiCI users perceive the interaction of these cues in order to improve their ITD sensitivity. Although all participants in this study had normal hearing, the results presented will lay the groundwork for studying binaural envelope cue competition in BiCI users.

Stimuli were presented through circumaural headphones while participants sat in a sound booth. On each trial, listeners indicated the perceived intracranial lateral location of a sound event. The stimulus was a 4 kHz pure tone modulated with a 100-Hz raised-cosine envelope. Pink noise was added to mask low-frequency distortion products. In the control condition, ITDs and ILDs were imposed on the stimulus to determine their extent of lateralization when presented alone. In the two-cue conditions, combinations of ITD and ILD with opposing values were used to determine how much each cue affected the other. Stimuli from all conditions were randomized and interleaved. To control for changes in the slope of the envelope when an ILD was imposed, the roll-off factor of the raised cosine was adjusted based on the intensity of the presented ILD.

This presentation will focus on the extent of lateralization due to either ITD or ILD envelopes cues presented alone or in competing conditions. Bias weights were estimated for envelope ITDs and ILDs. Cue bias weights were calculated from the difference of the natural cue present in the stimulus and the observed cue corresponding to the location of the listener's response.

This work was supported by NIH-NIDCD R01DC016839 and NIH-NIDCD R01DC03083 to RYL, NIH-NIDCD R03DC015321 to AK, and NIH-NICHD U54HD090256 to the Waisman Center.

PS 632

Emergence of ITD Selectivity in a Deep Neural Network Trained for Binaural Natural Sound Detection

Takuya Koumura; Hiroki Terashima; Shigeto Furukawa
NTT Communication Science Laboratories

Interaural time difference (ITD) is an important binaural cue for natural sound detection and localization. Some neurons in the auditory system respond selectively to sounds with specific ITDs. ITD selectivity is considered

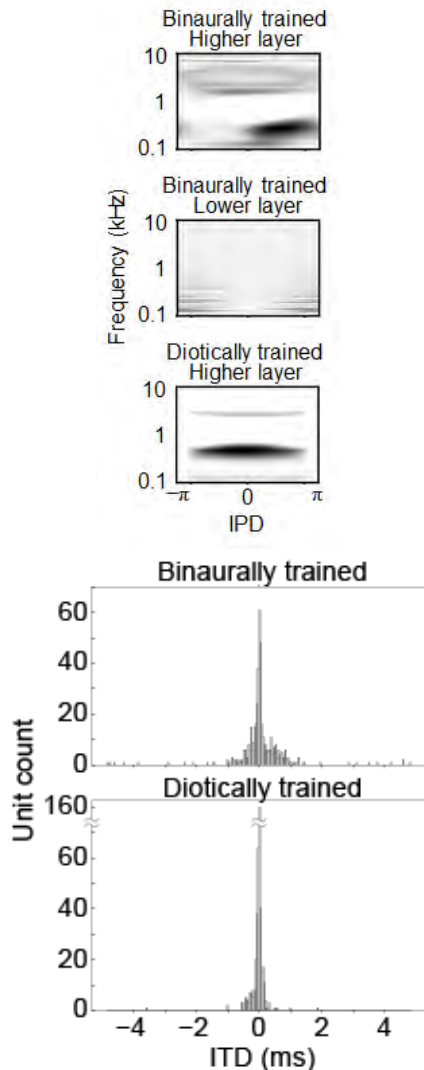
to be one of the neural mechanisms of binaural hearing. However, the primary function for which ITD selectivity evolved is not known. It could be possible that ITD selectivity can emerge only by sound detection and that performing sound localization might not be necessary for forming ITD selectivity.

This pilot study attempted to test this possibility by taking a computational approach. Specifically, we modeled the auditory system with a deep neural network (DNN). A DNN is a state-of-art machine learning model for sound recognition. Since a DNN processes a sound through its cascaded layers for recognition, it is suitable for modeling the auditory system that processes a sound for recognition through cascaded brain regions. We trained a DNN to detect acoustic events from natural sounds recorded with a dummy head microphone (Mesaros, Heittola, & Virtanen, 2016) and analyzed the trained DNN with neurophysiological methods (Koumura, Terashima, & Furukawa, 2018). We recorded single unit activities in the DNN in response to tones with various frequencies and ITDs.

Units in the lower layers did not show clear tuning to frequency or ITD, but some units in the higher layers exhibited frequency- and ITD-selective activities. The best ITD (the ITD which induces the largest unit activity) was distributed across the physiological range of humans (± 0.7 ms) with some units with their best ITD exceeding the range, as in the auditory system (Grothe, Pecka, & McAlpine, 2010). Moreover, the ITD tunings in a DNN trained on diotic sounds appeared to be symmetrical around the frequency axis, indicating insensitivity to the sign of the ITD. Their best ITDs were confined to smaller range than those in the DNN trained on binaural sounds. Although the evidence obtained so far is not yet very strong, these results may suggest that ITD selectivity emerged from optimization to binaural natural sound detection even without performing localization.

References:

- Grothe, B., Pecka, M., & McAlpine, D. (2010). *Physiological Reviews*, 90(3), 983–1012. <https://doi.org/10.1152/physrev.00026.2009>
- Koumura, T., Terashima, H., & Furukawa, S. (2018). *BioRxiv*, 308999. <https://doi.org/10.1101/308999>
- Mesaros, A., Heittola, T., & Virtanen, T. (2016). 2016 24th European Signal Processing Conference (EUSIPCO), 1128–1132. <https://doi.org/10.1109/EUSIPCO.2016.7760424>



PS 633

Interaural Time Differences: Lateralization Adapts to Stimulus Space

Nima Alamatsaz¹; Antje Ihlefeld²

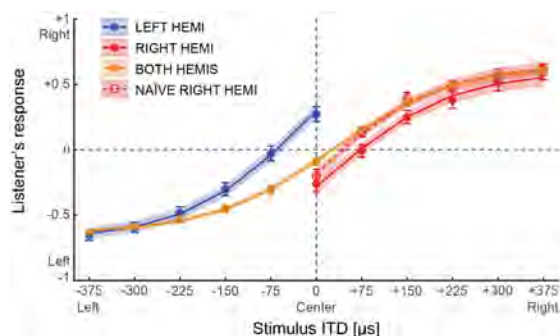
¹New Jersey Institute of Technology, Rutgers University; ²New Jersey Institute of Technology

A wide range of species relies on sound localization for both navigation and auditory scene analysis. For low-frequency sound, interaural time differences (ITDs) are the dominant cue for determining the direction of a source in the horizontal plane, a phenomenon called sound lateralization. The mechanisms by which the nervous system maps ITD into perceived sound direction are incompletely understood.

In anechoic spaces, a given source angle in the horizontal plane typically gives rise to the same ITD, across a wide range of source distances. However, in everyday environments where background sound and reverberant energy are often present, ITDs are much less reliable

indicators of source direction. This raises the possibility that when estimating source direction, a listener's interpretation of ITD changes depending on the context of the listening environment. Indeed, previous work shows plasticity in perceived sound direction across a wide range of conditions, including ear plugging, modifications to shape of the pinnae, prolonged exposure to constant interaural delays, in presence of preceding distractors, long-term procedural learning and short-term stimulus history. However, we have an incomplete understanding of short-term adaptation of sound lateralization based on the overall range of ITDs.

Here, we randomly assigned 34 naïve normally-hearing listeners to 4 groups. Using a target-pointer matching task without visual feedback, listeners of three groups were trained on ITD lateralization for 3 sessions. A fourth naïve control group was tested without training. All 4 groups of listeners then performed a lateralization task which asked them to identify and plot the internal image of low-frequency noise tokens. For both training and testing, one trained group (RIGHT HEMI) was only presented with positive ITDs (right hemisphere), the second trained group (LEFT HEMI) only with negative ITDs (left hemisphere), and the third trained group (BOTH HEMIS) with the full range of bilateral ITDs (both hemispheres). The naïve group was tested with positive ITDs only (NAÏVE RIGHT HEMI). Listener responses across different groups and stimulus conditions were analyzed with a Nonlinear Mixed-Effects Model (NLME). Results show robust response expansion in all unilaterally tested listeners towards the contralateral side, with a larger effect for the trained groups versus the naïve. In contrast, bilaterally trained listeners did not display any response bias. Together, these results show that perceived direction adapts rapidly to stimulus space. Results will be discussed in the context of assessing spatial perception in patient groups with impaired binaural cues, including bilateral cochlear implant users and cochlear implant users with single-sided deafness.



Perceived laterality from left (-1) to right (1). Circles show across-listener average laterality scores for each stimulus space condition (filled symbols for trained and open symbols for untrained listeners). Error bars show one standard error of the mean. NLME fits are shown by lines with ribbons indicating one standard error of the mean in the model predictions. For both trained and untrained listeners, stimulus space significantly affected where listeners lateralized based on ITD (NLME, y-intercept attributed to stimulus space, $t=12.61$, $p<0.001$, $DF=19599$, $AIC=1060.27$, $BIC=1154.89$, $\logLik=-518.14$, $r^2=0.779$).

PS 634

Normative Study of the Binaural Interaction Component of the Human Auditory Brainstem Response as a Function of Interaural Timing Differences

Carol A. Sammeth¹; Nathaniel T. Greene²; Andrew D. Brown³; Daniel J. Tollin⁴

¹Department of Physiology & Biophysics, University of Colorado School of Medicine; ²University of Colorado School of Medicine, Department of Otolaryngology; ³Department of Speech and Hearing Sciences, University of Washington; ⁴Department of Physiology & Biophysics, and Department of Otolaryngology, University of Colorado School of Medicine

When the sum of monaural right and left ear auditory brainstem responses (ABRs) is subtracted from the binaural ABR, the difference is the binaural interaction component (BIC). There are conflicting reports regarding the reliability of BIC measures in humans. This study examined BIC characteristics across a large number of normal-hearing adults using three interaural time differences (ITDs), and compared the BIC results to those from a behavioral ITD discrimination task.

Methods:

Subjects were 40 normal hearing adults (20 male, 20 female), aged 21 to 48 (median = 27), with no history of otologic or neurological disorders.

ABRs were recorded from electrodes at high forehead (Fz) referenced to the nape of the neck (7th cervical vertebra) with a nasion (Fpz) ground. Electrode impedance was 5 k Ω and balanced. EEG was amplified x50,000, analog filtered 30-3000 Hz, and post-hoc digitally filtered 100-3000 Hz. Stimuli were biphasic clicks presented at 14 per second (jittered) via Etymotic ER-2 insert earphones at 90 dB peSPL (55 dB nHL). During each run, 2000 each of interleaved right monaural, left monaural, and binaural stimuli were presented. Four runs were averaged for 8000 stimuli per condition. BIC was measured for ITD=0 (simultaneous bilateral) and +/- 500 and 750 microseconds. Subjects separately performed a touch screen lateralization task, with the same stimulus, to determine ITD discrimination threshold.

Results:

Most subjects produced a BIC, appearing as a negative trough ("DN1") around the latency of wave V roll-off; however, not all subjects had measurable or reliable BICs. BIC was most often found when a subject was relaxed or sleeping, and less often when a subject fidgeted or reported neck tension during testing, suggesting myogenic activity as a likely factor in disrupting BIC measurements.

When present, the BIC generally showed the expected

pattern of increased latency and decreased amplitude with increased ITD. For the task used, there was no clear relationship between the ABR BIC and the behavioral ITD discrimination threshold - subjects without a measurable BIC generally performed the task as well as those that produced a BIC.

Conclusions:

The fact that the human ABR BIC is not always present and is time consuming to measure limits its clinical utility unless stimuli and measurement parameters can be identified that produce a more robust response. Nonetheless, modulation of BIC characteristics across ITDs supports the concept that the BIC can be considered a biomarker of binaural brainstem processing.

Supported by NIH R01-DC011555

PS 635

Deep Neural Networks as Models of Real-World Human Sound Localization

Andrew Franci; Josh H. McDermott
Massachusetts Institute of Technology

The ability to localize a sound source by listening is a core component of audition, and has been a focus of hearing research for over a century. Sound localization has traditionally been studied using simple sounds and listening conditions, such as single noise bursts or tones in anechoic environments. However, in everyday life we localize sounds in environments with multiple sound sources, background noise, and room reverberation. At present we lack models that can explain these everyday abilities.

Recent engineering advances have led to artificial neural network models that perform at human levels for many perceptual tasks. Such network models are optimized to extract cues from the input that best support performance of the trained task. As a result, a trained model can reveal characteristics of near-optimal performance, and can provide hypotheses for biological systems that solve the same task. We have utilized this approach to build a model that localizes sound sources in noisy reverberant environments from binaural audio. Following optimization, the model accurately localized natural sounds in 3D space amid background noise and reverberation. Preliminary analysis of the model revealed some behavioral characteristics evident in human localization. Forcing the model to recognize as well as localize sounds caused notable drops in performance, suggesting the need for features specialized for localization, as are believed to be found in the auditory midbrain. The results indicate that deep learning can be harnessed to build models of sound localization in realistic conditions that can be fruitfully compared to biological sound localization systems.

PS 636

Using fNIRS to investigate effortful listening of normal and degraded speech with noise

Xin Zhou¹; Gabriel Sobczak²; Ruth Litovsky³

¹Waisman Center, University of Wisconsin-Madison;

²Medical School, University of Wisconsin-Madison;

³University of Wisconsin - Madison

Listening to speech with co-located noise can be challenging even for people who have normal hearing (NH). For cochlear implant (CI) users, this is harder due to degraded auditory input by the CI. Performance assessed with percent-correct word identification is typically better when the speech and noise are spatially separated, i.e., spatial release from masking. However, little is known about the cognitive load involved in effortful listening to degraded speech and in spatial release from masking. This study aimed to investigate whether a neural signature for release from effort could be identified by examining the cortical activity using functional near-infrared spectroscopy (fNIRS).

This study simulated listeners with single sided deafness (SSD) who receive a CI in the deaf ear. NH listeners were tested with stimuli presented through insert earphones. Speech sentences were either vocoded (8 channels) or unprocessed, and noise was vocoded, eight-channel 4-talker babble, presented at 75 dBA (at -10 and -15 dB SNR). Speech was presented to the left ear, with ipsilateral or bilateral noise.

fNIRS measures the concentration changes of hemoglobin in blood flow from extracerebral and cerebral tissues, comprising a mix of evoked and non-evoked (spontaneous) neural and systemic components. When quantifying the fNIRS event-evoked neural responses, it is essential to reduce confounding components. Two methods were implemented: (1) we extracted the neural response components from fNIRS data by minimizing the mutual information between systemic and neural components; (2) we used shorter (8 mm) than regular (3 cm) channels to measure responses only from the extracerebral and not from cerebral tissues, with which extracerebral responses in the regular channels could be removed.

We will present fNIRS findings pertaining to the impact of masking and unmasking noise on speech understanding in SSD simulations. Our preliminary results showed greater responses in the bilateral inferior prefrontal cortex (IPFCs) when attending to vocoded speech than to normal speech. These findings agree with previous studies using fNIRS and functional magnetic resonance imaging, that have reported the involvement of bilateral IPFCs in effortful listening to degraded speech. We

will further determine which method provides more consistent fNIRS measures of neural responses. We ultimately aim to investigate whether fNIRS could reveal the neural signature for the release from effort in CI users with SSD.

Supported by NIH-NIDCD (R01DC003083 to RL), UW-Madison's Office of the Vice Chancellor for Research, and a Core grant from NIH-NICHD (U54HD090256 to Waisman Center).

PS 637

Spectral Weighting of Interaural Time and Level Differences in the Lateralization of Complex Tones

G. Christopher Stecker

Vanderbilt University Medical Center

Spatial hearing in complex environments requires the auditory system to extract and encode binaural cues that vary over time and across frequency, and to integrate those cues across time, frequency, and cue type. By weighting the various cues appropriately, the integration process emphasizes the most reliable and informative cues. Appropriate weighting reduces errors that arise, for example, by reverberation or distortion by competing sounds. The current study focuses on the weighting of interaural time and level differences (ITD and ILD) across the spectral frequency components of complex sounds. The approach follows Stecker et al. [2013, *J Acoust Soc Am* 134:1242-52], who used an open-loop lateralization task to measure temporal weighting functions (TWF) for sounds varying simultaneously in ITD and ILD. Here, stimuli consisted of multiple frequency components, which were either sinusoids, trains of narrowband impulses, or narrow bands of noise. On each trial, listeners judged the lateral position of a single stimulus whose overall ITD and ILD varied from trial to trial over the range $\pm 400 \mu\text{s}$ and $\pm 4 \text{ dB}$. Within each stimulus, individual frequency components varied, randomly and independently, by an additional $\pm 100 \mu\text{s}$ and/or $\pm 1 \text{ dB}$. Listeners indicated the lateral position on each trial using a touch-sensitive display. Lateralization weights were estimated by multiple regression of rank-transformed responses onto the per-component ITD and ILD values on each trial. These weights comprise the spectral weighting function (SWF) and quantify the relative potency of ITD and ILD carried by each frequency component. In some conditions, per-component ITD and ILD values were manipulated independently in order to allow the simultaneous estimation of ITD and ILD weights, along with the corresponding ITD/ILD "trading ratio," at each frequency. Preliminary results based on SWFs spanning 1-8 kHz revealed greater weight on low-frequency components, consistent with a dominance of low-frequency cues in broadband sound localization [e.g., Wightman & Kistler 1992, *J Acoust Soc*

Am 91:1648-61]. Further analysis of independent ITD/ILD weights revealed that both cue types exhibited low-frequency dominance, but steeper SWF slopes were observed for ITD than for ILD. The results thus support a sizable though secondary role of ILD cues even at frequencies where ITD dominates. The dominance relationship reverses above 2 kHz, where neither cue is particularly potent in the face of competing low-frequency sound. Trading ratios at those frequencies favored ILD similarly to high-frequency sounds tested in isolation (i.e. 100-200 μ s/dB). Supported by NIH-NIDCD R01 DC016643.

PS 638

Hemispheric Processing Asymmetries for Fixed vs. Moving Auditory Stimuli

Barrett St George; Barbara Cone
The University of Arizona

Background Information

The purpose of this research was to measure the hemispheric processing asymmetries for fixed vs. moving auditory stimuli using auditory evoked potentials and perceptual methods. Previous research has established that there is a contralateral dominance of cortical processing for sound sources within a given hemisphere. Accompanying this general contralaterality, there seems to be a right hemisphere dominance for motion perception, specifically.

The auditory P300 event-related potential (ERP) is an electrophysiological measure that reflects the contralateral dominance for spatial listening tasks, at least for fixed stimuli. Yet previous results have been variable with respect to a right-hemispheric dominance for stimuli that evoke a perception of movement based upon interaural level differences. (Estes, Jerger, & Jacobson, 2002; Jerger & Estes, 2002). This present research was conducted to compare fixed vs. moving sound source perception. The main hypotheses were: 1) both fixed and moving stimuli will show a contralateral hemispheric dominance, 2) only moving stimuli will show a general rightward hemispheric dominance, and 3) perceptual laterality ratings will correlate with both amplitude and latency of P300.

Methods

20 right-handed, normal hearing young adults participated. Stimuli consisted of broadband random noise that were systematically varied by four factors: 1) duration, 2) inter-aural level difference (ILD) magnitude, 3) direction (right vs left) and 4) stimulus type (moving vs fixed). Stimuli were delivered through extended high-

frequency range headphones.

Perceptual laterality ratings for all stimuli were obtained from a listening task that consisted of 10 tokens of each stimulus parameter, presented in a randomized sequence.

P300 ERPs were obtained during listening tasks in which the standard stimulus consisted of a diotic token whereas the deviant stimuli were dichotic and reflected systematic differences in duration, ILD, direction and stimulus type. Listeners were asked to identify each stimulus as left, right or center. Hemispheric asymmetry patterns for all stimulus conditions were calculated from 16 electrodes sites, 8 for each hemisphere.

Results and Conclusion

Analyses to date show a strong effect for direction (right vs. left) with stimuli yielding a perception of right laterality showing larger P300 responses than left. There is also a strong effect for stimulus type with moving stimuli evoking a larger response than for fixed stimuli. These results are consistent with the hypotheses and suggest hemispheric differences for lateralized sounds created by interaural level differences. These findings may be useful in creating objective tests of spatial listening ability.

PS 639

Real-time Algorithm for Sound-Source Segregation with Binaural Cues Preserved

Marcos Cantu; H Steven Colburn
Boston University

An algorithm designed to compute a Time-Frequency (T-F) mask in real-time is evaluated here using virtual room acoustics and computational measures of speech intelligibility and sound source segregation. The advantage of this approach is that the T-F Mask can be applied independently to signals at the left and right ears, thereby preserving natural binaural cues for spatial hearing. Results of the preliminary evaluation suggest that the algorithm can boost speech intelligibility for a target talker from a specified "look" direction, while simultaneously suppressing the intelligibility of competing talkers.

A proposed Short-Time Target Cancellation (STTC) Assistive Listening Device (ALD) uses three pairs of microphones to compute a T-F mask that filters the signals from a fourth pair of microphones ([L,R]) in the user's ears. The "target cancellation" approach involves removing the Signal from a mixture and computing an estimate of the Noise. However, when there is little to no

phase difference between target and interferer, the target cancellation approach is ineffective; there is an interaction between frequency, microphone spacing and direction of arrival angle that yields wrapped absolute phase differences of zero at certain frequencies. A “piecewise” approach to constructing a Global Ratio Mask with three microphone pairs improves performance by providing a positive absolute phase difference for the STTC algorithm to work with. The STTC ALD computes T-F masks for three different microphone spacings (140, 80 and 40 mm). Each of the three Ratio Masks has frequency bands where the T-F tiles are being overestimated. However, the multiple ratio and binary masks can be interfaced to compute a Thresholded Ratio Mask which can look similar to the Ideal Binary Mask (IBM) and Ideal Ratio Mask (IRM).

Performance was evaluated with a mixture of three concurrent talkers in anechoic space using virtual room acoustics and computational measures of speech intelligibility and sound source segregation. Predictions of speech intelligibility were made with the Coherence Speech Intelligibility Index (CSII) and Sound Source Segregation was evaluated using the SDR and SIR measures in the BSS_EVAL toolbox. The results suggest that a significant improvement in speech intelligibility can be afforded with the proposed Short-Time Target Cancellation (STTC) Assistive Listening Device (ALD), while still preserving binaural cues for spatial hearing. The proposed device could conceivably provide much needed help to populations currently having difficulty following conversations in complex acoustic environments.

[Work Supported by NIH/NIDCD Grant DC000100.]

PS 640

Rapidly varying interaural phase difference cues within modulated tonal stimuli: Comparing lateralization cues from stimulus onset and cues from on-going amplitude modulation.

Nicholas R. Haywood; David McAlpine
Macquarie University, Department of Linguistics

In spatial-listening tasks, lateralization judgments are typically weighted strongly towards stimulus onsets, where stimulus amplitude is rising (e.g. Stecker & Hafter, 2002; Dietz et al., 2013). However, most environmentally relevant sounds are characterised by a continuous series of amplitude modulations. Here, we explored the extent to which lateralization judgements are influenced by rising-amplitude stimulus segments beyond the onset.

In Experiment 1 (preliminary), we assessed the relative importance of ongoing onsets in lateralization judgements using amplitude-modulated binaural beats (AMBBs; Dietz

et al., 2013). Stimuli comprised a 750-ms signal with an 8 Hz diotic AM/binaural beat (496/504 Hz carrier-tones). The carrier interaural phase difference (IPD) at onset was set to between 0° and ±270°. Subjects reported whether stimuli were heard to the left/right in a two-alternative, forced choice task. Lateralization reflected the IPD configuration present during the rising-amplitude segments as opposed to those at peak amplitude, consistent with previous studies. In additional conditions, the onset/offset ramps were preserved, but the modulation depth during the sustained portion of the stimulus was set to 0.66%, 0.33%, or 0%. For IPDs heard off-centre, removing the sustained AM reduced lateralization by ~50%. Therefore, whilst the onset influenced lateralization strongly, subsequent modulations also made a significant further contribution.

Experiment 2 (preliminary) extended the initial/onset AM cycle by 50%, inserting a flat-amplitude segment at mid-point/peak. Therefore, carrier IPDs during the rising slope of the onset cycle (0°-180°) were laterally opposed to those during subsequent cycles (180°-360°). As the number of cycles increased, listeners progressively lateralized away from the onset cycle. Irrespective of beat rate (8/16 Hz), listeners lateralized strongly away from onset for stimuli >250-ms, suggesting a time-constant for onset dominance. Lateralization appears determined by IPD information present at specific points within on-going modulation cycles.

In experiment 3 (preliminary), an unmodulated 8-Hz beating stimulus contained raised-cosine onset/offset ramps, each spanning 180° of the beat cycle (62.5-ms). Stimulus duration was varied in 62.5-ms increments, with the offset ramp either matching (0°-180°) or mismatching (180°-360°) IPDs of the onset ramp. For signal durations >250-ms, there was a subtle, but persistent reduction in the extent of lateralization (~5%) for mismatched-offset conditions, suggesting an IPD sensitivity during amplitude decrements. Control conditions employed rapid offsets (5-ms), to account for recency effects non-specific to envelope characteristics.

These experiments demonstrate that lateralization to AMBBs is not driven exclusively by information at sequence onset. Rather, listeners remain sensitive to IPD information throughout signals containing envelope fluctuations.

PS 641

Developing a Multilevel Objective Assay of Binaural Hearing Sensitivity

Spencer B. Smith¹; Trent Nicol²; Travis White-Schwoch²; Jennifer Krizman²; Nina Kraus²

¹*The University of Texas at Austin and Northwestern University*; ²*Northwestern University*

Background:

Binaural hearing is an integral contributor to speech-in-noise performance. However, because extensive training is required to achieve reliable psychophysical measures of binaural sensitivity, this skill is not commonly assayed in clinical settings. A clinical measure of binaural hearing sensitivity may have multiple applications from evaluating patients complaining of speech-in-noise deficits to fine tuning binaural hearing aids and cochlear implants.

The goals of this work were to 1) develop a rapid “multilevel” objective assay of binaural hearing sensitivity and 2) investigate predictive relationships between this objective assay and a spatial speech-in-noise test.

Methods:

Interaural phase difference (IPD) detection was objectively measured in 22 listeners with normal hearing using binaural stimuli with 180-degree phase inversions embedded in them. The stimuli were 80 Hz sinusoidally amplitude modulated tones with different carrier frequencies (500, 750, 1000, and 1250 Hz). In the control condition, the tones remained binaurally in phase throughout the duration of the 800 ms trial, whereas in the test condition, a 180-degree monaural phase inversion occurred in the carrier tone at 400 ms during an envelope null. Motivated by previous work, auditory evoked potentials approximately corresponding to different “levels” of the auditory nervous system (i.e., subcortex, midbrain, and cortex) were evaluated for evidence of neural IPD detection. Specifically, IPD-induced changes in neural phase locking strength to the carrier tones (subcortical) and SAM envelopes (midbrain) were evaluated, as were cortical acoustic change complex (ACC) amplitudes. Listeners also completed the Hearing in Noise Test; spatial release from masking scores (noise separated – noise collocated) were used as proxy measures of subjective binaural hearing benefit.

Results:

ACC responses to phase inversions were present in all participants; onset response amplitudes were negatively correlated with carrier tone frequency. Following the phase inversions in the test condition, envelope phase locking strength diminished and subsequently recovered, whereas phase locking to the carrier tones remained degraded. HINT spatial release from masking was not correlated with any objective measure of binaural hearing acuity.

Conclusions:

ACC responses to phase inversions of different carrier frequencies provide a straightforward and rapid within-subject measure of IPD detection. However, the present

results did not find a relationship between objective and subjective measures of binaural hearing, indicating that they are measuring different abilities. This may be due to the previous observation that speech spatial release from masking is driven by the “better ear” monaural signal-to-noise ratio when low pass masking noise is used; thus, spatial release from masking as measured by the HINT may not be an appropriate proxy of binaural hearing.

PS 642**The Size of an Auditory Scene: Role of Spatial Separation and Stimulus Similarity**

William A. Yost; M. Torben Pastore
Arizona State University

How many people can be perceived at a cocktail party? In other words, how many concurrent sound sources can be perceived in an auditory scene? If the number is large, then the auditory brain is probably doing substantial neural calculations. If so, devices that provide real or virtual information about an auditory scene may require large computational resources. If the number is small, then the opposite conclusions may be reached. The great majority of research involving multi-source auditory scenes have used a small number of sound sources, most often only two (a masker/distractor and signal/target). If the perceived scene is small, this work may indicate a good estimate of the human ability to process real auditory scenes. If not, then additional research is probably required to more fully characterize the perception of multi-source auditory scenes. This research project deals with several of these issues. Normal hearing listeners were asked to make same-different discriminations between multi-source stimuli presented with different spatial configurations among the sources in one set of experiments and different degrees of stimulus similarity in another set of experiments. The stimuli were 16 consonant-vowel (CV) pairs spoken by 10 males and 10 females. The CVs could be concatenated to make longer “word-like” utterances. The CVs were presented nearly simultaneously, from one or more loudspeakers in a 24 azimuthal loudspeaker array in a sound deadened room. Thus, the spatial configuration of the loudspeakers presenting sound, the CVs that were spoken, the number of concatenated CVs, the number of talkers, and which talkers were speaking were all varied in different conditions and experiments. The results indicate that listeners have great difficulty discriminating between auditory scenes when the number of sources is more than approximately four -- even four sound sources can lead to barely discriminable differences for some listeners in some conditions. Listeners have great difficulty in discriminating a change in the spatial configuration of the sources when there are more than three sound sources. If more than one variable (spatial

separation, CVs, and talker) changes between stimuli, listeners have great difficulty discriminating differences in an auditory scene when there are more than three sound sources. There was, however, substantial between listener variability. (Research supported by NIDCD and Oculus, VR LLC).

PS 643

A Physiology-Based Time-Frequency Mask Estimation Method for Auditory Scene Analysis

Kenny F Chou; H Steven Colburn; Kamal Sen
Boston University

Those who suffer from hearing-impairment lose the ability to focus on a single target in the presence of competing sounds. Many computational auditory scene analysis (CASA) algorithms for sound segregation have been explored to address this issue. The goal of many CASA algorithms is to estimate the “ideal binary mask”, which attenuates all non-target dominated time-frequency spectrogram tiles. These algorithms assume “oracle knowledge” and have little biological relevance. In this work, we present a physiology-based algorithm for separating spatially distributed sound sources via estimating a time-frequency mask. Our algorithm first encodes the sound mixture into spike trains, and separates its components according to their spatial locations, using a model of spatially tuned neurons in the avian midbrain. The spike train corresponding to the target of interest is then read-out by a cortical network model, based on the songbird auditory cortex analog. Finally, the output cortical spike trains are used to construct a time-frequency mask to isolate the target within a mixture. Our algorithm does not require training, retains binaural information, and can produce sounds with good intelligibility. This model can be used to study neural processes involved in sound segregation, and its ideas can potentially be used to improve the performance of hearing assistive devices (e.g., hearing aids and cochlear implants), as well as speech recognition technology, for auditory scene analysis.

Development III

PS 644

Notch-mediated Polarity Decisions in the Zebrafish’s Lateral Line

Adrian Jacobo¹; Agnik Dasgupta¹; Anna Erzberger¹; Kimberly Siletti²; A.J. Hudspeth¹
¹*Rockefeller University*; ²*Karolinska Institutet*

The lateral line of the zebrafish and other aquatic vertebrates is a specialized organ formed by a series of small patches of mechanosensory epithelium called

neuromasts. Each neuromast contains equal numbers of hair cells of two opposite polarities, half of them sensitive to caudad water movement and half to rostrad flow. The core planar-cell-polarity (PCP) proteins, which in many systems orient structures such as cilia and cuticular hairs, are asymmetrically enriched at the apical surfaces of hair cells. Vangl2—one of the core PCP proteins—always occurs at the posterior edge of an apical surface, regardless of the polarity of the hair bundle. Therefore, half of the hair cells in a neuromast have their bundles opposite the direction determined by the core PCP proteins, a phenomenon termed polarity reversal.

Because optimal sensitivity to directional stimuli requires that hair cells exhibit precise patterns of orientation, polarity reversal is essential to the organization of neuromasts and of the vestibular organs of all vertebrates, including mammals. It has recently been shown that *Emx2*, a homeobox transcription factor, is involved in the regulation of polarity reversals. *Emx2* is expressed specifically in a subpopulation of hair cells that show reversal of hair-bundle polarity, and *Emx2* overexpression or knockout mutant animals display uniformly polarized hair bundles. In the neuromast *Emx2* is expressed only by cells of caudad sensitivity.

Hair cells in the neuromast develop in pairs from a transit amplifying cell. After division of the progenitor, one of the hair cells begins to express *Emx2* and later develops a hair bundle of caudad sensitivity. Its sister cell remains *Emx2*-negative and forms a bundle of rostrad sensitivity. The mechanism of polarity reversal reliably produces a pair of hair cells of opposite polarity, but how the *Emx2* identity of the cells is specified after division has remained a mystery. In this work we show that knockout or overexpression of Notch produces polarity reversal phenotypes like the ones observed in *Emx2* mutants. Then, using a combination of mathematical modeling and experimental perturbations we demonstrate that the binary fate decision underlying polarity patterning is regulated by Notch mediated lateral inhibition.

PS 645

The Role of Wnt7b in Cochlear Morphogenesis and Hair Cell Planar Cell Polarity

Andre Landin Malt; Arielle Hogan; Maxwell Madani; Yuqiong Zheng; Xiaowei Lu
University of Virginia School of Medicine

The orientation and shape of the stereociliary hair bundle atop cochlear hair cells form V-shaped hair bundles that are uniformly oriented across the organ of Corti (OC). This process is controlled by the coordinated action of intercellular planar cell polarity (PCP) signaling

and a hair cell-intrinsic polarity machinery. However, while Wnt signaling has been implicated in otic development and hair cell differentiation, whether and how hair cell PCP is regulated by specific Wnt signals during development remain unknown.

There are a total of 19 Wnt ligands, many of which are expressed in the developing cochlea. Among them, we found that Wnt7b is dynamically expressed in the OC and adjacent cochlear epithelium during cochlear outgrowth and hair bundle morphogenesis. To determine whether Wnt7b plays a role in the establishment of hair cell PCP, we deleted Wnt7b in the cochlear epithelium using *Emx2Cre* and *Wnt7bflox* alleles. Analysis of Wnt7b conditional knockout (*Wnt7bcKO*) revealed mild hair bundle orientation and shape defects. Moreover, cochlear length was reduced, accompanied by four rows of outer hair cells in the apical turn of the cochlea. These findings suggest that Wnt7b regulates the establishment of hair cell PCP in the cochlea.

To further understand how Wnt7b mediates cochlear extension and hair cell PCP, experiments are underway to examine the asymmetric localization of core PCP proteins, including *Vangl2* and *Dishevelled2*. Furthermore, components of the cell-intrinsic PCP effectors, which consist of *Par3*, *Par6*, *Rac-PAK*, *Cdc42-aPKC* and *LGN/Gai/Daple* modules, have planar polarized distribution in the OC and together control hair bundle polarity independent of the intercellular PCP pathway. Therefore, we will also examine the localization of cell-intrinsic PCP effectors in *Wnt7bcKO* cochleae. These experiments will shed light on the specific role of Wnt7b in cochlear morphogenesis and hair cell PCP.

PS 646

The role of Hedgehog receptor Cdo in controlling cochlear hair cell formation

Elaine Y.M. Wong^{1,2,3}, Marcus Atlas^{1,4} and Rodney Dilley^{1,4}

¹*Ear Science Institute Australia*; ²*School of Biomedical Sciences, The University of Hong Kong*; ³*Curtin University*; ⁴*Ear Sciences Centre, The University of Western Australia*

Cdo (Cell adhesion molecule-related, down-regulated by oncogenes) is a novel receptor of the Hedgehog (Hh) pathway. Mutations in Cdo cause holoprosencephaly, a human congenital anomaly defined by forebrain midline defects prominently associated with diminished Hedgehog pathway activity. Cdo functions as a receptor of the Hh signalling and feedback network. Cdo enhances Shh signalling by acting as co-receptors with *Ptch1*, or via regulation of Gli transcription factors. A proper balance of Gli repressor and activators is required to mediate Hh

signalling during inner ear morphogenesis.

Cdo homozygous knockout mice have profound hearing loss. However, the role of Cdo in inner ear development is still unknown. To understand the function of Cdo receptor in the modulation of Hh signaling in mammalian inner ear development, we present the differential expression pattern of Cdo in the developing mouse inner ear. We found that the expression of Cdo at E12.5 marks the prospective organ of Corti, but by E16 Cdo is down-regulated in hair cells and becomes restricted to supporting cells, suggest that Cdo may have distinct roles in molecular pathways that direct cells towards different cell fates in cochlea. Besides, the otic vesicle-derived inner ear structures are under-developed, with reduced proliferation and premature cell cycle exit during prosensory specification and ectopic hair cells formation in the Cdo mutants. It is possible that Cdo in Hh signaling is required for inhibiting cells from differentiating into hair cells and specifying progenitor cells to generate the distinctly fated cell populations in the inner ear.

PS 647

The key transcription factor expression in the developing vestibular and auditory sensory organs: a comprehensive comparison of spatial and temporal patterns

Shaofeng Liu¹; Yan Chen²; **Wenyan Li**³; Huawei Li³
¹*Department of Otolaryngology-Head and Neck Surgery, Yijisan Hospital of Wanan Medical College*; ²*ENT Institute and Otorhinolaryngology Department of Affiliated Eye and ENT Hospital, State Key Laboratory of Medical Neurobiology, Fudan University*; ³*ENT Institute and Otorhinolaryngology Department, Affiliated Eye and ENT Hospital, State Key Laboratory of Medical Neurobiology, Fudan University, 2 NHC Key Laboratory of Hearing Medicine (Fudan University)*,

Inner ear formation requires that a series of cell fate decisions and morphogenetic events occur in a precise temporal and spatial pattern. Previous studies have shown that transcription factors, including *Pax2*, *Sox2*, and *Prox1*, play important roles during the inner ear development. However, the temporospatial expression patterns among these transcription factors are poorly understood. In current study, we present a comprehensive description of the temporal and spatial expression profiles of *Pax2*, *Sox2*, and *Prox1* during auditory and vestibular sensory organ development in mice. Using immunohistochemical analyses, we show that *Sox2* and *Pax2* are both expressed in the prosensory cells (the developing hair cells), but *Sox2* is later restricted to only the supporting cells of the organ of Corti. In the vestibular sensory organ, however, *Pax2* expression is localized in hair cells at postnatal day 7, while *Sox2*

is still expressed in both the hair cells and supporting cells at that time. Prox1 was transiently expressed in the presumptive hair cells and developing supporting cells, and lower Prox1 expression was observed in the vestibular sensory organ compared to the organ of Corti. The different expression patterns of these transcription factors in the developing auditory and vestibular sensory organs suggest that they play different roles in the development of the sensory epithelia and might help to shape the respective sensory structures.

PS 648

Expression of Norrin and Frizzled 4 in the Cochlea

Yushi Hayashi; Albert Edge

Department of Otolaryngology, Harvard Medical School

Introduction

Norrie disease is an X-linked recessive neurological syndrome whose symptoms include bilateral blindness with a prominent intraocular mass (pseudoglioma) and avascularity of the retina, mental retardation, and progressive sensorineural hearing loss beginning in adolescence. The disease is caused by mutations in the Ndp gene, which codes for the secreted protein, Norrin. Frizzled 4 (Fzd4) has been identified as the receptor for Norrin. Ndp or Fzd4 mutations result in vascular defects in the retina and cochlea, including enlarged vessels in the stria vascularis with vascular degeneration. Studies in both the retina and the cochlea have concluded that the neurological deficits associated with the disease are caused by this underlying vascular defect. To further elucidate the pathology of Norrie disease-related hearing loss, we looked at the sites and timing of expression of mRNA and protein of both receptor and ligand in the mammalian cochlea.

Methods

We harvested the mouse cochlea at E14, E18, P3 and P28 and performed immunohistochemistry for Norrin and in situ hybridization for Ndp mRNA and Fzd4 mRNA on whole mounts or cryosections.

Results

At E14, Norrin was expressed throughout the cochlear duct. The expression pattern changed dramatically between embryonic and adult stages. Upon formation of the organ of Corti (E18), Norrin expression was found primarily in the greater epithelial ridge, and this pattern of expression continued into postnatal (P3 and P28) stages. Norrin expression was not observed in the lateral wall at E18, but appeared in basal cells at P3, and in the spiral ligament at P28. Fzd4 was expressed in supporting cells and hair cells at E18 and at increasing levels at P3 and P28, with greater hair cell than supporting cell expression as the ear matured. Fzd4 was also expressed in endothelial cells in the lateral wall.

Conclusions

Expression of Fzd4 in hair cells, supporting cells and endothelial cells is likely to confer the ability to receive the signal from secreted Norrin. Immunohistochemical results for Norrin would be consistent with greater epithelial ridge cells providing Norrin to hair cells and supporting cells and the lateral wall providing the protein to endothelial cells.

PS 649

Wnt/ β -catenin Interacts with the FGF Pathway to Control Neuromast Development in Zebrafish Lateral Line

Dongmei Tang¹; Yingzi He¹; Huawei Li²

*¹Otorhinolaryngology Department of Affiliated Eye and ENT Hospital; ²ENT Institute and Otorhinolaryngology Department, Affiliated Eye and ENT Hospital, State Key Laboratory of Medical Neurobiology, Fudan University
²NHC Key Laboratory of Hearing Medicine (Fudan University),*

Control of cell proliferation is a critical process during the sensory organs development. While the canonical Wnt/ β -catenin signaling pathway plays a critical role in regulating cell proliferation and differentiation; the exact molecular mechanisms induced by Wnt/ β -catenin activation that mediate these changes in the development of sensory organs remains poorly defined. In this study, we use the zebrafish mechanosensory organ-lateral line neuromast to understand how cell proliferation is regulated during development. Our results showed that overactivation of the Wnt pathway promoted the neuromast proliferation, resulting in an increased expression of the specific FGF target genes and ultimately leading to significantly more proliferating cells and differentiated cells, whereas suppression of the Wnt signaling inhibited the cell proliferation and differentiation in neuromast and rendered a significant reduction of FGF markers expression. Meanwhile, blockade of FGF signaling using pharmacological inhibitor or transgenic line disrupted the cell proliferation and differentiation in the neuromast. Moreover, the proliferation induced by Wnt activation was totally inhibited after FGF inhibition. Conversely, overactivation of the FGF pathway by basic fibroblast growth factor (bFGF) treatment resulted in enhanced proliferation and increased hair cell formation during developmental stage similarly to Wnt activation, whereas no significant change in Wnt target gene expression were detected after over-activating FGF. Furthermore, bFGF treatment led to a partial rescue of neuromast defects in the absence of Wnt activity. In summary, these data suggest that FGF acts downstream of Wnt signaling during the periods of proliferation and hair cell differentiation stage and that the balance of the activation of Wnt and FGF signaling pathways is essential for proper neuromast development.

PS 650

Wnt-Fzd Signaling is Required for Type II Spiral Ganglion Neuron Peripheral Axon Turning

Satish Ghimire; Michael Deans
University of Utah

We previously reported that the core Planar Cell Polarity (PCP) protein VANGL2 acts non-cell autonomously to guide peripheral axons of Type II spiral ganglion neurons (SGN) during outer hair cell innervation. In *Vangl2* mutants, Type II fibers turn incorrectly towards the cochlear apex rather than towards the base. In contrast, mice lacking the Wnt receptor and core PCP protein FZD3 have a significantly less penetrant, milder turning phenotype. Since VANGL2 and FZD3 form an intercellular signaling complex that guides hair cell PCP, an outstanding question is whether FZDs are similarly required for axon turning or if VANGL2 functions independently in this context.

During PCP signaling VANGL2 and FZD3 are enriched on opposite sides of cells and oppose each other across the intercellular space between neighboring cells. We previously demonstrated that VANGL2 is asymmetrically localized on the basolateral membrane of organ of Corti supporting cells facing the cochlear apex. To determine whether FZD3 has a complementary distribution we evaluated 3XHA-Fzd3 transgenic mice in which 3XHA tagged protein expression can be sparsely induced by Cre recombinase, and observed 3XHA-FZD3 opposite of VANGL2, and facing the cochlear base. Since asymmetric protein distribution is thought to be established by WNT signaling gradients we evaluated Type II SGN turning in *Wnt5a* KOs, and *Pax2-Cre;Porcn* CKOs in which WNT release is blocked. While turning errors do not occur in *Wnt5a* KOs, hypomorphic canonical-WNT signaling phenotypes and axon turning errors were frequent in *Porcn* CKOs. These turning errors correlated with the loss of asymmetric VANGL2 protein distribution, suggesting that WNT-dependent protein localization precedes axon turning.

One explanation for the weak *Fzd3* phenotype is genetic compensation by other *Fzd* genes. Consistent with this hypothesis, *Fzd3* and *Fzd6* have similar patterns of expression and more significant, in *Fzd3;Fzd6* DKOs the majority of fibers (>50%) turn incorrectly towards the cochlear apex. In addition, *Fzd3* interacts genetically with *Vangl2* further demonstrating that Type II axon turning requires intercellular PCP signaling. Thus, while 35% of peripheral axons turn incorrectly in *Pax2-Cre;Vangl2* CKOs, turning is random when the CKO is evaluated on a *Fzd3* KO background. Based upon these results we propose that non-canonical WNT signaling leads to the polarized distribution of PCP proteins and intercellular PCP signaling between organ of Corti supporting cells. Formation of this PCP axis is required for the non-cell

autonomous function of VANGL2 to guide incoming Type II growth cones and bias their turning towards the cochlear base.

PS 651

GPSM2-GNAI specify the tallest stereocilia and define row identity in the hair bundle

Abby Tadenev¹; Anil Akturk¹; Nick Devanney¹; Pranav Dinesh Mathur²; Anna Clark²; Jun Yang²; **Basile Tarchini**¹

¹The Jackson Laboratory; ²University of Utah

The transduction compartment of inner ear hair cells, the hair bundle, is composed of stereocilia rows of graded height, a property essential for sensory function that remains poorly understood at the molecular level. We previously showed that GPSM2-GNAI are enriched at stereocilia distal tips, and required for their postnatal elongation and bundle morphogenesis - two characteristics shared with MYO15 (short isoform), WHRN and EPS8 proteins. Here we first performed a comprehensive genetic analysis of the mouse auditory epithelium to show that GPSM2-GNAI and MYO15-WHRN operate in series within the same pathway. To understand how these functionally disparate proteins act as an obligate complex, we then systematically analyzed their distribution in normal and mutant bundles over time. We discovered that WHRN-GPSM2-GNAI is an extra module recruited by and added to a pre-existing MYO15-EPS8 stereocilia tip complex. This enlarged complex is only present in the first, tallest row, and is required to stabilize larger amounts of MYO15-EPS8 than in shorter rows, which harbor MYO15-EPS8 only. In absence of GPSM2 or GNAI function, including in the epistatic *Myo15* and *Whrn* mutants, bundles retain an embryonic-like organization that coincides with generic stereocilia at the molecular level. We propose that GPSM2-GNAI confer on the first row its unique tallest identity and participate in generating differential row identity across the hair bundle.

PS 652

The Role of JAG1-Mediated Notch Signaling in Maturation of the Cochlea

Felicia Gilels; Jun Wang; Amy E. Kiernan
University of Rochester Medical School

The Notch signaling pathway plays multiple essential roles in the embryonic development of the sensory regions of the inner ear. Initially, Notch is required for establishing the sensory progenitors via the Jagged1 (JAG1) ligand. Subsequently, the Notch pathway is used again, via the Delta-like1 (DLL1) and Jagged2 (JAG2) ligands, in a process called lateral inhibition, which helps determine which cells will differentiate as hair cells, and

which as supporting cells. After birth, when the sensory regions are still immature, it is unclear whether Notch plays a role in the maturation or maintenance of the sensory regions. Interestingly, the Notch ligand JAG1, unlike the other ligands, becomes localized to supporting cells during embryonic sensory differentiation and continues to be expressed in supporting cells postnatally and into adulthood. To investigate the role of JAG1 in the postnatal sensory regions, we deleted JAG1 by crossing a conditional allele of *Jag1* (*Jag1^{fl/fl}*) to an inducible Cre allele (*Sox2CreER*) expressed in the sensory regions. To achieve deletion, we delivered tamoxifen at postnatal days (P)0 and P1, via intraperitoneal injection. We observed significant downregulation of JAG1 protein by P6 in all cochlea turns, indicating widespread deletion. To determine the effects of deletion of JAG1 in the cochlea, we assessed cochlear function by measuring auditory brainstem response (ABR) and distortion product otoacoustic emissions (DPOAE) thresholds across different frequencies. Results of these studies showed that loss of JAG1 caused significantly raised ABR thresholds across all frequencies. Interestingly, DPOAE thresholds were not affected at most frequencies, indicating that the main effects of JAG1 deletion occur within the inner hair cell pathway. Morphological analysis of the cochlea in plastic sections did not reveal any consistent cellular loss or cell fate changes, and the structure of the JAG1-deficient cochlea resembled controls. Synaptic analyses revealed only a mild decrease in synaptic puncta at one frequency, indicating synaptic defects were unlikely to account for the hearing deficits. To further understand the molecular consequences of JAG1 deletion, we undertook an RNA-seq analysis at P6. Results showed 411 genes were significantly upregulated while 137 were significantly downregulated. Pathway analyses revealed that Notch signaling, axonal guidance signaling, glutamate receptor signaling, and Rho family GTPases were the top pathways affected by loss of JAG1. Our results indicate that JAG1 plays an essential role in the development of hearing. A further understanding of postnatal Notch signaling will reveal important insights into cochlear maturation.

PS 653

Proteostasis is a prerequisite for cell polarity and is crucial to cochlear development and function

Stephen Freeman; Susana Mateo-sanchez; Ronald Pouyo; Pierre-bernard Vanlerberghe; Kevin Hanon; Giovanni Morelli; Laura Van Hees; Sophie Laguesse; Alain Chariot; Laurent Nguyen; Laurence Delacroix;
Brigitte Malgrange
University of Liege

Cell identity and function are reliant upon the polarized organisation of cellular components. In epithelia, this is best exemplified by the exquisite intrinsic polarity

displayed at the apical surface of mechanosensory hair cells of the auditory epithelium, which is instrumental for efficient sound perception. Generating this intrinsic polarity requires the regionalized enrichment of the polarity proteins LGN, GNAI3, and aPKC at the apical surface. We report here that normal proteostasis guarantees the proper localization of these molecules. We show that depletion of Elp3, a member of the Elongator complex, or chemical inhibition of proteasome function causes the accumulation of misfolded and aggregated proteins in the apical region of cochlear hair cells. These protein aggregates cause a local slowdown of microtubular trafficking and disrupt the compartmentalization and enrichment of intrinsic polarity proteins, both of which can be restored upon alleviation of protein misfolding using the chemical chaperone 4-phenylbutyric acid. Taken together, our study reveals an essential role for maintenance of proteostasis during the establishment of cell intrinsic polarity.

PS 654

Actin Severing Proteins are Necessary for Auditory Hair Cell Bundle Patterning and Maturation

Jamis McGrath; Benjamin Perrin
Indiana University-Purdue University Indianapolis

Mammalian auditory hair cells have V-shaped bundles of stereocilia precisely oriented such that they are deflected towards their vertex by sound-induced vibrations. Bundle patterning is critical to hair cell function and depends on several factors. The formation of a lateral apical domain devoid of stereocilia positions the bundle toward the medial side of the cell. The kinocilium, which is linked to the bundle, must then be pulled by associated microtubules toward the lateral wall of the cell. This drags the bundle by its vertex, resulting in its characteristic chevron shape. The microtubules that position the kinocilium interact with the lateral wall and apical domain, which include networks of cortical actin. The factors that mediate the likely interaction between the microtubule and actin networks are not fully defined. Here we show actin depolymerizing factor (ADF) and cofilin-1 (Cfl1), which efficiently sever actin filaments, contribute to stereocilia bundle patterning by remodeling actin to allow normal interaction with microtubules. Single ADF or Cfl1 knockout hair cells have mild defects in bundle morphology compared to double knockouts, which have severely dysmorphic bundles. ADF null hair cells heterozygous for cofilin knockout, termed cofilin monoalleles, show many of the same phenotypes as knockouts but have better cell survival. In comparison, bundle patterning is less affected in ADF monoallele mice. Mutant hair cells have a range of phenotypes. In many examples, the kinocilium is improperly positioned. Correspondingly, bundles have abnormal morphologies including being circular, flat, inverted or fragmented.

Actin filaments inappropriately accumulated in ADF/Cfl1 knockout cells, often forming a thick ring at the cell periphery. Kinocilia-associated microtubules in these cells were also disorganized, suggesting their regulation depends on interactions with actin. Together, these data suggest actin filaments at the cell cortex are pruned by ADF and cofilin-1 to permit a microtubule-based mechanism to polarize hair cell stereocilia bundles along the cochlear medial-lateral axis.

PS 655

Characterizing the Role of Sall1 in Development of the Mouse Cochlea

Alejandro Anaya-Rocha¹; Michael C. Kelly²; Elizabeth C. Driver¹; Matthew Kelley³

¹Laboratory of Cochlear Development, National Institute on Deafness and Other Communication Disorders, National Institutes of Health; ²Single Cell Analysis Facility, National Cancer Institute, National Institutes of Health; ³NIDCD

Townes-Brocks Syndrome (TBS) is a genetic disorder caused by a mutation of the Spalt Like Transcription Factor 1 (Sall1) gene. The Sall1 gene encodes a zinc finger transcriptional repressor that is involved in the development of many organs and tissues. TBS is characterized by several bodily malformations including abnormalities of the digits, kidneys, and genitals, and hearing impairment. Hearing loss is predominately sensorineural, with high frequencies affected more than low frequencies, and is slowly progressive. However, the cause of the hearing loss in TBS has not been examined in detail, so we sought to examine how deletion of Sall1 affects the development of the mouse cochlea. Previous single cell transcriptional profiling data from the lab has suggested that Sall1 is expressed in hair cells (HCs) and supporting cells (SCs) of the Organ of Corti at postnatal day 1 (P1). We used single molecule fluorescent in situ hybridization (smFISH) to confirm the expression of Sall1 in the inner ear at embryonic and neonatal stages. smFISH on cochlear sections obtained from embryonic day 16.5 (E16.5), P1, and P7 mice indicates Sall1 labeling in HCs and SCs, validating the single-cell RNA-seq data. Furthermore, immunohistochemistry shows SALL1 labeling in the developing sensory epithelium as early as E12.5 and persisting throughout development, until at least P7. Similarly, using a Sall1GFP knock-in reporter mouse line, we observed GFP expression in the pro-sensory domain at E14.5, and in HCs and SCs at E16.5 and P0. We used this Sall1GFPnull allele to examine whether Sall1 loss-of-function results in a cochlear phenotype. Sall1GFP/GFPcochleae appeared grossly normal, but examination of known HC and SC markers suggested there is a slight delay in maturation at E18.5. Since Sall1 mutations that

lead to TBS are thought to act as dominant-negatives, we are also using a Sall1-truncating dominant-negative allele, Sall1ΔZn, which mimics a mutation that causes TBS. Analysis of these mice should allow us to observe a more representative phenotype of the human disorder. Sall1ΔZn heterozygous mice have been shown to have high-frequency hearing loss, and we will examine both Sall1ΔZn/+ and Sall1ΔZn/ΔZn cochleae to determine the cause of the hearing deficit. Finally, we will use ChIP-seq to identify DNA binding targets of SALL1 in the cochlea. These studies will add to our understanding of the role of Sall1 in development of the mouse inner ear, and to how truncated SALL1 contributes to the hearing loss in individuals with TBS.

PS 656

Increased Notch signaling induces proliferation in the neonatal mouse cochlea

Luyi Zhou; Melissa McGovern; Michelle R. Randle; Brandon C. Cox

Southern Illinois University School of Medicine

Background: Previous studies have shown that overexpression of the Notch1 intracellular domain (N1ICD) in the embryonic cochlea results in the formation of ectopic sensory patches in non-sensory regions. This phenotype is restricted to the early embryonic stage, and was not observed when N1ICD was overexpressed after embryonic day (E) 14.5. However, using a different mouse model, our lab has recently observed ectopic hair cells (HCs) when N1ICD expression is increased in all non-hair cells at birth. In this study, we further investigated this phenotype.

Methods: Sox10rtTA::TetO-N1ICD::TetO-LacZ mice, as well as littermate controls lacking the TetO-N1ICD allele, were administered doxycycline in the diet to nursing mothers from postnatal day (P) 0 to P7 and doxycycline was injected in pups at P1. Mitotic tracer BrdU was injected twice a day from P3 to P6. Cochleae were collected at P7 and immunostained with myosin VIIa, Sox2, and BrdU.

Results: Cochlea with N1ICD overexpression had a disorganized organ of Corti with indistinguishable inner and outer HCs, but no change in HC numbers. However, we observed many ectopic HCs medial to the organ of Corti, among the spiral ganglion axons. These ectopic HCs lacked terminal HC markers, but contained presynaptic ribbon synapses and immature stereocilia bundles. Interestingly, in Sox10rtTA::TetO-LacZ control mice, we also observed some ectopic HCs. This suggests that Sox10 haploinsufficiency could contribute to the observed ectopic HC formation. Additionally, in the cochlea of Sox10rtTA::TetO-N1ICD::TetO-LacZ

mice, there was expanded expression of Sox2 medial and lateral to the organ of Corti, consistent with the location of widespread proliferation as indicated by the mitotic tracer BrdU. Unfortunately, we could not further investigate the impact of this mouse model on hearing because Sox10rtTA:TetO-N1ICD::TetO-LacZ mice had massive weight loss and died between P9 and P11. Further analysis indicated that these mice have a shorter small and large intestine with a thinner intestinal wall and gas trapped within the intestine. These intestinal abnormalities likely interfere with nutrition absorption and lead to fatality.

Conclusions: Our results indicate that increased Notch signaling at birth induces widespread proliferation and combined with Sox10 haploinsufficiency, induces ectopic HC formation in non-sensory region of the neonatal cochlea. Current investigation is underway to further characterize the Sox2 expansion and excessive proliferation, as well as elucidate the individual role of increased Notch signaling and Sox10 haploinsufficiency in the observed phenotype.

Funding: DOD W81XWH-15-1-0475.

PS 657

Conditional Knockout of p27Kip1 from Cochlear Hair Cells results in the Partial Conversion of Inner Hair Cells to an Outer Hair Cell like fate

Anshuman Singh; Laura House; Bradley J. Walters
UMMC

Previous studies demonstrate a well-established role for p27Kip1, the protein product of the Cdkn1b gene, as a tumor suppressor protein that inhibits CDK-cyclin complexes thereby arresting cells in G1 phase of the cell cycle. Similarly, it has been shown that p27Kip1 is expressed during cochlear development and promotes the quiescence of supporting cells and hair cells. More recently, it has been shown that the deletion of p27Kip1 can enhance Atoh1 mediated differentiation of supporting cells into hair cells via a cell cycle independent mechanism. In addition, transcriptomic profiling of inner and outer hair cells (IHCs and OHCs) revealed that Cdkn1b transcripts are approximately 8 fold more enriched in IHCs than OHCs. Combined, these data suggest that p27Kip1 may contribute to the differentiation of IHCs and OHCs, and that its absence may facilitate OHC differentiation. To test this, we conditionally deleted Cdkn1b by breeding the p27Kip1 floxed mouse line with either Atoh1CreER or OtoferlinCreER lines and inducing with tamoxifen (75 mg/kg, i.p.) at postnatal days (P) 0-1 or P6-7, respectively. The mice were sacrificed at P21 and cochleae were fixed and either immunostained or prepared for scanning electron microscopy.

Immunostaining for several proteins known to be enriched in either OHCs (e.g. prestin and oncomodulin) or IHCs (e.g. VGLUT3) revealed the upregulation of several OHC proteins and the downregulation of IHC proteins in p27Kip1-depleted IHCs. Interestingly, neuroplastin, which is enriched in the stereocilia of OHCs did not appear to be upregulated in p27Kip1-depleted IHCs, suggesting that the hair bundle may remain IHC-like in this model. This suggests that p27Kip1 deletion may result in an intermediate conversion of IHCs to OHC-like cells. Current studies are underway to assess the extent to which p27Kip1-depleted IHCs resemble OHCs using SEM to assess bundle morphology and RNA-seq to directly compare transcriptomic profiles. In addition, we are testing p27Kip1 deletion at earlier stages in development and developing a model to ectopically express p27Kip1 in OHCs.

PS 658

Lrrn1 Regulates Medial Boundary Formation in the Mouse Cochlear Epithelium

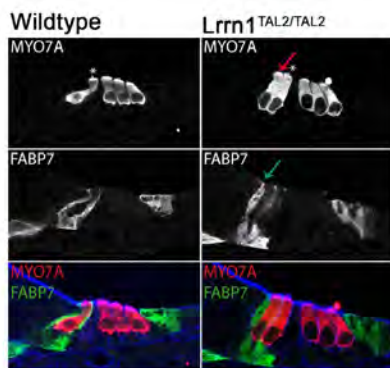
Helen Maunsell¹; Kathryn Ellis²; Elizabeth C. Driver¹; Matthew Kelley³

¹Laboratory of Cochlear Development, National Institute on Deafness and Other Communication Disorders, National Institutes of Health; ²Decibel Therapeutics; ³NIDCD

Many intersecting developmental pathways contribute to the distinct spatiotemporal cell patterning of the organ of Corti, the sensory epithelium of the cochlea. Among these is the canonical Notch signaling pathway, which is important for early medial-lateral boundary formation, and subsequent differentiation of sensory hair cells and neighboring supporting cells through lateral inhibition. We are investigating the role of a potential Notch interactor, leucine rich repeat protein 1, neuronal (Lrrn1), in the developing mouse cochlea. Lrrn1 has been shown to act downstream of the Notch modifier gene Lfng during chick midbrain-hindbrain boundary formation, and single-cell RNA sequencing data indicates that Lrrn1 is expressed by inner hair cells (IHCs) and inner phalangeal cells (IPhCs) in the neonatal mouse cochlea. In situ hybridization data confirmed the Lrrn1 expression pattern in neonates and also demonstrated a similar medial expression pattern at embryonic time points. Fate mapping using transgenic Lrrn1CreER; RosatdTomat mice indicates that Lrrn1 is expressed as early as E12.5, primarily in progenitors of IHCs, IPhCs, and border cells.

To assess the function of Lrrn1 in cochlear development, we generated Lrrn1 mutant mice using TALEN-mediated mutagenesis. While extra IHCs are occasionally observed in wild-type cochleae, we find that cochleae

of *Lrrn1* mutants have significantly more extra IHCs and associated IPhCs located medial to the endogenous row of IHCs compared to wild-type littermates. A similar phenotype can result from disrupted Notch signaling during early cochlear development. Since both IHCs and IPhCs are duplicated, we hypothesize that *Lrrn1* acts to regulate the boundary between sensory and non-sensory epithelium. Future experiments will examine whether inhibition of Notch enhances the *Lrrn1* phenotype by reducing Notch signaling in a *Lrrn1* mutant background, either by pharmacological inhibition of Notch in vitro, or genetic removal of one copy of *Notch1*. We will also use a cell-based assay to investigate if *LRRN1* modulates Notch signaling in Notch-sending (IHC) or Notch-receiving (non-sensory) cell types and determine whether *Lrrn1* deletion affects expression of Notch ligands or targets. We have found synaptic connections on extra IHCs in postnatal *Lrrn1* mutant cochleae, but preliminary results show that hearing is mostly unaltered in *Lrrn1* mutants. This project reveals a role for *Lrrn1* in mouse cochlear development and increases our understanding of the molecular signals that regulate mammalian auditory cell fate.



High magnification confocal images showing organ of Corti in transverse sections of basal cochleae from wildtype and *Lrrn1*^{TAL2/TAL2} mutant mice at P1. IHCs are labeled with anti-MYO7a (red) and inner phalangeal cells (IPhCs) are labeled with anti-FABP7 (green). F-Actin is labeled with phalloidin (blue). Asterisk indicates endogenous IHC. Green and red arrows respectively indicate extra IPhC and extra IHC in *Lrrn1*^{TAL2/TAL2} mutant.

PS 659

Expression of Class III Semaphorins and their Receptors in the Developing Chicken Inner Ear

M. Katie Scott; Jia Yue; Deborah J. Biesemeier; Joo Won Lee; **Donna M. Fekete**
Purdue University

Published work from our lab suggests that *Sema3D* and *Nrp2* may play a role during development of the basilar papilla (BP), the avian homolog of the mammalian organ of Corti. Class III Semaphorins (*Sema*) secreted ligands are most commonly known for their repulsive effects on neurites expressing Neuropilin (*Nrp*) and/or Plexin (*Plxn*) membrane-bound receptors. There

is, however, a growing body of literature supporting that *Sema* signaling also has alternative roles in development, such as boundary formation and vasculogenesis.

Using in situ hybridization and immunohistochemistry, we examined the expression of *Sema3D*, *Sema3F*, *Nrp1*, *Nrp2*, and *PlxnA1* in horizontal cross sections of the BP and vestibular organs of the inner ear in the chicken embryo at ages ranging from embryonic (E) day 5 to E10. The resulting expression patterns are consistent with several different functions for *Sema* signaling that extend beyond axon repulsion.

Sema3D expression flanks the sensory tissue in the cristae and the saccular macula (SM) on E5-E8. This localization could serve to repel the peripheral neurites of *Nrp2*- and *PlxnA1*-expressing neurons of the vestibular ganglion, thereby channeling them into the sensory domains. Subsequently, the expression of *Sema* signaling genes in the sensory hair cells of the BP, cristae, SM, and utricular macula on E8-E10 suggests that this signaling pathway could influence synaptogenesis. In the nonsensory epithelium lining the wall of the cochlear duct, *Sema3D* expression is found immediately adjacent to *Nrp1* and *PlxnA1*. This suggests a potential role in forming or maintaining a boundary between two nonsensory analgen that will become the hyaline cells and the tegmentum vasculosum. In the periotic mesenchyme, *Nrp1* colocalizes with tissue rich in capillaries while *Sema3D* immediately flanks this *Nrp1*-expressing tissue. The juxtaposition of *Sema3D* and *Nrp1* implicates a repulsive signaling activity that would restrict endothelial cell migration to a *Sema3D*-free region. In total, these expression data suggest that *Sema* signaling may serve multiple functions in and around the developing inner ear.

PS 660

Surface Tethering and GPI-dependent Release of Alpha-tectorin are Required for the Formation and Maturation of the Tectorial Membrane, Respectively.

Dong-Kyu Kim; Ali Almishaal; **Sungjin Park**
University of Utah

The tectorial membrane (TM) is an extracellular matrix (ECM) structure that hovers over the organ of Corti. The TM is formed by cochlear supporting cells and plays important roles in frequency tuning and amplification of auditory stimuli. Its exquisite architecture and unique position in an open luminal space of the scala media suggest that there should exist a structural organizer on the cell surface to prevent the diffusion of the TM components. The established ECM layer on the cell surface is, in turn, released from TM-producing cells when the TM grows and is eventually detached from

inner sulcus. Alpha-tectorin (Tecta) is the major non-collagenous protein of the TM and plays roles in crosslinking collagens and other TM components. We show that Tecta is tethered to the surface membrane via a GPI-anchorage. Specific removal of the GPI-anchorage from Tecta in vivo leads to disorganized aggregation of collagen fibrils, which is detached from the producing cells and lacks glycoproteins. Secreted Tecta without a GPI-anchorage is not incorporated into the collagen aggregates but uptaken by CD45+ phagocytes in the stria vascularis. On the other hand, conversion of Tecta into a transmembrane protein generates a thin layer of collagen network on the supporting cells, which does not grow. Excessive collages that are not captured on the cell surface form disorganized aggregates. Our study reveals the dual roles of GPI-anchorage of Tecta in TM development: surface tethering of Tecta is required for the organization of collagen networks and GPI-dependent release of Tecta mediates the growth of the TM. The stepwise printing of a new layer to the cellular surface of the developing ECM provides a novel insight into the morphogenesis mechanism of complex ECM structures.

PS 661

Notch and Wnt Signalling Interactions in the Formation of Inner Ear Sensory Organs

Magdalena Žak¹; Vincent Plagnol²; Nicolas Daudet¹

¹University College London; ²University College London Genetics Institute, London, UK

The inner ear is composed of distinct sensory organs responsible for sound detection and the perception of balance and head movements. The mechanisms controlling the embryonic formation of these organs and the non-sensory territories that separate them remain unclear. Our recent work has shown that several of the sensory organs arise by progressive segregation from a common 'pan-sensory' domain, in which Notch signalling propagates prosensory identity by lateral induction. To further characterise the molecular signals regulating the specification and segregation of the sensory organs, we performed a high-throughput transcriptome profiling of chicken otocysts after gain- and loss-of Notch function. Our bioinformatics analyses identified a great number of genes regulated by Notch, with a significant enrichment of key elements of Wnt signalling pathway. Furthermore, our ongoing functional studies indicate that canonical β -catenin/Wnt signalling regulates neurosensory specification and the spatial pattern of Notch activity in the early otocyst. Hence, the interplay between these two major signalling pathways could be critical for the normal specification and morphogenesis of inner ear sensory organs.

PS 662

Expression of Small VCP-Interacting Protein (Svip) in the Developing Mouse Cochlea

Ryosuke Yamamoto¹; Hiroe Ohnishi¹; Masahiro Fukui²; Takayuki Nakagawa¹; Koichi Omori¹; Norio Yamamoto¹

¹Department of Otolaryngology-Head and Neck Surgery, Graduate School of Medicine, Kyoto University; ²Institute for Virus Research, Kyoto University

Background

Small p97/VCP-interacting protein (Svip) encodes a cofactor of p97 protein. p97 is a regulator of endoplasmic reticulum-associated degradation (ERAD) pathway and SVIP functions as an inhibitory cofactor of p97 (Ballar et al., 2007). SVIP has a different role as a promoter of autophagy (Wang et al., 2011). Autophagy is one of the systems to degrade abnormal protein, organelle or virus within a cell body (Mizushima et al., 2010). Similar to other organs, autophagy is required for proper auditory function in the cochlea (Fujimoto et al. 2017) or vestibular development in the mouse inner ear and adequate chicken otic development (Magarinos et al., 2017). Therefore, we decided to identify the function of Svip gene during the developing mouse cochlea. Sox2 is a necessary transcription factor for the generation of sensory regions of the inner ear and is a marker of a prosensory region at an embryonic day 13.5 (E13.5) in the developing mouse (Kiernan et al., 2005).

Methods

As a first step to elucidate the function of Svip gene, we evaluated the expression of Svip in the developing mouse inner ear using reverse transcription polymerase chain reaction (RT-PCR) and in situ hybridization. For in situ hybridization, we hybridized sense and antisense probes for Svip to frozen mid-modiolar cochlear sections from mice at various embryonic days. Sox2 expression was used to clarify the sensory epithelial region within a developing mouse cochlea. We used the adult mouse testis as a positive control for Svip probe.

Results

RT-PCR showed the expression of Svip in the developing inner ear around E 13.5. In situ hybridization demonstrated that Svip mRNA expression in a part of the Sox2 positive region of the cochlea, exclusively in the apical turn of the cochlea at E13.5. At E15.5, its expression region expanded toward the basal turn of the cochlea. Svip expression was apparent in the apex at E13.5 and might spread from the apical to basal

turns although differentiation of the prosensory domain proceeds from the basal to apical turns. Svip might have a specific role during the development of the mouse cochlea.

Conclusions

We confirmed Svip expression in a part of the Sox2 positive prosensory region of the embryonic mice cochleae. Its expression was limited to the apical turn of the cochlea at E13.5 and expanded towards the basal turn at E15.5. Svip might have a role in a prosensory region of the developing mouse.

PS 663

Linking Mitochondrial Calcium Uptake, Metabolism, and Hair-cell Synapse Formation

Hiu-Tung Wong; Alisha Beirl; Katie Kindt
National Institute on Deafness and Other Communication Disorders

Background

Sensory hair cells rely on specialized ribbon synapses to facilitate rapid and sustained vesicle release. The structural protein Ribeye is a major component of the presynaptic ribbon. Ribeye has a putative NAD(H) binding domain that has been shown in vitro to regulate Ribeye-Ribeye interactions, an effect which has not been demonstrated in vivo. However, previous work has shown that in vivo Ribeye localization to the ribbon increased when the presynaptic L-type calcium channel Cav1.3 function is blocked during synapse development. We aim to investigate how ribbon formation is affected by NAD(H) redox homeostasis, and if Cav1.3-dependent activity promotes Ribeye localization to the ribbon through NAD(H) redox homeostasis.

Methods

We examined ribbon synapse development in lateral-line hair cells, which are easily manipulated and visualized and similar in structure and innervation to mammalian type II vestibular hair cells. Using pharmacology we disrupted hair-cell calcium and NAD(H) redox homeostasis in living zebrafish larvae. We also used stable transgenic zebrafish that express localized fluorescent biosensors to visualize subcellular calcium dynamics and NAD(H) redox in hair cells during pharmacological treatments. We quantified synaptic ribbon morphology by immunofluorescence staining of Ribeye.

Result

We have found that hair-cell mitochondria, an important organelle involved in NAD(H) redox homeostasis, are often closely associated with presynaptic ribbons. We

observed that mechanical stimulation of the hair cells induced mitochondrial calcium uptake adjacent to presynaptic ribbons in developing cells. This uptake was eliminated after blocking the mitochondrial calcium uniporter (MCU) or Cav1.3 channels. Interestingly, as hair cells mature, cytosolic NAD⁺/NADH ratio decreases. In addition, Ribeye has a NAD(H)-binding domain thought to be important for Ribeye self assembly. Therefore we predicted that mitochondrial calcium uptake, could alter NAD(H) redox and Ribeye self-assembly via Ribeye's NAD(H)-binding domain. To test this, we pharmacological blocked the MCU and found that, similar to Cav1.3 block ribbon size increased during ribbon formation. To examine the relationship between Cav1.3 and MCU with NAD(H) redox we measured the NAD⁺/NADH ratio in hair cells after these pharmacological treatments. We found NAD⁺/NADH ratio increased in developing hair cells after these treatments. To confirm whether NAD(H) redox could directly regulate ribbon assembly we treated developing hair cells with exogenous NAD⁺ or NADH and found that these treatments could increase or decrease ribbon assembly respectively.

Conclusion

These results suggest that in vivo Cav1.3-dependent mitochondrial calcium uptake may control ribbon assembly through cytosolic levels of NAD⁺. This mechanism couples synaptic function to synapse formation in the hair cell through changes in cellular metabolism.

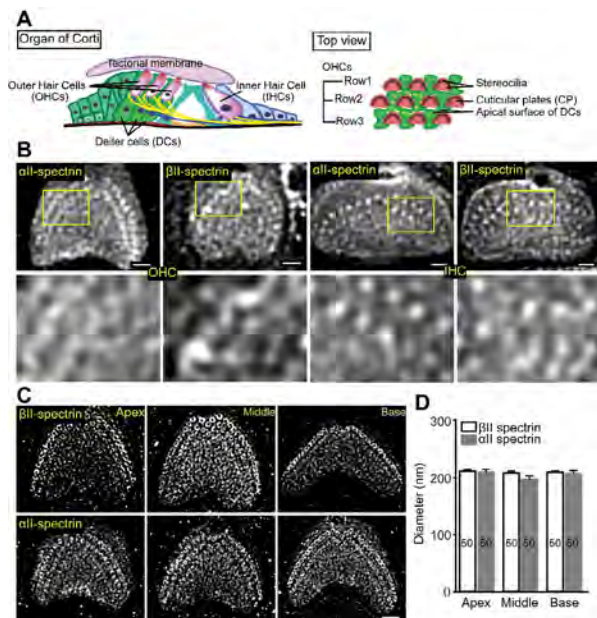
PS 664

Critical role of spectrin in hearing development and deafness

Jieyu Qi¹; Mingliang Tang¹; Weijie Zhu¹; **Renjie Chai²**
¹Southeast University; ²Key Laboratory for Developmental Genes and Human Disease, Ministry of Education, Institute of Life Sciences, Southeast University

Inner ear hair cells (HCs) detect sound through the deflection of mechanosensory stereocilia. Stereocilia are inserted into the cuticular plate of HCs by parallel actin rootlets where they convert sound-induced mechanical vibrations into electrical signals. Underpinning our ability to hear are the molecules that support these rootlets and enable them to withstand constant mechanical stresses. However, these structures remain unknown. We hypothesized that α - and β -spectrin subunits fulfill this role and investigated their structural organization in rodent HCs. We found spectrin formed ring-like structures around the base of stereocilia rootlets with super-resolution fluorescence imaging. These spectrin rings were associated with the hearing ability of mice. Further, HC-specific, β -spectrin knockout mice displayed profound deafness. Overall, our work has

identified and characterized structures of spectrin that play a crucial role in mammalian hearing development.



PS 665

Inhibitor-of-Differentiation 4 (Id4): a Dominant-Negative Helix-Loop-Helix Transcription Factor with Dose-Dependent Effects on Hair Cell Differentiation

Sara Weber; Ruth Moon; Miriam Gomez; Zoe Mann; Magdalena Žak; **Nicolas Daudet**
University College London

A complex network of basic Helix-Loop-Helix (bHLH) transcription factors regulates hair cell fate decisions during their embryonic production. The proneural bHLH Atonal-homologue 1 (Atoh1) promotes adoption of the hair cell fate. Atoh1 expression is repressed by bHLH members of the Hairy and Enhancer-of-Split (Hes) family, the major downstream effectors of Notch signalling during the lateral inhibition of hair cell formation. An additional class of dominant-negative HLH proteins, encoded by the Inhibitor of Differentiation (Id) genes 1-4, could also potentially interfere with Atoh1 and other bHLH proteins expressed in the inner ear. Among these, we found that Id4 is expressed within the prosensory domains of the developing inner ear, but does it act as a negative regulator of hair cell formation? We show that the overexpression of Id4 in the embryonic chick inner ear strongly inhibits Atoh1 expression and hair cell differentiation. However, Id4 is normally expressed in differentiating hair cells, indicating that at endogenous gene dosage, it is unlikely to interfere with Atoh1 function. Furthermore, there is no excess or premature differentiation of hair cells in the inner ear of

an Id4-deficient mouse model, even in conjunction to a pharmacological blockade of Notch activity in vitro. Whilst the precise role of Id4 remains unclear, these paradoxical findings highlight the critical importance of dosage in the bHLH proteins network at the core of hair cell fate decisions.

PS 666

Characterization of Myosin VIIA in the Cochlear and Vestibular Neurons of the Developing Mouse

Sarah Law; Molly Stout; Caroline Kernan; Haley Stronczek; Jennifer Rowsell
Saint Mary's College

Myosins are a superfamily of actin-based motor proteins that are involved in many cellular functions including transport, cell migration and growth cone motility. Myosin proteins have been found in different types of neurons including mature auditory and vestibular afferents. In order to determine whether myosins may play a role in the development of auditory and vestibular neurons, we characterized the expression of Myosin II, Myosin V and Myosin VIIA during mouse embryonic development. We used immunohistochemistry to determine the spatiotemporal expression pattern of Myosin II, Myosin V and Myosin VIIA from embryonic (E) day 9.5 to 13.5 in mice. Myosin II and V were not expressed during these embryonic ages in the auditory or vestibular neurons. Myosin VIIA was expressed in the cochleovestibular ganglion (CVG) neurons from E9.5-E12.5. The number of Myosin VIIA positive neurons decreased as development progressed. This may indicate that Myosin VIIA plays a role in an early developmental process such as delamination, migration, segregation or pathfinding of afferent nerve fibers of the CVG neurons.

PS 667

Pou3f4-Expressing Otic Mesenchyme Cells Promote Spiral Ganglion Neuron Survival

Paige Brooks; Meaghan Macrae; Katherine Rangoussis; Thomas M. Coate
Georgetown University

Nearly three in every 1,000 children in the United States are born with detectable hearing loss. Of these cases, about 80% can be accounted for by inherited genetic mutations (2017 GeneReviews), including the deafness gene DFNX2, the most common form of X-linked deafness. DFNX2 phenotypes result from mutations of the transcription factor Pou3f4, and typically include developmental malformations of the middle and inner ear, and profound lifelong hearing loss. Whereas Pou3f4 controls a wide array of genes

related to the development of the auditory system, our data indicate that Pou3f4 is also critical for maintaining auditory connectivity and hearing health into adulthood. In mouse, otic mesenchyme cells express Pou3f4 starting around E10.5 and continue to do so through adulthood. Throughout this protracted period, the Pou3f4-expressing mesenchyme cells surround the SGNs, and we have recently discovered a conspicuous and transient population of these cells that reside within the spiral ganglion. Initially following birth, SGN numbers are normal in Pou3f4 knockout mice (Pou3f4y/-) when compared with littermate controls (Pou3f4y/+). However, sometime before postnatal day 8, SGN density begins to decline in Pou3f4y/- mice with approximately 30% of SGNs ultimately lost. Overall, these data suggest that Pou3f4-positive mesenchyme cells facilitate SGN survival. To address the hypothesis that Pou3f4 directly regulates the expression of an SGN trophic factor, we are currently performing in vitro Pou3f4 Morpholino driven knock-down experiments and developing a Pou3f4 conditional knock out model. If Pou3f4 directly affects SGN survival, we expect reduced Pou3f4 to result in reduced SGNs. In ongoing experiments, we aim to identify the precise time point of Pou3f4-mediated SGN survival. Once this time point is identified, we plan to screen Pou3f4y/- and control ears to determine the genes that Pou3f4 is regulating to promote SGN survival.

PS 668

Conserved Roles for CHD7, the Chromatin Remodeler Mutated in CHARGE Syndrome, in Transcriptional Elongation of Genes Involved in Neural, Neural Crest, and Inner Ear Development

Elaine Ritter¹; Hui Yao¹; Ford Hannum²; Gilson Sanchez¹; Ethan Sperry³; Alina Saiakhova⁴; Daniel Fuentes⁵; Margot Bowen⁶; Adrienne Niederriter-Shami³; Jennifer M. Skidmore¹; Anshika Srivastava³; Laura Attardi⁶; Tomasz Swigut⁵; Joanna Wysocka⁷; Peter Scacheri⁴; Donna M. Martin⁸

¹Dept. Pediatrics, University of Michigan; ²Dept. of Biostatistics, University of Michigan; ³Dept. Human Genetics, University of Michigan; ⁴Dept. Genetics, Case Western Reserve University; ⁵Dept. Chemical and Systems Biology, Stanford University; ⁶Dept. Radiation and Cancer Biology, Stanford University; ⁷Depts. Chemical and Systems Biology, Radiation and Cancer Biology, Stanford University; ⁸Depts. Pediatrics and Human Genetics, University of Michigan

CHD7 is an ATP-dependent helicase that is critical for normal mammalian development. Heterozygous pathogenic variants in CHD7 cause multiple organ system malformations and CHARGE syndrome, which includes ocular Coloboma, Heart defects, Atresia of the choanae, Retardation of growth and development,

Genital hypoplasia and pubertal delay, and Ear abnormalities, including deafness and vestibular disorders. Central and peripheral nervous system impairment are common in CHARGE, yet the underlying mechanisms of CHD7 action in early neural and neural crest development are not well understood. Chd7Gt/+ mice exhibit dysplastic semicircular canals and mild mixed conductive-sensorineural hearing loss and are an excellent model for CHARGE syndrome. Reduced Chd7 function in the ear disrupts expression of genes involved in developmental patterning and neurogenesis. Here we explored potential roles for CHD7 in global regulation of gene transcription in the nervous system, including differentiation of stem cells toward neural epithelial progenitors, neural crest cells, and inner ear tissues. We used mouse embryonic stem cells (ESCs) null for Chd7 to study CHD7 in early neuronal development, during the transition of embryonic stem cells to neural progenitor cells (NPCs), and found that loss of Chd7 disrupts neuronal and glial differentiation without affecting proliferation or apoptosis. Transcriptome analysis via RNA-Seq on E10.5 and E12.5 otocysts from Chd7+/+ and Chd7Gt/+ mutant mouse embryos showed a length-dependent effect of Chd7 on gene transcription, with preferential effects on longer (>100 kb) genes. A milder length dependent effect was observed in heterozygous CHD7 mutation-positive human induced pluripotent stem cells (iPSCs) differentiated into neural crest cells (NCCs) when compared to isogenic patient derived iPSCs in which the variant was corrected via CRISPR/Cas9 gene editing. We also observed that genes with high CHD7 occupancy display low RNA polymerase II (Pol II) pausing and higher RNAPII throughout the gene body. Collectively, our findings support roles for CHD7 in chromatin events that regulate transcriptional elongation. Interestingly, length-dependent gene dysregulation has been described for Rett syndrome, Autism Spectrum Disorder, and Fragile X syndrome, suggesting possible links between the molecular etiologies of these disorders and CHARGE syndrome.

PS 669

Primary cilium plays differential roles during cochlear development

KyeongHye Moon¹; HongKyung Kim¹; Ji-Hyun Ma¹; Jeong-Oh Shin¹; Sun Myoung Kim²; Ping Chen²; Doris Wu³; Hyuk Wan Ko⁴; Jinwoong Bok¹

¹Yonsei University College of Medicine; ²Emory University School of Medicine; ³National Institute on Deafness and other Communication Disorders; ⁴Yonsei University College of Life Science and Biotechnology

Background

The primary cilium serves as a signaling center for several cellular pathways important for development

including Sonic hedgehog (SHH). Defects in the primary cilium are associated with a range of genetic disorders known as ciliopathies, which include hearing loss. Previous studies showed that ciliary defects resulted in a shortened cochlear duct and abnormal hair cell polarization. While the hair cell polarization defect is attributed to defective planar cell polarity (PCP) signaling, the cause for shortened cochlear duct and precise etiology of the hearing loss in ciliopathies remain unclear.

Methods

To understand the role of primary cilia in the inner ear, we analyzed three different ciliary mutants, Broad-minded (Bromi) mutant, Intestinal cell kinase (Ick) knockout (KO), and conditional knockout of *Ift88* (*Pax2-Cre*; *Ift88lox/lox*, *Ift88 cKO*). *Ift88 cKO* mutants lack the primary cilium, while Bromi and Ick mutants show abnormal morphology and length of the cilium.

Results

All three mutants exhibited shortened cochlear duct, extra rows of hair cells in the apex, premature hair cell differentiation, and decreased hair cell number. In addition, Bromi and *Ift88 cKO* developed ectopic vestibular-like hair cells in the Kölliker's organ and exhibited reversed hair cell differentiation wave. Moreover, the expression of an apical cochlear marker, *Msx1*, which requires high levels of SHH signaling, was reduced or absent. These phenotypes closely resemble those of mutants carrying defective SHH signaling. Indeed, *Ptch1* expression, which is a direct readout of SHH signaling, was compromised in the developing inner ears of the ciliary mutants. These results indicate that the major cause of cochlear phenotypes of ciliary mutants is misregulated SHH signaling. Interestingly, we observed that there is a transition from the primary cilia to the kinocilia at the onset of hair cell differentiation. Although we did not observe an obvious difference in their microstructures, there was a clear change in their ability to respond to SHH signaling. We are currently investigating how such transition contributes to mediate diverse roles of SHH signaling essential for cochlear development.

Conclusion

Taken together, our results demonstrate the complexity of ciliary mutants and the importance of the primary cilia in mediating multiple roles of SHH signaling during cochlear development.

Supported by the BK 21 PLUS Project for Medical Science, Yonsei University

PS 670

The Novel Roles of Transcription Factors *Atoh1* and *Neurod1* in Inner Ear Development

Iva Macova¹; Martina Dvorakova²; Romana Bohuslavova²; Kateryna Pysanenko³; Tetyana Chumak³; Josef Syka³; Bernd Fritsch⁴; Gabriela Pavlinkova²

¹*Institute of Biotechnology CAS, Vestec, Czechia;*

²*Institute of Biotechnology CAS;* ³*Institute of Experimental Medicine CAS;* ⁴*University of Iowa Department of Biology*

Background: Understanding the mechanism of inner ear development and its transcriptional regulation can help us in restoring hearing and balancing hearing disorder treatment. Inner ear development has been extensively studied, yet the precise transcriptional network is still unclear. In this project, we focus on the interactions of bHLH proteins and related downstream pathways. *Atoh1* is known as a necessary molecule for hair cell differentiation while *Neurod1* is important for neuroblast survival. However, their roles in other processes remain to be discovered.

Methods: Using immunostaining, in situ hybridization and dye tracing, we analyzed the inner ear phenotype of three conditional knock out mouse models with deletion of *Atoh1*, *Neurod1* and *Atoh1/Neurod1* driven by *Islet1-Cre*. We also evaluated hearing, balance and behavioral function using ABR, DPOAE, static rod and startle response tests.

Results: After conditional deletion of *Atoh1*, neither hair cells nor supporting cells were found in any part of the cochlea and innervation was lost as a result of missing neurotrophic support produced by the sensory epithelium. The *Neurod1CKO* cochlea was 40 % shorter than the control and the organ of Corti was disorganized in the apex. The mutant spiral ganglion contained only 17 % of the control number of neurons and this number was unchanged during postnatal development. The vestibular ganglion was enlarged and unlike the controls was not separated into inferior and superior parts. Innervation was totally disorganized, with the basal spiral ganglion innervating the base and the apex of cochlea and vestibular organs too; the vestibular ganglion innervating both the balance organs and the cochlea. Impaired tonotopic organization was also detected in the cochlear nucleus. These morphological changes impact hearing function. *Atoh1/Neurod1CKO* lack the sensory epithelium and nerve fibers form an unusual dense network with many knots and overshooting loops<./p>

Conclusions: Our results show that *Neurod1* is necessary for embryonic but not for postnatal survival

of spiral ganglion cells. We found its novel roles in the processes of neuroblast migration, ganglion separation and tonotopic organization. Besides being necessary for hair cell differentiation, Atoh1 could also play an important role in axon pathfinding as shown in the double mutant.

PS 671

Short Stature Homeobox 2 in Zebrafish Otic Development

Alejandra Laureano¹; Kathleen Flaherty¹; Hatem Sabaawy²; Kelvin Kwan¹

¹Rutgers University; ²Cancer Institute of New Jersey

INTRODUCTION

The Short Stature Homeobox 2 gene (SHOX2) was identified as a candidate transcription factor involved in early auditory neuron development. Zebrafish, like humans possess both orthologues of the SHOX gene family (SHOX and SHOX2), whereas mice only possess SHOX2. To better understand and recapitulate the role of SHOX2 in human inner ear development zebrafish was chosen as a model organism.

RESULTS

Zebrafish *shox2* has not been previously attributed to inner ear development. Utilizing in situ hybridization, we showed that *shox2* is dynamically expressed in many cell types during development and is present at 18 hours post fertilization (hpf) in the developing inner ear. Live cell imaging of fish harboring both *shox2* (*shox2:Gal4;UAS:mCherry*) and inner ear (*tg(pax2a:GFP)e1*) fluorescent reporters confirmed the presence of *shox2* in the otic vesicle at 18hpf. At 24hpf, fish with *shox2* (*shox2:Gal4;UAS:GFP*) and progenitor (*tgBAC(neurog1:dsRed)nl6*) reporters co-labeled cells in the developing statoacoustic ganglion. To assess the function of *shox2* in the developing inner ear, antisense morpholinos were used to reduce *shox2* transcript levels. Compared to controls, three day *shox2* morphants displayed behaviors suggestive of inner ear and neurological dysfunction which included circling, lack of avoidance behavior and spasms. To further determine the role of *shox2* in inner ear development, a *shox2* null mutation was generated using CRISPR/Cas9 and will be characterized.

DISCUSSION

The results suggest a role of *shox2* in early otic neurosensory development. We propose that *shox2* is essential for determining otic neuronal fate. Generation of *shox2* null reporter lines for cell lineage tracing will help determine whether otic cell fate is altered in the absence of *shox2*.

PS 672

Transcription factor ISLET1 regulates the development of spiral ganglion neurons

Martina Dvorakova¹; Iva Macova²; Simona Vochyanova¹; Romana Bohuslavova¹; Josef Syka³; Bernd Fritsch⁴; Gabriela Pavlinkova¹

¹Institute of Biotechnology CAS; ²Institute of Biotechnology CAS, Vestec, Czechia; ³Institute of Experimental Medicine CAS; ⁴University of Iowa Department of Biology

Background: The LIM-homeodomain transcription factor *Isl1* (ISL1) is expressed in prosensory precursors, neuroblasts, and in neurons of vestibular and spiral ganglia in the inner ear. However, the functional role of ISL1 in the development and maintenance of neurosensory cells in the inner ear is still not fully established. We generated a novel conditional deletion model of *Isl1* by using the cre-loxP system. Specifically, we used *Neurod1-cre* to eliminate floxed *Isl1*, as *NEUROD1* is essential for neuronal differentiation and survival, and negatively regulates hair cell differentiation during inner ear development.

Methods: *Neurod1-cre* was used to conditionally delete floxed *Isl1* in the ear. We used immunohistochemistry to establish morphological and cellular changes in the inner ear, specifically supporting cells, hair cells and neurons. We also studied the pattern of innervation in whole or dissected ears using lipophilic dye tracing in aldehyde fixed tissue.

Results: *Isl1*CKO mice were viable without any obvious abnormal motor activity behavior that would indicate defects in the vestibular system. Correspondingly, the vestibular organs were of normal size with hair cells and innervation indistinguishable from control littermates. The *Isl1*CKO cochlea was about 40 % shorter compared to controls. The sensory epithelium in the apex was disorganized with multiple rows of outer hair cells and inner hair cells differentiated among the outer hair cells. The disorganization of the epithelium was due to the accelerated differentiation of hair cells. The formation of the spiral ganglion of *Isl1*CKO mutants was impaired with many missing neurons, abnormal migration, and aberrant innervation. A number of misplaced spiral ganglion neurons was detected in the vestibular ganglion and in the area surrounding the cochlear nerve. The cochlear nucleus, the first integrative stage of the auditory pathway, was smaller in *Isl1*CKO mutants compared to littermate controls indicating an effect of reduced afferent input.

Conclusions: These data show that ISL1 regulates inner ear development and that its deletion causes significant

changes in both neuronal and sensory development. Accelerated hair cell differentiation indicates interactions of ISL1 and ATOH1 similar to the NEUROD1-ATOH1 interactions, providing negative feedback in hair cell maturation. Impaired migration of neurons indicates altered differentiation of neurons.

PS 673

Conditional Deletion of ISLET1 Leads to Dysfunctional Auditory Properties

Kateryna Pysanenko¹; Martina Dvorakova²; Iva Macova³; Simona Vochyanova²; Romana Bohuslavova²; Bernd Fritzscht⁴; Gabriela Pavlinkova²; Josef Syka¹

¹Institute of Experimental Medicine CAS; ²Institute of Biotechnology CAS; ³Institute of Biotechnology CAS, Vestec, Czechia; ⁴University of Iowa Department of Biology

Background: Expression studies, including our own, show that ISLET1 (ISL1), a LIM homeodomain (LIM-HD) transcription factor, is expressed in cells that will develop as either prosensory cells or neuroblasts. Since embryos lacking the *Isl1* gene die by embryonic day 10.5 (E10.5), the molecular mechanisms by which ISL1 affects the fate and maintenance of neurosensory cells in the inner ear remain to be investigated. We have developed a novel conditional deletion model of *Isl1* using *Neurod1-Cre* that eliminates *Isl1* in the inner ear (*Isl1cKO*). The morphological analyses showed abnormal innervation and formation of the spiral ganglion of *Isl1cKO*. Since *Isl1cKO* mice are viable, we evaluated how morphological changes in the cochlea affect the properties of auditory processing.

Methods: *Neurod1-cre* was used to conditionally delete floxed *Isl1* in the ear. We used immunohistochemistry to establish morphological changes in the formation of the inner ear. With the aim to evaluate physiological functions, we measured the distortion product otoacoustic emissions (DPOAE) and auditory brainstem responses (ABRs). In addition, we evaluated the responses to acoustical stimuli by recording single and multiple unit activity in the inferior colliculus.

Results: In the knock-out we observed an aberrant spiral ganglion with radial fibers present only in the base of the *Isl1cKO* cochlea. Misplaced spiral ganglion neurons were detected in the vestibular ganglion and in the area surrounding the cochlear nerve. The sensory epithelium in the apex was disorganized, with multiple rows of outer hair cells and inner hair cells differentiated among the outer hair cells. The morphological changes were associated with significant hearing impairment in adult mice. In comparison with controls, the DPOAEs in

Isl1cKO were absent or significantly decreased for low and middle frequencies but remained unchanged at the high frequency band. ABR thresholds were increased in a similar manner. Responses of inferior colliculus neurons in the *Isl1cKO* mice were characterized by a reduced tonotopic range, increased excitatory thresholds and various shapes of receptive fields from simple control-like to wide or multi-peaked receptive fields, reflecting the tuning impairment of *Isl1cKO* mutants.

Conclusions: A conditional deletion of the *Isl1* gene during development results in an abnormal innervation of the spiral ganglion, and disorganization of the sensory epithelium in the cochlea. The distorted organization of neurosensory cells in the cochlea during embryonic development leads to malfunction of the auditory system in adult *Isl1cKO* mice.

Supported by the Czech Science Foundation (17-04719S).

Genomics & Gene Regulation

PS 674

Cell-Specific Transcriptional Responses to Heat Shock in the Mouse Utricle Using RiboTag

Erica Sadler¹; Matthew Ryals¹; Lindsey A. May¹; Beatrice Milon²; Erich T. Boger³; Robert J. Morell³; Ronna Hertzano²; Lisa Cunningham¹

¹National Institute on Deafness and Other Communication Disorders, National Institutes of Health;

²University of Maryland Baltimore-School of Medicine;

³Genomics and Computational Biology Core, National Institute on Deafness and Other Communication Disorders, National Institutes of Health

Background

We have previously shown that heat shock protein HSP70 is induced in supporting cells and not hair cells after exposure to heat shock, suggesting that hair cells and supporting cells may respond differently to this stressor. Here we used the RiboTag method to compare the translational responses of hair and supporting cells to heat shock.

Method

We used the RiboTag pulldown method (Sanz et al. 2009, PNAS) to obtain cell-type-specific translational data on hair cells and supporting cells with and without heat shock. The RiboTag method allows for the use of distinct Cre drivers for each cell type to activate the RiboTag Rpl22-HA. Significantly differentially-expressed genes (DEGs) were determined using three analysis methods.

Significance was defined by an adjusted p-value < 0.05 and a log fold change > 1. Additionally, only genes that were significantly enriched in the RiboTag precipitate (IP) as compared to the input were used to determine differential expression between groups. Immunostaining was performed to validate the spatiotemporal expression patterns of proteins associated with several of the DEGs.

Results

RiboTag IP for hair cells and supporting cells without heat shock showed enrichment for known hair cell and supporting cell markers, indicating that the RiboTag method enriched for transcripts characteristic of the cell types of interest. GO analyses of these DEGs showed that supporting cells were enriched in transcripts related to a greater diversity of biological processes and molecular functions than hair cells. GO analyses were also performed on genes enriched in heat-shocked hair cells and supporting cells relative to their corresponding controls. Both hair cells and supporting cells were enriched for the biological process 'response to unfolded protein'; (GO:0006986). However, only heat-shocked supporting cells were enriched for regulation of cellular responses to heat (GO:1900034) and to stress (GO:0080135).

Conclusions

Our data indicate that utricular hair cells and supporting cells both respond to heat shock transcriptionally. Further analysis is needed to ensure that heat shock protein transcripts were not captured from background supporting cells in hair cell IP samples, which will be critical to determining if the previously-reported cell-type-specific differences in HSP70 expression occur at the transcriptional or translational levels.

This work was supported by the NIDCD Division of Intramural Research.

PS 675

Misregulation of Gene Expression in the CNS and Inner Ear of the raumschiff Zebrafish Mutant

Matthew Hill¹; Eliot Smith¹; Timothy Erickson²; Teresa Nicolson¹

¹Oregon Hearing Research Center and Vollum Institute, Oregon Health & Science University; ²East Carolina University

According to a 2001-2004 report by the National Health and Nutrition Examination Survey (NHANES), 35% of US adults over 40 years of age and 85% of US adults over 80 years of age show symptoms of vestibular dysfunction. Efforts to create new therapies to prevent and treat

balance diseases necessitate a better understanding of how detection of head position and coordination work. Zebrafish serve as an excellent model organism to identify the underpinnings of vestibular function and coordination due to the conservation of this critical sense. We isolated a new mutant deficient in balance, 'raumschiff', using ENU mutagenesis. We defined the critical interval on chromosome 25 using simple sequence length polymorphisms. RNAseq data analysis of mutant and sibling transcripts with the RNAMapper program revealed missense mutations in two candidate genes. Characterization and complementation analysis with fish carrying null alleles for the two candidate genes, *sall1b* and *rbl2*, is underway. Hair cell morphology and mechanotransduction, as analyzed by confocal microscopy of inner ear organs and FM labeling of lateral line hair cells respectively, are comparable to wild-type morphology and function. With respect to differential expression in mutants versus siblings, the RNAseq data also revealed striking up or down regulation of multiple genes. We used whole-mount in situ hybridization (ISH) to validate the changes in mRNA expression for several misregulated genes in the raumschiff mutants. The expression patterns of the misregulated genes were largely confined to specific regions of the brain, including neurons within the midbrain and hindbrain area. However, we also see upregulation of the gene *fosl1a* specifically in mutant inner ear maculae. These expression patterns suggest that the phenotype may involve both central processing and inner ear function. Moving forward, we aim to elucidate the pathway involving this mutation and possible translational applications.

PS 676

Developmental Modulation of Transcriptional Bursting During Organ of Corti Development

Jörg Waldhaus¹; Daniel Ellwanger²; Mary Lee¹; Michael Kain¹; Robert Durruthy-Durruthy²; Stefan Heller²

¹Kresge Hearing Research Institute, University of Michigan; ²Stanford University, School of Medicine, Department of Otolaryngology-HNS

Transcriptional profiling of single cells often results in zero-inflated data. Depending on the method applied technical noise and lack of sensitivity account for a significant amount of false negative data generated. In order to overcome this limitation algorithms capable to impute transcriptional data were developed, however, there are also numerous zero-values accurately reporting that no transcripts of a given gene were detected. Interestingly, studies focused on development reported an increase in the number of zeros detected per cell and vice versa a decrease in the number of genes detected per cell as maturation proceeds. We hypothesized that some of the

changes in gene expression during development not only correspond to genes simply being shut off but also result from expression changing between 1-state ON and 2-state ON/OFF modes.

To test the hypothesis we isolated single Deiter's cells from postnatal day 2, 21 and 63 and analyzed expression patterns of 92 different genes using single cell qRT-PCR. In support of previously published data we measured a decrease of genes detected per cell with increasing age. At single gene level we found candidate genes being constantly expressed across all investigated time points, as well as genes that were significantly up- or down-regulated with proceeding development. Specifically, the transcription factor Sox2 showed characteristic changes in gene expression pattern indicative of a transition from constitutively ON to 2-state ON/OFF mode, commonly known as transcriptional bursting, while protein was detected at all time points as shown by reporter fluorescence and antibody staining. We developed a novel data analysis strategy allowing us to analyze qPCR-data for bursting rate, burst intensity and burst length for each of the 92 genes analyzed. Single molecule Fluorescent In Situ Hybridization (smFISH) was performed to support our previous findings.

The data analysis strategy developed in this study contributes to the quickly growing field of single cell transcriptomics by providing an alternate approach for quantification and visualization of transcriptional kinetics from single cell qPCR data. Here we report transcriptional modulation of 92 candidate genes in Deiter's cells during organ of Corti development and maturation. This approach may be scaled up to 300 genes per cell and is intended to generate novel insights in gene regulation in the context of drug development at high resolution.

PS 677

Alternative Splicing-Dependent Regulation of REST Is Critical for Hearing

Yoko Nakano¹; Michael C. Kelly²; Atteeq U. Rehman³; Erich T. Boger⁴; Robert J. Morell⁴; Matthew Kelley⁵; Thomas B. Friedman⁶; **Botond Banfi**¹

¹*Department of Anatomy and Cell Biology, Carver College of Medicine, University of Iowa*; ²*Single Cell Analysis Facility, National Cancer Institute, National Institutes of Health*; ³*Department of Molecular and Human Genetics, Baylor College of Medicine*;

⁴*Genomics and Computational Biology Core, National Institute on Deafness and Other Communication Disorders, National Institutes of Health*; ⁵*NIDCD*;

⁶*Laboratory of Molecular Genetics, National Institute on Deafness and Other Communication Disorders*

Background

The DNA-binding protein REST forms complexes with

histone deacetylases (HDACs) to repress neuronal genes in non-neuronal cells. In differentiating neurons, the activity of the REST complex is reduced, and the target genes of REST are upregulated. The hair cells of the inner ear are also characterized by high expression of REST target genes, suggesting neuron-like regulation of REST activity in these cells. Transcriptional silencing is the main mechanism whereby REST is downregulated in differentiating neurons. In addition, alternative splicing of a frameshift-causing exon (i.e., exon 4) into Rest has been described in both neurons and hair cells. The splicing of exon 4 into Rest truncates the encoded protein upstream of a repressor and three zinc finger domains that are critical for REST function. The contribution of this splicing event to the downregulation of REST activity was not determined in any tissue prior to our study.

Results

Here we set out to determine whether inactivation by alternative splicing is redundant with other mechanisms of REST regulation. We found that mice heterozygous for the deletion of exon 4 of Rest have no apparent neurological defects, but lose all hair cells in the hearing organ and fail to respond to sound. The exceptional sensitivity of the ear to the deletion of exon 4 correlated with the particularly high contribution of exon 4 splicing to REST downregulation in hair cells. The hair cells and hearing of exon 4 knockout mice could be rescued with Vorinostat (SAHA), an FDA-approved HDAC inhibitor. These results led us to examine the cause of dominantly-inherited deafness in several related human subjects whose non-syndromic hearing loss had been linked to the REST-containing DFNA27 locus. Analysis of this genomic region revealed a novel variant of REST that prevented exon 4-dependent inactivation of the encoded protein.

Conclusions

Our data reveal the necessity for alternative splicing-dependent regulation of REST in hair cells, and identify a potential treatment for a group of hereditary deafness cases.

PS 678

A2ML1 and Otitis Media: Novel Variants, Differential Expression and Relevant Pathways

Eric Larson¹; Jose Pedrito Magno²; Melquiadesa Pedro³; Elisabet Einarsdottir⁴; Sven-Olrik Streubel⁵; Talitha Karisse Yarza⁶; Melissa Scholes⁵; Samuel Gubbels⁷; Stephen P. Cass⁸; Jeremy Prager⁵; Patricia Yoon⁵; Todd Wine⁵; Norman Friedman⁵; Juha Kere⁴; Kenny Chan⁵; Petri Mattila⁹; Herman Jenkins¹; Lena Hafren⁹; Charlotte Chiong³; Regie Santos-Cortez¹

¹*University of Colorado School of Medicine*; ²*University of the Philippines Manila-Philippine General Hospital*;

³*Philippine National Ear Institute*; ⁴*Biomedicum*

Helsinki; ⁵Children's Hospital Colorado; ⁶Philippine National Ear Institute; ⁷University of Colorado Anschutz Medical Campus; ⁸University of Colorado School of Medicine, Department of Otolaryngology; ⁹Helsinki University Hospital

A genetic basis for otitis media is established, however the role of rare variants in otitis media is largely unknown. Previously a duplication variant within A2ML1 was identified as a significant risk factor for otitis media in an indigenous Filipino population and in US children. In this report exome sequencing was performed using additional DNA samples from the indigenous Filipino population, Filipino cochlear implantees and Finnish families with otitis media. Nine novel, damaging A2ML1 variants identified in otitis media patients were rare or low-frequency in population-matched controls. In the indigenous population, both gingivitis and A2ML1 variants including the duplication variant and c.4061+1G>C were independently associated with otitis media. Sequencing of salivary RNA samples from indigenous Filipinos demonstrated lower A2ML1 expression according to carriage of A2ML1 variants. Sequencing of additional salivary RNA samples from US patients with otitis media revealed differentially expressed genes that are highly correlated with A2ML1 expression levels. In particular RND3 is upregulated in both A2ML1 variant carriers and high-A2ML1-expressors. These findings support a role for A2ML1 in keratinocyte differentiation within the middle ear and the potential application of ROCK inhibition in otitis media.

PS 679

Genomic Elements that Regulate Expression of Fbxo2

Byron Hartman; Stefan Heller

Stanford University, School of Medicine, Department of Otolaryngology-HNS

We seek to understand regulatory mechanisms of otic-specific genes and identify promoter and enhancer elements that drive gene expression in the inner ear. Here we investigate regulation of Fbxo2, which encodes the E3 ubiquitin ligase Fbx2, a highly specific and abundant inner ear protein shown to be important for cellular homeostasis. Lack of Fbx2 in mice leads to age-related hearing loss beginning at two months, associated with degeneration of cochlear supporting cells and changes in membrane integrity, followed by progressive degeneration of hair cells and spiral ganglia (Nelson et al., 2007). It is thought that Fbx2, a ubiquitin ligase substrate adapter protein with specificity for glycoproteins, plays an important role in protein quality control in the inner ear. Although it appears to function in cochlear maintenance, Fbxo2 is expressed

surprisingly early in development of the inner ear. In a previous microarray study, we found that Fbxo2 is one of the most abundant and specific genes in the developing otocyst as compared to other tissues of the early mouse embryo (Hartman et al., 2015). We generated Fbxo2-VHC knock-in reporter mice to further characterize expression of this gene and exploit it to access the otic sensory lineage for developmental studies (Hartman et al., 2018).

Here we aim to decipher how the robust and specific expression of Fbxo2 is regulated and identify cis-elements for directing future gene therapies specifically to the inner ear. Phylogenetic comparison of Fbxo2 across vertebrate species reveals several conserved noncoding regions, including a ~2kb promoter and nine highly evolutionarily conserved regions (ECRs) downstream. Several potential binding sites were identified in silico, including sites for Pax2/5/8, Gata3, and Sox10. Conservation and clustering of binding sites within the promoter and ECRs suggests combinatorial transcription factor binding. We used plasmid electroporation as a preliminary test of the activity of the 2kb promoter and found that it is sufficient to drive reporter expression in embryonic cochlea explants.

We hypothesize that Fbxo2 expression in the developing and adult mouse is regulated through multiple cis-regulatory modules located within the promoter and downstream ECRs. To test this, we produced a reporter mouse (Fbxo2*tdTomato) with a transgene that mimics the native 100kb Fbxo2 locus while condensing it to about 10kb by excluding non-conserved regions and replacing the Fbxo2 coding region with tdTomato. All nine of the ECRs were individually positioned similar to their native orientation and loxP and FRT sites were strategically included to allow subsequent excision of ECRs in two groups. The proximal ECRs 1-5 can be removed with Cre recombination while the distal ECRs 6-9 can be removed with Flip recombination. Germ line recombination was achieved by crossing the Fbxo2*tdTomato mouse line to Cre and/or Flip recombinase-expressing mouse lines. The full-length transgene determines whether all of the conserved elements are sufficient to confer the normal pattern of Fbxo2 expression, while Cre/Flip excision tests for necessity within the ECR clusters. We find that the fully intact Fbxo2*tdTomato reporter accurately recapitulates the major features of Fbxo2 expression and that downstream ECRs contain elements that enhance expression in otic cells and repress expression in off-target cells.

PS 680

The Cell-Type Specific Response to Noise in Adult Mouse Inner Ears

Beatrice Milon¹; Sunayana Mitra Mitra¹; Yoko Ogawa¹; Benjamin Shuster¹; Yang Song¹; Didier Depireux²; Ran Elkon³; Ronna Hertzano¹

¹University of Maryland Baltimore-School of Medicine;

²Otolith Labs; ³Tel Aviv University, Sackler Faculty of Medicine, Israel

While several studies have described changes in gene expression in whole cochleae following noise exposure, cell-type specific data are still largely missing. Filling this gap is important as we consider candidate genes and pathways that may underlie acquired hearing loss. Here, we used the RiboTag approach to characterize changes in gene expression following noise exposure when compared to unexposed (baseline) adult mice. We generated RiboTag;PrestinCreERT2 and RiboTag;Sox2CreERT2 mice to enrich for actively translated transcripts in outer hair cells (OHC) and supporting cells (SC), respectively.

Using a reporter gene, we first show that while PrestinCreERT2 induces recombination specifically in OHC, Sox2CreERT2 induces recombination both in SC and in glial cells (GC) of the spiral ganglion. We then optimized our noise exposure scheme to obtain a permanent threshold shift across all frequencies measured (8kHz, 16kHz, 24kHz and 32kHz) in 10-week old mice. Whole cochleae were harvested 6h after a mock noise exposure (baseline) or 6 hours and 24 hours post noise exposure and processed for RiboTag immunoprecipitation (IP) followed by RNA-seq of the input and IP samples. Our bioinformatics analyses combined an enrichment analysis between input and IPs, differential gene expression analysis, clustering analysis, gene ontology, cis-regulatory analysis and ligand-receptor pair predictions. We were able to detect cell-type specific changes in gene expression profiles following noise exposure. Our data reveal that 20% of the immune system up-regulated transcripts traditionally thought to originate from infiltrating immune cells are actually up-regulated in the OHC and SC. For example, transcripts for several inflammatory chemokines are significantly enriched specifically in OHC following noise exposure and gene expression of interleukin-receptors are induced in SC. Additionally, cis-regulatory analyses on genes down-regulated following noise exposure suggest several transcription factors as key regulators such as Ying-Yang 1 (YY1) in OHC and RFX4 in SC/GC.

In conclusion, the RiboTag approach combined with cell type-specific Cre mouse lines is an efficient method to enrich for transcripts from a specific cell-type and to

identify cell-type specific changes in expression profiles following noise exposure in the adult mouse cochlea. While dependent on enrichment analyses to determine the cell of origin for gene expression, it affords the advantage of eliminating a dissociation step, which is associated with activation of immediate early genes. This is particularly relevant in studies of noise exposure where some of these genes play a role in the early response to noise.

PS 681

The ATP-Dependent Chromatin Remodeler CHD7 is Critical for Proper Cochlear Length and Organization, and Auditory Nerve Formation

Vinodh Balendran¹; Lisa A. Beyer²; Jennifer M. Skidmore³; Jelka Cimerman¹; Elizabeth Hurd⁴; Yehoash Raphael²; Donna M. Martin⁵

¹Department of Pediatrics, University of Michigan;

²Kresge Hearing Research Institute, Department of Otolaryngology-Head and Neck Surgery, University of Michigan; ³Dept. Pediatrics, University of Michigan;

⁴Deputy Director, University of Edinburgh; ⁵Depts.

Pediatrics and Human Genetics, University of Michigan

Epigenetic regulation of gene transcription by chromatin remodeling proteins has recently emerged as an important contributing factor in inner ear development. Pathogenic variants in CHD7, the gene encoding Chromodomain Helicase DNA binding protein 7, cause CHARGE syndrome, which presents with malformations in the developing mammalian ear. Germline deletion of Chd7 in mice is embryonic lethal, whereas heterozygous Chd7 loss-of-function mice display mild mixed sensorineural/conductive hearing loss. Chd7 is broadly expressed in the mouse auditory epithelium as early as E13.5, yet the pathogenic effects of Chd7 loss in the cochlea have yet to be fully defined. Here we characterized auditory phenotypes after Chd7 deletion in the otocyst and surrounding mesenchyme (using Foxg1Cre), in the otic mesenchyme (using TCre), in hair cells (using Atoh1Cre), and in developing neuroblasts (using Ngn1Cre). Inner ears were examined using paintfilling, scanning electron microscopy, cochlear whole mount immunofluorescence, auditory brainstem response (ABR) and distortion-product otoacoustic emissions (DPOAEs) assays. Deletion of Chd7 in Foxg1Cre;Chd7Gt/flox mice resulted in disorganized, ectopic, and supernumerary rows of hair cells and disrupted innervation with excess axonal looping. Deletion of Chd7 in the mesenchyme by TCre led to normal cochlear morphology at E14.5. At P42, Atoh1Cre mutant mice exhibited elevated ABR thresholds at 32 kHz and depressed DPOAE levels at 24 kHz. Together, these observations suggest the presence of dosage-, tissue-, and time-sensitive roles for Chd7 in cochlear elongation,

hair cell morphology, and cochlear neuron organization. Interestingly, the otocyst and maturing neurons appear uniquely sensitive to Chd7 deficiency. These studies indicate that CHD7 acts to regulate cochlear size and epithelial and neuronal organization, providing novel information about roles for Chd7 in development of both auditory epithelia and neurons.

PS 682

Tropism of Adeno-Associated Viral Vectors in Adult Mammalian Inner Ear Cell Subtypes with Single and Dual Transduction

Ryotaro Omichi¹; Hidekane Yoshimura²; Seiji Shibata¹; Luk Vandenberghe³; Richard J. H. Smith¹

¹Department of Otolaryngology, Molecular Otolaryngology and Renal Research Laboratories, University of Iowa; ²Department of Otolaryngology, Molecular Otolaryngology and Renal Research Laboratories; ³Grousbeck Gene Therapy Center, Schepens Eye Research Institute and Massachusetts Eye and Ear Infirmary & Ocular Genomics Institute, Department of Ophthalmology, Harvard Medical School, & Harvard Stem Cell Institute

Background

Adeno-associated virus (AAV) transduction has been reported as an effective method of gene delivery to inner hair cells (IHCs) and outer hair cells (OHCs). Tropism of AAV is relevant to targeted cell transduction. In this study, we tested several AAV serotypes to define tropism.

Methods

Four-week-old C3H/FeJ mice were assigned to the different experimental groups, with at least four animals per group. 1 µL of AAV2/1, 2/2, 2/8, 2/9 CMV.EGFP.WPRE.bGH or AAV2/Anc80.AAP.CMV.EGFP.WPRE.bGH was injected into the left ear using the round window membrane + canal fenestration method we have previously described. Two weeks later, auditory brainstem responses (ABR) were measured. Cochleae were then harvested and dissected to evaluate transduction efficiency. Dual transduction was also studied using combinations of AAV2/2.CMV.EGFP, AAV2/2.CMV.mCherry, AAV2/9.CMV.EGFP and AAV2/9.CMV.mCherry.

Results

Cochlear transduction was serotype dependent. For IHCs, it was most robust with AAV2/2 (90%) and AAV2/Anc80 (100%). AAV2/8 and AAV2/9 transduced 70%-80% of IHCs. AAV2/1 transduction was poor at 10%. OHC transduction was most robust with AAV2/2 (80- 95%). Anc80 transduction was 30-65%; the remaining serotypes were not effective in transducing OHCs. Duals injection with AAV2/2.eGFP.WPRE and AAV2/2.mCherry was as efficient as single

injection with AAV2/2.eGFP.WPRE. Use of Anc80 was associated with significant hair cell loss in the middle and basal turns of the cochlea, while with AAV2/8, hair cell loss was restricted to the basal turn. No auditory compromise was observed, as measured by ABR.

Conclusion

Of the viral serotypes tested, in mature mice AAV2/2 provides the best transduction efficiency of both IHCs and OHCs without measurable hair cell loss or hearing damage. Transduction is equally robust with single vector and dual vector injections.

PS 683

HEar-Seq Targeted Gene Panel Identifies the Spectrum of Inherited Variants for Deafness in a Diverse Jewish Population

Zippora Brownstein¹; Fabio T.A. Martins¹; Maria Birkan¹; Suleyman Gulsuner²; Lara Kamal³; Nada Danial-Farran⁴; Ming Lee²; Bella Davidov⁵; Lina Basel-Salmon⁶; Moshe Frydman⁷; Chana Vinkler⁸; Michal Macarov⁹; Meirav Sokolov¹; Noga Lipschitz¹; Noam Shomron¹; Tom Walsh²; Moien Kanaan³; Staviv Allon-Shalev¹⁰; Mary-Claire King²; Karen B. Avraham¹

¹Tel Aviv University; ²University of Washington;

³Bethlehem University; ⁴Technion, Tel Aviv University;

⁵Rabin Medical Center; ⁶Tel Aviv University, Rabin Medical Center; ⁷Tel Aviv University, Sheba Medical Center; ⁸Wolfson Medical Center; ⁹Hebrew University; ¹⁰Emek Medical Center

More than 150 genes are involved in deafness worldwide, with different mutations in different populations. However, about half of cases of inherited deafness remain unsolved. The same is true for the Israeli Jewish population, which includes multiple ethnic groups, turning Israel into a microcosm of genetic diversity that harbors mutations in many deafness genes. This population mixture presents a challenge to determining the cause of deafness in unsolved cases, and next-generation sequencing (NGS) has proven an efficient tool for tackling this task. Using HEar-Seq panels, we sequenced 375 human and mouse deafness genes in 90 families with hearing loss from a variety of Jewish lineages. An additional 101 deaf singleton cases were subsequently evaluated for specific variants identified on the HEar-Seq panels. Community-specific founder mutations were identified and the corresponding phenotypes evaluated. Of the 90 families and 101 singletons evaluated, 46 families and 31 additional singletons carried mutations in genes on HEar-Seq. In total, 77/190 (41%) cases of deafness, involving 50 alleles in 23 genes were resolved. HEar-Seq raised the proportion of solved cases from 26% to 41% and the number of genes known to cause hearing loss in Jewish populations from 7 to 28. Specific variants

revealed clear genotype-phenotype relationships and clear association with specific Jewish ethnicities. These results have immediate impact on genetic counseling for the deaf in Israel and demonstrate the effectiveness of HEar-Seq panels in solving the genetics of deafness in a genetically diverse population such as Israeli Jews. We conclude that HEar-Seq analysis can assist in the development of a strategy for genetic counseling for hearing loss, optimizing efficiency, time, and cost.

PS 684

The Effect of Pulse Polarity on Neural Response of the Electrically-Stimulated Auditory Nerve in Children with GJB2 or SLC26A4 Gene Mutations

Angela Pellitteri¹; Jianfen Luo²; Lei Xu²; Xiuhua Chao²; Ruijie Wang²; Zhaomin Fan²; Haibo Wang²; Shuman He¹

¹The Ohio State University Wexner Medical Center;

²Shandong Provincial Hospital affiliated to Shandong University

Background: The most commonly identified causes for genetic deafness are GJB2 and SLC26A4 gene mutations. The goal of the present study was to investigate the effect of GJB2 and SCL26A4 gene mutations on auditory nerve function in children with cochlear implants (CI). Their results were compared to those measured in children with idiopathic hearing loss.

Methods: Study participants included 20 children with biallelic GJB2 mutations, 16 children with biallelic SLC26A4 mutations and 19 participants with idiopathic hearing loss. All except for two study participants with SLC6A4 mutations had Mondini malformation and enlarged vestibular aqueduct (EVA). All participants were Cochlear® Nucleus™ CI users. The electrically-evoked compound action potential (eCAP) was recorded in each participant at one basal, one middle and one apical electrode location using both anodic- and cathodic-leading biphasic pulses. The primary dependent variable (DV) of interest was the slope of eCAP Input/Output (I/O) function and it was estimated using statistical modeling with a linear regression function. eCAP amplitude, measured at the maximum comfortable level of the anodic stimulus (the anodic C level) and eCAP threshold were also compared between pulse polarities and among study groups. Effects of study group, stimulus polarity and electrode location on each DV were evaluated using Generalized Linear effect Mixed Models.

Results: The anodic stimulus resulted in steeper slopes of eCAP I/O functions, larger eCAP amplitudes at the anodic C level and lower eCAP thresholds in all subject groups and at all electrode locations. Children

with GJB2 mutations showed steeper slopes and larger eCAP amplitude than children in both the SLC26A4 and idiopathic hearing loss group. In addition, these subjects also showed smaller effect size of pulse polarity on eCAP amplitude. These data indicated that children with GJB2 mutations had better neural survival of auditory nerve fibers than children with SLC26A4 who had concurrent Mondini malformation and EVA and children with idiopathic hearing loss.

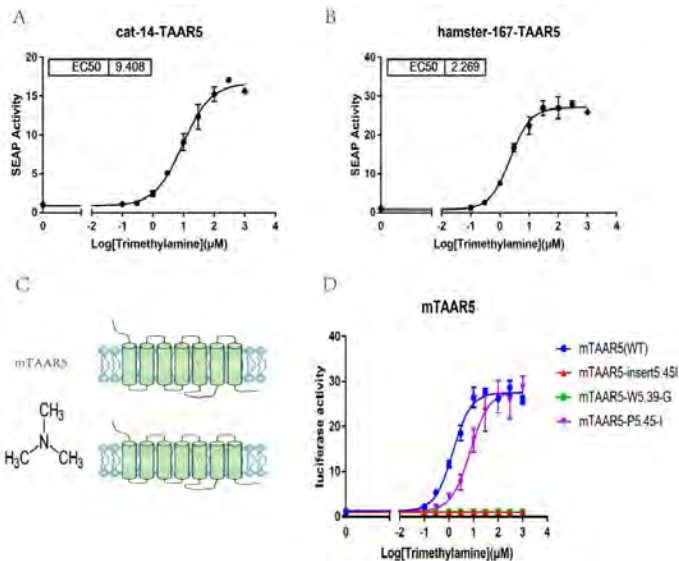
Conclusion: The results suggest that anodic stimuli are more effective in activating the auditory nerve fibers than cathodic stimuli in spite of GJB2 or SLC26A4 gene mutations. The results also provide evidence that children with hearing loss caused by the GJB2 gene mutation have better neural survival than those with the SLC26A4 mutation and concurrent Mondini malformation and EVA or idiopathic hearing loss.

PS 685

Identification of Ligands for Orphan Olfactory TAARs across Different Species

Lingna Guo¹; Zhengrong Xu²; Qian Li³; Renjie Chai⁴
¹Southeast University; ²Nanjing University; ³Shanghai Jiao Tong University School of Medicine; ⁴Key Laboratory for Developmental Genes and Human Disease, Ministry of Education, Institute of Life Sciences, Southeast University

Trace amine-associated receptors (TAARs) are G protein-coupled receptors (GPCRs) function as olfactory receptors that conserved in vertebrate, several TAARs have been proved to mediate innate animal behaviors by recognizing volatile amines. However, the majority of TAARs are orphan with unknown agonists. Here, we screened chemicals for orphan olfactory TAARs across different species using high-throughput screening assay, and we found new ligands such as spermidine, dopamine, and tryptamine. Moreover the homologous TAAR across different species usually showed similar response profiles. Loss-of-function analysis based on homologous sequence alignment indicated that Phe3.37 and Asp6.54 were the key points of TAAR9, while the site of Trp5.39 was necessary for activation of TAAR5. Overall, our work has identified new ligands for orphan olfactory TAARs and shed light on molecular basis of GPCRs.



PS 686

Deafness in a Noise-Resistant Bat Species

Nazrawit Retta¹; Katrina M. Schrode²; Hamad Javaid¹; Mohamed Lehar¹; Susanne Sterbing-D'Angelo¹; Cynthia Moss¹; Amanda Lauer¹

¹Johns Hopkins University; ²Johns Hopkins University School of Medicine

The echolocating big brown bat, *Eptesicus fuscus*, is known to be extremely resistant to noise-induced hearing loss. Echolocating bats are also thought to be protected from age-related hearing loss due to their dependence on high frequency hearing for survival over a long lifespan. In the present study, we performed hearing screening and quantitative analysis of cochlear sensory cells and neurons in big brown bats after reports that subjects from an inbred population were not performing normally in laboratory echolocation experiments and did not show neural activity in auditory nuclei. The presumably deaf bats lacked sound evoked auditory brainstem responses (ABR) and distortion product otoacoustic emissions (DPOAEs), which were robust in wild-caught members of the same species. Light and confocal microscopy of whole mount and sectioned cochleae revealed regions with missing inner and outer hair cells, spiral ganglion neurons, and medial olivocochlear efferent innervation. Regions missing hair cells were mapped through three-dimensional reconstruction of the cochleae. Spiral ganglion counts were estimated using stereological procedures. Damage was observed over extensive regions of the cochleae. In most cases, surviving hair cells were observed only in the most apical regions. Spiral ganglion neurons were missing. Damage patterns were more severe than what was observed in two mouse models of early-onset

deafness, the DBA/2J and C57BL/6J. Tissue from these mouse strains was harvested at ages when the hearing loss was profound. These results are surprising in bats, as they rely heavily on hearing for social communication and echolocation. The underlying cause or onset of the deafness is unknown; however, analysis of body condition and teeth did not indicate that the deaf bats were otherwise unhealthy or at the end of their lifespan. Neither were the animals exposed to any conditions known to induce hearing loss in other species. Further analysis will be conducted to determine how central auditory neurons are affected in the deaf bats. These bats present a rare opportunity to conduct a quantitative and comparative analysis of the pathobiology of deafness in a hearing specialist.

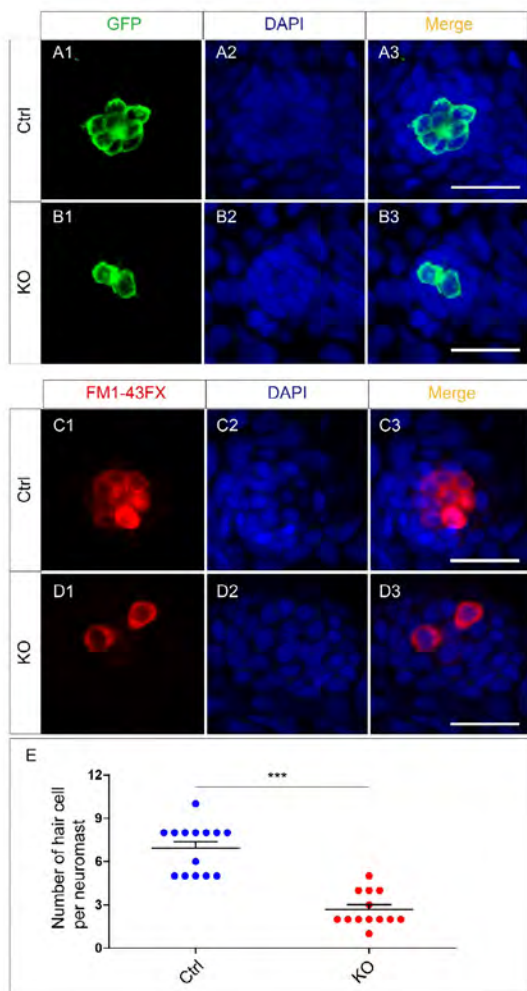
PS 687

slc4a2b Is Required for Hair Cell Development in Zebrafish

Fuping Qian¹; Dong Liu²; Renjie Chai³

¹Southeast University; ²Nantong University; ³Key Laboratory for Developmental Genes and Human Disease, Ministry of Education, Institute of Life Sciences, Southeast University.

Hair cells function as an important sensory receptor which can detect the movement in their environment. Hair cells in the inner ear can sense acoustic information, and in the aquatic vertebrates, hair cell can also detect movement, vibration, and pressure gradients in the surrounding water. A great many genes are responsible for the development of hair cells. According to the functional analysis, we found that loss of function of *slc4a2b* (solute carrier family 4, member 2b) gene, which was a member of anion exchanger family, can reduce the number of hair cell in zebrafish neuromasts, and further studies demonstrated it was due to the hair cell apoptosis. We therefore concluded that *slc4a2b* gene was of importance in the development of hair cell in zebrafish.



PS 688

Pericyte Abnormalities Precede Strial Capillary Basement Membrane Thickening in Alport Mice.

Dominic Cosgrove¹; Brianna Dufek¹; Daniel Meehan¹; Duane Delimont¹; Grady Phillips²; Grant Baxter²; Michael Anne Gratton²

¹Boys Town National Research Hospital; ²Washington University School of Medicine

Background: In 129 Sv autosomal Alport mice, the strial capillary basement membranes (SCBMs) progressively thicken between 5 and 9 weeks of age resulting in a hypoxic microenvironment with metabolic stress and induction of pro-inflammatory cytokines and chemokines. These events occur concomitant with a drop in endocochlear potential and a susceptibility to permanent noise-induced hearing loss under conditions that do not permanently affect age/strain-matched littermates. The current study aimed to gain an understanding of events that occur before the onset of SCBM thickening.

Methods: We performed RNAseq analysis on RNA from stria vascularis isolated from 3-week Alport mice and wild type littermates. Data was processed using

Ingenuity Pathway Analysis software and further distilled using manual procedures. To examine changes in the cellular architecture of the stria, we performed dual immunofluorescence analysis on whole mounts of the stria vascularis from these same animals stained with anti PDGFRB and anti-desmin (pericyte markers) antibodies.

Results: RNAseq analysis revealed significant dysregulation of genes involved in cell adhesion, cell migration, formation of protrusions, and both actin and tubulin cytoskeletal dynamics. Overall, the data suggested changes in the cellular architecture of the stria might be apparent. Dual immunofluorescence analyses of strial whole mounts showed evidence of pericyte detachment and migration as well as the formation of cellular protrusions on pericytes in z-stacked confocal images from Alport mice compared to wild type littermates. Interestingly, similar observations were recently reported for noise damaged stria vascularis (Hou et al., JARO, 2018).

Conclusions: Collectively, these findings suggest that the change in type IV collagen composition in the Alport SCBMs results in cellular insult to the pericyte compartment, activating detachment and altered cytoskeletal dynamics. These events precede SCBM thickening and hearing loss in Alport mice, and thus constitute the earliest event so far recognized in Alport strial pathology.

Supported by R01 DC015385

PS 689

Neurod1 Expression Reduces Schwannoma Cell Proliferation

Lintao Gu¹; Linjing Xu¹; Jennifer Kersigo²; Timothy A. Jones³; Bernd Fritzsche²; Marlan R. Hansen¹

¹University of Iowa Department of Otolaryngology Head and Neck Surgery; ²University of Iowa Department of Biology; ³University of Nebraska Lincoln

Background: Schwannomas commonly occur within the vestibular nerve and bilateral vestibular schwannomas (VSs) are a hallmark of Neurofibromatosis type 2 (NF2). Current therapeutic options are limited to surgery or radiation yet most patients become deaf and ultimately succumb to tumor burden. Development of treatment strategies that slow tumor progression while sparing inner ear function would be a superior solution. Here we explore a molecular approach that uses conditional Schwann cell (SC) expression of Neurod1, a proneuronal transcription factor, to potentially force schwannoma cells to exit the cell cycle.

Methods: The periostin (Postn)-cre line drives cre expression specifically in SCs. Crossing this cre line with a line containing floxed Nf2 gene (Postn-cre;Nf2f/f) leads to multiple schwannomas, including bilateral VSs. The Postn-cre;Nf2f/f mice were crossed with a Rosa26LSL-Neurod1 line that induces Neurod1 expression via cre-mediated excision of a stop codon, enabling the Rosa26 locus to drive Neurod1 expression. Auditory brainstem response (ABR) and vestibular evoked potentials (VsEPs) thresholds were serially recorded to longitudinally assess the effect of Neurod1 expression on auditory and vestibular function. We then compared EdU uptake in the vestibular ganglia of the various genotypes at 12 months. Primary human VS cell cultures were transduced with adenoviral vectors expressing Neurod1 or empty vector. Cell proliferation was assessed by EdU uptake. Finally, to determine the effect of Neurod1 expression on normal Schwann cell (SC) proliferation, we performed sciatic nerve axotomies in mice of the various genotypes and compared EdU uptake 7 days after injury.

Results: Deletion of Nf2 via cre expression led to elevated ABR and VsEPs thresholds over time compared to age-matched wild-type littermates demonstrating the effects of schwannoma growth on auditory and vestibular function. This effect was partially mitigated by Neurod1 expression. Further expression of Neurod1 significantly reduced schwannoma cell proliferation in animals lacking Nf2 and in human VS cultures. Sciatic nerve axotomy significantly increased SC proliferation in wild-type and Nf2-null animals. Interesting deletion of Nf2 results in reduced SC proliferation following axotomy compared to wild-type animals consistent with prior observations that dominant-negative Nf2 mutation leads to reduced SC proliferation. Further, expression of Neurod1 appears to reduce the proliferative capacity of both wild-type and Nf2-null SCs following nerve injury.

Conclusions: Expression of Neurod1 reduces schwannoma cell proliferation in mouse genetic models of NF2 and in human VS cultures. Molecularly interfering with schwannoma proliferation through conditional inactivation of cell cycle progression represents a potential novel approach to reduce schwannoma growth

PS 690

Characterizing Translational Changes in Mammalian Stria Vascularis as it Relates to Cisplatin Exposure

Ian Taukulis¹; Rafal Olszewski¹; Soumya Korrapati¹; Andrew Breglio²; Katharine Fernandez¹; Erich T. Boger³; Daniel Martin⁴; Robert J. Morell³; Lisa Cunningham⁵; Michael Hoa¹

¹NIDCD/NIH; ²National Institute on Deafness and

Other Communication Disorders, National Institutes of Health; ³Genomics and Computational Biology Core, National Institute on Deafness and Other Communication Disorders, National Institutes of Health; ⁴NIDCR/NIH; ⁵National Institute on Deafness and Other Communication Disorders, National Institutes of Health

Background: Cisplatin is a chemotherapeutic agent commonly used to treat patients with a variety of cancers, including head and neck cancer. However, cisplatin is ototoxic, and hearing loss is a significant side effect in treated patients. Recently, it has been shown the stria vascularis (SV) in cisplatin-treated mice exhibits long-term retention of cisplatin and is associated with a reduction in the endocochlear potential (EP). To better understand the effects cisplatin exposure has on the SV, we analyzed the transcriptional changes between normal and cisplatin-treated mouse SVs using single-cell RNA-Sequencing technology.

Methods: Stria vascularis were dissected from cisplatin-treated and placebo CBA/J P30 mice. One group was injected with a single dose of 14mg/kg of cisplatin and the other group was injected with saline as a control. The SV tissues were dissociated, and single cells were captured in droplets by the 10X Genomics platform, where the cells were lysed, and RNA was obtained and converted to cDNA libraries. The libraries were sequenced, and the resulting reads were mapped to generate gene counts. Gene count data was analyzed using Seurat and weighted gene co-expression network analysis (WGCNA), an unsupervised iterative gene co-expression analysis technique, to identify changes in RNA expression between treated and untreated strial cells.

Results: Using Seurat, differential RNA expression among specific cell types of the SV was performed. We validate differential gene expression between cisplatin-treated and untreated strial cell types using immunohistochemistry. WGCNA was used to identify modules of co-expressed genes. Using these modules, potential gene regulatory networks were constructed using network analysis tools. Focusing on gene regulatory networks involved in ion homeostasis, these genes were analyzed utilizing a druggable genome target database to identify pharmacologic agents with the potential to modulate the EP.

Conclusions: The use of cisplatin as a tool for perturbation of regulatory networks of the mammalian stria vascularis has larger implications for the future of cancer treatments in humans. A greater understanding of inner ear cellular processes affected by exposure to cisplatin will allow us to better define the cellular mechanisms of the endocochlear potential.

PS 691

CRISPR/Cas9-mediated targeted Y Chromosome Elimination In the Mammalian Auditory System

Yong Tao¹; Wen Kang¹; Xingle Zhao¹; Hao Wu²

¹Shanghai Ninth People's Hospital, Shanghai Jiao Tong University School Of Medicine; ²clinical auditory

Background

Turner syndrome happens when one of the X chromosomes is missing or partially missing, which affects one out of 2,500 females at birth. Turner syndrome can cause a variety of medical and developmental symptoms, including hearing loss. Common problems include chronic ear infections as well as conductive and sensorineural hearing loss, however, the mechanism underlying hearing loss is not fully understood. Lack of appropriate animal model to study the effect of X chromosome missing is one of the main reasons, as systemic X chromosome missing lead to multiple symptoms in the organ systems across the whole body. X chromosome elimination inside auditory system could be a more promising system to dissect the mechanism of hearing loss of Turner syndrome.

Methods

Neonatal and adult male inducible CRISPR/Cas9 knock-in mice (Cre recombinase-dependent expression of CRISPR associated protein 9 (cas9) endonuclease) were randomly assigned to the different experimental groups, at least 6 mice in each group. AAV8-CMV-Cre, AAV8-U6-Ssty2-gRNA-CMV-Cre, AAV8-U6-Ssty2&Rbmy1a1-gRNA-CMV-Cre were injected through cochleostomy in neonatal, canalostomy in adult respectively. Acoustic brainstem Response (ABR) were performed at 1, 2, 3 and 4 weeks old. Cochleae were harvested and dissected, and Cre induced tomato signals were used to label infected cells. MYO7A and TUJ1 antibodies were used to label hair cells (HC) and spiral ganglion neurons (SGN).

Results

Cas9 were successfully activated in SGNs and inner HCs after viral expressed Cre was delivered to the inner ear. DNA-FISH were performed in cochlear cells?, and Y chromosome signals was not detected in AAV8-U6-Ssty2&Rbmy1a1-gRNA-CMV-Cre injected group, which indicate Y chromosome could be selectively eliminated in SGN and HC in vivo. ABR analysis shown no significant difference incompared to the AAV8-CMV-Cre injection group, but 40dB SPL ABR threshold shifted were observed in other two groups after 2 weeks.

Conclusions

Viral vector carried sgRNA and Cre can induce genome

editing in vivo. Elimination Y chromosome in auditory system impaired ABR thresholds in mice, and karyotype analysis validated the Y chromosome deletion. It is feasible CRISPR/Cas9 gene editing to knock down gene in auditory system specific. Gene editing supply efficient and quick method to establish gene KO model in auditory system, which is novel tool for hearing research and drug screening.

PS 692

The Epigenetic Regulator CXXC Finger Protein 1 (Cfp1) is Required to Maintain Mature Differentiated Auditory Hair Cells

Chun-Yu Tung; David Skalnik; Benjamin Perrin

Indiana University - Purdue University Indianapolis

Mammalian auditory hair cells, which are maintained for the life of the organism, must have mechanisms to ensure that proper gene regulation persists over time. CXXC finger protein 1 (Cfp1) binds to unmethylated CpG dinucleotide DNA sequences where it can recruit Set1 histone H3-Lysine 4 methyltransferase complexes that deposit a chromatin modification that generally promotes gene expression. Cfp1 is required for differentiation in every cell type tested, but it is unknown whether it is also required in differentiated cells. To determine if Cfp1 activity is important for auditory hair cell maintenance, we used Atoh1-cre to delete the gene after cells were differentiated. Conditional Cfp1 knockout mice form apparently normal auditory hair cells and have auditory brainstem responses that are comparable to control mice at most sound frequencies. However, as mice age, Cfp1 conditional knockout mice have progressive high-frequency hearing loss that affects all tested frequencies by 9 weeks of age. Some hair cells are lost; however, hearing loss more closely corresponds to a progressive reduction in the number of synapses on inner hair cells as well as fusion and loss of stereocilia bundles. Together these data suggest that Cfp1 mediates ongoing epigenetic modifications that are required to maintain the integrity and function of differentiated auditory hair cells.

PS 693

Differential Gene Expression in Mature Cochlear Neurons and Macrophages After Selective Hair Cell Ablation

Tejbeer Kaur¹; Eric Tycksen¹; Vikrant Borse²; Mike Heinz¹; Mark E. Warchol

¹WASHINGTON UNIVERSITY SCHOOL OF

MEDICINE; ²Washington University in Saint Louis

Background

Loss of cochlear hair cells or afferent synapse can

cause gradual degeneration of spiral ganglion neurons (SGNs). Such neural loss can limit the efficacy of cochlear implants or any hair cell regenerative therapies. Therefore, it is of great interest to develop interventions that can prevent neural degeneration and promote SGN survival in injured cochlea. Hair cell death results in a sustained increase in macrophage numbers in the spiral ganglion. SGNs communicate with macrophages via the chemokine fractalkine (CX3CL1) that is expressed on SGNs and its receptor, CX3CR1, expressed on macrophages. Interruption of fractalkine signaling leads to diminished SGN survival after loss of cochlear hair cells, but the precise mechanisms by which macrophages or fractalkine regulate neural survival are unclear. The objective of this study was to determine the effects of fractalkine signaling on gene expression in both cochlear macrophages and SGNs following targeted deletion of cochlear hair cells.

Methods

Adult CX3CR1+/GFP:Pou4f3 DTR/+ and CX3CR1GFP/GFP:Pou4f3 DTR/+ mice were employed to induce diphtheria toxin (DT)- dependent selective hair cell ablation and CX3CR1+/GFP and CX3CR1GFP/GFP mice served as undamaged controls. The CX3CR1GFP/+ line retains fractalkine signaling, while CX3CR1GFP/GFP lack the fractalkine receptor. Mice were injected with DT and allowed to recover for two weeks. Cochleae were then harvested and subjected to tissue digestion to prepare a single cell suspension. Suspended cells were incubated with antibodies against CD45 (pan leukocyte marker) and CD90.2 (SGN marker) and subjected to FACS sorting. RNA was isolated from neurons and macrophages. Following ds-cDNA synthesis and fragmentation, sequencing was performed on an Illumina HiSeq-3000 using single 50 base reads. Data analyses was performed using StarFish and Limma-Voom. Differentially expressed genes were validated by qRT-PCR and immunohistochemistry.

Results

RNA-Seq identified ~500 differentially expressed genes in macrophages and ~600 such genes in SGNs between CX3CR1GFP/+ and CX3CR1GFP/GFP mice after hair cell ablation. In silico analysis-using KEGG and GO, revealed significant changes in multiple molecular and biological pathways in both macrophages and neurons of damaged CX3CR1 knockout animals. These include complement cascade, cytokine-cytokine receptor interaction, glutamatergic synapse and calcium signaling pathways. Validation of 20 genes by qRT-PCR revealed nearly 50% correlation with seq data.

Conclusions

The data suggest that deletion of CX3CR1 leads to changes in gene expression in both macrophages and neurons after selective hair cell ablation. Future studies will validate potential pathways and genes that may have neuroprotective or neurotoxic functions in injured cochlea.

PS 694

Methionine Sulfoxide Reductase Proteins are Indispensable for Auditory Function in Mice

Elodie M. Richard¹; Zubair M. Ahmed¹; Vadim N. Gladyshev²; Saima Riazuddin¹

¹University of Maryland, School of Medicine; ²Brigham and Women's Hospital and Harvard Medical School

Methionine sulfoxide reductases (MSR) are enzymes responsible for catalyzing the reduction of methionine-sulfoxides in damaged proteins. Previously, we and others, demonstrated that loss of MSRB3 function is associated with profound prelingual non-syndromic deafness in humans and mice. To decipher the role of other MSR proteins in the auditory pathway, we acquired or generated knock-out mouse models for MsrA, MsrB1 and MsrB2.

Contrary to MsrB3 knock-out mice, ABR measurements showed that all of these homozygous mutant mice have hearing at P16. MsrA and MsrB1 mutants have elevated hearing thresholds as compared to their wild-type littermates at 32kHz and 40 kHz frequencies (32 and 40kHz), as early as P90 and P60, respectively. While the hearing deficit worsens with age in MsrB1 knock-out mice, affecting lower frequencies, the hearing loss seems confined to higher frequencies in MsrA knock-out mice (P16 to P180). On the other hand, MsrB2 knock-out mice, from P16 to P180, did not exhibit any hearing deficit at all frequencies tested (8, 16, 24, 32 and 40kHz). A closer look at the organ of Corti epithelium of MsrA and MsrB1 knock-out mice did not reveal any apparent cytoarchitecture, hair cells or stereocilia abnormalities, compared to their control littermates. These data taken together with the absence of gross abnormalities observed in the stria vascularis and spiral ganglion suggest a more subtle alteration of the auditory apparatus. In both mutant mice, concomitant with the expression pattern of these two proteins in the spiral ganglion neurons and inner hair cells, MsrA and MsrB1 deficiency lead to wave 1 amplitude decrease at all tested frequencies, as early as P30. Taken together, our data show that the loss of MsrA or MsrB1 impact hearing ability and the observed deficit progresses with age. This study highlights that despite their common function and importance to maintain redox balance, Msr proteins play differential roles in the auditory pathway.

PS 695**A Single Cell Transcriptomic Characterization of the Stria Vascularis and Lateral Wall from the Adult Mouse Cochlea**

Jonathan B. Sellon; Kathy S. So; Gabriela Pregernig; Matthew Nguyen; Adam T. Palermo; John Lee; Joseph C. Burns

Decibel Therapeutics

The stria vascularis and cochlear lateral wall are widely believed to be essential for maintaining both endocochlear potential and the barrier between systemic circulation and inner ear fluids. Marginal (MCs), intermediate (ICs), and basal cells (BCs) of the stria vascularis have been shown to regulate both potassium concentration in endolymph and within the interstitial space. The blood-labyrinth barrier (BLB) has been shown to be maintained by endothelial cells (ECs) connected via tight junctions, an underlying basement membrane, pericytes (PCs), and perivascular-resident macrophage-like melanocytes (PVM/Ms). With age, strial capillaries have been shown to retreat coupled with significant declines in endocochlear potential. While the various cell types and functions of the stria vascularis have been characterized, the underlying transcriptional pathways controlling permeability of the BLB and maintenance of endocochlear potential have been largely uncharacterized.

To better understand how the ear maintains endocochlear potential and BLB integrity we conducted whole transcriptome profiling of the stria vascularis and lateral wall from the adult CBA/CaJ mouse (12 weeks old) cochlea using our previously optimized dissociation protocols for high-throughput single-cell RNA-Seq (scRNA-Seq). With our isolation techniques, we capture ~3,500 single cells per cochlea with ~2,000 genes detected per cell. Using an unbiased clustering approach and known cell type markers we characterize a wide variety of cell types in the stria vascularis including MCs, ICs, and BCs as well as ECs, PCs, and macrophages of the vasculature. Additional cell types characterized include immune cells, fibrocytes, and mesenchymal cells. To better understand transport properties of compounds through the BLB we examine a variety of drug related transporters, surface proteins, and other surface receptors of these cells. Furthermore, we compare transcriptional profiles of ECs in the strial vasculature to those surrounding spiral ganglion neurons from a separate single cell isolation to examine transport properties of ECs bordering endolymph spaces compared to those bordering perilymph spaces. Using this characterization we hope to understand the transcriptional pathways involved in strial damage as well as better predict and modulate compound permeability through the BLB into endolymph and perilymph spaces.

PS 696**Single Cell RNA Sequencing of Immortalized Multipotent Otic Progenitors**

Joseph Fantuzzo; Zhichao Song; Azadeh Jadali; Ronald Hart; **Kelvin Kwan**
Rutgers University

The inner ear is responsible for our ability to hear and balance. Encased in a bony labyrinth, the cochlea is the auditory organ that allows us to hear complex sounds and discern speech. Spiral ganglion neurons (SGNs) relay neural signals from the cochlea to the cochlear nucleus and is essential part of the auditory circuit. Improper development or damage to SGNs results in cell death and causes hearing loss. Use of otic progenitors to replace damaged SGNs is potential avenue for regeneration. Understanding the molecular changes in otic progenitors as they differentiate into neurons will accelerate efforts for regeneration. To understand this process, immortalized multipotent otic progenitors (iMOPs) were employed for single cell RNA sequencing (RNA-seq).

iMOP cells are clonal cell lines derived from developing murine otic progenitors. Under the appropriate culture conditions, iMOPs can differentiate into cells with bipolar neuronal morphology and fire action potentials. Even though iMOP cultures contain over 90% neuronal β -tubulin (TUBB3) expressing cells, the cultures are heterogenous because they contain cells at different stages of neuronal differentiation. Single-cell RNA-seq provided an unbiased classification of distinct populations of differentiating cells by employing dimensionality reduction methods for clustering. Analysis revealed at least three distinct cell populations during iMOP neuronal differentiation. The transcriptome changes between distinct cell populations predicted a differentiation trajectory from an otic progenitor into a neuron. Validation of the transcriptome changes using stranded RNA-seq and fluorescence in situ hybridization provided additional insight into the molecular mechanisms that underlie neuronal differentiation.

PS 697**Comparative Analysis of the Inner Ear Transcriptome Between Postnatal Days 2 and 7 using Single Cell RNA-seq**

Kevin Rose; Brian Herb; Yang Song; Beatrice Milon; Seth Ament; Ronna Hertzano
University of Maryland, Baltimore - School of Medicine

Sensory hair cells located in the inner ear are mechanoreceptors essential for hearing and balance. Loss of these sensory hair cells is a final common pathway in most forms of hearing loss and results in

permanent hearing impairment in both human and mouse as they do not spontaneously regenerate in mature mammals. In Contrast, early postnatal inner ear supporting cells are still able to differentiate into new hair cells in mouse but supporting cells lose this ability shortly after birth. Here we aim to better understand the gene expression differences between two postnatal time points (P2 and P7) where supporting cells can and cannot differentiate into hair cells. To obtain a global understanding, we have dissociated sensory epithelia from P2 and P7 wild type mouse cochleae and utricles and profiled gene expression in 445-4813 single-cells using the 10X Genomics Chromium platform. Here we report our analysis comparing gene expression in the various cell types identified using our approach between P2 and P7 as well as additional downstream gene regulatory analyses. We further provide full access to the analyzed dataset through the gEAR portal (umgear.org).

PS 698

Exploring the Roles of RFX 1, 3, and 7 Alone and in Concert in Hearing and Balance

Kathleen Gwilliam¹; Beatrice Milon²; Saumil Sethna³; Mark McMurray²; Sarath Vijayakumar⁴; Zachary Margulies¹; Sherri M. Jones⁴; Zubair M. Ahmed⁵; Ronna Hertzano²

¹University of Maryland, Baltimore-School of Medicine;

²University of Maryland Baltimore-School of Medicine;

³University of Maryland Baltimore; ⁴University of Nebraska Lincoln-College of Education and Human Sciences; ⁵University of Maryland, School of Medicine

The regulatory factor X (RFX) family consists of eight transcription factors, RFX1-RFX8, that are divided into four groups based on their functional domains and bind to the X-box promoter motif of genes to regulate transcription. Previous work from our laboratory has found a strong enrichment of the RFX binding motif in the promoter regions of newborn mouse inner ear hair cell-expressed genes. This enrichment suggests a potential role for the RFX family of transcription factors in the development and maintenance of the inner ear hair cells.

RFX1 and RFX3 are members of Group 1 of the RFX transcription factors, with RFX3 showing the highest expression out of the RFX members in P1 mouse hair cells. We established a double conditional knockout of Rfx1/3 from hair cells using the Gfi1-Cre mouse. This mouse had profound hearing loss secondary to rapid loss of outer hair cells throughout the length of the cochlear duct following the onset of hearing, between P12-14. RFX7 is the second highest RFX expressed in P1 mouse hair cells. Although not entirely identical

in terms of all functional domains, RFX7, a member of Group 3, includes the same DNA binding domain as RFX 1 and RFX3.

Here we further characterize the roles of Rfx1/3 in hair cell development using the Myo15-Cre and PrestinCreERT2 mouse models. Our data indicate that conditional deletion of Rfx1/3 up to P4 results in an early profound hearing loss, whereas deletion of these transcription factors from hair cells after P8 does not affect hearing. In addition, we generated conditional knockout mice for Rfx7 alone and in combination with Rfx1 or Rfx3. Our data show that while Rfx7 is highly expressed in hair cells, these conditional knockout mice have normal hearing and vestibular function.

These data support an established role for Group 1 of the RFX transcription factors in hearing. Ongoing work in the laboratory is focused on identifying the transcriptional cascade downstream of the RFX transcription factors in hair cells and other RFX combinations that may play a role in development of the vestibular hair cells.

PS 699

A Genome Wide Association Study in the UK Biobank Cohort Identifies a Large Number of Genome-wide Significant Loci Linked to Self-Reported Adult Hearing Ability

Helena RR. Wells¹; Maxim MB. Freidin¹; Fatin N. Zainul Abidin²; Antony Payton³; Piers Dawes⁴; Kevin Munro⁵; Cynthia C. Morton⁶; David R. Moore⁷; Frances MK. Williams¹; Sally J Dawson²

¹Department of Twin Research & Genetic Epidemiology, King's College London.; ²UCL Ear Institute, University College London.; ³Centre for Epidemiology, Division of Population Health, Health Services Research & Primary Care, The University of Manchester.; ⁴Manchester Centre for Audiology and Deafness, The University of Manchester.; ⁵The University of Manchester; ⁶Brigham and Women's Hospital, Harvard Medical School; ⁷Cincinnati Children's Hospital and the University of Cincinnati

Background

Age-related hearing impairment (ARHI) is the most common sensory impairment in the aging population; over a third of individuals develop this complex trait by the age of 65. It is a multifactorial disorder with both genetic and environmental components, with estimates of heritability ranging between 35 to 55%. It is expected to be a highly heterogeneous trait given that over 150 genetic loci have been identified in non-syndromic hereditary hearing loss alone. Previous genetic studies into ARHI have successfully identified a number of

promising candidate genes although only a very small number have reached genome-wide significance. However, replication of these findings across cohorts has been limited possibly due to varied phenotyping approaches and restricted sample sizes for genome wide analysis.

Methods

We performed two genome-wide association studies (GWAS) using self-reported hearing data from the UK Biobank (UKBB) study involving over 500,000 volunteers recruited between 40-69 years of age. Using a case control design we categorised participants based on answers to questionnaires regarding hearing ability (n=498,281) and hearing aid use (n=316,629). The 500,000 samples in the UK Biobank cohort were genotyped on one of two arrays; the Affymetrix UK BiLEVE Axiom array and the Affymetrix UK Biobank Axiom® array. The two arrays shared 95% coverage resulting in >800,000 genotyped SNPs. Imputation was carried out centrally by UKBB, primarily using the HRC reference panel and IMPUTE2. A linear mixed models approach was used to test for association between a total of 9,740,198 SNPs and the two hearing traits in white British participants. Final case control sample sizes for the association analysis were n=250,389 for self-reported hearing ability and n=253,918 for self-reported hearing aid use.

Results

A large number of SNPs were associated at genome-wide significant levels ($P < 5E-08$): 2,080 SNPs with hearing ability and 240 SNPs with hearing aid use. Conditional analysis with GCTA-COJO confirmed that these results represent at least 40 independent genome-wide significant loci. A number of these loci contain genes previously linked to congenital hearing loss such as EYA4, LMX1A and TRIOBP, however most loci appear to be novel associations with hearing.

Conclusion

Our study provides a new insight into genes which underlie susceptibility to adult hearing loss and thereby may be a first step towards a greater understanding of the pathological mechanisms involved.

PS 700

New Year, New gEAR: Better Performance, New Features, and More Data

Joshua Orvis¹; Brian Gottfried¹; Dustin Olley¹; Jayaram Kancherla²; Beatrice Milon¹; Yang Song¹; Hector Corrada-Bravo²; Anup Mahurkar¹; Ronna Hertzano¹

¹University of Maryland Baltimore-School of Medicine;

²University of Maryland College Park

The gene Expression Analysis Resource (gEAR) is an online portal for multi-omic data visualization, sharing, and analysis, and is supported by the NIDCD and the Hearing Restoration Project (HRP) to promote discovery in hearing research. In 2018, gEAR simultaneously faced a rapid expansion of its user base (over 300 active users) and a logarithmic increase in the scale of expression data uploaded to its database. The adoption of single-cell RNA-sequencing (scRNA-seq) techniques brings exciting new opportunities for analysis tools and consequently, new requirements for its large volume of data. In order to satisfy these requirements, we addressed major infrastructure bottlenecks by switching from relational databases to storing expression data in a fast, efficient binary data format. This improved performance across gEAR and in the new data uploader where scRNA-seq data can upload in minutes rather than hours.

Our scRNA-seq tool allows researchers to get quick preliminary analysis results with no programming experience. Analyses can be curated, saved, shared privately with others, or made public for direct referencing in a manuscript. Users also have greater flexibility in configuring how their datasets should best be presented. This includes customizing colors, new interactive plots, and the ability to toggle between available visualizations. We have also improved upon our integration with Epiviz, an interactive exploratory analysis tool for epigenetic data. The Epiviz genome browser supports genome navigation and allows multiple visualizations of data within genomic regions. Users can upload their epigenetic data and have it displayed in an Epiviz environment within their profile.

Finally, in addition to improving performance and features, over 40 published datasets have been curated and uploaded to allow users to perform a greater range of comparative analyses. The datasets include expression data from microarray, bulk RNA-seq, sequencing of sorted cells, scRNA-seq, and microRNA experiments from mouse, chick, zebrafish and human. The reference annotation has also been refactored to better support experiments in a variety of organisms and a history of Ensembl releases (currently 85-93).

PS 701

Systems Genetic Analysis of ABR Thresholds in The BXD Family of Mice Defines New Modulators of Age-Related Hearing Loss

Qing Yin Zheng¹; Fuyi Xu²; Xinyuan Ma¹; Eena Cheng¹; Weinan Du¹; Robert W. Williams²; Lu Lu²
¹Case Western Reserve University; ²University of Tennessee Health Science Center

The auditory brainstem response (ABR) test provides a non-invasive electroencephalographic assay of the inner ear and central auditory function in both man and mouse. A continuous series of brief pure tone pips (from 0 up to ~100 decibel) is presented to an anesthetized mouse at 29.3 per second; each stimulus evokes waves of activity in the brainstem that are computer-averaged to differentiate them from non-auditory background voltages. The intensity of the pips is reduced in steps until an ABR can no longer be discerned, thereby defining an ABR threshold, closely related to the hearing threshold.

Here, we mapped variation in ABR thresholds across a panel of 51 BXD recombinant inbred strains of mice. The use of this family of isogenic strains permits precision mapping of gene variants that control audition. In addition, this resource provides tight integration and comparison of data sets obtained across environments and laboratories, and offers the possibility to study trait covariance by exploiting powerful on-line bioinformatics resources. We quantified ABR threshold traits in 161 cases (2–4 per strain and sex), all close to one year-of-age with sound stimuli at 8, 16, and 32 kHz. We identified a significant QTL on chromosome 16 at 57–75Mb that modulates ABR thresholds at 8, 16, and 32 kHz in both sexes (likelihood ratio statistic values of ~22, genome-wide P ahl (PMID: 9447922), ahl2(PMC2862211), ahl4(PMC2756338), ahl8 (PMC2836023) hearing loss loci, as well as other hearing modifiers (PMC2864026, PMC2858224, PMC2862212). To our surprise, even as late as 12 months-of-age several BXD strains had good hearing—ABR thresholds even lower than 35 dB. This is notable because both DBA/2J and C57BL/6J parental strains are almost deaf at 32 kHz, suggesting a hearing protective allele in the new ahl locus.

PS 702

Large-Scale Functional Genomics of Hearing & Vestibular Disorders in Zebrafish

Kaili Liu¹; Cassidy Petree¹; Teresa Requena¹; Prathishtha Varshney¹; Shawn M. Burgess²; Gaurav Varshney¹
¹Oklahoma Medical Research Foundation; ²National Human Genome Research Institute

Approximately 360 million people worldwide (5% of the world's population) are affected by hearing loss. Indeed, one in every 500-1000 newborns is affected by the sensorineural hearing loss, making it one of the most common birth defects. Hearing loss is associated with a substantially reduced quality of life and overall health. Low-cost genomic sequencing technologies continually identify new mutations associated with human hearing loss, but their functional validation is unacceptably slow. There is an urgent need to fill this knowledge gap, which is required to develop new treatments that arrest or reverse hearing loss and improve patient outcomes. We found that 94% of human hearing loss genes have an orthologue in zebrafish, suggesting high functional conservation. Zebrafish are an ideal model organism to study hearing loss, given their external embryonic development, transparent body, accessible inner ear and the presence of lateral line neuromasts, which are functionally analogous to mechanoreceptors of the mammalian inner ear. In addition, zebrafish have been shown to effectively recapitulate disease phenotypes. Numerous publications have demonstrated the efficacy of gene targeting in zebrafish using CRISPR/Cas9 including a variety of tools and methods for guide RNA synthesis and mutant identification. While all the published techniques work, not all approaches are readily scalable to increase throughput. We recently described a CRISPR/Cas9 based high-throughput mutagenesis and phenotyping pipeline in zebrafish. Using this pipeline, we generated the loss of function alleles in 80 hearing loss genes selected from the hereditaryhearingloss.org database. We will present the mutagenesis pipeline, and phenotyping data from selected candidate genes showing various hearing and vestibular defects.

PS 703

Open Chromatin Dynamics in Prosensory Cells of the Embryonic Mouse Cochlea

Brent A. Wilkerson; Leah VandenBosch; Alex D Chitsazan; Mathew Wilken; Thomas Reh; Olivia Bermingham-McDonogh
University of Washington

To elucidate transcriptional control mechanisms specifying the cochlear prosensory cells that generate the hair cells and support cells critical for hearing function, we are mapping the cis-regulatory elements such as promoters and enhancers that precisely orchestrate where, when and how genes are expressed. More specifically, we compared chromatin accessibility using ATAC-seq in sorted prosensory cells (Sox2-EGFP+) and non-sensory cells (Sox2-EGFP-) from isolated embryonic cochlear ducts. In prosensory cells, we find more open chromatin regions near genes known

to be spatially restricted in expression to the prosensory region of the cochlear duct including Sox2, Prox1, Isl1, Eya1, Lfng, Gata3 and Pou4f3. Furthermore, we find significant enrichment for the consensus binding sites of Sox2, Six1 and Gata3—transcription factors required for prosensory development—in open chromatin regions of sorted prosensory cells. Over 1,700 regions displayed differential accessibility with developmental time (E12, E14.5 and E16) in prosensory cells, with most changes in the E12-14.5 window. Correlation analysis showed that accessibility in prosensory cells was more highly correlated to that in nonsensory cells than to that in other embryonic tissues. Our results reveal a dynamic landscape of open chromatin in prosensory cells with many potential implications for gene expression, chromatin structure and transcription factor-binding.

PS 704

Simple and efficient copy number variant analysis method for the Ion AmpliSeq custom panel.

Shin-ya Nishio¹; Hideaki Moteki²; Shin-ichi Usami³
¹*Department of Hearing Implant Sciences, Shinshu University School of Medicine;* ²*Department of Otorhinolaryngology, School of Medicine, Shinshu University;* ³*Department of Otorhinolaryngology, Shinshu University School of Medicine*

Background

Recent advances in molecular genetic analysis using next-generation sequencing (NGS) have drastically accelerated the identification of disease-causing gene mutations. Most next-generation sequencing analyses of inherited diseases have mainly focused on single nucleotide variants and short indels, although, recently, structure variations including copy number variations have come to be considered an important cause of many different diseases. However, only a limited number of tools are available for multiplex PCR-based target genome enrichment.

Methods

We developed a simple and efficient copy number variation visualization method for Ion AmpliSeqTM target resequencing data. Unlike the hybridization capture-based target genome enrichment system, Ion AmpliSeqTM reads are multiplex PCR products, and each read generated by the same amplicon is quite uniform in length and position. Based on this feature, the depth of coverage information for each amplicon included in the barcode/amplicon coverage matrix file was used for copy number detection analysis. We also performed copy number analysis to investigate the utility of this method through the use of positive controls and a large Japanese hearing loss cohort.

Results

Using this method, we successfully confirmed previously reported copy number loss cases involving the STRC gene and copy number gain in trisomy 21 cases. We also performed copy number analysis of a large Japanese hearing loss cohort (2,475 patients) and identified many gene copy number variants. The most prevalent copy number variation was STRC gene copy number loss, with 129 patients carrying this copy number variation.

Conclusion

Our copy number visualization method for Ion AmpliSeqTM data can be utilized in efficient copy number analysis for the comparison of a large number of samples. This method is simple and requires only easy calculations using standard spreadsheet software.

PS 705

Efficient delivery of AAV into mammalian inner ear in vivo via trans-stapes injection in adult guinea pig

Yilai Shu¹; Jinghan Wang¹; Xi Gu¹; Yuanyuan Xue¹; Luo Guo¹; Wenyan Li¹; Renjie Chai²; Huawei Li¹
¹*ENT Institute and Otorhinolaryngology Department, Affiliated Eye and ENT Hospital, State Key Laboratory of Medical Neurobiology, Fudan University, Shanghai, China.* ²*NHC Key Laboratory of Hearing Medicine (Fudan University);* ²*Key Laboratory for Developmental Genes and Human Disease, Ministry of Education, Institute of Life Sciences, Southeast University.*

Introduction: Lack of efficient delivery system into mammalian inner ear remains a major barrier to the studies of gene therapy and mammalian inner ear function. Adeno-associated viral (AAV) vectors have become the vector of choice for gene delivery in animal models in vivo. We report here the study of an AAV, Anc80L65, which substantially increased delivery into mammalian inner ear cells in vivo in adult guinea pig trans-stapes (oval window) injection and trans-round window injection.

Methods: To evaluate the efficacy of Anc80L65 in vivo, we delivered Anc80L65 that carry a reporter gene GFP in adult guinea pig by microinjection trans-stapes (oval window) or trans-round window in vivo. Auditory brainstem response (ABR) was used to measure hearing, one month after infection. The tissues were harvested later for analysis. We evaluated inner ear cells of cochlear for GFP signal by immunolabeling.
Results: Microinjection of Anc80L65 to adult guinea pig cochlea resulted in GFP signal in 95% of cochlear inner and 84% outer hair cells in trans-round window injection group with 20 dB difference of ABR compare to uninjected ear. In contrast, there were 51% outer and 90% inner hair cells GFP positive in trans-stapes (oval

window) injection group and it showed preservation of hearing with ABR differences less than 10 dB.

Conclusion: AAV can be efficiently delivered into mammalian inner ear cells in vivo trans-stapes (oval window) injection and trans-round window injection in adult animal. Trans-stapes injection which is very similar to stapes surgery in human can preserve hearing. The system can be used as virus-based therapy including regeneration and gene therapy in mammalian inner ear. We Established AAV-mediated gene therapy that can effectively transduce adult animal models toward its application as a potential therapy in human adult hearing loss.

Inner Ear: Drug Delivery

PS 706

Inner Ear and Serum Kinetics of the Ototoxin, 2-Hydroxypropyl-Beta-Cyclodextrin, Delivered via Intravenous, Intrathecal, and Intranasal Routes in the Mouse

Mark A. Crumling¹; Kristin M. Bullock²; Kim M. Hansen²; Michelle A. Erickson²; Anzela Niraula²; William A. Banks²; R. Keith Duncan¹

¹University of Michigan; ²Veterans Affairs Puget Sound Health Care System and University of Washington

A newly identified ototoxin, 2-hydroxypropyl-beta-cyclodextrin (HPBCD), is currently the most promising treatment for Niemann-Pick Disease Type C. Though visceral abnormalities are common in the disease, neurological manifestations are the cause of premature fatality. Various strategies have been employed to overcome poor uptake of HPBCD by the brain due to limited blood-brain barrier (BBB) permeability. In compassionate use trials, high intravenous (IV) doses have been used—with limited success—to penetrate the BBB with enough drug to treat neurological symptoms. In Phase 1-3 clinical trials, intrathecal (IT) delivery of HPBCD has given promising results in slowing disease progression, but all patients acquired significant hearing loss. An improved method of delivering HPBCD to the brain is needed. In this study, we compared the pharmacokinetics of IV and IT drug delivery with intranasal (IN) injections of HPBCD, hypothesizing that delivery to the brain via the nasal cavity would circumvent the BBB while limiting exposure to the inner ear. We used carbon-14 labeled HPBCD to examine the time course of serum and inner-ear HPBCD content after IV, IT, and IN administration in CD-1 mice. For each route, 10⁶ dpm (67 µg) of 14C-HPBCD was given, and HPBCD levels in serum and whole inner ear samples were determined by scintillation counting. For serum, IV and IT dosing produced similar kinetics, both approximating

exponential decay from a peak that occurred in minutes post-injection. IN administration resulted in a relatively linear increase in serum HPBCD over 2 hours, suggesting slow and minimal uptake by vasculature. For the inner ear, IV gave HPBCD concentrations that were about a tenth of serum, paralleling the serum time course. IT delivery resulted in ear concentrations that were about a tenth of serum, but they were essentially constant over two hours, perhaps reflecting direct communication of CSF and intracochlear fluids via the cochlear aqueduct. The peak inner-ear levels for IV and IT were approximately the same. IN delivery, however, resulted in a scatter of inner-ear HPBCD levels with no clear relationship to time, ranging from well below to far above the amounts seen with the other two delivery routes. This could be the consequence of variable uptake by or along olfactory/trigeminal neurons to give better or poorer access to CSF, or reflect access of the drug solution to the middle ear via the Eustachian tube, allowing very high or low inner ear levels depending on contact with the membranous windows.

PS 707

Development of Robust In Vitro and Ex Vivo Assays to Support Drug Discovery Programs

Ryan C. McCarthy; Changsuk Moon; Tian Yang; Noah Druckenbrod; Emma Alterman; Yong Ren; Joseph C. Burns; Janeta V. Popovici-Muller; Inmaculada Silos-Santiago

Decibel Therapeutics

The development of a robust toolbox of in vitro and ex vivo assays to support drug discovery are essential in preclinical research. Efficiently building confidence towards a set of therapeutic compounds requires the use of multiple in vitro and ex vivo assays that range in complexity and throughput. Here, we describe a series of assays developed to further our understanding of spiral ganglion neuron (SGN) response to exogenous therapeutics. The assays built out for the analysis of SGN neurite initiation, elongation, and/or synapse formation include: Neuro2a cells, primary dissociated SGNs, neonatal SGN explant cultures, adult modiolus explant cultures, and neonatal organotypic synapse assay. Neuro2a cells are derived from murine neuroblastoma and are described here as a more high-throughput method for initial compound testing. Primary murine dissociated SGN provide readouts including SGN survival, neurite initiation, and mean neurite length in response to compounds while neurite length is the primary readout for compound testing in the neonatal and adult explant cultures. A major advantage of using the neonatal organotypic synapse assay is that synapses can be visualized before and after exposure to neuroexcitatory molecules such as kainic acid and

glutamate. These assays vary in their physiological relevance, complexity, throughput, and responses to compounds and/or biologics. Here, we describe the development of each assay, their individual readouts, and summarize the advantages and disadvantages of each.

A major goal for the development of these assays was to build a robust and reliable pipeline of assays to quantify neurite outgrowth. Neurite outgrowth was quantified across all the assays in response to a variety of compounds and biologics. Through our testing of several classes of compounds we observed a clear heterogeneity in responses between assays. We demonstrate this heterogeneity here by highlighting neurite outgrowth quantification in response to two groups of therapeutics; neurotrophins and Rho-associated protein kinase (ROCK) inhibitors. Taken together, the variation in neurite outgrowth in response to compound treatment amongst these assays indicates that one must be cognizant of the possibility that their lead target or pathway will not be available or active in every assay.

PS 708

Distribution and Retention of Neurotrophin-3 in Cochlea

Qi-Ying Hu¹; Rachael Richardson²; Andrew Wise³; Rachel Stewart⁴; John Lee¹; Fuxin Shi¹

¹Decibel Therapeutics; ²1. Bionics Institute 2.

University of Melbourne, Department of Medical Bionics; ³1. Bionics Institute 2. University of Melbourne, Department of Medical Bionics; ⁴InviCRO

Hearing loss is one of the most common disabilities worldwide, however no approved treatment is currently available. Endogenous growth factors are established, successful therapeutic modalities in drug discovery, and while the neurotrophin family of proteins has been extensively studied as potential therapies, including for hearing loss, a systematic study of neurotrophin-3 (NT3) disposition in the inner ear has been lacking.

A number of studies, using both in life and staggered terminal imaging approaches were conducted to evaluate the cochlear distribution and retention of NT3.

Prior to the NT3 studies, capability of in life imaging of mouse cochlea via MicroCT to produce high resolution visualization and quantification of a mouse cochlea was confirmed. The cochlear distribution and retention of an iodinated contrast agent was measured and quantified in life over 6 hours following an intra-labyrinth infusion through the posterior semicircular canal.

Single-photon emission computed tomography (SPECT) offers higher sensitivity for quantification over CT. Single photon emission computerized tomography SPECT was utilized to assess the tissue distribution and retention of [125I] NT3, when administered via direct infusion into the posterior semicircular canal of adult mice. Via SPECT, in-life radioactivity was measured in the cochlea, the semi-circular canals, the rostral head, spine, and thyroid over 72 hours. Subsequently, the animals were further assessed via autoradiography. Animals were sectioned, and white light and autoradiographic images were acquired. Autoradiography revealed cochlear and semi-circular canal [125I] NT3 levels orders of magnitude higher relative to systemic levels.

In a separate study, the [125I] NT3 was infused into cochlea via cochleostomy at the base turn in adult guinea pigs. The effect of infusion volume, rate, and concentration on cochlea perilymph concentrations of NT3 over 2 weeks was assessed following a single infusion. Cochleae were harvested at various time points between 15 minutes and 2 weeks, and gamma radiation measurements were obtained from the whole cochlea as a means to determine the amount of NT3 remaining in the cochlea. Smaller volumes, slower infusion rates, and higher concentration resulted in higher levels of NT3, as measured by radioactive counts. Autoradiography on cochlear micro-sections was then used to acquire high resolution images. NT3 was detected in all the turns with highest concentration in the base.

In summary, two delivery routes in two rodent species revealed a similar retention and distribution profile for NT3 in the cochlea. The concentration gradient from base to apex was different for cochleostomy as opposed to the canalostomy. This study provides important disposition baseline on NT3 for the development of therapies for hearing loss. The methodology developed in this study will also be valuable for comparing drug delivery platforms for the cochlea.

PS 709

Functional Improvement and Target Engagement in Mouse Model of Synaptopathy Following Sustained Exposure via AAV8-Ntf3 Delivery

Trang Nguyen¹; Xichun Zhang¹; Lillian Smith¹; Changsuk Moon¹; Matthew Nguyen¹; Joseph Manna¹; Ning Pan¹; Guo-Peng Wang²; David Kohrman³; Gabriel Corfas⁴; Joseph C. Burns¹; Janeta V. Popovici-Muller¹; Inmaculada Silos-Santiago¹

¹Decibel Therapeutics; ²Kresge Hearing Research Institute, Dept. of Otolaryngology Head and Neck Surgery. University of Michigan; ³Kresge Hearing Research Institute, Dept. of Otolaryngology Head and Neck Surgery. University of Michigan; ⁴Dept. of

Neurotrophin-3 (NT3) is a neurotrophic factor known to support the survival and axonal growth of spiral ganglion neurons during development. Recent studies have indicated that NT3 can protect the cochlea from noise induced synaptopathy; however, sustained delivery to the inner ear remains a hurdle. In this study, we have used AAVs as an approach to deliver Ntf3 to the inner ear for a prolonged period of time.

CBA-CaJ mice administered with an intra-labyrinth (IL) injection of AAV8-Ntf3, two weeks before exposure to 97 dB noise, were found to have improved Auditory Brainstem Response (ABR) wave1 amplitude compared to control groups.

Levels of NT3 protein were quantified by ELISA and mRNA levels of Ntf3 and Vgf by qPCR. Intra-labyrinth administration of AAV8-Ntf3 resulted in increased Ntf3 mRNA levels in cochlear tissues as well as NT3 protein levels in the perilymph. In addition, mRNA levels of Vgf, a biomarker of neurotrophin activity, were increased in cochlear tissues. RNAscope was utilized to identify the cell types in the injected inner ear that expressed the Ntf3 transgene and Vgf. Both Ntf3 transgene and Vgf were found to be highly expressed in the spiral ganglion neurons.

AAV8-Ntf3 provides an excellent approach to deliver consistent levels of NT3 and maintain sustained exposure in the inner ear.

PS 710

Tropism of Engineered Serotypes in Adult Rodent Cochlea: Towards Translationally Relevant Vectors

Ning Pan; Kathryn Ellis; Xichun Zhang; Nancy Paz; Joseph C. Burns; Adam T. Palermo; Jonathon Whitton
Decibel Therapeutics

The development of AAV-based gene therapies for hearing and balance disorders depends on the identification of serotypes that target relevant cell-types in rodent models and primates. Previous studies have comprehensively assessed the tropism of natural AAVs in the neonatal and the adult cochlea. These studies have generally found that while many serotypes transfect inner hair cells in neonatal and adult rodents, outer hair cells are poorly transfected in adult rodent cochleae. While neonatal cochlear tropism is important for discovery efforts, the adult rodent ear has greater translational significance given the mapping between inner ear development in the altricial mouse and precocious humans.

Through directed evolution and rational design, several hyperinfective serotypes have been identified for the retina in rodents. In this survey, we assessed the tropism of natural and engineered serotypes in the adult rodent ear and identified several translationally relevant candidates that targeted inner hair cells, outer hair cells, and spiral ganglion neurons. Follow-up experiments will assess serotype tropism in primates.

PS 711

Factors Effecting Viral Vector-Mediated Gene Expression in the Cochlea

Sara Talaei¹; Anthony J. Ricci²

¹Stanford University - Department of Otolaryngology, Head and Neck Surgery; ²Stanford University

Gene delivery into the cochlea using viral vectors is a developing technology with multiple applications for the inner ear. Adeno-associated viruses (AAVs) are popular vectors because they are nonpathogenic, produce long-term gene expression and are capable of infecting most cell types. While there have been reports on gene expression variability due to application of different AAV types and injection methods including round window membrane injection, cochleostomy and canalostomy (Kawamoto et al., 2001, Yoshimura et al., 2018), more data is required for understanding the impact of parameters such as injection volume, animal strain and post-injection incubation time.

We investigated these parameters after injecting AAV DJ (Grimm et al., 2008) for expressing GFP in cochlear cells. By injecting 1 μ l AAV DJ with CMV promoter into the vestibular canal of C57/BL6 mice at P1, the percentage of infected inner hair cells (IHCs) and outer hair cells (OHCs) in the apex of cochlea were 73 \pm 20 (n=43) and 20 \pm 10 (n=40), respectively. There was no increase in number of infected HCs, from 1 to 10 weeks after injection. However, the intensity of expressed GFP in HCs was increased over time (e.g. 5 weeks after injection, the average fluorescent intensity was almost 5 times greater than the intensity at 2 weeks). In the contralateral cochlea less than 1% of HCs expressed GFP, suggesting that vectors could escape from the injected ear within the perilymphatic space to the contralateral ear, likely via the cochlea aqueduct (Stover et al., 2000). Increasing the injection volume from 1 to 2 μ l, raised the percentage of infected HCs significantly (i.e. IHCs from 80 \pm 11 (n=8) to 94 \pm 6 (n=8) and OHCs from 21 \pm 9 (n=6) to 43 \pm 2 (n=5)). There was no significant difference in hearing thresholds between groups. We also observed that 5 weeks after injection, the percentage of infected OHCs in CD1 mice was higher than C57/BL6 mice (i.e. 38 \pm 18 (n=9) compared to 19.8 \pm 10 (n=9)).

We conclude that AAV DJ is a potent vector for transducing cochlear cells. The onset of gene expression in-vivo, can happen as early as 1 week and last for at least 10 weeks after injection. Increasing the injection volume can increase the transduction rate, and gene expression levels can vary between strains.

Acknowledgements: NIH-NIDCD RO1 DC009913, Stanford Medicine Dean's Postdoctoral Fellowship, NIH-NIDCD core grant DC010363, Stanford OHNS core facilities supported by the Stanford Initiative to Cure Hearing Loss through the Bill and Susan Oberndorf foundation

PS 712

Gene Therapy Rescues Auditory and Vestibular Function in A Mouse Model with A Null Mutation of Ush1c Gene

Weinan Du¹; Gwenaelle S. Geleoc²; Quinn McDermott¹; Chelsea Zheng¹; Zihao Yu¹; Qing Yin Zheng¹

¹Case Western Reserve University; ²Boston Children's Hospital, Harvard Medical School

Usher syndrome type 1C (USH1C) is characterized by profound sensorineural deafness, vestibular dysfunction and childhood onset of retinitis pigmentosa. USH1C is associated with mutations in the USH1C gene which encodes for harmonin, a protein expressed in sensory hair cells of the ear and photoreceptor cells of the eye. Several USH1C mutations lead to absence of protein expression. Our goal is to assess gene replacement therapy for the treatment of USH1C associated with such mutations. For this purpose, our laboratory has established a novel Ush1c knockout (KO) mouse model by traditional gene targeting approach (Tian C et al, PMID: PMC2907663). Ush1c KO mice lack harmonin and display congenital deafness and vestibular dysfunction (circling behavior). To assess gene replacement therapy, we injected the harmonin vector (AAV2/Anc80L65.CMV.HarmB1.hGH) via semicircular canal microinjection at postnatal day 2 pups. At 4 weeks after microinjection, we measured Auditory Brainstem Responses (ABR) and performed several behavioral assays. Our results demonstrate improvement of auditory thresholds, along with reduced circling behavior and improved swimming capabilities in the treated Ush1c KO mice. Some unique gene rescuing features in this model will be further confirmed and reported. The data presented here suggest a biological method to restore the loss of function of Ush1c gene in a mouse model of Usher Syndrome.

PS 713

Biocompatibility and Permeability of Upconversion Nanoparticles into the Inner Ear following Transtympanic Administration in a Rat Model.

Rahul Mittal; Emre Ocak; Stefanie A. Peña; Mario M. Perdomo; Hannah Marwede; Jeenu Mittal; Adrien A. Eshraghi

University of Miami Miller School of Medicine

Introduction: Nanoparticle (NP) based drug delivery holds a great potential as a therapeutic strategy for auditory diseases. Although a number of NPs are available, upconversion NPs (UCNPs) offer several advantages such as high penetration depth, low autofluorescence background, higher drug retention property, large anti-stokes shifts, sharp emission bandwidths, and high photostability. However, before UCNPs can be used for inner ear drug delivery, it is essential to determine their ototoxicity, biocompatibility and permeability in the cochlea following transtympanic administration. The aim of the present study was to determine the effect of non-surgical administration of UCNPs through transtympanic delivery on the cochlear function and to assess any adverse effects on the auditory system. We also determined the bio-distribution of UCNPs in the various cochlear compartments.

Methods: UCNPs were injected transtympanically into rats. Rats that received phosphate buffer saline (PBS) or no injection served as the control group. Cochleae were harvested from UCNPs treated or control group and subjected to FITC phalloidin staining to visualize hair cells. Hearing thresholds were determined by Auditory Brainstem Recordings (ABRs) and Distortion Product Otoacoustic Emissions (DPOAEs). The presence of luminescent UCNPs inside cochlea was also determined. Cochleae were also subjected to histopathological examination to determine any pathological manifestations of UCNPs.

Results: We observed that UCNPs have no adverse effect on cochlea as there was no significant difference in the number of hair cells between UCNPs treated and control group. ABR thresholds and DPOAEs amplitudes did not differ significantly between UCNPs treated and control group. We also observed that transtympanic administration of UCNPs lead to their permeability into the inner ear. There were no pathological manifestations observed in the inner ears of rats receiving transtympanic administration of UCNPs similar to PBS-injected and control group.

Conclusion: The results of this study suggests that UCNPs are biocompatible with cochlea and do not exert any adverse effect on hearing function in our

rat model. Our data also suggests that transtympanic administration leads to permeability of nanoparticles into the inner ear and this delivery method appear to be promising for future use in clinical otology. The results of this study will lay the foundation for developing UCNPs based novel treatment modalities for auditory disorders.

PS 714

Demonstration of a Wirelessly-Controlled Implantable Microsystem with Refillable Reservoir for Murine Inner Ear Drug Delivery

Farzad Forouzandeh¹; Xiaoxia Zhu²; Meng-Chun Hsu¹; Joseph P. Walton³; Denis Cormier¹; Robert D. Frisina²; David A. Borkholder¹

¹Rochester Institute of Technology; ²Medical Engineering Dept., Global Center for Hearing & Speech Research, University of South Florida; ³Communication Sciences & Disorders Dept., Medical Engineering Dept., Global Center for Hearing & Speech Research, University of South Florida

Recent advances in protective and restorative biotherapies have created new opportunities to address auditory and vestibular disorders with site-directed, programmable drug delivery systems. Successful therapy development leveraging the transgenic, knock-in, and knock-out variants of human disease in the mouse model system requires advanced microsystems specifically designed to function with nanoliter precision and with system volumes suitable for implantation. Here we present a novel biocompatible, fully implantable, and scalable microsystem consisting of a phase-change peristaltic micropump and a refillable microreservoir. The structure of the peristaltic micropump is built around a commercially available catheter microtubing (250µm OD, 125µm ID), which can provide a biocompatible leak-free flow path while avoiding complicated microfluidic interconnects. In vitro pump characterization results are presented, demonstrating nanoliter resolution control over the drug delivery flow rate in the desired flow rates range (10-100 nL/min) by changing the actuation frequency. It is also shown that the presence of up to 10× maximum physiological backpressure (5 kPa), or a ±3 °C variation in the ambient temperature do not significantly affect micropump functionality. The microreservoir consists of a refilling port and a cavity area, fabricated in a 3D-printed platform and coated with Parylene-C enabling long-term biocompatibility. A silicone-based septum refilling port is fabricated and fitted tightly in a 3D-printed angled cylinder space, enabling 200 injections without leakage under up to 100× backpressure (50 kPa). The cavity area is fabricated by having polyethylene glycol as a sacrificial layer between two Parylene layers. This Parylene encapsulated cavity holds the drug in a biocompatible medium with zero-restoring force. The

micropump and the microreservoir are integrated into a planar form factor single-compartment structure, suitable for subcutaneous implantation. Subcutaneous implantation results demonstrate successful refilling of the microreservoir, wireless communication for reprogramming, and delivery of salicylate to the round window membrane niche with measurement of real-time shifts in distortion product otoacoustic emission (DPOAE) thresholds and amplitudes (DPgrams). This implantable and programmable micropump technology specifically designed for the mouse model system is poised to enable an enhanced level of control for biotherapy development. This microsystem is inherently scalable to larger species and for clinical applications in humans by appropriate scaling of the microtubing size and actuator volume.

Supported by NIH NIDCD award R01 DC014568

PS 715

Optimization of Adeno-associated Virus Transduction in the Mouse Cochlea

Graham Casey¹; Mark Brimble²; Andrew Davidoff²; Bradley J. Walters³

¹University of Mississippi Medical Center; ²St. Jude Children's Research Hospital; ³UMMC

Sensorineural hearing loss is one of the most prevalent disabilities and can arise from many sources. Such prevalence necessitates effective tools for studying the molecular machinery of cochlear cells. One highly adopted method for expressing genes of interest (GOIs) is Adeno-Associated Virus (AAV). While there are numerous AAV serotypes, their efficacy varies greatly and high titers are often required to transduce a majority of cochlear hair cells. This inefficiency could be due to many factors as gene delivery via AAVs occurs through many steps. First, the viral particle must bind to cell surface receptors and be internalized. Next, the viral particles must avoid degradation machinery and translocate to the nucleus to achieve gene expression. Finally, a complementary strand of the viral DNA must be synthesized by the cell so that transcription of the GOI can occur. Here, in the context of infection of cultured neonatal mouse cochleae, we tested 4 different hypotheses that have been shown in other cell types to improve GOI expression from AAV. Specifically we tested whether GOI expression in cochlear cells could be enhanced by (1) liposomal packaging of AAVs (2) pharmacological inhibition of proteasomal degradation (3) Self-complementary viral DNA that can bypass second strand synthesis (4) treatment with the EGFR inhibitor Tyrphostin 23. To assess the efficacy of these different conditions we produced AAV constructs to express GFP driven by the CMV promoter. We then explanted cochleae from neonatal mice and cultured them for 24 hours before infecting with AAV with and without the treatments listed above. We tested these conditions with three different AAV

serotypes (AAV1, AAV2, and AAVAnc80). Interestingly, the only treatment condition that resulted in significantly improved GFP expression in the cochleae was the Self-complementary AAV configuration, consistently shown in many cell types to have this effect. Despite having also been shown to improve transduction of AAV in other cell types; neither the proteasome inhibitors tested, liposomal packaging of AAV, nor treatment with Tyrphostin 23, enhanced AAV expression when applied to cochlea cells in culture. These results suggest that to enhance transgene expression for a given construct in the cochlea, it may be a better strategy, where possible, to design a construct that fits within the 2.35kb packaging capacity of Self-complementary vectors, than to attempt to boost expression levels with these pharmacological agents.

PS 716

AAV2.7m8 is a Powerful Viral Vector for Inner Ear Gene Therapy

Kevin Isgrig¹; Devin McDougald²; Jianliang Zhu³; Hong Jun Wang³; Jean Bennett²; Wade W. Chien¹

¹NIDCD, Johns Hopkins University; ²Perelman School of Medicine; ³NIDCD

Background: Adeno-associated viruses (AAVs) are popular vector choices for gene delivery in the inner ear due to their excellent biosafety profiles. While conventional AAVs are capable of transducing inner hair cells (IHC) in the cochlea to varying degrees, outer hair cells (OHC) and supporting cells are transduced less efficiently. In this study, we examined the transduction patterns of three synthetic AAVs (AAV2.7m8, AAV8BP2, AAV-DJ) in the neonatal mouse inner ear.

Methods: Neonatal (P0-P5) CBA/J mice were used in this study. Synthetic AAV-GFPs were injected into mouse inner ear using the posterior semicircular canal approach. Immunohistochemistry was used to assess the infection efficiency. ABR was used to assess auditory function.

Results: AAV2.7m8 transduced both IHCs and OHCs with very high efficiency. AAV8BP2 transduced the IHCs with high efficiency, but the transduction efficiency of OHCs was lower. AAV-DJ transduced the IHCs and OHCs at low levels. AAV2.7m8 also transduced the inner pillar cells and inner phalangeal cells with high efficiency. Mice that underwent AAV2.7m8 injections had similar ABR thresholds compared to non-injected controls.

Conclusions: Our study showed AAV2.7m8 transduced both IHCs and OHCs at high efficacy. Furthermore, AAV2.7m8 transduced inner pillar cells and inner phalangeal cells with high efficacy, making AAV2.7m8 an excellent choice for gene therapy targeting both cochlear hair cells and supporting cells.

PS 717

Verification of Therapeutic and Adverse effect of Hyper-viscus Biogel for Intratympanic Drug Delivery

Myung-Whan Suh; Yu-Jung Hwang; Tae-Soo Noh; Moo Kyun Park; Jun Ho Lee; Seung-Ha Oh
Seoul National University Hospital

Objective

Intratympanic (IT) drug delivery is one of the mainstream treatment for hearing loss (HL). But since the drug is usually injected in a fluid form, it is easily drained through the Eustachian tube. If the drugs can be delivered through a vehicle that lasts longer in the middle ear, more drug may be delivered into the inner ear. In this study we tested the hearing outcome in ototoxic hearing loss animals and compared the incidence of adverse inflammatory reaction.

Methods

Young male SD rats were used. IT dexamethasone (D) was delivered via two different vehicles: saline+D (10mg/ml), hyper-viscus biogel+D (10mg/ml) and hearing loss control group served as the control. Before ototoxic hearing loss, rats were treated with IT drug/vehicle injection. After four days, cisplatin (2mg/kg), gentamycin (120mg/kg) and furosemide (90mg/kg) were injected intravenously for two consecutive days. ABR threshold was measured before and after hearing loss for 60 days. Serial micro CT and endoscopy of the TM was performed to evaluate the adverse reaction. Histologic sections of the middle ear mucosa and tympanic membrane were evaluated after 60 days. The number of outer and inner hair cells were evaluated by means of whole mount confocal microscopy.

Results

The drug lasted in the middle ear for 41.1 ± 27.0 d in the biogel+D group and 1.1 ± 0.3 d in the saline+D group. The tympanic membrane perforation healed completely after 16.7 ± 11.9 d in the biogel+D group and 21.6 ± 12.6 d in the saline+D group. One ear with infection was found at day 12 in the biogel+D group. The mean hearing improvement (Δ threshold) at day 45-60 in the biogel+D group (30.0 ± 12.7 and 31.7 ± 21.8 dB SPL) was slightly better than that of the saline+D group (12.5 ± 14.4 and 21.4 ± 15.2 dB SPL) in 8 and 16 kHz. Proportion of ears with meaningful hearing improvement (≥ 15 dB) was 80.0% (biogel+D), 83.3% (saline+D), and 50.0% (control) at 8 kHz. It was 83.3% (biogel+D), 66.7% (saline+D), and 50.0% (control) at 16 kHz. There was no evidence of inflammation or infection in the histologic

sections of the biogel+D and saline+D group. Number of hair cell count was similar among all three groups.

Conclusions

The vehicle/drug sustained longer in the middle ear when it was carried with the hyper-viscus biogel. The incidence of post-injection infection was very low with the hyper-viscus biogel. Also, there was no evidence of middle ear inflammation in the histologic section of the biogel+D group. The mean hearing improvement and proportion of meaningful hearing improvement was slightly better in the biogel+D group compared to those of the saline+D group and control group. Hyper-viscus biogel may be a good vehicle for IT inner ear drug delivery.

PS 718

Hyper-viscus Biogel Vehicle Can Enhance the Quality of Inner Ear MRI Imaging

Myung-Whan Suh; Yu-Jung Hwang; Mina Park; Tae-Soo Noh; Moo Kyun Park; Jun Ho Lee; Seung-Ha Oh
Seoul National University Hospital

Objective

Intratympanic (IT) gadolinium delivery is one method to image the inner ear with MRI. But since the gadolinium is usually injected in a fluid form, it is easily drained through the Eustachian tube. If the gadolinium can be delivered through a vehicle that lasts longer in the middle ear, more gadolinium may be delivered into the inner ear. This may result in a better image quality of the inner ear MRI. In this study we tested the amount of perilymphatic enhancement with gadolinium delivered via three different vehicles.

Methods

Gadolinium (Gd-DTPA, Magnevist® or Gd-DO3A-butrol, Gadovist®) was injected into the middle ear in 13 Sprague-Dawley rats via the transtympanic route. Three different vehicles were used: biogel 1 (hyper-viscus biogel), biogel 2 (commercial biogel), and saline. MR images of the inner ear were acquired at 1.0, 1.5, 2.0, 2.5, 3.0, and 3.5 after intratympanic (IT) injection using an 9.4T Agilent MRI system. As for biogel 1, MR images were acquired up to day 10 (n=8). The normalized signal intensity was quantitatively analyzed at the scala vestibuli (SV), scala media, and scala tympani (ST). Then the normalized signal intensities (SIs) were compared between the three vehicles.

Results

When biogel 1 and biogel 2 were compared, SI was greater in the ears injected with biogel 1 compared to that injected with biogel 2. This difference was

most pronounced in the SV of the apical turn at 1.5 hr (normalized SI 3.3 vs. 1.0). The same pattern of difference was identified through out the whole cochlea (apical to basal) in both perilymphatic spaces (ST and SV) from post injection 1.0 to 3.5 hr. When biogel 1 and saline was compared, SI was greater in the ears injected with biogel 1 compared to that injected with saline. This difference was most pronounced in the SV of the basal turn at 3.5 hr (normalized SI 7.20 vs. 3.81). More importantly, the high SI lasted for 7 days in the ears injected with biogel 1 in the basal turn (normalized SI 2.10 vs. 1.18).

Conclusions

MRI gadolinium enhancement of the inner ear was greater when hyper-viscus biogel was used as the IT drug delivery vehicle. It seems that hyper-viscus biogel can deliver higher concentration of gadolinium into the inner ear compared to the commercial biogel. Also, it seems that hyper-viscus biogel can deliver gadolinium into the inner ear for a longer duration compared to saline. This may demonstrate that hyper-viscus biogel can be an effective vehicle for inner ear drug delivery.

PS 719

Diffusion of Small Molecule in Thermoreversible Hydrogel Across a Perforated Membrane

Arnuparp Santimetaneedol; Zihan Wang; Daniel N. Arteaga; Aykut Aksit; Charlotte PrevotEAU; Michelle Yu; **Harry Chiang**; Dimitrios Fafalis; Anil K. Lalwani; Jeffrey W. Kysar
Columbia University

Microperforations have been suggested as a means for enhancing current methods of drug delivery into the inner ear. The most common technique, intratympanic injection, relies on diffusion of drug across the round window membrane, a process that can be highly variable thus leading to inconsistent response and frequent side effects. The thermoreversible hydrogel poloxamer 407 shows promise as a drug carrier that can minimize the variability in diffusion of drug. In this study, we investigate the role of multiple microperforations as an adjunct to poloxamer 407 in diffusion across a membrane. We use horizontal diffusion cells separated by an artificial membrane to model drug delivery across the round window membrane. Using our system, we compared the permeances of therapeutic material dissolved in poloxamer 407 versus in saline across the membrane, with and without microperforations. First, we found that our experimental apparatus provides reliable and repeatable measurements of diffusion across a membrane. Second, the permeance of therapeutic material in saline across an unperforated artificial membrane was an order of magnitude higher than that

in poloxamer 407. Third, the permeance of therapy in saline increased with each additional perforation and with larger total perforation cross-sectional area ($p < 0.007$ for all PBS-based experiments), but the same association was not found with poloxamer 407. Rather, in poloxamer 407 experiments, only a large perforation increased the permeance of therapy ($p < 0.0001$), but multiple small perforations did not ($p = 0.153$). These results confirm that for drug dissolved in saline, multiple small perforations are an effective method for enhancing therapy diffusion without the clinical risks of large perforations. However, for drug carried in poloxamer 407, larger perforations are necessary. Perforations of these size may result in undesired consequences and warrant further investigation for clinical use.

PS 720

AAV Mediated Gene Therapy Restores Partial Auditory Sensitivity in Mouse Models of Autosomal Recessive Non-Syndromic Deafness DFNB31 and Usher Syndrome type IID

Hannah Goldberg¹; Yukako Asai²; Bifeng Pan¹; Kevin Isgrig³; Jun Yang⁴; Wade W. Chien³; Gwenaëlle S. Geleoc¹

¹*Boston Children's Hospital, Harvard Medical School;*

²*Boston Children's Hospital, Harvard Medical School;*

³*NIDCD, Johns Hopkins University;* ⁴*University of Utah*

Background: The PDZ domain-containing protein whirlin (WHRN), encoded by the WHRN gene is essential for both hearing and vision. WHRN is implicated in the stabilization, elongation and maintenance of the stereociliary bundles of the sensory hair cells in the inner ear. Two major WHRN splice variants have been shown to be expressed in auditory hair cells: the full-length isoform (FL-WHRN) of the protein is located on the tip and shaft of the stereocilia in inner hair cells (IHCs) and the ankle link complex in outer hair cells (OHCs); the short isoform (C-WHRN) is restricted to the tips of the stereocilia in both IHCs and OHCs. Distinct disruptions of one or both of these isoforms lead to a variety of phenotypic configurations including Usher Syndrome type IID (USH2D) and autosomal recessive non-syndromic deafness 31 (DFNB31).

Methods: To assess the efficacy of novel gene therapy approaches in mouse models of USH2D and DFNB31 (whirler), we used a synthetic viral vector, Anc80L65, encapsulating gene sequences encoding for FL-WHRN and C-WHRN. USH2D mice received FL-WHRN, while DFNB31 mice received either FL-WHRN or a combination of FL-WHRN and C-WHRN via injection to the inner ear at P1 to induce expression of the transgene in vivo. Efficacy of the treatment was assessed by comparing uninjected DFNB31 and USH2D mutants versus injected mutants at the cellular and systems level with analysis

of mechanosensitive transduction currents, protein expression, hair cell survival and analysis of ABR and DPOAE.

Results: Injection of FL-WHRN in USH2D mice was associated with both improved mechanotransduction in OHCs and IHCs and hair bundle morphology as analyzed with SEM. ABR recovery was variable, down to 45 dB thresholds for the best performer. In DFNB31 mice, injections of combined FL-WHRN and C-WHRN versus FL-WHRN only, did not lead to improved outcomes. Our data demonstrate that treatment at P1 with FL-WHRN leads to significant increase in mechanotransduction currents in OHCs, recovery of expression and correct localization of whirlin to the tips and base of the stereocilia, and improved hair cell survival in adults. ABR recovery was again variable for either treatment with best performers responding to ~60 dB sound intensities.

Conclusion: The variability of the recovery noted for both mouse models is likely due to technical variations. However, significant improvements seen in the best performers demonstrate that gene replacement strategies are viable for treatment of mouse models of USH2D and DFNB31.

PS 721

Inner ear pharmacokinetics and tissue distribution of the sustained-exposure dexamethasone formulation OTIVIDEX in various species - Predicting drug exposure in Meniere's disease patients

Xiaobo Wang; Rayne Fernandez; Natalia Tsivkovskaia; Scott Coleman; Jennifer Hou; Fabrice Piu
Otonomy, Inc.

Background: A major limitation in the development of effective drug therapies for inner ear disorders resides in the inability to routinely sample the inner ear compartment (perilymph) in human subjects. Due to technical challenges, possible permanent adverse effects and overall ethical concerns, human inner ear pharmacokinetic data are extremely sparse. To date, a handful of studies have reported on the drug levels achieved in the inner ear following intratympanic and systemic administration (methylprednisolone, dexamethasone). To further our understanding of drug exposure in humans following intratympanic administration, pharmacokinetics studies were conducted with OTIVIDEX (also known as OTO-104). OTIVIDEX is a thermosensitive, sustained-exposure formulation of the steroid dexamethasone, that is currently being developed for the treatment of Meniere's disease vertigo. Inner ear pharmacokinetic data were obtained in several rodent and large animal species. The distribution profile of OTIVIDEX was also investigated by examining

additional otic tissues and the auditory system. Finally, using allometric scaling, drug exposure levels in the inner ear of Meniere's disease patients administered with OTIVIDEX were projected.

Methods: Rodents and non-rodents served as subjects in these experiments. All animals received a single intratympanic administration targeting the round window membrane (IT-RWM) of OTIVIDEX at different doses. To ensure comparability of effects, drug volume administration was normalized to the perilymph volume across the different species. Dexamethasone levels in the perilymph were determined at different time points up to 12 weeks post dose, depending on the species. Dexamethasone levels were also determined in various otic and auditory tissues up to 7 days post dose. Liquid chromatography mass spectrometry methods were used to quantify dexamethasone levels.

Results: IT-RWM administration of OTIVIDEX resulted in significant and lasting dexamethasone inner ear exposure (perilymph) across species. Differences in the pharmacokinetic profile of OTIVIDEX were evident among the species evaluated, including C_{max}, AUC, and elimination kinetics. Exposure to other otic compartments (cochlear tissue, vestibular nerve) and the central auditory system (cochlear nucleus) was also observed. Projected human perilymph levels were determined using different allometric methods.

Conclusions: Intratympanic administration of OTIVIDEX resulted in exposure to various otic compartments and the central auditory system. The projection of OTIVIDEX levels in the inner ear compartment of Meniere's disease patients could be derived from pharmacokinetic data collected across several rodent and non-rodent species.

PS 722

Drug Metabolizing Enzymes and Transporters in the Cochlea: Expression and Mechanistic Implications for Ototoxicity of Analgesics

Stefanie Kennon-McGill; Melissa Clemens; Mitchell McGill
University of Arkansas for Medical Sciences

Acetaminophen (APAP) and non-steroidal anti-inflammatory drugs (NSAIDs) are the most commonly used drugs in the US, but may cause hearing loss in some people. Data from epidemiological studies indicate that chronic use of APAP and NSAIDs over the course of years increases risk of hearing damage. Additionally, numerous reports of rapidly progressive hearing loss in patients taking APAP/opioid combinations have been published. Importantly, though, little is known about the mechanisms of ototoxicity of these drugs. In other tissues,

the toxicity of APAP and some NSAIDs is dependent on drug metabolizing enzymes (DMEs), and transporters. Specifically, cytochrome P450 (Cyp) enzymes catalyze formation of toxic reactive intermediates, while UDP-glucuronosyl-transferases (UGTs), sulfotransferases (SULTs), and transporters promote drug clearance. However, expression of DMEs and transporters in cochlea has never been comprehensively studied. To address that, we compared expression of major Cyps, UGTs, SULTs, and transporters between cochlea and liver, an organ with high expression, in mice using qPCR and enzyme kinetics. Together, the tested DMEs and transporters account for metabolism of more than 50% of all clinically-relevant drugs. Expression of all Cyps was low in the cochlea compared to liver (mean±SE: 2.3±1%). Similar results were obtained for UGTs (13.4±2%) and SULTs (7±7%). Interestingly, expression of most transporters was also low (84±68%), with two major exceptions: *Abcg2/Bcrp* expression was similar between cochlea and liver, while expression of *Mdr1/P-gp*, which is generally thought to be highly expressed in liver and poorly expressed in the CNS, was 3-fold greater in cochlea. Importantly, both *Bcrp* and *P-gp* are known to protect other tissues from toxicity of cancer drugs by acting as extrusion pumps. Conclusions: Cyps, UGTs, and SULTs are poorly expressed in cochlear tissue, while *Bcrp* and *P-gp* are surprisingly highly expressed. Based on these data, it is unlikely that the mechanisms of APAP and NSAID ototoxicity involve reactive intermediates. Furthermore, our data support the hypothesis that certain transporters, namely *Bcrp* and *P-gp*, are critical for protection against ototoxicity of many drugs, including cancer chemotherapeutics.

PS 723

Intratympanic Delivery of a Calcium-Channel Blocker-Hydrogel: A Novel Therapeutic Approach to Otoprotection against Cisplatin-induced Ototoxicity

James Naples¹; Michael J. Ruckenstein²; Jarnail Singh³; Brandon C. Cox³; Daqing Li²

¹*Department of Otorhinolaryngology-Head and Neck Surgery, University of Pennsylvania;* ²*UNIVERSITY OF PENNSYLVANIA HEALTH SYSTEM;* ³*Southern Illinois University School of Medicine*

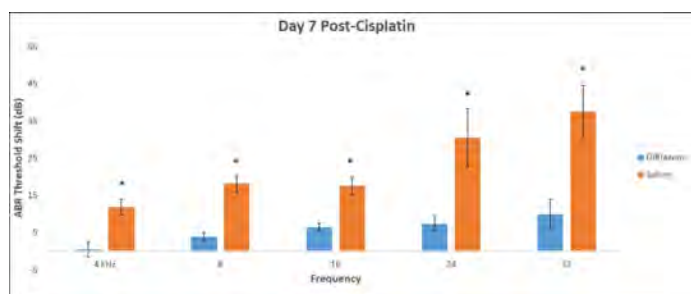
Background: Cisplatin-ototoxicity induces calcium-mediated apoptosis of cochlear hair cells. Previous work has demonstrated that intratympanic (IT) delivery of the calcium channel blocker diltiazem can provide otoprotection and reduce auditory brainstem response (ABR) threshold shifts in the setting of cisplatin-induced ototoxicity. However, when using the IT approach, a large portion of the drug is transported out of the middle-ear space via the Eustachian tube and therefore it is

unavailable for diffusion into the inner ear. Recently, a novel hydrogel approach for inner ear drug delivery has evolved with potential to allow sustained elution of drug into the inner ear. Here, we report our current study on the application of diltiazem embedded in chitosan glycerol phosphate-hydrogel (CGP-diltiazem) and delivered by IT injection to mice treated with cisplatin. We hypothesize that CGP-diltiazem will protect against cisplatin-induced ototoxicity and prevent hair cell death.

Methods: Baseline pure-tone and click-evoked ABRs were performed in 4 week old CBA/J mice. A control group (IT CGP-Saline, n=8) and treatment group (IT CGP-diltiazem 2 mg/kg, n=10) of mice underwent baseline ABR testing followed by IT administration on the same day as a single dose of intraperitoneal cisplatin (14mg/kg). Post-treatment ABRs were performed on day 7 post-cisplatin, followed by collection of the temporal bones. Cochleae were dissected using the whole mount method and stained with anti-myosin VIIa to label hair cells and Hoechst to locate their nuclei. Hair cell quantifications were performed in confocal images taken from two representative regions in each cochlear turn.

Results: The mean click-evoked ABR threshold shift on day 7 was 17.5 ± 1.25 dB in CGP-saline compared to 8 ± 1.08 dB in CGP-diltiazem treated mice. The mean threshold shift on day 7 in tone-evoked ABRs was significantly reduced at all frequencies in CGP-diltiazem treated mice compared to control CGP-saline mice. At 4, 8, and 16 kHz, the CGP-saline threshold shift was 11.8 ± 2.15 , 18.1 ± 2.15 , and 17.5 ± 2.33 dB respectively compared to CGP-diltiazem shifts of 0.5 ± 2.05 , 4 ± 1.18 , and 6.5 ± 1.01 dB respectively. The largest reduction in threshold shift was at 24 and 32 kHz, where CGP-saline had shifts of 30.6 ± 7.72 and 37.5 ± 7.01 dB, compared to CGP-diltiazem with shifts of 7.5 ± 2.01 and 10 ± 4 dB respectively. Preliminary hair cell quantifications demonstrate significant hair cell loss in the basal turn of the cochlea in CGP-saline treated mice, while CGP-diltiazem treated mice had more remaining hair cells.

Conclusions: A single IT dose of CGP-diltiazem (2 mg/kg) provides otoprotection against cisplatin-ototoxicity to hair cells and reduction in ABR threshold shifts in our mouse model. Our study indicates that this new approach may have translational potential and clinical application.



PS 724

High Concentration of TAT-DRBD Protects against Ototoxicity Induced by Cisplatin in Cochlear Organotypic Cultures

Weidong Qi¹; Renji Zhang²; Dalian Ding³

¹Department of Otolaryngology Head and Neck Surgery, Huashan Hospital, Fudan University; ²Fudan University; ³Center for Hearing and Deafness, State University of New York at Buffalo

TAT double-stranded RNA-binding domains (TAT-DRBD) was proved to can internalize siRNA efficiently through round window in vivo in a non-cytotoxic manner in our previous study. To gain a better understanding for the efficiency of this peptide vector mediated RNAi, we screened a valid siRNA targeting Ctr1(Slc31a1), a copper transporter seems to control the cellular accumulation of cisplatin, then transfected the siRNA by TAT-DRBD into hair cells in cochlear organotypic cultures with 10 μ M cisplatin and examined the samples for evidence of protective effect.

Cy3 labeled siRNA were shown to be present inside inner and outer hair cells after 6 hours transfected by TAT-DRBD, although the signals were very weak. 12 hours after transfection, strong fluorescence signals were observed with almost 100% of transfection efficiency. Compared with liposome vector LipoFiterTM, transfection with TAT-DRBD acquired lower knockdown efficiency (67% vs. 91%) in BRL cells, but without ototoxicity. Although the BM is composed of multiple cells, Gene expression still declined 47%. Specimens treated with 10 μ M of cisplatin sustained ~50% hair cell loss in middle turn; however, suppression of Ctr1 mediated by TAT-DRBD could attenuated the cisplatin-induced damage, 87% of hair cells survived.(P

It's amazing that high concentration (>400nM) of TAT-DRBD itself showed strong protective effect against cisplatin ototoxicity. After 48 hours treated with 10 μ M cisplatin/800nM TAT-DRBD, almost 100% hair cells on basilar membrane survived. Even in 50 μ M cisplatin, we also observed >90% hair cells survival.

Taken together these results suggest that reduce cisplatin uptake by blocking copper transporters can be considered as a feasible otoprotective strategy. TAT-DRBD is a potential candidate for both siRNA delivery in inner ear and cisplatin inhibitor against ototoxicity.

PS 725

Preferential Inner Hair Cell Transfection and Lack of Toxicity of Novel AAVs in Mature Guinea Pig Cochlea

Diane M. Prieskorn¹; Lisa A. Beyer¹; Sue J. DeRemer¹; Cindy Park-Windhol²; Luke Schissler²; Steven D. Pennock²; Jilin Liu²; Guo-jie Ye²; Mark S. Shearman²; **Yehoash Raphael¹**

¹*Kresge Hearing Research Institute, Department of Otolaryngology-Head and Neck Surgery, University of Michigan*; ²*Applied Genetic Technologies Corporation*

Introduction: Gene therapy presents a promising approach to restoring hearing loss caused by underlying genetic mutations. One of the major challenges of inner ear gene therapy, however, is identifying a viral vector which can infect target cells with high specificity and efficiency. In this study, we examined several engineered AAV capsids and their ability to infect various cell types in the adult guinea pig inner ear.

Methods: Hartley guinea pigs were infused with 5µl of AAV (1 x 10¹² vg/mL) via cochleostomy into the scala tympani of the inner ear. Auditory brainstem response (ABR) at 4, 8 and 20 kHz were used to assess hearing at baseline (prior to surgery), and 3 and 14 days post-operatively. Subjects were euthanized 2 weeks following virus inoculation. Epifluorescence was used to assess the infection efficiency.

Results: There were no significant differences in ABR thresholds observed across groups at any time point, although one animal had mild threshold elevation. Based on reporter gene fluorescence, these novel AAV-GFP viruses transduced mostly inner hair cells (IHC). A few outer hair cells (OHC) were also GFP-positive. Under the conditions used, none of the supporting cells were transduced. No GFP was seen in mesothelial cells lining the perilymphatic space where the vector was injected. These results indicate very high affinity to hair cells. In some ears, the basal cochleostomy resulted in hair cell transduction throughout the cochlear duct. A few hair cells in the contralateral ear were also positive.

Conclusions: The novel AAV-GFP vectors we tested were able to infect hair cells with high efficiency. Cochleostomy via scala tympani is a safe and efficient method to transduce IHCs in the adult guinea pig inner ear with no significant threshold shift. Normal thresholds and morphology indicated a lack of toxicity. The novel vectors may be useful for the investigation of gene therapy to correct hereditary hearing loss in mammalian models of human deafness associated with IHC mutations.

Supported by AGTC

PS 726

New vectorization approaches for inner ear gene therapy

Athanasia Warnecke¹; Jennifer Schulze¹; Axel Schambach¹; Hildegard Buening¹; Axel Rossi¹; Helena Wichova²; Hinrich Staecker²

¹*Hannover Medical School*; ²*University of Kansas School of Medicine*

Sensorineural hearing loss is a common disorder affecting more than 360 million individuals worldwide. Currently therapies for hearing loss range from sound amplification using hearing aids to cochlear implantation in severe cases. Advances in genetic diagnostics have demonstrated that there are over 100 genes causing non-syndromic sensorineural hearing loss. As our understanding of genetic hearing loss continues to improve, gene therapy for correction of hearing disorders can be developed to correct these diverse disorders. Limitations currently include in efficiency of current vector systems and size limitations in the size of gens that can be delivered. Current research has focused on adeno-associated viral (AAV) vectors as one of the most promising therapeutic long-term delivery systems for gene therapy to the human inner ear. AAV vectors have a limited packaging capacity and until now the development of synthetic vectors such as Anc 80 have suffered from limitations in consistent delivery to all cell types within the inner ear. We report the development of a range of capsid engineered AAV and pseudotyped lentiviral vectors that efficiently and consistently transduce a wide variety of cell types within the inner ear. In combination with cell specific promoters this vector toolbox would allow targeting of individual cells within the inner ear for a range of gene sizes. Vectors were evaluated in vitro using organ of Corti and spiral ganglion cultures and in vivo through delivery into the posterior semicircular canal of mice. Outcome measures included evaluation of transduction efficiency, cell type transduced with different capsid types and effect of vector on hearing and balance in control animals.

PS 727

Autonomous Programmable Intracochlear Drug Delivery System with Assessment of Delivery Pharmacokinetics

Vishal Tandon¹; Woo Seok Kang²; Marcello Peppi³; Andrew Ayoob⁴; Tremaan Spearman-White¹; Ernest Kim¹; Michael McKenna⁵; Sharon G. Kujawa⁶; Mark Mescher¹; Jason Fiering¹; William Sewell⁷; Jeffrey Borenstein¹

¹*Draper*; ²*Asan Medical Center*; ³*Frequency Therapeutics*; ⁴*Spiral Therapeutics*; ⁵*Eaton Peabody*

Laboratories, Massachusetts Eye and Ear & Department of Otolaryngology, Massachusetts Eye and Ear and Harvard Medical School & Otopathology Laboratory, Massachusetts Eye and Ear,; ⁶Department of Otolaryngology, Harvard Medical School and Eaton-Peabody Laboratories, Massachusetts Eye & Ear Infirmary; ⁷Eaton Peabody Laboratories, Massachusetts Eye and Ear, & Department of Otolaryngology, Massachusetts Eye and Ear and Harvard Medical School

Introduction:

A principal challenge in the treatment of sensorineural hearing loss is the development of safe and efficacious methods for administering therapeutics, along with accurate, quantitative pharmacokinetics assessment. Systemic delivery can have poor efficacy and undesirable side effects, whereas local delivery methods that rely on diffusion of drug through the round window membrane (RWM) can result in poor or uncontrolled drug distribution. Intracochlear drug delivery (ICDD), either through a trans-RWM or cochleostomy approach, increases bioavailability of the drug within the cochlea, and enables highly controlled dosing when combined with a precision fluid delivery system.

We have developed an autonomous, battery-operated, ICDD system comprising a micropump, programmable microcontroller, rechargeable battery, and enclosure for head-mounting onto guinea pigs. The pump uses electromagnetic actuators for bi-directional flow control and is integrated with a drug reservoir. To assess and interpret delivery performance, we used electrophysiological measurements, histological analysis, and computational modeling.

Methods:

We used DNQX, a glutamate receptor antagonist that blocks neurotransmission between IHCs and neurons, as a test drug for delivery in guinea pigs using a cochleostomy approach with our ICDD system. Decreased activity of the compound action potential (CAP) at various frequencies indicated the distribution of the compound. Measurement of DPOAEs served as an indicator of safety, as they should not be affected by DNQX. We tested the pump for periods of 1 hr - 5 days. Finally, we tested a new method for estimating cochlear pharmacokinetics, by delivering a 2- μ L bolus of a fluorescent tracer (FM 1-43 FX) directly into the scala tympani, sacrificing the animal after durations of 3 - 72 hours, and then measuring the fluorescence distribution in whole mount cochlear sections using confocal microscopy. We interpreted our results in the context of a pseudo-1D convection-diffusion model.

Results:

With a single battery charge, the micropump generated over 12,000 pump strokes, resulting in up to 6 mL of fluid pumped. Acute delivery of DNQX reduced CAP amplitudes and elevated CAP thresholds at the infusion site, with spreading of the DNQX effects consistent with diffusion-dominated transport. In initial chronic studies, we programmed the pump to automatically initiate drug delivery every other day for a period of one hour. We saw evidence of DNQX delivery after each delivery, but with diminished performance over time. DPOAEs were stable during both acute and chronic delivery. Finally, fluorescence analysis of distribution of the FM 1-43 FX after intracochlear delivery was also consistent with diffusion-dominated transport.

PS 728

Magnetic Nanoparticle Mediated Local Delivery of Adeno-Associated Virus Vectors with Neurotrophin Gene Ameliorates Noise Induced Hearing Loss in Rats

Subhendu Mukherjee¹; Trung Le²

¹Sunnybrook Research Institute, University of Toronto;

²Department of Otolaryngology - Head & Neck Surgery, Sunnybrook Health Sciences Centre Toronto

Introduction: Sensorineural hearing loss (SNHL), a very common sensory impairment in humans, results from damaged hair cells or spiral ganglion neurons. One common cause of SNHL is overexposure to noise leading to noise-induced hearing loss (NIHL). NIHL is a major health problem in the present era and often remains unrecognized and undertreated. Systemic drug administration is not adequate for inner ear diseases, mainly because of the blood-labyrinth barrier. Local drug delivery methods are currently being developed, however, the complexity of inner ear makes it one of the most challenging target organs for local drug delivery. In this study, we aim to use magnetic targeting of superparamagnetic iron oxide nanoparticles (SPIONs) to deliver adeno-associated virus (AAV) vectors with neurotrophin gene locally into inner ear using an external magnetic field. We examine the effect and efficiency of magnetic delivery of growth factors with respect to hearing preservation after noise exposure in a rat model.

Methods: Long-Evans rats were exposed to white noise to induce SNHL. AAV vector was coupled with brain-derived neurotrophic factor (BDNF) expressing gene and tagged onto SPIONs. The nanoparticles were delivered to the round window niche of the left ear 72 hr after noise exposure via a post-auricular incision. Right ear was used as the control. An external magnet was placed on the contralateral ear to pull the virus through the

round window into the inner ear. Immunofluorescence, qPCR, and ELISA were used to assess the expression level of BDNF, tracking marker (GFP), hair cells, and synaptic markers. Audiometry was used to evaluate the functional hearing effect of local delivery before and at different time points after noise exposure.

Results: The results indicated that magnetic targeting can deliver virus-tagged nanoparticles efficiently into the inner ear. We found an increased expression of BDNF and GFP in the cochlea of treated ears. There was no adverse effect of local delivery on inner ear hair cells and hearing of non-deafened rat. Furthermore, delivery of AAV.BDNF substantially reduced NIHL at high-frequency level in deafened rat. These results suggest the effectiveness of the magnetic delivery system.

Conclusion: Results from this study show that magnetic delivery of AAV.BDNF in inner ear protect hair cells and synapses effectively and reduce the degree of NIHL. This work potentially has a significant clinical implication to provide an effective approach to the local delivery of therapeutic drug to treat inner ear disorders.

PS 729

RNA interference and concomitant gene replacement as a treatment strategy for autosomal dominant and recessive non-syndromic hearing loss

Yoh-ichiro Iwasa; Ryotaro Omichi; Paul Ranum; Hidekane Yoshimura; Richard J. H. Smith
Department of Otolaryngology, Molecular Otolaryngology and Renal Research Laboratories, University of Iowa

Background

RNA interference (RNAi) is effective in preserving hearing in a murine model of ADNSHL caused by mutation of *Tmc1*. Generalizing this approach, however, to target the large number genetic variants implicated in ADNSHL is unlikely to be economically feasible. As an alternative, we sought a gene-specific therapy generalizable to both ADNSHL and ARNSHL. This approach is based on the use of RNAi to suppress both endogenous alleles of a specific deafness-associated gene while concomitantly providing gene replacement with a wild-type construct engineered to resist RNAi-mediated silencing. Herein, we describe our results to suppress both endogenous alleles of murine *Tmc1*.

Methods

Homozygous Beethoven mice (*Tmc1*^{Bth/Bth}) maintained on a C3HeB/FeJ background and wild-

type C3HeB/FeJ mice were used in this study. rAAV2/9 (1 μ L) carrying CMV-driven eGFP and an artificial miRNA construct validated to suppress wild-type and mutant *Tmc1* in vitro was introduced into the inner ear of mice at P30 using the round window membrane – semi-circular canal fenestration technique we have described. Two weeks later, single hair cells were isolated from the membranous labyrinth and cDNA was extracted by reverse transcription using the Smart-seq2 protocol. Products were quantitated by SYBR Green-based qRT-PCR.

Results and Conclusions

The artificial miRNA suppressed expression of both wild-type *Tmc1* and the Bth *Tmc1* alleles by more than 70% as compared to mRNA levels in non-injected mice. We will next investigate induced expression of the wild-type construct we have designed to resist RNAi-mediated silencing.

PS 730

Comparison of SENS-401 Inner Ear Tissue and Perilymph Exposure after Oral Administration in Rat, Guinea Pig and Cat

Jonas Dyhrfeld-Johnsen¹; Sonia Poli²; Daniel Smyth³
¹Sensorion; ²Onex; ³Cochlear

Documentation of the local target exposure of a candidate drug at effective doses in preclinical models is essential to successful translational drug development, as it informs the dose selection for, and design of, clinical trials. SENS-401 is a small molecule, clinical stage otoprotectant drug candidate with demonstrated efficacy in rat models of severe acoustic trauma and cisplatin-induced ototoxicity, also being investigated for the potential to preserve residual hearing after cochlear implant surgery. To further substantiate local target exposure in the inner ear for future clinical trials, we here compare inner ear tissue and perilymph exposure of SENS-401 after oral administration in two additional preclinical species relevant for otoprotective drug development, - guinea pig and cat.

Local exposure in the inner ear of male Wistar rats after oral gavage administration of a single 13.2 mg/kg dose of SENS-401 was compared to equivalent body-surface area scaled doses of 12 mg/kg SENS-401 (gavage) for male Duncan-Hartley guinea pigs and 10 mg/kg SENS-401 (oral capsule) for mixed gender domestic short hair cats. At defined time-points after oral administration, terminal blood samples and temporal bones were collected from groups of n=3-4 animals. Blood samples were centrifuged and collected plasma stored frozen until further analysis. The bulla of the temporal bones

were dissected to expose the cochlear apex and 2 μ L perilymph collected and frozen. The bony labyrinth of the cochlea was separated, distributed in medium after being broken by forceps and frozen. All samples were extracted with acetonitrile for HPLC-MS/MS quantification versus a known concentration standard curve.

SENS-401 achieved significant inner ear exposure after oral administration in all three species. From 1-4 hrs after oral administration, perilymph concentrations reached $\sim 435 \pm 245$ nM in rats, $\sim 530 \pm 125$ nM in guinea pigs and $\sim 175 \pm 60$ nM in cats, while inner ear tissue concentrations reached $\sim 510 \pm 40$ nM in rats, $\sim 610 \pm 150$ nM in guinea pigs and $\sim 1290 \pm 470$ nM in cats. Inner ear tissue exposures remained elevated for longer in larger animals (rat < guinea pig < cat). While average exposure ratios relative to plasma for perilymph only varied from 18.6-34.9% across species, the average inner ear exposure ratios ranged from 34.2% in rats to 142% in cats.

Although these data demonstrate some species differences, high nanomolar SENS-401 concentrations were achieved in both perilymph and inner ear tissue after oral administration in all three species. This demonstrates that local target exposure is not specific to a single species and thus otoprotectant efficacy may also be generalized.

Noise Injury II

PS 731

Outer Hair Cell Loss Causes Hearing Deficits in a Mouse Model of Blast Exposure

Tara Balasubramanian¹; Beatrice Mao¹; Scott Haraczy¹; Kamren Hollingsworth²; Ying Wang³; Rodrigo Urioste³; Donna Wilder³; Sajja Venkatasivasaisujith³; Yanling Wei³; Irene D. Gist³; Elizabeth C. Driver¹; Weise Chang¹; Tracy Fitzgerald⁴; Zahra N. Sayyid⁵; Alan G. Cheng⁶; Joseph B. Long³; Matthew Kelley⁷

¹Laboratory of Cochlear Development, National Institute on Deafness and Other Communication Disorders, National Institutes of Health; ²Laboratory of Cochlear Development, National Institute on Deafness and Other Communication Disorders, National Institutes of Health, Bethesda, MD; ³Blast-Induced Neurotrauma Branch, Center for Military Psychiatry and Neuroscience, Walter Reed Army Institute of Research; ⁴Mouse Auditory Testing Core Facility, National Institute on Deafness and Other Communication Disorders; ⁵Department of Otolaryngology-Head and Neck Surgery, Stanford University School of Medicine; ⁶Stanford University; ⁷NIDCD

The use of improvised explosive devices has become widespread in modern combat. As a result, soldiers are increasingly exposed to concussive blasts. Many wounded-in-action soldiers exhibit sensorineural deficits including hearing loss, tinnitus, and vertigo, as well as persistent headaches and balance-related issues. Although blast exposure has been linked to deficits in auditory and vestibular function, the effect of blast on the inner ear is not well understood. To assess the damage caused by concussive blasts, we examined the functional and morphological changes that occur in the inner ear after exposure to single or multiple blast waves. Following exposure to one or three blasts, mice were allowed to recover for specific periods of time between 24 hours and 90 days. Auditory and vestibular function were assessed using auditory brain stem response (ABR) and vestibular evoked potentials (VsEP). To determine the extent of structural changes, inner hair cells, outer hair cells, utricular hair cells, and spiral ganglion neurons were counted in both whole-mounted and sectioned tissue. ABR results indicated progressive threshold shifts at both high and middle frequencies while VsEP indicated no significant changes in utricular function. No difference in the number of inner hair cells or utricular hair cells was observed across conditions or time points. However, in the basal turn of the cochlea we found significant outer hair cell loss in triple blasted ears, and a trend of fewer surviving cells in single blasted ears, indicating a greater susceptibility of outer hair cells to damage by blast. The magnitude of outer hair cell loss increased with time, suggesting ongoing sensory hair cell death. Outer hair cell loss was not observed in regions of the cochlea that correlate with the observed elevated thresholds in mid-range frequencies. To determine whether loss in mid-frequencies could be a result of synapse elimination, we are in the process of examining the integrity of inner hair cell synapses in blast-exposed mice. However, our results suggest that the primary cause of blast-related hearing deficits is loss of outer hair cells.

PS 732

Lower Level Noise Exposure that Produces only Temporary Threshold Shift Modulates the Immune Homeostasis of Cochlear Macrophages

Mitchell D. Frye¹; Celia Zhang²; Bo Hua Hu²

¹Callier Center for Communication Disorders, University of Texas at Dallas; ²Center for Hearing and Deafness, State University of New York at Buffalo

Background

Noise exposure producing temporary threshold shifts (TTS) has been demonstrated to cause permanent changes to cochlear physiology and hearing function. Several explanations have been purported to underlie

these long-term changes in cochlear function, such as damage to sensory cell stereocilia, damage to synaptic connections between sensory cells and their innervation by spiral ganglion neurons, and demyelination of the auditory nerve. Though these structural defects have been implicated in hearing difficulty, cochlear responses to this stress damage remains poorly understood. Here, we report the activation of the cochlear immune system following exposure to lower level noise (LLN) that causes only TTS.

Methods

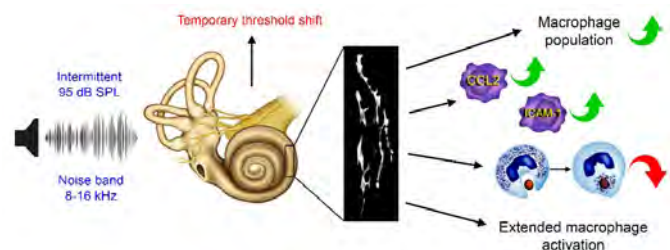
ABR thresholds were acquired for CBA/CAJ mice prior to noise exposure and following chronic exposure to an 8-16 kHz noise band at 95 dB SPL for 7 and 15 days. ABR measures were repeated 20 days post noise cessation to confirm a TTS. Using multiple morphological, molecular and functional parameters, we assessed the responses of macrophages, the primary immune cell population in the cochlea, to the LLN exposure.

Results

This study reveals that a LLN that causes only TTS increases the macrophage population in cochlear regions immediately adjacent to sensory cells and their innervations. Many of these cells acquire an activated morphology and express the immune molecules CCL2 and ICAM1 that are important for macrophage inflammatory activity and adhesion. However, LLN exposure reduces macrophage phagocytic ability. While the activated morphology of cochlear macrophages reverses, the complete recovery is not achieved at two months after the LLN exposure.

Conclusions

Taken together, these observations clearly implicate the cochlear immune system in the cochlear response to LLN that causes no permanent threshold change.



PS 733

The effects of blast injury on hearing in the small rodent model

Dan Lan¹; Jackson R Rossborough²; Roberta Allgayer de Moraes³; Jinahong Liu³; Laura Gomezllanos⁴; Curtis King⁵; Carey Balaban⁶; Suhrud M. Rajguru⁷; Michael Hoffer⁸

¹Department of Otolaryngology, University of Miami;

²Department of Biomedical Engineering, University of Miami; ³Department of Otolaryngology, University of Miami; ⁴Department of Otolaryngology, University of Miami; ⁵Lucent Technologies; ⁶Department of Otolaryngology, Neurobiology, Communication Sciences & Disorders, and Biogengineering, University of Pittsburgh; ⁷Department of Biomedical Engineering and Otolaryngology, University of Miami; ⁸Department of Otolaryngology and Neurological Surgery, University of Miami

Background

Mild traumatic brain injury secondary to blast and blunt head trauma is an increasingly recognized injury pattern with known acute and chronic sequelae. In order to best study these injury patterns researchers must find reliable methods of reproducing both injury mechanics and quantifiable injury patterns. While the small rodent model is not ideal for studying human injury and most humans are not typically exposed to blast, both models remain viable. The small rodent model is critical to examine the neuropathologic injury (grossly and at the cellular level) and blast is valid because it provides a reproducible injury that produces observable outcomes without significant amount of neurotrauma.

Methods

The tube design followed (Courtney 2012) with two coupled tubes. The driver section, which holds stoichiometric oxyacetylene fuel, is 26.7cm long with 16mm ID and 22 mm OD. The driver has an inlet port for the fuel along with an electric igniter coupled to one end. The driven section was 183cm long with 27mm ID and 34mm OD and has ports for pressure sensors that allow characterization of the impulse. A medical grade plastic film was used as a seal covering the open end of the driver section. The anesthetized animal is held in a wire cage at the long end driven section. A signal conditioner and data acquisition board along with two pressure sensors (PCB Piezoelectronics) controlled using custom LabView program were used to collect the data. Anesthetized animals were subjected to blast injury in the mild to moderate range 8-12 psi and then underwent hearing testing at defined intervals over a 28-day period using auditory brainstem testing (IHS, Inc., Miami, Florida)

Results

The animals had normal baseline hearing results over the four frequencies tested. At 24 hours post-blast the animals showed a profound hearing loss which slowly corrected over time. Significant hearing changes were seen in both low(12K) and high frequency (32 K) time points by seven days of recovery. All frequencies demonstrated significant improvement by the 21-day time point. The hearing results are shown in

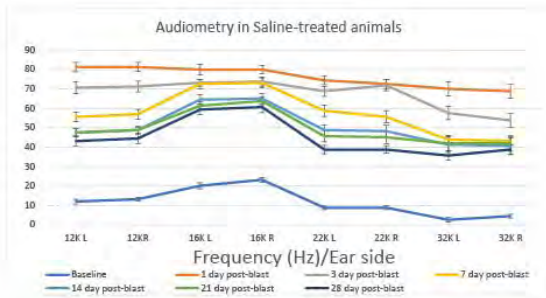
Figure 1

Conclusion

This hearing marker initially produces a profound effect (TTS) which improves over time to a more permanent hearing level (PTS) which is not the same as baseline. This response pattern allows us to examine how other treatments either improve or worsen with both acute as well as chronic outcomes.

References

Courtney et al. Rev Sci Instrum. 2012 Apr;83(4):045111
Figure 1 – Audiometry results in a rat model



PS 734

Betaine-homocysteine S-methyltransferase Deficiency Causes Increased Susceptibility to Noise-induced Hearing Loss Associated to Plasma Hyperhomocysteinemia

Silvia Murillo-Cuesta¹; Teresa Partearroyo²; Néstor Vallecillo³; Lourdes Rodríguez-de la Rosa¹; Adelaida M Celaya⁴; Giacomo Mandruzzato⁵; Steven H Zeisel⁶; María A Pajares⁷; Gregorio Varela-Moreiras⁸; **Isabel Varela-Nieto¹**

¹IIBM CSIC-UAM, CIBERER, IDIPAZ; ²Universidad CEU San Pablo, IIBm CSIC; ³IIBM CSIC-UAM; ⁴IIBM CSIC-UAM, CIBERER; ⁵MED-EL GmbH; ⁶University of North Carolina; ⁷CIB CSIC; ⁸Universidad CEU San Pablo

Nutritional imbalance is an emerging causative factor for deafness¹ and several epidemiological and experimental studies have linked alterations in methionine metabolism caused by folic acid and/or vitamin B12 deficiencies with age-related, noise-induced or sudden hearing loss. Betaine homocysteine S-methyltransferases (BHMTs) are methionine cycle enzymes that remethylate homocysteine, hence their malfunction leads to hyperhomocysteinemia.

Here, we have studied the expression of methionine cycle genes in the mouse cochlea and the impact of knocking out the Bhmt gene in the auditory receptor. We evaluated age-related changes in mouse hearing

by recording auditory brainstem responses at different moments from embryonic to adult stages, and following exposure to noise. Also we measured cochlear cytoarchitecture, gene expression by RNA-arrays and RT-qPCR, and metabolite levels in liver and plasma by HPLC.

Our results indicate that there is an age-dependent strain-specific expression of methionine cycle genes in the mouse cochlea and a further regulation during the response to noise damage. Loss of Bhmt did not cause an evident impact in the hearing acuity of young mice, but it produced higher threshold shifts and poorer recovery following noise challenge. Hearing loss was associated with increased cochlear injury, altered expression of cochlear methionine cycle genes and hyperhomocysteinemia. Our results suggest that BHMT plays a central role in the homeostasis of cochlear methionine metabolism and that Bhmt2 upregulation could carry out a compensatory role in cochlear protection against noise injury in the absence of BHMT.

Work supported by the Spanish MINECO/FEDER SAF2017-86107-R grant to IVN, U.S. National Institutes of Health DK056350 to SZ, and CEU-Banco Santander precompetitive (MUSPB047) and consolidation (MBS18C12) project to TP.

References 1: Partearroyo T et al. (2017). Front Mol Neurosci 10, 107. 2: Lasisi A et al. (2010) Otolaryngol Head Neck Surg 143, 826-830. 3: Martinez-Vega R et al. (2015) FASEB J 29, 418-432. 4: Martinez-Vega R et al. (2016) Front Aging Neurosci 8, 209.

PS 735

Epigenetic modification of histones in acquired hearing loss

Su-Hua Sha¹; Hao Xiong²; Haishan Long¹; Song Pan¹; Yuanping Zhu¹; Kayla Hill¹

¹Medical University of South Carolina; ²Sun Yat-sen Memorial Hospital, Sun Yat-sen University

Background: Post-translational modification of histones alters their interaction with DNA and nuclear proteins, influencing gene expression and cell fate. We investigated the effect of noise trauma and aminoglycoside antibiotics on histone H3 lysine 9 acetylation (H3K9ac) and dimethylation (H3K9me2) in the inner ear of adult CBA/J mice and postnatal cochlear explants, respectively.

Methods: Inhibitors of histone deacetylase (vorinostat) or G9a histone methyltransferase (BIX-01294) were utilized to evaluate the protective effects against inner ear trauma and alteration of H3K9ac or H3K9me2 expression in the cochlea by immunohistochemistry.

Also, inner hair cell (IHC) synaptic ribbons after noise exposure were counted. Noise exposure paradigm: CBA/J mice at the age of 12 weeks were exposed to an octave band noise with a frequency spectrum from 8–16 kHz for 2 hours at 101-dB sound pressure level to induce permanent hearing loss. Aminoglycoside treatment: explants of postnatal 3-day-old pups (p3) were treated with gentamicin to induce hair cell loss. CBA/J mice were treated at the age of 5 weeks with kanamycin, 700 mg/kg bid, for 15 days to induce permanent hearing loss.

Results: After noise exposure, H3K9ac decreased and H3K9me2 increased in outer hair cell (OHC) nuclei in the basal region of the cochlear epithelium and in marginal cells. Additionally, levels of histone deacetylases (HDAC1, 2, and 3) and G9a were increased in the cochlea. Treatment with vorinostat or BIX-01294 attenuated noise-induced loss of OHCs and noise-induced auditory threshold shifts. Treatment with vorinostat also reduced gentamicin-induced OHC loss in explants, but not in chronic models of kanamycin-induced ototoxicity. Our findings suggest that modification of histone H3 at lysine 9 is involved in the pathogenesis of acquired hearing loss and may offer a strategy for protection against acquired hearing loss. Our findings also caution of the potential differences in histone modification between acute and chronic inner ear traumata.

Acknowledgements: The research project described was supported by the grant R01 DC009222 from the National Institute on Deafness and Other Communication Disorders, National Institutes of Health.

PS 736

Noise Susceptibility in Cytomegalovirus -Positive and -Negative Guinea Pigs

Stefan Voigt; Moritz Gröschel; Arne Ernst; Dietmar Basta

Department of Otolaryngology at ukb, University of Berlin, Charité Medical School, Germany

The congenital cytomegalovirus (CMV) is the most common non-genetic cause of sensorineural hearing loss (SNHL) worldwide in humans. The congenital infection of guinea pigs with the guinea pig cytomegalovirus (GpCMV) is known to range from subtle auditory sensorineural and neurologic deficiencies to congenital deafness.

In this study the hearing thresholds (via auditory brainstem responses (ABR)) of normal hearing Dunkin Hartley guinea pigs (two groups: GpCMV -positive and -negative) were recorded one day before and 14 days after a noise exposure (2h, 5-20kHz, 115 dB SPL). Subsequently the animals were perfused with 4% PFA

and the cochleae were removed from the bullae. The Organ of Corti were stained and the outer hair cells loss was determined.

Whereas the pre-exposure thresholds between positive and negative guinea pigs do not differ, there was a significant difference between the ABR-thresholds after the noise exposure. Interestingly the hair cell count was not statistically different between the groups. These findings suggest a retro-cochlear origin of the different susceptibility to noise between GpCMV positive and negative animals.

PS 737

Fluvastatin Protects Against High Level Noise Induced Hearing Impairment and Cochlear Damage in CBA/CaJ Mice

Donna Whitton¹; Frederic Depreux²; Lyubov Czech²; Hunter Young²; Claus-Peter Richter³

¹Department of Otolaryngology; Interdepartmental Neurosciences Program; Knowles Hearing Center; Northwestern University; ²Department of Otolaryngology, Northwestern University; ³Department of Otolaryngology; Department of Biomedical Engineering; Knowles Hearing Center; Northwestern University

Background. We recently demonstrated in a guinea pig model of noise induced hearing loss that Fluvastatin, delivered directly to the ear by catheter attached to a minipump, protects the opposite ear from threshold elevation in response to noise exposure. Further, the protection is associated with retention of outer and inner hair cells (Richter et al., Scientific Reports, 2018). The inter-animal variability of responses in these outbred guinea pigs, however, is large and generally not optimal for biochemical studies of the mechanism of fluvastatin protection. In this study, we have instead moved to the inbred, CBA/CaJ mouse model.

Methods. We tested several methods for surgically implanting a catheter into a mouse cochlea through a cochleostomy. Fluvastatin was then delivered through the catheter attached to a minipump carried on the animal's back. After surgery and when the mice were awake, the animals were exposed to 110 dB SPL x 2 hr x 8-16 kHz in a sound booth, which we showed to cause permanent threshold shift (PTS). Tone evoked ABR measurements were made before surgery, 1,2,3 and 4 weeks after noise exposure. Animals were euthanized, cochleas were fixed by perfusion, then immunolabeled for CTBP2 and GLUR2. Immunolabeled cochleas were imaged on a confocal microscope. The images were exported into Imeris and Image J to locate and count presynaptic (CTBP2) and colocalized (CTBP2/GLUR2) puncta, representing synaptic ribbons and engaged

synapses respectively.

Results: In untreated (no fluvastatin), noise exposed animals ABR thresholds were elevated at 8, 16 and 32 kHz, but not 2 and 4 kHz. Twelve animals were surgically implanted and exposed to noise. Of the 12 surgically implanted animals, 3 animals were eliminated due to inadequate surgery. In five animals, fluvastatin completely protected against NIHL in the opposite ear at 8, 16 and 32 kHz; and in 4 animals, fluvastatin protected at one frequency only. The number of synaptic ribbons/inner hair cell and synapses/inner hair cell were averaged from sampled microscopical fields between 8 and 32 kHz. In mice exposed to noise alone, both the synaptic ribbons/IHC and synapses/IHC were decreased from control (untreated, unexposed) levels when measured 4 weeks after noise exposure. However, the ribbons/IHC and synapses/IHC in the noise+fluvastatin treated mice were similar to those of the control animals.

Conclusions: These studies support our previous work and demonstrate that fluvastatin protects against high level noise induced ABR threshold shift in two animal models. Moreover, protection from hearing loss is also associated with synaptic ribbons/IHC and synapses/IHC at the end of the study that are similar to the unexposed control. The CBA/CaJ mouse shows less variability in responses among individuals than did the Hartley guinea pigs and will serve as a good model for delving into the mechanism by which fluvastatin protects against noise induced hearing loss. Fluvastatin, already vetted in human medicine for other purposes, is a promising candidate for treatment of hearing loss in humans.

Acknowledgments: Supported by ONR grants #N00014-16-1-2508; N00014-18-1-2508; and the Department of Otolaryngology, Northwestern University.

PS 738

Probing Estrogen's Role in Hearing Physiology: Implications for Noise-Induced Hearing Loss

Benjamin Shuster¹; Beatrice Milon¹; Ryan Casserly¹; Mark McMurray¹; Shaun Viechweg¹; Kanisa Davidson¹; Didier Depireux²; Jessica Mong¹; Ronna Hertzano¹

¹University of Maryland Baltimore-School of Medicine;

²Otolith Labs

According to the World Health Organization (March 2018), 466 million individuals worldwide suffer from debilitating hearing loss. While hearing loss afflicts both men and women, significant sex differences in hearing have been well documented in a number of species, and are particularly well-documented in humans. An increasing body of literature suggests that the gonadal hormone estrogen plays a role in the

modulation of hearing and may account for differences in hearing between the sexes. Previous studies from our laboratory demonstrate that female mice are protected from a permanent threshold shift (PTS)-inducing noise exposure in comparison to males. In addition to an elevation in hearing threshold, another well-documented consequence of a PTS-inducing noise exposure is a decrease in auditory brainstem response (ABR) wave-1 amplitude, which reflects a decrease in synchronous neural firing at the level of the spiral ganglion. Previous work in our laboratory demonstrates that females display larger ABR wave-1 amplitudes than males at baseline and after a PTS-inducing noise exposure.

Here we present data investigating estrogen's potential protective capacity in the context of noise-induced hearing loss by utilizing a gonadectomy mouse model to control for levels of circulating gonadal hormones. The use of a gonadectomy model allows for the investigation of estrogen's protective effects, and avoids potential confounds of knockout models where the effects of gonadal steroids on normal brain development may be disrupted. In the first set of experiments designed to evaluate estrogen's protective effect in both sexes, gonadectomized male and female mice were continuously supplemented with either 17 β -estradiol or a vehicle control prior to a PTS-inducing noise exposure (8-16 kHz, 102.5dB SPL, 2h). Our data demonstrate that exogenous estrogen replacement confers protection following a PTS-inducing noise exposure to female but not male mice. Furthermore, our data show that exogenous estrogen replacement ameliorates the decrease in wave-1 amplitude in female mice following the noise exposure.

In a separate set of experiments designed to isolate estrogen's effect on ABR wave-1 amplitudes in female mice the physiological response to sound as measured by ABR was compared in gonadectomized females with and without estrogen supplementation using a within-subject comparison model. In addition, the general effects of estrogen on the peripheral auditory system are investigated using histological and RNA-sequencing approaches. Collectively, these data provide novel insights into the effect of estrogen on hearing physiology and the potential implications for NIHL.

PS 739

The contribution of Innate and Adaptive Immune Response in Recruiting Heterogeneous Immune Cells in the organ of Corti and Modulating Inflammation after Acoustic Trauma

Rai Vikrant¹; Megan B Wood²; Tetsuji Yamashita²; Jian Zuo¹

¹Department of Biomedical Sciences, Creighton

Research Background: Following inner ear acoustic trauma, the contributions of innate and adaptive immune response in sensory hair cell (HC) loss in the inner ear is poorly understood. Increasing evidence suggests that the loss of HC is exacerbated by inflammation of the cochlea mediated by chemokines, cytokines, and reactive oxygen species generated by either resident cochlear or infiltrating immune cells. However, the cause-and-effect data is lacking regarding the time of acoustic trauma and recruitment of cell type, their lineage, and the exact role of infiltrating immune cells in degenerating and regenerating the cochlear structure by modulating inflammation and protect hearing loss.

Methods: Immunostaining and flow cytometry was carried out to analyze the type of recruited immune cell population in the organ of Corti in response to acoustic trauma in C57BL/6 mice. Single-cell RNA sequencing was performed on Fgfr3iCre⁺; Atoh1-HA; Chrna9-GFP: tdTomato⁺ mice at P12, P26, and P33 to elucidate the recruited immune cell population. Auditory Brain Response was measured in mice anesthetized with tribromoethanol (Avertin). Cytokine profiling was done at the different time points of acoustic trauma. RT-PCR analysis of the cDNA extracted from HeLa and HEI-OC1 cells treated with recombinant high mobility group box (HMGB)-1 and interleukin (IL)-10 was used to analyze the effect on mediators of inflammation.

Results: Immunostaining, flow cytometry, and single-cell RNA sequencing reveal the presence of a heterogeneous population of recruited immune cells including macrophages, B cells, T-cells and Schwann cells in the organ of Corti in response to acoustic trauma. Flow cytometry data revealed CD45⁺ CD11b⁺ CX3CR1⁺ (cochlear macrophages), B220⁺ CD45⁺ (B cells), T cells, NK cells, myeloid cells, neutrophils, and immature macrophages in the organ of Corti. RT-PCR analysis showed that expression of HMGB-1, receptor for advanced glycation end products (RAGE), toll-like receptor (TLR)-2, TLR-4, IL-6, and tumor necrosis factor (TNF)- α was increased in cells treated with rHMGB-1 but decreased treated with IL-10.

Conclusions: Noise-induced trauma to the inner ear results in an innate and adaptive immune response and mediates the recruitment of the heterogeneous population of immune cells in the organ of Corti. HMGB-1 and proinflammatory cytokines secreted by the damaged cochlear structures enhanced the inflammation in the cochlea and anti-inflammatory activity of IL-10 secreted by immune cells attenuated the inflammation.

The secreted damage-associated molecular patterns (DAMPs) that initiate the inflammation, cytokines that modulate inflammation and macrophages that are polarized to instigate repair will give more insight in protecting hearing loss.

Supported in part by NIHR01DC015010, NIHR01DC015444, ONR-N00014-18-1-2507, USAMRMC-RH170030, ALSAC and LB692/Creighton.

PS 740

Unraveling NF- κ B Transcriptional Activity in the Auditory System

Kuu Ikäheimo; Anni Herranen; Ulla Pirvola
University of Helsinki

Nuclear factor kappa B (NF- κ B) is a transcription factor that has been assigned with many roles. It has been associated with development, inflammation, aging and injury. NF- κ B is a family of proteins: RelA, RelB and c-Rel, p50 (NF- κ B1) and p52 (NF- κ B2). The two latter ones are cleaved from the larger units p105 and p100, respectively, by the ubiquitin/proteasome pathway. Inactive NF- κ B is coupled to its inhibitors (I κ Bs) in the cytoplasm, but it can be rapidly released from this inhibition. Thereby, NF- κ B does not require new protein synthesis to act. Several prior studies have studied NF- κ B expression in the auditory system, but with inconsistent results. This maybe due to the variability in the antibodies used. To avoid problems with antibody specificity, we have studied NF- κ B transcriptional activity by histological methods using a well-established NF- κ B/LacZ reporter mouse line. We have studied this activity in the peripheral and central auditory pathway at adulthood. As NF- κ B transcriptional activity is often modulated by acute and chronic stressors, we have studied NF- κ B activity both after noise exposure and during aging. Our results show that NF- κ B transcriptional activity is absent from the resident cells of the organ of Corti, but that it predominates in the neuronal compartment of the auditory system, both in basal conditions and following acute and chronic stress. These data set the stage to decipher the various roles of NF- κ B in normal hearing physiology and in pathophysiology.

PS 741

Investigating the Role of the Lateral Wall Stress Response in Noise-Exposed CBA/Ca Mice

Anni Herranen; Kuu Ikäheimo; Ulla Pirvola
University of Helsinki

The CBA/Ca mouse strain is known to be particularly sensitive to noise at the young adult age. It has also been shown that noise exposure triggers activation of stress

signaling pathways in the organ of Corti and the lateral wall of CBA/Ca mice at young adulthood (Herranen et al. JARO 2018). In other studies, when young and older CBA/Ca mice were compared, older animals were found to be more resistant against noise-induced outer hair cell (OHC) loss (Ohlemiller et al. Hear Res 2000, 2018). Is this age-dependent change in OHC vulnerability due to mechanisms within the organ of Corti or do other parts of the cochlea or even systemic effects influence OHC vulnerability? Cells of the lateral wall are responsible, for example, for creating the endolymphatic potential (EP). The lateral wall also contains a rich vascular supply, which makes it a potential route of systemic factors for the regulation of OHC fate. We were interested to study whether stress signaling pathways are activated following noise exposure in the older, more resistant CBA/Ca cochleas, similar as in young adults. The young age group consisted of 2-month-old and the older group of 10-month-old mice. Both groups were exposed to 105 dB SPL for 2 h. They were studied either acutely after trauma for the detection of the stress response or 6 days post-trauma for the assessment of the extent of OHC loss. ABRs were recorded in non-exposed and exposed mice, in both the young and older age group. The stress response was assessed by immunohistochemistry using induction of p-c-Jun (Serine 73) and p-ERK immunostaining as a readout for the activation of JNK/c-Jun and ERK stress signaling pathways. Interestingly, the lateral wall stress response was mounted in both age groups acutely after noise exposure, despite the differential OHC vulnerability. These results suggest that the lateral wall stress response does not drive OHC pathology on its own. However, in young mice, the lateral wall stress response may together with systemic (metabolic) effects sensitize OHCs, perhaps via EP changes or changes in the inflammatory response. Based on these results, we discuss the possible pathophysiological roles of the lateral wall stress response in the noise-exposed cochlea.

PS 742

CRF Signaling Up-regulation Following Various Trauma Insults

Kathleen T. Yee; **Douglas E. Vetter**

*Dept. of Neurobiology and Anatomical Sciences,
University of Mississippi Medical Center*

Introduction: Our goal is to further elucidate the cells and molecular signaling cascades that are involved in cochlear protection. We previously described an apparently complete duplication in the cochlea of the molecular signaling system associated with the hypothalamic-pituitary-adrenal (HPA) axis. Typically, protective systems are suggested to center on neural/hair cell aspects of cochlear function (e.g. the

olivocochlear system). However, we suggest that these ideas miss a key aspect of the system- that the cochlea is first and foremost an organ much like any other that also happens to have a sensory function. We suggest that a “true” protective system should reside at a root level of the underlying organ, with the idea being that the overall organ needs to be protected, and if it is, then the specialized function is also protected. If this hypothesis is correct, a “true” protective system should be initiated via numerous types of insults, not just exposures to noise that target mainly the specialized function that we have used for many years.

Methods: Corticotropin releasing factor (CRF)-Cre mice were bred to floxed STOP td Tomato reporter mice (Ai14) to produce CRF-tdTomato reporter mice. Reporter mice were exposed to two different trauma paradigms: 1) Noise trauma paradigm- 2 hour noise (106-108db, 8-16kHz) with 2- 4 hour survival; or 2) Mild traumatic brain injury (mTBI) paradigm- a single mTBI impact delivered to the top of the skull followed by a 24 hour survival. Temporal bones were fixed, isolated and sectioned. Sections were immunostained with primary antibodies to red fluorescent protein (RFP), myosin VIIa, F4/80 (a macrophage marker), and Iba1 (a macrophage/microglia marker).

Results: (1) Noise trauma: The td Tomato reporter for CRF was up-regulated in the spiral limbus, spiral ligament, cochlear epithelium, and in the macrophage niche beneath the basilar membrane. (2) mTBI: CRF visualized by td Tomato was up-regulated in cochlear epithelium, in spiral limbus, spiral ligament and support cells. Preliminary indications are that myosin VIIa levels decrease in some hair cells. Some CRF-positive cells in the modiolar region and under the basilar membrane are F4/80 positive, while others co-label with Iba1.

Conclusions: Following both noise exposure and mild traumatic brain injury, CRF is up-regulated in various cells and regions of the cochlea. These data also indicate that some cells that are CRF+, are of macrophage lineage. CRF signaling may represent a core protective system in the cochlea.

Support: R21DC015124 (DEV), P30GM103328 (Confocal Imaging Core)

PS 743

Auditory Trauma Following Blast Exposure

Monica Benson¹; John Peacock²; Nathaniel T. Greene³; Daniel J. Tollin⁴

¹University of Colorado School of Medicine, Neuroscience Graduate Program, Department of Physiology and Biophysics; ²University of Colorado

School of Medicine, Department of Physiology and Biophysics; ³University of Colorado School of Medicine, Department of Otolaryngology; ⁴Department of Physiology & Biophysics, and Department of Otolaryngology, University of Colorado School of Medicine

Permanent hearing damage is known to occur following exposure to high intensity impulse noise events such as gunfire and the detonation of explosives. Damage from impulse noise exposure can include damage to the inner and outer hair cells in the cochlea, as well as gross morphological damage such as rupture of the tympanic membrane, dislocation of the middle ear ossicles, and delamination of the basilar membrane. A clearer understanding of how the auditory system responds to blast could help us better prevent auditory trauma.

Chinchillas are commonly used in studies of the auditory system and hearing loss due to similarities between human and chinchilla audiograms, and we have recently shown that chinchillas are well suited as a model of human impulse noise exposure compared to other common small laboratory species. Additionally, we have recently described the intracochlear pressures in response to high intensity sounds in both humans and chinchillas, allowing us to translate directly impulse noise exposures in both humans and chinchillas.

To investigate the mechanisms of hearing loss to impulse noise exposure in chinchillas, we conducted measurements of auditory trauma after exposure to single impulse noise events via a small-bore shock tube. Chinchillas were exposed to a range of peak shock wave intensities from 1 to 8 PSI (170-188 dB pSPL). Behavioral audiogramsto establish hearing thresholds as well as physiological measurements including auditory brainstem response (ABRs) and distortion product otoacoustic emissions (DPOAEs) were measured in each animal before, and then once a week for three weeks following the exposure.

Results show that individual exposures of $> \sim 1.5$ -2.0 PSI (~ 174 -177 dBpSPL) produce permanent hearing loss in chinchilla and the degree of loss scales with peak exposure level. If we assume that a given cochlear pressure producing hearing loss in the chinchilla produces a comparable hearing loss in the human ear, then we may use the previously characterized chinchilla and human middle-ear transfer functions to calculate the equivalent human exposure for the observed chinchilla exposure. We thereby infer that the pressures that a chinchilla 2 PSI (177 dB pSPL) exposure is equivalent to a human exposure of ~ 0.3 PSI (~ 160 dB pSPL), which is comparable to the exposure expected from firearm use.

Supported by DOD W81XWH-15-2-0002

Otoacoustic Emissions

PS 744

Changes in Distortion Product Otoacoustic Emission Maps with Posture and Fluid Shift Using Statistical Parametric Mapping

Allison Anderson¹; Keith Covington¹; Catherine Reike²; Abigail Fellows³; Jay Buckley³

¹University of Colorado Boulder; ²Dartmouth College Geisel School of Medicine; ³Space Medicine Innovations Laboratory

Distortion product otoacoustic emission (DPOAE) mapping may provide a comprehensive window into cochlear health. DPOAE mapping measurement techniques investigated to date, however, have not shown the necessary accuracy and precision to be used in clinical monitoring. Analysis techniques to extract meaningful information from maps have not demonstrated the accuracy and specificity needed for clinical applications. Novel data analysis methods were developed to assess DPOAE maps changes caused by shifting posture and inducing a fluid shift. The numerical methods were developed to analyze DPOAE amplitude maps in such a way that gross changes in map can be statistically identified. Statistical parametric mapping, a technique used for MRI imaging, was implemented to detect regional changes within the data as compared to a normative population.

Data was collected in two experiments: a Repeatability Cohort where maps were collected in the same group of subjects repeatedly over time, and a Posture Cohort where subjects were measured in supine, prone, and under lower body negative and positive pressure (LBNP/PP) in both postures. Statistical parametric mapping and random field theory were applied to DPOAE amplitude maps. A region of greatest change is found within the 5-7.5 kHz range and between ratios of 1.13 – 1.24. This is most pronounced in the prone LBPP condition, where amplitudes for the Postural Cohort were below the Repeatability Cohort. Global shifts in the maps were also found, where amplitudes were lower in LBPP and in atmospheric pressure, regardless of posture. Although the physiological mechanism for these changes is not known, through our statistical parametric mapping technique, it may provide a sensitive measure of regional changes in DPOAE maps.

Middle-ear Transmission and Generation of Stimulus-Frequency Otoacoustic Emissions (SFOAEs): Finite-Element Mouse Model

Hamid Motallebzadeh¹; Sunil Puria²

¹Harvard Medical School; ²Eaton-Peabody Laboratories

Background: Local reflections of tone generated traveling waves produce low-level sounds that travel back through the middle ear (ME) into the ear canal (EC) called SFOAEs. Previously we showed, in a mouse cochlea model, that random perturbation of the basilar membrane stiffness and hair-cell gain are the most influential parameters responsible for SFOAE generation and mostly from ½-octave basal to the best frequency location (Motallebzadeh & Puria, 2018). However, changes in a lumped representation of the reverse ME impedance ZMER significantly altered SFOAEs at the oval window. In this study we extend our previous model by replacing the lumped ZMER with an anatomically realistic, fully coupled ME. The model is being used (1) to characterize the mouse ME, (2) to investigate how ME parameters affect SFOAEs, and (3) to explore SFOAE generation due to OoC impedance irregularities.

Methods: The previous 3D finite-element model is extended by adding an EC, ME, and ME cavity (reconstructed from uCT images) and tested against measurements of ossicle velocity in the 2-60 kHz frequency range (Dong et al., 2013). To access the ossicles, the pars flaccida (PF) was removed during measurements and we similarly removed the PF for model validation. For the rest of the study, the intact PF model is used to calculate MEG-F, the ME pressure gain in the forward direction from the EC to the vestibule; and MEG-R, the ME pressure gain in the reverse direction from the vestibule to the EC. The model cochlear impedance (Zc) and ZMER are calculated as the vestibule-pressure to the stapes-volume-velocity ratio for forward and reverse drives, respectively.

Results: The model predicts that removing the PF shunts ME transmission below 10 kHz. In the 12-60 kHz range, the magnitude of MEG-F varies from about +18 to +32 dB, while MEG-R varies from -36 to -50 dB. Zc is resistive and is in the 1.5 to 2.5 T-Ohms range for the passive cochlea and varies from 1 to 5 T-Ohms for the low-level active cochlea. The magnitude of ZMER ranges from 0.2 to 1.5 T-Ohms. We plan to perform sensitivity analysis of the ME modifications on SFOAEs. We also plan to repeat our previous studies of the impedance irregularities of the OoC with spatial frequency that ranges from 1/8 to 8 OHC spacing along the cochlear length and SFOAEs generated from selective sites by increasing random perturbation from the base to the apex, in 10% increments.

Short-Latency Stimulus Frequency Otoacoustic Emissions Predict Cochlear Status

Joshua J. Hajicek¹; Carrick L. Talmadge²; Glenis R. Long³

¹University of Michigan, Kresge Hearing Research Institute; ²University of Mississippi, National Center for Physical Acoustics; ³The Graduate Center, City University of New York

Background

Stimulus frequency otoacoustic emissions (SFOAE) have characteristically and relatively long latencies commonly believed to arise due to distributed roughness along the cochlear partition. However, SFOAE responses also contain significant energy with shorter latencies. These are commonly ascribed to relatively basal linear reflections of cochlear traveling waves. However, this hypothesis neglects possible contributions from nonlinear reflectance. We propose that the short latency component 1) arises from a similar region as the reflection source emissions, 2) the amplitude of the short latency component reflects, in part, cochlear gain and thus, short latency SFOAE provide important information about cochlear status, 3) combining information obtained from the short and long latency SFOAE will be more sensitive to cochlear status.

Methods

SFOAE were collected from 14 human ears. Hearing thresholds were obtained using Bekesy tracking. Narrow band noise was used to mitigate effects of threshold fine-structure. SFOAEs were measured from 1-8 kHz using frequency swept probe- and suppressor-tones. SFOAEs were examined with the continuous wavelet transform and a least squares fitting procedure. SFOAE measurements were separated into short, long, and combined (short + long) latency components from where amplitude, phase, and phase gradient delays (the derivative of phase with respect to angular frequency) were computed. Responses were further parsed into 15 frequency bands and stepwise linear- and multiple-linear regression models were computed for each frequency band. The independent variables were the short, long, and combined amplitude, phase, and phase gradient delay, and hearing thresholds the dependent variable. Bayesian information criterion was used to select the most parsimonious regression models and prevent overfitting.

Results and Conclusions

Linear regressions revealed that individual components of amplitude, phase, or phase gradient delay were unable to significantly predict thresholds. Multiple linear regressions were significant for all frequencies and

indicated that phase and phase gradient delay were the most significant predictors in each model. The relative importance of short, long, or combined latency components was frequency dependent. The short latency components were important predictors at every frequency. Collectively, these results suggest that each component provides valuable information about cochlear status. Contributions from nonlinear reflectance and the interaction of short and long latency components will be discussed.

PS 747

Dependence of Distortion-Product Otoacoustic Emissions on Hearing Loss - Comparison of Experimental and Numerical Input/Output Functions

Dennis Zelle; Anthony W. Gummer; Ernst Dalhoff
University of Tübingen

Introduction

Distortion product otoacoustic emissions (DPOAEs) emerge in the healthy cochlea as a response of two simultaneously presented tones of frequencies f_1 and f_2 and mainly consist of two components, a nonlinear-distortion and a coherent-reflection component. Recently, it was shown that estimated distortion product thresholds (EDPTs) extrapolated from semi-logarithmic input-output (I/O) functions [1] predict behavioral thresholds in normal-hearing and hearing-impaired ears with high accuracy, if solely the nonlinear-distortion component is utilized [2]. However, DPOAE I/O functions based on the nonlinear-distortion component sometimes exhibit a considerable deviation from the expected semi-logarithmic growth behavior. Here, experimentally derived I/O functions evoked by short-pulse stimulation [2] are compared to numerically obtained I/O functions for $f_2 = 1 - 8$ kHz ($f_2/f_1 = 1.2$) using a nonlinear hydrodynamic cochlea model [3] with variable cochlear amplification in order to simulate various degrees of hearing loss.

Methods

The human cochlea is modeled as two arrays of locally damped oscillators representing the basilar and the tectorial membranes. Longitudinal coupling is provided by hydrodynamic force propagators and shearing resistance of the membranes [3]. Incorporating a simplified middle-ear model as a fourth-order mechanical oscillator enables the computation of DPOAEs in the ear canal. Integration of the differential equations for the smooth cochlea, i.e. without coherent reflection, was done directly in the time domain using the Dormand-Prince method (ODE45, Matlab). Incorporating a dimensionless scaling factor in the cochlear-amplifier

force enables simulation of various degrees of hearing loss.

Results

The cochlea model exhibits compressive amplification of traveling waves up to 43 dB at 4 kHz. The simulated I/O functions generally follow the experimentally established semi-logarithmic growth behavior enabling the computation of simulated EDPTs. However, deviation from optimal primary-tone levels yields non-monotonic I/O functions, which are also apparent in the experimental data. Decreasing the amplification force alters the shape and the slope of the simulated I/O functions and increases simulated EDPTs.

Conclusion

The analysis of simulated DPOAE I/O functions provides a link between DPOAE growth behavior and the nonlinear characteristics of the mechano-electrical transducer. Furthermore, the variation of I/O functions with decreasing cochlear amplification may be used to improve the sensitivity of objective parameters, such as the EDPT, to detect hearing loss.

[1] - Boege & Janssen, 2002. J. Acoust. Soc. Am. 111, 1810–1818.

[2] – Zelle et al., 2017. J. Acoust. Soc. Am. 141, 3203–3219.

[3] – Gummer et al., 2018. AIP Conference Proc. 1965, 090002.

PS 748

Time-Domain Analysis of Distortion-Product Otoacoustic Emission Components Using a Hydrodynamic Cochlea Model

Dennis Zelle; Ernst Dalhoff; Anthony W. Gummer
University of Tübingen

Introduction

Distortion-product otoacoustic emissions (DPOAEs) are used to noninvasively ascertain the functional state of the cochlea. According to a widely accepted model, the cubic distortion product at $2f_1-f_2$ consists of a nonlinear-distortion component, which is generated in the overlap region of the two primary tones, and a coherent-reflection component arising at the tonotopic place of the distortion-product frequency. Using short stimulus pulses instead of continuous primary tones, the two DPOAE components can be extracted by decomposing time-domain recordings into pulse-basis functions (PBFs) using a least-squares fit approach [1]. The present work utilizes a time-domain implementation of

a nonlinear hydrodynamic model of the human cochlea to simulate short-pulse DPOAE responses comprising both components.

Methods

The cochlea is modeled as two arrays of locally damped oscillators representing the basilar and the tectorial membranes [2], both of which are longitudinally coupled by shearing resistance. Direct coupling of the cochlea model with a fourth-order mechanical oscillator representing the middle ear enables the simulation of DPOAEs in the ear canal near the tympanic membrane. Matrix formulation of the equations of motion was used to solve the differential equations in the time domain using the Dormand-Prince method. In order to produce coherent reflection, inhomogeneity in the form of Gaussian distributed variations were incorporated in the stiffness of the basilar-membrane fibers and the cochlear-amplifier force. Subtraction of DPOAE signals simulated in a smooth model from DPOAE signals simulated in a model with inhomogeneity yields an estimate of the coherent-reflection components. The simulated DPOAE components are compared to band-pass filtered experimental data for $f_2 = 1$ to 8 kHz ($f_2/f_1 = 1.2$) from normal-hearing subjects taken from a recent study [3].

Results

In general, DPOAE responses simulated in a smooth cochlea show a distinct steady state with duration commensurate with the duration of the short-pulse stimulus. In contrast, incorporating inhomogeneity yields complex DPOAE responses similar to experimental data due to the occurrence of coherent-reflection components. Depending on the magnitude of the inhomogeneity, multiple reflections and spontaneous OAEs appear in the simulated signals.

Conclusion

Time-domain analysis of simulated DPOAE signals provides additional insights into their underlying components, which can be directly used to improve source separation of experimental DPOAE data.

References

- [1] Zelle et al., 2013. *J. Acoust. Soc. Am.* 134, EL64–EL69.
- [2] Nobili & Mammano, 1996. *J. Acoust. Soc. Am.* 99, 2244–2255.
- [3] Zelle et al., 2017. *J. Acoust. Soc. Am.* 141, 3203–3219.

PS 749

The Effects of Combined Forward- and Emitted-Pressure Level Calibrations on OAE Variability During Repeated Probe Fits

Carolina Abdala¹; Tom Maxim²; Christopher A. Shera¹; Karolina K. Charaziak¹; Ping Luo¹

¹University of Southern California; ²Keck School of Medicine, USC

OAE stimuli are often calibrated using in situ sound-pressure level (SPL) measurements taken at the probe microphone inserted into the subject's ear canal. However, SPL calibrations can produce errors in the specification of stimulus level due to standing-wave interference. These errors vary across individuals and between fit and refit in the same ear. Calibrating stimuli using forward-pressure level (FPL) is one way to mitigate the effects of this interference. Past work has studied the effect of FPL calibration on DPOAEs by utilizing intentional deep versus shallow probe fits in subjects. These studies have not considered the effect of standing-wave interference on the measurement of OAEs emerging from the cochlea, which can be reduced by expressing OAEs in emitted-pressure level (EPL) rather than SPL. In this study, we investigate the effect of FPL calibration on stimulus level combined with EPL correction to OAE levels during natural probe insertion and reinsertion. Distortion-product and stimulus-frequency OAEs were recorded in 20 normal-hearing young-adult subjects using in situ SPL calibration, FPL calibration alone, and FPL calibration + EPL conversion. Initial fit and refit measurements were made at low and moderate stimulus levels across a five-octave frequency range (0.5 to 16 kHz). Results show a significant effect of calibration procedure on OAE test-retest variability: Both the FPL and the combined FPL+EPL calibration schemes resulted in the overall lowest test-retest differences for DPOAE level at frequencies > 4 kHz. The benefit was modest, ranging on average from 0.5 to 2 dB. SFOAE level did not show significant effects of calibration method on any metric, likely due to reduced signal-to-noise ratios and compressive growth of the SFOAE at our chosen stimulus levels, rendering it insensitive to calibration effects. There were no significant differences in OAE inter-subject variability among the three calibration procedures.

Advanced calibration techniques that correct for ear-canal standing-wave interference on both the stimulus and OAE levels enhance the reliability of DPOAE measurements and reduce the dependence on probe position, even when variations in probe fit are small (i.e., not artificially induced). Although the improvements to test-retest reliability were modest, we posit that the benefit of FPL+EPL calibration would have been

greater had we tested a more heterogeneous group of subjects and better mimicked common clinical practice, in which repeated tests are often conducted by different audiologists.

PS 750

Low-Frequency Oscillatory Modulation of the Cochlear Amplifier by Selective Attention

Constantino Dragicevic¹; Bruno Marcenaro²; Marcela Navarrete³; Luis Robles⁴; Paul Delano⁵

¹*Departamento de Neurociencia, Facultad de Medicina, Universidad de Chile;* ²*Pontificia Universidad Católica de Chile;* ³*Universidad de Valparaíso;* ⁴*Programa de Fisiología y Biofísica, ICBM, Facultad de Medicina, Universidad de Chile;* ⁵*Departamento Otorrinolaringología, Universidad de Chile*

Evidence show that selective attention to visual stimuli modulates the gain of cochlear responses, probably through auditory-cortex descending pathways. At the cerebral cortex level, amplitude and phase changes of neural oscillations have been proposed as a correlate of selective attention. However, whether sensory receptors are also influenced by the oscillatory network during attention tasks remains unknown. Here, we searched for oscillatory attention-related activity at the cochlear receptor in humans. We used an alternating visual/auditory selective attention task and measured electroencephalographic activity simultaneously to distortion product otoacoustic emissions (a measure of cochlear receptor-cell activity). In order to search for cochlear oscillatory activity, the otoacoustic emission signal, was included as an additional channel in the electroencephalogram analyses. We found the presence of low frequency (<10 Hz) brain and cochlear amplifier oscillations during periods of selective attention to visual and auditory stimuli. Notably, switching between auditory and visual attention modulates the amplitude and the temporal order of brain and inner ear oscillations. These results extend the role of oscillatory activity network during cognition in neural systems to the receptor level.

Funded by Fondecyt 1161155, Proyecto ICM P09-015F and Fundacion Guillermo Puelma.

PS 751

Identifying the Origin Along the Cochlea of Stimulus Frequency Otoacoustic Emissions

Shawn Goodman¹; Choongheon Lee²; John J. Guinan³; Jeffery Lichtenhan²

¹*University of Iowa;* ²*Washington University in St Louis;* ³*Eaton-Peabody Laboratories, Massachusetts Eye and Ear; Graduate Program in Speech and Hearing and Bioscience and Technology, Harvard Medical School*

Background

Stimulus frequency otoacoustic emissions (SFOAEs) have been promoted as providing the most frequency-specific, non-invasive, objective measurement of cochlear amplification. However, there is controversy about where along the cochlea SFOAEs originate: (1) they originate only near their characteristic frequency (CF) place, or (2) substantial SFOAE fractions originate two octaves or more basal to their CF place. Specifying the spatial origin of SFOAEs will advance understanding cochlear mechanics and increase SFOAE clinical utility.

Methods

Salicylate or KCl solutions that depress outer-hair-cell (OHC) motility were perfused through scala tympani from a fenestra in the apical fourth cochlear turn to the cochlear aqueduct in the base of anesthetized guinea pigs. This perfusion reduced cochlear amplification sequentially from the lowest to highest CF regions. The injection rate was varied to achieve a constant flow rate of 0.5 mm/min of the solution front along scala tympani. This covered 1 octave in 5 minutes.

At one frequency per animal (N=16), SFOAEs were measured every 30 seconds using the double-evoked method (40 dB SPL probe tone and near-frequency 60 dB SPL suppressor tone). Interleaved were measurements of compound action potentials (CAPs) elicited by 40 dB SPL tone bursts at the SFOAE frequency.

Results

As the solution flowed from apex to base, the midpoints of the SFOAE reductions generally occurred later in time than the midpoints of the CAP reductions: by -3.6 to 11.9 minutes for SFOAE frequencies =4 kHz. Continued solution flow decreased SFOAEs to a low asymptotic value but seldom abolished the SFOAE. From the CAP reduction mid-point to the approximate time the asymptotic SFOAE was reached, was 6.6 to 17.4 minutes for SFOAE frequencies =4 kHz. As the perfusion decreased the SFOAE, the SFOAE phase change never exceeded 1 cycle and the phase was constant in the asymptotic region.

Conclusions

Most of the SFOAE originates basal of its CF region with the origin length greatest for frequencies = 4 kHz. SFOAE phase as a function of perfusion time is vastly different from previous reports of residual phase as a function of frequency obtained using swept suppressor tones. These differences show that the SFOAE and swept-suppressor residual originate from different cochlear processes.

Understanding the role of cochlear originated distortion products along the auditory pathway

Xiaohui Lin¹; Chantal Van Ginkel¹; **Wei Dong**²

¹VA Loma Linda Healthcare System; ²VA Loma Linda Health Care System and Otolaryngology, Loma Linda University

When the cochlea is stimulated with two or more tones, distortion products (DPs) are generated by the active process - the cochlear amplifier and its associated nonlinearity. Post-generation, DPs can travel reversely, and are able to be detected by a sensitive microphone in the ear canal, termed as distortion product otoacoustic emissions (DPOAEs). DPOAEs have been studied intensively and are used as noninvasive tools to probe cochlear mechanics in research and the clinic. On the other hand, the DPs also have been shown to travel forwardly in the cochlea in a similar manner as other external tones, i.e., going through similar signal cochlear processing. However, the role of the forward traveling DP components is not well understood even though they have been recorded at various levels of the auditory pathway, such as the cochlea, the auditory nerve, the brainstem, and the auditory cortex.

The current study explores the role of forward-traveling-DP components, i.e., the cubic difference tone (CDT) at frequency of $2f_1-f_2$ and the quadratic difference tone (QDT) at frequency of f_2-f_1 in gerbil, via simultaneous measurements at three levels along the auditory pathway: the ear canal, the basilar membrane, and the brainstem. Both CDTs and QDTs were characterized. The CDTs and QDTs were physiologically vulnerable to cochlear conditions, and decreased when the cochlea was damaged, suggesting their cochlear origin. The reverse traveling QDTs always appeared to be smaller than CDTs when measured in the ear canal. The forward traveling DP components of the CDTs and QDTs, when measured at the brainstem, were dependent on the primary frequency ratio of f_2/f_1 . The CDTs were greater when two stimulus tones were well separated in frequency (i.e., $f_2/f_1=1.25$); alternatively, the QDTs were much greater, even comparable to those of the primaries when the two stimulus tones were close to each other (i.e., $f_2/f_1=1.05$).

These measurements shed light on our understanding of the biological significance of DPs in signal processing along the auditory pathway. In addition, combining the non-invasive measurements of two-tone induced DPOAEs in the ear canal with the brainstem recordings at both primary and DP frequencies can certainly provide crucial information regarding intracochlear condition and the neuronal auditory pathway.

Anomalous DPOAE increase induced by contralateral acoustic stimulation, and its relation to “symmetrical” negative-delay components

Renata Sisto¹; Arturo Moleti²

¹INAIL Research; ²Università di Roma Tor Vergata

The medio-olivo-cochlear (MOC) reflex can be studied in humans by measuring the DPOAE response while exposing the subject to contralateral acoustical stimulation (CAS). The effect of CAS is normally a mild reduction (1-2 dB) of the DPOAE response level. Conversely, in some cases, it is possible to observe an enhancement of the response, particularly in elderly or pathological subjects. On the other hand, in a recent study (Sisto, Moleti, Shera, 2018) it has been shown that “symmetrical” negative-delay components can be observed in the time-frequency representations of the DPOAE response. These components have been interpreted as due to a spatial modulation of the distortion generator strength which is one of the possible realizations of “roughness”. Such a quasi-periodic amplitude modulation of the DPOAE response, lacking a causal phase counterpart, appears indeed in the time-frequency plot as a symmetrically delayed $1/f$ distribution around the zero-delay axis. In order to separate the “true” long-latency components related to place-fixed coherent backscattering from the tonotopic place $x(fDP)$ from those due to the modulation of the distortion generator, generated around $x(f_2)$, it is necessary to subtract the symmetrical component. Applying the subtraction procedure to a data subset in which an enhancement of the signal was observed during the CAS administration, one generally observes an increase of the symmetrically delayed components, whilst both the zero-delay and the asymmetric positive-delay components do not increase. The increase of the symmetrical component means increased modulation of the distortion generator strength, which may be an effect of CAS. Indeed, the decrease of the tuning factor due to CAS implies a broader DPOAE generation region, including gain irregularities on a larger spatial scale. Time-symmetrical components were mainly observed in elderly subjects and in neurological patients, in which these components become particularly large after CAS administration. The relation between CAS-induced DPOAE level changes and age is similar in Parkinsonian patients and in controls, with a significant age shift, suggesting that Parkinsonian patients suffer from early aging of the auditory function. Therefore, it would be worth investigating if the increase of the time-symmetrical DPOAE components could be proposed as a signature of a dynamical increase of this effect of roughness, to be used for the diagnosis of both aging and neurological diseases.

PS 754

Top-Down Modulation of Otoacoustic Emissions and Early Auditory Evoked Potentials by Visual Working Memory Load

Bruno Marcenaro¹; Alexis Leiva²; Vladimir Lopez¹; Constantino Dragicevic³; Paul H. Delano⁴
¹*Pontificia Universidad Católica de Chile*; ²*Audition and Cognition Center. Faculty of Medicine. University of Chile*; ³*Departamento de Neurociencia, Facultad de Medicina, Universidad de Chile*; ⁴*Faculty of medicine*

Selective attention requires focusing on relevant stimulus but also avoiding distracting stimulus from other sensory modalities. A growing line of evidence show that attention and working memory mechanisms are closely related, so that early modulation of sensory processing can impact subsequent working memory performance. Here, we ask whether distortion product otoacoustic emissions (DPOAEs), a sub product of the cochlear amplifier in the cochlea, and early cortical auditory evoked potentials N1 and P2 are modulated by selective attention and visual working memory load. Twenty subjects (twelve male, age range 20-31, mean age 25.2 years) with normal hearing performed a visual change detection task with varying working memory load (high load= 4 objects; low load = 2 objects). Auditory stimulus (frequency range 1250-2200 Hz) were delivered simultaneously with the task to measure DPOAEs, and N1-P2 evoked potentials. Individual visual working memory capacity was assessed using behavioral results. Results show that the amplitude of DPOAEs are modulated by working memory load and that working memory performance is correlated with P2 amplitude. This study helped to clarify the role of auditory efferent pathway in the regulation of cochlear responses and understand how early stimulus processing is related with working memory.

Funded by Fondecyt 1161155, Proyecto ICM P09-015F and Fundacion Guillermo Puelma.

PS 755

Level Dependence of the Coherent-Reflection Source of Cubic Distortion Product Otoacoustic Emissions

Vaclav Vencovsky¹; Ernst Dalhoff²; Anthony W. Gummer²; Ales Vetesnik¹
¹*Czech Technical University in Prague*; ²*University of Tübingen*

Distortion product otoacoustic emissions (DPOAEs) are generated by two simultaneously presented pure tones with close frequencies. They are generated (primary source) by the nonlinear mechano-electrical transducer in the outer hair cell. The lower sideband cubic DPOAE

with frequency 2f₁-f₂ is usually the strongest and generates a traveling wave in the cochlea which peaks at its tonotopic place located apically to the generation place. Impedance perturbations (roughness) at the 2f₁-f₂ tonotopic place can cause a second source of DPOAEs which interfere with the primary source contribution. A 2D nonlinear cochlear model is used to study the relationship between contributions of the primary and secondary sources at different levels of the pure tones. Simulation results are compared with experiments with normal hearing subjects. The aim of the study is to include information about the secondary source in the estimation of hearing threshold by DPOAEs.

PS 756

Stimulus Frequency Otoacoustic Emissions Generated by Suppression and Compression in a Nonlinear Cochlear Model

Vaclav Vencovsky¹; Ales Vetesnik¹; Anthony W. Gummer²

¹*Czech Technical University in Prague*; ²*University of Tübingen*

A pure tone presented to the ear evokes a traveling wave in the cochlea. This traveling wave may be reflected back due to inhomogeneity in the basilar membrane and organ of Corti. The reflected wave is transmitted back through the middle ear and creates a pressure wave in the outer ear canal which is called a stimulus frequency otoacoustic emission (SFOAE). SFOAEs must be extracted from the signal recorded in the outer ear canal where it is mixed with the input stimulus of the same frequency. An extraction method which is used in many experimental studies employs an additional tone of nearby frequency and higher intensity than the probe tone in order to suppress the traveling wave evoked by the probe tone. Another method, called the method of compression, is based on the fact that SFOAE amplitudes do not grow linearly with stimulus intensity. The response to a probe tone is derived from the scaled response obtained with a tone of higher intensity than that of the probe tone. The response is scaled by the ratio of the tone intensities. In humans, these two methods have been shown to yield similar results. However, SFOAEs simulated by a two-dimensional nonlinear cochlear model, which allows for the accurate measurement of true SFOAEs, show differences between the methods and so called true SFOAEs obtained with the model by removing the simulated inhomogeneity. The simulations indicate that both experimental methods are not accurate if the gain of the cochlear amplifier is smaller than approximately 40 dB.

Why Do Cubic Difference Tone DPOAE I/O Functions Rollover?

Mackenzie Mills; Robert Withnell
IU Speech & Hearing

Background:

Two stimulus tones presented to the ear will interact nonlinearly in the cochlea to produce cochlear distortion products and mutual suppression through saturation of the OHC gating function (Geisler et al., 1990). Distortion product otoacoustic emissions arise from two locations in the human cochlea; the first being the location of maximum wave interaction between two stimulus tones, the wave-fixed component, and a second location at the place of the distortion product characteristic frequency (Heitmann et al., 1996), the place-fixed component. The amplitude growth of these distortion products shows a complex behavior that is dependent on stimulus level, stimulus level ratio, and frequency ratio (Gaskill & Brown, 1990). Two-tone suppression (Withnell & Yates, 1998), a nonlinear feedback loop (Lukashkin et al., 2002) and/or a two-component phase interaction (Mauermann & Kollmeier, 2004) may influence the growth of the emissions. Two-tone suppression may explain stimulus-level dependent non-monotonic growth in species where the emission arises primarily from one cochlear location (e.g., guinea pig), although non-monotonic growth has also been described as arising out of a nonlinear feedback loop. The origin of the non-monotonic growth of this emission in primates has not yet been established. In particular, why does the scissor paradigm produce approximately monotonic growth?

Methods:

To investigate the possible effects of two-tone suppression and a two-component interaction on emission amplitude, we varied the stimulus level relationship and stimulus frequency ratio. Six stimulus conditions were used to investigate the effect of the place-fixed component on emission amplitude. $L1 = L2 + 10$; $f2/f1 = 1.17$ (Eqn. 1) $f2/f1 = 1.22$ (Eqn. 2) $L1 = L2$; $f2/f1 = 1.17$ (Eqn. 3) $f2/f1 = 1.22$ (Eqn. 4) $L1 = 80 + 0.137 \cdot \log_2(18/f2) \cdot (L2 - 80)$; $f2/f1 = 1.22 + \log_2(9.6/f2) \cdot (L2/415)^2$ (Eqn. 5) (Johnstone et al., 2006) $L1 = 0.45 \cdot L2 + 44$; $f2/f1 = 1.22$, (Neely et al., 2005) (Eqn. 6) $L1$ and $L2$ are the stimulus levels in dB SPL of the two stimulus tones and $f1$ and $f2$ are the stimulus frequencies in kHz. The variation in these equations are expected to alter the phase relationship between the two DPOAE components.

Ear canal sound pressure was measured using a ER10-B probe in response to two stimulus tones. Custom software in Matlab was used to generate stimuli, record

ear canal sound pressure, and perform data analysis. Time domain recordings were digitized using an RME Babyface audio device at a 96,000 kHz sampling rate and averaged. Emission amplitude and phase were examined for each stimulus condition using Matlab.

Results:

DPOAE I/O functions were obtained from human participants for each of the six stimulus equations. Equation 1 produced a DPOAE I/O function with non-monotonic growth with a dip at a moderate stimulus levels. The dip was examined for the contributions of a two-component interaction versus a consequence of being transduced by a nonlinearity, and the latter was found to be the dominant cause of the dip (Lukashkin et al., 2002). For a frequency ratio of 1.17, the emission is expected to be dominated by the place-fixed component and more closely resemble a one-component source. Non-monotonic I/O functions were observed with this frequency ratio as well. The results for $L1=L2$ I/O functions were similar, although the stimulus levels at which the non-monotonicities were observed were not the same, this presumably reflecting a difference in two-tone suppression effects. Equations 5 and 6 produced I/O functions with monotonic growth with phase as a function of stimulus level indicating that the two components were predominantly in phase. This was more evident as a general feature from equation 5 than equation 6.

Conclusion:

This study examined the effects of two-tone suppression, two-component interactions, and nonlinearity for DPOAE I/O function growth. The purpose of this study had two objectives: firstly, to investigate the impact of each of these three contributions on DPOAE I/O growth, and secondly, why the scissor paradigm is the optimal stimulus equation to produce I/O functions with monotonic growth. The significance of this study relates to the role that the two-component interaction has on the growth of DPOAEs, an impact that would be expected to be most pronounced at low-moderate stimulus levels.

PS 758

Amplitude and frequency modulation in synchronized spontaneous otoacoustic emissions from human ears

Han-Wen Lien¹; Tzu-Chi Liu¹; Shih-Feng Huang¹; Pa-Chun Wang²; Hau-Tieng Wu³; **Yi-Wen Liu¹**
¹National Tsing Hua University; ²Cathay General Hospital; ³Duke University

Background

The synchronized spontaneous (SS) otoacoustic emission (OAE) refers to the long-lasting oscillation

evoked by clicks after transient-evoked OAEs (TEOAEs) attenuate. As the name suggests, SSOAEs are closely related to spontaneous OAEs (SOAEs), but can be synchronously triggered by external stimuli. The spectral characteristics of SSOAEs are well understood (e.g., Wable and Collet, 1994), but their temporal dynamics are less explored (e.g., Sisto et al., 2001; Jdrzejczak et al., 2008). This research aims to extract human SSOAE components and study their time-varying features.

Methods

18 subjects of age 21-28 years were recruited. TEOAEs were measured by presenting a repetition of 3000 clicks with 59 ms intervals. The peak instantaneous amplitude was 31.3 ± 15.2 mPa. Responses were averaged to improve the signal to noise ratio. To search for SSOAEs, the response 20-50 ms after the click was analyzed via Fourier transform and ConceFT, a modern nonlinear time-frequency representation tool based on frequency reassignment and multi-tapering (Wu and Liu, 2018). Individual SSOAE components were extracted by custom-adjusted band-pass filters (BPF). Thus, their amplitude envelope (AE) and instantaneous frequency (IF) can be calculated using the Hilbert transform. For each subject, the OAE measurements were repeated on multiple days so results can be compared.

Results

SSOAEs were found in 18 out of 36 ears. By inspecting the signal after BPF and its AE and IF, it seems possible to categorize the SSOAE components into at least four different types. Type I exhibits in-phase amplitude modulation (AM) and frequency modulation (FM), and the long-term AE slowly decays (See Fig. 1 in the supplementary materials). Type II also shows a slowly decaying AE, but the AM and FM seems to be anti-phase (Fig. 2). Type III shows a relatively fast increasing AE, while the IF seems to converge within 50 ms (Fig. 3). Type IV demonstrates beating of two equally strong components (Fig. 4). Presently, the exact ratio of occurrence of these types is hard to estimate because of noise issues in some of the data.

Conclusions

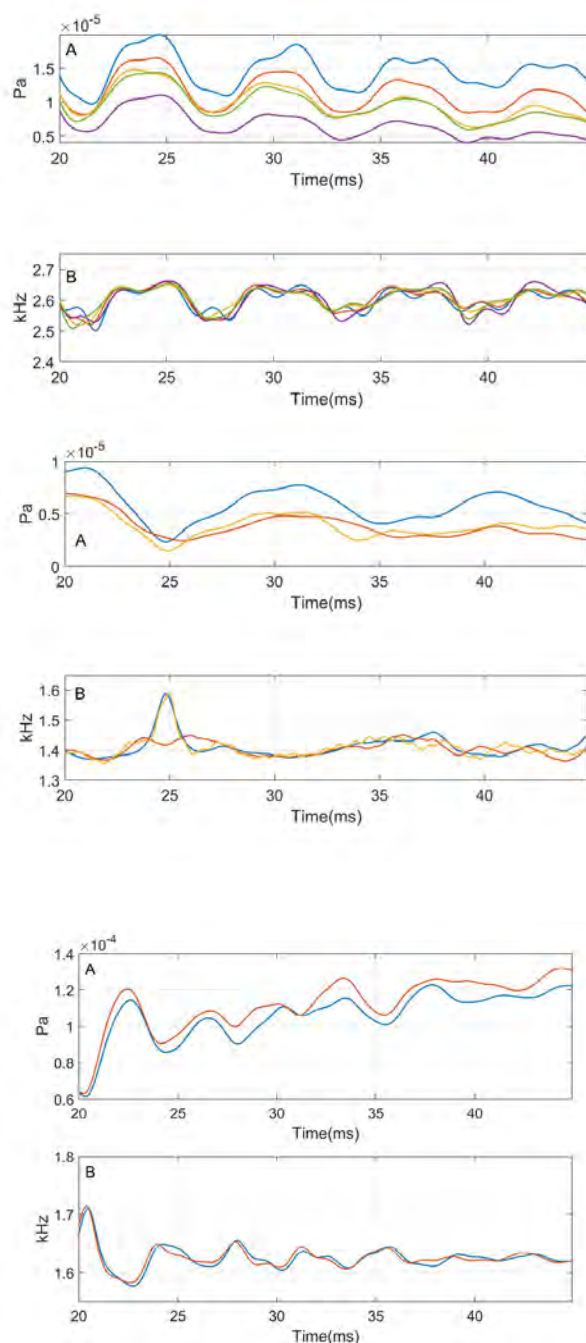
Though similarly triggered by clicks, the present results demonstrate clearly distinct types of SSOAEs in terms of the amplitude and frequency modulation. For the same ear, the AM and FM pattern stays consistent across multiple days. It is not clear whether the types observed here were caused by intrinsically different mechanisms, or they are just different modes that can be explained by one unified theory of cochlear mechanics.

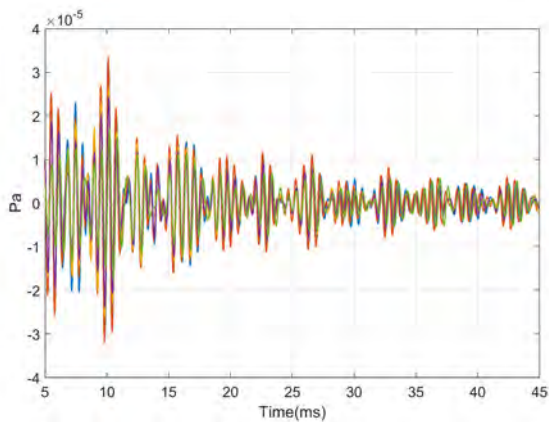
Fig. 1: Type-I SSOAE from a female subject. Colors represent results from different days. **A.** The amplitude envelope (AE). **B.** the instantaneous frequency (IF). The AE and the IF seem to be in-phase. Further analysis shows that the modulation frequency in the IF is about 164.5 ± 0.82 Hz (across different days), and the mean phase different is 0.02 cycle between the AE and the IF at the modulation frequency.

Fig. 2: Type-II SSOAE from a male subject. Colors represent different days. This time, the AE (panel A) and the IF (panel B) are anti-phase.

Fig. 3: Type-III SSOAE from a female subject. Colors represent two different days. The AE seems to have a rising trend with periodic fluctuations that is anti-phase with the fluctuation in the IF.

Fig. 4: Type-IV TE and SSOAE from a male subject. The signal after BPF seems to show two beating components.





Outer & Middle Ear: Mechanics

PS 759

Experimental Evaluation of a New Transcutaneous Bone Conduction Hearing Aid

Ivo Dobrev; Alex Huber; **Christof Röösl**
 Department of Otorhinolaryngology Head & Neck
 Surgery, University Hospital Zürich, University of Zurich

Objectives: Experimental evaluation of the performance of a new transcutaneous (surface mounted via adhesive pad) actuator of a bone conduction hearing aid, and its comparison with conventional bone-anchored actuators.

Methods: Pilot experiments were conducted on a Thiel embalmed whole head cadaver specimen. The electromagnetic actuators from a commercial bone conduction hearing aids (BCHA) (Baha® Power, and ADHEAR®) were used to provide stepped sine stimulus in the range of 0.1-10 kHz. Osseous pathways (direct bone stimulation or transcutaneous stimulation) were sequentially activated by mastoid stimulation via a percutaneously implanted screw (BI300), Baha® Attract transcutaneous magnet, 5-Newton steel headband, and skin surface adhesion (for ADHEAR®). The response of the skull was monitored as motions of the ipsi-, top and contra-lateral skull surface as well as the ipsi- and contralateral promontory. Surface motion was quantified by sequentially measuring ~200 points on the skull surface (~ 15-20mm pitch) via a three-dimensional laser Doppler vibrometer (3D LDV) system. Analogously, single point 3D velocity measurements were done at each promontory.

Results: 3D LDV data indicates that skull surface undergoes complex spatial motion with similar contributions from all motion components, under all coupling types. Actuator coupling type affects the spatial composition of the skull motion, specifically the ratio between the normal and tangent motion.

Conclusion: Comprehensive experiments, including simultaneous motion across the whole skull surface and promontories, allow for detailed exploration and differentiation of various coupling methods for current and potential future BCHA.

PS 760

Evaluation of an Efficient Numerical Computation of Pinna Resonance Sensitivity to Physiological Perturbations: Preliminary Results

Parham Mokhtari
 NICT / CiNet

Monaural auditory cues for sound-source localization are provided by head-related transfer function (HRTF) peaks and notches, which are generated mainly by acoustical resonance in the pinna (outer ear) cavities. Insofar as each person has a unique ear geometry, individual variation in sound localization performance may partly be attributed to the relative prominence of such cues. Conversely, geometry-related “sensitivity maps” may help identify any pinna-shape modifications that might enhance these auditory cues, and thereby the individual’s sound-localization performance.

Here, we calculate pinna-resonance sensitivity maps using finite-difference time-domain (FDTD) simulation of three-dimensional (3D) acoustic wave propagation and scattering. While human 3D pinna geometries were also measured by magnetic resonance imaging (MRI), we first evaluate our methods on a simplified pinna model comprising only one cavity (concha) with an elliptical cross-section. In particular, two methods are compared: (i) a baseline but computationally costly “direct perturbation” (DP) method, where the shift in each resonance frequency is calculated after inserting a single voxel at a time in and around the pinna-cavity air volume (thus requiring thousands of simulations); and (ii) a computationally much more efficient method that requires only one simulation for each resonance with the unperturbed pinna geometry, followed by calculation of an “acoustic radiation pressure” (ARP)-like quantity using the acoustic pressure and particle velocity at every voxel.

Our simulations with the pinna model (represented at isovoxel resolution 2 mm, total 2223 air-voxels) first revealed three resonances up to 15 kHz: (P1) a longitudinal mode at 4133 Hz with maximum farfield response at {ipsilateral azimuth 80 deg, elevation 0 deg}; (P2) a major-axis transverse mode at 8771 Hz with maximum response at {ipsilateral azimuth 55 deg, elevation 101 deg}; and (P3) a minor-axis transverse mode at 11139 Hz with maximum response at {ipsilateral azimuth 45 deg, elevation 169 deg}. Images

of the sensitivity maps for each resonance showed a reasonably good qualitative agreement between the two methods. Quantitatively, scatter-plots of the 2223 shifts in each resonance frequency obtained with the ARP-like versus the DP method confirmed close agreement, with correlation coefficients 0.92, 0.91, and 0.97 for P1, P2, and P3, respectively. Nevertheless, the two methods did not yield identical results, pointing to potentially systematic sources of mismatch, some of which will be discussed.

This work was supported by JSPS KAKENHI Grant Number JP17K00260.

PS 761

Middle ear transmission recovery during the spontaneous healing process of tympanic membrane perforations in gerbil

Glenna Stomackin¹; LingLing Cai²; Xiaohui Lin¹; Timothy Jung¹; **Wei Dong**³

¹VA Loma Linda Healthcare System; ²the Ninth People's Hospital Affiliated to Shanghai Jiaotong University, School of Medicine; ³VA Loma Linda Health Care System and Otolaryngology, Loma Linda University

Tympanic membrane (TM) perforations in patients are commonly caused by either trauma or infection. These perforations may spontaneously heal, however the spontaneously healed TMs are thickened and denser and thus patients still present conductive hearing loss (CHL) in the clinic. The current study explored hearing and middle ear (ME) transmission recoveries over the healing process post TM-perforation in gerbils.

Post mechanically induced TM perforation to either one-quarter (25%) or half (50%) removal of the pars tensa, hearing was evaluated by auditory brainstem responses (ABRs) and distortion product otoacoustic emissions (DPOAEs) weekly up to 4 weeks post. Between 5-6 weeks post, ME transmission was directly measured from the input to the output of the ME using three simultaneously recorded quantities and comparisons of each pair: pressure responses at the TM near the umbo (PTM) using an ultrasound Sokolich probe-tube microphone, velocity of the umbo (Vumbo) using a laser Doppler vibrometer, and pressure responses in scala vestibuli (PSV) produced by the motion of the stapes using a micro-pressure sensor. After in-vivo measurements, TMs of the left and right ears were harvested and the thicknesses were mapped via optical coherence tomography (OCT).

Consistent to published results, TM closure started at ~1-week post-perforation and was complete closed by 2

weeks. The thicknesses of the TMs at their perforation locations at week 5-6 were about 3 times thicker than normal TMs. ABR thresholds and DPAOEs showed size- and frequency-dependent manners over the recovery period. At week 1, ABR thresholds started to recover, especially at frequency region between 5-10 kHz, however, the DPOAEs showed further reduction. From week 2, both ABR thresholds and DPOAEs recovered progressively. By week 4, neither of them recovered completely, and significant reductions still existed at low-(30 kHz). The incomplete recovery was consistent with direct measures of the ME transmission in forward and reverse directions via PTM, Vumbo, PSV, and derived quantities, i.e., umbo transfer function (Vumbo/PTM) and middle ear pressure gain (PSV/PTM), which showed size- and frequency-dependent ME transmission losses due to the abnormalities of the healed TMs. Our results contributed to our understanding of ME transmission under these TM pathological conditions, the role of the TM in sound transmission and the CHL in patients over the spontaneously healing process.

PS 762

Two Procedures to Calibrate Microphones for High-frequency Auditory Experiments Yield Equivalent Results

Jonathan H. Siegel¹; Michael E. Ravicz²

¹Northwestern University; ²Eaton-Peabody Lab, Mass. Eye & Ear

Introduction: Only a few descriptions have appeared in the literature of procedures to calibrate microphones to measure sound levels in the ears of small rodents. Two have been described in detail. One procedure places the inlet of the uncalibrated probe tube microphone of an acoustic source designed for small mammals within 1 mm of the diaphragm of a 1/8" reference microphone (EPL Cochlear Function Test Suite Users'; Manual, ver. 1.0; Beranek, 1986). Acoustic excitation is provided via one of the acoustic source's internal earphones. It is assumed that the sound levels at the reference and uncalibrated probe tube microphone (including any contribution of non-uniform transmission modes) are the same, due to the small separation between them. The other uses a variant of the substitution method (e.g., Beranek, 1986), in which the excitation sound produced by a separate sound source is delivered through a damped tube to either the reference or probe tube microphone placed at the same location. A small auxiliary probe tube microphone placed within 1 mm of the microphone corrects for differences in sound pressure caused by differences in the local acoustic impedance of the reference and uncalibrated probe microphones (Siegel, 2002; Rasetshwane and Neely, 2011). This arrangement aims to apply uniform

plane wave excitation to the two microphones and is not limited by the output of the earphones in the acoustic source. In principle, these two calibration methods should yield equivalent sensitivities and frequency responses of the uncalibrated microphone. Here we test this assertion.

Methods: Each of the two calibration procedures was applied to two small-animal acoustic sources: the EPL Acoustic System and an otoacoustic emission probe designed by the first author for measurements in mice (the NU OAE probe). All measurements were made at Northwestern University. In both cases, the reference microphone was a Brüel & Kjaer 4138 1/8" condenser microphone. The auxiliary probe tube used in the second procedure was a Knowles FG 23742 with a 23.4 mm long x 0.66 mm ID probe tube. Sound pressure frequency responses were measured with chirp excitation and transfer functions calculated using SysRes (Neely and Stevenson, 2002).

Results: Microphone sensitivities and frequency responses for each probe tube microphone were found to be virtually identical at frequencies up to 60 kHz when measured by either procedure. Comparisons at higher frequencies could not be made due to the noise floor of the auxiliary probe tube microphone used in the second procedure.

Conclusions: The observation that the sensitivities and frequency responses measured using the two calibration procedures were virtually identical further validates both procedures. Sound levels measured using a microphone calibrated with either procedure should be equally accurate.

Funding: Supported by the Knowles Hearing Center, Northwestern University and the Massachusetts Eye and Ear.

PS 763

Effects of High-level Contralateral Noise on Simultaneous Measurement of Electrocochleography and Ear Canal Pressure in Normal-hearing Adults

Jessica Chen; Michael Simpson; Skyler Jennings
University of Utah

Background:

The middle ear muscle (MEM) reflex modulates incoming acoustic stimuli by stiffening the ossicular chain, thereby increasing middle ear impedance to low-frequency sounds. Activity of the MEM reflex in humans is often inferred by monitoring changes in impedance at the tympanic membrane (TM) using ear canal pressure measurements. The MEM reflex is also expected to

influence pre-neural and neural cochlear potentials as measured by electrocochleography (ECoChG). These cochlear potentials provide an estimate of the influence of MEM activity on the effective signal reaching the auditory nerve.

Simultaneous measurement of ear canal pressure and ECoChG is expected to reveal how MEM-related changes in acoustic impedance at the TM relate to the effective signal reaching the auditory nerve. This experiment tests the hypothesis that activation of the MEM reflex using contralateral acoustic stimulation (CAS) results in decreased cochlear microphonic (CM) amplitude across a range of frequencies (226-1356 Hz), consistent with a reduction in the effective signal reaching the auditory nerve.

Methods:

A probe microphone and a TM electrode were placed in the right ear canal to simultaneously measure ear canal pressure and the CM in adults with normal hearing. The ipsilateral probe was a tone complex and was presented with or without a high-level (80-90 dB SPL) broadband noise.

Results:

CM amplitude was reduced with compared to without CAS, regardless of probe frequency. In contrast, probe pressure in response to CAS increased for probe frequencies below 1000 Hz, consistent with greater TM impedance. For frequencies at and above 1000 Hz, CAS resulted in decreased probe pressure, consistent with greater TM admittance.

Conclusions:

CM amplitude decreased in response to CAS, regardless of the direction of pressure change in ear canal pressure, consistent with an MEM-induced reduction of the effective signal reaching the auditory nerve for frequencies between 226-1356 Hz. Greater TM admittance with CAS for frequencies at and above 1000 Hz did not result in increased CM amplitude, which is consistent with an additional MEM-related change in impedance occurring between the TM and cochlea.

PS 764

Lumped-Element Model of a Hearing Contact Lens for Tympanic Membrane Stimulation

Ainhitze Mendizabal; Daniela Wildenstein; Anthony W. Gummer; Ernst Dalhoff
University of Tübingen

Background

The main disadvantages of conventional hearing aids are their limited high-frequency capabilities in the case

of the preferred open-fit configuration (widely vented ear canal), the feedback of the amplified sound into the ear canal, and their visibility. The first two disadvantages limit the sound quality of aided hearing, and depend on the limits in the miniaturization of speakers and the relatively high degree of reflection of sound at the tympanic membrane, especially at high frequencies. Recently, alternative concepts based on direct mechanical stimulation of the tympanic membrane have been proposed (Fay et al. 2013, *Otol. Neurotol.* 34:912-921; Perkins 1996, *Otolaryngol. Head Neck Surg.* 114:720-728). Here, we investigate the modeling and design of a piezoelectric actuator (Schächtele et al. 2012 *IEEE Trans. Ultrason. Ferroelectr. Freq. Control* 59:2765-2776) used for driving a hearing contact lens placed directly on the tympanic membrane. The piezoelectric actuator is manufactured using micro-electromechanical systems (MEMS) technology, enabling easy scalability and providing high amplitudes and bandwidth despite its small dimensions.

With the aim of enabling a better understanding of the driving principles of such tympanic membrane actuators, we present a physically motivated model, which simulates the basic mechanical behavior of the hearing contact lens acting on the human ear. This model predicts the experimental response of the human ear to frequencies up to 10 kHz.

Methods

Experimental vibration data for the actuator were obtained using a Laser Doppler vibrometer under different load conditions, and in human temporal-bone experiments where the actuator was placed at the tympanic membrane, driving the middle ear and the cochlea. Middle-ear transmission was measured at the stapes in response to electrical stimuli to the actuator as well as sound-pressure stimulation of the eardrum without attached actuator.

Model parameters were fitted in separate steps to the series of experimental results for different load and stimulus conditions.

Results

Simulations show that the developed lumped-element model describes the performance of the piezoelectric actuator acting on the tympanic membrane as well as the coupling to the anatomical structures, in fair agreement with the experimental data up to frequencies of 10 kHz.

Conclusion

The model enables analysis of the coupling of the actuator to the tympanic membrane in individual experiments and optimization of the actuator, its fixation, and the silicone cap.

PS 765

Implications of Oblique Ear-Probe Insertions on Reflectance

Kren Rahbek Nørgaard¹; Efren Fernandez Grande¹; Søren Laugesen²

¹*Technical University of Denmark*; ²*Interacoustics Research Unit*

Measurements of the ear-canal reflectance using ear probes require estimating the characteristic impedance of the ear canal in situ. However, an oblique insertion of an ear probe causes difficulties in estimating this characteristic impedance. As a starting point for the investigation of this problem, oblique probe insertions into a uniform occluded-ear simulator are considered. The characteristic impedance of a uniform waveguide is closely related to the cross-sectional area and an oblique ear-probe insertion modifies the waveguide geometry in front of the ear probe into a short horn loading. Such an oblique ear-probe insertion introduces significant errors into measurements of the ear-canal reflectance, however, current measurement technology is neither able to identify nor compensate for these errors.

This poster gives an overview of the implications of oblique ear-probe insertions in measurements of the ear-canal reflectance and proposes a methodology that can detect and quantify them. This is achieved by estimating the characteristic impedance across multiple frequency ranges. If the ear probe is inserted at an oblique angle into the ear canal, these estimated characteristic impedances vary with this frequency range. Additionally, a method is proposed to compensate for the effects of an oblique ear-probe insertion on the measured reflectance in an otherwise uniform waveguide. This is achieved by estimating the incident measured impedance of the horn loading, i.e., the measured impedance were the uniform waveguide terminated by its characteristic impedance. This incident measured impedance then replaces the characteristic impedance when calculating the reflectance.

The proposed method is capable of accurately identifying and compensating for an oblique ear-probe insertion into the occluded-ear simulator, obtaining substantially similar reflectances with perpendicular and oblique ear-probe insertions. The method was able to reduce the variation of the measured ear-canal reflectance with insertion depth, however, more research is required to further assess the applicability of the method in real ears and to validate the measured ear-canal reflectance.

Do Ambient Pressure Changes Impact Coupling Efficiency of a Middle Ear Implant Actuator?

Ute A. Gamm¹; Nils K. Prentzler²; Max E. Timm²; Thomas Lenarz²; Hannes Maier²

¹Cochlear Deutschland GmbH & Co. KG; ²Hannover Medical School

Introduction: One of the options to treat moderate to severe sensorineural (SNHL) and mixed hearing loss (MHL) is the implantation of an active middle ear implant like the Cochlear™ Carina® implant. The actuator of the implant is fixed firmly to the skull and stimulates the ossicular chain either through coupling to the incus body or to the long process of the incus, stapes head or round window. Clinicians and recipients need assurance that the coupling will be stable over time, even under slow movements of the ossicular chain caused by changes in barometric pressure. This has not been systematically investigated in laboratory experiments where the coupling itself can be challenged in a controlled and reproducible way. We designed a study to test whether pressure fluctuations to the middle ear expected from events from daily life could potentially move the ossicular chain enough to change coupling efficiency of the actuator.

Methods: Experiments were performed on fresh frozen human temporal bones. Two daily-life pressure events were tested; Valsalva's manoeuvres (500 cycles of -40 hPa - +60 hPa) and jumping into a swimming pool and diving 3 meters deep (a step change of 300 hPa). To simulate Valsalva's manoeuvre a clinical tympanometer was used, and to simulate the larger pressure event of 300 hPa compressed air from the laboratory faucets was regulated and connected to the ear canal via a custom made attachment to the ear canal. Actuator coupling efficiency was measured before and after the pressure events through laser Doppler vibrometric measurement of stapes motion for a frequency range between 100 Hz and 10 kHz. The actuator coupling efficiency was expressed as equivalent free field sound pressure levels at 1 Vrms actuator input. Three different coupling configurations were tested; coupling to the incus body, coupling to a small hole to the incus body made by a surgical laser (standard procedure at Hannover Medical School) and coupling to the long process of the incus via an áWengen clip.

Results and conclusion: Preliminary data of this ongoing study is currently available for 4 temporal bones. All 3 coupling configurations connected the actuator securely to the ossicular chain. Small changes after pressure application of less than 7 dB were observed in individual cases and occurred after the 500 pressure cycles as well as the larger pressure event of 300 hPa. More data will be

collected in the following weeks allowing for more definite interpretation of the data.

PS 767

Actuator Performance for Different Coupling Configurations of the Cochlear™ Carina® Active Middle Ear Implant

Ute A. Gamm¹; Nils K. Prentzler²; Max E. Timm²; Thomas Lenarz²; Hannes Maier²

¹Cochlear Deutschland GmbH & Co. KG; ²Hannover Medical School

Introduction: The Cochlear™ Carina™ active middle ear implant (AMEI) can be used to treat moderate to severe sensorineural (SNHL) and mixed hearing loss (MHL). The implant can be coupled to multiple places on the ossicular chain, like the short and long process of the incus and the stapes head, as well as the round window. The decision, which coupling configuration will be used is highly dependent on the patient's situation; i.e. sensorineural or mixed hearing loss, ossification, absence of ossicles etc. More information about actuator efficiency for each coupling configuration could help the surgeon to make an informed decision on which type of coupling would most benefit their patient.

Methods: We carried out a temporal bone (TB) study where we measured and compared actuator output for different coupling configurations: coupling to the incus body, coupling to the incus to a hole made with a surgical laser, coupling to the long process of the incus using an áWengen clip and coupling to the stapes head using an áWengen clip. Actuator output was measured through laser Doppler vibrometric measurement of stapes motion for a frequency range between 100 Hz and 10 kHz. The actuator output was expressed as equivalent free field sound pressure levels at 1 Vrms actuator input.

Results: Preliminary data of this ongoing study is currently available for 4 temporal bones. For coupling to the incus body, with and without a laser hole, actuator output was stable at approximately 120 dB for the low frequency range between 100 and 1000 Hz. Above 1000 Hz actuator output varied between 100 and 140 dB for the four TBs, mostly describing a gradual rise up to 140 dB in output, followed by a dip at 6-8 kHz. Coupling to the long process of the incus resulted in varying results and coupling to the stapes was the most efficient. Coupling to the stapes led to an actuator output of 130 to 140 dB SPL_{eq} for the 100-1000 Hz range and up to 20 dB higher at frequencies higher than 2 kHz.

Conclusion: All 4 coupling configurations led to high actuator output with long-process coupling leading to most variable results. More data will be collected and presented at the conference.

PS 768

Novel Application of Ambient Pressure Tympanometry for Superior Semicircular Canal Dehiscence Screening

Anthony Thai¹; Zahra N. Sayyid²; Davood K. Hosseini²; Austin Swanson³; Yifei Ma²; Ksenia Aaron²; Yona Vaisbuch²

¹Stanford University School of Medicine; ²Department of Otolaryngology-Head and Neck Surgery, Stanford University School of Medicine; ³Stanford University

Background: Superior semicircular canal dehiscence (SSCD) consists of a defect in the bony layer overlying the superior semicircular canal. The syndrome consists of a wide range of symptoms, including autophony, aural fullness, and pulsatile tinnitus. The current diagnostic work-up consists of audiometry, vestibular evoked myogenic potentials (VEMPs) and a CT scan, but poor correlation exists between these diagnostic modalities. Ambient pressure tympanometry (APT) uses a microphone to record changes in sound intensity in the external ear canal while a speaker introduces a tone. However, in contrast to standard tympanometry, the recording occurs over time without introducing external pressure. This tympanometry technique is not utilized regularly and until now, was only used as the baseline measurement in patulous Eustachian tube tests. Here we introduce for the first time the use of APT test as a potential screening tool for SSCD.

Objective: To introduce the concept and the potential application of continuous APT tracing in screening for superior semicircular canal dehiscence (SSCD), and to propose a method for objectively distinguishing positive APT findings from noise.

Methods: Adult patients at a tertiary otology referral center. APT was performed randomly, and patients with computerized tomography (CT) scans of the temporal bone were retrospectively analyzed. Ears were divided into SSCD and control groups based on presence or absence of SSCD on CT imaging, and APT findings were analyzed in each group. Patients with diagnoses other than SSCD that could potentially affect tympanic membrane mobility were excluded.

Results: We describe 46 patients (72 ears) who underwent APT and CT imaging. In the SSCD group, 64.7% of patients displayed regular waves on APT, compared to 26.5% of patients in the control group (sensitivity: 64.7%, specificity: 73.5%). The average amplitude of positive waves in the SSCD group was 0.036 mL, compared to 0.014 mL for positive waves in the control group. We propose a novel algorithm for distinguishing true APT waves from noise using criteria

based on regularity, frequency and amplitude of the waves.

Conclusion: Characteristic wave patterns on APT, over time, may be indicative of otherwise unrecognized pathology, such as SSCD. APT is a simple, feasible and widely available tool that can help direct suspicion and inform diagnosis. The sensitivity and specificity of this potential screening tool will need to be confirmed in a larger, prospective study.

PS 769

Effect of Tensor Tympani on High Fidelity Sound Transmission Through the Middle Ear

Mohamed Diop; Elizabeth S. Olson
Columbia University College of Physicians and Surgeons

The tympanic membrane plays an important role in transmitting a wide range of frequencies with high temporal fidelity in the middle ear. Recent evidence suggests that tensor tympani may have a role in modulating the high-fidelity sound transmission in the middle ear by fine-tuning the tympanic membrane's response. These findings have motivated us to investigate the changes in high fidelity sound transmission by the eardrum when the tensor tympani is manipulated. To this purpose, we drive the ear of a fresh post-mortem gerbil with a 20 us click, a broadband stimulus that contains frequencies up to ~ 50 kHz, using a Tucker Davis Technologies stimulus generator and a JIX tm earbud speaker. The click stimulus is measured with a Sokolich probe tube ultramicrophone positioned near the ear canal. A Polytec laser interferometer is used to record the velocity response of the umbo and several locations on the TM when the tensor tympani is tightened. The TM velocity responses are processed by a LeCroy 200 MHz oscilloscope and the corresponding data is transferred to MATLAB for analysis. Preliminary results suggest that manipulating the tensor tympani may result in an increased ringing response on the umbo, implying that the tensor tympani may have some effect on fine-tuning high-fidelity sound transmission by the TM.

PS 770

Finite-element modelling based on optical coherence tomography and X-ray microCT data for the same human middle ear

Marzieh Golabbakhsh¹; Xuan Wang¹; Dan MacDougall²; Josh Farrell²; Thomas Landry²; W. Robert J. Funnell³; Robert Adamson⁴

¹Dept. BioMedical Engineering, McGill University, Canada; ²School of Biomedical Engineering, Dalhousie University, Canada; ³Depts. BioMedical Engineering

Optical coherence tomography (OCT) is an emerging imaging modality which is non-invasive and can be employed *in vivo*. There is interest in the clinical application of OCT for imaging of the middle-ear because it can record both static anatomy and vibrations. An akinetic swept-source laser system makes imaging of the full depth of the human middle ear possible in real-time and it provides both brightness mode (B-mode) images and phase-resolved Doppler vibrography measurements. We recorded vibrations at three different frequencies (500 Hz, 1 kHz and 2 kHz) in a human cadaver middle ear. We also have X-ray microCT images from the same specimen. A finite-element model was built based on geometry obtained from the microCT images. The material properties and boundary conditions of the model were obtained from previously reported studies. Model verification was performed by applying multiple finite-element solvers and comparing their simulation results. The simulated vibration pattern of the tympanic membrane in our model can be compared with the corresponding experimental OCT vibration data. This is a first step toward creating patient-specific models based on *in vivo* OCT measurements.

PS 771

In-vivo vibration measurements of the gerbil eardrum under quasi-static pressures

Orhun Kose¹; W. Robert J. Funnell²; Sam J. Daniel³

¹*Dept. BioMedical Engineering, McGill University, Canada;* ²*Depts. BioMedical Engineering and Otolaryngology - Head & Neck Surgery, McGill University;* ³*Depts. Pediatric Surgery and Otolaryngology - Head & Neck Surgery, McGill University*

Tympanometry is a relatively simple non-invasive test of the status of the middle ear. An important step toward understanding the mechanics of the middle ear during tympanometry is to make vibration measurements on the eardrum under tympanometric pressures. Our previous studies included post-mortem measurements at several points on the gerbil eardrum, showing the spatial pattern of the vibration response and the effect of static pressure steps. In this study, we measured *in vivo* vibration responses in nine gerbils under quasi-static pressures. Vibrations were recorded using a single-point laser Doppler vibrometer with five glass-coated reflective beads (diameter ~40 µm) as targets. The locations were the umbo, mid-manubrium, posterior pars tensa, anterior pars tensa, and pars flaccida.

As described in earlier studies (e.g., Maftoon et al., 2013), the unpressurized vibration magnitude was flat at low frequencies, increased until a resonance frequency at around 1.8–2.5 kHz, and became complex at higher frequencies. At both the umbo and mid-manubrium points, when the static pressure is increased to the largest positive pressure (+2500 Pa, eardrum retracted into the middle ear), the low-frequency vibration magnitude (measured at 1.5 kHz) showed a monotonic decrease, except for an unexpected dip at around +500 to +1000 Pa. This dip was not present for the pars-tensa and pars-flaccida points. The resonance frequency shifted to higher frequencies, to around 7–8 kHz at +2.5 kPa. On the negative-pressure side (eardrum bulging towards the ear canal), the low-frequency vibration magnitude decreased monotonically, with no dip, and the resonance frequency shifted to around 5–6 kHz at -2.5 kPa. There was more inter-specimen variability on the negative-pressure side than on the positive-pressure side. The low-frequency vibration magnitudes on the positive-pressure side were higher for the pars-tensa points than for the umbo and mid-manubrium points, while the magnitudes were similar at all four locations on the negative-pressure side. Most gerbils showed repeatability within less than 10 dB for consecutive cycles. For a few gerbils, measurements after sacrifice are also presented. The results of this study provide insight into the mechanics of the gerbil middle ear under tympanometric pressures.

PS 772

Morphometry of the Human Stapedial Annular Ligament from Multiphoton Imaging

Merlin Schär¹; Ivo Dobrev²; Michail Chatzimichalis³; Christof Röösl²; Alex Huber²; Jae Hoon Sim¹

¹*University Hospital Zurich;* ²*Department of Otorhinolaryngology Head & Neck Surgery, University Hospital Zürich, University of Zurich;* ³*Dorset County Hospital,*

Background: The annular ligament provides a compliant interface between the stapes and oval window. Previous studies were able to expose a three-layered structure of the ligament in cross sections but could not quantify the three-dimensional features along the full boundary in intact human samples. This represents a significant obstacle for the development of more accurate simulations of middle-ear behavior. In order to resolve this issue, the three-layered structure and complex spatial geometry along the complete boundary of an intact human annular ligament were investigated via multiphoton microscopy, which was thereby introduced as a novel tool for soft-tissue morphometry in the middle ear.

Methods: The region around the oval window niche with an intact stapes and annular ligament was extracted from a fresh-frozen human temporal bone of a 46-years old female. The morphometry of the annular ligament could be obtained from the unstained sample due to the second-harmonic generation of collagen and auto-fluorescence of elastin. Multiphoton scanning of the face layers on both the middle-ear and cochlear side of the annular ligament were conducted separately. Based on the two separate multiphoton scans, the face layers were manually segmented and registered to a high-resolution μ CT image of the same sample.

Results: The multiphoton scans of the human annular ligament showed that 1) the core layer is much thicker than the face layers, 2) the face layers between the middle-ear and cochlear side exhibit an asymmetric geometry with varying thickness and width along the footplate boundary, 3) the two face layers feature a divergent relative alignment, and 4) the face layer fiber composition varies along the boundary, most clearly observed at the collagen-reinforced anterior pole on the middle-ear side of the investigated sample.

Conclusion and outlook: Within the scope of this study, multiphoton imaging was introduced as a morphometrical tool for soft-tissue structures in the middle ear. The feasibility of this novel approach was demonstrated by using this modality to obtain the full sandwich beam structure of an intact human annular ligament along its complete boundary. The comprehensive workflow established for sample preparation, image processing, and 3D-feature analysis can be used for future investigations of more samples and the morphometry of other soft-tissue structures in the middle-ear. The resulting data may contribute to the refinement of existing and future numerical middle-ear simulations.

PS 773

Preliminary Investigations of Rupture of Human Tympanic Membrane subjected to High Pressure Loads

Payam Razavi¹; Haimi Tang¹; Koohyar Pooladvand¹; Cassia Larson²; John Rosowski³; Cosme Furlong¹; Jeffrey T. Cheng⁴

¹Center for Holographic Studies and Laser micro-mechaTronics, Mechanical Engineering Department, Worcester Polytechnic Institute; ²Harvard College; ³Eaton Peabody Lab, Massachusetts Eye and Ear Infirmary, Harvard Medical School; ⁴Eaton Peabody Laboratory, Massachusetts Eye and Ear Infirmary; Department of Otolaryngology, Harvard Medical School

Background:

ARO Abstracts

High-intensity impulsive sounds caused by blast waves (e.g., explosion, large caliber ordnance, etc.) can damage the Tympanic Membrane (TM), which leads to mild to severe conductive hearing loss. In order to improve the design of hearing protection and TM rehabilitation surgeries, it is important to understand the complex TM failure mechanisms under high amplitude excitations. To achieve this goal, we apply High-Speed Digital Image Correlation (HS-DIC) methods for full-field-of-view measurements of cadaveric human TMs subjected to high pressure excitations.

Method:

Fresh normal human post-mortem TMs are ruptured by rapidly pressurizing the middle-ear cavity (within 200 msec) to levels of tens of kPa using a custom-made loading apparatus. Two tubes are sealed into the middle-ear cavity through the facial recess to deliver the excitation and monitor the cavity pressure independently. The dynamic rupture process together with shape and in- and out-of-plane displacements and deformations (strains) of the entire TM surface are simultaneously quantified using a three-dimensional HS-DIC system at high frame rates (i.e., >100,000 frames per seconds). The results enable full investigation of displacements and deformations over the rapid time-course of TM response and TM failure mechanisms as well as quantitative comparisons of shape parameters (i.e., curvature, area, etc.) before and after TM rupture as well as during the pressurization.

Results:

The TM failure mechanism can be described in four sequential stages: 1- global TM displacement, 2- global TM expansion with dominant in-plane deformations, 3- local strain concentrations, and 4- local crack (the initial opening of a perforation) propagation mostly at the locations of local strain concentration. A preliminary analysis of crack location and propagation suggests the cracks occur and grow along both radial and circumferential fiber directions, with clear differences in propagation speed. Radial cracks occur rapidly and spread with speeds as high as 85 $\mu\text{m}/\mu\text{s}$, while circumferential cracks show two stages with an initial very slow crack propagation (< 0.5 $\mu\text{m}/\mu\text{s}$) followed by rapid propagation (~ 45 $\mu\text{m}/\mu\text{s}$) with signs of fiber delamination.

Conclusions:

We managed to perform preliminary measurements of 3D transient displacements and shape of the TM under high strain rates by HS-DIC methods in full-field of view. The results describe the high-displacement and high-strain rates of TM response from the initial stages of rapid pressurization up to complete TM failure. The high spatio-temporal resolution measurements allow

the determination of TM mechanical properties and the description of high pressure load induced TM injury failure mechanisms.

Funding:

This work is supported by NIDCD 5R01DC016079 and NSF MRI-CMMI-1428921. We thank the Massachusetts Eye and Ear and the Worcester Polytechnic Institute.

PS 774

Contribution of the Flexible Incudomalleal Joint to Hearing under Static Pressure Change

Birthe Warnholtz¹; Benjamin Sackmann²; Merlin Schär¹; Dmitrii Burovikhin²; Pascale Cuny¹; Michael Lauxmann²; Jae Hoon Sim¹

¹University Hospital Zurich; ¹Hochschule Reutlingen

While most of other mammals have an immobilized incudomalleal joint (IMJ), the IMJ in human ears is deformable allowing relative motion between the malleus and incus. Previous studies revealed that the mobility of the IMJ in human ears acts negatively to high-frequency hearing by causing a middle-ear sound transmission loss above 2 kHz. Then, a possible role of the flexible IMJ might be immediate adaptation of sound transmission to changes in surrounding conditions such as static pressure difference between the ear canal and middle-ear cavity. This study aims to examine middle-ear sound transmission under different static pressure for mobile and immobilized IMJ, and to explore roles of the flexible IMJ in human ears for adaptation to static pressure change. An artificial ear canal attached to the annular rim of the eardrum in cadaveric temporal bones, and static pressure change in the range of -500 to 500 dPa was made within the artificial ear canal, using an air pump. Then, dynamic stimulation in the frequency range of 0.5-10 kHz was integrated into the static pressure chamber, and motion of the middle-ear ossicular chain was measured using a 3D Laser Doppler vibrometer (LDV). Such measurements were performed before and after the IMJ was artificially immobilized. The immobilization of the IMJ was made by replacing the synovial fluid in the IMJ with glue. The static and dynamic simulation could be integrated without considerable interference each other, and three-dimensional (3D) motion components were constructed for each of three middle-ear bones from the measurement with the LDV. With the static pressure change in the ear canal, relative sliding of the two articular surfaces (i.e., articular surfaces of the malleus and incus) was observed for the mobile IMJ whereas the relative sliding was prohibited by immobilizing the IMJ. The middle-ear structures were stiffened by static pressure changes in the ear canal, and middle-ear sound transmission differed with the static pressure change. The stiffening of the middle-

ear structures along the audible frequency range was also confirmed by examination using a wide-band tympanometry. The mobility of the IMJ in the human middle ear is presumed to provide a spatial buffer for static pressure change and thus minimize attenuation of middle-ear sound transmission by the static pressure change. Such a role of the IMJ can be emphasized as an immediate response to static pressure change surrounding ears because pressure equalization by the Eustachian tube has time lags.

PS 775

Comparative Study of the Tympanic Membrane in Normal and Experimentally Simulated Pathological Ears by Modal Analysis

Haimi Tang¹; Payam Razavi¹; Nima Maftoon²; John Rosowski³; Cosme Furlong¹; Jeffrey T. Cheng⁴

¹Center for Holographic Studies and Laser micro-mechanics, Mechanical Engineering Department, Worcester Polytechnic Institute; ²Systems Design Engineering, University of Waterloo; ³Eaton Peabody Lab, Massachusetts Eye and Ear Infirmary, Harvard Medical School; ⁴Eaton Peabody Laboratory, Massachusetts Eye and Ear Infirmary; Department of Otolaryngology, Harvard Medical School

Background:

We are developing a High-speed Digital Holographic (HDH) system to measure acoustically induced transient displacements and shapes of live mammalian Tympanic Membrane (TM) for research and clinical applications. Currently, the HDH system measures the shape of the entire TM with a resolution of about 120 μm , and sound-induced displacements with temporal resolutions of less than 20 μsec . The full-field of view measurement technique and the high spatial and temporal resolution of the TM shape and transient displacement measurements allow us to apply Experimental Modal Analysis (EMA) to extract complex mode shapes including their amplitudes, damping, and natural frequencies to quantitatively compare vibrations of different TMs or changes in these modal parameters introduced by different experimentally simulated pathologies. The work we will describe is a temporal-bone test of the ability of our measurements and analyses to separate and identify normal middle ears from those with artificial pathologies that include middle-ear fluid and ossicular abnormalities.

Method:

Transient displacements in response to broadband acoustic clicks and the shape of cadaveric human TMs are measured before and after different simulated middle-ear pathologies. After the control (normal middle ear) measurement, the middle ear is filled to different levels of fluid (saline) and measurements

repeated. Measurements are also performed after removal of fluid and introduction of stapes fixation and incudo-stapedial (IS) joint interruption. The transient responses are compensated by the shape information to calculate the out-of-plane motion of the entire TM. The displacements to sound-pressure transfer functions of the out-of-plane motion are then analyzed to determine natural frequencies, damping and mode shapes. Modal Assurance Criterion (MAC) matrices extracted from mode shapes, weighted by the natural frequency and damping of each mode, are used to compare control and different pathological conditions.

Results:

Preliminary displacements, shape measurements and modal analysis were performed on two cadaveric human TMs before and after various simulations. One finding is that the damping ratio of the TM at each natural frequency in the normal ear decreases as frequency increases. We also see differences in identified modal shapes and natural frequencies before and after the various manipulations. These analyses will be continued in order to identify trends in the data associated with the different pathologies and test the sensitivity of MAC matrix to differentiate between pathologies.

Conclusion:

High spatio-temporal resolution measurements of TM shape and the determination of the out-of-plane TM full-field motions allow modal analysis to compare vibrations of the TM after inducing different simulated pathologies. In particular, the combination of holographic measurements and modal analysis allows quantitative characterization of the TM that could be potentially used for diagnostic purposes.

Funding:

This work is supported by NIDCD 5R01DC016079 and NSF MRI-CMMI-1428921. We thank the Massachusetts Eye and Ear and the Worcester Polytechnic Institute.

PS 776

Imaging of the gerbil incudostapedial joint

Sajjad Feizollah¹; Majid Soleimani¹; **W. Robert J. Funnell²**

¹*Dept. BioMedical Engineering, McGill University, Canada;* ²*Depts. BioMedical Engineering and Otolaryngology - Head & Neck Surgery, McGill University, Canada*

Developing an accurate mechanical model of the behaviour of a biological system requires understanding of both the geometry and the material properties of its components. There have been previous attempts to model the incudostapedial joint, but quite simplified

geometries were used and we have found that the responses of models of the joint are very sensitive to its geometry. The gerbil is a common choice of animal for hearing experiments, and gaining structural information about its incudostapedial joint will be valuable for developing more realistic models of its mechanics. We are studying the anatomy of the joint in a state as close as possible to that in the living animal. Considering the delicacy of the incudostapedial joint, in addition to using the whole bulla for imaging, we also embedded the whole bulla in methacrylate to stabilize the ossicles and then extracted a small sample containing only the joint for imaging. We used a Zeiss Xradia 520 Versa X-ray microscope in our study as the main imaging modality. To obtain better imaging of the soft tissues, we used phosphotungstic acid (PTA) as a contrast agent and also used phase contrast. We also used a tissue-clearing method to further examine the soft-tissue components of the joint under a Zeiss Z.1 light-sheet microscope. To complement our X-ray and light-sheet observations, we also examined conventional histological sections. The results of the different methods are compared and discussed.

PS 777

Resting Ambient Pressure Tympanometry Provides Key Information Suggesting Alternative Diagnoses in Patients Tested for Patulous Eustachian Tube

Anthony Thai¹; Zahra N. Sayyid²; Davood K. Hosseini²; Austin Swanson³; Yifei Ma²; Jennifer Y. Lee²; **Yona Vaisbuch²**

¹*Stanford University School of Medicine;* ²*Department of Otolaryngology-Head and Neck Surgery, Stanford University School of Medicine;* ³*Stanford University*

Background: Patulous eustachian tube (PET) is a condition in which the Eustachian tube remains open frequently, leading to symptoms such as autophony, aural fullness and sensation of ear pressure. These symptoms overlap with other otologic conditions, including superior semicircular canal dehiscence (SSCD). Previous researchers have suggested the use of acoustic impedance and standard tympanometry to indirectly observe respiration-synchronous movements of the tympanic membrane in the presence of PET. This test is usually performed at rest and with forced respiration through the mouth, both nostrils and the ipsilateral nostril. Healthy individuals are expected to present with no regular waves while PET patients may display wave patterns consistent with respiratory rates.

Objective: To introduce the use of baseline ambient pressure tympanometry (APT) recording, which is already part of PET work-up, to identify patients with potential alternative otologic conditions

Methods: Adult patients at a tertiary referral center. PET testing was performed on all patients referred to our PET clinic. The APT recording at baseline was retrospectively analyzed and compared to patient medical records, with a focus on diagnoses confirmed on computerized tomography (CT). To identify positive waves, we analyzed amplitude and frequency of APT waves, assessing for regularity of waves and comparing wave frequency to patient heart rates.

Results: PET testing was performed on 141 patients (277 ears). Analyzing the baseline APT recording, we identified 71 patients (111 ears) with regular, sinusoidal wave patterns that are inconsistent with respiratory rates (50.3% of patients, 40% of ears). Of these patients, 26 had temporal bone CT scans. Imaging studies confirmed alternative pathologies in 8 patients, including 5 cases of SSCD, 3 cases of tegmen dehiscence, 1 case of jugular bulb dehiscence and 1 case of cholesteatoma. Conclusion: APT is a simple, feasible test that is already performed in PET tympanometry testing, although focus is placed on waves resulting from patient maneuvers. This study suggests that interpretation of the baseline APT recording may direct suspicion toward other otologic diagnoses in patients receiving PET testing.

PS 778

Regular Wave Patterns on Ambient Pressure Tympanometry in Patients with Pulsatile Tinnitus-associated Pathologies

Anthony Thai¹; Zahra N. Sayyid²; Davood K. Hosseini²; Austin Swanson³; Yifei Ma²; Yona Vaisbuch²

¹Stanford University School of Medicine; ²Department of Otolaryngology-Head and Neck Surgery, Stanford University School of Medicine; ³Stanford University

Background: Tinnitus is a common problem worldwide, with prevalence of 15-20%, and is pulsatile in approximately 4% of cases. Various otologic conditions can present with pulsatile tinnitus, some of which are treatable, including encephalocele, glomus tumors, vascular wall anomalies, and palatal or middle ear myoclonus. However, these conditions have overlapping presentations and can be challenging to diagnose.

Ambient pressure tympanometry (APT) uses a microphone to record changes in sound intensity in the external ear canal while a speaker introduces a tone. However, in contrast to standard tympanometry, the recording occurs over time without introducing external pressure. This tympanometry technique is currently only used as the baseline measurement in patulous Eustachian tube tests.

Here, we present a case series of patients with various pulsatile tinnitus-associated pathologies that display regular wave patterns on APT.

Objective: To introduce the potential use of continuous APT in the screening of pathologies associated with pulsatile tinnitus

Methods: Adult patients at a tertiary otology referral center. APT was performed randomly, and medical records, including imaging, were retrospectively reviewed. APT findings were objectively characterized using an algorithm based on regularity, frequency and amplitude of the waves.

Results: APT was performed on 589 patients (1035 ears). We identified 156 patients (258 ears) with regular wave patterns on APT. From this group, we identified 9 distinct diagnoses, including superior semicircular canal dehiscence (23 patients, 34 ears), glomus tumors (5 patients, 6 ears), carotid dehiscence (3 patients, 4 ears), myoclonus (3 patients), inner ear hydrops (3 patients), jugular bulb dehiscence (2 patients), sigmoid sinus dehiscence (2 patients), encephalocele (2 patients), and aberrant carotid artery (1 patient).

Conclusion: Characteristic wave patterns on APT over time may be indicative of otherwise unrecognized pathology associated with pulsatile tinnitus. APT is a simple, feasible and widely accessible tool that can help with diagnosis or direct suspicion.

PS 779

Derivation of a Simplified Middle Ear Model Using System Identification

Jim Easter¹; Nathaniel T. Greene²; Daniel J. Tollin³; Ted Argo⁴; Tim Walilko⁵

¹Cochlear Boulder LLC; ²University of Colorado School of Medicine, Department of Otolaryngology;

³Department of Physiology & Biophysics, and Department of Otolaryngology, University of Colorado School of Medicine; ⁴Rocky Mountain Division, Applied Research Associates, Inc; ⁵Applied Research Associates, Inc. Health Effects and Risk Assessment Group

Our study of acoustic injury from very high-pressure events (e.g., blast) has created a need for a simple, computationally efficient middle ear model able to accept a predicted pressure input in the EAC after attenuation by hearing protection and to return energy transmitted (SV pressure and cochlear volume velocity) to the inner ear. The transmitted energy is then used with a damage model by mapping it to hair cell and synaptic injury, and ultimately to loss of auditory function.

The method employed to derive the simplified model draws upon a set of techniques developed within the discipline of System Identification. These techniques combine 1) an experimental design methodology to yield the most useful guiding data set with a decision process for candidate model selection, 2) optimization within the selected model family, 3) model validation, and 4) useful simulation. Using these techniques, a nonlinear model may be found which gives accurate prediction of a chosen output variable without attempting representation of physical quantities within its structure.

The input data for this model were a set of pressure waveforms recorded from experiments using a mobile shock tube (ARA, Littleton, CO). Simulated blast waves with peak pressures of 0.3 – 12 psi (160 – 192 dBp) were recorded at the skin surface and within the EAC of cadaveric human specimens. Parallel experiments were conducted in human temporal bones using a blast emulator delivering high pressure (120 – 165 dB SPL) pure tones from 10 Hz to 12800 Hz directly to the EAC. Stapes velocities were recorded by laser Doppler velocimetry (Polytec, Inc.), while SV and ST pressures were measured with fiber optic probes (FISO, Inc.).

The data from each of 43 frequencies at a given presentation level were used as input to System Identification Toolbox (Mathworks, Inc.), yielding a nonlinear Hammerstein-Wiener model optimized for that frequency. The individual models were then combined to yield a composite model giving good prediction of SV pressure in response to EAC pressure across the spectrum of interest. The composite model was validated against shock tube pressure data, and found to capture both the sharp rise time and long duration characteristic of blast waves.

This model will be used in concert with hearing protection and neurophysiological injury modules developed for this project to improve prediction of auditory degradation from high-pressure events.

Funding for this project is administered by Dr. Richard Shoge (MRMC) under Contract Number W81XWH-15-2-0002.

PS 780

The eardrums report both eye movement and eye position: the full EMREO map

David LK. Murphy¹; Cynthia D. King¹; Stephanie Schlebusch¹; Rachel Landrum¹; Christopher A. Shera²; Jennifer M. Groh¹

¹Duke University; ²University of Southern California

After every eye movement, the brain must realign the visual and auditory reference frames in order to co-locate sights and sounds. Exactly where, when, and how such visual-auditory spatial integrations occur is not fully understood. We recently discovered that the eardrum oscillates beginning a few milliseconds before saccades and continuing until well into ensuing periods of fixation (Gruters, Murphy et al PNAS 2018). Information about at least the horizontal direction and length of saccades appear to be reflected in the phase and magnitude of these eye movement-related eardrum oscillations (EMREO). Here, we sought to assess the full spatial characteristics of this signal in both vertical and horizontal dimensions, including the relative contributions of eye displacement vs. absolute (initial or final) eye position.

We found that EMREOs depend on both horizontal and vertical saccade components, varying predominantly with eye displacement, but modulated by absolute (initial or final) position as well. In toto, EMREO appear to represent combinations of these saccade parameters such that any saccade corresponds to a specific eardrum oscillation. These results demonstrate that detailed information about the relationship between visual and auditory reference frames is present in the earliest stage of the auditory pathway.

Future work delving into the relationship between EMREO and the transduction of incoming sounds will be needed to ascertain their effects on the processing of auditory spatial locations in relation to the visual scene. While the frequency and magnitude of EMREO suggest that they may be related to middle ear muscle contractions, the underlying mechanisms that generate them are unknown. As an initial assessment of EMREOs connection to middle ear function, we are estimating the correspondence between tympanometry measures and EMREO recordings (King et al, Association for Research in Otolaryngology Midwinter Meeting 2019).

PS 781

The Eardrums Move When the Eyes Move: Potential Future Clinical Implications

Cynthia D. King¹; David LK. Murphy¹; Stephanie Schlebusch¹; Rachel Landrum¹; Christopher A. Shera²; Jennifer M. Groh¹

¹Duke University; ²University of Southern California

Our brains integrate information received from visual and auditory stimuli in order to make sense of the three dimensional world around us. However, it is not known where this integration occurs within the brain. Recent findings from our laboratory have identified a phenomenon where, in the absence of auditory stimuli,

both eardrums begin synchronous, low-frequency oscillations just prior to saccadic eye movements. These eye movement-related eardrum oscillations (EMREO) change in amplitude and direction with changes in saccade amplitude and direction. This discovery suggests that connections between the visual and auditory systems likely begin as early as the auditory periphery (Gruters, Murphey et al, PNAS 2018).

Our present goal is to further characterize this phenomenon and assess the feasibility for use in future clinical research. To evaluate the replicability of the EMREO, and to develop an animal model for future neurophysiologic testing, we recorded eardrum oscillations from one rhesus monkey in ~30 one-hour sessions over a two-month period. The monkey was head-restrained and made spontaneous saccades in a dark room. Microphones placed in both ear canals recorded the oscillations and eye movements were tracked with a video eye tracker. Analysis shows a reliably recorded EMREO in approximately 5 minutes of recording time (Schlebusch et al, *Advances and Perspectives in Auditory Neuroscience* conference 2018). Similar analysis of recordings from human subjects suggests that a reliable response can also be seen with brief recording times, suggesting potential value in future clinical research.

To further characterize the EMREO in humans, we examine the relationship between traditional measures of middle-ear function (e.g., compliance) and salient features of the EMREO. Ten normal hearing subjects participated in visual tracking tasks, divided into one-hour sessions across several days. Subjects were seated, facing a monitor, and stable head position was maintained using a chinrest. Microphone recordings and eyetracking were similar to the nonhuman primate experiment. Middle-ear tympanometric measurements were obtained prior to each recording session. This allows investigation of the relationship between variations in middle-ear measurements and the structure of the EMREO.

Ongoing parallel research in our laboratory seeks to assess the full spatial characteristics of the EMREO, including the relative contributions of eye displacement vs. absolute (initial or final) eye position (Murphy et al, *Association for Research in Otolaryngology Midwinter Meeting* 2019).

Speech Perception: Musicianship, Models & Mechanisms

PS 782

Online Assessment of Statistical Learning Through Event-Related Potentials

Madeline Hsiang¹; Jiayue Liu²; David LK. Murphy¹; Tobias Overath¹

¹*Duke University*; ²*Xi'an Jiaotong University*

Statistical learning, the identification of probabilistic patterns (e.g. the syllable or phoneme order within a language), is a fundamental component of language acquisition (Saffran et al., 1996). This mechanism facilitates the rapid segmentation of incoming words, optimizing the way we process language. Click-detection during segmentation of continuously presented non-words has been proposed as an online measure of such statistical learning during language acquisition.

In a previous behavioral study from our lab, participants listened to a stream of concatenated tri-syllabic non-words and were asked to respond to clicks that were either placed between words (at the beginning of syllable 1, S1) or within words at the beginning of the second or third syllables (S2, S3). In accordance with previous studies (Gomez et al., 2011; Franco et al., 2015), reaction times (RT) for all click positions grew over the course of the experiment. This increase over time suggests that there is an interaction between the segmentation process and click-detection process and that, as learning occurs, cognitive resources are shifted away from click detection and towards word segmentation. Our results also showed that RT for the detection of S3 clicks was faster than S1 clicks during explicit learning, replicating the behavior observed in syllable detection tasks (Batterink, 2015), but contradicting previous studies comparing clicks at positions S1 and S2 over the course of the task (Gomez et al., 2011; Franco et al., 2015).

The present study sought to track the emergence of statistical learning online by recording EEG while participants listened to a stream of concatenated tri-syllabic non-words and responded to clicks (S1, S2, or S3). In particular, we hypothesized that, as participants learn the statistical rules governing the sound stream, differences in the P3 component to click targets will emerge depending on click position, reflecting the behavior observed in our previous study. In addition, we predicted an earlier response differentiation at the latency of the P50, reflecting altered auditory processing of the clicks themselves. Finally, we hypothesized that the magnitude of the neural effects observed would be reflected in the magnitude of statistical learning of each individual listener. Analyses of data are still ongoing. The

approach of tracking behavioral and neural changes as statistical learning emerges over time will yield important insights for validations of language acquisition methods.

PS 783

Event-related Potential Correlates of Auditory Frequency Discrimination

Cyan McFarlane¹; Jonathan Neukam¹; Mario Svirsky²; Robert Froemke³

¹NYU School of Medicine; ²New York University School of Medicine; ³(1) Department of Neuroscience and Physiology, (2) Neuroscience Institute, (3) Department of Otolaryngology-HNS, (5) Skirball Institute, New York University School of Medicine

Background

Poor frequency discrimination can hinder speech perception in listeners with hearing impairment, particularly those with cochlear implants (CIs). In this study we explore potential physiological indices of frequency discrimination based on electroencephalography (EEG). More specifically, we examine the extent to which the N1/P2 potential may be a useful correlate of tone discrimination in normal hearing listeners and CI users.

Materials & Methods

Ag/AgCl electrodes were placed at Fz with a nasion ground and referenced to the mastoid contralateral to the stimulated ear. N1/P2 amplitude were recorded and measured from -200ms to 500ms. Stimuli consisted of a target, 1000Hz tone and six non-target foils symmetrically placed (mel scale) above and below the target tone, presented via insert earphones to the right ear. The level of difficulty level was individually set before running the actual experiment to avoid floor or ceiling effects. The target stimulus was presented one third of the time and the remaining two thirds were foils. The task was to correctly identify stimuli as target or non-target. Feedback was provided to subjects after each response.

Results

All normal hearing listeners exhibited N1/P2 complexes for all four response categories: true positives, false positives, true negatives, and false negatives. Grand average waveforms showed that the N1 amplitude of a true positive response (target tone correctly identified) was larger (-5.09uV) than that of a false negative response (-3.47uV; target tone incorrectly identified as a foil). P2 amplitudes were not affected by any response category.

Discussion

It has been well documented that the N1/P2 complex has large contributions from the frontal cortex which

is involved in decision making and executive function. Because the physical stimulus is the same in the case of a true positive and a false negative, differences in amplitude may be related to underlying identification processes and perceptual confusion. However, it is crucial to verify that these differences are reliable and that they exist at the individual level. Past experience in our lab has shown that cortical measures can be obtained in CI users in this experiment paradigm. It would be of interest to determine whether the same patterns are observed in CI users, and to determine whether it is possible to track changes in frequency discrimination or to quantify spectral resolution through objective EEG measures.

PS 784

Musical Experience, Pitch Perception, and Tone Language Discrimination through Noise

Elizabeth Marvin¹; Hannah Dick²; Anne Luebke³

¹University of Rochester Eastman School of Music;

²University of Rochester; ³University of Rochester Medical Center

Music and speech share many sound attributes. Some earlier studies have postulated a 'musician' advantage on speech-in-noise processing for intonation languages, though other studies have failed to replicate this advantage. Moreover, it is also unclear whether there is a 'musician' advantage for processing pitch and contours found in tonal languages. We assessed hearing-in-background-noise abilities in a Sino-Tibetan tonal language using a two-alternative forced choice (2-AFC) discrimination test of Cantonese tones 1, 2, and 4 in the presence of quiet and speech-shaped broadband background noise (2-AFC-C-HINT). We also assessed fine pitch discrimination using Sek & Moore's temporal fine structure test (TFS) in both quiet and in noise. So as to remove any confounding variables we excluded subjects with absolute (or perfect) pitch. To explore these questions we recruited 58 subjects (23 music majors, native English speakers; 21 non-music majors, native English speakers, and 14 non-music majors, native tonal language speakers (Mandarin and Vietnamese)). All participants exhibited normal audiometric thresholds in both ears. There was no significant difference between our three groups in detecting differences in Cantonese syllables in the presence of background noise (C-HINT). We also compared TFS discrimination in quiet and in noise across these same groups and found significant differences in TFS performance across groups, but only in the quiet conditions (Kruskal-Wallis; data were not normally distributed). Post-hoc analysis revealed that differences were entirely due to the tone-language group, whose fine pitch discrimination was less accurate than the other two groups. This may reflect

the fact that pitch contour discrimination is categorical for tone-language speakers, but not for speakers of intonational languages such as English. The small pitch differences tested by TFS fall within a linguistic category for tone-language speakers (only) and are not relevant for linguistic meaning. With regard to musical experience, music majors were better at TFS discrimination but not at discrimination of lexical tones (C-HINT) in noisy backgrounds, where native tone language speakers excelled.

Taken together, our findings do not confirm that there is a 'musician' advantage on the ability to discriminate lexical tones in noisy backgrounds; yet musical training does improve ability to discriminate the narrow pitch excursions found in the TFS test battery.

This research was supported by grants from P30 DC05409 (NIH), BCS-1840677 (NSF) and the University of Rochester Provost Multidisciplinary Award.

PS 785

Deriving Spectro-Temporal Properties of Hearing from Speech Data

Hynek Hermansky; Lucas Ondel
Center for Language and Speech Processing, The Johns Hopkins University

Introduction

Speech evolved to be heard well. Subsequently, properties of hearing should emerge in engineering systems for processing speech. In support of this hypothesis, recent techniques for data-driven machine recognition of speech are applied to derive spectro-temporal filters, which emulate auditory cortical receptive fields observed in mammalian auditory cortices.

Experimental setup

The architecture of a convolutive deep neural network is set up in such a way that the first net layer is performing linear spectro-temporal filtering of an auditory-like spectrum, followed by a sequence of two hidden layers, yielding posterior probabilities of 39 speech sounds of the American English. The net is trained on roughly 60 hours of high-quality speech data (Wall Street Journal data) to classify center parts of each speech sound.

Results

We found the filters, which impulse responses span several hundreds of milliseconds and which enhance dominant modulations in speech. Ripple analysis of the obtained spectro-temporal filters shows the overall sensitivity to spectro-temporal modulation, which is qualitatively consistent with observed sensitivities of human hearing to such modulations. Further, each

filter selectively suppressing different parts of speech spectrum. Found hearing-like properties of the filters, which were derived from speech data without any explicit use of the hearing knowledge, supports our hypothesis about the evolution of human speech.

Implications

Assuming that human cognition is able focus only on reliable processing streams in the cortex, the adaptive frequency selectivity of the whole hearing chain could account for observed resilience of human speech communication to frequency localized noises. Automatic speech recognition techniques, which are based on this concept are under development.

PS 786

Talker Change Detection: A comparison of human and machine performance

Neeraj Kumar. Sharma¹; Shobhana Ganesh²; Sriram Ganapathy²; Lori L. Holt¹
¹*Carnegie Mellon University*; ²*Indian Institute of Science, Bangalore*

The automatic analysis of conversational audio remains challenging, in part due to the presence of multiple talkers speaking in turns, often with rich intonation, loudness variation, and overlapping speech. The majority of prior work on psychoacoustic speech analysis and system design has focused on single-talker speech signals, or overlapping talkers as in the cocktail party effect. There has been much less focus on how listeners detect a change in talker or probing the acoustic dimensions significant in characterizing a talker's voice in conversational speech. This study examines human talker change detection (TCD) in multi-party speech utterances using a novel behavioral paradigm in which listeners indicate the moment of perceived talker change. By relating the reaction time in TCD to acoustic dimensions using a modeling approach, human reaction time can be well predicted using the distance between acoustic features before and after change instant, and model prediction improves with duration of speech before the change instant. Further, the study highlights that the human performance is superior to several on-line and off-line state-of-the-art machine TCD systems.

PS 787

Validation of a Forced-Choice (2-AFC) Speech-In-Noise Test Against the HINT Test: Effects of Musical Training and Musical Aptitude on Auditory Filtering Abilities

Elizabeth Marvin¹; Hannah Dick²; Charles Babb³; **Anne Luebke**³
¹*University of Rochester Eastman School of Music*;
²*University of Rochester*; ³*University of Rochester*

The ability to understand speech in the presence of background noise is a critical skill, and this skill is often assessed using the Hearing-in-Noise Test (HINT), which requires a verbal response. We were interested in designing a test similar to HINT that did not require a verbal response. We were also interested whether there is a ‘musician’; advantage in HINT results, with “musicianship” parsed by music major, musical training, musical experience, and/or musical aptitude. To explore these relationships, we recruited 46 adults (18-30 yrs; 25 music majors) with normal audiometric thresholds whose first language was English. After recruitment, they then completed a musical experience/sophistication survey, underwent musical aptitude testing using Gordon’s Advanced Measure of Musical Audiation (AMMA), and we tested their mid-level DPOAEs (0.5 to 8 KHz) to assess any underlying peripheral impairments. We then assessed their speech-in-noise ability by administering the HINT test adaptively, and our new two-alternative forced choice (2-AFC) HINT test, with same-different discrimination at differing SNR levels, to determine 2-AFC HINT thresholds. The 2-AFC HINT test consists of sentence pair sets, where “different” pairs included one changed word that rhymed with the original. Sentence sets were balanced for word order, grammatical function, and word frequency of the rhyming word in an American English corpus, and a phonemic distance metric. We found no significant differences in DPOAE amplitudes between music majors and other majors. We also found no significant differences between the adaptive HINT score and many other measures of musicianship (major, years training, age begun training, and AMMA score). Our 2-AFC-HINT test exhibited d’; and c validity, and was correlated with both adaptive HINT and AMMA score. One possibility for a lack of a ‘musician’; advantage between our music major and other-major groups is they were very similar with respect to age, years of musical study, and when they began music study, and only differed by musical aptitude, weekly hours playing and practicing, suggesting that there are multiple parameters that may influence the ‘musician’; advantage. Moreover, we have validated our 2AFC-HINT test with the adaptive HINT test, enabling assessments of speech-in-noise in minimally-verbal populations. The 2AFC-HINT offers a test that is easier and less expensive to administer, which may encourage its use earlier in the diagnostic process.

This research was supported by grants from P30 DC05409 (NIH), BCS-1840677 (NSF) and the University of Rochester Provost Multidisciplinary Award.

PS 788

The Effect of Broadening Auditory Filters on Perception of Speech in Noise with Linear and Nonlinear Hearing Aids

Sungmin Lee¹; C. T. Justine Hui²; Takayuki Arai²; Chin-Tuan Tan¹

¹University of Texas at Dallas; ²Sophia University

Reduced frequency selectivity in listeners with sensorineural hearing loss is usually associated with the broadening auditory filters. Previous studies have shown that broadened auditory filters spectrally smear speech, which makes speech perception more difficult, particularly in noisy environments. Current assistive hearing devices may not directly address this supra-threshold deficit in their compensation strategy. At the same time, other studies have shown that hearing aids have helped to improve speech perception in noise. The objective of this study is to systematically study the outcome of linear and nonlinear hearing aids on recovering speech perception in noise with broadened auditory filters.

In the present study, we looked at speech perception by hearing impaired listeners, both unaided and aided with either linear or nonlinear hearing aids, in both noisy and clean conditions. We estimated the auditory filters of hearing impaired listeners by measuring their psychoacoustic tuning curves (PTCs) centered at 500 Hz, 1000 Hz and 2000 Hz, using the fast PTC method (Sek and Moore, 2011). The measurement was repeated in three conditions: unaided, linearly amplified and nonlinearly amplified in accordance to the NAL-R and NAL-NL2 prescription formulae respectively. We also carried out a speech intelligibility test using the Maryland consonant-vowel nucleus-consonant (CNC) word list both in quiet condition and noisy condition at 10 dB SNR with babble noise.

We computed the Q-factor of their PTC’s; Q_{10} , which is the ratio of the centre frequency of the auditory filter to the bandwidth of the filter, measured at 10 dB below the peak. Lower Q_{10} value is associated with broader auditory filters. We also compared the Q_{10} values centered at 500 Hz, 1000 Hz and 2000 Hz to the speech recognition scores in both quiet and noise. In the unaided conditions, the Q_{10} values of hearing impaired listeners decrease from 1.8 at 500Hz to about 1.5 at 2000Hz. With amplification, the auditory filters were narrowed to Q_{10} values around 2.5 at all three frequencies. We observed similar outcome in both linearly and nonlinearly aided conditions. Higher speech recognition scores in noise were found in aided conditions. Further analyses will be performed to correlate between speech recognition performance and Q_{10} values in each individual listener.

PS 789

Rotated Faces Reduce Listening Benefit of Visual Speech Cues Despite Preserved Temporal Coherence

Sara Fiscella; Ross K. Maddox
University of Rochester

Many conversations take place in noisy environments, yet people are generally able to focus on the person with whom they are speaking and understand what is being said. It is well established that speech understanding is greatly improved when a listener is able to see the face of the person speaking. One contributor to this benefit is the visual representation of linguistic cues, such as place of articulation. However, our previous work has shown that even for nonlinguistic stimuli, temporal coherence alone between the auditory and visual modalities can offer a listening benefit. Here we sought to disentangle these two mechanisms by perturbing the linguistic component of the visual stimuli while perfectly preserving the temporal coherence. We did so by a simple rotation of the visual stimuli.

We engaged listeners in an audio-visual speech comprehension task in which they were presented with high context target sentences and asked to type the words they heard. The sentences were presented in three levels of two-talker maskers (faces not shown) at signal-to-noise ratios of 0, -3, and -6 dB. At each masking level we tested four visual conditions: normal visual speech, ± 90 degree rotation, 180 degree rotation, and a still image face control. Consistent with previous experiments, comprehension was highest with the unrotated face and lowest for the static face control. Performance on the rotated conditions was also worse than the unrotated condition. Because audio-visual temporal coherence was preserved, this performance decrement can be attributed to the disruption of visual linguistic cues by the rotation.

PS 790

Overtone Focusing in Tuvan Throat Singing

Christopher Bergevin¹; Brad Story²; Joy Williams¹; Jennifer Steeves¹; Natasha Mhatre³; Chandan Narayan¹

¹York University; ²University of Arizona; ³University of Toronto Scarborough

“Throat singers” from central Asia are well known for their unique song vocalizations. In particular, singers from Tuva (a federal subject of Russia) have become popularized in part due to the exploits of the late physicist Richard Feynman. A salient example is “Khoomei”, a style that creates an otherworldly

yet organic sound. Deeply steeped in folk tradition, Tuvan “overtone singing” is achieved without the aid of external apparatus (e.g., a lamellophone). However, the underlying vocal tract biomechanics required for throat singing are not well understood. To elucidate such mechanisms, this study combines several approaches: detailed spectral analysis of a variety of song from several Tuvans, dynamic and volumetric structural MRI of a Tuvan singer, and computational airway modulation modeling. Preliminary results indicate that singers produce source patterns that give rise to a dense array of harmonics (i.e., “overtones”), which are kept relatively stable across time. Singers simultaneously modify their vocal tract to create narrowly “focused” filter states [i.e., highly accentuated formant(s)] that can be modulated independent of the source and other focused states (if present). Model results suggest a focused state arises from a singer’s ability to merge two formants to (greatly) enhance the amplitude of one or two harmonics. Tongue tip position and inclusion of the piriform cavities appear important to help produce a focused state, while position of the back of the tongue controls aspects of “pitch”. Comparisons are also explored with “Western” singers, who produce overtone focused song that has both significant similarities and differences relative to the Tuvans.

PS 791

Relation between Gray Matter Volume and Speech-in-noise Performance in Tinnitus Patients with Normal Hearing Sensitivity

Yihsin Tai; Somayeh Shamsavarani; Rafay Khan; Sara Schmidt; Fatima Husain
University of Illinois at Urbana-Champaign

Our recent study (Tai & Husain, JARO, 2018) using the Quick Speech-in-Noise (QuickSIN) test suggested that normal-hearing individuals with tinnitus performed significantly worse at 5-dB signal-to-noise ratio (SNR) condition compared with controls. Although structural changes such as reduced gray matter (GM) volume in brain regions critical for speech-in-noise (SiN) recognition have been reported in tinnitus, these changes have not been linked to SiN performance. The aim of the present study is to examine the relationship between SiN scores at 5-dB SNR condition and GM volumes. Pure-tone audiometry and QuickSIN test were conducted on seven individuals with bilateral tinnitus (mean: 47.43 years) and 14 non-tinnitus individuals (mean: 44.86 years); all participants had bilateral normal hearing sensitivity (≤ 25 dB HL up to 8 kHz). Tinnitus severity estimated by Tinnitus Functional Index (TFI) suggested a mild handicap (mean: 21.03, range: 1.2-40.8). T1-weighted structural MRI images were obtained from all participants, and GM volume assessed using

whole-brain voxel-based morphometry was compared between groups. Additionally, regression analyses were performed to examine the correlation between whole-brain GM volume and SiN scores in each group. SiN performance at 5-dB SNR in both ears was poorer in the tinnitus (mean: 71.43%) relative to the non-tinnitus group (mean: 82.86%), but did not reach statistical significance. No significant correlation was found between SiN and TFI scores. Using uncorrected p-value, preliminary results showed decreased GM volume in the right middle temporal gyrus (MTG), right inferior temporal gyrus (ITG), left cingulate gyrus, left precuneus, left insula, and bilateral inferior frontal gyri in the tinnitus group compared with the non-tinnitus group. However, only changes in the right MTG reached statistical significance (corrected for multiple comparisons). Regression analyses, using uncorrected p-value, revealed a negative correlation between GM volumes in the right ITG and SiN scores within the tinnitus group and a positive correlation between GM volumes in the left middle frontal gyrus (MFG) and SiN scores within the non-tinnitus group. Our findings in the non-tinnitus group suggest that regions of the prefrontal cortex are associated with better SiN performance, echoing the work of Wong et al. (2010, Ear and Hearing); however, the same pattern was not observed in the tinnitus group. This is an ongoing study; more data, along with a region-of-interest analysis on brain regions associated with speech recognition, are required to better understand the relation between brain structural changes and SiN recognition in tinnitus.

PS 792

Perceptual Learning of Spectrally Degraded Speech may be Impaired by Auditory Distraction in Adolescence

Katrina Potter¹; Fariha Mostafiz²; Julia Huyck¹
¹Kent State University; ²Northeast Ohio Medical University

Adolescents are still maturing both in terms of their naïve (untrained) performance and training-induced learning on some auditory tasks. One potential contributor to this late maturation is attention, which is known to develop well into adolescence. Previous work indicated that adults must attend to spectrally degraded (noise-vocoded, NV) speech to learn to understand it. The aim of this study is to evaluate the role of attention in adolescents'; learning to comprehend NV speech. Listeners aged 10-17 years were exposed to a series of 6-band NV sentences. All listeners completed a five sentence pre-training test and a 20 sentence post-training test, during which they listened to the sentences and reported what they heard. During the training phase, listeners were divided into three groups: Two groups were simultaneously exposed both to 15 NV sentences and to a series of amplitude-

modulated noises that sounded as though they were approaching (increasing in amplitude) or departing (decreasing in amplitude). One of these groups was asked to detect infrequent departing noises in a series of approaching noises. The other group listened to the NV sentences and attempted to repeat them aloud. The third group served as control listeners, and played a video game in silence. Preliminary data show that all three groups improved slightly between the pre- and post-training tests and that those who attended to the NV speech did not improve any more than those who had no training or who attended to the noises. This outcome suggests that, unlike adults, at least some adolescents are unable to benefit from experience with NV speech if it is accompanied by competing auditory stimuli. Thus, immature auditory attention may interfere with adolescents' ability to learn to understand degraded speech under conditions where there are auditory distractions. All three groups improved over the 20 sentences of the post-training test, indicating they were able to learn to comprehend NV speech when it was presented alone. If this preliminary result holds, it suggests that adolescent listeners adjusting to new hearing aids or cochlear implants may benefit most from listening to speech in quiet environments with few distractions.

PS 793

Hearing Impairment Reduces the Fluctuating-Masker Benefit for High-Rate but not for Low-Rate Modulated-Noise Maskers

Kenneth K. Jensen; Joshua G.W. Bernstein
Walter Reed National Military Medical Center

Introduction

Normal-hearing (NH) listeners can extract and integrate speech fragments revealed in momentary dips in the level of a fluctuating masker, yielding a fluctuating-masker benefit (FMB) for speech understanding relative to a stationary-noise masker where no dips are present. Hearing-impaired (HI) listeners generally show less FMB, suggesting a dip-listening deficit attributable to suprathreshold spectral or temporal distortion. However, HI listeners are typically tested at higher SNRs to achieve similar baseline stationary-noise performance to NH listeners. The reduced FMB might at least partially result from different test SNRs, reduced absolute audibility of otherwise unmasked speech segments, or age differences.

Methods

This study examined the FMB for nine age-matched NH-HI listener pairs, while simultaneously equalizing audibility and performance at a fixed SNR in stationary noise. Nonsense syllables were masked by stationary

noise, 4- or 32-Hz sinusoidally amplitude-modulated (SAM) noise, or an opposite-gender interfering talker. Stationary-noise performance was equalized by adjusting the size of the available response set for each individual listener. Audibility was equalized for each NH-HI listener pair by first low-pass filtering at 4 kHz and then by applying intensity filtering to remove stimulus components with intensities less than the HI absolute threshold plus 10 dB. Thus, each NH and HI listener pair was presented with the same signal processing and had the same signal audibility.

Results

After audibility was equalized between the two listener groups, the response set size required to yield a fixed level of performance in stationary noise was not found to be significantly different between the NH (12.4 syllables) and HI listeners (14.8 syllables). The HI listeners showed a clear 4.5-dB reduction in FMB for 32-Hz SAM noise, but the same amount of FMB as the NH listeners for 4-Hz SAM noise. There was a non-significant trend toward a 2-dB reduction in FMB for an interfering talker.

Discussion

These results suggest that once audibility and age differences are controlled, HI listeners do not exhibit a general dip-listening deficit for all fluctuating maskers, but rather a specific temporal-resolution deficit that affects performance for high-rate modulated maskers. [The views expressed in this article are those of the authors and do not reflect the official policy of the Department of Army/Navy/Air Force, Department of Defense, or U.S. Government.]

PS 794

Computational Model for the Modulation of Speech-in-noise Comprehension Through Transcranial Electrical Stimulation

Mikolaj A. Kegler; Tobias Reichenbach
Department of Bioengineering and Centre for Neurotechnology, Imperial College London

Background

Transcranial electrical stimulation (TES) can non-invasively modulate neuronal activity in humans. Recent studies have shown that TES with an alternating current that follows the envelope of a speech signal can modulate the comprehension of this voice in background noise (Wilsch et al., 2018). However, how exactly TES influences cortical activity and influences speech comprehension remains poorly understood. Here we present a computational model for speech coding in a spiking neural network and employ it to investigate the effects of TES on the coding of speech in noise.

Methods

Based on previous work, we established a computational model of a spiking neuronal network that encodes natural speech through entraining network oscillations in the theta and gamma frequency range (Hyafil et al., 2015). We used the network's spiking output to classify speech in different levels of background babble noise. We then investigated the effect of different external currents on the network dynamics as well as on the neural output and the associated speech coding. Finally, we analysed the behaviour of the computational model and its speech classification performance in different conditions to optimize the stimulation paradigm for enhancement of natural speech processing.

Results

The computational model generated coupled oscillations in the theta and the gamma frequency range. In agreement with experimental results, the slower theta oscillations reliably predicted the onsets of syllables and provided a temporal reference frame for the faster activity in the gamma band that encoded phonemes. Classifying speech in different levels of background noise yielded results comparable to normal human performance, with a 50% speech recognition threshold at approximately -1 dB SNR. Simulating the effect of simultaneous external current with a range of different temporal patterns and stimulation intensities we were able to identify the parameters that impeded as well as enhanced the neural coding of speech in noise.

Conclusions

The developed model provides an insight into the neural mechanisms through which speech in noise can be processed in the auditory cortex and how TES can enhance this processing. Moreover, our computational model allows to optimize the temporal pattern of the stimulation for improving speech-in-noise comprehension.

References

- Hyafil et al. (2015) *Elife*, 4, e06213.
- Wilsch et al. (2018) *NeuroImage*, 172, 766-774.

Acknowledgements

This study was supported by the EPSRC Centre for Doctoral Training in Neurotechnology for Life and Health. We thank Alexandre Hyafil, Shabnam Kadir and Milos Cernak for helpful comments and fruitful discussions.

Network Model to Quantify the Effect of Reduced Audibility on Cognitive Processes

Curtis Alcock; James Rankin
University of Exeter

Background: Speech understanding involves the dynamic interaction of different systems including hearing, vision, language, memory and attention (Cong and Liu 2014; Davis and Johnsrude 2007) enabling inference under uncertainty from highly variable input (Kleinschmidt and Jaeger 2015; Friston 2010). These dynamic interactions make isolating one system's contribution from another challenging, confounding attempts to quantify the impact of reduced audibility on cognition (Davis & Johnsrude 2007). However, acoustic and visual inputs are known to activate mental representations of candidate words, which compete to produce a winner (Vitevitch & Luce 2016). Ambiguity results in recruitment of additional resources (cognitive load) until a match is found (Pirog Revill et al. 2008; Rodd, Davis, and Johnsrude 2005). Here we propose a novel network approach that quantifies increased ambiguity as a proxy for cognitive load, and models the contribution of different systems (e.g. lip-reading, memory) in resolving the ambiguity.

Methodology: We modelled the relationship of phonemes, visemes (Bear and Harvey 2017) and words to one another as a network. Thus multiple phonemes (e.g. /m/, /b/, /p/) might relate to a single viseme (lips closed), and a word relate to multiple phonemes sequentially (c, a, t). We then created nearest neighbour relationships between each word that differed in pronunciation from another by substitution (e.g. cats → cots, caps etc.), deletion (cats → cat) or addition (cat → cast) of a single phoneme (Vitevitch and Luce, 2016). Finally we weighted each word by how frequently it occurs in the SUBTLEX-US corpus (Brysbaert and New 2009), a measure shown to predict processing speed and ambiguity resolution (Ellis 2002). To simulate reduced audibility, we presented stimulus words to our model which activated candidates affected by the removal of a set of phonemes (e.g. the voiceless fricatives), quantifying the resulting ambiguity using Shannon Entropy (Shannon 1948).

Results: Entropy increased across all phoneme categories, demonstrating a need to recruit additional information to resolve the ambiguity resulting from reduced audibility. However, recruiting word frequency reduced the average entropy by 48%, visemes by 72%, visemes plus word frequency by 85%.

Conclusion: Our model offers a novel extensible method for quantifying in silico the impact of reduced audibility,

whilst isolating the contribution of recruited sensory/cognitive resources, with effect size quantified through increase/decrease in entropy. So far we have looked at the effect of removing phoneme classes on context-independent words, but our network-based approach is generalisable across all systems contributing to speech understanding.

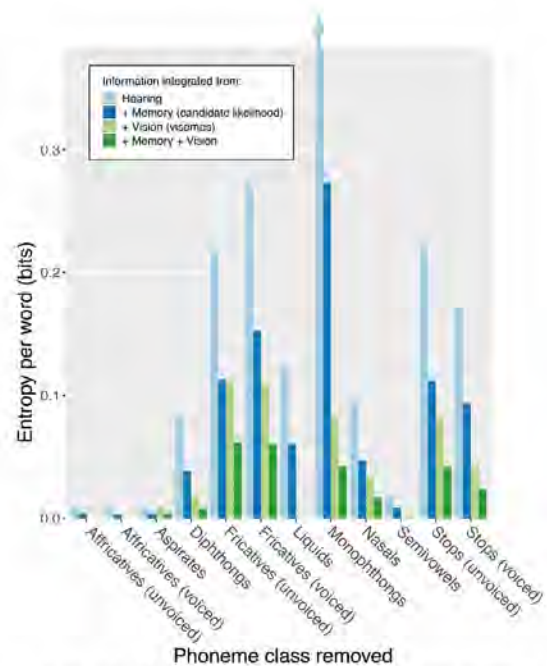


Figure 1: Mean increase in entropy (ambiguity) per word, resulting from removal of phoneme class as a proxy for reduced audibility.

Reduced audibility, as simulated here by the removal of a phoneme class (e.g. unvoiced fricatives), increases the number of possible words activated in the listener's perception when a stimulus word is presented (e.g. spot → pot, pots, spots). This results in an increase in ambiguity which a listener must resolve by recruiting additional information (e.g. from lip-reading, lexical knowledge, context) to the available auditory information. Ambiguity is quantified in 'bits' using Entropy (Shannon 1948), which can be regarded as a measure of the additional information required to resolve that ambiguity, and therefore a proxy for increased cognitive load. Bars represent the increase in ambiguity over and above recognition of the stimulus word first time, accurately (i.e. 0 bits = no ambiguity, 1 bit = two equally likely possibilities). Integrating visual lip-reading information (i.e. visemes), or long-term memory effects (i.e. how likely the word is to occur) cumulatively reduces this ambiguity by constraining the possibilities. Top-down/bottom-up processing can therefore be understood as the integration of information available to the listener within the time-frame of perception.

Musical Aptitude Predicts Auditory Filtering in Young Adults and Children with Autism Spectrum Disorder (ASD)

Loisa Bennetto¹; Jordan Schramm²; Jessica Keith¹; Paul Allen²; Anne Luebke²

¹University of Rochester; ²University of Rochester Medical Center

Daily communication rarely occurs in quiet environments; background noise is often present, degrading the acoustic signal, in fact, approximately 17% of American adults report difficulty hearing in a noisy environment. Moreover, parents and teachers often report that children with autism spectrum disorder (ASD) have difficulty attending to and understanding speech in noisy environments. To explore the relationship between musical aptitude and auditory filtering in adults, we first recruited 56 normal-hearing adults (20 dB HL@0.5-4kHz; 25 dB HL @ 8kHz in both ears) between 18-30 years, who then were tested for their musical aptitude and their hearing-in-noise abilities. Musical aptitude was assessed with Gordon's Tonal Imagery Melody subtest of the Musical Aptitude Profile (MAP T1). Hearing-in-noise ability was assessed for both speech (HINT) and music (newly designed MINT). We found that signal-to-noise ratios from MINT (non-language based test) and the HINT (speech based test) were highly correlated with each other.

We also comprehensively characterized the nature of auditory filtering abilities in children with ASD (n=33) compared to well matched controls (n=32), using speech-shaped noise and synthesized babble as maskers, and speech and non-speech as signals, and assessed musical aptitude and surveyed musical experiences. We found that children with ASD exhibited impaired hearing-in-noise (HINT) abilities when compared to TD controls (p 0.001). Hearing in noise difficulties in ASD were not specific to speech targets, as children with ASD also showed impaired auditory filtering on a tones-in-noise test (TINT). Moreover, performance on the TINT and HINT was significantly related across both groups. Hearing in noise (for speech and tones) is related to years of musical training and was also related to musical aptitude in both groups, though children with ASD and TD controls did not differ in their average musical aptitude score (Intermediate Measures of Music Audiation; IMMA).

Our findings provide evidence that children and adults with higher musical aptitudes exhibit enhanced abilities to hear in background noise, and suggests the importance of musical training in improving hearing-in-noise abilities across multiple domains.

This research was supported by grants from NIH NIDCD R21 DC011094 (Luebke & Bennetto, multi-PI), P30 DC05409 (CNCS), and Clinical & Translational Science Institute Awards (UL1 RR024160 & TL1 RR024135). Special thanks to Sigfrid Soli and Daniel Freed at the House Ear Institute in Los Angeles, CA for customized software, Ranisha Nelson, Alyssa Lord, Ruth Davis, and Jiashu Li for help with data collection

and processing, and we also thank the children and families who participated in these studies.

PS 797

Pupillometry Studies in Individuals with Single-sided Deafness: impact of trial inclusion criteria

Sara Misurelli¹; Emily Burg²; Tanvi Thakkar³; Taylor Fields⁴; Stefanie Kuchinsky⁵; Ruth Litovsky³

¹Department of Surgery, Division of Otolaryngology, University of Wisconsin School of Medicine and Public Health; ²Waisman Center, University of Wisconsin-Madison; ³University of Wisconsin - Madison; ⁴Neuroscience Training Program; ⁵Audiology and Speech Pathology Center, Water Reed National Military Medical Center; Department of Hearing and Speech Sciences, University of Maryland

Individuals with hearing loss describe listening to speech in noise as effortful. Speech intelligibility in a clinical setting is reported as percent of words correctly repeated. However, this measure fails to capture the amount of effort to maintain that level of performance. In this study, we measured both speech intelligibility and pupillary response, a measure that has is shown to be correlated with listening effort, in listeners with single-sided deafness (SSD, normal hearing in one ear and deaf in the other). This is a timely population to study, given that some of these individuals are now pursuing cochlear implantation in attempt to improve speech intelligibility and possibly decreased listening effort in noise. However, raw data in this population is subject to artifacts, such as blinking and lack of task engagement. Numerous decisions must be made when deciding to keep or discard data. Yet the literature lacks evidence as to which trial inclusion criteria should be used and how these decisions influence the pupil response data. We examined the effect of two trial inclusion criteria (1) accepted percentage of "blinks", or data interpolation, and (2) accepted percentage of intelligibility, which is related to task engagement.

Nine patients with SSD listened to sentences presented from a loudspeaker in front in two conditions—quiet or with interfering sentences. Maximum pupil dilation was calculated using blink criteria of <15% (tracks with >15% discarded), and no blink criteria (all tracks included regardless of %blinks). Similarly, tracks were discarded for tracks with intelligibility criteria of <60%, versus using no limitation on percent correct.

Results indicated higher maximum peak dilation when listening with interferers than in quiet, suggesting that adding interferers resulted in more effortful listening. When discarding tracks based on blinks, a small drop in the overall peak dilation was observed for both

conditions, compared to no blink criteria; however, the relationship between conditions remained unaffected. When discarding based on intelligibility, there was a reduced effect of the interferer. This suggests that intelligibility criteria can affect differences between listening conditions more than blink criteria. These findings may motivate use of more lenient blink criteria, which would facilitate larger amounts of data retention. The long-term goal of this study is to investigate the role of trial inclusion criteria decisions on pupil response and establish best practices using different analysis methods (e.g., peak-picking and growth curve analysis).

Work supported by NIH-NIDCD R01DC003083(RYL) and a Core grant from NIH-NICHD U54HD090256(Waisman Center).

PS 798

Valence of Mating but not Restraint Vocalizations is Perceived Differently by Male and Female mice

Zahra Ghasemahmad¹; Bhavya Sharma²; Drishna Karthic Perumal²; Rishitha Panditi²; Krish Nair²; Jeff Wenstrup²

¹Northeast Ohio Medical University, Kent State University; ²Northeast Ohio Medical University;

Introduction:

Many studies have addressed the significance of mouse ultrasonic vocalizations (USVs) for facilitating social behavior. However, few studies have addressed the significance of other categories of vocalizations frequently emitted in conjunction with USVs in natural vocal sequences. Here we recorded and analyzed acoustic features of mating and restraint vocalizations based on the behavioral state of the sender. We then performed playback experiments using exemplars of mating and restraint vocal sequences to examine behavioral responses of male and female mice.

Methods:

Vocalizations and behavior of CBA/CAJ mice (n=54; ages p90-p180) were recorded during mating and restraint. For mating, we defined low and high arousal states, then compared acoustic features in vocalizations recorded during the two states. Restraint vocalizations were reported previously (Grimsley et. al, 2016). In playback experiments, we selected five representative exemplars of natural vocal sequences from restraint and from the higher arousal state of mating. On the test day, male and female mice were presented with either mating or restraint vocalizations for 20 minutes. We video-recorded and analyzed 19 different behaviors before, during, and after stimulus presentation.

Results:

Mating vocalization analysis: Vocalizations emitted during the higher arousal state of mating included higher percentages of low frequency harmonic (LFH) calls and complex USVs, compared to the lower arousal state. Syllables emitted in the higher arousal state had higher rates, longer durations, and higher amplitude ($p < 0.005$).

Playback experiment: Both mating and restraint vocal sequences increased attending and head orientation toward the speaker ($p < 0.0005$). In response to mating sequences, females decreased locomotion and increased alert postures and escape behaviors. In contrast, males increased exploratory behaviors (locomotion and rearing) ($p < 0.05$). In response to restraint sequences, both males and females increased aversive behaviors including speaker-escape, twitching, and lunge and sniff ($p < 0.0005$) (All comparisons: MANOVA with repeated measures).

Conclusion:

These results suggest that mice communicate internal state via social vocalizations. Thus, spectrotemporal features of mating vocal sequences change with intensity or arousal of mating behaviors. Our previous findings showed that restraint vocalizations also have characteristics distinct from vocalizations in other contexts. Further, vocal sequences linked to mating but not restraint, change the behavior of listening male and female mice in different ways: In response to playback of mating vocalizations, males were more exploratory, while females displayed reduced locomotion and more alert behaviors. Vocalizations linked to restraint, however, increased escape behaviors for both sexes, in accord with the negative affect of this behavioral state.

PS 799

Auditory and Cognitive Moderators of the Relationship Between Speech Recognition and Short-Term Memory

Adam K. Bosen; Michael F. Barry
Boys Town National Research Hospital

In listeners with various forms of hearing loss, short-term memory is often correlated with speech recognition outcomes. Direct examination of this correlation is confounded by variations in both short-term memory and the amount of auditory information available across individuals with hearing loss. To characterize the relationship between available auditory information, speech recognition, and short-term memory, we measured sentence recognition and serial recall within listeners with normal hearing across vocoded speech conditions of varying difficulty. Listeners heard and repeated PRESTO sentences, lists of digits, and lists of consonant-vowel-consonant words presented through

16, 8, and 4 channel noise band vocoders. As expected based on previous work, performance on digit lists was unaffected by the number of channels in the vocoder, but accuracy for sentences and word lists decreased with decreasing number of vocoder channels. This approach precisely controlled the amount of available auditory information, which allowed us to characterize how available auditory information moderated the relationship between short-term memory and speech recognition. To account for additional sources of variability, we also measured fluid intelligence and various forms of attention (sustained attention, inhibition-concentration, and attentional shifting). Preliminary results indicate that performance across attention and intelligence tasks was correlated but separable, and that performance on these tasks is correlated with memory span and speech recognition across vocoder conditions. These results suggest that the relationship between speech recognition and short-term memory may not be a simple causal structure, and that additional aspects of cognitive function, as well as the available auditory information, should be considered moderators of this relationship.

PS 800

Audibility and Subjective Preference in Self-Adjustment of Hearing Aid Gain

Trevor Perry; Peggy B. Nelson
University of Minnesota

Self-adjustment of hearing aid gain is a feasible solution for increasing user engagement and customization of hearing aids, potentially improving comfort and satisfaction with amplification. Self-adjustment of gain may become an important tool for programming over-the-counter hearing aids or similar devices targeted toward individuals with mild-to-moderate hearing loss. However, if people with hearing loss choose gain settings which are comfortable but undercut speech audibility, improvements in communication and quality of life could be limited. Previous work found that people with mild-to-moderate sensorineural hearing loss made consistent self-adjustments when listening to speech at 65 dBC in quiet or noisy backgrounds, but inter-listener variability in gain preferences was large. Although listeners often selected less gain than their NAL-NL2 prescriptive fit, speech recognition was similar between the self-adjusted fits and the prescriptive-fits (Nelson, Perry, Gregan, & VanTasell, Trends in Hearing 2018.) The audibility of speech depends upon hearing sensitivity and the levels of the speech and competing sounds. For people with mild-to-moderate losses, speech at moderate levels in quiet is often intelligible with little or no amplification. For speech in noise, audibility is mainly determined by the noise level, not the gain. Thus the potential that self-adjustment might commonly result in suboptimal gain

has not yet been fully examined.

The present study assessed whether self-adjustment of gain will lead to reduced speech recognition under conditions in which gain has a larger effect on speech audibility, namely, when speech is presented in quiet at low levels. Participants with mild-to-moderate hearing loss were fitted with their NAL-NL2 prescriptive targets. Then, in a sound-treated booth, participants self-adjusted gain using the Ear Machine© software interface while listening to speech passages in quiet, presented at 45, 55, or 65 dBA. New settings were also created by cutting the gain in the high frequencies (>1200 Hz) from the self-adjusted fit so as to further reduce the predicted intelligibility. Participants completed a series of blinded, paired comparisons between the prescriptive fit, the self-adjusted fit, and the reduced-gain fit while listening in the same speech conditions as before. Participants rated the fits on satisfaction, clarity, loudness, comfort, sound quality, and overall preference. Data will be presented connecting listener preferences to gain levels and intelligibility. The preference ratings will shed light on the range of gains that listeners find acceptable and highlight the trade-offs participants made during self-adjustment between audibility and subjective preference factors.

Funded by NIH grant R01 DC013267 to PN

PS 801

Self-Reported and Measured Hearing Difficulties in Noise in a Population of Normal-Hearing to Mildly Hearing-Impaired Adults.

Guillaume Andeol¹; Thibaut Fux¹; Jean Christophe Bouy¹; Clara Suied¹; Annie Moulin²

¹*Institut de recherche biomédicale des armées*; ²*Lyon Neuroscience Research Center*

Speech in noise performance differ widely among a population of normal-hearing to mildly hearing-impaired adults. However, it is unclear whether speech in noise performance measured in tests is related or not to the listener's subjective assessment of his/her own speech in noise abilities.

In the present study, speech in noise performance was measured with the French version of the Oldenburg Matrix test (namely the Framatrix), and the French language version of Noble and Gatehouse's Speech, Spatial and Qualities of hearing questionnaire (SSQ) was used for the self-report measure. One hundred listeners participated, aged from 18 to 50 (mean = 34 ± 7).

Pure-tone audiometry was evaluated per octave from

125 Hz to 12.5 kHz in both ears of each subject. The Matrix test consist in sentences presented in a voice shaped noise, in free field, using an adaptive procedure to identify the 50% threshold. Three consecutive tests were performed for each subject and the best threshold of the three was considered. The SSQ scores were calculated on the full scale and subscales, and using the new 15 items SSQ short-form (15iSSQ).

There was no significant correlation between low and mid-frequencies hearing thresholds and the SSQ score, or the Matrix test thresholds. However, the SSQ scores decreased significantly as high frequency thresholds (HFT ie the average of 4-8-12.5 kHz thresholds) increased. Matrix test SNR threshold decreased significantly with decreasing HFT and decreased significantly with increasing SSQ scores, and SSQ speech scores. However, the variance in SSQ scores and SSQ speech scores explained by the Matrix test seemed to be low. Those results reflect dissimilarities between self-report and test measurement of speech in noise abilities.

PS 802

Audiovisual Cues Influence the Categorical Perception of Clear and Degraded Speech

Gavin Bidelman; Lauren Bush; Alex Boudreaux;
Lauren Sigley
University of Memphis

Inherent to speech perception is the need to properly group acoustic information into meaningful linguistic-phonetic units, the process of categorical perception (CP). Beyond providing a smaller and more manageable perceptual space, CP might also aid degraded perception if categories are more resistant to noise than surface acoustic features of the speech signal. Combining audiovisual (AV) cues also enhances speech recognition, particularly in noisy environments. Here, we investigated the degree to which visual cues from a talker aid listeners'; speech categorization amidst noise interference. In Exp. 1, we parametrically varied signal-to-noise ratio (SNR) [clean, +10 dB, -5 dB] while listeners classified an acoustic-phonetic continuum whose percept varied from /u/ to /a/. Listeners'; psychometric functions were steeper and their responses faster for clean speech. However, noise-related changes in CP were only observed at the lowest SNR. Similarly, identification of tokens with clear phonetic labels (i.e., continuum endpoints) was invariant to noise, whereas ambiguous tokens (i.e., those not producing clear phonetic percepts) declined with decreasing SNR. These results suggest that phonetic representations of speech are more resistant to external noise degradation than corresponding acoustic representations. In Exp.

2, we measured speech identification in severe (-15 dB SNR) levels of noise for stimuli presented in either the auditory-only or combined AV modalities. Identification curves were sharper for AV compared to A-only speech suggesting visual cues enhance speech CP. While noise in the auditory channel expectedly weakened speech categorization (i.e., shallower slopes), interestingly, the addition of visual cues of the talker largely counteracted noise-related decrements in performance. Collectively, results show that (i) beyond providing grouping mechanisms, mapping speech sounds to categories aids its perception in "cocktail party" environments and (ii) visual cues help lattice the formation of auditory-phonetic categories to further enhance speech identification.

PS 803

Linguistic, Perceptual, and Cognitive Factors Underlying Musicians' Benefits in Noise-Degraded Speech Perception

Jessica Yoo; Gavin Bidelman
University of Memphis

Previous studies have reported musicians'; have better speech-in-noise (SIN) recognition than nonmusicians. Others have failed to observe this "musician SIN advantage." Here, we aimed to clarify equivocal findings and determine the most relevant perceptual and cognitive factors that do and do not account for musicians'; benefits in SIN processing. We measured performance in musicians and nonmusicians on a battery of SIN recognition, auditory backward masking (a marker of attention), fluid intelligence (IQ), and working memory tasks. We found that musicians outperformed nonmusicians in SIN recognition but also demonstrated better performance in IQ, working memory, and attention. SIN advantages were restricted to more complex speech tasks featuring sentence-level recognition with speech-on-speech masking (i.e., QuickSIN) whereas no group differences were observed in non-speech simultaneous (noise-on-tone) masking. This suggests musicians'; advantage is limited to cases where the noise interference is linguistic in nature. Correlations showed SIN scores were associated with working memory, reinforcing the importance of general cognition to degraded speech perception. Lastly, listeners'; years of music training predicted auditory attention scores, working memory skills, general fluid intelligence, as well as SIN perception (QuickSIN scores), implying that longer durations of musical training enhance perceptual and cognitive skills. Overall, our results suggest (i) enhanced SIN recognition in musicians is due to improved parsing of competing linguistic signals rather than signal-in-noise extraction, per se and(ii) cognitive factors (working memory, attention, IQ) at least partially drive musicians'; SIN advantages.

PS 804

Pathology-Specific Brain Oscillations Serve as Underpinnings of Tinnitus and Its Modulation

Ethan Firestone¹; Hao Luo¹; Edward Pace¹; Bin Liu¹; Bora Agabigum¹; Na Zhu²; Xueguo Zhang¹; John Moran³; Jinsheng Zhang¹

¹Wayne State University; ²University of Michigan - Flint;

³Henry Ford Health System

Tinnitus, or phantom auditory perception, is associated with a host of neural signatures, but identification of definitive biomarkers and an undisputed etiology has been stunted due to the presence of confounding disorders such as hearing loss. Thus, we attempted to solve this issue, in a rat model, by employing a combination of behavior tests, multi-structure electrophysiological recordings, and auditory cortex electrical stimulation (ACES), a therapy we have previously reported to suppress tinnitus in rats. For induction of tinnitus and hearing loss, we subjected rats to loud-noise exposure (10 kHz, 120 dB, 2 hrs), and used the gap prepulse inhibition of the acoustic startle reflex behavior paradigm to separate traumatized subjects into tinnitus(+) and tinnitus(-) groups. We then recorded electrophysiological activity simultaneously in the dorsal cochlear nucleus (DCN), inferior colliculus (IC), and auditory cortex (AC), both before and after ACES. Our neural spike results showed that acoustic trauma led to hyperactivity and hyperbursting in the IC and DCN of tinnitus(-) and tinnitus(+) rats, respectively, while the latter group also displayed hypersynchrony in the AC. Looking at the local field potential, hearing loss-alone was associated with broadband elevation of spectral power and coherence, throughout, and enhanced phase-phase cross-frequency coupling (CFC) between theta and various demarcations of gamma rhythms within the DCN and between its contacts to the IC and AC. Pathological signaling in tinnitus(+) rats was honed to high-powered, hyper-coherent gamma oscillations that resonated across the auditory axis, along with increased broadband coherence in the AC and exacerbated theta-gamma CFC between the DCN and the other two structures. Furthermore, we studied functional connectivity via transfer entropy, and it revealed that hearing loss-alone involved widespread elevation of information transfer, while this facet was only exacerbated within the AC and in top-down connections between the IC-DCN and AC-DCN, in rats with tinnitus. Finally, ACES-induced tinnitus suppression was paralleled by decreased hyper-coherent, cortical signals, elevated background noise, and restoration of natural connectivity along the auditory axis. Our findings illuminate novel metrics for teasing apart compounded auditory disorders, provide foundation for future causative studies, and will contribute

to development of efficacious, clinical treatments for tinnitus.

PS 805

Dorsal cochlear nucleus fusiform-cell plasticity is altered in salicylate-induced tinnitus

David T. Martel; Thibaut Pardo-Garcia; Susan E. Shore

University of Michigan

Introduction: Following tinnitus-induction, dorsal cochlear nucleus (DCN) fusiform cells show altered stimulus-timing dependent plasticity (StDP), increased spontaneous synchronization and increased spontaneous firing rates (SFR). Pathologically enhanced neural activity correlates with tinnitus behavior (Marks et al., 2018). Salicylate, which induces tinnitus at high doses, increases NMDAR activity in the auditory pathway (Basta et al., 2008). Eliciting fusiform cell StDP requires NMDAR activation; furthermore, blocking NMDA receptors alters StDP timing rules and decreases cross-unit synchronization in DCN fusiform cells (Stefanescu and Shore, 2015). Thus, systemic NMDAR activation with salicylate (Guitton et al, 2003) should alter fusiform-cell StDP, subsequently increasing SFR and synchrony, thereby inducing tinnitus. Herein, we examined mechanisms underlying salicylate-induced tinnitus and recording in vivo single-unit responses from fusiform cells pre- and post-salicylate administration.

Methods: Tinnitus was induced in guinea pigs with systemic salicylate (i.p. 350 mg/kg). Two behavioral methods were used to assess tinnitus: 1) gap-prepulse inhibition of acoustic startle (GPIAS) and 2) operant conditioning in which guinea pigs were trained to cross a box when hearing a sound. Silence probe trials were randomly presented and guinea pigs with tinnitus were expected to increase their crossing rates during silent trials (Ruttiger et al., 2003). Next, single-unit recordings were obtained using multichannel NeuroNexus electrodes placed into the DCN fusiform cell layer after ketamine/xylazine anesthesia. Fusiform cells were identified by electrode position within the DCN and sound-evoked responses at best-frequency (BF) (Stabler et al., 1996). StDP timing rules were measured as the percent change in firing rate as a function of bimodal (auditory-somatosensory) stimulation interval (+/-20ms, +/-10ms, +/-5ms). The stimulus paradigm consisted of somatosensory stimuli (via transdermal electrodes placed over C2; square-wave electrical pulses at the sub-contraction threshold, 1 kHz rate, 100 us/phase), and 40 dBSL acoustic stimuli at the most common unit BF for each animal.

Results: Guinea pigs administered salicylate showed increased crossing rates during silence compared

to baseline as well as impaired GPIAS. In addition, fusiform-cell SFR and synchrony were significantly increased and correlated with the behavioral measures of tinnitus. Furthermore, tinnitus-frequency-specific StDP timing rules were shifted towards long-term potentiation compared to baseline and non-tinnitus-frequencies.

Conclusions: These results suggest salicylate-induced tinnitus has a similar pathophysiology in DCN to that underlying noise-overexposure. Further studies are necessary to cross-validate GPIAS and operant conditioning using noise-overexposure for tinnitus induction.

PS 806 - WITHDRAWN

PS 807

Ventral cochlear nucleus bushy cells contribute to enhanced auditory brainstem response amplitudes in tinnitus

David T. Martel; Susan E. Shore
University of Michigan

Introduction: Noise exposure results in increased spontaneous firing rates (SFR) and cross-unit spontaneous synchrony in tonotopically-restricted groups of dorsal cochlear nucleus (DCN) fusiform cells, which correlate with behavioral measures of tinnitus (Wu et al, 2016). Noise exposure can also result in increased SFR in ventral cochlear nucleus (VCN) bushy cells (Voegler et al, 2011, Bledsoe et al, 2012). Bushy cells exhibit high onset firing rates (OFR) that are synchronized with neighboring cells (Winter and Palmer, 1990), likely providing a significant contribution to the auditory brainstem response (ABR) as waves II-V arise predominantly from the bushy cell pathway (Melcher et al, 1996). Humans with tinnitus have demonstrated enhanced later ABR wave amplitudes (Schaeffe and McAlpine, 2011; Gu et al, 2012), suggesting that bushy cells may play a role in tinnitus. Here we examined the role of the bushy cell pathway in tinnitus generation by recording ABRs and simultaneous single unit activity from bushy cells in animals with behaviorally-verified tinnitus.

Methods: Guinea pigs were exposed to unilateral narrowband noise (1/2 octave, centered at 7 kHz, 97 dB SPL) for two hours to induce temporary threshold shifts. Tinnitus was assessed using gap/prepulse-inhibition of acoustic startle (GPIAS; Turner et al, 2006), and quantified using distribution differences between pre- and post-exposure GPIAS values (Tinnitus Index, TI). Tinnitus was assessed ($p < 0.05$; Student's t-test; 8 weeks after noise-exposure), the animals were anesthetized with ketamine/xylazine, ABRs measured, and 16-channel probes stereotaxically inserted into the VCN. Individual

ABR wave I-V amplitudes were manually identified and normalized by the corresponding wave I amplitude (8, 12, 16, 20, 24 kHz; 0.5 ms rise/fall time, 5 ms duration, cos² gating). Spontaneous and tone-evoked activity were simultaneously recorded from multiple VCN bushy cells recorded with a multichannel recording electrode. Synchrony was computed as peak normalized cross-correlation coefficients; significance was defined as four standard deviations above the mean correlation.

Results: ABR wave amplitude ratios correlated with computed from GPIAS tinnitus indices. Furthermore, bushy cells in tinnitus animals show higher SFRs, greater OFRs and lower first-spike-latencies compared to those in non-tinnitus animals. Synchrony was significantly elevated in animals with tinnitus and correlated with enhanced SFR. Further, SFR, synchrony and onset firing rates correlated with frequency-matched tinnitus indices.

Conclusions: Tinnitus-related alterations to bushy cell firing patterns may underlie enhanced ABR wave amplitude ratios and potentially tinnitus pathology. Future studies are necessary to reconcile tinnitus-related pathology throughout the cochlear nucleus.

PS 808

Deficits in Gap Prepulse Inhibition of the Acoustic Startle (GPIAS) in a Mouse Model of Acute and Chronic Tinnitus.

So Young Park¹; Min Jung Kim¹; Shi Nae Park¹; Dong Kee Kim²; Hyo Jeong Yu¹; Jung Mee Park¹

¹*Department of Otorhinolaryngology-Head and Neck Surgery, College of Medicine, The Catholic University of Korea;* ²*Department of Otorhinolaryngology-Head and Neck Surgery, College of Medicine, Daejeon St. Mary's Hospital*

Objective: Tinnitus research provides insights into neural mechanisms of tinnitus and ultimately leads to the development of effective tinnitus therapies. Behavioral animal models for tinnitus have been divided into conditioning- and reflex-based types. The latter type named gap prepulse inhibition of the acoustic startle (GPIAS) utilizes acoustic startle modification and tinnitus gap-filling hypothesis. GPIAS-based models have been most commonly developed in rats. Now increasing number of studies are being conducted on mice with a wide range of genetically engineered strains. Despite the popularity of GPIAS method, its validity and reliability remain controversial. In this study we induced tinnitus in C57BL/6J mice by using either salicylate toxicity or noise trauma and investigated the gap detection performance to verify the presence of tinnitus and to establish a new mouse model of acute and chronic tinnitus. We also aimed to confirm the consistency and validity of GPIAS-

based tinnitus mouse models.

Methods: Male 1-month old C57BL/6 mice were randomly allocated into the control, SIT (salicylate-induced tinnitus), and NIT (noise-induced tinnitus) groups (n = 7, each) to conduct two separate experiments using common controls. To induce tinnitus, mice in the SIT group were injected with intraperitoneal sodium salicylate (350 mg/kg) for five consecutive days, and mice in the NIT group were exposed to 16 kHz narrow band noise (NBN) at 110 dB SPL for 2 hours with the right ear plugged. All mice underwent auditory brainstem response (ABR), distortion product otoacoustic emission, GPIAS, and prepulse inhibition of the acoustic startle (PPIAS) at several time points before, during, and after tinnitus induction until 2 weeks/1 month in the SIT/NIT groups. GPIAS test used three different carriers (16/24 kHz NBN and broadband noise, BBN at 70 dB SPL), which were matched to the prepulse sound for PPIAS. The serial GPIAS/PPIAS parameters were compared with the baseline and with the controls by repeated measures analysis of variance. GPIAS reduction without PPIAS reduction implies the presence of tinnitus. The number of mice showing 'tinnitus-positive' behavior defined as GPIAS reduction > 95% confidence interval of the mean pre-induction baseline was counted within each group at each time point.

Results: The SIT group showed 15-dB temporary threshold shifts in ABR during the salicylate treatment. The noise-exposed ears demonstrated permanent hearing loss, the most severe at 16 kHz followed by 32 kHz. Both salicylate toxicity and unilateral noise trauma resulted in deficits in GPIAS, i.e. tinnitus behavior. At most time points, 16-/24-kHz GPIAS decreased significantly compared with its own baseline and also with the controls, which was recovered in the SIT group and maintained in the NIT group. The frequency of the carrier has no different effect on both GPIAS reduction and the number of tinnitus-positive mice at each time point. Nevertheless, GPIAS reduction was the clearest when 16-kHz carrier was used, which can be attributed to the best GPIAS in 16-kHz carrier in normal mice. A statistical significance of GPIAS reduction must have depended on the better baseline gap detection performance without tinnitus rather than larger GPIAS reduction with tinnitus.

Conclusion: Our study confirmed the consistency and validity of the GPIAS-based mouse models of tinnitus. GPIAS could be optimized for tinnitus assessment by employing 16 kHz NBN carrier at 70 dB SPL. The choice of a carrier frequency corresponding to the region of highest hearing sensitivity in the species studied and a repeated measures design are emphasized for reliable results. We suggest that C57BL/6 mice can be used as a simple mouse model of both acute and chronic tinnitus for future studies.

PS 809

Safety and Effects of Intratympanic Botulinum Toxin: A Rat Study

Jung Mee Park; Min Jung Kim; So Young Park; Shi Nae Park

Department of Otorhinolaryngology-Head and Neck Surgery, College of Medicine, The Catholic University of Korea

Background: Middle ear myoclonic tinnitus (MEMT) is an unusual condition caused by repetitive contractions of middle ear muscles (MEMs), i.e. tensor tympani and stapedius muscles. To date, management of MEMT is largely limited to supportive therapy and/or few pharmacological agents with uncertain efficacy. Tenotomy of MEMs could be a treatment option for intractable MEMT, but it is an invasive procedure under operating room setting. Therefore, intratympanic injection of botulinum toxin that may induce paralysis of MEMs could be an alternative treatment modality. This animal study was conducted to investigate safety of botulinum toxin to inner ear structures as well as to examine its effect on MEMs prior to clinical studies.

Methods: Male Sprague-Dawley rats aged 1 month were divided into 3 subgroups according to the sacrificing day after botulinum toxin injection: 3 days (3D), 1st week (1W), and 3rd week (3W). After initial hearing tests using ABR and DPOAE, one ear was randomly assigned as the experimental ear, the other, as the control ear. Experimental ears were intratympanically injected with 0.1 ml of botulinum toxin A, whereas control ears were injected with saline. Final hearing tests and collection of MEMs with cochleas were done according to the subgroup for analysis. Cochleas were evaluated for morphologic changes, and degenerations of MEMs were evaluated through electron microscopic study.

Results: There were no significant changes in hearing thresholds of all experimental ears in all 3 subgroups (P>0.05). Cochlear morphologic studies also did not show significant changes in the organ of Corti, spiral ganglion, or stria vascularis, indicating safety of botulinum toxin to inner ear structures. MEM sections obtained from the experimental ears showed some significant alterations in muscle ultrastructures compared to the control ears, such as loss of myofibrils and crystalalysis in mitochondrias.

Conclusion: Intratympanic injection of botulinum toxin do not seems to have ototoxic effect on inner ear function. Muscular degenerations of tensor tympani and stapedius muscles were observed in electron microscopic analysis after intratympanic botulinum injection, suggesting its possible use as a MEM-inactivating substance. Further transitional clinical study may support the therapeutic use of intratympanic botulinum toxin for the management of MEMT.

PS 810

Biological verification of optimal GPIAS parameter in salicylate induced tinnitus mouse

So-Young Chang¹; Min Young Lee²; Ilyong Park³; Ji Eun Choi²; Jae-Hun Lee¹; Nathaniel Carpena²; Phil-Sang Chung²; Jae Yun Jung²

¹Beckman Laser Institute Korea, College of Medicine, Dankook University; ²Department of Otorhinolaryngology-Head & Neck Surgery, College of Medicine, Dankook University; ³Department of Biomedical Engineering, College of Medicine, Dankook University

Background:

Tinnitus is the phantom sound in the ears without external auditory stimulation. The treatment of tinnitus mostly relies on tinnitus retraining and curative therapeutic modality does not exist because of unclear underlying pathophysiology. Thus, appropriate animal model for tinnitus is required to investigate the molecular mechanism. Salicylate (SS), a component of the aspirin, can cause reversible tinnitus by high dose. Gap-Prepulse Inhibition of the Acoustic Startle Reflex (GPIAS) is a paradigm for detecting tinnitus objectively in animal. We induced tinnitus using SS in mouse, and optimal (showing less variable, and efficiently reduced GPIAS after SS) parameter was determined. In addition, protein (such as VGLUT 1&2 and TRPV1) expressions in cochlea, spiral ganglion neuron (SGN), and cochlea nucleus (CN) are compared among control and various GPIAS outcomes using the optimal parameter to verify the functional outcome.

Materials and Methods:

For the optimization of GPIAS parameters, various inter-stimulus interval (ISI) (0 to 100 ms) and startle pulse duration (20, 40 and 60 ms) were tested to normal mice without any treatment. For the induction of tinnitus, SS (250, 300 and 350 mg/kg) with different concentration was injected intraperitoneally three consecutive days. Then GPIAS, of which the parameters that were determined in present study, was tested 2 h after each SS injection. ABR was performed to evaluate the hearing threshold before and after salicylate injection. Using the parameters GPIAS were measured. Epifluorescence analysis of cochlea, SGN and CN was performed. VGLUT 1&2 and TRPV1 expression were compared among various GPIAS outcome subjects.

Results:

In the untreated mice, 20 ms of ISI and 20 ms of startle pulse duration showed highest reduction of startle reflex with the gap-prepulse and showed least variability. Among the three different concentrations of SS, 250 mg/kg failed to reduce the GPIAS. In contrast, concentration

of 300 mg/kg resulted in reduction of averaged GPIAS (<50%). However, results of concentration of 350 mg/kg SS were variable and showed large hearing threshold shift. The expression of VGLUT 1 in CN was significantly decreased after SS injection compare to the control, while the expression of VGLUT2 in CN was significantly increased compared to the control. In addition, the expression of TRPV1 in CN was significantly increased after SS injection. Expression of each protein varied by GPIAS outcome, subjects with reduced GPIAS at sacrifice showed relatively larger difference to control while ones who did not show smaller difference in CN.

Conclusions:

Modified GPIAS parameters significantly reduced the GPIAS value after SS injection, which indirectly proves the existence of tinnitus. After SS injection VGLUT2 and TRPV1 increased while VGLUT1 decreased. Moreover, there was tendency showing correlation of GPIAS result at sacrifice day with such protein expression.

Acknowledgements:

This study was supported by Basic Science Research Program through the National Research Foundation of Korea (NRF) funded by the Ministry of Education, Science and Technology (NRF-2017R1A6A3A11031784), and supported by Leading Foreign Research Institute Recruitment Program through the National Research Foundation of Korea (NRF) funded by the Ministry of Science and ICT (MSIT) (NRF-2018K1A4A3A02060572).

PS 811

Modulation of Shock Tube Blast Overpressure and Related Auditory Changes

Srinivas Kallakuri¹; Mirabela Hali²; Andre Kuhl²; Catherine Martin³; Ariane Kanicki⁴; Rodney Braun²; Richard Altschuler⁴; Avril Genee Holt²

¹Wayne state University; ²Wayne State University School of Medicine; ³University of Michigan; ⁴University of Michigan, Kresge Hearing Research Institute

Introduction: A high percentage of blast exposed Veterans report tinnitus or hearing deficits. Currently, animal models of blast induced tinnitus and hearing loss are generated using a shock tube to produce blast over pressures (BOP) of various intensities under controlled conditions. However, much of the shock tube data is related to the intensity of the BOP with no detailed information related to the spectral characteristics. The ability to measure and modulate the spectral content of the BOP may allow improvements in animal models to better study tinnitus and hearing deficits.

Methods: BOP was generated by a custom-built shock tube under two distinct set-ups with a driver chamber

connected either to a 6-meter-long shock tube (LST) or to a 2.43 meter-short shock tube (SST). Desired BOP was produced with compressed helium and calibrated Mylar sheets. Pressure measurements were analyzed for spectral content characteristics. Separately, anesthetized male Sprague Dawley rats were exposed to BOP using these two shock tube settings (n=2 per set-up). Auditory brainstem responses (ABR) were measured within 24 hrs and 2 weeks after. Cochleae were harvested and processed for hair cell counts.

Results: The SST resulted in a higher peak overpressure than the LST (25.83 vs. 23.91 psi). The LST produced peak sound pressure levels (SPLs) between 160-180 dB while the SST produced \leq 160 dB and involved higher frequencies. ABR threshold (TH) shifts were found 24 hours after exposure in animals subjected to BOP using the LST. In animals exposed to BOP by SST, permanent TH shift was observed at high frequencies. All animals showed a measurable ABR wave 1 with a reduced amplitude. Two weeks post ABRs revealed hearing recovery at low frequencies (4, 12, 20 kHz) with low wave 1 amplitudes at higher frequencies (25, 32, 36 kHz). Wave 1 amplitude values for the animals blasted in the SST tended to be the lowest. Cytocochleograms revealed loss of hair cells in the base of cochlea. This loss was more prominent in animals exposed to BOP by SST. These animals also showed hair cell loss in the middle (5-15% missing) of the cochlea also.

Discussion: Our results suggest that BOP using SST results in louder dB SPLs resulting in higher ABR thresholds, smaller Wave I amplitudes and more hair cell loss in the base and middle of the cochlea. These results suggest that the degree of cochlear injury is dependent upon BOP characteristics.

PS 812

Nucleus Accumbens Affected by Noise Induced Hearing Loss and Hyperacusis

Anaam Alkharabsheh; Yuying Liu; **Wei Sun**
State University of New York at Buffalo

Noise exposure is a common cause of hearing loss and hyperexcitability in the central auditory system induced by hearing loss may cause tinnitus and hyperacusis. Recent studies suggested that limbic system may also play a critical role of tinnitus and hyperacusis generation. Nucleus accumbens (NAc), an important area of limbic system, may not only influence the loudness of tinnitus, it may also control the generation. However, the function changes in the limbic system after hearing loss and tinnitus/hyperacusis are still not clear. In our recent studies, we found that noise exposure in the early age of developmental

period can cause hyperacusis, measured by reduced reaction time to acoustic stimuli. We also found that hyperacusis is accompanied by increased activity of in the auditory cortex (AC) and the inferior colliculus (IC). In this study we examined the c-Fos staining of rats after developed hearing loss and hyperacusis. Hearing loss was evaluated by the ABR test and operant conditioning behavioral test was used to measure hyperacusis. Our preliminary experiment found that the number of c-Fos positive cells in NAc of the rats with hearing loss showed significant reduction compared to the control group. However, the number of c-Fos positive cells in the NAc of rats with hyperacusis increased significantly. These results suggest that a long term hearing loss may cause depression of NAc activity and hyperexcitability in the NAc may be related to hyperacusis. Low-level noise, even though it may not cause permanent hearing loss at early-age may still be a risk factor for hyperacusis.

PS 813

Uncovering the Role of Aberrant Cortical Oscillations, Thalamocortical Dysrhythmia, and Central Gain Enhancement in Animals with Behavioral Evidence of Tinnitus

Sarah Hayes; Greg Sigel; Ashley Schormans; Björn Herrmann; Brian Allman
University of Western Ontario

Over the past few decades, a variety of theories have been put forth to suggest how tinnitus might emerge from disrupted activity in the auditory cortex, including aberrant oscillations, thalamocortical dysrhythmia (TCD), or enhanced central gain. In the present study, we used rat models to investigate the interplay of these putative neural correlates of tinnitus, and specifically examined (1) whether tinnitus induced by different insults (acute-noise exposure; sodium salicylate, SS) share the same cortical disruptions, and (2) if direct pharmacological manipulation of GABAergic neurotransmission in the auditory pathway is sufficient to induce tinnitus. In our first experimental series, we compared the changes in spontaneous oscillations in the auditory and frontal cortices immediately after loud noise exposure versus systemic injection of SS. Although both insults induced behavioural evidence of tinnitus (as confirmed by the quiet-trial errors made during our two-alternative forced-choice paradigm), only SS altered the oscillatory profile; findings which reveal that tinnitus can indeed emerge in the absence of aberrant cortical oscillations. Next, to investigate the potential for TCD to generate tinnitus, we micro-injected pharmacological agents (THIP or Gabazine) into the medial geniculate body (MGB) via chronically-implanted infusion cannulae. Contrary to our prediction, local manipulation of GABAergic neurotransmission in the MGB did not cause behavioural

evidence of tinnitus, despite producing significant disruption of thalamocortical signaling as measured by spontaneous cortical oscillations. Finally, we examined the putative link between tinnitus and central gain enhancement by comparing the sound-evoked local field potentials in auditory cortex following acute-noise, SS and MGB micro-infusion (THIP; Gabazine). Surprisingly, no consistent relationship was observed between the manipulations that enhanced central gain and those that induced behavioural evidence of tinnitus. Taken together, our collective results show that there is not a clear link between tinnitus and the presence of aberrant cortical oscillations, TCD, or central gain enhancement. Consequently, it seems reasonable to suggest that perhaps the known tinnitus inducers (acute-noise and SS) generate phantom sound perception through truly disparate mechanisms, or alternatively, through shared mechanisms not investigated in the present study (e.g., disrupted neural networks; loss of cortical inhibition; etc.).

PS 814

A Loss of Inhibition in the Auditory Cortex Increases Spontaneous Activity and Induces Tinnitus in Rats

Ashley Schormans; Krystal Beh; Sarah Hayes; Brian Allman

University of Western Ontario

Despite decades of research studying the neural correlates of tinnitus, the underlying causal mechanisms remain elusive. Noise exposure, a common tinnitus inducer, is known to disrupt the balance of excitation and inhibition in the auditory pathway. Related to this, previous animal studies have reported that various auditory structures (e.g., auditory cortex; inferior colliculus; dorsal cochlear nucleus) show increased spontaneous firing rates following noise exposures capable of inducing tinnitus. Beyond these correlative studies, however, it is unclear whether impaired inhibitory neurotransmission and a resultant increase in spontaneous firing rates actually cause (rather than simply coexist with) tinnitus. In the present study, we used rat models to investigate if a loss of cortical GABAergic inhibition was indeed sufficient to induce spontaneous and sound-evoked hyperactivity, as well as cause phantom sound perception. In our first experimental series, *in vivo* extracellular electrophysiological recordings were made in the primary auditory cortex (A1) using a 32-channel electrode that was inserted perpendicular to the cortical surface so as to record across all cortical layers simultaneously, before and after local micro-infusion of the GABA-A antagonist, Gabazine. As predicted, Gabazine micro-infusion increased the spontaneous spiking activity in the majority of cortical layers, as

well as increased the sound-evoked spike counts and response durations. Armed with this effective dosing of Gabazine, in our second experimental series, we then assessed the effect of blocking GABAergic inhibition in A1 on rats performing a two-alternative forced-choice behavioral paradigm that could screen them for the presence/absence of tinnitus. As expected, when the vehicle control (aCSF) was micro-infused into A1 prior to behavioral testing, the rats' performance was unaffected compared to baseline, such that they only mistakenly identify a few quiet trials as though a steady narrowband noise (NBN) was being presented (i.e., aCSF: $3 \pm 1\%$ quiet trials misidentified as NBN). In strong contrast, micro-infusion of Gabazine caused rats to mistakenly identify $30 \pm 7\%$ of quiet trials as NBN; findings indicative of tinnitus-positive behavior. Importantly, this error profile was consistent with that observed in these same rats following tinnitus induction via a 15-minute noise exposure. Thus, we conclude that a loss of GABAergic cortical inhibition is sufficient to induce phantom sound perception. In the future, it would be interesting to use this direct pharmacological approach to examine if a loss of inhibition in subcortical areas could also manifest as tinnitus.

PS 815

Contrasting Changes in Nitric Oxide Synthase Expression in the Auditory Cortex and Inferior Colliculus of Rats in a Tinnitus Model

Hannah Maxwell¹; Jennifer Schofield²; Martine Hamann²; Bas M.J. Olthoff³; Nadia Pilati⁴; Charles Large⁴; Mark Cunningham¹; Sarah E. Gartside³; Adrian Rees¹

¹Newcastle University; ²University of Leicester;

³Institute of Neuroscience, Newcastle University;

⁴Autifony Therapeutics Limited

There is considerable interest in discovering biological signatures for tinnitus (the perception of a phantom sound) to improve our understanding of its origins, and develop effective treatments. The expression of neuronal nitric oxide synthase (nNOS), the enzyme that catalyses nitric oxide production, is upregulated in the ventral cochlear nucleus in animals with tinnitus (Zheng et al., 2006; Coomber et al., 2015). To determine whether tinnitus is associated with changes in nNOS in higher parts of the auditory system, we used immunohistochemistry to investigate the expression of nNOS in the auditory cortex and inferior colliculus of rats that had undergone unilateral acoustic over exposure and tinnitus testing.

Anaesthetised Long Evans rats were noise exposed (16 kHz tone at 116 dB, 1 hour) with the left ear plugged. Subsequently they were tested for tinnitus with the gap-pre-pulse inhibition of the acoustic startle paradigm.

Animals with reduced inhibition of acoustic startle were classified as 'tinnitus'. Tinnitus and (unexposed) control rats were deeply anaesthetised and transcardially perfused with 4% paraformaldehyde. Brains were removed, cryoprotected and sectioned. Rabbit anti-nNOS antibody was applied to free floating 30µm coronal sections and detected using goat anti-rabbit Alexa 568 antibody. Labelling was visualised with a Nikon A1 confocal microscope and labelling intensity was compared between tinnitus and control animals.

Expression of nNOS varied across the auditory cortex: nNOS labelled somata were concentrated in layers II, V and VI while neuropil labelling was highest in layers III and IV. The overall intensity of nNOS labelling across the auditory cortex was significantly reduced in tinnitus animals compared to controls and did not differ between hemispheres. Reduced intensity of labelling was observed both in the somata and in the neuropil forming 'background'; across all regions of the auditory cortex. In the inferior colliculus, somata with dense nNOS expression are numerous in the dorsal and lateral cortices. Cells in the central nucleus contain nNOS positive puncta, however overall nNOS expression is much lower than in the cortices. In the dorsal cortex there were significantly more nNOS positive cells in tinnitus animals versus controls: mean labelling intensity was non-significantly higher. There were no differences in labelling between control and tinnitus animals in the central nucleus or lateral cortex. The contrasting changes in nNOS expression in the auditory cortex and inferior colliculus observed in tinnitus animals suggest an important role for the modulation of synaptic activity by nitric oxide in the pathophysiology of tinnitus.

Coomer, B., Kowalkowski, V.L., Berger, J.I., Palmer, A.R. and Wallace, M.N. (2015) 'Modulating central gain in tinnitus: changes in nitric oxide synthase in the ventral cochlear nucleus', *Front Neurol*, 6, p. 53.

Zheng, Y., Seung Lee, H., Smith, P.F. and Darlington, C.L. (2006) 'Neuronal nitric oxide synthase expression in the cochlear nucleus in a salicylate model of tinnitus', *Brain Res*, 1123(1), pp. 201-6.

PS 816

Combined Blast and Concussive Impact-Induced Tinnitus, Hearing Loss and Related Traumatic Brain Injuries in Rats

Hao Luo¹; Bin Liu¹; Ethan Firestone¹; Edward Pace¹; Dalian Ding²; Bo Pang³; Norair Adjamian³; Lauren Kassa³; Srinivas Kallakuri³; Ayeshah Sarfaraz³; Linda Zhu⁴; John Moran⁵; Shaowen Bao⁶; Richard Salvi⁷; Jinsheng Zhang¹

¹Wayne State University; ²Center for Hearing and

Deafness. State University of New York at Buffalo; ³Wayne state university; ⁴University of Michigan-Flint; ⁵Henry Ford Health System; ⁶University of Arizona; ⁷University at Buffalo

Blast and its secondary concussive impact from shrapnel and debris are known to cause tinnitus, hearing impairment, and related traumatic brain injuries, particularly among military personnel and veterans. We have previously reported that blast-alone induces tinnitus, which is accompanied by temporary ABR threshold shift, chronic degradation of wave 1 amplitude, early-onset hyperactivity in the dorsal cochlear nucleus (DCN) and inferior colliculus (IC), and delayed hyperactivity in the auditory cortex (AC). However, the mechanisms driving combined blast and concussive impact-induced tinnitus, hearing loss, and related mild traumatic brain injuries remain unclear. To shed light on these disorders, we subjected rats to combined blast and concussive-impact and followed up by obtaining behavioral measures of tinnitus and hearing dysfunction, assessing immunohistochemical changes, and multi-channel electrophysiological recordings simultaneously in the DCN, IC, and AC. We found that blast-plus-impact induced chronic tinnitus and hearing loss, caused severe inner and outer cochlear hair cell loss, and increased microglial activity in the central auditory structures. Electrophysiologically, tonotopic mapping results showed that both tinnitus(+) and tinnitus(-) groups exhibited reduced high-frequency-representations in the DCN, IC, and AC compared to the control group, illustrating significant neuroplasticity. The neural spike results showed that tinnitus(+) rats displayed increased spontaneous firing rates (SFR) and bursting in the AC and elevated neural synchrony in the DCN, yet all three of these measures were depressed in the IC. At the local field potential level, both tinnitus(+) and tinnitus(-) rats showed decreased coherence, phase lock index (PLI), and cross-frequency coupling (CFC), compared with control rats. However, among traumatized subjects, tinnitus(+) rats exhibited higher coherence, PLI, and CFC values in the DCN and AC, especially in gamma bands, than the tinnitus(-) rats. When studying sound driven responses, the tinnitus(+) rats showed enhanced central gain in the DCN and IC, but decreased central gain in the AC, suggesting that central gain change was not necessarily correlated with hyperactivity along the auditory pathway, under the current experimental condition. Taken together, compared to blast alone, combined blast and concussion may generate more severe and chronic tinnitus along with compromised hearing and complex central changes. These trauma-induced anatomical, neurophysiological, and inflammatory changes in the auditory centers may contribute to a better understanding of tinnitus

and hearing loss under certain traumatic conditions, which could assist in the development of efficacious treatments.

PS 817

Relationship of Sex and Stress Level to Chronic Tinnitus Development After Sound Exposure

Alexandra Niemczura¹; Ryan Longenecker²; Chae Kim²; Jasmine Grimsley²; Jeff Wenstrup²; Alexander Galazyuk²

¹Northeast Ohio Medical University, Kent State University; ²Northeast Ohio Medical University

Background

Stress and chronic tinnitus often occur comorbidly, but their relationship is poorly understood. In mice, we used behavioral and hormonal assays to assess whether sex and stress level are associated with signs of chronic tinnitus following sound exposure.

Methods

Forty-eight adult (P90-P270; 24 male, 24 female) CBA/CaJ mice were utilized in this study. At P90 and prior to sound exposure, baseline levels of plasma corticosterone, gap-induced prepulse inhibition of the acoustic startle reflex (GPIAS), and open-field behavior were acquired. Twenty-four experimental animals were anesthetized with ketamine/xylazine (100/10 mg/kg, i.p.) and underwent unilateral sound exposure to induce tinnitus (12.5 kHz center frequency, ~8-17 kHz bandwidth, for 1 hour at 116 dB SPL). Controls underwent sham exposure. Animals were returned to their home cage for 3 months, during which chronic tinnitus developed in a subset of sound-exposed mice. Post-exposure measurements of plasma corticosterone, open-field behavior, and GPIAS (10 sessions for each mouse) were then collected. Hearing thresholds were assessed using auditory brainstem responses (ABRs) immediately prior to, 1 day after, and 3.5 months after sound exposure as described previously (Longenecker & Galazyuk, 2016). Startle responses were automatically classified (Grimsley et al., 2015) and behavioral signs of tinnitus were assessed for each individual (Longenecker et al., 2018). The presence of chronic tinnitus was indicated by a significant reduction in GPIAS from pre- to post-exposure.

Results

Plasma corticosterone level increased from pre- to post-exposure in sound-exposed females with signs of chronic tinnitus ($p < 0.05$). However, there was no change in corticosterone level for sound-exposed males

with signs of tinnitus, or in sound-exposed males or females without signs of tinnitus ($p > 0.05$). This suggests that sex and chronic tinnitus development after sound exposure interact to affect corticosterone level. There was no change in thigmotaxis (wall-hugging behavior) from pre- to post-exposure ($p > 0.05$), indicating that development of sound-induced tinnitus does not affect behavioral signs of stress in males or females.

Conclusions

Future analyses include assessing whether baseline stress level predicts chronic tinnitus development after sound exposure and whether vocal behavior is affected in mice with signs of chronic tinnitus. Greater understanding of the relationship between stress and tinnitus will enable greater knowledge of how chronic tinnitus develops, which individuals are at increased risk, and how stress level differs in affected individuals.

Hearing in Aging: Temporal Processing Deficits Throughout the Brain

Chair: Björn Herrmann

SYMP 58

Addressing Hearing Loss from a Public Health Perspective

Adele Goman

John Hopkins University

Hearing loss is a major public health issue, affecting nearly two thirds of older adults. The number of adults with better-ear hearing loss is anticipated to rise from 29 million in 2020 to over 45 million by 2060 given the aging population. Recent epidemiologic research has highlighted independent associations between hearing loss and poorer health outcomes among older adults. Yet despite the high prevalence of hearing loss, interventions remain underutilized. Several barriers to hearing care, including accessibility challenges, limit utilization. Addressing hearing loss from a public health perspective to overcome these barriers is both timely and critically important.

SYMP 59

How Sensitivity to Frequency and Amplitude Modulation Changes with Age and Hearing Loss

Kelly L. Whiteford; Heather A. Kreft; Andrew J. Oxenham

University of Minnesota

Acoustic communication requires sensitivity to frequency and amplitude modulation (FM and AM). A long-standing hypothesis has been that slow-rate FM at low carrier frequencies is represented by precise, phase-locked spike timing in the auditory nerve, whereas fast-rate FM is coded by a cochlear place-based mechanism. We measured individual differences in sensitivity to slow- and fast-rate FM, along with sensitivity to AM and frequency selectivity. The results show strong correlations between detection of both slow and fast FM, and similar effects of age and frequency selectivity on both rates of FM. The results instead suggest a unitary code for FM.

SYMP 60

Alpha Oscillations Index the Temporal Dynamics of Effortful Listening

Björn Herrmann¹; Burkhard Maess²; Ingrid S. Johnsrude¹

¹The University of Western Ontario; ²Max Planck Institute for Human Cognitive and Brain Sciences

The ability to exert cognitive effort during listening is crucial for speech perception in the presence of background sound, and may be an important factor that determines listening success in older people with hearing difficulties. Neural alpha oscillations in parietal cortex may provide a promising index for the assessment of effort as its power increases when individuals listen for subtle acoustic changes in sounds. It is, however, less clear how alpha oscillations are modulated by prior knowledge about when in time cognitive effort must be exerted during listening. In electroencephalography (EEG) and magnetoencephalography (MEG) experiments (N>100), we investigated how alpha power in a gap-detection task is affected by knowledge about when a near-threshold gap occurs within 10-s white noise sounds. Within one recording block, the gap occurred either within the first or the second half of the sound, and participants (21-33 years) were informed prior to each block. The precise position of the gap within the specified half was unknown to participants. Reaction times indicate that participants shifted their attention to either the first or second half of the sound, depending on the anticipated gap occurrence. EEG data showed a peak in alpha power at parietal electrodes either within the first or the last 5 seconds after sound onset, depending on whether participants were instructed to focus on the first versus second half of the sound. When detecting supra-threshold gaps, reaction times again indicated that participants shifted their attention to either the first or second half of the sound, but alpha power was less sensitive to this manipulation. These results suggest that investment of effort is needed to modulate alpha power. MEG data show that alpha power in superior parietal cortex was sensitive to the manipulation of gap

occurrence (first vs. second half), but that alpha-power in superior temporal cortex remained enhanced throughout sound presentation (relative to baseline), independent of gap occurrence. MEG data from older people (54-72 years) show similar context-dependent modulations of alpha power, but activity originated rather from inferior parietal cortex. The data show that alpha oscillations are sensitive to when in time cognitive effort is exerted during listening, but also that the neural sources differ between younger and older people.

SYMP 61

Age-Related Changes in Neural Coding of Envelope Cues: Peripheral Declines and Central Compensation

Aravindakshan Parthasarathy¹; Edward Bartlett²; Sharon G. Kujawa¹

¹Department of Otolaryngology, Harvard Medical School; Eaton-Peabody Laboratories, Mass. Eye and Ear Infirmary; ²Depts of Biology and Biomedical Engineering, Purdue University

Middle aged and older adults with normal hearing thresholds often exhibit a decreased ability to process complex sounds in challenging listening conditions. These age-related declines in neural encoding of sounds can arise from changes in the peripheral auditory system and the central auditory pathway. At the auditory periphery, there is a progressive loss of synapses between the inner hair cell and the auditory nerve with age that occurs independent of changes in hearing thresholds. Functional consequences of this cochlear synaptopathy remain poorly understood, but may include altered temporal coding of sound in the early auditory pathway. Using neural population based envelope following responses, we demonstrate that these temporal processing deficits arise at the earliest neural generators and are strongly correlated with the underlying synaptopathy. When faced with these degraded inputs from the auditory periphery, the central auditory pathway attempts to compensate for them by increasing its activity. By comparing the synaptic inputs measured using local field potentials to the spiking outputs of neurons in the inferior colliculus, we show an age-related increase in activity in the auditory midbrain in response to complex sounds. This has implications for speech processing, where the representation of periodicity envelope cues abnormally increase with age. Taken together, these results suggest that temporal processing along the ascending auditory pathway is affected due to peripheral declines in neural processing with age. The work is supported by the Department of Defense (W81XWH-15-1-0103 to SGK) and the NIH (NIDCD R01DC011580 to ELB).

SYMP 62

Age-Related Temporal Processing Deficits Along the Auditory Pathway

Hanin Karawani¹; Lindsey Roque²; Alanna Schloss²; Samira Anderson³

¹Department of Hearing and Speech Sciences, University of Maryland; Department of Communication Sciences and Disorders, University of Haifa; Department of Otorhinolaryngology-Head and Neck Surgery, Rambam Health Care Campus; ²Department of Hearing and Speech Sciences, University of Maryland; ³Department of Hearing and Speech Sciences, University of Maryland; Neuroscience and Cognitive Science Program, University of Maryland

Degraded temporal processing associated with aging contributes to speech perception difficulties in older adults and may affect the ability to distinguish between words based on temporal cues. The present study investigates the neurophysiological mechanisms that may contribute to these behavioral deficits along different levels of the auditory pathway, from periphery to midbrain to cortex. Age-related differences in perception and neural encoding of vowel duration cues were assessed by obtaining perceptual identification functions to naturally-produced words differing along a 9-step vowel duration continuum ("wheat" vs. "weed") and by recording frequency-following responses (FFR) and cortical auditory-evoked responses to the endpoints of this continuum in normal-hearing younger (ages 20-30) and older (age 55-70) adults. Multiple linear regression was used to determine how well neural representation of these vowel duration cues predicts behavioral performance. Older adults had shallower slopes on the identification function, poorer subcortical phase-locking, and delayed cortical latencies compared to younger adults. High-frequency pure-tone thresholds predicted variance in perception, but subcortical and cortical variables predicted significant additional variance.

SYMP 63

Neural Tracking of the Speech Envelope Across the Lifespan: Disentangling the Neural Consequences of Age and Sensorineural Hearing Loss Related to Speech Understanding in Noise

Lien Decruy; Jonas Vanthornhout; Tom Francart
The Katholieke Universiteit Leuven

Objectives: When we grow older, understanding speech in noise becomes more challenging. Studies have shown that these difficulties cannot be entirely explained by the typical reduced audibility of high frequencies with advancing age. For example, older adults with normal hearing thresholds perform more poorly on speech-in-

noise tests compared to their younger counterparts. To investigate the neural consequences of aging related to speech-in-noise difficulties and the effect of sensorineural hearing loss, we measured the neural tracking of the speech envelope in normal hearing (NH) and hearing impaired (HI) persons across the lifespan. Methods: We recorded the EEG of 47 NH (17-82 years) and 14 HI (21-80 years) participants who were provided with linear amplification. During the EEG, participants were asked to listen to stories, and to recall Matrix sentences to obtain a direct link with behaviorally measured speech understanding. To obtain different speech understanding levels, the target talker was embedded in a speechweighted noise or competing talker. Envelope tracking was estimated by first training a linear decoder, then applying the decoder and reconstructing the envelope from EEG and finally correlating it with the original envelope. To investigate the effect of hearing loss, HI participants were age-matched with NH adults. Results & Conclusions: For both NH and HI adults and across different ages, we found an increase in envelope tracking with increasing speech understanding. This is promising for the development of an objective measure of speech understanding based on envelope tracking, which could offer complementary information to behavioral speech audiometry. Furthermore, we found that age affects envelope tracking non-linearly with an increase from 50 years on. One explanation for this envelope overrepresentation is that middle-aged and older adults need more cognitive resources, to perform the same task as their younger counterparts. The decreased connectivity between brain regions with advancing age can also be linked with this. Lastly, sensorineural hearing loss, seems to result in an additional increase in envelope tracking on similar speech understanding levels. We suggest that this increase is due to a combination of factors, such as amplification, the need for higher SNRs and/or more cognitive resources and enhanced envelope sensitivity. Acknowledgements: This project has received funding from the ERC under the European Union's Horizon 2020 research and innovation programme (No 637424 to Tom Francart) and the KULeuven Special Research Fund (OT/14/119). Research of Jonas Vanthornhout is funded by a PhD grant of the Research Foundation Flanders (FWO).

SYMP 64

Increased Speech Representation in Older Adults Originates from Early Response in Higher Order Auditory Cortex

Christian M. Brodbeck¹; Alessandro Presacco¹; Stefanie Kuchinsky²; Samira Anderson³; Jonathan Z. Simon⁴

¹Institute for Systems Research, University of Maryland; ²Audiology and Speech Pathology Center,

Water Reed National Military Medical Center; Department of Hearing and Speech Sciences, University of Maryland; ³Department of Hearing and Speech Sciences, University of Maryland; Neuroscience and Cognitive Science Program, University of Maryland; ⁴Institute for Systems Research, Department of Electrical and Computer Engineering, Department of Biology, University of Maryland;

Compared to young adults, older adults are known to have increased difficulty comprehending speech, especially in challenging acoustic environments. Yet, somewhat paradoxically, previous research has found that older adults' cortical responses track the acoustic envelope of continuous speech signals more robustly than those of younger adults. We investigated this puzzle with magnetoencephalography (MEG) to determine the anatomical origin of this difference. Results indicate that older adults' cortical responses are not simply magnified versions of young adults' responses, but that they recruit additional regions, ventral to core auditory cortex. Older adults' responses in this region occurred with very low latencies for cortical processing, with their increased amplitude peaking at ~ 30 ms. This finding is consistent with theories suggesting age-related changes to bottom-up processing of acoustic signals in auditory cortex. In addition, older adults further showed increased responses at a substantially longer latency of ~ 200 ms, suggesting that higher level processing may also be altered.

SYMP 65

Benefits of Recruiting Age-Matched Normal-Hearing Control Groups in Cochlear Implant Speech Processing Research

Brittany N. Jaekel; Rochelle Newman; Matthew Goupell
University of Maryland

A growing number of cochlear-implant (CI) candidates are middle-aged and older adults, many who lost their hearing from presbycusis. When studying speech perception in CI users, it may be necessary to compare CI listener and age-matched normal-hearing (NH) listener performance. Older listeners process speech differently than younger listeners; for example, speech rate effects on phoneme perception (Jaekel et al., 2017) and reliance on speech-repair mechanisms (Jaekel et al., 2018) differ with age. Thus, differences due to aging rather than hearing status may contribute to some differences in speech processing between younger NH and older CI listeners.

Tribute to David Lim

Chair: Allen Ryan

SYMP 66

Fine Structure of the Middle Ear: The Contributions of David J Lim

Sung Moon
David Geffen School of Medicine, UCLA

The mammalian middle ear, an air-filled cavity in the temporal bone, functions to transfer vibrations of the tympanic membrane to the inner ear fluid. The lining mucosa of the middle ear, continuous with that of the nasopharynx through the Eustachian tube, consists of a variety of cells such as ciliated cells and secretory cells. The ciliated cells are populated densely in the Eustachian tube but scarcely in the mastoid air cells, indicating a directional movement of the middle ear clearance. Lectin studies show the heterogeneity of the secretory cells, producing mucin-type or serum-type glycoproteins. In addition to mucins, the middle ear mucosa secretes antimicrobial molecules including defensins and lysozyme, which create a highly effective barrier against pathogens and contribute to maintaining the sterility of the middle ear cavity, along with the mucociliary system. The round window membrane allows the cochlear fluid to move in response to sound vibrations, but this membrane can serve as a route for pathogen molecules to permeate into the inner ear, resulting in cochlear inflammation. Major contributions of Dr. David Lim to the middle ear research will be reviewed further, and the clinical implications will be discussed.

SYMP 67

David J. Lim: Contributions to the Development and Utilization of Auditory Cell Lines

Federico Kalinec
Department of Head and Neck Surgery, David Geffen School of Medicine at UCLA

David Lim's scientific work included important contributions to many different areas of Hearing Research. Well known are, for instance, David's influence in the use of Electron Microscopy techniques to elucidate the structure of the cochlea and his studies on otitis media and Menieres Disease. Less known, however, are David efforts aimed to develop auditory cell lines and promote their use. In 1999, in collaboration with Dr. John S. Rhim, David reported the development of a cell line from middle ear epithelium of chinchillas immortalized by infection with adenovirus 12-simian virus 40 hybrid virus. This initial work was immediately followed, in 2001 and 2002, by the establishment, using the same technique, of two additional lines, one from middle ear epithelium

and the other from eustachian tube epithelium of rats. Simultaneously, and always in collaboration with Dr. Rhim, David's group started working with human auditory cells. This effort crystallized in the generation of a line from human middle ear cells obtained from explants of fresh human middle ear epithelium harvested from patients undergoing neurotologic surgery for acoustic neuromas at the House Ear Clinic. In this case, cells were immortalized by using a retrovirus containing the e6/e7 genes of human papillomavirus type 16. In the following years two more auditory cell lines were developed at David's Lab, a rat spiral ligament cell line and a human inner ear cell line. While the first has been already used in several studies on homeostasis and inflammation of the inner ear, the human inner ear cell line is still in process of characterization. In this presentation I will discuss David ideas behind the development of cell lines from the auditory apparatus, and the importance of these cell lines as models for the study of inflammatory responses and the search for new drugs and biological agents for the treatment of hearing diseases.

SYMP 68

David J. Lim: Innate Immunity, Inflammation and New Therapeutic Targets in Otitis Media

Jian-Dong Li

Institute for Biomedical Sciences, Georgia State University

Innate immunity and inflammation play critical roles in eradicating pathogens in the ear. However, dysregulated host innate immune and inflammatory response often results in middle ear and inner ear immunopathology and hearing loss. The innate immune and inflammatory mediators and the molecular mechanisms underlying their regulation remain largely unknown. Over the past several decades, Dr. David Lim and his colleagues have made significant contributions to improve our understanding of the key innate immune and inflammatory mediators and the underlying molecular mechanisms in the pathogenesis of otitis media. (1). Identification of innate immune molecules and their regulatory mechanism in otitis media. They demonstrated the antimicrobial activity of innate immune molecules including lysozyme and the beta defensins secreted from middle ear epithelial cells against *Streptococcus pneumoniae*, *Moraxella catarrhalis* and nontypeable *Haemophilus influenzae* (NTHi). NTHi upregulates β -defensin 2 via Toll-like receptor (TLR)-dependent IRAK-TRAF-MAPK p38 pathway in middle ear epithelial cells. In addition, they also found that internalized NTHi induced cytosolic receptor NOD2-mediated induction of β -defensin 2 which contributes to the protection against NTHi-induced otitis media. Interestingly, NTHi and interleukin 1 (IL-1) α synergistically up-regulated

β -defensin 2 via the p38 MAP kinase pathway. (2). Positive and negative regulation of middle ear infection-induced inner ear inflammation. Cochlear inflammatory diseases, such as tympanogenic labyrinthitis, are associated with acquired sensorineural hearing loss. The positive and negative regulators underlying the tight regulation of cochlear inflammation remain largely unknown. In addition, the molecular mechanism involved in cochlear protection from inflammation-mediated tissue damage has yet to be understood. Dr. Lim and his colleagues have demonstrated that NTHi induced Chemokine (C-X-C motif) ligand 2 (CXCL2) via ERK2-dependent activation of c-Jun in inner ear fibrocytes. Moreover, NTHi also induced SLF-derived monocyte chemotactic protein 1 (MCP-1)/CCL2 in inner ear inflammation through CCR2-mediated recruitment of monocytes. Importantly, IL-10 plays a critical role in modulating cochlear inflammation through inhibition of MCP-1/CCL2 expression in spiral ligament fibrocytes (SLFs). (3). Demonstration of the therapeutic potential of adenovirus-mediated intratympanic gene delivery of β -defensin 2 for experimental otitis media. In summary, Dr. David Lim has made outstanding contributions to advance our understanding on regulation of innate immune and inflammatory responses in the pathogenesis of otitis media and identify novel therapeutic targets for treating otitis media.

SYMP 69

David J. Lim's Research on the Inner Ear

Peter Santi

University of Minnesota

I was fortunate to have known David J. Lim most of my professional career. Although we never collaborated on a publication, we had many discussions on the structure and function of the inner ear. David was not only a great colleague but a truly good person who encouraged everyone and nurtured our field in profound ways. David not only produced outstanding research, but he also established the ARO and developed a society that brought together clinicians, basic scientists, and international participants. This special symposium provides only a glimpse of his outstanding contributions and my role will be to review his research contributions on the inner ear. One of his first publications in 1969 on the inner ear used a newly developed technology called scanning electron microscopy (SEM). Using SEM, he provided the first 3-dimensional view of the inner ear and the complex internal anatomy of the hair cells and supporting cells of the scala media, which provided a good description of normal anatomy of the mammalian cochlea. He then focused on the tectorial membrane and the presumptive cells (interdental cells) that produce it.

His attention then turned to the mechanisms of cochlear damage after acoustic overstimulation and ototoxic drugs, using SEM and transmission electron microscopy (TEM). The stria vascularis and the outer hair cells were also investigated by David, to understand the role of fluid transporting enzymes in the cochlea and to relate cochlear micromechanics with structure. In addition to these inner ear studies, he also maintained an active research program on otitis media and how it affected inner ear structures. I will show some data from these studies and try to put them in context to other research developments in the field.

Inner-Ear Structure & Function

PD 73

Presynaptic Nicotinic Receptors Enhance Transmitter Release from Efferent Neurons on Cochlear Hair Cells.

Yuan-yuan Zhang¹; Isabelle Roux²; Elisabeth Glowatzki³; Paul A. Fuchs⁴

¹Johns Hopkins University School of Medic; ²National Institute on Deafness and Other Communication Disorders; ³Johns Hopkins University; ⁴Johns Hopkins University School of Medicine

Research Background: Cochlear hair cells are subject to synaptic inhibition by efferent neurons projecting from the brainstem (olivocochlear efferents). Release of acetylcholine (ACh) activates $\alpha 9\alpha 10$ -containing acetylcholine receptors in hair cells, increasing intracellular calcium to activate nearby calcium-dependent potassium channels. Efferent synapses are directed to outer hair cells in the mature cochlea. Prior to the onset of hearing, functionally identical efferent synapses inhibit inner hair cells. These synapses are lost at the onset of hearing. Recent studies have shown that transmitter release from efferent terminals is subject to modulation through several mechanisms. Here we demonstrate presynaptic nicotinic receptors that increase the probability of ACh release from efferent terminals on both inner and outer hair cells.

Methods: Apical cochlear turns were excised from mice ranging from 8 to 11 days of age, providing intracellular recordings from inner or outer hair cells with functional efferent synapses. Whole-cell, tight-seal recordings were made to record post-synaptic currents occurring spontaneously, or after drug application. A nearby 'puffer' pipette was used to apply nicotine (1 mM) for 0.5 seconds. Other drugs were applied by bath perfusion. All experiments were performed at room temperature.

Results and Conclusions: Puffer application of nicotine gave rise to a burst of synaptic currents in inner hair cells. These synaptic currents were due to the activation of SK-type, calcium-dependent potassium channels subsequent to calcium entry through the hair cell's $\alpha 9\alpha 10$ -containing ACh receptors. This effect was robust, occurring reliably and repeatedly in the great majority of inner hair cells. Several features of this response were of interest. After brief nicotine application transmitter release could continue for many seconds. Furthermore, after repeated nicotine exposures, 'spontaneous' synaptic currents became more frequent for the duration of the experiment. Efferent terminals on outer hair cells have intrinsically lower probabilities of release, nonetheless it was possible to show that nicotine also activated transmitter release onto some outer hair cells. The mechanism by which nicotine acts is under investigation, but preliminary experiments suggest that blockade of N, P/Q calcium channels (that support efferent transmitter release) does not entirely prevent the effect of nicotine.

Funding

Supported by NIDCD R03DC013374 to IR, NIDCD R01DC006476 and R01DC012957 to EG, NIDCD R01DC016559 and the John E. Bordley Professorship to PF and the David M. Rubenstein Fund for Hearing Research.

PD 74

Which mechanisms underlie the heterogeneity in spontaneous rates of spiral ganglion neurons?

Mamiko Niwa¹; Eric D. Young²; Elisabeth Glowatzki³; Anthony J. Ricci¹

¹Stanford University; ²Johns Hopkins School of Medicine; ³Johns Hopkins University

Type-I spiral ganglion neurons (SGNs) receive inputs from inner hair cells (IHCs). SGNs can be divided into 2~3 subgroups based on their spontaneous rate (SR) of action potential firing (Liberman, 1978). Their SRs are correlated with sound intensity threshold, sensitivity to amplitude modulated sounds, speed of adaptation and resistance to masking noise (Joris and Yin, 1992; Rhode and Smith, 1985; Costalupes et al., 1984). Although SR is a behaviorally relevant parameter of SGNs, the molecular mechanisms underlying SR heterogeneity is not well understood. Our study examined properties of the IHC/SGN synapse after hearing onset, focusing on potential mechanisms of heterogeneity. We performed whole-cell, voltage-clamp recordings from single SGN's terminal endings of C57BL6 mice (postnatal days 17~21 and 28~36) and measured EPSCs in the absence and presence of 40 mM K^+ stimulation. Fibers were located on the pillar or

modiolar side of IHCs, where high SR and low SR fibers preferentially terminate, respectively (Liberman, 1982).

Most recorded fibers showed low to no EPSCs in the standard physiological solution containing 5.8 mM K⁺. Fibers showed a clear onset of response to 40 mM K⁺, and the EPSC rate increased gradually to a peak and then declined during continuous 40 mM K⁺ application. The peak EPSC rate significantly increased with age (from P20 to P30; p=0.0293, rank sum test). When analyzed separately by terminal location, the peak rate of pillar fibers significantly increased from P20 to P30 (p=0.0017, Two-Way ANOVA), while the modiolar fibers did not change (p=0.892). We also examined how EPSC amplitude, area (EPSC integrated over time), and the number of elementary events per EPSC (#events/EPSC, determined by deconvolution) change over the time course of 40 mM K⁺ stimulation. Assuming that each EPSC is generated by summation of multiple vesicle fusions, the higher #events/EPSC indicates desynchronization of elementary events. Modiolar fibers showed decline in both amplitude and area while the EPSC rate increased to peak, whereas pillar fibers sustained amplitude and area during the same time period. In P30 pillar fibers, #events/EPSC started off high at the response start and declined as the response progressed to peak, whereas in P30 modiolar fibers, #events/EPSC started off low and increased toward the peak response. That the dynamics of #events/EPSC differ between pillar vs. modiolar locations implicates a (to be determined) differential presynaptic mechanism exists between pillar vs modiolar fibers.

Funding sources: NIDCD R01DC009913 to AR, R01DC006476 and R01DC012957 to EG, F32DC013721 to MN

PD 75

Characterizing the Role of CIB2 in Maintaining Ca²⁺ Homeostasis in the Auditory Hair Cells

Arnaud P.J. Giese¹; Shawn M. Crump²; Saima Riazuddin³; Gregory I. Frolenkov⁴; Zubair M. Ahmed³
¹University of Maryland School of Medicine; ²University of Kentucky; ³University of Maryland, School of Medicine; ⁴Department of Physiology, University of Kentucky

CIB2 encodes a Calcium and Integrin Binding protein 2 (CIB2). In the inner ear, CIB2 is localized toward the tips of the stereocilia of sensory hair cells, near the tip link-MET complex. We previously showed that CIB2 interacts with TMC1 and TMC2 and is essential for mechanotransduction in auditory hair cells (Giese et al, 2017). Among the known missense mutations of CIB2 that have been reported in humans suffering with profound prelingual hearing loss, two of these mutations

(p.Glu64Asp and p.Phe91Ser) affect the interaction of CIB2 with TMC1 and TMC2, while the p.Ile123Thr and p.Arg186Trp mutations only impaired the Ca²⁺ buffering of CIB2 and not interaction with TMC1/2, and thus are excellent candidates to explore the potential role of CIB2 in maintaining Ca²⁺ homeostasis in the auditory hair cells. Here, we report that mice carrying a p.Arg186Trp mutation of *Cib2* (*Cib2*^{R186W}). The *Cib2*^{R186W} homozygous mice have profound hearing impairment at P16 and have defect in FM1-43 dye uptake. We investigated the molecular impact of this variant on the components of the mechanotransduction complex and Ca²⁺ homeostasis in the hair cells. Furthermore, the development, staircase formation and maintenance of hair cells stereocilia were investigated with high-resolution scanning electron microscopy and compared with the *Cib2* total knockout mice. Results of these studies will be presented.

Support: This work was supported by the NIDCD/NIH grants R01DC012564 (Z.M.A./G.I.F.).

PD 76

Using optical coherence tomography (OCT) to obtain morphometric measurements within intact living and postmortem gerbil cochleae

Nam-Hyun Cho¹; Michael E. Ravicz²; **Sunil Puria**²
¹Harvard Medical School; ²Eaton-Peabody Lab, Mass. Eye & Ear

Background: Anatomical measurements within the organ of Corti (OoC) are critical for understanding physiological processes related to hearing. However, much of our knowledge of OoC anatomy comes from measurements on histological slices of chemically fixed and stained cadaveric tissue. While this has been the gold standard, its shortcomings include: an uncertain relationship to the original in-vivo anatomy, preparation-related distortions of the OoC cytoarchitecture, and being limited to a primarily 2D view. Finite-element models require accurate 3D anatomical descriptions of the OoC cytoarchitecture. In this work, we used optical coherence tomography (OCT) to obtain this information for intact in-vivo and postmortem gerbil cochleae. In addition, we also made vibrometry measurements in the same reference frame.

Methods: We used a Thorlabs Ganymede-III-HR 905-nm OCT system with a 100-kHz high-speed camera, and custom VibOCT software written in LabVIEW. VibOCT provides imaging and vibrometry acquisition using GPU-based near-real-time processing of acquired A-line data to extract displacement waveforms and spectra in response to tones. Respective axial (in water) and lateral resolutions are approximately 2.2 μm and 8 μm with the 36-mm objective lens used. Our axial resolution

is higher than most previous studies, and the noise floor is typically < 1 nm. We report 2D B-scan and 3D-volume C-scan images in the apical region of the gerbil cochlea. Custom SyncAv software provided the ear-canal sound stimulus, measured the ear-canal pressure, and triggered the vibrometry measurements in VibOCT.

Results: We observed in-vivo features and postmortem changes in cochlear morphology not seen previously. Reissner's membrane (RM) shows significant curvature for the in-vivo condition that remains for up to 45 min. postmortem, but by 140 min. postmortem the RM is nearly flat. The flat RM shape resembles what has been reported in previous histological studies with normal cochleae. This suggests that a change occurs in the static fluid-pressure difference between the scala media and scala vestibuli > 45 min. postmortem. The distance between the stria vascularis and Hensen-cell border decreases postmortem, indicating a flattening of those cells. Much of the cellular structure of the OoC, including 3 distinguishable rows of outer hair cells, is clearly visible in-vivo, but appears less distinct postmortem. Vibrometry measurements of multiple structures at multiple radial locations in the postmortem condition indicate a low-pass-like response. These in-vivo and postmortem images of the intact cochlea provide an opportunity to reassess previously published histological and physiological results. [Work supported by NIDCD R01-DC007910].

PD 77

Mitochondrial Networks Play a Role in Hair Cell Function in the Zebrafish Lateral Line

Andrea L. McQuate; David W. Raible
University of Washington

Mitochondria are implicated in many types of hearing impairments, including those brought on by age, noise exposure, and heritable disorders. Yet little is known about hair cell mitochondrial morphology, or whether disruption of hair cell mitochondria results in hearing loss. We use the zebrafish lateral line as a model for inner ear hair cells. With a combination of super resolution imaging and 3D reconstruction of mitochondria, we have found that hair cell mitochondria in the zebrafish lateral line are highly networked, with over 80% of the total mitochondrial volume consisting of a single network. We did not find this networked mitochondrial morphology, however, in adjacent supporting cells, despite their similar shape and proximity to hair cells. We are performing a CRISPR screen to identify genes that regulate mitochondrial morphology and dynamics, and testing these for altered hair cell function and susceptibility to damage. The hair cells of CRISPR mutants for the gene *opa1*, involved in the fusion of the inner mitochondrial

membrane, demonstrate a fragmented mitochondrial network phenotype and abnormal mitochondrial calcium buffering. These results suggest that the networked morphology of hair cell mitochondria might play a distinct role in hair cell function.

PD 78

Cochlear Purinergic Receptors Contribute to In Vivo Spontaneous Activity in the Developing Auditory System

Travis A. Babola¹; Calvin Kersbergen¹; Han Chin Wang²; Dwight E. Bergles²

¹*Johns Hopkins University;* ²*JHMI*

Spontaneous electrical activity is a prevalent feature of the developing nervous system, which has been shown to influence the maturation and survival of neurons, as well as refinement of circuits in the brain. In the auditory system, bursts of activity are initiated in the cochlea when ATP is released by inner supporting cells (ISCs) within Kölliker's organ (greater epithelial ridge). This periodic release of ATP induces inward currents, crenations (cell shrinkage), and calcium waves in ISCs, ultimately leading to depolarization of inner hair cells (IHCs). Subsequent release of glutamate and activation of spiral ganglion neurons transmits these bursts into the central nervous system, where it propagates through developing auditory centers. While key components of this signaling pathway have been explored, the receptors that mediate the effects of ATP remain undefined, limiting our ability to define functional consequences of this activity. Our studies indicate that activation of purinergic autoreceptors on ISCs is a critical initial step in the cascade of events that lead to efflux of potassium into the extracellular space and depolarization of IHCs. Using whole cell patch clamp and DIC imaging, we found that spontaneous currents and crenations of ISCs were inhibited by chelation of intracellular calcium or by inhibition of phospholipase C, suggesting that metabotropic, Gq-coupled receptors are required. ISC activity was abolished by the P2ry1 antagonist MRS2500 and dramatically reduced in P2ry1^{-/-} mice. Moreover, confocal imaging of cochleae from mice expressing GCaMP3 revealed that spontaneous calcium waves in Kölliker's organ were eliminated by MRS2500, indicating that P2ry1 is responsible for initiating spontaneous activity in ISCs. Loose patch recordings from SGNs in cochlear whole mounts from P2ry1^{-/-} mice or in the presence of MRS2500 revealed a marked reduction in SGN burst firing. Additionally, *in vivo* administration of MRS2500 dramatically reduced cochlear-driven neuronal calcium transients in the auditory midbrain of mice expressing the genetically encoded calcium indicator GCaMP6s, indicate that P2ry1 is responsible for triggering bursts of activity in ISCs and adjacent hair cells prior to hearing

onset. Unexpectedly, inhibition of P2ry1 with MRS2500 eventually led to tonic firing of SGNs, and spontaneous, non-burst firing of SGNs was enhanced in P2ry1^{-/-} mice, suggesting that P2ry1 also suppresses IHC excitability. Together, these results indicate that P2ry1-dependent signaling is a key regulator of IHC excitation in the cochlea, responsible for both triggering bursts of action potentials and limiting tonic firing.

PD 79

Normal Patterns of In Vivo Spontaneous Neural Activity in the Developing Auditory System Require Cochlear Supporting Cell Potassium Release, Mechanotransduction Channels, and Efferent Input

Calvin Kersbergen¹; Travis A. Babola¹; Sally Li¹; Paul A. Fuchs²; Ana Belen Elgoyhen³; Ulrich Müller²; Dwight E. Bergles⁴

¹Johns Hopkins University; ²Johns Hopkins University School of Medicine; ³Universidad de Buenos Aires;

⁴JHMI

Prior to sensory input, intrinsically-generated bursts of neural firing with distinct temporal and spatial arrangements are found along sensory neural pathways. In the auditory system, pre-hearing activity is initiated by ATP release from Inner Supporting Cells (ISCs) in the developing cochlea, leading to coordinated potassium release from ISCs via calcium-activated chloride channel TMEM16a, depolarization of nearby Inner Hair Cells (IHCs), and burst firing in Spiral Ganglion Neurons (SGNs). Our recent work suggests that this activity propagates to central auditory nuclei, where spontaneous calcium transients occur bilaterally in discrete patterns along the tonotopic axis in the Inferior Colliculus (IC). Additional contributions to spontaneous activity patterns have been identified, such as developmental medial olivocochlear (MOC) synapses onto IHCs, resting mechanotransduction currents, and spontaneous calcium action potentials in IHCs during the pre-hearing period. To assess how spontaneous activity patterns are altered with loss of these individual components, we performed widefield epifluorescence calcium imaging in the IC of un-anesthetized Postnatal day 6 (P6)-P8 *Snap25:GCaMP6s* mice with genetic deletion of TMEM16a, TMIE, or the Alpha9 nicotinic receptor.

Previous studies demonstrated that *Pax2Cre;TMEM16a^{fl/fl}* mice exhibit reduced spontaneous inward currents in ISCs, leading to a reduction in spontaneous depolarizations in IHCs and loss of correlated calcium transients in SGNs. *In vivo*, the frequency and amplitude of spontaneous calcium transients in the IC was also reduced in *Pax2Cre;TMEM16a^{fl/fl}* mice. However, residual patterned activity in the IC remained, perhaps due to incomplete deletion of TMEM16a and/or homeostatic changes in excitability. *Alpha9^{-/-}* mice exhibited no changes in the

frequency, amplitude, or duration of events; however, individual events were less correlated between the right and left IC, leading to highly lateralized activity. Mice with a gain-of-function mutation in the Alpha9 receptor, which exhibit smaller, but more prolonged, IPSCs in IHCs during this period, did not exhibit any changes in event amplitude, frequency, bilateral correlation, or event duration. A similar phenotype to *Alpha9^{-/-}* mice was observed in *TMIE^{-/-}* animals, where loss of mechanotransduction channels during the pre-hearing period also resulted in more pronounced asymmetric activity between right and left IC, as well as a small decrease in event amplitude and increase in event half-width. Together, these results suggest that a complex interplay of cochlear signaling *in vivo* generates and modulates the spontaneous neural firing throughout the auditory system prior to hearing onset, and that the precise pattern of neuronal activity during this period controls the global representation of sound in neural circuits that span both hemispheres.

PD 80

Precise Coupling Between Stereocilia and the Tectorial Membrane Depends on Stereocilia Elongation

Leonardo R. Andrade¹; Mhamed Grati²; Seham Ebrahim³; Felipe Salles³; Uri Manor¹; Bechara Kachar²
¹Waite Advanced Biophotonics Center, The Salk Institute for Biological Studies; ²NIDCD, NIH; ³NIH

The proper connection between inner ear cochlear hair cell stereocilia and the overlying tectorial membrane (TM) is critical for normal hearing. The TM is a gelatinous extracellular structure composed mostly of type II collagen fibers, alpha-, and beta-tectorins. In mammals, the tallest row of stereocilia from both inner (IHC) and outer hair cells (OHC) physically interact with the lower side of the TM forming, respectively, two morphological features: the Hensen's stripe and concave W-shaped imprints. The imprints correspond to the sites of OHC stereocilia-tectorial membrane junction (STJ) required for synchronization and amplification of hair bundle deflection during sound-induced oscillations of the organ of Corti. Mutant mouse models for several human deafness genes have revealed that proper stereocilia elongation and organization is critical for normal hearing. Here, we use scanning electron microscopy to show what happens to the STJ of mouse mutants with short stereocilia bundles, with planar cell polarity (PCP) disruption, and with stereocilia degeneration during aging. Adult mutants whose stereocilia are very short (e.g. *MyoXVa^{-/-}*, *EPS8^{-/-}*) showed an overall well-preserved TM but no STJ imprints. *Whirlin^{-/-}* mice whose stereocilia decrease significantly in height along the apical-basal axis of the sensory epithelium present many STJ imprints in the apical turn TM, few in the

middle, and none in the basal region of the cochlea. Mice with PCP defects (e.g. MyoVI^{-/-}, NMIIC^{-/-}, CD2^{-/-}) or with disorganized bundle morphology (e.g. SANS^{-/-}, TMHS^{-/-}) exhibit abnormal STJ in correspondence with their stereocilia morphology. In two year old mice, the TM surprisingly contains all the normal imprints from OHC stereocilia long after the disappearance of OHCs, revealing limited plasticity or turnover of the TM surface. However, the Hensen's stripe significantly thickens compared to younger mouse TM, which we hypothesize is due to a lifetime of mechanical interaction with IHC stereocilia. Our data suggest that the coupling between stereocilia and tectorial membrane requires proper stereocilia elongation and precise bundle formation. More specifically, we conclude that the lack of STJ in short stereocilia mutants is a key component of the pathophysiology of their associated mutations. The fact that the adult TM has limited plasticity is relevant to gene therapy and age-related hearing loss research.

Beyond the Mouse: Comparative Approaches to Investigate Auditory Encoding

Chairs: Christine Koppl & Sonja Pyott

SYMP 70

Using small mammals to understand big humans: Comparative animal models to understand auditory circuitry

Philip X. Joris
University of Leuven

The choice of animal models is based on a complex mixture of practical concerns, societal norms, scientific questions, technical possibilities, and existing knowledge. We have used a combined approach of single-cell and mass-potential recording in different species to interpret cochlear potentials measured in humans with normal hearing, resulting in estimates of human frequency tuning and phase-locking. In other experiments, we have used different species because they enable different technical approaches, leading to a multi-faceted view of binaural processing. Comparative approaches are thus rewarding both for intrinsic and technical reasons and can be an essential component of our scientific armamentarium.

SYMP 71

Monkey Business: What marmosets teach us about the central mechanisms of human hearing and vocal communication

Steven J. Eliades
University of Pennsylvania

Vocal communication is a fundamental behavior common to both humans and many animal species and plays a role in reproductive success and maintaining social groups. Despite this importance, neural and behavioral mechanisms related to communication remain poorly understood. Here, we present recent work in our laboratory showing how marmosets, a New World monkey species, reproduce many communicative behaviors seen in humans. We further demonstrate the role of the auditory system in vocal communication, and the similar mechanisms shared by marmosets and humans. Finally, we highlight opportunities in marmosets to manipulate neural processing, yielding valuable potential insights into human speech mechanisms.

SYMP 72

From man to mouse to fish: developing clinically relevant models of Usher syndrome

Erwin van Wyk
Radboud University Medical Center

Usher syndrome is genetically heterogeneous and affects both hearing and vision. Despite the insights into the role of Usher syndrome genes in hair bundle development revealed by mouse mutants, much remains to be learned about Usher gene function in the retinal photoreceptors. To further understand the role of Usher syndrome-associated proteins, we have generated and characterized zebrafish (*Danio rerio*) *ush2a* mutant models. Examination of the retinal pathology in these zebrafish disease models provides parallel insight into the cochlear pathology. This work shows that zebrafish is an excellent disease model and, moreover, provides a unique model to evaluate novel therapeutic strategies.

SYMP 73

Neurophonic from owls to mammals: the emergence of extracellular fields

Paula T. Kuokkanen
Humboldt-Universität zu Berlin

Extracellular field potentials (EFPs) are clinically important signals that arise from various underlying neural sources. Our recent work shows that the auditory frequency-following EFP (neurophonic) in mammals and owls exhibits highly similar characteristics despite different contributing sources. In the barn owl's nucleus laminaris, the EFP originates predominantly from spiking in the afferent axons with little contribution from the synapses and postsynaptic laminaris neurons. In contrast, in chicken and mammals, the neurophonic has mainly synaptic origins. The comparison of EFPs generated from anatomically different but well-characterized circuits from different species offers unique opportunities to unravel their sources and clinically relevant contributions.

SYMP 74

What the naked mole rat tells us about mammalian hearing

Catherine Barone
University of Illinois Chicago

The African naked mole-rats (NMRs) are subterranean rodents with poor high frequency hearing and limited ability to localize sound compared. Our recent anatomical characterization indicates that the NMR cochlea undergoes stunted maturation that results in unique patterns of peripheral synaptic organization and altered expression of ion channels compared to other mammals, including gerbil and mouse. Our even more recent functional auditory assessments, complemented with genetic analyses, indicate multiple mechanisms that may result in their relatively poor hearing compared to other mammals. This work provides essential comparative insight into the peripheral mechanisms shaping frequency-selectivity and sound localization.

Genetic Landscape of Hearing Loss

PD 81

Sequencing Platforms for Deafness: Expectations, Realities and Perspectives

Hela Azaiez¹; Kevin T. Booth²; Gongxin Yu²; Daniel Walls²; Ann Black-Ziegelbein²; Richard J. H. Smith³
¹*Molecular Otolaryngology and Renal Research Laboratories, Department of Otolaryngology, University of Iowa*; ²*Molecular Otolaryngology and Renal Research Laboratories, Department of Otolaryngology, University of Iowa*; ³*Department of Otolaryngology, Molecular Otolaryngology and Renal Research Laboratories, University of Iowa*

Background

Genetic testing for inherited disorders has been revolutionized with the advent of next generation sequencing (NGS), and nowhere is this more evident than in the study of genetic hearing loss. Deafness-associated genes can be screened for genetic variants using several platforms that differ based on the genomic regions that are covered - whole genome sequencing (WGS), whole exome sequencing (WES) and disease-specific targeted gene panels (TGP). In this study, we assessed the coverage of known deafness-associated genes across these three sequencing platforms to compare diagnostic accuracy and yield.

Methods

One hundred patients from a multiethnic cohort with varied types of hearing loss underwent WES and targeted deafness-gene sequencing using a specific platform we

have developed (OtoSCOPE). In addition, WGS was completed on 10 of the 100 samples. Bioinformatic analysis was completed using a custom pipeline and was limited to genes and mutations associated with deafness. Sanger sequencing was performed to validate genomic variants.

Results

Average depth-of-coverage of deafness-associated regions using OtoSCOPE was >400 reads/base, as compared to WES (70 reads/base) and WGS (31 reads/base). Accordingly, coverage at 30X was 96.5% with OtoSCOPE, 53% with WES and 50% with WGS. WGS offered the most uniformly distributed coverage across all regions. The drop in coverage depth correlated with a decline in base and variant quality, ambiguity in zygosity and most notably a lower detection rate of genomic variants especially for WES. A comparison of variant lists generated for patients after filtering for quality and minor allele frequency ($\leq 2\%$) showed that many OtoSCOPE-detected variants were missed in WES. Of missed variants, some were of clinical significance as they were causally linked to deafness. Detection of copy number variations (CNVs) also varied, with OtoSCOPE showing the most robust and accurate detection rate especially for heterozygote CNVs.

Conclusion

WES currently has the lowest variant detection rate when compared to WGS and targeted panel-based testing of deafness-associated genes. Several factors must be considered when choosing and implementing a clinical diagnostic test, including test sensitivity, accuracy, turn-around-time and cost. For deafness, targeted gene panels remain the most sensible choice for comprehensive clinical-based genetic testing as they offer the highest diagnostic yield at the lowest cost.

PD 82

Excess of missense variants in sensorineural hearing loss genes in sporadic Meniere disease

Alvaro Gallego-Martinez¹; Teresa Requena¹; Pablo Roman-Naranjo¹; Patrick May²; **Jose Antonio Lopez Escamez**¹

¹*Centre for Genomics and Oncology GENYO*;

²*Luxemberg Centre for System Biomedicine*

Background: Autosomal dominant familial Meniere's disease (MD) has been associated with rare variants in six genes (*COCH*, *DPT*, *DTNA*, *PRKCB*, *FAM136A* and *SEMA3D*) in single families with incomplete penetrance and variable expressivity in the phenotype. The aim of this study was to determine the contribution of rare variants in sensorineural

hearing loss (SNHL) genes, including familial MD genes, to sporadic MD by targeted exome sequencing.

Methods: A diagnostic panel with 69 genes was designed for the genetic diagnosis of MD. Nine hundred thirty DNA samples (890 cases and 40 controls) were pooled (each pool = 10X) and genomic libraries were generated by HaloPlex PCR target enrichment system. Paired-end sequencing was performed in a Nextseq500 instrument. BWA and GATK were used for alignment and quality controls. Variant calling was made through VarScan2 and the estimated minor allelic frequencies (MAF) were compared with three population datasets: total gnomAD, Non-finnish European from gnomAD and Spanish population from CIBERER variant server database (<http://csvs.babelomics.org/>), excluding patients with hearing loss. KGGseq suite (grass.cgs.hku.hk/limx/kggseq) was used for the prioritization of rare variants. Gene burden analysis was carried out to assess the interaction of multiple rare variants on the same gene on the phenotype.

Results: Patients with sporadic MD showed an excess of missense variants in SNHL genes that were not found in the controls. An enrichment of rare missense heterozygous variants with unknown significance was observed in familial genes FAM136A, PRKCB and SEMA3D in singletons (p-adjusted $\cdot 11$). Remarkably, a burden of missense variants was found in several SNHL genes including *GJB2*, *USH1G*, *SLC26A4*, *ESRRB*, *CLDN14* and *POU4F3* in patients with sporadic MD (p-adjusted, range 6.8×10^{-3} to 6.6×10^{-11}). A novel synonymous variant with unknown significance was found in the *MARVELD2* gene in three unrelated patients with MD. Two non-hearing loss genes, *ADD1* and *NFKB1* also showed a significant burden of missense variants.

Conclusions:

1. A burden of rare variants in SNHL genes may contribute to heritability in MD.
 2. The interaction of several variants with an additive effect in the same or different genes can also explain variable expressivity in familial MD.
 3. Some singletons may have a compound heterozygous recessive inheritance.
- Funded by Meniere Society, UK and the Luxembourg National Research Fund (INTER/Mobility/17/11772209).

PD 83

Identification of *SLC12A2* as a Candidate of Nonsyndromic Sensorineural Hearing Loss in Human

Hideki Mutai¹; Koichiro Wasano²; Yukihide Momozawa³; Yoichiro Kamatani³; Fuyuki Miya⁴; Sawako Masuda⁵; Noriko Morimoto⁶; Kiyomitsu Nara¹; Satoe Takahashi²; Tatsuhiko Tsunoda⁴; Kazuaki Homma²; Michiaki Kubo⁷; Tatsuo Matsunaga¹
¹National Hospital Organization Tokyo Medical Center; ²Northwestern University Feinberg School of Medicine; ³Center for Integrative Medical Sciences, RIKEN; ⁴Tokyo Medical and Dental University; ⁵National Hospital Organization Mie Hospital; ⁶National Center for Child Health and Development; ⁷RIKEN Center for Integrative Medical Sciences

Genes associated with hereditary hearing loss are highly heterogeneous. One of the reasons of unsuccessful diagnosis for hereditary hearing loss would be due to unidentified responsible genes. Using whole exome analysis, we identified two missense and a splice site variants of *SLC12A2*, encoding Na⁺, K⁺, Cl⁻ cotransporter 1 (NKCC1), as the best candidates in three families with nonsyndromic sensorineural hearing loss. *SLC12A2* plays critical roles in homeostasis of K⁺-enriched endolymph. Multiple strains of *Slc12a2* deficient mice have shown congenital and profound deafness. Importance of *Slc12a2* for proper inner ear function has also been demonstrated in zebrafish; however, no human variant of *SLC12A2* has been reported to associate with hearing loss. All the subjects with heterozygous *SLC12A2* variants showed congenital, severe to profound hearing loss. All the variants were found on or at the splice site of exon 21 in *SLC12A2*. *In vitro* splicing assay revealed that the splice site variant failed to incorporate exon 21, suggesting that this variant likely produces non-frameshift, truncated isoform of *SLC12A2*. The transcript of *SLC12A2* that lack exon 21 was endogenously expressed in mammalian brains, but not in the cochleae, suggesting tissue-specific role of the exon 21-encoded region. Heterologous expression of recombinant *SLC12A2* protein with both missense variants or the truncated isoform in HEK293T cells resulted in significantly decreased Cl⁻ influx as compared to cells expressing wild type recombinant *SLC12A2* protein, indicating that these *SLC12A2* mutants are functionally impaired. Immunohistochemical analysis demonstrated that *SLC12A2* was located on several types of cells in the non-human primate cochlea such as basolateral membrane of the stria marginal cells, where the cells play critical role in accumulation of K⁺ from surrounding area and secretion into the endolymph. Taken together, our study suggests that *SLC12A2* is responsible for hereditary hearing loss in human.

Mutation in the Clarin-2 Gene Cause Hearing Loss in Human and a Zebrafish Model Reveals the Likely Cause of that Hearing Loss

Suhasini R. Gopal¹; Barbara Vona²; Reza Maroofian³; Hela Azaiez⁴; Kevin T. Booth⁵; Kate Clancy¹; Neda Mazaheri⁶; Gholamreza Shariati⁷; Alireza Sedaghat⁸; Ruben Stepanyan¹; Richard J. H. Smith⁹; Thomas Haaf¹⁰; Hamid Galehdari⁶; Kumar N. Alagramam¹
¹Department of Otolaryngology, University Hospitals Cleveland Medical Center, School of Medicine, Case Western Reserve University; ²Institute of Human Genetics, Julius Maximilians University Würzburg; ³Molecular and Clinical Sciences Institute, St George's University of London, Cranmer Terrace; ⁴Molecular Otolaryngology and Renal Research Laboratories, Department of Otolaryngology, Department of Otolaryngology, University of Iowa; ⁵Molecular Otolaryngology and Renal Research Laboratories, Department of Otolaryngology, University of Iowa; ⁶Department of Genetics, Faculty of Science, Shahid Chamran University of Ahvaz; ⁷Department of Medical Genetics, Faculty of Medicine, Ahvaz Jundishapur University of Medical Sciences; ⁸Diabetes Research Center, Health Research Institute, Ahvaz Jundishapur University of Medical Sciences; ⁹Department of Otolaryngology, Molecular Otolaryngology and Renal Research Laboratories, University of Iowa; ¹⁰Institute of Human Genetics, Julius Maximilians University Würzburg

Background

The Clarin-2 gene encodes a putative four transmembrane protein closely related to tetraspanins. Its amino acid sequence in human, mice and zebrafish is well conserved and mutations in the paralogous gene, Clarin-1, have been causally linked to hearing loss in humans (Usher syndrome IIIA), mice and zebrafish. Therefore, we hypothesized that Clarin-2 is essential for hearing in vertebrates.

Methods and Results

To investigate the functional consequence of mutation in Clarin-2, we generated zebrafish carrying a *clm2* knockout (KO) allele using CRISPR/Cas9 technology. *clm2*^{+/KO} zebrafish were normal at all ages, however, *clm2*^{KO/KO} larvae exhibited poor startle response (poor hearing) and a balance defect 6 days post fertilization. Hair cells in *clm2*^{KO/KO} displayed abnormal morphology with short and disrupted hair bundles and a significantly reduced number of mature ribbon synapses. The mechanotransduction function of *clm2*^{KO/KO} hair cells, as reflected by microphonic potentials, was significantly attenuated. Consistent with the *clm2*^{KO/KO} phenotype, we showed that *clm2* mRNA is restricted to hair cells

within the inner ear. Additionally, Clrn2-YFP fusion protein expressed in zebrafish hair cells localized to the hair bundle and plasma membrane. These data demonstrate that Clrn2 is an essential hair cell protein, and its defect results in loss of hearing and balance in zebrafish.

To test whether mutation of *CLRN2* causes hearing loss in humans, we screened an ethnically diverse cohort of patients with hearing loss and identified a missense mutation in an extended consanguineous Iranian family segregating autosomal recessive non-syndromic sensorineural hearing loss (ARNSHL). When the mutant Clrn2*-YFP protein was transiently expressed in zebrafish hair cells, it failed to localize to the hair bundle or plasma membrane. In addition, *in silico* and *in vitro* analyses using mini-gene assays revealed defective splicing and a shift in the reading frame as a result of this missense variant.

Conclusion

Taken together, these findings establish CLRN2 as a key player in auditory function and incriminate it in the pathophysiology of hearing loss.

PD 85

Rescue of SYNE4/Nesp4 Deafness in a Mouse Model for Human Hearing Loss

Shahar Taiber¹; Prathamesh Thangaraj Nadar-Ponniah¹; Ofer Yizhar-Barnea¹; Yukako Asai²; Jeffrey R. Holt³; Karen B. Avraham¹
¹Tel Aviv University; ²Boston Children's Hospital, Harvard Medical School; ³Boston Children's Hospital & Harvard Medical School

Pathogenic variants in *SYNE4* are known to lead to deafness in humans from Israel (Horn H, Brownstein Z et al, *J Clin Invest*, 2013) and Turkey (Masterson J et al, *Balkan Med J*, 2018). The *Syne4* gene encodes a protein that is part of the linker of nucleoskeleton and cytoskeleton (LINC) complex in the nuclear envelope, named Nesprin 4 (Nesp4). LINC complexes couple nuclear components to the cytoskeleton and mediate nuclear polarization. In an attempt to rescue the hearing loss of a Nesp4 knock-out mouse, we used the synthetic AAV, Anc80L65. We cloned the coding sequence of *Nesp4* into the AAV backbone and generated AAV-CMV-Syne4-EGFP expression vectors. A single injection of virus preparations was made into the posterior-semicircular-canal of *Nesp4*^{-/-}, *Nesp4*^{+/-} and wild-type mice at P0-P2. We then evaluated the transfection efficiency two weeks after injection using whole-mount immunofluorescence. Based on GFP fluorescence, the majority of inner hair cells and a variable amount of outer hair cells were transduced. To determine whether viral transfection resulted in prolonged Nesp4 expression, we transfected HEK293T cells with AAV-CMV-Syne4-EGFP or AAV-CMV-EGFP as a control. Injected mice were evaluated for hearing using open-field ABR at P15, just

after the mice acquire the ability to hear, and P30, when *Nesp4*^{-/-} mice are known to lose their remaining hearing capacity. The treated mice appear to have a small but significant level of rescue of hearing loss. Morphological assessment of treated and control ears demonstrated that while the inner hair cells are unchanged, a greater number of outer hair cells appear to survive in *Nesp4*^{-/-} injected inner ears than in non-injected *Nesp4*^{-/-} ears. Currently, *Nesp4*^{-/-} organ of Corti explants are being examined at earlier time points in order to characterize the developmental dynamics of *Nesp4*-mediated function. As the *Nesp4* knock-out mouse phenotype mimics the human one, these mice are a relevant model for development of gene therapy to rescue hearing loss.

PD 86

Targeted Allele Suppression Prevents Progressive Hearing Loss in the Mature Murine Model of Human TMC1 Deafness

Hidekane Yoshimura¹; Seiji Shibata¹; Paul Ranum¹; Hideaki Moteki²; Richard J. H. Smith¹

¹Department of Otolaryngology, Molecular Otolaryngology and Renal Research Laboratories, University of Iowa; ²Department of Otorhinolaryngology, School of Medicine, Shinshu University

Background

To date, several reports describe successful auditory restoration following intra-cochlear gene therapy in neonatal mouse models of genetic deafness. While these outcomes represent important advances, the neonatal murine inner ear is only partially developed and undergoes structural maturation until the onset of hearing at postnatal day 14-15 (P14-15). At P1-2, it is temporally equivalent to the human cochlea prior to 26-weeks gestational age, suggesting translation of neonatal murine studies to human subjects would require *in utero* intervention. Studies in mature animals are needed to assess the effect of gene therapy, however delivering gene therapy to mice after the first postnatal week has been precluded by ossification of the bony labyrinth. To address this challenge, we developed a surgical approach in which round window membrane injection is combined with semi-circular canal fenestration. Using this technique, we aimed to assess the effect of gene therapy in the fully developed murine inner ear.

Methods

We used the *Beethoven* (*Bth*)-heterozygous mouse, a murine model of human *TMC1* deafness (DFNA36). The mice carry a dominant-negative missense mutation in the *Tmc1* gene and exhibit progressive hearing loss. Using a single intracochlear injection of an artificial microRNA (miRNA) carried in an adeno-associated virus (AAV) vector and delivered at P15-16, P56-60 or P84-90, we

determined whether selective suppression of the mutant *Tmc1* allele prevented hearing loss as measured by auditory brainstem response audiometry, prolonged IHC survival as documented by immunohistochemistry, and changed in IHC stereocilia morphology as visualized by scanning electron microscopy.

Results

We show that RNA-interference-mediated gene silencing slowed progression of hearing loss, improved inner hair cell survival, and prevented stereocilia bundle degeneration in the mature *Bth* mouse. In mice injected at P15-16 and P56-60, progression of hearing loss was halted but not reversed. In mice treated at P84-90, hearing loss continued at a rate indistinguishable from untreated ears.

Conclusions

We present the first successful application of cochlear gene therapy in an adult mouse model of progressive human deafness and demonstrate that RNAi mitigates progression of hearing loss in the mature *Bth* mouse. Our results show that for *TMC1*-related deafness, microRNA-based allele suppression prevents but does not reverse hearing loss and that there is an upper time limit before which intervention must occur. Proof that gene therapy is effective in mature murine ears constitutes a significant step towards its application in human subjects.

PD 87

The Formin Protein Fhod3 Is a Novel Hearing Loss Gene Involved In Regulating Stereocilia Lengths

Ely Cheikh Boussaty¹; Leonardo R. Andrade²; Pezhman Salehi³; Juemei Wang⁴; Takahiro Ohyama⁴; Uri Manor²; Rick A. Friedman¹

¹Division of Otolaryngology, Head and Neck Surgery, Department of Surgery, University of California, San Diego; ²Waite Advanced Biophotonics Center, The Salk Institute for Biological Studies; ³Department of Biomedical Sciences, Creighton University, School of Medicine; ⁴USC-Tina and Rick Caruso Department of Otolaryngology-Head & Neck Surgery, Zilkha Neurogenetic Institute, USC Keck School of Medicine, University of Southern California

Formins are actin-regulatory proteins most commonly associated with the elongation of parallel actin bundles via their ability to polymerize actin filaments. Two formin genes thus far have been genetically associated with hearing loss – *mDia1* and *Diaph3* – and were discovered to be pathological in cases of increased activity, either due to overexpression or due to abnormally constitutive activity due to mutations in their autoinhibitory domains. However, even though inner ear sensory hair cell stereocilia are comprised of long parallel actin filaments,

no formins have yet been shown to localize to or regulate stereocilia actin specifically. We identified Fhod3, a formin gene within a peak SNP interval on chromosome 18, in a meta-analysis genome-wide association study (GWAS) of age-related hearing loss (ARHL) in C57BL/6J x DBA/2J F1 intercross mice. In situ hybridization revealed Fhod3 expression in auditory hair cells and spiral ganglion neurons of the cochlea in neonatal mice. Immunofluorescence staining using several antibodies targeting different Fhod3 epitopes indicates that Fhod3 localizes to outer and inner hair cell stereocilia in mice, rats, and guinea pigs. Interestingly, no Fhod3 deleterious polymorphisms were identified in the DBA/2J strain, but quantitative PCR showed significantly increased inner ear expression of Fhod3 in DBA/2J when compared to C57BL. To study the effects of Fhod3 overexpression *in vivo*, we generated and characterized inner ear tissue specific Fhod3-cACT: Pax2-Cre transgenic mice. Auditory Brainstem Responses (ABR) measured at 6 and 12 weeks postnatally show that Fhod3 overexpression in the inner ear leads to progressive high frequency (24 and 32 KHz) hearing loss. Scanning and transmission electron microscopy imaging of Fhod3-cAct transgenic mice cochlea show that Fhod3 overexpression is associated with loss of the shortest row of the inner and outer hair cell stereocilia in basal regions of mouse cochlea. These data show for the first time a clear role for a formin protein in stereocilia structure and function. In conclusion, our results support the hypothesis that Fhod3 is involved in regulating the lengths of hair cell stereocilia, and that overexpression of Fhod3 disrupts proper stereocilia length regulation. Understanding the mechanism by which Fhod3 regulates stereocilia structure and function will lend new insight towards the physiopathology of progressive hearing loss and may identify new therapeutic targets for age-related hearing loss.

PD 88

Characterization of Copy Number Variations in POU3F4 in Chinese Cases with Hearing Loss Using MPS Dataset

Yu Lu; Jia Geng; Jing Cheng; Huijun Yuan
Medical Genetics Center, First Affiliated Hospital, Army Medical University

Background: *POU3F4*, also known as DFNX2, is the most common causative gene account for X-linked nonsyndromic hearing loss (HL) subjects. Temporal bone computer tomography (CT) of male hearing loss subjects with *POU3F4* mutations showed bilateral malformations of enlarged internal auditory canal (IAC), and absent cochlear modiolus, defined as incomplete partition type III (IP-III). About 43% females carrying *POU3F4* heterozygous mutations present with milder hearing loss and variable inner ear malformations.

Several copy number variations (CNVs) have been reported, none was in Chinese population. We explore to detect possible CNVs in Chinese hearing loss subjects using in-house MPS dataset.

Methods: In this study, massively parallel sequencing (MPS) of known HL genes was performed in 12,247 Chinese subjects with hearing loss. SNVs, indels, CNVs and SVs were analyzed using in-house bioinformatics pipeline. Sanger sequencing confirmed the breakpoints and segregation of the CNVs identified in the HL families.

Results: Three CNVs with different partial exon deletions were identified in coding region of *POU3F4* gene in three male HL subjects. One partial exon deletion causes truncated protein, and two long range deletions include start code of *POU3F4* gene. The audiograms of these subjects showed congenital profound hearing loss. Sanger sequencing indicated the three CNVs were all inherited from mothers with normal hearing carrying heterozygous CNVs.

Conclusion: This study reported for the first time the CNVs in *POU3F4* gene coding region associated with DFNX2 in Chinese hearing loss population. Although CNVs of *POU3F4* gene were uncommon, they can improve the molecular diagnosis of undiagnosed cases with inner ear malformation that failure to identify SNVs or indels.

Receptors, Afferents, Brains & Behaviors

PD 89

Striola and Crista Central Zone of the Vestibular Organs Are Required for Rapid, Transient Vestibular Activities

Kazuya Ono¹; Omar López Ramirez²; Antonia González Garrido²; Sarath Vijayakumar³; Sherri M. Jones³; Ruth Anne Eatock²; Doris Wu⁴
¹NIDCD; ²University of Chicago; ³University of Nebraska Lincoln-College of Education and Human Sciences; ⁴National Institute on Deafness and other Communication Disorders

Vestibular sensory epithelia have a specialized central region, known as the striola in otolith maculae and central zone in semicircular canal cristae. Differences between central and surrounding regions (extrastriolar and peripheral zones) are evident in the accessory structures, sensory hair bundles, synaptic morphology, Ca²⁺ binding protein expression, and afferent terminal diameter and physiology. Afferents from central regions have higher conduction velocities, more irregular spike timing, and show greater sensory adaptation than afferents from peripheral regions. These properties suggest that the striolar and central zones provide input to fast reflexes

that maintain balance and gaze during rapid head motions. Linear vestibular evoked potentials (VsEP) generated by jerk stimuli applied to the head are thought to be generated by signals in striolar afferent neurons. Despite these proposed functions, the precise role of the striola/central zones has not been tested in an animal model.

We have generated a “loss of striola/central zone” mouse model by deleting *Cyp26b1*, which encodes one of the retinoic acid degradation enzymes expressed in the prospective striola/central zones of vestibular sensory organs during development. *Foxg1-Cre*-mediated conditional knockouts of *Cyp26b1* (*Cyp26b1* cKO) are viable and they show loss of striola/central zone based on molecular, anatomical, and physiological analyses. *Cyp26b1* cKO also showed remnant or absence of VsEP, providing direct evidence that linear VsEP is generated by the striola. Despite the loss of VsEP, low-frequency VOR was unaffected in *Cyp26b1* cKO. No chronic vestibular deficits such as head tilt or circling behaviors were detected, and general motor skills and swimming ability also appeared normal. However, *Cyp26b1* cKO mice have trouble crossing a narrow balance beam, suggesting that the coordination of vestibular-motor function is compromised. Taking together the VsEP and behavioral results, we propose that the striola/central zones of the vestibular organs are not critical for low-frequency vestibular function but are critical for signaling high-frequency (transient) head motions and performing challenging vestibulo-motor activities.

Supported in part by grant R01 DC012347.

PD 90

Infrared Photo-sensitivity in the Vestibular Neuroepithelium is Modulated by TRPV4

Federica Maddalena Raciti¹; Weitao Jiang²; Suhru M. Rajguru³

¹Department of Physiology and Biophysics, University of Miami; ²Department of Biomedical Engineering, University of Miami; ³Department of Biomedical Engineering and Otolaryngology, University of Miami

Introduction: Pulsed infrared radiation (IR) is being investigated as a non-invasive technique for altering activity of excitable cells such as nerve and muscle. However, the mechanisms of action of IR are poorly understood. Previous studies suggest that IR induced intracellular $[Ca^{2+}]$ changes as a result of activation of temperature-dependent Transient Receptor Potential (TRP) channels. In the present work, we investigated the mechanisms underlying IR responses in the vestibular neuroepithelium focusing on the role of the thermosensitive TRP channels. We hypothesized

that IR-activation of TRPV4 channels modulates $[Ca^{2+}]$ leading to glutamate release from vestibular hair cells and the observed excitatory and inhibitory post-synaptic responses.

Materials and Methods: The University of Miami Institutional Animal Care and Use Committee approved all procedures. Bilateral eye movements were recorded and characterized during pulsed IR stimulation of vertical semicircular canals *in vivo* in a rat model to assess the activity of the vestibular system (ISCAN Inc, Woburn, MA). Results were analyzed using custom MATLAB program. IR at 1860nm (200 μ s, 200Hz, various radiant exposures) was directed at the vestibular neuroepithelium via a 200 μ m dia. optical fiber. IR evoked eye movements were measured before and after the neurotransmission was impaired upstream by an acute treatment with Neomycin (100 mM), causing hair cells loss, or downstream by perfusion of CNQX (100 μ M), a competitive AMPA/kainate receptor antagonist. Furthermore, the IR response was also recorded prior to and after reducing the temperature below the activation threshold of the TRPV4 (<26°C) with perfusion of temperature-controlled artificial perilymph. TRPV4 channels were targeted pharmacologically with specific blockers (GSK2193874 and HC067047) perfused at different concentrations.

Results and Discussion: The IR evoked amplitude of eye movement reduced significantly following treatment with both CNQX and Neomycin. The amplitude of IR-evoked eye movement, also, reduced significantly with temperatures lower than TRPV4 activation threshold as well as after the perfusion of TRPV4 channel blockers. The eye movement recovered at the physiological temperatures and after washout of the compounds suggesting that TRPV4 channels play an important role in IR activation of the vestibulo-ocular motor pathway.

Conclusion: These results suggest that IR stimulation primarily affects vestibular hair cells and that TRPV4 channels within the vestibular neuroepithelium drive the photothermal responses.

Funding NIH/NIDCD

1R01DC008846and 1R01DC013798

PD 91

The Role of Quantal and Non-Quantal Synaptic Transmission in Auditory Frequency Phase Locking of Calyx-Bearing Vestibular Afferent Neurons

Marta M. Iversen; Brandon R. Pope; Richard D. Rabbitt
University of Utah

Introduction

Dimorphic and calyx-only vestibular afferent neurons

respond to auditory frequency (AF) sound and vibration by firing action potentials at precise times relative to the stimulus waveform (phase locking). Calyx-bearing afferents synapsing on type I hair cells respond to AF stimuli up to several kilohertz, and are much more sensitive than bouton-only afferents synapsing on type II hair cells^[1]. A unique feature of these AF sensitive afferents is that they receive both quantal (Q) and non-quantal (NQ) transmission from hair cells^[2]. It is unknown how, or if, these two forms of synaptic input combine to excite AF phase locked action potentials in vestibular afferent neurons. In this report, we examine in silico the potential contributions of Q and NQ transmission to AF phase locking in vestibular afferent neurons.

Methods

A mathematical model of a space-clamped vestibular afferent neuron was constructed in the Hodgkin-Huxley framework. Ionic currents included typical sodium, potassium, and leak currents, a fast calcium current and a calcium-dependent after-hyperpolarization current^[3]. Q and NQ synaptic inputs from vestibular hair cells modulated at auditory frequencies were used to drive action potential generation. The NQ input was simulated using a compartmental model of ionic buildup in the synaptic cleft and modulation of a passive NQ current^[4,5]. The quantal input was simulated with either quantized, log-normally distributed, excitatory postsynaptic currents (EPSCs), or with modulated multiquantal release (MEPSCs)^[6,7]. The potential contributions of non-quantal and quantal inputs were examined numerically.

Results

Simulations indicate that NQ synaptic input to vestibular afferents is likely to play two important roles in shaping vestibular responses to sound and vibration. First, NQ transmission generates a rectifying current that moves the voltage toward action potential threshold. Second, the small AF modulation of the NQ component increases the probability a single EPSC will trigger an action potential at a precise phase of the stimulus even if EPSC arrival times are random. Phase locking is stronger when stimulus strength dependent multi-quantal release is included.

Conclusion

Results offer an explanation why calyx-bearing vestibular afferents are the most sensitive to AF sound and vibration, and why these afferent neurons are preferentially excited in clinical tests that use AF stimuli.

Funding

References

- [1] Curthoys, *Front Neurol* (2017).
- [2] Holt, *J Neurophysiol* (2007).
- [3] Nguyen, *Eur Phys J Spec Top* (2010).
- [4] Contini, *J Physiol* (2017).
- [5] Highstein, *Proc Natl Acad Sci USA* (2014).
- [6] Highstein, *J Neurophysiol* (2015).
- [7] Li, *Neuron* (2014).

PD 92

In Vivo Mapping of Graded Linear Acceleration in Central Vestibular Pathways

Srinivasu Kallakuri; Mirabela Hali; Andre Kuhl; Rodney Braun; Avril Genene Holt
Wayne State University School of Medicine

Introduction: The vestibular system is crucial for posture, gait, and the perception of head and body position in space. Damage to this system can manifest as dizziness, imbalance, and poor postural control. Linear acceleration has been reported to result in measurable vestibular short-latency evoked potentials (VsEPs). The precise central neurons that contribute to the production of VsEPs are not well delineated. Manganese acts as a calcium surrogate and accumulates in active neurons. The paramagnetic nature of manganese permits visualization of these active neurons. Therefore, we have combined VsEP and manganese-enhanced magnetic resonance imaging (MEMRI) to assess vestibular function and visualize activity in central neurons responding to varying magnitudes of jerk stimulation (nonuniform linear acceleration).

Methods: Following anesthesia, each male Sprague Dawley rat (n=5) was attached to a mechanical shaker via a ceramic nut that had previously been attached with dental cement and centered on bregma. Each animal was then subjected to a jerk stimulation (either 500 g/s, 2500 g/s, or 6000 g/s). Manganese chloride was administered just prior to stimulation. Typically, 200-400 jerk stimuli were delivered per trial. Each trial was repeated a total of 15 times with a ten-minute interval after every five trials. Responses were recorded (CED power 1401 data acquisition system and Spike2 software) and analyzed using custom MATLAB scripts. Animals were also subjected to baseline, 24-hour post, and 2-week post stimulation MRI to assess manganese uptake in vestibular nuclei (lateral, medial, superior, and spinal vestibular nuclei).

Results: For each of the jerk stimuli the response latency for P1 was ~ 1 ms after the stimulus onset. While each of the jerk stimuli resulted in VsEP, the 500 g/s stimulus resulted in the least robust signal, with the greatest signal observed after 2500 and 6000 g/s. Repetitive high-intensity stimulation appeared to result in diminished P1 amplitudes and earlier onset. All the vestibular nuclei (VN) had significantly elevated manganese uptake following stimulation versus baseline. Manganese uptake was least in animals administered jerks of 500 g/s. Greatest manganese uptake was observed in vestibular nuclei of animals subjected to jerks of 2500 g/s and 6000 g/s.

Discussion: Our results demonstrate graded increases in manganese uptake in vestibular nuclei corresponding to increases in linear acceleration, particularly in the spinal vestibular nucleus. MEMRI and VsEP are promising tools which can be used to non-invasively map vestibular activity.

PD 93

Neural Correlates of Galvanic Vestibular Stimulation in the Alert and Behaving Macaque

Kathleen E. Cullen¹; Annie Kwan²; Patrick Forbes³; Diana Mitchell²; Dale Roberts¹; Jean-Sébastien Blouin⁴
¹*Johns Hopkins University*; ²*McGill University*; ³*Delft University of Technology*; ⁴*University of British Columbia*

The vestibular system encodes sensory information that is vital for a range of behaviors, including reflexes, balance, navigation and perception. In everyday life, the vestibular system is typically activated in concert with other sensory modalities (i.e., proprioceptive, somatosensory and visual) leading to our sense of self-motion. However, in the laboratory it is possible to selectively activate the sensory organs of the vestibular system (the semicircular canals and otoliths) by applying electrical currents over the mastoid process. This tool – termed galvanic vestibular stimulation (GVS) - evokes stereotypical ocular and postural responses as well as virtual sensations of motion that have been well described in humans. Yet, exactly how this non-invasive tool activates the vestibular system remains an open question. Conflicting views suggest that preferential GVS activation of either canal or otolith afferents drive the evoked responses. This controversy in turn leads to misconceptions of experimental procedures and/or misinterpretations of clinical observations. To link neuronal and behavioural responses, we recorded eye movements and individual vestibular afferent activity while applying transmastoid GVS in alert macaques. We found that GVS predominately evoked torsional eye movements, similar to those reported in humans. Our single unit recordings further revealed that canal and otolith afferents are similarly activated by GVS, and

afferents with greater intrinsic variability show greater response modulation. Notably, GVS-evoked responses of both canal and otolith afferents overturn previous expectations that GVS induces responses that are invariant across stimulation frequency, and also differed markedly from their response to natural motion. The dynamics of GVS-evoked primary vestibular afferent activity could be explained by a stochastic model of repetitive activity in vestibular afferents. Taken together, these results reveal the neural correlates underlying GVS-evoked perceptual, ocular and postural responses – a fundamental step into understanding the representation and use of such information in the brain that is critical to advance the applicability of GVS for biomedical uses in humans.

PD 94

A Novel Virtual Reality Technique to Adapt Heading Perception in the Horizontal Plane in Unilateral Vestibular Loss

Daniel Martin; Benjamin T. Crane
University of Rochester

Introduction: After acute unilateral vestibular loss, patients experience vertigo which often improves over time, yet, remains a major detractor of quality of life. Heading perception in the horizontal plane in patients with chronic loss has been previously evaluated. These patients have inertial heading perception which is deviated, such that straight ahead is more likely to be perceived as toward the side of the lesion. This experiment aimed to correct this with a novel virtual reality adaption stimulus.

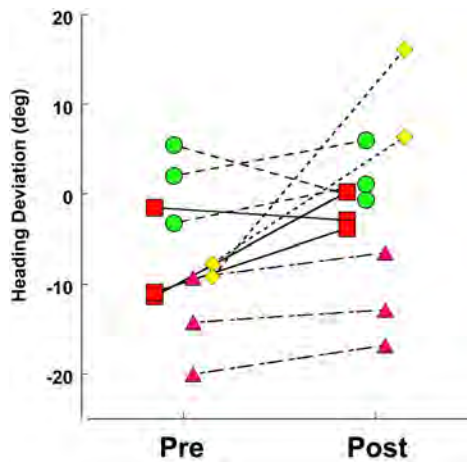
Methods: Subjects were asked to report inertial heading direction using a forced choice task to establish a baseline heading perception (point of subjective equality). They were then placed in a virtual reality environment which consisted of white dots on a black spherical background (i.e. "star-field"). The sphere has a radius of 50 virtual meters. The star-field consists of 500 dots randomly placed along the spherical surface. The stars are circles that are 6 pixels in diameter on a 1080×1200 screen. The sphere has a 40°/sec angular speed either clockwise or counter-clockwise. Every frame 10% of the stars in the star-field randomly change their location, giving a 90% visual coherence. Direction of star-field rotation was tailored to each subject to return heading perception to straight ahead (counter-clockwise for a rightward bias). While in the environment, subjects were asked to fix gaze on randomly spawning objects which move with the environment. Once fixated upon, the object disappears and a new object respawns one second later. Subjects were exposed to the environment for a total of ten minutes. Subsequently, the subject's;

post VR inertial heading perception was measured in the same method as before. Subjects repeated this protocol an average of 2.75 times (range 2-3) over the course of one month.

Results: Four patient were enrolled. Pathology was unilateral and included prior labyrinthectomy, vestibular neuritis, acoustic neuroma removal with subsequent gentamicin injection and long standing idiopathic hypofunction. Average age was 47 (range of 36-59). Three were female. Initial inertial PSE was deviated $7.3 \pm 7.1^\circ$ (mean \pm SD) from center. After adaption, average PSE was $0.6 \pm 8.5^\circ$ with an average change of $6.7 \pm 8.6^\circ$. Paired two tailed T-test confirmed significance of adaption technique ($p=0.03$).

Conclusion: Heading deviation after unilateral vestibular loss can be adapted back into the normal range. This may be feasible as a vestibular rehabilitation protocol in the future.

Support: R01-DC013580



PD 95

The Vestibular Implant: Restoring the High-Frequency Visual Stabilization Abilities

Raymond Van de Berg¹; Nils Guinand²; Florence Lucieer¹; Maurizio Ranieri²; Samuel Cavuscens²; Dmitrii Starkov³; Jean Philippe Guyot²; Herman Kingma¹; Stefano Ramat⁴; Angélica Perez-Fornos²
¹Division of Balance Disorders, Faculty of Health Medicine and Life Sciences, Department of Otorhinolaryngology and Head and Neck Surgery, School for Mental Health and Neuroscience, Maastricht University Medical Center; ²Service of Otorhinolaryngology and Head and Neck Surgery, Department of Clinical Neurosciences, Geneva University Hospitals.; ³Faculty of Physics, Tomsk State University; ⁴Department of Electrical, Computer and Biomedical Engineering, University of Pavia

Introduction. The vestibular implant seems feasible as a clinically useful device in the near future. Previously, the first functional benefit was shown by restoring the dynamic visual acuity during walking. Recently, the functional head impulse test (fHIT) was developed to selectively test the high-frequency visual stabilization abilities. This case study investigated the feasibility of restoring the high-frequency visual stabilization abilities with a vestibular implant, using the fHIT.

Methods. A 72-years old female with bilateral vestibulopathy and fitted with a modified cochlear implant incorporating three vestibular electrodes (MED-EL, Austria), was selected for this study. After training and understanding the fHIT, she underwent 6 trials of the fHIT: 1) System off; 2) System on, baseline stimulation; 3) System on, positive 3dB modulation around baseline; 4) System on, negative 3dB modulation around baseline; 5) System off, no delay after condition 4; 6) System off, 25 minutes delay after condition 4. Electrical vestibular stimulation was provided by the electrode close to the lateral ampullary nerve on the left side. Each trial of the fHIT (BEON Solutions, Italy) consisted of at least 16 horizontal head impulses (randomly to each side). During the impulses, the patient had to look at a computer screen at a distance of 1.5 meter while randomly oriented Landolt C-optotype letters appeared for 80 milliseconds. After each impulse, the patient had to report which Landolt C-optotype letter was displayed. The percentage of correct answers during the trial was registered for left and right impulses, and compared to the other trials.

Results. Electrical vestibular stimulation was able to improve the high-frequency visual stabilization abilities. The percentage of correct answers improved from 19-44% (minimum-maximum) in the conditions without the system on, to 75-94% (minimum-maximum) in the condition with negative 3dB modulation around the baseline (table 1).

Conclusion. It is possible to improve the high-frequency visual stabilization abilities by the vestibular implant. This functional benefit of the vestibular implant illustrates again the feasibility of this device for clinical use in the near future.

Table 1. Percentage (and absolute number) of correctly determined Landolt C-optotypes during different test conditions.

Condition	Side	
	Left (Implanted)	Right
System _{off}	25 (5/20)	20 (4/20)
System _{on} baseline	50 (8/16)	56 (9/16)
System _{on} +3dB	38 (6/16)	25 (4/16)
System _{on} -3dB	94 (15/16)	75 (12/16)
System _{off} 0min	44 (7/16)	38 (6/16)
System _{off} 25min	38 (6/16)	19 (3/16)

Restoration of the High-Frequency, Angular Vestibulo-Ocular Reflex with a Vestibular Implant in Humans

Nils Guinand¹; Raymond Van de Berg²; Erich Schneider³; Maurizio Ranieri¹; Samuel Cavuscens¹; Herman Kingma²; Jean Philippe Guyot¹; Angélica Perez-Fornos¹
¹*Service of Otorhinolaryngology and Head and Neck Surgery, Department of Clinical Neurosciences, Geneva University Hospitals;* ²*Division of Balance Disorders, Faculty of Health Medicine and Life Sciences, Department of Otorhinolaryngology and Head and Neck Surgery, School for Mental Health and Neuroscience, Maastricht University Medical Center;* ³*Brandenburg University of Technology Cottbus—Senftenberg,*

Background: vHIT (video Head Impulse Test) has become a gold standard in vestibular testing. It allows side specific, independent assessment of the 6 semicircular canals in the high frequency range. Therefore vHIT is an optimal test for the evaluation of the performance of vestibular implants, which are devices designed to primarily restore the canal function in patients with a severe bilateral vestibulopathy loss (BV). The purpose of this study was to evaluate whether it is possible to restore the high-frequency, angular vestibulo-ocular reflex (aVOR) with a vestibular implant prototype.

Methods: Three patients with severe BV were fitted with a vestibular implant prototype. The device consists in a modified cochlear implant (MED-EL, Innsbruck, Austria) with vestibular electrodes implanted in the ampullae of each semicircular canal. The high-frequency, aVOR was assessed using the vHIT (EyeSeeCam system) while motion-modulated electrical stimulation was delivered via one of the implanted vestibular electrodes (S1 – posterior ampullary nerve, S2 – lateral ampullary nerve, S3 – superior ampullary nerve). Results obtained with different gains were compared to control measurements obtained with the vestibular implant switched off.

Results: Upon stimulation, the shape of the aVOR response changed. When positive transfer function slopes were used, the shape of the aVOR improved for both excitatory and inhibitory head impulses in S1, but only for excitatory head impulses in S2 and S3. It was accompanied by a concomitant decrease in the frequency of compensatory saccades. Inverting the polarity of the slope of the linear transfer function resulted in an inversion of the aVOR response in S1 and S3, as well as an increase in the frequency and amplitude of compensatory saccades in S3, mainly for inhibitory head impulses. For S2, the response appeared similar to that observed in the system OFF condition. All patients presented low aVOR gains (<0.20) when the system was not activated, as expected.

Conclusions: Using the vHIT, these results demonstrate that it is possible to restore the high-frequency aVOR using motion-modulated electrical stimulation of the vestibular afferents, delivered with a chronically implanted, prototype vestibular implant. This result extends previous findings, confirming that our device successfully restores multimodal vestibular function, providing clear evidence that a vestibular implant might become an effective rehabilitation alternative for patients with a BVL in a near future.

Activity-Dependent Development of the Auditory Inner Ear

Chairs: Tobias Moser & Snezana Levic

SYMP 75

Persistent spontaneous activity in the auditory system of deaf mice

Dwight Bergles
Johns Hopkins University School of Medicine

The developing organ of Corti generates spontaneous activity that propagates throughout the auditory system before hearing onset to initiate cellular maturation and circuit refinement. To understand how this activity is influenced by loss of genes linked to deafness, we monitored the activity of spiral ganglion neurons (SGNs) in isolated cochleae, and auditory neurons in vivo in unanesthetized mice prior to hearing onset. Our studies indicate that spontaneous activity is preserved despite disruption of the mechanotransduction apparatus or abolishment of glutamatergic excitation of SGNs, indicating that these neurons exhibit robust homeostatic responses to preserve spontaneous activity during this critical developmental period.

SYMP 76

Mechanisms that Regulate Spiral Ganglion Neuron Subtype Specification in the Auditory System

Ulrich Müller
Johns Hopkins University School of Medicine

Type I SGNs transmit sound information from cochlear hair cells to the CNS. Using transcriptome analysis of thousands of single neurons, we demonstrate that murine type I SGNs consist of several molecularly distinct subtypes. Subtype-specification is initiated prior to the onset of hearing during the time frame when auditory circuits mature. Gene mutations linked to deafness that affect hair cell function disrupt spontaneous activity in the auditory system and SGN subtype specification. We conclude that activity dependent mechanisms are critical for the specification of different subtypes of SGNs, which

likely have distinct functions for transmitting sound information to the CNS.

SYMP 77

Developmental maturation of inner hair cell ribbon synapses

Christian Vogl

Institute for Auditory Neuroscience, University Medical Center Göttingen

Prior to the onset of hearing, inner hair cell (IHC) ribbon-type presynaptic active zones undergo a range of molecular and structural refinements. These developmental processes are essential to shape the high-throughput exocytic release machinery and establish the characteristic presynaptic morphology of these monosynaptic connections. During this transitional period, IHC ribbon counts progressively decrease as multi-ribbon active zones are streamlined to harbor predominantly single ribbons. To date, the molecular key players as well as the underlying pathways involved in this highly dynamic process remain largely elusive. To address this issue, we combined super-resolution microscopy with EM tomography and functional imaging.

SYMP 78

Spatio-temporal pattern of the action potential firing in developing inner hair cells.

Régis Nouvian

Institute for Neurosciences of Montpellier

Sensory inner hair cells (IHCs) of the cochlea, the organ of hearing, fire action potentials during development. This presensory activity likely drives refinement of the ascending auditory pathway. Using patch-clamp recordings and calcium imaging, we show that IHCs fire spontaneous bursts of action potentials independently of their position along the tonotopic axis and that proximal auditory hair cells tend to have synchronized activity. These data therefore suggest that the specification of the higher auditory center would depend to the synchronization of a discrete number of auditory sensory cells

SYMP 79

Spontaneous and coordinated Ca²⁺ activity of cochlear sensory and non-sensory cells drives the maturation of OHCs and their innervation

Walter Marcotti

The University of Sheffield

Outer hair cells (OHCs) are specialized sensory cells conferring the fine tuning and sensitivity of the mammalian cochlea to acoustic stimuli. Their mature

functional characteristics are acquired during early stages of immature development. We found that waves of Ca²⁺ activity in the non-sensory cells act, via ATP-induced activation of P2X receptors, to synchronize the spontaneous firing activity of OHCs. By genetically manipulating spontaneous Ca²⁺ signalling in mice *in vivo*, we also found that OHC maturation and the refinement of their afferent innervation are orchestrated by complementary spontaneous Ca²⁺ signals originating in OHCs and non-sensory cells from the immature cochlea.

SYMP 80

Spontaneous activity in developing hair cells is required for proper synaptic refinement in the developing auditory neuron-hair cells synapse

Snezana Levic

Brighton and Sussex Medical School, University of Sussex

An important blueprint of the developing nervous system is the appearance of patterned spontaneous action potentials (SAPs) which is very likely obligatory for proper neural wiring and synapse formation in the developing visual system. In the developing auditory system, rhythmic membrane activity in spiral ganglion neurons (SGNs) and its removal has a profound impact on the population and morphology of neurons in the cochlear nucleus (CN). Thus, one of the prevalent models is that peripheral neural activity in the developing auditory system may shape the structure, wiring, and survival of CN neurons. Auditory hair cells (HCs) fire SAPs before the onset of hearing, but SAPs are not necessary for the projection of SGNs to the cochlear epithelia. Evidently, developing epithelia devoid of HCs continue to receive neural projections, raising questions on the etiology and functions of SAPs in the auditory system. Meanwhile, the stark coincidence that cannot be ignored is the appearance of SAPs during HC-SGN synapse formation and its cessation following synapse formation. The origin of SAPs may be intrinsic to the developing HC, but ATP released from supporting cells sculpted its structure. Evidence suggested that SAPs in the developing auditory pathway are major determinant of proper tonotopic maps along the auditory axes. However, the exact roles of pre-synaptic SAPs and postsynaptic activity in the developing auditory primary receptors remain elusive. SAPs produce rhythmic changes in intracellular Ca²⁺ (Ca²⁺_i). An important factor in regulating Ca²⁺_i levels is calcium-induced calcium release (CICR), a positive feedback process whereby the increase of Ca²⁺_i begets activation of Ca²⁺ release from the ryanodine (Ry) sensitive stores. The roles of CICR in the maintenance of SAP structure is unknown. In this report, we used a naturally occurring Ry receptor

(RyR) mutant chicken with altered, chronic Ca²⁺i handling to demonstrate that reduced Ca²⁺i produces robust changes in K⁺ current expression, resulting in the attenuation of SAPs in developing HCs. Moreover, SAPs can be restored upon increased external Ca²⁺. Cessation of SAPs in developing HCs did not alter initial pre- and post-synapse formation. Rather, in the absence of HC activity, there was increased misalignment of the pre- and post-synaptic elements. Remarkably, complete loss of the juxtaposition of pre- and postsynaptic elements, followed by loss of withdrawal of post-synaptic densities occurred when pre-and post-synaptic activities were attenuated. We propose that SAPs in the developing HCs strengthen and maintain synapse formation in a “Hebbian” activity-dependent manner.

Benefits and Limitations of Perceptual Fusion Within and Across Modalities

Chairs: Lina Reiss & Ruth Litovsky

SYMP 81

Combining Information Within and Between Senses

Martin S. Banks

University of California - Berkeley

Humans use multiple sources of sensory information to estimate environmental properties. For example, the eyes and hands both provide relevant information about an object’s shape. The eyes estimate shape using binocular disparity, perspective projection, etc. The hands supply shape information from tactile and proprioceptive cues. Combining information across cues can improve estimation of object properties but may come at a cost: loss of single-cue information. We observed that single-cue information is indeed lost when cues from within one sensory modality (disparity and texture gradients in vision) are combined, but not when different modalities (vision and haptics) are combined.

SYMP 82

How Does the Brain Develop its Capacity to Integrate Information from Multiple Senses?

Barry E. Stein

Wake Forest School of Medicine

Neurons in the superior colliculus (SC) serve as an excellent model to understand how the brain crafts its ability to synthesize information from different senses (auditory, visual, tactile). However, this capacity is not inborn. Its gradual maturation is directed by cross-modal experience, thereby ensuring its operational features become adapted to the environment in which it will be used. Thus, compromising auditory-visual

experience by noise-rearing or dark-rearing precludes the development of A-V integration capabilities. These development factors, the likely neural site at which cross-modal experience is encoded, and the effect of multisensory integration on overt SC-mediated behavior will be discussed.

SYMP 83

The Impact of Dynamic Interaural Time Differences on Auditory Object Formation and Sound Source Lateralization in Bilateral Cochlear Implant Listeners

Tanvi Thakkar; Alan Kan; Ruth Litovsky

University of Wisconsin - Madison

In complex environments, normal hearing (NH) listeners can usually separate the location of different sound sources with ease, in spite of the acoustic input having multiple interaural time differences (ITDs) that are interleaved over time. This is because NH listeners typically weight onset ITDs more heavily than the dynamically-changing, ongoing ITD to form the percept of an auditory object that is located in space. However, recent data showed that bilateral cochlear implant (BiCI) listeners experience difficulties in sound source lateralization in the presence of time-varying ITDs presented on electrical pulse trains. In this work, we systematically vary the amount of stable and dynamic ITD cues in an electrical stimulus to understand the mechanisms that might be disrupting good lateralization and auditory object formation (AOF) in BiCI listeners. Using synchronized research processors, we presented trains of biphasic electrical pulses (100 pulses-per-second, 300-millisecond duration), presented on an interaural pair of electrodes determined by a pitch-matching task. We systematically manipulated the number of pulses that carried the same ITD (either 0, -800 μ s or +800 μ s within a trial), starting from the onset. Remaining pulses had a dynamically-changing ITD that, on average, pointed to a location in the same or opposite hemifield as the onset but the ITD imposed on each pulse could vary by ± 40 μ s. Listeners responded by indicating the perceived location of the auditory object on an image of a face shown on a computer monitor. Listeners were also instructed to indicate how many sounds were perceived, ranking them from most to least dominant. Each stimulus condition was randomly interleaved and presented a total of 20 times. When stable and dynamic ITDs pointed in opposite hemifields, at least five pulses with stable ITDs are required in order for an auditory object to be correctly lateralized. In contrast, when stable and dynamic ITDs pointed in the same hemifield, the auditory object was usually correctly lateralized regardless of number of pulses with stable ITDs. AOF was unrelated to the number of pulses with stable ITDs. However, the most dominant

source was always reported in the direction of the stable ITD while any secondary sources, if perceived, were reported towards the direction of the dynamic ITD. These findings suggests that BiCI listeners may benefit from a sound coding strategy that has a stable ITD in a few pulses so that a sound object can be correctly localized in a complex auditory environment.

SYMP 84

Duplex Pitch Perception in Hybrid Cochlear Implants

Damien Bonnard; Adam Schwalje; Inyong Choi
University of Iowa

A duplex theory of pitch perception explains that pitch sensation of a complex tone becomes salient by combining excitation pattern-based pitch from low-frequency resolved harmonics and temporal pitch from unresolved high-frequency harmonics. As hybrid cochlear implant (CI) users receive low-frequency information in acoustic stimulation and high frequency in electric within the same ear, a question arises whether they can benefit from duplex pitch perception. We found that, from our 2AFC inharmonicity-detection experiment, hybrid CI users do have duplex pitch perception, which indicates their ability to combine electric and acoustic stimulation as a single auditory object.

SYMP 85

Indiscriminate Binaural Fusion Leads to Interference for Speech Perception and Impairs Auditory Object Segregation

Lina Reiss
Oregon Health and Science University

Hearing-impaired individuals often exhibit abnormal binaural fusion based on pitch cues, fusing sounds differing in pitch by up to 3-4 octaves across ears into a single auditory object. We present evidence that such indiscriminate binaural fusion leads to averaging and smearing of mismatched spectral information, such that speech perception can be worse with two ears than one. Further, indiscriminate fusion impairs the segregation of auditory objects based on pitch differences, such as different voices in a cocktail party environment. Obligatory binaural fusion, with a concomitant loss of information from individual streams, may occur before object formation and segregation.

SYMP 86

Audiovisual Plasticity Following Long-Term Monocular Deprivation

Jennifer Steeves
York University

A growing body of research shows that complete deprivation of the visual system from early blindness results in changes in the remaining senses and recruitment of visual cortices for this purpose. A unique model for examining partial visual deprivation is early unilateral eye enucleation where one half of the visual input is eliminated during postnatal brain maturation. Our lab has shown that some aspects of auditory processing are enhanced and there is less susceptibility to audiovisual illusions such as the McGurk Effect following unilateral eye enucleation. These effects appear to be supported by altered auditory/audiovisual neural substrates.

Hair Cells: Mechanotransduction & Synaptic Transmission

PD 97

A Myosin Molecular Motor Directly Stimulates Actin Polymerization to Drive Stereocilia Growth

Melanie Barzik¹; Carlos Aguilar²; Rui Gong³; Arik Shams¹; Fangfang Jiang⁴; Jesse Werth¹; Christian Faaborg-Andersen¹; Randall Harley¹; Daniel C. Sutton⁵; Andrew Parker²; Elizabeth Wilson¹; Tracy Fitzgerald⁶; Yasuharu Takagi⁷; James Sellers⁷; Steve Brown²; Thomas B. Friedman¹; Gregory Alushin³; Michael Bowl²; **Jonathan Bird**⁴

¹Laboratory of Molecular Genetics, National Institute on Deafness and Other Communication Disorders; ²Mammalian Genetics Unit, MRC Harwell Institute; ³Laboratory of Structural Biophysics and Mechanobiology, The Rockefeller University; ⁴Dept of Pharmacology and Therapeutics, University of Florida; ⁵Program in Molecular and Human Genetics, Department of Genetics, Baylor College of Medicine; ⁶Mouse Auditory Testing Core Facility, National Institute on Deafness and Other Communication Disorders; ⁷Laboratory of Molecular Physiology, National Heart, Lung and Blood Institute

Stereocilia hair bundles are actin-based mechanosensors that detect sound and acceleration. The ATPase myosin-15 (MYO15) shapes hair bundle architecture using two protein isoforms that independently: 1) drive stereocilia elongation during development, and 2) postnatally maintain shorter rows of mechanosensitive stereocilia. Disruption of either isoform causes human deafness, DFNB3. During development, a shorter MYO15 isoform is hypothesized to traffic an 'elongation complex'; of WHRN, EPS8, GNAI3 and GPSM2 to stereocilia tips; the major site of actin polymerization during hair bundle growth. How these proteins regulate actin polymerization remains unknown. We investigated this question using an ENU-induced *Myo15* missense allele (*jordan*), originally identified from a phenotype-driven mouse mutagenesis screen.

Homozygous *jordan* mice exhibit ABR thresholds of ≥ 45 dB SPL at 4-weeks of age (controls 18-24 dB SPL), progressing to ≥ 80 dB SPL by 12-weeks of age (controls 18-28 dB SPL). SEM analyses revealed that, similar to *Myo15 shaker-2* mutants, hair bundles from *jordan* cochleae have additional rows with stereocilia not elongating to wild-type lengths. Using P7-P14 mice, we confirmed that MYO15 and the elongation complex proteins localize to stereocilia tips in wild-type animals, but are absent from the short hair bundles of *shaker-2* mutants as previously reported. Interestingly, despite *jordan* hair cells having short bundles, MYO15 and the elongation complex proteins were still localized to stereocilia tips, indicating that trafficking of these molecules alone is not sufficient to drive growth.

We used purified wild-type and mutant MYO15 to analyze how the *jordan* mutation interferes with stereocilia elongation. The *jordan* mutant protein has a severe ATPase defect relative to wild-type, but is mechanically active in gliding filament assays, consistent with MYO15 trafficking the elongation complex in *jordan* hair cells. Single-particle cryo-electron microscopy was used to determine the structure of wild-type and *jordan* MYO15 bound to filamentous actin (F-actin). Wild-type MYO15 modulates the conformation of F-actin, an effect diminished in the *jordan* mutant, which disrupts a residue within the actin-binding interface. *In vitro* pyrene-actin and single filament TIRF microscopy assays show that wild-type MYO15 strongly stimulates actin polymerization, and this activity does not require elongation complex proteins. Importantly, this stimulatory effect is blocked by the *jordan* mutation, suggesting that this activity of MYO15 is essential for stereocilia elongation *in vivo*. Our results support a fundamentally new model for stereocilia growth, where MYO15 traffics proteins essential for elongation, but also directly stimulates actin polymerization at the stereocilia tip to control hair bundle architecture.

PD 98

Biochemical Properties of TMC1 Suggest a Dimeric, Two-Pore Structure for the Hair-Cell Transduction Channel

Nurunisa Akyuz¹; Bruce Derfler¹; Walrati Limapichat¹; Sanket Walujkar²; Lahiru Wimalasena²; Jeffrey R. Holt³; Marcos Sotomayor²; David P. Corey⁴

¹Harvard Medical School; ²The Ohio State University; ³Boston Children's Hospital & Harvard Medical School; ⁴Harvard Medical School, Department of Neurobiology

The TMC1 and TMC2 proteins are critical components of the mechanotransduction complex in vertebrate inner-

ear hair cells, and have been proposed as pore-forming subunits of the force-gated transduction channel. To understand TMC proteins, we sought insight into the atomic structure of TMC1. We first synthesized and purified mouse and human TMC1. A variety of tests—including FRET, native gels, size-exclusion chromatography, chemical crosslinking, multi-angle light scattering and cryo electron microscopy—suggest that TMC1 assembles as a dimer. The predicted secondary structure and hydrophobicity suggest an architecture with ten transmembrane domains.

The dimeric stoichiometry, and a distant sequence similarity between TMCs and the TMEM16 family of anion channels and lipid scramblases, suggest that TMCs may have a tertiary structure and topology similar to TMEM16 with ten transmembrane domains. We used Phyre2 and I-TASSER to align TMC1 with TMEM16A, for which the atomic structure has been solved. TMEM16A dimerizes at an interface involving the tenth transmembrane domain, and each subunit of the dimer has an separate ion conducting pore, bounded by transmembrane domains S4-S7—a configuration strikingly different from well-known ion channels with a central pore bounded by three to six subunits. To ask whether S4-S7 of TMC1 might also enclose a pore, we used molecular dynamics simulations of the predicted structure of TMC1 embedded in a lipid membrane and surrounded by a salt solution. Simulations showed that the putative S4-7 pore of TMC1 is accessible to water and to potassium ions, suggesting that it can be an ion conduction pathway. Details of the TMC1 pore are different from that of TMEM16; specifically, TMC1 has some conserved acidic residues at the outer pore where TMEM16 has acidic residues, consistent with the hair-cell channel being cation-selective.

The likely dimeric structure of TMC1, together with the dimeric structure of PCDH15 elucidated with X-ray crystallography and cryo-EM, suggest a mechanotransduction complex in which each subunit of the PCDH15 dimer interacts with one subunit of the TMC1 dimer, to open a pore in that subunit. Other proteins such as LHFPL5, which interacts with both PCDH15 and TMC1, may also be integral members of the complex.

PD 99

Cysteine Substitution Identifies the Pore-forming Region of TMC1 in Hair Cell Sensory Transduction Channels

Bifeng Pan¹; Xiao-Ping Liu¹; Nurunisa Akyuz²; Bence György³; Carl Nist-Lund¹; Kiyoto Kurima⁴; Yukako Asai⁵; David P. Corey⁶; Jeffrey R. Holt⁷

¹*Boston Children's Hospital, Harvard Medical School*; ²*Harvard Medical School*; ³*Department of Neurobiology, Harvard Medical School, Massachusetts General Hospital*; ⁴*NIDCD/NIH*; ⁵*Boston Children's Hospital, Harvard Medical School*; ⁶*Harvard Medical School, Department of Neurobiology*; ⁷*Boston Children's Hospital & Harvard Medical School*

Background

Molecular identification of ion channels that mediate sensory transduction has been a major focus in the field of sensory biology for many years, yet, the proteins that form sensory transduction channels required for hearing and balance have not been definitively identified. TMC1 and TMC2 have been proposed as possible pore-forming subunits, but the pore region itself has not been identified.

Methods

We generated 17 unique cysteine substitutions in TMC1 and packaged the coding sequences into AAV2/1 vectors. The vectors were injected into the inner ears of P1 mice that lacked expression of endogenous *Tmc1* and *Tmc2*. Injected ears were dissected at P7 and the organs of Corti were cultured for an additional 8 to 10 days. We used the rapid hair bundle deflections and the whole-cell, tight-seal technique to record sensory transduction currents from 566 inner hair cells. We applied four different cysteine modification reagents (methanethiosulfonate: MTS) in native mouse sensory hair cells.

Results

We identified thirteen TMC1 residues that altered the biophysical properties of hair cell mechanosensory transduction. Five residues were rapidly modified by MTS reagents to confer changes in whole-cell current amplitudes, three sites caused changes in single-channel current amplitudes and eleven sites altered calcium selectivity, and cysteine substitution at one site blocked current almost entirely.

Conclusions

The data support a revised TMC1 topology with ten transmembrane domains and identify four TMC1 transmembrane domains that line the permeation pathway of mechanosensory transduction channels in mammalian auditory and vestibular hair cells. We conclude TMC1 is a major pore-forming subunit of the hair cell sensory transduction channel.

PD 100

An Uncharacterized Motif within the N-Terminus of Mouse TMC1 Contributes to ER Retention in Heterologous Cell Line

David Soler¹; Manikandan Mayakannan²; Suhasini R. Gopal²; Andrew Sloan¹; Thomas McCormick³; Ruben

Stepanyan²

¹*The Department of Neurosurgery & the Brain Tumor and Neuro-Oncology Center, University Hospitals Cleveland Medical Center and the Case Comprehensive Cancer Center*; ²*Department of Otolaryngology, University Hospitals Cleveland Medical Center, School of Medicine, Case Western Reserve University*; ³*The Department of Dermatology & The Murdough Family Center for Psoriasis, University Hospitals Cleveland Medical Center, School of Medicine, Case Western Reserve University*

Hair cell mechanotransduction, which converts sound-evoked mechanical stimuli into electrical signals, lies at the heart of sound detection in vertebrates. Considerable effort has been put forth to identify proteins that comprise the hair cell mechanotransduction apparatus. TMC1, a member of the transmembrane channel-like (TMC) family, emerged recently as a key protein expected to form a mechanotransduction channel in the hair cells. However, the inability of TMC1 to traffic through the endoplasmic reticulum in heterologous cellular systems has hindered efforts to characterize its function and fully identify its role in mechanotransduction. We developed a novel approach that allowed for identification of uncharacterized retention signals within the intracellular region of a membrane protein of interest. We took advantage of the ability of Aquaporin 3 (AQP3) to unequivocally display intense plasma membrane staining in HEK293 cells with very little fluorescence from internal membranes when C-terminally tagged with GFP. We then used this construct as a fluorescent reporter, in order to identify possible novel ER retention signals located at TMC1 N-terminus. The fusion protein, comprising of 183 amino acid N-terminus of mouse TMC1 and AQP3-GFP, displayed an ER-like localization pattern. Moreover, we were able to pinpoint that the N-terminus of TMC1 contains an uncharacterized ER retention motif between amino acids 138-168, which precludes the AQP3-GFP from trafficking to the plasma membrane; the resulting reticular pattern is reminiscent of TMC1 localization in heterologous cells. In addition, this ER retention motif leads to a significant decrease in AQP3-GFP reporter intensity, suggesting that it may function as a degron. Using this approach, we additionally detected the presence of a novel Golgi localization signal positioned between amino acids 93-137, which unlike the ER retention signal, does not preclude plasma membrane localization of AQP3. In conclusion, we have successfully applied AQP3-GFP based constructs to effectively identify novel intracellular retention signals in the N-terminus of mouse TMC1. These signals are dissimilar to any known ER/Golgi retention motifs and they may perturb the proper trafficking of TMC1 to the plasma membrane in heterologous cells.

Supported by NIDCD grant DC015016 (R.S.) and by the Center for Clinical Research and Technology at University Hospitals Cleveland Medical Center (R.S.)

PD 101

Stereocilia Tip Complexes Depend on Transduction and PCDH15 for Differential Localization

Jocelyn F. Krey¹; Paroma Chatterjee¹; Jonathan Bird²; Peter G. Barr-Gillespie¹

¹Oregon Health & Science University; ²Dept of Pharmacology and Therapeutics, University of Florida

Hair bundles of inner hair cells (IHCs) have a unique architecture essential for mechanotransduction. Stereocilia are tall and thick in row 1 (the tallest), have intermediate height and are thick in row 2, and are short and thin in row 3. Recent evidence suggests that row 1 stereocilia have a complex of GPSM2, GNAI3, WHRN, MYO15A isoform 2 (MYO15A-S), and EPS8 at their tips. By contrast, MYO15A isoform 1 (MYO15A-L), EPS8L2, TWF2, CAPZB, and other proteins are localized to row 2 and 3 tips. Here we used mutant mice to examine the role of transduction and stereocilia links on the development of IHC bundles and how row 1 and 2 complexes are formed. In apical IHCs of wild-type mice, row 1 stereocilia grew continuously in height between postnatal day 0.5 (P0.5) and P7.5. By contrast, row 2 stereocilia grew until P0.5, then shrank by P4.5, showing that heights of the two rows were differentially controlled. Homozygous *Pcdh15(av3J)* mutants, which lack tip-links, had altered bundle shape and variable stereocilia height within rows at P7-P9. Bundles of *Tmc1;Tmc2* double knockout (*Tmc* DKO) mice, which lack mechanotransduction and Ca(2+) entry but maintain tip links, had four or more rows of stereocilia of reduced but near-uniform diameter and much shorter staircase spacing than in WT at P7-P9. Mice mutant for *Tmie*, which also lack transduction while maintaining tip links, had a bundle phenotype identical to that of *Tmc* DKOs. In both *av3J* and transduction mutants, the row 1 proteins MYO15A-S and EPS8 redistributed to all stereocilia tips, but in different relative proportions. In *av3J* bundles, both row 1 and the shorter rows all contained similar, high amounts of EPS8/MYO15A-S at their tips, whereas in transduction mutants, EPS8/MYO15A-S remained more abundant in the tallest row than in other rows. Row 2 complex proteins, including EPS8L2 and MYO15A-L, localized to both row 1 and 2 tips in *av3J* and transduction mutants; MYO15A-L puncta were reduced in intensity in all mutants and exhibited variable presence at tips. Our results suggest that both transduction and PCDH15 help generate the unique molecular identity and morphology of rows 2 and 3. In wild-type bundles, transduction and PCDH15 prevent row 1 proteins from accumulating in shorter mechanotransducing rows, and help stabilize

row 2 proteins in those rows. Distinct complexes of proteins in rows 1 and 2 may then allow row 1 stereocilia to continue to elongate while row 2 stereocilia shorten.

PD 102

The Dynamic Strength of the Tip-Link Bond in Hair Cells

Eric M. Mulhall¹; Darren Yang²; Andrew Ward²; David P. Corey³; Wesley P. Wong²

¹Department of Neurobiology, Harvard Medical School; ²Program in Cellular and Molecular Medicine, Boston Children's Hospital; ³Harvard Medical School, Department of Neurobiology

The tip link is a critical component of the mechanotransduction complex in vertebrate hair cells, which converts vestibular and auditory mechanical stimuli into an electrical signal by gating a transduction channel at its base. The tetrameric tip link is composed of parallel dimers of PCDH15 and CDH23, bonded in trans at their N-termini through a unique handshake interface, the structure of which has been resolved by X-ray crystallography (Sotomayor et al., 2012). Electron microscopy and structural studies show that each protein of the tip link likely exists as a parallel dimer (Kachar et al., 2000; Dionne et al., 2018). How strong is the tip link bond? How can just two bonds faithfully maintain the tip link over long times? Could sufficiently loud noise break the bond?

We used single-molecule dynamic force spectroscopy to measure the force-dependent kinetics of the tip-link bond and the response to force of the tip-link structure itself. We first created fusion proteins containing a single N-terminal binding domain of mouse CDH23 and PCDH15. Individually attached through DNA tethers to beads, the CDH23 and PCDH15 N-terminal constructs were allowed to bind. The antiparallel dimer bond was then assayed for mechanical strength on a new, ultra-passivated optical tweezer system. We find that—compared with classical cadherins such as E-cadherin—tip link cadherins have several novel and distinguishing biophysical characteristics.

We also measured the force-dependent kinetics of the native tetrameric tip link using fusion proteins that contained full length extracellular domains fused to antibody Fc domains for dimerization. We find that when one of the two CDH23-PCDH15 pairs of the tetrameric complex unbinds, it is able to re-bind quickly enough to ensure that the complex as a whole remains stable, greatly enhancing its lifetime. This phenomenon occurs at low forces, but at high forces the effect is diminished and the strength of the tetramer is only twice that of the dimer. The tip link can thus act as a mechanical circuit breaker for large forces. We show how low Ca²⁺ or deafness mutations in the bond interface destabilize the link. Overall, the tip link acts as both a faithful transducer of mechanical stimuli at

physiologically relevant forces, but also as a mechanical circuit breaker at damaging forces.

PD 103

Mechanical relaxation of the hair bundle is not correlated with Ca²⁺-dependent slow adaptation

Giusy A Caprara; Andrew Mecca; Anthony Peng
University of Colorado Anschutz Medical Campus

Hair cells of the inner ear are mechanosensory cells that transduce mechanical forces arising from sound waves and head movement to provide our senses of hearing and balance. Sound deflects the hair bundle, a crosslinked cluster of stereocilia on the apical surface of a hair cell, causing the opening of mechanically sensitive ion channels to start the mechanotransduction process. The mechanotransduction complex is built around the tip-link, an extracellular filament that connects the top of the shorter stereocilia with the side of the next taller row. One important property of the kinetics of mechanotransduction currents is a decline in current during a sustained displacement stimulus, a process called adaptation. Adaptation can be divided into multiple different components. The mechanism underlying Ca²⁺-dependent slow (motor) adaptation is documented in non-mammalian and low frequencies hair cells and resulted in the motor model of adaptation. In the model, myosin motors climb along the sides of stereocilia to generate resting tension in the tip-link. Upon stimulation of the hair bundle, Ca²⁺ influx through mechanotransduction channels cause unconventional myosin 1C to release tension by sliding down the sides of the stereocilia, thus causing mechanotransduction channels to close (Holt, et al., 2002; Howard & Hudspeth, 1987). A key to this climbing and slipping model was the mechanical relaxation that correlated with observed slow adaptation during displacement of the hair bundle with a flexible fiber (Howard & Hudspeth, 1987). This correlation has not been rigorously tested. Using rat and gerbil auditory and vestibular hair cells, high-speed imaging, and pharmacology, we tested the correlation between Ca²⁺-dependent adaptation and mechanical relaxation of the bundle when using a fluid jet stimulation. Our results show that myosin motors are important for Ca²⁺-dependent slow adaptation, but the mechanical relaxation of the bundle is not correlated with the amount of the adaptation in cochlear hair cells. To better control how force is delivered to a hair bundle, we also investigated vestibular hair cells using a flexible fiber to stimulate the hair bundle. Also in this case the mechanical relaxation of the bundle and the adaptation were not linked. Our results show that the motor model unlikely is the molecular mechanism behind the Ca²⁺-dependent adaptation, and we require a new model of slow adaptation in hair cells.

PD 104

Targeted deletion of synaptosomal-associated protein 25 (SNAP-25) impairs synaptic function of auditory inner hair cells

Charlotte Calvet¹; Ghizlene Lahlou¹; Margot Tertrais²; Nicolas Michalski³; Céline Trébeau³; Sylvie Nouaille³; Andrea Lelli⁴; Jacques Boutet de Monvel²; Paul Avan⁵; Vincent Michel²; Christine Petit⁴; Didier Dulon⁶; Saaid Safieddine²

¹UPMC; ²INSERM UMRS 1120; ³Institut Pasteur;

⁴Génétique et Physiologie de l'Audition, Institut Pasteur; ⁵University of Auvergne; ⁶University of Bordeaux

The synapses of auditory hair cells, the inner hair cell (IHC), have unique morphological, molecular and physiological characteristics. They are ribbon synapses capable of releasing glutamate at high rates and with a high degree of temporal precision over several minutes. Despite their striking structural differences, IHC synapses share with conventional CNS synapses several fundamental mechanisms of regulated synaptic vesicle exocytosis. Transduction of the sound stimulus into an electrical signal occurs when the IHC depolarizes, resulting in rapid calcium influx at the active zone and binding of Ca²⁺ ions to otoferlin, the calcium sensor, thereby triggering the fusion of synaptic vesicles with the presynaptic plasma membrane. In addition, IHC synapses are equipped with the presynaptic scaffold proteins piccolo, bassoon and RIM, and they also share with CNS synapses most of the SNARE proteins involved in synaptic vesicular trafficking and membrane fusion, including syntaxin, SNAP25 and VAMP. Although the presence of the neuronal SNARE transcripts in IHCs is well documented, the expression of their corresponding proteins remains controversial. In particular it has been reported that the lack of SNAP-25 has little or no effect on IHC synaptic exocytosis probed in organotypic culture of organs of Corti (Nouvian et al., 2011). This led to a surprising conclusion suggesting that IHC may operate without neuronal SNAREs. The knockout of SNAP-25 in mice results in embryonic lethality in the homozygote mutants, whereas the heterozygote mice show normal phenotype. This has prevented so far to address the consequences of SNAP-25 dysfunction in the function of mature IHC ribbon synapses, and its possible downstream effects on the development of afferent auditory neurons. Here, we developed a conditional SNAP-25 knockout to address these questions. We found that mice whose IHCs lack SNAP25 are viable and profoundly deaf with normal DPOAEs, indicating normal function of outer hair cells. The results suggest that deafness in these mice is due to a failure of the IHC synapse, and/or of its afferent synaptic contacts.

Acknowledgements:

This work was supported by the French government funds managed by *Agence Nationale de la Recherche*.

Age-Related Hearing Loss in Animals

PS 818

Effect of Atorvastatin on Age-related Hearing Loss: an Animal Model Study

Oak-Sung Choo¹; Yeong Chul Kim¹; Yun yeong Lee¹; Seong Jun Choi²; Yun-Hoon Choung¹

¹*Department of Otolaryngology, Ajou University School of Medicine;* ²*Department of Otorhinolaryngology-Head and Neck Surgery, Soonchunhyang University School of Medicine*

Background: Age-related hearing loss brings out difficulties in communication, decreased quality of life, isolation, loneliness, and frustration. Elderly people with hearing loss are more likely to have cognitive decline and impairment. Treatment for hearing preservation is limited and drugs are not developed yet. Among candidate drugs for hearing preservation, the action of atorvastatin in hearing loss is still under debate. Up to date, atorvastatin has been reported to prevent noise-induced hearing loss and delay the deterioration of inner ear function in aging. Opposing theories have also been proposed such as the cause for irreversible hearing loss and increase in blood glucose. Thus, the aim of this study was to investigate the effect of atorvastatin in age-related hearing loss (AHL) using C57BL/6J mice.

Materials and Methods: 6 months old C57BL/6J mice were classified into six groups; candidate drug A (atorvastatin) dosage #1, atorvastatin dosage #2, candidate drug B, combination of atorvastatin dosage #1 and candidate drug B, combination of atorvastatin dosage #2 and candidate B, and control group. All candidate drugs were injected via oral gavage 5 days a week for a total of 6 months. ABR thresholds were measured before the study, after 3 months, and after 6 months of the study. We also analyzed the 1) body weight, 2) Blood tests including clinical chemistry 3) ABR (8, 16, 32 kHz), and 4) histology (H&E). The mechanism studies were used for HEI-OC1 cells.

Results: By the end of the study, the mice were 12-months-old, and ABR results showed increase of ABR threshold in all groups. However, we were able to observe the preservation of hearing in atorvastatin dosage #1 compared to the control group in all frequencies. Blood test results proved that none of the candidate drugs showed any signs of toxicity including the kidney, liver, and the heart. Furthermore, all blood test results were within the

normal reference intervals for C57BL/6J mouse model.

Conclusions: We believe that the atorvastatin may have high potential for hearing preservation in AHL. Further studies will be relevant to prove the effect of atorvastatin in AHL, other than its originally known effect, with more knowledge of its mechanisms and targets.

PS 819

Electrocorticographic Measures in the Auditory Cortex of Aging Mice

Jeffrey Rumschlag; Khaleel A. Razak
UC Riverside

Background

As humans age, auditory temporal processing declines, resulting in communication deficits. Translational biomarkers of auditory system deficits will allow for testing of pharmacological and/or behavioral interventions to improve auditory processing. Responses to auditory stimuli can be measured as electrical activity recorded from the surface of the cortex and can be compared across age. This study uses the FVB strain of mice as a model for normal auditory aging.

Responses to amplitude-modulated (AM) auditory stimuli, which rely on auditory temporal processing have been examined in relation to age in humans. We recorded the EEG responses of mice of different ages (3-, 6-, 12-, and 20 months-old) to AM noise, to examine altered temporal processing with age. Phase-amplitude coupling (PAC) describes how the phase of a low-frequency oscillation modulates the amplitude of a higher-frequency oscillation. Patterns of PAC are related to sensory processing, but if this changes with age is unclear. Therefore, we calculated PAC from EEG signals recorded from mice at different ages.

Methods

Baseline EEG activity and responses to auditory stimuli were recorded from mice at different ages. Baseline EEG power spectra were calculated by averaging the fast Fourier transform of 1-second time bins over the course of the recording. PAC was calculated over the course of the baseline recordings, separated into movement and non-movement conditions. The stimuli consisted of AM broadband noise, including a swept-frequency AM chirp. Responses to these stimuli were measured by calculating the inter-trial phase coherence (ITPC). Group comparisons were made using a Monte Carlo cluster algorithm.

Results

Baseline EEG power shows a trending increase across frequencies with age. Phase-amplitude coupling (PAC) showed frequency-specific trending differences between

younger and older mice. For all age groups, during movement, PAC of low frequencies to high frequencies increased. The magnitude of this movement-related increase may be different in older mice.

Responses to the amplitude-modulated broadband noise chirp stimuli were more consistent, as indexed by higher ITPC, in 6mo mice compared to 3mo mice. The changes between responses of 6 and 12mo mice are frequency-specific, mimicking a change shown in aging humans.

Conclusions

The measures of baseline activity may show important differences in the way that auditory cortical activity changes with age. The results from this study suggest that the response to amplitude-modulated noise and phase amplitude coupling may be useful for examining the effects of age on auditory processing.

PS 820

The Erlong (erl) Mutation of Cadherin 23 Gene (Cdh23) Causes Early Onset of Sensory Cell Pathogenesis and Provokes Intense Immune Responses in the Cochlea

Bo Hua Hu¹; Celia Zhang¹; Weinan Du²; Qing Yin Zheng²

¹Center for Hearing and Deafness, State University of New York at Buffalo; ²Case Western Reserve University

Background

Age-related hearing loss allele (*ahl*) of *Cdh23* gene causes auditory dysfunction and sensory cell pathogenesis in the cochlea. Our previous study has shown that C57BL/6J mice display an increased immune activity in the cochlea as their age increases. Here, we report that a novel *Cdh23* mutation (*erlong*, *erl*) causes rapid progression of sensory cell pathogenesis, and this progression is accompanied by an enhanced immune cell activity in the cochlea.

Methods

Cdh23^{erl/erl} mice and wild-type mice were used in the current study. The animals were sacrificed at the age of 4, 6 or 8 weeks. The cochleae were collected for assessment of sensory cell pathogenesis and immune activities. The number of sensory cell loss was quantified using DAPI nuclear staining. Immune activities were assessed by examining immune cells, including macrophages and neutrophils, as well as by detecting immune cell expression of immune functional proteins, MHC-II and CD68. These immune profiles

were analyzed in multiple cochlear partitions including the scala tympani, the neural region of the osseous spiral lamina, the basilar membrane and the lateral wall.

Results

Cdh23^{erl/erl} mice displayed a rapid deterioration of cochlear function. Using the ABR thresholds measured at 4 weeks as the base-level, we found an average threshold shift of 25 dB at 8 weeks. Consistent with this functional loss, sensory cell loss started at 4 weeks, and rapidly progressed at 8 weeks. As compared with the cochleae harvested at 4 weeks, the cochleae collected at 8 weeks displayed a significant increase in the number of CD45-Iba1-positive cells in the regions of the basilar membrane, the osseous spiral lamina, and the luminal surface of the scala tympani. In addition, immune cells on the surface of the basilar membrane transformed from a branched shape to a rounded or amoeboid shape, a morphological sign of inflammatory activation. Cells with an amoeboid shape exhibited strong expression of CD68, an indication of inflammatory activation. MHC-II, an antigen presentation protein, is a marker of inflammatory activation. MHC-II positive cells were identified at 4 weeks in *Cdh23^{erl/erl}* mice. These cells were present in the lateral wall and in the neural region within the osseous spiral lamina. Their number further increased at 8 weeks.

Conclusions

The current study reveals an enhanced inflammatory activity in the cochleae of *Cdh23^{erl/erl}* mutant mice. This inflammatory activity is associated with the rapid progression of sensory cell pathogenesis.

PS 821

A Plausible Role of ATP-Purinergic Signaling in Age-Related Hearing Loss and Alzheimer's Disease

Hong-Bo Zhao; Yan Zhu; Shu Fang

Dept. of Otolaryngology, University of Kentucky Medical Center

Background: Alzheimer's disease (AD) is a neurodegenerative disorder characterized by a progressive loss of memory and cognitive decline. Hearing is an important neural-sensory input for central neural system and cognition. Hearing loss can reduce sensory input leading to cognitive decline. Noise exposure known to damage the cochlea can lead to more general cognitive dysfunction. Moreover, recent studies demonstrated that noise can induce irreversible degeneration of synapses between inner hair cells (IHCs) and auditory nerves leading to hidden hearing loss (HHL), which can eventually induce difficulty hearing and understanding. ATP-purinergic signaling

plays an important role in many aspects in the cochlear function and hearing. Our previous studies revealed that deficiency of ATP-gated P2X receptors can increase susceptibility to noise stress and may be associated with age-related hearing loss. In this study, we explored a role of ATP-purinergic receptors in age-related hearing loss and a possible link to AD.

Methods: P2X2 knockout (KO) mice and P2X7 KO mice were used. ABR threshold, DPOAE, and cochlear microphonics (CM) were recorded to assess cochlear and hearing function. The ribbon synapse degeneration was examined by immunofluorescent staining for CtBP2.

Results: In young ages, hearing function in P2X2 KO mice measured as ABR threshold had no significant difference in comparison with WT mice. As age increased, P2X2 KO mice demonstrated accelerated age-related hearing loss. Immunofluorescent staining showed that ribbon synapses were significantly reduced as age increased. In comparison with noise-exposed mice, aged mice had similar ribbon synapse reduction.

Conclusions: These data suggest that ATP-purinergic signaling may play a role in age-related hearing loss, possibly linking to AD.

Supported by NIH R01 DC 017025 and DC 017025-01S1

PS 822

Age-Related Alterations of Resident Macrophage Activity in Mouse and Human Cochlea

Kenyaria Noble; Ting Liu; Annemarie Lam; Bradley A. Schulte; Jeremy Barth; Hainan Lang
Medical University of South Carolina

Background: Age-related hearing loss (presbycusis) is one of the most common chronic disorders of the older adult population. Recent studies show that resident macrophages in the cochlea, undergo dramatic morphological changes in response to pathological conditions, though how these changes relate to immune response/signaling activity is not clear. Here we used transcriptomic analysis and 3D supra-confocal imaging to assess macrophage function in the cochlear lateral wall and auditory nerve of aged mice. Macrophage interactions with other cochlear cells also were examined in human temporal bones from older donors.

Methods: Young adult and aged CBA/CaJ and CX3CR1^{GFP} mice were used in the study. Auditory brainstem response was used to assess auditory function. Transcriptomic analysis (RNA-seq) was conducted on the cochlear lateral wall and auditory nerve

of young adult and aged mice. Enrichment analysis of differentially expressed genes was performed with the MetaAnalysis function in IPATHWAY (Advaita Bio) and ToppFunn (ToppGene Suite). Macrophage morphology and cell-cell interactions were examined by quantitative 3D supra-resolution confocal microscopy using markers of macrophage activation (Iba-1, CD68, Isolectin-B4) for mouse and human temporal bone.

Results: Transcriptomic analysis confirmed that immune response was enhanced in the cochlear lateral wall and auditory nerve of aged mice. This included upregulation of mRNAs associated with macrophage identity (including *Emr1*, *Itgam*, *Cx3cr1*) and activation (*Aif1*, *CD68*, *Fcer1g*). Among innate immune response genes, 19 were regulated in the auditory nerve and 26 in the lateral wall (log FC > 1.5, adjusted p-value < 0.05), with 6 genes in common. Macrophage morphologies in the aged mouse cochlea were consistent with activation, displaying rounding and reduced cellular projections. CD68⁺ macrophages were observed in the stria vascularis and spiral ligament. Isolectin-B4 binding, an indicator of immune cell activation, was observed in both the lateral wall and auditory nerve. Macrophage numbers were increased in the aged CX3CR1^{GFP} auditory nerve. In temporal bones of older humans, numerous Iba1⁺ macrophages with rounded morphology were detected in areas of cellular degeneration. Auditory nerve macrophages often localized with axons of neuronal cells while lateral wall macrophages were often present near micro-vessels.

Conclusions: Our data suggests that enhancement of the innate inflammatory response is a significant pathological component of the ageing process in the cochlear auditory nerve and lateral wall. Currently, we are assessing the pro-inflammatory or anti-inflammatory phenotype of macrophages in these two cochlear sub-regions to determine how abnormal immune cell signaling contributes to degeneration of the aged cochlea and presbycusis.

PS 823

IGF-1 Delayed Age-Related Hearing Loss in DBA/2J Mice

Desislava Skerleva¹; Fukuichiro Iguchi¹; Tatsuya Katsuno¹; Hiroe Ohnishi²; Tomoko Kita²; Norio Yamamoto²; Juichi Ito³; Koichi Omori²; Takayuki Nakagawa²

¹Department of Otolaryngology-Head and Neck Surgery, Graduate School of Medicine, Kyoto University; ²Department of Otolaryngology-Head and Neck Surgery, Graduate School of Medicine, Kyoto University; ³Shiga Medical Center Research Institute

Objective

Previously, we have reported the therapeutic potential of recombinant human (rh) IGF-1, Mecasermin, for the treatment of sensorineural hearing loss (SNHL) with acute onset in animal models and patients with sudden SNHL. In animal models, rhIGF-1 exhibited protection of cochleae against excessive noise, ischemia, aminoglycosides or CI electrode insertion by protection of sensory hair cells and regeneration of afferent synapses. Here, we examined the potential of rhIGF-1 for attenuation of early-onset progressive hearing loss in DBA/2J mice.

Materials and Methods

To reveal the time course of age-related hearing loss in DBA/2J mice (n = 30), we performed ABR and DPOAE at ages of 3, 4, 6 and 8 weeks, followed by histological assessments. We determined the timing for local application of rhIGF-1 as 4 weeks of age, when the progressive hearing loss was initiated without massive loss of hair cells. A piece of gelatin hydrogel soaked with rhIGF-1 was applied on the round window membrane of the left ear of each animal, while the right ear was preserved without any surgical treatment. Functional analysis was done before and at day 14, day 21 and day 28 after surgery. On day 28, the experimental animals were sacrificed for histological estimations. Immunohistochemistry for myosin VIIa, CtBP2 and GluA2 was employed for quantitative assessments of hair cells and ribbon synapses.

Results

Four-week-old DBA/2J mice were selected for the lowest ABR thresholds, highest DPOAE amplitudes, and preservation of OHC and IHC that were observed in comparison with the other ages. ABR threshold shifts were significantly lower in rhIGF-1-treated ears at 25 kHz and 32 kHz at day 28 after the surgery (Two-way ANOVA, $p < 0,05$). DPOAE showed significant elevation at 32 kHz in rhIGF-1 treated ears at day 21. Wave I amplitude exhibited significant reduction in control ears at 25 kHz and 32 kHz at day 14 and day 21 (Two-way ANOVA, $p < 0,05$). Histological analysis showed significant preservation of the outer hair cells (Paired t-test, $p < 0,05$) and ribbon synapses (Paired t-test, $p < 0,0001$) only in the basal region of the cochlea.

Conclusion

rhIGF-1 already showed its safety in the clinical local application for sudden SNHL. Our data confirmed partial delay of hearing loss and preservation of OHC and ribbon synapses after rhIGF-1 treatment, therefore, it might be of great value for clinical application in the progressive hearing loss.

Acknowledgments

This work was supported by KAKENHI (Grants-in-Aid for Scientific Research (C) (26462557 and 17k11325).

PS 824

Differences in rates of hearing loss by female and male CBA/CaJ mice (*Mus musculus*) for pure tones varying in duration

Anastasiya Kobrina; Micheal L. Dent
University at Buffalo, SUNY

Mice are frequently used to study and model age-related hearing loss (ARHL) due to similarities in the human and mouse cochleae and in genetic makeup. Mice emit ultrasonic vocalizations (USVs) that may be used for communication purposes, similar to speech in humans. Previous electrophysiological research showed that the CBA/CaJ mouse strain is an appropriate model for late-onset hearing loss. These mice exhibit sex differences in auditory brainstem responses (ABRs) for pure tones between 12 and 15 months of age, with males showing higher ABR thresholds than females (Henry, 2004, *Hearing Research*). Mice also exhibit ARHL for detection of USVs and pure tones when measured using behavioral methods, however, much later in life than previously estimated by electrophysiological methods (Kobrina and Dent, 2016, *Hearing Research*). In addition, mice showed hearing loss differences between the sexes for USVs but not for 42 kHz tones, contradicting previous physiological studies. The goal of the current research was to use operant conditioning procedures to measure aging audiograms and temporal summation functions in CBA/CaJ mice. In order to reach this goal, 62 adult CBA/CaJ mice were trained and tested using an accelerated longitudinal study design. Mice were trained on a detection task using operant conditioning procedures with positive reinforcement. Aging audiograms were constructed using thresholds for 8, 16, 24, 42, and 64 kHz pure tones. Temporal summation functions were constructed for 16 and 64 kHz pure tones ranging from 20 to 800 ms in duration. The results revealed that mice retain pure tone hearing late into their lifespan, with high frequency hearing loss preceding low frequency hearing loss. Similarly to humans, mice benefit from pure-tone duration increases across lifespan, however this benefit decreases with age. Generally, male mice lose hearing at a faster rate than females. CBA/CaJ mice lose hearing for pure tones varying in duration in a manner that parallels humans. These results highlight the importance of measuring hearing in awake, trained, behaving subjects when comparing ARHL across different species. This work was supported by F31 DC016545 and R01 DC012302

Age-related Hearing Loss is Associated with an Imbalance Between Excitation and Inhibition in the Cochlea and Brainstem

Katrina M. Schrode¹; Hamad Javaid²; James H. Engel¹; Amanda Lauer²

¹Johns Hopkins University School of Medicine; ²Johns Hopkins University

The auditory system processes acoustic stimuli through a combination of excitatory and inhibitory processes. In the cochlea, ribbon synapses provide excitatory drive from hair cells to spiral ganglion neurons, while efferent synapses from olivocochlear neurons serve a primarily inhibitory function. The ventral cochlear nucleus (VCN) receives excitation primarily from the auditory nerve and secondary sources. At least five sources of inhibition shape these responses, including inhibitory interneurons, ipsilateral dorsal cochlear nucleus, superior olivary nuclei, and cortex. Previous studies have separately identified age-related auditory nerve damage and loss of central inhibition. The current study investigated how excitatory and inhibitory pathways in the cochlea and cochlear nucleus are concurrently altered by age-related hearing loss. We aged adult CBA/CaJ mice to at least 20 months. We measured auditory brainstem responses (ABRs) to assess auditory sensitivity and synchrony in auditory nerve/brainstem pathways. From these mice, we harvested cochleas and brains for immunohistochemistry. In the cochleas, we labeled afferent or efferent synapses with antibodies against c-terminal binding protein 2 or synaptic vesicle protein 2, respectively. We also labeled hair cells with a myosin 6 antibody. We labeled brain sections with anti-vesicular glutamate transporter 1 (VGLUT1) or anti-glutamic acid decarboxylase 65 (GAD65) to identify excitatory or inhibitory synapses, respectively. ABR thresholds were moderately increased in animals over 20 months of age compared to young adult animals (~10 week old). Outer hair cells and the occasional inner hair cell were missing at many frequencies in the older animals; we quantified synapses on those hair cells that remained. Older animals had about half as many ribbon synapses inner hair cells as young adults, but the total area of labeled efferent synapses in the inner hair cell region was slightly increased in older animals. Outer hair cells had fewer, but larger, efferent synapses in old mice compared to young adults. VGLUT1 labeling in the VCN was slightly decreased in old mice compared to young, while GAD65 labeling was approximately halved. Transmission electron microscopy confirmed synaptic degeneration in the VCN of old animals. These significant changes in the anatomy of the aging auditory system signify an imbalance in excitation and inhibition in both the cochlea and brainstem. This imbalance likely contributes to hearing in noise and temporal processing deficits in

addition to age-related loss of sensitivity. Furthermore, increased efferent innervation with age may exacerbate the loss of sensitivity by reducing cochlear activity to a greater than normal extent.

PS 826

Autophagic Gene Expression Changes in the Mouse Cochlea Associated with Age-Related Hearing Loss

Lauren R. Paganella¹; Bo Ding²; Xiaoxia Zhu³; Jennifer A. Pineros³; Robert D. Frisina³

¹Chemical and Biomedical Engineering Dept., Global Center for Hearing and Speech Research, University of South Florida - Tampa; ²Communications Sciences and Disorders Dept., Global Center for Hearing & Speech Research, University of South Florida; ³Medical Engineering Dept., Global Center for Hearing & Speech Research, University of South Florida

BACKGROUND: Age related hearing loss (ARHL), also known as presbycusis, is the most common type of hearing loss affecting the elderly, for which no treatments currently exist. Autophagy, a cellular process that maintains homeostatic energy levels, degrades organelles, and recycles nutrients, is disrupted with age in some physiological systems. However, it is not clear how autophagy is involved in ARHL. Therefore, our goal in this study was to identify any significant expression changes in cochlear autophagic pathway biomarkers through the screening of gene expression banks that include autophagic pathway genes.

METHODS: Nine young adult (4-5 month, 4 female, 5 male), eighteen middle-aged (10-15 month, 10 female, 8 male), and fifteen old (21.5-34 month, 8 female, 7 male) CBA/CaJ mice were used. Mice were separated into four groups according to age and degree of hearing loss. Auditory brainstem responses (ABRs) and distortion product otoacoustic emission (DPOAE) amplitudes and thresholds were tested. GeneChip data (Affymetrix) were extracted from cochlea tissue samples and transcriptional expression patterns of 414 autophagy-related genes were subjected to one-way ANOVA analysis using GraphPad Prism. Linear regression and correlation tests were used to confirm relations between genotype and phenotype. Candidate genes for screening were selected from the Human Autophagy Database and other autophagy databases.

RESULTS: Our study identified 42 probes (37 genes) with significant expressional changes correlating with aging. Among these, 30 probes (26 genes) showed correlation with the ABR and DPOAE auditory measurements. Unc-51 like kinase 2 (ULK2) and BCL2 interacting protein 3 like (BNIP3L), which are genes

associated with the initiation and nucleation steps of autophagy, show *decreased* gene expression with age and correlate with ABR and DPOAE thresholds. BNIP3L is important for the activation and phosphorylation of the BECLIN1 complex. Interestingly, the gene expressions of protein high chain 3 (LC3), frequently used markers to assess autophagy during elongation, also declined with age. We also found that there was an age-related dynamic change of LC3 protein expression in our *in vivo* cochlea samples, indicating additional mechanisms of post-transcriptional modification.

CONCLUSION: Focusing on the strategy of preventatives or treatments for the initiation, nucleation, and elongation steps of autophagy could utilize interventions for preventing or treating key aspects of ARHL. Future experiments will utilize proteomics to determine the role of functional proteins related to autophagic pathways and identification of post-translational protein changes in cochlear ARHL.

Work supported by NIH grant P01 AG009524 from the Nat. Inst. on Aging.

PS 827

Role of Mitochondrial Thioredoxin in Cochlear Antioxidant Defense and Aging

Mi-Jung Kim¹; Chul Han¹; Hyo-Jin Park¹; Karessa White¹; Dalian Ding²; Christina Rothenberger³; Emily Bui³; Kaitlyn Evans³; Isabela Caicedo¹; Upal Bose³; Paul Linser⁴; Richard Salvi⁵; Shinichi Someya⁶
¹University of Florida, Department of Aging and Geriatric Research; ²Center for Hearing and Deafness, State University of New York at Buffalo; ³University of Florida; ⁴University of Florida, Whitney Lab; ⁵University at Buffalo; ⁶Aging and Geriatric Research

Backgrounds: The mitochondrial thioredoxin 2 (TXN2) system is one of the major antioxidant defense systems in mitochondria. There are three major players in the TXN2 system: thioredoxin 2 (TXN2), thioredoxin reductase 2 (TXNRD2), and peroxiredoxin 3 (PRDX3). In mitochondria, NADPH-dependent TXNRD2 catalyzes the reduction of oxidized TXN2 (TXN2_{oxi}) to regenerate reduced TXN2 (TXN2_{red}). Subsequently, TXN2 catalyzes the reduction of oxidized PRDX3 (PRDX3_{oxi}) to regenerate reduced PRDX3 (PRDX3_{red}) which plays a role in the removal of hydrogen peroxide (H₂O₂) in cells. In the current study, we investigated the roles of Txn2 in cochlear antioxidant defense and aging using wild-type (Txn2^{+/+}) and Txn2 heterozygous knockout (Txn2^{+/-}) mice that have been backcrossed onto the CBA/CaJ strain for 4 generations.

Methods: To investigate the role of Txn2 in cochlear aging, we performed auditory brainstem response

(ABR) hearing tests to measure ABR thresholds, wave I latencies, and wave I amplitudes in Txn2^{+/+} and Txn2^{+/-} mice at 5, 15 and 24 months of age. To confirm these physiological test results, we performed histological analyses to assess hair cell loss, spiral ganglion neuron density, and stria vascularis thickness in the cochlea from young and old Txn2^{+/+} and Txn2^{+/-} mice. To investigate the role of Txn2 in cochlear antioxidant defense, we measured antioxidant defense (activities of thioredoxin- and glutathione-related enzymes, catalase, and superoxide dismutase), mitochondrial function (mRNA levels of mitochondrial biogenesis markers and mitochondrial DNA copy numbers), and oxidative damage (levels of 8-oxoguanine and protein carbonyl) parameters in the inner ears from young Txn2^{+/+} and Txn2^{+/-} mice. To conform these *in vivo* test results, we performed oxidative stress tests followed by cell viability tests in the mouse HEI-OC1 cell lines transfected with scrambled siRNA (si-Con) and siRNA targeted to mouse Txn2 (si-Txn2).

Results: There were no differences in ABR thresholds at 4, 8, 16, 32, or 48 kHz between Txn2^{+/+} and Txn2^{+/-} mice at 5, 15, or 24 months of age. There were no differences in the numbers of hair cells between Txn2^{+/+} and Txn2^{+/-} mice at 5 or 24 months of age. Consistent with the physiological and histological test results, there were no differences in any of the mitochondrial function, oxidative damage, or antioxidant defense parameters in the inner ears between young Txn2^{+/+} and Txn2^{+/-} mice. Furthermore, Txn2 knockdown did not affect cell viability under oxidative stress conditions in the HEI-OC1 cell line.

Conclusions: These results show that mitochondrial thioredoxin is not essential for maintaining cochlear antioxidant defense under normal physiological conditions or during aging.

Funding: This study is supported by NIH/NIDCD grants R01 DC012552 (S.S.) and R01 DC014437 (S.S.).

PS 828

Ibuprofen Prevents Key Aspects of Age-Related Hearing Loss through Prestin Mechanisms in Outer Hair Cells of CBA/CaJ Mice

Parveen Bazard¹; Bo Ding²; Tanika T. Williamson³; Xiaoxia Zhu¹; Robert D. Frisina¹

¹Medical Engineering Dept., Global Center for Hearing & Speech Research, University of South Florida;

²Communications Sciences and Disorders Dept., Global Center for Hearing & Speech Research, University of South Florida; ³Medical Engineering Dept., Global Center for Hearing and Speech Research, University of South Florida

Introduction: Oto-acoustic emissions are sounds emitted by cochlear outer hair cells, (OHCs). OHCs are responsible for sound amplification and decline with age, as part of age-related hearing loss (ARHL). Here, we investigated the effects of ibuprofen; a frequently used clinical drug, on auditory functions in aging CBA/CaJ mice to understand possible roles of anti-inflammatory agents in prevention of presbycusis.

Methods: Physiological Experiments: 19 month old CBA mice were used, and fed chow feed containing ibuprofen (Envigo, Madison, WI; 375 ppm) for six months. Control mice were fed the same chow with no drug. Auditory brainstem responses (ABRs) and distortion-product otoacoustic emissions (DPOAEs) were recorded using TDT Biosig systems at different time points of the study: baseline, 2nd month, 4th month, 6th month.

Western Blot Experiments: The HEI-OC1 hair cell line was used for *in vitro* western blots. Cells were treated with different doses of ibuprofen for 24 hr, and/or salicylate, and analysed for prestin protein expression.

Results: At the start, DPOAEs amplitudes and thresholds, which measure OHCs functionality, were normal for both groups for their age. During the treatment period, DPOAEs amplitude levels were not changed for ibuprofen animals whereas there was a steady decline for controls. Similarly, DPOAEs thresholds were not changed over the treatment duration for ibuprofen animals, whereas the control group displayed a steady increase in thresholds due to ARHL. Interestingly, there were no significant differences in age-related ABR threshold changes between control and treatment groups, suggesting that ibuprofen may prevent OHCs aging effects versus other cochlear processes. Since prestin is the motor protein expressed in OHCs and required for OHC motility, we investigated the effects of ibuprofen on prestin levels *in vitro* with HEI-OC1 cells. Initial western blot experiments indicated that there was a dose dependent response in prestin levels, i.e., an increase in protein levels for low ibuprofen doses and decrease for high doses. Increases in prestin levels were observed for salicylate treatment as well. Future experiments will be focused on molecular studies with cell and animal tissue samples to better understand the cellular and molecular mechanisms involved in cochlear ibuprofen therapeutic treatments.

Summary: Since loss of hair cells in the aging ear occurs, and is a cellular mechanism of ARHL, our studies demonstrate the possible important role of ibuprofen in treatment of certain aspects of ARHL in aging mammals.

Supported by NIH grant P01-AG009524 from the National Inst. on Aging.

PS 829

P43 ROS-induced activation of DNA damage responses drives senescence-like state in post-mitotic cochlear cells: implication for hearing preservation

Corentin Affortit¹; Florence François¹; Bernard Malfroy-Camine³; Nesrine Benkafadar¹; Jean-Luc Puel²; **Jing Wang¹**

¹INSERM, University Montpellier; ²INM, Inserm, Univ Montpellier; ³MindSet Rx

Background - Introduction:

In our aging society, age-related hearing loss (ARHL) has become a major socio-economic issue. Reactive oxygen species (ROS) may be one of the main causal factors of age-related cochlear cell degeneration. We examined whether ROS-induced DNA damage response drives cochlear cell senescence and contributes to ARHL from cellular up to system level.

Methods:

Here, we examined the molecular basis responsible for ROS-induced cochlear cell damage from the cellular to the whole system. In addition, to identify a protective strategy that would be suitable for clinical use, we evaluated the efficiency of hearing preservation with systemic administration of EUK-207 a synthetic superoxide dismutase/catalase mimetic in adult senescence accelerated mouse prone 8 (SAMP8) mice.

Results:

Our results revealed that sub-lethal concentrations of hydrogen peroxide (H₂O₂)-exposure initiated a DNA damage response illustrated by increased γ H2AX and 53BP1 expression and foci formation mainly in sensory hair cells, together with increased levels of p-Chk2 and p53. Interestingly, post mitotic cochlear cells exposed to H₂O₂ displayed key hallmarks of senescent cells, including dramatically increased levels of p21, p38 and p-p38 expression, concomitant with decreased p19 and BubR1 expression and positive senescence-associated β -galactosidase labelling. Importantly, the synthetic superoxide dismutase/catalase mimetic EUK-207 attenuated H₂O₂-induced DNA damage and senescence phenotypes in cochlear cells *in vitro*. Furthermore, systemic administration of EUK-207 reduced age-related loss of hearing and hair cell degeneration in senescence accelerated mouse prone 8 (SAMP8) mice.

Conclusion:

Altogether, these findings highlight ROS-induced DNA damage responses drive cochlear cell senescence and contribute to accelerated ARHL. EUK-207 and likely other anti-oxidants with similar mechanisms of action could potentially postpone cochlear aging and prevent ARHL in humans.

Assessment of Mitochondrial DNA Mutations in the Cochleae of CBA/CaJ, C57BL/6 and Polg mutator mice

Shinichi Someya¹; Christina Rothenberger²; Emily Bui²; Upal Bose²; Kaitlyn Evans²; Elena Hoogland²; Lambert Lee²; Dalian Ding³; Richard Salvi⁴
¹*Aging and Geriatric Research*; ²*University of Florida*;
³*Center for Hearing and Deafness. State University of New York at Buffalo*; ⁴*University at Buffalo*

Backgrounds: Mutations in mitochondrial DNA (mtDNA) impair oxidative phosphorylation function and cause a variety of mitochondrial disorders. mtDNA mutations have also been implicated in age-related neurodegenerative diseases, including age-related hearing loss (AHL). The most common genetic defects observed in individuals with mtDNA diseases are point mutations or deletions in mtDNA. Up to now, more than 100 different mtDNA deletions have been identified in individuals with mtDNA diseases, including KSS (Kearns-Sayre syndrome), CPEO (chronic progressive external ophthalmoplegia), and Pearson syndrome. mtDNA depletion or reduced mtDNA copy number is also associated with respiratory chain dysfunction in the substantia nigra neurons of Parkinson's Disease patients. In the current study, we investigated the role of mtDNA deletions, point mutations and copy numbers in cochlear aging using CBA/CaJ, a model of late onset AHL, C57BL/6J, a model of early onset AHL, and *Polg* mutator mice, a model of premature aging.

Methods: We measured mtDNA deletion frequencies and mtDNA copy numbers in the inner ear tissues from male CBA/CaJ mice at 3-5 and 24-25 months of age, and C57BL/6J and *Polg* mutator mice at 3-5 and 15-18 months of age using the digital PCR-based method of the mtDNA deletion and copy number assays.

Results: CBA/CaJ mice displayed a 4-fold increase in mtDNA deletion frequencies in the inner ears compared to young CBA/CaJ mice, while middle-aged *Polg* mutator mice displayed a 13-fold increase in mtDNA deletion frequencies in the inner ears compared to age-matched WT mice. However, there were no differences in mtDNA deletion frequencies between young and middle-aged C57BL/6J mice. There were also no differences in mtDNA copy numbers in the inner ears between young and old CBA/CaJ mice, young and middle-aged C57BL/6 mice or young and middle-aged *Polg* mutator mice.

Conclusions: These results suggest that mtDNA deletions play a role in the development of late onset AHL in CBA/CaJ mice and early onset AHL in *Polg* mutator mice, but not in early onset AHL in C57BL/6 mice. In

addition, aging does not result in a reduction in mtDNA copy number in the inner ear of CBA/CaJ, C57BL/6 or *Polg* mutator mice.

Funding: This study is supported by NIH/NIDCD grants R01 DC012552 (S.S.) and R01 DC014437 (S.S.).

PS 831

Discrimination of Harmonic and Inharmonic Tone Complexes based on Temporal Fine Structure: a Comparison of Mongolian Gerbils with Normal and Compromised Cochlear Function

Henning Oetjen¹; Friederike Steenken¹; Christine Köppl²; Georg M. Klump³

¹*Cluster of Excellence Hearing4all, Dept. of Neuroscience, Carl von Ossietzky University*;

²*Department of Neuroscience, School of Medicine and Health Sciences, Carl von Ossietzky University Oldenburg*; ³*Cluster of Excellence Hearing4all, Department of Neuroscience, Carl von Ossietzky University*

Background

Several studies have reported perceptual difficulties in supra-threshold situations for listeners with normal auditory thresholds. One possible explanation for this so-called hidden hearing loss is a reduction in the number of auditory-nerve fibers (review by Liberman and Kujawa 2017, *Hear Res* 349: 138-147). It has been suggested that such a fiber loss results in a deficit in temporal processing (Moore 2014, *Auditory processing of temporal fine structure: Effects of age and hearing loss*, *World Scientific*). Moore and Sek (2009, *Int J Audiol* 48: 161-171) developed, for humans, the TFS1 test measuring the ability for discriminating harmonic and inharmonic tone complexes based on the temporal fine structure. Here we investigated the behavioral sensitivity of Mongolian gerbils with different degrees of cochlear dysfunction for discriminating harmonic and inharmonic tone complexes. Establishing a psychoacoustic animal model for the TFS1 test will provide a better understanding of the mechanisms underlying supra-threshold perception of temporal fine structure with hidden hearing loss.

Methods

We studied young (under 18 month) untreated gerbils, young gerbils that had either 40µM or 70µM ouabain briefly applied to the round window, inducing a synaptopathy, and old (over 36 month) gerbils with various degrees of age-related hearing loss. Gerbils were trained in a repeated background Go/No-Go procedure with food rewards to discriminate TFS1 stimuli, i.e., harmonic tone complexes from inharmonic tone complexes with the same fundamental frequency and component starting phase. Hit rate and false alarm rate were measured to calculate

the sensitivity d' ; and discrimination threshold (criterion $d' = 1$). Tone complexes with fundamental frequencies of 200 Hz and 400 Hz and center frequencies of 1600 Hz and 3200 Hz were used. A filter with a bandwidth that included 7 adjacent frequency components of the complex around the center frequency and with slopes of 30 dB/octave was applied. Pink noise was added to mask distortion products. The component tone level was 60 dB SPL and the stimulus duration was 0.4 s including 25 ms Hanning ramps.

Results and Conclusions:

Preliminary data demonstrate that gerbils are able to discriminate between harmonic and inharmonic tone complexes, similarly to humans. A comparison with normal hearing humans showed better discrimination thresholds for young normal hearing gerbils and poorer discrimination thresholds for old gerbils. In ouabain-treated gerbils, the sensitivity varied considerably, being on average lower than observed in young untreated gerbils.

Funded by the DFG, SPP 1608

PS 832

Mitochondrial fission and sequent mitophagy rescue HEI-OC1 from oxidative stress-induced cellular senescence

Hanqing Lin; Zhongwu Su; Jiaqi Pang; Hao Xiong; Yiqing Zheng
Sun Yat-sen Memorial Hospital, Sun Yat-sen University

Background: Mitochondria are dynamic organelles, which constantly go through fission and fusion to provide energy to all kinds of cellular activities. Mitochondrial fission has very much to do with mitochondrial function and the underlying molecular machinery involve dynamin-related protein1(DRP-1) in cellular senescence. However, the role of DRP-1 in cellular senescent model remains unclear. **Methods:** H₂O₂ treatment was to induce cellular senescence. Population doubling rate, CCK8 assay and senescence associated β -galactosidase stain were performed to evaluate cellular senescence. Genesilencing by siRNA, ATP assay, mtDNA assay, mitochondrial probe staining, Western blot and immunocytochemistry were performed to detect the dynamics of mitochondria and mitophagy in HEI-OC1 cells. **Results:** In this study, we found that oxidative stress induced mitochondrial fragmentation during induction cellular senescence by treatment of 1mM hydrogen peroxide(H₂O₂). Mitochondrial fission and sequent mitophagy were initiated but both levels decreased in a senescent HEI-OC1 cell model. Moreover, inhibition of DRP-1 by 50 μ M of mitochondrial division inhibitor-1(Mdivi-1) lowered the levels of fission and mitophagy thus enhanced oxidative

stress-induced senescence. **Conclusions:** Altogether, these results indicate that mitochondrial fission and mitophagy together eliminate dysfunction mitochondria and DRP-1 may be protective against oxidative stress-induced senescence by initiating mitochondrial fission and mitophagy to remove dysfunction mitochondria.

PS 833

Gene Expression and Auditory Physiology Analyses to Determine the Roles of Connexin 30 and 43 in Age-Related Hearing Loss

Jennifer A. Pineros¹; Xiaoxia Zhu¹; Bo Ding²; Parveen Bazard¹; Robert D. Frisina¹

¹Medical Engineering Dept., Global Center for Hearing & Speech Research, University of South Florida;

²Communications Sciences and Disorders Dept., Global Center for Hearing & Speech Research, University of South Florida

Introduction: Connexin proteins (Cx) are essential for formation of gap junctions, the intercellular pathways between cells; and Cx gene expression has been discovered in various cochlear regions. Mutations in Cx genes, such as Cx26 [FJR1] have been linked to human nonsyndromic deafness. However, no studies have been conducted on Cx's involvement in age-related hearing loss (ARHL). Also, the locations of Cx isoforms as matrix components in the cochlea are not identified. We analyzed age-associated changes and identified locations of Cx30 and Cx43 for future translational advances to treat ARHL.

Materials and Methods: CBA/CaJ mice (N=40) were classified into four groups according to age and degree of hearing loss, and an Affymetrix GeneChip equipped with transcriptional expression assessment for the mouse genome was used to measure gene expression. The results were analyzed with one-way ANOVA and linear regression. To confirm our GeneChip results, RT-qPCR was conducted for *in vitro* and *in vivo* samples. Furthermore, to test aging trends, an *in vivo* experiment with young (3 mon, n=4) and old (30 mon, n=4) samples was analyzed. Auditory brainstem response (ABR) and distortion product otoacoustic emissions (DPOAE) were recorded to measure hearing threshold changes.

Results and Discussion: All members of the Cx family were analyzed using GeneChip, but only Cx30 and Cx43 exhibited significant expressional changes with age. Moreover, both genes showed a correlation with ARHL hearing threshold changes. For our *in vitro* SV-K1 cell study, only Cx30 was detected using RT-qPCR, suggesting Cx30 but not Cx43 is expressed in the young adult stria vascularis (SV) and a trend of down-regulation with age is apparent for Cx 30. Since Cx43 is expressed in the cochlea *in vivo*, we hypothesize that expression of Cx43 is found in areas other than SV. Although only Cx30 and Cx43 gene

expressions were found to change with cochlear aging, age-related post-transcriptional modification of other members of the Cx family cannot be excluded. Therefore, proteomics and immunohistochemistry analysis are also underway to quantify the roles of the connexin family in ARHL.

Summary: Our study suggests a trend of down-regulation of Cx30 in the cochlea, with only Cx30 being detected in the SV cell line, while the location of Cx43 in the cochlea is not known precisely. Our long-term goal is to determine how aging affects the connexin family in different functional regions of the cochlea, and the impact on potential treatment options for ARHL.

Support: NIH grant P01 AG009524.

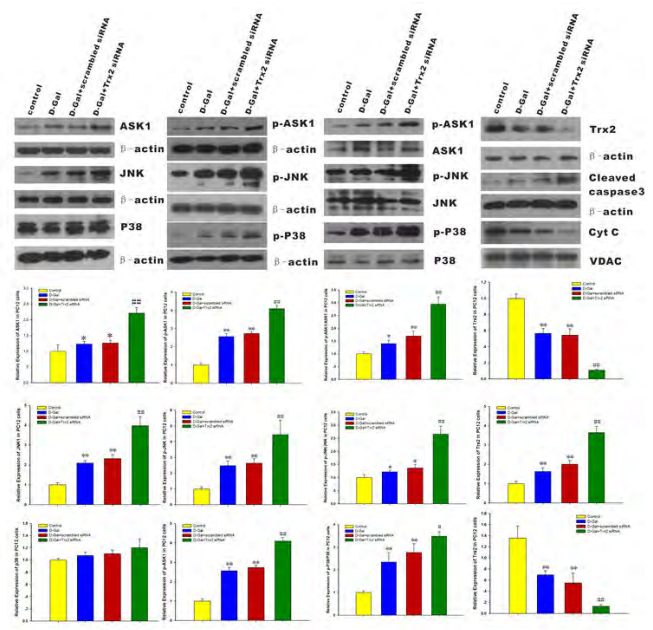
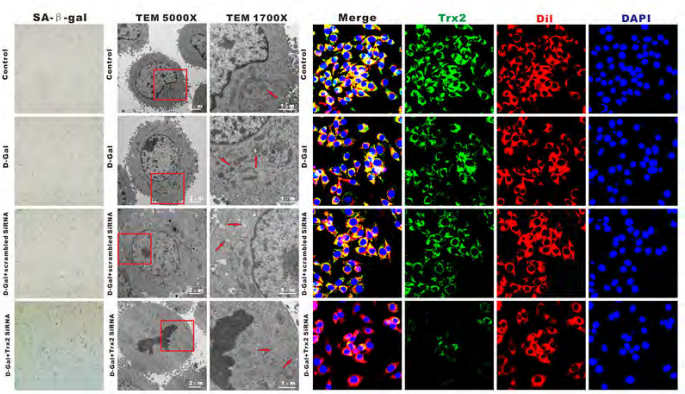
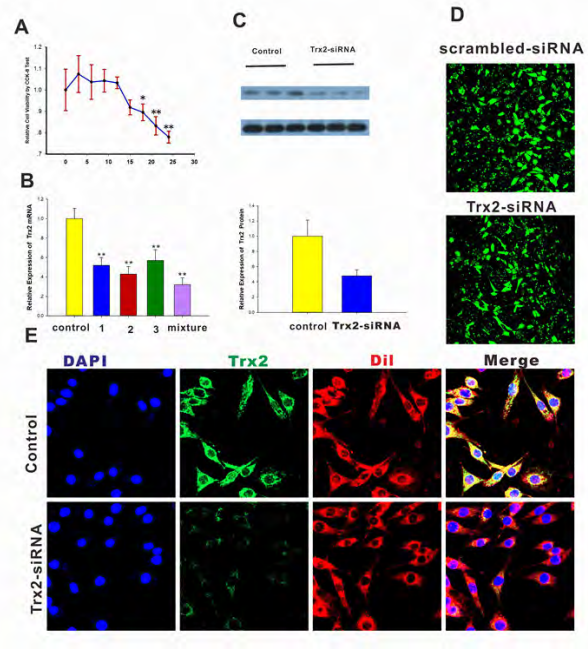
PS 834

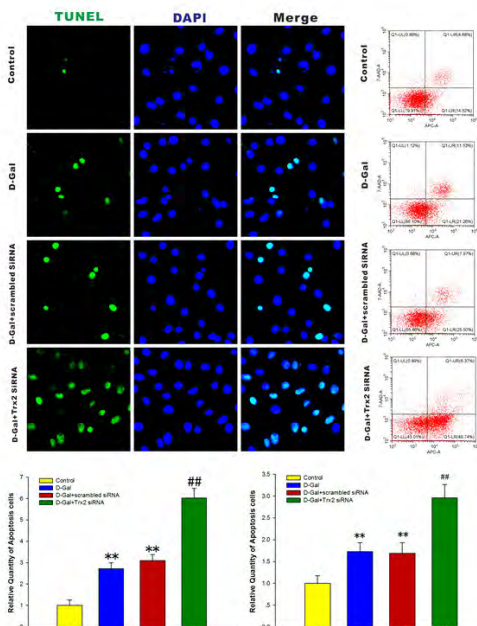
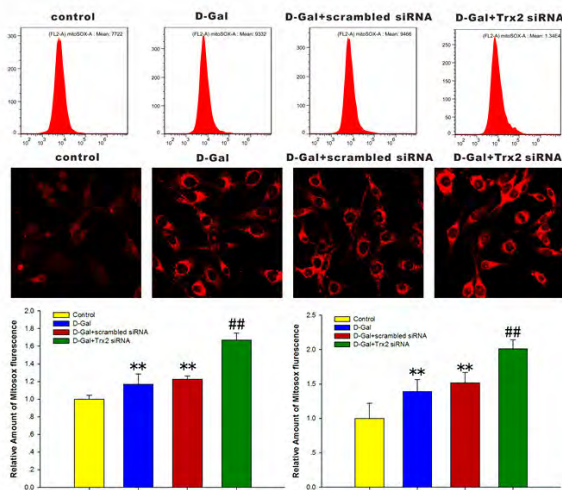
Decreasing of Trx2 Increases ROS Generation and Activates ASK1-JNK/p38 Apoptotic Signal Pathway in Auditory Cortex of the Mimetic Aging Rat Model.

Haiying Sun; Baoai Han; Yongqin Li; Jie Yuan
Otolaryngology Department, Union Hospital, Tongji Medical College, Huazhong University of Science and Technology

Central presbycusis, which refers to age-associated deterioration in the central auditory system, can impair sound localization as well as speech perception. Available evidence indicates that the mechanism of presbycusis involves oxidative stress and apoptosis. Thioredoxin2 (Trx2),

plays an important role in scavenging abnormal ROS and maintaining redox balance in the cell. Trx2 tightly controlling of Apoptosis signal-regulating kinase 1 (ASK1) is a major contributor in regulating apoptosis. To date, little is known about the function of Trx2 and ASK1, as well as its downstream c-Jun-NH (2)-terminal kinase (JNK) / p38 in the central presbycusis. Here, we explored the association between Trx2 mediated abnormal regulation of ASK1-JNK/P38 apoptosis signal pathway and central presbycusis by using mimetic aging models induced by D-galactose (D-Gal) in both vitro and vivo. Our results demonstrate that compared with control groups, the level of Trx2 was decreased significantly while the activity of ASK1-JNK/P38 signal pathway were dramatically increased in the auditory cortex of mimetic aging group. Furthermore, Knockdown of Trx2 resulted in increasing activity of ASK1-JNK/P38 signal pathway and dramatically increasing ROS level, cell Senescence, apoptosis and death. Taken together, our research demonstrated the significant protective function of Trx2 in preventing presbycusis by maintain mitochondrial integrity, reducing ROS generation, and preventing the activity of ASK1-JNK/P38 apoptosis signal pathway.





PS 835

Upregulation of the GABAAR Gamma1 Subunit in the Inferior Colliculus of Fischer Brown Norway rats Increases throughout Early Adulthood and Peaks during Middle-age.

Lauren Robinson; Oren Barat; **Jeffrey Mellott**
Northeast Ohio Medical University

The γ_1 subunit of GABA_A receptor is upregulated with age in the inferior colliculus (IC). Given that the γ_1 subunit can increase the efficacy of GABAergic transmission, increased expression of γ_1 is possibly a homeostatic mechanism compensating for the age-related loss of GABAergic input. We recently reported that the γ_1 subunit is upregulated in both glutamatergic or GABAergic neurons

in aged animals. Here we show that show the γ_1 subunit is substantially upregulated in young adulthood and reaches its strongest expression in middle-age. We assessed Fischer Brown Norway rats in four age groups: “young adult-early” (2-3 months); “young adult-late” (4-7 months); “middle-aged” (19-22 months); “aged” (28-30 months). Brain sections, perfused with 4% paraformaldehyde, were immunostained for GAD67 (Millipore; MAB5406), anti-GABA_A γ_1 (Alomone Labs; AGA-016 and Bioss Antibodies; bs12078R) and NeuroTrace (Molecular Probes; N-21480). We classified cell bodies as expressing γ_1 based on the presence of immunofluorescent γ_1 puncta along the membrane, distinguishing dense expression (≥ 10 puncta) versus sparse expression (< 10 puncta). A total of 20,836 IC cells were quantified.

Expression of γ_1 was similar across IC subdivisions and for both glutamatergic and GABAergic cells. The percentage of cells expressing γ_1 increased significantly from young adult-early (21%) to young adult-late ages (48%) to middle-aged (68%) and aged (67%). When we distinguished dense vs. sparse expression, we found that dense expression peaked at middle-age, when 39% of γ_1 -expressing cells were dense. The percentage of cells classified as “dense” was significantly lower at other ages (13%, 32%, and 18% in the young adult-early, young adult-late and aged groups, respectively).

Our data lead to two main conclusions regarding GABA_A γ_1 subunit expression in the IC. First, γ_1 expression has increased significantly by 4-7 months (“young-adult”-early), substantially earlier than previously realized. Second, dense expression of γ_1 subunit peaks at middle age, then decreases at later ages. This suggests that age-related changes in GABAR subunit composition may not simply track changes in hearing thresholds. Rather, changes in GABAR composition may show multiple phases, with early phases reflecting a reduction of peripheral input and later phases reflecting a balance of multiple compensatory changes occurring throughout the auditory system.

PS 836

Modulation of autophagy by miR-34a/ATG9A/TFEB pathway in cochlear hair cell death and age-related hearing loss

Hao Xiong; **Jiaqi Pang**; Yongkang Ou; Haidi Yang; Yiqing Zheng
Sun Yat-sen Memorial Hospital, Sun Yat-sen University

Previous studies have shown that impaired autophagy induced by increased miR-34a in aging cochlea is correlated with cochlear hair cell death and plays a critical role in the pathogenesis of age-related hearing loss (AHL). However, the detailed mechanisms underlying miR-34a modulation of autophagy in cochlear hair cell death is largely unknown. Here we

show that miR-34a regulates nuclear localization and activity of the transcription factor EB (TFEB), a master transcription factor, which drives expression of autophagy-related-genes and impairs autophagic flux in hair cells like HEI-OC1 cell. Moreover, ATG9A, one of miR-34a's targets, interacts with TFEB and also modulates nuclear translocation of TFEB. In addition, autophagy enhancement by rapamycin promotes TFEB nuclear translocation in HEI-OC1 cell with either miR-34a overexpression or ATG9A inhibition, which restores the autophagic flux and attenuates HEI-OC1 cell death. Importantly, rapamycin alleviates cochlear outer hair cells loss, inner hair cell synaptic ribbon loss and delays the development of AHL in old C57BL/6 mice, an animal model of AHL. This protective effect seems to be partly attributable to the preservation of TFEB nuclear translocation and autophagic flux in rapamycin-treated cochlea. Our results support a link between autophagy modulation by miR-34a/ATG9a/TFEB pathway and cochlear hair cell survival, which may serve as a potential target for AHL treatment.

PS 837

Decreased Auditory Nerve Population Activity in Aged Gerbils

Friederike Steenken¹; Rainer Beutelmann²; Henning Oetjen¹; Georg M. Klump³; Christine Köppl⁴
¹Cluster of Excellence Hearing4all, Dept. of Neuroscience, Carl von Ossietzky University; ²Cluster of Excellence "Hearing4all"; ³Cluster of Excellence Hearing4all, Department of Neuroscience, Carl von Ossietzky University; ⁴Department of Neuroscience, School of Medicine and Health Sciences, Carl von Ossietzky University Oldenburg

Introduction

Gerbils are an attractive presbycusis model due to their good low-frequency hearing and short life expectancy (Cheal, 1986, Exp Aging Res 12(1): 3-21). The origin of age-related hearing loss is still debated (Gleich et al., 2016, Exp Gerontol 84: 61-70). Here, mass potentials (or neural noise) recorded at the round window (RW) of quiet-aged Mongolian gerbils (*Meriones unguiculatus*) were used to measure the neural index of the auditory nerve in response to broadband noise. This has been shown to be a sensitive metric for the number of active auditory nerve fibers, including low-spontaneous-rate fibers (Barel et al., 2017, PLoS One 12(1):e0169890).

Methods

An electrode was placed in the RW niche of Mongolian gerbils under ketamine/xylazine anesthesia. Third-octave band noise (300 ms) with center frequencies of 1.6-16 kHz was presented monaurally at 60 dB SPL in

stimulus pairs of opposite polarities. Only the steady-state response (last 200 ms) was analyzed. The mean of the responses to both polarities was calculated, eliminating the cochlear microphonic, and the power spectral density (PSD) computed. A neural gain was obtained by dividing point-by-point the PSD of the unstimulated by the stimulated condition. Finally, a neural index for each frequency band was derived by integrating the area under the neural gain curve, resulting in an auditory-nerve excitation pattern across frequency.

Results

In a total of 9 aged (23-39 months) and 38 young adult (4-8 months) ears, the neural index of young gerbils peaked broadly at two frequencies, as previously shown. The overall auditory-nerve excitation of aged gerbils was significantly reduced compared to that of young adults (mixed-model ANOVA, $p < 0.001$). Post-hoc tests for each frequency band showed significant reductions between 1.6 and 3.3 kHz and at 16 kHz, with similar trends at all other frequencies. On average, the decrease of the neural index indicated a loss of about 28% of auditory nerve fibers, and up to 45% at 2.5 kHz.

Conclusions

Gleich et al. (2016) showed a numerical decrease in ribbon synapses in aged gerbils, with the largest loss, near 40%, in apical regions. Consistent with that, the neural index suggests losses of active auditory nerve fibers of a similar magnitude. Importantly, both metrics show the clearest loss in low-frequency cochlear regions. This was unexpected, since synaptopathy after noise exposure preferentially affects low-spontaneous-rate fibers that, in the gerbil, predominate at high frequencies.

Supported by the Deutsche Forschungsgemeinschaft (DFG), priority program 1608.

PS 838

Role of Transforming Growth Factor (TGF) in Presbycusis

Mark A. Bauer¹; Parveen Bazard²; Bo Ding³; Xiaoxia Zhu²; Robert D. Frisina²

¹Medical Engineering Department, Global Center for Hearing and Speech Research, University of South Florida; ²Medical Engineering Dept., Global Center for Hearing & Speech Research, University of South Florida; ³Communications Sciences and Disorders Dept., Global Center for Hearing & Speech Research, University of South Florida

Introduction. We hypothesize that Inflammation is associated with age-related hearing loss (ARHL-presbycusis), one of the top three chronic medical

disorders of the elderly. TGF plays roles in inflammation, differentiation and cell proliferation. The TGF protein family is also involved in noise-induced hearing loss (NIHL). As NIHL can have similar mechanisms to ARHL, the TGF family could be involved in ARHL. Therefore, to test our hypothesis, the inflammatory modulator TGF family and its associated receptors (TGFs and epidermal growth factor receptor-EGFR) were investigated to determine if inflammation is a mechanism for cochlear ARHL.

Methods. Auditory brainstem responses (ABRs) and distortion product otoacoustic emissions (DPOAEs) were used to characterize auditory function in young (Y, 1.5 months, n=4) and old (O, 24-31 months, n=4) CBA/CaJ mice. Following auditory testing, SV tissue (*in vivo*) samples were dissected from the cochleae, and extracted RNA was then analyzed for gene expressions using qPCR. For *in vitro* experiments, stria vascularis-SVK1 cells were used. Cisplatin and hydrogen peroxide were administered to SVK1 cells for a period of 24 hours to mimic cochlear aging and inflammation. Extracted RNA samples were then analyzed for the genes listed above using qPCR. The gene expression candidates were TGF α , β 1, β 2, β 3, TGF β 1, TGF β 2, TGF β 3 and EGFR.

Results. ABRs and DPOAEs revealed elevated hearing thresholds with aging (24-31 months) compared to young adult animals (1.5 month old). All gene expressions of the TGF gene family and associated receptors were examined in SV-K1 cells and for the *in vivo* cochlear tissue. The *in vivo* samples mostly matched the *in vitro* samples with TGF Beta 1, TGF Beta 2, TGF β 2, TGF β 3, and EGFR genes being *downregulated* with age/cellular stress, while TGF β 1 was *upregulated*. TGF Beta 3 and TGF α were the two outliers, as their gene expression levels were not consistent between *in vivo* and *in vitro* experiments, suggesting that there may be subtle mechanism differences in inflammatory reactions between strial cells as a single unit and the more general *in vivo* tissue response.

Conclusions and Future Work: Our findings strongly suggest that the TGF family and their associated receptors are involved in cochlear ARHL. These cytokines can be both anti-inflammatory and pro-inflammatory depending upon the mechanisms involved. Future work will explore mechanistic pathways and therapeutic potentials of anti-inflammatory drugs in the treatment and prevention of ARHL.

Supported by: NIH grant P01 AG009524 from the Nat. Inst. on Aging.

PS 839

Nicotinic Cholinergic Receptor Subunits in Inferior Colliculus, Medial Geniculate Body, and Auditory Cortex: Distribution and the Impact of Aging

Troy M. Hackett¹; Lynne Ling²; Donald M. Caspary³
¹Department of Hearing and Speech Science, Vanderbilt University Medical Center; ²Department of Pharmacology, Southern Illinois University School of Medicine; ³Department of Pharmacology and Department of Surgery, Division of Otolaryngology, Southern Illinois University School of Medicine

Age-related hearing loss is a complex disorder impacting 30-50% of the United States population aged 65 or older. In public settings, seniors frequently have difficulty understanding speech potentially leading to social withdrawal and depression. Studies have shown that older individuals can maintain speech understanding in the face of degraded temporal information by increasing use attentional and cognitive resources. Attentional resources are brought into play when difficult to identify acoustic signals ascend the central auditory neuraxis. Cholinergic neurons in brainstem and basal forebrain are activated under attentional demand releasing acetylcholine activating nicotinic cholinergic receptors (nAChRs) and muscarinic receptors in inferior colliculus (IC), medial geniculate nucleus (MGB) and primary auditory cortex (A1). In the present study we examined the impact of aging on the expression of four nAChR subtypes (a4, b2, a7, b4) in the major divisions of the IC, MGB, and A1. Secondly, we mapped the locations of excitatory and inhibitory neurons containing mRNA transcripts of these subunits. Aging negatively impacted or altered nAChRs in all three structures. Saturation binding showed age-related losses of nAChRs across layers of A1 and in MGB, while competition binding studies were suggestive of an age-related subunit switch within the IC. Significant age-related reductions in a4 and b2 transcript density were observed in all three regions, while a7 was reduced in IC and A1, but not MGB. In A1, the majority of excitatory (>80%) and inhibitory (>50%) neurons in L2-L6 expressed a4 and b2 subunit transcripts, whereas a7 nAChRs were expressed by ~60% of both neuronal classes. In MGB, where nearly all neurons are excitatory, >90% expressed a4 and b2, while only ~20% contained a7 subunit message. In the IC, the majority of excitatory neurons expressed a4, b2, and a7 subunits, a4 was detected in 80% of neurons containing a7 also expressed a4 and b2. Collectively these data indicate modest but highly consistent age-related cholinergic hypofunction in the central auditory system likely reflecting the need for increased attentional effort required for adequate speech understanding seen in the elderly. Expression of a4, b2, and a7 nAChRs is generally robust in A1, MGB, and IC, but varies by location and neuronal class, indicating regional and cell-type specific patterns of expression.

Effects of Estrogen Inhibition on Age-Related Hearing Thresholds and Autophagy Changes in Mice

Xiaoxia Zhu¹; Bo Ding²; McKenzie Watson³; Carlos Cruz³; Tanika T. Williamson⁴; Robert D. Frisina¹

¹Medical Engineering Dept., Global Center for Hearing & Speech Research, University of South Florida;

²Communications Sciences and Disorders Dept., Global Center for Hearing & Speech Research,

University of South Florida; ³Chemical & Biomedical Engineering Dept., Global Center for Hearing and

Speech Research, University of South Florida;

⁴Medical Engineering Dept, Global Center for Hearing and Speech Research, University of South Florida

Introduction: Estrogen is an important steroid trophic hormone supporting the function of many cells. Several reports characterize the effects of estrogen-deficiency on hearing in women, suggesting its inhibition may play a role in age-related hearing loss, but the mechanisms are not clear. Autophagy is a highly conserved catabolic process essential for embryonic development and adult cellular homeostasis. Evidence has linked compromised autophagic processes to age-related disorders, such as Parkinson's and Alzheimer's diseases. In light of this, here we tested the hypothesis that estrogen can regulate autophagy, and possible involvement of autophagy on cochlear aging and hearing changes.

Methods: The stria vascularis cell line, SV-K1, was used as an *in vitro* model. Treatments, such as tamoxifen (TAX, an estrogen antagonist) and 17- β estradiol were administered to SVK-1 cells. In addition, two month (mon) old young adult CBA/CaJ mice (N= 18) were divided into three groups: females with ovariectomy (OVX) at 2 mon old, intact females, and male controls. These groups were treated with TAX (20mg/kg/day, intraperitoneal [IP] 2weeks) at 12 mon old. The animals underwent measurement of auditory brainstem responses (ABRs).

Results: Significant ABR threshold elevations (10-30 dB) at different frequencies were observed at 10 months (12 mon old) in the OVX group compared to pre-OVX (2 mon old). Age-related minor ABR threshold shifts were similar between 2 mon and 12 mon old in both female groups and male controls. In addition, for the mice treated with TAX at 12 month old, the female controls showed ABR thresholds shifts, between 12 and 16 mon, larger than the OVX and male groups. The pattern of LC3 expression in the aged cochlea was different from the young adult expression: LC3I was decreased and LC3II increased in the aged cochlea, suggestive of autophagy inhibition with aging. This is similar to our *in vitro* findings with the autophagy inhibitor chloroquine using the SV-K1 cell line. In contrast, 17 β -Estradiol treatment *in vitro* decreased expression

levels of the autophagy markers LC3 and p62 compared to vehicle control treatment, suggesting estrogen may help prevent age-related autophagy blocking. However, TAX blocked these LC3II and p62 expression changes induced by 17 β -Estradiol. We also observed that TAX alone didn't change the LC3 and p62 expressive patterns compared with vehicle control treatment.

Conclusion: Inhibition of estrogen may lead to age-related autophagy pathway modulations and hearing threshold changes.

Work Supported by NIH grant P01 AG009524 from the Nat. Inst. on Aging.

PS 841

Aldosterone Regulates Na-K-Cl Co-transporter (NKCC1) Currents Through the Modification of Its Intracellular Location

Bo Ding¹; Parveen Bazard²; Harish Chittam³; Venkat Bhethanabotla³; Joseph P. Walton⁴; Robert D. Frisina²

¹Communications Sciences and Disorders Dept., Global Center for Hearing & Speech Research,

University of South Florida; ²Medical Engineering Dept., Global Center for Hearing & Speech Research,

University of South Florida; ³Chemical & Biomedical Engineering Dept., Global Center for Hearing and

Speech Research, University of South Florida;

⁴Communication Sciences & Disorders Dept., Medical Engineering Dept., Global Center for Hearing & Speech Research, University of South Florida

Introduction: Degeneration of a specialized cochlear organ, the stria vascularis (SV) is involved in age-related hearing loss (ARHL). SV marginal cells contain Na⁺-K⁺-2Cl⁻ co-transport protein (NKCC1), which generates the potassium rich endolymphatic fluid and endolymphatic potential, the battery which powers auditory signal transduction. Recently, we demonstrated that NKCC1 expression is decreased in the aging cochlea compared to young cochlea, and treatment with aldosterone (ALD) increases NKCC1 expression. Here, we investigated possible mechanisms of how ALD alters NKCC1 currents in an *in-vitro* model using whole cell electrophysiology and molecular methods.

Methods: SH-SY5Y cells were differentiated from a neuroblast-like state into mature human neurons with retinoic acid. To confirm NKCC1 expression levels, quantitative qRT-PCR and western blots were performed. Whole-cell electrophysiology used standard patch clamp techniques, utilizing a 700-B Multiclamp amplifier and 1440-A data acquisition unit (Molecular Devices). Recordings were performed using thick-walled borosilicate glass micropipettes (5-6Mohms) at room temperature.

Results: qRT-PCR and Western Blot experiments confirmed that both undifferentiated and differentiated cells express NKCC1 at gene and protein levels. Differentiated cells were used for whole-cell patch clamping. Cells were continuously perfused with extracellular solutions containing 1 μ M ALD. An increase in outward K⁺ currents was observed after approximately 10 minutes following 1 μ m of ALD, compared to pre-ALD currents. This was reversed by fluid washout. These K⁺ currents were blocked following 1 μ M application of tetraethyl ammonium (TEA) in the bath. To test for mechanisms of how NKCC1 modulates ALD activity-elicited currents, experiments were designed to inhibit NKCC1 action or expression, by using bumetanide- an NKCC1 channel blocker. Initial experiments indicate that ALD was not as effective in altering the current response in the presence of bumetanide as compared to controls- no bumetanide. Alterations in the plasma membrane expression of NKCC1 were detected during the ALD treatment with dose and time-dependent responses. NKCC1 immunoreactivity during ALD treatment was *higher* than non-treatment as measured by membrane fractions, but this immunoreactivity was *decreased* for the cytoplasmic fractions. In addition, qRT-PCR didn't detect mRNA expressional changes, suggesting that post-transcriptional modifications contribute to the alterations in dynamic protein expression of NKCC1. Further experiments are underway to quantify the role of NKCC1 knock-outs for regulation of ALD-elicited ion currents.

Summary: These results elucidate the cellular and molecular mechanisms by which ALD modulates NKCC1 channel expression and function through the distribution and relocation of NKCC1 in cells.

Support: NIH grant P01-AG009524 from the Nat. Inst. on Aging.

Auditory Brainstem III

PS 842

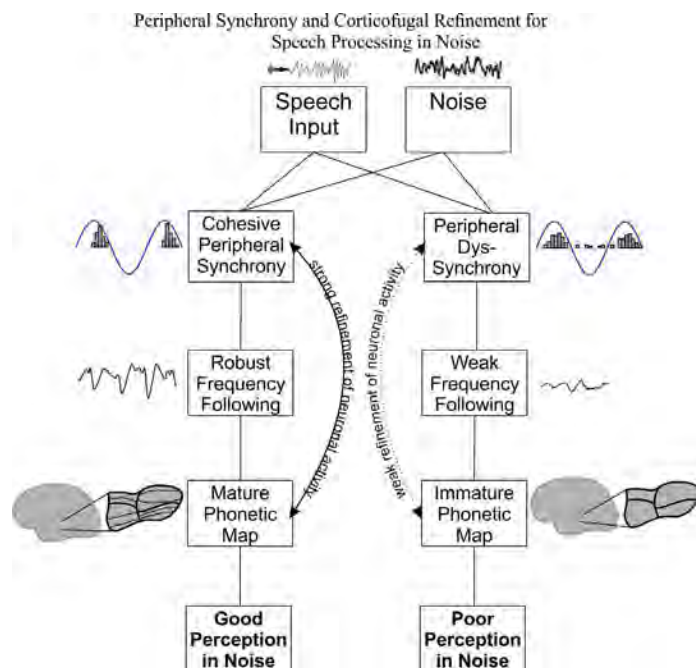
Effects of Noise and Age on the Infant Brainstem Response to Speech

Gabriella Musacchia¹; Silvia Ortiz-Mantilla²; Cynthia Roesler²; Sree Rajendran²; Julie Morgan-Byrne²; April Benasich²

¹University of the Pacific; ²Rutgers University

Background noise makes hearing speech difficult for people of all ages. This difficulty can be exacerbated by co-occurring developmental deficits that often emerge in childhood. Sentence-type speech-in-noise (SIN) tests are available clinically but cannot be administered to very young individuals. Our objective was to examine the use of an electrophysiological test of SIN, suitable for infants, to track developmental trajectories. Speech-evoked

brainstem potentials were recorded from 30 typically-developing infants in quiet and +10 dB SNR background noise. Infants were divided into two age groups (7-12 and 18-24 months) and examined across development. Spectral power of the frequency following response (FFR) was computed using a fast Fourier Transform. Cross-correlations between quiet and noise responses were computed to measure encoding resistance to noise. Older infants had more robust FFR encoding in noise and had higher quiet-noise correlations than their younger counterparts. No group differences were observed in the quiet condition. These data show that by two years of age, infants show less vulnerability to the disruptive effects of background noise, compared to infants under 12 months.



PS 843

Assessing Contributions of Magnitude and Phase in Classification of Frequency Following Responses

Steven Losorelli¹; Blair Kaneshiro¹; Gabriella Musacchia²; Nikolas Blevins³; Matthew Fitzgerald¹

¹Stanford University; ²University of the Pacific; ³Department of Otolaryngology-Head and Neck Surgery, Stanford University School of Medicine

Speech and music perception are challenging for hearing-impaired listeners. Clinicians have few objective tools to determine the source of a patient's perceptual difficulties. For those using hearing aids and cochlear implants, better prognostics are needed to distinguish between instances where 1) auditory deficits arise from the delivery of a deficient signal, or 2) the stimulus signal is intact, but the

patient has not yet learned to assign a label to it. Recent research has used electroencephalography (EEG) to discriminate auditory signals from quantifiable patterns of neural activity. One such response is the frequency following response (FFR), the steady-state component of the auditory brainstem response that is phase-locked to features of the auditory stimulus.

We recently demonstrated that a machine-learning approach called classification can be used to decode stimulus labels from speech and music FFRs with high accuracy in normal-hearing (NH) listeners. While this approach does not involve pre-selecting known features of interest, we seek to further understand which features of the response drive classification. A strength of classification is its ability to operate over various representations of the input signal. Here, we explore how time- and frequency-domain features contribute to decoding accuracy.

We presented NH participants (n=13) with six 135ms stimuli—three speech (/ba/, /da/, /di/) and three musical note ('piano', 'bassoon', 'tuba') sounds—while FFR trials were recorded. All stimuli had similar fundamental frequencies but varied in overall spectral and temporal characteristics. We then passed time and frequency (FFT magnitude, phase, real/imaginary coefficients) representations of 200-repetition FFR trial averages into the classifier. Classification was performed over the full time course of the response as well as in shorter, overlapping temporal windows. Classification of real/imaginary FFT components, which fully characterize the response, produced an overall accuracy of 68% ($p < 0.001$) - similar results to classification of the time-domain representation of the response (accuracy=68%, $p < 0.001$). Classifying only FFT magnitudes or phase angles produced accuracies of 41% and 56%, respectively (both p -values < 0.001). These results suggest that both FFT magnitude and phase angle contribute complementary information used in classification to predict stimulus labels from the FFR. Further development of appropriate stimuli and analysis techniques could benefit hearing-impaired populations in clinical settings.

PS 844

The Effect of Carrier Type on Brainstem Neural Representation of Vcoded Speech

Saradha Ananthakrishnan; Danielle Yurjevich
Towson University

Noise- and sine-vocoders have been extensively used to simulate cochlear implant speech processing in listeners with normal hearing. Behavioral studies have established an advantage for sine-vocoders over noise-vocoders for particular aspects of speech recognition (e.g. gender identification, vowel recognition). However, it is unclear

if the improved speech recognition associated with sine-vocoders exists in the neural representation of vocoded signals at the level of the brainstem in listeners with normal hearing. Ananthakrishnan, Luo, and Krishnan (2017) found no statistically significant effect of carrier type (sine- vs. noise-vocoder) on the brainstem neural representation of the fundamental frequency (F0) in listeners with normal hearing; however, the comparison was carried out at a fixed number of 8 channels. The aim of the current study is to determine if there is an effect of carrier type (sine-wave or noise-band) on brainstem neural representation of F0 when the channel number is varied for a vocoded speech signal. In this study, the Frequency Following Response (FFR), a scalp-recorded electrophysiological response reflecting phase-locked activity from the rostral brainstem, was used to study the effects of varying the carrier type (sine vs. noise) and number of channels (1,2,4,8,16,32) of a vocoded speech signal on brainstem neural representation of F0 in 9 listeners with normal hearing. FFRs were subjected to temporal and spectral analyses, including an examination of waveform amplitudes, autocorrelation analysis, and Fast Fourier Transform (FFT) analysis. Preliminary qualitative analyses and descriptive statistics suggest that average F0 strength in the brainstem neural response is greater for sine- as compared to noise-vocoded signals when the number of channels is lower, i.e. 1,2 and 4. The average F0 strength in the neural response is similar for the two carriers when the number of channels is 8, and stronger for noise- as compared to sine-vocoded signals at 16 and 32 channels. Inferential statistics are required to describe the data thoroughly. Future directions include analysis of spectral FFRs to determine the effect of varying the carrier type on neural representation of other acoustic features such as formant-related frequencies present in vocoded speech.

PS 845

Diagnosis of Cochlear Synaptopathy in Mouse using Masked Auditory Brainstem Responses

Kirupa Suthakar¹; M. Charles Liberman²

¹*Eaton-Peabody Lab, Massachusetts Eye and Ear Infirmary, Harvard Medical School*; ²*Mass. Eye and Ear Infirmary*

Cochlear synaptopathy preferentially targets synapses of low spontaneous rate (LSR) auditory nerve fibers (ANFs) with high thresholds and long response latencies (Furman et al 2013, *J Neurophysiol* 110:577). Owing to their wide dynamic ranges and relative resistance to noise masking, LSR ANFs are likely important in difficult listening environments. Since high-spontaneous-rate (HSR) ANFs, with low thresholds, saturate at lower masker levels than LSR fibers, we hypothesized that the dynamics of ABR responses masking could be

used to non-invasively diagnose cochlear synaptopathy, specifically that loss of LSR ANFs would 1) decrease the level of a broadband masker at which the probe response disappeared and 2) decrease the normal masker-induced increase in response latencies.

CBA/CaJ mice were exposed at 7 wks to 8-16 kHz noise at 97.5 dB SPL for 2 hrs and compared to unexposed age-matched controls. After a 1 wk recovery, ABRs and DPOAEs at half-octave intervals from 5.6 to 45.2 kHz were measured. Masked ABRs were performed at two frequency regions: 8kHz, where exposed animals show no synaptopathy, and 32 kHz where there is significant synaptopathy. The masking ABR paradigm consisted of fixed level (80 dB SPL) tone-pip probes (8 or 32 kHz) with simultaneous presentations of audiometrically shaped continuous masking noise of varying levels (8 kHz: octave band centered around 8 kHz; 32 kHz: high-pass noise above 22.6 kHz).

ABR and DPOAE thresholds in exposed animals were normal from 5.6–32.0 kHz, but elevated by ~15 dB at 45.2 kHz. Cochlear histopathology confirmed a 40-50% loss of inner hair cell synapses around the 32 kHz place and subtotal loss of outer hair cells at the basal tip. Changes in suprathreshold masking of ABRs were observed in the synaptopathic (32kHz) region. Paradoxically, the masker level required to reduce the probe response by 50% was increased in the synaptopathic animals, which we attribute to threshold elevations at regions basal to the 32-kHz probe. As seen in prior study (Mehraei et al. 2016, *J Neurosci* 30:3755), the normal masker-induced shift in ABR latency, especially peak 4, was greatly attenuated in the synaptopathic group for the 32 kHz probe, but not the 8 kHz probe. These data suggest that changes in masker-induced ABR latency, rather than amplitude, may provide useful diagnostic markers of cochlear synaptopathy.

Research supported by a grant from NIDCD (DC000188)

PS 846

Pushing the Envelope-Following Response to the Limit: Influence of the Stimulus Envelope on its Sensitivity to Cochlear Synaptopathy

Viacheslav Vasilkov¹; Markus Garrett²; Sarah Verhulst¹

¹Ghent University; ²Oldenburg University

Recent animal studies show that subcortical envelope-following responses (EFRs) are promising diagnostic markers of cochlear synaptopathy, i.e. loss of afferent synapses between the inner-hair-cells and auditory-nerve fibers. Although noise- or ageing-induced changes in animal EFR magnitudes were directly associated with a histologically validated loss of synapses, the translation

of EFR metrics to individualized human diagnostics of synaptopathy is not straightforward. Human EFR metrics require a relative recording paradigm, and cannot always be robustly measured when other sensorineural hearing deficits co-exist.

To design sensitive EFR markers for humans, this study combines a computational modeling approach with recordings to evaluate the diagnostic potential of EFRs evoked by stimuli with different envelope shapes. A human auditory periphery model was adopted to simulate subcortical EFRs and cochlear synaptopathy was simulated by selectively reducing different inner-hair-cell synapse types and numbers. Normal and impaired audiograms were implemented by manipulating the frequency-specific degree of cochlear filter gain. EFR reference data were recorded from young (yNH) and older listeners with normal (oNH) or impaired (oHI) audiograms. A 4-kHz carrier was amplitude modulated (AM) with a 120-Hz periodicity in all stimuli which were either presented with the same rms or peak-to-peak as the reference 100% sinusoidally AM tone (70 dB SPL). Three envelope conditions were tested: a 25% (1) or 50% (2) duty-cycle squared envelope and a ten-harmonic-complex envelope (3).

EFR magnitudes were calculated by adding up spectrum peaks at 120 Hz and available harmonics above the noise floor. Both experimental and modeling results show that stimuli with more “peaky” envelopes, i.e. (1), evoke substantially stronger EFR magnitudes than the reference SAM tone of equal intensity. The spread of individual EFR magnitudes covered a wider dynamic range and showed above-noise floor EFRs in all of the yNH and part of the oNH group, demonstrating an increased robustness of the suggested metrics. Using the model, we studied the effect of different synaptopathy and cochlear gain loss profiles on the EFR magnitudes evoked by stimulus (1). The simulations corroborate the observed spread in the empirical data which showed reduced EFR magnitudes in both oNH and oHI listeners compared to yNH EFRs. Taken together, our results suggest that oNH and oHI listeners both suffered from cochlear synaptopathy and that modifying the EFR stimulus envelope can yield more sensitive EFR markers.

Funding German Research Foundation (DFG PP1608 VE924/1-1; VV), DFG Cluster of Excellence (EXC1077/1 “Hearing4all”; MG) and European Research Council (ERC 678120; SV)

PS 847

Integrated ABR & VsEP System for Auditory and Vestibular Function Testing

Dingxuan Zeng; Wei Liu; Xiaojie Yang; **Fangyi Chen**
Southern University of Science & Technology

Here we presented an auditory & vestibular function testing system with: 1) integrated electronics system with high-resolution ADC & DAC for accurate stimulus generation & response sampling in both ABR & VsEP tests; 2) animal holders for both systems; 3) software system for presenting results and analyzing data. The ABR system has the capability of measuring up to four animals at the same time, and thus greatly increases the throughput of hearing screening. The speakers has a flat spectrum and can be calibrated on-site for generating more than 90 dB SPL sound up to 60 kHz. We verified our ABR system with the TDT one, and results showed similar sensitivity. The VsEP system has a specially-designed animal head-holder, which is conducive to produce more reliable results during the vertical acceleration. The recorded data can be saved in text format for post-processing on different platforms.

Supported by

The National Natural Science Foundation of China (8177188 and 81470701 to FC) and 2018 Shenzhen Basic Research Fund (JCYJ20170817111912585 to FC)

PS 848

Consequences of Cochlear Synaptopathy in Noise-Exposed Middle-Aged Adults

Tim Schoof; Tim Green; Stuart Rosen
University College London

Evidence for cochlear synaptopathy using non-invasive measures in humans remains limited. However, previous research has predominantly focused on young adults with normal hearing thresholds whose suspected synaptopathy has solely been based on self-reports of noise exposure history. It is quite likely that measurable synaptopathy only becomes evident later in life through the combined effects of ageing and noise exposure.

Here we investigated incidence of cochlear synaptopathy in humans by focusing on normal-hearing middle-aged adults (45-60 years old) with self-reported noise exposure history. We compared the data to a young control group (18-35 years old) without much noise exposure history. In addition, we investigated the potential consequences of synaptopathy for speech perception in noise.

To assess cochlear synaptopathy, we measured ABR wave I amplitudes in response to clicks presented at three different levels (95, 105, 115 dB peSPL), and envelope

following responses (EFRs) in response to a 2.8 kHz transposed tone amplitude modulated at 176 Hz at three different modulation depths (0, -4, and -8 dB). To quantify the degree of cochlear synaptopathy, we computed the slope of the click ABR wave I amplitude across levels and the spectral magnitude of the EFR at F0 across modulation depths.

To examine the potential effects of cochlear synaptopathy on speech perception in noise, we measured speech reception thresholds (SRTs) for both consonants (VCVs) and (IEEE) sentences at two different levels (40 and 80 dB SPL). SRTs are measured in two conditions, one where both the target and background noise are diotic (N_0S_0), and another where the target signal is inverted in polarity in one ear (N_0S_π) leading to a phase disparity across the ears. We computed the binaural intelligibility level difference (BILD) by taking the difference between the N_0S_0 and N_0S_π conditions. Of particular interest is the relationship between our electrophysiological measures of cochlear synaptopathy and our behavioural speech-in-noise measures.

Given that cochlear synaptopathy is thought to selectively affect high-threshold low spontaneous rate fibres, we hypothesise that clicks presented at lower levels and transposed tones with shallower modulation depths will not be encoded as robustly in individuals with cochlear synaptopathy. We therefore predict that the middle-aged group will show shallower ABR and EFR slopes compared to the young controls. In addition, we expect that individuals with shallower ABR and EFR slopes will perform more poorly on the speech-in-noise task, particularly at higher stimulus levels.

PS 849

Hidden Hearing Loss and Selective Attention in the Brainstem

Marina Saiz-Alia¹; Antonio E. Forte¹; Tobias Reichenbach²

¹*Department of Bioengineering, Imperial College London;* ²*Department of Bioengineering and Centre for Neurotechnology, Imperial College London*

Cochlear synaptopathy or hidden hearing loss can be caused by noise exposure and ageing. It refers to the damage of higher-threshold auditory-nerve fibers and may account for the differences in the ability of normal hearing threshold listeners when communicating in challenging environments (Bharadwaj et al., 2014). However, it remains unclear if the condition actually occurs in humans, how it can be best diagnosed, and how exactly it impacts speech-in-noise processing.

Recently we proposed a method for measuring the brainstem's response to natural non-repetitive speech and employed it to show that the auditory brainstem

already plays a role in selective attention to speech (Forte et al., 2017). We thereby observed individual differences in the modulation of the brainstem response by selective attention: some subjects showed large attentional modulation while others exhibited only little modulation. We therefore wondered if the strength of the attentional modulation correlates with hearing ability and if it relates to cochlear synaptopathy.

We approached this issue through a computational model and experimental measurements. First, to explore the effects of hidden hearing loss, we developed a realistic computational model of the auditory-brainstem response (ABR) to speech based on an existing model (Zilany et al., 2014). We employed it to investigate the neural response to continuous speech at different stages in the brainstem, and to explore the effects of hidden hearing loss. We found significant responses and characteristic latencies for neural signals generated at the level of the auditory-nerve fibres, the cochlear nuclei and the inferior colliculus (IC). The latency of the response of the IC matched the latency that we found experimentally, suggesting that the scalp-recorded brainstem response to speech is dominated by the IC.

Secondly, we assessed young healthy listeners for speech-in-noise comprehension, lifetime noise exposure, the middle ear muscle reflex, binaural hearing and different brainstem measures, including the brainstem response to continuous speech and its modulation by selective attention. We found that there was considerable variability in all measures across the participants. However, only few of the objective measures were able to explain the differences in speech-in-noise comprehension between the participants. Interestingly, the modulation of the brainstem response by selective attention correlated with the performance in the speech-in-noise task. Our findings suggest that the attentional modulation in the brainstem response can inform on hearing ability and potentially on hidden hearing loss.

References

- Bharadwaj et al. (2014). *Frontiers in systems neuroscience*, 8, 26.
Forte et al. (2017). *eLife*, 6, e27203.
Zilany et al. (2014). *The Journal of the Acoustical Society of America*, 135(1), 283-286.

PS 850

Derived-band Envelope Following Responses as a Frequency-specific Marker of Cochlear Synaptopathy

Sarineh Keshishzadeh¹; Markus Garrett²; Sarah Verhulst¹

¹Ghent University; ²Oldenburg University

Cochlear synaptopathy compromises the coding of supra-threshold sound and reduces the amplitude of envelope following responses (EFRs) in subjects with normal hearing thresholds. However, a frequency-specific assessment of synaptopathy is complicated because the sources contributing to the EFR can stem from a broad cochlear frequency region and depend on the stimulus specifics (e.g., bandwidth, carrier type, off-frequency maskers). To address the need for more sensitive and frequency-specific diagnostic metrics, we hypothesize that derived-band EFRs, constructed by spectral subtraction of EFRs in response to amplitude-modulated white-noise carriers with different bandwidths, can provide a frequency-specific assessment of synaptopathy.

To test this hypothesis, we first simulated derived-band EFRs to 70-dB-SPL, 100% modulated (SAM, 120 Hz) broadband noise carriers using a computational model of the human auditory periphery with different configurations of synaptopathy. The white-noise stimuli were bandpass filtered with low cutoff frequencies of 0.25, 0.5, 1, 2 and 4 kHz and a high cutoff frequency of 22 kHz. The spectral subtraction of the simulated EFR responses resulted in derived-band EFRs limited to the [0.25-0.5], [0.5-1], [1-2] and [2-4]-kHz frequency regions and the simulations revealed a dominant contribution of the [2-4]-kHz derived-band to the broadband EFR. We witnessed a reduction of simulated EFR amplitudes which was caused by increasing degrees of synaptopathy in the frequency region corresponding to the derived band. To validate our model predictions, which propose the use of the derived-band EFR as a frequency-specific marker of synaptopathy, we recorded EFRs to the designed stimuli in 11 young normal-hearing listeners. The observed dominant contribution of the [2-4]-kHz frequency band and the predicted range of individual variability of EFR amplitudes confirmed the model simulations. Our study suggest that individual differences in the [2-4]-kHz derived-band reflect different states of auditory-nerve integrity. In support of this observation, no meaningful correlation was observed between the EFR amplitudes and distortion product otoacoustic emissions thresholds at 3 kHz.

Based on the experimental results and model simulations, we conclude that the [2-4]-kHz derived-band is the most dominant frequency region for the generation of the EFR to broadband noise. Moreover, the model simulations support that inter-subject variability in the derived-band EFR is a promising relative diagnostic measure of synaptopathy in the absence of outer-hair-cell loss.

Funding: European Research Council (ERC) under the European Union's Horizon 2020 research and innovation programme (RobSpear: 678120)

PS 851

Reafferent Processing in the Human Auditory Brainstem: Auditory Brainstem Responses to Self-Produced Sounds

Parker Tichko; Erika Skoe
University of Connecticut

Many sounds listeners encounter in their daily lives are the outcome of their motor actions, such as self-generated sounds (e.g., speech, singing, snapping) and self-initiated sounds (e.g., sounds that are tied to a button press). How does the nervous system differentiate between self- and externally produced sounds? One hypothesis, the corollary-discharge (CD) hypothesis, posits that information about motor actions is propagated forward to sensory areas (i.e., an “efference copy” or “corollary discharge”) that is then used by an internal model to generate predictions on self-generated or self-initiated sounds (Sperry, 1950; von Holst & Mittelstaedt, 1950). If the generated or initiated sound matches the prediction, a subtractive, suppression effect is predicted to occur, allowing the organism to remain alert to external sounds in the environment, while reducing its sensitivity to self-generated (reafferent) sounds.

A large body of research has studied reafferent sound processing that occurs at cortical levels of the auditory system. For instance, in human and non-human animals, self-generated sounds have been shown to result in the suppression of cortical auditory-evoked potentials (Heinks-Maldonado et al., 2005; Knolle, Schröger, & Kotz, 2013; Houde, Nagarajan, Sekihara, & Merzenich, 2002; Liu, Behroozmand, & Larson, 2010). Moreover, in humans, suppression effects have been demonstrated for both self-generated sounds, such as speech sounds, and self-initiated non-verbal sounds, such as acoustic stimuli triggered by a button box (Martikainen, Kaneko, & Hari, 2005; Baess et al. 2009). Yet, little human work has investigated reafferent processing in lower level auditory structures, such as the auditory brainstem, that interface directly with the motor system (e.g., cerebellum). Here, we investigated reafferent processing in the subcortical auditory system using a novel paradigm for recording auditory brainstem responses (ABRs) where participants controlled the presentation of an auditory click stimulus. During the experiment, we first recorded ABRs while participants initiated an auditory click stimulus train by repeatedly pressing a button box. Next, we recorded participants’ ABR while they passively listened to an identical presentation of the click stimulus train without using the button box. Unlike suppression effects that have been reported in cortical auditory responses, our analyses suggest that the amplitude of the ABR waveform is enhanced to self-initiated sounds relative to

externally generated sounds with an identical acoustic and timing structure. This finding is consistent with recent work suggesting that phase-locked neural responses, those with an auditory brainstem source, are enhanced during sensorimotor synchronization to external acoustic rhythms (Nozaradan et al., 2016).

PS 852

Increased Central Auditory System Gain in Listeners with Decreased Background Noise Tolerance

Erika Skoe; Sarah Camera; Jennifer Tufts
University of Connecticut

Listeners vary considerably in their willingness to tolerate background noise. Small studies of healthy, normal-hearing young adult listeners suggest that central auditory system (CAS) gain may be a physiological basis of decreased tolerance for background noise (Harkrider and Tampas 2006; Tampas and Harkrider 2006). These studies used an extreme grouping approach, in which one group had a high level of intolerance to background noise and the other group had normal levels of background noise tolerance. This grouping approach, in combination with small sample sizes, raises questions about the replicability and generalizability of the findings. Here we ask whether CAS activity can account for group-level differences in listeners’ willingness to tolerate background noise when tolerance scores are in the typical range and the groups represent high and low ends of this typical range. In 56 young adults with clinically-normal audiograms, CAS gain was measured from the suprathreshold auditory brainstem response (ABR), using the amplitude of ABR Wave V. ABR Wave I amplitude served as our measure of peripheral auditory system activation.

Consistent with previous, smaller-scale studies, we find that lower tolerance for background noise is associated with increased CAS activation (i.e., larger Wave V amplitudes) when the lower- and higher-tolerance groups are compared. This group difference is evident in the ABR Wave V amplitude across a range of stimulus presentation rates, from slow to fast rates (3-90/sec). The groups, however, are matched in terms of ABR Wave I amplitude and have similar levels of environmental noise exposure, as measured by body-worn dosimeters that recorded sounds levels for one week.

Recent work has advanced the theory that CAS hyperactivity can arise when the input to the CAS is reduced, as might occur when peripheral receptors become hypoactive following noise-induced damage. Our findings suggest that peripheral system hypoactivity (i.e., reduced Wave I) is not a requisite condition for CAS hyperactivity. Instead of findings suggest

that idiosyncratic physiological variations in CAS gain may underlie normal variation in behavioral tolerance for background noise.

PS 853

fMRI and ABR Assessment of Ascending Auditory Pathway Function Associated with Lifetime Noise Exposure in Normally-Hearing Listeners

Rebecca Dewey¹; Susan Francis¹; Hannah Guest²; Garreth Prendergast²; Rebecca E. Millman³; Christopher J. Plack²; Deborah Hall⁴

¹*Sir Peter Mansfield Imaging Centre*; ²*Manchester Centre for Audiology and Deafness*; ³*Manchester Centre for Audiology and Deafness, NIHR Manchester Biomedical Research Centre*; ⁴*University of Nottingham, and NIHR Nottingham BRC*

Noise exposure has been shown to cause permanent damage to hair-cell synapses, apparent as physiological changes in the ascending auditory pathway. It is unclear whether this can be detected in the human brain. This study examined the link between lifetime noise exposure and responses within the ascending auditory pathway using auditory brainstem responses (ABR) and functional MRI (fMRI). The primary hypothesis tested for an effect of noise exposure group (high > low).

62 volunteers (age 25-40 years) with clinically-normal audiometric thresholds (≤ 20 dB HL; 0.5-8 kHz) were recruited to 'low' and 'high' lifetime exposure groups using a Noise Exposure Structured Interview.

Click responses were measured using a BioSemi ActiveTwo system with electrodes on the vertex/Cz, and mastoids. ABR data were processed by first rejecting noisy epochs, averaging across trials and filtering, before automatic detection of peaks for waves I and V. ANCOVAs were performed on these amplitudes using sex and group as between-subject factors and age as a covariate.

fMRI was acquired on a Philips Ingenia 3.0T scanner. The sound stimulus comprised 24-seconds broadband noise presented using OptoACTIVE headphones during active noise cancellation. fMRI data were corrected for physiological noise, image distortion and head motion, and general linear model analysis performed to model onset and sustained stimulus responses. A region of interest (ROI) analysis was then performed on the GLM beta-estimates for functionally-defined subcortical auditory nuclei and auditory cortex. ANCOVAs were performed on the onset and sustained beta-estimates of the fMRI responses with factors group (between-subjects), region-of-interest (within-subjects), and age as a covariate.

There was no significant effect of noise exposure on

the ABR amplitude of waves I and V ($F=0.41$; d.f.=1,57; $p=0.523$ and $F=1.42$; d.f.=1,57; $p=0.238$, respectively).

fMRI responses were more robust to the onset than for sustained responses. The fMRI onset response differed significantly between noise exposure groups (high > low; $F=4.170$; d.f.=1,59; $p=0.046$); with a significant difference across ROIs ($F=77.121$; d.f.=4,236; $p < 0.001$), but no interaction. Significance of group was not reached for the sustained responses ($F=3.269$; d.f.=1,59; n.s.), likely due to lower beta-estimates but the trend was in the same direction, the effect of region was again significant ($F=47.443$; d.f.=4,236; $p < 0.001$). Similar ANCOVAs showed no effect of tinnitus or sound-level tolerance on fMRI responses.

This is the first fMRI demonstration of the physiological effects of lifetime noise exposure in humans with clinically-normal audiometric thresholds.

This work is supported by the Medical Research Council, MR/L003589/1 awarded to the University of Manchester.

PS 854

Effects of Early-Onset Deafness on Cochlear Nucleus and Auditory Brainstem Nuclei in the Mongolian Gerbil

Maïke Vollmer¹; Elena Eninger²; Johanna Knorz²; Barbara Kellner²; Otto Gleich³

¹*Department of Otorhinolaryngology-HNS, University Hospital Magdeburg, Germany*; ²*Comprehensive Hearing Center, University Hospital Würzburg, Germany*; ³*Department of Otorhinolaryngology-HNS, University Hospital Regensburg*

Peripheral hearing loss can result in morphological changes along the entire auditory pathway. The extent of these changes depends on several factors, such as the species and the degree, type, onset, and duration of hearing loss. Especially early-onset, long-term deafness is associated with pronounced degenerative changes. Using the Mongolian gerbil, the present study evaluated the effects of early-onset bilateral deafness on morphological changes in the lateral superior olive (LSO) and its excitatory (anteroventral cochlear nucleus, AVCN) and inhibitory (medial and lateral nucleus of the trapezoid body, MNTB and LNTB) input nuclei.

Gerbils were deafened around hearing onset (P13-P20) by systemic administration of Kanamycin and the loop diuretic Bumetanide. Deafness was confirmed by the absence of auditory brainstem responses (>95 dB SPL). After 3-4 months of deafness, the four different nuclei were investigated in frontal brain sections.

Light microscopic analysis of Nissl-stained sections was performed to quantify the cross-sectional area of the nuclei and the size, number, and density of neurons. Because directional hearing is dependent on the intact balance between excitatory and inhibitory inputs in auditory brainstem nuclei, GABA- and Glycin-immunostained sections were used to evaluate deafness-induced changes in the number and density of inhibitory neurons in LNTB and LSO. Analyses were separately performed for high, middle, and low frequency regions of the given nuclei. Age-matched normal-hearing adult gerbils served as controls.

The AVCN and the LSO displayed deafness-induced reductions in cross-sectional areas that were not observed in the LNTB or the MNTB. Moreover, with the exception of the LNTB, early-onset deafness resulted in a significant reduction in cell size. The changes in cell size were independent of the tonotopic organization of the nuclei. Cell count and cell density were not affected by early-onset deafness. Specifically, GABA- and Glycin-immunostained sections showed no difference in the number and density of inhibitory neurons in LNTB and LSO between deaf and normal-hearing animals.

The combination of Kanamycin and Bumetanide proved effective in deafening gerbils during early development. Deafness-induced changes occurred along the auditory pathway from AVCN to the target nucleus LSO. Reductions in soma size were observed in most nuclei. Moreover, the cross-sectional areas of AVCN and LSO were reduced following early-onset deafness. The observed morphological changes may contribute to functional degradations in directional hearing.

Supported by DFG VO 640/2-2.

PS 855

Classification of Electrophysiologic Responses to Speech Processed Through an Acoustic Simulation of a Cochlear Implant

Vivian Lou¹; Steven Losorelli¹; Blair Kaneshiro¹; Gabriella Musacchia²; Steven Gianakas¹; Nikolas Blevins³; Matthew Fitzgerald¹

¹Stanford University; ²University of the Pacific;

³Department of Otolaryngology-Head and Neck Surgery, Stanford University School of Medicine

To maximize speech understanding, post-lingually deafened recipients of cochlear implants (CI) face a lengthy period of adaptation to a signal that is degraded relative to that heard by individuals with normal hearing (NH). CI recipients often have difficulty accurately describing what they hear, and when they fail to identify a sound, it is unclear whether they are receiving insufficient information from the implant or have not learned the

appropriate label for a given sound. Thus, both clinicians and researchers would benefit from objective methods to assess sound identification regardless of the reporting ability of a patient. The frequency following response (FFR) is an obligatory evoked potential that closely tracks the stimulus features of a sound. We have previously demonstrated in NH individuals that a classification algorithm applied to the FFR can predict stimulus labels to both syllables and musical stimuli. As a first step toward extending this approach to clinical populations, we investigate whether classification can accurately label responses to stimuli processed through a noise vocoder.

Thirteen NH participants (aged 18-35) participated in a two-session experiment. In each session, we first recorded 2500 sweeps of the FFR to each of six vowel stimuli (/hɔ/, /hʌ/, /hi/, /hi/, /hu/, and /hʊ/). Participants subsequently completed a vowel identification task using these same stimuli without feedback. In one session (vocoded condition), the vowels were vocoded using an 8 of 22 channel peak-picking noise vocoder with 8 dB per octave filter slopes; the other session used the unaltered vowels (intact condition). No participant reported prior exposure to vocoded speech, and the order of each condition was randomly assigned. Vowel labels were predicted from FFRs using a classification algorithm (linear discriminant analysis); resulting confusion matrices were then compared to perceptual responses.

Participants identified vowels with high accuracy in both intact (77-98% for single vowels) and vocoded conditions (50-92%). The FFR classification algorithm also labeled vowels in the intact condition, but with a lower accuracy (70-89%). Notably, the classification algorithm was more accurate for the vocoded condition (92-100%). These results suggest that vocoding preserves and may enhance features of the vowels that contribute to accurate classification. While our findings suggest that a classification approach may be feasible with hearing-impaired individuals who receive a degraded signal, we need to better understand the relationship between perceptual responses and the neural features on which the classification algorithm bases its predictions.

PS 856

Delayed Bilateral Implantation in Children Promotes Aural Preference in Brainstem Processing of ITDs

Melissa J. Polonenko; Claire Salloum; Blake C. Papsin; Karen Gordon
Hospital for Sick Children

Objective: To evaluate brainstem processing of interaural timing differences (ITD) in children who received bilateral cochlear implants (CIs) with limited delay (2 years).

Background: Perception of binaural cues is important for localizing sound and listening in noisy environments. Two CIs stimulate the bilateral auditory pathways, but prolonged unilateral stimulation promotes asymmetric brainstem development that persists with bilateral experience. We hypothesized that these developmental brainstem asymmetries could impede binaural processing in the brainstem.

Methods: Thirty-two children who received their first CI at age (mean±SD) 1.9±1.1 years old and used two CIs for 1.8±0.8 years participated: 15 children received CI2 with minimal to no delay (0.41±0.46 years) and 17 children used CI1 for 5.2±2.6 years before receiving CI2. Electrophysiological measures of brainstem activity were evoked by biphasic electrical pulses presented at 11 Hz at maximum comfortably loud levels. Stimuli were presented unilaterally and bilaterally at ITDs ranging from 0-2 ms leading from both ears. Peak latency differences across ITD were assessed using linear mixed effects regression.

Results: Peak latencies of unilaterally evoked brainstem responses were more asymmetric in children with long (0.18±0.13 ms) than short (0.01±0.14 ms) inter-implant delays ($F(1,31)=15.4$, $p<0.001$). Bilateral responses contained multiple peaks at latencies corresponding to the unilateral wave V latencies for ITDs $>\pm 0.4$ ms. The latency difference between these bilateral peaks increased with ITD (slope: $t(80.3)=-3.3$, $p=0.001$), but were smaller for ITDs leading from CI2 versus CI1 in the long delay group (hemifield*group: $t(86.6)=-3.0$, $p=0.004$). This hemifield asymmetry for peaks in the bilateral responses increased with larger asymmetries in unilateral response latencies ($\chi^2(1)=8.6$, $p=0.003$). To assess binaural integration, bilateral responses were compared with the sum of the unilateral responses (binaural difference (BD)) across ITDs. BD latency increased with ITD (slope: $t(27.9)=16.3$, $p<0.001$), but at a slower rate for ITDs leading from CI2 than CI1 for the long delay group (ITD*hemifield: $t(37.8)=-3.4$, $p=0.002$). This hemifield difference in ITD processing worsened logarithmically with years delay to bilateral implantation ($R^2=0.30$, $F(1,30)=12.9$, $p=0.001$), even after correcting for asymmetries in unilateral responses ($R^2=0.39$, $F(1,30)=19.2$, $p=0.001$).

Conclusion: Brainstem processing of ITDs is affected by a period of unilateral stimulation in development, even after years of bilateral CI experience. After correcting for asymmetries in unilateral brainstem responses, children with long inter-implant delays continue to exhibit asymmetric ITD processing compared to their peers with minimal delay to bilateral implantation, which may compromise binaural hearing development.

PS 857

The Representation of Speech in a Biophysically Detailed Model of the Ventral Cochlear Nucleus

Melih Yayli; Ian C. Bruce
McMaster University

Biophysically detailed representations of neural network models provide substantial insight to underlying neural processing mechanisms in auditory systems. For simple biological systems the behavior can be represented by simple equations or flow charts. But for complex systems more detailed descriptions of individual neurons and their synaptic connectivity are typically required. Creating extensive network models allows us to test hypotheses, apply specific manipulations that cannot be done experimentally and provide supporting evidence for experimental results. Several studies have been made on establishing realistic models of the cochlear nucleus (Manis and Campagnola, *Hear. Res.*, 2018; Eager et al, *Proc. 10th Aust. Int. Conf. on Speech Science and Technology, SST. 2004*), the part of the brainstem where sound signals enter the brain, both on individual neuron and networked structure levels. These models are based on both in vitro and in vivo physiological data, and the models successfully demonstrate certain aspects of the neural processing of sound signals. Even though these models have been tested by using tone bursts and isolated phonemes as stimuli, the representation of speech in the cochlear nucleus and how it may support robust speech intelligibility remains to be explored with these detailed biophysical models. In this study, a biophysically detailed model of microcircuits in the cochlear nucleus is created based on Manis and Campagnola (*Hear. Res.*, 2018). We have updated this model to take inputs from the new phenomenological auditory periphery model of Bruce et al. (*Hear. Res.*, 2018). Different cell types in the cochlear nucleus are modelled by detailed cell models of Rothmann and Manis (*J. Neurophys.*, 2003). Networked structures are built out of them according to published anatomical and physiological data. The outputs of these networked structures are used to create neurograms to investigate the representation of different phonemes and words and are compared to published physiological data (Blacburn & Sachs, *J. Neurophys.*, 1990; Delgutte, *The Handbook of Phon. Sci.*, 1997; Delgutte et al., *Psychophys. and Physio. Adv. in Hear.*, 1998). The ultimate goal of this study is to incorporate physiologically-detailed models of brainstem processing into neural-based predictors of speech intelligibility.

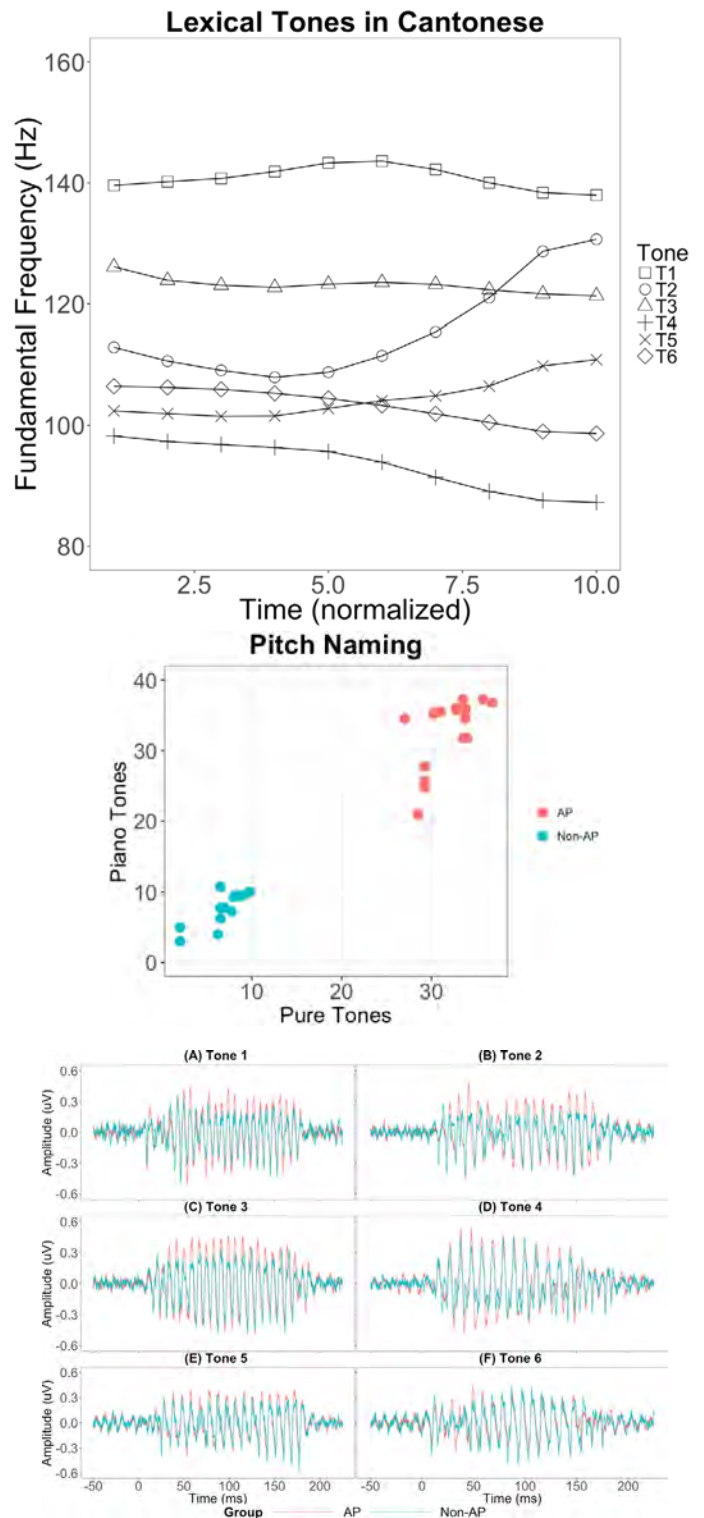
[Supported by the Turkish Ministry of Education and the Natural Sciences and Engineering Research Council of Canada (Discovery Grant No. 261736).]

Neural Encoding of Pitch in Individuals with Absolute Pitch

Akshay Maggu¹; Joseph Lau²; Patrick Wong²; Mary Waye²

¹Kresge Hearing Research Institute; ²The Chinese University of Hong Kong

Absolute pitch (AP) is a rare ability to name a given pitch without any reference to another pitch. AP is known to be influenced by cultural (Baharloo et al., 1998) and genetic factors (Zatorre, 2003). AP has a higher reported prevalence in speakers of East-Asian tone languages (Deutsch et al., 2004, 2006), which may in turn be associated with the perception of lexical tones (Burnham et al., 2015). Whether or not the processing of AP is influenced by lower-level auditory perceptual processes is a matter of ongoing debate. In order to test the effects of AP on lower-level auditory perceptual encoding, we examined the Frequency Following Response (FFR) to pitch from individuals with AP. FFR is an auditory event-related potential that is considered to originate from the inferior colliculi of the auditory brainstem for stimuli with a fundamental frequency (F0) greater than 100 Hz (Bidelman, 2018), and it captures the neural representation of acoustic signal (F0). Because AP and lexical tone perception may be linked behaviorally (Burnham et al., 2015), we investigated the role of auditory perceptual processes in AP processing by comparing the FFR to six Cantonese lexical tones (Figure 1) from speakers of Cantonese with AP and those without AP. Based on a test of pitch naming of piano and pure tones (Baharloo et al., 1998), we selected 17 Cantonese-speaking subjects with AP and 13 Cantonese-speaking subjects without AP (Figure 2). We compared these two groups of subjects across four measures of FFR, namely, Stimulus-to-Response Correlation, Pitch Error, Root-Mean-Square amplitude (RMS), and Signal-to-Noise Ratio. We found that the subjects with AP outperformed the subjects without AP on all measures of FFR (Figures 3 and 4). These findings suggest that AP is linked to enhanced encoding of F0 in the early stages of the ascending auditory pathway at least in speakers of a tone language. These findings add to the growing literature concerning the role of cortical (Zatorre et al., 1998) and subcortical contribution to AP.



roles of neurotrophic signaling in shaping functional properties of developing NM neurons.

Two-hour bath application of BDNF significantly reduced total K_V current at E13. Membrane time constant and input resistance increased due to reduction in low-voltage activated potassium (K^+_{LVA}) current. Interestingly, membrane capacitance—an indirect measure of neuronal size—also increased compared to control neurons; suggesting a possible role of BDNF-TrkB signaling in dendrite maintenance during early development. Action potentials (APs) had slower fall rate and longer half width due to reduction in high-voltage activated potassium (K^+_{HVA}) current. These effects were less dramatic at E15. A reduction in total K_V current was only observed at lower membrane voltages, indicating a decrease in K^+_{LVA} . In agreement with this, time constant and input resistance increased while AP kinetics remained similar. BDNF showed an opposite effect on some intrinsic properties at E18. For example, we observed a slight increase in total K_V current with no difference in passive membrane properties compared to control neurons. However, AP kinetics improved, indicating that BDNF increased K^+_{HVA} current only. The effect of BDNF was blocked with a potent and selective antagonist of the TrkB receptor. We observed no changes in membrane capacitance beyond E15, suggesting minimal contribution of BDNF to dendrite regulation. In stark contrast, application of NT-3 reduced K_V current (mainly K^+_{HVA}) at E18 but not at E13. In summary, neurotrophic signaling plays a dynamic and bidirectional role in regulating K_V current and AP properties of developing NM neurons. This directional effect reversed between E15 and E18, a developmental time period corresponding to hearing onset and functional refinement. Our findings suggest that neurotrophic signaling promote the maturation of functional phenotypes of developing auditory brainstem neurons.

PS 860

Neural Coding of Vowels in Interrupted Noise: Effect of Glimpse Duration

William J. Bologna; Michelle R. Molis; Brandon M. Madsen; Curtis J. Billings
VA RR&D NCRAR

Speech communication is difficult when background sounds fluctuate in level and intermittently mask portions of the speaker's intended message. Listeners can interpret the message by "glimpsing" brief audible segments of speech when the background level is relatively low. This complex perceptual ability is highly variable across individuals, even among younger adults with normal hearing sensitivity. One potential source of variability in glimpsing is the fidelity of neural coding of

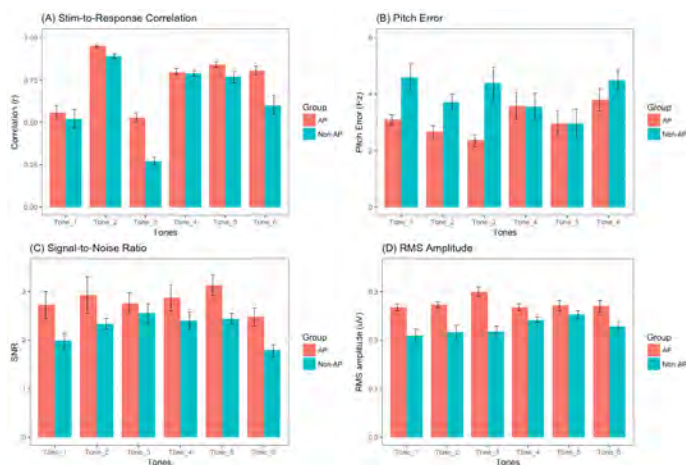


Figure captions

Figure 1. Lexical tones in Cantonese. (F0 ranges: T1: 135–146 Hz, T2: 105–134 Hz, T3: 120–124 Hz, T4: 85–99 Hz, T5: 102–113 Hz, T6: 100–106 Hz).

Figure 2. Distribution of AP and Non-AP subjects across the identification of piano (Y-axis) and pure tones (X-axis).

Figure 3. Averaged FFR waveforms of AP and Non-AP group for lexical tones 1-6 (A)-(F).

Figure 4. Comparison of AP and Non-AP groups across the six lexical tones of Cantonese for (A) Stimulus-to-Response Correlation; (B) Pitch Error; (C) Signal-to-Noise Ratio; and (D) RMS Amplitude. Overall, the AP group outperformed the Non-AP group on all the FFR measures. Error bars = ±SEM.

PS 859

Neurotrophic factors regulate functional properties in the developing auditory brainstem

Hui Hong; Momoko Takahashi; Jason Tait Sanchez
Northwestern University

Neurotrophins are proteins that regulate development, maintenance and function of nervous systems. Fundamental to this is the role of brain-derived neurotrophic factor (BDNF) and neurotrophin-3 (NT-3) – along with their respective high-affinity tyrosine receptor kinase, TrkB and TrkC. The diverse expression patterns of neurotrophins in the vertebrate nervous system provide a unique opportunity to investigate the establishment of normal structure and function during neuronal ontogenesis. For example, in the chicken cochlear nucleus magnocellularis (NM), the expression of TrkB receptors is present at embryonic (E) day 7, reduced by E15 and minimal at E18. The expression of TrkC receptors stays constant with maturation; however, their functional role is largely unexplored. Using patch-clamp electrophysiology, we report here the diverse

speech cues during dips in the level of a masker. The degree of fidelity may depend on glimpse duration. Longer glimpses of speech may provide sufficient time for brainstem neurons to phase-lock to important speech cues. Conversely, brief glimpses of speech may not be well encoded at the level of the brainstem. As such, a physiological measure of brainstem coding of glimpses of varying durations may help explain how processing limitations impact speech understanding in noise and contribute to the variability observed in behavioral studies. In this study, electrophysiological recordings of the envelope following response (EFR) were elicited from younger adults with normal hearing thresholds in response to synthetic vowels in quiet and in interrupted noise. A steady-state vowel /a/ was synthesized with a characteristically female fundamental frequency (230 Hz) that is well represented by phase-locked activity in the EFR. Speech-shaped noise was interrupted at different rates by rectangular gating functions and mixed with the vowel at a negative signal-to-noise (SNR) ratio, such that the final stimuli contained vowel glimpses of varying durations. Responses in quiet contained a phase-locked representation of the periodicity envelope of the vowel, measured using the magnitude of the response at the fundamental frequency and associated harmonics. Responses during glimpses in interrupted noise revealed vowel coding that approached the response strength obtained in quiet, but longer glimpses generally resulted in more robust coding than shorter glimpses. Results will be discussed in terms of the role that bottom-up neural coding plays in glimpsing. Future studies will investigate individual differences in neural coding as a potential contributing factor to the variation in speech recognition in fluctuating backgrounds. [Work supported by NIH TL1TR002371/R01DC015240 and VA/RR&D I01RX002139].

PS 861

Auditory Brainstem Responses to Speech and Click Stimuli in Preterm Infants

Kerry Walker¹; Beth Prieve¹; Linda Hood²
¹*Syracuse University*; ²*Vanderbilt University*

Background:

Speech-stimuli evoked auditory brainstem response (sABR) provides information about sub-cortical spectral and temporal processing of an individual's ability to encode complex sounds contributing to cognitive functioning. Understanding the processing of complex stimuli is particularly important in preterm infants, who have a high prevalence of delayed or disordered language in toddlerhood. Previous studies have shown that sABR is sensitive in detecting language and auditory processing disorders in school-age children

(Cunningham et al., *Clin Neurophysiol*, 112, 158-67, 2001) and can be measured in infants (Anderson et al., *JASA*, 137, 3346-55, 2015). Because click-evoked ABR is the standard-of-care for detection of congenital hearing loss in preterm infants, it is hypothesized that sABR may be highly correlated with later language ability at older ages. The current study is a first-step towards this investigation, with the purpose being to describe the timing characteristics of sABR and click-evoked ABR in preterm infants tested at four different gestational ages (GA).

Methods:

Speech-evoked ABR was measured in 36 preterm infants to a 40 ms synthesized /da/. Testing was completed in newborns aged 33 weeks GA (n=10) and 35 weeks GA (n=7) in the neonatal intensive care unit. Infants aged between 48-52 weeks GA (n=12) and 62-66 weeks GA (n=7) were tested in a quiet or sound-treated room. The Intelligent Hearing Systems SmartEP was used to collect sABR to /da/ presented at 80 dB SPL. The sABR was measured in one ear in which wideband acoustic absorbance, otoacoustic emissions and click-evoked ABR were considered normal.

Results:

All ABR absolute and interpeak latencies were visually detected 100% of the time at all ages and significantly correlated with GA. The presence of sABR waves increased with GA. The absolute latencies of waves associated with the onset (A) and offset (O) of the stimulus, as well as those associated with the envelope following response (EFR), decreased with GA. However, there was not a significant correlation between the A-O interpeak latency and GA.

Conclusions:

Speech-evoked ABR responses were measurable in premature infants with more waves, onset, offset and those associated with the EFR, being detectable with development. The development of interpeak latency (I-V) of the click-evoked ABR and onset-offset (A-O) sABR were different than each other in premature infants. The non-significant A-O interpeak latency with GA indicates similar rates of change across age for their respective sub-cortical generator sites. [Funding: NIH-NIDCD R01DC011777]

Low-Sound-Level Auditory Processing and the Effects of Noise Exposure

Warren M. H. Bakay¹; Christopher J. Plack¹; Michael A. Stone²

¹Manchester Centre for Audiology and Deafness;

²Manchester Centre for Audiology and Deafness, NIHR Manchester Biomedical Research Centre

Introduction

Sub-clinical hearing loss appearing only at low-sound-levels has been reported in humans with no change in absolute thresholds (Stone, Moore, & Greenish, 2008), and with small but sub-clinical changes in thresholds (Vinay & Moore, 2010). Low-sound-level deficits are contrary to the suspected mechanism of Hidden Hearing Loss (HHL): cochlear synaptopathy of high-threshold fibres (Kujawa & Liberman, 2009; Furman et al., 2013; Hesse & Bakay et al., 2016). These low-level sub-clinical hearing deficits occur in individuals with a history of exposure to high-level noises. Since traditional hearing losses compress hearing range, this low-sound-level impairment should occupy a larger portion of that reduced range.

Goal

To quantify low-sound-level deficits and determine their correlation to sound exposure history, and to determine whether they affect speech comprehension in people with sub-clinical hearing loss.

Methods

Participants were recruited between the ages of 30 and 70 and underwent a screening session of standard clinical measures: Pure Tone Audiometry (PTA), Tympanometry, Threshold Equalising Noise (TEN) tests, and Interaural Timing Difference (ITD) threshold testing). Participants were grouped based on noise exposure determined using the Noise Exposure Structured Interview (NESI).

Thresholds were determined at three different levels of TEN noise: 0dB (unmasked, 12dB SL and 24dB SL. Preliminary results suggest a difference in TEN test thresholds between the 12dB and 24dB masking levels.

Subjects with elevated PTA at 4kHz but not at 1kHz were invited for electrophysiological testing, comprising the Auditory Brainstem Response (ABR) and Auditory Steady State Response (ASSR). These were recorded using Biosemi electrodes from multiple sites, including in the ear canal using tiroprades.

Octave band chirp stimuli to induce ABRs were presented in two different frequency bands (750-1500Hz, and 2.5–5 kHz) and three different intensity levels (100dB SPL, 30dB SL, and 15dB SL). ASSR stimuli were presented

in two different complexes (2 carriers, 2 modulators, with 2 octaves between carriers, at 750Hz/3kHz, and 1kHz/4kHz).

Finally, participants underwent psychophysical tasks to determine their ability to differentiate small changes in frequency (frequency difference limens) and amplitude modulation depth, at 5 different frequencies (750Hz, 1kHz, 3kHz, 4kHz, 6kHz) and the effect that noise exposure history has on these tasks.

Acknowledgements

This research was supported by grant MR/M023486/1 from the Medical Research Council (MRC) and was sponsored by the University of Manchester.

Auditory Cortex: Plasticity

PS 863

Neuroinflammation Mediates Noise-Induced Synaptic Imbalance and Tinnitus

Weihua Wang¹; Li Zhang²; Alexander Zinsmaier¹; Genevieve Patterson¹; Emily Leptich¹; Savannah Shoemaker¹; Edward Pace³; Jinsheng Zhang³; Sungchil Yang⁴; Shaowen Bao¹
¹University of Arizona; ²UNIV OF ARIZONA; ³Wayne State University; ⁴City University of Hong Kong

Hearing loss is a major risk factor for tinnitus, hyperacusis and central auditory processing disorder. Although recent studies indicate that hearing loss causes neuroinflammation in the auditory pathway, the mechanisms underlying hearing loss-related pathologies are still poorly understood. We examined neuroinflammation in the auditory cortex following noise-induced hearing loss (NIHL) and its role in tinnitus in rodent models. Our results indicate that NIHL is associated with elevated expression of proinflammatory cytokines and microglial activation—two defining features of neuroinflammatory responses—in the primary auditory cortex (AI). Genetic knockout of tumor necrosis factor alpha (TNF- α) or pharmacologically blocking TNF- α expression prevented neuroinflammation and ameliorated the behavioral phenotype associated with tinnitus in mice with NIHL. Conversely, infusion of TNF- α into AI resulted in behavioral signs of tinnitus in both wildtype and TNF- α knockout mice with normal hearing. Pharmacological depletion of microglia also prevented tinnitus in mice with NIHL. At the synaptic level, the frequency of miniature excitatory synaptic currents (mEPSC) increased and that of miniature inhibitory synaptic current (mIPSC) decreased in AI pyramidal neurons in animals with NIHL. This excitatory-to-inhibitory synaptic imbalance was completely prevented by pharmacological blockade of TNF- α expression. These

results indicate that noise-induced neuroinflammation leads to perturbations in the excitation-inhibition balance, which may impair central auditory processing.

PS 864

Noise-Induced Plasticity in the Brainstem, Auditory Cortex and Anterior Cingulate: Implications for Functional Connectivity and Acoustic Hyper-Reactivity

Krystyna Wieczerek; Kaela Scott; Björn Herrmann; Sarah Hayes; Brian Allman
University of Western Ontario

It is well-established that noise exposure (NE) can affect areas of the brain outside the classical auditory pathway (e.g., hippocampus; cerebellum). At present, however, it is not clear whether the nature and extent of noise-induced plasticity observed in the auditory cortex is also present in higher-order cortical areas (e.g., anterior cingulate), and if the functional connectivity between these brain regions is affected by noise exposure. In the present study, we exposed rats to loud noise (120 dB SPL broadband noise for 2h), and compared the magnitude and time-course (pre-NE, 2 days and 7 days post-NE) of noise-induced plasticity in the brainstem, auditory cortex, and anterior cingulate. We used (1) electrophysiological recordings, including auditory brainstem responses (ABR), spontaneous oscillatory activity, and 40 Hz auditory steady state responses (ASSR), as well as (2) reflexive behavioral responses to sound via the acoustic startle reflex. For passively-listening animals with chronically-implanted electrodes, we found that neither the auditory cortex nor the anterior cingulate demonstrated changes in spontaneous oscillations post-NE, whereas sound-evoked responses showed a differential effect in these brain regions, characterized by enhanced central gain in only the auditory cortex. Adding to this regional disparity, the inter-trial coherence of the 40 Hz ASSR in the auditory cortex was unaffected by NE, yet this metric was significantly decreased in the anterior cingulate, providing evidence of reduced synchronization of these neural ensembles. Furthermore, there was an early (2 days) and persistent (7 days) reduction of the phase-locking value between auditory cortex and anterior cingulate post-NE; findings which suggest that noise-induced hearing loss leads to dysfunctional network activity. At the level of the brainstem, there was a ~50% reduction in cochlear output (i.e., reduced ABR wave I amplitude) at 7 days post-NE; however, these same rats showed an increase in their reflexive reactivity to moderately-loud sounds (i.e., increased startle responses). Overall, we observed a differential time-course between the onset of cortical plasticity (at 2 days post-NE) and the brainstem-mediated reflexive behavior to moderately-loud sounds

(at 7 days post-NE). Collectively, the present work highlights the complex and regionally-specific plasticity observed throughout subcortical and cortical areas in the days following noise-induced hearing loss.

PS 865

Early-Life Stress Impairs Perceptual Gap Detection in Gerbils

Yi Ye; Michelle M. Mattingly; Merri J. Rosen
Hearing Research Group, Dept. Anatomy & Neurobiology, Northeast Ohio Medical University

Developmental stress (early-life stress, ELS) is known to have widespread effects on learning, cognition, and emotional regulation. Brain regions involved in these functions (e.g. frontal cortex, amygdala, and hippocampus) project to auditory cortex (ACx) and are especially vulnerable to developmental stress. However, despite the increased plasticity of the ascending auditory system during critical periods of development, it is unexplored whether developmental stress affects basic auditory perception and ACx function. The ability to detect short gaps in ongoing sound, when measured by gap-inhibition of the acoustic startle response (gap-PPI of the ASR), is known to require ACx. We thus tested whether early-life stress caused impaired behavioral detection of short gaps using gap-PPI, and whether ELS affected gap detection thresholds in ACx neurons.

ELS gerbils (n=23, 10F/13M) were maternally separated and restrained for 2 hrs/day at unpredictable times from their 9th postnatal day (P9) through P24. They were compared with Control animals (n=16, 9F/7M). Gap detection thresholds were obtained using gap-PPI of the ASR at two age points: over three sessions from P33-P39 (during adolescence) and over three sessions from P83-P89 (during adulthood). Blood corticosterone levels were acquired at P33, immediately following the first session of acoustic startle testing. In separate groups of ELS and Control animals, gap detection thresholds of individual neurons were measured using extracellular recordings in primary ACx.

The ELS group exhibited lower blood corticosterone levels than Controls in response to an acute stressor (the first session of acoustic startle), indicating that the ELS induction protocol was effective in inducing stress (ELS animals frequently show lower CORT levels after an acute stressor). In adolescence, the ELS group had higher (poorer) gap detection thresholds than controls. This difference in detection lasted into adulthood (although at a smaller magnitude). The ability to detect shorter (< 100ms) gaps was more impaired by ELS than the ability to detect longer (> 150ms) gaps; this suggested the involvement of ACx, as cortical

inactivation is known to impair detection of shorter gaps only. ELS also affected auditory learning: ELS animals showed less improvement in gap detection thresholds across sessions than controls. Our results indicate that early life stress, which is known to affect higher-order cognition, also impairs basic sensory perception, and this effect is maintained into adulthood. We will compare these perceptual results with electrophysiological recordings, to determine whether gap detection thresholds of auditory cortical neurons reflect the poorer gap detection abilities of ELS animals.

PS 866

Early-Life Stress Disrupts Amplitude Modulation Detection in Gerbils

Kate A. Hardy¹; Ramya Gutta¹; Merri J. Rosen²
¹*Northeast Ohio Medical University*; ²*Hearing Research Group, Dept. Anatomy & Neurobiology, Northeast Ohio Medical University*

Stress during adulthood impairs auditory learning in rodents and induces various neural changes in auditory cortex. Despite the heightened plasticity of sensory systems during critical periods of development, the effects of *developmental* stress (early-life stress, ELS) on auditory perception and learning are largely unexplored. ELS is known to affect various cognitive processes including learning, attention, and memory. Brain areas involved in these functions (e.g. frontal cortex, amygdala, and hippocampus) project to auditory cortex and are especially vulnerable to stress during development. Here we test the idea that ELS may disrupt a specific auditory percept known to require an intact auditory cortex.

To assess the effects of ELS on auditory perception and auditory learning capacity, Mongolian gerbils were tested with an operant amplitude modulation (AM) depth detection task previously shown to require an intact auditory cortex. During postnatal days (P) 9-24, ELS animals were maternally separated and restrained for two hours at random times on ten non-consecutive days. Beginning at P28, both ELS and Control animals were trained using a conditioned avoidance procedure to detect sinusoidal amplitude modulation in a broadband noise. After reaching criterion performance at a fully-modulated depth, animals were tested daily for seven days to determine their AM depth detection thresholds, calculated using a signal detection theory framework.

ELS animals mastered procedural learning for the basic task (detecting a fully-modulated AM depth at criterion level) more quickly than Controls. However, across the subsequent 7 days of perceptual learning, ELS animals exhibited higher (poorer) depth detection thresholds

than Controls. Further, while Controls improved their thresholds over testing days, ELS animals did not. These differences could not be attributed to task proficiency or proxies for attention or motivation.

Our findings indicate poorer auditory perception and perceptual learning in animals that had experienced ELS. This outcome occurred even though the ELS animals had better initial proficiency on the basic task than Controls. This better initial procedural learning may have been affected by differential anxiety-based activity during exposure to the new environment and the challenging task, an idea supported by suppressed corticosterone levels during acute stressors known to occur in ELS rodents. The deficits in perception of time-varying signals and perceptual learning implicate changes at the level of auditory cortex and frontal cortex, regions required for AM perception and auditory learning.

PS 867

An Investigation into the White Matter Deficits associated with Tinnitus and Hearing Loss

Rafay Khan; Sara Schmidt; Somayeh Shahsavarani; Yihsin Tai; Fatima Husain
University of Illinois at Urbana-Champaign

Tinnitus, the perception of sound in the absence of an external source, has been attributed to both changes in the periphery (e.g. hearing loss) and changes in the central auditory pathways and the cortex. It is unclear, however, what specific neural changes occur that cause the generation and persistence of tinnitus. More confusing still is the precise nature of the association between hearing loss and tinnitus – a majority of tinnitus patients have decreased hearing sensitivity, but half of those with hearing loss do not have tinnitus. Neuroanatomy can be broadly divided into 3 components – grey matter, white matter and cerebrospinal fluid. White matter (WM) consists mainly of nerve fibers and their myelin sheaths (also called tracts). Changes in WM tracts could play an important role in the generation and persistence of tinnitus, and only a handful of studies have attempted to investigate these changes to date, with mixed findings. Of those studies, even fewer have attempted to parse out the impact of hearing loss within tinnitus. In this study, we attempted to distinguish WM differences between those who had tinnitus and hearing loss (TIN-HL) and those who had tinnitus but no hearing loss (TIN-NH), by using the MRI technique of diffusion tensor imaging (DTI). DTI measures the diffusion of water molecules in WM tracts, and provides information about the microstructural integrity and orientation of targeted tracts. Preliminary data from our current study (TIN-NH (n =11, mean age = 44.82) vs TIN-HL (n=36, mean age = 56.03) suggests

five regions of difference between the two groups – the left anterior thalamic radiation (ATR), right inferior fronto-occipital fasciculus, right inferior longitudinal fasciculus, forceps minor, and forceps major (both located in the cerebellum). These regions demonstrated deficits in TIN-HL subjects compared to TIN-NH subjects, using a FWE correction threshold of $p < 0.05$. Studies have noted the involvement of the left ATR in general hearing loss, and the cerebellum has been shown to be a sufficient generator of tinnitus. The two fasciculi implicated here may be associated with the non-perceptual aspects of tinnitus, and are believed to be associated with speech generation. These findings shed further light on our understanding of tinnitus, its relationship to hearing loss, and other cognitive factors. This is an ongoing study, and the inclusion of more TIN-NH subjects (typically a much smaller proportion of the tinnitus population than TIN-HL) will help us further understand the neural differences observed.

PS 868

Learning for Fun: Auditory Training in Mice using Wheel-Running as a Reward

James L. Sinclair; Jennifer F. Linden
UCL Ear Institute

Running wheels are among the most common forms of environmental enrichment recommended for laboratory mice (Olsson and Dahlborn, 2002 *Lab Anim*). Wheel running appears to be intrinsically rewarding for mice, as demonstrated by reports that even wild mice will voluntarily use running wheels placed in nature (Meijer and Robbers, 2014 *Proc R Soc B*). Use of running wheels has also been shown to enhance neurogenesis, learning, and memory in mice (van Praag et al., 2000 *Nature Rev Neurosci*).

Less explored is the question of whether or not running wheels could be used as an effective reward for operant conditioning in mice, for example in auditory discrimination tasks. Will mice perform repeated trials of behavioural tasks in order to obtain short bouts of wheel-running as a reward? If so, could this strategy be used to train mice in their home cages, without any need for food or water restriction?

We describe the development and validation of an inexpensive (~£40) device for training mice on behavioural tasks in the home cage, using wheel-running as a reward. The device consists of a standard plastic running disk for mice, mounted on a custom 3D-printed plastic housing designed to fit inside a medium-sized rodent cage. An Arduino microcontroller inside the housing transmits information from a rotary encoder and other sensors to a computer via Bluetooth, enabling remote monitoring of wheel usage and remote triggering of the wheel brake.

We tested the effectiveness of behavioural training with this device in pilot experiments involving two strains of mice commonly used in auditory research (CBA/Ca and C57BL/6). We observed that mice rapidly became accustomed to the presence of the device in their home cages. When the wheel was left unbraked, one C57 mouse ran up to 4.5 hours per night in bouts of 2.5 +/- 2.3 min (123 bouts). In ongoing experiments, we are determining how well-motivated mice are by access to the wheel if it is unbraked for only short bouts of running (e.g., 30 s), and whether mice can learn to trigger unbraking of the wheel (e.g., by stepping on a pedestal). Our goal is to use this approach for go/no-go auditory discrimination training in mice.

Supported by the Medical Research Council (MR/P006221, J.F.L.).

PS 869

Assessment of Auditory Performance in a Mouse Model of Cross-Modal Plasticity

Ye-Hyun Kim¹; James H. Engel¹; Katrina M. Schrode¹; Hey-Kyoung Lee²; Amanda Lauer²
¹Johns Hopkins University School of Medicine; ²Johns Hopkins University

Background

Cross-modal plasticity refers to functional enhancement of remaining senses following deprivation or loss of a sensory modality. Previous studies have demonstrated enhanced neural responses including increased sensitivity and frequency selectivity in the auditory cortex *in-vitro* following short-term visual deprivation in adult mice (Petrus et al., 2014). This cross-modal plasticity is mediated by enhanced synaptic transmission and circuit refinement in the thalamocortical layers in the cortex (He et al., 2012; Meng et al., 2015, 2017; Petrus et al., 2015). However, whether these visual deprivation-induced cross-modal neural changes translate into improved auditory perception and performance remains unclear.

Methods

To investigate the cross-modal influence of visual deprivation on auditory behaviors, CBA/CaJ mice underwent binocular enucleation at 3-4 weeks old. Young adult mice were trained on conditioned lick suppression tasks to test tone detection and frequency discrimination. Mice were also tested for acoustic startle response (ASR) and prepulse inhibition (PPI) to evaluate performance on behaviors that do not require learning. Auditory brainstem response (ABR) and middle latency response (MLR) were measured to screen for the effects of visual deprivation on non-behavioral hearing functions. Both enucleated and sighted control mice were housed and maintained in normal 12 hour light-dark schedule throughout the entire experimental procedure.

Results

Control and enucleated mice showed similar tone detection sensitivity and frequency discrimination in the conditioned lick suppression test. Compared to control mice, enucleated mice exhibited more stable performance in tone detection across test days, while their performance in frequency discrimination was more variable when a randomly roving level was introduced to the stimuli.

Both control and enucleated mice showed normal reactivity to sound as measured by ASR. However, when the startle stimulus was presented in noise, control mice showed significantly increased ASR amplitude compared to the enucleated mice. Furthermore, control and enucleated mice displayed no significant difference in PPI, indicating similar auditory temporal acuity and responses to changes in frequency. In addition, there was no significant difference between groups for ABRs or MLRs, suggesting normal synchronous neural population responses in brainstem and auditory-thalamocortical pathways.

Conclusions

Our findings hint toward the possibility that, while visual deprivation-induced cross-modal plasticity occurs at the synaptic and circuit levels, it may not directly influence basic auditory functions. Assessment of more complex auditory behavior in visually deprived adult animals may reveal behavioral enhancements, but laboratory mice are not ideally suited for such experiments.

PS 870

Inhibitory strength is differentially altered along the corticostriatal circuit during task learning in normal-hearing and hearing-loss animals

Nihaad Paraouty; Joey A. Charbonneau; Todd M. Mowery
New York University

Background

Developmental hearing loss (HL) leads to deficits in auditory perceptual abilities. When peripheral deficits are treated, perceptual thresholds often return to control values. However, on many non-perceptual (cognitive) tasks, difficulties may persist. This suggests that regions downstream of the primary auditory cortex (ACx) are sensitive to developmental HL. One such region, which is highly involved in language development, is the auditory striatum. Accordingly, we have recently shown that animals that have recovered from HL continue to show significant changes in inhibitory synaptic properties in the striatum (Mowery et al., 2017). More precisely, reduced inhibitory synaptic strength in the striatum does not resolve during recovery from developmental HL.

During associative learning, Sarro et al. (2015) reported a decrease in cortical inhibitory synaptic strength in layer 2/3 neurons. Here, we asked whether learning produces a similar change in inhibition in ACx layer 5 neurons and their target medium spiny neurons (MSNs) in the striatum. Our primary aim was to determine how initially reduced inhibitory synaptic strength is compensated for in HL individuals as they learn an auditory task.

Methods

Adult Mongolian gerbils were trained on an amplitude-modulation (AM) rate discrimination task using an appetitive reinforcement operant conditioning procedure. The animals were trained to initiate each trial by a nose poke, and a 12-Hz AM stimulus indicated the availability of a food pellet (Go stimulus), versus a 4-Hz AM stimulus which signaled the absence of a reward (Nogo stimulus). A sensitivity measure, d' , was computed for each animal across training days. Following each training session, a corticostriatal brain slice was obtained and inhibitory synaptic properties were recorded from ACx layer 5 pyramidal neurons and their target MSNs in the auditory striatum.

Results

Our preliminary data indicate that in NH gerbils, inhibitory strength (IPSP amplitude) is reduced during associative learning in the striatum. For HL animals, in which IPSP amplitude is already reduced, we observe an increase in IPSP amplitude during associative learning. Although the inhibitory synaptic changes that occur in NH and HL animals are opposite in polarity, they each permit learning to occur. That is, initially reduced inhibitory synaptic strength in HL animals moves towards an apex that is approximate to the reduction in inhibitory strength seen in NH animals.

Conclusions

These results suggest that a transient change in inhibition accompanies learning for both NH and HL animals. It also demonstrates how the brain can overcome permanent cellular deficits induced by developmental deprivation.

PS 871

Mismatch Negativity as a Neural Marker of Adaptive Plasticity in Monaural Sound Localization.

Alzaher Mariam; Cloé Verlhac; Pascal Barone;
Mathieu Marx
CerCo

Sound localization and speech in noise segregation abilities rely on binaural integration derived from interaural disparities. In unilateral deafness, binaural processing is altered leading to spatial hearing deficits and the development of adaptive compensatory

strategies expressed by a functional reorganization of the auditory cortex. The aim of the present study is to search for an association between the behavioral deficit in spatial hearing and auditory cortical representation assessed by Mismatch Negativity (MMN). Twenty normal hearing (NH) subjects underwent an oddball paradigm in bin- or monaural condition. The standard sound (100ms pink noise, 10 ms fade in/out) was positioned at a location of 50°, and deviant sound at 10°, 20° and 100° of separation from the standard position.

In the binaural condition, an MMN was observed for each deviant positions. The amplitude of the MMN was progressively higher and the peak latency was shortened with the increasing spatial separation from the standard. In monaural conditions, we observed a similar variation in MMN characteristics when the plugged ear was opposite to the standard. However, the latency at 100° of deviation, which was consequently ipsilateral to the ear plugged, appeared later with values similar to that observed with the other deviant positions. When the earplug was ipsilateral to the standard, no significant MMN was elicited at 10 and 20° of separation, although a slight significant MMN was present at 100° with a delayed latency compared to the binaural condition.

Subjects underwent a sound localization task in a free field with 12 loudspeakers positioned in a semi-circular array. In monaural conditions, we observed the known deficits in sound localization with responses shifted towards the non-plugged side. Further, we showed that the absence of MMN signal corresponds to the location of the deviant stimuli for which the subjects present RMS errors greater than the sound separation in the oddball protocol when the plugged ear was ipsilateral to the standard.

Ongoing experiments on patients with unilateral and bilateral hearing loss revealed compensatory strategies in sound localization in long-duration deaf patients compared to deafened NH subjects. These results will be analyzed and correlated with respect to the MMN values.

Altogether, our results established a link between cortical MMN values and spatial hearing accuracy that can be used as a marker of auditory functional compensatory strategies in unilateral or bilateral deaf patients.

Grant Support. ANR VIRTUALHEARING3D

PS 872

The Effects of Short Term Hearing Loss on Adult Perception and Cortical Cellular Properties

Kelsey L. Anbuhl; Todd M. Mowery; Dan H. Sanes
New York University

A brief period of adult-onset hearing loss (HL) can induce transient changes to auditory perception (e.g., Formby et al., 2003), and these may be associated with homeostatic changes to central nervous system cellular properties (e.g., Clarkson et al., 2016; Zhuang et al., 2017). Here, we tracked the relationship between perceptual performance and auditory cortex (ACx) cellular properties before, during, and after placement of bilateral earplugs. Adult gerbils were trained on an amplitude modulation (AM) rate discrimination task, using an appetitive Go-Nogo paradigm ("Go" stimuli were AM rates between 4.5 to 12 Hz, and the "Nogo" stimulus was 4 Hz AM (broadband noise carrier, 100% depth modulation). Psychometric functions were collected daily until animals reached asymptotic performance (3 sessions in which false alarm (FA) rates were 2, and the number of trials per AM rate was >15). Animals then received bilateral earplugs and performance was again assessed daily for 10 sessions (sound level raised by 40 dB to compensate for earplugs). The plugs were then removed, and performance was again assessed daily at the original sound level. Prior to HL, gerbils exhibited AM rate thresholds of 4.9 ± 0.05 Hz ($n=5$; average \pm SEM). Immediately following HL, gerbils exhibited poorer AM rate thresholds of 5.3 ± 0.16 Hz, but recovered to pre-HL performance levels within 4-10 days.

To assess whether the ACx adapted to HL, we recorded excitatory (EPSP) and inhibitory postsynaptic potentials (IPSP), and intrinsic firing rate in ACx layer 2/3 neurons using thalamocortical brain slices obtained from a separate group of animals ($n=7$). These recordings were obtained after 2 or 10 days of earplugs. After just 2 days of HL, excitatory synaptic strength began to increase, but inhibitory synaptic strength was unchanged. The threshold current required to evoke an action potential was much lower after 2 days of HL, while the maximum current-evoked (600 pA) discharge rate only began to decline after 2 days of earplugs. These results suggest that, at the cellular level, HL induced compensatory changes occurred both rapidly (e.g., increased EPSP amplitude) and slowly (e.g., firing rate). Taken together, these results indicate that short term HL can disrupt perceptual performance even when sound attenuation is compensated, and suggest that changes to CNS cellular properties may affect cortical processing underlying perception.

Support: T32-MH019524 and R01-DC014656

Experimental Auditory Training for Older Listeners Using Rate Discrimination: Effects on Perceptual and Neural Measures

Samira Anderson¹; **Alessandro Presacco**²; Lindsay DeVries³; Edward W. Smith³; Alyson Schapira³; Rachel Robinson³; Reynier Hernandez³; Matthew Goupell⁴; Sandra Gordon-Salant⁴

¹*Department of Hearing and Speech Sciences, University of Maryland; Neuroscience and Cognitive Science Program, University of Maryland;* ²*Institute for Systems Research, University of Maryland, College Park;* ³*Department of Hearing and Speech Sciences, University of Maryland, College Park;* ⁴*University of Maryland*

Introduction: Older individuals, with and without hearing loss, have difficulty understanding speech that is degraded by noise, reverberation, fast talkers, or accented talkers. Central temporal auditory processing deficits in older individuals contribute to these difficulties, and have been observed on behavioral tasks (Fitzgibbons & Gordon-Salant, 1995) and electrophysiologic measures of neural processing (Anderson et al., 2012). This study seeks to understand the neural encoding mechanisms that contribute to central temporal auditory processing deficits and attempt to remediate those deficits through auditory perceptual training. The first phase of our investigation of hierarchical auditory training methods is to evaluate the effectiveness of auditory training focused on a simple judgment in the temporal domain: rate discrimination. The hypotheses are: 1) rate discrimination training will improve perception and neural encoding of trained pulse-rate stimuli; 2) rate discrimination training will improve perception of near-generalization stimuli, but not of far-generalization stimuli; and 3) older listeners will show comparable improvements in perceptual learning and neural processing as younger listeners, but at a slower rate of learning.

Method: Participants are younger normal-hearing, older normal-hearing, and older hearing-impaired listeners. They undergo pre- and post-training neurophysiology measures and behavioral measures, in addition to training sessions with pulse-train stimuli. The neurophysiology measures are auditory steady-state responses (ASSRs) to 1024 sweeps of each of four pulse trains (100, 200, 300, 400 pulses per second, pps), each 30 ms in duration, presented at 75 dB SPL. Pre-post behavioral measures are: 1) rate discrimination at four rates (two of which are near-generalization stimuli); 2) gap detection, gap duration discrimination, and tempo discrimination to 5-tone sequences (mid-generalization); and 3) recognition of time-compressed speech, reverberant speech, and speech in noise (far-

generalization). Training stimuli are the 100 pps and 300 pps pulse trains used in the ASSR measures. Participants train over 9 sessions; each training session consists of four blocks/pulse rate, with 60 trials/block (total of 240 trials/pulse rate).

Results: Preliminary results show that patterns of learning with pulse trains vary across participants. Many participants, both younger and older, exhibit significant improvements at the post-training assessments for both behavioral and electrophysiological measures.

Conclusions: Experimental training with temporally based acoustic stimuli holds promise for improving auditory temporal processing among older listeners. [Research supported by NIH/NIA grant P01 AG055365.]

PS 874

Transcriptome analysis for deafness: intracellular signal transduction signaling pathways regulate neuroplastic change in the auditory cortex

Sang-Yeon Lee¹; Ho Sun Lee²; Min-Hyun Park²

¹*Seoul National University Hospital;* ²*Seoul National University, College of Medicine*

Background: Hearing loss leads to synaptic changes in auditory neurons and their networks, and functions in the central auditory system as the consequence of interplay of genes and proteins. However, cellular and molecular mechanisms leading to deaf-induced neuroplasticity in the auditory cortex (AC) remains unclear.

Objective: To examine the differential expression genes (DEGs) and their associated molecular signaling pathways in the AC following auditory deprivation through the whole RNA-Seq analysis.

Methods: Sprague-Dawley rats induced bilateral deafness by cochlear ablation were maintained for 12 weeks until their auditory cortices were harvested. RNA-seq analysis was performed to reveal transcript and gene expressed in each sample, then, these values are used for comparison analysis of differentially expressed genes between samples.

Results: RNA-seq analysis identified 72 DEGs, out of which 19 were clearly upregulated (>1.5-fold, P < .05) and 53 were significantly downregulated (*Bdnf*, *Nr4a1*, *Ntf3*, *Dusp1*, *Dusp6*, *Gadd45g*, *c-Fos*), tumor necrosis factor (e.g. *Edn1*, *Junb*, *Ptgs2*, *c-Fos*), and cyclic adenosine 3',5'-monophosphate (e.g. *Bdnf*, *Gli1*, *c-Fos*) signaling pathways in regulating change of gene expression after bilateral deafness. The expression patterns of interest DEGs, including *Fos*, *Arc*, *Ntf3*, and *Gli1*, from the RNA-seq analysis were in line with that in RT-qPCR.

Conclusion: Bilateral deafness induced the changes in signaling transduction pathways participated robust of a variety of transcription factors and subsequent gene expressions in the AC, suggesting that auditory deafferentation can evoke neuroplasticity and long-term functional changes via an interplay of genomic and non-genomic actions. Through RNA-seq analysis, long-term auditory deprivation induced the robust changes of gene expression, a variety of transcription factors and their complex interaction at specific gene promoters in the AC of rats. Especially, activation of intracellular signal transduction signaling pathways that regulate DEGs may suggest the long-lasting process of neuroplasticity in the AC.

PS 875

Auditory Nociception Test (ANT) to Assess Pain Hyperacusis in Rats

Senthivelan Manohar¹; Henry Adler¹; Kelly Radziwon²; Richard Salvi¹

¹University at Buffalo; ²State University of New York at Buffalo

Normal hearing listeners begin to experience auditory pain at sound levels around 130 dB SPL. However, individuals with pain-hyperacusis experience painful sensations within and around the ear and face at sound levels as low as 80-90 dB SPL. Efforts to understand the mechanisms underlying pain hyperacusis have been hampered by the lack of animal behavioral models that are able to “report” on what sounds evoke or modulate pain. To address this issue, we developed the Auditory Nociception Task (ANT) to evaluate how sound stimulation modulates thermal pain sensitivity in both normal hearing rats and in rats with high frequency, noise-induced hearing loss. The ANT paradigm uses the tail-flick latency to assess a rat’s sensitivity to thermal pain delivered to the tail. The rat’s tail is immersed into water maintained at 52 °C. The time it takes for the rat to remove its tail from the warm water (latency) is representative of the level of thermal nociception. To determine how auditory stimulation interacts with thermal nociception, the tail-flick latency was measured in quiet or in a wide range of testing noise (70-120 dB SPL, 2-20 kHz.) Because the auditory and pain pathways converge in the central nervous system, tail-flick latency provides a readout of the central pain network. To determine if noise-induced hearing loss could affect central pain sensitivity, we measured the auditory-tail-flick latency input/output function before and after inducing a high-frequency, noise-induced hearing loss. Consistent with earlier studies, we found an audio-hypoalgesia effect for 80-90 dB SPL noise. Because extremely high intensity sounds can induce auditory pain, we hypothesized that thermal pain would increase when higher intensities

were presented. Consistent with our hypothesis, we discovered for the first time that intensities equal to or greater than 110 dB decreased thermal tail-flick latencies (audio-hyperalgesia). Because hyperacusis is often associated with hearing loss, we speculated that hearing loss might disturb audio-hypoalgesia. As anticipated, we found that high-frequency, noise-induced hearing loss disturbed thermal pain sensitivity and showed audio-hyperalgesia for 80-90 dB SPL noise. Our results provide functional evidence for the convergence of sensory information from the auditory and pain pathways in the central nervous system. Moderate- intensity sounds induce audio-hypoalgesia, whereas high-intensity sounds induce audio-hyperalgesia. Surprisingly, high-frequency noise-induced hearing loss disturbed the central pain pathway and we found evidence of audio-hyperalgesia for lower level noise, providing important new clues relevant to pain-hyperacusis and the potential contribution of central pain mechanisms.

PS 876

Interactive Learning Environment for Use in Auditory Rehabilitation: Usability Study

Dragana Barac-Cikoja¹; Kevin Cole²; Ashleigh Collis¹; Kelsey Ugucioni¹; Ellen Delp¹; Andrea Kottlowski³

¹Gallaudet University, Department of Hearing Speech and Language Sciences; ²NOVA Web Development; ³Gallaudet University

A computer-based auditory training/counseling program has been developed that allows an individual to experience the benefits and limitations of his/her hearing device in a variety of simulated real-life listening situations. The program is based on self-directed exploration of the relationship between acoustic factors that affect hearing/sound processing, and technological solutions and communication strategies that are aimed at improving sound detection, speech comprehension and the overall listening experience. This study investigated the system’s usability in auditory rehabilitation (AR) from the perspective of AR clients. Six hearing device users participated in the study. They completed exercises that included different types of visual interfaces that allowed them to: (i) manipulate the signal to noise ratio using a control panel, (ii) detect incidental sounds and identify their source locations using a graphic interface, and (iii) change the soundscape and optimize listening conditions by moving an avatar in a virtual space. The exercises involved listening to speech, music, or environmental sounds in noisy backgrounds common to a restaurant, living room, office, street, or car. Objective measures of the participant’s exploratory activities and his/her immediate feedback on the corresponding listening experience were collected and analyzed. In addition, the participants evaluated each graphic interface using (i) the

Task Load Index (Hart and Staveland, 1988) to rate the ease of use, and (ii) the System Usability Scale (Brooke, 1986) to assess its usefulness in demonstrating hearing device functionality in different listening conditions. Clinical application of the system based on the findings will be discussed.

PS 877

Contribution of observational learning to an auditory discrimination task

Nihaad Parouty; Joey A. Charbonneau; Dan H. Sanes
New York University

Background

Observational learning has been observed in many species, from insects to primates. In principle, it diminishes an individual's error trials, thereby improving the chance of survival and reproduction. Here, we asked whether Mongolian gerbils can learn an auditory discrimination task through observation of a trained demonstrator. Our primary aim was to determine whether animals learn only the motor task, or whether they also learn about the auditory stimulus contingencies.

Methods

Demonstrator gerbils were first trained on an amplitude modulation (AM) rate discrimination task using an appetitive reinforcement operant conditioning procedure. The task required animals to initiate each trial by entering a nose-poke, and to discriminate between a 12-Hz AM stimulus which signalled the availability of a food pellet (Go stimulus), versus a 4-Hz AM stimulus which signalled the absence of a reward (Nogo stimulus). Once demonstrator gerbils performed the task with a $d' > 1.5$, a naive observer was placed in an observation chamber immediately next to the test chamber, and remained there while the trained demonstrator performed > 80 Go trials and > 20 Nogo trials. The observer's performance was then assessed in a subsequent test phase.

Results

In the first experiment, a group of naive observer gerbils each observed a separate same-sex littermate that was trained on the task (i.e., demonstrators). The observers ($n=4$) required between 4 to 8 days to learn the task at the following criterion: a sensitivity of $d' > 1.5$, and a false alarm rate $< 30\%$. In the second experimental group, naive observers were paired for 5 consecutive days with demonstrator gerbils, but were not tested until after the 5th session. The observers were tested alone after the 5th observation session, and on subsequent days. Task acquisition for these observer gerbils ($n=3$)

required between 5 to 7 days to reach the same criterion performance. In the third experiment, to determine whether naive gerbils could learn the task without experimenter training or observation of a demonstrator, a naive animal was placed in the testing chamber and a second naive animal was placed in the observing chamber. During this pairing, the nose poke and food tray were absent. Following a > 15 min pairing period, the nose poke and food tray were returned to the testing chamber and the naive observer was tested alone. The observers ($n=4$) in this experiment displayed no task acquisition across 5 days of testing. In comparison to these results, we have previously found that when gerbils are individually trained by an experimenter on the AM discrimination task ($n=51$), the time to reach criterion performance is 12 to 29 days (mean=19).

Conclusions

Task acquisition was found to be improved as a result of observation, compared to subjects that do not have the observational experience, and also as compared to experimenter-trained animals. Future experiments will test whether auditory experience alone can contribute to task learning.

PS 878

Excitation and Inhibition in Auditory and Visual Cortices after Long Term Deafness: a RT-qPCR, Immunocytochemistry and Evoked Potential Analysis

Marianny Pernia¹; Ivan Diaz¹; Ana Colmenarez¹; Ignacio Plaza¹; Casto Rivadulla²; Miguel Merchan¹
¹*Instituto de Neurociencias de Castilla y Leon*;
²*Universidad de La Coruña*

Bilateral cochlear lesions were performed in adult male Wistar rats by removing the middle ear ossicles and puncturing the cochlea with a needle under deep anesthesia. Immunocytochemical, molecular and electrophysiological analysis were made 90 days after lesion. We demonstrate by Auditory brainstem responses (ABRs) and spiral ganglion cell counting a bilateral and profound deafness in all animals of our experimental group.

We assessed long-term gene expression changes by RT-qPCR of GluR2 and GABA-Aa1 in auditory cortex (AC) and visual cortex (VC). Also, we analyze in both cortical areas quantitative immunocytochemistry for c-Fos and Arc/Arg3.1 and proteins related to excitatory and inhibitory neurons as GluR2/3, GAD67 and Parvalbumine. A functional evaluation of visual cortex activation was also made by recordings of visual evoked potentials (VEPs).

Present RT-qPCR results confirmed c-Fos and Arc/Arg3.1 immunocytochemical results previously published by us (Pernia et al., 2017). Also, a significant increase in GAD67 and GABA-Aa1 gene expression was shown in the AC but not in VC.

By quantitative immunocytochemistry both AC and VC showed a significant increase of immunoreactivity for Parvalbumine and GAD67.

AMPA glutamate receptors significantly increase in the AC and decrease in the VC. In sum, the present study reports evidence that permanent hearing loss in adult rats induces decrease in activation of VC in which we suggest it underlies a global increase in AC inhibition. The authors will discuss these findings to try to reach an accurate interpretation.

PS 879

Testing the central gain theory: Loudness growth correlates with central auditory gain enhancement in two rodent models of hyperacusis

Benjamin D. Auerbach¹; Kelly Radziwon¹; Richard Salvi²

¹State University of New York at Buffalo; ²University at Buffalo

The central gain model of hyperacusis proposes that loss of auditory input can result in maladaptive neuronal gain increases in the central auditory system, leading to the over-amplification of sound-evoked activity and excessive loudness perception. Despite the attractiveness of this model, and supporting evidence for it, a critical test of the central gain theory requires that changes in sound-evoked activity be explicitly linked to perceptual alterations of loudness. Here we combined an operant conditioning task that uses a subject's reaction time to auditory stimuli to produce reliable measures of loudness growth with chronic electrophysiological recordings from the auditory cortex and inferior colliculus of awake, behaviorally-phenotyped animals. In this manner, we could directly correlate daily assessments of loudness perception with neurophysiological measures of sound encoding within the same animal. Using this novel psychophysical-electrophysiological paradigm, we compared the effect of high-dose salicylate and a mild acoustic trauma that reliably resulted in temporary hearing loss and neural hyperactivity. Both salicylate and acoustic trauma induced parallel changes to loudness growth and evoked response-intensity functions consistent with temporary hearing loss and hyperacusis, albeit with distinct time courses and region-specific differences in the magnitude of gain enhancement. Most importantly, we found a striking correlation between behavioral and electrophysiological response changes

following both manipulations that co-varied on an individual animal basis. These results provide strong support for the central gain model of hyperacusis and demonstrate the utility of using an experimental design that allows for within subject comparison of behavioral and electrophysiological measures, thereby making inter-subject variability a strength rather than a limitation.

PS 880

Comparison of Single Cell Spike Rate and Timing in the Brainstem in Response to Cochlear Implant and Acoustic Stimulation

Michaela Müller¹; Barbara Beiderbeck¹; Benedikt Grothe²; Michael Pecka³

¹Graduate School of Systemic Neurosciences, Ludwig Maximilian University of Munich; ²Graduate School of Systemic Neurosciences, Biocenter, Section of Neurobiology, Department Biology II, Ludwig Maximilian University of Munich; ³Biocenter, Section of Neurobiology, Department Biology II, Ludwig Maximilian University of Munich

Hearing impairment and deafness is the most frequent sensory deficit today and deprives patients from interaction with their environment. Specifically, spatial hearing is essential for communication as well as navigation in everyday life. The cochlear implant (CI) allows for the functional restoration of hearing, in particular the basic understanding of speech. Unfortunately, sound localization in complex environments is still severely limited in patients with bilateral CIs and its restoration thus remains one of the central obstacles of CI research.

Interaural Time Difference (ITD) is the dominant binaural cue for sound localization and speech comprehension in noisy environments. Neuronally, ITD sensitivity is based on the integration of excitatory and inhibitory synaptic inputs from both ears by brainstem neurons in the medial superior olive (MSO) and the lateral superior olive (LSO). Current implantation and stimulation techniques as well as behavioral performance levels imply that CI users might predominately make use of the LSO pathway. Recent in vivo recordings in the LSO demonstrated that during normal hearing, inhibition and excitation interact with microsecond precision during ITD processing (Beiderbeck et al., 2018). However, the mechanisms underlying this precise temporal integration of individual inputs and potential differences in temporal precision during electrical stimulation are not understood.

Here, we obtained in vivo electrophysiological recordings from single neurons in the brainstem of Mongolian Gerbils (*Meriones unguiculatus*). We characterized the temporal precision of action potential firing in response to click-train stimuli of varying inter-click-intervals (ICI)

in binaural neurons of the LSO and their upstream, monaural inputs, namely the cochlear nucleus (CN) and medial nucleus of the trapezoid body (MNTB). To assess potential differences in temporal precision between acoustic and electrical stimulation, complementary data are obtained in normal hearing animals and animals that underwent deafening and cochlear implantation.

Our results demonstrate that electrical stimulation differs from acoustical stimulation throughout the auditory brainstem. We observed dramatically higher spike probability and reduced jitter for the electrical stimulated cells both in CN and MNTB. Ultimately, we aim to identify basic principles of binaural integration in the auditory brainstem during acoustic and CI-based spatial hearing.

PS 881

The Role of Talker Variability on Word Learning in Adults with Cochlear Implants and with Normal-Hearing

Jasenia Hartman¹; Jenny Saffran²; Ruth Litovsky³
¹*Neuroscience Training Program, University of Wisconsin-Madison*; ²*Department of Psychology, University of Wisconsin-Madison*; ³*University of Wisconsin - Madison*

Word learning is a core component of language acquisition that occurs throughout an entire lifespan. Previous studies have shown that individuals with cochlear implants (CIs) have poorer word-learning abilities than their normal-hearing (NH) peers. While these deficits have been associated with CI listeners'; perceptual difficulties in identifying the speech sounds corresponding to the word forms, the learning paradigms used in prior studies may be exacerbating this problem. In previous word-learning studies, CI listeners were only exposed to a single talker, thereby receiving limited knowledge about their language. Recent studies have shown that exposure to multiple talkers enhances word learning for children with NH by highlighting which acoustic dimensions are relevant for word identity, and which are unrelated. Little is known about whether the same effect occurs in adult listeners with NH and with CIs. The purpose of the present experiment is to examine the role of talker variability on word learning in CI and NH adult listeners.

Adults with NH and with CIs learn to associate 8 English pseudowords with 8 novel objects. Half of the words are spoken by a single talker, while the other half are spoken by multiple talkers (n = 8). Participants are tested on their ability to learn the words using a novel talker in a two-alternative-forced choice task (2-AFC). Test phases consist of easy and hard trials where word choices differ by multiple phonetic features or a single phonetic

feature, respectively. In both the learning and test phases, listeners receive an audiovisual presentation of the talker to facilitate phonetic processing. Learning accuracy and reaction time were assessed via eye-tracking. Accuracy is validated via mouse-click.

Preliminary results from NH participants suggest that listeners learn words spoken by multiple talkers better than words spoken by a single talker. Although mouse-clicks revealed similar performance between the two conditions, eye-tracking data showed that listeners took longer to fixate towards the target object during the single-talker condition compared to the multiple-talker condition. Interestingly, the multiple talker learning phase led to increased accuracy in fixating to the target for the easy trials, but not for hard trials. We will evaluate if CI participants also benefit from talker variability, and whether their performance is similar to, or reduced relative to NH participants. Such findings will reveal whether talker variability can be advantageous to CI listeners.

Work supported by NIH-NIDCD R01-DC003083 to RYL, and NIH-NICHD U54HD090256 to the Waisman Center.

PS 882

Effects of Prolonged Low-Level Noise on Loudness Growth vs Startle Reflex Amplitudes

Xiaopeng Liu¹; Kelly Radziwon²; Guang-Di Chen¹; Richard Salvi³

¹*Center for Hearing and Deafness, SUNY at Buffalo*; ²*State University of New York at Buffalo*; ³*University at Buffalo*

Background: The auditory cortex (AC) is remarkably plastic and can alter its performance based on prior sound stimulation. This was clearly illustrated by a series of studies in cats in which prolonged, non-traumatic exposures (less than 80 dB SPL) to band limited noise depressed sound-evoked activity in AC tuned to the noise, but enhanced responses to AC neurons tuned to the edges of the noise. The perceptual/behavioral consequence of these neurophysiological changes in the AC are poorly understood. In order to gain insights on the perceptual and behavioral consequences of long-term, non-traumatic noise exposures, we measured: (1) acoustic startle reflex (ASR) amplitude input/output function and (2) behavioral reaction time-intensity (RT-I) functions reflecting loudness growth. The ASR is a pre-attentive, reflex response dominated by neural circuits in the brainstem. In contrast, the behavioral RT-I functions used to assess loudness growth engage complex neural circuits involving auditory perception, attention, motor control and decision making.

Methods: For the ASR studies, we used 18 rats; 10 rats were exposed to 18-24 kHz narrowband noise presented at 85 dB SPL for 6 weeks. The 8 remaining rats were used as sham controls. The ASR was evoked by narrowband noises centered at 4, 8 or 20 kHz and presented at intensities from 70-100 dB SPL. Startle reflex amplitude/intensity functions were recorded before and immediately after the exposure. Eight rats were behaviorally trained and RT-I functions were obtained at 4, 8, 20 and 40 kHz at intensities from 30-90 dB SPL before and immediately after the 18-24 kHz exposure.

Results: Immediately after the 18-24 kHz noise exposure, mean ASR amplitudes at 4 kHz were substantially larger than baseline at all intensities, moderately larger than baseline at 8 kHz and similar to baseline at 20 kHz. ASR amplitudes were stable/unchanged in the Control group. In contrast, RT-I functions were largely unaltered by the 18-24 kHz noise exposure. Importantly, the 85 dB exposure did not alter behavioral thresholds and therefore was non-traumatic.

Summary: Our results showed that prolonged exposure to the 18-24 kHz noise presented at 85 dB SPL enhanced ASR amplitudes at 4 and 8 kHz, frequencies below the 18-24 kHz noise, suggesting an increase in low-frequency gain in the ASR brainstem reflex network. Despite the increase in low-frequency ASR amplitudes, RT-I functions, a surrogate measure of loudness growth, remained unchanged.

Research supported by grants from NIH (R01DC014693 and R01DC014452)

Auditory Prostheses VI: Audiovisual Integration & Speech Perception

PS 883

Pre-operative Audiovisual Integration as a Predictor of Post-operative Speech Recognition in Adults with Cochlear Implants

Aaron Moberly¹; Kara Vasil¹; Christin Ray¹; David Pisoni²

¹The Ohio State University; ²Indiana University

Background: Cochlear implants (CIs) provide the listener with a degraded auditory input, and speech recognition abilities of adult CI users remain highly variable. This variability has been partially attributed to demographic and clinical factors, such as age or severity and duration of hearing loss, as well as cognitive functions, such as working memory capacity. There is some evidence from cross-sectional studies that multimodal (i.e., audiovisual, AV) integrative abilities vary among CI listeners, and that these integrative abilities may relate to speech recognition outcomes. This study sought to take a longitudinal

approach to investigate whether pre-operative AV integrative skill would predict post-operative speech recognition abilities in adults who receive CIs. The main hypothesis was that individuals with better pre-operative AV integration would demonstrate greater auditory-only (A-only) speech recognition after implantation.

Methods: Data were collected longitudinally from 25 adults at two time points: immediately before CI surgery, and 6 months after device activation. Pre-operative speech recognition performance was measured in A-only, visual-only (V-only), and multimodal AV fashion for City University of New York (CUNY) sentences, and relative gain scores of visual gain and auditory gain during AV sentence recognition were computed as the main predictors. At 6 months after CI activation, participants were tested in the A-only condition on several measures of open-set speech recognition: isolated words, words in meaningful sentences, words in sentences in multi-talker babble, words in semantically anomalous sentences, and words in high-variability multi-talker sentences. Linear regression analyses were performed with A-only post-operative speech recognition scores as outcomes and visual gain and auditory gain measures as predictors to determine whether pre-operative AV integration ability would predict post-operative A-only speech recognition performance.

Results: Both visual gain and auditory gain scores predicted scores of A-only sentence recognition for all sentence types, in both quiet and in babble ($r = 0.45$ to 0.59 , $p = .007$ to $.042$). In contrast, visual gain and auditory gain scores did not significantly predict isolated word recognition.

Conclusions: Multimodal AV integrative ability prior to cochlear implantation significantly predicts speech recognition outcomes at 6 months after CI for sentence recognition in quiet and in babble, but not for isolated word recognition. Findings suggest that pre-operative AV integrative skills accounts for approximately 20 to 35% of the variance in post-operative A-only sentence recognition. Moreover, the results suggest a differential role of AV integrative ability in sentence versus word recognition in CI users, a finding that deserves further exploration.

PS 884

The Contribution of Voice Pitch Contour to Emotion Recognition

Harley J. Wheeler¹; Anna Tinnemore²; Monita Chatterjee³

¹Dept. of Communication Sciences & Disorders, James Madison University; ²Dept of Hearing & Speech Sciences, University of Maryland, College Park; ³Boys Town National Research Hospital

Understanding the role of prosodic cues in speech—which include harmonic pitch, intensity, and duration information—to emotion perception by normal-hearing listeners will also yield insight relevant to perception of emotion by cochlear implant users, for whom some of these cues are reduced due to device limitations. Previous examinations of vocal prosody's contribution to communication of emotion have been conducted with the intent of isolating prosodic features by removal of semantic content through use of low-pass filters at 400-600 Hz. However, these studies may have included F1 information, or cut off higher-frequency excursions of F0, due to the overlap of these two features in the frequency domain.

The current study investigated the contribution of prosodic cues isolated by conversion of emotionally-spoken stimuli to “hummed” versions—this process did not use low-pass filtering but eliminated other speech cues—to emotion identification. Participants with normal hearing performed an emotion identification task in which semantically-neutral sentences in either the original or “hum” (Type of speech) conditions were to be categorized as *Angry, Happy, Neutral, Sad, or Scared*. Based on previous findings using LPF and preliminary data from our laboratory, we hypothesized that identification performance with our “hummed speech” would be poorer than when listening to the original stimuli. These impacts were expected to be larger for conditions measured using an “adult-directed” material set, for which prosodic cues are subtler than “child-directed” speech, as child-directed speech has been shown in associated studies to generally perform at ceiling in emotion identification tasks. Due to talker variability in voice emotion communication, we also hypothesized effects of Talker, Type of speech, and Emotion. Analyses showed significant effects of Type of speech (poorer performance with the hummed stimuli) and Talker/ material set (male or female talker of adult- or child-directed stimuli), as well as a significant interaction between Type of speech and Talker. Reaction time showed similar main effects. Analyses of effects of emotion category on identification accuracy and reaction time showed significant effects, showing main effects of Emotion and interactions with the Type of speech.

Results indicated that F0 contour alone did not fully convey vocal emotion information. However, reasonable accuracy in emotion recognition was achieved with “hum” stimuli. Although cochlear implant users can access both duration and intensity cues (present in our “hum” stimuli), lack of salient F0 contour information and highly-degraded phonetic cues likely explains their difficulty with vocal emotion recognition.

PS 885

Association of Speech Processor Technology and Speech Recognition Outcomes in Adult Cochlear Implant Users

Peter R. Dixon¹; David Shipp²; Kari Smilsky²; Vincent Lin³; Trung Le³; Joseph Chen⁴

¹*Department of Otolaryngology - Head & Neck Surgery, University of Toronto, Canada; Institute of Health Policy, Management & Evaluation, University of Toronto;* ²*Sunnybrook Cochlear Implant Program, Sunnybrook Health Sciences Centre, Toronto;*

³*Department of Otolaryngology - Head & Neck Surgery, Sunnybrook Health Sciences Centre Toronto, Canada;*

⁴*Department of Otolaryngology - Head & Neck Surgery, Sunnybrook Health Sciences Centre Toronto; Institute of Health Policy, Management & Evaluation, University of Toronto*

Research Background.

Cochlear implant (CI) performance has improved dramatically since the introduction of the first multichannel device in 1978. This improvement has been attributed to expanded candidacy criteria and advancements in CI system technology. In a healthcare environment that emphasizes efficiency of spending, determining the relative contribution of technological advancements to improved outcomes has important implications for policy-makers, clinicians, and patients. The date of implantation has been used as a measure of technological sophistication, but this metric fails to account for technological advancements that occur *after* the date of implantation including innovations of speech processors and speech processing strategies. We aimed to determine the association of advancements in speech processor technology with improvements in speech recognition outcomes.

Methods.

A retrospective analysis of a registry of adult unilateral CI recipients was carried out. Advancements in speech processor technology were operationalized by year of their market availability. The primary outcome measures were Consonant-Nucleus-Consonant (CNC) word recognition and Hearing in Noise Test (HINT) in quiet sentence recognition scores. Multivariable generalized linear models were fitted to estimate the effect of speech processor novelty on CNC and HINT scores, each accounting for clustering of scores within patients, the era of implantation, and several patient characteristics known to influence speech recognition outcomes.

Results.

From 1991 – 2016, 1,111 CNC scores and 1,121 HINT scores were collected from 351 patients who had complete data, 99 (28.2%) of whom had upgraded

their speech processor since implantation. Mean post-implantation CNC score was 53.8% and increased with more recent year of implantation ($p < 0.001$, Analysis of Variance [ANOVA]). Median HINT score was 87.0% and did not vary over eras of implantation ($p = 0.06$, ANOVA). Observed changes in patient characteristics over surgical eras were consistent with expanding candidacy criteria. Each 5-year increment in speech processor novelty was independently associated with an increase in CNC score by 2.85% (95% confidence limits [CL] 0.26, 5.44%) and was not associated with change in HINT scores ($p = 0.30$).

Conclusion.

Newer speech processors are associated with improved CNC scores independent of the year of device implantation and expanding candidacy criteria. We suggest that era of implantation may not be a sufficient measure of technological sophistication since additional speech outcome variability is explained by accounting for year of processor release. The implications of these findings with respect to appropriate interval of speech processor upgrades is discussed.

PS 886

Audio-visual Sentence Identification in Early-deafened, Late-implanted Cochlear Implant Users

Dana Kort; Rolien Free; Deniz Başkent; **Christina Fuller**

University Medical Center Groningen

Background The early-deafened, late-implanted (EDLI) cochlear-implant (CI) users are deafened during language acquisition, but implanted after a long period of auditory deprivation, a factor that might influence understanding of auditory speech negatively. On the other hand, compared to the typical, post-lingually deafened CI users, many EDLI CI users rely on visual only or audiovisual communication, including sign language. We hypothesized that potentially low EDLI CI outcome performances for auditory speech perception may be compensated by visual cues, such as provided by lipreading.

Methods The inclusion criteria for EDLI group were hearing loss onset 16 years of age, and >1 year CI experience. The control group of post-lingually deafened CI users were age- and gender-matched with the EDLI group. Identification of meaningful sentences was measured using three modalities: 1) audio only; 2) visual only; 3) audiovisual.

Results Thus far 11 EDLI and 7 control CI users were included. The preliminary results show that while EDLI scored lower on auditory sentence identification than controls (67% versus 98%, on average), they also

compensated this by using lipreading cues (audiovisual sentence recognition 79% versus 97%). The use of lipreading was also implied in visual only sentence identification scores, where EDLI scored significantly higher than controls for visual sentence identification (26% versus 5%).

Conclusions EDLI CI users have a lower, though not significantly lower, sentence identification for audio only than post-lingually deafened CI users. EDLI, however, significantly outperform post-lingually deafened CI users in the visual only condition. Lastly, EDLI greatly profit from the addition of visual cues for enhancing auditory sentence identification. An explanation for the better visual sentence identification and the benefit for audiovisual communication could be that the cross-modal effects of a language acquisition based largely on visual cues (lipreading or sign language) on the auditory cortex persist after implantation, and provide the EDLI CI user with a benefit for audiovisual communication. Finally our newly developed audiovisual sentence identification test is capable of capturing performance differences for audiovisual communication in EDLI. The current outcomes could support implantation in EDLI, despite the auditory deprivation period.

Funding: This abstract is supported by the Mandema Stipendium of University Medical Center Groningen, an otological neurotological stipendium from the Heinsius-Houbolt Foundation, and the VICI grant No. 918-17-603 from the NWO and the ZonMw.

PS 887

Effects of Aging on Voice Emotion Recognition in Cochlear Implant Users and Normally Hearing Adults

Shauntelle A. Cannon; Monita Chatterjee
Boys Town National Research Hospital

Introduction: Facial and voice emotion recognition, as well as overall social cognition, are negatively affected by age-related changes in normally hearing (NH) adults. Older NH adults have also demonstrated deficits in phoneme discrimination, gender discrimination, and voice pitch discrimination in cochlear implant (CI) simulation studies. These deficits may also impact their perception of voice emotion. The effects of aging on voice emotion recognition in NH listeners attending to spectrally-degraded stimuli are not known, nor are the effects of aging on adult CI users. The objective of the present study is to explore age-related effects on voice emotion recognition in NH adults listening to CI-simulated speech, and to compare these changes to age-related changes in adult CI users'; voice emotion recognition in unprocessed (clean) speech.

Methods: Participants included 44 NH adults and 18 post-lingually deafened adult CI users. The CI users ranged in age from 29.6-74.5 years while the NH adults were split into three age groups: younger (25-39 years), middle-aged (40-55 years) and older (age 60-75 years). Stimuli consisted of 12 emotion-neutral sentences spoken by a male and female talker in 5 emotions (happy, sad, scared, angry, neutral) in an adult-directed manner. For NH adults, these sentences were presented in four conditions: unprocessed speech and 16-channel, 8-channel, and 4-channel noise-band vocoded (NBV) speech. The adult CI users only listened to unprocessed speech. The participant's task was to choose which emotion was being conveyed by the talker in a single-interval, five-alternative, forced-choice paradigm.

Results: Preliminary results indicate declines in overall percent correct scores and increased reaction time with both age and increasing spectral degradation. The younger adults showed better performance than the middle-aged and older adults group on voice emotion recognition in all conditions of spectral degradation. Results also suggest age-related effects on percent correct and reaction times scores within the CI group alone.

Conclusions: These results confirm that age-related declines in voice emotion recognition are present in normally hearing adults, both with unprocessed and CI-simulated speech. They further suggest that similar age-related declines may occur in listeners with CIs. Further analyses quantifying the effects of age and spectral resolution, and their interactions, are ongoing. Limited ability to recognize and respond to a talker's intended emotion can negatively impact social interactions in aging adults. These results have important implications in the aging population of adults with NH and with CIs, as declines in the quantity and quality of social interactions and in social cognition have been associated with declines in quality of life. [Work supported by NIH/NIDCD grant no. R01 DC014233 and R01 DC014233 04S1]

PS 888

Social Factors and Individual Outcomes in Cochlear Implant Users

Erin O'Neill; Peggy B. Nelson
University of Minnesota

Background: Cochlear implants (CIs) can significantly improve the quality of life for people with profound sensorineural hearing loss, but individual users struggle to varying degrees with listening environments, which can negatively impact social well-being. While improved hearing outcomes and increased social engagement are two primary goals for those who receive CIs, little is

known about the interplay between an individual's social behavior in everyday life and their relative success with the device. In this study, our aim was to assess the social engagement and listening patterns of CI users in daily life and relate those measures to both subjective and objective hearing outcomes.

Methods: Ecological Momentary Assessments (EMAs) collected using a Smartphone app, along with self-report questionnaires, were used to probe patterns of listening behavior in CI users in natural environments. These results were compared with those of normal hearing (NH) adults to detect differences in social engagement and overall quality of life. Speech perception measurements were also completed by the CI users to uncover possible correlations between listening or social behaviors and overall success with the device.

Results: Preliminary data suggest that CI users consistently report more difficulty listening in everyday environments than NH peers, but also tend to be in environments with overall lower levels of background noise. Compared to NH adults of the same age, CI users are much more likely than peers to be around other people but not actively engaging with them and to seek out environments that alleviate listening effort. Individual differences in social behaviors and their relation to laboratory test results will be reported.

Conclusions: Overall, these data suggest that systematic differences exist between how CI users and NH adults navigate and manipulate listening and social environments in everyday life, with CI users expending more effort, despite the positive benefits of cochlear implants.

Acknowledgements: This work is supported by a grant from the National Science Foundation Research Training: Understanding the Brain, awarded to the University of Minnesota Graduate Training Program in Sensory Science: CogniSense.

PS 889

The Effect of Visual Distraction on the Speech Understanding of Listeners with Cochlear Implants

Anna Tinnemore¹; Sandra Gordon-Salant²; Matthew Goupell²

¹*Dept of Hearing & Speech Sciences, University of Maryland, College Park;* ²*University of Maryland*

Intro: Listeners with cochlear implants (CIs) can often understand speech well using a combination of auditory and visual cues. Their experience with hearing loss creates a reliance on visual cues for maximum speech understanding. Everyday listening environments contain many challenges to speech understanding in the auditory

domain (including the degraded signal presented from a CI), as well as many visual distractions. Previous research has shown that normal-hearing listeners are sometimes affected by visual distractions. Speech understanding performance may decline with visual distraction or the addition of a secondary visual task, especially when the speech is distorted (e.g., with a foreign accent). Currently, the effect of visual distraction and a secondary task on the performance of CI listeners is unknown. This study investigated the hypothesis that older CI listeners would be able to ignore visual distractions in the environment, and would be minimally affected by the demands of a secondary task due to their experience switching attention between environment and facial cues.

Method: Participants were middle-aged and older (>45 years) CI users. IEEG sentences were recorded in an audiovisual (AV) mode by both unaccented and accented talkers. Videos were presented with a solid background or with the target talker embedded in a busy sidewalk scene. Listeners were asked to repeat the sentences presented in background noise while either ignoring the sidewalk scene or engaging in a visual secondary task with the scene. Thus, each listener saw three AV conditions with each talker (solid-colored background, background scene, and background scene with secondary task), and one visual condition where only the secondary task was required.

Results: Preliminary results from nine participants show highest speech understanding performance for unaccented speech with and without the background video. Accented speech caused a significant reduction in performance in all distraction conditions with no differences between conditions. There was an interaction between accent and secondary task where listeners performed worse on unaccented speech when performing the secondary task as compared to when they were not.

Discussion: These results tentatively suggest that listeners with CIs can suppress irrelevant visual information despite their reliance on visual cues for speech understanding. Listeners are negatively affected by the demands of a secondary task as well as when speech is spoken with a foreign accent. [Research supported by NIH/NIA grant R01 AG051603.]

PS 890

Influence of Competing Talker Loudness and Training-Data Quantity on EEG-based Auditory Attention Decoding Performance

Stephanie Haro¹; Michael Nolan²; Gregory Ciccarelli²; Paul Calamia²; Joseph Perricone²; James O'Sullivan³; Nima Mesgarani⁴; Thomas Quatieri⁵; Christopher Smalt²

¹Harvard University; ²Bioengineering Systems and Technologies, MIT Lincoln Laboratory; ³Columbia University; ⁴Zuckerman Institute for Brain Research, Columbia University, Program in Neurobiology and Behavior, Columbia University, Department of Electrical Engineering, Columbia University; ⁵Bioengineering Systems and Technologies, MIT Lincoln Laboratory & Graduate Program in Speech Hearing Bioscience & Technology; Harvard Medical School

State of the art hearing aids are still limited in noisy environments, especially those with multiple talkers. Usage would greatly benefit from the device selecting and amplifying only the desired attended talker stream, in contrast to uninformed amplification and/or noise reduction. The process of detecting the attended talker in the presence of two or more talker streams is termed auditory attention decoding (AAD). Inspired by the naturally occurring pauses of the attended talker during a two-talker narrative stimulus, this work examines whether the dynamic loudness ratio of competing talkers influences AAD performance.

AAD is performed using a temporal response function (TRF) decoding technique; it predicts the attended stimulus envelope from a sliding window of 64 channel electroencephalogram (EEG) data (O'Sullivan, 2014). 14 subjects were instructed to attend to a specific talker (male or female) when presented two concurrent talker narratives and switch their attention to the other talker half way through the experiment. We hypothesized that AAD system performance would be improved by constraining training to regions dominated by the attended talker instead of regions that contain a mixture of competing talkers.

To test our hypothesis, both the quantity and quality (envelope loudness ratio) of the training data were controlled. Across our 14 subjects, we found that 14 minutes is necessary and sufficient to achieve an accuracy that is equivalent to decoding performance derived from 28 minutes of data. Leave-one out cross validation methods were used to achieve 59.1% (SE = 0.5%) and 59.5% (SE = 0.5%) accuracies respectively. Performance did not improve when training was constrained to samples that were dominated by the attended talker, contrary to our hypothesis. Furthermore, we used a separate, single talker data set to push this

concept further. Preliminary results, on a single subject that performed both competing talker and single talker listening tasks, found that training with 14 minutes of single talker training data underperforms the decoder trained on 14 minutes of mixed talker data on the same multi-talker evaluation (52.3% vs 69.1% single decoder accuracies).

Future work includes confirming these results using nonlinear deep neural network TRF methods to show that they are independent of the decoding method. We hope to use these results to derive a subject specific training protocol that could eventually be implemented in an audiology clinic for attention-decoder based hearing-aid fitting.

PS 891

Cognitive and Auditory Factors for Speech and Music Perception in Older Adult Cochlear Implant Users

Xin Luo; Courtney Kolberg; Kathryn Pulling; Tamiko Azuma
Arizona State University

Background

Cochlear implant (CI) users struggle with speech recognition in noise and music perception and their performance has a high inter-subject variability. This study aimed to examine the relative contributions of specific cognitive and auditory variables to the performance of older CI users under challenging listening tasks.

Methods

Working memory was measured using auditory digit span, visual letter span, and dual-modality memory tasks with directed or divided attention, as well as reading span with a distracting sentence judgment task. Temporal resolution was measured using amplitude modulation detection and gap detection in noise, while spectral resolution was measured using spectral ripple discrimination. This study included words in noise (WIN) and AzBio sentence recognition in noise as two speech recognition tests, and a music perception test of melodic contour identification. To examine the separate effects of age and hearing loss, the performance of ten older CI users was compared to the performance of ten older age-matched, normal-hearing (NH) adults and ten young NH adults.

Results

The young NH adults had significantly higher auditory digit span and visual letter span than older NH adults and CI users, while the two older groups had similar performance in these working memory tests. For all the other measures, there was a significant age effect observed for young and older NH adults and a significant

hearing loss/CI effect observed for older NH adults and CI users. Backward stepwise regressions revealed that, for older CI users, the duration of CI use and spectral resolution were the strongest predictors of speech recognition in noise, and only reading span weakly predicted melodic contour identification. For older NH adults, the gap detection threshold and auditory digit span with directed attention were the strongest predictors of speech recognition in noise. No significant predictors were identified for young NH adults'; speech recognition in noise and music perception, possibly due to the small variation and ceiling effects in their performance.

Conclusions

These results suggest that sensitivity to bottom-up spectral and temporal cues and working memory involved in top-down processing of context cues differentially contribute to speech and music perception for different listener groups. For CI users, increasing the spectral resolution appears to be the key to improve speech recognition in noise.

PS 892

Assessing Cognitive Load in Cochlear Implant Users Using a Recall Task and Pupillometry

Yue Zhang; Mickael Deroche; Alexandre Lehmann
McGill University

Although most adults with severe to profound hearing loss who receive cochlear implants (CIs) derive some benefit regarding speech recognition in quiet, substantial variability and individual differences in both speech performance and life quality still exist. Specifically, CIs do not transmit salient pitch percept due to the envelope-based coding strategies. This limits CI users'; performance on various tasks that rely on a fine sense of pitch, such as music and speech perception, prosody and speaker recognition, and competing speakers segregations. Furthermore, this lack of auditory saliency could also contribute to the elevated listening effort reported among CI users. It is likely that the lack of pitch information requires CI users to invest additional cognitive effort during the ongoing auditory stream to map the degraded signal inputs from the CI device to the phonological representations stored in their memory. Therefore, this current project aims to develop a robust task to measure the increased cognitive load of CI users and its negative impact on their short-term memory due to the poor pitch fidelity via CIs, using both behavioral task and pupillometry.

Testing materials are either French or English words (for native French or English participants respectively), with the F0 of these words manipulated in 4 conditions: 1) a monotonised condition where F0 remains steady at a fixed value; 2) a naturally intonated condition where

F0 is unprocessed; 3) an exaggerated condition where natural F0 pattern is doubled on a logarithmic scale; 4) an inverted condition where the natural F0 pattern is flipped upside-down on a logarithmic scale. Participants wear eyetracking glasses for tracking pupil size variations throughout the experiment. After the presentation of each word, they are required to repeat the word they heard. At the end of each 10-word list, participants are required either to recall as many words as possible from the previous 10 words, or to move on to the next list. It is hypothesised that the degraded pitch information will affect both the decoding of the acoustic signals during word recognition and the encoding of words for the recall task.

30 normal hearing and 30 CI adults will be recruited. The experiment will present a more comprehensive picture of the elevated listening effort experienced by CI users and its impact on their cognitive abilities. Furthermore, the additional cognitive load and the resulted memory impairment should also demonstrate the importance of improving the pitch availability in CI devices.

Auditory Prostheses VII: Brainstem & Cortex

PS 893

Optimizing Electrode Pairs

Hannah E. Staisloff; Justin Aronoff
University of Illinois at Urbana Champaign

Currently in clinics, bilateral cochlear implant maps are created by pairing electrodes in the two ears. These pairings are dependent on the frequency allocations and rely solely on the relative distance of electrodes from the end of the electrode array. Better performance may result by pairing electrodes based on a bilateral task, but it is unclear if different bilateral tasks would yield the same pairings. To investigate that, six bilateral Nucleus users were tested in Experiment 1. Three different bilateral tasks were used to determine the optimal bilateral pairs, one based on interaural time differences (ITDs), one based on interaural level differences (ILDs), and one based on pitch matching.

All three measures were acquired with five reference electrodes and multiple comparison electrodes. For each reference electrode, the optimal bilateral pair for ITD and ILD sensitivity was the pair that yielded the lowest threshold. The optimal bilateral pairs for pitch matching were based on the electrodes that yielded the same pitch. The results suggest that the optimal pairs based on ITDs, ILDs, and pitch matching differed.

Experiment 2 was conducted to determine if altering the frequency allocations, such that electrodes that

were optimally paired across ears received the same frequency allocation, yielded improved performance. Programs were created where the electrodes that were optimally paired were based on the ITD measure, the ILD measure, or the pitch matching measure from Experiment 1. Participants were assessed on tests of spectral resolution, pitch perception, and localization. Preliminary results suggest that the different programs yielded differences in performance.

PS 894

Dorsal Acoustic Stria Lesions Reduce Short-Latency IC Responses to Electrical Stimulation of the Dorsal Cochlear Nucleus

Stephen McInturff¹; Osama Tarabichi²; Vivek V. Kanumuri²; Nicolas Vachicouras³; Stéphanie P. Lacour³; Daniel J. Lee⁴; M. Christian Brown⁵
¹*Eaton-Peabody Laboratories, Massachusetts Eye and Ear, Harvard Program in Speech and Hearing Bioscience and Technology*; ²*Eaton-Peabody Laboratories, Massachusetts Eye and Ear, Harvard Medical School*; ³*École Polytechnique Fédérale de Lausanne*; ⁴*Department of Otolaryngology, Harvard Medical School*; ⁵*Eaton-Peabody Laboratories, Massachusetts Eye and Ear, Harvard Medical School, Harvard Program in Speech and Hearing Bioscience and Technology*

Introduction

Electrical stimulation of the cochlear nucleus (CN) is provided by the auditory brainstem implant (ABI), a hearing prosthesis used by human subjects with absent or damaged auditory nerves. The ABI stimulates CN neurons, but which neurons and subdivisions of the CN are activated is not known. Neurons project out of the CN through three acoustic stria: the dorsal (DAS), intermediate (IAS), and the ventral (VAS) acoustic striae. Here, in order to determine whether neurons projecting out the DAS and IAS are activated by the ABI, we compare how responses change after cutting these striae.

Methods

Using anesthetized CBA/CaJ mice, surgical exposure of dorsal CN (DCN) and IC were performed using a posterior craniotomy. A 3- or 4- channel conformable stimulating array microfabricated at the *École Polytechnique Fédérale de Lausanne (EPFL)* was placed on the DCN to provide monopolar electrical stimulation. Electrically evoked auditory brainstem responses (eABRs) were recorded with needle electrodes in the skin, and multi-unit neural activity was recorded with a 16-channel recording probe (NeuroNexus) placed in the central nucleus of the contralateral inferior colliculus (IC). Successively deeper cuts were made between the stimulated DCN and the

midline until a noticeable change in responses was identified. Placement of cuts was confirmed in Nissl-stained transverse sections by comparing sections to our previous database of labeled axons in the acoustic striae to determine if the cut severed: 1) the DAS and IAS, or 2) DAS only.

Results/Conclusion

Before cuts, IC responses to electric stimulation formed a broad peak with latencies between 0.42 +/- 0.18 and 9.4 +/- 1.85 with a local minimum at 3.25 +/- 0.87ms, which used as to distinguish early vs. late responses. Following a DAS/IAS cut (n = 17), or a DAS-only cut (n = 5), early responses were significantly attenuated ($p = 4.5 \times 10^{-10}$) while late responses remained unaffected ($p = 0.33$). Cuts reduced the amplitudes of peaks in the eABR but not their latencies.

These results suggest that the earliest IC responses to DCN electrical stimulation are mediated by DCN pyramidal/fusiform cells (whose axons exit the CN via the DAS). The IAS does not significantly contribute to these responses. In contrast, the later IC responses are mediated by cell types whose axons project out the uncut VAS. Thus, VCN cells, perhaps multipolar or bushy cells, may be stimulated by the human ABI even when the electrode array is on the surface of the DCN.

PS 895

Electrophysiological correlates of dichotic streaming in bilateral CI users.

Andrew Dimitrijevic¹; Brandon T. Paul¹; Mila Uzelac²; Varia Sajeniouk¹; Vincent Lin³; Trung Le³; Joseph Chen⁴

¹Sunnybrook Research Institute; ²University of Western Ontario; ³Department of Otolaryngology - Head & Neck Surgery, Sunnybrook Health Sciences Centre Toronto; ⁴Department of Otolaryngology - Head & Neck Surgery, Sunnybrook Health Sciences Centre Toronto, Canada; Institute of Health Policy, Management & Evaluation, University of Toronto

Background:

Cochlear implant (CI) users often have difficulty following conversations in the presence of distracting talkers. This requires selective attention to intended stream and perhaps suppression of an ignore stream. Previous work in normal hearing (NH) humans has shown selective attention to left versus right concurrent auditory streams are associated with specific neural markers: 1) increased "neural tracking" to the attend stream compared to the ignore stream and 2) alpha event-related synchronization (ERS) ipsilateral to the attend side. Neural tracking measures include cross correlation and temporal response functions between the EEG

(electroencephalogram) and the speech envelope. The purpose of this study was to determine whether neural signatures of perceptual stream segregation could be quantified in CI users and whether this measured could be related to performance.

Methods:

Two speakers positioned at +/- 45 degrees and at 1.5 meters away from the CI users and normal hearing (NH) listeners were used for stimulus presentation. The stimuli consisted of 4 to 7 pairs of digits presented to each speaker. Prior to each trial, a cue indicated which side the participant was instructed to attend to. The number of digits and attend side varied randomly across trials. The task was to recall the last digit presented on the cued side. A 64-channel EEG (electroencephalogram) recorded while subjects performed the task. Temporal response functions between the speech envelope and the EEG were separately performed for attend and ignore stimuli. Time-frequency analysis was also separately performed.

Results: CI users performed the task at 80-90% behavioural accuracy and NH controls performed near 100% accuracy. Neural tracking measures indicated that the attend stream evoked larger responses than the ignore stream peaking near 100 ms. The magnitude of the neural tracking measure was greater in NH compared to CI users. We also observed a cue-evoked alpha ERS in the ipsilateral hemisphere however, this effect appeared to be larger in CI users compared to NH listeners.

Conclusion: Our results indicate that neural tracking measures to sound objects are possible to record in CI users. Similar neural tracking signatures exist in bilateral CI users and NH listeners. The increase cortical alpha synchrony compared to NH maybe related to greater cognitive resources dedicated to this task in CI users compared to NH.

PS 896

Relationships Between Stimulus Intensity and fNIRS Responses in Cochlear Implant Users.

Hamish Innes-Brown; Darren Mao; Colette McKay
Bionic Ear Institute

Background: A totally objective and reliable method to program a cochlear implant (CI) is crucially needed in the CI clinic, especially for infants. Use of electrically-evoked compound action potentials have proven inadequate for this purpose when used alone, while cortical electrophysiological measures such as cortical auditory evoked potentials show more promise but are inefficient and subject to electrical artifact. Our earlier

published work with normal-hearing adults [1] showed that hearing thresholds and comfortably-loud levels could be estimated using functional near-infrared spectroscopy (fNIRS) responses. The objective of this study is to extend this work to develop an objective method to program a CI using fNIRS.

Methods: Five adults with existing CIs participated and were imaged while listening to tones via direct audio-input into a calibrated research processor. Tones were presented at a sub-threshold level, and at five supra-threshold levels spanning the electrical dynamic range. fNIRS responses were recorded in the bilateral auditory and pre-frontal cortices, and response amplitude was compared across stimulation levels.

Results and conclusions: fNIRS responses on average increased as a function of stimulus intensity. The fNIRS response is easy to measure in CI users and is not subject to electrical artefacts. Preliminary data with CI users are consistent with our earlier work using acoustic stimuli in normal and hearing impaired adults and children, and shows promise for objective programming of CIs.

1. Weder S, Xhou X, Shoushtarian M, Innes-Brown H, McKay CM. (2018). "Cortical processing related to intensity of a modulated noise stimulus - a functional near-infrared study," *J.Assoc.Res.Otolaryngol.* 19(3):273-286.

Acknowledgements: We thank Xin Zhou, Nicola Anglin, Virginia Roncagliolo, and Nicola Horvarth for assistance with recruitment and data collection. CM was supported by Veski and Lions fellowships, HIB by an NHMRC fellowship. The Bionics Institute acknowledges the support it receives from the Victorian Government through its Operational Infrastructure Support Program.

PS 897

Utilizing the Cochlear Implant to Characterize Electric Potentials During Transcranial Electric Stimulation

Phillip Tran; Matthew L. Richardson; Fan-Gang Zeng
University of California, Irvine

Non-invasive transcranial electric stimulation (tES) can be used to treat a number of neurological disorders such as epilepsy, depression, and tinnitus. However, delivering the required current to deep neural structures is often ineffective because of shunting through low-impedance pathways. We attempt to quantify the amount of current reaching a target by utilizing the cochlear implant (CI). A specific aim is to develop an empirical method for optimizing stimulation strategies that can target deeper structures, including the auditory nerve, for the treatment of tinnitus. In our study, non-invasive tES consisted of charge balanced, biphasic pulse stimuli being delivered

to five CI subjects from electrode pairs on the scalp and/or ear canal. Voltage levels within the inner ear target were recorded using CI back-telemetry. Conversely, CI stimulation was delivered via the intracochlear electrode array and surface potentials were recorded at 64 scalp electrode sites. Gain measures indicate substantial current spread, with a maximum of 2.2% recorded at the inner ear target during tES (mastoid-to-mastoid). Similarly, CI stimulation produced a maximum of 1% gain, measured at the scalp electrode nearest the CI return. Gain varied as a function of electrode montage according to a point source model that accounted for five distances: Active stimulation to CI, return to CI, active to monopolar reference, return to monopolar reference, and active to return. Within the same electrode montages, current gain patterns varied across subjects suggesting the importance of tissue properties, geometry, and electrode positioning. These results provide us with a starting point to improve neural excitation of deep structures; in particular, to optimize stimulation parameters that can activate the auditory nerve and effectively suppress tinnitus.

PS 898

Brain responses to silent lip reading in normal hearing, CI users, and CI candidates.

Andrew Dimitrijevic¹; Brandon T. Paul¹; Varia Sajeniouk¹; Antoine Shahin²; Mila Uzelac³; Trung Le⁴; Vincent Lin⁴; Joseph Chen⁵

¹*Sunnybrook Research Institute*; ²*UC Davis Center for Mind and Brain*; ³*University of Western Ontario*; ⁴*Department of Otolaryngology - Head & Neck Surgery, Sunnybrook Health Sciences Centre Toronto, Canada*; ⁵*Department of Otolaryngology - Head & Neck Surgery, Sunnybrook Health Sciences Centre Toronto; Institute of Health Policy, Management & Evaluation, University of Toronto*

Background: Previous work in human and animals have shown that deafness is associated with auditory cortex activation in response to visual stimuli. In CI users, greater degrees of auditory cortex activation to visual stimuli were associated with poor speech perception outcomes. The purpose of this study was to examine whether similar relationships exist in CI users and those waiting for a CI.

Methods: Normal hearing (NH), CI users, and those waiting for a CI ("pre-operative") were tested on a speech lip-reading paradigm using a silent movie as a stimulus. The movie consisted of a person uttering a single syllable animal lasting approximately 2.5 sec. The task was to watch the movie clip and indicate via keyboard the perceived word. A 64-channel EEG (electroencephalogram) recorded while subjects performed the task.

Results: Behavioral identification of the movie syllable object did not differ between all three groups. Evoked responses (P1/N1) were observed to the onset of the movie. Brain source analysis revealed that in NH and CI users, the visual cortex was maximally activated. In the pre-op population, the peak activity occurred in auditory temporal lobe regions. Time-frequency analysis indicated a robust alpha desynchronization that localized to occipital cortex in all three subject groups.

Conclusion: Cortical evoked potentials and brain oscillatory activity represent different aspects of neural processing. Evoked potentials appear to represent early sensory processing and show an abnormal generator in the pre-op population. No differences were observed in the brain oscillations between the groups suggesting similar post-sensory, cognitive neural networks are engaged resulting in similar behavioral identification outcomes.

PS 899

Next-Generation Auditory Brainstem Prosthesis for Profound Hearing Loss Using Array of Penetrating Silicon-Based Microelectrodes

Martin Han¹; Nicholas Nolta¹; Pejman Ghelich¹; Douglas McCreery²

¹University of Connecticut; ²Huntington Medical Research institutes

Background: For persons with deafness who cannot benefit from cochlear implants, including neurofibromatosis type 2 patients and a subset of cochlear implant users, some hearing may be restored by an array of stimulating electrodes implanted in their cochlear nucleus (CN). Major challenges are: (1) to develop a generalizable device design for the human cochlea nucleus, and (2) to determine how to modulate sound to electrical impulses in the auditory brainstem.

Methods: In this study, we have developed and chronically implanted arrays of penetrating silicon-based 3D microelectrode arrays into cats' cochlear nucleus. These are three-dimensional, four-shanked devices that feature five to eight independent electrode sites on each penetrating shank as compared to the single-tip microwire devices. This allows access to the tonotopic organization of the cochlear nucleus while also minimizing the number of penetrations into the brain. The silicon shanks combine the deep reactive ion etching technique and mechanical shaping of the probes' tip region, yielding a mechanically sturdy shank and a sharpened tip to reduce insertion force into the cochlear nucleus (Han, 2012). Significant progress has been made to streamline and advance this technology toward clinical translation. The cochlear nucleus device also included macroelectrodes that reside on the surface of the nucleus. The neuronal activity induced by modulated electrical stimuli applied through

both types of electrodes were recorded by another 3D array of also silicon 3D microelectrode arrays implanted in the inferior colliculus.

Results: Chronic animal study has been conducted. Results showed that the temporal modulation of the neuronal activity induced by the modulated stimuli applied in (penetrating) or on (surface) the CN was very similar across a range of modulation frequencies and modulation depths, especially for transient modulation simulating the periodicity of speech.

Conclusion: This concordance should greatly facilitate development of an auditory brainstem implant using surface electrodes and silicon-based penetrating microelectrodes in an integrated manner in order to convey both the loudness and pitch of sound. Advances in the device technology will also facilitate the clinical translation.

Acknowledgments: This work was supported by NIH grants R01DC013412 (DM) and R01DC014044 (MH).

PS 900

Cortical Processing of Frequency Changes in Cochlear Implant Users

Fawen Zhang¹; Chun Liang²; Gabrielle Underwood¹; Kelli McGuire¹; Jing Xiang³; Chelsea Blankenship⁴

¹University of Cincinnati; ²University of Cincinnati, Shenzhen maternity and child healthcare hospital; ³cincinnati children's hospital; ⁴University of Cincinnati/Cincinnati Children's Hospital Medical Center

Backgrounds

For cochlear implant (CI) users, speech and music tasks that heavily rely on the detection of frequency changes in sounds (e.g., speech perception in noise, talker gender identification, music melody perception, etc.) are extremely challenging (Kenway et al., 2015). However, little is known about how the auditory system processes frequency changes at the cortical level in CI users. Acoustic change complex (ACC) is a type of cortical auditory evoked potential elicited by changes in acoustic features (e.g., frequency, duration, and intensity etc.) embedded in an ongoing stimulus. Data in non-CI users have shown that the ACC threshold (the minimum magnitude of acoustic changes required to evoke the ACC) is in agreement with behavioral auditory discrimination threshold and the ACC amplitude is related to the salience of the perceived acoustic change (He et al., 2012; Liang et al., 2016). Examining how the brain processes frequency changes in CI users has important impact on the identification of appropriate assessment tools and the understanding of potential abnormalities in the brain function of CI users.

Methods

Sixteen post-lingually deafened adult CI users (age range from 20-66 years) participated in this study. Each CI ear was tested individually. All participants underwent a psychoacoustic test of frequency change detection, electroencephalographic (EEG) recordings, and speech tests (CNC words, AzBio sentence in quiet and noise, and Triple digit test). For the psychoacoustic test and EEG recordings, stimuli were 1-sec tones (base frequency of 0.25, 1, and 4 kHz) containing different magnitudes of upward frequency changes (0%, 5%, and 50%) at 500 ms from the stimulus onset. The frequency change occurred for an integer number of cycles of the base frequency and the change occurred at 0 phase (zero crossing), thus there were no audible transients when the frequency change occurred (Dimitrijevic et al., 2008). All test stimuli were presented in the sound field at the most comfortable level.

Results

Data analysis is still ongoing. The correlations between the ACC measures (amplitude and latency) and behaviorally measured frequency change detection thresholds (FCDTs) and speech perception performance will be examined. The effect of the base frequency on the FCDT and ACC measures will be examined.

Conclusions

The results will inform if the ACC evoked by frequency changes can serve as a useful objective tool in assessing frequency change detection capability and predicting speech perception performance in CI users.

PS 901

Loudness Integration by Auditory Brainstem Implant (ABI) and Cochlear Implant Users

Mahan Azadpour; William Shapiro; Mario Svirsky
New York University School of Medicine

Auditory brainstem implants (ABI) are clinically used to restore hearing to deaf patients who cannot benefit from cochlear implants (CI) due to damaged or nonviable auditory nerves or malformed/missing cochleas. ABIs bypass the auditory nerve and deliver electrical stimulation to the brainstem, using electrodes that are placed on the cochlear nucleus. Unfortunately, speech perception with ABIs is much worse than that obtained with CIs despite the fact that both devices encode information using similar trains of amplitude-modulated pulses delivered to different electrodes. The reasons for this difference between ABI and CI users are not well understood. In fact, little is known about how auditory processing of pulse train stimuli differs for ABI and CI users. This study investigates loudness integration by ABI and CI users in response to different numbers of stimulation pulses and inter-pulse intervals.

These data can illuminate differences in the properties of neurons stimulated by each device, and perhaps help interpret differences in speech perception outcomes. We assessed changes in perceived loudness as new pulses were added to a comfortably-loud reference pulse train in both ABI and CI users. The reference stimulus consisted of 6 pulses with 100ms inter-pulse intervals. Several experimental stimuli were created by inserting different numbers of pulses at different inter-pulse intervals after each one of the reference stimulus pulses (except the last one to maintain stimulus duration). We measured the change in current amplitude that was required for the experimental stimuli to match the loudness of the reference stimulus. The results from both ABI and CI subjects confirmed that current amplitude of the experimental stimuli had to be reduced to achieve matched loudness to the reference stimulus. However, the patterns of current reduction as a function of inter-pulse interval and number of additional pulses varied across ABI subjects, and differed for ABI and CI subjects. ABI and CI patterns sometimes differed when the number of added pulses was only one, suggesting that auditory response to a single pulse could differ for the two subject groups. The observed difference in loudness integration by ABI and CI subjects may be related to how cochlear nucleus and auditory nerve neurons respond to electrical stimulation pulses. Neural response behaviors (such as refractoriness and adaptation) could affect the way stimulation pulses are represented neurally and integrated for perception. These results suggest that biophysical properties that underlie neural response behaviors may differ for cochlear nucleus and auditory nerve neurons.

PS 902

Do Both Anodic and Cathodic Phases of Analog Stimulation Contribute to Rate Pitch?

Natalia Stupak¹; Monica Padilla²; David M. Landsberger³
¹New York University School of Medicine; ²University of Southern California Keck School of Medicine; ³NYU School of Medicine

It is assumed that in a biphasic pulse, both phases produce stimulation. Therefore, one would anticipate that for a fixed pulse rate, a biphasic pulse train, a cathodic (pseudo)monophasic pulse train and an anodic (pseudo) monophasic pulse train would produce the same rate pitch. However, with analog stimulation, the situation is less obvious. Unlike a biphasic pulse in which the anodic and cathodic phases are short and temporally adjacent, the anodic and cathodic phases of an analog signal are long and temporally separated. That is, if a neural population responds to both anodic and cathodic phases, a 100 pulse per second (pps) biphasic pulse train will produce firing every 10 ms. However, if the neural

population responds to both phases of an analog 100 Hz signal then one might expect it to respond every 5 ms.

Stupak et al. (2017) demonstrated that in monopolar mode, analog stimulation at a given frequency was scaled to have a similar pitch as monopolar biphasic pulse trains at the corresponding rate. This may suggest that the auditory system is responding to only one phase of the analog stimulation. Had it responded to both phases of the stimulation, it would likely have been perceived as having double the rate pitch. That is, a 100 Hz analog signal would have been rated as having a rate pitch more similar to a 200 pps pulse train than a 100 pps pulse train.

We reasoned that if the auditory system were only responding to one phase of an analog signal, then a bipolar analog signal may be perceived as having double the rate pitch as a monopolar signal. That is, for every cycle of an 100 Hz bipolar stimulus presented between electrodes A and B, an anodic phase would be presented twice (once on electrode A and once on electrode B).

In the present experiment, we compared the rate pitch of analog single electrode stimulation in monopolar and bipolar modes to determine if bipolar analog stimulation provides a rate pitch similar to monopolar stimulation at the same frequency or double the frequency. A parallel control experiment was conducted comparing rate pitch with monopolar and bipolar biphasic pulse trains. Early results suggest that for a given frequency, monopolar and bipolar analog stimulation provide similar rate pitches. These data potentially argue against the idea that the auditory system tracks both phases for rate pitch.

Support provided by the NIH/NIDCD (R01 DC012152).

PS 903

Cortical Auditory Evoked Potentials to Gaps in Tones: Comparison with Behavioral Gap Detection and Speech Perception in Cochlear Implant Recipients

Chelsea Blankenship¹; Fawen Zhang²

¹University of Cincinnati/Cincinnati Children's Hospital Medical Center; ²University of Cincinnati

Introduction: Speech recognition performance among cochlear implant (CI) recipients is highly variable and is influenced by their ability to perceive changes in frequency, intensity, and timing within the acoustic signal (i.e., temporal resolution). Behavioral gap detection threshold (GDT) tests, a common measure temporal resolution, require active participation which is infeasible for infants and young children. Cortical auditory evoked potentials (CAEP or P1-N1-P2 complex), have been used as a potential objective

measure of temporal resolution. While within-frequency gap detection (identical pre- and post-gap frequency) is most commonly assessed, across-frequency (different pre- and post-gap frequency) is thought to be more important for speech understanding. However limited studies have examined the across-frequency GDTs and its correlation with speech perception in CI recipients. The purpose of the study is to evaluate behavioral and electrophysiological measures of temporal processing and speech recognition in NH and CI recipients.

Methods: Post-lingually deafened adult CI recipients (N=15 ears, Mean=50.4 years) and age/gender-matched NH individuals were recruited. Speech perception was assessed with the CNC word, AzBio sentence, and BKB Speech-in-Noise test. Behavioral GDTs were measured for within-frequency (2kHz pre- and post-gap tone) and across-frequency conditions (2kHz pre-gap to 1 kHz post-gap tone) using an adaptive, two-alternative, forced-choice paradigm. CAEPs were measured with a 40-channel Neuroscan system for eight conditions (4 gap durations for both within- and across-frequency conditions). The gap durations were customized based on the subjects'; behavioral GDT: 1.) Threshold (θ or behavioral GDT), 2.) Supra-threshold ($\theta \times 3$), 3.) Sub-threshold ($\theta/3$), and 4.) Reference (No gap).

Results: CI recipients demonstrated significantly poorer speech understanding (CNC:70.53%;AzBio:65.47%; BKB:+8.18dB) compared to NH listeners (CNC:99.13%; AzBio:99.17%; BKB:-0.65dB, $p < 0.001$). A significant difference in behavioral GDTs between groups was not found for within-frequency (CI:9.6ms; NH:2.0ms) or across-frequency (NH:58.75ms; CI:82.44ms; $p > 0.05$). Data analysis has been finished for NH listeners. The pre-gap CAEP did not differ among gap or frequency conditions. The within-frequency CAEPs evoked by the gap-in-tones showed progressively increased amplitude with increases in gap duration, while the across-frequency CAEP did not differ with increases in gap duration. CI recipient data analysis is ongoing, preliminary results (N=4) show variable responses with some CAEPs displaying a similar trend of increased amplitude with increased gap duration.

Conclusions: CI recipients have significantly poorer speech perception performance with similar within- and across frequency GDTs. Further analyses will examine: 1.) group differences in CAEP amplitude and latency, 2.) the correlation among speech perception, behavioral GDTs, and CAEP amplitude and latency.

Auditory Brainstem Implant Array Position and Auditory Outcomes

Dana Egra-Dagan¹; Barbara S. Herrmann²; Mary E. Cunnane³; Samuel R. Barber⁴; M. Christian Brown⁵; Daniel J. Lee⁶

¹Eaton Peabody Lab, Massachusetts Eye and Ear infirmary; ²Department of Otolaryngology, Department of Audiology, Massachusetts Eye and Ear Infirmary, Harvard Medical School; ³Department of Radiology, Massachusetts Eye and Ear Infirmary; ⁴University of Arizona College of Medicine; ⁵Eaton-Peabody Laboratories, Massachusetts Eye and Ear, Harvard Medical School, Harvard Program in Speech and Hearing Bioscience and Technology; ⁶Department of Otolaryngology, Harvard Medical School

Background: The auditory brainstem implant (ABI) provides most patients with sound detection and speech pattern perception that aids lip reading. A few ABI users, however, are able to achieve open-set speech perception through audition alone. The underlying factors contributing to ABI outcome variability are not well understood. The goal of this study is to correlate ABI electrode array position with perceptual data. We hypothesize that differences in ABI array position may explain some of the variance in perceptual outcomes.

Methods: Retrospective review of adult ABI subjects with Neurofibromatosis type 2 (NF2) and non-NF2 etiologies with postoperative head computed tomography (CT) and perceptual data. Using the imaging methods of Barber, S. et al. (2017, *Ear and Hear.* 38(6):e343-e351), three-dimensional (3D) electrode array position was classified based on angles from the horizontal using posterior and lateral views and on distances between the proximal array tip superiorly from the basion (D1) and laterally from the midline (D2). Perceptual data included the number of electrodes that provided auditory sensation, level of speech perception (from no sound to open-set word recognition of monosyllables) and psychophysical threshold levels (T).

Results: CT imaging was analyzed from 15 NF2 and non-NF2 ABI subjects. Although the 3D orientation of the ABI array exhibited a variety of angles, all arrays were posteriorly tilted from the lateral view and most were medially tilted from the posterior view. ABI positions relative to the basion and midline showed mean distances of 1.58 ± 0.43 cm and 1.0 ± 0.3 cm for D1 and D2, respectively. The number of electrodes that provided auditory sensation ranged from 8 to 16 (out of a total of 21). Speech perception outcomes ranged from no sound detection to open-set recognition of monosyllabic words. The two subjects with open-set recognition had arrays that when viewed from posterior were oriented superiorly (neither having much tilt medially or laterally).

Conclusion: ABI array position based on postoperative 3D CT reconstruction varies widely and may contribute to the range of auditory outcomes seen in this specialized patient cohort.

PS 905

EEG Oscillations and Entrainment in Cochlear Implant Users While Watching “The Office”: Neural Correlates of Listening Effort and Speech Encoding with Continuous, Naturalistic Stimuli

Brandon T. Paul¹; Varia Sajeniouk¹; Joseph Chen²; Trung Le³; Vincent Lin³; Andrew Dimitrijevic¹

¹Sunnybrook Research Institute; ²Department of Otolaryngology - Head & Neck Surgery, Sunnybrook Health Sciences Centre Toronto ; Institute of Health Policy, Management & Evaluation, University of Toronto, Canada; ³Department of Otolaryngology - Head & Neck Surgery, Sunnybrook Health Sciences Centre Toronto

Background. Cochlear Implant (CI) users commonly report difficulty when listening to speech in adverse listening environments. As a result they must expend more listening effort (LE) to understand speech, but prolonged LE can lead to fatigue and even discontinued CI use. The neural mechanisms of LE are not well understood, but could provide valuable information to a clinician during the rehabilitation process. Here we measured brain oscillations using electroencephalography (EEG) while CI users were presented with naturalistic stimuli in different levels of background noise. The objective was to determine if self-reported LE correlated to alpha oscillations (8-12 Hz) and if these oscillations explained individual differences in EEG entrainment to the speech envelope.

Methods. Adult CI users (N = 18) watched the television show “The Office” using their everyday CI setting. Sound was delivered in a circular 8 speaker array. The front facing speaker played the sound of the show while the other speakers played multitalker babble. Three signal-to-noise ratios (SNR) were used +5, +10, and +15 dB. In addition to a 64-channel EEG recording, the audio output of the movie stimulus was simultaneously digitized as a channel on the EEG amplifier. EEG was recorded for 15 minutes for each of the SNRs. Subjective reports of task difficulty (i.e., watching and following the television show) were assessed using the NASA Task Load Index for each of the SNRs.

During analysis, the CI artifact was attenuated offline by using second-order blind identification (SOBI) ICA algorithm. The audio speech envelope and the EEG was low-pass filtered at 10 Hz. We used temporal response functions (TRFs) to predict 30-second intervals of

EEG activity from the audio envelope, and the quality of that prediction was taken as a measure of speech entrainment. Time-frequency analysis was used to quantify the power of alpha oscillations. In addition, cortico-acoustic coherence was measured.

Results. Preliminary results suggest that in the +5 dB SNR listening condition, LE was associated with increased cortico-acoustic coherence, increased speech entrainment, and reduced alpha oscillations. These results were not found in the +15 and +10 dB SNR conditions.

Conclusions. Both spontaneous EEG alpha activity and sensory encoding of the speech signal are related to LE. Project supported by the Barberian Scholarship Fund.

PS 906

Intra-Individual Correlations Between EEG Alpha Oscillations and Self-Reported Listening Effort Ratings During a Speech-in-Noise Task in Cochlear Implant Users

Brandon T. Paul¹; Joseph Chen²; Trung Le³; Vincent Lin³; Andrew Dimitrijevic¹

¹*Sunnybrook Research Institute*; ²*Department of Otolaryngology - Head & Neck Surgery, Sunnybrook Health Sciences Centre Toronto*; *Institute of Health Policy, Management & Evaluation, University of Toronto, Canada*; ³*Department of Otolaryngology - Head & Neck Surgery, Sunnybrook Health Sciences Centre Toronto*

Background. Cochlear implant (CI) users commonly indicate that a significant amount of listening effort (LE) is required to overcome difficulty with understanding speech in challenging environments, such as in noise or with competing talkers. Over time, chronic LE can exhaust the listener and sometimes lead to discontinued CI use. The physiological processes underlying LE are not well understood, making it difficult to target these mechanisms to assist with rehabilitation. Our past research in both normal-hearing (NH) and CI users has however found that inter-individual differences in frontal alpha oscillations (8-12 Hz brain rhythms) in the electroencephalogram (EEG) correlate with self-reported LE in a speech-in-noise perception task, suggesting this activity is a candidate neural marker of LE. In contrast to inter-individual differences, the goal of the current study is to determine if *intra*-individual changes in alpha activity can explain different degrees of LE exerted within the same CI user.

Methods. In an 8-speaker free field, eleven CI users were presented three spoken digits in multi-talker babble noise at different signal-to-noise ratios (SNRs).

Owing to large individual differences in speech in noise understanding, the range of SNRs was adjusted on an individual basis so that they were scaled to each CI user's range of effort ability. For each of the 180 trials, listeners verbally reported the digits that they heard, and rated LE on a 1-10 scale. During this time we recorded the 64-channel EEG. We used beamforming to extract sources of single-trial alpha activity during digit presentation, which thereafter were correlated to LE ratings using partial Spearman (rank) correlations in order to control for the changing SNR levels.

Results. Cluster-based permutation tests on these correlations revealed significant relationships between self-reported listening effort and alpha activity in right frontal brain regions in the majority of CI users. These areas are consistent with networks associated with attention and speech comprehension.

Conclusions. Results suggest that alpha activity indexes self-reported listening effort and can be used as an objective neural marker of LE in CI users and may help clinicians understand when a CI user is exerting a high degree of effort. Project support provided by MED-EL.

PS 907

Response Strength and Response Spread in Primary Auditory Cortex Using Different Pulse Shapes With Cochlear Implants: Is There a "Best/Optimal/Efficient" Stimulation Strategy?

Victor Adenis¹; Pierre Stahl²; Dan Gnansia²; Jean-Marc Edeline¹

¹*NeuroPSI UMR CNRS 9197*; ²*Oticon Medical, Vallauris, France*.

Many research efforts are still dedicated on improving the coding strategies of cochlear implants (CI). They all point out that the stimulation mode, the pulse shape and grounding schemes can exert either moderate, or drastic, consequences on the response strength, spread of excitation and nerve excitability. Several strategies are currently used to implement sound loudness such as increasing the pulse amplitude or the pulse duration. Here, we compared responses from auditory cortex neurons to stimulations delivered through a CI for which several parameters were modified such as the pulse amplitude, the pulse duration and the pulse shape. Experiments were performed in urethane anesthetized guinea pigs. The tonotopic gradient of the primary auditory cortex (AI) was first established by inserting an array of 16 cortical electrodes (2 rows of 8 electrodes separated by 1mm and 350µm within a row). A dedicated stimulation array (300µm) was then inserted in the cochlea (4 electrodes inserted in the 1st basal turn) and its connector was secured on the skull. The

cortical electrodes were placed back in auditory cortex at the exact same location as before the CI insertion. Twenty levels of charges were used to activate the auditory nerve through a dedicated stimulation platform. Stimulations were performed by increasing the pulse duration (PD) or pulse amplitude (PA) with either symmetric, asymmetric or ramped pulses. Asymmetric pulse shapes and ramped pulses were also tested for a given level of injected charge. For asymmetrical pulses, the ratio between the pulses phases increased from 1/1 to 1/10; for ramped pulses the angle was from 88 to 57°. On average, the firing rate (FR) evoked by the pulse duration (PD) and pulse amplitude (PA) strategies was similar and it was often similar with the asymmetric and ramped pulses. However, in many animals FR was lower than with pure tones. The spatial recruitment was often similar with the PA and PD strategy and with asymmetric and ramped pulse, but it was often lower than the one obtained with pure tones played at 75dB SPL. Group data suggest that equivalent cortical activation can be achieved with PA or PD strategy, with symmetric, asymmetric or ramped pulses. In individual cases, comparing the FR dynamic range and the spatial recruitment obtained with PA, PD, asymmetric pulses or ramped pulses, suggests that a particular strategy or pulse shape can be useful for limiting the spatial activation while still eliciting large FR changes.

PS 908

Effect of Current Steering and Current Focusing on Spectral Resolution

Monica Padilla¹; David M. Landsberger²

¹University of Southern California Keck School of Medicine; ²NYU School of Medicine

Introduction: Current steering and current focusing have each been proposed as methods of improving spectral representation. Current steering typically involves simultaneous stimulation on two adjacent physical electrodes creating an electric field such that the peak of stimulation is between the two physical electrodes. This technique is often used to increase the number of stimulation sites beyond the number of physical electrodes. Current focusing is a technique in which simultaneous stimulation is provided out-of-phase on multiple electrodes to reduce the spread of the electrical field and provide more precise stimulation. In this study, we investigate the effect of current steering and current focusing separately and together on a task (SMRT) that is dependent on spectral resolution.

Methods: Spectral resolution performance was measured using the SMRT task (Aronoff and Landsberger, 2013) in nine Advanced Bionics users. Experimental maps for monopolar (MP; no steering and no focusing), monopolar

virtual channels (MPVC; steering and no focusing), partial tripolar stimulation (TP+1; focusing and no steering) and virtual tripolar (VTP; steering and focusing) stimulation, were created using BEPS+ research software on BTE research processors. Maps were loudness balanced to the subjects'; clinical maps. SMRT was measured for four runs per strategy per subject.

Results: Preliminary results suggested that many subjects benefit from current focusing, while others perform better without current focusing. Most subjects benefited from current steering. Average performance across subjects suggests that both current steering and current focusing improve spectral resolution. However, the effects are not yet statistically significant.

Conclusions: Preliminary results show that both current focusing and current steering tend to improve performance on a task that depend on spectral resolution. However, there is great deal of variability across subjects and either focusing or steering can be detrimental for some subjects.

Support provided by the NIH/NIDCD (R01 DC012152), as well as Advanced Bionics for subject testing.

Hair Cells: Anatomy & Function

PS 909

The MRTF-SRF Circuit in Hair Cell Function and Maintenance

Tingting Du; Jung-Bum Shin
University of Virginia

Filamentous actin (F-actin) constitutes the structural basis of all hair cell features required for mechanoreceptor function, most prominently the hair bundle and the cuticular plate. Characterizing how the hair cell governs its F-actin dynamics is thus imperative for understanding the development, function and maintenance of the hair cell. Serum response factor (SRF) is a versatile transcription factor that is abundantly expressed in many cell types. It has been described in depth as an essential transcriptional regulator of cytoskeletal genes involved in actin dynamics. The myocardin-related transcription factor (MRTF) operates as a cofactor: dependent on the ratio of monomeric to filamentous actin, MRTF shuttles between the cytosol and the nucleus and regulates SRF-dependent transcription. Based on the importance of F-actin-based structures in the hair cell, we posited that the MRTF-SRF circuit might be essential for actin cytoskeleton homeostasis and mechanotransduction function in the hair cell.

To investigate the role of SRF in hair cell development and function, we generated a hair cell-specific *Srf* knockout mouse line. Our studies showed that deletion of *Srf* in hair

cells does not affect hair cell development, but causes rapid postnatal deterioration of the hair bundle in inner hair cells, and weakening of the cuticular plate in outer hair cells, resulting in profound hearing loss by wean age, especially affecting low frequencies.

We next developed a *Mrtf-b-2xHA* knock-in mouse model as a way to report MRTF-SRF circuit activity. In combination with recombinant anti-HA antibodies tagged with GFP and modified to be membrane-permeable ("Fluobody" and "Flashbody"), this tool can be used to visualize the nucleo-cytoplasmic shuttling of MRTF and SRF activity in the living hair cell. With this tool in hand, we will test whether the MRTF-SRF circuit is disturbed during ototoxic insults such as noise and mechanical damage, demonstrating the significance of the MRTF-SRF circuit for understanding a broad spectrum of sensorineural hearing loss phenotypes.

PS 910

Inner Ear Mitochondria Characterized By EM Tomography And Metabolic Analysis Into Distinct Subpopulations

Anna Lysakowski¹; Joseph Lesus¹; Steven Price¹; Kevin Arias¹; Vidya Babu¹; Sofia Sobkiv¹; Meet Patel¹; Anuj Kambalyal¹; Francisco Padron¹; Peymaun Mozaffari¹; Jacob Kulaga¹; Laila Ghatalah¹; Rose Bahari¹; Nora Laban¹; Bhoomi Desai¹; Mark H. Ellisman²; Guy Perkins²

¹University of Illinois at Chicago; ²School of Medicine, University of California, San Diego

The central hypothesis of this study is that *mitochondria in hair cells and inner ear sensory epithelia are non-homogeneous and that structural and molecular differences they exhibit are related to their differential responses to ototoxic insults, such as aminoglycoside toxicity and noise*. It is likely that due to variations in physical structure and corresponding molecular composition, the various sub-populations of hair-cell mitochondria are differentially affected by ototoxic insults, such as aminoglycoside antibiotics and chemotherapeutics. EM tomography and graphic reconstruction methods were used in the morphological analysis. Our results indicate that there are three different-sized populations of mitochondria in the vestibular sensory epithelium (based upon volume and surface area measurements): large (found in the subcuticular region of central zone type I vestibular hair cells); medium (in all hair cells and afferents); and small (in efferent boutons). We are also investigating mitochondria in the cochlea. By reconstructing several examples of each type, we are determining the average volume and surface area of each type, and the number and type of cristae (tubular, lamellar or tubulo-lamellar). In addition, we are investigating the number, size, and locations of

crista junctions (intersections of the cristae with the inner mitochondrial membrane) in relation to other significant structures within the cell. As one example of our structural findings, we found that in many hair cells, the cristae of mitochondria adjacent to the cuticular plate or to a striated organelle (SO) are perpendicular to, and polarized toward, this organelle. This means that, for example, these cristae, which are lamellar, align end-on with the cuticular plate and that the crista junctions (CJs) open towards the SO on that side of the mitochondrion. Short videos help us to determine the asymmetry in the distribution of CJs. Crista junctions, which function as barriers to the diffusion of molecules inside mitochondria, thus concentrating the oxidative phosphorylation complexes that generate ATP, are also thought to be key regulators for the release of apoptotic effectors. Finally, we are also attempting to characterize the three size sub-populations in vestibular hair cells by Seahorse Bioanalyzer analysis of oxygen consumption rates (OCR) and extracellular acidification rates (ECAR), with the goal of determining which sub-population is most sensitive to ototoxic antibiotics. We conclude that there are significant differences in morphology among these three mitochondrial sub-populations.

PS 911

Structural and Functional Analyses of Age-related Changes in Outer Hair Cell Mitochondria.

Guy Perkins¹; Jeong Han Lee²; Michael Anne Gratton³; Seojin Park²; Mincheol Kang⁴; Saeyeon Ju⁵; Mark H. Ellisman¹; **Ebenezer N. Yamoah**²

¹School of Medicine, University of California, San Diego; ²University of Nevada Reno; ³Washington University School of Medicine; ⁴University of Nevada, Reno; ⁵University of California, San Diego

Background: Since the mitochondrial theory of cell aging was proposed in the 1970s, evidence for mitochondrial structure/function correlates testing this theory has been sought. In the brain, mitochondrial size and size heterogeneity increase with age whereas mitochondrial membrane potential and metabolic competence (COX activity) of the largest mitochondria decrease with age and are correlated with a decrease in complex I-linked state 3 respiration. However, the basic mitochondrial structure does not change. We are investigating changes in mitochondrial structure and function in cochlear outer hair cells (OHC) in aged (15, 18 and 24-month) CBA mice compared to young mice of 3 months age.

Methods: We used fluorescence microscopy, histology, electron microscopy and tomography in the experimental analyses.

Results: We found that mitochondrial size and size

heterogeneity had increased and the number density of mitochondria had decreased in 18-month OHCs. Whereas, there was no change in mitochondrial volume density or mitochondrial membrane architecture or crista density with age. These findings suggest that mitophagy decreases and mitochondrial quality control deteriorates in the aged OHC.

Conclusions: In the auditory brainstem, the mitochondria in an associated adherens complex (MAC) have cristae oriented perpendicular to the synaptic membrane and increased density of crista junctions facing this membrane. Most of the mitochondria in the OHC are in close proximity to the subsurface cisternae (SSC). Because a high level of a calcium-ATPase has been found in the SSCs of OHCs, we are investigating whether there is a polarized orientation of cristae and an increased density of crista junctions towards the SSC, which may enhance the ATP-mediated modulation of calcium fluxes at the SSC

Funding: NIH AG051443-01A1, AG060504-01 (ENY)

PS 912

Cellular differences in the cochlea of C57BL/6 and CBA mice may underlie their difference in susceptibility to hearing loss

Huihui Liu¹; Genglin Li²; Hao Wu³

¹*Department of Otolaryngology Head & Neck Surgery, The Ninth People's Hospital, Shanghai Jiao Tong University School of Medicine, Shanghai, China.*
²*Ear Institute, Shanghai Jiao Tong University School of Medicine;*
³*Otolaryngology-Head and Neck Surgery, Shanghai ninth people's Hospital, Shanghai Jiao Tong University School of Medicine; Ear Institute, Shanghai Jiao Tong University School of Medicine;*
³*clinical auditory*

Background

Hearing is an extremely delicate sense that is particularly vulnerable to insults from the environment, including drugs and noise. Unsurprisingly, mice of different strains show different susceptibility to hearing loss. In particular, the CBA mice maintain relatively stable hearing over age while the C57BL/6J (C57) mice show a steady decline of hearing, making them a popular animal model for late onset hearing loss. We suspect that the different susceptibility to hearing loss between the two mouse strains may be due to the morphological and functional differences in their cochleae, and we believe revealing these differences could provide insights for uncovering cellular and molecular mechanisms for late onset hearing loss.

Methods

Experiments were carried out in juvenile CBA and C57 mice (4 weeks) with normal hearing. Auditory brainstem responses (ABRs), whole-cell patch-clamp recording and whole-mount cochlea staining were used to examine morphological and functional differences in the cochleae of the two mouse strains.

Results

While both the ABR threshold and Wave I latency are comparable between the two mouse strains, the C57 mice have a smaller Wave I amplitude. This difference in the Wave I amplitude is probably due to the less number of spiral ganglion cells found in the C57 mice, as the number of ribbon synapses per inner hair cell (IHC) are comparable between the two mouse strains. Next, we compared the outer hair cell (OHC) function and we found OHCs from the C57 mice have a larger non-linear capacitance, suggesting they could provide more mechanical amplification. Lastly, we examined the IHC functions, and we found IHCs from the C57 mice have a large Ca²⁺ current, release more synaptic vesicles, and recycle synaptic vesicles more quickly.

Conclusion Taken together, our results suggest that excessive exocytosis from IHCs in C57 mice raises the possibility of glutamate toxicity, which could be exacerbated by more amplification from OHCs found in these animals. The glutamate toxicity accumulates over time and eventually leads to late onset hearing loss.

PS 913

Expression Of The BK Channel γ Subunit LRRc52 (γ 2) In Mouse Inner Hair Cells And The „BK Channel Activation Paradox“

Isabelle Lang¹; Barbara A. Niemeyer²; Martin Jung³; Peter Ruth⁴; Jutta Engel¹

¹*Saarland University, Dept. Biophysics and CIPMM, Hearing Research;*
²*Saarland University, Dept. Biophysics and CIPMM, Molecular Biophysics;*
³*Saarland University, Institute for Medical Biochemistry and Molecular Biology;*
⁴*University of Tübingen*

The mammalian inner hair cell (IHC) transduces sound into depolarization, followed by transmitter release resulting in neuronal activation. The big conductance, voltage and Ca²⁺-activated K⁺ (BK) channels of the mature IHC are responsible for fast repolarization of the receptor potential and for the small time constant of the IHC, enabling it to respond very quickly to changes in membrane potential. BK channels of the mammalian IHC, which are localized at the IHC neck, are spaced at a large distance from Ca_v1.3 Ca²⁺ channels at ribbon synapses. Although they activate at negative voltages (V_{half} ~ -50 mV; Marcotti et al., J Physiol 2004)

they are - unlike non-mammalian hair cells - largely insensitive to Ca^{2+} influx, a paradox that has not been resolved so far.

Ca^{2+} -independent activation of BK channels at negative potentials can be caused by the newly detected γ subunits, the LRRC proteins 26, 52, 55 or 78, which upon heterologous expression shift the voltage of half-maximum activation of the BK current by -140 mV, -100 mV, -50 mV, -20 mV, respectively (Yang and Aldrich, PNAS, 2012).

We consistently detected mRNA for LRRC52 but not for LRRC26 in cDNA synthesized from mRNA harvested specifically from IHCs of organs of Corti of 3-week-old wildtype (WT) mice using a nested PCR approach. Fluorescence immunolabeling for LRRC52 using confocal microscopy revealed perfect co-localization with spot-like immunoreactivity for BK α , the pore-forming subunit, at the IHC neck. This co-localization was confirmed using a proximity ligation assay, which indicates that both proteins are localized within a distance of less than 40 nm.

LRRC52 protein being absent from IHC until P10 was co-expressed and co-localized with BK protein at the onset of hearing at P12 and later on. In three-week-old IHCs of BK α knockout mice, LRRC52 was not expressed. In IHCs of $Ca_v1.3$ -deficient mice, which lack BK α protein, LRRC52 was missing, too.

In sum, LRRC52 is an intrinsic γ subunit of the mouse IHC BK channel complex from the developmental upregulation of BK channel expression at the onset of hearing onwards and is a strong candidate for causing the Ca^{2+} -independent activation of BK currents at negative voltages in mouse IHCs.

Supported by IRTG1830, SFB 894 and Saarland University.

PS 914

Lateral Line Hair Cell Activity Modulates the Latency of Zebrafish Startle Responses

Yagmur I. Ozdemir¹; Elias T. Lunsford²; Mohamed A. Ramy¹; Rana Barghout¹; Peter Cho¹; Christina A. Hansen¹; Ashley R. Carter¹; James C. Liao³; Josef G. Trapani¹

¹Amherst College; ²University of Florida/The Whitney Lab for Marine Bioscience; ³The Whitney Laboratory for Marine Bioscience

Aquatic animals use proprioceptive multi-sensory information to adjust their motion to their environment. Zebrafish larvae (*Danio rerio*) display startle responses to potentially threatening stimuli with a fast body

contraction called a C-bend that projects them away from the source of danger. The lateral line of zebrafish consists of superficial hair cells that detect hydrodynamic changes, which may modulate the directionality and latency of startle responses. To further investigate the contributions of the lateral line to startle responses, we ablated lateral line hair cells of zebrafish larvae with neomycin. To elicit startle responses, we used pulses of 470 nm light to stimulate hair cells in a transgenic zebrafish line that expresses Channelrhodopsin2 (ChR2) in ear and lateral line hair cells. We then examined the latency and kinematics of resulting startle responses using time-locked high speed videos and field potential recordings. Ablation of lateral line hair cells resulted in a significant decrease in the latency of both field potentials and C-bends, indicating that lateral line inputs may serve an inhibitory role in the startle response circuit. By recording from two locations simultaneously, we also observed that afferent neuron activity in the lateral line is largely absent during periods of motor root activity. This finding highlights a potential reciprocal relationship between muscle activity during fictive swimming and hydrodynamic sensation by the lateral line. These findings fit well with motor control theories where an efference copy is used by an organism to predict or silence proprioception during locomotion and suggest that a lack of this input can modulate behavior, including the latency of startle responses during swimming.

PS 915

Electrical Stimulation Induces Morphological Changes in Lateral-Line Organs of Larval Zebrafish

Hanqi Yao¹; Mark E. Warchol²; Josef G. Trapani¹; Lavinia Sheets²

¹Amherst College; ²Washington University School of Medicine in St Louis

Hybrid cochlear implants are an increasingly popular option for patients with residual low-frequency hearing. However, close to 10% of patients with hybrid cochlear implants lose their residual hearing over time (Woodson et al., 2010). One possible explanation is that continuous electrical stimulation from the implant results in disruption to the morphology, innervation, and/or activity of hair cells. For instance, patients with residual acoustic hearing experienced delayed hearing loss after implant activation (Kopelovich et al., 2015). Moreover, 10-V electrical stimulation in rat cochleotypic explants led to 50% reduction in afferent nerve fibers innervating the organ of Corti (Kopelovich et al., 2015). Due to complex factors such as cochlear inflammation and surgical techniques, further studies on this topic are sparse. Here, to further investigate the effects of electrical stimulation on hair cells and afferent neurons, we exposed larval zebrafish to electrical stimulation. To

mimic a cochlear implant's electrical signal, we utilized a custom-built stimulation chamber and exposed free-swimming larvae to 200 Hz square-wave stimulation for 24 hrs. We then used confocal microscopy and antibody labeling to visualize the morphology and innervation of hair cells and presynaptic ribbon bodies. Preliminary results indicated experimental larvae had drastically fewer hair cells per neuromast and Ribeye puncta than control larvae immediately post-exposure. In addition, treated larvae exhibited uneven size and brightness of their Ribeye puncta, frayed terminal fields of afferent neurons, and pyknotic nuclei within hair cell structures of the lateral line. Our data suggest that prolonged electrical exposure causes changes in hair cell morphology and innervation. Ongoing experiments are aimed at determining whether damage persists in larvae following varying post-stimulation recovery periods, measuring physiological changes following stimulation by recording evoked and spontaneous activity from afferent neurons and examining the latency and kinematics of acoustic startle responses. Together, our results could provide information toward improving cochlear implant technology.

PS 916

High resolution imaging of marmoset inner ear hair cells

Leonardo R. Andrade¹; Sammy Novak²; Tong Zhang²; Melissa Wu²; Zac Davis²; Mathias LeBlanc²; John Reynolds²; **Uri Manor**¹

¹*Waite Advanced Biophotonics Center, The Salk Institute for Biological Studies*; ²*Salk Institute for Biological Studies*

Mouse models are indispensable for biomedical research, including hearing loss research. Mutations that cause defects in inner ear sensory hair cell structure and function in mice often lead to discoveries of novel deafness mutations in humans, and vice versa. However, there remain significant differences between the genetics and cell biology of primate versus rodent sensory hair cells. Mice lose all their hearing and most of their hair cells within 1-2 years, while the primate lifetime and hearing function can last at least an order of magnitude longer, sometimes up to and beyond 100 years in the case of humans. Thus, the mechanisms and extent of inner ear subcellular and cellular turnover are likely to differ between rodents and primates. To better understand the mechanisms of age- and noise-related hearing loss in humans, we are working to establish the marmoset as a model system for studying hearing loss and function. Marmosets are primates and share many features in common with humans. The lineage that became marmosets separated from us more recently (~30 MYA) than the lineage that became mice (~90

MYA). However, marmosets live ~10 years (in the wild, longer in the lab) so they can be studied longitudinally, as contrasted with macaques whose lifespan can be up to 25-40 years. Here we present high resolution imaging data that highlights the increased homology between marmoset and human hair cells in comparison to rodents. Using scanning electron microscopy, we show that marmoset inner ear sensory hair cells have ≥ 4 rows of stereocilia, whereas mouse hair cells only have 3. We also use Airyscan immunofluorescence imaging to show that the tip link protein cadherin-23, an essential component of the mechanotransduction machinery, localizes to the upper tip link density of three rows of stereocilia in marmoset, as opposed to two rows in the rodent. These data suggest that primate hair cells have a larger number of mechanotransduction channels than rodent hair cells, which has important implications for both their physiology as well as their longevity. These data furthermore demonstrate the feasibility of using only slightly modified tissue preparation and staining protocols developed for imaging mouse inner ear sensory tissue to study marmoset hair cell structure and function. Future directions include longitudinal studies of marmoset hearing function and hair cell structure, as well as the development of transgenic marmoset models for probing turnover of hair cell and spiral ganglion neuron components throughout the aging process.

PS 917

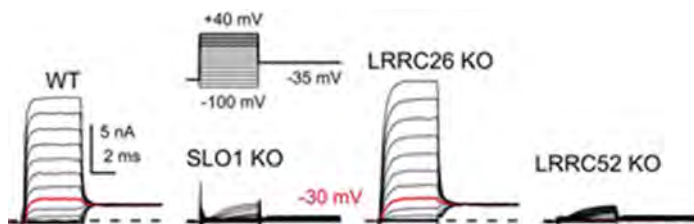
The Unique Gating Range of Inner Hair Cell Calcium- and Voltage-activated BK Channels is Defined by Gamma2, but not Gamma1, Regulatory Subunits

Christopher Lingle; Aizhen Yang-Hood; Shelby Payne; Xiaoming Xia; **Mark A. Rutherford**
Washington University in St. Louis

Both inner and outer hair cells of the mammalian cochlea robustly express Ca^{2+} - and voltage-activated BK-type K^{+} channels (Thurm et al., 2005). Some evidence indicates that inner hair cell (IHC) BK channels are essential for the precise timing of high-frequency cochlear signaling (Oliver et al., 2006). BK channels in both IHCs and outer hair cells have the unique property that they begin to be activated near -60 mV, even in the absence of Ca^{2+} . The gating range of BK channels is known to be influenced by a family of leucine-rich-repeat-containing (LRRC) regulatory subunits (gamma1: LRRC26; gamma2: LRRC52; gamma3: LRRC55) (Yan and Aldrich, 2012). At present, only gamma1 is known to unambiguously be a BK regulatory subunit in native cells, while gamma2 has been shown to be a partner of the Slo3 pH-regulated K^{+} channel in mammalian sperm (Zeng et al., 2015). Here, using KO mice, we address whether a member of the gamma subunit family may partner with the BK

channel pore-forming subunits in mouse IHCs. In WT IHCs, a fast voltage-dependent outward current ($I_{K,f}$), sensitive to the BK-selective blocker iberiotoxin (IbTx), begins to be activated around -60 mV. This current is absent in IHCs from BK KO mice (*Kcnma1^{-/-}*), but is unaltered in gamma1 KO mice (*Lrrc26^{-/-}*). In contrast, IHCs from gamma2 KO mice (*Lrrc52^{-/-}*) exhibit complete loss of BK current activation up to about +50 mV. Above +50 mV, an outward current absent in IHCs from BK KO mice begins to appear in gamma2 KO mice, indicative that BK channels are present but lack the regulatory components necessary to define the physiological gating range. An unexplained aspect of the results is that the gating range of BK currents in WT IHCs is left-shifted by about 40 mV relative to heterologously expressed gamma2-containing BK channels, suggesting there may be some additional factor regulating IHC BK current. These results establish that LRR52, thought to be a sperm-specific partner of the Slo3 K⁺ channel, is also a BK regulatory subunit and is critical in defining the unique properties of IHC BK channels.

Fig. 1. LRR52 regulates IHC BK current. IHCs of the indicated genotypes were stimulated with the indicated voltage-protocol. Red trace is at -30 mV. Slo1 KO defines currents in the complete absence of BK. LRR52 KO abolishes BK activation negative to +50 mV. XE991 inhibited KCNA current and 4-AP inhibited non-BK Kv current.



PS 918

Targeted Deletion of *Pou4f3* from Hair Cells Causes Apoptotic Hair Cell Death Followed by Loss of Supporting Cells in the Mouse Cochlea

Jarnail Singh¹; Michelle R. Randle²; Brandon C. Cox¹
¹Southern Illinois University School of Medicine; ²SIU School of Medicine

Germline knockout and mutational studies have previously demonstrated the critical role of the transcription factor *Pou4f3* in regulating hair cell (HC) survival during embryonic development. We recently demonstrated that deletion of *Pou4f3* from HCs in the neonatal, juvenile, and adult mouse cochlea causes massive HC loss at all

ages of deletion. Here, we investigated the mechanism of HC death after *Pou4f3* deletion and the long term effects of HC loss on supporting cells (SCs) and spiral ganglion neurons (SGNs). We used the CreER-loxP system (*Prestin^{CreERT2}·Pou4f3^{loxP/loxP}*) to delete *Pou4f3* from outer hair cells (OHCs) at juvenile and adult ages and *Atoh1-CreERTM·Pou4f3^{loxP/loxP}* to delete *Pou4f3* from both OHCs and inner hair cells (IHCs) at the neonatal age. Tamoxifen was injected on two consecutive days, in neonatal mice at postnatal day (P) 0 and P1, in juvenile mice at P12 and P13, and in adult mice at 4 weeks and 8 weeks of age. After *Pou4f3* deletion at 4 weeks of age, we observed many TUNEL-positive HCs 5-7 days after tamoxifen injection. This suggests that HCs die by apoptosis after *Pou4f3* deletion. We are currently measuring expression changes for genes associated with HC survival and apoptosis, as well as genes thought to be downstream of *Pou4f3*, using real-time qPCR. To study the long term effects of HC loss caused by *Pou4f3* deletion, we analyzed samples 16 weeks after *Pou4f3* deletion at neonatal, juvenile, and adult ages (4 weeks and 8 weeks). In the samples where *Pou4f3* was deleted from OHCs at the juvenile and adult ages, we observed occasional loss of some IHCs in all cochlear turns, but this was variable. However, there was a significant loss of SCs irrespective of the age when *Pou4f3* was deleted. We are currently performing similar studies to investigate whether SGN survival is impacted. In conclusion, *Pou4f3* deletion from HCs, regardless of the age it was deleted, causes apoptotic death of HCs, followed by a delayed loss of SCs.

Funding: Supported by NIH/NIDCD R01 DC014441

PS 919

The Mechanism of PKA Modulation on BK Currents in Chick Hair Cell

Jun-Ping Bai¹; Omolara Lawal¹; Na Xue²; Joseph Santos-Sacchi³; Dhasakumar Navaratnam⁴
¹Department of Neurology, Yale University School of Medicine, New Haven, CT; ²Department of Otolaryngology - Head & Neck Surgery, Shanghai Ninth People's Hospital, Shanghai JiaoTong University School of Medicine; ³Department of Surgery (Otolaryngology), Yale School Of Medicine; ⁴Department of Neurology and Neuroscience, Yale University School of Medicine, New Haven

Changing kinetics of large-conductance potassium (BK) channels in hair cells of nonmammalian vertebrates, including the chick, plays a critical role in electrical tuning, a mechanism used by these cells to discriminate between different frequencies of sound. Hair cells in the auditory epithelium are arranged tonotopically and show a gradual change in oscillation frequency

that corresponds to the cell's tonotopic location. BK channels show large openings in response to a rise in intracellular Ca^{2+} at a hair cell's operating voltage range. BK channels consist of an alpha subunit and a variable number of ancillary subunits. The interaction of these channels with protein kinase A (PKA) are well studied in other tissues, but little is known of the effects of PKA on BK channels in hair cells.

Recordings were made of tall hair cells from freshly isolated basilar papilla from E21 chicks, when hearing is mature. Recordings were obtained in the whole cell mode. Hair bundle heights were measured as a reference of its tonotopic location. Cells were recorded in the presence of blockers of KCNQ and small conductance Ca^{2+} dependent (SK) channels, to isolate BK currents.

Our data show that changes in extracellular Ca^{2+} in contrast to intracellular Ca^{2+} have distinct effects on the size and I-V relationships of the outward current in hair cells. Reducing extracellular Ca^{2+} and blocking voltage gated Ca^{2+} channels with $20 \mu\text{M}$ CdCl_2 both resulted in a reduction in the size of the current and a right shift in the I-V relationship. In contrast, buffering intracellular Ca^{2+} with EGTA resulted in a significant reduction in the size of the outward current with no change in its I-V relationship. Activation of PKA, unexpectedly, owing to the expression of the STREX variant in these cells, increased the size of the current and had no effects on its I-V relationship. We determine that Ca^{2+} induced Ca^{2+} release plays a significant role in BK channel activation in tall hair cells and provide data for the existence of a synaptic Ca^{2+} cistern that has been shown to be present in short hair cells, recipients of efferent innervation.

(Supported by NIH-NIDCD R01 DC007894)

Hair Cells: Mechanics & Motility

PS 920

A Three-state Kinetic Model for Prestin

Koichiro Wasano¹; Satoe Takahashi²; Samuel Rosenberg²; **Kazuaki Homma²**

¹National Institute of Sensory Organs, National Hospital Organization Tokyo medical Center; ²Northwestern University Feinberg School of Medicine

Background

Prestin is a voltage-driven molecular motor that is abundantly expressed in the lateral membrane of the outer hair cells (OHCs). This motor activity is the basis of OHC somatic electromotility. Although the importance of prestin for normal cochlear operation has been demonstrated, the molecular mechanism of how prestin

converts the changes in the cell membrane electric potential into mechanical work remains largely elusive. We show that a kinetic model containing three distinct voltage-dependent conformational states fully explains various electrophysiological characteristics of prestin, which cannot be explained by the widely accepted kinetic model containing only two voltage-dependent conformational states.

Methods

HEK293T-based stable cell lines that heterologously express wild-type and mutated prestin constructs with C-terminally attached mTurquoise2 were established. Whole-cell nonlinear capacitance (NLC) recordings were performed using either sinusoidal (2.5-Hz, 120-150 mV amplitude) or ramp (from -150 mV to +50 mV or from +50 mV to -150 mV) voltage stimuli superimposed with two sinusoidal stimuli (391 (f_1) and 781 (f_2) Hz, 10 mV amplitude). For stimulus frequency-dependent NLC measurements, f_1 was set at 195 ($f_2=391$), 391 ($f_2=781$), 781 ($f_2=1563$), 1563 ($f_2=3125$), and 3125 ($f_2=6250$) Hz. Recording pipettes were filled with an intracellular solution containing (mM): 140 CsCl, 2 MgCl₂, 10 EGTA, and 10 HEPES (pH 7.3). Cells were bathed in an extracellular solution containing (mM): 120 NaCl, 20 TEA-Cl, 2 CoCl₂, 2 MgCl₂, 10 HEPES (pH 7.3). Osmolarity was adjusted to 304 mOsm⁻¹ with glucose. Current data were collected and analyzed by jClamp (SciSoft Company, New Haven, CT) (Santos-Sacchi et al., 1998).

Results

We determined the apparent valence of the voltage-sensing charge (z_{app}) of prestin and its mutants from NLCs measured under various experimental conditions. We found that introduction of a three-state kinetic model is indispensable for explaining: (i) the prepulse effect on z_{app} , (ii) the dual Lorentzian stimulus frequency-dependence of z_{app} , and (iii) the stimulus frequency-dependent increase of z_{app} unexpectedly found in some prestin mutants.

Conclusions

The widely accepted two-state model can still be accepted as the norm for evaluating the voltage-driven motor activity of prestin. However, this practical exercise would not unravel the molecular mechanism of prestin.

PS 921

Effect of Efferent Activity on Hair Bundle Mechanics

Chia-Hsi Lin; Dolores Bozovic
UCLA

Hair cells in the auditory and vestibular systems receive both afferent and efferent innervations. A number of prior

studies have indicated that efferent regulation serves to diminish the overall sensitivity of the auditory system. The efferent pathway is believed to affect the sensitivity and frequency selectivity of the hair cell by modulating its membrane potential. However, its effect on the mechanical response of the hair cell has not been established. In the current work, we explore how stimulation of the efferent neurons affects the mechanical responsiveness of an individual hair bundle. We explored this effect on *in vitro* preparations of hair cells in the sacculus of the American bullfrog. We performed experiments using a two-compartment recording chamber, which exposes the hair cell's apical and basolateral surfaces to endolymph and perilymph solutions, respectively. Using a suction electrode, the entire saccular nerve was stimulated with either pulse trains or DC offsets. Efferent stimulation of both types routinely resulted in an immediate increase of the frequency of hair bundle spontaneous oscillations for the duration of the stimulus. Enlarging the stimulus amplitude, pulse length and/or the pulse frequency led to oscillation suppression. Additionally, we explored the phase-locking properties of spontaneously oscillating saccular hair bundles exposed to a mechanical stimulus. Hair bundles were mechanically stimulated using elastic fibers, and their motion was recorded with a high-speed camera. The response plotted over a range of stimulus frequencies and amplitudes forms a diagram known as an Arnold Tongue. The Arnold Tongues of hair cells undergoing efferent stimulation demonstrated an overall desensitization, frequency shift, as well as a broadened frequency selectivity, with respect to those of unstimulated cells. These mechanical responses to efferent activity are consistent with the inhibitory feedback commonly observed from efferent stimulation. Finally, the addition of *d*-tubocurarine or strychnine to the perilymph bath reversibly eliminated the aforementioned responses to efferent modulation.

PS 922

Theory Predicts the Experimental Variations Associated with the Potential of Maximum Voltage Sensitivity for Outer Hair Cells

Varun K.A. Sreenivasan¹; Vivek Rajasekharan²; William E. Brownell²; **Brenda Farrell**²
¹University of New South Wales; ²Baylor College of Medicine

Introduction. We and others have reported that the density of the displacement charge associated with the sensors in the lateral membrane of outer hair cells (OHC) decreases with cell size. We also observe that the potential of maximum voltage sensitivity, $V_{0.5}$ of this charge increases as the density decreases for OHCs isolated from the guinea pig. By comparing our measurements with theory we now show how the

relationship between the potential of maximum voltage sensitivity and density is explained. **Theory.** Kim and Warshel (e.g., J. Phys. Chem. B 2016 120: 418) use a fluctuation-dissipation relation to calculate the charge movement (Q) associated with voltage sensors. They show that Q is equal to the product of the voltage-independent capacitance of the membrane ($C_{L,Eq}$) when the voltage sensors exhibit minimal effect on Q (i.e., at hyperpolarized and depolarized potentials) and the potential difference between these quasi-equilibrium states (ΔV_{min}). This relationship was derived from the fluctuation-dissipation relation that shows $C_{L,Eq}$ is equivalent to the product of κT (κ : Boltzmann's constant T : temperature) and the variance of the charge detectable in the external circuit at the equilibrium states. When described in terms of the membrane potential when two states are equally occupied (i.e., $V_{0.5}$) it predicts that a plot of $V_{0.5}$ versus $Q/C_{L,Eq}$ will produce a negative slope of magnitude $\frac{1}{2}$ with intercept: $V_{d,min}$ representing the quasi-equilibrium voltage for one of the states. **Method.** Recordings were obtained with whole-cell patch clamp voltage clamp assay on outer hair cells isolated from guinea pig. The membrane capacitance of lateral membrane (C_{LW}) where the voltage sensors reside (i.e., $C_{LW} \equiv C_{L,Eq}$) was determined from the measured capacitance. Q and C_{LW} vary along the basal-apical axis of the cochlea providing data to determine the slope. We determine the mean $\langle V_{0.5} \rangle$ and $\langle Q/C_{LW} \rangle$ by grouping the data (bin width 5 pF) based upon the electrical size of the lateral membrane. **Results.** We find that $\langle V_{0.5} \rangle$ increases as $\langle Q/C_{LW} \rangle$ decreases and calculate a $V_{d,min}$: ~ 32 mV when fixing the slope to $\frac{1}{2}$ (R^2 : 0.844, P -value: 0.00008). Values reported with OHCs from rat also lie on this relationship. **Conclusion.** Theory offers an explanation for our observations, reconciles reported variations of $V_{0.5}$, and helps suggest whether this potential will be coincident with the resting potential *in vivo* as expected for optimum hearing.

PS 923

Towards Recovery of the Energy Landscape of the Pillar Bond of Outer Hair Cells with Force Spectroscopy

Brenda Farrell; Vivek Rajasekharan
Baylor College of Medicine

Introduction. The lateral wall of outer hair cell (OHC) contains two membranes the plasma membrane and the outermost lateral cisternae membrane that are sandwiched together by a cortical lattice. This cytoskeleton is composed of circumferential F-actin rings that are crosslinked axially by spectrin with *pillar* linkages that project perpendicular to connect the membranes. Our working model is that the *pillar* forms by anion exchanger 2 (AE2) within the plasma

membrane with F-actin and spectrin on the cortical lattice as proposed (Hearing Research 1997: 110-141), where AE2 contributes either fully to the linkage or forms part of a multicomponent linkage. To accommodate prestin within the membrane we propose that AE2 is hexagonally-close packed with a rhombus unit cell (60 x 60 nm), and 20 prestin dimers are semi-ordered within the liquid-crystal membrane associated with two AE2s, two protein 4.1s, one F-actin filament, and one $\alpha 2\text{-}\beta\text{V}$ spectrin tetramer. Lipids make up the remaining area to provide for 1 protein per 80-100 lipids. This model with a gap of 60 nm provides for a linker and prestin density of $640/\mu\text{m}^2$ and $6415/\mu\text{m}^2$ and a circumferential F-actin distance of 53 nm and requires that each monomer of prestin contributes to produce ~ 1.7 fC of charge/ μm^2 . The goal is to test and refine this model. Here we describe an approach to determine the *energy landscape* of the *pillar* bond. **Methodology.** We combine force spectroscopy with technology used to form membrane nanotubes from cells. This is achieved because the force to rupture the initial bonds is separate from the extrusion of the membrane nanotube. Force spectroscopy experiments involve separating a complex with application of a force and determining the probability distribution of the rupture force (f^R) at each experimentally measured loading rate. The lifetime of the bond is then determined from the distribution of f^R at each loading rate with the distance to the barrier, energy of transition state barrier(s) and rate(s) calculated with theories. In our case the experiment entails measuring rupture of one membrane-cytoskeleton bond, and establishing the number of bonds sharing the point load. **Conclusion.** We report the methodology employed to obtain the probability histograms of rupture of single membrane-cytoskeleton bonds in cells, especially differences relative to *in vitro* single-molecule experiments. We demonstrate that this methodology can reveal the characteristics of the OHC pillar-bond.

PS 924

Novel Role of Prestin in Echolocating Mammals?

Maria Morell¹; A. Wayne Vogl²; Lonneke L. IJsseldijk³; Marina Piscitelli-Doshkov⁴; Ling Tong⁵; Sonja Ostertag⁶; Marisa Ferreira⁷; Natalia Fraija-Fernandez⁸; Kathleen M. Colegrove⁹; **Jean-Luc Puel**¹⁰; Stephen A. Raverly¹¹; Robert E. Shadwick⁴

¹Inserm Unit 1051, Institute for Neurosciences of Montpellier; ²Department of Cellular and Physiological Sciences, The University of British Columbia; ³Department of Pathobiology, Faculty of Veterinary Medicine, Utrecht University; ⁴Zoology Department, The University of British Columbia; ⁵Virginia Merrill Bloedel Hearing Research Center, University of Washington; ⁶Department of Fisheries and Oceans Canada; ⁷Marine Animal Tissue Bank,

Portuguese Wildlife Society, Estação de Campo de Quiaios; ⁸Marine Zoology Unit, Cavanilles Institute of Biodiversity and Evolutionary Biology, Science Park, University of Valencia; ⁹Zoological Pathology Program, University of Illinois at Urbana-Champaign; ¹⁰INM, Inserm, Univ Montpellier; ¹¹Animal Health Center, Ministry of Agriculture

Prestin is an integral membrane motor protein located in outer hair cells (OHCs) of the mammalian cochlea. It is responsible for electromotility and required for cochlear amplification. Generally, prestin is expressed only in the basolateral membrane of OHCs. However, here we report that in five species of echolocating whales and two species of echolocating bats, specific labeling for the protein prestin was also observed in the cuticular plate and stereocilia of OHCs and inner hair cells (IHCs), in addition to the basolateral membrane. These labeling patterns were obtained using immunofluorescence technique and were confirmed using immuno-electron microscopy. Conversely, prestin labelling in cochleas from rats that were processed concurrently with cochleas from echolocating mammals showed only the typical staining of the basolateral membrane of OHCs. These findings provide morphological evidence that prestin can have a role in cochlear amplification in the basolateral membrane up to 120-180 kHz. We propose that the species of toothed whales and bats studied here have an additional mechanism involved in hearing based on a broader use of the motor properties of prestin. This study improves our understanding of the mechanisms involved in sound transduction in echolocating mammals and suggests a convergent evolution amongst widely different groups that echolocate.

PS 925

mRNA Profiles of OHCs Lacking Electromotility in Vivo

Jing Zheng¹; Yingjie Zhou¹; Kazuaki Homma²; Satoe Takahashi²; Mary Ann Cheatham¹

¹Northwestern University; ²Northwestern University Feinberg School of Medicine

Background

The unique motor protein, prestin, provides the molecular basis for outer hair cell (OHC) somatic electromotility (Zheng et al., 2000). Loss of prestin (prestlin knockout (KO), Liberman et al., 2002) or expression of mutant prestin that lacks electromotility *in vivo* (499-prestin knockin (KI), Dallos et al., 2008) results in an ~ 50 dB threshold shift and OHC loss by 6 weeks of age (Wu et al., 2004; Cheatham et al., 2015). The unexpected OHC loss discovered in both prestin mouse models raises the question of whether electromotility, or some other

aspect of prestin's activity, is required for OHC survival. If so, are common pathways/mechanisms involved? To define the molecular bases underlying OHC death, we performed single cell RNA sequencing (scRNA-seq) to analyze mRNA profiles.

Methods

OHCs were collected from apical turns in WT, prestin-KO, and 499-prestin-KI mice at P28 (n=3 for each) and processed in parallel for library preparation using a SMART-Seq V4 Ultra Low Input RNA Kit (Clontech). scRNA-seq and basic bioinformatics analysis were performed by the NUSeq Core Facility at Northwestern University as described previously (Takahashi et al., 2018). Pathway analyses were performed using Metascape, MetaCore, and Ingenuity Pathway Analysis.

Results

Compared to WT, expression of 525 genes in prestin-KOs and 413 genes in 499-prestin KIs were significantly different (FDR adjusted, $p < 0.05$). Among them, 47 genes were up-regulated and 54 genes were down regulated in both mouse models. Except for non-coding RNA/tRNA processing, we did not find common pathways or enriched ontology clusters that were significantly different from WT among these two prestin mouse models. This result is consistent with the fact that each mouse model showed distinct but abnormal changes in neuronal innervation patterns and in the distribution of several membrane proteins (Takahashi et al., 2018). The most significant changes in prestin-KOs occurred for genes involved in stress-induced apoptosis, consistent with OHC loss observed in mice lacking prestin. However, these enriched apoptosis gene clusters were not found in 499-prestin KIs that showed even greater OHC loss, suggesting that OHC death in KO and 499-KI occurs via different pathways.

Conclusions

scRNA-seq using OHCs from prestin-KO and 499-prestin KI mice did not reveal common pathways that are differentially regulated when compared to WT. This observation suggests that different mechanisms underlie OHC loss even though these two mouse models exhibit similar changes in sensitivity and frequency selectivity.

(Work supported by the American Hearing Research Foundation and the Knowles Hearing Center).

PS 926

Kinetic Membrane Model of Outer Hair Cells

Kuni H. Iwasa

NIH

Outer hair cell (OHC) motility is essential for the sensitivity, frequency selectivity, and the dynamic range of the mammalian ear. This motility is based on piezoelectric properties of membrane protein SLC26A5 (prestin). It is driven by the receptor potential that is generated by the sensory hair bundle of the each cell. Even though such a biological role of this motility has been confirmed by using mutant animals, the mechanism, with which OHC motility plays this role, has not been fully understood.

In previous reports(*), mechanical power output of OHC has been evaluated assuming a two-state model of the motile protein with a simplified one-dimensional (1D) model for the OHC, which is rather phenomenological. Here the previous treatment is extended by introducing a more physical membrane model. As in the previous treatment, the power output of an OHC is evaluated by imposing a viscous and elastic loads in parallel with the cell. Consistent with the previous 1D model, the maximal power output is near mechanical resonance frequency, where the movement of prestin charge nearly cancels out the structural membrane capacitance of OHCs.

The present model predicts that nonlinear capacitance is sensitive to both turgor pressure and external elastic load. An increased elastic load reduces the peak height and broadens the voltage dependence of nonlinear capacitance. The peak voltage shifts in the negative direction if turgor pressure is lower, and in the positive direction if the turgor pressure is higher, as the elastic load increases. The critical turgor pressure corresponds to the volume strain of 0.065. However, mechanical power output of OHCs was not as sensitive to turgor pressure as nonlinear capacitance is.

The maximum power output of the membrane model is higher than the estimates based on the 1D model by up to 20%, corroborating the previous analysis: for OHCs to cover the entire auditory range, multiple modes of motion in the cochlear partition is required: Because the elastic load cannot be significantly larger than that of OHC for high power output, resonance at higher acoustic frequency range requires small inertial load associated with OHC. This result appears to be consistent with recent observations on the motion of organ of Corti with optical coherence tomography (OCT) technique.

*) Iwasa KH: Biophys J. 111(2016)2500-2511, doi: 10.1016/j.bpj.2016.10.021; Iwasa KH: Sci Rep. 7(2017)12118, doi: 10.1038/s41598-017-12411-6.

PS 927

Chaotic Dynamics Enhance the Sensitivity of Inner Ear Hair Cells

Justin Faber; Dolores Bozovic
UCLA

Hair cells of the auditory and vestibular systems are capable of detecting sounds that induce sub-nanometer vibrations of the hair bundle, far below the stochastic noise levels of the surrounding fluid. Hair cells of certain species are also known to oscillate without external stimulation. The role of these spontaneous oscillations is not yet understood, but they are believed to be a manifestation of an underlying active mechanism. As this active process constitutes an important topic in auditory research, a deeper understanding of spontaneous motility could impact our understanding of the extreme sensitivity of hearing. We previously demonstrated that these spontaneous oscillations exhibit chaotic dynamics. Nonlinear systems that exhibit chaos have been shown to be highly sensitive to small perturbations. We therefore propose that hair cells exploit the nature of chaotic dynamics to achieve their sensitivity of detection. We will present experimental measurements of spontaneous and stimulated hair bundle oscillations, which were obtained from the sacculus of the American bullfrog. By varying the Calcium concentration and the viscosity of the Endolymph solution, we were able to modulate the degree of chaos in the hair bundle dynamics. We found that the hair bundle was most sensitive to weak stimulus when poised in a weakly chaotic regime. These results agree well with our numerical simulations of a chaotic Hopf oscillator.

PS 928

SLC26A5 (Prestin) Interaction With Anions

Tatiana Sukhanova¹; Silvia Ravera²; Qiang Song³; Nancy Carrasco²; Dhasakumar Navaratnam⁴; Joseph Santos-Sacchi⁵

¹*Yale School of Medicine, Department of Surgery (Otolaryngology)*; ²*Yale School of Medicine, Cellular and Molecular Physiology Department*; ³*Department of Surgery (Otolaryngology) and Neurology, Yale University School of Medicine*; ⁴*Department of Neurology and Neuroscience, Yale University School of Medicine, New Haven*; ⁵*Department of Surgery (Otolaryngology), Yale School Of Medicine*

Prestin (SLC26A5) is a motor protein present in the membrane of outer hair cells in the inner ear of mammals. It is a member of the SLC26 anion transporter family, whose members are responsible for binding and transport of various mono- and divalent anions across membranes. We are currently working on cryo-EM structural studies of prestin, and require evidence of

functionality of our purified protein. The aim of this work was to study conformational changes in prestin resulting from established interactions with the monovalent halide anions (Cl, I, F) and gluconate. Interaction was determined via tryptophan (Trp) fluorescence measures. Prestin was extracted and purified from a HEK cell line, conditionally expressing prestin-YFP. The Trp assay shows changes in Trp fluorescence resulting from conformationally-induced changes in the exposure of these residues within prestin upon anion binding (concentrations ranging from 0.1 to 100 mM).

Each halide was able to reduce Trp fluorescence, indicating conformational changes due to binding. For Cl, reduction plateaued above 1 mM at 90% of initial value. This value is near the reported Cl K_d for prestin. The reduced fluorescence indicates a change in the conformation of the protein (reduced tryptophan exposure), in agreement with the effects of Cl on OHC NLC and motility. We have begun to use the scintillation proximity assay (SPA) to further assess binding of I-125 to prestin.

Supported by NIH-NIDCD R01 DC000273, R01 DC016318 and R01 DC008130 to JSS and DN.

PS 929

SLC26A5 Membrane Protein Purification for Structure Analysis

Qiang Song¹; Alexei Surguchev¹; Jun-Ping Bai²; Dhasakumar Navaratnam³; Joseph Santos-Sacchi⁴

¹*Department of Surgery (Otolaryngology) and Neurology, Yale University School of Medicine*; ²*Department of Neurology, Yale University School of Medicine*; ³*Department of Neurology and Neuroscience, Yale University School of Medicine, New Haven*; ⁴*Department of Surgery (Otolaryngology), Yale School Of Medicine*

Prestin is the outer hair cell motor responsible for cochlea amplification. Based on threading analysis including cysteine scanning mutagenesis

prestin is modeled to have a 7+7 inverted repeat structure that has been observed in a number transporters. Based on homology and phylogenetic relationships prestin is most closely related to UraA, Slc26Dg and AE1, proteins that have structural data in two conformations (inside open – UraA and SLC26Dg, outside open –AE1). However, prestin has a mechanical response which has no equivalent in other transporter proteins.

Prestin-YFP was purified using a combination of His/ Ni affinity chromatography and size exclusion chromatography from a stably expressing HEK293 cell line. We explored a number of detergents and found

N-Dodecyl-beta-Maltoside Detergent (DDM) to be effective in extracting the protein. We established that exchanging LMNG at its critical micellar concentration for DDM allowed for a monodispersed preparation. Several forms were identified including one corresponding to its monomeric form and one that corresponded to a tetrameric or dimeric form. Negative staining confirmed uniform particle size. Presently our efforts are concentrated on obtaining monodispersed prestin after scaling up biochemical purification to allow incorporation into nanodiscs.

Funding

This study is supported by NIH-NIDCD R01 DC000273, R01 DC016318 and R01 DC008130

PS 930

Attempts at solving SLC26A6 (A6) structure by Cryo-EM

Alexei Surguchev¹; Alberto Rivetta²; Frederick Sigworth²; Dhasakumar Navaratnam³; Joseph Santos-Sacchi⁴

¹Department of Surgery (Otolaryngology) and Neurology, Yale University School of Medicine;

²Cellular and Molecular Physiology, Yale School Of Medicine;

³Department of Neurology and Neuroscience, Yale University School of Medicine;

⁴Department of Surgery (Otolaryngology), Yale School Of Medicine

Prestin, a member of the SLC26 family of anion transporters, is responsible for motility of outer hair cells. It is believed to function by responding to membrane voltage changes producing intra-molecule charge movements, resulting in conformational changes transmitted to the OHC lateral membrane. The current 7+7 inverted repeat model is based on homology modeling of three distant family members SLC26Dg, UraA, and AE1. However better structural information is long overdue in order to get a clearer understanding how prestin functions on a molecular level. We choose human SLC26A6 (A6) which has 40% identity (65% allowing for conservative substitutions), and is expected to be a superior structure to model prestin to. A6 is an anion-exchanger/transporter expressed in the apical membrane of the kidney proximal tubule. It transports oxalate, sulfate, and bicarbonate. Previously, we reported the use of insect cells for expression of A6 from a baculovirus infected SF9 cells. We optimized the expression conditions, and perform a two-step purification procedure of affinity and SEC chromatography in the presence of the non-ionic detergent DDM. The resulting SEC profile consists of two distinct peaks. The first peak was non-symmetrical and represented A6 dimers or larger protein oligomers. The second peak was symmetrical, and represented A6

monomers. Fractions from both peaks were separately analyzed by negative staining (NS) EM. The NS revealed that both peaks were particle size dependent, however only particles from peak two were homogenous and monodispersed. On the other hand, particles from peak one were of diverse sizes and shapes, and showed a significant degree of aggregation. The fraction from peak two were concentrated, and used to prepare frozen grids for Cryo-EM. Data generated from Cryo-Em pictures will be analyzed by Relion for particle classification, 2D analysis, and 3D reconstruction. In case data from A6 in DDM detergent proves to be of subpar quality for 3D reconstruction, we will attempt to reconstitute A6 into lipid nanodisc and repeat the Cryo-EM data acquisition and analysis.

PS 931

The Frequency Response of Outer Hair Cell Motility Indicates a Voltage Dependent Cellular Compliance Governed by Prestin.

Joseph Santos-Sacchi¹; Kuni H. Iwasa²; Winston Tan³

¹Department of Surgery (Otolaryngology), Yale School Of Medicine; ²NIH; ³Yale University

The outer hair cell (OHC) of the organ of Corti underlies a mechanically based process that enhances hearing, termed cochlear amplification. The cell possesses a unique motor protein, prestin, which senses voltage and consequently changes conformation to cause significant cell length changes, termed electromotility (eM). Prestin's voltage sensor generates a capacitance that is both voltage and frequency dependent, peaking in magnitude at a characteristic membrane voltage (V_h) that can be greater than the cell's linear capacitance. Consequently, the OHC membrane time constant is multifarious depending upon resting potential and frequency of AC stimulation. After precisely correcting for this influence on the whole-cell voltage clamp time constant, we find that OHC eM is low pass in nature, substantially attenuating in magnitude within the frequency bandwidth of human speech. The frequency response is slowest at V_h , with a cut-off near 1.5 kHz, but increases up to six-fold in a U-shaped manner as holding voltage deviates from V_h . NLC mirrors this pattern. Bath viscosity influences on eM alone cannot account for such behavior, nor can they be combined with a sigmoidal voltage-dependent OHC stiffness (He and Dallos, JARO, 1:64-81, 2000). However, viscous drag combined with kinetics of prestin, resulting in the bell-shaped "gating compliance" of prestin (Iwasa, JASA, 107: 2764-2766, 2000), is in line with our observations. How OHC eM influences cochlear amplification at higher frequencies needs reconsideration and may require considering loads on the cell.

Hair Cells: Synapses

PS 932

Modelling the Dynamical Properties of the Vestibular Hair Cell Synapse

Aravind Chenrayan Govindaraju¹; Imran Quraishi²; Karolina G. Simcic³; Anna Lysakowski⁴; Ruth Anne Eatock³; Robert M. Raphael¹
¹Rice University; ²Yale University; ³University of Chicago; ⁴University of Illinois at Chicago

In the past few decades, electrophysiological experiments have provided data on the physiology and function of ion channels and pumps within the sensory epithelia of the vestibular inner ear. In mammals and other amniotes, a striking feature of these epithelia is the presence of cup-shaped synaptic terminals (calyces) made by primary afferent neurons on specialized mechanosensory cells (type I hair cells). These are the only postsynaptic calyces reported in the nervous system, with the flow of information from hair cell to calyx. Recent work has shown that type I hair cells transmit to calyces by two mechanisms: (1) conventional release of glutamate from vesicles ("quantal") and (2) unconventional flow of ions from the hair cell into the cleft and the postsynaptic calyx ("non-quantal"). Details of this complex transmission remain unknown, and the relevant compartments (cells and synaptic cleft) are hard to access, hindering the measurement of ion concentrations and potentials. As a complementary approach, we are creating a mathematical model of the vestibular hair cell-calyx synapse (VHCC) with the goal of predicting and accounting for both quantal and non-quantal transmission modes and their interactions. The VHCC model incorporates the specific location and surface density of ion channels (MET, HCN, Kv, Ca_v, Na_v) and pumps (Na-KATPase, KNCC, KCC) expressed in hair cells and calyces, along with measurements of cell and calyx geometry from electron micrographs. The dynamic behavior of the system is determined from measured or estimated open probabilities, conductance, and activation times of the channels. The VHCC model is implemented in COMSOL and Matlab using a variant of the cable equation along with K⁺ electrodiffusion in the cleft, simplified Hodgkin-Huxley-style ion currents, and stochastic vesicle release along an axisymmetric parametric surface. In its current state, our model can mimic patterns found in voltage recordings from the vestibular hair cell synapse. This model will allow us to test the effects of changing parameters such as voltage, ion concentration, and cytosolic regulatory factors such as cAMP, on the gamut of channels and pumps. The VHCC model can be extended to

simulate inputs from multiple calyces/dendritic trees. Consolidation of these details into a representative model will help explain how head motions are encoded by the vestibular inner ear and allow us to test ideas about the special roles of type I-calyx synapses.

Supported by NIH-NIDCD R01 DC012347

PS 933

The Distribution of Synaptic Architectures in Utricular Hair Cells: Analyses Across Spatial Scales

Johnny J. Saldate¹; Ivan A. Lopez²; Richard Schalek³; Jeff Lichtman³; Mark Terasaki⁴; Felix Schweizer¹; Larry Hoffman¹

¹Geffen School of Medicine at UCLA; ²Department of Head and Neck Surgery, David Geffen School of Medicine; ³Harvard University; ⁴University of Connecticut Health Center

Presynaptic regions within hair cells of inner ear sensory epithelia are characterized by synaptic ribbons, electron-dense structures exhibiting multiple morphologies enshrouded by neurotransmitter-containing vesicles. Ribbon complexes exhibit architectural heterogeneity within and between hair cells, which evidence suggests has physiological correlates. However, the 3D ultrastructure of ribbon complexes has not been extensively explored. Therefore, a comprehensive understanding of ribbon archetypes represents an important step in understanding their specific contributions to processing within sensory epithelia. We approached this objective through serial ultrastructural analyses to elucidate the 3D architecture of ribbon complexes in murine utricular hair cells. Utricles from C57BL/6 mice were harvested, fixed (4% paraformaldehyde, 2% glutaraldehyde), and prepared for ATUM-SEM (automated tape-collecting ultramicrotomy and scanning electron microscopy) as previously described (Terasaki et al. 2012, Kasthuri et al. 2014). Sections were obtained at 30 and 50 nm thicknesses, and imaged at 4 and 3 nm/pixel, respectively. We also utilized an immunohistochemical approach in cryosectioned and whole-mounted tissue, followed by high-resolution confocal microscopy, to examine defined sub-populations of hair cells within striolar and extra-striolar utricular regions.

Ribbon complexes in utricular hair cells conformed to two general architectures. As previously described, individual micrographs revealed simple architectures, characterized by a single ribbon body, exhibiting spheroid, ellipsoid, or bar morphologies surrounded by clear vesicles. While many spheroid or ellipsoid ribbons conformed to the expected structures in serial reconstructions, 2D-apparent bar-type ribbons were most often found upon reconstruction to be sections

of a "plate", resembling ribbons found in retinal rods. Such plates extended more than 0.5 μm along the presynaptic membrane. Some plates extended $>1 \mu\text{m}$ into the hair cell cytoplasm. Other architectures were found to be ribbon clusters, represented by multiple ribbons exhibiting mixed morphologies (bars/plates or spheroids/ellipsoids). Adjacent ribbons within a cluster were separated by, and potentially share, a single "sheet" of vesicles. Close apposition with the presynaptic membrane was very limited in some cases but quite extensive in others. Presynaptic contact was made most often by only 1-2 ribbons of a given cluster, strongly implying the existence of mechanisms to shuttle vesicles from distal ribbons to the active zone. These results provide strong support for the ability to identify cluster architectures through immunohistochemistry, providing the capability to examine architectural distributions over large regions of vestibular epithelia. The architectural heterogeneity of utricular hair cell synaptic ribbons may underlie broad physiological heterogeneity in spontaneous and dynamic postsynaptic activity.

PS 934

Acute Disruption of Synaptic Ribbons in Auditory Hair Cells Reduces the Rate of Exocytosis without Altering its Temporal Precision

Adolfo E. Cuadra¹; Geng-Lin Li²

¹Biology / Morrill II; ²University of Massachusetts

Ribbon synapses are found in both the retina and the cochlea where synaptic transmission must operate over a broad dynamic range of graded membrane potentials. However, the exact functions of synaptic ribbons are not clearly understood. In particular, it is unknown if synaptic ribbons play a role in exocytosis of high temporal precision from auditory hair cells, which is required for phase-locking. In the present study, we performed paired patch-clamp recording in hair cells and auditory afferent fibers in the bullfrog amphibian papilla, a hearing organ responding to sounds of 100 Hz ~ 1 kHz. To reveal functions of synaptic ribbons, we dialyzed hair cells with a FITC-tagged ribbon binding peptide (10 μM) via the patch clamp pipette and applied fluorescence-assisted light inactivation (FALI) to disrupt synaptic ribbons. We first applied strong step depolarization (-30 mV, 500 ms) to hair cells and recorded the presynaptic capacitance jump (ΔC_m) and the excitatory postsynaptic current (EPSC) simultaneously. We found that FALI markedly reduced ΔC_m , from 140.3 ± 34.5 to 59.3 ± 16.9 fF (n=9). Consistently, FALI reduced the initial EPSC peak to $68.4 \pm 7.5\%$ (n=9), but the sustained release was reduced to a greater degree, to $31.8 \pm 5.9\%$, suggesting that disruption of synaptic ribbons reduces the rate of exocytosis by slowing down synaptic vesicle recruitment. Next, we applied intermediate step depolarization (-55

mV, 5 s) to induce exocytosis at a low rate and we found that neither the rate nor the amplitude of EPSC events was affected, suggesting disruption of synaptic ribbons selectively impairs fast synaptic vesicle recruitment. In addition, neither the rise time nor the decay time constant of EPSC events was affected by FALI, suggesting synaptic vesicle fusion is not altered. Finally, we applied physiologically relevant sinewave stimulation to hair cells. Consistent with the findings with strong step depolarization, we found both the rate and amplitude of EPSCs were reduced by FALI (Rate: 197.8 ± 62.1 vs. 106.53 ± 53.3 Hz; Amplitude: 118.1 ± 25.9 vs. 59.8 ± 14.3 pA; before and after FALI, n=7). The temporal precision of exocytosis, i.e. the phase-locking of EPSC events, was not significantly altered (vector strength, 0.64 ± 0.05 vs. 0.69 ± 0.05 , before and after FALI, n=7). Taken together, our results suggest synaptic ribbons function as an "accelerator" for synaptic vesicle recruitment, which is required for exocytosis at a high rate.

PS 935

Recovery of Spontaneous and Evoked Spikes after Threshold Stimulation of Zebrafish Hair Cells

Wisdom E. Yevudza; Emily C. Isko; Daniil Frolov; Samuel A. Short; Thomas F. Sommers; Alexander J. Ordoobadi; Josef G. Trapani
Amherst College

Zebrafish detect hydrodynamic changes in their environment via the lateral line system, which encodes such changes within sequences of action potentials (spike trains) evoked by stimulation of sensory hair cells. Previous studies highlight the role of the hair cell ribbon synapse in the onset time of first evoked spikes, aka first spike latency (FSL). Less is known about the ribbon's role in adaptation of FSL or in the onset time of the first spontaneous spike after offset of stimulation (FSSL). We performed experiments with larval zebrafish to probe the mechanisms underlying FSL and FSSL and recovery of each following threshold stimulation of hair cells. Specifically, hair cells that express Channelrhodopsin-2 (ChR2) in transgenic larvae were optically stimulated with focused flashes of 470 nm light to evoke just single spikes in lateral line afferent neurons. Following hair cell stimulation at a threshold intensity, we determined the mean evoked FSL. Next we obtained the latency of the first spontaneous spike (FSSL) following the threshold stimulation. We also stimulated at threshold intensity in a paired-pulse paradigm and varied the inter-stimulus time interval between both pulses. In this manner, we seek to determine the recovery time for evoked FSLs. By comparison of the time required for recovery of threshold FSL to the time for recovery of spontaneous spikes (FSSL), we aim to gain insight into hair cell mechanisms that determine the time course of each

process and whether they share similar properties. Together, our experiments may provide insight into the rates of depletion and refilling of particular synaptic vesicle pools including the readily releasable pool at the hair cell's ribbon synapse.

PS 936

Calcium Dependence of Inner Hair Cell Transmitter Release in Near Physiological Conditions

Lina Maria Jaime Tobon¹; Tobias Moser²

¹*Institute for Auditory Neuroscience, University Medical Center Göttingen; Synaptic Nanophysiology Group, Max Planck Institute for Biophysical Chemistry; Collaborative Research Center 889, University of Göttingen; IMPRS Neuroscience Program;* ²*Institute for Auditory Neuroscience, University Medical Center Göttingen; Synaptic Nanophysiology Group, Max Planck Institute for Biophysical Chemistry; Collaborative Research Center 889, University of Göttingen*

Inner hair cells (IHC) are the gateway of sound stimuli to the auditory pathway. They are responsible for transforming mechanical sound-borne vibrations into electrical signals and conveying this information to the afferent spiral ganglion neurons. Upon stimulation, the receptor potential triggers the opening of voltage-gated Ca²⁺ channels, mediating the fusion of vesicles and the consequent release of neurotransmitter from the presynaptic active zone to the postsynaptic bouton (for review, Moser & Vogl, 2016).

The coupling between Ca²⁺ influx and exocytosis critically determines how the acoustic stimulus is encoded at the synapse between the IHC and the spiral ganglion neuron. The Ca²⁺ nanodomain hypothesis of exocytosis control proposes that only few Ca²⁺ channels in nanometer proximity to the vesicular release site govern the Ca²⁺ concentration that drives the release of a synaptic vesicle (Moser et al. 2006). However, validation of the Ca²⁺ nanodomain hypothesis by paired pre- and postsynaptic recordings that provide high resolution and specificity is required. Moreover, it remained unclear whether the Ca²⁺ nanodomain-like control operates in IHC synaptic transmission under physiological conditions. Here, we performed paired pre- and postsynaptic patch-clamp recordings in near physiological conditions on murine IHCs ribbon synapses after the onset of hearing.

To determine the apparent Ca²⁺ dependence of glutamate release, the presynaptic Ca²⁺ influx was altered by depolarizing the IHC with 2 ms voltage steps from -58 mV to -17 mV. These short stimuli were used to avoid synaptic vesicle pool depletion. The relationship of EPSC charge (Q_{EPSC}) and Ca²⁺

charge (IHC Q_{Ca}) was approximated by a power function yielding an apparent Ca²⁺ cooperativity (*m*) of 2.3. This suggests that few Ca²⁺ channels control vesicle fusion during physiological sound encoding.

Additionally, two independent manipulations to alter the single Ca²⁺ channel current or the number of open Ca²⁺ channels were carried out. 1 mM Zn²⁺ was perfused to cause a rapid flicker block of the Ca²⁺ channel (Winegar & Lansman, 1990) and reduce the apparent single channel current. This manipulation revealed a supralinear relationship between Q_{EPSC} and IHC Q_{Ca} (*m* = 4.8), most likely reflecting the high intrinsic Ca²⁺ cooperativity at the Ca²⁺ sensor. Conversely, slow wash-in of 2 μM Isradipine to gradually reduce the number of open Ca²⁺ channels, yielded a more linear Ca²⁺ dependence with a power of 1.7. Taken together, these findings support that physiological sound encoding relies on few Ca²⁺ channels to control vesicle fusion in a Ca²⁺ nanodomain-like fashion.

PS 937

Synaptic Changes in Cochlear Hair Cells of *Tmc* Mutant Mice

John Lee; Gwenaëlle S. Geleoc; Jeffrey R. Holt

¹*Boston Children's Hospital, Harvard Medical School*

Background:

Tmc1 and *Tmc2* form sensory transduction channels in auditory and vestibular hair cells. Mice with targeted deletion of *Tmc1* (*Tmc1Δ*) exhibit deafness, while those lacking both (*Tmc1Δ;Tmc2Δ*) lack sensory transduction, are deaf, and have vestibular dysfunction. Single-channel properties also differ between TMC1 and TMC2. Hair cells that express TMC2 have higher calcium selectivity and higher single-channel conductance than those that express TMC1. While hair bundle morphology and function, and hair cell survival have been assessed in *Tmc* mutant mice, consequences of absent and/or impaired sensory transduction on the development and/or maintenance of ribbon synapses have not been examined. Cochlear and vestibular hair cells utilize these ribbon synapses to mediate synchronous release of glutamate-filled vesicles for temporally precise transmission of auditory cues. Absent or altered numbers of synaptic ribbons contribute to abnormal synaptic transmission, impaired speech-in-noise discrimination, and perceptual anomalies like tinnitus. The purpose of this study was to determine if synaptic differences exist between wild-type mice and mutant mice that lack *Tmc1*, *Tmc2* or both across multiple ages. Characterizing the consequences of impaired/absent sensory transduction on ribbon synapses will be informative when assessing the effectiveness of restoring sensory transduction via gene therapy strategies.

Methods:

Cochlea from wild-type, *Tmc1Δ*, *Tmc2Δ*, and *Tmc1Δ;Tmc2Δ* mice were harvested at various time points (P7, P10, P14, P21, P28) and immunostained with antibodies to C-terminal binding protein 2 (CtBP2), glutamate receptors (GluA2/3), and myosin7a (Myo7a). Each cochlea was microdissected and frequency maps were generated using apex-to-base length measurements. Confocal z-stacks of the 8.0, 11.3, 16.0, 22.6, and 32.0kHz regions were obtained and image stacks were ported to Imaris, an image analysis software. 3-D projections were generated and the average number of synapses per inner hair cell were counted using Imaris' "Spot Detection" feature.

Results:

Differences in the number of synapses in *Tmc1Δ;Tmc2Δ* mice were evident at several developmental time points, suggesting *Tmcs* may be required for normal development and maintenance of synapses. Synapse counts in *Tmc1Δ* mice resembled those in *Tmc1Δ;Tmc2Δ* mice, while counts in *Tmc2Δ* mice were similar to those of WT mice.

Conclusions:

Differences in the number of IHC ribbon synapses observed in *Tmc* mutant mice suggest sensory transduction is required for maintenance of cochlear synapses. More specifically, the absence of *Tmc1* appears to result in the changes observed, suggesting single-channel properties of *Tmc1* (smaller conductances, lower Ca²⁺ permeability) and/or the developmental shift from *Tmc2* to *Tmc1* play crucial roles in regulating IHC synapses.

PS 938

Dual AAV-Mediated Gene Therapy Restores Hearing in a DFNB9 Mouse Model

Omar Akil¹; Frank Dyka²; Charlotte Calvet³; Alice Emptoz⁴; Ghizlene Lahlou³; Sylvie Nouaille⁵; Jacques Boutet de Monvel⁶; Jean-Pierre Hardelin⁷; William Hauswirth²; Paul Avan⁸; Christine Petit⁹; Saaid Safieddine⁶; Lawrence Lustig¹⁰

¹Department of Otolaryngology, University of California San Francisco; ²Department of Ophthalmology, University of Florida, College of Medicine; ³UPMC; ⁴Genetics and Physiology of Hearing Laboratory Inserm, Institut Pasteur; ⁵Institut Pasteur; ⁶INSERM UMRS 1120; ⁷INSERM; ⁸University of Auvergne; ⁹Génétique et Physiologie de l'Audition, Institut Pasteur; ¹⁰Department of Otolaryngology-Head & Neck Surgery, Columbia University Medical Center

INTRODUCTION: Autosomal recessive genetic defects account for most cases of profound congenital deafness forms. Adeno-associated virus (AAV)-based

gene therapy is a promising treatment option, but it is limited by a potentially short therapeutic window and the constrained packaging capacity of the AAV vector. In this study we focus on the otoferlin (*OTOF*) gene underlying DFNB9, one of the most prevalent genetic forms of congenital deafness. We adopted a dual AAV approach allowing us to extend the limited packaging capacity (< 5 kb) of the AAV vector, and deliver the entire coding sequence of the otoferlin cDNA (6 kb) to the mouse inner hair cells. The otoferlin cDNA was split into two parts, which were inserted into two expression cassettes sharing a recombinogenic bridging sequence. These recombinant vectors were packaged in two individual AAV2 capsids. Upon co-infection of the same cell, the two AAV recombinant vectors formed head-to-tail concatamers that recombined, leading to the production of the full-length otoferlin.

METHODS: A single injection of the two recombinant vectors was made into the left cochleas of mutant mice lacking otoferlin (*Otof*^{-/-} mice) on P10, P17, or P30. ABR recordings and immunofluorescence analysis of the injected cochleas were performed to determine otoferlin expression and hearing recovery in these mice.

RESULTS AND CONCLUSION: We report here, for the first time that single cochlear delivery of a fragmented cDNA by a dual-AAV vector approach can effectively restore the production of the full-length protein in a DFNB9 deaf mouse model, and results in a long-lasting restoration of hearing. Remarkably, this local gene therapy not only prevented deafness in *Otof*^{-/-} mice when administered before hearing onset, but also reversed the deafness phenotype in a sustained manner when administered well after hearing onset. These results are highly significant for the future design of gene therapy trials in DFNB9 patients.

PS 939

A Gene Therapy Approach with Split AAVs Partially Rescues IHC Exocytosis and Hearing in Otoferlin-Knock-Out Mice

Hanan Al-Moyed¹; Andreia Cepeda²; SangYong Jung³; Tobias Moser⁴; Sebastian Kügler⁵; Ellen Reisinger¹

¹University Medical Center Göttingen, Dept. for Otorhinolaryngology; ²University Medical Center Goettingen, Department of Otorhinolaryngology; ³Institut for Auditory Neurosciences, University Medical Center Göttingen; ⁴Institute for Auditory Neuroscience, University Medical Center Göttingen; Synaptic Nanophysiology Group, Max Planck Institute for Biophysical Chemistry; Collaborative Research Center 889, University of Göttingen; ⁵Viral Vectors Lab, Dept. of Neurology, University Medical Center Goettingen

Mutations in *OTOF* mostly cause profound deafness due to a lack of signal transduction from inner hair cells (IHCs) to spiral ganglion neurons. Apart from a 40% reduction of afferent synapses found at mouse *Otof*-knock-out IHCs, the inner ear is structurally intact, which predestines this form of deafness to be ameliorated with gene therapy. However, the 6kb coding sequence of *otof*erlin remained an obstacle for gene transfer, since so far none of the viral vectors that can transport such large foreign sequences proved to be suitable for the transfer of *otof*erlin to IHCs. We overcame this challenge by splitting the *otof*erlin cDNA to two adeno-associated viruses (AAVs). AAVs are small non-pathogenic parvoviruses with low immunogenicity but a packaging limit of ~5kb. AAVs form long head-to-tail virus genome multimers in the nuclei of infected cells. This intrinsic feature allows a re-assembly of split coding sequences encoded on separate AAVs, which can be enforced by introducing splice sites or overlapping sequences for homologous recombination at the respective virus genome ends. In this study, we injected two AAV vectors each encoding one half of *otof*erlin cDNA at postnatal day 6 or 7 through the round window membrane into the cochlea of *Otof*-KO mice. Immunohistochemistry revealed the expression of full-length *otof*erlin in up to 50% IHCs (average 25%). Remarkably, *otof*erlin was not expressed in other cell types than auditory hair cells, despite the AAV transduced also supporting cells and spiral ganglion neurons. Using patch-clamp electrophysiology of IHCs, we assessed exocytosis of the readily releasable pool of synaptic vesicles and sustained exocytosis, two processes for which *otof*erlin is essential. In dual-AAV transduced *Otof*-KO IHCs, fast exocytosis, elicited by 5-20ms depolarization steps to -14mV, exocytosis was fully rescued. For longer depolarization steps, synaptic vesicle fusion was partially restored, reaching 50-70% of wild-type vesicle replenishment rates.

At the age of three to four weeks, we recorded auditory brainstem responses (ABRs). Acoustic click stimuli elicited ABRs with thresholds of typically 50dB, which were mostly independent of IHC transduction rates. The amplitudes of ABR waves at 80dB were smaller than in wild-type controls, and increased with higher IHC transduction rates. For tone bursts, we found thresholds of 50dB in the best animals at 8 and 12 kHz.

In summary, our data indicate that a dual-AAV approach is well suitable to transduce IHCs with full-length *otof*erlin cDNA and to partially rescue hearing in mouse models for DFNB9.

PS 940

Live 4D Imaging of Spontaneous Activity in Zebrafish Hair-cell Organs Using Light-sheet Fluorescent Microscopy

Qiuxiang Zhang¹; Alisha Beiri¹; Katie Kindt¹; Osama Hamdi²

¹National Institute on Deafness and Other Communication Disorders; ²Howard University

Spontaneous activity has been observed in many different regions of the nervous system among many different species. In the developing mammalian auditory system, waves of calcium signals triggers periodic bursts of action potentials in the afferent neurons before the onset of hearing. However, the origin and role of spontaneous activity is still an important area of research. Part of the challenge in this area of research is the difficulty in mimicking the *in vivo* environment required to generate and study this activity.

Zebrafish is a unique and highly advantageous animal model that has been used to study the activity of hair cells and afferent neurons *in vivo*. Activity in these cells in both the inner ear and lateral-line system can easily be measured in intact zebrafish. For this work, we use genetically encoded calcium and ATP sensors in zebrafish, combined with a self-constructed light-sheet fluorescence microscopy (LSFM) system to image spontaneous activity *in vivo*. LSFM is particularly advantageous – it relies on selective plane illumination that minimizes photobleaching and phototoxicity while retaining sensitivity. We have used the zebrafish model and this microscopy system to capture 4D *in vivo* recordings over extended periods of time, to study spontaneous activity in the developing zebrafish lateral-line system and inner ear.

By this approach, we are able to measure spontaneous calcium activity from hair cells and afferent neurons. We can detect spontaneous calcium signals in hair cells in both apical mechanosensory bundles and in basal presynaptic regions of hair cells as well as in postsynaptic afferent terminals simultaneously. Our experimental results indicate that spontaneous activity increases during hair-cell development and decreases after hair cells mature. Simultaneously imaging from presynaptic hair cells and postsynaptic afferents shows synchronized spontaneous activity. This indicates that spontaneous activity may function strengthen the pre- and post-synaptic neuronal connections. We are also investigating the role of supporting cells and efferent neurons in the hair-cell spontaneous activity *in vivo* using genetic, pharmacological and imaging approaches. Overall, developing this model to understand how spontaneous activity is generated and changes during development will help us understand the specific role of this activity in synapse formation and maintenance.

PS 941

Using Zebrafish to Correlate Hair-cell Activity with Neomycin Resistance and Susceptibility

Daria Lukasz; Katie Kindt

National Institute on Deafness and Other Communication Disorders

Hair cells, the primary sensory cell of the auditory system, rely on calcium for proper development and function. Once human hair cells are destroyed, they do not regenerate, and this contributes to the estimated 45 million cases of hearing loss in the United States. Exposure to ototoxins such as aminoglycoside antibiotics can result in hair-cell death. Although differential susceptibility to aminoglycosides has been reported within hair cell organs of various species, including zebrafish, why some hair cells live and others do not after treatment is unclear. One possibility is that functional differences among hair cells, either in regard to mechanotransduction or synaptic transmission, could confer resistance or susceptibility to a specific subset of cells. Using the zebrafish lateral line, our group discovered that approximately only 30% of lateral-line hair cells are synaptically “active”. This functional distinction among seemingly indistinguishable hair cells has led us to hypothesize that activity differences could contribute to susceptibility to ototoxins such as the aminoglycoside neomycin.

To answer this question, we are conducting functional calcium imaging in transgenic zebrafish expressing genetically encoded calcium indicators (eg: GCaMPs) in lateral-line hair cells. Our transgenic zebrafish lines enable us to measure evoked mechanotransduction as well as synaptic and mitochondrial calcium signals within hair cells *in vivo*. After collecting activity measurements, we apply neomycin or neomycin-Texas Red solution to larvae, track cell survival, and draw correlations between survival, activity, and uptake. Using this approach, we can identify different types of calcium signals within hair cells and determine whether they confer resistance or susceptibility to ototoxins.

Currently we have found that synaptically “active” cells are more resistant to neomycin ototoxicity. Additionally, these synaptically “active” cells also contain significantly less neomycin. Similarly, hair cells with mitochondrial calcium loading show similar resistance to the antibiotic and contain significantly less of it. This correlation between functional activity and resistance to neomycin ototoxicity suggests that calcium activity can influence whether a hair cell lives or dies when exposed to ototoxins. We are currently expanding our analysis to include mechanotransduction and developmental age. Overall, identifying how activity-dependent signals provide protection is critical to the development of otoprotective or even regenerative therapies.

PS 942

GluD1 Deficiency Causes Progressive High-Frequency Hearing Loss and Insufficient Efferent Synapse Formation on Outer Hair Cells

Takamori Takeda¹; Taro Fujikawa¹; Yuriko Sakamaki²; Masato Fujioka³; Yoshiyuki Kawashima¹; Taku Ito¹; Ayane Makabe¹; Takeshi Tsutsumi¹; Michisuke Yuzaki⁴

¹Dept. of Otorhinolaryngology, Tokyo Medical and Dental University; ²Research Core, Tokyo Medical and Dental University; ³Dept. of Otorhinolaryngology - Head and Neck Surgery, Keio University School of Medicine; ⁴Dept. of Neurophysiology, Keio University School of Medicine

GluD1, a member of the delta subfamily of ionotropic glutamate receptors, is expressed in cochlear hair cells and plays an essential role in normal hearing at high frequencies (Gao et al., Mol Cell Biol 2007). However, little is known regarding the specific localization and physiological role of GluD1 in the cochlea. First, we examined immunolabeling for Cbln1, a C1q-like synaptic organizer that forms a complex with postsynaptic GluD1 (Yuzaki, Annu Rev Physiol 2018), and showed its localization in synaptic clefts of efferent boutons on adult rat outer hair cells. Then, we analyzed *GluD1*-null mice to assess progression of hearing loss using auditory brainstem response and distortion product otoacoustic emissions, and examined morphological changes of hair cell synapses using light and transmission electron microscopes. *GluD1*-null mice showed significant cochlear threshold shifts; hearing loss started at frequencies of 22.4 kHz and higher, and progressed faster in all frequencies. Interestingly, in the middle turn (16 – 32 kHz) of *GluD1*-null mouse cochlea at 9 months of age, the number of efferent boutons was lower and average area of each bouton was larger compared to wild type ($p = 0.01$, respectively), although the number of inner and outer hair cells was not affected. There were no obvious abnormalities in ultrastructure of efferent synapses on outer hair cells or the distribution and density of synaptic vesicles in the presynaptic terminals. Thus, GluD1 deficiency causes a reduction in numbers of synapses and compensatory enlargement of synaptic terminals, resulting in progressive high-frequency hearing loss. Similarly, abnormalities in synapse number and connections are found in the cerebellum of GluD2 and Cbln1 deficient mice (Kurihara et al., J Neurosci 1997; Hirai, et al., Nat Neurosci 2005). We conclude that GluD1 has an essential role in synapse formation and maintenance of outer hair cell efferents.

The Use of CRISPR-Cas9 Genome Editing *In Vivo* to Probe The Role of Ca_V1.3 Ca²⁺ Channel Isoforms in Synaptic Transmission of Mouse Auditory Hair Cells

Jean-Christophe Leclère¹; Margot Tertrais²; Thibault Peineau²; Yohan Bouleau²; **Didier Dulon**²

¹University of Brest; ²University of Bordeaux

Transmitter release at auditory hair cell ribbon synapses is known to be regulated by presynaptic L-type Ca_V1.3 calcium (Ca²⁺) channels which are constituted of long (Ca_V1.3_L) and short (Ca_V1.3_S) C-terminal isoforms, with respectively slow (sec) and extremely fast (ms) time inactivation (Scharinger et al., 2015; Vincent et al., 2017). The expression of Ca_V1.3_L and Ca_V1.3_S results from the alternative splicing of exon 43 in the *CACNA1D* gene. Ca_V1.3_S channel isoforms have a truncated regulatory C-terminal region that allows a more efficient Ca²⁺-dependent binding of calmodulin (CaM) to the IQ and pre-IQ domains, generating then a fast inactivation of the Ca²⁺ current. Ca_V1.3_L isoforms, harboring a complete regulatory C-terminal region with a proximal and a distal domain (PCRD for “proximal C-terminal regulatory domain” and DCRD for “distal C-terminal regulatory domain”) display poor and slow inactivation. The specific role of these Ca_V1.3 channel isoforms in auditory hair cells remain unknown. Here we investigated the impact on the hearing function of a specific hair cell genome editing of exon 43 to stop the encoding of Ca_V1.3_L isoform while maintaining the encoding of Ca_V1.3_S isoforms, through CRISPR-Cas9 technology, *in vivo*, in postnatal mice. We found that a hair cell specific targeting of the Ca_V1.3_L isoform generated severe deafness in mice with normal otoacoustic emissions, indicating an auditory hair cell synaptopathy. Electrophysiological patch-clamp recordings in auditory inner hair cells of these mice showed a normal fast and transient exocytosis of synaptic vesicles that was, however, associated with a severe defect in the sustained component of exocytosis, indicating a deficit in the recruitment of synaptic vesicles to the hair cell active zone. Our results show that a specific exon silencing with CRISPR-Cas9 technology, *in vivo*, in postnatal mice, in a specific type of cells, such as the auditory hair cells, is possible. Our work demonstrates, for the first time, that the slowly inactivating Ca_V1.3_L isoform, likely by allowing a deep and sustained Ca²⁺ diffusion into the hair cell active zone, is essential to mobilize distant synaptic vesicles for an endless and inexhaustible auditory synaptic transmission by hair cells.

Cyclic AMP and cochlear inner hair cell synapse excitotoxicity

Sriram Hemachandran; Steven H. Green

The University of Iowa

Cochlear Inner hair cells (IHC) transmit sound stimuli by releasing the neurotransmitter glutamate onto the afferent nerve fibers, type 1 spiral ganglion neurons (SGNs). During noise exposure the IHCs release excess glutamate leading to increased influx of Ca²⁺ in the SGNs, which causes excitotoxic damage to and loss of synapses or “synaptopathy.” In an *in vitro* model of noise-induced cochlear synaptopathy (Wang & Green, 2011), an organotypic cochlear explant culture is exposed to a glutamate agonist such as kainic acid (KA) to cause excitotoxic damage to and loss of synapses on IHCs.

SGN activity is directly modulated by the lateral olivocochlear (LOC) efferent projection. CGRP, one of the neuropeptides released by LOC efferents, potentiates KA excitotoxicity *in vitro*. The CGRP receptor recruits cyclic AMP (cAMP) as a second messenger and cAMP appears to be necessary and sufficient for potentiation of KA. However, cAMP may signal through the kinase PKA or through the Exchange Factor Activated by cAMP (EPAC). Here we distinguish between alternative signaling pathways for effects of cAMP.

Organotypic cochlear explants were exposed for 2 hr to KA at a concentration (0.01 mM) that, alone, does not cause significant synapse loss. In combination with cAMP (1 mM), significant synapse loss is observed. (cAMP alone does not cause synapse loss.) A synapse is defined as colocalized CtBP2 (ribbon) and PSD95 immunofluorescent puncta. We also used Oregon Green-BAPTA to monitor Ca²⁺ influx into cultured SGNs and found that, while 0.01 mM KA cAMP potentiated Ca²⁺ influx into cultured SGNs caused by KA. Potentiation by cAMP of excitotoxic damage to synapses was not prevented by inhibition of PKA (H-89) but was prevented by an EPAC inhibitor (ESI-09) and was mimicked by an EPAC-specific activator (8-cpt-cAMP).

These data show that an atypical cAMP signaling pathway potentiates excitotoxicity at synapse on IHCs and can be recruited by the LOC efferents via the neuropeptide CGRP. This might be a consequence of modulation of Ca²⁺ mobilization by the EPAC pathway, a possibility we are now investigating. Interestingly, an effect of cAMP on synapse regeneration appears to be due to PKA signaling, suggesting that selective targeting of downstream cAMP signaling pathways may be of value therapeutically for noise-induced synaptopathy.

Modulation of Potassium Permeation in the Diffusion-limited Synaptic Cleft Between Type I Hair Cells and Calyx Afferents in the Vestibular System

Donatella Contini¹; Gay R. Holstein²; Jonathan J. Art¹
¹University of Illinois College of Medicine; ²Icahn School of Medicine Mount Sinai

In the vertebrate nervous system, ions accumulate in diffusion-limited synaptic clefts during ongoing activity. Such accumulation can be demonstrated at large appositions such as the hair cell – calyx afferent synapse in the central region of the vestibular semicircular canal epithelium. Type I hair cells influence discharge rates in their calyx afferents by modulating the potassium concentration in the synaptic cleft, $[K^+]_{\text{cleft}}$, which depolarizes both hair cell and afferent. Dual recordings from hair cells and associated afferents have demonstrated that, in spite of a decreased driving force due to potassium accumulation, hair cell depolarization elicits sustained outward currents in the hair cell, and a maintained inward current in the afferent. We have used kinetic and pharmacological dissection of the hair cell conductances to understand the potential interdependence of channel gating and permeation in the context of these restricted extracellular spaces. From a holding potential of -100 mV, a rapid calcium influx in response to depolarization leads to activation of a large, calcium-activated potassium conductance, BK. This can be blocked by agents that disrupt either calcium influx or the elevation of $[Ca^{2+}]_i$, as well as by the specific K_{Ca} 1.1 blocker, Iberiotoxin. The efflux of K^+ from the BK conductance elevates $[K^+]_{\text{cleft}}$, which can speed the activation and slow the deactivation of a second potassium conductance, $K_{(LV)}$. Elevation of $[K^+]_{\text{cleft}}$ or chelation of $[Ca^{2+}]_o$ linearizes the $I_{K_{(LV)}}$ steady-state I–V curve, consistent with extracellular potassium competitively relieving a Ca^{2+} -block of the K_{LV} pore. From a holding potential of -70 mV, depolarization-induced potassium flux through the combined BK and K_{LV} conductances may be sufficient to increase the K_{LV} conductance to levels necessary to compensate for any decrease in the driving force that results from elevating $[K^+]_{\text{cleft}}$. As a result, the total hair cell potassium current is maintained throughout the depolarization. This leads to a sustained inward current in the post-synaptic calyx afferent that adds to its other intrinsic currents. At synapses where individual quanta are large, a maintained inward current could depolarize an afferent to potentials that are sufficient for generating an action potential at the peak of an EPSP. At synapses where quanta are small, the maintained inward current might simply increase the frequency of regenerative oscillatory behavior in the afferent.

Topographic Visualization of the Acoustic Radiation in Normal Hearing and Deaf Subjects via Semi-Automated Tractography

S. Bryn Dhir¹; Kwame Kutten¹; Muwei Li²; Andreia Faria¹; J. Tilak Ratnanather¹
¹Johns Hopkins University; ²Vanderbilt University

Background

The acoustic radiation (AR) is the final stage of the auditory pathway. It consists of white matter (WM) fibers coursing from the medial geniculate body (MGB) of the thalamus to the Heschl's gyrus (HG) which contains the auditory cortex. The AR presents a challenge for automated tracking WM fibers in diffusion tensor imaging (DTI) as it is partly obscured by the optic radiation tract. Specifically, visualization of the AR is complicated (Maffei *et al.* 2017) and it is thought to be impossible to generate AR from DTI scans (Behrens *et al.* 2007; Berman *et al.* 2013). Probabilistic tracking such as dynamic programming (DP) can deal with such types of crossing fibers (Ratnanather *et al.*, 2013). Li *et al.* (ARO 2013) previously showed that DP could be used to generate the AR but with reference to a single-subject atlas. This extended study shows how the topography of the AR can be reliably visualized in native space across several subjects with and without hearing loss (HL) and at different scanner strengths.

Methods

DWI and T1 scans at 1.5T for 10 subjects with no HL and five subjects with HL were acquired, as well as at 3T for one of the subjects with HL and a single-subject atlas. Scans were rigidly registered and DWI data was processed through DTIStudio and MRICloud (Jiang *et al.* 2006; Mori *et al.*, 2016) to yield whole brain images of fractional anisotropy (FA), color orientation maps, eigenvalues and eigenvectors. The MGB and HG were manually segmented in the color map and T1 image, respectively. The AR on each side was generated via DP (Li *et al.* 2014) and visualized in 3D.

Results

The post-mortem lateral, posterior, anterior and superior visualization results of Maffei *et al.* (2017) were confirmed across all 17 scans. Specific topography of the AR at 1.5T was identified with the genu, stem and fan bundle and was replicated at 3T. The FA of the AR was found to be lower in the left side for subjects with HL ($p < 0.005$, Wilcoxon rank-sum).

Conclusions

It is possible to reconstruct and visualize the AR in clinical DTI scans across several subjects and at

different scanner strengths. The ability to visualize the AR in such scans may allow for applications in clinical pathology, such as in vestibular schwannomas.

Funding

Research supported by NIH grant P41-EB015909 and National Organization for Hearing Research.

PS 947

Cortical Tonotopic Maps in Tinnitus and Hearing Loss

Elouise A. Koops¹; Remco J. Renken²; Cris P. Lanting³; Pim Van Dijk⁴

¹Univeristy Medical Center Groningen, University of Groningen; ²University Medical Center Groningen, University of Groningen; ³Radboudumc; ⁴Dept. of Otorhinolaryngology, University Medical Center Groningen

Introduction

The presence of clinical hearing loss, associated with neural plasticity, increases the chances of developing tinnitus. The specific pathophysiology involved in tinnitus remains elusive. A striking feature of the auditory cortex is its tonotopic organization. Several studies have suggested a relation between hearing-loss-induced tonotopic reorganization and tinnitus. This large fMRI study intended to clarify the relation between hearing loss, tinnitus and tonotopic reorganization. We focused on participants with high-frequency sensorineural hearing loss, both with and without tinnitus. This allowed us to investigate to what extent reorganization is a consequence of hearing loss, and whether reorganization is specifically related to tinnitus.

Methods

Functional magnetic resonance imaging (fMRI) was used to investigate the association between tonotopic reorganization, hearing loss and tinnitus. In the current study, we quantified changes in the tonotopic maps in relation to tinnitus and hearing loss. Principally, bilateral cortical responses to sound stimulation were measured in a total of 90 participants. Three groups of participants were included: a hearing loss group with tinnitus, a hearing loss only group and a control group with normal hearing. Loudness matched pure tone stimuli (0.25 – 8 kHz) were presented in the MRI scanner while participants performed an unrelated visual task to control for attention effects.

Results

With the aid of principal component analysis, we found a considerably larger increase in activation level in response to 8 kHz stimulation in both groups with hearing loss compared to the control group. Secondly,

the tonotopic map in tinnitus appears very similar to the tonotopic map of the hearing loss group; this finding is in line with the similar hearing thresholds for the tinnitus and the hearing loss groups. The shift towards higher frequencies is more pronounced in the hearing loss group compared to the tinnitus group.

Conclusion

High-frequency sensorineural hearing loss is associated with increased responsiveness to high frequency stimuli, in a loudness matched protocol. As a result, the tonotopic map shifts toward high frequency responsiveness. The presence of tinnitus in addition to hearing loss does not appear to influence the major framework of the cortical tonotopic map, except for a less-pronounced shift to high-frequencies in tinnitus. These changes could imply a reduced cortical ability to adapt to hearing loss.

PS 948

Pupillary Light Response Reveals Covert Attention to Auditory Space and Object

Hsin-I Liao; Haruna Fujihira; Shigeto Furukawa
NTT Communication Science Laboratories

Our previous study (Liao et al., ARO 2018) showed that the pupillary light response (PLR) reflects the focus of auditory spatial attention, presumably based on the underlying mechanism of a unified crossmodal spatial attention between audition and vision. When the listener was attending to the left or right ear via a voice instruction during an experiment, the pupil size changed in accordance with the luminance of the visual field corresponding to the attended ear side. In the current study, we further examined whether the PLR is sensitive to not only the attention directed to the space per se but also to that directed to an auditory object, which is associated with space. The investigation provided insights into entangle auditory mechanisms underlying attention to 'where'; and 'what';.

We conducted an experiment in which two different sentences from a coordinate response measure (CRM) corpus (Japanese version, Furukawa & Kominato, 2012) were presented dichotically via a headphone, one from a female talker and the other from a male talker. Each sentence was repeatedly presented twice, for a total duration of around 6 s. Before the sentence presentation, a voice instruction saying 'left'; or 'right'; (attend-to-location condition), or 'female'; or 'male'; (attend-to-gender condition) was given to define the target sentence. In each trial, participants were instructed to pay attention to the entire target sentence, memorize its content, and recall after the sound presentation. The pupil diameter was monitored throughout each trial. The participant was instructed to

fixate a spot at the center of a monitor. The left and right visual fields on the monitor had a disparity in luminance.

Result showed that pupil size changed in accordance with the target sound-source location, not only when the target sound was defined by location but also by gender. Specifically, average pupil size during the sound presentation was larger when participants attended to the ear-side where the visual field was darker than the other side (attention-to-location condition), or when the target was presented at the darker side despite the fact that it was defined by the gender of the talker (attention-to-gender condition). The overall results indicate that the PLR reflects the focus of auditory attention not only when attention is directed to a particular space by endogenous spatial cue but also when attention is allocated to a particular auditory object via non-spatial characteristics.

PS 949

Hearing Complaints are Associated with Greater Rates of Cortical Thinning in a Cohort Enriched for Alzheimer's Disease Risk

Taylor Fields¹; Sterling Johnson²; Ozioma Okonkwo²; Ruth Litovsky³

¹Neuroscience Training Program; ²Wisconsin Alzheimer's Disease Research Center; ³University of Wisconsin - Madison

Previous studies indicate that auditory dysfunction among cognitively normal adults can predict future cognitive decline and incident dementia, but little is known about the biological basis of these associations. Alzheimer's disease (AD) has been associated with a signature pattern of cortical thinning that is distinct from healthy aging and present prior to overt clinical decline. The AD cortical signature includes temporal and parietal regions known to be involved in complex auditory perception. The aim of this study was to investigate whether subjective hearing complaints (SHCs) are associated with greater rates of cortical thinning in these regions, as a potential neural substrate of auditory dysfunction in AD.

Participants (N=124) enrolled in the Wisconsin Registry for Alzheimer's Prevention (WRAP) underwent longitudinal anatomical magnetic resonance imaging (MRI) and completed a 5-item hearing questionnaire at separate visits. We included participants who were clinically unimpaired at their most recent visit and who had at least two MRI scans with at least one year between their earliest and most recent MRI. Regional cortical thickness was measured using a set of automated tools (Freesurfer) to reconstruct the brain's cortical surface from structural MRI data. Multivariable linear regression

was used to examine the association between average SHCs and annualized change in thickness ([thickness at most recent MRI - thickness at first MRI]/interval between first and most recent MRI) for regions of interest (ROIs) previously found to be affected in early AD. All analyses were adjusted for age at most recent MRI, sex, and literacy.

SHCs were associated with significantly greater rates of cortical thinning in inferior and middle temporal gyri, fusiform gyrus, precuneus, superior parietal cortex, and supramarginal gyrus. There was a trend towards greater rates of thinning in inferior parietal cortex among individuals with greater SHCs but no associations with rates of thinning in entorhinal cortex, parahippocampal cortex, or temporal pole.

These findings demonstrated greater rates of cortical thinning in several AD signature regions among clinically unimpaired adults with greater SHCs. Higher rates of atrophy in these regions may be responsible for early auditory deficits observed in individuals who go on to develop symptomatic AD. Accordingly, additional follow-up studies would reveal whether thinning in these cortical regions mediates an association between SHCs and prospective decline in cognitive status.

Work funded by the National Institutes of Health (NIA and NIDCD)

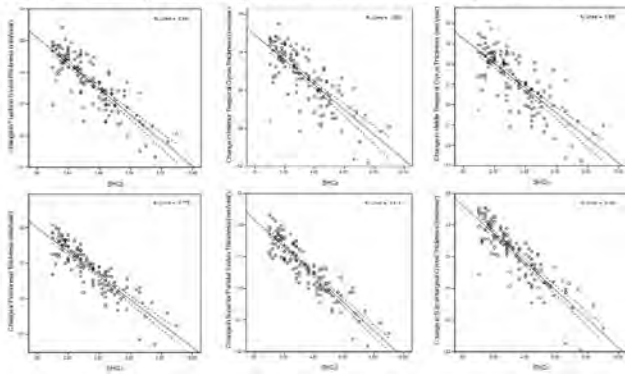
Table 1: Participant characteristics (n=124)

Characteristic	Value
Age at most recent MRI, y, mean (SD)	63.1 (6.1)
Female, n (%)	87 (70.2)
APOE ε4 carrier, n (%)	47 (37.9)
Family history positive, n (%)	86 (69.4)
Interval between first and most recent MRI, y, mean (SD)	3.0 (1.4)
Education, y, mean (SD)	16.5 (2.5)
WRAT-III Standardized Reading Score, mean (SD)	107.8 (9.6)
Average SHCs, y, mean (SD)	3.4 (1.8)

Table 2: SHCs are associated with greater rates of regional cortical thinning.

ROI	B (SE)	p-value
Entorhinal Cortex	-.001 (.005)	.752
Fusiform Gyrus	-.004 (.002)	.047
Inferior Parietal Cortex	-.003 (.002)	.091
Inferior Temporal Gyrus	-.007 (.003)	.037
Middle Temporal Gyrus	-.006 (.002)	.006
Parahippocampal Cortex	.001 (.002)	.677
Precuneus	-.003 (.001)	.010
Superior Parietal Cortex	-.004 (.001)	.005
Supramarginal Gyrus	-.004 (.002)	.006
Temporal Pole	-.008 (.005)	.122

Figure 1: Scatter plots of change in thickness vs. SHCs for significant ROIs.



PS 950

Cortical Processing Related to Intensity of a Modulated Noise Stimulus - a Functional Near-Infrared Study

Stefan Weder¹; Xin Zhou²; Mehrnaz Shoushtarian³; Hamish Innes-Brown⁴; Marco D. Caversaccio⁵; Colette McKay⁶

¹Department of Otorhinolaryngology, Head and Neck Surgery, Inselspital Bern, University of Bern,;

²Waisman Center, University of Wisconsin-

Madison; ³The Bionics Institute; ⁴Bionic Ear Institute;

⁵Department of Otorhinolaryngology, Head and Neck Surgery, Inselspital Bern, University of Bern; ⁶The Bionics Institute

Sound intensity is a key feature of auditory signals. A profound understanding of cortical processing of this feature is therefore highly desirable. This study investigates whether cortical functional near-infrared spectroscopy (fNIRS) signals reflect sound intensity changes and where on the brain cortex maximal intensity-dependent activations are located. The fNIRS technique is particularly suitable for this kind of hearing study, as it runs silently. Twenty-three normal hearing subjects were included and actively participated in a counterbalanced block design task. Four intensity levels of a modulated noise stimulus with long-term spectrum and modulation characteristics similar to speech were applied, evenly spaced from 15 to 90 dB SPL. Signals from auditory processing cortical fields were derived from a montage of 16 optodes on each side of the head. Results showed that fNIRS responses originating from auditory processing areas are highly dependent on sound intensity level: higher stimulation levels led to higher concentration changes. Caudal and rostral channels showed different waveform morphologies, reflecting specific cortical signal processing of the stimulus. Channels overlying the supramarginal and caudal superior temporal gyrus evoked a phasic response, whereas channels over Broca's area

showed a broad tonic pattern. This data set can serve as a foundation for future auditory fNIRS research to develop the technique as a hearing assessment tool in the normal hearing and hearing-impaired populations.

PS 951

The Effect of Profound Hearing Loss: Meta-analysis of Bilateral and Unilateral Structural MRI Studies

Francis A.M. Manno¹; Rachit Kumar¹; Raul Rodríguez-Cruces¹; Condon Lau²; J. Tilak Ratnanather³

¹JHU; ²City University of Hong Kong; ³Johns Hopkins University

Introduction: Bilateral and unilateral hearing loss has a profound effect on speech and language development and elicits underlying functional deficits; nevertheless, little is known concerning structural reorganization. Studies of individuals with bilateral hearing loss have revealed increased gray matter and decreased white matter in Heschl's gyrus (Emmorey et al., 2003; Smith et al., 2011), left posterior superior temporal gyrus (STG) white matter deficits, (Shibata, 2007) and cortical thinning (Li et al., 2012); however, one report has indicated preserved left > right Heschl's gyrus asymmetry (Penhune et al., 2003). Neuroimaging studies of bilateral hearing loss give clues as to how reorganization occurs, as the lack of binaural input appears to alter left Heschl's gyrus by changing gray matter (GM) and white matter asymmetry.

Objective: Determine a cluster-wise meta-analytic approach to assess the effect of hearing loss in humans using structural MRI studies.

Methods: A PubMed search identified approximately n = 5000 studies concerning MRI structural analyses of bilateral or unilateral hearing loss. Approximately n = 46 studies were identified as using MRI techniques to assess structural alterations, such as VBM (n = 11), CT (n = 3), and DTI (n = 6). From these, n = 20 studies reported MNI coordinates which we utilized for coordinate-based activation likelihood estimation (ALE) meta-analysis. The input variables were: threshold method, uncorrected p value, chosen p value threshold = 0.01, minimum ALE value > threshold = 0.00595, volume > threshold = 20952 mm³, chosen min. cluster size = 50 mm³.

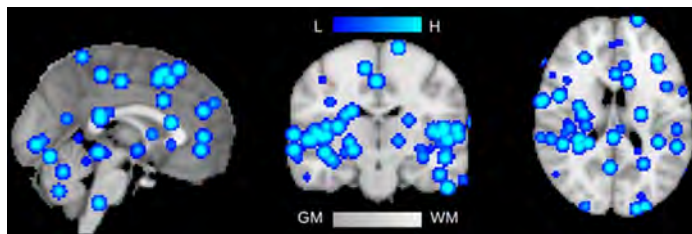
Results: The meta-analysis of hearing loss studies yielded n = 281 foci of at least 50 mm³ from 445 MRI scans of patients (Figure color bars of high and low density and GM and WM). Above 200 mm³ volumes, 9 clusters of significance were found: 1) 592 mm³ | MNI: -43.2/-22.8/8.1, Left STG GM Brodmann area (BA) 13, 2) 584 mm³ | MNI: 44.9/-21.6/5.3, Right Insula, sub-lobar GM BA 13, 3) 272 mm³ | MNI: 41.1/-25.6/12.9, Right Transverse Temporal Gyrus GM BA 41, 4) 256 mm³ |

MNI: 25.1/-14.7/20.4, Right Sub-lobar Lentiform Nucleus GM Putamen, 5) 240 mm³ | MNI: -17.6/- 58.4/-16.3, Left Cerebellum Anterior Lobe Culmen GM, 6) 240 mm³ | MNI: 53.2/- 20.6/0.8, Right STG GM BA 22, 7) 232 mm³ | MNI: -49.5/-5.9/-8.4, Left STG GM BA 22, 8) 224 mm³ | MNI: -1.9/-36.1/-8, Left Cerebellum Anterior Lobe Culmen GM, and 9) 208 mm³ | MNI: 30.9/-38.4/16.5, Right Sub-lobar Caudate GM Caudate Tail. The random effects analysis FWHM with a focus = 9.57 output a maximum ALE score = 0.00755, p = 0.000155. Hearing loss had a profound global effect across the brain based on the meta-analysis of MNI clusters.

Conclusion: The meta-analysis of bilateral and unilateral hearing loss studies reveals widespread alterations not only in STG or the Sylvian fissure, but globally across the brain, in the cortex, subcortex and brainstem. Future studies should determine the difference between bilateral and unilateral hearing loss and should distinguish an effect of hearing loss on different age populations.

DOI 10.17605/OSF.IO/7Y59J
<https://osf.io/7y59j/>

Smith KM, et al., *Cereb Cortex*. 2011 May;21(5):991-8. Emmorey K, Allen JS, Bruss J, Schenker N, Damasio H. *Proc Natl Acad Sci U S A*. 2003 Aug 19;100(17):10049-54. Penhune VB, Cismaru R, Dorsaint-Pierre R, Petitto LA, Zatorre RJ. *Neuroimage*. 2003 Oct;20(2):1215-25. Li J, et al., *Brain Res*. 2012 Jan 9;1430:35-42. Shibata DK. *AJNR Am J Neuroradiol*. 2007 Feb;28(2):243-9.



PS 952

Profound Bilateral and Unilateral Hearing Loss Alters Large Scale Macroscopic Cortical Asymmetry and Yakovlevian Torque

Francis A.M. Manno¹; Rachit Kumar¹; Raul Rodríguez-Cruces¹; Condon Lau²; J. Tilak Ratnanather³

¹JHU; ²City University of Hong Kong; ³Johns Hopkins University

Introduction: Bilateral and unilateral hearing loss has a profound effect on speech and language development in children and elicit functional deficits; nevertheless, little is known concerning structural reorganization. Studies of bilateral deaf individuals have revealed increased gray

matter and decreased white matter in Heschl's gyrus (Emmorey et al., 2003; Smith et al., 2011), superior temporal gyrus (STG) white matter deficits (Shibata, 2007), and cortical thinning (Li et al., 2012). Neuroimaging studies of bilateral hearing loss give clues as to how reorganization occurs, as the lack of binaural input appears to alter Heschl's gyrus and the temporal lobe by changing gray matter and white matter relationship.

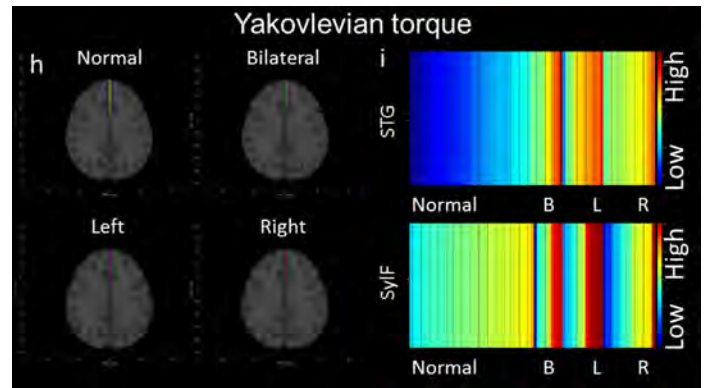
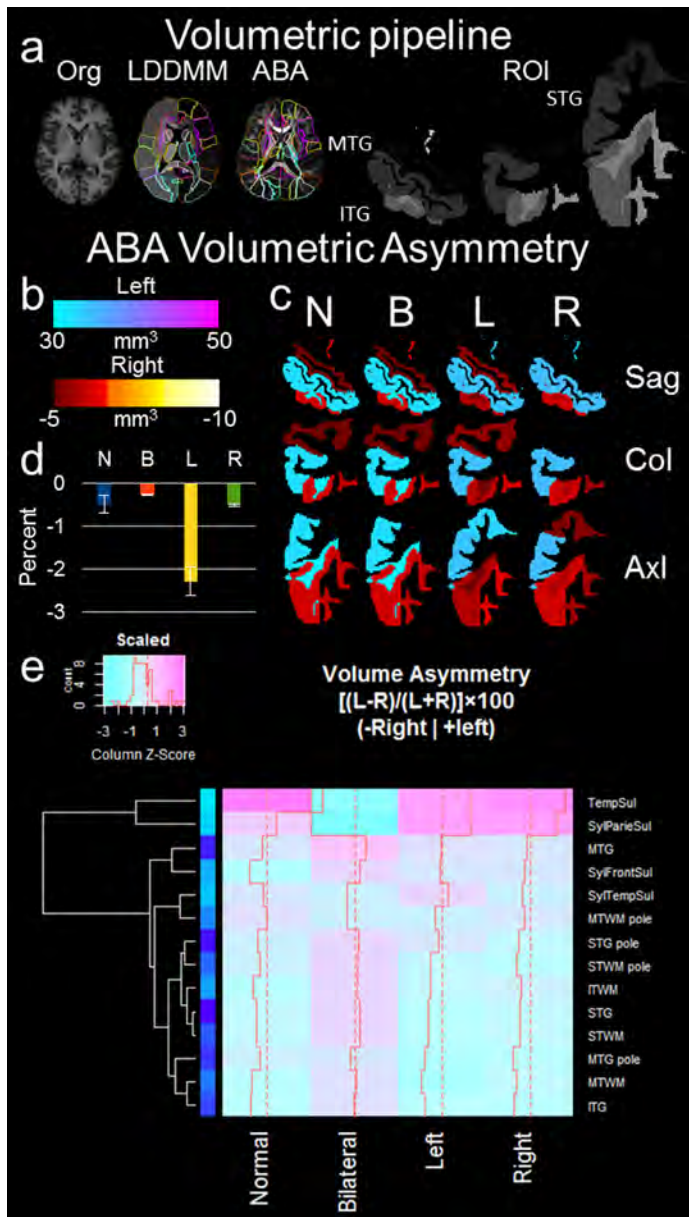
Objective: Assess the effect of bilateral and unilateral hearing loss using MRI volume based morphometry and shape metrics (Fig. a).

Methods: 42 children (n = 18 bilateral, prelingual) or unilateral hearing loss (left n= 10, right n= 14, perilingual) participated with 43 age and sex matched controls (range 6 months to 18 years). Children were from an homogeneous group having profound sensorineural hearing loss (≈ 90 db) bilaterally or unilaterally. Air and bone-conduction thresholds as well as speech recognition thresholds were assessed. Structural MRI three-dimensional (3D) sagittal T1-weighted magnetization-prepared rapid gradient-echo (MP-RAGE) sequences assessed volume and shape metrics using a segmentation pipeline (Mori et al., 2016). Specifically, asymmetry was defined as [(L-R)/(L+R)]×100 which produces an index ranging from -100 (larger right volume) to +100 (larger left volume) and Yakovlevian torque, a metric of hemispheric twist, defined as distortion between the translation of the native space brain onto MNI space based on the affine matrix – here greater distortion indicates greater twist of a subject's brain to fit to their MNI registered template (Fig. b).

Results: Volume metrics indicated bilateral and left and right unilateral hearing loss individuals were similar to controls, but asymmetry metrics were significantly different between hearing loss groups and controls (Fig c). Left unilateral hearing loss was most pronounced (Fig. d). A metric of hemispheric twist revealed little global Yakovlevian torque due to hearing loss (Fig h); however, local torque in regions such as the STG and Sylvian fissure were grossly affected (Fig i). Hearing loss not only affected traditional metrics assessed with MRI, but hearing loss also resulted in a twist of the brain around an axis due to singled sided hearing or bilateral deafness.

Conclusion: We assessed three unique groups of children to determine how brain metrics change due to hearing loss. Hearing loss affected traditional volumetric analysis of grey matter and white matter in addition to shifting asymmetry of volume. Shape metrics revealed the shift of volume may be due to the brain twisting about the axis to compensate for hearing on one side versus the other.

Smith KM, et al., *Cereb Cortex*. 2011 May;21(5):991-8.
Emmorey K, Allen JS, Bruss J, Schenker N, Damasio H. *Proc Natl Acad Sci U S A*. 2003 Aug 19;100(17):10049-54.
Penhune VB, Cismaru R, Dorsaint-Pierre R, Petitto LA, Zatorre RJ. *Neuroimage*. 2003 Oct;20(2):1215-25.
Li J, et al., *Brain Res*. 2012 Jan 9;1430:35-42.
Shibata DK. *AJNR Am J Neuroradiol*. 2007 Feb;28(2):243-9.
Mori et al., *IEEE CS*. 2016 Aug;18(5):21-35.



PS 953

Plastic changes within the auditory cortex after removal of the vestibular schwannoma

Oliver Profant¹; Jaroslav Tintera²; Filip Jiru²; Zdenek Fik³; Jan Betka³; Veronika Svobodova³; Diana Kucharova³; Josef Syka⁴

¹Department of Auditory Neuroscience, Institute of Experimental Medicine, The Czech Academy of Sciences; ²MR Unit, Institute of Clinical and Experimental Medicine; ³Department of Otorhinolaryngology and Head and Neck Surgery, 1st Faculty of Medicine, Charles University in Prague, University Hospital Motol; ⁴Institute of Experimental Medicine CAS

Introduction: Vestibular schwannoma (VS) is the most common tumor of the temporal bone. Symptomatology of the VS includes sensorineural hearing loss (SNHL; the most frequent symptom), tinnitus and vertigo. Treatment of the VS (active – surgery or radiotherapy, passive - observation) depends on several factors (size of the tumor, state of hearing, concomitant pathologies, overall health, patient's wish).

Aim: The aim of our study was to identify central changes related to asymmetric hearing loss/deafness caused by the tumor removal.

Material and methods: Eighteen patients were included in our study. Patients underwent auditory examination (pure tone audiometry, speech audiometry, ABR, OAE), MRI (resting state, event related functional MRI, MR spectroscopy, MR morphometry and tractography) before the surgery, and 3 months, 1 year and then every year after the surgery (2 patients were followed up to 2 years after the surgery). We used the retrosigmoid approach with the aim to remove the tumor and preserve hearing.

Results: All patients had useful hearing prior to surgery

(Gardner-Robertson 1 or 2). In all cases the tumor was completely removed with a good function of the facial nerve and minimal postoperative complications. In 6 cases hearing was preserved after the tumor removal. The fMRI showed no abnormality in the activation of the auditory cortex (AC) prior to the surgery, with the resting state showing the strongest connectivity between AC regions. Postoperative fMRI showed strong differences between the activations in patients with preserved hearing, compared to the group with single sided deafness. Individual differences in time course of the plastic changes were present in patients with postoperative deafness.

Conclusion: Hearing loss caused by the removal of the VS produces plastic changes in the auditory system, in some cases by already 3 months after the surgery. These changes include differences in the functional activation of the AC.

PS 954

Neural Correlates of Speech-in-Noise Variance in Cochlear Implant Users

Inyong Choi¹; Ann Holmes²; Subong Kim³; Adam Schwalje¹; Andrew S. Liu⁴; Phillip E. Gander⁵; Youngmin Na⁶; Jihwan Woo⁶; Bob McMurray⁷; Timothy D. Griffiths⁸

¹University of Iowa; ²Department of Psychology and Brain Sciences, University of Iowa; ³Department of Communication Sciences and Disorders, University of Iowa; ⁴Department of Otolaryngology - Head and Neck Surgery, University of Iowa Hospitals and Clinics; ⁵Department of Neurosurgery, Department of Otolaryngology, The University of Iowa; ⁶Department of Biomedical Engineering, University of Ulsan; ⁷Department of Psychology and Brain Sciences, The University of Iowa; ⁸Wellcome Centre for Human Neuroimaging, University College London; Institute of Neuroscience, Newcastle University

Understanding speech in noise (SiN) is essential for communication in everyday settings, but the ability to successfully navigate SiN differs dramatically especially in cochlear implant (CI) users. Variation in the neural encoding of acoustic information, measured as early auditory-cortical evoked responses, is known to contribute to the variance in speech perception outcomes, while its interaction with cognitive processing mediated by frontal cortex is unclear. Understanding the relative contributions of sensory encoding fidelity and cognitive factors can guide clinical interventions. Here, we explored relationships between the evoked responses from key regions of the speech-processing chain including auditory cortex (AC), supramarginal gyrus (SMG, BA40), inferior frontal gyrus (IFG, BA44), and performance in SiN understanding.

Previous electroencephalographic (EEG) studies showed increased inferior frontal gyrus (IFG) activity in the clean speech condition (Bidelman & Howell, 2016), whereas an fMRI study showed increased IFG activity associated with the increased listening effort (Wild et al., 2012). We hypothesized that stronger and faster AC and SMG responses predict better performance, and increased amplitude and latency of evoked responses from IFG predict difficulty in SiN understanding. We tested evoked responses to consonant-vowel-consonant spoken words in multi-talker babble background in CI users. We found that poor CI performers exhibit stronger late response (later than around 700ms after the word onset) in the left IFG, whereas good CI performers show stronger early AC and SMG responses. Our results suggest that the interplay between temporo-parietal and frontal cortical activity can predict SiN understanding performance of CI users. This study will define several fundamental mechanisms of neural processes required for successful speech-in-noise understanding and will provide an insight to a better understanding of individual variances in CI benefits.

This work was supported by NIDCD P50 DC000242 31A1 (PI: Gantz).

PS 955

Modality-specific Resetting of Segregation During Bistable Perception of Auditory Streams

Nathan C. Higgins¹; Breanne D. Yerkes¹; David F. Little²; Jessica E. Nave-Blodgett¹; Mounya Elhilali²; Joel S. Snyder¹

¹University of Nevada Las Vegas; ²Johns Hopkins University

Bistability is a perceptual phenomenon during which the repeated presentation of stimuli elicits alternating interpretations that switch back and forth in an unpredictable manner. This pattern of switching is similar for auditory and visual stimuli. Whether there is a common cognitive process that operates perceptual switching independent of sensory modality or a distributed system specific to the relevant sensory percepts, remains unknown. To test the extent of modality independence, an auditory streaming paradigm was designed to examine the effect of perceptual streaming in the presence of auditory and visual distractors. Triplets of low-high-low pure tones (ABAs) were used to create a bistable perception of 1- or 2-streams and participants responded continuously via button press to indicate their percept. Presented in separate auditory or visual blocks, the auditory distractor was a 500 ms iterated ripple noise (centered at 1, 2, or 3 kHz), and the visual distractor was a 500 ms flash of red, green, or blue on the fixation screen. Distractor types (Auditory or Visual) were presented in separate 7 minute

blocks (8 trials per block; 100 ABAs per trial); within each block distractor type and time of distractor presentation within the ABA pattern were counterbalanced. Over the first 20s of each trial--in which no distractors were present--no significant difference in the reported percepts (N=38 subjects) between 1- versus 2-streams was observed between auditory and visual blocks. The proportion of reported 1- versus 2-streams, however, sharply deviated upon introduction of the distractors with significantly more 1-stream percepts reported for blocks with auditory distractors (paired t-test; $t_{(37)} \geq 3.68$; $p < 0.001$, Bonferroni corrected). In a separate analysis, ABA epochs were binned into 3 sec time windows and separated by percept (either 1- or 2-streams) at sound onset. When perceiving 1-stream, introduction of an auditory, visual, or no distractor resulted in an equal likelihood of switching to a 2-stream percept over the ensuing 3 seconds. Conversely, during epochs in which 2-streams were perceived, a significant effect of the auditory distractor was observed, evidenced by a significant shift to 1-stream, while the introduction of the visual distractor had no significant effect in the same circumstance. This pattern of results (modality and percept-direction specific switching) is consistent with a model of cognitive bistability in which bottom-up processing of distractors is modality specific.

PS 956

O-15 Water PET Study of Speech in Noise Processing in Cochlear Implant Patients

Phillip E. Gander¹; Laura Ponto²; Inyong Choi³; Bob McMurray⁴; Timothy D. Griffiths⁵

¹Department of Neurosurgery, Department of Otolaryngology, The University of Iowa; ²Department of Radiology, The University of Iowa; ³University of Iowa; ⁴Department of Psychology and Brain Sciences, The University of Iowa; ⁵Wellcome Centre for Human Neuroimaging, University College London; Institute of Neuroscience, Newcastle University

One of the most important issues in hearing impairment (HI) is difficulty with speech in noisy real-world environments. Recent research in normal hearing listeners indicates that auditory cortex is active while abstracting speech objects from noise and provides input to fronto-temporal networks for further perceptual, attentional, and semantic analysis. We want to understand whether these are the same neural mechanisms that support the changes a cochlear implant user experiences as they adapt to their new hearing condition, and how these mechanisms relate to successful hearing outcomes.

Here we report a proof-of-concept study to determine if we could robustly and reliably measure brain activity to speech in noise at a single subject level, so that we will be able to track individual subjects after implant activation

over the long term as their experience with the implant changes. We sought to: 1) demonstrate activity in a fronto-temporal network to speech in noise in each single subject, 2) determine reliability by testing on the same stimulus conditions at two different sessions separated by weeks, 3) compare activity between cochlear implant and normal control subjects, and 4) compare activity to sentences in noise and words in noise.

We measured [¹⁵O]Water positron emission tomography (PET) blood flow in a group of 9 cochlear implant patients and 10 age-matched normal hearing controls while they listened to 2-min blocks of continuous sentences in noise or noise alone (matched on RMS sound level). On a given run for speech in noise (+7 dB), 30 unique sentence tokens (~2.5 sec length) were presented (1.5 sec inter stimulus interval). We acquired 12 scans (6 each condition, random order) to allow for single subject inference. Six control subjects were scanned in a repeat session with the same sentence in noise stimulus, and two control subjects were scanned with a word in noise stimulus (-3 vs 13 dB). PET data were analyzed in SPM12 using a flexible factorial model.

We found robust activations in single subjects for the contrast speech in noise vs noise in auditory cortex (lateral Heschl's gyrus, planum polare, and planum temporale) and inferior frontal cortex (frontal operculum and inferior frontal gyrus) bilaterally (p

In the normal hearing control subjects we found similar brain activations in the fronto-temporal network in each subject with no differences to the cochlear implantees at the group level. In the six subjects that returned for a repeat sentence in noise session we found very high correlations across the whole brain (all $r < 0.9$). In the two subjects that completed a second session of a word in noise task, fronto-temporal activity was very similar to the sentence in noise data.

Our results support a similar model for speech in noise processing in cochlear implant patients and normal hearing listeners, that can be reliably detected across sessions. These findings support the possibility of conducting a longitudinal study to assess the changes in cochlear implantee performance.

PS 957

Auditory Spatial Attention over 360°

Genesis Rivera; Jeffrey Mock; Edward Golob
University of Texas at San Antonio

Attending to a specific region of space has behavioral benefits. For example, reaction times are fastest to stimuli at an attended location, and progressively slow down with greater distance from the focus of attention

(termed an "attention gradient"). Prior studies suggest that auditory spatial attention gradients indeed appear in the frontal azimuth plane, however, research on the full azimuth plane is limited. The current study tests properties of auditory attention gradients by manipulating two variables: the attended location and the range of speaker locations. Subjects were surrounded by a 360° speaker array, and they pressed one of two buttons in response to amplitude-modulated white noise (25 vs. 75 Hz, $p=.50/.50$, 1.2 sec SOA, 70 dB SPL). In each block of trials most sounds were presented from one speaker that was the focus of attention ("standard location"), with occasional shifts to the other speakers. In Experiment 1 ($n=25$) a speaker range of 180° was tested in both the front and back hemispace, with standard locations at the left, midline, and right. When the standard location was on the left (270°) or right (90°), reaction times progressively increased with greater shifts from the standard ($p<.001$), indicating a spatial attention gradient. In the right hemispace bottom-up attention capture was greater for shifts at the back vs. the corresponding front locations ($p';s<.01$). In the left hemispace capture was comparable for front vs. back locations. For midline standards (0°, 180°) there were significant gradients when focusing on the front standard ($p<.01$), but not for the back standard. In two additional experiments ($n';s=29$ and 24) the speaker range covered the 360° range with either 5 or 8 speakers equally spaced apart in the array. In both experiments reaction times were fastest at each standard location, and were slower at the remaining locations, which had comparable reaction times ($p';s < .01$). These findings show that under a restricted range of locations attention gradients adopt complex shapes due to front-back and left-right asymmetries. When a full 360 range of locations is tested, attention gradients become much more uniform over space.

PS 958

Pupillometry as an objective measure of listening effort and sustained attention in young and ageing populations

Gabriela Bury¹; Sijia Zhao¹; Alice Milne¹; Maria Chait²
¹University College London; ²UCL Ear Institute, University College London

BACKGROUND

Listening in noisy environments does not only depend on hearing acuity but also on the brain's ability to focus attention on a specific sound source amidst concurrent, irrelevant sounds. Understanding this capacity is central to understanding listening and deficits in listening in natural environments. Here, we aimed to explore the use of pupillometry as an objective measure of the effort associated with sustained attention in young and aging listeners.

METHODS

Young (aged 18 to 35) and older (over 60) participants with normal hearing completed a listening task of varying levels of difficulty. The task involved sustaining attention on a target sound-stream for ~30s and detecting occasional silent gaps. Difficulty was manipulated by increasing the number of distractor streams (0, 1 or 2 distractor streams). Streams were widely spaced in frequency (at least 2 ERB) such that the presence of distractor streams was associated with informational but not energetic masking.

Pupil Dilation Response (PDR) was measured throughout the experiment. PDR was analysed across conditions and related to individual task performance.

RESULTS

Behavioural results indicated that performance decreased across conditions in both young and older groups. Individual variability was high. To make sure that the measured pupil dynamics reflected attentive tracking as opposed to disengagement from the task in the more difficult conditions, PDR analysis was performed on successful trials only (100% hit rate, up to 1 Fa). In both groups, results showed increased, sustained pupil dilation as a function of task difficulty. PDR results were related to individual and group performance. PDR to distractor gaps was shown to reliably represent the amount of cognitive resources applied to the listening task.

CONCLUSIONS

Pupillometry can be used as a measure of effort to sustain attention over long (~30 sec) durations in both young and ageing populations.

Human Development

PS 959

Brainstem Correlates of Listening Difficulties in Children

Chelsea Blankenship; David R. Moore; Audrey Perdeu; Lisa L. Hunter
University of Cincinnati/Cincinnati Children's Hospital Medical Center

Children with listening difficulties (LiD) but 'normal'; audiometry may have sub-clinical hearing deficits that affect speech in noise abilities. The medial olivocochlear (MOC) bundle and middle ear muscle reflex (MEMR) are thought to influence speech perception in low and higher levels of background noise, respectively. Wolter (2014, Aud Neurology) found lower frequency suppression is abolished by transection of the stapedius (e.g., MEMR), while higher frequency MOC activity (4 kHz) was preserved. Saxena (2015, IJA) reported shallower MEMR growth slopes in children with listening difficulties. Wideband MEMR growth analyzed spectrally may reveal higher frequency MOC activity in addition to lower

frequency MEMR activity. Likewise, auditory brainstem response (ABR) amplitude and MEMR growth functions may provide a useful measure of neural integrity at the level of the brainstem.

Children with LiD (n=64, 6-12 yrs) based on validated parent questionnaires (ECLiPS, Barry, 2015, Ear Hear.) and age-matched typically developing (TD) children (n=56) were recruited from clinical services and website advertisements at Cincinnati Children's. Over a two-day period, children completed a variety of behavioral and physiological tests including audiometric thresholds (0.25-16kHz), click-evoked ABR, and wideband MEMR using a custom research system (Keefe, 2017, JARO). Two-channel ABR (alternating polarity, 11.1/second) was recorded using ear canal electrodes from 75 to 90 dB nHL in 5-dB steps. Ipsilateral and contralateral MEMR were measured in 5-dB steps using a wideband probe (click) and activators of broadband noise (BBN; 45-90 dB SPL) and pure-tones (0.5, 1, 2 kHz; 60-105 dB SPL). MEMR growth functions (change in reflex absorbance with increases in intensity level) were calculated for various spectral regions from .25 to 8 kHz.

All participants had normal audiometric thresholds in the standard frequency range (≤ 20 dBHL; 0.25-8 kHz). MEMR growth functions showed systematic increases in absorbance at 0.71 and decreased absorbance at 1.41 and 4 kHz. The slope of the MEMR growth function showed a similar, systematic change in absorbance at 0.71 and 1.41 kHz for TD and LiD groups. However, the LiD group showed flat functions at 4 kHz. ABR results (Wave I, III, V) displayed a systematic and similar decrease in latency and increase in amplitude with increases in stimulus intensity for both the TD and LiD group. Further analyses will examine correlations between ABR amplitude (Wave I and V) and MEMR growth functions, as well as effects of EHF hearing loss, history of PE tubes and speech in noise performance.

Supported by NIH: R01DC014078

PS 960

The Relationship between Auditory Sequence Processing and Language Skill in Children: Do Working Memory, Attention or Musical Training act as Mediators?

Faye Smith¹; Manon Grube²; Sukhbinder Kumar³; Timothy D. Griffiths⁴

¹Newcastle Auditory Group; ²Aarhus University; ³Newcastle University; ⁴Wellcome Centre for Human Neuroimaging, University College London; Institute of Neuroscience, Newcastle University

Research Background: Previous work has demonstrated a robust relationship between the

processing of nonverbal, basic auditory sequences and language skill in children (PMID 22951739). Understanding the role of basic auditory processing in language development is important for clarifying the nature of language difficulties. This study aims to extend the previous findings by investigating whether working memory, attention or musical training mediate the relationship between auditory sequence processing and language skill.

Method: A large sample of 239 11-year-old children completed eight auditory sequence tasks in a classroom setting: 3 pitch sequence tasks, 3 rhythm tasks, a dynamic ripple discrimination task and an auditory working memory task. Standardized language, literacy and nonverbal ability tasks were administered individually alongside a computerized auditory attention task. Participants were asked about their history of musical training.

Results: Replicating PMID 22951739, a significant relationship was demonstrated between the first principal components of language and auditory skill ($r=.317$, $p<.001$). More specifically, language skill correlated with auditory analysis of short pitch sequences and the detection of both deviation from isochrony and detection of a more abstract change in sequence regularity. Mediation analyses revealed that these relationships did not depend on nonverbal ability, auditory working memory, auditory attention or musical training.

Conclusion: This study supports previous findings of a relationship between auditory sequence processing and language ability in children. As previously shown, at this point in development sensitivity to deviations from basic rhythmic and melodic features is particularly important. Crucially, these relationships are not mediated by key higher order skills of nonverbal ability, auditory working memory and auditory attention, nor are they mediated by musical training.

PS 961

Development of Early Communication Skills of Normal and Hearing Impaired Children in Korea

Jiyeong Yun; Eunsung Lee; Kieun Lee; Hyunwook Song; Jinsook Kim
Hallym University

Background: Given the importance of early communicative skills for the later developments, the evaluation of speech and language could be crucial for understanding the developmental process and planning the intervention program of the Hearing Impaired (HI) children. However, a limited attention span and the less comprehension of instructions have made the speech and language assessment in HI children challenging.

Four tools, Korean MacArthur-Bates Communicative Development Inventories (M-B CDI K), Sequenced Language Scale for Infants (SELSI), Communication and Symbolic Behavior Scales Developmental Profile (CSBS DP) checklist and behavior sample were known to be efficient for evaluating the communicative skills in very young age for both HI and Normal Hearing (NH) children. The aim of this study was to investigate the development of early communication skills in NH and HI children and to compare the performance between chronological and hearing ages of HI children. **Methods:** The data were collected from 40 children including 21 NH and 19 HI children ranging from 4 to 56 months of age. Participants were divided into six periods of month groups, 4-6 months, 7-9 months, 10-12 months, 13-15 months, 16-18 months, and 19-24 months to observe the periodical developmental process. Participants were tested regularly every 2 to 3 months using the four evaluation tools. And the HI children were intervened by recently developed program of Korean auditory, language and cognitive rehabilitation for infants from the beginning of evaluation. Developmental progress depending on chronological age between NH and HI groups, developmental progress depending on hearing age between NH and HI groups, and developmental progress between chronological and hearing ages in HI group were analyzed systematically. **Results:** The NH group showed better performance than the HI group significantly in chronological age ($p < 0.05$). The HI group showed similar or better performance than NH group in hearing age. The scores of hearing age showed better than those of chronological age significantly in all assessment tools ($p < 0.05$) except the production score of M-B CDI K between chronological and hearing ages in HI group. **Conclusions:** The hearing age showed higher performance than the chronological age showing the influence of intervention. In HI group, the increasing speech scores of CSBS DP checklist and behavior sample in hearing age also showed strong proof of intervention effect between 13-15 and 16-18 months groups. Thus, it is recommended to intervene HI children for enhancing communicative skills for facilitating developmental progress as early as possible.

PS 962

Neural Processing of Speech in Children with Sensorineural Hearing Loss

Axelle Calcus; Stuart Rosen; Lorna Halliday
University College London

Previous research has shown that even a mild (21-40 dB HL) or moderate (41-70 dB HL) sensorineural hearing loss (MMHL) can impair cortical processing of speech sounds, as evidenced by differences in event-related potential responses (P1-N1-P2-N2 and MMN)

between children with MMHL and chronological age-matched normally hearing (NH) controls (Koravand et al., 2013). However, to date no studies have examined speech processing at the subcortical level in children with MMHL. Moreover, the effects of amplification on the neural encoding of speech are still poorly understood, with previous data suggesting a significant benefit at the subcortical (Anderson et al., 2013) but not the cortical level (Billings et al., 2007).

The aims of this project were to (i) investigate the cortical and subcortical processing of speech sounds in children with MMHL and (ii) evaluate the effects of amplification on the neural processing of speech in this group. Cortical and subcortical EEG activity evoked by speech stimuli (/ba/-/da/) were simultaneously recorded in 18, 8- to 16-year-old children with MMHL and 16 age-matched NH controls. Subcortical processing was assessed using the frequency following response (FFR), an EEG component that reflects the encoding of the fundamental frequency (F0) and first few harmonics of complex auditory signals such as speech. Cortical measures included the MMN and the intra-class correlation (ICC) coefficient. For the MMHL group, stimuli were presented both unamplified (70 dB SPL), and with a frequency-specific gain (without compression) based on their individual audiograms.

Results revealed that as a group, children with MMHL had smaller ICC coefficients than NH controls in both unamplified and amplified conditions, and did not show an MMN. In contrast, at the subcortical level, they showed an FFR that was smaller than that of NH controls in the unamplified condition only. With simulated amplification, children with MMHL demonstrated an FFR that was comparable to that observed in NH controls. Our findings suggest that the neural processing of unamplified speech may be impaired at both subcortical and cortical levels in children with MMHL. However, consistent with previous studies in adults, amplification might benefit auditory processing at subcortical but not cortical levels in children with MMHL. This may be explained by increasing multi-sensory integration that occurs at successive levels of the auditory system: whereas the inferior colliculus processes unimodal information, the auditory cortex processes multimodal information. Alternatively, our findings may reflect the later maturation of the auditory cortex compared to the inferior colliculus.

Acknowledgements

This research was supported by the People Programme (Marie Curie Actions) of the European Union's Seventh Framework Programme FP7/2007-2013/under REA grant agreement n° FP7-607139 (iCARE).

References

Anderson, S., Parbery-Clark, A., White-Shwoch, T., Drehobl, S., & Kraus, N. (2013). Effects of Hearing Loss on the Subcortical Representation of Speech Cues. *J. Acoust. Soc. Am.* 133(5), 3030-3038

Billings, C., Tremblay, K., Souza, P. & Binns, M. (2007). Effects of Hearing Aid Amplification and Stimulus Intensity on Cortical Auditory Evoked Potentials. *Audiology & Neurotology*, 12, 234-246.

Koravand, A. Jutras, B., & Lassonde, M. (2013). Auditory event related potentials in children with peripheral hearing loss. *Clinical Neurophysiology*, 124, 1439-1447.

Inner Ear: Anatomy & Physiology

PS 963

Changes in Inner Hair Cell Function Contribute to the Late-onset Hearing Loss in GJB2 V37I Mutation Knock-in Mice

Xin Lin¹; Gen Li²; Yunfeng Hua¹; Tao Yang³; Genglin Li¹; Hao Wu⁴; Lei Song¹

¹Otolaryngology-Head and Neck Surgery, Shanghai ninth people's Hospital, Shanghai Jiao Tong University School of Medicine; Ear Institute, Shanghai Jiao Tong University School of Medicine; ²Department of Otolaryngology-Head and Neck Surgery, Ninth People's Hospital, Shanghai Jiao Tong University School of Medicine; ³Otolaryngology-Head and Neck Surgery, Shanghai ninth people's Hospital, Shanghai Jiao Tong University School of Medicine; Ear Institute, Shanghai Jiao Tong University School of Medicine; ⁴clinical auditory

Background: V37I mutation of GJB2 gene is highly associated with late-onset progressive hearing loss, especially in East Asia populations. GJB2 encodes Connexin 26 (Cx26), one of the connexin families that form gap junctions. We generated a V37I knock-in (KI) mouse model (Chen et al. 2016) that produces progressive hearing loss, similar to the phenotype of human carriers. Here, we take advantage of this animal model and investigate cellular mechanisms of this disease.

Methods: ABRs and Endocochlear Potentials (EPs) were measured in age-matched homozygous and wild-type (WT) mice. H&E and fluorescence stainings were used to evaluate cochlear morphology. Whole-cell patch-clamp recording of inner hair cells (IHCs) was performed to identify their functional changes. To explore the impact of potassium accumulation, middle ear injection of KCl and noise exposure was applied to stress the inner ear.

Results: Starting from week 15, homozygous animals develop a mild progressive hearing loss above 16 kHz.

Morphological assessments do not find significant hair cell loss, Stria Vascularis atrophy or Spiral Ganglion neuron loss between homozygous and WT mice. Further functional analyses show EPs in homozygous mice are slightly reduced (~ 10 mV, 4-100 weeks), which explains the reduction of Q10 in ABR Wave I forward masking tuning curves. Elevated ABR thresholds are accompanied with prolonged Wave I latencies. CTBP2 and GluR2 punta are reduced in homozygous mice. Capacitive changes (ΔC_m), calcium charges (Q_{Ca}) and calcium currents (I_{Ca}) of IHCs are significantly changed in homozygous animals. To evaluate the impact of potassium ion accumulation in the inner ear, we performed a one-time injection of KCl solution (150 mM) in the middle ear cavity. Post-injection results show a greater increase of ABR Wave I latency in homozygous animals over the time period of 10 days. Band-pass noise exposure (8-16kHz, 100 dB SPL, 2 hours) elevated thresholds in homozygous mice with further prolonged ABR wave I latencies and decreased amplitudes that do not recover over the two-week post-exposure time period. Synapse counts show a significant reduction in the affected middle turns in homozygous mice. Taken together, our data suggest that GJB2 V37I mutation causes late-onset hearing loss by rendering inner hair cell synaptic function more vulnerable to the environmental insults.

Conclusions: V37I mutation-induced hearing loss is mainly due to synaptic changes in IHCs associated with potassium accumulation around hair cells.

PS 964

Loss of Oncomodulin Correlates with Changes in Outer Hair Cell Morphology

Preston Simpson; Andrew Cox; Craig Heflick; Leslie Climer; **Dwayne D. Simmons**
Baylor University

The exquisite sensitivity of mammalian hearing is due to cochlear outer hair cells (OHCs) that serve as a feedback mechanism capable of rapid motile responses that tune the signal received by the inner ear. Oncomodulin (Ocm) is a major calcium buffer in OHCs and a member of the parvalbumin protein family. Targeted deletion of Ocm leads to early progressive hearing loss in adult mice, suggesting that calcium regulation is significant to OHC function and may even play a role in aging. Significantly, Ocm knockout (KO) mice show a progressive elevation of distortion-product otoacoustic emissions (DPOAEs) beginning in high frequencies and suggesting a progressive loss of electromotile responses in OHCs. Early studies of slow motility, electromotility and lateral stiffness suggest the involvement of an actin-spectrin network of the cortical cytoskeleton that can be modified by calcium. Prestin (SLC26A) is an OHC transmembrane

protein primarily responsible for OHC electromotility and may also be modified by calcium levels within OHCs. Based on previous localization studies in OHCs, we hypothesize that a lack of Ocm may affect the OHC cytoskeleton and eventually lead to changes in OHC electromotile responses. We first investigated the morphological overlap of Ocm with prestin. We took high resolution confocal images of OHCs labeled with prestin and Ocm for wild-type (WT) mice at different ages and with different strain backgrounds. There is significant colocalization between Ocm and prestin in WT mice that may decrease with age, suggesting the potential for spatial interaction between the two proteins. After the onset of elevated DPOAE thresholds in Ocm KO mice, we found that OHCs may express prestin abnormally and may have abnormal cell shapes: OHCs are less circular and appear to collapse in on themselves. We are investigating prestin and Ocm interactions using co-immunoprecipitation and differences in the actin cytoskeleton in Ocm KO mice. Based on these preliminary results, we conclude that Ocm plays a role in the regulation of the actin cytoskeleton in OHCs, which may lead to changes in electromotile responses.

PS 965

Dysferlin Direct Protein-Protein Interactions Support Involvement of Dysferlin in Apoptotic Pathways of Hair Cells as Predicted by Structurally Similar Otoferlin

Dennis G. Drescher; Marian J. Drescher; Priyanka Annam
Wayne State University

Background

Previously, we demonstrated that exposure of the adult rat to 118 dB SPL noise upmodulated annexin-A2, which co-localizes with dysferlin in OHC stereocilia and at the IHC base. Heidrych (2008) obtained evidence that otoferlin C2D-C2E domain directly binds the "cell-death protein" PDCD6 and that the otoferlin carboxy domain interacts with FKBP8, which would bind the anti-apoptotic protein Bcl-2. We now investigate direct interactions of these proteins linking ferlins to cell atrophy.

Methods

Rat dysferlin-specific in-frame molecular domains, PDCD6, and annexin-A2 were inserted into pRSET-A, expressed in bacteria, the proteins isolated and examined by western blot and direct PPI with K_D determined by SPR. Immunohistochemistry was performed for dysferlin, PDCD6, FKBP8, and ryanodine receptors on 5- μ m sections of rat cochleas, with 3,3'-diaminobenzidine detection which permits direct morphological assessment. Skeletal muscle was

utilized for positive controls. For SPR, we employed a GE 3000 instrument. Ligand protein was amine-coupled onto a CM5 chip. Target-protein analyte was presented in concentration series and BIA-evaluation software was used for kinetic curve fitting and deriving association-dissociation constants.

Results

We found by SPR that dysferlin interacts via the C2D-C2E region with PDCD6, with $K_D = 1 \times 10^{-8}$. The PDCD6 protein was also found to interact with annexin-A2, the latter thought to be important in repairing cell membranes after lesion, with a $K_D = 2 \times 10^{-8}$. Thus dysferlin C2D-C2E and annexin-A2 are likely to compete in binding to PDCD6, and we have localized PDCD6 exclusively to cochlear hair cells, concentrated at supranuclear sites, particularly in IHCs. We have immunolocalized FKBP8, the putative dysferlin and Bcl-2 binding partner, to the tectorial membrane and cochlear hair cell in adult rat. Ryanodine receptors, a target of Bcl-2, have been immunolocalized to the base of OHCs, subserving efferent innervation, and to stereociliary sites.

Conclusions

We have obtained evidence supporting a role for dysferlin in interacting with PDCD6 which directly interacts with PDCD6IP (AIP1, ALIX), which in turn couples to stereocilia ankle protein ezrin. Given dysferlin/annexin-A2 mutual binding to PDCD6, alternate protein complexes may underlie the hair-cell response to noise. We have immunolocalized FKBP8 to peripheral sites of the tectorial membrane for the adult rat cochlea, which would be consistent with dysferlin interaction with FKBP8, given that dysferlin immunoreactivity extends from apical aspects of the stereocilia to the tectorial membrane. We also detected ryanodine receptor immunoreactivity in stereocilia, prominent in the apical turn, consistent with dysferlin/ryanodine receptor interaction.

PS 966

Characterization of Circadian Genes and Proteins in the Human Cochlea

Jacopo Fontana¹; Evangelia Tserga¹; Christopher Cederroth¹; Francois Lallemand¹; Ivan A. Lopez²; **Barbara Canlon**¹

¹*Karolinska Institutet*; ²*Department of Head and Neck Surgery, David Geffen School of Medicine*

Circadian rhythms provide an internal representation of time allowing for organisms to adapt to changing environments such as the light-dark cycle, temperature and feeding. Circadian rhythms are highly conserved across all organisms and are controlled by a molecular machinery that has a periodicity of approximately 24 hours. The main molecular clock machinery consists of

two transcription factors, CLOCK and BMAL1 that regulate *Per* and *Cry* gene transcription. Their protein products form a co-repressor complex that bind to the CLOCK/BMAL1 dimer and inhibit their transcriptional regulation. In the mouse cochlea, the mRNA of the core clock genes, *Per1*, *Per2*, *Bmal1*, *Clock*, and *Rev-Erb* have been shown to have circadian oscillations. Moreover, we identified 7211 genes in the mouse cochlea that have circadian expression and a large proportion of them are regulating cell signaling, hormone secretion and inflammation and nearly 2/3 of these genes showed maximal expression at nighttime. It is likely that the findings obtained from the mouse cochlea will have similar properties in human cochlea since the circadian regulation in mammalian species is highly homologous. However, this has never been tested in human cochlear samples before and is the purpose of this study. The expression pattern of core clock components (mRNA and proteins) in the human cochlea will be presented. Using immunocytochemistry and RNAscope technology we will characterize the expression of the core clock machinery in the human cochlea. These findings could have important implications with reference to the circadian regulation of the human auditory system and understanding variations that result from noise trauma and pharmacological treatment of auditory disorders.

PS 967

How is the Tectorial Membrane Formed? Ducts, vesicles and Ca²⁺ transients in Interdental Cells of the Developing Cochlea

Thore Schade-Mann¹; Pauline Schepsky²; Stefan Münkner²; Tobias Eckrich²; Jutta Engel³

¹Saarland University, Tübingen University Hospital;

²Saarland University; ³Saarland University, Dept. Biophysics and CIPMM, Hearing Research

Background

The formation of the tectorial membrane (TM) is an integral part of cochlear maturation. Beginning at around embryonic day 16, different types of proteins are secreted into the space of the developing cochlear duct by distinct cell types including the interdental cells (IDCs) of the spiral limbus. By postnatal day 12 (P12), the onset of hearing in mice, the TM is a complex, highly organized acellular structure comprised of different glycoproteins, some of which are specific to the inner ear, e.g. alpha- and beta-tectorin. Maintenance of the TM including slow turnover of its proteins is essential for normal hearing.

Methods

Cryosections of mouse cochleae were labeled with fluorescent antibodies and studied with a confocal laser-scanning microscope. Acutely explanted whole mount preparations of neonatal mouse cochlea were studied

by live cell imaging using the membrane markers FM4-64 and CellMask Deep Red to investigate the morphology of IDCs and the neonatal spiral limbus. Using Fluo-8 AM and confocal microscopy, we recorded spontaneous and ATP/UTP-evoked calcium signals in IDCs from P1 to P18. Relative fluorescence changes in IDCs were analysed with FIJI and parameters of the Ca²⁺ transients such as interspike interval, amplitude, time to peak, peak duration and decay time were extracted using a custom-made routine.

Findings

IDCs have a variable and complex anatomy. Towards the lateral margin of the spiral limbus they are perfectly aligned in a column-like fashion divided by the teeth of Huschke, extracellular protrusions from the core of the spiral limbus. Upon maturation of the cochlea, these interdigitations become more pronounced. There is evidence supporting the hypothesis of secretory activity in IDCs: Some IDCs form duct-like structures that are filled with a TM-like substance. Furthermore, we observed large intracellular vesicles (0.5 - 1 µm) moving within the IDCs. The occurrence of spontaneous calcium transients and the oscillation characteristics of ATP/UTP-triggered calcium signals changed between P1 and P18 suggesting that those Ca²⁺ signals triggered age-dependent exocytosis of vesicles containing TM material. Further experiments are needed to identify exocytotic processes in IDCs of the developing cochlea.

Supported by DFG SFB 1027 and Saarland University.

PS 968

Increased Neurotrophin 3 (NT3) expression by cochlear supporting cells improves gap detection and alters neuronal activity in the dorsal cochlear nucleus

Lingchao Ji¹; Calvin Wu²; David T. Martel²; M. Charles Liberman³; Susan E. Shore²; Gabriel Corfas¹

¹Dept. of Otolaryngology, Head and Neck Surgery, University of Michigan; ²University of Michigan; ³Mass. Eye and Ear Infirmary

We have previously shown that the neurotrophic factor Neurotrophin 3 (NT3) derived from cochlear supporting cells plays critical roles in the formation of synapses between inner hair cells (IHCs) and type I spiral ganglion neurons (Wan et al., eLife 2014). We demonstrated that over-expression of NT3 by supporting cells increases IHC synapse numbers and enhances amplitudes of ABR peak 1. In contrast, reduced NT3 levels lead to a reduction in the number of IHC synapses and peak 1 amplitude. These results suggest that the levels of supporting cell-derived NT3 could influence how animals process auditory signals. To explore this, we are testing

the behavioral and physiological phenotypes of mice with increased or decreased NT3 levels, focusing on pre-pulse inhibition (PPI) or gap inhibition of the startle response and spontaneous and sound-evoked neuronal activity in the dorsal cochlear nucleus (DCN).

We are using mice with inducible supporting cell NT3 over-expression or knockout of the *Ntf3* gene starting at the neonatal stage. These mice carry a *Plp1*/*CreER^T* transgene in combination with either *Ntf3^{stop}* or *Ntf3^{flox/flox}* alleles. Tamoxifen is injected daily from P1–P7 and ABRs and DPOAEs are measured in mutants and age-matched controls when mice reach adulthood (8 wks). Acoustics startle responses, as well as PPI and gap-inhibition of startle, are used to assess stimulus detectability, sensory gating, temporal processing, and tinnitus. Then, *in vivo* single unit recordings from the dorsal cochlear nucleus (DCN) are performed to measure spontaneous and evoked activity, including bursting, synchrony, and response gain. Finally, NT3 mRNA levels in the cochlea are measured by real-time quantitative RT-PCR and the number of hair cells and IHC synapses are quantified using immunostaining and confocal microscopy.

As expected, mice with NT3 over-expression (*Plp1*/*CreER^T*:*Ntf3^{stop}*) showed normal ABR and DPOAE thresholds but increased ABR peak 1 amplitudes. These mutants showed no differences in startle amplitudes and performance in the PPI test. Remarkably, mice over-expressing NT3 showed significantly greater gap-inhibition of startle compared with controls. These mice also exhibited increased evoked firing rates and reduced spontaneous neural synchrony of DCN neurons. Real-time quantitative RT-PCR verified the increased expression of cochlear *Ntf3*. Together, these results indicate that the increased number of IHC synapses resulting from NT3 over-expression leads to altered sound coding in DCN, which could underlie the improved gap detection, potentially reflecting enhanced sensory processing. Studies of mice with reduced NT3 expression are underway.

Research supported by grants from NIDCD (R01 DC004820 and R01 DC017119) and the American Tinnitus Association

PS 969

Effect of Selective Inner Hair Cell Loss on Acoustic Reflexes in Carboplatin Treated Chinchillas

Monica Trevino; Eliza Granade; Hannah Swanner; Edward Lobarinas
University of Texas at Dallas

Abstract: The acoustic reflex is an involuntary response of the middle ear stapedius muscle to moderately loud sound. This response results in a measurable decrease

in the admittance of the ossicular chain, reducing acoustic input to the inner ear. Diagnostically, the acoustic reflex (AR) threshold and amplitude are widely used in comprehensive hearing assessments. Approximately 65% of Audiologists in the US include the AR as part of their standard hearing test battery to evaluate retrocochlear pathways, corroborate hearing thresholds, and detect nonorganic hearing loss. Robust reflexes can be obtained in patients with mild to moderate sensorineural hearing losses associated with loss of outer hair cells (OHC) but are substantially diminished or abolished by severe to profound hearing loss. Remarkably, the relationship between the AR and inner hair cells (IHC), the primary conduits of acoustic information, is unknown. To answer this important question, we assessed the presence and amplitude of the AR in chinchillas before and after carboplatin treatment that reliably and selectively destroys IHC. We hypothesized that a substantial IHC loss would result in a significant reduction of the acoustic reflex amplitude or abolish the response.

Methods: Free feeding young adult chinchillas (1-3 years-of-age), housed in an enriched environment were used in this study. Ipsilateral ARs were obtained in awake animals using a Tymstar middle ear clinical analyzer. Stimuli were presented at a fixed level of 95 dB HL (91-100 dB SPL) for the 4 kHz tonal stimulus, low pass noise, high pass noise, and broadband noise. To control for potential OHC dysfunction, distortion product otoacoustic emissions (DPOAEs) were measured using a commercially available system. Following baseline measures, animals were treated with 75 mg/kg of carboplatin (i.p.), a dose shown to produce 50-80% selective IHC loss. Post-carboplatin assessments were performed three weeks post-treatment.

Results and Conclusions: As expected, carboplatin treatment had no effect on DPOAEs, suggesting OHC survival and function. However, contrary to our hypothesis, ARs either remained unchanged or showed increased amplitudes. These results suggest that a robust population of IHCs is not necessary for the AR. The enhancement of the response may suggest lower level compensatory gain or higher order downstream projections from the central auditory system in response to reduced cochlear output following IHC loss. The overall findings of this and subsequent experiments could have a substantial impact on the understanding and clinical interpretation of AR.

PS 970

Age-related cochlear and vestibular pathologies in African vervet monkeys

Dalian Ding¹; Weidong Qi²; Haiyan Jiang¹; Richard Salvi³; Masaru Tanokura⁴; Shinichi Someya⁵

¹*Center for Hearing and Deafness. State University of New York at Buffalo;* ²*Department of Otolaryngology*

Although a variety of experimental animal models such as mice, rats, guinea pigs, and chinchillas have been extensively used to study age-related pathological changes in the inner ear, the anatomical structures of the inner ear in these small animals differ somewhat from humans. In the current study, we investigated age-related hair cell damage in the inner ears of non-human primate African vervet monkeys (*Chlorocebus aethiops sabaeus*) that were housed in the Wake Forest Primate Center. The ages of subjects were 1-8 years (n=3) and 23-26 years (n=4). For quantification of cochlear hair cells, the whole cochlear epithelium was micro-dissected out, stained with hematoxylin and mounted on glass slides as a surface preparation. The cochlear hair cells were counted over the entire length of cochlear basilar membrane and the data used to construct cochleograms. For quantification of vestibular hair cells, the macula of saccule, macula of utricle, and crista ampulla were dissected out and mounted on glass slides for hair cell counting in several small regions in order to obtain hair cell density measurements. No hair cell loss was observed in the cochlea and no change in hair cell densities were observed in the utricle, saccule or crista in young vervet monkeys. However, in old monkeys, approximately 50% of the outer hair cells were missing along the entire length of the cochlear basilar membrane, in contrast to the typical base-to-apex gradient of hair cell loss often seen in rodents. Hair cell densities were reduced approximately 60% in all the vestibular organs. Together, these results suggest that non-human primate vervet monkeys may be a useful experimental model for studies of age-related inner ear pathologies.

PS 971

Novel N-ethyl-N-nitrosourea-induced dominant mutation in the *KIT* gene causes deafness and hypopigmentation in Bama miniature pigs

Cong Xu; Wei Ren; Weiwei Guo; Hui Zhao; Shiming Yang
PLA General Hospital

Background Mutations in *KIT* gene can lead to multiple defects including congenital deafness and hypopigmentation in human beings. In mouse models with *KIT* mutations, similar defects were identified. However mutant mice exhibited progressing hearing loss rather than congenital deafness in humans. Furthermore, huge differences in inner ear development process, morphology and electrophysiology between human and mouse also

limit the application of mice as an ideal deafness model. According to our previous studies, Bama miniature pig is an ideal mammalian model for otologic research. Therefore, N-ethyl-N-nitrosourea (ENU) was used to generate a novel pig model with *KIT* c.2418T>A mutation, resulting in substituting aspartic acid with glutamic acid, exhibiting deafness and hypopigmentation.

Method We performed random mutagenesis of the porcine genome by ENU treatment and a whole genome linkage analysis to identify sites of mutations. Auditory Brain Response (ABR) was measured to evaluate hearing thresholds. Immunofluorescence was performed to locate *kit* protein expression in pig cochlea. Celloidin embedded H&E sections scanning electron microscopy was performed for the morphology of cochlea.

Result We identified and characterized a novel ENU-induced autosomal dominant inheritance model of severe hearing loss and pigmentation abnormalities in the Bama miniature pigs. A whole genome linkage analysis identified that the c.2418T>A mutation in exon 17 of the *KIT* gene resulted in substituting a conserved aspartic acid with glutamic acid (p. D806E), which encodes a class III receptor tyrosine kinase, was linked to deafness and hypopigmentation in a dominant inheritance pattern. Immunofluorescence analysis revealed *KIT* protein expression in the stria vascularis and spiral ganglion of the wild-type pig cochlea. Histological analyses of the *KIT*^{D806E/+} cochlea showed major disruption of the organ of Corti and thinning of stria vascularis. Furthermore, the auditory hair cells were absent or severely diminished and the supporting cells displayed severe abnormalities.

Conclusion *KIT* p. D806E mutations may associate with deafness and hypopigmentation in Bama miniature pigs and might be a candidate gene of human hereditary hearing loss. This *KIT*^{D806E/+} porcine model provides us with a powerful tool for studying the mechanism of *KIT* gene function and developing therapies to combat hereditary hearing loss.

Figure 1

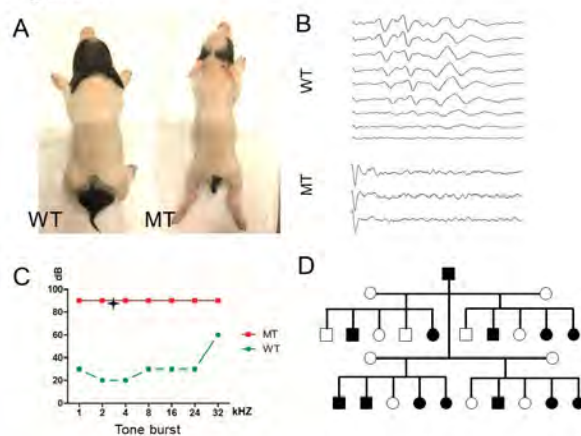


Figure 2

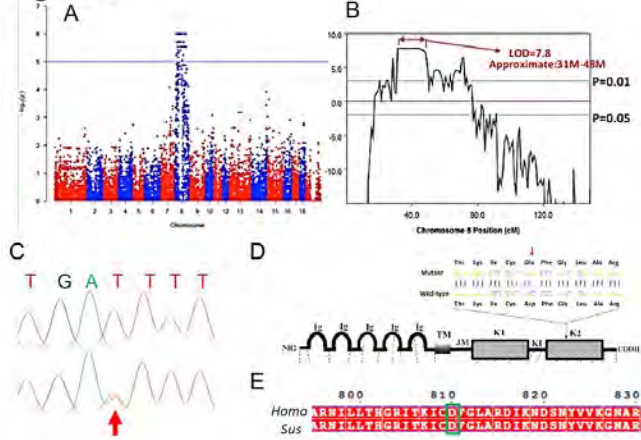


Figure 3

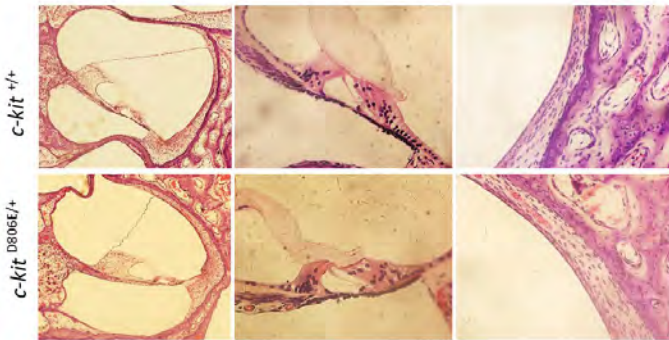


Figure 4

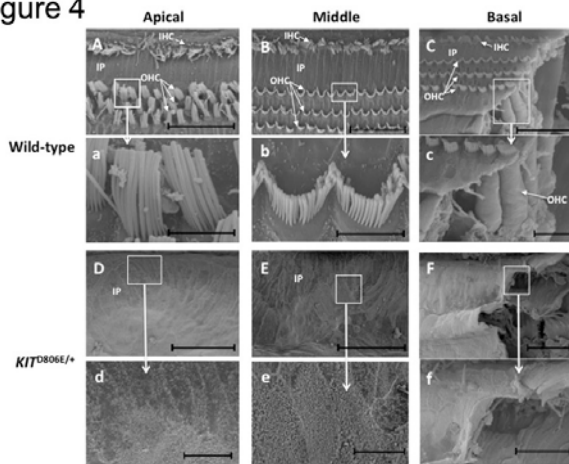
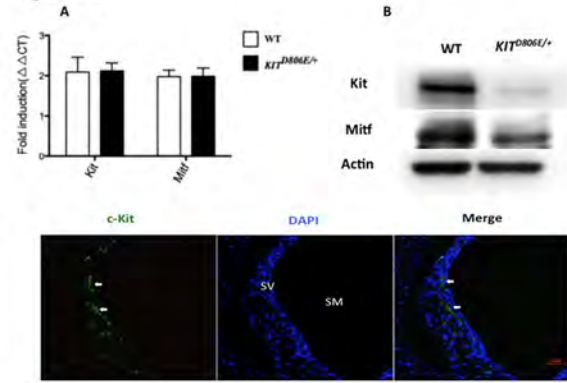


Figure 5



PS 972

Light Sheet Microscopy of the Gerbil Cochlea

Kendall A. Hutson; Caroline Naso; Stephen H. Pulver; Gilberto D. Graña; Douglas C. Fitzpatrick
University of North Carolina at Chapel Hill

Light sheet (LS) microscopy provides a rapid and complete 3D image of the cochlea while its unique structure and anatomical orientation remain intact. Constituents of the basilar membrane and organ of Corti can be fluorescently stained, or antibodies applied to visualize specific elements such as hair cells. Compared to confocal or light microscopy, LS has the advantage of representing the entire cochlea without requiring dissection of the basilar membrane or reconstruction from sectioned material. The LS technique preserves anatomical relationships with the external surface of the cochlea including landmark structures such as the round and oval window. Here, we used anti-Myosin to label hair cells of normal-hearing and kanamycin/furosemide treated gerbil cochleae to trace the cochlear spiral and derive frequency maps that retain these 3D relationships. In addition, we seek to compare the geometrical arrangement of the cochlea with the magnitudes and polarities of the summing potential (SP) recorded from different turns of the cochlea. The expectation is that the 3D frequency organization can provide insights into how physiological responses are affected by the curvature of the cochlea.

Our findings demonstrate that LS material can be used to visualize inner and outer hair cells of gerbils with minimal histological processing. The frequency maps obtained by applying the frequency - distance equation of Müller, 1996 (*Hear Res* 94: 148-156, 1996), were visually and quantitatively indistinguishable from those using whole-mount preparations, but with the added dimension of depth. Cytochleograms obtained from kanamycin/furosemide treated animals were similar to those from whole-mounts of animals receiving the

same ototoxic drug dosages. Furthermore, this material provides the actual (curvilinear), radial (shortest) and angular (degrees) distance between frequencies along the basilar membrane *in situ*. Additionally, the 3D LS material illustrates where frequencies “go around the bend” of the modiulus relative to one-another and relative to the location of a recording electrode. Physiologically, the SP changes in size and polarity as a function of stimulus frequency, intensity and recording location. Recordings from the scala tympani of different turns of the cochlea often show opposite polarities, indicating they are on different sides of the dipole produced by the responding elements. The identification of recording locations and 3D architecture with LS microscopy can help to identify the center of gravity of different sources of the SP, including inner and outer hair cells and the auditory nerve.

PS 973

Navigating the Acoustic Territory of Bald (*Haliaeetus leucocephalus*) and Golden (*Aquila chrysaetos*) Eagles

JoAnn McGee; Peggy B. Nelson; Julia B. Ponder; Jeff Marr; Patrick Redig; Christopher Milliren; Christopher Feist; Andrew Byrne; Edward J. Walsh
University of Minnesota

Although much is known about the basic auditory biology of birds, especially species within the order Passeriformes, very little is known about the auditory biology and vocal attributes of raptors, other than the barn owl, *Tyto alba*. One goal of ongoing work in this area is to mount a framework within which a comparison of the auditory and vocal features of raptors can be made within the broader avian taxonomy. To that end, we report here on the auditory characteristics and the acoustic properties of a subset of calls comprising the vocal repertoire of bald and golden eagles, two iconic representatives of the diurnal raptor community. Using the auditory brainstem response (ABR) to explore the receptive auditory space of each species, we report that threshold-frequency curves overlap extensively and bear a strong resemblance to sensitivity curves of many songbirds. The overall finding from the auditory biology aspect of this investigation is that the best frequency of both species is approximately 2.0 kHz, with thresholds falling off at a rate of approximately 15 dB/octave below best frequency and by approximately 55 dB/octave above best frequency. Latencies and amplitudes of ABR peaks considered as a function of both stimulus level and frequency also overlap extensively. These findings collectively suggest that eagles operate as auditory generalists as a first approximation of their responses to acoustic stimulation. Regarding vocal characteristics, the bulk of acoustic energy carried by a subset of calls

comprising the vocal repertoire of bald eagles falls within the most sensitive band of audible frequencies. Most calls studied as a part of this investigation were tonal in nature, harmonically structured, high pitched and exhibited distinctive nonlinear characteristics. Though relatively simple from a categorical perspective, bald eagle calls varied in complexity within individual callers. Although the availability of golden eagle calls is limited, the acoustic properties of an overlapping collection of call types in both vocal repertoires will be discussed. Generally, findings reported here indicate that both eagle species navigate the same basic acoustic territory and communicate, forage and interact socially using the same essential acoustic bandwidth.

This work was supported by Department of Energy grant #DE-EE0007881.

PS 974

Seasonal Hair-cell Density Changes in Male Plainfin Midshipman: a Teleost Fish with Divergent Reproductive Strategies

Nicholas Lozier; Joseph Sisneros
University of Washington

Unlike mammals, fish add vestibular and auditory hair cells throughout their lifetime. Plainfin midshipman fish (*Porichthys notatus*) offer a unique opportunity to study hair cell turnover because changes in inner ear hair-cell density have been correlated with seasonal enhancement of auditory sensitivity and reproductive-related acoustic communication. In this mating system there are two male sexual phenotypes, referred to as type I and type II males. During the summer mating season, type I males vocalize to attract reproductive females while type II males eavesdrop and employ a sneak spawning strategy to steal fertilizations. Previously, females were shown to undergo reproductive state-dependent increases in hair cell density that were concurrent with enhanced peripheral auditory sensitivity, which likely increases the detection and localization of potential mates. It is unknown if similar reproductive state-dependent changes in hair cell density occur in midshipman males (types I and II) that have divergent mating strategies. Here we sought to quantify hair cell density in the auditory sensory epithelia of non-reproductive type I males in comparison to reproductive females, type I, and type II males. We hypothesized that increased seasonal enhancement in auditory sensitivity is concurrent with increased hair cell density and would likely be adaptive for all three sexual phenotypes. Because a seasonal increase in auditory sensitivity is known to occur in type I males we predict that type I males would also exhibit seasonal increases in inner ear hair-cell density. We stained the inner ear auditory sensory epithelia with phalloidin and counted

hair-cell stereocilia bundles in representative marginal and central regions of the sensory epithelia. Hair cell density was significantly lower in the sensory epithelia of winter, non-reproductive type I males compared to all three summer, reproductive sexual phenotypes. In sum, our results suggest reproductive state-dependent increases in hair cell density occur in all three sexual phenotypes, and that these changes are likely associated with the observed reproductive-state dependent enhancement of auditory sensitivity. Such changes in hair cell density may be adaptive for midshipman to facilitate conspecific detection and localization during the breeding season.

PS 975

Effect of swim bladder removal on auditory lagena sensitivity in the plainfin midshipman fish (*Porichthys notatus*)

Brooke Vetter; Joseph Sisneros
University of Washington

The plainfin midshipman fish (*Porichthys notatus*) is an established neuroethological model for investigating mechanisms of acoustic communication and is an ideal species for studying social acoustic behaviors because the reproductive success of this species is dependent on the production and reception of social acoustic signals. It is thought that plainfin midshipman detect acoustic particle motion using their three otolithic inner ear end organs (sacculle, utricle, and lagena) that act as biological accelerometers. Recent work from our lab demonstrated that midshipman possess intra- and inter- sexual dimorphisms of the swim bladder that likely enhance the detection of sound pressure. The swim bladders of female midshipman have rostral extensions that project close to the inner ear, especially the lagena, while nesting males lack such rostral swim bladder extensions. The presence of the swim bladder extensions in females should enhance sound pressure sensitivity. We tested the hypothesis that the female swim bladder indirectly enhances sound pressure detection of the lagena. Evoked lagena potentials were recorded from reproductive females with intact (control condition) and removed (treated condition) swim bladders. Evoked potentials were recorded from the lagena in control females with intact swim bladders up to 1005 Hz, while lagena potentials were only elicited from treated fish that had swim bladders removed at frequencies up to 505 Hz. Furthermore, females with intact swim bladders had lower thresholds (higher sound pressure sensitivity) than treated females, with control females demonstrating an average threshold that was 6 dB lower at the characteristic frequency (85 Hz) than females without swim bladders. These findings suggest that the midshipman lagena is sensitive to sound pressure indirectly via the rostral swim bladder extensions, which

likely enhance the detection of social acoustic signals.

PS 976

Pig As a Big Animal Model for Hearing Research

Shi-ming Yang
PLA General Hospital

[Introduction] An animal model is critical for clinical research regarding human diseases. As usually, most hearing research were done on the mice and rat and so on as a small animal model. It is necessary to explore a big animal model to better understand the hearing of human being.

[Method] In the present study, we observed the morphology of inner ear of the pig, as well as the electrophysiology and the inner ear development of pigs, while the pig models with genetic hearing loss were set up.

[Results] The pig cochlea provides an excellent model for the human Corti's Organ. We found that the cochlea of pig has three and half turns and the average length of the cochlea is 39 mm, 25% longer than a human cochlea, which is suitable for perfectly implant electrode as the same one using in clinic. The threshold and waveforms of the auditory brainstem response of pigs are mature from birth. We took advantage of a hearing loss model found in Rongchang pigs, studied the spontaneous mutation in a non-regulatory region of melanocyte-specific promoter of microphthalmia-associated transcription factor gene (*Mitf*). The mutation generated a novel repressor and eliminated the expression of *Mitf-m*. It consequently caused the early degeneration of intermediate cells of cochlear stria vascularis and a profound hearing loss, the typical phenotype of Waardenburg syndrome in humans. Our results demonstrated the sole dysfunction of *Mitf-m* isoform sufficiently causes deafness and depigmentation in pigs. The study provides the first evidence of systemic functional *de novo* enhancer in mammal. Moreover, the hiPS cells with a green fluorescent protein reporter were surgically injected into the scala tympani through the round window and then electrode array was inserted into the cochlea of Rongchang pigs. The results from the Rongchang pig model provided the first evidence that electrical stimuli can guide hiPS cell migration and improve the function of cochlear implants in pigs. Furthermore, we report that the pilot study of large-scale production of SOX10 mutant causes inner ear malformation in pigs by ENU mutagenesis.

[Conclusion] Taking together, our studies have established the pig models as an ideal big animal model for hearing researches.

PS 977

Partial Loss of Cx26 Reduces Endocochlear Potential (EP) but Shows Normal Hearing

Shu Fang; Yan Zhu; Jin Chen; Chun Liang; Hong-Bo Zhao

Dept. of Otolaryngology, University of Kentucky Medical Center, Lexington, KY 40536

Background: Cx26 (*GJB2*) mutations are responsible for >50% of nonsyndromic hearing loss; most deafness mutations are autosomal recessive deafness mutations, which can affect as many as 3 of every 1,000 babies. The frequency of carriers with heterozygous mutations is even higher. In the clinic, these heterozygous-mutation carriers usually show normal hearing. However, the underlying mechanisms for maintaining normal hearing and potential susceptibility to hearing-damaging factors, such as noise, in these heterozygous mutation carriers remain unclear. In this study, we investigated mechanisms underlying normal hearing in these heterozygous mutation carriers by using heterozygous Cx26 deletion mice.

Methods: As described in our previous studies, Cx26 conditional knockout (cKO) mice, which were created by a Cre-FloxP technique, were used. ABR threshold, DPOAE, EP, and cochlear microphonics (CM) were recorded to assess cochlear and hearing function. Cx26 expression in the cochlea was quantitatively examined by immunofluorescent staining.

Results & Discussion: As reported in previous studies, homozygous Cx26 cKO mice with Cx26 completely deleted in the cochlea had severe hearing loss. However, as demonstrated by heterozygous Cx26 mutation carriers in the clinic, heterozygous Cx26 cKO mice demonstrated normal hearing as measured by ABR threshold. However, EP in Cx26 heterozygous deletion mice was significantly reduced. Immunofluorescent staining also showed that Cx26 expression in the cochlea in the heterozygous Cx26 cKO mice was almost reduced to the half level of WT mice. Our previous studies demonstrated that connexin gap junctions in cochlear supporting cells are required for active cochlear amplification, even though hair cells have no connexin gap junctional expression (Yu and Zhao, 2009; Zhu et al., 2013; Zong et al., 2017). Deletion of Cx26 can reduce DPOAE, i.e., active cochlear amplification, leading to late-onset hearing loss (Zhu et al., 2013, 2015). In this study, we found that unlike homozygous Cx26 deletion mice, DPOAE in heterozygous Cx26 cKO mice was not decreased in comparison with that in WT mice, suggesting that active cochlear amplification in the heterozygous Cx26 cKO mice was not reduced, even the driving force EP was reduced.

Conclusions: These data may reveal a mechanism underlying normal hearing in heterozygous Cx26 cKO

mice and heterozygous mutation carriers; heterozygous Cx26 deletion may retain active cochlear amplifying normally to maintain normal hearing even the driving force EP is reduced.

Supported by NIH R56 DC 015019 and R01 DC 017025

PS 978

Paired Measurements of Cochlear Function and Structure in Dutch-Belted Rabbits with Noise-Induced Hearing Loss

Hariprakash Haragopal¹; Holly Johnson²; Soichi Tanda²; Mark Berryman²; Mitchell Day²

¹Department of Biological Sciences; ²Ohio University

Physiological measures of cochlear function, such as auditory brainstem responses (ABRs) or distortion product otoacoustic emissions (DPOAEs), are useful for assessing hearing loss. Inferring structural damage to the cochlea, such as loss of hair cells, from physiological measures requires paired measurements of the two. Here, we directly compared per cent cochlear inner and outer hair cell (IHC and OHC, respectively) survival to thresholds of ABRs and DPOAEs in Dutch-belted rabbits (a strain used in central auditory studies) following noise overexposure. In order to induce sensorineural hearing loss, we bilaterally exposed anesthetized rabbits to uncorrelated, octave-band noises centered on 750 Hz and presented at 133 dB SPL for either 60 or 90 min. Click-evoked and frequency-specific ABRs were measured before and 2 weeks after exposure. Click-evoked ABR threshold shifts were, on average, 10 and 52.5 dB for noise durations of 60 and 90 min, respectively. For male and female rabbits exposed over a 90-min duration, pre- and post-exposure DPOAEs were additionally measured, then rabbits were sacrificed for cochlear histological processing. Threshold shifts were strikingly different between males and females for both ABRs and DPOAEs: those of females clustered at relatively high levels, whereas those of males had a broad range that overlapped with the female range but spread down to as low as 5 dB (ABR) or -6 dB (DPOAE). Cochlear sections were stained with a hair cell-specific fluorescent marker and hair cells were counted using a confocal microscope. Each cochlear frequency location of each overexposed cochlea fell into one of three categories: majority survival of both IHCs and OHCs; majority survival of IHCs, but near or total wipe-out of OHCs; or near or total wipe-out of both IHCs and OHCs. OHC survival could be predicted, equally well, from either ABR or DPOAE threshold shifts and followed a step function: majority survival switched to near or total wipe-out above critical threshold shifts of 40 dB for ABR and 20 dB for DPOAE. IHC survival also began to decrease above the same critical threshold shifts, but was highly variable within a range from 0 to 100% survival. In summary, we

found: 1) male rabbits were, on average, less susceptible to noise overexposure; 2) OHCs were more susceptible to overexposure than IHCs; and 3) majority survival or wipe-out of OHCs could be directly predicted from either ABR or DPOAE threshold shifts.

PS 979

Rapid Mitochondrial Calcium Uptake is Critical for Hearing Preservation in Mice

Manikandan Mayakannan¹; Steven Walker¹; Aditi Deshmukh¹; Elizabeth Perea¹; Danqi Wang²; Kumar N. Alagramam¹; Ruben Stepanyan¹

¹Department of Otolaryngology, University Hospitals Cleveland Medical Center, School of Medicine, Case Western Reserve University; ²Swagelok Center for Surface Analysis of Materials, Case Western Reserve University

Deflections of hair cell stereocilia lead to the opening of mechanotransduction cation-permeable channels with high selectivity for Ca²⁺. To balance Ca²⁺ influx during stimulation, stereocilia possess plasma membrane Ca²⁺ ATPase (PMCA) pumps and Ca²⁺-binding proteins. Mitochondrial Ca²⁺ uptake also contributes to clearing Ca²⁺ inflowing from stimulated stereocilia, which is consistent with densely localized mitochondria arranged in a belt beneath the cuticular plate structure supporting the stereocilia. Apart from acting as large-capacity calcium stores, mitochondria also fuel PMCA pumps by elevating production of adenosine 5'-triphosphate (ATP), thereby reinstating Ca²⁺ balance. Mitochondria may be thrust to play a more prominent role in Ca²⁺ removal in basal, high frequency, outer hair cells (OHCs) during stimulation, since the basal OHCs have larger mechanotransduction currents but shorter and thinner stereocilia with fewer PMCA pumps. Therefore, we investigated the effect of rapid mitochondrial Ca²⁺ uptake on Ca²⁺ homeostasis within the hair cells, and the cochlear function in general, by utilizing an FVB/NJ mouse line-based model with mitochondria that lack an apparent capacity to rapidly uptake Ca²⁺. In these mice, we observed an initial high frequency hearing loss at one month of age, which progressed to profound deafness in about 6 months. In young postnatal mice, which lack rapid mitochondrial Ca²⁺ uptake, gross cochlear morphology, as well as hair cell Ca²⁺ levels, mitochondrial superoxide levels, and the number of developed inner hair cell (IHC) ribbon synapses were not altered. At three months of age, a significant loss of OHC bundles was observed in these mice, and IHC stereocilia started to show early signs of degeneration. In conclusion, mitochondrial Ca²⁺ uptake is not required for the normal development of cochlea but is likely necessary for hair cell preservation and hearing maintenance.

Supported by NIDCD grant DC015016 (R. S.) and by the Center for Clinical Research and Technology at University Hospitals Cleveland Medical Center (R. S.)

PS 980

Evaluation of Human and Computer-assisted Quantification of Hair Cells in Full-length Cochlea

Leandro Almeida¹; Sylvain Berlemont¹; Susanna Malmström²; Sylvie Cosnier-Pucheu²

¹Keeneye; ²Cilcare

Approximately 15% of the worldwide population suffers from hearing disorders, which can be due to many different factors (acoustic trauma, aging, drug toxicity...). Histological techniques to quantify cochlear hair cell number, in association with auditory function, are commonly used to evaluate the efficacy of drug candidates involved in hearing protection and recovery. The results are most commonly presented in a cochleogram. The detection, and counting procedure requires much attention and expertise, in addition to the time spent. The objective of this study was to develop and validate software to detect and count live inner and outer hair cells in fluorescent images of whole cochleae. Furthermore to parametrize the results automatically in a cochleogram.

Method

The entire membranous and sensory Sylvain spiral containing the organ of Corti was dissected out as half-turns from decalcified cochleae, as a flat surface preparation. The hair cells in each fragment were immunolabeled for anti-Myosin-VIIa. The fragments were then mounted on a microscope slide and images acquired on a confocal microscope. A group of 3 expert users manually counted blindly all hair cells in 6 rat cochleae (~4000 cells/cochlea), three controls and three treated with cisplatin. A deep learning algorithm was developed and used for the detection and counting of hair cells in three dimensional fluorescent image stacks of the whole cochlea. The images were then grouped together from apex to base, to create a cochleogram of hair cell density.

Results

With the fully automated detection and counting software we achieved an average precision rate of 79.8%, defined by area under the recall and precision curve. This is in tune with the variability of 18.3±0.6% observed in the user data set. Optimizing the rates of the algorithms leads to a sensitivity of 78.8% and a precision of 88.2%. We also computed the detection and metrics along the length of the fragments providing an average precision cochleogram.

Conclusion

This new software validated in rat cochleae permits to obtain semi-automatically and rapidly a cochleogram of cell density.

Effect of Increased Outer Hair Cell Infection and Whirlin Long Isoform in Whirlin Mutant Mice

Kevin Isgrig¹; Jianliang Zhu²; Claire Cheng²; Hannah Goldberg³; Inna A. Belyantseva²; Thomas B. Friedman⁴; Lisa Cunningham⁵; Gwenaelle S. Geleoc³; Wade W. Chien¹

¹NIDCD, Johns Hopkins University; ²NIDCD; ³Boston Children's Hospital, Harvard Medical School; ⁴Laboratory of Molecular Genetics, National Institute on Deafness and Other Communication Disorders; ⁵National Institute on Deafness and Other Communication Disorders, National Institutes of Health

Background: In a previous study, we reported that when AAV8 carrying the cDNA sequence for the long whirlin isoform (AAV8-whirlin) was injected locally into the whirler (*Whrn^{wi/wi}*) mutant mouse ear *in vivo*, auditory function was improved. However, the hearing recovery was incomplete. In this study, we explore whether increased outer hair cell (OHC) transduction and the presence of both long and short whirlin isoforms would further improve auditory function in whirlin mutant mice.

Methods: Neonatal (P0-P5) mice were used in this study. To increase OHC infection, Anc80L65 carrying the long whirlin isoform (Anc80-whirlin) was delivered to whirler (*Whrn^{wi/wi}*) mutant mice via posterior canal injection. To assess the effect of whirlin isoforms, AAV8 carrying the long whirlin isoform (AAV8-whirlin) was delivered to the *Whrn^{tm1b}* mutant mouse, which lacks the long whirlin isoform but expresses the short whirlin isoform. Hearing outcome was assessed using auditory brainstem responses (ABR).

Results: Delivery of Anc80-whirlin to neonatal *Whrn^{wi/wi}* mutant mice resulted in increased outer hair cell infection compared to AAV8-whirlin. Infected *Whrn^{wi/wi}* hair cells have increased stereocilia length, comparable to what has been reported with AAV8-whirlin. However, improvement in ABR thresholds in *Whrn^{wi/wi}* mutant was incomplete with Anc80-whirlin, similar to what was observed with AAV8-whirlin. When AAV8-whirlin was injected into neonatal *Whrn^{tm1b}* mutant mice, the ABR thresholds were initially similar to non-injected *Whrn^{tm1b}* mutant mice at P30. However, injected *Whrn^{tm1b}* mutant mice had longer hearing preservation compared to non-injected *Whrn^{tm1b}* mutant mice over time.

Conclusions: In *Whrn^{wi/wi}* mutant mice, increased OHC infection by Anc80-whirlin did not result in improved hearing recovery compared to AAV8-whirlin. In *Whrn^{tm1b}* mutant mice, delivery of the AAV8-whirlin long isoform cDNA resulted in prolonged hearing preservation compared to non-injected *Whrn^{tm1b}* mutant mice.

Inner Ear: Innervation & Synaptic Transmission

PS 982

Inactivating Kv Currents in Type II Hair Cells of the Mouse Utricle

Vicente Lumbreras¹; Anna Lysakowski²; Ruth Anne Eatock¹

¹University of Chicago; ²University of Illinois at Chicago

Vestibular type II hair cells have large outwardly rectifying K⁺ conductances that are activated by depolarizing receptor potentials and repolarize the hair cell, contributing to sensory adaptation. Their molecular composition is not fully known despite their prominent effect on the receptor potential. K_V1 voltage-gated potassium channels have the appropriate voltage dependence and are expressed in vestibular hair cells (Scheffer et al., J Neurosci 35:6366, 2015; Correia et al., Neuroscience 152:809, 2008). Here we investigate K_V1 contributions in mouse type II hair cells with the Kv1-selective channel blocker, α-dendrotoxin (αDTX). We recorded whole-cell voltage-dependent currents from type II hair cells in semi-intact preparations of the mouse utricle (postnatal days 5-12). Recorded cells were mapped to central (striolar) or peripheral (extrastriolar, ES) epithelial zones, which have more adapting and more tonic afferent response dynamics, respectively. Recording solutions were L-15 medium (bath) and KCl-based (pipette) at room temperature. Holding potential was -64 mV, similar to average resting potential. Following 100-ms prepulses to -124 mV, 400-ms depolarizing steps evoked outward current with sustained (I_{SS}) and inactivating (I_A) components. I_A activated at substantially more positive voltages (V_{1/2} -8 mV (48 cells)) than I_{SS} (V_{1/2} -22 mV (56), p<0.0001). I_A inactivation was usually monoexponential in striola (11/14 cells, τ = 124±8 ms), and usually double-exponential in ES (29/39 cells; τ's of 19±1 ms and 177±16 ms) with a dominant slow component (23/29 cells). Because of the additional fast component, ES I_A inactivated more than striolar I_A (47±2% vs. 31±3%, p=0.0004). The prominent inactivation in ES type II cells affects voltage responses to injected currents and may reduce sensory adaptation and nonlinear rectification of ES afferent firing. 10-100 nM αDTX blocked I_A more than I_{SS}. The half-blocking dose for I_A is consistent with certain Kv1 channels (K_D 1-25 nM) (Alexander et al., Br J Pharmacol 172:5904, 2015), including Kv1.1, which is strongly expressed by mouse utricular hair cells (Scheffer et al. 2015). Homomeric Kv1.1 channels do not inactivate, however; Kv1 channel inactivation is mediated by Kv1.4 α subunits. Kv1.4 is strongly expressed in mouse and pigeon vestibular hair cells (Scheffer et al. 2015; Correia et al. 2008). We report Kv1.4-like immunoreactivity in adult rat utricle that is consistent

with a role for Kv1.4 in type II cells. Thus, I_A in mouse utricular type II hair cells may flow through heteromeric Kv1 channels comprising Kv1.1 and Kv1.4 subunits. Funding: NIDCD R01DC012347

PS 983

Pou3f4 In Otic Mesenchyme Regulates Spiral Ganglion Neuron Innervation Patterns In The Mammalian Cochlea

Mansa Gurjar; Vinodh Balendran; Maeher Grewal; Thomas M. Coate
Georgetown University

Precise synapse formation between spiral ganglion neurons (SGNs) and sensory hair cells during cochlear development is essential for normal hearing function. Determining the molecular basis of cochlear innervation may aid in the development of therapeutics for people with sensorineural hearing loss. Our present studies focus on how otic mesenchyme cells regulate this process by influencing SGN peripheral axon guidance and ribbon synapse maturation. Loss-of-function mutations in the Pitt-Oct-Unc (POU)-domain transcription factor *Pou3f4* on the X-chromosome are an underlying cause of X-linked nonsyndromic hearing loss (DFNX2). Our model suggests that *Pou3f4*, which is specifically expressed by otic mesenchyme cells, controls the expression levels of various Ephs and Ephrins as part of SGN axon guidance. I will discuss our preliminary findings on how *Pou3f4* normally inhibits *Efna1* (Ephrin-A1) and *Efna2* (Ephrin-A2) ligand expression. Preliminarily, chromatin immunoprecipitation assays show *Pou3f4* protein is associated with *Efna1* and *Efna2*, and that Ephrin-A1 and Ephrin-A2 attract growing SGN processes in *in vitro* culture assays. Additionally, RNAScope assays show *Efna1* and *Efna2* mRNA are normally expressed in otic mesenchyme cells (like *Pou3f4*), as well as other cell types in the cochlea at E15. Our initial analysis of *Efna1* knockout tissue shows that cochleae lacking Ephrin-A1 have impaired axon outgrowth when compared to WT littermate controls. *Efna1* knockout cochleae also show a slight delay in prosensory domain development, so Ephrin-A1 may also be involved in additional aspects of cochlear development. I will further discuss our ideas for future work to evaluate hearing related phenotypes associated with the loss of *Efna1* and *Efna2* and investigate their Eph receptor binding partners on SGNs.

PS 984

Is Cochlear Innervation Altered in the Absence of TRPA1 channels?

Sara J. Torres-Gallego; **Kasey Schock**; Gregory I. Frolenkov; A. Catalina Vélez-Ortega
Department of Physiology, University of Kentucky

TRPA1 channels are highly expressed in somatosensory nociceptive neurons and in the cochlea. In the former, TRPA1 channels are essential for nociceptive responses and inflammatory pain. In the latter, their function remains unknown given that mice lacking functional TRPA1 channels (*Trpa1*^{-/-}) exhibit normal hearing thresholds, vestibular function and hair cell mechanotransduction (Bautista, *et al.*, PNAS, 2006; Kwan, *et al.*, Neuron, 2006). However, analysis of the waveform of auditory brainstem responses (ABR) to supra-threshold click stimuli revealed statistically significant larger Wave I amplitudes (generated by the activity of the auditory nerve) and smaller Wave V amplitudes (generated by the activity from higher levels of the auditory brainstem) in *Trpa1*^{-/-} mice than in wild type controls.

Ratiometric calcium imaging of early postnatal cochlear explants showed long-lasting calcium responses to the local delivery of TRPA1 agonists in Hensen's cells. These responses often propagated to the Kolliker's organ where they could trigger the previously-described self-propagating ATP-dependent calcium waves. These ATP-dependent calcium waves in the Kolliker's organ occur spontaneously before the onset of hearing and are believed to be crucial for the proper wiring of auditory nerve pathways (Tritsch, *et al.*, Nature, 2007). Therefore, we wondered whether the absence of TRPA1 channels could lead to deficits in cochlear innervation that could explain the differences we found in the ABR waveforms to the supra-threshold stimuli.

To evaluate cochlear innervation patterns in the adult cochlea we (i) performed immunolabeling against CtBP2/RIBEYE to quantify synaptic ribbons and (ii) are using antibodies against tyrosine hydroxylase to selectively label type II spiral ganglion neurons. Our results show no differences in inner hair cell synaptic ribbons between *Trpa1*^{-/-} mice and wild type controls. However, our ongoing analysis of the type II afferent fibers indicates abnormalities in *Trpa1*^{-/-} mice.

We conclude that TRPA1 channels may play a role in the early development and/or refinement of cochlear innervation and, in particular, of the type II spiral ganglion neurons.

Supported by NIDCD/NIH R01DC014658 to G.I.F, and by the Hearing Health Foundation 2018 ERG to A.C.V.

PS 985

A New Category of Hidden-Hearing Loss in Humans with Blast-Induced Tinnitus

Anthony T. Cacace; John L. Woodard
Wayne State University

The term “hidden hearing loss” is described when normal hearing sensitivity is manifest in the context of normal sensory cell populations typically measured functionally via transient evoked or distortion product otoacoustic emissions (TEOAEs or DPOAEs), combined with a reduced number of ribbon synapses and abnormal nerve fiber counts. Additionally, if experimental testing is performed before and after a noise-trauma study, then the amplitude of Wave I of the auditory brainstem response or the amplitude N1 wave of the compound action potential using electrocochleography is used to help validate this effect. With these measures, the post-test response amplitude is diminished in comparison to the pre-test condition. It is also noteworthy that the “hidden hearing loss” phenomenon has primarily been confirmed behaviorally, physiologically, and histopathologically in animal experiments, but not in humans.

Recently, in a sample of 22 adults with BINT, approximately 30% of the ears had normal hearing sensitivity measured by pure tones in the standard frequency range (0.25-8.0 kHz), 54% had mild-to-profound high-frequency sensorineural hearing loss (SNHL), 7% had moderate-to-moderately severe flat SNHL, 2% had classic reverse slope SNHL (i.e., where hearing loss is worse in the low frequencies (1 kHz) and normal in the higher frequency range (>2-8 kHz), and 7% had reverse slope hearing loss with concurrent moderate-to-severe high-frequency SNHL.

In this sample, the normal hearing group can be broken down into two specific categories: **1)** those ears with normal hearing sensitivity (0.25-8.0 kHz) with normal DPOAEs, as would be expected (having DPs above the noise floor over the entire measurement bandwidth (0.842-7.996 kHz); and **2)** those ears with normal hearing sensitivity (0.25-8.0 kHz) with various degrees of DPOAE anomalies in the higher frequency range. In the latter group, this effect was overtly obvious and contrary to theoretical and practical expectations.

Implicit in the original description of hidden hearing loss was the presence of normal sensory cell integrity. This new category shows that hidden hearing loss can occur when a valid biomarker of outer hair cell function is distinctly abnormal, particularly in the presence of normal middle-ear function. These effects were not acute findings and were found in males ranging in age from 29-58 years. Herein, we will describe these anomalies and attempt to account for their expression.

Supported by DoD Grant W81XWH-11-2-0031 to (AT Cacace, Humans; J-S. Zhang, Animals).

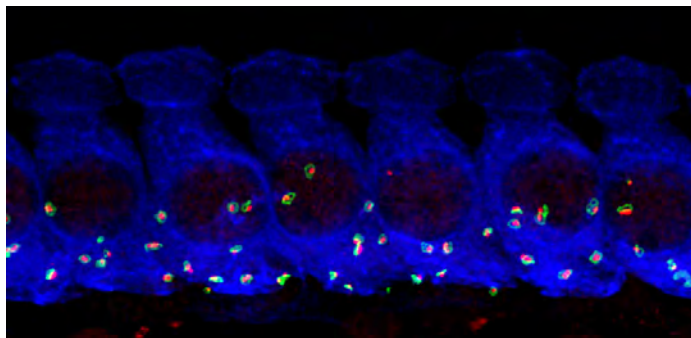
PS 986

Ribbon Synapse Morphology Before and After Noise Exposure in Vglut3 WT and KO IHCs: Glutamate-dependent and Glutamate-independent Effects

Jay Gantz; Jason Carlquist; Babak V-Ghaffari; Kyunghee Kim; Mark A. Rutherford
Washington University in St. Louis

Glutamate is required for synaptic transmission and is the driver of noise-induced excitotoxicity at synapses between cochlear inner hair cells (IHCs) and auditory nerve fibers (ANFs). The effects of glutamate deprivation or glutamate overexposure on synapse morphology are unclear. Therefore, we used vesicular glutamate transporter-3 (Vglut3) mice to examine how the presence or absence of vesicular glutamatergic transmission affected the morphology of IHC-ANF synapses in unexposed or noise-exposed mice aged 9-11 weeks. Methods: Cochlea from WT or Vglut3 KO mice were imaged either before or two weeks after 2 hours of 100 dB, 8–16 kHz noise exposure. We developed a reproducible, high-throughput, semi-autonomous workflow to measure the 3D morphology of presynaptic ribbons (anti-CtBP2) and postsynaptic AMPA receptors (anti-GluA3) using confocal microscopy immunohistofluorescence. Synapse location on the modiolar-pillar and habenular-cuticular axes was also measured. We used Imaris image processing software to define synapses as surface objects, and Matlab custom procedures to pair presynaptic ribbons with postsynaptic GluA3 clusters, as well as to remove unpaired or erroneously paired objects. Control experiments determined the range of microscope settings over which object volume estimates were reproducible and robust for between-group comparisons. Results: Genotype – Ribbons and GluA3 clusters were fewer and larger in Vglut3 KO synapses than WT synapses in apical-, mid-cochlear, and basal regions in unexposed or exposed mice. Noise, ribbons – Two weeks after noise exposure in WT, mid-cochlear ribbons were fewer in number and larger than unexposed ribbons. Surprisingly, although KO ribbons were unchanged in number after noise exposure, they were larger than unexposed ribbons in the mid-cochlear region. Noise, AMPARs – In WT and KO, GluA3 clusters tended to be larger after exposure but the effect was smaller and less robust than for ribbons. Tonotopy – In unexposed WT and KO, apical ribbons were larger and fewer than midcochlear ribbons. Position – In WT but not in KO, ribbons and GluA3 clusters were significantly larger on the modiolar side than the pillar side of the IHC. After noise exposure in WT, the midcochlear modiolar-pillar volume gradients were diminished. Conclusions:

1) Vesicular glutamatergic transmission has a significant effect on synapse morphology in unexposed mice and on changes in morphology after noise exposure. 2) In general, when synapses were fewer in number they tended to also be larger (comparing KO vs WT, exposed vs unexposed, apical vs mid-cochlear). 3) Changes in ribbon volume after noise exposure in the KO suggest a mechanism of glutamate-independent synaptic plasticity.



PS 987

Auditory neurons' biophysical properties are correlated with their terminal position along the base of the inner hair cell.

Alexander Markowitz¹; Radha Kalluri²

¹Neuroscience Graduate Program; ²Department of Otolaryngology

The auditory nerve consists of subclasses of type I spiral ganglion neurons (SGN) that differ in their spontaneous discharge rate, threshold, and dynamic range. Additionally, their morphologies differ by synaptic location: high-threshold SGN fibers terminate primarily on the modiolar-side of the inner hair cell, while low-threshold SGN fibers terminate primarily on the pillar-side of the inner hair cell. The mechanisms differentiating the *in vivo* responses of SGN subclasses remain unclear and are of interest due to high-threshold SGN exhibiting higher susceptibility to degeneration via noise-induced synaptopathy. Previous studies have shown that the biophysical properties of SGN are heterogeneous, but have not linked specific biophysical phenotypes to individual SGN subclasses. Our goal is to test whether the biophysical properties of SGN correlate with the spatial position of SGN terminals on inner hair cells.

Our approach takes advantage of the *in situ* organization of the SGN subclasses by using acute semi-intact preparations of rat cochleae (P1-P16), where the somata, afferent fibers, and spatial organization with hair cells remain intact. We performed simultaneous patch-clamp recordings and single-cell labelling to record the biophysical properties of neurons and classify each neuron's morphology. The morphology was classified

using a two-tier system. First, we identified which side of the inner hair cell the afferent fiber contacts using a bimodal scale (modiolar versus pillar). Then, we measured where the contact was made along the length of the inner hair cell from the basal pole to the cuticular plate. The addition of the more resolved spatial axis under the inner hair cell provides a continuous axis against which we mapped the biophysical properties of SGN.

We measured multiple parameters from each SGN in current- and voltage-clamp modes. These included resting potential, current thresholds and outward current magnitudes. In a multi-variate linear regression model, we show that the biophysical properties of SGN are significantly correlated with their synaptic position along the base of the inner hair cell ($r^2 = 0.61$, RMSE = 0.15, $p=0.001$). These data are the first to show a link between cellular biophysics and previously described SGN subclasses. We will discuss the implications of these findings in relation to the so-called "in vivo spontaneous-rate classes"; that are believed to be important for intensity coding.

PS 988

A vestibular ganglion model examines the role of KCNQ and HCN channels on spike-timing regularity

Christopher Ventura¹; Radha Kalluri²

¹Neuroscience Graduate Program; ²Department of Otolaryngology

Variability in spike-timing regularity is a hallmark feature used to classify vestibular ganglion neurons (VGN). Differences in regularity reflect the type of information encoded by these neurons, yet the origins of regularity are not fully understood. Recent recordings from the terminals of vestibular neurons suggest that hyperpolarization-activated mixed-cationic current (I_H), may be needed for highly regular firing. However, we have shown that activating the I_H current is insufficient to produce highly regular firing in disassociated VGN *in vitro*. We suggest that this is caused by an interaction between I_H and low-voltage-gated potassium currents (I_{KL}), which we believe become ubiquitously upregulated in all VGN over development. Using a single compartment vestibular neuron model, we show that activating I_H in the presence of I_{KL} recruits larger I_{KL} and drives spiking toward irregularity. I_H has a significant impact on spike-timing regularity only when I_{KL} is small or not present. Based on these results we hypothesize that in some neurons highly regular firing will require a simultaneous reduction in the size of I_K and activation of I_H . This hypothesis is appealing because a portion of the I_{KL} current is carried by KCNQ channels which can be closed by activating mAChRs, facilitating a reduction in overall I_{KL} . For this to be possible, KCNQ components must be dominant in a sub-group of VGN. Ongoing work will test for this sub-

population amongst VGN.

PS 989

Dopaminergic and Cholinergic Regulation of Afferent Neuron Activity During Motor Behaviors in the Lateral Line System of Larval Zebrafish

James C. Liao¹; Elias T. Lunsford²; Dimitri A. Skandalis²

¹*The Whitney Laboratory for Marine Bioscience;*

²*University of Florida/The Whitney Lab for Marine Bioscience*

In zebrafish, modulation of lateral line activity is thought to occur during swimming through the activity of efferent neurons. Here, we investigate how dopaminergic and cholinergic efferent neurons regulate spontaneous afferent neuron activity during motor behaviors in 4-6 day post fertilization larval zebrafish. Simultaneous afferent neuron and ventral motor root recordings using the DRD1 dopamine antagonist SCH-23390 revealed no change in spontaneous afferent spike activity during fictive swimming. We next turned on dopaminergic efferent neurons using 470nm pulses of light in Tg(DAT:ChR2) fish while simultaneously recording from afferent neurons. Our results showed that, consistent with our pharmacological results, dopaminergic activity does not influence spontaneous afferent spike activity. However, in a small subset of recordings, putative afferent activity increased during swimming, was tightly locked to blue light pulses, and degraded over multiple pulses. This suggested that in rare cases dopaminergic efferents can increase the spiking rate of afferents. To look at population level activity in cholinergic efferents located in one side of the hindbrain, we backfilled neuromasts in GcAMP6s fish to be able to monitor calcium activity (typically four to six labelled somata). We hypothesized that left- and right-populations of cholinergic efferents would be active in antiphase, corresponding to swimming phase. Instead, we observed that all efferents were active throughout the motor event, suggesting that afferent activity is broadly attenuated without regard to swimming phase or neuromast location. We next photo ablated the efferents using 30 second near-UV confocal laser pulses, then recorded spontaneous afferent spiking activity. Both control and sham-operated fish exhibited suppression of afferent activity during fictive swim events, but firing rates of photo ablated fish during swims were indistinguishable from firing rates in an equivalent period prior. Thus cholinergic hindbrain efferents are sufficient for the observed suppression of afferent activity during swims, and coarsely suppress all afferents rather than selectively tuning responses.

Suppression of afferent neuron spike rate has been shown to occur during motor behaviors through the

activity of efferent neurons. Two efferent neurotransmitter phenotypes, dopaminergic and cholinergic, are thought to play roles in modulating the sensitivity of the lateral line system in zebrafish. We investigated the contributions of dopaminergic and cholinergic efferent neurons in regulating the activity of the afferent neurons in 4-6 day post fertilization larval zebrafish. Simultaneous afferent neuron and ventral motor root recordings using the DRD1 dopamine antagonist SCH-23390 revealed no change in spontaneous afferent spike activity during fictive swimming. We next turned on dopaminergic efferent neurons using 470nm pulses of light in Tg(DAT:ChR2) fish while simultaneously recording from afferent neurons. Our results showed that, consistent with our pharmacological results, dopaminergic activity does not influence spontaneous afferent spike activity. However, in a small subset of recordings, putative afferent activity increased during swimming, was tightly locked to blue light pulses, and degraded over multiple pulses. This suggested that in rare cases dopaminergic efferents can increase the spiking rate of afferents. To look at population level activity in cholinergic efferents located in one side of the hindbrain, we backfilled neuromasts in GcAMP6s fish to be able to monitor calcium activity (typically four to six labelled somata). We hypothesized that left- and right-populations of cholinergic efferents would be active in antiphase, corresponding to swimming phase. Instead, we observed that all efferents were active throughout the motor event, suggesting that afferent activity is broadly attenuated without regard to swimming phase or neuromast location. We next photo ablated the efferents using 30 second near-UV confocal laser pulses, then recorded spontaneous afferent spiking activity. Both control and sham-operated fish exhibited suppression of afferent activity during fictive swim events, but firing rates of photo ablated fish during swims were indistinguishable from firing rates in an equivalent period prior. Thus cholinergic hindbrain efferents are sufficient for the observed suppression of afferent activity during swims, and coarsely suppress all afferents rather than selectively tuning responses.

PS 990

The Role of D1-like and D2-like Dopamine Receptors in Lateral Olivocochlear Efferent Function

Jingjing Sherry Wu¹; **Marco Manca**²; Kushal Sharma³; Eunyoung Yi³; Elisabeth Glowatzki⁴

¹*Harvard Medical School;* ²*Johns Hopkins University School of Medicine;* ³*Mokpo National University;*

⁴*Johns Hopkins University*

In the cochlea, dopamine (DA) is released from lateral olivocochlear (LOC) efferents that innervate the dendrites of type I auditory nerve fibers (ANFs). Using RT-PCR

and genetic deletion of dopamine receptors, Maison *et al.* 2012 characterized expression patterns and knock-out phenotypes of specific dopamine receptor subtypes. These data suggest that D1-like and D2-like DA receptors play an important role in lateral efferent function and are possibly involved in protection of the hair cell afferent synapses from noise exposure.

To further understand the effects of dopaminergic LOC input in the cochlea, we investigated the effects of D1-like and D2-like receptor agonists on ANF firing, using whole-cell or extracellular loose patch recordings in excised cochlear tissue (Wu *et al.*, 2016). Secondly, utilizing several transgenic reporter mouse lines for D1-like and D2-like receptors, we further confirmed the expression pattern of dopamine receptors in the cochlea. Finally, we examined the expression of other molecular components involved in DA signaling in the cochlea.

Type I ANF recordings in 3-4 week old rats demonstrate that DA reduces the spontaneous firing in a dose-dependent fashion. Preliminary results show that D2-like receptors agonists elicited a stronger effect reduction of ANF firing compared to D1-like receptor agonists. In *Drd1-TdTomato* mice, expression of D1-like receptors is found in most if not all type I ANFs, whereas in *Drd2-Cre* mice, D2 receptor are found to be expressed in the dopaminergic LOC efferents. These results are consistent with previous immunostaining results by Maison *et al.* 2012. Finally, immunostaining against the vesicular monoamine transporter 2 (VMAT2) shows dense labeling in the inner spiral bundle region, further supporting the idea that dopamine is released from the lateral efferent terminals.

This work was supported by NIDCD grants R01DC006476 and R01DC012957 to EG and by a grant of the Korea Health Technology R&D Project, Republic of Korea (HI17C0952) to EY.

PS 991

CMV in Newborn Mice Induces Loss of Synapses Followed by Reduction in Spiral Ganglion Cells Accompanied by Progressive Hearing Loss

Shelby Payne¹; Song Zhe Li²; Cathy Yea Won Sung³; Mark A. Rutherford¹; William J. Britt³; **Keiko Hirose**¹
¹Washington University in St. Louis; ²Washington University School of Medicine; ³University of Alabama at Birmingham

Congenital CMV occurs in 1/200 newborns in the United States, and 10% of infants born with CMV develop hearing loss. The mechanism of hearing loss caused by congenital CMV infection is unknown. The murine model of congenital CMV infection that we have developed using peripheral viral inoculation in newborn mice

induces hearing loss in approximately 60% of infected mice (Smith strain, 200pfu/P1 mouse). A flat threshold shift of 15-30 dB was typical in those mice that acquired hearing loss. Viral DNA can be detected in the brain and cochlea within days post infection, and infectious virus was recovered from the cochlea by day 8. The majority of CMV infected cells in the inner ear were endothelial cells and resident macrophages. Viral infection of sensory cells has not been observed. A robust inflammatory response was detected within days post infection with peak responses seen two weeks after infection. Threshold shift was observed in the majority of mice, detected by P35 without apparent histologic changes in the sensory epithelium. Loss of spiral ganglion cells and disruption of inner hair cell synapses appeared to be the most consistent pathology observed in mice when infected with CMV as newborns. Virally induced inflammation in the ganglion and the lateral wall during development of the auditory periphery may both contribute to hearing loss that is observed in this model of hearing loss associated with congenital CMV infection.

PS 992

Cochlea-specific deletion of Cav1.3 calcium channels before birth excludes causative role of the efferent feedback system for IHC immaturity in systemic Cav1.3^{-/-} mice and unravels pitfalls of conditional mouse models

Stephanie Eckrich¹; Dietmar Hecker¹; Katharina Sorg¹; Kerstin Blum¹; Kerstin Fischer¹; Stefan Münkner¹; Gentiana Wenzel¹; Bernhard Schick²; Jutta Engel³

¹Saarland University; ²University of Saarland;

³Saarland University, Dept. Biophysics and CIPMM, Hearing Research

Ca_v1.3 voltage-gated Ca²⁺ channels are crucial for the function of inner hair cells (IHCs): before the onset of hearing (postnatal day 12 in mice), IHCs generate Ca²⁺ action potentials that drive terminal maturation of IHCs and the auditory pathway. In mature IHCs, Ca²⁺ currents elicit transmitter release. IHCs of deaf systemic Ca_v1.3^{-/-} mice remain immature with persistent expression of SK2 and lack of BK K⁺ channels. SK2 channels mediate transient efferent inhibition of neurons from the superior olivary complex (SOC) onto the spontaneously active immature IHC. Ca_v1.3 is expressed in SOC neurons and plays an important role for their survival, health and function. Persistence of SK2 channels and lack of BK channels in IHCs of systemic Ca_v1.3^{-/-} may thus result from malfunctioning SOC neurons [Hirtz (2011) J Neurosci 31:8280]. To separate these multiple roles of Ca_v1.3 in IHCs and auditory pathway, we analyzed *Pax2::cre;Cacna1d-eGFP^{fl^{ex}/fl^{ex}}* and *Pax2::cre;Cacna1d-eGFP^{fl^{ex}/-}* mice with a cochlea-

specific Ca_v1.3 knockout from embryonal day 9.5 coupled to GFP (flex switch) reporter function [Satheesh (2012) HumMolGen 21:3896; Ohyama (2004) Genesis 38:195].

We analyzed Ba²⁺ currents through Ca_v1.3 channels using whole-cell patch clamp recordings of IHCs from 3 week-old mice. Expression of IHC proteins was studied by immunolabeling of whole-mount organs of Corti. Auditory brainstem responses (ABR) and distortion product otoacoustic emissions (DPOAE) were recorded from 4-6 week-old mice to assess hearing function.

Lack of Ba²⁺ currents, profound hearing loss, persistence of SK2 channels and lack of BK channels in *Pax2::cre;Cacna1d-eGFP^{flex/-}* mice recapitulated the phenotype of systemic Ca_v1.3^{-/-} mice. In addition, we noticed GFP toxicity resulting in death of basal coil IHCs of *Pax2::cre;Cacna1d-eGFP^{flex/flex}* but not *Pax2::cre;Cacna1d-eGFP^{flex/-}* mice, which was most likely caused by high GFP concentration and small repair capacity. Moreover, the success of *Pax2*-driven *cre* in inactivating both *Cacna1d-eGFP^{flex}* alleles was limited, leading us to mainly study *Pax2::cre;Cacna1d-eGFP^{flex/-}*. Notably, IHCs of control *Cacna1d-eGFP^{flex/-}* mice without *cre* expression showed a significant reduction in Ca_v1.3 channel cluster sizes and currents, suggesting that the intronic construct interfered with gene translation or splicing.

The Ca_v1.3^{-/-}-like phenotype of *Pax2::cre;Cacna1d-eGFP^{flex/-}* mice indicates that during terminal differentiation, K⁺ channel expression is intrinsically regulated by the IHC rather than the efferent input. Additionally, the pitfalls found in our mice are likely to be a general problem of many genetically modified mice with complex or multiple gene-targeting constructs, showing that great caution and appropriate controls are required.

Funded by CRC894, EU-project MRTN-CT-2006-35367 („CavNet“) and Saarland University

PS 993

Change of paired-click ABR detection threshold after acoustic trauma; analysis in relation to synaptopathy

Jae-Hun Lee¹; Nathaniel Carpena²; So-Young Chang¹; Ji Eun Choi²; Min Young Lee²; Phil-Sang Chung²; Jae Yun Jung²

¹Beckman Laser Institute Korea, College of Medicine, Dankook University; ²Department of Otorhinolaryngology-Head & Neck Surgery, College of Medicine, Dankook University

Backgrounds and Objective:

Hearing ability could be altered without change in

hearing threshold. Synaptopathy which is reduction of synaptic connection between inner hair cell and auditory nerve fiber is considered as one of the responsible pathomechanism. In animal, this could be measured functionally using the amplitude of peak 1 among ABR waveform and reduction of peak 1 amplitude indicates the diminished synaptic connection. In human, there is still controversy. Several reports failed to demonstrate the change of peak 1 amplitude after acoustic overexposure in human. Reduction of temporal resolution which is thought to be related to decrease of the low firing rate with high threshold synapses could be an alternative ways to measure synaptopathy. Paired click detection threshold is a way to measure temporal resolution by identifying amplitude of ABR waveform of second click stimulus with varying time gap between two clicks. Thus, the purpose of this study is to identify correlation between paired click detection threshold to the peak 1 amplitude and population of presynaptic ribbon within inner hair cell in rat acoustic overexposure model.

Materials and Methods:

Twenty-four SD rats were used in this study. Synaptopathy was induced by narrow band noise exposure (16 kHz with 1 kHz of bandwidth, 105 dB SPL, 2 hours). ABR was measured (8, 12, 16, and 32 kHz) before, 1, 3, 7, and 14 days after noise exposure; and paired-click ABR was recorded before, 7, and 14 days after noise exposure. ABR recovery threshold was determined as an inter-stimulus interval (ISI), which is one step above the first ISI after reaching less than 50 %. For histological analysis, ribbon synapses were immunostained and quantified. The correlations among the ABR peak 1 amplitude, number of ribbon synapses, and paired-click ABR was analyzed.

Results:

In the results, peak 1 amplitude, ABR recovery threshold, and the number of synaptic ribbons were changed after noise exposure. Statistical reduction of peak 1 amplitude, number of synaptic ribbons and increase of paired click detection threshold was observed at 16 and 32 kHz. The correlation between peak 1 amplitude and ABR recovery threshold was significant at 16 and 32 kHz. The correlation between number of synaptic ribbons and ABR recovery threshold was also significant at same frequencies.

Conclusion:

Our results indicate that peak 1 amplitude of ABR and the number of synapses were highly correlated with ABR recovery threshold after noise exposure. This suggest that paired click ABR would serve as an additional tool for the assessment for expected synaptopathy or hidden hearing loss.

Acknowledgements:

This study was supported by the Ministry of Science, Information and Communications technology (ICT) and Future Planning grant funded by the Korean Government (NRF-2017R1D1A1B03033219), and supported by Leading Foreign Research Institute Recruitment Program through the National Research Foundation of Korea (NRF) funded by the Ministry of Science and ICT (MSIT) (NRF-2018K1A4A3A02060572).

PS 994

Genetic Deletion of the Sodium-Activated Potassium Channels KNa1.1 and KNa1.2 Alters Activity of the Primary Auditory Neurons and Auditory Function in Mice

Daniël O. J. Reijntjes¹; Jeong Han Lee²; Seojin Park²; Nick Schubert¹; Marcel van Tuinen¹; Sarath Vijayakumar³; Sherri M. Jones³; Timothy A. Jones⁴; Michael Anne Gratton⁵; Xiao-Ming Xia⁵; Ebenezer N. Yamoah²; Sonja J. Pyott⁶

¹University Medical Center Groningen; ²University of Nevada Reno; ³University of Nebraska Lincoln-College of Education and Human Sciences; ⁴University of Nebraska Lincoln; ⁵Washington University School of Medicine; ⁶University of Groningen, University Medical Center Groningen, Groningen, Department of Otorhinolaryngology and Head/Neck surgery

Background

Na⁺-activated K⁺ channels have been shown to modulate firing rate in the auditory midbrain (Bhattacharjee et al., 2002; Kaczmarek et al., 2005). We hypothesized that these channels might also regulate activity of the peripheral auditory system. Therefore, we examined the expression of the Na⁺-activated K_{Na} 1.1 (Slack/SLO2.2) and K_{Na} 1.2 (Slick/SLO2.1) channels in the spiral ganglion neurons (SGNs) and examined the contribution of these channels to *in vivo* and *in vitro* function of the SGNs using K_{Na} 1.1/1.2 wildtype and knockout mice.

Methods and Results

Using RNAseq and single molecule fluorescent *in situ* hybridization (smFISH) techniques, we identified K_{Na} 1.1- and K_{Na} 1.2-encoding transcripts in SGNs. Genetic deletion of K_{Na} 1.1/1.2 channels in mice resulted in reduction of the amplitude of supra-threshold (wave I) auditory responses despite normal absolute thresholds and normal numbers of SGNs and afferent synapses. Whole-cell voltage clamp examination of SGNs isolated from wildtype (WT) mice revealed Na⁺-activated outward K⁺ currents in some but not in all SGNs. This conductance was absent in SGNs isolated from K_{Na} 1.1/1.2 double knockout (DKO) mice. SGNs from DKO mice also

displayed altered membrane properties, including reduced AP latencies, thresholds and amplitudes, when examined under whole-cell current clamp configuration.

Conclusions

These findings indicate that K_{Na} 1.1/1.2 channels are important regulators of SGN response properties and that the absence of these channels results in reduced auditory supra-threshold responses without morphological loss of the SGNs or auditory synapses. This demonstrates that K_{Na} 1.1/1.2 channels are essential for normal auditory function and that early forms of hearing loss may be manifested through functional changes in SGN properties. Expression of K_{Na} 1.1/1.2 channels in some but not all SGNs suggests that K_{Na} 1.1/1.2 channels may help establish populations of SGNs with variations in threshold sensitivities.

PS 995

Local Expression and Selective Activation of Sodium-Activated Potassium and Voltage-Activated Sodium Channels in Primary Auditory Neurons.

Jeong Han Lee¹; Seojin Park¹; Mincheol Kang²; Xiaodong Zhang³; Maria Cristina Perez-Flores²; Hannah Ledford³; Wenying Wang²; Victor Matveev⁴; Nipavan Chiamvimonvat³; **Ebenezer N. Yamoah**¹

¹University of Nevada Reno; ²University of Nevada, Reno; ³University of California, Davis; ⁴New Jersey Institute of Technology

Background: Sodium influx through diverse voltage-dependent sodium (Nav) channels can activate sodium-activated potassium (kcnt1/2) channels. Previous work from our research team indicates that in spiral ganglion neurons (SGNs), activation of kcnt1/2 channels underlies the generation of the fast afterhyperpolarization (AHP) following brief 2-3-ms action potentials (APs), suggesting sodium entry through transient sodium channels may be the source of kcnt1/2 activation. In contrast, in other neurons, sodium entry via persistent sodium current underlies activation of kcnt1/2 channels. The source of sodium for Kcnt1/2 channel activation remains unknown.

Methods: We used smFish, immunocytochemistry, fluorescence resonance energy transfer (FRET), and patch-clamp electrophysiology to examine the expression, function and interaction of kcnt1/2 and Navs in SGNs.

Results: We found distinct localization of kcnt1/2 and Nav1.4/1.6 mRNA and protein expression, but not other Nav subtypes, at the postsynaptic terminals of afferent nerve endings of SGNs. We studied channel activity in whole-cell and cell-attached patches from SGNs and report a unique specificity of physical coupling, such

that *kcnt1/2* and *Nav1.4/1.6* are < 20 nm apart. These findings were confirmed using FRET experiments. The physical coupling between *kcnt1/2* and *Nav1.4/1.6* have functional implications; null deletion of *kcnt1/2* reduced the expression levels of *Nav1.4/1.6* at the postsynaptic terminals. Indeed, the temporal and spatial association between *kcnt1/2* and *Nav1.4/1.6* establishes sodium nanodomain at the synaptic terminals, which regulate AP firing and postsynaptic responses. These findings provide the first evidence to demonstrate local synthesis and coupling between channels, and illustrate the functional importance of nanodomain sodium.

Conclusions: *Kcnt1/2* and Nav channels are expressed in SGNs and contribute to the regulation of the SGN excitability and synaptic functions. Morphological distinctions of the afferent synaptic terminal and the close association between *kcnt1/2* and *Nav1.4/1.6* channels establish submembrane sodium domains which regulate auditory synapse responses.

Funding: NIH 1R01DC015135, 1R01DC015252-01 (ENY)

PS 996

Deletion of β -Secretase BACE1 Causes Hearing Loss Through Synaptic Disorganization and Hypomyelination of Nerve Fibers in the Auditory Periphery

Marlen Dierich¹; Stephanie Hartmann²; Nadine Herrmann³; Philip Moeser²; Konstantin Tziridis²; Achim Schilling²; Sabine Hessler²; Sandra Lehnert²; Dominik Oliver¹; Tobias Moser⁴; Holger Schulze²; Christian Alzheimer²; Tobias Huth²; **Michael Leitner**⁵
¹*Philipps-University Marburg*; ²*University of Erlangen-Nürnberg*; ³*Institut for Auditory Neurosciences, University Medical Center Göttingen*; ⁴*Institute for Auditory Neuroscience, University Medical Center Göttingen*; *Synaptic Nanophysiology Group, Max Planck Institute for Biophysical Chemistry*; *Collaborative Research Center 889, University of Göttingen*; ⁵*Medical University of Innsbruck*

β -site APP cleaving enzyme 1 (BACE1, also known as β -secretase) gained much scientific attention, as it is crucially involved in the processing of amyloid precursor protein, which is central in the pathogenesis of Alzheimer's disease (AD). However, there is increasing evidence for important physiological functions of BACE1 in the healthy brain. As nothing is known about the role of BACE1 in the auditory system, we utilized mice with genetic deletion of the enzyme to unravel its importance for the physiology of the auditory pathway. We found that genetic loss of BACE1 causes significant hearing loss in mice (BACE1-KO) as demonstrated

by increased thresholds and reduced amplitudes of auditory brainstem responses (ABR) and decreased distortion product otoacoustic emissions (DPOAE). As in wild-type mice BACE1 was strongly expressed in efferent olivocochlear terminals and in neurons of the spiral ganglion (SGN), these findings indicated that hearing loss in BACE1-KO mice was caused by a loss of sound sensitivity due to impaired information processing in afferent neurons of the auditory periphery. Indeed, using immunohistochemistry and confocal microscopy we found that SGN fibers close to the organ of Corti appeared disorganized and were abnormally swollen. The postsynaptic compartment also was disorganized as demonstrated by ectopic overexpression of PSD95 far outside the synaptic region in BACE1-KO mice. Furthermore, in the BACE1-KO by far fewer SGN fibers were myelinated than in wild-type mice and, if detectable at all, myelination did not extend all the way to the distal fiber endings in the majority of those fibers in BACE1-KO mice. Taken together, our findings demonstrated that expression of BACE1 is essentially required for establishment of normal fiber architecture, myelination and, synaptic connections in the auditory periphery and thus for normal hearing. This work was supported by Deutsche Forschungsgemeinschaft (DFG) through priority programme SPP1608 (grant to M.G.L.).

Inner-Ear Mechanics II

PS 997

3-D Finite Element Model of the Chinchilla Ear for Modeling Sound Transmission from Ear Canal to Cochlea

Paige Welch; **Kyle Smith**; Marcus Brown; Rong Gan
University of Oklahoma

Introduction: Research on acoustic signal transmission in the ear has provided insight into understanding the pathologies and disorders of the ear such as acute otitis media. To this end, 3-D finite element (FE) models of the chinchilla and human ear were created for analyzing middle ear functions and modeling sound transmission throughout the ear. Chinchilla models are often used in hearing research due to the animal's similarity in hearing range to that of humans. However, a 3-D FE model of the chinchilla ear including a spiral cochlea has yet to be created. In this study, we constructed a 3-D FE model of the chinchilla spiral cochlea and connected it to our previously published chinchilla middle ear model (Wang and Gan, 2016). We aim to understand the transmission of sound from ear canal to cochlea using this completed model.

Materials and Methods: The left bulla of an adult chinchilla was harvested for X-ray micro-CT (μ CT) scanning. A total of 519 μ CT images containing the entire

middle ear cavity and cochlea were segmented in Amira software. All surfaces of the model built in Amira were imported and meshed in HyperMesh (Altair Computing). The two and a half turn cochlea model consisted of the scala vestibuli, scala tympani, helicotrema, basilar membrane, and supporting structures. The length of the basilar membrane was approximately 16 mm. This model was connected to the middle ear model through the oval window and round window. A 90 dB pressure over the frequency range of 100-10,000 Hz was applied in the ear canal 2 mm away from the TM to derive the middle ear transfer function and cochlear pressures in ANSYS.

Results and Discussion: Results from FE analysis showed that displacement along the basilar membrane normalized with respect to the footplate displacement at various frequencies agreed with cochlea function results from published studies. That is, high frequencies localized near the base while lower frequencies localized near the apex. The model-derived data were compared with experimental results from chinchillas.

Conclusion: This study resulted in a 3-D FE model of the entire chinchilla ear. While aiming to use the model to understand sound transmission from ear canal to cochlea, future applications include experimental studies to validate the model. (Supported by DOD W81XWH-14-1-0228)

PS 998

Contralateral Suppression of Chirp-Evoked Auditory Brainstem Responses

Yi Shen; Amanda K. Tolen
Indiana University Bloomington

The dispersion of the cochlear traveling wave can be indirectly studied in humans by measuring chirp-evoked auditory brainstem responses (ABR). A strong ABR is obtained when the frequency glide in the chirp effectively counteracts the traveling delays from the base to the characteristic place across frequencies. In the current study, this technique was used to study the effect of contralateral broadband stimulation on the cochlear traveling wave delay. Auditory brainstem responses were measured for three types of harmonic complexes with periodic low-to-high frequency glides (i.e. periodically repeating chirps), covering a broad frequency range (180 - 7920 Hz). The fundamental frequency of the complexes was 90 Hz and the three complexes had different rates in their frequency glides. The duration for each complex was 178 ms. During the data acquisition, the three complexes were presented to the test ear, and they were randomly interleaved and repeated 500 times. The presentation level for the

complexes was 60 dB SPL. In separate conditions, the contralateral ear was presented with either no stimulus or a broadband noise (100 – 9000 Hz) at 80 dB SPL. The order of the two conditions was counter-balanced across listeners. Based on data collected from a group of young, normal-hearing listeners, the responses to the three different chirp stimuli were suppressed when the contralateral broadband noise was presented. The contralateral stimulation did not significantly affect the dependency of the response amplitude on the three different chirp stimuli, neither did it influence ABR latency. Results suggest that contralateral broadband stimulation suppresses the responses in the ipsilateral cochlea, but this suppression may occur without significant changes to the cochlear traveling wave delay.

PS 999

Preliminary study of the Inner Ear Mutual Mechanics between Cochlea and Vestibular in Finite Element Simulation

Junfeng Liang¹; Marcus Brown¹; Paige Welch¹; Rong Gan¹; Abderrahmane Hedjoudje²; Chenkai Dai¹
¹*University of Oklahoma;* ²*Johns Hopkins University School of Medicine*

Background: In vertebrates, the inner ear consists of two main functional parts: the [cochlea](#), dedicated to hearing and the [vestibular system](#), dedicated to [balance](#). These two parts are connected by lymphatic fluids, which fill the two bony labyrinth sections separated by the membranous labyrinth. The fluid flow of the endolymph is central to the function of the angular balance sense and the perilymphatic fluid plays an essential role in the cochlea. Very few research investigates both parts of the inner ear in mechanics. In this project we try to simulate mechanics in cochlea and vestibular simultaneously.

Methods: A 3-D finite element (FE) model of the chinchilla's inner ear consisting of the cochlea and vestibular was created to simulate the inner mechanics change in response to sound stimulation and head rotation. The model was established using images acquired with micro-CT of a chinchilla inner ear. Mechanical simulations (head rotation) and sound stimulation were carried out for the morphology of the chinchilla's semicircular canal/cochlea using known physical properties of the basilar membrane, ampulla, endolymph and perilymph.

Results: The frequency sensitivity and displacement of the basilar membrane/ampulla in response to both sound stimulation and mechanical rotation were simulated in the FE model. These results demonstrate the mutual effect of sound stimulation and mechanical rotation on basilar membrane in cochlea and ampulla in

the vestibular semicircular canal.

Conclusions: The presented simulation studies the full inner ear function including hearing and balance, which is a crucial step toward the development of a comprehensive FE model of the entire chinchilla's ear for acoustic-mechanical analysis.

Acknowledgements: This work was supported by DOD W81XWH-14-1-0228 and NIDCD R01DC009255.

PS 1000

A computational model for hidden hearing loss: synaptopathy vs. myelin defects

Maral Budak¹; Michal Zochowski¹; Victoria Booth¹; Karl Grosh²; Gabriel Corfas³
¹University of Michigan; ²University of Michigan, Ann Arbor; ³Dept. of Otolaryngology Head and Neck Surgery. University of Michigan

Hidden hearing loss (HHL) is an auditory neuropathy characterized by normal hearing thresholds but reduced amplitude of the sound-evoked auditory nerve compound action potential (CAP). It has been proposed that in humans HHL leads to speech discrimination and intelligibility deficits, particularly in noisy environments. Animal models originally indicated that HHL can be caused by moderate noise exposures or aging, and that loss of inner hair cell synapses could be its cause. However, Wan and Corfas (2017) provided evidence that transient loss of cochlear Schwann cells also causes HHL in mice. In this animal model, HHL occurs early in the demyelination process and persists for the animal's lifespan even after Schwann cells regenerate and axons remyelinate. The only histological finding in the mice after Schwann cell regeneration is a permanent disruption of the heminode at the AN peripheral terminals, i.e., while in the normal ear all heminodes are located at the same distance from the hair cell, in the remyelinated animals the heminodes are disorganized, and some unmyelinated segments are observed. Moreover, Choi et al. (2018) showed that patients with a subtype of Charcot-Marie-Tooth disease (CMT1A), a genetic demyelinating peripheral neuropathy, present symptoms of hidden hearing loss. This study supports the hypothesis that demyelination is another mechanism for hidden hearing loss. We constructed a reduced biophysical model for a population of inner hair cells (IHCs) with 15 postsynaptic auditory nerve (AN) fibers to test the impact that synaptopathy or disruption of heminode position have on the transmission of action potential. We then used a probabilistic model to simulate neurotransmitter release from the IHC's synapses in response to different sound levels. Neurotransmitter released at the IHC-AN synapse causes brief axonal depolarizations in the

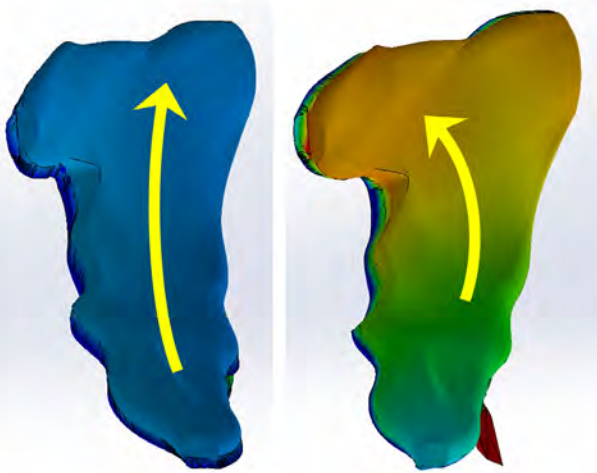
biophysical models. To simulate heminode defects, we varied the position of heminodes in the different axons to model the pathology seen after remyelination. We found that the amplitude of simulated sound-evoked auditory nerve CAPs is lower and has a greater delay when the heminodes are disorganized, i.e., they are placed at different distances from the hair cell rather than at the same distance as seen in the normal cochlea. Thus, our model confirms that heminodal disruption causes desynchronization of AN spikes leading to a loss of temporal resolution and reduction of the sound-evoked auditory nerve CAP. We also simulated synaptopathy by removing high threshold IHC-AN synapses and saw that the amplitude of simulated sound-evoked auditory nerve CAPs decreases while delay remains the same, supporting experimental results in noise-exposed animals. This model can be used to further study the effects of synaptopathy or demyelination on auditory function.

PS 1001

Guinea Pig Sacculle Finite Element Model - Spanning the dynamic range of VEMP testing

Zach Land¹; Jacob Jones¹; Ian S. Curthoys²; Wally Grant³; **Julian L. Davis**¹
¹University of Southern Indiana; ²The University of Sydney; ³VA Tech

Otolith organs are recognized as transducers of head acceleration. They respond to mechanical stimulus in the range up to their natural frequency. Previous work has shown that the guinea pig utricle has natural frequencies between 300-800 Hz (Land et al 2018). This is within the range of testing for Vestibular Evoked Myogenic Potential (VEMPs), usually between 500-2000Hz. VEMPs are one method of assessment of otolith function. However, 1200 Hz of frequency left in the testing range suggests that other organs are sensitive to the higher range of VEMP testing. This work uses finite element models to demonstrate the sacculle to be a much stiffer organ than its counterpart, thereby translating into higher natural frequencies. The natural frequencies of the sacculle organ are still within the range of stimulus during VEMP testing. These results imply that the Utricle and Sacculle work together to span the dynamic range of VEMP testing and that they can do so by adjusting structural characteristics of the otolith organs themselves.



PS 1002

A Theoretical Model for Vesicle Fusion of Auditory Hair Cells

Jaeyun Yoo; Woo Seok Lee; Kang-Hun Ahn
Chungnam National University

In auditory hair cells, precise timing of synaptic transmission is important to great features of hearing such as sound localization and speech recognition. Thus, understanding the nature of the synaptic fusion in auditory hair cells is key to understand hearing mechanism. Full collapse fusion and kiss-and-run have been suggested as mechanisms for vesicle fusion. To investigate a detail of the dynamics of fusion, we performed numerical simulations based on an electronic circuit model incorporating the pore dynamics. Spontaneous fusion arises in a various manner where we find sudden full fusion and kiss-and-run type fusion. Our numerical results imply that the key factor to determine the fusion type is the interplay between the calcium concentration and the noise strength involved in the pore opening.

PS 1003

Temporal Prediction as a Principle Behind Cochlea Tuning

Freddy Trinh¹; Ben D. B. Willmore¹; Andrew J. King¹; Nicol S. Harper²
¹Department of Physiology, Anatomy and Genetics, University of Oxford; ²University of Oxford

Neurons in the sensory systems are tuned to diverse but specific features of the sensory environment. Over the years, several theoretical principles – notably sparse coding – have been proposed which explain how this specific tuning may be the result of adaptation to the

statistical regularities of natural sensory stimuli. The cochlea transduces sound waves into electrochemical signals by filtering them using impulse response functions that can be approximated using gammatone filters. It has been suggested that the shape of these filters can be accounted for by efficient, sparse representation of sound in the cochlea (Lewicki, 2002, *Nat Neurosci* 5:356-363; Smith & Lewicki, 2006, *Nature* 439:978-982).

We suggest an alternative principle: that the peripheral auditory system is governed by temporal prediction, meaning that predictive information of auditory stimuli is preferentially encoded. Recent experimental findings indicate that retinal neurons might be optimised for temporal prediction (Palmer et al., 2015, *Proc Natl Acad Sci* 112:6908-6919), and theoretical work also suggests that temporal prediction may explain many aspects of receptive fields in both primary auditory and visual cortex (Singer et al., 2017, *bioRxiv*). We ask if the same principle can explain the features of the peripheral auditory system, more specifically the cochlea.

We trained a feedforward network with one hidden layer to predict the immediate future values of raw sound waveforms based on the most recent past values. We used an auditory dataset that is representative of the natural soundscape, and a crucial component of our model was the addition of Gaussian noise to the training set. We interpret the input weights to each hidden unit as the impulse response of a section of the basilar membrane.

The tuning characteristics of the hidden units show ringing and resemble gammatone filters, which approximate the impulse response functions reported for both the basilar membrane and auditory nerve fibres. The hidden units are tuned to frequencies over a wide range, and their density is inversely proportional to best frequency, while the filter bandwidth is proportional to best frequency. The filters are asymmetric in time and enable biologically plausible real-time encoding. Overall, a simple model optimized for temporal prediction can capture several distinct features of the peripheral auditory system.

PS 1004

Acoustic Evaluation of Graft Materials for Tympanoplasty

Iman Ghanad¹; Salwa F. Masud²; Nicole Black³; Elliott D. Kozin⁴; Jeffrey T. Cheng⁵; Aaron K. Remenschneider⁶

¹Mass Eye and Ear, Harvard Medical School; ²Harvard Medical School; ³Harvard John A. Paulson School of Engineering and Applied Sciences, Harvard University; ⁴Wyss Institute for Biologically Inspired Engineering, Harvard University; ⁵Eaton Peabody Laboratory,

Massachusetts Eye and Ear Infirmary; ⁴Massachusetts Eye and Ear Infirmary; Department of Otolaryngology, Harvard Medical School; ⁵Eaton Peabody Laboratory, Massachusetts Eye and Ear Infirmary; Department of Otolaryngology, Harvard Medical School; ⁶Department of Otolaryngology, University of Massachusetts Medical School; Massachusetts Eye and Ear Infirmary; Department of Otolaryngology, Harvard Medical School

Background: The tympanic membrane (TM) contains a delicate circular and radial collagen architecture that imparts acoustic properties allowing sound transfer across a range of frequencies. In tympanoplasty, commonly used autologous grafts do not recapitulate the native TM architecture, and may restrict sound transfer function in reconstructed TMs. Variability in hearing results following tympanoplasty may be explained, in part, due to utilized graft materials. In this study, we perform mechanical and acoustical analyses on several commonly used materials in tympanoplasty both *in vitro* and in a temporal bone model to determine reliability of results and differences in sound transfer function between materials.

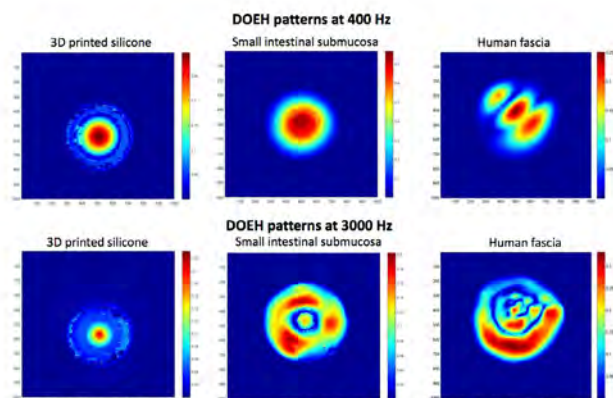
Methods: Graft materials evaluated included human fascia, porcine intestinal submucosa (SIS), and 3D printed silicone grafts. Digital opto-electronic holography (DOEH) and laser Doppler vibrometry (LDV) were used to measure sound induced surface motions and velocity of graft materials in an artificial annulus. Young's modulus for each graft material was determined through tensile testing. Wideband acoustic immittance was used to assess the mechanics of the TM. Cadaveric temporal bones were then utilized to obtain baseline stapes velocity with intact TM. Controlled TM perforations were created and graft materials used to reconstruct perforations. Sound induced stapes velocity and power reflectance were obtained for each material in the temporal bone setup.

Results:

In an artificial annulus, non-autologous graft materials and autologous graft material showed simple surface motion patterns at lower frequencies (400 Hz), with a limited number of displacement maxima. At higher frequencies (>1000 Hz) the displacement of non-autologous grafts were organized with multiple areas of high displacement separated by regions of lower displacement. In contrast, autologous graft materials revealed asymmetric and less regular holographic patterns. LDV measured velocity of SIS and 3D printed silicone sheet revealed consistency among measured samples, while fascia demonstrated non-regular velocity with high variability. Tensile testing revealed significant differences in Young's modulus between materials. In 6 human temporal bones,

perforation closure for each graft material was confirmed by endoscopic evaluation and detected differences in ear canal and middle ear pressure. In all reconstructed TMs, stapes displacement was higher than in perforated TMs, with peak displacement shifting between 500 Hz to 2 kHz. Wideband acoustic immittance demonstrated an increase of power reflectance in all reconstructed TMs below 2 kHz.

Conclusion: Motion patterns among graft materials utilized to reconstruct perforated TMs showed differences in material structures and mechano-acoustic properties, which may influence postoperative hearing outcomes following TM reconstruction.



PS 1005

Quantifying the Mechanisms of Cochlear Bone Conduction in the Chinchilla Inner Ear

Peter Bowers¹; Michael E. Ravicz²; John Rosowski³
¹Harvard University; ²Eaton-Peabody Lab, Mass. Eye & Ear; ³Eaton Peabody Lab, Massachusetts Eye and Ear Infirmary, Harvard Medical School

Bone-conduction hearing occurs when vibrations applied to the skull and body cause the transmission of sound energy to the inner ear. While there are multiple pathways for such energy transmission, the inner-ear based sources of bone conduction include several mechanisms, whose effects combine in unknown ways, and their effect on hearing is frequency dependent. These mechanisms are commonly referred to as cochlear fluid inertia, cochlear compression and expansion, and sound pressure transmission via "third-window" pathways to the inner ear.

We use physical measurements of intracochlear sound pressure and electrophysiologic measurements of compound action potentials (CAPs) to estimate the auditory response to bone-conduction stimulation in chinchilla. These measurements made before and after systematic manipulations of the auditory system allow

us to estimate the relative importance of the different inner-ear mechanisms of bone conduction to hearing.

Interruption of the incudostapedial joint allows inner-ear mechanisms to be isolated from external (ear canal compression) and middle-ear (ossicular inertia) bone-conduction sources. Occlusion of the oval and round window reduces the effect of cochlear fluid inertia and emphasizes the effects of cochlear compression and sound pressure transmission via other cochlear windows. The contributions of cochlear compression and other-cochlear-window mechanisms to bone conduction are quantified by comparing intracochlear sound pressure measurements and skull velocity measurements during normal bone-conduction stimulation and direct mechanical stimulation of the brain.

A lumped-element circuit model for bone conduction is being developed from a previously defined air-conduction model. The model mimics the experimental conditions and is fit to the intracochlear sound pressure and CAP data. The model cochlear network is being extended from the simplified air-conduction model to incorporate additional pressure and volume-velocity sources representative of inner-ear bone-conduction mechanisms. The geometry of the cochlear scalae guides estimates of inertance and compression-controlled parameters, while the geometry of the cochlear and vestibular aqueducts guides estimates of the additional pathways to and from the inner ear. Additionally, the effect of pathology, such as otosclerosis and superior canal dehiscence, is investigated by changing the model structure and estimating the cochlear drive before and after manipulation.

PS 1006

3D Finite Element Modeling of Blast Wave Transmission from the External Ear to the Cochlea

Marcus Brown; Xiao Ji; Rong Gan
University of Oklahoma

Introduction: Blast exposure-induced injuries affect the health and quality of life for veterans in the US after the wars in Iraq and Afghanistan. The auditory damage is often caused when a person is subjected to blast exposures. While damage to the tympanic membrane (TM) can be observed non-invasively, examining the damage to the inner ear is difficult to quantify. Finite element (FE) model of the ear provides a tool that allows for the prediction of the inner ear function changes when the external ear is exposed to a blast. Previous works have modeled the cochlear response when subjected to a harmonic, acoustic pressure input, but the inner ear mechanics have not been studied when the ear is exposed to a blast wave. In this study, we utilized a FE

model of the human ear, which includes the ear canal, middle ear, and an uncoiled, two-chambered cochlea, to simulate the cochlear response to blast overpressure at the entrance of the ear canal and compared the results to experimental data.

Methods: The FE model components include the ear canal, ossicular chain, TM, middle ear suspensory ligaments/muscle tendons, middle ear cavity, round window membrane, and cochlea with the basilar membrane (BM) and two chambers. The material properties used for the structural components were described in Gan et al. (2007). There were three fluid domains: the air in the ear canal and middle ear cavity and the cochlea fluid. An overpressure waveform recorded from the blast tests on human cadaver ears was applied at the entrance of the ear canal, and the pressure transmission through the ear canal and middle ear into the cochlea was calculated in ANSYS. The TM and stapes movements and cochlear BM motion were derived in the time domain.

Results and Discussion: Results from the FE model exhibited significant displacements of the flexible membranes and tissues of the ear. The stapes displaced up to 60 μm in the piston direction with cochlear pressures and BM displacements as high as 80 kPa and 23 μm , respectively. These simulated results would undoubtedly cause damage to the inner ear.

Conclusions: A 3D FE model of the entire ear was used to simulate the mechanics of the cochlea when the ear was exposed to blast overpressure. Future experimental studies will measure cochlear pressure during blast exposure for model validation and evaluation of hearing protection devices for the inner ear. (Supported by DOD W81XWH-14-1-0228)

PS 1007

Evaluation of the Spatial Distribution of the Human Skull Mechanical Properties for better Understanding of Bone-conducted Hearing

Ivo Dobrev¹; Woonhoe Goo²; Christof Rösli¹; Namkeun Kim²

¹Department of Otorhinolaryngology Head & Neck Surgery, University Hospital Zürich, University of Zurich; ²Department of Mechanical Engineering, Incheon National University

Objectives: For a better understanding of bone-conducted hearing, the sound wave propagation in a human skull should be investigated, and the Young's modulus of the skull is a significant factor to determine the wave speed in the skull. Therefore, we measured the spatial distribution of the Young's modulus of the skull and compared it with published values.

Methods: In a pilot experiment, a Thiel preserved human cadaver head was used to measure Young's modulus of the skull bone. The specimen was first scanned via computed tomography (CT) and Magnetic resonance imaging (MRI) to determine the approximate shape and thickness distribution of the skull bone and soft tissue within the head. Based on the volumetric data, several areas of the skull were selected, from which test samples were extracted, including: ipsi- and contralateral mastoid, temporal and parietal bones, forehead, as well as anterior and inferior sections of the occipital bone. Two to three samples were extracted from each section, each measuring approximately $2.5 \times 1.5 \times 20$ mm². Each sample was scanned with μ CT (12 μ m voxel size) to define its microstructure and corresponding bone volume fraction between the cortical bone and the cancellous bone. After all volumetric scans, samples were individually fit into a micro tensile-compression stage, with a maximum range of 2 kN. Several tension-compression loading cycles within the linear elastic range were applied to each sample, after which the tensile load was increased until failure, providing experimental values for both Young's modulus and ultimate tensile strength. Theoretical values of the Young's modulus were also predicted based on μ CT data in combination with composite- and curved-beam theory.

Results: Due to the variation of the ratio between the cortical bone and the cancellous bone through the skull, Young's modulus of the skull also varied from 300 MPa to 10 GPa.

Conclusion: Merging experimental data from multiple imaging domains, including MRI, CT, μ CT volumetric data with tension-compression tests, allows for detailed exploration of the skull bone material properties and its spatial variation. Such multi-domain data could be used for improving existing numerical models and for optimization of the design of bone conduction hearing aids.

Keywords: Young's modulus, human skull, micro tensile stage, MRI, CT, μ CT, bone conduction, beam theory.

PS 1008

Experimental and Simulation Evaluation of the of Bone Conduction Surface Wave Propagation

Ivo Dobrev¹; Namkeun Kim²; Stefan Stenfelt³; Alex Huber¹; Christof Rösli¹

¹Department of Otorhinolaryngology Head & Neck Surgery, University Hospital Zürich, University of Zurich; ²Department of Mechanical Engineering, Incheon National University; ³Linköping University

Objectives: Experimental and simulation (finite element

model, FEM) investigation of bone conduction sound propagation by surface waves of the skull bone and their dependence on osseous and non-osseous stimulation site and coupling method of the bone conduction hearing aid (BCHA).

Methods: Experiments were conducted on five Thiel embalmed whole head cadaver specimens. The electromagnetic actuators from a commercial bone conduction hearing aids (BCHA) (Baha® Cordelle and Power, and BoneBridge®) were used to provide a stepped sine stimulus in the range of 0.1-10 kHz. Osseous pathways (direct bone stimulation or transcutaneous stimulation) were sequentially activated by mastoid stimulation via a percutaneously implanted screw, Baha® Attract transcutaneous magnet and a 5-Newton steel headband. Non-osseous pathways (only soft tissue or intra-cranial contents stimulation) were activated by stimulation on the eye, neck, and dura via a 5-Newton steel headband, as were compared with equivalent stimulation on the mastoid or forehead. The response of the skull was monitored as motions of the ipsi-, top and contra-lateral skull surface. The surface motion was quantified by sequentially measuring ~200 points on the skull surface (~ 15-20mm pitch) via a three-dimensional laser Doppler vibrometer (3D LDV) system. Experimental data for stimulation via screw implant was compared with predictions from a finite element model of the human head (LIUHead).

Results: 3D LDV data indicates that the skull surface undergoes complex spatial motion with similar contributions from all motion components, under all stimulation modes. BCHA coupling type affects the spatial composition of the skull motion, specifically the ratio between the normal and tangent motion. Stimulation in the proximity of the base of the skull, results in wave motion primarily at the inferior section of the skull, below 3-4kHz. Experimental data and FEM predictions are qualitatively comparable.

Conclusion: Comprehensive experiments, including simultaneous motion across the whole skull surface, with various stimulation positions and coupling methods, allow for detailed exploration and differentiation of the individual contributions of the various bone conduction stimulation conditions and pathways.

Keywords: Bone conduction pathways, 3D Laser Doppler Vibrometer, surface waves, scanning velocimetry, cadaver head, coupling method, finite element model.

Inner-Ear Therapeutics II

PS 1009

Next Generation Gene Therapy Improves Hearing, Balance, and Secondary Outcomes in Mouse Models of Genetic Inner Ear Disorder

Carl Nist-Lund¹; Bifeng Pan¹; Amy Patterson¹; Yukako Asai¹; Wu Zhou³; Hong Zhu²; Tianwen Chen²; Sandra Romero³; Jennifer Resnick⁴; Daniel B. Polley⁴; Gwenaelle S. Geleoc¹; **Jeffrey R. Holt**

¹*Boston Children's Hospital, Harvard Medical School;*

²*Department of Otolaryngology University of Mississippi Medical Center;* ³*MEE;* ⁴*Eaton-Peabody Laboratories, Massachusetts Eye and Ear; Dept. of Otolaryngology, Harvard Medical School*

Background

Genetic mutations cause up to fifty percent of deafness worldwide, yet hearing aids or cochlear implants, the current standards of care, provide only partial restoration for a limited patient population. To develop biologic treatments to prevent or delay the effects of pathogenic inner ear mutations, we designed gene replacement therapies using synthetic adeno-associated viral vectors (sAAVs) to deliver the coding sequence for Transmembrane Channel-Like (*Tmc*) 1 or closely related *Tmc2* into sensory hair cells. Mice that carry *Tmc1* and *Tmc2* mutations are profoundly deaf, have severe vestibular deficits, and do not breed well.

Methods

The coding sequence for *Tmc1ex1* with a CMV promoter and WPRE sequence were cloned into AAV2 plasmids, which were packaged into sAAV capsids. sAAV-*Tmc1* vectors were injected into the inner ears of P1 mice that carried genetic deletions in endogenous *Tmc1*, *Tmc2* or *both*. To assay for recovery of function, we measured hair cell sensory transduction, ABRs, DPOAEs, neuronal responses in auditory cortex and acoustic startle responses. To investigate recovery vestibular function, we measured vestibular-ocular reflexes, open-field behavior and rotarod performance.

Results

We find that a single injection of sAAV-*Tmc1* via the round window membrane in *Tmc1*-null mice enhanced hair cell survival. sAAV-*Tmc1*-transduced hair cells recovered sensory transduction. ABR thresholds in sAAV-*Tmc1*-injected ears were improved to 35 dB in some cases. Mirroring the peripheral recovery, we observed cortical recovery, as measured by multi-unit recordings from auditory cortex. We also found restoration balance behavior, as well as, rotational and

translational vestibular ocular reflexes in *Tmc1/2* double mutant mice. As a secondary consequence of the hearing and balance recovery, we found that injected mice had improved breeding frequency, litter survival and growth rates.

Conclusions

The data demonstrate sAAV-*Tmc1* gene therapy promotes recovery in the auditory system at the cellular, organ, systems and behavioral levels. In the vestibular system we found evidence for recovery of semicircular canal and otolith organ function and enhanced performance on balance tasks. These preclinical data suggest *Tmc* gene therapy may be well-suited for further development and perhaps translation to clinical application.

PS 1010

Sirtuin 1 and Autophagy Attenuate Cisplatin-induced Hair Cell Death in The Mouse Cochlea and Zebrafish Lateral Line

Ting Zhan; Jiaqi Pang; Hao Xiong; Haidi Yang
Sun Yat-sen Memorial Hospital, Sun Yat-sen University

Cisplatin-induced ototoxicity is one of the major adverse effects in cisplatin chemotherapy, and hearing protective approaches are unavailable in clinical trial. Recent work unveiled a critical role of autophagy in cell survival in various types of hearing loss. Since the excessive activation of autophagy can contribute to apoptotic cell death, whether the activation of autophagy increases or decreases the rate of cell death in cisplatin ototoxicity is still being debated. In this study, we showed that cisplatin induced activation of autophagy in the auditory cell HEI-OC1 at the early stage. We then used rapamycin, an autophagy activator, to increase the autophagy activity and found that the cell death significantly decreased after cisplatin injury. In contrast, treatment with the autophagy inhibitor 3-methyladenine (3-MA) resulted in reduced autophagy activity and significantly increased cell death. In accordance with the vitro results, rapamycin alleviated cisplatin induced death of the lateral line hair cells in zebrafish and cochlear hair cells in mice. Notably, we first found that cisplatin-induced increase of Sirtuin 1 (SIRT1) in the HEI-OC1 cells modulated the autophagy function. The specific SIRT1 activator could successfully prevent the increase of hair cell death both in HEI-OC1 cells and in the cochlea of mice after cisplatin exposure. These findings demonstrate that there is a protective way for the sensory hair cells to rescue themselves by raising SIRT1 expression and autophagy activity at the early stage of cisplatin injury. SIRT1 and autophagy activation can be suggested as potential therapeutic strategies for overcoming the cisplatin-induced ototoxicity.

Study on protection effect of inner ear in administration of Adalimumab to noise induced hearing loss model mice

Yohei Yamamoto¹; Kazuma Sugahara²; Hiroshi Yamashita²

¹Yamaguchi University Hospital; ²Department of Otolaryngology, Yamaguchi University Graduate School of Medicine

Background:

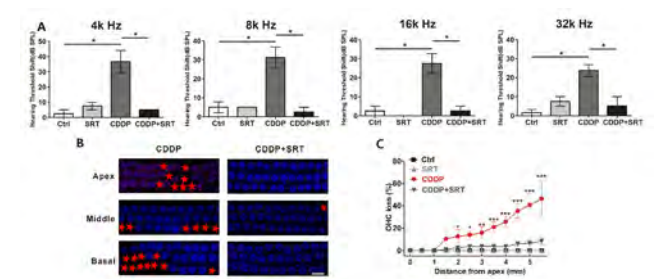
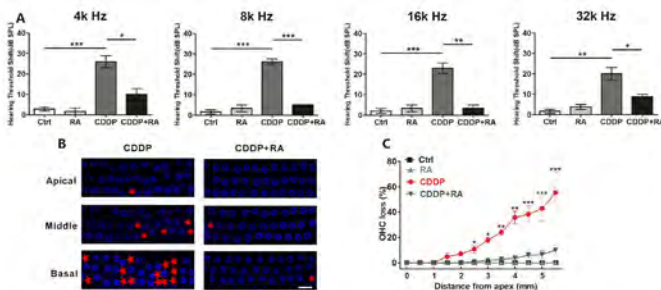
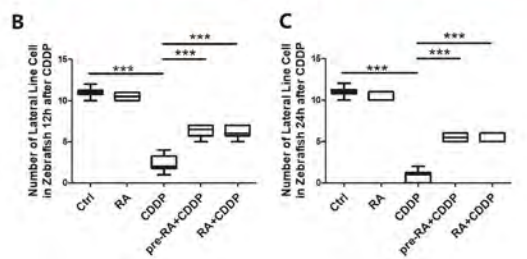
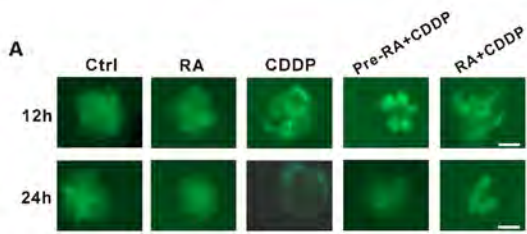
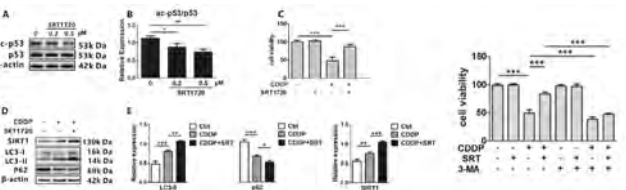
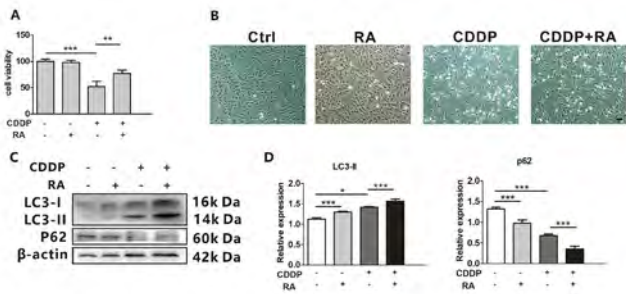
In noise induced hearing loss, it is suggested that inflammatory cytokines increase in the inner ear and are involved in hearing loss through impairment of hair cells and decrease of cochlear blood flow. TNF α , a major mediator of the inflammatory response, is also known to increase after acoustic injury, and it has been reported that hearing loss could be suppressed by suppressing TNF α . We considered that administration of Adalimumab which is an anti human monoclonal antibody preparation before acoustic disorder could obtain inner ear protective effect and examined changes in ABR threshold and hair cell loss rate before and after acoustic disorder in mice.

Method:

Animals were males of CBA/N mice and were 6-7 weeks old and weighing 20-25 g were used. An acoustic load of 130 dB SPL, 5 hours was set with octave band noise of center frequency 4 kHz which is PTS model of our team. Animals were divided into two groups, Adalimumab administration group and Control group, and the ABR before loading was measured. Adalimumab of 10 mg/kg or physiological saline was administered intraperitoneally 1 hour before acoustic loading. Furthermore, ABR was measured 7 days after the acoustic load, and the change of the ABR threshold before and after the load was compared. After that, the cochlea was quickly decapitated and the cochlea was taken out, then stained with phalloidin to compare the deficiency ratio of hair cells.

Result:

In our assumption, we predicted that the Adalimumab treatment group had better ABR threshold rise than the Control group and that the hair cell defect rate was also lower. However, ABR threshold after acoustic load tended to have a tendency for threshold value to increase at each frequency in Adalimumab administered group. In addition, even in comparison of the hair cell depletion rate by phalloidin staining, the deficiency rate tended to be higher in the Adalimumab administration group, in particular, a significant difference was obtained on the basal rotation side.



Discussion:

TNF α is also involved in inner ear disorder, but on the other hand it is suggested that it may be involved in maintaining the function of the inner ear. That is, there is a possibility that TNF α increases and internal ear disorder that induces inflammatory response may occur, but conversely if too much suppressing TNF α , there is a possibility that the homeostasis of the inner ear will not be adversely affected.

PS 1012

Comparison of the Otoprotective Profiles of Antioxidant and Anti-apoptotic Compounds in Ex Vivo models of Cisplatin-induced Hearing Loss

Pranav D. Mathur; Phillip Uribe; Stephanie Szobota; Anne Harrop-Jones; Fabrice Piu; Alan C. Foster; Bonnie Jacques
Otonomy, Inc.

Background: Hearing loss is a serious adverse effect of widely used platinum-based chemotherapies, and a large percentage of patients treated with cisplatin will develop some degree of hearing loss. In the inner ear, hair cells, spiral ganglion neurons and the stria vascularis are all susceptible to cisplatin-induced damage, and dysfunction of any of these cell types can contribute to hearing loss. Hair cell death is thought to result from the formation of DNA-crosslinks and enhanced levels of reactive oxygen species which activate cell death pathways. Research from the ear and other organ systems has identified several classes of compounds that may prevent this type of cell death; some of these include antioxidants and inhibitors of apoptosis. Here, we compared the otoprotective profiles of these classes of molecules in clinically relevant ex vivo models of cisplatin-induced hearing loss (CIHL) to determine their relative therapeutic potential.

Methods: P2-P4 Sprague-Dawley rats were used for all experiments. Whole organ cochlear explants were established, allowed to acclimate overnight, then were pre-treated for 1.5 hours with various concentrations of otoprotectant compounds prior to co-incubation with cisplatin for 48-72 hours. Explants were then fixed and stained for hair cell and SGN markers and cells were quantified. To evaluate protection of the stria vascularis, dissociated strial cells were expanded in culture for 48-72 hours, then were similarly pre-incubated in the otoprotectants, with subsequent co-incubation with cisplatin for 22 hrs. Strial cultures were stained for marginal cells and caspase activation.

Results: In our ex vivo assay system, both antioxidants and apoptosis inhibitors were found to be protective against hair cell, SGN and marginal cell damage

at clinically relevant doses of cisplatin. While this protection was dose-responsive, it varied as a function of the concentration and degree of cisplatin damage. Interestingly, there were differences in how these classes of therapeutics impacted the SGNs and hair cells.

Conclusions: Comparative ex vivo evaluation of two classes of otoprotective compounds identified clear dose-responsive protection of hair cells, SGNs and marginal cells, although their protective capacity and range of effective dose varied depending on cell type. This suggests there may be different mechanisms of cisplatin-induced damage among the vulnerable cell types in the cochlea and demonstrates the ability of ex vivo models to identify these differences and screen for compounds with broad otoprotective profiles.

PS 1013

Can Mannitol be Used to Decrease Cisplatin Level and Reduce Its Ototoxic Effects in the Cochlea?

Ayesha Noman¹; Trung Le²

¹Sunnybrook Hospital; ²Department of Otolaryngology - Head & Neck Surgery, Sunnybrook Health Sciences Centre Toronto, Canada

Introduction: Cisplatin is a chemotherapeutic medication used to treat many types of cancers. It has been known to cause ototoxicity as it induces hearing loss by increasing ROS and activating the pathway leading to hair cell apoptosis. There is currently no FDA approved medication for cisplatin induced hearing loss even though researchers have spent years focusing on combating cisplatin-based ototoxicity at the level of the hair cell. Since the discovery of cisplatin accumulation in the stria vascularis, scientists are uncovering new ways to alter the pharmacokinetics of cisplatin. Mannitol, a diuretic medication which has been shown to adjust the permeability of the blood-labyrinth barrier, may have a potential to extract cisplatin from the cochlea (inner ear). In this study, our hypothesis is that mannitol will allow cisplatin to egress the inner ear and thus decreasing its perniciousness.

Methods: To study whether mannitol alters the pharmacokinetics of cisplatin in the inner ear, rats will be divided into three groups. The groups will be administered with either 1) cisplatin with mannitol, 2) cisplatin without mannitol, or 3) saline. The perilymph, CSF, and serum matrices will be collected from rats at different time points after injection. Cisplatin concentrations will be detected using LC MS/MS after derivatization of cisplatin using diethyldithiocarbamate (DDTC) and measuring the Pt-DDTC complex.

Furthermore, rats will be divided into the above-mentioned groups to study the otoprotective properties

of mannitol. The rats will be subjected to a clinically relevant cisplatin regime comprising of 3 cycles. Each cycle consists of 4 days of injections followed by a 10-day recovery period. Auditory experiments will be performed post injection and recovery periods. Auditory Brainstem Response (ABR) and Distortion Product Otoacoustic Emission (DPOAE) will be measured to monitor changes in hearing threshold.

Expected Results: Mannitol administration prior to cisplatin injections may increase the clearance of cisplatin from the perilymph and CSF indicated by a greater reduction in Pt-DDTC complex levels over time and it may reduce hearing loss noted with a lower threshold potential for each frequency.

Conclusion: By manipulating the blood labyrinth barrier and preventing long-term retention of cisplatin in the cochlea, mannitol can reduce cisplatin ototoxicity in susceptible tissues of the inner ear. Our results will demonstrate the role of mannitol in the manipulation of the blood labyrinth barrier and provide an important therapeutic strategy to prevent cisplatin ototoxicity, a direct implication in hearing rehabilitation in cisplatin chemotherapy.

PS 1014

Protective Effects of Salvianolic acid B Against Cisplatin-Induced Ototoxicity in the zebrafish lateral line and in an auditory-derived cell line.

Zhiwei Zheng; Chengfu Cai

First Affiliated Hospital of Xiamen University

Hair cell is specifically sensitive to oxidative stress, and this is the mainly mechanism that induces cell apoptosis in most ototoxic insults-induced ototoxicity. Reducing reactive oxygen species (ROS)-mediated oxidative damage through antioxidant mechanisms has the therapeutic potential for the prevention of auditory sensory loss. In this regard, it is of great interest to determine whether antioxidants could alleviate ototoxicity through ameliorating mitochondrial dysfunction caused by ototoxic insults. Salvianolic acid B (SalB), a natural bioactive component from *Alvialia miltiorrhiza* Bge, is a potent antioxidant and has been reported to exert protective effect in various types of cells. Here we have determined the effectiveness of SalB on cisplatin-induced ototoxicity *in vitro* in HEI-OC1 culture cells. The cell viability, apoptosis, ROS production, mitochondrial membrane potential and changes in the apoptotic signal pathway were investigated. Our results showed that SalB significantly protected against cisplatin-induced apoptotic features and decreased caspase-3 activity in the HEI-OC1 cells. Treatment of the HEI-OC1 cells with SalB decreased the intracellular ROS production

and reduced the expression of Bax and cleaved caspase-3 compared to their significant increase after cisplatin treatment. Then, the protective effect of SalB were further explored *in vivo* in a transgenic zebrafish (*Brn3C: EGFP*) model. Our data demonstrated that SalB markedly decreased the TUNEL staining and protected against cisplatin-induced hair cell loss of the neuromasts in the zebrafish lateral line. Taken together, these results suggest that SalB has otoprotective effects against cisplatin-induced hair cell death and could be an effective candidate for the prevention of cisplatin-induced ototoxicity.

PS 1015

Differential Protective Effects of Berbamine Analogs from Aminoglycoside-Induced Hair Cell Death

Alexandria M. Hudson¹; Gavin M. Lockard¹; Bruce E. Blough²; Peter S. Steyger³; Allison B. Coffin¹

¹Washington State University, Vancouver; ²RTI International; ³Oregon Health & Science University

Aminoglycosides are used worldwide due to their potent antibacterial properties and low cost, surpassing expensive antibiotics with fewer harmful side effects. However, their use is often coupled with permanent hearing loss that affects 20% of patients requiring these life-sustaining antibiotics. To date, there are no FDA-approved drugs that prevent damage from aminoglycosides. Our goal is to develop a drug that prevents aminoglycoside-induced hearing loss. A previous study by our lab identified four compounds that share a modified quinoline scaffold and strongly protect zebrafish lateral line hair cells by attenuating aminoglycoside uptake, likely via partial block of the mechanotransduction channel (MET). The present study builds on previous work, investigating analogs of berbamine, our most protective compound, to determine the core protective structure and the specific molecular targets that are responsible for protection. Recent findings suggest that co-treatment of our analogs with aminoglycosides robustly protect hair cells from ototoxic damage at higher potencies than the parent compounds. Some analogs were found to be particularly efficacious and blocked uptake of aminoglycosides, implying those structures likely mitigate damage via a transient block of the MET channel. Additional gentamicin washout experiments further demonstrate that some analogs may attenuate aminoglycoside hair cell damage via intracellular mechanisms in addition to transiently blocking the MET channel. Hair cell protection also varied depending on the combination of analog and aminoglycoside. Certain analogs protected hair cells from multiple aminoglycosides while others only prevented neomycin damage. These data suggest

multiple pathways of protection and are consistent with the literature on aminoglycosides activating different mechanisms of damage. Future studies will continue exploration of the derivative chemical structure to refine the functional groups for optimization as an otoprotectant for aminoglycoside toxicity. This work demonstrates that we have promising lead compounds for further development to meet the therapeutic goal of devising a protective hearing loss drug.

PS 1016

Inhibition of Protein Nitration Mitigates Cisplatin-Induced Inactivation of STAT3-Mediated Anti-Apoptotic Signaling in Organ of Corti Cells

Rita Rosati¹; Monazza Shahab¹; William Neumann²; Samson Jamesdaniel¹

¹Wayne State University; ²Southern Illinois University Edwardsville

Background

JAK/STAT pathway is one among the several oxidative stress-responsive signaling pathways that appear to play a critical role in facilitating cisplatin-induced ototoxicity. Our studies indicated that cisplatin treatment decreases the levels of cochlear LMO4, which acts as a scaffold for IL6-GP130 protein complex. Cisplatin-induced nitration and degradation of LMO4 could destabilize this protein complex, which in turn could compromise the downstream STAT3-mediated cellular defense mechanism. Therefore, we hypothesized that the destabilization of IL6-GP130 complex, due to cisplatin-induced nitration and downregulation of LMO4, impedes JAK1 dependent recruitment/activation of STAT3 and thereby compromises the transcription of anti-apoptotic genes and facilitates cisplatin-induced ototoxicity. In this study, we investigated the link between cisplatin-induced nitrate stress and STAT3-mediated apoptosis by using a cell culture model.

Methods

UB/OC1 cells, an immortal cell line derived from the mouse embryonic organ of Corti, were used to investigate the effects of inhibition of nitration on STAT3-mediated anti-apoptotic signaling in cisplatin-induced ototoxicity. SRI110, a peroxydinitrite decomposition catalyst that prevented cisplatin-induced decrease in LMO4 levels and ototoxicity, was used to inhibit nitrate stress. The expression, phosphorylation, and nuclear localization of STAT3 were assessed by immunoblotting/immunostaining with anti-STAT3 and anti-pSTAT3. JAK/STAT pathway RT2 Profiler PCR Array was used to assess cisplatin-induced changes in the expression of genes associated with the IL6/STAT3 signaling pathway, with and without SRI110 co-treatment.

Results

Cisplatin treatment decreased the expression levels, phosphorylation, and nuclear localization of STAT3. Inhibition of nitration by SRI110 co-treatment prevented cisplatin-induced inactivation of STAT3 and promoted its nuclear localization. Treatment of UB/OC1 cells with cisplatin up regulated the expression of Cdkn1a and Cebpd and down regulated the expression of Bcl2l1, Ccnd1, Egfr, Fas, Il6st, Jak1, Jak2, Jak3, Src, Stat3, and Tyk2, which are genes associated with the IL6/STAT3 signaling pathway. Inhibition of cisplatin-induced nitrate stress by SRI110 co-treatment reversed the cisplatin-induced changes in the expression levels of Bcl2l1, Ccnd1, Jak2, Jak3, and Src and significantly attenuated the changes in the expression levels of Cdkn1a, Egfr, Fas, Il6st, Jak1, Stat3, and Tyk2.

Conclusion

Collectively, these results suggest that the inhibition of cisplatin-induced nitration prevents the inactivation of STAT3 probably due to the stabilization of the IL6-GP130 complex, which in turn enables the transcription of anti-apoptotic genes and thereby helps to mitigate cisplatin-induced ototoxicity.

PS 1017

Ebselen Attenuates Aminoglycoside-Induced Ototoxicity in Mice

Rende Gu; Jennifer Homan; Jonathan Kil
Sound Pharmaceuticals, Inc.

Background Aminoglycosides (AG) such as tobramycin and amikacin are commonly used in CF patients with recurrent pulmonary infections. It has been well established that AGs can compromise auditory and vestibular function and result in ototoxicity. Prior studies demonstrate that ebselen can prevent and treat sensorineural hearing loss in animals and humans. The goal for this study is to investigate the efficacy of ebselen in reducing AG-induced ototoxicity both in vitro and in vivo.

Methods P0-1 SW mice cochlea were cultured on filter membranes. After 24 hours, 50% of the medium was replaced with medium containing ebselen or DMSO (control). Thirty minutes later, tobramycin or amikacin was added to a final concentration of 0.5 or 1.0 mM, respectively. Cultures were maintained for another 48 hours. Cochlea were fixed and immuno-stained with Myosin-VIIa and several morphologic criteria were used to assess the damaged vs undamaged regions. SW mice (12-16 weeks) received daily tobramycin injections (200 mg/kg/sc) or daily amikacin injections (500 mg/kg/sc) for 14 days. In a different group of mice, daily

ebesen injections (20 mg/kg/ip) or vehicle injections (DMSO/saline) preceded each AG injection by 30 minutes. ABRs were performed at baseline, 2, 4, 6 and 8 weeks after the last injection.

Results Epifluorescence whole mount microscopy indicate that the undamaged region of the organ of Corti was significantly longer in the ebesele/tobramycin cochlea than the tobramycin cochlea (2.2 +/- 0.65 vs. 1.2 +/- 0.22 mm). Similar improvements were observed in the ebesele/amikacin vs amikacin cochlea (4.36 +/- 0.44 vs. 2.33 +/- 0.18 mm). Tobramycin (200 mg/kg/d) or amikacin (500 mg/kg/d) x 14 days, induced a mild to moderate hearing loss at all frequencies tested (4, 8, 16, and 32 kHz). After 8 weeks, ebesele/AG treatment resulted in significantly less threshold shift at 8 kHz when compared to tobramycin (2.8 vs 22.3 dB) or amikacin (3.2 vs 14.6 dB). At 4 kHz, ebesele/AG vs tobramycin (-0.3 vs. 12.7 dB) or amikacin (3.6 vs 11.8 dB). At 16 kHz, ebesele/AG vs tobramycin (8.8 vs. 11.3 dB) or amikacin (3.6 vs 11.4 dB). At 32 kHz, ebesele/AG vs tobramycin (8.8 vs. 10.7 dB) or amikacin (1.1 vs 10.2 dB).

Conclusions In both experiments, tobramycin appeared more ototoxic than amikacin. Ebesele treatment can attenuate aminoglycoside-induced ototoxicity in neonatal cochlear cultures and in adult mice following repeat administration. These data support the testing of ebesele in humans exposed to repeat daily doses of tobramycin or amikacin.

PS 1018

Induction of redox-active gene expression by CoCl₂ ameliorates oxidative stress-mediated injury of mouse auditory cell lines

Jhang Ho Pak¹; Jong Woo Chung²; Hae Ri Baek²; Sujin Ryu²; Min Young Kwak³; Yehree Kim⁴

¹*Department of Convergence Medicine, University of Ulsan College of Medicine and Asan Institute for Life Sciences, Asan Medical Center;* ²*Department Of Otorhinolaryngology-Head And Neck Surgery, Asan Medical Center, University Of Ulsan College Of Medicine;* ³*Seoul Asan Medical Center;* ⁴*Asan Medical Center*

Free radicals formed in the inner ear in response to high-intensity noise are regarded as detrimental factors for noise-induced hearing loss (NIHL). The present study was designed to understand the preconditioning effect of cobalt chloride (CoCl₂), a well-known hypoxia mimetic, on oxidative stress-mediated cytotoxicity. Treatment of mouse auditory cells (HEI-OC1) with 100~200 μM CoCl₂ for 6 h promoted cell proliferation, concomitant with increases in the expressions of two redox-sensitive transcription factors (hypoxia-inducible factor 1α; HIF1α,

erythroid 2-related factor 2; Nrf2) and an antioxidant enzyme (peroxiredoxin 6; Prdx6). Hydrogen peroxide (25 μM) treatment for 24 h resulted in the induction of HEI-OC1 cell death and the reduction of these protein expressions, which was restored by pretreatment with CoCl₂. Knockdown of HIF1α or Nrf2 attenuated the preconditioning effect of CoCl₂, indicating that they play important roles in CoCl₂-mediated protective mechanism to oxidative injuries. Luciferase reporter analysis with a murine Prdx6 promoter revealed that HIF1α and Nrf2 transactivated Prdx6 gene expression. Therefore, the protective effect of CoCl₂ is achieved through distinctive signaling mechanism involving HIF1α, Nrf2, and Prdx6.

PS 1019

Evaluating Autophagy Compounds as Potential Therapies for Mammalian Aminoglycoside-Induced Hair Cell Loss

Clara Draf¹; Taylor Wyrick²; Eduardo Chavez³; Kwang Pak³; Allen F. Ryan⁴

¹*Department of Surgery / Otolaryngology, University of California, San Diego;* ²*Department of Otorhinolaryngology, Head and Neck Surgery, St. Elisabeth- Hospital, Clinic of the Ruhr University of Bochum;* ³*Department of Surgery / Otolaryngology, University of California, San Diego;* ⁴*Department of Surgery / Otolaryngology, University of California, San Diego; San Diego VA Medical Center;* ⁴*Department of Surgery / Otolaryngology; Department of Neurosciences, University of California, San Diego; San Diego VA Medical Center*

Background: Autophagy allows cells to safely degrade and recycle dysfunctional components. There is evidence of autophagy participation in hair cell (HC) damage. However, whether autophagy functions to protect or damage HCs remains unclear. Our goal was to perform a high throughput screen of compounds targeting different aspects of autophagy and their effects on HC death due to aminoglycoside ototoxicity.

Methods: The SELLECKChem autophagy compound library consisting of 154 compounds was used to screen an *in vitro* mouse model of ototoxicity. Organ of Corti (oC) from postnatal day 3-5 pou4f3/GFP transgenic mice in which HCs express green fluorescent protein (GFP) were utilized. The oC were micro-dissected, the apical turns discarded, and basal and middle turns were divided into segments (micro-explants). Each micro-explant was placed into a single well of a 96-well plate. Triplicate of each compound were treated with 200μM of gentamicin (GM) plus three dosages of a test compound, with an additional triplicate testing only the highest dose. Three wells with micro-explants containing media alone served as negative controls. For positive ototoxicity controls,

three wells were treated only with GM. The samples were then maintained in culture for 72 hours post GM treatment. Explants were photographed every 24 hours and HCs counted for each day.

Results: The majority of the 154 autophagy-inducing or -inhibiting compounds had no effect on GM-induced HC loss. However, a subgroup of compounds exhibited a significant, dose-dependent protective effect. Another subset enhanced HC loss, even in the absence of GM.

Conclusions: The disparate results obtained with the autophagy compounds tested point out the complexity of autophagy events that influence HC responses to aminoglycosides. Moreover, our study evaluated many autophagy compounds that have not been tested previously on HCs. Our findings could serve as a basis for further studies with these compounds as potential drug targets.

PS 1020

Statins Offer Protection against Cisplatin-induced Ototoxicity in Mice and Humans

Katharine Fernandez¹; Thomas Townes²; Paul Allen³; Carmen Brewer⁴; Deborah Mulford⁵; LaGuinn P. Sherlock⁶; Shawn Newlands⁵; Candice Ortiz²; Nicole Schmitt⁷; Lisa Cunningham⁸

¹NIDCD/NIH; ²Walter Reed National Military Medical Center, Bethesda, MD; ³University of Rochester Medical Center; ⁴NIDCD; ⁵Department of Otolaryngology, University of Rochester Medical Center, Rochester, NY; ⁶Army Public Health Center / Walter Reed National Military Medical Center; ⁷National Institute on Deafness and Other Communication Disorders, NIH, Bethesda, MD; ⁸National Institute on Deafness and Other Communication Disorders, National Institutes of Health

Introduction:

Though highly effective as a life-saving antineoplastic agent, cisplatin often induces ototoxic damage that results in a permanent sensorineural hearing loss. Induction of heat shock proteins (HSPs), including heme-oxygenase-1 (HO-1, also known as HSP32), reduces cisplatin-induced hair cell death *in vitro* (Baker et al., 2015). Statins, a class of drugs used in the clinical management of high cholesterol, can activate HO-1 and decrease reactive oxygen species (ROS; Beltowski et al., 2008). Recent animal studies have shown that pravastatin (Park et al., 2012) and atorvastatin (Jahani et al., 2016) reduce cochlear injury in noise exposed mice, while simvastatin protects against aminoglycoside-induced sensory hair cell death *in vitro* (Brand et al., 2011). Here we are examining the potential for statin co-therapy to reduce cisplatin ototoxicity in mice and humans.

Methods

Animals: Adult CBA/CAJ mice underwent distortion product otoacoustic emission (DPOAE) and auditory brainstem response (ABR) testing to evaluate auditory function pre- and post-cisplatin treatment. Mice were administered Lovastatin (40 or 60 mg/kg) once daily while undergoing 3 cycles of cisplatin administration which consisted of 3 mg/kg/day for 4 days followed by 10 recovery days. Upon completion of treatment, cochleas were collected for histological analysis.

Humans: A retrospective analysis was conducted using patient data from multiple sources that included audiograms collected before, during, and after cisplatin treatment. Changes in hearing were calculated relative to pre-treatment baseline audiograms, and the presence of hearing loss was identified according to ASHA criteria and graded using the TUNE ototoxicity scale.

Results

Lovastatin reduced cisplatin-induced sensory hair cell death and hearing loss in mice. In humans our data suggest reduced incidence and severity of cisplatin-induced hearing loss in statin users relative to individuals who were not on a concurrent statin therapy. Both retrospective and prospective studies in humans are ongoing.

Conclusions

Statins have been in clinical use for decades with few reports of side effects and have recently been reported to exert mild anti-tumor properties (Ledo et al., 2018). Concurrent use of a statin co-therapy with cisplatin-based chemotherapy may offer a low-risk approach to minimizing ototoxicity without jeopardizing the success of cancer treatment.

This work was supported by the NIDCD Division of Intramural Research

PS 1021

Lasting SENS-401 Protection of Cochlear Hair Cells in Organ of Corti Explant Cultures following Gentamicin Ototoxic Insult In Vitro

Audrey Broussy; Montserrat Bosch-Grau; Jonas Dyhrfeld-Johnsen
Sensorion

Aminoglycoside antibiotics are used to treat life-threatening bacterial infections but can cause hearing loss due to cochlear hair cell death. While many efforts have been made to develop strategies for aminoglycoside ototoxicity prevention, no pharmaceutical treatment

is currently approved. SENS-401 is a small molecule, clinical stage oral drug candidate which has previously demonstrated enhanced hearing outcomes through otoprotection with enhanced outer hair cell survival rat models of severe acoustic trauma induced hearing loss and cisplatin induced ototoxicity. We here present in vitro results suggesting a potential efficacy of SENS-401 in the treatment of hearing loss from aminoglycoside ototoxicity. Organ of Corti explants from P3 Wistar rat pups were cultured in 24 well plates and hair cells loaded with FM1-43 dye for 4h after which the culture medium was changed for 24h incubation. Following a baseline scan, medium for groups of cultures (n=2-5) were changed to 1 mM gentamicin for 24h. Live cell imaging was performed every 6h for 120h with quantification of the fluorescence density of FM1-43 normalized to group mean at baseline. The assay was initially validated in two repeated experiments using co-application of the reference compound minocycline (10 and 100 μ M; Corbacella et al. 2004, Wei et al. 2005), reproducing the reported otoprotective effect at 24h (1.6-2.1 fold enhanced hair cell survival), but also demonstrating that this effect was transient until ~36h post gentamicin application with no lasting otoprotection at 120h. Co-application of 1-3 μ M SENS-401 with gentamicin in three repeated experiments resulted in an early, milder enhancement of outer hair cell survival most robustly observed at 36h after gentamicin application (1.2-1.7 fold enhanced hair cell survival), however in contrast to minocycline, SENS-401 showed robust and lasting otoprotective effects 120h after gentamicin administration reaching 1.5-2 fold enhancement of hair cell survival in two out of three experiments. These preliminary results suggest that SENS-401 would be potential treatment for hearing loss due to aminoglycoside ototoxicity, consistent with a mechanism of action able to reduce hair cell death through both the extrinsic and intrinsic apoptotic pathways. Further experiments will determine the extent of functional otoprotection against aminoglycoside toxicity by oral administration of SENS-401 in vivo.

PS 1022

Protective Effect of Anti-oxidant Avenanthramide-C on Ototoxicity

Alphonse Umugire¹; Munyoung Choi²; Dami Kim¹; Sungsu Lee²; Hyong-Ho Cho²

¹Department of Biomedical Science, College of Medicine, Chonnam National University Graduate School, BK21 PLUS Center for Creative Biomedical Scientists at Chonnam National University; ²Hearing and Neurotology lab, Department of Otolaryngology-Head and Neck Surgery, Chonnam National University Hospital

Introduction

Sensorineural hearing loss has no adequate chemicals to prevent or treat so far. Noise exposure instigates various physical damages and cellular changes within the cochlear hair cells that result in hearing loss. ROS found in the cochlea orchestrates cascade reactions with different molecules within the cochlea and disrupt normal physiological mechanisms, and results in hair cell death. Avenanthramide (AVN) extracted from oat possesses antioxidant properties and exert protection on various cell types. In this present study, we wanted to investigate whether AVN-C can protect auditory hair cell and preserve hearing from ototoxicity.

Methods

Wild type C57BL/6 mouse was randomly used in 6 to 12 per individual study. Mouse tissue fluid samples were analyzed using Liquid Chromatography-mass spectrophotometry to detect AVN-C in mouse tissue fluids. Mice were subjected under noise stimuli centered at 100 dB, 8 kHz for 6 hours once a day for 7 days with or without pre-treatment of 10 mg/kg of AVN-C. ABR thresholds measurement were done. Outer hair cells were visualized by immunohistochemistry using confocal microscope. HEI-OC cells were treated with AVN-C and gentamicin in vitro; flow cytometry and RT-qPCR were conducted.

Results

AVN-C reached its climax into mouse serum after 1 hour post I.P. injection and decreased with time, to be washed out within 6 hours. Furthermore, AVN-C crossed blood brain barrier and peaked within 2 hours. The permeability of AVN-C towards blood labyrinth barrier was outlined by its presence into perilymph and noise exposure enhanced its clearance. Pre-treatment of AVN-C 24 hours contributed to preserve hearing to temporary threshold shift noise. Moreover, in Permanent threshold shift with 100 dB for 7 days, AVN-C proved to procure prominent protection to noise overstimulated subjects, one month post noise exposure. Cochlea histological analysis demonstrated loss of outer hair cells (OHCs) in noise induced only group, and preservation of OHCs in AVN-C pre-treated subjects confirming the noteworthy protective effect provided by AVN-C over noise overexposure. AVN-C exhibited protective effect, and thwarted the toxicity caused by Gentamicin when treated to HEI-OC cell culture 24 hours in advance to Gentamicin. Several apoptotic and reactive oxygen species (ROS) genes were downregulated by AVN-C.

Conclusion

AVN-C provided a significant protective effect over ototoxicity in noise overexposed wild type subjects, and revealed to be a good candidate molecule for future therapy on sensorineural hearing loss.

PS 1023

cAMP Enhancer, Forskolin Prevents Cisplatin-induced Hearing Loss Promoting Non-sensory Supporting Cell Survival

Yeon Ju Kim¹; Oak-Sung Choo²; Young Sun Kim¹; Jeong Hun Jang¹; **Yun-Hoon Chung**²
¹Ajou University School of Medicine; ²Department of Otolaryngology, Ajou University School of Medicine

Background: The sensory epithelium of the inner ear contains mechano-sensory cells, known as hair cells, each of which is surrounded by non-sensory supporting cells. Supporting cells are directly connected to adjacent supporting cells with gap junctions that allow ions and small molecules up to 1 kDa. Our previous studies showed that pharmacological regulation of gap junctions prevents cisplatin-induced ototoxicity. From this study, we encountered with some questions. Which molecules (< 1kDa) can propagate the ototoxicity through the gap junction channels and which GJ-controlling chemicals can specifically induce the prevention of hearing loss without influencing the anti-cancer effect of cisplatin? The purpose of this study was to find specific small molecules passing through gap junction channels and their control chemicals in the process of cisplatin-induced auditory cell death and suggest new mechanisms to prevent ototoxic hearing loss.

Methods: Chemical reagent (2-APB, Ru360, Forskolin, SQ22536, KT5823 and DAGi) regulating different small molecules passing gap junctions were used to analyze the changes in ototoxicity against cisplatin. We selected agents and explored their oto-protective activity and cellular mechanisms in response to systemic cisplatin treatment with *in vitro* and *in vivo* studies. And also the effect of the identified chemical on anticancer effect of cisplatin was evaluated using nude mice.

Results: Treatment with forskolin, an inducer of cyclic adenosine monophosphate (cAMP) significantly prevents House Ear Institute-Organ of Corti 1 (HEI-OC1) cell death against cisplatin and gap junction enhancer markedly increases the cell viability. *In vivo* administration of forskolin reduced the hearing threshold shifts with activating cAMP response element binding protein (CREB) in the supporting cells under cisplatin treatment. Additionally, treatment of forskolin enhanced the chemotherapeutic effects of cisplatin in A549 xenograft tumor model for lung cancer, while protecting inner ear from ototoxicity.

Conclusions: We propose that the increase of cAMP promotes supporting cell survival through PKA/CREB phosphorylation, finally resulting in increase of hair cell survival after cisplatin damage. cAMP enhancer, forskolin may be a suitable candidate to prevent hearing loss from the use of cisplatin.

Acknowledgments : This research was supported by the Basic Science Research Program through the National Research Foundation of Korea (NRF) funded by the Ministry of Education, Science, and Technology (NRF-2015R1A2A15055956).

PS 1024

Mitigating Cisplatin Ototoxicity by Targeting the Unfolded Protein Response in a Novel Mouse Model

Stephanie L. Rouse; Jiang Li; Ian R. Matthews; Elliott H. Sherr; Dylan K. Chan
University of California, San Francisco

Background: Cisplatin is a widely used chemotherapeutic drug, despite a common side effect of irreversible sensorineural hearing loss. Oxidative stress has been implicated in cisplatin-induced ototoxicity, leading to development of candidate therapies, but more upstream targetable mechanisms have not been fully explored. In endoplasmic reticulum (ER) stress, misfolded proteins accumulate in the ER, activating the unfolded protein response (UPR) in an effort to restore proteostasis. Severe ER stress induces apoptosis. Recent work from our group implicated the UPR in genetic and noise-induced hearing loss, strengthening the link between ER stress, UPR upregulation, and hearing loss. In the current study, we sought to investigate the UPR as a target to prevent cisplatin ototoxicity.

Methods: Using a novel single-dose cisplatin ototoxicity model (5.5 mg/kg intraperitoneal (IP) injection in 8-wk-old Balb/C mice), we measured pure-tone ABR thresholds and UPR expression via qPCR for CHOP, BiP, S-XBP1 and caspase 3. Hair cells were counted by whole-mount immunohistochemical staining for MyoVIIa and actin. In a complementary *in vitro* model, HEK cells were treated with 50 μ M cisplatin for 48 hours and then processed for qPCR analysis.

Results: This optimized model of cisplatin ototoxicity in mice produced consistent, high-frequency, permanent threshold shifts with no weight loss or morbidity. We saw isolated 50-dB shifts in 32-kHz ABR thresholds up to PID21 with no change at 8 and 16 kHz. Upregulation of genes representing the three major arms of the UPR \square CHOP, BiP, and XBP-1 \square was seen after cisplatin exposure in HEK cells and WT Balb/C mice, showing that cisplatin induces ER stress. We then tested the

efficacy of the small-molecule UPR and stress response modulator ISRIB (Integrated Stress Response Inhibitor), which activates eIF2B and leads to decreased synthesis of the pro-apoptotic protein Chop (C/EBP-homologous protein). A single concurrent IP dose of ISRIB (10 mg/kg) reduced cisplatin-induced 32-kHz threshold shifts by 38 dB SPL (32-kHz ABR thresholds: 90.0 ± 9.1 for vehicle-treated vs. 52.0 ± 12.0 dB SPL (mean ± SD) for ISRIB-treated (n=6 for each; p < 0.001)) and basal-turn hair-cell death by 49.4% (57.2% ± 20% (vehicle) vs. 7.8% ± 11.8% (ISRIB); p < 0.01) in this mouse model.

Conclusions: Pharmacologic downregulation of the pro-apoptotic arm of the UPR significantly attenuates cisplatin-induced hearing loss and ototoxicity in this novel mouse model optimized for consistent threshold shifts and minimal toxicity. These results suggest further investigation of the UPR as a promising target for preventing cisplatin-related ototoxicity.

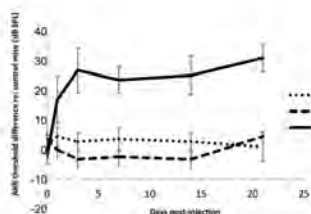


Figure 1. Single-dose cisplatin model of ototoxicity. 8-wk-old WT Balb/C mice were injected with 5.5 mg/kg cisplatin (CP) or vehicle (control) in a single intraperitoneal dose. Pure-tone ABR thresholds were measured at 8, 16, and 32 kHz on post-injection days (PID) 0, 1, 3, 7, 14, and 21 (n=6 CP, 3 control mice). The difference between CP and control group ABRs is shown here (difference in means ± SEM).

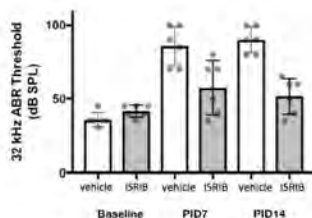


Figure 2. ISRIB protects against cisplatin-induced ototoxicity. Pure-tone 32 kHz ABR thresholds were measured at baseline, post-injection day (PID)7, and PID14 in 8-week-old WT Balb/C mice after IP injection of 5.5 mg/kg cisplatin + 10 mg/kg ISRIB (n=6, grey) or cisplatin + vehicle (n=6, white).

Ototoxicity II

PS 1025

Lower Ototoxicity and Absence of Hidden Hearing Loss point to Gentamicin C1a and Apramycin as Promising Antibiotics for Clinical Use

María Beatriz Durán Alonso¹; Masaaki Ishikawa²; Nadia García-Mateo¹; Alen Čusak³; Iris López-Hernández¹; Marta Fernández-Martínez⁴; Marcus Müller⁵; Lukas Rüttiger⁶; Wibke Singer⁶; Hubert Löwenheim⁶; Gregor Kosec³; Štefan Fujs³; Luis Martínez-Martínez⁷; Thomas Schimmang¹; Hrvoje

Petkovic³; Marlies Knipper⁶

¹Institute of Biology and Molecular Genetics (IBGM); ²Tübingen Hearing Research Center (THRC); ³Acies Bio, d.o.o.; ⁴University Hospital Marqués de Valdecilla IDIVAL; ⁵Hearing Research Center, Department of Otolaryngology - Head & Neck Surgery, University of Tübingen Medical Center; ⁶University of Tübingen; ⁷University Hospital Reina Sofia

Background: Spread of antimicrobial resistance and shortage of novel antibiotics have led to an urgent need for new antibacterials (Maura *et al.* 2016, *Curr Opin Microbiol* 33: 41-46; Tacconelli *et al.* 2018, *Lancet Infect Dis* 18: 318-327). Although aminoglycoside antibiotics (AGs) exhibit potent antimicrobial activity, their use has been largely restricted due to serious side-effects, mainly nephrotoxicity and ototoxicity (Forge and Schacht 2000, *Audiol Neurootol* 5: 3-22; Huth *et al.* 2011, *Int J Otolaryngol* 2011: 937861). It is therefore of great importance to identify AGs of strong antibacterial activity that lack their most harmful side effects.

Methods: A large number of AGs were tested against a series of multidrug-resistant clinical isolates of the ESKAPE panel; of these, five AGs showing strong antibacterial activity were selected to evaluate their ototoxicity. A stepwise approach was followed, aiming at setting up a protocol that could be used in future high-throughput screenings. *In vitro* tests were initially conducted by assessing the viability of two established otic cell lines following AG treatment, and subsequently on murine cochlear organotypic cultures, by analysing hair cell survival. *In vivo* work was then carried out on a guinea pig model, following local round window application of the AGs.

Results: Commercial gentamicin mixture (GM), the GM congener gentamicin C1a (GM C1a), apramycin (Apra), paromomycin (Paro) and neomycin (Neo) were selected for ototoxicity testing. *In vitro* analyses confirmed GM and Neo as the most toxic of the tested AGs, and Apra and Paro as those with the lowest toxicity; interestingly, GM C1a appeared to be less toxic than GM. Regarding the *in vivo* work, a dose-dependent effect of AGs on outer hair cell (OHC) survival and compound action potentials (CAPs) showed that GM C1a and Apra were the least toxic. Strikingly, although no changes were observed in CAP thresholds and OHC survival following treatment with low concentrations of Neo, GM and Paro, the number of inner hair cell (IHC) synaptic ribbons and the CAP amplitudes were reduced. This indication of hidden hearing loss was not observed with GM C1a or Apra at such concentrations.

Conclusion: These findings have: (a) validated our screening approach, approach that will now be used for high-throughput testing of newly isolated AG congeners, (b) revealed the IHCs as the inner ear's most vulnerable element to AG treatment, and (c) identified GM C1a and Apra as promising bases for the development of clinically useful antibiotics.

PS 1026

Development of Clinically Relevant Ex Vivo Models of Cisplatin-Induced Hearing Loss

Phillip Uribe; Pranav D. Mathur; Stephanie Szobota; Anne Harrop-Jones; Fabrice Piu; Alan C. Foster; Bonnie Jacques
Otonomy, Inc.

Background: Platinum-based chemotherapies are commonly used to treat many forms of cancer; however, they are highly ototoxic and many people treated with cisplatin develop significant hearing loss. This is particularly problematic in children where hearing loss can dramatically impact language acquisition and social skills. In the inner ear, the cells most susceptible to cisplatin damage are the hair cells, spiral ganglion neurons (SGNs) and marginal cells of the stria vascularis, and damage to any of these cell types can contribute to hearing deficits. To identify otoprotective agents that may prevent cisplatin-induced hearing loss (CIHL), clinically relevant models are needed that mimic the range of mild to severe hearing loss observed in patients. Thus, we sought to develop a comprehensive array of ex vivo models of CIHL that can be used as screening tools for otoprotectants with therapeutic potential. These included cisplatin-exposed cochlear explants to differentially evaluate damage to hair cells and SGNs as well as a novel ex vivo model of stria vascularis damage.

Methods: P2-P4 Sprague-Dawley rats were used for all experiments. Whole organ cochlear explants were established, allowed to acclimate overnight, then treated for 24-72 hours with various concentrations of cisplatin. Explants were fixed and stained for hair cell and SGN markers to evaluate cell death/viability. For evaluation of marginal cells, the stria vascularis was isolated, cut into small pieces or dissociated in trypsin, then seeded onto culture plates. Strial cells were expanded for 48-72 hours, then were exposed to cisplatin for 22 hours. Cell death was determined by activated Caspase 3.

Results: A clear dose response in hair cell and SGN damage was observed for cisplatin between 3.0 and 50 μM when explants were treated for 48-72 hours. Interestingly, the damage profile was different between hair cells and SGNs, with each having a characteristic

dose range of maximal cell loss, suggesting that cisplatin-sensitive cell types may respond differently depending on their clinical dosing regimen. A dose response for marginal cell damage in strial cultures was also observed with cisplatin between 10 and 100 μM .

Conclusions: An optimized, comprehensive set of clinically relevant ex vivo models of mild to severe CIHL using neonatal cochlear explants to assess hair cell and SGN damage was developed. In addition, a novel model to evaluate cisplatin-induced damage in the marginal cells of the stria vascularis was developed. Combined, these models represent good screening tools for the evaluation of otoprotective compounds against CIHL.

PS 1027

Exosomes Mediate Intercellular Communication in the Inner Ear

Andrew Breglio¹; Lindsey A. May¹; Nora Welsh¹; Shimon Francis¹; David Anderson²; Ronald Petralia¹; Ya-Xian Wang¹; Matthew Wood³; **Lisa Cunningham**¹
¹*National Institute on Deafness and Other Communication Disorders, National Institutes of Health*; ²*National Institute of Diabetes and Digestive and Kidney Diseases*; ³*Department of Physiology, Anatomy and Genetics, University of Oxford*

Introduction: We have previously demonstrated that induction of heat shock proteins (HSPs) is protective against ototoxic drug-induced hair cell death, and that this protective effect is non-cell-autonomous (May et al., 2013; Baker et al., 2015, Francis et al., 2017). Here we investigated the roles of secretory exosomes as mediators of non-autonomous protective signaling in the inner ear. Exosomes are endosomally-derived extracellular vesicles that carry protein, lipid, and nucleic acid cargo and can interact with target cells either by being internalized or by signaling through cell surface receptors. Signaling via exosomes can alter function in target cells. Exosomes are emerging as important mediators of intercellular signaling in a variety of systems.

Methods: Whole-organ cultures of utricles from adult mice were heat shocked, and exosomes were purified from media surrounding heat shocked utricles. Isolated exosomes were applied to utricle cultures in the presence or absence of neomycin. Hair cell counts were performed on fixed, myosin 7a-labeled utricles. Exosomes were quantified using nanoparticle tracking analysis. Exosome biogenesis was inhibited using spiroepoxide, an inhibitor of neutral sphingomyelinase 2. Exosome cargo was analyzed using mass spectrometry and RNA-Seq.

Results: Our data indicate that heat shocked utricles release exosomes—a type of extracellular vesicle—and that these exosomes carry a variety of proteins, including HSP70. Isolated exosomes were sufficient to improve the survival of hair cells exposed to neomycin, while inhibition of exosome biogenesis using spiroepoxide abolished this protective effect. Toll-like receptor 4 (TLR4) expression on hair cells was necessary for the protective effect of exosomes.

Conclusions: Our results indicate that exosomes are a previously-undescribed mechanism of intercellular communication in the inner ear; they can mediate a critical role in hair cell survival, and they may have potential as a therapy modality for hearing loss.

This work was supported by the NIDCD Division of Intramural Research.

PS 1028

The Role of Retrograde Intraflagellar Transport Genes in Aminoglycoside-induced Hair Cell Death

Tamara Stawicki¹; Tor Linbo²; Liana Hernandez²; Lauren Parkinson¹; Danielle Bellefeuille¹; Edwin Rubel²; David W. Raible²

¹Lafayette College; ²University of Washington

Background

Aminoglycoside antibiotics cause hair cell death which can lead to hearing loss and vestibular dysfunction in patients taking these medications. Mutations in a number of cilia-associated genes lead to resistance to neomycin-induced hair cell death. Of these genes two different retrograde intraflagellar transport (IFT) mutants seem to show comparable levels of reduced hair cell death but differing levels of reduced neomycin uptake into hair cells with the retrograde motor gene, *dync2h1*, showing a greater reduction than the IFT-A adaptor molecule gene, *wdr35* (Stawicki et al., 2016).

Methods

The effect of retrograde IFT genes on aminoglycoside induced hair cell death was investigated by exposing animals to aminoglycosides and counting hair cells. Additionally, to look at aminoglycoside and FM1-43 uptake animals were exposed to neomycin-Texas Red or FM1-43 and the level of fluorescence in hair cells was quantified.

Results

To further investigate whether different classes of retrograde IFT genes differently affect aminoglycoside entry into hair cells we investigated mutants in the retrograde IFT motor gene, *dync2h1* and three additional IFT-A adaptor genes, *ift122*, *ift140*, and *wdr19*. We found that mutations in all these genes lead to reduced hair cell

death in response to neomycin as well as a significant reduction in aminoglycoside and FM1-43 entry into hair cells comparable to what had previously been seen in *dync2h1* mutants. To test whether *dync2h1* and *wdr35* are really protecting hair cells via different mechanisms, as we had originally hypothesized due to the differences in uptake in these mutants, we investigated these mutants' response to gentamicin, which has been shown to involve a slightly different cell death mechanism than neomycin. We found that mutations of both genes lead to a similar level of resistance to gentamicin-induced hair cell death. We also generated double mutants and found that there was no additive protection to neomycin-induced hair cell death in these animals.

Conclusions

We conclude that mutation of either retrograde IFT motor genes or adaptor molecule genes will significantly impair aminoglycoside uptake into hair cells and thus reduce hair cell death in response to these drugs.

PS 1029

Upregulation of Transient Receptor Potential Vanilloid 1 (TRPV1) Exacerbates Aminoglycoside-Induced Hearing Loss

meiyan Jiang¹; Hongzhe Li²; William Meier¹; Anastasiya Johnson¹; Yuan Zhang¹; Farshid Taghizadeh¹; Allan Kachelmeier¹; Peter S. Steyger¹
¹Oregon Health & Science University; ²VA Loma Linda Healthcare System

Background: Clinically-essential aminoglycoside antibiotics, particularly gentamicin, can induce permanent loss of cochlear sensory cells, leading to life-long hearing loss. Previously, we have demonstrated experimentally that cell lines expressing Transient Receptor Potential Vanilloid-1 (TRPV1) channels preferentially take up gentamicin, and that agonists or antagonists of TRPV1 can modulate this uptake. In other models, inflammatory signaling increases cellular expression of TRPV1.

Aim: We hypothesized that inflammatory signaling upregulates cochlear expression of TRPV1 *in situ*, increases aminoglycoside entry into hair cells *in vitro*, and, is required to potentiate cochlear uptake of aminoglycosides and cochleotoxicity *in vivo*.

Methods: C57BL/6, *Trpv1*^{-/-} or *Tlr4*^{-/-} mice, or cochlear coil explants from *Pcdh15*^{-/-} mice, received saline (controls), or 1 mg/kg (1 µg/ml) lipopolysaccharides (LPS), as a model of bacterial infection, prior to treatment with (fluorescently-tagged) gentamicin for 1 hour. Fixed cochleae were processed for TRPV1 immunofluorescence. Cochlear uptake of (fluorescently-tagged) gentamicin was assessed by confocal

microscopy or enzyme-linked immunosorbent assays. For chronic ototoxicity studies, we followed the method of Koo, Quintanilla-Dieck et al. (2015) with a modified dose of 850 mg/kg kanamycin twice daily for 15 days, and both auditory brainstem responses and distortion product otoacoustic emissions were obtained using an extended frequency range (4-48 kHz).

Results: In fixed cochleae, TRPV1 is immunolocalized near the apical membranes of hair cells and adjacent supporting cells in the sensory epithelium, as well as marginal cells in the stria vascularis. Exposure to immunostimulatory LPS, significantly increased cochlear expression of TRPV1 *in situ* in wildtype mice, but not in *Trpv1^{-/-}* or *Tlr4^{-/-}* mice. LPS also significantly increased outer hair cell uptake of gentamicin, including outer hair cells from *Pcdh15^{-/-}* mice lacking functional MET apparatus, *in vitro*. *In vivo*, exposure to lipopolysaccharides exacerbated aminoglycoside-induced auditory threshold shifts and outer hair cell loss in wildtype mice, but not in *Trpv1^{-/-}* mice.

Conclusion: These data suggest that upregulating cochlear expression of TRPV1 is required to exacerbate aminoglycoside-induced cochleotoxicity in models of systemic bacterial infection, *in vivo*.

Supported by R01 DC04555, R01 DC012588, and P30 DC005983.

PS 1030

Screening Hair Cell Toxicity in Autophagy Library using the zebrafish lateral line

Yoshinobu Hirose; Kazuma Sugahara; Makoto Hashimoto; Hiroshi Yamashita
Department of Otolaryngology, Yamaguchi University Graduate School of Medicine

Zebrafish lateral line hair cells are physiologically and morphologically similar to inner ear hair cells. As the zebrafish lateral line is located on the body surface, damage to the hair cells can be rapidly assessed. Therefore, the zebrafish lateral line is an effective system for the evaluation of drugs that damage or protect hair cells. We have been used to screen protective effect of supplement and herbal medicines drugs, and damage effect of anti-cancer drugs.

Autophagy is one of the mechanisms of cells to break down intracellular proteins. It is a mechanism found in eukaryotic organisms from yeast to humans, preventing the accumulation of abnormal protein in the cell, recycling proteins when protein synthesis is excessive or when the nutrient environment deteriorates. It is involved in maintenance of homeostasis of living organisms by eliminating pathogenic microorganisms invaded into the cytoplasm. In addition, it is known to

be involved in programmed cell death in the process of ontogeny, occurrence of diseases such as Huntington's disease, and inhibition of canceration of cells.

There will be a possibility that autophagy plays an important role in the inner ear. In this research, we have used the zebrafish lateral line to screen a library of 94 Autophagy drugs (Cancer Research Institute of Kanazawa University Drugs Set) that induce or inhibit autophagy for hair cell toxicity.

5 dpf Zebrafish embryos of the AB wild-type strain were produced by paired mating of adult fish. For drug library screening, 5-dpf larval zebrafish were incubated with 2 μ M YOPRO-1 (Invitrogen) in embryo medium for 20 min. Zebrafish were then rinsed three times in embryo medium. Zebrafish larvae were exposed to the drug library for 1 or 6 h (screened separately) and then anesthetized with MS222 and imaged by fluorescence microscopy to determine whether hair cells were lost or showed evidence of damage. For drugs identified as potential ototoxic drugs from the initial screen and confirmatory retesting, dose response testing was performed. Anti-parvalbumin was used as a primary antibody, hair cells were immunostained. Hair cells from the SO1, SO2, O1, and OC1 neuromasts were counted with a fluorescent microscope.

This study will show the effect of autophagy in the hair cells.

PS 1031

Toxic effects of 3,3'-iminodipropionitrile on utricle in adult mice

Shan Zeng¹; Wenyan Li²; Huawei Li²

¹*ENT Institute and Otorhinolaryngology Department, Affiliated Eye and ENT Hospital, State Key Laboratory of Medical Neurobiology, Fudan University, 2 NHC Key Laboratory of Hearing Medicine (Fudan University);* ²*1 ENT Institute and Otorhinolaryngology Department, Affiliated Eye and ENT Hospital, State Key Laboratory of Medical Neurobiology, Fudan University. 2 NHC Key Laboratory of Hearing Medicine (Fudan University)*

Utricles are vestibular sense organs that is believed having limited ability to repair itself in mice. Since genetic therapy to vestibular hair cell regeneration is still the most promising cure for hair cell injury, it's very important to establish a reliable and convenient mouse vestibular injury model. This work sought to investigate the toxic effect in adult mouse utricle by IDPN injected *in vivo* and to explore the self-recovery mechanism of adult mouse utricle. Different dose of IDPN were intraperitoneal injected to adult mouse (P30). Utricle Hair cell (HCs) and Supporting cells (SCs) were counted after injury. Swim test and rotating VOR test were employed to evaluate vestibular function after IDPN injected. Spontaneous proliferation of supporting cells were observed in severe

injured utricle. RT-qPCR showed transient up-regulated of Hes5 & Hey1 and fluctuating up-regulated of Axin2 & β -catenin after IDPN administration. These results conclude us that IDPN induced vestibular cells loss is dose-dependent as well as the vestibular function. Type I HCs are more vulnerable to IDPN. Single time intraperitoneal injection of IDPN can be used to establish appropriate injured utricle model in adult mouse *in vivo*. Rotating VOR test is more accurate to evaluate vestibular function than behavior and swim test. Vestibular function would recover when HCs loss was light which required no proliferation of hair cells and supporting cells. Limited SC spontaneous regeneration only happened in severe injured utricle when SCs loss is significant which might induced by transient up-regulated of Notch signaling and fluctuating up-regulated of Wnt signaling. **Key words** IDPN, Utricle, Vestibular function, Self-regeneration

PS 1032

Cisplatin Entry Routes and Ototoxicity in Mammalian Sensory Hair Cells

Siân R. Kitcher; Richard T. Osgood; Guy Richardson; Corné J. Kros
University of Sussex

Background

Cisplatin is a potent chemotherapy drug used to treat solid malignancies, but causes irreversible sensorineural hearing loss in almost all patients treated. Hearing loss induced by cisplatin is due to the death of basal-coil outer hair cells (HCs). This pattern of damage is also seen after treatment with the aminoglycoside (AG) antibiotics, known to enter cochlear HCs through their mechano-electrical transducer (MET) channels. Evidence from the zebrafish lateral line has shown that functional mechano-electrical transduction is required for cisplatin-induced HC death (Thomas et al 2013 *J Neurosci* 33:4405; Vargo et al 2017 *Front Cell Neurosci* 11:393). We therefore sought to investigate whether cisplatin enters mouse cochlear HCs via the MET channel.

Methods

Organotypic cochlear cultures were prepared from CD-1, $Myo7a^{+/Sh6J}$ or $Myo7a^{Sh6J/Sh6J}$ mice at postnatal day 2 and incubated for 24 h prior to use. To assess ototoxin-induced damage, cultures were incubated with 5 μ M cisplatin or 50 μ M Texas Red-conjugated cisplatin (CPTR) for 48 h prior to fixation, immunohistochemistry and quantification of HC survival. MET currents were recorded from outer HCs during exposure to 100 μ M cisplatin using the whole-cell configuration of the patch-clamp technique. To assess loading and cellular distribution of fluorescently-conjugated ototoxins,

cultures were incubated with CPTR or Texas Red-conjugated gentamicin (GTTR) for short (10 min) or long (24-72 h) time periods and then imaged live or fixed and imaged by confocal microscopy.

Results

After treatment with 5 μ M cisplatin, the survival of outer HCs in cultures prepared from $Myo7a^{Sh6J/Sh6J}$ mice was significantly higher than that observed in cultures prepared from $Myo7a^{+/Sh6J}$ mice. Cisplatin did not, however, block MET currents when applied to outer hair cells at a concentration of 100 μ M. Cultures prepared from wild-type mice show no evidence of loading with CPTR after a duration of 10 minutes (a time frame within which GTTR clearly loads). Over longer incubation periods loading is seen in surviving HCs in both $Myo7a^{Sh6J/Sh6J}$ and $Myo7a^{+/Sh6J}$ cultures.

Conclusions

Although cisplatin may enter into cultured mouse cochlear hair cells via the MET channel, the rate of entry must be slow and cannot be measured by electrophysiology or visualised with fluorescent imaging. The MET channel is unlikely to be the only route of entry as transduction-deficient hair cells load with CPTR over longer durations. Functional mechano-electrical transduction is, however, required for toxicity.

Supported by Action on Hearing Loss and the MRC

PS 1033

GTTR Induces the Formation of Membranous Cytoplasmic Bodies in Cochlear Hair Cells

Richard T. Osgood; Siân R. Kitcher; Corné J. Kros; Guy Richardson
University of Sussex

Background

Treatment with aminoglycoside (AG) antibiotics can lead to kidney damage due to cytotoxic effects on proximal tubule cells and, in the inner ear, permanent sensorineural hearing loss caused by the death of sensory hair cells. Whilst AGs have been demonstrated to enter hair cells by endocytosis, their primary route of entry is believed to be via the mechano-electrical transducer (MET) channel. Indeed, AGs are not toxic to hair cells with non-functional MET channels, such as those in the $Myo7a^{Sh6J/Sh6J}$ mouse, and a number of MET channel blockers can protect hair cells from AG toxicity.

Methods

Here we use cochlear cultures, gentamicin conjugated to Texas Red (GTTR), and ultrastructural analysis by

transmission electron microscopy (TEM) to investigate the relationship between the distribution of GTTR in the hair cell, cytological changes, and ototoxicity.

Results

Using a low-dose, long-duration *in vitro* assay we find GTTR is slightly more ototoxic to basal-coil outer hair cells than the parent compound, gentamicin (LD50 GTTR = 0.9 μ M, LD50 gent = 2.0 μ M). Whilst GTTR (0.2 μ M) does not load rapidly (within 10 mins) into the hair cells of *Myo7a^{Sh6J/Sh6J}* mice, when hair cells in both wild-type and *Myo7a^{Sh6J/Sh6J}* mice are exposed to a 5-10 fold higher concentration (1-2 μ M) over longer periods (24-48 h) GTTR is observed in discrete punctate structures *and* within the cytoplasm. TEM reveals the primary ultrastructural change caused by GTTR in wild-type hair cells after 24 h is the presence of multi-lamellar, lipid-rich inclusion bodies that are comparable to those observed in proximal tubular cells during AG treatment *in vivo*, with a proportion of the bodies contained within a limiting membrane. The morphology of these structures is similar to those observed in the myeloid/zebra bodies that are found in lysosomal storage disorders. Using a concentration of non-conjugated gentamicin with a toxicity comparable to GTTR, such lipid-rich inclusion bodies are not observed in wild-type hair cells after 24 h.

Conclusions

These results show that the appearance of multi-lamellar inclusion bodies in GTTR-treated cultures precedes hair cell death, and that hair cells in *Myo7a^{Sh6J/Sh6J}* cultures are protected from GTTR over 48 h, despite the presence of such structures. The significance of these inclusions for toxicity therefore remains unclear; however either AG entry through the MET channel, or more likely, given the cytosolic localisation of GTTR in *Myo7a^{Sh6J/Sh6J}* hair cells, functional mechano-electrical transduction itself *is* required for ototoxicity.

PS 1034

Gut Microbiota Regulates Cochlear Immunity and Cisplatin Induced Inflammation

Soumen Roy; Carolyne Smith; Raquel Costa; Bathai Edwards; Jonathan Badger; Amiran Dzutsev; Shurjo Sen; Simone Difilippantonio; Misty Peck; Giorgio Trinchieri
NCI

Research backgrounds: Nearly 360 million people worldwide suffer from profound deafness (report from the World Health Organization). 40%-80% of cancer patients develop permanent hearing loss due to the exposure of life-saving drugs, such as cisplatin. Unfortunately, mammalian hair cells cannot regenerate once they are damaged due

to various ototoxic insults. Although cisplatin has a shorter half-life in systemic circulation, however, the clearance of protein-bound platinum drug remains a critical challenge in the clinic, which might be impacted by local or systemic cochlear immunity. Recently it is established that the gut microbiota regulates chemotherapy and immunotherapy. In addition, gut microbiota also play a very important role in drug metabolism and tissue homeostasis. However, the role of gut microbiota in cisplatin-induced ototoxicity is not known. We hypothesize that gut microbiota regulates a defined subset of immune cells in the cochlea and cisplatin-induced inflammation.

Methods: Immunohistochemistry is a great tool for identifying various cell types in whole tissue or in a section of the cochlea and provides spatial information. However, it cannot simultaneously capture the entire immune cell profile within the cochlea for a higher degree of quantification. Here, for the first time, we utilized high-dimensional flow cytometry to study the complex populations of leukocytes in the cochlea. The whole murine cochlea is processed into single cell suspensions; myeloid and lymphoid cells are stained with the following antibodies: Live/ dead, B220, CD45, CD11b, CD11c, Ly6G, Ly6C, F4/80, Siglec F, MHC-II, CXCR2, CD3, CD4, CD8, NK1.1. In addition to this high-resolution multispectral imaging for localizing tissue-resident immune cells, Inductively Coupled Plasma Mass Spectrometry (ICP-MS) for platinum clearance, RNA-seq for gene expression and flow cytometry-based ROS quantifications are done for better understanding the cochlear immunity and inflammation.

Results: By utilizing high-dimensional flow-cytometry techniques we defined cochlear immunity in the untreated cochlea, which has different immune cell frequencies compared to blood-borne immune cells. Our preliminary data further indicates that gut microbiota play a significant role in maintaining a specific subset of immune cells in the cochlea, which ultimately regulate cochlear inflammation via facilitating platinum clearance. Additionally, our preliminary data shows the presence of different frequency of immune cells in sensory regions, stria vascularis and in vestibular regions.

Conclusions: Understanding the role of gut microbiota in cisplatin toxicity and cochlear immunity will help us to reduce drug-induced ototoxicity, which will maximize the therapeutic window of the cancer drugs and ultimately enhance the quality of life of cancer patients.

PS 1035

Expression Patterns of Wnt and Notch Signaling in Cochlear Hair Cell Injury Models

Hao Chiang¹; Niliiksha Gunewardene¹; Albert Edge²

¹Department of Otolaryngology and Laryngology, Harvard Medical School and Eaton-Peabody Laboratory, Massachusetts Eye and Ear Infirmary; ²Department of Otolaryngology, Harvard Medical School

Supporting cell proliferation and hair cell generation in the postnatal cochlea can be achieved with the appropriate activation or inhibition of signaling pathways. We have recently shown that hair cell damage influences Wnt signaling. We sought here to document the expression patterns of Wnt and Notch signaling pathways after hair cell injury. We compared canonical Wnt activity in a TCF/Lef:H2B-GFP reporter mouse line among 3 *in vivo* injury models: (1) aminoglycoside-induced hair cell loss in newborn mice; (2) diphtheria toxin (DT)-induced hair cell ablation in Gfi1-Cre driven inducible DT receptor (DTR) newborn mice; and (3) noise exposure in adult mice. We further dissected the expression of regulators of Wnt signaling in Gfi1-Cre;iDTR mice by qRT-PCR. The localization of altered genes was visualized by RNAscope technology. We next explored the expression of Notch signaling in Gfi1-Cre;iDTR newborn and noise-exposed adult mice by qRT-PCR. A reduced Notch effector expression in Gfi1-Cre;iDTR and an increased Notch effector expression in noise-exposed adult mice suggests that Notch inhibition might facilitate hair cell generation. We also asked if pharmacological perturbation could reverse the signaling activity. Treatment with gamma-secretase inhibitor LY-411575 alone or in combination with GSK3 β inhibitor CHIR99021 partially decreased the active Notch signaling based on qRT-PCR. LY-411575 and a combination of LY-411575 and CHIR99021 also partially reversed the reduced *Atoh1* expression induced by noise exposure. Our findings demonstrate changes in signaling induced by damage to the postnatal cochlea and show that that this dynamic signaling can be altered by manipulation of these pathways in both newborn and adult animals.

PS 1036

Gentamicin Subtype Permeation of The Hair Cell Mechanotransducer Channel

Yohan Song¹; Mary E. O'Sullivan²; Robert Greenhouse²; Alan G. Cheng²; Anthony J. Ricci²

¹Stanford University School of Medicine; ²Stanford University

Introduction: Aminoglycosides are a widely used antibiotic against gram-negative bacteria whose side effect is ototoxicity. Ototoxicity derives from the selective loss of the sensory hair cells. Hair cells are sensitive to

aminoglycosides because these compounds permeate through the large nonselective mechanoelectric transducer channels located in the stereocilia. The recent ability to separate hospital gentamicin into its individual subtypes demonstrated a variation in ototoxicity that did not always correlate with changes in antimicrobial activity (See abstract by O'Sullivan). Present work investigates whether differences in ototoxicity are due to alterations of channel permeation by the subtypes.

Methods: Ototoxicity was assayed using a tissue culture protocol (described in O'Sullivan abstract). MET channel permeation was measured using the whole cell voltage clamp technique on rat outer hair cells (Postnatal day 8) and mechanically stimulating hair bundles using a stiff glass probe attached to a piezo electric stack. In this way, a 6-point dose response curve could be generated at different holding potentials for each drug concentration. MET currents were separated from other conductances using stimuli that elicit maximal on and off responses.

Results: All 7 tested compounds reduced the MET current in a dose-dependent manner at negative potentials. Each acted as a permeable blocker having little effect on MET currents at positive potentials. Differences in temporal block of the MET current for several compounds show that drugs can enter and block at different rates. EC50s for block were very similar for 6/7 compounds while one additional compounds were much less permeable. There was not a clear correlation between permeation and ototoxicity.

Discussion: Each of the subtypes of gentamicin acts as permeable blockers of the MET channels. The lack of correlation between permeation and ototoxicity suggests that hair cell access does not limit drug action within the cell. This begs the question as to what additional variations might be responsible for changes in ototoxicity? These changes might be related to additional actions within the hair cell that might include ribosome interaction and ability to alter protein synthesis, actions on alternative sites such as PIP2 or voltage-gated potassium channels. Data demonstrate that gentamicin remains permeable to hair cells despite multiple modifications altering charge ratios.

Acknowledgements: This work was supported by grants RO1 DC003896 and R01 DC014720.

Prosthetic Devices

PS 1037

Intralabyrinthine vs Distant Reference Electrodes for Multichannel Vestibular Prosthesis in Rhesus Monkeys

Pengyu Ren¹; Abderrahmane Hedjoudje¹; Guoliang Wang¹; JoongHo Ahn¹; Mehdi Rahman¹; Peter

Boutros¹; Charles C. Della Santina²; **Chenkai Dai**³
¹*Johns Hopkins University School of Medicine*; ²*Johns Hopkins University*; ³*University of Oklahoma*

Background: Maximizing the selectivity and efficacy of vestibular nerve branch stimulation is a key goal in development of a vestibular implant (VI) intended to restore sensation of 3-dimensional head movement in individuals disabled by chronic bilateral loss of labyrinthine hair cell function. The optimal location for a reference electrode to return current delivered by intraampullary stimulating electrodes has not yet been determined. Generally, “monopolar” stimulation using a distant reference electrode outside the temporal bone elicits bigger responses at lower thresholds but incurs more vestibulo-ocular reflex misalignment due to greater current spread. In contrast, bipolar stimulation between two closely-spaced intra-ampullary electrodes near the target nerve branch can achieve more focal stimulation but requires higher current and more electrodes and a stimulator with multiple independent current sinks. We hypothesized that a compromise between these – placing a near reference in the common crus – could achieve better alignment than a distant-reference monopolar design while still only requiring 4 electrodes and a single current sink.

Methods: To test above hypothesis, four rhesus monkeys were implanted with electrodes in each of three semicircular canals with two reference electrodes: one in the common crus and the other in musculature outside the temporal bone. Safety, performance, surgery and reliability were compared between these two references to provide evidence for better reference electrode option in common crus or musculature. 3D electrically-evoked vestibulo-ocular reflex (eeVOR) responses were recorded using each of the two reference electrodes for a comparison.

Results: Both reference electrode locations yielded eeVOR responses that aligned approximately with the target canal for at least one stimulating electrode per ampulla. Compared to using a distant reference, stimulation via a common crus reference achieved a slight but significant reduction in eeVOR misalignment, required higher stimulus current to achieve a given eeVOR magnitude, and yielded higher facial nerve activation threshold and wider dynamic range of stimulus current from eeVOR response threshold to onset of visible facial movement. Reliability was good for both reference electrode locations, which yielded stable results over 36 months of episodic use.

Conclusions: When a VI is constrained to have only a single reference electrode for stimulation – as is the case for a system based on a commercially available cochlear

implant stimulator with a single reference electrode channel and current sink – positioning the reference electrode in the common crus can achieve a slight but significant improvement in eeVOR misalignment and dynamic range.

Funding: Support: NIH/NIDCD R01DC009255 and R01DC13526

PS 1038

The Effect of Stimulation and Reference Electrode Location on Electrically-evoked Vestibulo-Ocular Reflex Eye Movements in Chinchillas

Margaret Chow¹; Kristin Hageman¹; Peter Boutros¹; Brian Morris¹; Angela Tooker²; Dale Roberts¹; Razi Haque²; Charles C. Della Santina²
¹*Johns Hopkins School of Medicine*; ²*Lawrence Livermore National Laboratory*

Background: Frequency modulation of pulsatile stimulation targeting vestibular nerve endings in the three semi-circular canals (SCCs) has been shown to partially restore the angular vestibulo-ocular reflex (aVOR), but suboptimal strength and selectivity of the electrode-nerve interface due to current spread in the labyrinth can result in responses that are weak and/or poorly aligned with the target canals. Seeking to optimize electrode array design to determine spatial tolerances for surgical implantation, we systematically varied stimulation and reference electrode locations and quantified effects on the magnitude and alignment of 3D binocular aVOR responses to prosthetic electrical stimulation targeting the SCCs in alert chinchillas.

Methods: We fit five chinchillas with head posts and binocular scleral coils for tracking 3D eye movements. After characterizing normal 3D eye movement responses to head rotation, we implanted a polyimide vestibular electrode array with 26 otolith, 24 SCC, and 2 distal reference contacts into the left ear of each animal. Trains of cathodic-first, charge-balanced, symmetric biphasic current pulses were delivered to head-fixed animals in darkness, eliciting sensation of a ‘virtual’; head movement and driving purely electrically-evoked 3D aVOR responses. Eye movements were recorded during sinusoidal pulse frequency modulation stimuli at a constant current amplitude and pulse phase duration using various stimulation electrodes on arrays with 8 electrode contacts separated by 150 um center-to-center (each 101um in diameter) along a linear array inserted into each SCC’s ampulla and a return electrode in the common crus. Holding stimulus conditions constant, the magnitude of the 3D aVOR responses peaked at one optimal electrode in each of the three SCCs in all five animals.

Results: In all five animals, the magnitude of the maximum eye velocity produced from a stimulating/electrode pair could be fit to an exponential model as a function of the distance of the stimulating electrode from the optimal electrode. Due to poor ocular response and therefore poor goodness-of-fit (R-squared

Conclusions: Anatomical and surgical variation can cause the response decay distance to vary significantly between animals and canals. However, in order to obtain well-aligned and strong vestibular response in the form of ocular reflexes, placement must be optimized. These data indicate that a surgeon has a position tolerance of about 200um to place an optimal stimulation electrode.

PS 1039

The Effect of Common Crus Reference Electrode Depth on Electrically-evoked Vestibulo-Ocular Reflex Eye movements in Rhesus Macaque

Brian Morris¹; Margaret Chow²; Abderrahmane Hedjoudje³; Kantapon Wiboonsaksakul¹; Dale Roberts¹; Kathleen E. Cullen¹; Roland Hessler⁴; Charles C. Della Santina¹

¹Johns Hopkins University; ²Johns Hopkins School of Medicine; ³Johns Hopkins University School of Medicine; ⁴MED-EL GmbH

Background: Prosthetic electrical stimulation targeting vestibular nerve endings in semicircular canals (SCCs) can partially restore the angular vestibulo-ocular reflex (aVOR), but suboptimal strength and selectivity of the electrode-nerve interface due to current spread can result in responses that are weak or poorly aligned with the target canals. This is especially a problem for a vestibular implant based on a cochlear implant stimulator that only has a single reference electrode channel. Modeling and a review of archival data suggested that inserting a vestibular implant's return electrode deeply in the common crus (CC) should yield better responses than a distant reference outside the temporal bone or a shallow CC electrode. To test this hypothesis, we examined 3D aVOR responses as a function of CC electrode location in a rhesus monkey implanted unilaterally with an electrode array comprising 3 CC reference electrodes, 11 ampullary stimulating electrodes and a distant reference.

Methods: Stimuli were trains of cathodic-first, charge-balanced, symmetric biphasic current pulses delivered to a head-fixed animal in darkness, eliciting sensation of 'virtual'; head rotations and driving purely electrically-evoked 3D aVOR responses. For each stimulating and reference electrode pair, 3D aVOR response were recorded using scleral coil oculography as a function of pulse current over 0-300 uA, with pulse duration and

pulse train frequency held constant. Reference electrode comparison focused on the one ampullary electrode per SCC that yielded the largest aVOR response.

Results: Compared to responses elicited using a distant reference, stimuli returned via the deepest common crus reference elicited a greater maximum eye velocity and lower misalignment for each ampulla (t-tests on CC/distant reference ratio: p=0.0209 and 0.0077, respectively). For 300 uA stimuli returned via the distant reference, the aVOR component aligned with the target SCC ranged from 26 to 46°/s and 3D misalignment ranged from 36 to 75°. Using the deepest CC reference, velocity ranged from 36 to 181°/s and misalignment from 3.7 to 57°.

Conclusion: Prosthetic stimulation using intra-ampullary vestibular implant electrodes yield stronger and more selective ampullary nerve stimulation when current is returned to a deeply inserted common crus electrode as a reference, as opposed to a distant reference. Common crus reference electrodes further from the vestibule yielded performance intermediate between the deep common crus and distant references. These data suggest that when a stimulator only has one reference electrode channel, placing the reference in the common crus near its junction with the vestibule achieves superior performance.

PS 1040

Combined Ionic Direct Current and Pulse Frequency Modulation to Improve Dynamic Range of Vestibular Canal Stimulation

Felix Aplin; Dilawer Singh; Charles Della Santina; Gene Fridman
Johns Hopkins University

Introduction: Vestibular prostheses emulate normal vestibular function by electrically stimulating the vestibular system using pulse frequency modulation (PFM). Spontaneous activity at the vestibular nerve may limit the dynamic range elicited by PFM. One proposed solution is the co-application of ionic direct current (iDC) to inhibit this spontaneous activity and PFM to modulate afferent firing rate. We tested the hypothesis that a tonic iDC baseline delivered in conjunction with PFM to the vestibular semicircular canals could improve the dynamic range of evoked eye responses.

Methods: Wild-type chinchillas were treated bilaterally with intratympanic gentamicin to mimic human vestibular dysfunction and implanted with microcatheter tubes in the left posterior and superior semicircular canals. Animals were adapted to both constant iDC offset and a pulse frequency baseline and then modulated via pulse frequency steps. Responses to stimulation were

assessed by recording vestibulo-ocular reflex (VOR) direction and velocity with an eye tracking rig.

Results: Modulation of the vestibular nerve produced VOR responses aligned to the stimulated canal. Introduction of an iDC baseline lead to a statistically significant increase in eye response velocity for VOR movements elicited via a down modulation of pulse frequency, without influencing the direction of eye rotation.

Conclusions: Our results suggest that a tonic iDC baseline may inhibit spontaneous activity in the vestibular nerve and thus increase the dynamic range available to pulsatile vestibular modulation. However, the magnitude of the effect was small compared to the total dynamic range of the system and so may not be pragmatically useful as a tool to improve existing stimulation strategies. Further research into iDC delivery for vestibular canal stimulation should focus on more promising iDC modulation strategies.

PS 1041

Using Vestibular Prosthesis to Restore Yaw Rotation Perception in Primates with Bilateral Vestibular Hypofunction

Kantapon Wiboonsaksakul; Oliver R. Stanley; Charles C. Della Santina; Kathleen E. Cullen
Johns Hopkins University

The vestibular system senses movement of the head and provides information crucial for appropriate reflexes and vestibular perception. Patients with bilateral loss of vestibular function not only experience disequilibrium, visual instability, and dizziness due to impaired vestibular reflexes but also suffer from loss of vestibular perception. To help improve the quality of life of these patients, there has been a recent focus on the development of devices to replace vestibular function. One emerging approach has been centered on a prosthesis that senses head rotation and translates the movement into ampullary stimulation, substituting for the damaged vestibular periphery. Recent experiments in our groups have characterized the efficacy of our vestibular prosthesis on the vestibulo-ocular reflex (VOR) and vestibulocollic reflex in nonhuman primates. However, to date, its ability to restore vestibular perception in nonhuman primates has not been explored. Here, we investigated the use of the vestibular prosthesis to restore yaw rotation perception in primates. A unilaterally vestibular-deficient rhesus monkey was trained to distinguish between passive left and right yaw rotations in a two-alternative forced-choice discrimination task. After the performance stabilized, the monkey underwent prosthetic implantation on the normal side, resulting in

a bilateral vestibular hypofunction (VOR gain < 0.15 bilaterally). We quantified the task performance and generated psychometric curves in light (with visual cues) and in darkness (without visual cues) for pre-surgery (unilaterally deficient), post-surgery (bilaterally deficient), and prosthesis (bilaterally deficient with prosthesis on) conditions. Prior to the surgery, the supra-threshold (30 deg/s at 1 Hz) performance in darkness was stable at ~75%, and dropped to near chance (~55%) after the implantation. Using the standard stimulation mapping, initial sessions with the prosthesis on showed an increase in performance to ~60%, indicating an improvement in yaw rotation perception. Future work will investigate the neural correlates of the perceptual improvement, in addition to employing a comparable psychophysical-based methodology in human patients.

PS 1042

Electrically Evoked Compound Action Potentials obtained in humans with a Hybrid Cochlear-Vestibular Implant

T. A. Khoa Nguyen¹; Konrad Schwarz²; Samuel Cavuscens³; Maurizio Ranieri³; Nils Guinand³; Raymond Van de Berg⁴; Herman Kingma⁴; Silvestro Micera⁵; Jean Philippe Guyot³; **Angélica Perez-Fornos**³

¹*Division of Functional Neurosurgery, Department of Neurology, Inselspital Bern*; ²*MED-EL*; ³*Service of Otorhinolaryngology and Head and Neck Surgery, Department of Clinical Neurosciences, Geneva University Hospitals*; ⁴*Division of Balance Disorders, Faculty of Health Medicine and Life Sciences, Department of Otorhinolaryngology and Head and Neck Surgery, School for Mental Health and Neuroscience, Maastricht University Medical Center*; ⁵*Bertarelli Foundation Chair in Translational Neuroengineering, EPF Lausanne*

Research Background: To characterize electrically evoked compound action potentials (eCAPs) using electrodes implanted in the cochlea and in the peripheral vestibular system.

Methods: Patients with bilateral vestibular loss and severe hearing loss received a hybrid cochlear-vestibular implant (MED-EL, Austria). We recorded eCAPs in 4 implanted patients for three setups: i) a cochlear setup, where stimulation and recording electrode were in the cochlear array; ii) a mixed setup, where the stimulation electrode was in the cochlear array and the recording electrode in a vestibular branch or vice versa; and iii) a trans-canal setup, where the stimulation electrode was in one vestibular branch and the recording electrode in another vestibular branch. In one subject, we additionally measured eCAPs during continuous stimulation to

investigate potential adaptation mechanisms.

Results: We successfully recorded eCAPs for all setups. Cochlear-vestibular and vestibular-vestibular eCAPs exhibited similar morphology as cochlear-cochlear eCAPs with two peaks. However, peak-to-peak voltages for cochlear-cochlear eCAPs were markedly larger than for the other setups. Amplitude growth functions for all setups displayed sigmoidal shape with distinct segments below and above threshold. Recovery functions for cochlear-cochlear eCAPs had a clearer exponential shape than the other setups. The investigation of eCAPs during continuous stimulation revealed very fast adaptation of the responses.

Conclusions: Our findings suggest that eCAP recordings with a vestibulo-cochlear implant could be used to reduce erroneous activation of non-target neurons by primarily guiding electrode placement during surgery. Post-operatively, the recordings could be leveraged to aid implant programming and as supplemental information about neuronal activation during chronic use.

PS 1043

Controlled Modulation of Posture with a Vestibular Implant in Humans

Angélica Perez-Fornos¹; Stephane Armand²; Maurizio Ranieri¹; Samuel Cavuscens¹; Céline Cretallaz¹; Raymond Van de Berg³; Herman Kingma³; Jean Philippe Guyot¹; Nils Guinand¹

¹Service of Otorhinolaryngology and Head and Neck Surgery, Department of Clinical Neurosciences, Geneva University Hospitals Geneva, Switzerland;

²Willy Taillard Laboratory of Kinesiology, Department of Clinical Neurosciences, Geneva University Hospitals;

³Division of Balance Disorders, Faculty of Health Medicine and Life Sciences, Department of Otorhinolaryngology and Head and Neck Surgery, School for Mental Health and Neuroscience, Maastricht University Medical Center

Research background: To investigate the possibility of evoking controlled postural responses using electrical stimulation delivered by a vestibular implant prototype (VI) in humans.

Methods: Three patients suffering from bilateral vestibular hypofunction received a VI providing 1-3 electrode branches implanted in the ampullae of the semicircular canals. Postural responses were evaluated during 20s trials of the Unterberger test without any electrical stimulation and upon electrical stimulation (charge-balanced biphasic pulse trains, 200µs/phase, 400 pulses-per-second) at different current intensities up- and down-modulated around a constant baseline current. Patient demographics and electrical stimulation

parameters are presented in Table 1. Whole-body postural responses were recorded using a 12-camera motion capture system (Oqus7+, Qualisys AB, Göteborg, Sweden).

Results: Without electrical stimulation, the angular rotation of the patients'; trunk was negligible (gray plots in Figure 1). Upon electrical stimulation, we observed a significant negative correlation between current intensity and trunk rotation in two patients (S1 and S2 in Figure 1). The results for S3 showed a slight, non-significant trend. Linear body motion (distance and direction) was variable and uncorrelated to electrical stimulation. Results for head motion were practically identical, demonstrating that the patients'; whole body moved "in-bloc".

Conclusions: These results demonstrate, for the first time in humans, that whole-body motion can be controlled and modulated using electrical stimulation delivered to the ampullary nerves in humans. These results are very encouraging, suggesting that vestibular implants could potentially provide useful cues to address disabling postural deficiencies (e.g., imbalance) and consequently decrease fall risks.

Table 1. Patient demographics and electrical stimulation details.

ID	Sex	Implanted side	Vestibular electrode	Current amplitudes[µA]
S1	M	left	PAN	300, 325, 350 (baseline), 375, 400
S2	F	left	SAN	300, 325, 350 (baseline), 375, 400
S3	M	left	PAN	250, 300, 350 (baseline), 400, 450

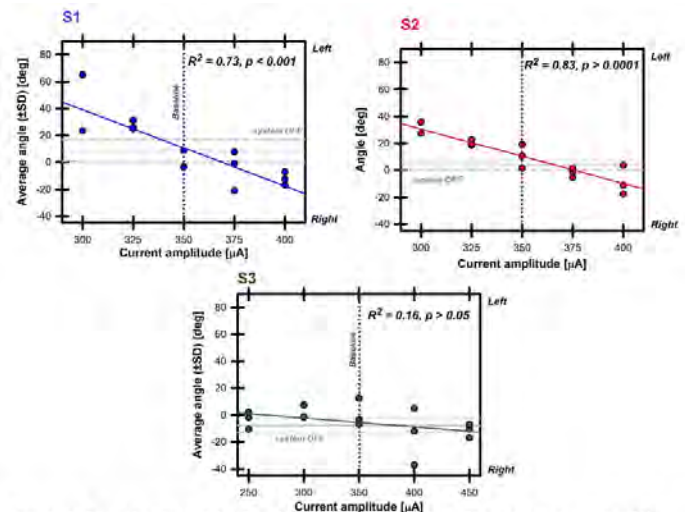


Figure 1. Angular trunk rotation of the three tested patients in each experimental condition. Gray plots represent results without electrical stimulation (system OFF). Colored plots (S1: blue, S2: red, S3: green) present results in the different electrical stimulation conditions. The pink dotted bars mark the "baseline" electrical stimulation level to which the patients were adapted and around which currents were up- and down-modulated.

Regeneration II

PS 1044

In vivo simultaneous ectopic expression of Neurog1 and Neurod1 converts cochlear glia cells into neurons

Xiang Li; Chao Li; Guangqin Wang; Zhenghong Bi; Zhiyong Liu

Institute of Neuroscience, CAS Center for Excellence in Brain Science and Intelligence Technology, Shanghai Institutes for Biological Sciences, Chinese Academy of Sciences

Cochlear spiral ganglion neurons (SGN) receive inputs from inner hair cells and send outputs into cochlear nucleus. Damage or degeneration of SGN will cause hearing impairment. Previous *in vitro* studies indicate that glia cells (that can be marked by *Plp1-CreER+* strain) can be reprogrammed into SGNs by ectopic induction of *Ascl1* alone or together with *Neurod1*. Whether it is the case *in vivo* remains unclear. Here, we addressed this question by simultaneous induction of *Neurog1* and *Neurod1*, which are key bHLH transcriptional factors for SGN development, in cochlear glia cells at neonatal ages. We first generated a new conditional *Rosa26-LSL-Neurog1*3xHA-P2A-Neurod1*3xFlag-T2A-EGFP* /+ knock in mouse strain in which cells with *Neurog1* and *Neurod1* expression can be visualized by EGFP. Secondly, *Plp1-CreER+;Rosa26-LSL-Neurog1*3xHA-P2A-Neurod1*3xFlag-T2A-EGFP* /+ (heterozygous) and *Plp1-CreER+; Rosa26-LSL-Neurog1*3xHA-P2A-Neurod1*3xFlag-T2A-EGFP* / *Rosa26-LSL-Neurog1*3xHA-P2A-Neurod1*3xFlag-T2A-EGFP* (homozygous) strain were experimental group, whereas *Plp1-CreER+; Rosa26-LSL-EGFP* /+ (heterozygous) strain was used as control group. Both groups were given tamoxifen at P0/P1 and analyzed at various ages. As expected, high level expression of *Neurog1* and *Neurod1* protein were observed in experimental but not control group. Furthermore, in control group, all EGFP+ cells were Sox10+ glia cells and we never observed cells expressing both EGFP and neuronal markers such as *Tuj1* and *Map2*. In contrast, in experimental group, 40%-70% EGFP+ cells that expressed *Tuj1* and *Map2*, which were defined as glia-derived new SGNs and frequently observed at P6, P16 and P42. Those new SGNs also decreased expression of glia cell markers Sox10 and Sox2. Interestingly, 5% of those new SGNs also expressed *Gata3* and/or *Mafb*. Notably, such coexpression of EGFP and *Gata3/Mafb* was observed in two copies (homozygous experimental group) but not one copy (heterozygous experimental group), suggesting a dose-dependent efficiency of reprogramming glia into SGN by *Neurog1* and *Neurod1*.

Thirdly, we also manually picked EGFP+ cells that resembled SGN morphology in experimental

group (heterozygous or homozygous) and EGFP+ cells in control group. Our real-time PCR assays showed that, relative to EGFP+ glia cells in control group, new SGNs (EGFP+ in experimental group) significantly enriched *Neurog1*, *Neurod1*, *Tuj1* and *Map2*. Taken together, we concluded that *Neurog1* and *Neurod1* can convert glia cells into SGNs *in vivo*.

PS 1045

A Highly Supplemented Medium Thins F-actin Bands and Stimulates Proliferation of Supporting Cells in Murine Utricles

Mikolaj Kozlowski; Jeffrey Corwin; Mark Rudolf
University of Virginia

Background

In mice, thickening of junction-associated F-actin bands is correlated ($r=0.98$) with postnatal restriction of supporting cell (SC) proliferation. Neither thickening nor restriction occurs in SCs of non-mammals that readily replace hair cells (Burns *et al.*, 2008; 2013). We investigated the potential interplay of F-actin band thickness and SC proliferation in the murine utricle using EFICVP6, a culture medium containing EGF, FGF2, IGF1, vitamin C, and inhibitors of GSK3B, HDAC, and TGFBR1 that McLean *et al.* (2017) developed for expanding dissociated cochlear cells.

Methods

We cultured utricles from P0, P2, P4, P8, P16, and adult mice for 72h in EFICVP6 or control medium and measured S-phase entry using EdU. In other experiments we fixed groups of utricles 24h, 48h, 72h, 96h, and 120h after the start of cultures and measured widths of the adherens junction regions (AJRs) spanning the circumferential F-actin bands that bracket the junctions between neighboring SCs. We cultured other utricles for up to 5 days, adding EdU for the final 24h to determine when S-phase entry occurred.

Results

When P0 utricles were cultured with EFICVP6 and EdU for 72h, Sox2+ SCs increased S-phase entry 8.6-fold ($1,107\pm 279$ vs 128 ± 39 in control medium). Utricles explanted from P2, P4, and P8 mice and cultured with EFICVP6 contained 581 ± 111 , 136 ± 34 , and 11 ± 4 EdU-labeled SCs, respectively, while those from P16 and adults had comparable numbers to the P8 utricles. Thus, even the robustly stimulatory EFICVP6 medium appears to lose effectiveness as neonatal mouse utricles mature.

P8 mouse utricles cultured 72h in control medium showed a 17% reduction of mean AJR width compared

to utricles fixed immediately post-dissection (1.87 ± 0.21 vs 2.26 ± 0.12 μm). However, the widths in P8 utricles cultured 72h in EFICVP6 medium decreased by 52% to 1.09 ± 0.07 μm , which was followed by increases in EdU labeling during the subsequent 48h. In P8 mouse utricles cultured in EFICVP6 medium for 120h, with EdU present for the final 24h, 79 ± 34 Sox2+ SCs were EdU-labeled while only 2 ± 2 were in the control medium.

Conclusions

In short-term cultures EFICVP6 medium stimulates substantial SC proliferation in newborn mouse utricles, but becomes less effective as SCs mature. However, with longer exposure to the EFICVP6 medium the circumferential F-actin bands of SCs in P8 utricles start to thin and that appears to partially reverse the maturational restriction of mammalian SC proliferation, since it is followed by increased S-phase entry.

(Supported by NIDCD R01-DC000200 to JTC and F30-DC016806 to MR)

PS 1046

Combinatorial expression of transcription factors *Atoh1*, *Gfi1* and *Pou4f3* enable the production of ectopic hair cells in the Greater Epithelial Ridge region of the neonatal mouse cochlea

Amrita A. Iyer¹; Hsin-I Jen²; Rizwan Yousaf³; Melissa McGovern⁴; Tiantian Cai⁴; Onur Birol⁵; Sunita Singh⁴; Hongyuan Zhang⁴; Revathi Ravella⁴; Andrew Groves⁶
¹Department of Molecular and Human Genetics, Baylor College of Medicine; ²Program in Developmental Biology Baylor College of Medicine; ³Department of Neuroscience, Baylor college of Medicine; ⁴Department of Neuroscience, Baylor College of Medicine; ⁵Program in Developmental Biology, Baylor College of Medicine; ⁶Department of Neuroscience, Department of Molecular and Human Genetics, Baylor College of Medicine

Inner ear hair cells enable the perception of sound waves through the process of mechano-transduction, rendering them indispensable for hearing. Regeneration of these hair cells occurs naturally in non-mammalian vertebrates like fishes, amphibians and birds. In mammals, these hair cells regenerate at young ages to a minimal extent, in response to specific genetic interventions. One such intervention is the ectopic expression of transcription factor *Atoh1*. It is known that the expression of a transcription factor cocktail comprising *Atoh1*, *Gfi1* and *Pou4f3* can reprogram the transcriptomic signature of mouse embryonic stem cells towards that of inner ear hair cells. However, the effects of these transcription factor combinations on the underlying hair cell genetic network, and the cell types responsive to such reprogramming signals *in vivo*, remain unknown.

We targeted the *Rosa26* locus to allow conditional overexpression of *Atoh1* alone (*Rosa26-A*), *Gfi1*, *Atoh1* (*Rosa26-GA*) and *Gfi1*, *Atoh1*, *Pou4f3* (*Rosa26-GAP*) each. The mice harboring these conditional alleles were bred with the *Sox2^{CreERT2}* strain to achieve overexpression in nonsensory cells of the neonatal cochlea after tamoxifen administration at P1. Immunostaining for hair cell (*Myo7a*, Phalloidin) and supporting cell (*GLAST*) markers was performed after harvesting these cochleae at P8. In response to the combinatorial transcription factor expression, a significantly larger number of ectopic hair cells were generated in the greater epithelial ridge (GER) region of the experimental animals in comparison to the wild type control animals. In the experimental animals, we also observed the presence of GER cells interspersed among the ectopic hair cells which were positive for supporting cell marker, *GLAST*. Our next steps include the determination of alterations in the transcriptomic signature and epigenetic profile of these ectopic hair cells as well as supporting cells through RNA-seq and ATAC-seq respectively.

Through this work, we aim to compare and understand the effect of additional transcription factors *Gfi1* and *Pou4f3* with *Atoh1*, in turning on specific gene networks to reprogram distinct cell populations of the neonatal mouse cochlea into hair cells. Understanding the principles governing mammalian hair cell regeneration may enable achievement of efficient therapeutic strategies for treating human hearing loss.

PS 1047

Transplantation of human pluripotent stem cell-derived cells into the selectively ablated mouse organ of Corti

Hiroki Takeda¹; Anna Dondzillo²; Jessica Randall²; Samuel Gubbels²

¹Kumamoto University and University of Colorado Anschutz Medical Campus; ²University of Colorado Anschutz Medical Campus

Sensorineural hearing loss is caused by the irreversible degeneration or loss of cochlear hair cells in most cases. Stem cell based approaches represent one potential therapeutic option for cochlear hair cell regeneration. The development of this therapy will require a detailed understanding of the process of differentiation from pluripotent stem cells to cochlear hair cells *in vitro*, as well as the conditions that will allow for engraftment and terminal differentiation to functional cells *in vivo* upon transplantation. Here we report on the *in vitro* differentiation of human embryonic stem cells and cochlear transplantation of these cells to the neonatal transgenic mouse cochlea. First, we differentiated

human embryonic stem cells (hESCs) to the preplacodal ectoderm (PPE)-like cells using a previously reported method (Leung, et al. 2013). We then transplanted these differentiated cells into the selectively-ablated neonatal mice cochlea through the round window membrane. Finally we evaluated the localization of transplanted ESC-derived progenitors within the cochlea at several time points after transplantation. We found that hESCs differentiated into PPE-like progenitors as identified by immunocytochemistry and qPCR for up to 14 days *in vitro*. Furthermore, some of the transplanted cells at day 7 of differentiation engrafted in the organ of Corti and some, albeit limited, engrafted cells expressed supporting and/or hair cell markers at 29-30 postnatal days.

PS 1048

Do Highly Conserved Protein Sequences in Non-Mammalian Vertebrates Modulate Hair Cell Regeneration in Zebrafish?

Regina Tsay¹; Jordan Donaldson¹; Robert Boney¹; Phillip Uribe²; Allison B. Coffin¹

¹Washington State University Vancouver; ²Otonomy, Inc.

Hair cells can be damaged from a variety of sources, including excessive exposure to noise or ototoxic drugs, and mammalian hair cells are unable to regenerate after damage. In contrast, non-mammalian vertebrates exhibit robust and often rapid regeneration of hair cells. Our goal is to identify genes that are responsible for hair cell regeneration in innately regenerative species. Previously, we characterized amino acid-level differences between regenerative and non-regenerative vertebrates and identified conserved protein sequences in regenerators that are divergent in mammals and may therefore contribute to differential regenerative capacity. Using our bioinformatics analysis we identified several novel targets as potential modulators of hair cell regeneration, including the catecholamine metabolism protein catechol-O-methyltransferase (COMT), the metabolic regulator inositol hexakisphosphate kinase 2a, the E3 ubiquitin ligase SHRPH, and the telomere-binding protein TERF1. We used CRISPR-Cas9 technology to individually knock out these target genes in transgenic Brn3c:mGFP or myob6:EGFP zebrafish, then determined the effects on hair cell development and regeneration in the lateral line. Zebrafish embryos were co-injected with sgRNA targeting tyrosinase, a gene responsible for pigmentation, to provide a phenotypic readout for CRISPR efficacy. Preliminary results suggest that COMT may influence lateral line development. Ongoing experiments will examine the effects of COMT and the other target genes on hair cell regeneration. We are also using pharmacological

manipulations of the target proteins to further investigate their role in hair cell regeneration. Collectively, these studies enhance understanding of the variety of genetic regulators responsible for hair cell regeneration in non-mammalian species and present new targets to stimulate regeneration in the cochlea.

PS 1049

Inner Ear Vestibular Organs of Vestibular Schwannoma Patients Reveal Features of Sensory Cell Precursors

Tian Wang¹; Davood K. Hosseini²; Grace S. Kim³; Sara E. Billings³; Zahra N. Sayyid²; Yona Vaisbuch²; Robert K. Jackler³; Ivan A. Lopez⁴; Alan G. Cheng⁵

¹Department of Otolaryngology-Head and Neck Surgery, Stanford University School of Medicine; ²Department of Otolaryngology-Head and Neck Surgery, The Second Xiangya Hospital, Central South University; ³Department of Otolaryngology-Head and Neck Surgery, Stanford University School of Medicine; ⁴Department of Otolaryngology-Head and Neck Surgery, Stanford University School of Medicine; ⁵Department of Head and Neck Surgery, David Geffen School of Medicine; ⁵Stanford University

Background:

Hair cells are mechanoreceptors required for vestibular function, and their degeneration is the primary cause of balance dysfunction in humans. Prior work shows that hair cell regeneration occurs after drug damage in mouse and guinea pig utricles - an otolithic organ responsible for detecting linear acceleration. Moreover, hair cell regeneration has been observed in human utricles damaged by aminoglycosides *in vitro*. However, whether hair cell regeneration occurs spontaneously in human utricles *in situ* is not known. Here, we characterized utricles harvested from patients with and without vestibular schwannoma and compared them to live donors'; and cadaveric utricles.

Methods:

Utricles were prepared as whole mount and sections and processed for immunohistochemistry and *in situ* hybridization. Hair cells and supporting cells expressing early hair cells markers (Pou4f3 and Gfi1) were quantified. Patient demographics, audiologic data, and other pertinent health information were collected.

Results:

Utricles were collected from patients with vestibular schwannoma (13), recurrent meningitis (1), and cholesteatoma (1). The average age of vestibular schwannoma patients was 50.5±16.7 years. The tumor size ranged from 0.77 to 18.48 cm². All patients had hearing loss with a pure tone average (PTA) of

72.8±28.1 dB and word discrimination ranging from 0% to 80%. Sixty-seven percent of patients experienced vestibular dysfunction. For patients without vestibular schwannoma, the average age was 58.5±3.5 years. PTA was 94.5±12.0 dB and word discrimination ranged from 44% to 80%. Neither patient had any vestibular dysfunction. For live donors and cadavers (4), the average age was 69.8±8.6 years. They had no history of hearing or vestibular deficits.

Hair cell density in utricles from vestibular schwannoma patients (19.8±9.0 per 10,000µm²) was significantly lower than live donor/cadaveric patients (68.4±7.5 per 10,000µm²) and non-vestibular schwannoma patients (43.0±29.0 per 10,000µm²). No significant difference in supporting cell density was found among groups. In utricles from vestibular schwannoma patients, more than 10% of supporting cells (Myosin7a-/Sox2+) expressed Pou4f3 or Gfi1, which we validated using *in situ* hybridization. By contrast very few (<5%) supporting cells in non-vestibular schwannoma and live donors/cadaveric utricles expressed Pou4f3 and Gfi1.

Conclusions:

Utricles from patients with vestibular schwannoma had significantly fewer hair cells and more hair cell precursors than live donors'; and cadaveric utricles.

Funding:

This work was supported by **NIDCD/NIH R21DC015879**, National Natural Science Foundation of China 81670938 (T.W.), **NIDCD/NIH RO1DC013910**, and California Initiative in Regenerative Medicine RN3-06529 (A.G.C.) and the Oberndorf family.

PS 1050

An in vivo model for thyroid regeneration and folliculogenesis

Yoshinori Takizawa¹; Manabu Iwadate²; Yo-Taro Shirai³; Seiji Hosokawa⁴; Shioko Kimura³

¹Department of Otorhinolaryngology, Seirei Mikatahara General Hospital; ²Department of Thyroid and Endocrinology, Fukushima Medical University School of Medicine.; ³Laboratory of Metabolism, National Cancer Institute, National Institutes of Health, Bethesda, Maryland, USA; ⁴Department of Otorhinolaryngology/Head and Neck Surgery, Hamamatsu University School of Medicine,

While thyroid is considered to be a dormant organ, when required, it can regenerate through increased cell proliferation. However, the mechanism for regeneration remains unknown. Nkx2-1(fl/fl);TPO-cre mouse thyroids exhibit a very disorganized appearance because their thyroids continuously degenerate and regenerate. In mouse thyroids, a cluster of cells are found near the

tracheal cartilage and muscle, which are positive for expression of NKX2-1, the master transcription factor governing thyroid development and function. In the present study, we propose that this cluster of NKX2-1-positive cells may be the precursor cells that mature to become thyroid follicular cells, forming thyroid follicles. We also found that phosphorylation of AKT is induced by NKX2-1 in the proposed thyroid progenitor-like side-population cell-derived thyroid cell line (SPTL) cells, suggesting the possibility that NKX2-1 plays a role in differentiation through the modulation of AKT signaling. This study revealed that Nkx2-1(fl/fl);TPO-cre mice provide a suitable model to study in vivo regeneration and folliculogenesis of the thyroid.

PS 1051

Hydrogels as Matrix for Neuritogenesis of Spiral Ganglion Neurons

Verena Scheper¹; Noushin Kakuan¹; Anayancy Osorio-Madrado²; Thomas Lenarz¹; **Jana Schwieger**¹
¹Hannover Medical School; ²University of Freiburg

Background: Bridging the distance between electrode contacts and neurons to be excited is a prerequisite for neuroprostheses to improve the electrical stimulation and therefore the nerve-electrode-interaction. In the context of cochlear implants spiral ganglion neuron (SGN) dendrites may grow out of the bony modiolus towards the fluid filled scala tympani where they are faced with an unattractive environment and do not proceed growing towards the electrode array. Here we investigate different hydrogels as matrix for neuritogenesis.

Methods: Alginate and chitosan in different viscosities were investigated in vitro for their feasibility as matrix for SGN-neuritogenesis. SGN-explants were harvested from neonatal rats (postnatal day 3-5) and cultivated for 5 days in alginate or on chitosan. Alginate from brown algae species *Lessonia nigrescens* (very flexible) and *Lessonia trabeculata* (very stiff) consists of copolymers of D-mannuronic acid (M) and L-guluronic acid (G). Depending on the crosslinking-cation, its concentration and the ratio of the copolymers we received alginates of varying mechanical properties. Chitosan is a co-polysaccharide of β(1→4)-linked D-glucosamine (GlcN) and N-acetyl D-glucosamine (GlcNAc), mainly produced by N-deacetylation of chitin. In this work, different concentrations of a highly-deacetylated chitosan (DA: 2.5%), high molecular weight and low polydispersity index was used. Explants were cultured in A) softer alginate (pure *L. trabeculata*, 0.65% in NaCl) crosslinked by 2mM BaCl-addition or B) stiffer alginate (1:1 mixture of *L. nigrescens* and *L. trabeculata* 0,65% in NaCl), crosslinked by BI) 2mM BaCl-addition or BII) 20mM BaCl-addition.

Additionally, explants were cultivated on CI) 0.7%, CII) 1.0%, CIII) 1.3% or CIV) 2.0% Chitosan. All conditions were cultured with medium containing either 50ng/ml BDNF, or 100ng/ml CNTF, or 50ng/ml BDNF+100ng/ml CNTF or 10% fetal bovine serum (positive control) or no supplements (negative control). The number and length of neurites growing in contact with the gels were detected.

Results: The number and length of outgrowing neurites was significantly increased in BI) ultra-high viscosity-alginate compared to lower viscosity alginate. Neurons did adhere on the 2.0% chitosan but did not grow onto the surface or into the gel. In contrast, hydrogels of lower chitosan concentrations supported the outgrowth of neurites on their surface. In all used hydrogels, the addition of growth factors positively influenced the outgrowth but CNTF did result in the longest neurites detected.

Conclusion: Alginate as well as chitosan are promising matrixes for the neurogenesis of SGN to bridge the neuron-electrode gap, especially if they are combined with growth factors.

PS 1052

Importance of Atf5a and Atf5b in Hair Cell Development and Regeneration in the Larval Zebrafish Lateral Line

Roberto Rodriguez¹; Luis Colon¹; Aranza Torrado¹; Gaurav Varshney²; Martine Behra¹

¹University of Puerto Rico, Medical Sciences Campus;

²Oklahoma Medical Research Foundation

Hair cell (HC) loss is the leading cause of deafness and other hearing and balance disorders. HCs are mechanoreceptors in sensory epithelia of the vertebrate inner ear, which is deeply embedded in the skull and therefore difficult to access and study. HCs are lost because of defective development, or lack of regeneration after ototoxic damage. Remarkably, some lower vertebrates like birds, amphibians and fish can regenerate HCs. In amphibian and fish larvae, HCs are also found in the lateral line (LL), a superficial sensory organ that is composed of skin-deep stereotypically distributed patches named neuromasts (NMs) that only persist in adult fish. NMs contain HCs surrounded by support cells (SCs) that have been demonstrated to be HC progenitors. Because of easy access for manipulation and observation, zebrafish NMs became a prime *in vivo* tool for molecular studies of HC development and regeneration. I will be using this tool to assess the role of the *activating transcription factor 5* (*atf5*) gene in those two processes. This gene is known for its importance in proliferation of progenitor cells and was shown to be crucial in mice for maintenance, and

possibly regeneration, of olfactory sensory neurons (OSNs), which are sensory cells closely related to HCs. In zebrafish, there are two *atf5* orthologues: *atf5a* and *atf5b*. We found that *atf5a* is strongly expressed in olfactory epithelia, and weakly in NMs, whereas *atf5b* is strongly expressed in NMs but not in nasal pits, pointing to a potential complementary or redundant function in NMs. Using CRISPR-Cas9 technology, we generated loss-of-function *atf5a* and *atf5b* lines. Preliminary analysis of one of *atf5a*-KO alleles (*atf5a^{upr3}*) showed no overt developmental or regeneration phenotype, and homozygotes were viable and raised to adulthood. However, we found that *atf5b* gene expression was strongly upregulated in homozygote *atf5a^{-/-upr3}* NMs. We are currently establishing stable *atf5b*-KOs as well as double *atf5a/atf5b*-KOs lines, in which we will assess HC development and regeneration. These mutant lines will allow to dissect the respective role and contribution of each *atf5* ortholog. While one gene might be able to compensate for the other, at least in NMs where they are both expressed, we expect that when both *atf5a* and *atf5b* gene products are missing, HC development and regeneration will be strongly affected. Our work will shed light on this still understudied gene family in the context of the Biology of Hearing.

PS 1053

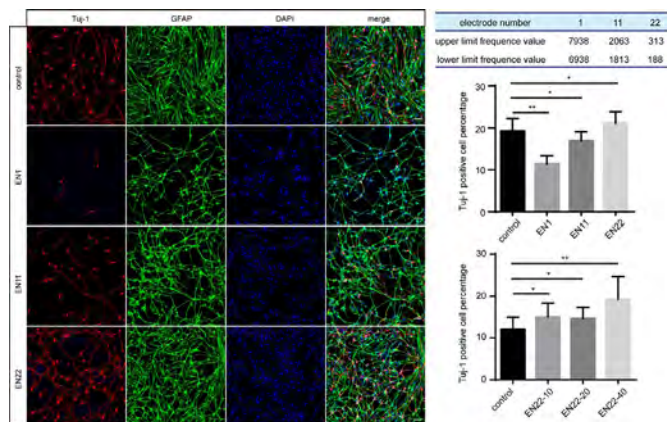
Cochlear Implant-Based Electrical Stimulation Modulates Neural Stem Cell-Derived Neural Regeneration

Rongrong Guo¹; Mingliang Tang¹; Renjie Chai²

¹Southeast University; ²Key Laboratory for Developmental Genes and Human Disease, Ministry of Education, Institute of Life Sciences, Southeast University, Nanjing, China.

Cochlear implantation is now the best therapeutic method for the profound sensorineural hearing loss. However, insufficient numbers of functional spiral ganglion neurons hinder the clinical effects of cochlear implantation. Stem cell transplantation is believed to provide a novel strategy for spiral ganglion neuron regeneration after injury. Some obstacles still need to be overcome, such as low survival, less migration into the site of the injury, uncontrolled differentiation and lack of functional regenerative neurons. It is promising to modulate neural stem cells behavior to address the mentioned issues by novel technologies. Here, a device capable of electrical stimulation was designed by combining cochlea implant and graphene substrate. Neural stem cells or primary spiral ganglion neurons were cultured on the graphene substrates and subjected to electrical stimulation transduced from sound by cochlear implant. Cell behaviors were further studied. It was found that this device was biocompatible for both neural stem cells and spiral ganglion neurons.

More importantly, prolonged electrical stimulation could promote neurite outgrowth of spiral ganglion cells, which may be through enhanced development of growth cone located on the tips of neurites. Furthermore, the results show that prolonged electrical stimulation with complex frequency induced neural stem cell death and apoptosis. Interestingly, electrical stimulation could promote neural stem cells to proliferate and enhance the differentiation into neurons when high-frequency stimulation was removed. Current study provides experimental evidence for understanding the regulatory role of electrical stimulation in stem cells, and highlights the potentials of this abovementioned device in stem cell therapy for hearing loss treatment.



PS 1054

Supporting Cells in the Adult Mouse Cochlea Convert into Hair Cells After Reprogramming with Multiple Hair Cell Transcription Factors

Melissa McGovern¹; Rizwan Yousaf²; Amrita A. Iyer³; Hsin-I Jen⁴; Tiantian Cai¹; Onur Birol⁵; Sunita Singh¹; Revathi Ravella¹; Hongyuan Zhang¹; Andrew Groves⁶
¹Department of Neuroscience, Baylor College of Medicine; ²Department of Neuroscience, Baylor college of Medicine; ³Department of Molecular and Human Genetics, Baylor College of Medicine; ⁴Program in Developmental Biology Baylor College of Medicine; ⁵Program in Developmental Biology, Baylor College of Medicine; ⁶Department of Neuroscience, Department of Molecular and Human Genetics, Baylor College of Medicine

In the mature mammalian cochlea, sensory hair cells (HCs) detect sound stimuli from the environment and transduce them to the brain. These HCs do not regenerate; any HC loss is therefore permanent leading to hearing loss. In contrast, non-mammalian supporting cells (SCs), which surround HCs, spontaneously regenerate lost HCs throughout the life of the animal. Additionally, some immature SCs in the neonatal mammalian cochlea are able to spontaneously regenerate into HCs after damage.

Furthermore, neonatal SCs and cells of the greater epithelial ridge adjacent to inner HCs respond to the ectopic expression of the HC transcription factor *Atoh1* by differentiating into HCs. In the mature cochlea, however, expression of *Atoh1* alone does not induce the conversion of SCs into HCs.

To determine whether mature SCs can convert into HCs, we have targeted the ROSA locus with three conditional alleles that each drive expression of one of three combinations of HC transcription factors: *Atoh1* alone (Rosa26-A), *Gfi1* and *Atoh1* (Rosa26-GA), or *Gfi1*, *Atoh1*, and *Pou4f3* (Rosa-GAP). When combined with either *Sox2*^{CreERT2} or *Lfng-CreER*, these lines express each set of transcription factors as well as the GFP reporter in SCs. Gene expression was induced at postnatal day (P) 21 and analyzed at P28, P35 and P42. Ectopic expression of *Atoh1* alone did not induce any supernumerary inner or outer HCs, however combined ectopic expression of *Gfi1* and *Atoh1* produced a small number of ectopic inner HCs at P35. Experiments analyzing the combined ectopic expression of *Gfi1*, *Atoh1*, and *Pou4f3*, as well as expression of these genes in the context of HC damage are underway.

Currently the best treatment options for hearing loss are hearing aids and cochlear implants. While these enable users to re-gain some lost hearing, they provide an incomplete recovery. Additionally, as clinical trials for gene therapies are becoming more common, identifying genes that are capable of producing new HCs in the mature cochlea may provide therapeutic approaches for hearing restoration in humans.

PS 1055

Distinctive Proliferative Features of Neonatal Mouse Organ of Corti Supporting Cells

Marie Kubota; Byron Hartman; Stefan Heller
 Stanford University, School of Medicine, Department of Otolaryngology-HNS

Background

Lost cochlear hair cells are not spontaneously regenerated in adult mammals. Nevertheless, after induced hair cell loss, some supporting cells in the neonatal organ of Corti do re-enter the cell cycle and generate new hair cells in vivo. Moreover, when isolated from neonatal cochlear ducts, some neonatal supporting cells are able to proliferate in culture and can give rise to clonal colonies that ultimately harbor newly generated hair cell-like cells. In this study, we examine and compare the ability of different neonatal supporting cell subtypes to give rise to floating colonies (spheres) when cultured in low density.

Methods

Cochlear ducts obtained from postnatal day 2 mice were dissociated and batches of cells were cultured for

7 days in different reagent cocktails to identify the most optimal conditions for sphere formation. Quantitative assessments of the spheres included their number, size, and morphology. Subsequent culture for another 14 days in media that support cell differentiation was applied to quantify the number of cells that upregulated hair cell markers. Using the most optimal sphere-formation conditions, we quantified the abilities of fluorescence activated cell sorted supporting cell subtypes to form spheres. For these experiments we used Lfng-GFP, Sox2-GFP, Fgfr3-iCre/TdTomato mice, and combinations of these strains. Our subsequent goal is to obtain transcriptomic and genomic information of individual supporting cells and analyze the inherent differences between cells that re-enter the cell cycle and cells that do not. Single cell RNA-Seq and ATAC Seq are the methods that will be used for these assessments.

Results

We observed distinct differences between growth conditions in their effects on sphere morphology. For example, a cocktail of GSK3b inhibitor, EGF, FGF-2, and IGF-1 was most potent to elicit growth of spheres with dense morphology (solid spheres) and generated significantly more hair cell-like cells after further culturing compared to spheres with acellular inclusions (hollow spheres). Supporting cells that are adjacent to hair cells showed robust proliferative ability compared to other cell types, and efficiently gave rise to hair cell-like cells. We identified conditions that hypothetically allow us to identify potential genomic and transcriptomic differences among supporting cells that ultimately correlate with their ability to re-enter the cell cycle.

Conclusions

We found neonatal supporting cell subtypes that are able to re-enter the cell cycle after single cell dissociation. We hypothesize that transcriptomic and genomic analyses will reveal clues why these cells have this distinct regenerative capability.

PS 1056

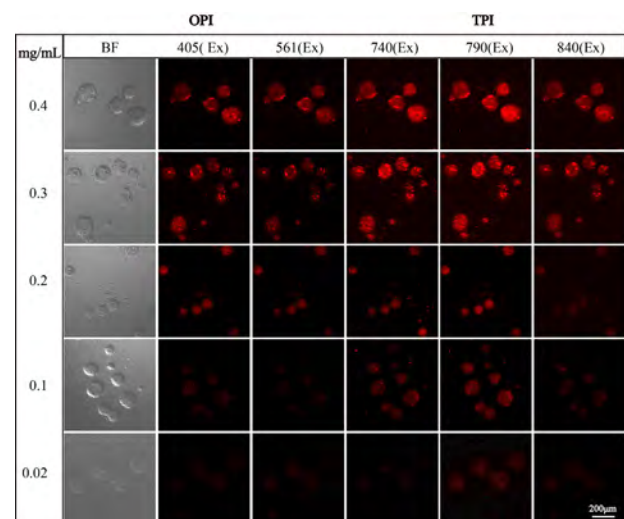
Two-photon imaging tracks neural stem cells via iridium complex-encapsulated polymeric nanospheres

Dan Li¹; Rongrong Guo¹; Mingliang Tang¹; Renjie Chai²

¹Southeast University; ²Key Laboratory for Developmental Genes and Human Disease, Ministry of Education, Institute of Life Sciences, Southeast University

Iridium (III) complexes have been demonstrated as promising probes in two-photon imaging which could be applied to dynamically track transplanted stem cells in stem cell-based therapies. Herein, we report a polymeric

nano-capsules loaded with Ir(MDQ)₂acac with excellent stability by double emulsion method. The Ir(MDQ)₂acac nano-capsules presented high biocompatibility and effective fluorescent labeling rate when it was incubated with mouse neural stem cell (NSC) culture system. More importantly, the Ir(MDQ)₂acac nano-capsules performed both one- and two-photon imaging properties with stable fluorescence lasting for 72 h. Furthermore, data from *in vivo* tracking in nude mice demonstrated that the Ir(MDQ)₂acac nano-capsules fluorescence in NSCs can be stably monitored for up to 21 days. Our results open up an insight into the clinical potential of iridium complex-encapsulated polymeric nanospheres for two-photon imaging in stem cell tracking.



PS 1057

Trans-differentiation of supporting cells into hair cells in explant cultures of chick basilar papillae following exposure to streptomycin

Mami Matsunaga; Tomoko Kita; Hiroe Ohnishi; Norio Yamamoto; Koichi Omori; Takayuki Nakagawa
Department of Otolaryngology-Head and Neck Surgery, Graduate School of Medicine, Kyoto University

Objective: To explore novel strategies for inducing hair cell regeneration in mammalian cochleae, one possible way will be revisiting the process of hair cell (HC) regeneration in the avian basilar papilla (BP). In the avian BP, there are two modes for HC regeneration; direct conversion, or trans-differentiation of supporting cells (SCs) into HCs and proliferation of SCs followed by differentiation into HCs. We focused on the former mode, which can occur in the mammalian cochlea, although its capacity is limited. In the current study, we analyzed alterations in cell populations in explant cultures of chick BPs after exposure to streptomycin (SM) aiming to reveal time courses for HC regeneration through SC direct conversion.

Methods: BPs were dissected from P1 chicks and maintained in DMEM for 24 h. BP explants were exposed to 78 μ M SM for 2 days in order to induce HC loss. Afterwards, the explants were cultured in DMEM with 1% FBS for additional 6 days. The samples were collected on days *in vitro* (div) 2, 4, 6, and 8. Immunohistochemistry for myosin VIIa and sox2 and nuclear staining with DAPI was performed in whole-mount preparation. The specimens were viewed with a confocal microscope. We quantified total cell numbers by counting DAPI-positive nuclei, Sox2 -positive cells, myosin VIIa -positive cells and myosin VIIa and sox2-double positive cells within the sensory epithelium.

Results: On div 2, no myosin VIIa-positive cell was found. On div 4, 6% of cells in the sensory epithelia exhibited myosin VIIa expression, and over 90% myosin VIIa-positive cells were also positive for sox2, indicating that SC trans-differentiation had already initiated, and most of myosin VIIa-positive cells were in the process of trans-differentiation. Specimens of div 6 showed similar cell populations to those of div 4. No significant increase of myosin VIIa-positive or myosin VIIa and sox2-double positive cells between div 4 and 6. Interestingly, increase of myosin VIIa-positive and myosin VIIa and sox2-double positive cells and decrease of sox2-positive but myosin VIIa-negative cells was found between div 6 and 8, suggesting that SC direct conversion actively occurred between div 6 and 8.

Conclusions: Present findings demonstrate that trans-differentiation of SCs initiated within 48 h after exposure to SM, while during exposure to SM, no trans-differentiation of SCs occurred. On the other hand, the activity for trans-differentiation of SCs was once saturated between div 4 and 6, and was re-boosted between div 6 and 8.

PS 1058

ErbB Family Signaling Drives Proliferation of Greater Epithelial Ridge (GER) Cells *In Vitro*

Patricia White; Jingyuan Zhang

University of Rochester Medical Center

Hearing is the ability to detect and perceive sound, an important quality in human activities. Hearing loss may happen when cochlear hair cells (HCs) are damaged or lost due to various factors, such as ototoxic insults and exposure to noise. In mammals, HCs are not regenerated once they die, resulting in permanent hearing impairment. However, in other vertebrates, the adjacent supporting cells (SCs) spontaneously proliferate and differentiate into new HCs, leading to functional re-establishment. Here we report on the effects of expressing constitutively activated ERBB2

receptors (CA-ERBB2) in mouse cochlear SCs. We used transgenic strategy to achieve ERBB2 gain-of-function activity at early stage. We used a transgenic construct that expresses an active form of *ErbB2* (CA-*ErbB2*), a rat version of *ErbB2* with a V654E substitution. CA-*ErbB2* activation in cochleae can be accomplished by crossing Tet-on CA-*ErbB2* line with an inner ear specific rtTA line, Sox10-rtTA line (Walters and Zuo 2015). Such expression is under temporal control by doxycycline application to the cochlear culture at postnatal age day 2 (P2) or to the animals from P0 to P2. *In vitro*, significant proliferation was observed in SCs and in the neighboring greater epithelial ridge (GER) cells upon CA-ERBB2 activation. We are currently investigating the downstream targets of CA-ERBB2 by using a variety of inhibitors to block several regenerative pathways. In contrast, no significant increase of proliferation by SCs was observed *in vivo* when pups were induced to express CA-ERBB2 from feeding the dams with doxycycline food. The lack of response suggests that proliferation *in vivo* is more tightly regulated in comparison to the environment in culture.

PS 1059

Vesicle Autonomous Maturation into Inner Ear Organoids

Liqian Liu; R. Keith Duncan

University of Michigan

The derivation of inner ear organoids from pluripotent stem cells is an exciting advancement with potential applications from disease modeling to regenerative medicine. However, there remains considerable heterogeneity in the size and cellular complexity of the organoids and in the efficiency of differentiation from otic vesicle intermediates. This heterogeneity could arise from diffusible factors and contact cues from ill-defined "non-otic" cells in the surrounding aggregate. Greater control over the microenvironment during vesicle maturation could reduce heterogeneity in efficiency and outcomes. Notably, native otic vesicles show some autonomy in organogenesis, differentiating *in vivo* into vestibular and cochlear domains under mesenchyme-free culture conditions. In this study, we sought to examine whether stem cell-derived otic vesicles were autonomous in their ability to generate cyst-like organoids. Aggregates of mouse embryonic stem cells (R1/E) were treated sequentially with factors to induce the formation of non-neural ectoderm, otic placode, and then otic vesicles. The vesicles were isolated from aggregates on day 10 (D10) to D16, the time period when Pax2+/Sox2+ vesicles are clearly delineated from the rest of the aggregate. The size of the freshly dissociated vesicles almost doubled from D10 to D16 (average diameter of 115 to 200 μ m), but the

average thickness of the epithelium (~30 µm) did not vary with time. To test autonomous differentiation, vesicles from D10, D12, and D14 aggregates were embedded in Matrigel and cultured in organoid maturation media for several days. When D10 vesicles were cultured in isolation for an additional 8 days, they became larger, growing from an average diameter of 115 to 350 µm, and thinner, decreasing in thickness from an average of 30 to 20 µm. A histogram of the thickness-to-diameter ratio revealed two distinct morphologies, small-thick vesicles and large-thin “cysts”. No matter when the vesicles were isolated from the aggregates (D10-D14), about 60% adopted a cyst-like appearance by the equivalent D16 in ex-aggregate cultures. A sample of the D16 cysts were examined by immunohistology (N=5), and each contained cells that were positive for MyoVIIa and Sox2. Culturing these cysts to equivalent D20 revealed MyoVIIa-positive cells with protruding phalloidin-positive hair bundles. We conclude that vesicle maturation into inner ear organoids is autonomous and independent of non-otic cells in the remaining aggregate. While all isolated vesicles consistently expressed Pax2, indicating an otic fate, only 60% differentiated into organoids, suggesting early fate specification. Our approach may help elucidate factors that ultimately determine competence for organoid maturation.

PS 1060

Lin28 promotes proliferation and neural cell fate in adult cochlear glial cells after damage

Judith S. Kempfle¹; Ngoc-Nhi Luu²; Marco Petrillo³; Reef Al-Asad³; Andrea Zhang³; Albert Edge⁴

¹Massachusetts Eye and Ear Infirmary, Eaton-Peabody Laboratories; ²University Department of Otolaryngology, Head and Neck Surgery;

³Massachusetts Eye and Ear Infirmary; ⁴Department of Otolaryngology, Harvard Medical School

Background: Sensorineural hearing loss is irreversible and can be caused by loss of inner ear neurons or hair cells. Regeneration of these cell types from remaining endogenous cells offers a future alternative to implantable hearing devices. RNA-binding protein Lin28 and transcription factor Sox2 are crucial for proliferation of progenitor cells and neurogenesis. We found that in the postnatal inner ear, proteolipid protein 1 (Plp1), a marker for glial cells is co-expressed with Sox2 in peripheral glia of the inner ear and double positive cells can act as progenitor cells for neurons *in vitro*. Transient upregulation of Lin28 promoted proliferation of Plp1-positive glial cells from the spiral ganglion *in vitro*, and subsequent neurogenesis, confirming a role for Lin28 during early stages of progenitor differentiation. This study suggests that Lin28 can exert a similar role after damage *in vivo*.

Methods: Adult 6 week old *Plp-Cre-ER;Rosa26^{tdTomato}*

mice or *Plp-CreER;Lin28^{TetO/+};Rosa26^{tdTomato}* mice underwent ouabain treatment to selectively ablate spiral ganglion neurons *in vivo*. Cell death was histologically confirmed in a control group after 7 days. Animals were injected with Tamoxifen followed by Doxycycline to transiently upregulate Lin28 for 3 days around day 7 after Ouabain surgery. Animals were then analyzed for gene expression and with immunohistochemistry 7 days and 1 month after treatment.

Results: Control mice demonstrated increased proliferation of glial cells with significant glial scar, but without conversion of glial cells into neurons based on marker expression. Mice that underwent transient overexpression with Lin28 showed upregulation of proneural markers and tracing of glial cells from *Plp-CreER;Lin28^{TetO/+};Rosa26^{tdTomato}* mice revealed co-labeling with neural markers.

Conclusion:

Lin28 promotes proliferation and neural fate of adult inner ear glial cells after damage *in vivo*.

PS 1061

A Small Molecule Neurotrophin-3 analogue Promotes Spiral Ganglion Neuron Outgrowth and Synaptogenesis In Vitro

Judith S. Kempfle¹; Christine Hamadani²; Carolina Amador³; Boris Kashemirov³; Albert Edge⁴; Charles McKenna³; David Jung⁵

¹Massachusetts Eye and Ear Infirmary, Eaton-Peabody Laboratories; ²Massachusetts Eye and Ear Infirmary;

³University of Southern California; ⁴Department of Otolaryngology, Harvard Medical School; ⁵Department of Otolaryngology, Harvard Medical School/ Massachusetts Eye and Ear,

Background:

Improvement of spiral ganglion neuron (SGN) survival, neurite outgrowth, and synaptogenesis may lead to significant gains for deaf and hearing-impaired patients. There has therefore been intense interest in the use of neurotrophic factors in the cochlea to promote both survival of SGNs and re-wiring of inner hair cells (IHCs) by SGNs following synaptic loss. Brain-derived neurotrophic factor (BDNF) and neurotrophin-3 (NT3) act through their respective receptors, TrkB and TrkC, and are critical for SGN development and maintenance. In various model systems, BDNF and NT3 have both been shown to promote SGN survival, SGN neurite outgrowth, and synaptogenesis between SGNs and IHCs.

We have previously shown that a small molecule BDNF-analogue (7,8-dihydroxyflavone; DHF) promotes SGN neurite outgrowth and synaptogenesis *in vitro*.

1Aa is a small molecule that mimics the activity of Neurotrophin-3 (NT3). However, its activity on SGNs has not been described. We synthesized 1Aa and assessed the ability of soluble 1Aa to promote SGN neurite outgrowth and synaptogenesis *in vitro*.

Methods:

Dissected SGNs or organ of Corti explants of neonatal cochleas (CBA, p4) were plated and treated *in vitro* with 1Aa, DHF, 1Aa+DHF (all at 400nM) or media alone. To evaluate for synaptogenesis, explants were pre-treated with kainic acid treatment (glutamatergic synaptotoxicity). Tissue was fixed for immunohistochemistry using neural and synaptic markers. After imaging with confocal microscopy, neurite outgrowth was measured with ImageJ and synaptogenesis in explants was evaluated with AMIRA.

Results:

The small molecule NT3 analogue 1Aa demonstrated ability to stimulate neurite outgrowth in SGN cultures at a significantly higher level compared to controls. Combination with DHF resulted in comparable outgrowth. Furthermore, in organotypic organ of Corti explant cultures with attached spiral ganglion neurons, 1Aa stimulated synaptic regeneration significantly better than control cultures following synaptotoxic kainic acid treatment.

Conclusions:

An NT3 small molecule analogue demonstrates neurotrophic properties as measured by neurite outgrowth length and synaptic regeneration *in vitro*.

PS 1062

Expression of Transcription Factors that Regulate Differentiation and Survival in Regenerated Hair Cells of the Neonatal Mouse Cochlea

Michelle R. Randle¹; Kaley A. Graves¹; Brandon C. Cox²

¹SIU School of Medicine; ²Southern Illinois University School of Medicine

Supporting cells (SCs) in the mouse cochlea have the ability to spontaneously regenerate hair cells (HCs) after damage is induced during the first postnatal week via two different mechanisms: mitotic regeneration or direct transdifferentiation. However, hearing is not restored and most regenerated HCs do not survive more than a week after they differentiate. We hypothesized that regenerated HCs are lacking transcription factors that are required for differentiation and/or survival which causes their death. There are several genes that play a role in HC survival and regeneration, including *Atoh1*, *Barhl1*, *Gfi1*, *Pou4f3*, and *Six1*. We have previously shown that 100% of regenerated HCs express *Barhl1*

and ~93% express *Pou4f3*, indicating that their impaired survival is not caused by the lack of expression of these two genes. In this study, we investigated the expression patterns of *Six1*, *Gfi1*, and *Atoh1* using fate-mapping and mitotic tracing techniques to identify regenerated HCs. To fate-map regenerated HCs, we injected *Prox1^{CreERT2}::ROSA26^{tdTomato/+}::Pou4f3^{DTR}* mice with tamoxifen at postnatal day (P) 0 and diphtheria toxin (DT) at P1 and used immunofluorescence to examine *Six1* expression. At P7, all HCs and SCs expressed *Six1* in control samples and all fate-mapped, regenerated HCs also expressed *Six1* in experimental samples. This indicates that the lack of *Six1* is not the cause of HC mortality. Experiments are ongoing to examine *Atoh1* and *Gfi1* expression in regenerated HCs. Due to a lack of quality antibodies for these two proteins, we are breeding *Prox1^{CreERT2}::ROSA26^{tdTomato/+}::Pou4f3^{DTR}* mice with *Atoh1^{GFP+/+}* or *Gfi1^{GFP+/-}* knockin reporter lines to investigate the expression of *Atoh1* and *Gfi1* in fate-mapped, regenerated HCs. To examine *Atoh1* and *Gfi1* in mitotically regenerated HCs, we crossed *Atoh1^{GFP+/+}* or *Gfi1^{GFP+/-}* mice with *Pou4f3^{DTR}* mice to ablate HCs. Mice were injected with DT at P1, followed by BrdU from P3-P6. At P7 in *Atoh1^{GFP+/+}* and *Gfi1^{GFP+/-}* controls, GFP expression was present in 100% of HCs and no BrdU-positive HCs were observed. In experimental *Atoh1^{GFP+/+}::Pou4f3^{DTR}* and *Gfi1^{GFP+/-}::Pou4f3^{DTR}* mice, there were 5-14 BrdU-positive HCs, all of which had robust GFP expression. We conclude that the impaired survival of regenerated HCs is not due to the lack of *Six1* expression; however additional data is needed to determine if *Atoh1* or *Gfi1* expression is lacking in regenerated HCs. We also plan to investigate additional transcription factors that regulate HC survival and/or differentiation. Understanding why regenerated HCs die is a critical step in achieving HC regeneration in adult mammals.

Funding: NIDCD R01 DC014441

PS 1063

Identification of Neural Stem Cells from Postnatal Mouse Auditory Cortex

Li Tao; Zhenjie Liu; Yiyun Jiang; Xin Deng; Zhengqing Hu
Wayne State University

Background

Auditory signals are processed in multiple central nervous system structures including the auditory cortex (AC). Development of stem cell biology provides the opportunity to identify neural stem cells (NSCs) in the central nervous system. NSCs are known to self-renew and differentiate in two brain structures: subventricular and subgranular zones. However, it is unclear whether

NSCs exist in the AC. The aim of this study is to determine whether there are cells in the AC possessing NSC features.

Methods

Postnatal mouse AC tissues were dissected and dissociated into singular and small cell clumps, which were suspended in the culture medium to observe potential neural sphere formation. EdU incorporation and Ki67 immunostaining were utilized to determine cell proliferation. AC-derived spheres were examined by reverse transcription PCR and immunofluorescence to determine expression of NSC genes and proteins. Additionally, AC-spheres were cultured in the presence or absence of astrocyte-conditioned medium (ACM) to study neural differentiation.

Results

The results of this study show that AC-derived cells were able to proliferate to form neurospheres, which expressed multiple NSC genes and proteins including Sox2 and Nestin. AC-NSCs were found to differentiate into cells expressing neuronal and glial cell markers. However, the neuronal generation rate is low in the culture medium containing nerve growth factor, approximately 8%. In order to stimulate neuronal generation, AC-NSCs were cultured in the culture medium containing ACM. In the presence of ACM, approximately 29% AC-NSCs differentiated into cells expressing neuronal marker class III β -tubulin (TUJ1). It was observed that the length of neurite outgrowths of AC-NSC-derived neurons in the ACM group was significantly longer than that of the control group. Additionally, synaptic protein immunostaining showed that expression of synaptic protein of the ACM group was significantly higher than the control group.

Conclusions

These results suggest that ACM is able to stimulate neuronal differentiation, extension of neurites and expression of synaptic proteins. Identifying NSCs in the AC and determining effects of ACM on NSC differentiation will be important for the auditory research.

PS 1064

Neural Crest Cell Injection as a Strategy to Treat Congenital Strial Deafness

Justine M. Renaud; Martín L. Basch
Case Western Reserve University

During inner ear development, neural crest cells migrate through the cochlea to form the intermediate cells of the stria vascularis as well as the glial cells of the spiral ganglion. This process requires several transcription factors such as Sox10, Mitf, as well as specific genes such as *ednrb*. In the absence of these transcription

factors, neural crest cells do not reach their target sites in the cochlea. The absence of intermediate cells interferes with the function of the stria vascularis and the establishment of the endocochlear potential, resulting in congenital strial deafness. Knockout (KO) or conditional knockout mice for these genes have been developed as models of congenital strial deafness.

Our aim is to determine whether multipotent neural crest cells and/or melanoblasts can replace the missing intermediate cells in a strial deafness mouse model, and subsequently to restore strial function and thus hearing. For this project, we studied the injection of GFP-labeled neural crest cells into neonatal *EdnrB* KO mice. We first characterized and confirmed the absence of intermediate cells in the cochlea of KO mice by immunostaining using CD44 as a marker of neural crest cells. We then measured the elevation of hearing thresholds by auditory brainstem response (ABR). We confirmed the location of the injection site and the survival of injected cells by immunostaining at multiple time points post injection. The impact of the cell injections on ABR thresholds were then measured at 21 days after surgery. Here we demonstrate that we have optimized the protocol to deliver neural crest cells with potential therapeutic effects into the lateral wall of the cochlea in neonatal mice.

This research was supported by the Hartwell Foundation.

PS 1065

Chd7 is Enriched at Cis-Regulatory Elements in Immortalized Multipotent Otic Progenitors

Azadeh Jadali; Zhichao Song; Jihyun Kim; Kelvin Kwan
Rutgers University

Spiral ganglion neurons (SGN) that reside within the cochlea convey neural information in the auditory circuit. Loss of SGNs from loud noise exposure contributes to progressive hearing loss. Otic progenitors are viable options for SGN cell replacement therapies. Understanding the molecular basis of otic progenitor differentiation into SGNs accelerates efforts for replacement therapies.

Using an immortalized otic progenitor (iMOP) cell line, chromodomain helicase DNA binding protein 7 (CHD7) was identified as a chromatin remodeling factor involved in the initial stages of neuronal differentiation. Knockdown of CHD7 in iMOP cells prevented neuronal differentiation into iMOP-derived neurons. To identify the genome-wide binding sites of CHD7, chromatin immunoprecipitation followed by deep sequencing (ChIP-seq) in proliferating iMOPs and iMOP-derived neurons was accomplished. Sequence alignment of CHD7 binding sites suggested a

functional role at enhancers and promoters. However, a large number of CHD7 binding sites remain undefined. Correlation of these regions with various histone marks suggests these sites could be novel cis-regulatory elements. Single cell fluorescence *in situ* hybridization after CHD7 knockdown suggested that transcription of genes near novel cis-regulatory elements were altered. We propose that CHD7 serves as a licensing factor at cis-regulatory elements to regulate transcription.

PS 1066

Stimulus-Evoked Activity in Vestibular Nucleus Neurons is Reduced After Hair Cell Regeneration as Measured by cFos Accumulation in Adult Mice

Emmanuel Jauregui¹; Kelli Hicks¹; James Phillips²; Jennifer Stone²

¹University of Washington Department of Otolaryngology; ²University of Washington Department of Otolaryngology and Virginia Merrill Bloedel Hearing Research Center

In adult mice, vestibular function is lost after hair cell destruction and does not appear to be restored, even though about half of the hair cell population (all of them type II) is regenerated. Regenerated hair cells acquire many features characteristic of native hair cells, including mechanotransduction and afferent nerve synapses. These observations raise the question of whether regenerated hair cells can respond to vestibular stimuli and convey information centrally. The immediate early gene cFos accumulates in vestibular nucleus neurons after sinusoidal galvanic stimulation of the vestibular nerve in rats (Holstein et al. *Front Neurol* 2012). In adult mice, we tested whether phosphorylated cFos (phospho-cFos) accumulates in vestibular nucleus neurons after rotational stimulation under normal conditions and during regeneration.

An established transgenic mouse line with the human diphtheria toxin receptor (DTR) inserted into the *Pou4f3* gene, a hair cell-specific transcription factor, was used to achieve conditional and selective ablation of vestibular hair cells upon injection of diphtheria toxin (DT). Adult *Pou4f3*^{+/+} wildtype (WT) mice and *Pou4f3*^{+/DTR} (DTR) mice were injected with DT. At 78 days post-DT, individual mice were placed in a beaker at the periphery of a rotating platform ($r=28$ cm) and subjected to sinusoidal centrifugation (0.01 Hz, pk-pk 600°/s) for 10 minutes. At 45 minutes after stimulation, mice were killed by cardiac perfusion with aldehydes. Brains were sectioned, and immunocytochemistry was performed to label phospho-cFos.

Non-stimulated WT mice had few phospho-cFos-labeled neurons in vestibular nuclei. However, labeled neurons were seen reliably in nucleus solitarius and dorsal motor nucleus of the vagus, which served as positive controls. In contrast to non-stimulated WT mice, stimulated WT mice, with or without DT, had numerous phospho-cFos-labeled neurons in vestibular nuclei. Labeled nuclei were not uniformly distributed; the majority were found in medial parvocellular and spinal vestibular nuclei. An increase in labeled cells was also noted after stimulation in other brainstem regions (e.g., nucleus prepositus hypoglossi), while phospho-cFos labeling in positive control regions was unchanged. In comparison, stimulated DTR mice at 78 days post-DT resembled non-stimulated mice, with perhaps even fewer phospho-cFos-labeled nuclei in spinal and medial vestibular nuclei.

These findings demonstrate that, under normal conditions, rotation evokes focal changes in phospho-cFos labeling in vestibular nuclei that are lost when only regenerated type II hair cells are present. We are currently examining evoked changes in phospho-cFos labeling in stimulated DTR mice immediately after damage and at later stages of regeneration.

PS 1067

Forced Expression of Gfi-1 Enhances Atoh1-Induced Cochlear Hair Cell Regeneration

Jae-Jun Song¹; Melih Acar²; Yoshihisa Ueda³; Hugo J. Bellen⁴; Yehoash Raphael⁵

¹Department of Otorhinolaryngology-Head and Neck Surgery, Korea University Guro Hospital; ²Celgen; ³Department of Otolaryngology, Kurume University Hospital, Kurume; ⁴Jan and Dan Duncan Neurological Research Institute, Baylor College of Medicine, Houston; ⁵Kresge Hearing Research Institute, Department of Otolaryngology-Head and Neck Surgery, University of Michigan

Forced expression of Atoh1 can induce ectopic hair cells *in vitro* and *in vivo* in the auditory and vestibular epithelium, but the efficiency declines as the tissue matures. The growth factor independent 1 (GFI-1) is a zinc finger protein shown to participate in the development of several systems including the final differentiation of hair cells. Here we tested the combined effect of viral-mediated overexpression of *Atoh1* and *GFI-1* on the number of ectopic hair cells formed in explants of developing auditory epithelia and in mature ears *in vivo*. In explants from developing cochleae of newborn pups we detected no ectopic hair cell in control ears whereas numerous ectopic hair cells were found in the treated explants, with more cells in Atoh1+Gfi1 cultures than Atoh1 alone. In mature guinea pig ears treated *in vivo*,

the Gfi1 + Atoh1 vector injection induced almost twice as many hair cells compared to Atoh1 alone. Some but not all ectopic cells located lateral to the outer hair cell area expressed prestin and those medial to the inner hair cells did not. The data demonstrate the utility of the dual-gene transfection strategy for enhancing the number of newly generated hair cells. The ability to augment *Atoh1* induced hair cell regeneration with another gene should provide a useful experimental tool for enhancing the understanding and improving the outcomes of such regenerative protocols.

Supported by NIH-NIDCD grants R01-DC014832 and P30-DC005188, and by the R. Jamison and Betty Williams Professorship.

PS 1068

Roles of Differentially Expressed Transcription Factors in Atoh1-Mediated Supporting Cell Transdifferentiation to Outer Hair Cells in Mature Cochleae

Zhenhang Xu¹; Rai Vikrant¹; Joe. R Frank²; Emma A Malloy³; Pezhman Salehi¹; **Jian Zuo**¹

¹*Department of Biomedical Sciences, Creighton University, School of Medicine;* ²*Department of Neuroscience, College of Arts and Sciences, Creighton University;* ³*Department of Biology, College of Arts & Sciences, Creighton University*

Background: In non-mammalian vertebrates, auditory hair cell (HC) death induces adjacent supporting cells (SCs) to transdifferentiate into new HCs, however, this process is absent in juvenile and adult mammals. Ectopic expression of the transcription factor *Atoh1* has shown to induce SC trans-differentiation to HCs in neonatal but not in adult rodents. Recent studies using combination of *Atoh1* and other transcription factors have shown promise in inducing SC conversion into HCs in mature murine cochleae (Walters et al., Cell Reports 2017). However, the morphology of the converted HC (cHCs) are still not mature enough and the conversion efficiency is not ideal to perform a normal hearing function. Recently, we have performed single cell and bulk RNA sequencing analysis of the conversion in mature cochleae and identified 51 transcription factors that are differentially expressed between cHCs and endogenous OHCs and SCs. Among these, we have shown that *Isl1* is a co-reprogramming factor that promotes *Atoh1*-mediated conversion both *ex vivo* and *in vivo* (Yamashita et al., PLoS Genetics 2018). Here we propose to identify additional transcription factors for improving the efficiency and completion of the conversion.

Methods: Cochlear explants from *Atoh1*-GFP mice are used for electroporation of identified transcription

factors together with *Atoh1*, cultured for 7-14 days and further analyzed for expression of HC markers (*Myo7a*), *Atoh1*-reporter, and transcription factor-reporter. Those transcription factors that increase *Atoh1*-mediated conversion rates will be further analyzed *in vivo* by creating transgenic mouse lines combined with *Atoh1*-ectopic expression mouse lines that will specifically target SCs in the mature cochlea. Their roles in HC regeneration in mouse models with noise-induced outer hair cell loss will be further analyzed.

Results: Among the 51 differentially expressed transcription factors we first focused on several that are highly expressed in OHCs but not in cHCs, aiming at increasing conversion rate and maturation. The first set includes *Sall1/3*, *Ikzf2*, *Rfx7*, *Pknox2*, *Rest*, *Six2*, *Lbh*, *Sall3*, *Arid3b*, and *Hmg20a*.

Conclusion: Differentially expressed transcription factors between cHC3 and OHC provided resources to identify additional factors that promote HC regeneration in mature cochleae. Such factors can be therapeutic targets and combinatory therapy using *Atoh1* and other transcription factors will likely be effective in treating hearing loss.

Supported in part by NIHR01DC015010, NIHR01DC015444, ONR-N00014-18-1-2507, USAMRMC-RH170030, and LB692/Creighton.

PS 1069

NG2-Derived Resident Pericytes Control Sprouting Angiogenesis in the Cochlea

Xiaohan Wang¹; Han Jiang²; Jinhui Zhang²; Allan Kachelmeier³; Manfred Auer⁴; **Xiaorui Shi**⁵
¹*Boston Children's Hospital, Harvard Medical School;* ²*Oregon Hearing Research Center, Department of Otolaryngology / Head & Neck Surgery, Oregon Health & Science University;* ³*Oregon Health & Science University;* ⁴*Life Sciences Division, Lawrence Berkeley National Laboratory;* ⁵*Oregon Hearing Research Center, Department of Otolaryngology / Head & Neck Surgery, Oregon Health & Science University*

Background: Angiogenesis is critical to tissue regeneration and repair under wound healing, hypoxic, and chronic ischemia conditions. Can vessels be regenerated in the damaged adult ear? The question is important because loss of vessel density is seen in a wide variety of hearing disorders, including in loud sound-induced hearing loss, ageing-related hearing loss, and genetic hearing loss. Progression in blood vessel pathology can parallel progression in hearing loss. However, new vessel growth in the ear has not been studied, nor has the role of angiogenesis in hearing. **Methods:** In this study, we use integrated approaches which include primary

cochlear cell lines (e.g., endothelial cell and pericyte), stria tissue explants, and genetically engineered pericyte fluorescent reporter mice in conjunction with an InCuCyte® zoom measurement system, 3D Matrigel® matrix, and transgenic and pharmacological pericyte depletion models to determine whether new vessels can be regenerated from adult mouse cochlea. **Results:** We demonstrate, for the first time, that new vessels can be regenerated in adult mouse cochlea by activation of vascular endothelial growth factor-A (VEGF-A) signaling. Most important, we discovered the progenitors of tip cells for new vessel growth are not pre-existing endothelial cells but converted NG2-derived pericytes. Depletion of NG2⁺ pericytes by pharmacological and genetic approaches impair sprouting angiogenesis *in vitro* and cause vascular regression and high frequency hearing loss *in vivo*. **Conclusions:** Our data highlight the vital role pericytes play in adult vascular regeneration. Resident pericytes self-convert to tip cells, lead sprouting angiogenesis, and are essential for maintaining the microvascular structure critical for auditory function. *This research was supported by NIH/NIDCD R21 DC016157 (X.Shi), NIH/NIDCD R01 DC015781 (X.Shi), NIH/NIDCD R01-DC010844 (X.Shi), NIH P30-DC005983 (Peter Barr-Gillespie), Medical Research Foundation from Oregon Health and Science University (OHSU) (X.Shi), and P01GM051487-20 (Manfred Auer). We would like to thank Drs. Neng Lingling and Wenjing Zhang (Shi lab, Oregon Hearing Research Center, OHSU) for their initial work in establishing a primary pericyte cell line from the stria vascularis in the Shi lab.*

PS 1070

Sustainable Hair Cell Regeneration and Clinically-Significant Hearing Recovery Through Pharmacologic Silencing of *Hes1* Expression Using siRNA Nanoparticle Technology

Richard D. Kopke¹; Xiaoping Du²; Matthew B. West²; Wei Li²; Qunfeng Cai²; Ibrahima Youm²; Xiangping Huang²; Weihua Cheng²; Don Nakmali³; Elaine E. Hamm³; Richard E. Gammans³; Donald L. Ewert²
¹Hough Ear Institute; Oklahoma Medical Research Foundation; Departments of Physiology and Otolaryngology, University of Oklahoma Health Sciences Center; ²Otologic Pharmaceuticals, Inc.; ³Hough Ear Institute; ³Otologic Pharmaceuticals, Inc.

Disabling hearing loss affects over 300 million people worldwide. The cumulative loss of cochlear hair cells (HC) due to acoustic or ototoxic insults or age-related attrition is the most common human pathologic correlate of sensorineural hearing loss (SNHL). This hearing loss is clinically-irreversible in humans, as there is no FDA-approved therapeutic agent that regenerates HCs and restores hearing function. Our approach to address this

unmet medical need employs localized delivery of small interfering ribonucleic acids (siRNAs) encapsulated within biodegradable nanoparticle (NP) matrices to induce the regenerative response and promote functional recovery. Our sustained-release siRNA-based therapeutic is designed to induce *Atoh1* expression and phenotypic conversion of supporting cells (SCs) into functionally-mature HCs by transient, targeted silencing of the Notch pathway effector protein, *Hes1*.

Using a combination of *in vitro* organotypic model systems and a noise-induced SNHL loss model in adult guinea pigs, we have demonstrated that poly(lactic-co-glycolic acid) (PLGA) NPs are non-toxic and readily endocytosed by SCs and, when loaded with *Hes1* siRNA, are capable of regenerating toxin- and noise-ablated inner and outer HCs in a dose-dependent manner, even in high-frequency basal regions of the cochlea. In noise-injured guinea pig cochleae surgically-infused with *siHes1* NPs, treatment-specific HC restoration and clinically significant (10-20 dB) hearing recovery were consistently observed across a broad tonotopic range, beginning at three weeks and extending out to nine weeks post-treatment, indicating a sustainable therapeutic response. Moreover, both ectopic and immature HCs bearing morphological and immunohistological evidence of *de novo* synthesis were uniquely observed in noise-injured cochleae treated with *siHes1* NPs, consistent with a regenerative response. As substantial loss of SCs through *siHes1*-mediated transdifferentiation may negatively impact the structural integrity and functional fidelity of the cochlea, complementary approaches to potentiate *siHes1* NP regeneration or repopulate SCs through cell division may enhance the therapeutic efficacy of this approach. In light of this rationale, we have found that staged inhibition of GSK3 β followed by *Hes1* silencing resulted in synergistic increases in HC numbers, consistent with a priming effect induced by Wnt pathway activation. We are currently expanding upon the promising results from our initial *siHes1* NP *in vivo* studies to ascertain whether greater functional recovery can be achieved using this augmented formulation.

As we have demonstrated that siRNA-loaded PLGA NPs readily traverse the round window membrane and achieve intracochlear silencing, a minimally-invasive middle ear approach for facile clinical implementation may be on the horizon.

Surgical Innovation

PS 1071

Acoustically Evoked Cochlear Response Magnitudes in Cochlear Implant Patients Using High Intensity Low Frequency Tone Bursts

William Riggs; Meghan Hiss; Jameson Mattingly; Oliver Adunka
The Ohio State University

Introduction: The advent of electro-acoustic stimulation in patients with cochlear implants (CIs) has ushered in an era of recording acoustically evoked cochlear potentials through the cochlear implant electrode array. This technology has many potential benefits, one of which may better understand individual patient's pattern of cochlear hair cell loss as well as areas of residual hair cell presence. This could potentially be important for post-operative mapping of the CI. Therefore, this study investigated how cochlear responses are affected by recording location with a CI in place.

Methods: Fourteen patients (ages 1-71 years) receiving an Advanced Bionics CI were prospectively included. Electrocochleography (ECochG) responses were recorded through the electrode array of the CI using high intensity low frequency long duration tone bursts (.25, .5 kHz). The first harmonic distortion magnitude at four intra-cochlear locations (E1, E5, E9, E13) along the length of the cochlea were immediately measured following CI insertion.

Results: The data demonstrates that the first harmonic magnitude was maximal at the apical most electrodes for both .25 and .5 kHz. On average the response was greatest at .5 kHz compared to .25 kHz. Interestingly, there was a steeper slope for each electrode as the recording location moved apically for .25 kHz compared to .5 kHz.

Conclusion: These preliminary findings indicate that in our cohort the first harmonic magnitude evoked by high intensity low frequency tones recorded from various locations along the cochlear spiral typically increased in a linear fashion from basal to apical regions (i.e. as the electrode location approaches the apical region amplitudes typically increased).

PS 1072

Angular positioning of prosthesis in stapes surgeries

Pascale Cuny¹; Nawaf Alsolami²; Birthe Warnholtz¹; Ivo Dobrev³; Christof Rössli³; Alex Huber³; Jae Hoon Sim¹

¹University Hospital Zurich; ²King Fahad Armed Forces Hospital; ³Department of Otorhinolaryngology Head & Neck Surgery, University Hospital Zürich, University of Zurich,

In stapedotomy surgeries, the longitudinal direction of the piston prosthesis should ideally be perpendicular to the stapes footplate. However, angular deviation of the prosthesis from the ideal angular position is unavoidable due to anatomical constraints and surgical conditions. This study aims to explore effects of angular positioning of the piston prosthesis on surgical outcomes and to provide surgical guidelines related to practical tolerance of the angular positioning maintaining effective surgical outcomes. Incus stapedotomy with a Kurz NiTiBond prosthesis (0.4-mm dia.) with two different hole sizes of 0.5- and 0.6-mm diameters on the stapes footplate has been assessed. Angular position of the prosthesis relative to the footplate was modulated by rotating the stapes about the long and short axes of the footplate. The tympanic membrane was acoustically stimulated in the frequency range of 0.25-10 kHz, and motion of the prosthesis was measured using a Laser Doppler vibrometer. Further, micro-computed tomography (micro-CT) data of the middle-ear bones were used for anatomical analysis of angular positioning of the prosthesis. The results showed that changes of angular position of the prosthesis relative to the stapes footplate do not cause significant changes of prosthesis motion until a certain angular position threshold, and sharply attenuate prosthesis motion when the angular position reaches the threshold. The angular tolerance generally covers the allowable region for prosthesis crimping in incus stapedotomy. The angular tolerance becomes smaller with a smaller size of the fenestra. In incus stapedotomy, it is recommended that prosthesis crimping should be located closer to the tip of the incus when the head of the stapes is offset anteriorly and/or the footplate is thickened by otosclerosis.

PS 1073

A Bone Conducting Distortion Product Otoacoustic Emissions System for Low Resource Settings

Aseem Jain¹; Sanjay Elangovan¹; Gianluca Croso¹; John P. Carey²; Francis Creighton³

¹Johns Hopkins University; ²Department of Otolaryngology—Head and Neck Surgery, Johns Hopkins University School of Medicine; ³Johns Hopkins Department of Otolaryngology

Research Background

According to the World Health Organization, unidentified hearing loss is the most common and significant disability impacting pediatric development. Globally, over 32 million children have debilitating hearing loss, and 90% come from developing countries. Otoacoustic emission (OAE) testing is the most commonly used screening test for newborn hearing. However, OAE devices currently on the market are ill-suited for global healthcare settings: they are extraordinarily expensive, ranging from \$2,500-\$25,000, and poorly function in dynamic, noisy healthcare settings in the developing world. To overcome these issues our group has created a novel, affordable, bone conduction OAE system, designed to address limitations in new born screening in developing countries and low resource settings.

Methods

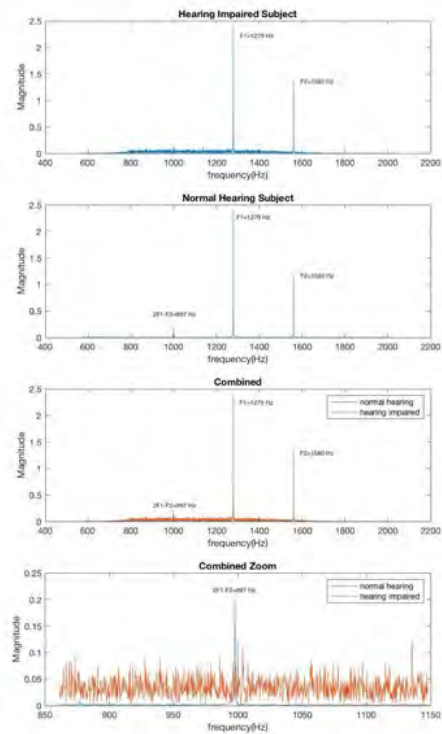
The device consists of two bone transducers mounted on a headband and an in-ear microphone. To test for dpOAEs, the user places a microphone in the ear canal while the bone transducers vibrate at two frequencies, f_1 and f_2 , in which $f_2/f_1 = 1.22$. Unlike stimulation of dpOAEs through air conduction (where a tone is sent through the ear canal to stimulate the dpOAE in the inner ear), bone conduction allows for separation of the stimulus signal and the dpOAE output signal. This method has allowed for a simplification of signal processing and eliminated the need for a high-quality speaker, drastically reducing the production price to sixty-five dollars. This system also uses a peak detection algorithm and band pass filters to both filter external noise and automate the detection of dpOAEs, presenting the user with a “pass” or “refer” output, thus reducing the training needed for practitioners.

Results

5 normal hearing adult subjects were tested in settings with background noise levels of 30dB. Bone conduction f_1 and f_2 were presented 40dB above noise floor. In all cases, the expected dpOAE signal was able to be detected by the signal processing algorithm, despite background noise. As a control a congenitally deafened adult subject was also tested using the system and showed no dpOAE response.

Conclusions

Initial results validate that this bone conducting OAE system can accurately detect dpOAEs in noisy backgrounds. This system can provide a low-cost, easy to use method for new born hearing screens in developing nations and low resource settings. Future goals include further reducing the price and ease of use of the device, and validating this system in the new born population.



PS 1074

Optimization of Fibroblast Alignment and Collagen Deposition on 3D-Printed Biodegradable Polyurethane Tympanic Membrane Grafts In Vitro and In Vivo

Nicole Black¹; Michelle Walsh²; Dhrumi Gandhi³; Jeffrey T. Cheng⁴; Iman Ghanad⁵; Elliott D. Kozin³; John Rosowski⁶; Jennifer Lewis⁷; Aaron K. Remenschneider⁸

¹Harvard John A. Paulson School of Engineering and Applied Sciences, Harvard University; Wyss Institute for Biologically Inspired Engineering, Harvard University; Eaton Peabody Laboratory, Massachusetts Eye and Ear Infirmary; ²Harvard John A. Paulson School of Engineering and Applied Sciences, Harvard University; Wyss Institute for Biologically Inspired Engineering, Harvard University; ³Massachusetts Eye and Ear Infirmary; Department of Otolaryngology, Harvard Medical School; ⁴Eaton Peabody Laboratory, Massachusetts Eye and Ear Infirmary; Department of Otolaryngology, Harvard Medical School; ⁵Mass Eye and Ear, Harvard Medical School; ⁶Eaton Peabody Lab, Massachusetts Eye and Ear Infirmary, Harvard Medical School; ⁷Harvard John A. Paulson School of Engineering and Applied Sciences, Wyss Institute for Biologically Inspired Engineering; ⁸Department of Otolaryngology, University of Massachusetts Medical School; Massachusetts Eye and Ear Infirmary; Department of Otolaryngology, Harvard Medical School

Background: The tympanic membrane (TM) contains

an exquisite radial and circular fibrous collagen microarchitecture that plays a role in sound conduction. However, current tympanoplasty and myringoplasty graft materials, including fascia and cartilage, lack this microarchitecture. Even when remodeled, reconstructed TMs contain isotropic tissues and, frequently, result in suboptimal hearing outcomes. By 3D printing biodegradable materials with increased stiffness along the print path, we hypothesize that fibroblasts will remodel the graft into an anisotropic, biomimetic collagen microarchitecture.

Methods: A novel 3D printable biodegradable poly(ester urethane urea) (PEUU) is synthesized. Polycaprolactone is used as a control material. Grafts are 3D printed in linear print paths using speeds of 5, 10, 15, and 20 mm/s and in circular/radial print paths. Tapping-mode atomic force microscopy (AFM) is used in phase mode to visualize the arrangement of hard and soft domains in the polyurethane. Green fluorescent protein expressing human neonatal fibroblasts (GFP-HNDFs) are seeded onto grafts *in vitro*. After 7 and 14 days in culture, grafts are visualized using confocal microscopy. For *in vivo* studies, chinchilla models are utilized to generate chronic 50% TM perforations transcanal. After one month, animals undergo underlay tympanoplasty using circular/radial PEUU grafts. Post-operative healing is assessed via otoendoscopy at 1 and 3 months. After 3 months, animals are euthanized, and the temporal bones are fixed and embedded in celloidin. Specimens are then sectioned, stained with hematoxylin and eosin, and histopathologically described.

Results: A PEUU formulation is successfully synthesized and 3D printed via heated direct ink write extrusion. AFM demonstrates greater alignment of hard domains at increased print speeds, corresponding to increased densification hardening. Directionality demonstrates 3-fold improvement in alignment of GFP-HNDFs along the print path at 20 mm/s print speeds as compared to 5 mm/s, unlike in polycaprolactone controls. Confocal microscopy of circular/radial grafts demonstrates alignment of GFP-HNDFs and collagen I in a radial orientation on the lateral surface of the grafts and circumferential orientation on the medial surface. Otoendoscopic evaluation of reconstructed TMs *in vivo* demonstrates incorporation of PEUU grafts with preserved architecture. Histologic analysis of PEUU grafts demonstrates extracellular collagen deposition along the circular/radial print path.

Conclusion: Grafts utilizing 3D printed PEUU at high print speeds can guide cellular elongation and collagen deposition along custom print paths. Thus, TM grafts can be 3D printed to guide biomimetic repair of the TM, potentially leading to improved patient audiometric outcomes following tympanoplasty.

PS 1075

Test-Retest Variability in Recordings of Low Frequency Cochlear Microphonic Waveforms Using Canal Electrodes in Normal Hearing Subjects

Ming Zhang¹; Pinky Raju²

¹LSUHSC; ²TTUHSC

Cochlear Microphonics can be recorded using electrocochleography. Its test-retest variability is an important factor in monitoring any changes in cochlear status or any effects of a treatment. Such importance has been recognized by experts in the field (Ferraro, Mayerhoff, Park, etc.) through their multiple reports on the variability related to the electrocochleography. Their reports have defined several components in the electrocochleogram such as action potentials (AP), summation potentials (SP), and/or ratios of SP over AP, recorded with a tympanic membrane electrode or an ear canal electrode. However, reports on variability related to cochlear microphonics recorded with a canal electrode have not been identified in the literature to our knowledge. So, our study was on the cochlear microphonics. Hair cells, mainly the outer hair cells, involve two forms of responses: besides the acoustic form (i.e., otoacoustic emission), electrical form (i.e., cochlear microphonics) is also important. Such importance has been more recognized in recent years as more reports on cochlear microphonics can be found. Newer trend sees emergence of cochlear microphonic waveforms recorded with extracochlear electrodes, which were evoked with a toneburst instead of a conventional stimulus (i.e., clicks). Compared to the click-evoked, the toneburst-evoked is of more frequency specific. As noise contaminates lower frequency otoacoustic emission recordings (e.g., 500 Hz) more than higher frequency recordings (e.g., 2000 Hz), we focused on using low frequency tonebursts together and canal electrodes. Therefore, for methods, electrocochleography, a canal electrode like Tiptrodes, and a toneburst at 500 Hz were adopted to record the cochlear microphonic waveforms. The data were collected from human subjects with normal hearing. The recording were performed through four sessions at different time points in a frame of about ten days. All recordings were performed in a same consistent manner by a same examiner. The amplitudes of the cochlear microphonic waveforms were measured from each of recordings. The amplitudes and their differences among data obtained at four different time sessions were compared. For comparison, the amplitudes were converted into dB in reference to microvolt. The results show that amplitudes changed in recordings among four different time sessions. The range of the differences among the four time sessions is 0.81 dB. In conclusion, variation exists in test-retest recordings but is not substantially when recordings

are performed in a same consistent manner. The low frequency cochlear microphonic waveforms recorded using a canal electrode can be potentially used to monitor some of cochlear status.

PS 1076

DNA Methylation May Affect Response to MEK Inhibitors in Primary Human Vestibular Schwannomas

Christine T. Dinh¹; Olena Bracho¹; Juan Young¹; Rahul Mittal¹; Denise Yan¹; Esperanza Bas¹; Michael Ivan¹; Jacques Morcos¹; Fred F. Telischi¹; Cristina Fernandez-Valle²; Xue-Zhong Liu¹

¹University of Miami Miller School of Medicine; ²Burnett School of Biomedical Sciences, University of Central Florida College of Medicine

Background: Neurofibromatosis Type 2 (NF2) is a genetic tumor disorder characterized by bilateral vestibular schwannomas (VS), which can lead to hearing loss, balance, and other neurological sequelae. Currently, there is no cure for NF2. Although some chemotherapeutic agents in clinical trial show promise in tumor stabilization, drug response is only seen in a subset of NF2 patients. The variability in drug response may reflect genetic and epigenetic differences in individual tumors. We investigate the NF2 mutational spectrum and DNA methylation profiles of cultured primary human VS that are responsive and not responsive to PD0325901, a MEK (mitogen-activated kinase kinase) inhibitor.

Methods: Tumor was harvested from seven consecutive patients undergoing VS surgery at the University of Miami/Jackson Memorial Hospital. Multiplex Ligation-Dependent Probe Amplification (MLPA) was utilized to assess NF2 mutations of each tumor. Dissociated primary human VS cells were cultured and treated with vehicle and different concentrations of PD0325901. Crystal violet assays were performed to determine cell viability after 72 hours *in vitro*. DNA methylation analysis was performed using the Infinium MethylationEPIC kit and compared between VS that responded (>20% reduction in viability) and didn't respond to PD0325901.

Results: NF2 mutations were identified in all seven VS. PD0325901 did not significantly reduce viability in two of seven VS (29%). Five VS (71%) showed >20% reduction in cell viability at the highest concentration of PD0325901 tested. In the two non-responding VS, DNA methylation analysis identified hypermethylation of a CpG site in the promoter region of the *ELMOD1* (Engulfment and cell motility domain 1) gene, which confers greater tumor aggressiveness and drug resistance. Furthermore, differentially methylated regions (DMR) of genes associated with non-MEK

merlin pathways were found in non-responding VS.

Conclusion: MEK inhibition with PD0325901 did not effectively reduce cell viability in all primary human VS. Non-responding VS demonstrated hypermethylation in the promoter region of *ELMOD1* gene and aberrant methylation of CpGs associated with non-MEK pathways. These findings identify potential mechanisms of drug resistance and response in NF2-associated VS. Further investigations into tumor heterogeneity and the impact on drug resistance are important steps in developing a precision medicine algorithm for selecting best therapies for NF2 patients.

PS 1077

Key Anatomical Landmarks for CT-Based Measurements in Cochlear Implant Users

Nicole Jiam¹; Melanie Gilbert²; Jonathan Mo³; Daniel Cooke¹; Charles J. Limb²

¹University of California San Francisco; ²Dept of Otolaryngology-Head and Neck Surgery, University of California, San Francisco; ³Johns Hopkins University

Advances in high-resolution imaging technology have led to dramatic improvements in our ability to localize cochlear implant electrodes within the cochlea. Preliminary studies from our lab suggest that imaging data obtained using flat panel computed tomography (CT) scans may be used to develop customized frequency allocation maps for cochlear implant users based on their own individual anatomy and electrode placement, rather than a manufacturer-specific default frequency allocation map (as is currently the standard of care). Further refinement and implementation of such customized frequency maps may ultimately lead to improvements in pitch perception, a fundamental problem with cochlear implant-mediated sound perception. The process of deriving precise localization measurements from CT images relies upon identification of fine detail anatomic marker, with several anatomic factors affecting the final measurements obtained through these methods. In this study, we sought to examine the impact of fine detail anatomic marker selection on final cochlear duct length measurements, cochlear implant electrode localization, and frequency map calculations. We identified the following cross-sectional marker selection points that are requisite steps to cochlear duct length calculation: round window localization (center vs. proximal edge vs. distal edge), x-axis localization (center vs. medial edge vs. lateral edge), y-axis localization (basilar membrane vs. Reissner's membrane), z-axis localization (modiolus center identification), and helicotrema/apex identification. In addition, we assessed the impact of cochlear implant electrode localization (mid-scalar vs. lateral wall) on frequency map allocation. We examined 15 secondary

reconstructions of FPCT imaging obtained from 12 cochlear implant users. Preliminary results show that round window position determination influences cochlear duct length calculation. Specifically, we observed a difference of 1.6mm (SD 1.5; p=0.037) in cochlear duct length when taking starting point measurements at the center versus proximal edge of the round window. Clinically, this translates to a difference of 6 semitones. Additional analyses are ongoing. Improvements in our understanding of the impact of fine detail anatomic marker selection on cochlear measurements will allow us to get closer to the development of radiologic gold standards for cochlear implant electrode localization. These methods should lead to greater accuracy of cochlear implant electrode frequency map allocation that may ultimately improve pitch perception in cochlear implant users.

PS 1078

The Application of CineMRI in Evaluation of Upper Airway Obstruction Levels in Pediatric OSAS

Shan He; Jie Chen

Department of Otolaryngology, Shanghai Children's Medical Center Affiliated with Shanghai Jiaotong University School of Medicine

Abstract Objective: To explore the role of cineMRI in the localization of upper airway obstruction in pediatric OSAS **Method:** Eleven persistent OSAS and 11 complex OSAS underwent cineMRI from June 2017 to March 2018. Each patient was imaged midline sagittal and axial magnetic resonance cine image. The obtained sagittal and axial images were displayed in cine format, creating a real-time "movie" of airway motion, to make a personalized treatment for each child. Polysomnography was performed to evaluate the effectiveness of cineMRI directed treatment for pediatric OSAS. **Result:** CineMRI could effectively define the upper airway obstruction level. There was a significant improvement in AHI (P=0.019) and saturation nadir (P<0.005). **Conclusion:** The cineMRI is useful in evaluating the upper airway obstruction in those patients who have persistent OSA symptoms after tonsillectomy or adenoidectomy, or in those patients who have complex systemic disease.

PS 1079

Novel Three-Dimensionally Printed Bony Implants for Biomimetic Reconstruction Following Canal Wall Down Mastoidectomy

Renee Friedman¹; Nicole Black²; Samuel R. Barber³; Elliott D. Kozin⁴; Jennifer Lewis⁵; Aaron K. Remenschneider⁶

¹Harvard John A. Paulson School of Engineering and Applied Sciences, Harvard University; Wyss Institute for Biologically Inspired Engineering, Harvard

University; ²Harvard John A. Paulson School of Engineering and Applied Sciences, Harvard University; Wyss Institute for Biologically Inspired Engineering, Harvard University; Eaton Peabody Laboratory, Massachusetts Eye and Ear Infirmary; ³University of Arizona College of Medicine; ⁴Massachusetts Eye and Ear Infirmary; Department of Otolaryngology, Harvard Medical School; ⁵Harvard John A. Paulson School of Engineering and Applied Sciences, Wyss Institute for Biologically Inspired Engineering; ⁶Department of Otolaryngology, University of Massachusetts Medical School; Massachusetts Eye and Ear Infirmary; Department of Otolaryngology, Harvard Medical School

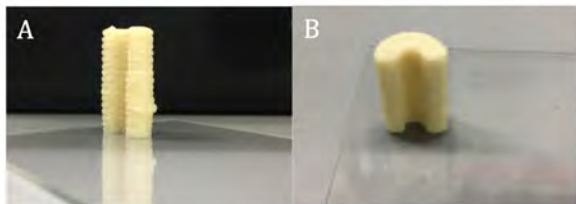
Background: During a canal wall down (CWD) mastoidectomy, the ear canal wall is removed in order to extirpate difficult to reach mastoid and middle ear disease. The resultant tympanomastoid compartment requires routine cleaning for the life of the patient, impairs middle ear sound transfer function by a minimum of 15dB, and requires water precautions to prevent caloric vertigo and mastoid infections. Current strategies to limit such problems include mastoid obliteration using autologous or synthetic materials, ear canal wall removal and reconstruction and 'soft wall'; reconstructive techniques. Each method has limitations and none has gained widespread adoption. Modern advances in filamentary extrusion three dimensional (3D) printing techniques may permit rapid, real time canal wall reconstruction using autologous materials. Herein, we aim to create high aspect ratio autologous bony implants with similar mechanical properties and structural integrity to the native ear canal wall in order to improve surgical and hearing outcomes for patients undergoing CWD mastoidectomies.

Methods: Bone pate is harvested from cadaveric mastoids and further grinded down to a fine powder. It is then dried and purified. A G-code print path is coded using anatomical measurements from CT scans of an example anonymous patient. The path encodes for 3D printing of a semi-cylindrical shell structure shaped like the ear canal wall with rapidly customizable dimensions. A novel bone pate-containing ink is created for 3D filamentary extrusion printing. The ink is used to print the ear canal wall structure. Post-printing, structures are dried and crosslinked to obtain desired geometry. Implants undergo compression testing using native human temporal trabecular bone as a control. Implants are also seeded with human neonatal dermal fibroblasts (HNDs) to assess cytotoxicity.

Results: Implants were successfully 3D printed with ink containing >50 wt% bone pate using a 1.36mm diameter straight nozzle at 18psi. For testing, implants were printed with dimensions of 5mm inner radius, 7mm outer

radius, and heights up to 2cm. Compression testing of crosslinked 3D printed implants yielded a compressive Young's Modulus of 8.929 GPa \pm 0.58GPa, which was similar to the Compressive Young's Modulus of native human trabecular bone that was found to be 9.755GPa \pm 1.2GPa. Through confocal microscopy and Live/Dead (ThermoFisher) staining, we observed that >95% of the HNDFs on the implants appeared to be alive, suggesting high biocompatibility of the final implant material.

Conclusion: Bony implants composed of a novel bone pate-containing ink can be 3D printed to high aspect ratios for ear canal wall reconstruction following CWD mastoidectomy. The mechanical properties of the implants mimic those of native trabecular bone and the implant material is nontoxic to HNDFs. Future studies will examine the reconstructive abilities of these implants using CT scans of cadaver implantation and *in vivo* implantation in animal models for canal wall reconstruction.



3D printed bony implants made of bone pate, fibrinogen, and pluronic. (A) Side view of implant. (B) Top view of implant.

PS 1080

microRNA profiling in the human inner ear perilymph of cochlear implant patients

Helena Wichova; Matt Shew; Jennifer Nelson-Brantley; Jacob New; Hinrich Staecker
University of Kansas School of Medicine

Objective: Hearing loss is common and caused by a wide range of molecular and cellular pathologies. Diagnosis of hearing loss depends of a combination of physiologic testing, patient history and in some cases genetic testing. No biopsy or equivalent procedure exists to diagnose inner ear disorders. MicroRNAs are short ribonucleic acids that regulate a variety of cellular processes. They have been found to be reliable markers for a variety of disease processes. In particular, a variety of miRNAs that are markers for neurodegenerative disease have been identified in cerebrospinal fluid. The goal of this study was to determine if miRNA populations in human perilymph could be used to understand the underlying pathology of the inner ear.

Study design: Prospective sampling and analysis

Subjects and Methods: Patients undergoing surgery in

which the inner ear is opened as part of the procedure (cochlear implantation, stapedectomy) were recruited. Two to 5 ml of perilymph was collected and analyzed using Affymetrix GeneChip miRNA 4.0 microarrays. A functional analysis of significant miRNAs was done using the IPA Ingenuity software package and a machine learning program that correlated miRNA profiles to hearing loss data and implant function

Results: miRNAs could be isolated from the inner ear fluid of all patients. Evaluation of miRNAs demonstrated the presence of miRNA populations that are predicted to interact with genes expressed in the inner ear. Additional analysis of miRNA populations demonstrated that perilymph miRNAs could be linked to pathways including regulation of apoptosis, autophagy, and neurotrophin signaling.

Vestibular Testing

PS 1081

Inter-rater differences of VOR gains using Video Head Impulse Test: A reliability study.

Jennifer Millar¹; Yoav Gimmon²; Michael C. Schubert²
¹Johns Hopkins Medical Institutions; ²Johns Hopkins University Department of Otolaryngology

Background: The purpose of this study is to assess inter-rater reliability of the vestibular head impulse test (VHIT). We hypothesized that there would be no differences in same day VHIT results by two examiners in patients with dizziness.

Methods: To date, 37 patients have been tested with the VHIT (Otometrics, Natus) for VOR gain in each semicircular canal by two examiners within a single clinic visit. The reported VOR gains are based on the software analysis algorithm that uses the area under the curve method. Each semicircular canal impulse plot was examined and "bad" (blink artifact, noise, an abnormally high gain, goggle slippage) trials were removed. 18 of the 37 subjects had at least one semicircular canal requiring the impulse data to be amended; only 8 patients are reported below for this preliminary abstract.

Results: A 2-Factor (examiner and semicircular canal) ANOVA compared VOR gains differences; Intraclass correlation examined similarity in VOR gains between E1 and E2 across semicircular canal function. Our results show three primary findings (Table 1): 1) Each examiner showed differences in VOR gain between the vertical and horizontal semicircular canals ($p < 0.00001$); 2) There was a significant difference in VOR gain between E1 and E2 ($p < 0.0002$); 3) Single measure Intraclass Correlation for each canal revealed strong correlation between examiners for the horizontal semicircular canal VOR gain

(left – 0.87 ; Right – 0.88), but weak to moderate for the vertical semicircular canal gains (RA -0.15 – LP 0.36 ; LA 0.57 – RP 0.69).

Conclusion: Our preliminary analysis suggests variability in vertical semicircular canal VOR gains between two examiners as measured using VHIT. A possible confound with this result is that E1 was more experienced in conducting VHIT.

References:

1. Weber KP, Aw ST, Todd MJ, McGarvie LA, Curthoys IS, Halmagyi GM. Head impulse test in unilateral vestibular loss: vestibulo-ocular reflex and catch-up saccades. *Neurology*. 2008 Feb 5;70(6):454-63. PMID: 18250290
2. MacDougall HG, McGarvie LA, Halmagyi GM, Curthoys IS, Weber KP. Application of the video head impulse test to detect vertical semicircular canal dysfunction. *Otol Neurotol*. 2013 Aug;34(6):974-9. PMID: 23714711

This work is supported by Department of Defense grant, W81XWH-15-1-0442.

Table 1:

Examiner	Yaw L (mean ± 1 sd)	Yaw R (mean ± 1 sd)	L Anterior (mean ± 1 sd)	R Posterior (mean ± 1 sd)	L Posterior (mean ± 1 sd)	R Anterior (mean ± 1 sd)
E1	0.82/±0.18 (95% CI 0.15)	0.90/±0.17 (95% CI 0.14)	0.63/±0.14 (95% CI 0.11)	0.76/±0.08 (95% CI 0.08)	0.90/±0.13 (95% CI 0.11)	0.91/±0.17 (95% CI 0.15)
E2	0.82/±0.14 (95% CI 0.12)	0.92/±0.12 (95% CI 0.10)	0.54/±0.24 (95% CI 0.2)	0.83/±0.10 (95% CI 0.09)	0.85/±0.38 (95% CI 0.22)	0.65/±0.21 (95% CI 0.18)

PS 1082

Video Ocular Counter-Roll (vOCR): A New Clinical Test of Otolith-Ocular Function

Shirin Sadeghpour¹; Francesco Fornasari²; Jorge Otero-Millan³; David Zee⁴; John P. Carey⁵; Amir Kheradmand⁶

¹Department of Neurology, Johns Hopkins University, School of Medicine, Baltimore²Vita-Salute San Raffaele University; ³Department of Neurology, Johns Hopkins University, School of Medicine; ⁴Department of Neurology, Neuroscience, Ophthalmology, and Otolaryngology & Head and Neck Surgery, Johns Hopkins University, School of Medicine; ⁵Department of Otolaryngology—Head and Neck Surgery, Johns Hopkins University School of Medicine; ⁶Department of Neurology and Otolaryngology & Head and Neck Surgery, Johns Hopkins University, School of Medicine.

Introduction

Video-oculography (VOG) devices are now widely used

for quantification of vestibular function. The video head impulse testing (vHIT) evaluates semicircular canal function. However, a comparable VOG method for evaluation of otolith-ocular function is lacking. During a static head tilt, there is a change in torsional position of the eyes in the opposite direction of the head tilt, which is driven by the otolith inputs. Here, we investigated whether VOG quantification of this ocular counter-roll (vOCR) can be used along with vHIT to detect loss of vestibular function at the bedside.

Methods

We examined feasibility of vOCR testing at the bedside using simple lateral head-on-body and whole-body tilts of 30 degrees. We recruited patients who had vestibular loss from resection of vestibular schwannoma within three weeks (acute), four weeks to six months (subacute), and more than six months (chronic) following the surgery. We also recruited a group of age-matched healthy controls. The vOCR and vHIT measurements were compared among the patient groups and healthy controls.

Results

The average vOCR values from patients were significantly lower compared with the healthy controls during both head-on-body and whole-body tilts (p-values<0.05). In the acute group, vOCR was reduced on the side of vestibular loss compared to the healthy side (p-values<0.05). This asymmetry was more pronounced with the whole body tilt than with the head-on body tilt in the acute and subacute groups, but resolved in the chronic group (p-values>0.5). The average vHIT gains on the side of vestibular loss were lower than the healthy side in all acute, subacute, and chronic groups (p-values<0.05)

Conclusion

vOCR can be easily applied at the bedside to detect and track loss of otolith-ocular function at different stages of recovery from vestibular loss. In acute stage, both vOCR and vHIT show an asymmetry with lower gains on the side of vestibular loss. While vHIT asymmetry persists, vOCR asymmetry resolves over time.

PS 1083

Evaluation of Vestibular-Ocular Reflex Using Head Impulse Testing in Patients with Benign Paroxysmal Positional Vertigo

Inon Kim; Min Pyo Hong; Ji Hyung Kim; Hye In Choi; Eun Jin Son
Yonsei University College of Medicine

Current pathophysiologic explanation of benign paroxysmal positional vertigo(BPPV) describes the

characteristic symptoms are caused by free-floating or dislocated otoconia in the semicircular canals(SCC). It is also assumed that the function of the vestibular receptors in the SCC are intact. The video head impulse test (vHIT) can provide precise information about the vestibulo-ocular reflex (VOR) to stimuli in the high-frequency range. In this study, we aimed to evaluate the VOR function using vHIT in 3 SCC planes (lateral, anterior, posterior SCC) in BPPV. Thirty-five patients clinically diagnosed with BPPV were included. VOR function was assessed using rapid head impulse in the planes of 3 SCC in both directions. Gain and presence of corrective saccades were analyzed for the affected and the normal ears. The mean gains of VOR during vHIT were within normal range for LSCC plane in both the affected (1.00 ± 0.12) and normal ears(1.07 ± 0.13), but gain was decreased in 9 cases (25.7%). Mean VOR gains were comparable to normal subjects for ASCC and PSCC. Presence of overt and covert saccades in ipsilateral LSCC were more common in BPPV patients with confirmed nystagmus compared to those without.

In patients with BPPV symptoms, the VOR in the horizontal plane measured during rapid head impulses was normal for both affected and normal ears. However, further studies are needed to clarify possible differences among involved SCC, or recurrent BPPV.

PS 1084

Accuracy of Detecting Saccades in Clinical Horizontal Head Impulses

Athanasia Korda¹; John P. Carey²; Ewa Zamaro¹; Marco D. Caversaccio¹; Georgios Mantokoudis¹

¹Department of Otorhinolaryngology, Head and Neck Surgery, Inselspital Bern, University of Bern,

²Department of Otolaryngology—Head and Neck Surgery, Johns Hopkins University School of Medicine.

Background: Clinicians performing a horizontal head impulse test (HIT) are looking for a corrective saccade, a corrective eye movement towards the direction of a deficient slow phase response of the vestibulo-ocular reflex (VOR), however, the detection of such saccades is a challenge. The aim of this study is to assess an expert's likelihood of detecting corrective saccades in subjects with vestibular hypofunction.

Methods: In a prospective cohort observational study we assessed 365 horizontal HITs performed clinically by an expert neurootologist in seven patients with unilateral deficient VOR. All HITs were recorded simultaneously by videooculography, which served as a gold standard for saccade detection. We evaluated saccades latency and amplitude, head velocity and gain in order to identify relevant parameters and cut-offs for optimal saccade

detection by an expert physician. Mixed effects logistic regression was used to test whether the physician identified a saccade more frequently with increasing latency, amplitude, gain, and velocity (univariate and all together), with patient and session within patient as random effects. Additionally, we adjusted for HITs direction towards the healthy or pathological side in additional models.

Results: The probability of saccade detection was 8 times higher for HIT towards the pathological side ($P=0.029$). In addition, an increase in saccade amplitude resulted in an increased probability of detection (Odds ratio (OR) 1.77 (1.31 - 2.40) per degree, $P<0.001$). The sensitivity to detect a saccade amplitude of 1 degree was 92.9%, specificity 79%. Sensitivity was 100% and specificity is 72% when the saccade velocity is equal or greater than 43 deg/s. Saccade latency and VOR gain did not significantly influence the probability of the physician identifying a saccade (OR 1.02 (0.94 - 1.11) per 10 ms latency and OR 0.84 (0.60 - 1.17) per 0.1 VOR gain increase).

Conclusions: The saccade amplitude is the most important factor for accurate saccade detection in clinically performed head impulse tests. The probability of saccade recognition doubles with an increment of 1° saccade amplitude. Contrary to current knowledge, saccade latency and VOR gain play a minor role in saccade detection. This is not expected since covert saccades are more difficult to detect compared to overt saccades with longer latencies. The role of saccade latency in relation to the head movement should be further investigated in future studies.

PS 1085

The functional Head Impulse Test (fHIT) and Oscillopsia in patients with Bilateral Vestibulopathy (BV)

Tessa van Dooren¹; Florence Lucieer²; Angélica Perez-Fornos³; Nils Guinand³; Jean Philippe Guyot³; Herman Kingma²; Stefano Ramat⁴; Raymond Van de Berg²

¹Department of Otorhinolaryngology and Head and Neck Surgery, Division of Balance Disorders, Maastricht University Medical Center, School for Mental Health and Neuroscience; ²Division of Balance Disorders, Faculty of Health Medicine and Life Sciences, Department of Otorhinolaryngology and Head and Neck Surgery, School for Mental Health and Neuroscience, Maastricht University Medical Center; ³Service of Otorhinolaryngology and Head and Neck Surgery, Department of Clinical Neurosciences, Geneva University Hospitals; ⁴Department of Electrical, Computer and Biomedical Engineering, University of Pavia

Introduction. Bilateral vestibulopathy (BV) is a chronic condition in which vestibular function is impaired or absent on both sides. Oscillopsia is one of the main symptoms of BV. It is attributed to the loss of the VOR function, and consequently gaze stabilisation. Oscillopsia can be quantified objectively by functional vestibular tests, and subjectively by questionnaires. Recently, a new technique for visual stabilization abilities was developed: the functional head impulse test (fHIT). This study compared the fHIT with the DVA treadmill test and Oscillopsia Severity Questionnaire (OSQ) in the context of objectifying dynamic visual acuity and the experience of oscillopsia in patients with BV.

Methods. Inclusion criteria comprised: 1) summated slow phase velocity of nystagmus of $<20^{\circ}/s$ during bithermal caloric tests, and 2) torsion swing tests gain of $<30\%$ and/or phase $<168^{\circ}$. During the fHIT (BEON Solutions, Italy) patients were seated in front of a computer screen at a distance of 1.5 meters. During a passive horizontal head impulse an optotype (Landolt C) was shortly displayed. Patients reported the seen optotype by pressing the corresponding button on a keyboard. The percentage correct answers was registered for leftwards and rightwards head impulses. During DVA treadmill patients were positioned 2.8 meters from a computer screen. Static visual acuity was determined during stance, followed by the assessment of the DVA during walking at 2, 4 and 6 km/h. When four out of five optotypes (Sloan letters) were correctly identified, the corresponding logMAR was registered. Every patient completed the Oscillopsia Severity Questionnaire (OSQ), developed by the Division of Balance Disorders in Maastricht.

Results. In total 23 patients were included. This study showed a correlation between the severity of oscillopsia experienced by the patient, as tested by the OSQ, and the fHIT for both rightwards ($r_s = -0.559$; $p = 0.006$) and leftwards ($r_s = -0.396$; $p = 0.061$) head impulses. No correlation between DVA treadmill and OSQ outcomes, or between DVA treadmill and fHIT was found. fHIT was completed in all patients, 52% of the patients was not able to complete the DVA treadmill on all speeds.

Conclusion. The fHIT seems to be a more suitable test than the DVA treadmill to objectify oscillopsia in BV patients, since it is more sensitive and can be completed in more patients.

PS 1086

Development of real-time video-oculography using high quality infrared video Frenzel, yVOG-Glass.

Makoto Hashimoto¹; Yosuke Okinaka¹; Hironori Fujii¹; Kazuma Sugahara¹; Yoshinobu Hirose¹; Shunsuke Tarumoto¹; Takuo Ikeda²; Hiroshi Yamashita¹

¹*Department of Otolaryngology, Yamaguchi University Graduate School of Medicine;* ²*Tsudumigaura Medical Center for Children with Disabilities*

Background

It is essential to use an infrared CCD camera in clinical examination of the vestibular system. Devices are currently available that can quite accurately record human eye movements, based on the principle of video-oculography (VOG). We devised an original VOG (HI-VOG) system using a commercialized infrared CCD camera, a personal computer and public domain software program (ImageJ) for data analysis. In the present study, we revised the VOG and image filing system for real-time 3D analysis of nystagmus, and developed high quality video Frenzel (yVOG-Glass).

Methods

The video image from a Frenzel with high quality image camera was captured at 60 frames per second at a resolution of 640*480 pixels. For real-time analysis of the horizontal and vertical components, the X-Y center of the pupil was calculated. For real-time analysis of torsional components, the whole iris pattern was overlaid with the same area of the next iris pattern, and the angle at which both iris patterns showed the greatest match was calculated.

Results

Accurate measurements of horizontal, vertical and torsional eye movement were taken while recording the video image in real-time. For quantitative analysis, the slow phase velocity of each occurrence of nystagmus and the average value of the slow phase velocity were analyzed automatically.

Conclusion

Using the yVOG-Glass system, it was possible to perform real-time quantitative 3D analysis of nystagmus from video images recorded with high quality video Frenzel.

Two-axis Magnetic Eye Tracking during Self-generated Head Motion in Freely Moving Mice

Shan Zhu¹; Hui Ho Vanessa Chang²; Kathleen E. Cullen¹

¹Johns Hopkins University; ²McGill University

The measurement of eye movements has proven to be a vital tool for neuroscientists, providing a window into a brain functions ranging from basic reflexes to cognitive processes such as attention. Mice have become a major experimental model for neuroscience research over the past decade. Thus, given an emerging focus understanding how the brain senses and generates action, it is essential to begin tracking eye movements in mice during natural voluntary behaviors. While video-oculography is now commonly used for eye tracking, a current limitation of this technology is that it can only be used to measure eye movements when the head is restrained and cannot be used to monitor eye movements in freely moving mice. Thus, it is necessary to develop more applicable techniques. A recent study (Payne & Raymond, 2017) demonstrated that magnetic sensing can provide reliable eye movement tracking in freely moving mice. However, a limitation of this method is that it assumes only the presence of horizontal eye movements. Yet, during natural behaviors, the eye moves both horizontally and vertically. Accordingly, we developed a two axes magnetic sensing method to concurrently measure both horizontal and vertical eye movements. We implanted each mouse with two pairs of magnets and sensors; each magnet (horizontal and vertical) was implanted in the eye under the conjunctiva, and each sensor was then oriented in order to detect the induced change in magnetic fields due to eye rotation. To validate our method, we conducted horizontal and vertical vestibular-ocular reflex (VOR) testing in head-restrained mice to evoke the eye movements. An inherent challenge of this method is that a given sensor will have some residual sensitivity to eye movement in the orthogonal plane, since the orientations of both magnets are not likely to be perfectly perpendicular. Thus, to address this issue we used nonlinear mapping approach to separate horizontal and vertical eye movement signals. Compared with the eye position data recorded simultaneously with the iSCAN system (video-oculography), our post-processed data showed that a magnetic-based method can measure two-axis eye movements with high accuracy ($r^2 > 0.90$). Taken together, we conclude that magnetic eye tracking can be generalized to two axes, to provide real-time horizontal and vertical eye movement tracking in freely moving mice.

A Comparison of Cervical Vestibular Evoked Myogenic Potential (cVEMP) Metrics in Meniere's Disease patients

Kimberley S. Noij¹; Barbara S. Herrmann²; John J. Guinan³; Steven D. Rauch⁴

¹Massachusetts Eye and Ear; ²Department of Otolaryngology, Department of Audiology, Massachusetts Eye and Ear Infirmary, Harvard Medical School; ³Eaton-Peabody Laboratories, Massachusetts Eye and Ear; Graduate Program in Speech and Hearing and Bioscience and Technology, Harvard Medical School; ⁴Massachusetts Eye and Ear Infirmary, Harvard Medical School

Background: The cervical vestibular evoked myogenic potential (cVEMP) is used to evaluate the function of the saccule and inferior vestibular nerve. To obtain a cVEMP, the saccule is acoustically or mechanically stimulated resulting in a primarily ipsilateral inhibition of the sternocleidomastoid (SCM) muscle that is measured by SCM electromyography (EMG). The cVEMP has been used to evaluate patients with Meniere's Disease (MD) for two decades. Over that time, a variety of cVEMP metrics have been studied, including amplitude, threshold, frequency tuning and interaural asymmetry ratio. Only a few studies have compared different cVEMP metrics in MD patients and a comparison across studies is complicated by methodological differences. The purpose of this study was to investigate the value of different cVEMP metrics in separating MD patients from an age-matched control group.

Methods: cVEMPs were prospectively collected in thirty patients with unilateral definite MD and twenty-three age matched controls. All subjects underwent cVEMP testing on both sides, using 500, 750, 1000 and 2000 Hz tone bursts. Sound level functions were obtained at each frequency, which allowed the calculation of normalized peak-to-peak amplitude (VEMP_n), VEMP inhibition depth (VEMP_{id}), cVEMP threshold, frequency tuning ratio and interaural asymmetry ratio (IAR). For the analyses, ears were separated into three groups: affected MD, unaffected MD and control.

Results: Based on receiver operating characteristic (ROC) curves, 500 Hz cVEMP threshold, VEMP_n and VEMP_{id} were similarly good at distinguishing affected MD ears from healthy controls, with area under the curves (AUCs) of >0.828 and optimal sensitivities and specificities of at least 80% and 70%. A combination of the best three metrics (500 Hz cVEMP threshold, VEMP_n and VEMP_{id}) yielded slightly larger AUCs (>0.880). Tuning ratios and IAR were not as effective in separating healthy from affected ears, with AUCs ranging from 0.540-0.702.

Conclusion: The cVEMP metrics most useful in the evaluation of patients with MD are the threshold, VEMPn and VEMPid, using 500 Hz tone burst stimuli. The frequently used IAR is less effective in separating MD patients from healthy controls and is not recommended.

PS 1089

Otolith Type I Hair Cell Bundle Deflection by VEMPs Testing Induced Endolymph Flow

Wally Grant¹; Joseph Welker¹; Ian S. Curthoys²
¹VA Tech; ²The University of Sydney

Introduction: Vestibular otolithic organs are recognized as transducers of head acceleration and function as such up to their undamped natural frequency (UDNF). It is well recognized that these organs respond to frequencies above their UDNF of approximately 650 Hz for humans, with responses up to 2 to 3 kHz. A mechanics model for transduction displacement of these organs was developed that predicts the response below the UDNF as an accelerometer and above that frequency as a seismometer [Grant and Curthoys, 2017]. Striolar Type I hair cell bundles (HCB) respond to seismometer mode stimulus above the UDNF. This stimulus motion induces endolymph flow in the otolith striolar region holes that are free of gel and column filament layer material where HCB reside. The endolymph induced flow produces a drag force on freestanding or weakly attached HCB, causing their deflection and activation. This work involves model simulation of fluid flow stimulus for striolar HCB deflection.

Methods: Two simulation methods were employed for this study: (1) 2-D model of a HCB hole filled with endolymph. Navier-Stokes equations were converted to vorticity and stream functions eliminating pressure terms. The simulation used Reynolds numbers of 10^{-3} to 10^{-4} , a viscously dominated flow with negligible fluid inertia effects; the resulting equations were solved using finite differences. (2) Computational Fluid Dynamics (CFD) 3-D fluid flow model of endolymph flow around a HCB was combined with a Finite Element Analysis (FEA) structural model of a striolar Type I HCB [Nam et al., 2005]. These two models were solved interactively at each time step. The velocity and pressures from the CFD model interacted with a FEA model determining the transient bundle deflection in a freestanding HCB. In another case the HCB was attached to the otoconial layer.

Results: (1) This simulation showed that the fluid flow, initiated by the endothelial layer motion, followed the stimulus with negligible time lag. The induced flow was circular in nature and produced sufficient velocity to deflect HCB. (2) Type IHCBs required small deflections to open ion channels with realistic fluid flow stimulation

from VEMPs.

Conclusions: Both simulations show that freestanding or weakly attached bundles followed the neuro-endothelial layer motion with negligible time lag. Bundle deflections were sufficient to activate hair cells.

References:

1. Grant and Curthoys (2017). *Hearing Research* 353:26-35.
2. Nam et al. (2005). *J Vest Res* 15:263-278.

PS 1090

Measures of Hydrops Following Exposure to Simulated Wind Turbine Emissions in Healthy Individuals

Joel J. Stanek; Michael J. Sullivan; Peggy B. Nelson; Meredith E. Adams
University of Minnesota

Background: Some individuals living in proximity to wind turbines report otologic symptoms including aural fullness, tinnitus, and vertigo. The infrasonic component of wind turbine generated noise has been suggested as a possible etiology. A mechanism by which infrasound could induce these symptoms has yet to be confirmed. Our work aimed to assess for a hydropic response to simulated infrasound through the use of electrocochleography (ECoG) and vestibular evoked myogenic potentials (VEMP) in healthy volunteers.

Methods: Twelve healthy adult volunteers ages 19-31 were included in the study. Subjects were randomized to undergo ECoG and either cVEMP or oVEMP in sequential order. Baseline summing potential/action potential (SP/AP) ratio and VEMP thresholds were recorded. Subjects then attended to peak-enhanced infrasound simulated from recordings of a research wind turbine ranging in intensity from 85-100 dB SPL for a 10-minute period. ECoG and VEMPs were repeated immediately following the stimulus. Testing was repeated after an additional 10-minute period if a change from baseline had been noted. Participants were asked to rate their symptoms before and after listening with a validated simulator sickness questionnaire (SSQ). Statistical analysis was performed with a Wilcoxon signed-rank test for paired, nonparametric data.

Results: Quality ECoG tracings sufficient for analysis were obtained in 8/12 (67%) participants. In this group, there was no significant change from baseline in SP/AP ratio after infrasound exposure

(mean difference -0.01, $p = 0.44$). One participant demonstrated an increase in SP/AP ratio from 0.23 to 0.39 following infrasound exposure that returned to 0.20 when repeated 10 minutes after exposure. In contrast, a second participant demonstrated a decline from 0.30 to 0.19 and remained at 0.18 10 minutes after exposure. There were no significant changes in cVEMP or oVEMP thresholds from baseline (mean difference 0.8 dB, $p = 0.77$; mean difference 0.8, $p = 1.0$, respectively). SSQ scores did not differ from baseline after exposure (mean difference 2.8, $p = 0.18$). The most common subject-reported symptoms included general discomfort, fatigue, and ear fullness which were rated as mild or moderate. No participants experienced vertigo or motion sickness.

Conclusions: In a cohort of healthy individuals, no significant change from baseline was seen in SP/AP ratio, cVEMP or oVEMP thresholds, or SSQ scores after infrasound stimulus. The observed changes in SP/AP ratio in two individuals is of unclear clinical significance. Subsequent work will examine the effects of infrasound in symptomatic individuals living near wind turbines.

PS 1091

Effect of a Trans-Cranial Vibration System on Nystagmus and Nausea Associated with Vestibular Testing

Didier Depireux¹; Robert True²; Jonathan Akers¹; Jack Daggitt¹; Thomas Hardart¹; Jeffrey Morgan¹; Samuel Owen¹

¹Otolith Labs; ²True Technologies

Background: Vestibular disorders can be difficult to diagnose and can vary in symptoms and fluctuate in severity. It is typically hard to determine which vestibular system (left/right) might be causing the vestibular disorder, as both sides normally work in unison. Testing the vestibular function in each side of a patient is typically done with "caloric testing", which allows testing the left and right vestibular systems separately. However, caloric testing leads to nausea in most patients, and part of the clinical test is spent waiting for the patient to recover. Many patients undergoing caloric testing experience nausea to the point that some patients cannot complete the test, while others need a long period of time to recover from the nausea and dizziness induced by the testing.

Objective: Primary: To measure the efficacy of a transcranial vibrating system of our design (TCVS) at preventing nausea in subjects undergoing vestibular (particularly caloric) testing, as measured by the reduction from baseline of symptoms associated with (caloric)-testing

Secondary: To show that the use of the TCVS does not change the clinical measures obtained by caloric testing.

Methods: Subjects were randomly assigned to "TCVS first" or "TCVS second" groups. For a subject assigned to the "TCVS first" group, they underwent the standard caloric testing, with Warm Right, Cold Right, Warm Left and Cold Left conditions (WR/CR/WL/CL), with the TCVS being turned on 15 seconds prior to the first condition (WR); the TCVS remains turned on throughout the 4 conditions. It is turned off 15 seconds after the end of the last condition (CL). For subject assigned to the "TCVS second" group, the TCVS is placed against the mastoid at the same time as the VNG device is placed on their head, but the TCVS is not turned on until the second set of conditions. The operating parameters of the TCVS (frequency, bone conduction level, applied pressure and location) are as determined from a preliminary study presented at ARO18.

A minute following each set of 4 conditions (WR/CR/WL/CL), subjects are handed a visual analogue scale for dizziness and a visual analogue scale for nausea, asking them to rate the severity of their dizziness (if any) and their degree of nausea. Above a critical score, the time to recovery is also measured. Clinical parameters derived from the vestibular testing is later read by a blinded audiologist.

Results: Results indicate that the dizziness and nausea experienced by healthy subjects and by patients is significantly reduced with the TCVS. Vestibular patients unable to complete the caloric testing under the standard set of 4 conditions (WR/CR/WL/CL) can now undergo the entire set. For the healthy subjects and those patients who could complete both tests (with and without the TCVS), the clinical parameters extracted from the caloric testing are not statistically changed by the use of the TCVS.

Conclusions

We have developed a non-pharmaceutical intervention that is remarkably effective at mitigating and sometimes completely preventing caloric testing-induced dizziness and nausea. In the near future, we will expand our research to medical conditions for which reduction of dizziness would result in improvement of quality of life, such as vestibular migraines, vestibular neuritis and Ménière's disease.

Investigating the Link Between Visual Sensitivity and Seasickness

Tyler Churchill¹; Ashley Zaleski-King²; Joshua G.W. Bernstein²; Douglas S. Brungart²

¹United States Naval Academy; ²Walter Reed National Military Medical Center

One trigger for motion sickness is dynamic visual motion, particularly when the visual motion is mismatched with other sensory inputs. Previous studies have shown that the subjective estimates of visual vertical (SVV) of individuals with clinically significant balance and dizziness symptoms are more sensitive to interference from a dynamic visual background than healthy controls. It is also possible that individuals who are not actively dizzy but who are unusually susceptible to motion sickness may also exhibit relatively high levels of visual sensitivity. Instructors who teach sailing to Navy midshipmen often find that inexperienced sailors experience motion sickness when at sea, where visual inputs are either unavailable or in opposition to information obtained from the vestibular and/or somatosensory systems. They also report that more experienced sailors tend to be less sensitive to seasickness, which may reflect an acquired reduction in visual sensitivity.

In order to investigate these observations, a preliminary study of visual sensitivity and motion sickness was conducted on twelve students in a sailing class. Students who consented for the study first provided demographic information and filled out the Motion Sickness Susceptibility Questionnaire (MSSQ) and the Motion Sickness Assessment Questionnaire (MSAQ). Then, to assess visual sensitivity, participants completed a virtual reality implementation of the Rod and Disk Test (RDT) that required participants to use buttons on a game controller to orient the image of a rod superimposed on a background of rotating dots into the vertical position. The results showed some indications of a systematic relationship between visual sensitivity and motion sickness susceptibility, and a trend toward a reduction in motion sensitivity in students who repeated the RDT after the sailing class. A follow-up study is now planned that will use a ship bridge simulator capable of incrementally increasing sea states. During and following their time in the simulator, participants will report their level of seasickness. This method will allow collection of participant seasickness data for specific simulated sea state conditions. It is hoped that the RDT test will be a useful tool for predicting seasickness susceptibility and reduce the necessity for new sailors to rely on preemptive medication that are costly and have undesirable side effects. If visual sensitivity can be found to predict the amount to which a person is prone to seasickness,

sailing populations could develop more targeted and effective seasickness mitigation procedures.

The views expressed in this talk are those of the authors and do not necessarily reflect the official policy or position of the Department of the Army, the Department of the Navy, the Department of the Air Force, the Department of Defense, or the U.S. Government.

Development IV

PD 105

Cochlear Neuroblasts Mature into Spiral Ganglion Neurons in a Shh-dependent Manner

Lok Sum Wong¹; Doris Wu²

¹NIDCD/NIH; ²National Institute on Deafness and other Communication Disorders

Hearing loss in patients suffering from auditory nerve damage cannot be alleviated because cochlear neurons do not regenerate in human. Thus, greater effort is needed to identify key factors that help direct proper neural development and establish correct wiring between the cochlea and brain in order to replace these cells. An essential gene that is known to be involved in early spiral ganglion (SG) development in mice is Sonic hedgehog (*Shh*), which encodes a secreted molecule that expresses in a subset of cells within the developing SG. Previously, we have shown that conditional knockout (cKO) of *Shh* in the SG resulted in a shorter cochlea and premature differentiation of mechanosensory hair cells in the cochlear epithelium. In addition to the requirement of this ganglionic source of *Shh* for cochlear development, *Shh* is also important for the formation of the SG because the size of SG is much reduced in the *Shh* cKO. To address how *Shh* signaling pathway regulates the formation of SG neurons, a combination of *in situ* hybridization, fate mapping, and cell cycle labeling techniques were used. We have identified that Patched (*Ptc1*), the receptor for the SHH ligand, is expressed strongly in the dividing neuronal progenitors juxtaposed to the post-mitotic, *Shh*-positive nascent SG neurons. Furthermore, fate mapping results indicate that nascent SG neurons only express *Shh* transiently and this expression is down-regulated as neurons become more mature. Based on this intricate relationship between *Shh* and *Ptc1* expression patterns, we propose that SHH secreted by nascent neurons guide neighboring *Ptc1*-expressing neuroblasts toward terminal mitosis. Post-mitotic neurons express *Shh* promptly and they replace previously-born neurons that begin to or have already downregulated *Shh* expression. As a result, there is a continual presence of

Shh that came from sequential production of nascent SG neurons, which signals back to adjacent *Ptc1*-expressing neuroblasts to form a feedback loop. The loss of *Shh* disrupted this chain of cellular events and resulted in a smaller SG. By understanding how the dynamic expression pattern of *Shh* is being regulated will provide insights for developing more effective interventions for treating auditory neuropathy.

PD 106

Morphogenesis of Type I Spiral Ganglion Neurons and the role of Sema 3a/Nrp1 signaling.

Homero L. Cantu¹; Michael Papazian¹; Nathalie Spita²; Thomas M. Coate¹

¹Georgetown University; ²John Hopkins School of Medicine

Proper connectivity of spiral ganglion neurons (SGNs) and hair cells is necessary for conveying sound information to the brain. The majority of SGNs are composed of type I fibers that innervate inner hair cells (IHCs) in the organ of Corti and transmit the vast majority of sound input. However, very little is known about the molecular mechanisms that mediate type I SGN innervation patterns on IHCs. Classic studies in the cat auditory nerve (by Liberman et al.) suggested two distinct morphological and functional populations of type I SGNs: thin SGNs with low rates of spontaneous discharge tend to innervate the modiolar side of the IHCs, and thicker SGNs with higher rates of spontaneous discharge tend to innervate the pillar cell side of IHCs. Using genetic SGN sparse labeling, confocal imaging, and morphometric analyses, we have begun to characterize the developmental time course of type I SGN innervation of mouse IHCs. Interestingly, at early stages, the average diameter of fibers contacting the modiolar side of the IHC is significantly lower than the diameter of fibers contacting the pillar side of the IHC. But, at P8 these differences are not apparent. Our data show that, around the onset of hearing and through P30, type I SGNs on the modiolar side of the IHC become thicker compared to those on the pillar cell side of the IHC. Using genetic models, we are attempting to identify signaling factors that may play a role in this pattern of innervation. My preliminary data show that Semaphorin- 3A (Sema3A) and its main receptor Neuropilin-1 (Nrp1) may control the distribution of type I SGNs. Sema3A is a secreted member of the semaphorin family and known to act as a chemorepellent that induces growth cone collapse. Via in situ hybridization, we identified the expression of Sema3a around IHCs in the developing cochlea suggesting a potential role in the innervation pattern of type I SGNs. Nrp1 protein is detectable on SGN processes and enriched in fibers projecting toward the pillar cell. We will examine

several Nrp1 and Sema3a mutant models to determine the extent to which Sema3A/Nrp1 interactions control type I SGN synaptic organization at the IHC. We will also determine the extent to which these factors are necessary for hearing acuity.

PD 107

Cellular and Molecular Mechanisms of Sensory Organ Segregation in the Embryonic Inner Ear

Ziqi Chen¹; Nicolas Daudet²

¹Ear Institute, University College London; ²University College London

The inner ear contains multiple sensory organs separated by non-sensory epithelial domains. These organs are specified during early otic development and become gradually individualised by segregation from a common Sox2-expressing pan-sensory domain. Some of the genes and signalling pathways essential for sensory organ specification and segregation have been identified. However, the basic cellular mechanisms of segregation are still unexplored. In this study, we analysed the changes in cell fate and cell morphology during the segregation of the lateral and anterior cristae in the embryonic chick otocyst. We found that their segregation is coupled to striking changes in cell morphology. The cells at the interface of the prospective cristae and the pan-sensory domain enlarge, become elongated and progressively align before down-regulating Sox2 expression. Multicellular rosettes and phosphorylated myosin regulatory light chain staining are present throughout the otocyst, suggesting that cell rearrangements mediated by acto-myosin contractility could contribute to sensory organ segregation. We are now testing this hypothesis using genetic and pharmacological manipulations of actomyosin contractility. We have also developed a new organotypic culture method that will enable us to study in real-time the dynamics of sensory organ specification and segregation in the chick and mouse inner ear using time-lapse imaging.

PD 108

Sensory Hair Cell Differentiation Requires De novo Changes in Chromatin Accessibility during Notch-mediated Lateral Inhibition

Haoze (Vincent) Yu¹; Litao Tao²; Juan Llamas¹; Suhasni Gopalakrishnan³; Talon Trecek⁴; Yassan Abdolazimi³; Neil Segil⁵

¹Department of Stem Cell Biology and Regenerative Medicine, Keck School of Medicine, University of Southern California; Caruso Department of Otolaryngology, Keck School of Medicine, University of Southern California; ²Department of Stem Cell Biology and Regenerative Medicine; Caruso Department of

Otolaryngology, Keck School of Medicine, University of Southern California; ³Department of Stem Cell Biology and Regenerative Medicine, Keck School of Medicine, University of Southern California; ⁴Department of Stem Cell Biology and Regenerative Medicine, Keck School of Medicine of the University of Southern California; Caruso Department of Otolaryngology, Keck School of Medicine, University of Southern California; ⁵Department of Stem Cell Biology and Regenerative Medicine, and Caruso Department of Otolaryngology - Head and Neck Surgery, Keck School of Medicine, University of Southern California

Background. The epigenetic basis for the formation of mechanosensory hair cells is poorly understood. During development of the mouse organ of Corti, hair cells and supporting cells differentiate within a pool of prosensory progenitors, by a process involving Notch-mediated lateral inhibition. To better understand the mechanisms of gene regulation that govern hair cell and supporting cell differentiation, we explored the chromatin landscape of FACS-purified cells from the organ of Corti at various embryonic stages, as well as during supporting cell transdifferentiation *in vitro*. Our results indicate that in contrast to the prevailing theory that enhancer accessibility is broadly permissive within a particular tissue lineage, as has been described in the crypts of small intestine, we observed that hair cell differentiation requires *de novo* opening of a large proportion of the distal elements controlling hair cell-specific gene expression, and identified some of the transcription factors involved.

Method. We profiled chromatin accessibility and the enhancer histone mark (H3K27ac) on FACS-purified primary cell types from the developing organ of Corti, by μ ATACseq and Assay for Transposase-Mediate-ChIPseq (ATM-ChIPseq), two methods developed in our lab to study the epigenome with small numbers cells.

Results. We detected 16,431 newly accessible (open) distal chromatin regions in the differentiating hair cells, compared to undifferentiated prosensory progenitors and differentiating supporting cells. A subset of these potential regulatory DNA elements is marked by the presence of nucleosomes containing histone H3 acetylated at lysine 27 (H3K27ac), an indication of active gene enhancers. These include genes involved in both Notch-mediated lateral inhibition, and hair cell differentiation. Motif-enrichment-analysis revealed a group of transcription factor binding sites highly enriched in hair cell-specific distal elements, including the POU-family motif. Chromatin structure data collected from Pou4f3-mutant hair cells showed that the chromatin accessibility of 3,095 hair cell distal elements (~20% of total), are Pou4f3-dependent, including ones near

known Pou4f3 target genes. Over-expression of Pou4f3 in mouse embryonic fibroblasts is sufficient to convert a subset of these lineage-specific elements into a hair cell-like configuration.

Conclusion. Pou4f3 is likely to be one of the pioneer factors necessary for hair cell differentiation, responsible for creating newly accessible enhancers to stimulate the expression of hair cell specific genes. Our results also appear to contradict the model of broad, lineage-specific chromatin accessibility, which predicts that potential enhancers required for differentiation are maintained in an accessible, and poised state in the undifferentiated, equipotent progenitors.

PD 109

Zika Virus Pathogenesis in the Developing Avian Inner Ear

Ankita Thawani¹; Nabilah H. Sammudin¹; Hannah Reygaerts¹; Vidhya Munnamalai²; Richard J. Kuhn¹; Donna M. Fekete¹

¹Purdue University; ²The Jackson Laboratory

Zika virus (ZIKV) is a tropical pathogen primarily transmitted by mosquitos. Although infected adults mainly present with mild febrile symptoms, the vertical transmission of ZIKV from an infected pregnant mother to the fetus can result in severe congenital defects in the developing brain and eye. Common pathologies include microencephaly, ventriculomegaly, retinopathy and brain calcifications. In addition to these neurological defects, the spectrum of congenital ZIKV syndrome extends to sensorineural hearing loss. Around 6% of newborns exposed prenatally to ZIKV presented with diminished otoacoustic emissions and auditory brainstem responses, hence indicating sensorineural hearing loss, perhaps originating in the cochlea. A key knowledge gap is the lack of information on the spatial and temporal susceptibility of the developing inner ear to ZIKV infection. Various cellular and animal models show that ZIKV is neurotropic and infection of neural progenitors by ZIKV represses cell proliferation and leads to cell death. We hypothesized that inner ear neurosensory cell populations, such as delaminating neural progenitors of the statoacoustic ganglion, prosensory epithelia of vestibular and auditory organs, and immature hair cells, may be preferentially susceptible to ZIKV infection when compared to non-neurogenic epithelial domains. To test this, ZIKV was injected directly into the otic primordium of chicken embryos *in ovo* on embryonic days (E)2, E3, E4 or E5, followed by harvests every other day until 8 days post infection. Short-term harvests were used to analyze cell death and to explore which inner ear cell types were most susceptible to infection at each stage of injection. Long-

term harvests showed evidence of pathogenic effects on ear morphogenesis. Our data showed strong inner ear infection in 32% of the embryos, including sensory epithelial infection in both vestibular and auditory organs. The statoacoustic ganglia and periotic mesenchyme were also targets for ZIKV infection. A preference for sensory over non-sensory epithelial infection in the inner ear labyrinth was not apparent. Infection was found in the sensory cochlea as late as E13; however, the later stages of harvest showed stronger sensory cochlear infection, when the hair cells are born and maturing. This study supports the conclusion that ZIKV may contribute to hearing loss by directly infecting tissues of the inner ear. The study is supported by NIDCD grant R21DC016732.

PD 110

Live Imaging of Centriole Movements in Nascent Utricular Hair Cells

Yosuke Tona¹; Doris Wu²

¹NIDCD/NIH; ²National Institute on Deafness and other Communication Disorders

Hair cells of the inner ear transduce sound and head movement information in the form of vibrations into chemical signals. This function of hair cells relies on the hair bundle on the apical cell surface that is comprised of a kinocilium and a number of stereocilia organized in a stair-case fashion. Proper orientation of the hair bundle is essential for signal transduction because hair cells are excited only when the hair bundle is deflected toward the direction of its kinocilium. It is known that hair bundles in the chicken basilar papilla (cochlea) are established by the migration of the kinocilium from the center of the apical surface towards the edge. After the kinocilium acquires its final position, the staircase stereocilia are then built adjacent to the kinocilium. Previously, we have shown that the line of polarity reversal (LPR) in the vestibular maculae of the mouse is established by the restricted expression of the transcription factor *Emx2* to one side of the prospective LPR in the macula, which causes all the hair bundles within the region to reverse their orientation from the default position by approximately 180 degrees. The mechanism(s) whereby the downstream effectors of *Emx2* mediate hair bundle reversal is not known. To gain insight into the role of *Emx2* in reversing hair bundle orientation, we compared the process of hair bundle establishment in hair cells across the LPR using live imaging of mouse utricular explants between embryonic day 13.5 to 14.5. In these preparations, the establishment of the kinocilium in tdTomato-positive hair cells were tracked by following the trajectory of the two Gfp-labeled centrioles, of which the mother centriole forms the base of the kinocilium. Our results showed that the centrioles in the utricular hair cells appears to take

on a more direct trajectory from the center of the apical surface to reach the final destination in the periphery than what was described in the chicken papilla. Additionally, the trajectory of the centrioles is similar between *Emx2*-positive and negative hair cells, despite their final position is located on opposite ends of the cell. These results suggest that by the time the kinocilium begins to acquire its position on the cell surface, the *Emx2*-positive and negative hair cells are already intrinsically different from each other, which guides the kinocilia to their respective positions. Experiments designed to examine hair bundle establishment in gain and loss of *Emx2* mutants are currently underway.

PD 111

Multi-directional signals regulate the dynamics of cochlear hair cell induction and organization

Tomoko Tateya¹; Susumu Sakamoto²; Fumiyoshi Ishidate³; Tsuyoshi Hirashima⁴; Itaru Imayoshi⁵; Ryoichiro Kageyama²

¹Department of Otolaryngology-Head and Neck Surgery, Graduate School of Medicine, Kyoto University; ²Institute for Frontier Life and Medical Sciences, Kyoto University; ³World Premier International Research Initiative-Institute for Integrated Cell-Material Sciences (WPI-iCeMS), Kyoto University; ⁴Department of Pathology and Biology of Diseases, Graduate School of Medicine, Kyoto University; ⁵Graduate School of Biostudies, Kyoto University

Auditory hair cells (HCs) and supporting cells differentiate from common precursors in the prosensory domain of developing cochlear epithelium. HCs are eventually aligned along the length of the cochlea in a regular pattern; however, how one row of inner HCs (IHCs) and three rows of outer HCs (OHCs) are organized is not well understood. The transition from prosensory cells to differentiating HCs is the initial process of HC organization. It occurs in a short period, approximately mouse embryonic day 14-16, too rapid to analyze using fixed samples. We investigated the transition process from prosensory cells to differentiating HCs using dynamic visualization of *Atoh1* expression by three-dimensional time-lapse imaging of *Atoh1*-EGFP fusion mouse cochlear explants. We crossed two transgenic lines, *Atoh1*-EGFP, and mCherry reporter mice for the visualization of *Dll1* or *Hes5*. Overnight live imaging was performed on cochlear explants of the double transgenic mice. The fluorescence intensity and position of individual cells in prosensory domain were detected at each time frame, and labeled cells were tracked over time by Imaris software. In our study, the live imaging parameters including laser power of the confocal microscope was different with each acquisition, so as to minimize both laser toxicity and

maximize the fluorescent signal. We made comparisons and perform statistical analyses among time-lapse imaging experiments after digital image processing. We defined the relationship among low-level GFP, high-level GFP, Dll1 and Hes5, and confirmed that a change in GFP intensity can be interpreted as cell fate commitment. HC induction initially occurs at the medial edge of the prosensory domain to form IHCs and subsequently at the lateral edge to form OHCs. We also administered Hedgehog or Bmp4 signaling inhibitors before time-lapse imaging, and the effects of these inhibitors on the patterning in transition process offered a model suggesting that multi-directional signals from outside of the prosensory domain regulate the dynamics of IHC and OHC induction and organization. Our time-lapse imaging approach is novel and complements the existing literature on HC differentiation and organization in the developing cochlea.

Normal & Impaired Binaural Hearing

PD 112

Listeners With No More Than “Slight” Hearing Loss Who Exhibit Deficits in Binaural Detection Also Exhibit Deficits in the Ability to Discriminate Changes in Interaural Time and Interaural Intensity

Leslie R. Bernstein; Constantine Trahiotis
University of Connecticut Health Center

Background

The results of recent experiments conducted in our laboratory have demonstrated consistently that listeners who would be classified via pure-tone audiometry as having no more than “slight” hearing loss may exhibit substantial deficits when tested in a binaural detection task. Specifically, binaural detection thresholds were found to be elevated for listeners whose absolute thresholds at 4 kHz exceeded 7.5 dB HL, but were not greater than 25 dB HL. Notably, deficits in binaural detection were found for such listeners when they were tested with stimuli having center frequencies which spanned the range 250 Hz to 8 kHz, in octave steps. Here, we show that such listeners also exhibit degraded sensitivity to changes in interaural temporal differences (ITDs) and interaural intensive differences (IIDs).

Methods

We measured 1) detection of tonal signals presented in the NoS π configuration; 2) sensitivity to changes in ITD; 3) sensitivity to changes in IID. Bands of Gaussian noise 100-Hz-wide served as maskers in the detection task and as reference and target stimuli in the discrimination tasks. The center frequencies of the stimuli were either 500 Hz (where the fine-structures of the stimuli convey changes in binaural temporal information) or 4 kHz (where the envelopes of the stimuli

convey changes in binaural temporal information). As in our previous experiments, in order to maximize sensitivity to envelope-based ITDs, the stimuli centered at 4 kHz were the transposed counterparts of tones and 100-Hz-wide Gaussian noises centered at 125 Hz.

Results and conclusions

The NoS π binaural detection thresholds replicated the outcomes of our previous two studies [Bernstein and Trahiotis, *J. Acoust. Soc. Am.* **144**, 292-307 (2018); Bernstein and Trahiotis, *J. Acoust. Soc. Am.* **140**, 3540-3548 (2016)]. That is, once again, we found that detection thresholds were elevated for listeners having pure-tone thresholds at 4 kHz > 7.5 dB HL as compared to listeners having pure-tone thresholds at 4 kHz 7.5 dB HL also exhibited elevated threshold-ITDs and threshold-IIDs at both center frequencies. These outcomes will be discussed within the framework of a modern cross-correlation-based quantitative model of binaural processing that includes both well-accepted stages of peripheral auditory processing and well-accepted types of internal noise.

[Research supported by the Office of Naval Research (ONR Award No. N00014-15-1-2140)]

PD 113

Monaural Temporal Sensitivity and its Implications for Binaural Hearing in Normal-Hearing and Cochlear-Implant Listeners

Sean R. Anderson¹; Alan Kan²; Ruth Litovsky²
¹*Waisman Center, University of Wisconsin-Madison;*
²*University of Wisconsin - Madison*

Sensitivity to interaural time differences (ITDs) and monaural temporal fluctuations is more variable within and across cochlear-implant (CI) users compared to normal hearing (NH) listeners. Since computation of ITDs in the brainstem relies on exquisitely precise temporal encoding, sensitivity to ITDs may be limited by poor encoding of temporal information in either ear. This study explored how sensitivity to and utility of envelope ITDs change when temporal encoding is poorer in one ear for NH and CI listeners. We hypothesized that if binaural sensitivity is mediated by the fidelity of temporal encoding in each ear, then sensitivity to and utility of ITDs would be predicted by temporal sensitivity in the poorer ear.

In NH listeners, fidelity of temporal encoding was manipulated by reducing the depth of modulation for sinusoidally amplitude-modulated acoustic pulse trains and tones, with carrier frequencies at 4000 and 8000 Hz. Computational models of the auditory nerve (Zilany et al., 2014) confirmed that reducing modulation depth results in poorer phase locking to amplitude modulation (AM).

Stimuli were presented at 65 dB SPL via circumaural headphones or insert earphones.

In CI users, fidelity of temporal encoding was indexed using an AM rate discrimination task on single electrodes. Stimuli were 3000 or 4000 pulse per second pulse trains with sinusoidal AM. All stimuli were presented at comfortable level via direct stimulation of electrodes 4, 12, 16, or 20 in either ear using the RF Generator (Cochlear, Ltd.).

Monaural temporal sensitivity was measured using a three-interval, two-alternative forced-choice discrimination task, where AM rate was greater for one of the latter two intervals. Binaural temporal abilities were measured using a: (1) same/different AM rate identification task was used, where a single interval was presented and listeners were instructed to report whether the AM rate was the same in both ears; (2) lateralization task, where listeners were asked to report the perceived intracranial location given a specific ITD.

In general, shallower modulation depths in one ear resulted in higher same/different AM rate identification thresholds and smaller ranges of lateralization in NH listeners. For CI users, there was evidence of a relationship between sensitivity to changes in AM rate presented monaurally, and same/different AM rate sensitivity and ITD lateralization. Together these results suggest that binaural abilities may be limited by the ear with poorer temporal encoding.

Work supported by NIH-NIDCD R01-DC003083 to RYL, NIH-NIDCD R03-DC015321 to AK, and NIH-NICHD U54HD090256 to the Waisman Center.

PD 114

The Effect of Spectral Resolution on Dichotic Listening Performance and Effort

Kristina DeRoy Milvae¹; Stefanie Kuchinsky²; Olga A. Stakhovskaya³; Matthew Goupell⁴

¹University of Maryland College Park; ²Audiology and Speech Pathology Center, Water Reed National Military Medical Center; Department of Hearing and Speech Sciences, University of Maryland; ³Department of Hearing and Speech Sciences, University of Maryland; ⁴University of Maryland

Introduction

Bilateral cochlear implantation is becoming more common but is typically sequential. This leads to differences in the duration of deafness and sometimes the functionality of the two ears, which may limit binaural benefits. Measures of performance and listening effort, the cognitive resources used to achieve a given level

of performance, could give complementary information about binaural perception. Listening effort, measured with pupillometry, increases with decreasing spectral resolution and may be sensitive to changes in auditory processing that occur with no significant change in speech understanding. It is not known if differences in the spectral resolution of the two ears affect the listening effort required to attend to one ear and recall what was heard. Therefore, spectral resolution was varied across ears in normal-hearing (NH) listeners to simulate symmetric and asymmetric cochlear-implant (CI) listening. It was hypothesized that less effort would be required to attend to relatively more clear speech in the presence of relatively more degraded speech.

Methods

NH listeners completed a dichotic listening experiment with unprocessed and 4- and 16-channel vocoded digits presented monotically and dichotically. Listeners were directed to attend to their right ear and report the digits heard in that ear. The accuracy of digit recall was measured to assess performance in each condition. Pupil dilation was continuously monitored as a proxy for listening effort.

Results

Preliminary results of this experiment show high performance with and without interfering digits in the unattended ear. There is also a trend for pupil size to be higher in dichotic conditions than in monotic conditions. The processing of the attended ear affected pupil size, with poorer spectral resolution related to larger pupil dilation, but the processing of the unattended ear did not lead to differences in pupil dilation.

Discussion

These preliminary results suggest that additional listening effort is required to attend to one ear when interfering speech is presented to the other ear. In addition, results suggest that the spectral resolution of the attended ear has a larger impact on listening effort than that of the unattended ear. Since objective measures of listening effort contribute additional information about auditory processing, and CI listeners report high listening effort, its measurement may inform clinical decisions regarding the timing of bilateral cochlear implantation.

[Work supported by NIH T32DC000046 (trainee K.D.M.) and R01DC014948 (M.J.G).]

PD 115

Decrease in Sound Localization Latency as a Function of Age in Infants and Young Children

Martin Eklöf; Filip Asp; Erik Berninger
Department of Clinical Science, Intervention and Technology, Karolinska Institutet

Background

Eye gaze is an innate response to auditory events. Sound localization latency (SLL) of responses may be studied objectively using gaze as a measure of sound localization behavior. The aim was to study the effect of age on SLL in normal-hearing children.

Methods

Twelve healthy and normal-hearing children (aged 26 to 160 weeks) participated in this study as part of another study (1). An array of twelve loudspeaker/display-pairs spanning ± 55 degrees azimuth in the frontal horizontal plane was used for measuring sound localization responses. An ongoing auditory-visual stimulus presented at 63 dB SPL(A) was shifted to randomly assigned loudspeakers with 1.6 sec pauses of the visual stimulus, beginning at each azimuthal shift. The subjects' saccades towards target were modeled by fitting an arctangent-function to the gaze samples after each loudspeaker shift, i.e. a trial. The time from an azimuthal shift of the sound to the 50%-point of the arctangent-function was defined as the trial latency. The median across the test (24 trials) was defined as SLL.

Results

Preliminary results show that young children aged 26-160 weeks exhibited a mean SLL of 800 ms. The mean SLL was significantly larger compared to normal hearing adults (250 ms, $n=8$; Eklöf, Asp, Berninger, in manus). The children exhibited a decrease in SLL as a function of age with a slope of 3.5 ms/week, as determined by linear regression ($p=.004$).

Conclusions

Sound Localization Latency decreased with age in normal-hearing infants and young children.

References

1 Asp F, Olofsson Å, Berninger E. Corneal-Reflection Eye-Tracking Technique for the Assessment of Horizontal Sound Localization Accuracy from 6 Months of Age. *Ear Hear.* 2016;37(2):e104-18.

PD 116

Neural Correlates of Speech Spatial Release from Masking

Spencer B. Smith¹; Trent Nicol²; Jennifer Krizman²; Travis White-Schwoch²; Nina Kraus²
¹The University of Texas at Austin and Northwestern University; ²Northwestern University

Background:

Spatial release from masking (SRM) is a binaural phenomenon defined as the improvement in speech-in-noise perception when speech and noise are spatially separated versus collocated. Despite being a widely documented perceptual ability, the neural processes underlying SRM and its breakdown are poorly understood, particularly for individuals with normal audiograms. In this study, we developed an electrophysiologic measure of SRM and investigated its relationship with perceptual SRM.

Methods:

Frequency following responses (FFR) to a speech token ("da") were recorded from 22 normal hearing listeners in three conditions analogous to those in the Hearing in Noise Test (HINT): Speech Front, Speech Front/Noise Front, and Speech Front/Noise Side. FFR envelope and fine structure spectral amplitudes and phase locking strength were computed for each condition. Neural SRM was calculated as the spectral amplitude and phase locking difference between Speech Front/Noise Side and Speech Front/Noise Front, respectively. Perceptual SRM was calculated from each participant's HINT performance.

Results:

The neural consequence of collocated speech and noise is to increase the neural representation of the F0, as FFR F0 spectral amplitudes were larger on average in the Speech Front/Noise Front condition versus Speech Front. Fine structure spectral amplitudes were larger in the Speech Front/Noise Side condition relative to the Speech Front/Noise Front condition; subtracting these two measurements yielded a neural SRM. Phase locking strength mirrored spectral amplitude findings. Perceptual and neural SRM were only weakly correlated; however, when participants were split into "high" and "low" perceptual SRM groups, larger neural SRM was observed in the high perceptual SRM group than in the low perceptual SRM group.

Conclusions:

To our knowledge, this study is the first to investigate neural signatures of SRM in humans using complex speech stimuli. Our observation that F0 spectral amplitudes grew in the Speech Front/Noise Front condition relative to Speech Front is consistent with recent modeling and human EEG

data demonstrating that the FFR envelope is driven by high frequency channels. That SRM can be measured neurally and, at least at the group level, is related to perceptual SRM indicates that some perceptual variation in spatial speech-in-noise performance is reflected in the FFR. This finding has important implications not only for studying neural mechanisms underlying spatial speech-in-noise performance variation but also for fine tuning binaural hearing aids and cochlear implants.

PD 117

Changing the Frequency-dependent Weighting of the Localization Cues

Norbert Kopco¹; Rene Sebens²; Peter Loksa²; Ondrej Spisak²; Maike Ferber³; Aaron Seitz⁴; Frederick Gallun⁵; Bernhard Laback⁶

¹P. J. Safarik University and Boston University; ²P. J. Safarik University; ³Austrian Academy of Sciences and P. J. Safarik University; ⁴University of California, Riverside; ⁵VA RR&D NCRAR; ⁶Austrian Academy of Sciences

Which cues the auditory system uses to determine the sound source location largely depends on the sound's frequency content. For low-frequency (LF) narrowband sounds, the interaural time difference (ITD) is the dominant cue, while for high-frequency (HF) narrowband sounds, the interaural level difference (ILD) dominates. For mid-frequency narrowband sounds, ITD and ILD appear to have about equal weights in determining the perceived location. We recently showed that the ITD/ILD weighting for a narrowband stimulus can be changed by visual feedback training in a virtual acoustic environment [Ferber et al., JASA, 143, 1813 (2018)]. Here, we examined whether a similar or stronger adaptation can be achieved by visually guided training on broadband stimuli in a real reverberant environment. This training eliminates issues related to the fidelity of the virtual environment, like limited externalization or audio-visual binding, thus potentially enhancing adaptation. Separate groups of 12 listeners each were trained either to increase the HF weighting or the LF weighting for broadband stimuli. The stimuli consisted of 2 or 4 one-octave noise bands, together covering the range 0.7 - 11.2 kHz, presented from neighboring speakers selected from a range of 11 speakers spanning the angles of -56° to 56° with separation of 11.25°. Visual feedback, co-located either with the HF components or the LF components, was used to instruct the subjects about the correct target location. On each training trial, the audio-visual stimulus was played continuously while the listener performed a head-turn towards it and then back to straight ahead, so that both static and dynamic cues were available while the visual signal guided auditory adaptation. This training was successful for the HF group, but not for the

LF group. However, the changes in spectral weighting only partially generalized into changes in the ITD/ILD weights. Additionally, we explored whether using a simple computer game-like adaptive discrimination task is sufficient to induce reweighting. The game training was found to be less effective. These results show that frequency-dependent weighting of the binaural cues can be modified in the real environment, as well as in the virtual environment, as shown in Ferber *et al.* (2018). The results are likely to have implications for training of bilateral cochlear-implant listeners and for creation of adaptive virtual auditory environments. [Supported by: Danube Partnership project APVV DS-2016-0026, H2020-MSCA-RISE-2015 #691229]

PD 118

What's so Monaural about "Monaural Spectral Cues"?

M. Torben Pastore; William A. Yost
Arizona State University

While binaural difference cues specify a range of locations, called the "cones of confusion," spectral cues from approximately 4-20 kHz can specify a unique location on the cone of confusion, provided there is sufficient bandwidth in the high-frequency range. Spectral cues derived especially from direction-specific interference with the pinnae can allow listeners to determine the front-back location of a sound source, thereby avoiding front-back reversals (FBRs) on the azimuth plane that intersect with a given cone of confusion. Such spectral cues are most often conceived of and referred to as "monaural spectral cues." As such, front-back reversals ought to be avoidable for a stationary listener with just the use of one ear.

We tested this hypothesis with seven single-sided deaf listeners implanted with a cochlear implant in the deafened ear, turning off the cochlear implant, leaving only the healthy ear for localization. Stationary listeners reported the loudspeaker location of 3-sec. duration Gaussian noises filtered to 2-8 kHz randomly presented from one of six loudspeakers 60 degrees apart from each other. The same experiment was carried out for eight normal hearing listeners, with one ear acutely occluded with an earplug. Earplug attenuation was measured in the sound field at 0° azimuth using pulsed-warble tones presented at octave frequencies from 0.250-8 kHz with a narrowband noise masker presented at 50 dB EM (effective masking) to the unoccluded ear using an insert earphone. The acute normal hearing listeners were then presented with the test stimuli 4 dB below their measured monaural detection threshold for the 2-8-kHz stimuli.

For normal hearing listeners with two healthy ears, front-back reversals are relatively rare for the high-frequency

stimuli presented in these experiments. For both monaural groups tested in these experiments, however, listeners were at chance in determining front from back sound source location, suggesting that using spectral cues may involve more than just monaural processing. (Research supported by NIDCD and Oculus, VR LLC).

PD 119

Model-based Meta-analysis of Sound Externalization Cues

Robert Baumgartner¹; Piotr Majdak²

¹Acoustics Research Institute, Austrian Academy of Sciences; ²Acoustics Research Institute, Austrian Academy of Sciences

The perceptual association of an auditory signal with a sound source located somewhere externally around the listener is natural but requires complex signal processing to be achieved artificially in virtual or augmented realities presented via headphones. Very little is known about the cues required to guarantee the natural percept of sound externalization. We aim to shed light onto the diversity of cues causing degraded sound externalization with spectral distortions by conducting a model-based meta-analysis of psychoacoustic studies. As potential cues we considered monaural and interaural spectral-shapes, spectral and temporal fluctuations of interaural level differences, interaural coherences, and broadband inconsistencies between interaural time and level differences in a highly comparable template-based modeling framework. Mere differences in sound pressure level between target and reference stimuli were used as a control cue. Our investigations revealed that the monaural spectral-shapes and the strengths of time-intensity trading are potent cues to explain previous results under anechoic conditions. However, future experiments will be required to unveil the actual essence of these cues.

Work supported by FWF J3803-N30 and Oculus Research, LLC.

Speech Perception

PD 120

The Dynamics of Lexical Access Change Depending on Listener Needs in Cochlear Implant Users: The Effect of Sentence Context

Francis X. Smith; Bob McMurray

Department of Psychology and Brain Sciences, The University of Iowa

At a central level, the process of mapping incoming speech to lexical candidates is characterized by competition. As the input unfolds multiple words are activated and compete until a single word is recognized. Previous work has found that cochlear implant patients exhibit different

dynamics of lexical access than normal hearing listeners (McMurray, Farris-Trimble, & Rigler, 2017; Farris-Trimble, McMurray, Cigrand & Tomblin, 2014). Post-lingually deaf CI users slow processing somewhat and experience more competition between target words and similar sounding competitors. In contrast, pre-lingually deaf CI users exhibit a “wait-and-see” approach. They slow down dramatically, and as a result show less competition from onset competitors (e.g., *wizard* and *whistle*), since they have heard more of the word when lexical access initiates, along with increased competition from offset competitors (*wizard/lizard*). Much of the work examining this process (in both NH and CI users) has examined words in isolation (Dahan, Magnuson, & Tanenhaus, 2001; McMurray, Tanenhaus, & Aslin, 2002). This is less ecologically valid, and the simple demands of processing multiple words simultaneously could alter CI users’ dynamics. For example, a “wait-and-see” approach that delays lexical access could be detrimental in longer sentences as listeners fall increasingly behind with each word. In the present study, experienced cochlear implant patients were tested in a Visual World Paradigm study to characterize the dynamics of lexical access. Listeners heard a target word and selected its picture from a screen containing pictures of the target word and several competitors. Eye-movements were monitored over time to gauge the strength by which each word was competing. Words were spoken either in isolation or in semantically neutral sentences (e.g., “please click on the ____ to continue”). Sentence lengths and the position of the target word in the sentence varied to prevent participants from ignoring the sentence altogether. Relative to words in isolation words in sentence contexts showed slightly faster activation of the target word, along with increased competition from onset competitors and decreased competition from offset competitors. This suggests faster and more incremental processing. However, in sentence contexts, both competitors remained active relative to an unrelated word later into the trial. This suggests that in sentence context CI users may maintain competitor activations longer to potentially deal with misheard words. Thus, sentence context seems to encourage more rapid lexical access while CI users simultaneously maintain competitors to be flexible in the face of potential errors.

PD 121

Comparing the Perceptual Strategies of Normal-Hearing and Hearing-Impaired Listeners in a Consonant Discrimination Task

Léo Varnet¹; Chloé Langlet¹; Christian Lorenzi²; Diane Lazare³; Christophe Micheyl⁴

¹Laboratoire des systèmes perceptifs, Ecole Normale Supérieure; ²Laboratoire des systèmes perceptifs, Ecole Normale Supérieure (UMR 8248); ³Institut Arthur Vernes; ⁴Starkey Hearing Technologies

Understanding what acoustic cues human listeners rely on to discriminate speech sounds in noise, how they use such cues, and how these perceptual strategies are impacted by hearing loss, is an important step toward designing more effective speech-processing algorithms for hearing-impaired or normal-hearing individuals.

In this study, recordings of natural speech signals are altered by the addition of a 'blob noise'. The times and frequencies of the blobs are selected so that they are likely to enhance, or degrade, certain spectrotemporal regions of the signal, which were identified (in earlier experiments using the reverse correlation method) as corresponding to acoustic cues used by listeners for discriminating the plosive consonant; one cue (primary) corresponds approximately to the transition of the second and third formants, while the other (secondary) corresponds approximately to the first formant. By systematically, and independently, varying the blob-to-noise ratio for these two blobs, we could infer the relative importance (or perceptual weight) of these perceptually relevant acoustic cues, for a given listener.

We used this approach in three groups of listeners: listeners with a normal audiogram ('normal-hearing'); listeners with high-frequency sloping hearing loss; and listeners with an approximately flat, or shallowly sloping, audiogram. We hypothesized that the perceptual importance of the higher-frequency cue would be reduced, relative to that of the lower-frequency cue in listeners with high-frequency sloping hearing loss, compared to listeners with normal-hearing, and listeners with 'flat' hearing loss, even after the application of frequency-dependent amplification to restore high-frequency audibility.

The results turned out to be consistent with our hypothesis. Furthermore, the substantial interindividual variability in cue-weighting strategies among hearing-impaired individuals, which is apparent in the data, suggests a need for individually-tailored speech-in-noise processing in these two populations, if more effective speech-enhancement in noise is to be achieved.

PD 122

Noise Exposure May Diminish the Musician Advantage for Perceiving Speech in Noise

Erika Skoe; Sarah Camera; Jennifer Tufts
University of Connecticut

Although numerous studies have shown that musicians have better speech perception in noise (SPIN) compared to non-musicians, other studies have not replicated the "musician advantage for SPIN." One factor that has not been adequately addressed in previous studies is

how musicians'; SPIN is affected by routine exposure to high levels of sound. We hypothesized that such exposure diminishes the musician advantage for SPIN. In the current study, environmental sound levels were measured continuously for one week via body-worn noise dosimeters in 56 college students with diverse musical backgrounds and clinically-normal pure tone averages. SPIN was measured using the Quick Speech in Noise Test (QuickSIN). Multiple linear regression modeling was used to examine how music practice (years of playing a musical instrument) and routine noise exposure predict QuickSIN scores. We found that noise exposure and music practice were both significant predictors of QuickSIN, but they had opposing influences, with more years of music practice predicting better QuickSIN scores and greater routine noise exposure predicting worse QuickSIN scores. Moreover, mediation analysis suggests that noise exposure suppresses the relationship between music practice and QuickSIN scores. Our findings suggest a beneficial relationship between music practice and SPIN that is suppressed by noise exposure.

PD 123

'Normal' Hearing Thresholds and Figure-Ground Perception Explain Significant Variability in Speech-in-Noise Performance

Emma Holmes¹; Timothy D. Griffiths²

¹*Wellcome Centre for Human Neuroimaging, University College;* ²*Wellcome Centre for Human Neuroimaging, University College London; Institute of Neuroscience, Newcastle University*

Speech-in-noise (SIN) perception is a critical everyday task that varies widely across individuals and cannot be explained fully by the pure-tone audiogram. One factor that likely contributes to difficulty understanding SIN is the ability to separate speech from simultaneously-occurring background sounds, which is likely not well assessed by audiometric thresholds. A basic task that assesses the ability to separate target and background sounds is auditory figure-ground perception. Here, we examined how much common variance links speech-in-noise perception to figure-ground perception, and how this relationship depends on the properties of the figure to be detected.

We recruited 96 participants with normal hearing (6-frequency average pure-tone thresholds < 20 dB HL). We presented sentences from the Oldenburg matrix corpus (e.g., "Alan has two old sofas") simultaneously with multi-talker babble noise. We adapted the target-to-masker ratio (TMR) to determine the participant's threshold for reporting 50% of sentences correctly. Our figure-ground stimuli were based on Teki et al.

(2013; PMID 23898398) in which each 50 ms time window contains random frequency elements. Figure frequencies either remained fixed or changed over time, mimicking the formants of speech. Participants had to discriminate gaps that occurred in the “figure” or “background” components—a task that cannot be performed based on global stimulus characteristics. We adapted the TMR to determine the participant’s 50% threshold for discriminating gaps in the figure-ground stimuli.

Average audiometric thresholds at 4-8 kHz accounted for 15% of the variance in SIN performance, despite recruiting participants with hearing thresholds that would be considered clinically ‘normal’. Figure-ground performance explained a significant portion of the variance in SIN performance that was unaccounted for by variability in audiometric thresholds. Performance with different figure-ground stimuli explained different portions of the variance, suggesting they index different reasons why people find SIN difficult.

These results in normally-hearing listeners demonstrate that SIN performance depends on sub-clinical variability in audiometric thresholds. In addition, the results show that we can better predict SIN performance by including measures of figure-ground perception alongside audiometric thresholds. Importantly, the results support a source of variance in speech-in noise perception related to figure-ground perception that is unrelated to audiometric thresholds. Given previous work demonstrates cortical contributions to both speech-in-noise and figure-ground perception, this shared variance likely arises at a central level. Overall, these results highlight the importance of considering both central and peripheral factors if we are to successfully predict speech intelligibility when background noise is present.

PD 124

Examining the Relationship between Pupillary and Neural Indices of Effortful Listening

Stefanie Kuchinsky¹; Jane S. Rose²; Ronella N. Rosenberg²; Aidan L. Marshall-Cort²

¹*Audiology and Speech Pathology Center, Walter Reed National Military Medical Center; Department of Hearing and Speech Sciences, University of Maryland;*

²*University of Maryland*

Background

The effort required to understand speech can vary substantially across task conditions and individuals, even when recognition accuracy is similar. The Framework for Understanding Effortful Listening has defined effort as the mental resources that are engaged to achieve a given level of speech recognition performance. However, the extent to which commonly used measures of effort

(e.g., pupillometry) index these resources is not well understood. To help address this gap, we simultaneously collected functional neuroimaging and pupillometry data during a challenging word recognition task.

Following previous research, we predicted that more challenging listening conditions would be associated with (1) greater pupil dilation and (2) greater activity within executive function neural systems, and (3) that these effects would be correlated across individuals.

Method

Sixteen younger, normal-hearing adults (ages 18-30) repeated aloud 180 NU-6 words presented in speech-shaped noise at two signal-to-noise ratios (SNRs). These SNRs were selected to yield 50% and 80% word recognition accuracy within each individual. Pupillometry and functional MRI (fMRI) data were collected throughout the main experimental task. A sparse-sampling multiband fMRI sequence (TR = 6.4 sec) allowed for word stimuli and oral responses to occur in the absence of volume acquisition noise.

Pupillary data were analyzed using growth curve analysis (GCA). Individual differences in GCA parameters were modeled as regressors at the second level of the general linear model describing the fMRI data.

Results

Preliminary analyses examined changes in pupillary and neural responses to words presented at a harder compared to an easier SNR. These contrasts were associated with a larger pupil size and greater cingulo-opercular (CO) activity in frontal cortex. Furthermore, these measures were related: individuals who exhibited a larger effect of SNR on pupil size also engaged more extensive CO activity.

Conclusion

In line with previous work, greater pupil dilation and frontal cortex activity were associated with recognizing speech in poorer SNRs. Importantly, these indices covaried across individuals, supporting the notion that pupillometry may be used to track at least some aspects of the executive function resources that underlie effortful listening.

Planned analyses will also examine the how components of the pupillary response track changes in executive functioning on a trial-by-trial basis. This research has implications for developing validated measures of effort that can be used to comprehensively assess the challenges that people face in adverse listening conditions.

This work is supported, in part, by NIH/NIDCD R03 DC015059 (SEK).

Individual Variability in Temporal Fine Structure Processing Underlying Speech-in-noise Intelligibility in Listeners with “Normal” Audiograms

Aravindakshan Parthasarathy¹; Sandra Romero Pinto²; Kenneth E. Hancock³; Daniel B. Polley³

¹*Department of Otolaryngology, Harvard Medical School; Eaton-Peabody Laboratories, Mass. Eye and Ear Infirmary;* ²*Eaton-Peabody Laboratories, Massachusetts Eye and Ear; Program in SHBT, Division of Medical Sciences, Harvard Medical School;* ³*Eaton-Peabody Laboratories, Massachusetts Eye and Ear; Dept. of Otolaryngology, Harvard Medical School*

The audiology database of the Massachusetts Eye and Ear Infirmary contains hearing tests from over 100,000 adult patients. Using clustering statistics, we characterized the preponderance of audiogram shapes among patients ranging from 18-79 years old. Here, we focused on the youngest cohort (18-35 years), approximately half of whom come to the audiology clinic with normal bilateral audiograms but report complaints of “decreased hearing”. We then recruited young adult subjects with normal audiograms into a study that identified neurophysiological and psychophysical signatures of diminished hearing that are not captured by conventional clinical tests.

Among our 22 subjects with clinically normal audiograms, we noted substantial variability in their subjective hearing quality and performance on a speech-in-noise task. Because stimulus temporal fine structure (STFS) cues are known to be vital for hearing in noise, we characterized monaural and binaural STFS processing with a complementary set of physiological and behavioral tests. Electrophysiological encoding of monaural STFS cues were characterized by measuring neural synchronization in the frequency following response to a 500Hz tone with frequency modulation (FM) ranging from 0-10Hz. Processing of binaural STFS cues were characterized by measuring the following response to changes in inter-aural phase delays (IPDs) of a 500Hz tone. Parallel behavioral tests assessed FM and binaural IPD psychophysical detection thresholds. Hearing in noise abilities were assessed using a digit comprehension task paired with measures of pupil diameter to assess cognitive load.

Neural phase-locking to the FM stimulus was strongly correlated with psychophysical estimates of FM detection threshold and speech-in-noise intelligibility. A strong correspondence was also noted between neurophysiological and behavioral measures of IPD processing. The cognitive load as measured by pupil

diameter was modulated by signal-to-noise ratio and binaural cues in hearing in noise tasks. These brainstem measures of FM and IPD phase-locking serve as a useful biological marker, and may identify neural signatures for suprathreshold hearing impairments in listeners with no overt hearing loss. Our ongoing work is focused on developing a multivariate model to predict individual differences in speech-in-noise intelligibility.

PD 126

Visual Speech Cues Increase the Relative Importance of Low-Frequency Speech Information

Joshua G.W. Bernstein¹; Jonathan H. Venezia²; Ken W. Grant¹

¹*Walter Reed National Military Medical Center;* ²*VA Loma Linda Healthcare System*

Introduction

Many hearing-aid fitting algorithms include the optimization of a model-based speech-intelligibility prediction as part of their prescriptive formula. Although the relative importance of individual frequency regions has been established for auditory-only (AO) speech, most speech communication takes place face-to-face with access to visual speech cues. Previous research with individual narrow speech bands suggests that the relative importance of low-frequency speech information increases under auditory-visual (AV) conditions. However, frequency-importance function estimates can change depending on whether individual bands are presented in isolation or combined with other bands. This study evaluated AO and AV frequency-importance functions for broadband speech.

Methods

Eight hearing-impaired and four normal-hearing listeners were presented with /a/-consonant-/a/ speech tokens filtered into four one-third octave bands, each separated by an octave to minimize band-on-band energetic masking (298-375, 740-945, 1890-2381, and 4762-6000 Hz). On each trial, the signal-to-noise ratio (SNR) in each band was selected randomly from a 10-dB range. This range was determined independently for each band such that the speech was just audible at the lowest SNR and the combination of four bands yielded 45% correct average performance. AO and AV conditions were tested with the same auditory stimuli. Band-importance functions were estimated using three different analyses examining the relationship between performance and the SNR in each band: (1) single-band correlations that assumed the independence of each band; (2) multiple regression considering the SNRs in all bands simultaneously; and (3) multiple regression also including band-interaction terms.

Results

All three analyses yielded similar results, suggesting that the independence assumption was valid, at least for speech bands that are separated by an octave and yield low performance (~15% correct) in isolation. For AO speech, all four bands contributed equally to performance. For AV speech, the lowest one or two frequency bands had significantly higher weights than the two highest bands. None of the band-interaction coefficients were significant.

Discussion

These results corroborate previous findings for individual narrow bands and extend them to broadband speech. AV conditions shifted the frequency-importance function for consonant perception toward lower frequencies, consistent with the idea that high-frequency speech information is redundant with place-of-articulation information available from lipreading. A different set of frequency-importance functions may be required to accurately predict AV speech intelligibility. [The views expressed in this article are those of the authors and do not reflect the official policy of the Department of Army/ Navy/Air Force, Department of Defense, Department of Veterans Affairs, or U.S. Government.]

PD 127

Behavioral and electrophysiological evidence of incidental learning across continuous speech

Yunan Wu¹; Ran Liu²; Sung-Joo Lim³; Lori L. Holt¹
¹Carnegie Mellon University; ²MARi; ³Boston University

Language learning requires that listeners generalize across acoustically variable speech sounds to recognize linguistically-relevant units like words and phonemes. Although a growing literature on auditory category learning guides understanding of the mechanisms available to support this learning, most studies have examined learning across isolated sound exemplars like individual phonemes or words. In contrast, real-world learning typically takes place across fluent, continuous speech. How do listeners learn across acoustically variable continuous speech when they do not have *a priori* information about the temporal window across which learning must occur? We hypothesized listeners discover temporal 'islands of reliability' in highly variable, continuous speech signals that are consistently associated with behaviorally relevant actions and events. Further, we predicted that listeners learn to treat the acoustics in these temporal windows as functionally equivalent, leading to behavioral and representational change consistent with category learning. Here, native English participants played a videogame in which actions directed at alien creatures were consistently associated with acoustically-variable Mandarin Chinese

target words embedded in continuous Mandarin speech spoken by 4 native talkers (2 female). Control words were also embedded in the continuous speech and were presented equally as often as target words; but control words were not associated with any particular action or event. Participants played the videogame for 3.5 hours across 5 days, with no prior knowledge of Mandarin. Neither overt categorization decisions nor overt feedback were involved in the videogame. Following training, an overt post-training categorization test revealed robust learning of target words that persisted at least 10 days and generalized to novel utterances and talkers. Comparison of pre- versus post-training electroencephalography responses to continuous Mandarin revealed that target words, but not control words, elicited an enhanced auditory evoked N100 response in central electrodes associated in prior research with word segmentation. This suggests that incidental learning under conditions in which behaviorally relevant actions and events align with functional units in continuous speech leads to more robust speech category learning than passive distributional learning through mere exposure.

Age-Related Changes in Humans & Mice

PD 128

Hearing Disability in the United States Adults Results from the American Community Survey 2012-2016

Chuan-Ming Li¹; Howard J. Hoffman²; Le Chen¹; Christa L. Themann³

¹National Institute on Deafness and Other Communication Disorders (NIDCD); ²National Institute on Deafness and Other Communication Disorders (NIDCD), National Institutes of Health (NIH); ³National Institute for Occupational Safety and Health (NIOSH), Centers for Disease Control and Prevention (CDC)

Background: Serious hearing loss (disability) limits the ability of many individuals to function independently. In 2013, the National Center for Health Statistics (NCHS) revised and updated their Urban–Rural Classification Scheme of Counties, based on population density, to examine health disparities. We used this classification to analyze the Census Bureau's American Community Survey (ACS), which is uniquely capable of generating small area estimates of reported disabilities to document disparities at local administrative levels.

Methods: The ACS collects data from a rolling sample of 250,000 households each month on over 40 topics, including disability, in the civilian non-institutionalized U.S. population. Since 2008, the ACS has asked about difficulties with hearing ("deaf or have serious difficulty

hearing"). By aggregating five years of data collection, the ACS can generate reliable estimates for small geographic areas. Prevalence of hearing disability was estimated from the 2012-2016 ACS by sex, age, race/ethnicity, the economically-depressed Appalachian area, and the 2013 NCHS Urban–Rural County Classification. ArcGIS hot spot analysis tool was used to identify clusters with high or low prevalence of hearing disability.

Results: Prevalence of hearing disability in adults was 4.6%; 5.4% for males and 3.7% for females ($p < 0.001$). Prevalence increased with age: 1.1%, 3.5%, and 15.2% for 18-44, 45-64, and 65+ years ($p < 0.001$). Prevalence was highest in rural micropolitan (5.8%) and noncore (5.6%) areas, decreasing with increasing population density; lowest prevalences were in small metro (5.2%), medium metro (4.7%), large fringe metro (3.9%), and large central metro metropolitan (3.5%). Prevalence was higher in Appalachia (4.7%) compared to elsewhere (4.0%, $p < 0.001$). American Indians/Alaska Natives (6.9%) and non-Hispanic whites (5.5%) had higher prevalence than non-Hispanic African Americans (2.8%) or Hispanics (2.8%). States in the East South Central region had the highest (5.7%) and the Middle Atlantic region the lowest (3.9%) prevalence of hearing disability. West Virginia had the highest prevalence (7.7%) of hearing disability among all states.

Conclusion: Hearing disability disparities in the U.S. exist for males, selected racial/ethnic groups, impoverished (Appalachia) and low-density rural geographic areas.

PD 129

Evidence for Age-related Cochlear Synaptopathy in Humans Unconnected to Speech-in-Noise Intelligibility Deficits

Peter T. Johannesen; Byanka C. Buzo; Enrique A. Lopez-Poveda
University of Salamanca

Cochlear synaptopathy (or the loss of primary auditory synapses) remains a subclinical condition of uncertain prevalence. Here, we investigate whether it occurs in humans, and whether it contributes to suprathreshold speech-in-noise intelligibility deficits. For 94 human listeners with normal audiometry (aged 12-68 years; 64 female), we measured click-evoked auditory brainstem responses (ABRs), self-reported lifetime noise exposure, and speech reception thresholds (SRTs) for sentences (at 65 dB SPL) and words (at 50, 65 and 80 dB SPL) in steady-state and fluctuating maskers. Based on animal research, we assumed that the shallower the rate of growth of ABR wave-I amplitude versus level, the higher the risk of suffering from synaptopathy. We found that wave-I growth rates decreased with increasing age but not with increasing noise exposure. SRTs were not

correlated with wave-I growth rates, and mean SRTs were not statistically different for two subgroups of participants ($N=14$) with matched audiograms (up to 12 kHz) but different wave-I growth rates. Altogether, the data are consistent with the existence of age-related but not noise-related synaptopathy. In addition, the data dispute the notion that synaptopathy contributes to suprathreshold speech-in-noise intelligibility deficits. [We thank James M. Harte, Niels H. Pontoppidan and Filip Rønne for useful discussions. Work supported by the Oticon Foundation (ref. 15-3571), Junta de Castilla y León (ref. SAP023P17), MINECO (ref. BFU2015-65376-P), and the European Regional Development Fund].

PD 130

Age-Related White-Matter Integrity Declines in the Auditory "Where" Pathway Predict Greater Spatial Hearing Difficulty in Older Listeners

James W. Dias¹; Carolyn M. McClaskey¹; Kelly C. Harris²

¹Medical University of South Carolina; ²Medical University of South Carolina-Dept of Otolaryngology-Head & Neck Surgery

Interaural differences in the intensity and timing of audible speech provide important information for detecting, locating, and selecting a talker from among other talkers in noisy listening environments. Older listeners typically experience more difficulty in such "cocktail party" scenarios, thought to be associated in part with declines in interaural information processing. The neural mechanisms that underlie auditory spatial perception in young normal-hearing adults are fairly well understood. However, how these neural mechanisms change with age and affect the spatial perception of older adults requires further investigation. Here we examined the extent to which age-related differences in the fractional anisotropy (FA) of interhemispheric white-matter tracts of the corpus callosum predicted age-group differences in the ability to identify spoken digits spatially cued by interaural timing differences and speech-in-noise identification when interaural timing provided no spatial information (Quick Speech-in-Noise Test). FA is a metric of white-matter integrity, the higher values of which have been associated with better cognitive and perceptual processing. Native-English-speaking younger ($N = 27$, 19-30 years of age) and older ($N = 35$, 56-83 years of age) listeners with pure-tone audiometric thresholds less than or equal to 35 dB HL at conventional audiometric frequencies between 250 Hz and 3,000 Hz participated in this study. Audiometric thresholds were unrelated to our speech and white-matter metrics. Replicating previous work, younger listeners correctly identified more spatially-cued speech than older listeners, but

non-spatial speech-in-noise identification did not differ between age-groups. Younger listeners also exhibited greater FA in callosal tracts connecting left and right orbito-frontal, superior-frontal, anterior-frontal, motor, superior-parietal, posterior-parietal, and occipital cortices, but the FA of tracts connecting left and right temporal cortices did not differ between age groups. Greater white-matter FA in tracts connecting left and right superior-frontal, anterior-frontal, and posterior-parietal cortices – all cortical areas previously associated with the dorsal auditory “where” pathway – predicted better spatially-cued speech identification, but not non-spatial speech-in-noise identification. In contrast, we found that the white-matter FA of tracts connecting left and right motor cortex predicted identification of spatially-cued speech and non-spatial speech-in-noise. The results suggest that the integrity of interhemispheric white-matter connecting cortical areas previously implicated in spatial hearing is important for preserving the interaural timing information used in spatial perception. As white-matter integrity declines with age, so too does spatial hearing ability. The results also suggest that white matter associating motor cortices plays an important role in speech processing, consistent with literature showing motor cortex involvement in speech perception.

PD 131

Structural Cingulate Cortex Changes Are Associated to Cochlear Aging

Chama Belkhiria¹; Rodrigo Vergara²; Simon San Martin¹; Alexis Leiva¹; Bruno Marcenaro³; Melissa Martínez⁴; Carolina Delgado⁴; Paul H. Delano⁴

¹*Audition and Cognition Center. Faculty of Medicine. University of Chile;* ²*Neuroscience Department, Faculty of Medicine, University of Chile;* ³*Pontificia Universidad Católica de Chile;* ⁴*Faculty of medicine. Av. Independencia,*

Introduction: Age-related hearing loss or presbycusis is characterized by bilateral progressive hearing loss and impaired speech understanding especially in noisy environments. Several studies in humans have found brain structural changes in patients with hearing loss, including grey matter volume reduction in the right temporal lobe and correlations between hearing impairment and smaller gray matter volume in the auditory cortex. However, whether cognitive decline and the atrophy of brain regions in presbycusis patients are specifically associated to the cochlear receptor cell loss is unknown. We hypothesized that cochlear amplifier dysfunction in presbycusis is a major contributor for cognitive decline and structural brain changes in elderly population.

Methods. 96 patients aged over 65 years were included from cross-sectional data from the ANDES cohort. These

subjects had mini mental state examination (MMSE) score over 24 and were evaluated by neuropsychological and audiological evaluations, including pure tone audiometric (PTA) thresholds and distortion product otoacoustic emissions (DPOAEs). Data were divided into three groups: (i) a control group with normal hearing levels, (ii) presbycusis group with preserved cochlear function (PCF) and (iii) a group with presbycusis and cochlear dysfunction (CD). Grey matter volumes and cortical thickness were calculated from 3-Tesla MRI whole-brain T1-weighted images using automatic Freesurfer segmentation.

Results. The patients mean age was 73.62 ± 5.34 years, with 63 female and with an average hearing of 25.35 ± 10.91 dB. When comparing structural differences between hearing impairment groups, the parahippocampus volume and the anterior and posterior cingulate cortex thickness were significantly more atrophied in the CD group. Only in the CD group there were significant correlations between cingulate cortex atrophy and impairment in working memory, episodic memory, language and visuo-constructive abilities.

Conclusions. Cochlear dysfunction was associated with brain structural changes mainly in non-auditory areas and was associated with impairment in cognitive domains beyond auditory processing. Our findings suggest that the presbycusis patients with loss of outer hair cells have more severe alterations in the neural structures related to the effortful network than those with more preserved cochlear amplifier function. The absence of DPAOE in mild presbycusis patients could be an early risk factor for executive dysfunction or cingulate cortex atrophy.

Funded by Proyecto Anillo ACT1403 and Fondecyt 1161155.

PD 132

Functional and Cellular Mechanisms Underlying the Transition from Hidden to Overt Hearing Loss in a Mouse Model.

Jeong Han Lee¹; Mincheol Kang²; Seojin Park¹; Daniël O. J. Reijntjes³; Xiaodong Zhang⁴; Maria Cristina Perez-Flores²; Sarath Vijayakumar⁵; Sherri M. Jones⁵; Timothy A. Jones⁶; Wenying Wang²; Nipavan Chiamvimonvat⁴; Sonja Pyott³; Ebenezer N. Yamoah¹
¹*University of Nevada Reno;* ²*University of Nevada, Reno;* ³*University Medical Center Groningen;* ⁴*University of California, Davis;* ⁵*University of Nebraska Lincoln-College of Education and Human Sciences;* ⁶*University of Nebraska Lincoln*

Background: Age-related hearing loss (ARHL) or presbycusis is the most prevalent sensory deficit, and, with increasing life expectancy, ARHL is predicted to

vastly impact the wellbeing of our society. Recent studies have demonstrated that signs of ARHL may begin much earlier than previously recognized. In some cases, sensory and neural defects, such as hair cell (HC) loss, synaptic dysfunction, and spiral ganglion neuron (SGN) loss, are observed before other inner ear pathology. These findings suggest that early but “silent” mechanisms underly the development of ARHL and that slowing, stopping or reversing these mechanisms would prevent the progression of ARHL. We used this motivation to determine the functional and cellular mechanisms underlying the gradual transformation of hidden to overt hearing loss in the KNa1.1/1.2 null mouse model.

Methods: We employed measurements of the auditory brainstem response (ABR) and distortion product otoacoustic emissions (DPOAEs), single molecule fluorescent in situ hybridization (smFish), histology, immunocytochemistry, patch-clamp electrophysiology and calcium imaging to characterize auditory function and SGN physiology in WT and mutant mice.

Results: Compared to their wildtype litter mates, KNa1.1/1.2 null mutants showed hidden HL (HHL), defined by reduced and delayed wave I ABR amplitudes by four weeks of age. This HHL was not associated with alterations in the sensorineural (hair cell, SGNs and synaptic) structures. However, SGNs isolated from KNa1.1/1.2 null mutants demonstrating HHL showed reduced postsynaptic responses and altered membrane properties, including reduced AP latencies, thresholds and amplitudes. The increased excitability of SGNs resulted in changes in Ca²⁺ transients and sustained intracellular Ca²⁺ levels. These features of HHL, persisted until 3 to 4-months of age, when there is significant increase in ABR absolute threshold together with a reduction in SGN size and total numbers. Concurrently, surviving SGNs showed robust reduction in membrane excitability. We report corresponding apoptotic SGNs degeneration, which is mediated by increased activated Caspase 3 and 9 mechanisms. Continued experiments will outline the sequence of molecular and cellular mechanisms that define the transformation from HHL to overt HL in this mouse model.

Conclusions: We conclude that there are sequential alterations of synaptic and neural properties that underlie the transition from HHL to HL that begin with without overt morphological changes in the hair cells, SGNs and their synaptic connections. However, the increased absolute hearing threshold is associated with morphological abnormalities the in KNa1.1/1.2 null mouse model.

Funding: NIH AG051443-01A1, DC016099-01

PD 133

Age-Dependent Changes in Gene Expression and Synaptic Function in Mouse Auditory Brainstem

Mahendra Singh¹; Pedro Miura²; Daphne Cooper²; David Knupp²; **Robert Renden**¹; Haley Torres³

¹*Department of Physiology and Cell Biology; University of Nevada, Reno School of Medicine;* ²*Department of Biology; University of Nevada, Reno;* ³*Molecular Biosciences Graduate Program; University of Nevada, Reno*

Hearing acuity and sound localization are affected by aging, and may contribute to cognitive dementias. While loss of hair cells and sensorineural conduction has been well documented, little is known regarding short-term synaptic plasticity in central auditory nuclei. Age-related changes in expression of coding (mRNA) and circular RNA (circRNA) species in C57BL/6J mice were examined by RNA-seq. Total RNA-seq profiling of auditory brainstem including the superior olivary complex showed differential expression of hundreds of protein-coding mRNAs between young (8-day and 1-month old) and 18-month old samples — including upregulation of genes involved in synapse assembly and the immune system, and downregulation of genes involved in cholesterol biosynthesis and myelination. Expression of circular RNAs (circRNAs), a newly appreciated class of largely non-coding RNAs, were also profiled and were found to globally increase during aging. In particular, circRNAs generated from synaptic-related genes were increased in older mice.

Age-related changes in synaptic transmission properties were evaluated at the calyx of Held, a sign-inverting relay synapse in the circuit for sound localization. Synaptic timing and short-term plasticity were degraded in older mice. Surprisingly, oral supplementation with acetyl-L-carnitine (ALCAR), an anti-inflammatory agent that facilitates mitochondrial function, fully reversed synaptic transmission delays in aged mice to reflect transmission in juvenile adults. These findings support ALCAR supplementation as an adjuvant to improve CNS performance.

In an attempt to correlate expression changes with physiology and rescue by ALCAR, markers for reactive astrocytes were evaluated in the medial nucleus of the trapezoid body of young and older mice, and older mice treated with ALCAR. Myelin thickness in ventral stria projection axons was also evaluated, in an attempt to link timing errors to decreased axonal myelination. In addition, we will use expression profiling in MATH5-CRE positive bushy cells labeled with tdTomato in young and aged mice, and aged mice treated with ALCAR, to identify neuronal expression changes due to ALCAR treatment.

PD 134

The Interplay Between the Effects of Noise Exposure and Aging on Neural Adaptation in the Mouse Inferior Colliculus

Lucy A. Anderson; Jennifer F. Linden; Roland Schaette
UCL Ear Institute

Exposure to even a single episode of loud noise can damage synapses between cochlear hair cells and auditory nerve fibres, causing hidden hearing loss (HHL) that is not detected by audiometry. We have recently shown that midbrain neurons from young adult mice with noise-induced HHL showed less capacity for adaptation to loud environments, conveyed less information about sound intensity in those environments, and adaptation to the longer-term statistical structure of fluctuating sound environments was impaired, suggesting a potential explanation for why many people with seemingly normal hearing struggle to follow a conversation in loud background noise.

Aging can also have a substantial impact on hearing function, and it has recently been shown that noise exposure at a young age can accelerate age-related hearing loss. How noise-induced HHL and aging interact in their impact on central auditory processing has not been investigated yet.

Here we investigated the interplay between the effects of noise-induced HHL and aging on functional hearing by measuring the ability of neurons in the auditory midbrain of 4-month-old and 24-month-old mice to adapt to sound environments containing quiet and loud periods. At 3 months, the mice were either exposed to octave-band noise (8-16 kHz) at 100 dB SPL for 2 hours under anaesthesia or subjected to a sham exposure. Neural recordings from the inferior colliculus took place one month or 21 months later. We tested the capability of neurons to adapt to sound level using noise stimuli that changed intensity every 50ms. Intensities were drawn with 80% probability from a 12-dB range (high-probability region, HPR) centred on either 44, 56, 68, or 80 dB SPL, and with 20% probability from the rest of the intensity range

ABR measurements showed a significant effect of age on hearing thresholds, but no effect of noise exposure and no interaction between noise exposure and aging. Recordings from the inferior colliculus of anaesthetized mice showed that old mice had significantly higher adapted thresholds for quiet sound environments (HPRs around 44 and 56 dB SPL), but not for loud sound environments (HPRs around 68 and 80 dB SPL). The adaptation depth was thus significantly reduced by the

effect of age. Moreover, rate-level-functions of neurons recorded from old mice had a tendency to be steeper than those recorded from young mice, possibly due to recruitment. These results suggest a complex interplay between age- and noise-induced hearing loss on central auditory processing.

Acknowledgements

This research was supported by Action on Hearing Loss through International Project Grant G80.

PD 135

SIRT1 protects cochlear hair cell and delays age-related hearing loss via autophagy

Jiaqi Pang¹; Hao Xiong²; Yongkang Ou¹; Haidi Yang¹; Lan Lai¹; Yiqing Zheng¹

¹*Sun Yat-sen Memorial Hospital, Sun Yat-sen University;* ²*Medical University of South Carolina*

Age-related hearing loss (AHL) is typically caused by the irreversible death of hair cells. A growing body of evidence proves that SIRT1 regulates a series of cellular processes as a protective effect against age-related dysfunction. Autophagy is one of cellular processes regulated by SIRT1. The role of the modulation of SIRT1 and autophagy in hair cell death and the development of AHL are not yet understood. In accordance with our previous work, reduced SIRT1 and impaired autophagy were proved in the organ of corti of the aged C57BL/6 mice, with the severe outer hair cells death and the high ABR threshold. In the auditory cell HEI-OC1, SIRT1 modulated autophagy. The underlying mechanism may be associated with the deacetylation of ATG9A by SIRT1. Moreover, SIRT1 inhibition facilitated cell death via autophagy inhibition, whereas, autophagy activation reversed the SIRT1 inhibition media cell death. Importantly, SIRT1 activation by the supplement of resveratrol altered the organ of corti autophagy impairment of the aged C57BL/6 mice and delayed AHL. These results show that the modulation between SIRT1 and autophagy have an important role in the hair cell death and the progressive hearing loss in aging. Deacetylation of ATG9A involves in the regulation of autophagy by SIRT1. And the supplement of SIRT1 activator resveratrol can be a [strategy](#) to delay the AHL. Our findings uncover a novel mechanism that why SIRT1 inhibition facilitates hair cell death and hearing loss.

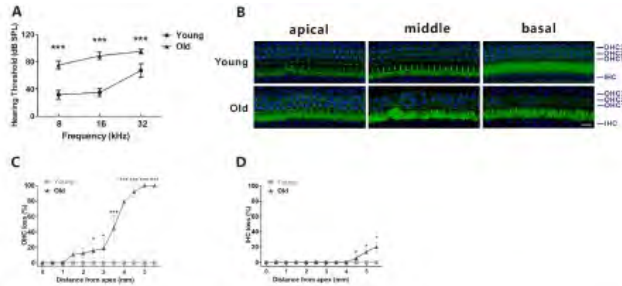


Fig. 1 Aged C57BL/6 mice develop AHL.

(A) ABR thresholds increased with aging in C57BL/6 mice at 8, 16 and 32 kHz ($n = 13$). (B) Surface preparations were stained with DAPI (blue) and Myosin VIIa as a HC marker (green). Scale bar, 10 μm . (C-D) HC counts obtained at different ages ($n = 3$). Data represent the mean \pm SEM. * $p < 0.05$, ** $p < 0.01$, *** $p < 0.001$. Young, mice of 2 months old; Old, mice of 12 months old. OHC, outer hair cell; IHC, inner hair cell.

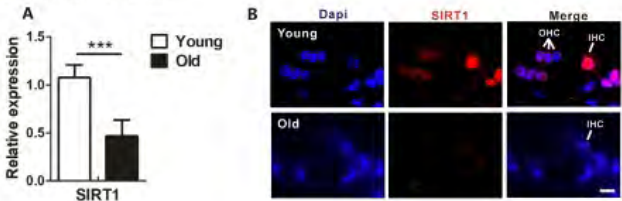


Fig. 2 SIRT1 is reduced in the organ of Corti of the aged C57BL/6 mice.

(A) SIRT1 mRNA were detected using qPCR in the total tissue of cochlea. (B) SIRT1 were detected in HCs. Cell nuclei were counter stained with DAPI (blue) and SIRT1 (red) ($n = 4$). Scale bar, 10 μm . Data represent the mean \pm SEM. * $p < 0.05$, ** $p < 0.01$, *** $p < 0.001$. Young, mice of 2 months old; Old, mice of 12 months old. OHC, outer HC; IHC, inner HC.

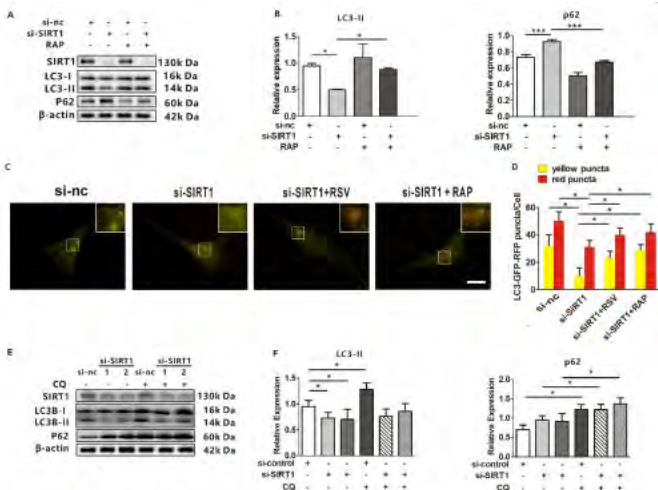


Fig. 5 SIRT1 modulates autophagosome formation in HEI-OC1 cells

(A-B) Western blots and densitometry analysis for autophagy marker LC3-II and p62 in si-SIRT1 and its control with or without RAP (10 μM , $n = 3$). (C) Fluorescence images of mRFP-GFP-LC3 in HEI-OC1 cells treated with a si-control, si-SIRT1 (40nM), si-SIRT1 with RSV (5 μM) and si-SIRT1 with RAP (10 μM). Scale bars: 10 μm . (D) Quantity analysis of yellow and red puncta was detected in 10 cells/experiment ($n = 3$). (E-F) Western blots and densitometry analysis for SIRT1 and autophagy marker LC3-II and p62 in si-SIRT1 and its control (40nM) with or without CQ (5mM, $n = 5$). Data represent the mean \pm SEM. * $p < 0.05$, ** $p < 0.01$, *** $p < 0.001$. si-nc, control of si-SIRT1; RSV, resveratrol; RAP, rapamycin; CQ, chloroquine.

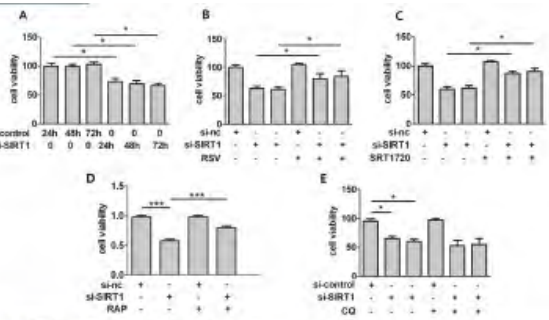


Fig. 6 SIRT1 inhibition leads to cells death via autophagy.

(A) The CCK8 assay was performed to examine cell viability of HEI-OC1 cells for si-SIRT1 (40 nM) and its control at different time after transfection ($n = 5$). (B) The CCK8 assay was performed to examine cell viability of HEI-OC1 cells for si-SIRT1 and its control (40nM) with or without RSV (5 μM , $n = 5$). (C) The CCK8 assay was performed to examine cell viability of HEI-OC1 cells for si-SIRT1 and its control (40nM) with or without SIRT1720 (0.5 μM , $n = 5$). (D) The CCK8 assay was performed to examine cell viability of HEI-OC1 cells for si-SIRT1 and its control (40nM) with or without RAP (10 μM , $n = 3$). (E) The CCK8 assay was performed to examine cell viability of HEI-OC1 cells for si-SIRT1 (40 nM) and its control with or without CQ (5mM, $n = 5$). Data represent the mean \pm SEM. * $p < 0.05$, ** $p < 0.01$, *** $p < 0.001$. si-SIRT1 1 and 2, two kinds of si-SIRT1; si-nc, control of si-SIRT1. RSV, resveratrol; RAP, rapamycin; CQ, chloroquine.

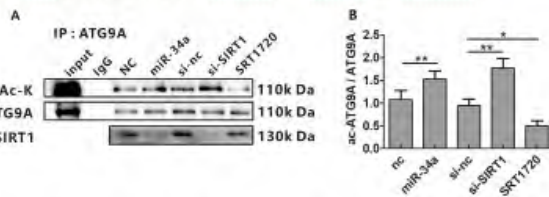


Fig. 7 SIRT1 deacetylates ATG9A in HEI-OC1 cells

(A) Acetylation levels of ATG9A were measured by IP Western blotting analysis in miR-34a mimics and its control (40nM), si-SIRT1 and its control (40nM) and SIRT1720 (0.5 μM , $n = 3$). (B) Values were expressed as quantification of the acetylated ATG9A/total ATG9A. Data represent the mean \pm SEM. * $p < 0.05$, ** $p < 0.01$. NC, control of miR-34a mimics; miR-34a, miR-34a mimics, si-nc, control of si-SIRT1.

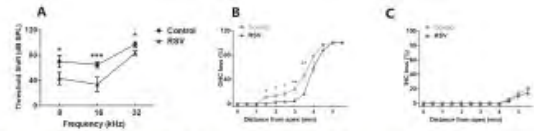


Fig. 8 SIRT1 activation alleviates hair cell loss and delays age-related hearing loss in C57BL/6 mice.

(A) ABR thresholds decreased with RSV treatment (4000 mg/kg/d, $n = 8$) mice compared with the aged C57BL/6 mice at 8, 16 and 32 kHz. (B-C) HC counts obtained for the control and RSV treatment ($n = 4$). Data represent the mean \pm SEM. * $p < 0.05$, ** $p < 0.01$, *** $p < 0.001$. control, mice of 10 months old with normal feed; RSV, mice of 10 months old with 4000 mg/kg/d RSV feeding started at the age of 2 months old. OHC, outer hair cell; IHC, inner hair cell.

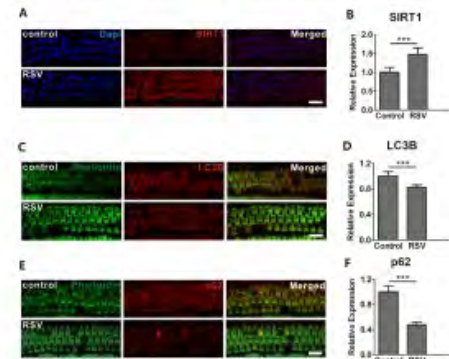


Fig. 9 Increase in SIRT1 expression corrects the OHC autophagy impairment in the aged C57BL/6 mice.

(A-B) Immunohistochemical and densitometry analysis of SIRT1 protein location in OHCs for the control and RSV treatment ($n = 4$). Surface preparations were stained with DAPI (blue) and SIRT1 (red). Scale bar, 10 μm . (C-D) Immunohistochemical and densitometry analysis of LC3B protein location in OHCs for the control and RSV treatment ($n = 4$). Surface preparations were stained with Phalloidin (green, located OHC cytoplasm) and LC3B (red). Scale bar, 10 μm . (E-F) Immunohistochemical and densitometry analysis of p62 protein location in OHCs for the control and RSV treatment ($n = 4$). Surface preparations were stained with Phalloidin (green, located OHC cytoplasm) and p62 (red). Scale bar, 10 μm . Data represent the mean \pm SEM. * $p < 0.05$, ** $p < 0.01$, *** $p < 0.001$. control, mice of 10 months old with normal feed; RSV, mice of 10 months old with 4000 mg/kg/d RSV feeding started at the age of 2 months old.

PD 136**Differential Sensitivity to Schroeder-Phase Harmonic Complexes in the Gerbil Cochlear Nucleus**

Hsin-Wei Lu¹; Philip H. Smith²; Philip X. Joris³
¹*KU Leuven*; ²*University of Wisconsin, Madison*;
³*University of Leuven*

Schroeder phase stimuli consist of equal-amplitude harmonic complexes with a specific phase spectrum which gives interesting properties to envelope and temporal fine structure. The envelope can vary from very peaky (phase curvature 0) to nominally flat (phase curvature +1 or -1), whereas the temporal fine structure can be an upward (negative phase curvature) or downward (positive phase curvature) frequency sweep within each fundamental period. Such rapid frequency changes are a common feature of speech and music. Psychoacoustic studies have shown strong effects of the phase spectrum in Schroeder stimuli on masking or timbre discrimination, but underlying physiological mechanisms are little studied.

We hypothesize that marked sensitivity to Schroeder-phases must first arise in the cochlear nucleus, where auditory afferents carrying timing information of cochlear activation converge differentially onto various cell types. We use single-cell recordings to study supra- and subthreshold responses in anesthetized Mongolian gerbils. Schroeder-phase stimuli were presented with fundamental frequency (F0) at 50, 100, or 200 Hz, phase curvature at ± 0 , ± 0.25 , ± 0.5 , ± 0.75 , and ± 1 , and sound intensity at 40-60 dB SPL.

We obtained responses from primary-like, primary-like with notch, chopper, ideal onset (Oi), and pauser-buildup units. Among all the cell types tested, Oi units showed clear preferences for either positive or negative phase curvature in their mean firing rates. Furthermore, they also showed very high vector strengths (>0.95) at these preferred curvatures and some even fire spikes entrained to F0. This is surprising as Oi units, presumably octopus cells, are known to be most sensitive to sounds with rapid changing temporal envelope, yet they could fire sustained, entrained spikes to flat-envelope Schroeder stimuli. Such phase-sensitive responses were less frequently observed in other cell types.

We conclude that monaural phase-sensitivity is initiated in the cochlear nucleus. The different degrees of sensitivity in each cell type may provide a new window on studying the structure-function relations in this circuit.

PD 137**Reduced Vesicle Pool Size at the Endbulb of Held Parallels Compromised Synaptic Transmission during Age-Related Hearing Loss**

Shengyin Lin¹; Yong Wang¹; Robert W. Ariss²; **Ruili Xie**¹

¹*Department of Otolaryngology, Ohio State University*;
²*University of Toledo Medical School*

Synaptic transmission at the auditory nerve central terminal, specifically the Endbulb of Held, is compromised during aging, which leads to reduced auditory input to the cochlear nucleus and contributes to perceptual deficits of age-related hearing loss. It remains unclear what age-related changes at the Endbulb of Held synapse underlie the declined physiological function. In this study, we investigated both physiology and anatomy of the same Endbulb of Held synapses in three age groups of CBA/CaJ mice at 2-4 months (young), 17-19 months (middle-aged) and 27-30 months (old). To evaluate the physiological function, we performed whole-cell patch clamp recording from bushy neurons in parasagittal slices of cochlear nuclei, while electrically stimulating the auditory nerve to activate the Endbulb of Held synapses. Fluorescent dye (Alexa Fluor 488) was included in the electrode solution to label the target bushy neurons, which were preserved in the brain slice upon completion of physiological recording. The brain slices were then fixed and immunostained against vGluT1 antibody to label synaptic vesicles with fluorescent marker (Alexa Fluor 647). vGluT1-labeled synaptic endings onto the target bushy neurons were imaged using confocal microscopy and subsequently quantified. Compared to the young mice group, Endbulb of Held synapses in the middle-aged and old groups showed not only deteriorated synaptic transmission, but also significantly reduced total area of vGluT1-labeled puncta surrounding target bushy neurons. It suggests that the synaptic vesicle pool decreases in size at the Endbulb of Held terminal during aging, which presumably underlie the compromised synaptic transmission. Interestingly, the total number of labeled puncta surrounding recorded bushy neurons were not significantly different among three age groups. Therefore, the number of total active zones may remain stable among surviving Endbulb of Held terminals during age-related hearing loss.

PD 138**D-stellate Neurons of the Ventral Cochlear Nucleus Decrease in Auditory Nerve-Evoked Activity during Age-Related Hearing Loss**

Yong Wang; Ruili Xie

Department of Otolaryngology, Ohio State University

D-stellate neurons are the major inhibitory neurons in the ventral cochlear nucleus that receive auditory nerve

inputs and provide widespread inhibitory innervation to other principal neurons of the cochlear nucleus. Neural inhibition is well known to decrease in strength during aging. However, it is unclear how the physiological activity of D-stellate neurons changes with age during the development of age-related hearing loss. In the present study, we performed whole-cell patch clamp recording in acute brain slices to investigate the auditory nerve evoked responses in D-stellate neurons using three age groups of CBA/CaJ mice at 2-4 months (young), 17-19 months (middle-aged), and 27-30 months (old). Under current clamp recording, electrically stimulating the auditory nerve evoked tonic spikes that lasted throughout the stimulus trains in young mice. In middle-aged mice, the firing rate of evoked spikes decreased over time within the stimulus train, and in some cells dropped to complete failure toward the end of stimulus trains. In old mice, auditory nerve stimulation only evoked spikes during the early phase of the stimulus trains, but failed to trigger any spikes throughout the later phase. The decreased overall activity of D-stellate neurons with age suggests that inhibitory innervation from D-stellate neurons to other principal cochlear nucleus neurons is weakened during age-related hearing loss. The fast adaptation in firing rate within the stimulus trains in middle-aged and old mice indicates that inhibition quickly fades upon sustained auditory activity during age-related hearing loss, which could be due to compromised synaptic transmission at the aged auditory nerve synapses onto D-stellate neurons.

PD 139

Inhibitory Synapses onto Medial Olivocochlear Neurons in the Ventral Nucleus of the Trapezoid Body

Lester Torres Cadenas; Matt Fischl; Catherine Weisz
NIH / NIDCD

Synaptic inputs onto medial olivocochlear (MOC) efferent neurons in the brainstem ventral nucleus of the trapezoid body (VNTB) are poorly understood. Excitatory, glutamatergic inputs originate in the cochlear nucleus, but the source, strength, or identity of neurotransmitters at putative inhibitory synaptic inputs have not been characterized. We performed whole-cell voltage-clamp electrophysiological recordings in MOC neurons to investigate inhibitory synaptic inputs. MOC neurons in the VNTB were identified for recordings in brainstem slices from P12-P23 mice using ChAT-IRES-cre mice crossed with a tdTomato reporter mouse line to label cholinergic neurons. MOC identity was confirmed by co-labeling tdTomato positive neurons with an antibody against choline acetyltransferase (ChAT), by confirming co-labeling of tdTomato with a retrograde tracer applied to the cochlea, and by filling the neuron with biocytin

during the recording followed by DAB staining to confirm characteristic MOC neuron morphology. During voltage-clamp recordings, spontaneous post-synaptic currents (sPSC) occurred that were partially sensitive to the AMPA type glutamate receptor blocker CNQX. The reversal potential of remaining sPSCs corresponded to the chloride reversal potential, indicating inhibitory synaptic currents. Application of both gabazine and strychnine further reduced sPSC frequency, demonstrating the presence of GABAergic and glycinergic synaptic transmission. Electrical stimulation delivered via a micropipette was used to evoke neurotransmitter release from subsets of pre-synaptic axons, while evoked (e)PSCs were measured in postsynaptic MOC neurons. Excitatory and inhibitory synaptic inputs were both evoked from axons originating primarily from the same ear. ePSCs in MOC neurons using 'paired pulse'; stimulation at inter-stimulus intervals (ISI) from 10-500 ms suggests that there is a depression of inhibitory synaptic inputs at an ISI of 10 ms. Immunohistochemical analysis also provided evidence for the existence of inhibitory synapses around MOC neurons. To determine the source of inhibitory inputs to MOC neurons, focal glutamate uncaging to activate MNTB somata was performed while recording from MOC neurons. MNTB activation evoked PSCs in the MOC neuron, confirming the MNTB as the source of inhibitory synaptic inputs. Our work indicates that MOC neurons in the VNTB receive inhibitory inputs in addition to glutamatergic inputs, both from the same ear. Future work will further characterize the effect of inhibitory neurotransmission on MOC function.

PD 140

Organizational Features of the Auditory Periphery shapes the Development of Tonotopically Distributed Membrane Properties in Cochlear Nucleus Neurons

Lashaka S. Jones¹; Weise Chang²; Zoe Mann³; Matthew Kelley⁴; R. Michael Burger¹

¹*Lehigh University*; ²*Laboratory of Cochlear Development, National Institute on Deafness and Other Communication Disorders, National Institutes of Health*; ³*Centre for Craniofacial and Regenerative Biology*; ⁴*NIDCD*

Tonotopic organization is the fundamental organizing principle of the auditory system. In the avian cochlea, this pattern arises along the basilar papilla and is defined partially by hair cell morphological and physiological gradients from base to apex. The BP imparts tonotopic organization on to central auditory neurons via the 8th nerve which provides primary input to Nucleus magnocellularis (NM). A primary function of NM neurons is to preserve or improve temporal precision of

phase-locked discharges to sounds, a key physiological feature for sound localization. These neurons are able to accomplish this task at relatively high frequencies due to tonotopically distributed intrinsic membrane properties. These include distributed expression of voltage-gated ion channels along the tonotopic gradient. Additionally, 8th nerve synapse number and size varies similarly along this gradient.

One unresolved question is how tonotopic properties in the brain arise during development? One hypothesis is that tonotopically distributed properties first develop in the ear which then, in turn, instructs the development of intrinsic properties centrally. An alternative, but not mutually exclusive, hypothesis is that central neurons develop independently of the ear instead relying on central cues to establish tonotopic patterns. We investigated this question using a “BMP7-manipulated” chick model. Previous work by the Kelley lab (Mann et al, 2014) showed that a gradient of Bone morphogenetic protein 7 (BMP7) is a primary driver of tonotopic patterning of hair cells along the BP. Overexpression of BMP7 in the developing otocyst results in a shift toward low frequency-like phenotypes along the entire BP.

We overexpressed BMP7 in-ovo using an RCAS viral vector to create chicks with a “BMP7-manipulated” or “low-frequency like” ear. We examined the development of intrinsic cellular properties within these animals. To investigate NM neuron excitability along the tonotopic axis, we used whole-cell current clamp to inject ramp stimuli into NM neurons. This enabled the measurement of slope threshold (ST) and integration period (IP) values, which are known to differ significantly among high and low characteristic frequency NM neurons (HCF, LCF) (Oline et al, 2016). Our results suggest that ST and IP value distributions across NM shift toward values expressed in control low characteristic frequency neurons. These data are the first to suggest that intrinsic membrane properties of central neurons are driven by the organizational features of the peripheral sensory epithelium.

PD 141

The Olivocochlear Reflex Strength is Correlated with Behavioral Performance in a Visual Selective Attention Task with Broadband Noise Distractors but no with Distress Calls in Chinchillas.

Macarena Bowen¹; Gonzalo Terreros²; Macarena Ipinza¹; Felipe N. Gomez-Moreno³; Luis Robles⁴; Paul H. Delano⁵

¹*ICBM, Facultad de Medicina, Universidad de Chile;*

²*Instituto de Ciencias de la Salud, Universidad de*

O'Higgins; ³*Departamento de Biología y Química, Facultad de Ciencias Básicas, Universidad Católica*

del Maule; ⁴*Programa de Fisiología y Biofísica, ICBM, Facultad de Medicina, Universidad de Chile;* ⁵*Faculty of medicine. Av. Independencia,*

Background

The auditory efferent network comprises descending projections from the auditory cortex to the superior olivary complex, from where medial olivocochlear (MOC) bundle emerges ending in the outer hair cells of the cochlea. MOC function can be assessed by measuring the effects of contralateral acoustic stimulation (CAS) on the amplitude of distortion product otoacoustic emissions (DPOAEs). One of the possible functions of the efferent system is the modulation of cochlear sensitivity during selective attention to visual stimuli. In this work, we studied the relationship between MOC reflex variability and visual attention performance, hypothesizing that inter-subject variability of MOC reflex is related to the capability of avoiding auditory distractors. For this, we analyzed the effect of two types of auditory distractors: (1) broad-band noise (BBN) as an irrelevant artificial stimulus and (2) chinchilla distress vocalizations as relevant ecological stimuli.

Methods

We measured the MOC reflex using contralateral BBN in ten awake chinchillas. After that initial measure, chinchillas were trained in a two-choice visual discrimination task. The behavioral performance was evaluated in a 12 days protocol divided into three blocks of 4 days: without auditory distractors (base-line), with BBN and with four different male chinchilla vocalizations (F0= 537 – 854 Hz), as auditory distractors.

Results

CAS-induced DPOAE amplitude changes had an average of 0.75 ± 1.23 dB across all frequencies. During the presentation of vocalization auditory distractors a significant increase in latency of correct responses was observed between the first day with vocalization (2025.11 ± 493.4 ms) and day 3 base-line (1373.81 ± 314 ms), day 3 and 4 of BBN (1416.62 ± 570.1 , 1381.43 ± 386.6 ms) and day 4 of vocalization (1513.9 ± 569.3 ms) (RM-ANOVA on Ranks, Tukey *post-hoc*, $p < 0.05$). Significant Spearman correlations among MOC reflex magnitudes and behavioral performance during first day with noise as distractor – latency of responses ($r = 0.7$, $p = 0.03$) and accuracy ($r = -0.8$, $p < 0.01$) – were found.

Discussion

Our results show a correlation between MOC strength and behavioral performance during selective attention to visual stimuli only when using BBN as auditory distractor.

Unexpectedly, vocalizations did not correlate with MOC strength, but affect behavioral performance by decreasing accuracy and increasing the latency of responses. Supported by FONDECYT 1161155 and Fundacion Guillermo Puelma.

PD 142

Differential Effects of Ipsi- and Contralateral Forward Masking Measured with Auditory Brainstem Responses in the Mongolian Gerbil

Maike Schaper; **Thomas Kuenzel**

Institute for Biology 2, Department of Chemosensation, RWTH Aachen University

Forward masking means that the presentation of one auditory stimulus influences the response to another stimulus presented later. Here, both sounds can be delivered to the same ear (ipsilateral) or the masker could be presented to the opposite ear (contralateral). One possible mechanism for masking could be short term neural adaptation. However, this is not a sufficient explanation for contralateral masking in monaural stations of the auditory pathway. Here, commissural or descending connections must be involved. An evaluation of masking effects on early stations of the auditory pathway could thus be useful to understand the connectivity in the auditory system. In order to do this, we recorded auditory brainstem responses from anesthetized mongolian gerbils. We analyzed ABR thresholds for broadband and tonal stimuli and also analyzed latencies and amplitudes of all ABR wave components individually. In our hands, mongolian gerbils had ABR thresholds to 0.1 ms broadband clicks of -0.3 ± 5.7 dB SPL ($n=15$). Thresholds to 6-12kHz pure tones were even lower (-6.4 ± 6 dB SPL, $n=11$). Preceding the click stimulus with the presentation of 50ms / 70dB SPL / 1ms gap broadband noise maskers to the contralateral ear strongly elevated ABR thresholds (by 19 ± 7.5 dB SPL for clicks, by 23.6 ± 9.2 dB SPL for tones). All ABR wave components except wave III showed increased latencies and reduced amplitudes. Interestingly, for ABR wave III the amplitudes in response to medium sound pressure levels were increased above control levels in the masked condition. For the early components (I-III), but not for later waves IV and V/VI, latencies and amplitudes became increasingly similar to the control condition with increasing ipsilateral stimulus levels. When we compared these results to the ipsilateral forward masking condition several differences became evident: Ipsilateral masking with identical stimulus conditions was much more powerful (63.3 ± 2.9 dB SPL threshold increase). Even when we applied softer ipsilateral masker levels which caused threshold elevation comparable to the contralateral masking condition (e.g. 26.7 dB SPL for 35 dB SPL masker level), increasing the stimulus level in this condition never caused recovery of

wave amplitude and latencies. We also used monopolar electrocochleographic recordings close to the round window to confirm these differences. Thus our study suggests that different mechanisms underly ipsi- and contralateral masking and furthermore that contralateral masking can have differential effects on the individual generator regions of the ABR.

PD 143

Effect of Anesthesia on Open Field Auditory Brainstem Response in Rats

Noor-E-Seher Ali; Anthony J. Ricci
Stanford University

Background: Auditory brainstem responses (ABRs) are a non-invasive hearing test used to physiologically assess the auditory pathway and peripheral function. To perform ABRs on animals, the combination of ketamine and xylazine is commonly used for their sedative and muscle relaxant properties. This helps minimize myogenic noise and reduced artifacts during recordings. A previous study done in mice showed ABR peak latency and thresholds are significantly increased in the anesthetized condition compared to the awake condition (Van Zanten et al, 2004). The objective of this study is to determine the effects of ketamine and xylazine over the duration of anesthesia on ABR thresholds, amplitude, width, and latency of wave 1.

Methods: Six Sprague Dawley rats approximately 20 days old were used for this experiment. They were anesthetized by administering 100mg/kg ketamine and 16 mg/kg xylazine intraperitoneally. We varied stimulus duration and rise time to optimize ABR testing parameters and ended up using a 5 ms stimulus with a 0.2 ms rise time. The rat was positioned ten centimeters away from the free field speaker, and an ABR recording was done every ten minutes for an average of 155 ± 20 minutes. No additional anesthesia was given. Threshold was defined as the lowest stimulus intensity at which the waveform was at least 3 standard deviations above the noise floor. Amplitude was calculated from baseline of noise floor to maximum point of wave one. Latency was calculated from 0 to time of first peak. Width of wave one was calculated at half maximum.

Results: On an average, the initial ABR was recorded 17 minutes after anesthesia injection. Thresholds across frequencies minimally changed throughout the duration (± 10 dB). Amplitude of wave 1 initially increased and stabilized around 40 minutes after initial anesthesia. At that point, in some rats, the amplitude plateaued ($n=2$), continued increasing ($n=1$), or fluctuated ($n=3$). Latency of wave 1 decreased over time reaching a plateau at 88 ± 15 minutes ($n=4/5$). Width of wave 1 decreased over time by 23% over 151 ± 16 minutes ($n=4/5$).

Discussion: The level of anesthesia alters several components of ABR measurements. Threshold was not sensitive to anesthesia level, whereas amplitude, latency, and width were. Waiting 40 minutes after giving anesthesia provides larger and stable wave one amplitudes. Latency and width decrease over duration of anesthesia. It is imperative to be consistent with timing of the ABR after anesthesia induction to reduce variance when investigating parameters other than threshold.

Cochlear Mechanics: Facts & Fancies

PD 144

Scanning fiber optic SDOCT-based probe for intra-cochlear imaging and displacement measurement

Nathan C. Lin; Elika Fallah; C. Elliott Strimbu;
Christine Hendon; Lisa Olson
Columbia University

The introduction of spectral domain Optical Coherence Tomography (SDOCT) system has revolutionized auditory mechanics, with its millimeter-range penetration depth and ability to measure simultaneous displacements from numerous structures. Imaging and displacement measurement of the cochlear sensory tissues can be done either through the bone in the apical region, or through the round window membrane. Here we are introducing a novel method to study cochlear mechanics by coupling the SDOCT system to a fiber optics probe. The probe, 140 μm in width with a focal length of 250 μm , can access the cochlea's sensory tissue in difficult-to-access regions, or through small cochleostomies. Moreover, it has a controllable lateral scanning range up to 200 μm for imaging cochlear structures, and the scanning range can be decreased and ultimately stopped to pinpoint the location for displacement measurements using Spectral Domain Phase Microscopy (SDPM). We will demonstrate the function of the probe with in vivo imaging and displacement measurements in the gerbil cochlea.

PD 145

Buildup of Reticular Lamina Traveling Wave Amplification in the Mouse Cochlea

James B. Dewey¹; Brian E. Applegate²; John S. Oghalai³

¹*Department of Otolaryngology - Head & Neck Surgery, University of Southern California*; ²*Department of Biomedical Engineering, Texas A&M University*; ³*USC Caruso Department of Otolaryngology - Head and Neck Surgery*

Until recently, our understanding of in vivo cochlear mechanics has largely been based on measurements of basilar membrane (BM) motion. It is well established

that sound-evoked BM traveling waves are amplified by outer hair cell-generated forces, that these forces only amplify BM motion near the traveling wave peak, and that amplification accumulates from one location to the next over the amplifying region. However, new measurements have revealed that traveling waves on the reticular lamina (RL), at the apical surface of the outer hair cells, are quite different than BM traveling waves, and are amplified over a broad region extending throughout the cochlear base. It remains unclear whether RL traveling wave amplification builds up independently from BM amplification, and whether RL amplification in far basal regions contributes to amplification at the wave's peak. Here we used an optical coherence tomography-based approach to examine the spatial buildup of RL traveling wave amplification in the mouse cochlear apex. While monitoring BM and RL responses to a fixed probe tone, we swept a second suppressor tone in frequency to selectively reduce the amplification provided by different cochlear regions. This allowed us to map the region over which amplification of the probe response had built up. For probe frequencies near the characteristic frequency (CF) of the measurement site, we found that suppressor tones up to an octave higher in frequency could partially suppress BM and RL responses to the probe. This indicates that BM and RL traveling waves share a common buildup region that extends ~ 1.2 mm basal to their peaks, and that RL amplification further basal does not contribute to amplification more apically. To directly assess the buildup of amplification distant from the RL traveling wave peak, we also examined the suppression of RL responses to below-CF tones, and found that such responses were unaffected by above-CF suppressor tones that stimulated regions basal to the measurement site. This confirms that amplification of RL motion distant from the traveling wave peak does not build up significantly, and is primarily a local phenomenon. We conclude that while outer hair cell-generated forces amplify the RL traveling wave throughout its basal extent, these forces only build up in regions of the wave where BM motion is also amplified. The mechanical properties of the BM and organ of Corti likely interact to spatially tune the longitudinal buildup of amplification.

Supported by NIDCD/NIH grants DC014450, DC013774, and DC016211.

PD 146

Temporal Limits of Dynamic Compression in the Organ of Corti

Anna Vavakou; Nigel P Cooper; Marcel van der Heijden
Erasmus MC

Acoustic signals are subjected to nonlinear processing in the cochlea. The functional correlate of these

nonlinearities, dynamic range compression, is fundamental to hearing but the mechanisms are poorly understood. The main problem is the lack of data on the micromechanics within the organ of Corti. Owing to recent improvements of Optical Coherence Tomography (OCT) vibrometry it is now possible to record vibrations inside the intact cochlear partition and to study the mechanisms of dynamic compression in fine detail. Using OCT we have recently provided a mapping of sound-evoked vibrations inside the Organ of Corti (Cooper et al, Nat. Commun. 9:1354, 2018), and reported a tightly delineated hotspot of vibrations that included the Deiters cells and the outer hair cells (OHC). One of the key findings of that study is the wide range of frequencies over which the hotspot response is nonlinear. Unlike the BM, for which the nonlinearity is restricted to a narrow frequency band near the characteristic frequency (CF), the hotspot shows compression over a wide frequency range, down to at least 6 octaves below CF.

The scope of our current work is to describe the temporal properties of the mechanical nonlinearity in the hotspot. The main question is: for stimuli having fluctuating amplitudes, can the compressive mechanism “keep up” with these fluctuations when they get faster, or does it fail to track fast intensity fluctuations, giving rise to hysteresis and release from compression? In a previous study of BM recordings (Cooper and van der Heijden, Adv. Exp. Med. Biol. 894:267), we found both hysteresis and release from compression around CF and interpreted them in terms of an automatic gain control mechanism that needs some time (a few 100 microseconds) to adjust the sensitivity to the stimulus intensity. In the current study we apply a similar measurement scheme to probe the speed of compression of low-tail (\ll CF) components in the hotspot. We found the nonlinear mechanism to be sluggish (“lowpass”), having a cutoff frequency of 2-3 kHz in the 13-25 kHz region of the gerbil cochlea. We interpret this result in terms of an OHC-controlled gain control mechanism and identify the 2-3 kHz cutoff frequency with lowpass filtering of the receptor potential by the OHC cell membrane.

PD 147

Proving Hair Cell's Mechano-transduction Using Two-tone Suppression Measurements

Wenxiao Zhou; Jong-Hoon Nam
University of Rochester

When two sound tones are delivered to the cochlea simultaneously, they interact with each other in a suppressive way, referred to as two-tone suppression (2TS). This nonlinear response is ascribed to the saturation of the outer hair cell's mechano-transduction.

Thus, 2TS can be used as a non-invasive probe to investigate the fundamental properties of cochlear mechano-transduction.

We analyzed existing 2TS data using a nonlinear cochlear model. The computational model incorporates cochlear fluid dynamics, organ of Corti mechanics and outer hair cell electrophysiology. Experimental observations such as compressive nonlinearity and frequency glide were reproduced with the model. Simulated results demonstrate such nonlinear responses are related with nonlinear mechano-transduction. The threshold of 2TS and rates of low-side suppression are dependent on mechano-transduction properties. By comparing model responses to existing 2TS measurement data, we estimate the intrinsic characteristics of mechano-transduction such as sensitivity and adaptation. When mechano-transduction sensitivity at the basal location (characteristic frequency of 17 kHz) being at 1.3 A/m, the simulation results agree with 2TS measurements. The model also demonstrates how the outer hair cell's adaptation alters the temporal pattern of 2TS by modulating mechano-electrical gain and phase.

[Supported by NIH NIDCD R01 DC014685]

PD 148

Implications of Recent OCT Data for the Kinematics of the Organ of Corti

Elisa Boatti¹; Julien Meaud²

¹*Georgia Institute of Technology;* ²*G.W.W. School of Mechanical Engineering and Petit Institute for Bioengineering and Bioscience, Georgia Institute of Technology*

The organ of Corti has a key role in the transduction of sound stimuli into electrical signals directed to the brain. However, a full understanding of its structures and function has not yet been achieved. In the last years, major advancements in the experimental techniques allowed for unprecedented accessibility of the organ of Corti and accuracy of the measurements. The most recent experimental observations should be carefully included in the development of new organ of Corti models, and taken into account for the assessment of the existing models, such that the predicted results can provide meaningful insights into cochlear mechanics and help explain the phenomena observed experimentally. In this work, we adopt simple kinematic models for the organ of Corti and compare their results to recent OCT data collected from mice. Specifically, our goal is to test the validity of typical modeling assumptions and to explore the role of organ of Corti structures extensibility. We first focus on the motion of the basilar membrane, tectorial membrane and reticular lamina, for which OCT measurements are available, and subsequently

we derive the predicted motion of the outer hair cells and of their hair bundles. In particular, we show that the common assumption of an inextensible reticular lamina cannot reproduce correctly the experimental measurements related to its radial displacement. We also observe that the reticular lamina extensibility may play a role in low-frequency attenuation of the hair bundles deflection for high sound pressure levels, possibly providing a mechanism of protection against unsafe high-level sound. On the other hand, the tectorial membrane extensibility appears to play an important role in the frequency tuning of the hair bundles deflection, especially around the characteristic frequency. This confirms the idea that the tectorial membrane is crucial for passive cochlear filtering, as already reported in previous studies. We therefore conclude that the extensibility of the organ of Corti structures is important for the correct sound stimuli transduction and should be taken into account to develop accurate organ of Corti models. This research is supported by grants NIH 1R56DC016114 and NIH 1R01DC016114.

PD 149

Measurements of Cochlear-Partition Motion in Human Cadavers Challenge the Classic Model of Basilar Membrane Motion

Stefan Raufer¹; John J. Guinan²; Hideko H. Nakajima²
¹*Eaton-Peabody Laboratories, Massachusetts Eye and Ear; Graduate Program in Speech and Hearing and Bioscience and Technology, Harvard University;*
²*Eaton-Peabody Laboratories, Massachusetts Eye and Ear; Graduate Program in Speech and Hearing and Bioscience and Technology, Harvard Medical School*

Background: In the mammalian cochlea, sound produces motion of the basilar membrane (BM) resulting in vibrations in the organ of Corti that are detected by mechanosensitive cells. BM motion has been extensively studied in experimental animals, but the human cochlear partition (CP, including the BM) anatomy is vastly different from the anatomy of experimental animals. In laboratory animals, the osseous spiral lamina (OSL) is short and vibrates very little, while the BM spans the width of the CP and its cross-sectional motion is like a simple beam. In contrast, in humans the OSL occupies a much larger percentage of the CP width in the base and the vibration profile of the CP is poorly understood.

Methods: We quantified the CP anatomy from histological sections and measured the transverse motion along the width of the CP in the cochlear base of fresh cadaveric temporal bones to pure-tone stimuli with laser-Doppler vibrometry.

Results: Our anatomical work shows that the human CP consists of the OSL and the BM, and that these

two structures are connected by a soft-tissue structure, which we name the CP “*bridge*” (not present in laboratory animals). In response to a tone at a frequency near or below the local best frequency (BF, here typically ~15 kHz), the motion of the OSL is like a stiff plate hinged near the modiolus with the transverse motion increasing almost linearly along the OSL to the bridge region. The motion increased in the region of the CP bridge and BM with the maximum vibration near the border between the bridge and the BM. This behavior contrasts findings in experimental animals where the maximum CP motion is near the center of the BM width. On average, BM motion accounted for only ~27% of the total volume displacement of the human CP at frequencies below the BF, and for ~46% at the BF in this passive preparation.

Conclusions: Human CP motion differs greatly from that in laboratory animals. In humans, the relatively wide OSL and the attached CP bridge region vibrate with a magnitude comparable to the BM. Classic BM motion, which forms the basis for physically-motivated cochlear models, cannot be assumed to apply to humans. The mechanisms for mechanotransduction, such as the shearing motion between the tectorial membrane and hair-cell bundles, may be profoundly affected by the unique CP anatomy and motion in humans.

[Supported by NIH/NIDCD R01-DC013303, and American Otological Society].

PD 150

A Base to Apex Model of the Mammalian Cochlea

Aritra Sasmal; Karl Grosh
University of Michigan, Ann Arbor

Building a physiologically-based mathematical model of the cochlea able to replicate the highly tuned and nonlinear response at the base, as well as the less sharply-tuned (nearly low-pass) and weakly nonlinear responses at the apex, has presented a longstanding challenge to cochlear mechanics modelers. Two additional features in the apical response that are usually ignored in most models are the departure from the exponential tonotopic map and the surprisingly small reflections of the pressure field at the helicotrema. Further, recent measurements using optical coherence tomography (OCT) has shown that the basilar membrane (BM) centric view of cochlear mechanics is incomplete. The differential motion within the organ of Corti (OoC) implicates more complex dynamics and has necessitated the formulation of a more complete theory that includes the motion of the tectorial membrane (TM) and the reticular lamina (RL). In this paper, we develop a computational model of the guinea pig cochlea to simulate its response from the base to the apex. Two key insights provide the appropriate physical

mechanisms to produce high fidelity results at the apex. First, the geometric taper of the scalae increases both the added fluid mass and the viscous damping, resulting in the prediction of the non-exponential tonotopic map observed at the apex. Secondly, incorporation of the geometry of the OoC, most importantly the angle that the outer hair cells make with the BM, serves to significantly reduce the effect of the active process on the BM but not on the RL. A model incorporating these elements predicts the transition from basal to apical mechanical tuning. Furthermore, we show that the RL moves out of phase with the BM below the characteristic frequency of the location at low sound pressure levels, and moves in phase with the BM post mortem, in line with recent experiments at the base of the gerbil and mouse. We extend this model to explain the change in shape of the neural tuning curves from base to apex. This work is supported by NIH-04084.

PD 151

Evidence for Flexoelectricity in Stereocilia Bundle Limit Cycles

Qian Deng¹; William E. Brownell²; Pradeep Sharma³
¹*Xi'an Jiaotong University*; ²*Baylor College of Medicine*;
³*University of Houston*

Introduction. Cochlear transduction is highly non-linear in terms of its sensitivity, its frequency selectivity, and its extraordinary dynamic range, which features a compressive non-linearity. Inner ear mechanics have been subjected to a variety of non-linear analytic approaches. The notion of Hopf bifurcation and the pertinent dynamical formalism are often used to describe stereocilia bundle dynamics and explain the idiosyncratic and nonlinear phenomenology of the hearing mechanism. Such a description is attractive but, in general, it has provided only modest insight into the physical mechanisms responsible. A dynamic limit cycle defines the Hopf bifurcation. The system is critically unstable at the edge of the limit cycle and enters oscillation with minimal provocation. We have explored the role of membrane flexoelectricity in generating a limit cycle in the stereocilia bundle. Flexoelectricity is a universal electromechanical coupling that exists in all dielectric substances. It is prevalent in soft matter and becomes relevant when one dimension of the material approaches the nanoscale. Bending artificial lipid bilayers results in a change in electrical polarization (the electricity that comes from flexing). An electrical field across the membrane causes it to bend (known as the converse flexoelectric effect).

Method. We have previously shown how piezoelectric-like membrane electromechanics leads to a linear model of stereocilia bundle motility. Here, we retain the well-

defined physical quantities such as membrane bending modulus, geometrical characteristics and other features of the earlier model and incorporate well-accepted principles of soft matter physics.

Result. The model now reveals that the natural reciprocity of membrane flexoelectricity is essential in inducing the limit cycle and the instability state known as a Hopf bifurcation. Two key control parameters are the biomembranes'; bending modulus and charge screening by cations.

Conclusions. Earlier assertions that the cochlea amplifies the acoustic stimuli through its exceptional electromechanical energy conversion property are confirmed and insights as to how physical properties such as biomembrane mechanics and the impact of cations on surface charge emerge as parameters that significantly affect the stability of the system and hence the hearing mechanism.

Funding. The financial support from NSFC (Grant No.11672222); the Fundamental Research Funds for Chinese Central University (XJJ2016071); and NIH/NIDCD (R01 DC000354) are gratefully acknowledged.

Auditory Cortical Plasticity

PD 152

Combining Stimulation Place and Rate to Improve Cochlear Implant Pitch Perception

Ray Goldsworthy

University of Southern California

Cochlear implants provide unique insight into how frequency is encoded into spatiotemporal properties of the auditory nerve. In normal hearing, pure tones of a given frequency produce an auditory nerve response that necessarily covaries in its spatial and temporal response properties. Consequently, it is difficult to characterize the relative importance of spatial versus temporal response properties of the auditory nerve for conveying tonal pitch. Cochlear implants provide independent control over stimulation place and timing, thus allowing the relative contributions to be examined. We are measuring frequency discrimination thresholds for frequencies between 100 and 3200 Hz as conveyed by place, rate, and combined place and rate of stimulation in adult cochlear implant users. Results to date indicate that stimulation place and rate combine perceptually to produce a singular sense of pitch. Moreover, frequency discrimination with combined place and rate is better than with place alone for frequencies as high as 800 Hz. Above 800 Hz, stimulation rate does not seem to contribute to the combined pitch percept; however, rate pitch has been shown to be highly plastic in cochlear implant users, so we speculate that

with experience the contribution of rate to the combined pitch percept can be extended to frequencies above 800 Hz. We interpret the results as indicating that stimulation timing can be used in cochlear implant sound processing to enhance frequency resolution for frequencies at least as high as 800 Hz.

PD 153

Simultaneous Measurement of Steady-State and Transient Electrically-Evoked Auditory Change Complex (eACC) Responses in Cochlear Implant Users

Deborah A. Vickers¹; Axelle Calcus¹; Lindsey N. Van Yper²; Jaime Undurraga³

¹University College London; ²Department of Linguistics, The Australian Hearing Hub, Macquarie University, Sydney; ³Macquarie University

Background

The auditory change complex (ACC) is a cortical response to a change in an ongoing stimulus. It can be used to objectively measure discrimination abilities. We have previously measured eACC responses for electrode discrimination following CI activation and observed different rates of change over time in the presence of and the amplitude of the response.

The current work explored a range of stimulus parameters to determine if both the electrical steady state responses and transient responses can be recorded in cochlear implant users with the same stimuli indicating the discrimination abilities at different stages in the auditory pathway.

Objectives

To determine if both the steady state and transient responses could be measured simultaneously for the same stimuli in cochlear implant users

To determine how/if at all this differed from normal hearing listeners

Methods

Eight normal hearing were tested acoustically and five adult post-lingually deaf cochlear implant users with Nucleus 24 devices were tested using direct stimulation to explore responses to changes in stimulus frequency. Discrimination tasks with the same stimuli were conducted to determine if stimuli that were discriminable behaviourally also produced a detectable electrophysiological response. For implant users this was conducted on the six most apical electrodes together with other measures of electrode discrimination.

Stimuli were constantly switched without gaps to maximise the estimate of the change response. A range

of parameters were explored to understand the limits of electrical hearing and make comparisons with normal hearing abilities. Two switching rates (6.4 and 2 Hz) were used. The steady state and transient responses were observed.

Results

Preliminary findings suggest that for normal hearing listeners both steady state and transient responses were present for both the fast and slow switching conditions but for the cochlear implant users these responses were only observed for the slower switching rate (2Hz). Further details of the exploration of the parameter set will be presented.

Conclusions

Potential interpretation of the findings is that the neural generators of the steady-state response may be adapted by electrical stimulation which is not observed for normal hearing listeners

PD 154

Downward Cross-modal Plasticity in Single-sided Deafness: Cooperation and Competition between Hearing and Vision

Yufei Qiao¹; Xuesong Li²; Hang Shen³; Xue Zhang²; Yang Sun²; Wenyang Hao¹; Bingya Guo¹; Daofeng Ni¹; Zhiqiang Gao¹; Hua Guo²; **Yingying Shang**¹

¹Department of Otorhinolaryngology, Peking Union Medical College Hospital; ²Center for Biomedical Imaging Research, Department of Biomedical Engineering, School of Medicine, Tsinghua University; ³Department of Neurology, Peking Union Medical College Hospital

Cross-modal plasticity has been widely demonstrated to occur in deafness, manifesting as increased involvement of the auditory cortex in the processing of other senses, such as vision, when compared to normal hearing individuals. However, it remains unclear whether similar cross-modal plasticity occurs in partial auditory-deprived individuals. To investigate this, we enrolled individuals with a typical partial auditory-deprivation, single-sided deafness (SSD), into functional MRI (fMRI) scans under resting state and a visuo-spatial working memory task. Eighteen left single-sided deafness subjects (LSSD), 18 right single-sided deafness subjects (RSSD) and 18 normal hearing controls (NH) underwent the fMRI scan. All SSD subjects had a long-term severe to profound sensorineural hearing loss with the duration of deafness longer than 2 years. Contrary to previous findings in bilateral deafness, our study revealed decreased activation in the auditory cortex in both LSSD and RSSD compared to NH during the visual task, especially in RSSD. Furthermore, weaker activation was also observed in the visual cortex in RSSD than NH. The

activation levels in both the auditory and visual cortices had a positive correlation with residual hearing abilities, including speech recognition in noise and sound localization in RSSD. Moreover, there was a positive correlation between performance in the visual task and hearing abilities in both LSSD and RSSD. These observations suggest that SSD can lead to a downward cross-modal plasticity: the more hearing ability lost, the fewer brain resources in the auditory cortex can be applied to visual tasks. In addition, the prefrontal cortex was also observed to be less activated during the visual task while the resting state fMRI revealed increased functional connectivity between the prefrontal cortex and the auditory cortex in RSSD, suggesting prefrontal resources were recruited less by vision but more by hearing. Together these findings may indicate that auditory and visual cortices cooperate with each other during visual processing. When hearing is partially deprived, there may be an underlying competition for brain resources between hearing and vision. Our findings in this pilot study of partial auditory-deprived individuals enrich the understanding of cross-modal plasticity in the brain.

PD 155

Role of peripheral BDNF for auditory perceptual learning?

Marlies Knipper¹; Philipp Eckert¹; Marie Manthey¹; Lucas Matt¹; Philine Marchetta¹; Wibke Singer¹; Peter Ruth¹; Thomas Schimmang²; Peter Pilz¹; Lukas Rüttiger¹

¹University of Tübingen; ²Institute of Biology and Molecular Genetics (IBGM)

Background:

While novel studies indicate that perceptual learning is not linked with permanent changes in cortical circuitry but rather with changes that are gated in a task- or context-dependent fashion, the molecular substrate of perceptual learning is still elusive. It is currently speculated that perhaps changes in synaptic weights restricted to a limited set of task-specific synapses play a crucial role (Irvine DRF Hearing Res. 2018, Zhang Y-X et al. *Amitay S* 2016, *Plos One*). BDNF is gradually upregulated in the cochlea and ascending auditory pathway onwards from prior hearing onset (postnatal day P4) (Singer et al., Knipper, *Neuropharmacol* 2014). Previously, we showed that peripheral BDNF in the cochlea or lower brainstem regions, but not in the central higher cortical brain regions is fundamental for improved and optimized auditory fidelity with hearing onset [Zuccotti A et al. Knipper, 2012, *J Neuroscience*, Chumak T et al., 2016, *Mol Neurobiol*]. This improved auditory fidelity included greater sensitivity of auditory fibers, lower hearing thresholds, and enlarged dynamic

range and inhibitory strength in the inferior colliculus related to lowering of spontaneous firing rate. We here asked to what extent these BDNF driven changes in auditory fidelity may influence memory-related shaping of auditory skills and auditory perceptual learning.

Methods:

Using conditional BDNF Pax2 KO mice, lacking BDNF in the cochlea, DCN and IC, we compared auditory fine structure analysis, auditory steady state response (ASSR), LTP and LTP-dependent task performance in BDNF WT and mutant mice, and investigated changes in markers for excitatory and inhibitory neuronal activity using high-resolution confocal microscopy and quantitative westernblot approaches.

Results:

Fundamental differences were found between BDNF Pax2 WT and KO mice at the molecular, functional, and behavioral level. The findings are discussed in the context of a role of BDNF for auditory perceptual learning in lower auditory brainstem regions.

Funding:

This work was supported by the Deutsche Forschungsgemeinschaft DFG-Kni-316-10-1, FOR 2060 project RU 713/3-2, SPP 1608 RU 316/12-1; KN 316/12-1; the Brain & Behavior Research Foundation NARSAD Young Investigator Grant 20748, BFU2013-40944; DFG KFO134.

PD 156

Probing the limits of compensatory plasticity and perceptual recovery following auditory neuropathy

Jennifer Resnick; Daniel B. Polley

Eaton-Peabody Laboratories, Massachusetts Eye and Ear; Dept. of Otolaryngology, Harvard Medical School

The auditory system employs a variety of rapid gain control mechanisms to adjust neural coding sensitivity to match transient shifts in acoustic signal energies. In addition to these “fast acting” gain control systems, central auditory neurons also exhibit slower gain control that adjusts neural excitability following long-lasting reductions in auditory input strength, for example, a deprivation of afferent input from the ear. While there is a general notion that increased “neural amplification” following a partial blockade of input from the ear is enabled by changes in inhibitory strength, the time course and cell type-specific circuitry modifications that underlie slow changes in central auditory gain remain unknown.

Here we performed chronic, cell type-specific 2-photon calcium imaging to simultaneously visualize sound-evoked GCaMP signals in genetically identified

inhibitory PV (parvalbumin expressing) neurons alongside neighboring PPy (putative pyramidal) cells in the auditory cortex of awake adult mice, before and after a controlled loss of afferent input from the cochlea. This approach allowed us to track the daily dynamics in identified cell types, at different spatial and temporal scales following peripheral insult. We found an increase in spontaneous activity in PPy cells on the day of the insult followed by an increase in PV spontaneous activity 24 hours later. Tone-evoked activity in both cell types was initially depressed, but then recovered and even surpassed baseline levels two weeks after injury. For more temporally complex stimuli, such as tones embedded in background noise, both PPy and PV cells showed an increase in response thresholds that didn't recover during the two weeks that followed the insult. Using a supervised learning model we found that while all tone detection deteriorated initially, recovery was limited to simple, but not complex, tone detection.

Our imaging data demonstrated complete cellular and network recovery for simple stimuli, but persistent coding deficits for more complex stimuli such as tones in noise. To explore the perceptual implications of these observations, auditory operant behavioral measurements were performed in head-fixed mice before and two weeks following nerve damage. As predicted from our imaging data, mice showed complete perceptual recovery for detecting tones in silence despite a massive loss of auditory nerve input. However, tone detection in noise remained impaired.

Collectively, our work provides new insight into slow compensatory plasticity in PV and PPy neurons in the auditory cortex that restores neural encoding of rudimentary, but not complex, sounds after peripheral deafferentation.

PD 157

Sound Localization Training Using Augmented Reality

Sungyoung Kim¹; Inyong Choi²; Adam Schwalje²
¹Rochester Institute of Technology; ²University of Iowa

Sound localization is a critical aural skill for identification of the position of a target object. However, hard-of-hearing listeners tend to rely more on visual cues for localization, which often causes a false sense of the invisible target's position as well as poor performance of speech perception in noise. A previous study showed that auditory training could assist in restoring directional selectivity of the auditory cortex. Improving on this idea by using the concept of gamification will potentially enable hard of hearing listeners to enhance auditory directional sensitivity and separate target sound source(s) from environmental noises. The authors have developed an

immersive sound localization training protocol using an augmented reality (AR) based game. Using enhanced proximity and realism of AR technologies, this game aims to offer fast and effective training as well as high level of involvement and engagement with a trainee, a common feature of e-learning and game-based learning. The game has been developed through two stages: (1) proof of the concept of sound localization training using a head-mounted display and (2) implementation in a hand-held device (a cellular phone and tablet PC) for broader dissemination. During the first stage, listeners (including both normal hearing and hard-of-hearing groups) participated in a seven-week sound localization training. In each trial, the trainee estimated an invisible target location, and then both true and estimated locations would be "visually" displayed in a Microsoft HoloLens, a head-mounted AR device. Through the isomorphic presentation, the trainee could "see" the mismatched sound position and learn to quantify corresponding sonic difference. The training results show that listeners could improve sound localization even with four training sessions over two weeks, while the progress differs across individuals. With the proved concept—efficacy of sound localization training using an AR device, we converted the training module to a training game; the game mission is to catch an invisible thief who makes a noise in a room, by throwing a net in the direction of the noise. Similar to other action games, the task gets more challenging for higher levels: decreasing the target sound level, adding maskers (non-target sound sources), moving the target sound, forcing time limits, and more. Within the game, we plan to measure pre- and post-game change in behavioral performances (speech-in-noise performance) and neurophysiological (EEG) correlates of sound localization and their relevance to speech perception in noise.

PD 158

Impaired Vesicle Replenishment at the Inner Hair Cell Ribbon Synapse leads to Impaired Sound Envelope Coding in the Inferior Colliculus

Maike Pelgrim¹; Markus Jeschke²; Nicola Strenzke¹
¹Department of Otolaryngology, University Medicine Göttingen; ²German Primate Center, Göttingen

Most mutations in the hair cell specific synaptic protein otoferlin lead to prelingual deafness DFNB9. However, even clinically deaf subjects may respond to rare sound stimuli presented in a soundproof chamber, and some patients maintain relatively well-preserved hearing thresholds while suffering from abnormal loudness adaptation and poor speech perception. Here, we analyzed the responses of single units of the anteroventral cochlear nucleus and inferior colliculus of mice carrying the human relevant Ile515Thr mutation

in otoferlin. Previous experiments had demonstrated normal sound thresholds but abnormal adaptation and delayed recovery from adaptation in single spiral ganglion neurons *in vivo*, which was ascribed to a defect of vesicle replenishment in inner hair cells. Like in spiral ganglion neurons, the responses of mutant cochlear nucleus neurons were relatively normal at low stimulation rates and declined when the stimulus rate was increased. The firing rates of multipolar/stellate cells which have long integration time constants were relatively normal. In contrast, those of octopus cells and bushy cells which serve as coincidence detectors were drastically reduced. In single neurons of the inferior colliculus, thresholds and spontaneous spike rates were normal, but evoked rates and dynamic ranges were slightly reduced in the mutants. However, in a paired pulse paradigm, significantly longer silent intervals were required for the recovery of spiking. There was an enhanced adaptation and increase in the rate of spike failures in response to amplitude modulated tones with modulation frequencies between 16 and 64 kHz, while the temporal precision of amplitude modulation coding was normal. In another more severely affected otoferlin mutant ("Pachanga"), only very few sound-responsive neurons were found in the IC, which all displayed high thresholds, an onset-type response and a strong dependence on the stimulus rate. In summary, we used two otoferlin-deficient mouse models to show that certain defects of the temporal properties of sound encoding at the inner hair cell ribbon synapse cannot be compensated in the auditory brainstem. A delayed recovery from forward masking entails a deficit in the encoding of rapid fluctuations of sound intensity, such as amplitude modulation and silent gaps in noise. Our findings are consistent with the speech perception deficits in human patients and suggest that testing for gap detection ability would be the most useful clinical test for auditory synaptopathy with auditory fatigue.

PD 159

Unilateral Congenital Deafness Affects Deprived Ear Representation from the Brainstem to the Cortical Level.

Peter Hubka¹; Monique Hajduk¹; Jochen Tillein²; Andrej Krai³

¹*Institute of Audioneurotechnology & Department of Experimental Otology, Hannover Medical School, Hannover;* ²*MED-EL Germany GmbH;* ³*Institute of AudioNeuroTechnology & Dept. of Experimental Otology, ENT Clinics, Hannover Medical University*

Unilateral congenital deafness leads to developmental structural and functional reorganization of the auditory pathways resulting in overall hearing ear preference

and suppression of the auditory input originating from the inexperienced ear. It is, however, not completely understood where this functional disadvantage initiates and how it progresses along the auditory pathways. Here, we have approached this problem by studying electrically evoked auditory brainstem responses (eABR) and cortical activation in a natural model of congenital deafness – adult bi- and unilaterally congenitally deaf cats.

In the present study, 4 hearing control, 4 bilaterally congenitally deaf cats (bCDC) and 4 unilaterally congenitally deaf cats (uCDC) were used. All animals were bilaterally electrically stimulated by cochlear implants (CI). For ABRs, single biphasic electric pulses (200 μ s/phase) were delivered to CI in broad bipolar configuration. The cortical responses were evoked by a train of 3 biphasic electric pulses (200 μ s/phase, 500 Hz). Intensities up to 12 dB above ABR threshold were used. The ABRs were recorded using Ag-AgCl subcutaneous wire electrodes placed caudo-ventrally from the respective pinna and at the head vertex. Local cortical activations (local field potentials and multiunit activities) were recorded using linear multichannel arrays (16 channels) covering all layers of the primary auditory cortex. The overall morphology, peak amplitudes, activation latencies and relation to binaural cues (interaural time and level differences \square ITD and ILD, respectively) were evaluated.

In uCDC, analysis of the eABRs reveals smaller peak amplitudes to electric stimulation of the deaf ear in comparison to the hearing one. This reduction in the brainstem activation cannot be explained by auditory deprivation alone since no difference in the peak amplitudes of eABR signals was found between bCDCs and hearing controls. The cortical responses showed shift in favor of the hearing ear irrespective of the recorded cortical hemisphere. Binaural stimulations showed dominance of the hearing ear resulting in weakly modulated ITD functions. The ILD functions were dominated by the intensity function of the hearing ear with small effects of the deaf ear input.

The present results show a weaker response to the deprived ear stimulation already at the level of the brainstem in adult uCDCs. The electric activation of the deprived auditory nerve could, however, evoke responses up to the level of the primary auditory cortex in these animals. Nevertheless, abnormal incongruent representations of the binaural spatial cues were found in their primary auditory cortices.

Supported by Deutsche Forschungsgemeinschaft (Exc 1077)

PD 160

Neuromodulation and Plasticity for a Rodent Model of Cochlear Implant Use

Erin Glennon¹; Jasmin Multani¹; Ioana Carcea²; Mario Svirsky³; Robert Froemke⁴

¹Department of Neuroscience and Physiology, New York University School of Medicine; ²Rutgers University - Newark; ³New York University School of Medicine;

⁴Department of Neuroscience and Physiology, Neuroscience Institute, Department of Otolaryngology-HNS

Cochlear implants are neuroprosthetic devices that can provide hearing to deaf patients. However, learning rates and peak speech perception performance with cochlear implants are highly variable across patients (Blamey et al. *Audiol Neurootol* 2013). Adaptation to cochlear implants is believed to require neuroplasticity within the central auditory system (Fallon et al. *J Neural Eng* 2009). However, mechanisms by which behavioral training enables plasticity and improves outcomes are poorly understood. Here we investigate the hypothesis that neural mechanisms that promote plasticity in the rodent auditory system are key to optimizing cochlear implant usage, and might be especially helpful in cases of poor performance. We focus on noradrenergic modulation of rat auditory cortex by the locus coeruleus, which can enable robust and long-lasting neural and behavioral changes (Manunta and Edeline *J Neurophysiol* 2004; Martins and Froemke *Nat Neurosci* 2015; Sara Curr Opin Neurobiol 2015)

We developed a new surgical approach for cochlear implantation in adult rats (King et al. *J Neurophysiol* 2016). Our approach allows insertion of an 8-channel electrode array covering up to 360 degrees in the cochlea and allows rats to freely behave while using the implant to perform auditory tasks. Rats are trained on a go/no-go task, and self-initiate trials to respond to a target tone. Previously, we showed in normal hearing animals that this task requires auditory cortex, and that this task is sensitive to cortical modulation and plasticity (Froemke, Carcea et al. *Nat Neurosci* 2013; Carcea et al. *Nat Commun* 2017).

Here we examined the effect of pairing locus coeruleus stimulation with an auditory stimulus on auditory learning when a new sound becomes the target. This was done both in normal hearing and cochlear-implanted rats. For both groups, initial training was done using acoustic stimuli and without locus coeruleus-auditory pairing. In the case of cochlear-implanted animals the new target was delivered by intracochlear electrical stimulation after implantation whereas in the normal hearing animals the new target was a tone of different

frequency. Prior to each daily behavioral training session for the new target, rats underwent a 5-10 min pairing session. Pairing accelerated learning in each case, with respect to animals that did not receive it. We used fiber photometry to monitor neural activity of noradrenergic locus coeruleus neurons, showing strong responses to novel auditory stimuli and noxious stimuli. During auditory learning, normal hearing animals display dynamic locus coeruleus activity, specifically during the acquisition of the new meaning of reward relevant tones. These studies indicate that neuromodulation can play a powerful role in shaping outcomes with cochlear implant use and training. Furthermore, native variability in cochlear implant use outcomes might reflect a difference in level of engagement of neuromodulatory systems across subjects.

Clinical Otolaryngology & Pathology

PD 161

Burden of Ear, Nose and Throat - Voice, Speech and Language Disorders Based on United States Health Surveys, 2011-2016

Howard J. Hoffman¹; Robert A. Dobie²; Katalin G. Losonczy¹; Christa L. Themann³; Mabel L. Rice⁴; Valerie B. Duffy⁵; Helen S. Cohen⁶; Charles C. Della Santina⁷

¹National Institute on Deafness and Other Communication Disorders (NIDCD), National Institutes of Health (NIH); ²The University of Texas Health Science Center at San Antonio; ³National Institute for Occupational Safety and Health (NIOSH), Centers for Disease Control and Prevention (CDC); ⁴University of Kansas; ⁵College of Agriculture, Health, and Natural Resources, University of Connecticut; ⁶Baylor College of Medicine; ⁷Johns Hopkins University

Introduction: The Global Burden of Disease 2010 (GBD 2010) produced worldwide estimates for a wide array of health conditions, including an estimate that more than 500 million people have disabling hearing loss. American data were used extensively in GBD 2010. The National Institute on Deafness and Other Communication Disorders (NIDCD) conducts and supports research on disorders of Ear, Nose and Throat – Voice, Speech and Language (ENT–VSL) and has sponsored nationally-representative health surveys to collect epidemiologic, population-based information on prevalence and risk factors for these health conditions.

Objective: To estimate the United States burden of ENT–VSL disorders.

Methods: Two US health surveys were analyzed: (1) National Health Interview Survey (NHIS) and (2) National Health and Nutrition Examination Survey (NHANES),

which are conducted continuously on the civilian, non-institutionalized US population. NIDCD collaborated with the National Center for Health Statistics (NCHS) in developing the 2012 NHIS Voice, Speech, and Language Supplement (voice, swallowing, speech and language questions); 2014 NHIS Hearing Supplement (hearing, tinnitus and hyperacusis questions); and 2016 NHIS Balance Supplement (balance, dizziness and falls questions). NIDCD also sponsored the first national survey of the chemical senses (olfaction/smell and gustation/taste questions) in NHANES, 2011–14. Prevalences were calculated using NCHS-provided weights for the survey years; US population estimates are standardized to the 2015 population (315.8 million).

Results: Reported prevalence of moderate-or-worse hearing difficulty in children and adults was 6.5% (20.6 million); mild-or-worse was 15.7% (49.5 million). Prevalence of moderate-or-worse tinnitus in adults was 3.2% (7.8 million). Combined moderate-or-worse hearing/tinnitus prevalence was 8.0% (25.4 million); prevalence of combined mild-or-worse hearing/tinnitus problem was 20.7% (65.3 million). Prevalence of reported moderate-or-worse balance/dizziness problems (BDP) in children and adults was 3.7% (11.4 million); mild-or-worse BDP prevalence in last 12 months was 13.1% (40.4 million). Prevalence of moderate-or-worse smell/taste problems, adults aged 40+, was 7.8% (11.8 million). The prevalence of moderate-or-worse voice-swallowing-speech-language (VSSL) disorders in children and adults was 3.1% (9.7 million); mild-or-worse VSSL problems lasting one or more weeks in last 12 months was 7.2% (22.0 million). Accounting for multiple conditions in individuals, the combined prevalence of moderate-or-worse ENT–VSL disorders was approximately 17.4% (54.8 million); mild-or-worse ENT–VSL disorders was 42.4% (133.9 million). Speech and language disorders are more common in children but, overall, the combined prevalence of ENT–VSL disorders is highest in older adults.

Conclusion: About one in six Americans have disabling (moderate-or-worse) impairments of hearing and/or other sensory or communication disorders.

PD 162

Accelerating Clinical Access and Implementation of Novel Hearing Therapeutics by Early Health Economic Modelling

Evie C. Landry¹; Matthew Su²; Mirre Scholte³; Rishi Mandavia²; Helen Blackshaw²; Maroeska Rovers³; Anne Schilder⁴

¹University of British Columbia | Ear Institute University College London; ²Ear Institute University College London; ³Radboud University; ⁴Ear Institute University College London | University Medical Centre Utrecht

Background:

A key challenge facing health systems today is to identify and avoid unnecessary health innovations and accelerate access those that are necessary. This process can be guided by applying health economic modelling at the early stages of development of new therapeutics to direct product development, market access, and pricing.

This is very relevant and timely to the field of age-related sensorineural hearing loss (ARHL), where biotechnology, pharmaceutical and device companies have identified an unmet market need and have dedicated sizeable investments in the development of novel (drugs, genes, cells) hearing therapeutics.

To assess the potential added value of these novel hearing therapeutics, we developed an early health economic model comparing novel regenerative hearing therapeutics with the current standard of care for people with ARHL.

Methods:

A decision analytic model was developed to assess the costs and effects of using novel regenerative hearing therapeutics in patients over the age of 50 with ARHL. This was compared to the current standard of care, including hearing aids and cochlear implants. Input data was derived from systematic literature searches and expert opinion. The study adopted a healthcare perspective of the UK National Health Service (NHS). Four different but related analyses were conducted: 1) headroom analysis to explore the maximum potential value; 2) threshold analysis to search for the minimum effectiveness needed for the innovation to be cost-effective; 3) formal cost-effectiveness to assess the cost per quality adjusted life-year (QALY) gained; and 4) sensitivity analyses, including both deterministic and probabilistic, and scenario analyses to evaluate relevant uncertainty.

Results:

The decision model showed that novel therapeutics for ARHL have potential value both in terms of improved patient outcomes, as well as cost-effectiveness. The base case analysis revealed an ICER of £11,690/QALY (95% CI: £8,810/QALY-£19,058/QALY) for regenerative hearing therapeutics compared with the current standard of care. Results of the threshold analysis revealed that novel hearing therapeutics had to be 75% effective or greater at restoring hearing to the normal range (pure tone average of ≤ 25 dB) to remain cost-effective. Finally, the most important uncertainties identified were the estimates of efficacy, uptake, and cost of the novel hearing therapeutics used in the model.

Conclusions:

Early health economic modelling shows that with novel regenerative hearing therapeutics for ARHL, QALYs can be gained in a cost-effective fashion under current willingness to pay thresholds.

PD 163

The Better Hearing Rehabilitation (BEAR) Study in Denmark. Study Population Characteristics and Perspectives

Anne Wolff¹; Sabina Storbjerg Houmøller²; Gérard Loquet³; Jesper Hvass Schmidt²; Vijay Narne⁴; Michael Gaihede⁵; Dan Dupont Hougaard⁶; Dorte Hammershøi⁷
¹*Department of Otolaryngology, Head & Neck Surgery and Audiology, Aalborg University hospital;* ²*Dept. of Otolaryngology, Head and Neck Surgery and Audiology, Odense University Hospital, Dept. of Clinical Research, University of Southern Denmark, Odense Patient data Explorative Network (OPEN), Region of Southern Denmark;* ³*Department of Clinical Medicine, Aalborg University. Department of Electronic Systems, Aalborg University;* ⁴*Department of Clinical Research, University of Southern Denmark;* ⁵*Department of Otolaryngology, Head & Neck Surgery and Audiology, Aalborg University Hospital, Department of Clinical Medicine, The Faculty of Medicine, Aalborg University;* ⁶*Department of Otolaryngology, Head & Neck Surgery and Audiology, Aalborg University hospital.* ⁷*Department of Clinical Medicine, The Faculty of Medicine, Aalborg University;* ⁷*Department of Electronic Systems, Aalborg University*

A recent report from WHO noted that 360 million people in the world have hearing loss. Despite efforts to provide hearing aids (HA) to people in need, hearing loss remains an unmet need. In Denmark, for example, 20% of HA owners do not use their HA regularly which results in wasted clinical resources and a lack of rehabilitation. To improve the treatment, we propose to revise diagnostic techniques and HA fitting practices based on individual hearing profiles, set of expectations, and lifestyles. To achieve this, a cooperative project "BEAR" has been launched between three national universities, three hospitals, and the HA industry in Denmark. This resulted in the building of a database of over 30,000 patient records, collected by two audiology departments (Aalborg and Odense, Denmark), from January 2017 until April 2018 from 1,963 hearing impaired patients. Data obtained describe procedures which are currently used in clinical audiology across Denmark and allow to explore which measures are available for each patient and what type of HA fitting they have received. Records consisted of audiometric data (air and bone conduction, uncomfortable levels, speech reception thresholds,

speech discrimination scores, stapedius reflex and tympanometry, Tinnitus Handicap Inventory), quality of life evaluation using questionnaires (health related quality of life [15-D], Health Related Questionnaires, Charlson Comorbidity Index), HA outcome measures using questionnaires (Speech, Spatial and Qualities of Hearing scale [SSQ-12], International Outcome Inventory for Hearing Aids [IOI-HA]) and HA fitting data (HA types, log data, fitting rationale and real-ear measurements). The database has a gender ratio of 126 males for 100 females, a mean age at 67 years (range from 19 to 100 years) and a mean hearing threshold in the better hearing ear of 40 dB HL (four frequencies average). 71.9 percent of the patients are first time HA users, as against 28.1 percent for patients with previous HA experience. Preliminary analyses show on average significant improvement in hearing abilities with HA (from IOI-HA and SSQ-12). However, substantial number of participants (18%) did not derive enough benefit from HA. Further analysis will be directed towards finding the possible reasons and grouping the participants based on HA benefit, demographic and audiological data. This will enable us to identify the areas, among contemporary standard examinations and hearing fitting strategies, which would be relevant to explore, change or further develop to provide a better HA fitting and thereby a greater user satisfaction.

PD 164

Clinical Optical Coherence Tomography Doppler Vibrometry of the Middle Ear

Dan MacDougall¹; Josh Farrell¹; Matthew Jahns²; Christine Morrison³; David Morris³; Matthew Farrell⁴; Drew Hubley⁴; **Robert Adamson**⁵
¹*School of Biomedical Engineering, Dalhousie University, Canada;* ²*School of Biomedical Engineering, Dalhousie University;* ³*Nova Scotia Health Authority;* ⁴*Audioptics Medical Inc.;* ⁵*School of Biomedical Engineering and Dept. Electrical & Computer Engineering, Dalhousie University, Canada*

Optical coherence tomography (OCT) is emerging as an important new diagnostic modality in otolaryngology for its ability to produce depth-resolved images of middle ear structures non-invasively and without exposing the patient to ionizing radiation. An important feature of optical coherence tomography is its ability to make phase-resolved measurements that allow the vibration of ear structures in response to sound to be measured. This capability has remained largely confined to experimental work due to the lack of a Doppler middle ear OCT system with a sufficient level of integration to allow clinicians to use it regularly in their practice. We report on Ossiview, a fully integrated OCT imaging and Doppler vibrometry system designed for clinical use.

The system, which is designed to be used by a single operator during patient examinations, can perform 2D and 3D B-mode imaging and multi-frequency Doppler vibrometry. It consists of a handpiece with integrated camera, microphone, speaker and scanning mirrors tethered to a console containing the OCT backend optics, data processing and synchronization electronics and a host computer. The system is portable and easy-to-use with an intuitive software interface and real-time graphics engine. Experiences and challenges with deploying the system in the clinic will be discussed. The applicability of OCT Doppler vibrometry to clinical otolaryngology will be discussed with reference to individual case seen at the Nova Scotia Health Authority site.

PD 165

Liquid-Infused Tympanostomy Tubes Allow for Biofouling Resistance and Improved Fluid Transport Properties

Ida Pavlichenko¹; Nicole Black²; Michael Kreder¹; Sam Peppou-Chapman¹; Dhrumi Gandhi³; Elliott D. Kozin³; Jennifer Lewis¹; Joanna Aizenberg⁴; Aaron K. Remenschneider⁵

¹Harvard John A. Paulson School of Engineering and Applied Sciences, Wyss Institute for Biologically Inspired Engineering; ²Harvard John A. Paulson School of Engineering and Applied Sciences, Harvard University; Wyss Institute for Biologically Inspired Engineering, Harvard University; Eaton Peabody Laboratory, Massachusetts Eye and Ear Infirmary; ³Massachusetts Eye and Ear Infirmary; Department of Otolaryngology, Harvard Medical School; ⁴Harvard John A. Paulson School of Engineering and Applied Sciences, Harvard University; Wyss Institute for Biologically Inspired Engineering, Harvard University; ⁵Department of Otolaryngology, University of Massachusetts Medical School; Massachusetts Eye and Ear Infirmary; Department of Otolaryngology, Harvard Medical School

Acute otitis media (AOM) and otitis media with effusion (OME), are the leading causes of healthcare visits worldwide, affecting more than 700 million people each year and instigating a considerable patient morbidity. By 3 years of age, 25-40% of children have had ≥ 3 episodes of AOM; following an episode of AOM, approximately 50% of children have an effusion behind the tympanic membrane at one month, 20% at two months and 10% at three months. Current treatment of recurrent and persistent AOM and OME requires the placement of tympanostomy tubes (TTs) into the tympanic membrane (TM). The primary purpose of TTs is to equalize the pressure in the middle ear, drain effusion, and allow for the delivery of topical antibiotic drops to the middle ear. However, contemporary TTs have limitations that often

cause otorrhea, occlusion of the lumen, and premature extrusion, resulting in TT replacement surgeries; damage to the TM; and failure to transport topical antibiotic drops to the middle ear.

To address these challenges, we developed novel TTs with rationally designed shapes and sizes fabricated using versatile three-dimensional (3D) printing and injection molding methods, and utilized a surface modification technique employing silicone elastomeric materials infused with lubricating oils, that form a durable immobilized slippery layer on the surface of the elastomer. To demonstrate an improved efficacy of the novel TTs, we tested *in-vitro* 1) the adhesion of human TM keratinocytes and bacterial cell lines commonly present in an infected middle ear (*P. aeruginosa*, MRSA, *S. epidermidis*, and *M. catarrhalis*), and 2) screened the optimal design parameters of the tubes (shape and dimensions, flange geometries, monomer/ cross-linker ratio) that allow for a guided enhanced fluid flow. We demonstrate that the liquid-infused TTs show a drastic reduction ($\sim 99\%$) in adhesion of both human keratinocytes (the cell line primarily responsible for clogging and premature extrusion of TTs), and AOM bacterial strains. The fluidic tests show that while water, antibiotic drops, and mucus droplets do not penetrate the lumen of commercial ear tubes, these fluids selectively and controllably flow through the lumen of the liquid-infused TTs with similar (or smaller) dimensions, and require applying ~ 20 -30% lower breakthrough pressure. In conclusion, we demonstrate that the rational design of the TT geometry and surface properties can significantly improve the efficacy of the TTs in terms of the biofouling resistance, drainage of the effusion from and delivery of the therapeutic drops of interest into the middle ear.

PD 166

Operationally-defined Auditory Synaptopathy is Relatively Common in Humans but Does Not Correlate with Hearing-In-Noise Performance

Sofia Pevzner¹; Bridget Kosilla²; Sarah Schwartzer³; Richard Hoben¹; Mark Parker⁴

¹St. Elizabeth's Medical Center; ²Vanderbilt University; ³Northwestern University; ⁴Tufts University School of Medicine

Hearing in noise (HIN) is a primary complaint of both the hearing impaired and the hearing aid user. Both auditory nerve (AN) function and outer hair cell (OHC) function contribute to HIN, but their relative contributions are still being elucidated. Due to their electromotility function, OHCs play a critical role in HIN by fine tuning the response of the basilar membrane. Further, animal studies suggest that auditory synaptopathy, the loss of synaptic contact between hair cells and the AN, may be another cause of HIN difficulty.

We have developed a clinical database of over 280 adults where we collect 109 subject variables such as age and sex; HIQ measures such as pure tone audiometry (0.25-20 KHz); objective perception of HIN difficulty, and subjective HIN measurements including the QuickSIN test, 45% time compressed WR in 10% reverberation and WR in the presence of 0 SNR ipsilateral speech-weighted masking noise. We correlate these variables with OHC function measured by DPOAE amplitude and threshold of (1-8 KHz), and AN function measured by CAP peak latency, peak amplitude, and ratio to summing potential evoked using 4 kHz centered tone pips presented at 30, 40, 50, and 60 dB SL, and clicks presented at 70 dB SPL.

While there is strong evidence that auditory synaptopathy occurs in animal models, there is debate as to whether auditory synaptopathy is clinically significant in humans, likely because of disparate methods of measuring noise exposure in humans and our high variability in susceptibility to hearing impairment. Rather than use self-reported noise exposure, another option is to assume that the general population exhibits a range of noise exposures and resulting otopathologies and define auditory synaptopathy operationally as low auditory compound action potential (CAP) amplitude.

Applying this operational-definition of synaptopathy to our clinical database provides evidence that auditory synaptopathy is not only present in persons with hearing thresholds within normal limits (WNL), but at an incidence as much as 45%, may be a relatively common occurrence. The data further demonstrate that persons with hearing WNL may exhibit HIN difficulties, persons with hearing WNL may exhibit two distinct types of undetected otopathologies (auditory neuropathy and/or OHC dysfunction), and HIN performance is primarily governed by OHC, rather than AN, function.

PD 167

An Approved Drug Mitigates ER Aggregation of Usher 3A-Associated Human Clarin1-N48K Protein and Restores Hair Cell Mechanotransduction in a Humanized Zebrafish Model

Suhasini R. Gopal; Yvonne T. Lee; Ruben Stepanyan; Brian M. McDermott; **Kumar N. Alagramam**
Department of Otolaryngology, University Hospitals Cleveland Medical Center, School of Medicine, Case Western Reserve University

Here we assess the functional consequences of the N48K mutation in the gene Clarin1 (*CLRN1*) that causes the hearing and vision disorder, Usher syndrome type IIIA (USH3A). We also investigated whether the pathological processes that lead to progressive hearing loss in this disease can be pharmacologically prevented.

To do so, a humanized zebrafish model was created by expressing human Clarin1 with the USH3A-associated mutation, N48K, in a Clarin1 knockout zebrafish line. The hearing, balance and swimming abnormalities of the mutant zebrafish larvae were investigated, and protein localization examined using a fluorescent tag. Previous studies showed that *CLRN1*^{N48K} causes a glycosylation defect that results in the mutant protein being retained in the ER, with only a fraction of the protein reaching the hair cell bundle, the mechanosensory structure of the inner ear. We hypothesized that the small quantity of *CLRN1*^{N48K} that reaches the hair bundle does so via an unconventional secretory pathway, and that the pharmaceutical activation of this pathway could be therapeutic. One approved drug in particular, a SERCA inhibitor, which activates this unconventional secretory pathway, enhances the localization of *CLRN1*^{N48K} to hair bundles and also attenuates the progressive loss of hair cell function in *clrn1* knockout larvae that express *CLRN1*^{N48K}. These findings thus highlight the potential of this approved drug as a therapeutic to prevent hearing loss in *CLRN1*^{N48K} USH3A patients and, by extension, other monogenic disorders associated with ER-aggregation of mutant protein.

PD 168

Clinical Development of Intratympanic, Sustained-Exposure Formulation of the NMDA Receptor Antagonist Gacyclidine for the Treatment of Tinnitus

Jeff Anderson; Jennifer Hou; Xiaobo Wang; Rayne Fernandez; Natalia Tsivkovskaia; Fabrice Piu
Otonomy, Inc.

Background: Tinnitus, the perception of sounds without a correlated external auditory stimulus, is widely prevalent, occurring in approximately 10% of the US adult population. Tinnitus can be a significant quality of life problem in many patients by impacting sleep, concentration, hearing, and emotional state. Heightened activation of NMDA receptors on cochlear afferent synapses, resulting from cochlear injury, may be particularly important in generating tinnitus. Gacyclidine, a high-affinity and selective antagonist of NMDA receptors, was formulated to provide sustained exposure to the cochlea following intratympanic injection. OTO-311, a thermosensitive, poloxamer-based formulation of gacyclidine was tested in a Phase 1 clinical study to evaluate its safety and plasma pharmacokinetics. OTO-313, a medium-chain triglyceride-based formulation of gacyclidine, is being developed to provide superior gacyclidine exposures to the inner ear compared to OTO-311.

Methods: The safety and plasma pharmacokinetics

of OTO-311 administered by intratympanic injection was evaluated in a randomized, placebo- and sham-controlled Phase 1 study. OTO-311 (0.15, 0.3, and 0.6 mg) was evaluated in 12 healthy subjects per dose cohort (8 subjects, OTO-311; 2 subjects, placebo; and 2 subjects, sham). Safety and tolerability were assessed by vital signs, ECG, clinical laboratory tests, otoscopy, audiometry, tympanometry, and physical examinations. Blood samples were obtained at appropriate time points and concentrations of plasma gacyclidine were quantified. To determine if OTO-313 yields better gacyclidine exposures compared to OTO-311, rats were dosed intratympanically with either OTO-311 or OTO-313 and perilymph was sampled for determination of gacyclidine concentrations.

Results: OTO-311 administered as a single intratympanic injection was safe and well-tolerated in healthy subjects, with no serious adverse events and no early discontinuations due to adverse events. Peak plasma concentrations of gacyclidine occurred by 1 to 2 hours post-administration in a dose-dependent manner. In rat studies, intratympanic administration of OTO-313 provided for a longer duration of gacyclidine exposure in the inner ear than OTO-311. Thus, OTO-313 is being developed for the treatment of tinnitus and is planned to be evaluated in a randomized, double-blind, placebo-controlled Phase 1/2 study in patients with moderate-severe, acute, unilateral tinnitus.

Conclusions: OTO-311 was safe and well-tolerated after intratympanic administration in healthy subjects. Rat pharmacokinetic studies indicate that OTO-313 provides a more sustained exposure of gacyclidine within the cochlear compared to OTO-311, supporting further development of OTO-313. Therefore, a Phase 1/2 study will evaluate the safety, PK, and exploratory efficacy of intratympanic OTO-313, an improved formulation of gacyclidine for otic delivery, in patients with tinnitus.

Inner-Ear Genomics & Gene Regulation

PD 169

Sequencing a Baby for an Optimal Outcome: A Genomic Future for Newborn Screening

Anne Giersch¹; Jun Shen²; Yvonne Chekaluk³; Razan Basonbul⁴; Kathryn Gregory¹; Jennifer Hochschild⁵; Linda Johnson³; Lauren McGrath³; Genevieve Medina⁶; Juliana Manganella⁶; Evette Ronner⁴; Michael Cohen⁷; Margaret Kenna⁸; Cynthia C. Morton⁹
¹Brigham and Women's Hospital, Harvard Medical School; ²3. Department of Pathology, Brigham and Women's Hospital, Harvard Medical School; ⁴ Laboratory for Molecular Medicine, Partners Personalized Medicine; ³ Brigham and Women's Hospital; ⁴ Massachusetts Eye and Ear;

⁵Harvard University; ⁶Boston Children's Hospital; ⁷Massachusetts Eye and Ear, Harvard Medical School; ⁸Boston Children's Hospital, Harvard Medical School; ⁹Brigham and Women's Hospital, Harvard Medical School

SEQaBOO (SEQuencing a Baby for an Optimal Outcome) is a research project integrating high-throughput genomic approaches into routine newborn screening. In this project, we are testing the hypothesis that rapid discovery of the etiology of a newborn's hearing impairment via whole genome sequencing will benefit clinical management of an infant with deafness.

Background: Congenital deafness and other subtle birth defects are recognized in newborns through newborn screening, allowing early interventions that limit life-long disabilities. Genetic factors contribute to the majority of congenital hearing loss in the US. Etiologies are highly heterogeneous, and pathogenic variants in hundreds of genes have already been identified. Development of whole genome sequencing (WGS) technologies provides a new opportunity as well as challenge for researchers and clinicians dedicated to improving the lives of these newborns. Investigations are underway to assess whether genetic etiologies of congenital disorders can be more accurately and efficiently defined and whether improved genetic diagnosis translates into superior clinical care.

Methods: The project will enroll approximately 500 newborns who do not pass their initial newborn hearing screen along with their biological parent(s) (trios) for WGS. Active enrollment began in July 2018. If parent(s) choose not to enroll in WGS, they may choose to participate in an annual survey. Genetic information pertinent to the infant's hearing will be returned to the child's otolaryngologist. Annual surveys ascertain general health, including speech and language development, in addition to hearing status, and parental attitudes toward genomic sequencing. In addition, parents will be offered the option of receiving for themselves results from the American College of Medical Genetics and Genomics recommended list of genes (ACMG59) with potential high medical importance.

Summary: SEQaBOO aims to analyze and assemble genomic datasets, perform clinical genomic research of deafness identifiable through newborn screening, and explore implications of integration of genomic sequencing into newborn screening. All of this will inform the care and management of newborns with congenital deafness and allow investigation of factors associated with society's acceptance of this technology for "optimal outcome" of a newborn baby.

Biological Insights from 31 Genomic Risk Loci for Hearing Difficulty

Gurmanna Kalra¹; Beatrice Milon²; Alex Casella¹; Yang Song²; Ronna Hertzano²; Seth Ament^{*1}

¹University of Maryland, Baltimore - School of Medicine; ²University of Maryland Baltimore-School of Medicine

Age-related hearing loss (ARHL) affects approximately 25% of those aged 65-74 and 50% aged 75 and older. Family and twin studies suggest that heritable factors contribute strongly to ARHL, yet specific loci remain largely unknown. Here, we integrated GWAS and published expression data with newly generated cochlear epigenomic data to characterize genetic risk loci and biological for hearing loss.

We conducted a multi-trait GWAS meta-analysis of hearing-related traits in the UK Biobank (n=323,978) and identified 31 genome-wide significant loci for self-reported hearing difficulty ($p < 5e-8$). In addition, gene-based analyses supported genetic associations with 577 genes (FDR < 0.05). Risk-associated genes were enriched specifically for expression in cochlear epithelial and non-epithelial cells, indicating relevance to the auditory system. A Gene Ontology (GO) enrichment analysis revealed a single enriched term: sensory perception of mechanical stimulus ($q = 9.18e-5$). In addition, we found a significant enrichment for Mendelian deafness genes, with 14 of 103 known Mendelian deafness genes reaching a nominal level of significance ($p < 0.01$).

To determine the enrichment of hearing difficulty risk loci in regulatory regions, we generated ATAC-seq data from mouse newborn cochlear epithelial and non-epithelial cells and identified open chromatin regions. We mapped homologous open chromatin regions to the human genome and tested for enrichment of heritability in these conserved regions using stratified LD score regression. We validated our open chromatin regions using a database of known ear enhancers (VISTA Enhancer Browser) and found significant overlap ($p < 1.0e-4$). Heritable risk for hearing difficulty was enriched 9-fold in epithelial open chromatin regions; 2.08% of all SNPs are in the annotated regions, and these SNPs capture 19.46% of the total SNP heritability ($p = 5.22e-8$).

Causal variants and target genes at individual risk loci were predicted via fine-mapping. Integrating protein-coding annotations and Hi-C data with the ATAC-seq and GWAS data. We identified 7 missense variants in six genes, of which, three have not previously been associated with hearing loss in humans. Our analyses of non-coding risk-associated SNPs predict

regulatory effects on nearby genes and identified 250 predicted SNP-gene interactions. Of note, within this list we identified predicted regulatory effects of risk-associated SNPs on *SOX2* and *LMX1A*, which are well characterized transcription factors expressed in hair cell progenitors and non-sensory domains of the developing cochlea, respectively. These results are significant because they identify new candidate genes as well as regulatory domains as risk-associated genomic regions for hearing difficulty.

PD 171

Gene Regulatory Networks Mapping and Druggable Genome Target Identification Using Stria Vascularis Single-cell/Single-nucleus Transcriptomes

Soumya Korrapati¹; Madeline Pyle¹; Ian Taukulis¹; Erich T. Boger²; Daniel Martin³; Robert J. Morell²; Michael Hoa¹

¹NIDCD/NIH; ²Genomics and Computational Biology Core, National Institute on Deafness and Other Communication Disorders, National Institutes of Health; ³NIDCR/NIH

Introduction: The stria vascularis (SV) is responsible for the high positive potential in the endolymph known as the endocochlear potential (EP). EP is key to proper hair cell function. Human temporal bone histopathology studies have implicated SV in the pathophysiology of Meniere's disease. Despite the importance of SV in the development and maintenance of the EP, our understanding of the involved gene regulatory networks remains limited. We previously generated both single cell and single nucleus RNA seq datasets of SV from P30 mice. Using computational analyses, we aim to identify possible druggable targets related to gene regulatory networks involved in EP maintenance.

Methods: Expression profiles of single cell and single nucleus strial transcriptomes were analyzed using weighted gene co-expression network analysis (WGCNA) to identify gene modules. Gene ontology and protein-protein interaction analyses were performed on the gene modules to identify potential gene regulatory networks. Select WGCNA gene modules were input into Pharos, a database describing over 20,000 protein targets and the availability of FDA approved drugs or small molecule ligands for each. Only targets with approved drugs of known mechanism of action (Tclin) or targets shown to bind small molecule ligands (Tchem) were considered. Targets affiliated with Meniere's disease in Pharos were also cross referenced with P30 WGCNA gene modules.

Results: Using the WGCNA pipeline, P30 SV genes were delineated into modules of co-expressed genes, including

SV cell type-specific gene modules. We demonstrate the utility of analyzing these gene modules to identify potential gene regulatory networks, which helped in resolving differences in gene expression between the single cell and single nucleus transcriptomes. Druggable genome target analysis using Pharos demonstrates that most P30 WGCNA gene modules contain Tclin drug target genes and all modules contain Tchem drug target genes.

Conclusions: We demonstrate the utility of an unsupervised iterative co-expression analysis technique like WGCNA on single cell and single nucleus transcriptomes. We generated potential gene regulatory networks using this technique along with identifying related druggable gene targets within the SV. Hypothesis testing based on these analyses may improve our understanding of mechanisms of EP maintenance and potentially diseases where SV pathology is implicated.

PD 172

Inhibition of Lysine-Specific Demethylase 1 Causes Epigenetic Activation of *Atoh1* in the Neonatal and Adult Cochlea

Niliksha Gunewardene¹; Takahisa Watabe¹; Quan Wang²; Tyler Gibson¹; Nicolai Hathiramani¹; Dunia Abdul-Aziz¹; Albert Edge³

¹Department of Otolaryngology and Laryngology, Harvard Medical School and Eaton-Peabody Laboratory, Massachusetts Eye and Ear Infirmary; ²Harvard Medical School, Eaton-Peabody laboratories, Massachusetts Eye and Ear; ³Department of Otolaryngology, Harvard Medical School

Epigenetic modifiers regulate the folding of DNA into heterochromatin or euchromatin and thus regulate gene transcription. The hair cell expressed transcription factor *Atoh1* is maintained in a bivalent state, defined by the simultaneous presence of active and repressive epigenetic marks. In the inner ear, *Atoh1* is upregulated during embryonic development, but downregulated in adults. Our current understanding of the epigenetic regulation of *Atoh1* in the inner ear is limited due to the technical difficulty of harvesting sufficient cell numbers for analysis.

Employing a published method to expand Lgr5+ cochlear progenitors in organoids, we screened a collection of epigenetic modifiers for their effect on development of hair cells. Lysine-specific demethylase 1 (LSD1) is commonly associated with gene repression and plays a vital role in regulating the fate of several cell lineages. We found that pharmacological and genetic inhibition of LSD1 potentiated hair cell differentiation, above what was achieved by manipulating the Wnt/Notch pathways. This was accompanied by expression of mature hair cell

genes.

Utilizing a recent adaptation of the CRISPR/Cas9 tool that permits genomic localization of LSD1 to putative promoter or enhancer regions, we demonstrated targeted *Atoh1* repression by LSD1. Cochlear progenitor cells infected with nuclease-inactivated Cas9 (dCas9) fused to LSD1 and short guide RNA sequences targeting the *Atoh1* promoter or 3'; enhancer regions had significant downregulation of *Atoh1* and other mature hair cell markers including *Myo7a*.

LSD1 was enriched at regulatory regions of the *Atoh1* gene in cochlear progenitors and LSD1 inhibitor-treated cells showed increased levels of activating histone marks, H3K4me and H3K4me2 at *Atoh1* promoter and enhancer regions.

Application of the LSD1 inhibitor to cochlear explants obtained from neonatal mice resulted in significant supporting cell proliferation and generation of additional hair cells *in situ*. In adult mice exposed to noise at levels that resulted in deafness, treatment with the LSD1 inhibitor activated *Atoh1* expression, and lineage tracing experiments revealed the generation of "new" hair cells. Collectively, these experiments highlight the potential for LSD1 to alter the chromatin structure and regulate *Atoh1* expression in the neonatal and deaf adult cochlea.

PD 173

Cellular mapping of human hearing loss genes using single cell transcriptomic data

Kevin Yu¹; Stacey Frumm¹; Katharine Lee¹; Lauren Byrnes²; Daniel Wong²; Julie Sneddon²; Aaron Tward¹
¹UCSF Department of Otolaryngology-Head and Neck Surgery; ²UCSF Department of Anatomy and Diabetes Center

Background: Mendelian hearing loss in humans has been associated with well over 100 distinct genes for which specific mutations are known. In most cases we do not have a deep understanding of how these specific mutations cause hearing loss. Further, in most cases we do not know the timing of expression of these genes during development or which distinct subsets of cells express these genes.

Methods: We performed single cell RNA sequencing using the 10X Genomics platform on dissociated cochleas from E12.5, E14.5, E16.5, E18.5, P2, and adult mouse cochlea. We then analyzed data using a custom analysis pipeline that includes CellRanger for demultiplexing and mapping transcripts, followed by our novel CellFindR algorithm that applies iterative rounds of graph-based nearest neighbor clustering via a decision rule to identify all distinct cell states within a

sample. Once distinct cellular subsets were identified in an unbiased fashion, the developmental timing and distinct cell populations that express all known hearing loss genes were determined.

Results: We identified over 60 distinct cell states present within the adult cochlea. We identified distinct clusters of expression of human hearing loss genes. Although the plurality of hearing loss genes were expressed within hair cells, there were distinct clusters of expression identified in adult animals mapping to marginal cells, melanocytes, various supporting cell populations, neurons, distinct populations of fibrocytes, and Schwann cells. Although many hearing loss genes were expressed throughout development and into adulthood, distinct subsets of hearing loss genes were expressed exclusively after P2, or exclusively at earlier timepoints during embryonic life. Notably, those genes expressed exclusively during embryonic life had an enrichment of genes known to be causative of gross inner ear abnormalities.

Conclusions: Genetic hearing loss can result from defects in many cell types beyond hair cells. Future gene therapeutic approaches should be targeted to the appropriate cell type and with the appropriate timing to ameliorate these defects.

PD 174

Development of Genome Editing Tools for Inner Ear Application

Veronica Lamas¹; Mingqian Huang¹; Yi-Zhou Quan¹; Yong Tao²; Yi Zhong¹; Yamin Li³; Qiaobing Xu³; Zheng-Yi Chen¹

¹Mass Eye and Ear infirmary, Harvard University;

²Shanghai Ninth People's Hospital, Shanghai Jiao

Tong University School Of Medicine; ³Department of Biomedical Engineering, Tufts University

Background: CRISPR/Cas9-mediated genome editing has been successfully used to rescue hearing in mouse models of human genetic hearing loss by liposome-mediated ribonucleoprotein (RNP) delivery targeting hair cells. To treat diverse forms of genetic hearing loss, it is essential to target diverse inner ear cell types. Further, the ability to study editing events in situ will enable the correlation between editing efficiency and hearing recovery. Development of editing tools applicable to large wild type animal models will accelerate editing-based therapy to humans.

Methods: To develop new delivery vehicles, we used a combinatorial library approach to synthesize degradable lipid-like nanoparticles capable of delivery with high efficiency and low toxicity. The bioreducible lipid nanoparticles (bLNPs) were tested for delivery and

editing in mouse inner ear in vivo. To determine inner ear cell types for delivery and genome editing, we screened and identified X-linked genes, and used immunolabeling to study editing events with cell type specificity in wildtype mice. Expression of X-linked genes was studied in large animal pig inner ear.

Results: We identified numerous bLNPs capable of delivering Cre recombinase protein into multiple inner ear cell types. The bLNPs were shown to deliver editing RNP (Cas9 protein and gRNA) into mouse inner ear with hair cell editing, demonstrating that the bLNPs represent a new class of liposomes for inner ear delivery of editing agents. We identified X-linked genes with widespread inner ear expression, and showed editing of X-linked genes at multiple inner ear cell subtypes in wildtype mice due to disruption of single functional copy gene that can be directly visualized by immunolabeling. Expression of X-linked genes was confirmed in pig inner ear by immunolabeling. Genes with important inner ear functions were identified by the in vivo editing study.

Conclusion: We have developed a platform to synthesize and characterize biodegradable lipid-like nanoparticles capable of RNP delivery of editing agents in multiple inner ear cell types. We take advantage of studying X-linked genes in wildtype animal so edited cell types can be identified at cellular level. Our platform is efficient to screen for new delivery vehicles to target diverse inner ear cell types for editing, which can be applied to wildtype animal models across species and in human samples, which should speed up development of editing-based therapy for human genetic hearing loss.

PD 175

The creation of LOXHD1b gene knockout zebrafish

Shunsuke Tarumoto¹; Youichi Asaoka¹; Kazuma Sugahara²; Yoshinobu Hirose²; Yousuke Takemoto¹; Makoto Seiki¹; Hiroshi Yamashita²

¹Yamaguchi University; ²Department of Otolaryngology, Yamaguchi University Graduate School of Medicine

Background

Deafness caused by *LOXHD1* gene mutation is clinically autosomal recessive inheritance and progressive. Hereditary families caused by *LOXHD1* gene mutation has been also reported in Japan. Reported by Grillet et al. as a causative gene of hereditary hearing loss, the *LOXHD1* gene is considered to be the causative gene of DFNB77 and expressed in hair cells in mouse. We used zebrafish as an experimental animal. In zebrafish, hundreds of eggs are produced at once, and eggs and embryos are transparent and can be easily observed

after spawning. Genetic modification technology can be easily introduced. zebrafish was selected as an experimental animal because zebrafish is useful in conducting screening of medicines such as therapeutic drugs in the future. We verified that the *LOXHD1b* gene was expressed in hair cell bundles of zebrafish by in situ hybridization. We report that we created the *LOXHD1b* gene knockout zebrafish by using the CRISPR-Cas9 system and studied the morphology and physiological function of stereocilia of hair cells of *LOXHD1b* gene knockout zebrafish.

Method

We injected Cas9 RNA and *LOXHD1b* mRNA into the zebrafish eggs of the first cell phase and the second cell phase using the CRISPR - Cas9 system. We crossed the injected F0 generation zebrafish and wild type zebrafish, and grew the F1 generation zebrafish. We cut the tail of the F1 generation zebrafish, recovered the genomic DNA, and performed genotyping with Heteroduplex Mobility Assay (HMA). A hetero mutant pattern was observed by electrophoresis. In the nucleotide sequence, deletion of the base on the N terminal side of the PAM sequence was observed. As a result of mating heterozygous mutants, electrophoretic patterns of homozygous mutants were obtained.

Result

Immunohistochemistry for anti parvalbumin antibody was performed on zebrafish at 1 day post fertilization. In the wild type, the stereocilia of hair cells of the lateral line are normal, whereas in the homozygote the stereocilia of hair cells of the lateral line are shortened and decreased. For behavior, individuals rotating in part of the homozygote zebrafishes and those sinking from the head were observed.

Prospect

Detailed morphological observation of stereocilia of hair cells in *LOXHD1b* homozygote will be carried out using electron microscope. In addition to the *LOXHD1b* gene, Knockout of *LOXHD1a* gene is also being prepared, and these gene mutation zebrafish Establishment of the human hearing disorder model used is expected to be useful for screening future therapeutic agents.

PD 176

SoxC transcription factors are required for establishment of sensory cell fate in the inner ear

Ksenia Gnedeva¹; Xizi Wang¹; Haoze (Vincent) Yu²; Litao Tao³; Talon Trecek¹; Juan Llamas²; Welly Makmura¹

¹*Department of Stem Cell Biology and Regenerative Medicine, Keck School of Medicine of the University of Southern California; Caruso Department of Otolaryngology, Keck School of Medicine, University of Southern California;* ²*Department of Stem Cell Biology and Regenerative Medicine, Keck School of Medicine, University of Southern California; Caruso Department of Otolaryngology, Keck School of Medicine, University of Southern California;* ³*Department of Stem Cell Biology and Regenerative Medicine; Caruso Department of Otolaryngology, Keck School of Medicine, University of Southern California*

Background:

Differentiation of hair cells - the sensory receptors of the inner ear – depends on the embryonic expression of the transcription factor Atoh1. However, the molecular determinants initiating the early establishment of hair cell fate, upstream of Atoh1, remain largely unknown. We explored the role of two members of the SoxC gene family—*Sox4* and *Sox11*—who's transient expression in the sensory epithelia during embryonic development is limited to the period just prior to hair cell differentiation. We have previously shown that loss of one allele each of *Sox4* and *Sox11*, results in vestibular ataxia and hearing deficiency, while homozygous conditional knockout of both genes yields stunted vestibular and hearing sensory organs that fail to produce hair cells (Gnedeva et al., 2015).

Methods:

Using Sox2-GFP and p27^{kip1}-GFP reporter mouse lines, we purified proliferating and post-mitotic progenitor cells from the developing organ of Corti, and utilized RNA- and ATAC- sequencing to assess molecular events associated with prosensory domain establishment in the organ. Using these data, we then identified changes in gene regulation caused by the conditional deletion of SoxC genes prior to hair cell differentiation. We also analyzed the effects of overexpression of *Sox4* or *Sox11*, using Anc80-AAV gene delivery vector, to assess their role in hair cell differentiation and regeneration.

Results:

Our data suggest that SoxC transcription factors regulate early establishment of hair cell fate. We demonstrate that SoxC factors are required for maintaining accessibility

of the promoters and enhancers of key hair cell-specific genes, including *Atoh1*, in the post-mitotic progenitor cells of the organ of Corti. Further, we demonstrate that over-expression of *SoxC* in supporting cells of the mature utricle, and in organ of Corti progenitor cells, is sufficient to promote hair cell differentiation.

Conclusions:

Our data uncovers early chromatin remodeling events that determine hair cell fate initiation in the post-mitotic progenitor cells of the organ of Corti. Our results further suggest *SoxC* transcription factors as key regulators of sensory fate determination and potential new targets for regenerative medicine approaches to treat hearing loss and balance disorders.

SAVE THE DATES

JANUARY 25-29, 2020

43rd Annual MidWinter Meeting

San Jose Convention Center
San Jose, California

FEBRUARY 20-24, 2021

44th Annual MidWinter Meeting

Renaissance SeaWorld
Orlando, Florida

FEBRUARY 5-9, 2022

45th Annual MidWinter Meeting

San Jose Convention Center
San Jose, California

FEBRUARY 11-15, 2023

46th Annual MidWinter Meeting

Renaissance SeaWorld
Orlando, Florida

Association for Research in Otolaryngology

19 Mantua Road
Mt. Royal, NJ 08061

www.aro.org